

Institute of High Current Electronics SB RAS  
National Research Tomsk Polytechnic University  
Tomsk Scientific Center SB RAS

# **International Congress on Energy Fluxes and Radiation Effects**

*Abstracts*

September 21–26, 2014  
Tomsk, Russia

Tomsk  
Publishing House of IAO SB RAS  
2014

## General Chairman of the Congress

Gennady Mesyats Russian Academy of Sciences

## Chairman of Program Committee

Nikolay Ratakhin Institute of High Current Electronics SB RAS

## Local Organizing Committee:

A. Markov	Chairman, Institute of High Current Electronics SB RAS, Tomsk, Russia
N. Landl	Co-Chairman, Institute of High Current Electronics SB RAS, Tomsk, Russia
V. Shklyaeв	Institute of High Current Electronics SB RAS, Tomsk, Russia
Yu. Akhmadeev	Institute of High Current Electronics SB RAS, Tomsk, Russia
I. Pegel	Institute of High Current Electronics SB RAS, Tomsk, Russia
N. Labetskaya	Institute of High Current Electronics SB RAS, Tomsk, Russia
E. Chudinova	Institute of High Current Electronics SB RAS, Tomsk, Russia
E. Petrikova	Institute of High Current Electronics SB RAS, Tomsk, Russia
O. Krycina	Institute of High Current Electronics SB RAS, Tomsk, Russia
S. Onishenko	Institute of High Current Electronics SB RAS, Tomsk, Russia
A. Shnaider	Institute of High Current Electronics SB RAS, Tomsk, Russia
K. Kostikov	Institute of High Technology Physics, TPU, Tomsk, Russia
A. Bogdan	Institute of High Technology Physics, TPU, Tomsk, Russia

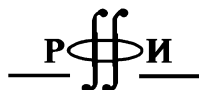
## Conferences:

18<sup>th</sup> International Symposium on High Current Electronics

12<sup>th</sup> International Conference on Modification of Materials with Particle Beams and Plasma Flows

16<sup>th</sup> International Conference on Radiation Physics and Chemistry of Condensed Matter

Congress is sponsored by



## Edited by:

Boris Kovalchuk, Gennady Remnev, Nikolai Koval, Valery Krivobokov, Vladimir Lopatin, Viktor Lisitsyn

---

**International Congress on Energy Fluxes and Radiation Effects: Abstracts.** — Tomsk: Publishing House of IAO SB RAS, 2014. — 542 pp.

This book comprises the abstracts of the reports (presentations) for the oral and poster sessions of International Congress on Energy Fluxes and Radiation Effects (EFRE-2014). The Congress combines three International Conferences held in Tomsk: Symposium on High Current Electronics, Conference on Modification of Materials with Particle Beams and Plasma Flows, and Conference on Radiation Physics and Chemistry of Condensed Matter. The program of the Congress covers a wide range of technical areas and modern aspects of pulsed power technology, ion and electron beams, high-power microwaves, sources of plasma and particle beams, modification of material properties, pulsed power applications in chemistry, biology and medicine, physical and chemical non-linear processes in inorganic dielectrics under the action of particle and photon beams, and physical principles of radiation-related technologies.

---

ISBN 978-5-94458-146-4

## CONTENTS

Plenary Session .....	5
<b>18<sup>th</sup> International Symposium on High Current Electronics .....</b>	<b>7</b>
<b>INTENSE ELECTRON AND ION BEAMS</b>	
Oral Session.....	9
Poster Session.....	25
<b>PINCHES, PLASMA FOCUS AND CAPILLARY DISCHARGE</b>	
Oral Session.....	54
Poster Session.....	65
<b>HIGH POWER MICROWAVES</b>	
Oral Session.....	79
Poster Session.....	87
<b>PULSED POWER TECHNOLOGY</b>	
Oral Session.....	114
Poster Session.....	128
<b>DISCHARGES WITH RUNAWAY ELECTRONS</b>	
Oral Session.....	149
Poster Session.....	163
<b>PULSED POWER APPLICATIONS</b>	
Oral Session.....	179
Poster Session.....	189
<b>12<sup>th</sup> International Conference on Modification of Materials with Particle Beams and Plasma Flows.....</b>	<b>207</b>
<b>BEAM AND PLASMA SOURCES</b>	
Oral Session.....	209
Poster Session.....	218
<b>FUNDAMENTALS OF MODIFICATION PROCESSES</b>	
Oral Session.....	245
Poster Session.....	253
<b>MODIFICATION OF MATERIAL PROPERTIES</b>	
Oral Session.....	264
Poster Session.....	290
<b>COATINGS DEPOSITION</b>	
Oral Session.....	353
Poster Session.....	367
<b>NANOSCIENCE AND NANOTECHNOLOGY</b>	
Oral Session.....	390
Poster Session.....	398

<b>16<sup>th</sup> International Conference on Radiation Physics and Chemistry of Condensed Matter .....</b>	<b>415</b>
ELEMENTARY PROCESSES	
Oral Session.....	417
Poster Session.....	432
NONLINEAR EFFECTS	
Oral Session.....	451
Poster Session.....	474
SURFACE PHENOMENA	
Oral Session.....	486
Poster Session.....	489
PHYSICAL BASIS OF RADIATION-RELATED TECHNOLOGIES	
Oral Session.....	498
Poster Session.....	508
METHODS OF TESTING	
Oral Session.....	526
Poster Session.....	527
<b>Author Index.....</b>	<b>532</b>

**MODERN TRENDS AND DEVELOPMENT IN HIGH-DOSE LUMINESCENT MEASUREMENTS**

V.KORTOV, S.NIKIFOROV, S.ZVONAREV, YU.USTYANTSEV

Ural Federal University, Mira Street, 19, Ekaterinburg, 620002, Russia, [vskortov@mail.ru](mailto:vskortov@mail.ru), +7.343.375-44-43

At present there is an intensive development of radiation technologies employing high-dose radiation to modify material properties, sterilize medical products and to perform other industrial processes. High-dose detectors are used in radiation monitoring of nuclear power station (NPS) equipment and storages for spent nuclear fuel. Such detectors are necessary also after large accidents at NPS (like Chernobyl and Fukushima). In most cases measurement of radiation doses as high as several dozens or hundreds of kGy is required.

This talk presents the results of thermoluminescent and dosimetric property investigations of some high-dose detectors. On the basis of this analysis one can conclude:

- At present several successful researches on luminescent and dosimetric properties of some materials suitable for high-dose detector manufacture have been carried out. A number of such materials can be expected to increase, as there is no tissue equivalence requirement for high-dose luminescent detectors.
- Highly sensitive luminescent detectors (e.g.  $\alpha$ -Al<sub>2</sub>O<sub>3</sub>:C, LiF:Mg,Cu,P) can be used to measure both low doses in personal radiation monitoring and high doses in radiation technologies.
- Crystals with deep traps are very prospective for high-dose measurements, because efficient filling of the deep traps starts with high-dose irradiation. Deep traps exist in non-irradiated  $\alpha$ -Al<sub>2</sub>O<sub>3</sub>:C crystals (TLD-500 detectors) and are found after intensive irradiation under high-temperature heating. It was shown that TL peak height at T<sub>m</sub>=430 K of TLD-500 detectors changes linearly in the range from 1,5 kGy to 80 kGy.
- High-dose detectors should be radiation-resistant. Higher radiation resistance is typical for low-dimensional materials (glass, ceramics), nano- and hetero-structures.
- A great role in the change of TL and dosimetric properties of detectors after high-dose irradiation is played by the processes of new trapping center formation including those with the aggregate defects involved.
- It is necessary the development of special annealing procedures after high-dose detector irradiation.

The existing experimental challenges in development and use of high-dose TL detectors are not significant and will be resolved.



# **18<sup>th</sup> International Symposium on High Current Electronics**



**Co-Chairmen:**

- Boris Kovalchuk Institute of High Current Electronics, Tomsk, Russia  
 Gennady Remnev Institute of High-Technology Physics, TPU, Tomsk, Russia

**International Advisory Committee:**

- Vasily Glukhikh D.V. Efremov Scientific Research Institute of Electrophysical Apparatus, St. Petersburg, Russia  
 Francis Lassalle Centre d'Etudes de Gramat, Gramat, France  
 Alexander Litvak Institute of Applied Physics RAS, Nizhny Novgorod, Russia  
 Michael Mazarakis Sandia National Laboratories, Albuquerque, New Mexico, USA  
 Mikhail Petelin Institute of Applied Physics RAS, Nizhny Novgorod, Russia  
 Efim Oks Institute of High Current Electronics SB RAS, Tomsk, Russia  
 Vladislav Rostov Institute of High Current Electronics SB RAS, Tomsk, Russia  
 Nikolai Ratakhin Institute of High Current Electronics SB RAS, Tomsk, Russia  
 Marek Sadowski Soltan Institute for Nuclear Studies, Warsaw, Poland  
 Edl Schamiloglu University of New Mexico, Albuquerque, USA  
 Victor Selemir All-Russian Research Institute of Experimental Physics, RFNC – VNIIEF, Sarov, Russia  
 Valery Shpak Institute of Electrophysics UB RAS, Yekaterinburg, Russia  
 Valentin Smirnov National Research Institute "Kurchatov Institute", Moscow, Russia  
 Vasily Ushakov Institute of Power Engineering, TPU, Tomsk, Russia  
 Yuriy Usov Institute of Power Engineering, TPU, Tomsk, Russia  
 Mikhail Yalandin Institute of Electrophysics UB RAS, Yekaterinburg, Russia  
 Yuriy Yushkov Institute of Power Engineering, TPU, Tomsk, Russia  
 Evgenij Grabovski Troitsk Institute for Innovation and Fusion Research (TRINITI), Troitsk, Russia  
 Sergey Rukin Institute of Electrophysics UB RAS, Yekaterinburg, Russia  
 Victor Tarasenko Institute of High Current Electronics SB RAS, Tomsk, Russia

**Sessions:**

- Intense electron and ion beams  
 Pinches, plasma focus and capillary discharge  
 High power microwaves  
 Pulsed power technology  
 Discharges with runaway electrons  
 Pulsed power applications



**HARD X-RAY GENERATION IN A RADIAL FOIL ROD-PINCH DIODE***S.A.SOROKIN**Institute of High Current Electronics SB RAS, 2/3 Akademichesky Ave., Tomsk 634055, Russia,  
E-mail: s.sorokin@rambler.ru, Phone: +7(382-2) 492322*

Experimental results of the low-impedance diode formation in a radial foil rod-pinch diode are presented. In these experiments, an aluminum foil is placed between concentric electrodes of a rod-pinch diode. The radial foil is subjected to the current pulse from the MIG generator (1 MV, 1.5 MA, 80 ns) and is accelerated in the axial direction by the  $\mathbf{J} \times \mathbf{B}$  force. The largest  $\mathbf{J} \times \mathbf{B}$  force at small radii close the anode rod leads to the largest foil mass axial displacement and the formation of a radial gap between the anode rod and the remaining foil. Strongly-pinched self-magnetically-limited electrons flow to the tip of the rod, once sufficiently high gap voltage is reached. A point-like hard x-ray source is formed at the rod tip. The foil thickness and the length of the rod extension beyond the radial foil are chosen so that the foil plasma moves past the end of the rod at the peak of generator current. Several successive intense bremsstrahlung pulses are formed as the result of current reconnections in the foil and rod plasmas.

## DYNAMICS OF THE MOLTEN METAL IN A VACUUM ARC CATHODE SPOT: SPLASHING THRESHOLD<sup>1</sup>

G.A. MESYATS\*, N.M. ZUBAREV\*\*

\*Lebedev Physics Institute, RAS, Leninskii pr. 53, Moscow, 119991, Russia

\*\*Institute of Electrophysics, UB, RAS, ul. Amundsena 106, Yekaterinburg, 620016, Russia, nick@iep.uran.ru, +7(343)2678776

It is known [1] that microcraters are formed on the cathode during the operation of a vacuum arc. Their occurrence is related to the extrusion of the metal molten due to Joule heating by the pressure of the cathode plasma. In the present work, we study the principal parameters that govern the behavior of a liquid metal (for definiteness, we consider molten copper) at near-threshold currents (an arc cannot be ignited if the discharge current is below the threshold value,  $I_c \approx 1.6$  A [1,2]).

Possible regimes of motion of the liquid are convenient to analyze with the use of two dimensionless groups: the Weber and Reynolds numbers,  $We = \rho U^2 D / \sigma$  and  $Re = UD / \nu$ , where  $D$  is the characteristic size of the region occupied by the liquid,  $U$  is the velocity of its extrusion,  $\sigma$  is the surface tension coefficient of the liquid, and  $\nu$  is its kinematic viscosity. For liquid copper whose temperature is a little above the melting point, we obtain  $We \approx 360$  and  $Re \approx 960$  [3].

We suppose that the problem concerning the extrusion of the molten metal from a microcrater is similar to the classical hydrodynamic problem of a liquid drop impact on a solid surface. According to Refs. [4,5], the condition under which a regular behavior of a liquid upon droplet impact on a plane solid surface (its spreading over the surface) will go into a singular behavior (splash accompanied by formation of jets and secondary drops) is the following:  $K \approx We^\alpha \times Re^{2(1-\alpha)} \geq K_s$ , where  $K_s \approx 1320$  and  $\alpha \approx 0.817$  ( $K$  is the splashing parameter and  $K_s$  is its critical value). This criterion allows one to determine threshold values of the pressure ( $P_s$ ) and of the electric current passing through a cell of an arc cathode spot ( $I_s$ ):

$$I_s = \frac{\pi P_s D_0^2}{4 u_i \gamma_i}, \quad P_s = \frac{K_s \rho^{1-\alpha} \sigma^\alpha \nu^{2(1-\alpha)}}{2^{(1+\alpha)/3} D_0^{2-\alpha}},$$

where  $D_0 = 2^{1/3} D$  is the diameter of a hemispherical microcrater,  $u_i$  is the characteristic velocity of the ions,  $\gamma_i$  is the ion erosion rate (mass removed per unit charge). If these values are exceeded, i.e.,  $I \geq I_s$ , or, which is the same,  $P \geq P_s$ , the regular regime of extrusion of the molten metal from the crater becomes singular. We obtain with the help of this formulas (see details in Ref. [3]) that  $I_s \approx 1.4$  A and  $P_s \approx 5.5 \times 10^7$  Pa. Recall that the threshold arc current  $I_c$  is  $\sim 1.6$  A. Thus, the conditions under which the formation of jets and drops of liquid metal extruded from a crater becomes possible almost coincide with the threshold conditions for a self-sustaining vacuum arc.

The estimates obtained count in favor of the supposition of the critical importance of hydrodynamic processes in self-sustaining electric arcs. In particular, in the context of the idea that the formation of liquid metal jets is necessary for the initiation of new explosive-emission centers [1], these estimates give grounds to relate the existence of a threshold current for electric arcs to the existence of a threshold for singular hydrodynamic processes in liquid metals (i.e., a threshold for the formation of microjets and microdrops of a liquid metal extruded from a crater). In other words, it is possible to identify the threshold current of an electric arc,  $I_c$ , with the threshold current for splashing of the liquid metal from the crater,  $I_s$ .

### REFERENCES

- [1] G. A. Mesyats // *Phys. Usp.* – 1995. – V. 38. – P. 567.
- [2] I. G. Kesaev // *Cathode Processes in an Electric Arc.* – Moscow, Nauka, 1968.
- [3] G. A. Mesyats and N. M. Zubarev // *J. Appl. Phys.* – 2013. – V. 113. – P. 203301.
- [4] G. E. Cossali, A. Coghe, and M. Marengo // *Exp. Fluids.* – 1997. – V.22. – P.463.
- [5] C. Bai and A. Gosman // *SAE Technical Paper.* – 1995. – P. 950283.

<sup>1</sup> This work was supported by the Russian Foundation for Basic Research (grant no 14-08-00235 and 13-08-96010\_r\_ural) and by the Presidium of the Russian Academy of Sciences in the framework of the program 29P.

## COMPARATIVE ANALYSIS FOR DIFFERENT MATHEMATICAL MODELS IN ELECTRON OPTICS

V.YA. IVANOV

*ICT RAS, 6 Lavrentiev prosp., Novosibirsk, 630090, Russia, vivanov.48@mail.ru, +7(913)486-9002*

The problem formulations in electron optics are very multifarious. It is well common to split them onto two main classes: non linear self-consistent problems of high-current beams, and precision problems of the image electronic devices. Different physical problems generate the set of different mathematical models. Thus, the efficiency of any particular model depends on the features of the physical problem formulation. In the paper we make the comparative analysis of computational efficiency for four mathematical models: pseudoviscosity method, “pipe-current” method, aberration approach and principal ray method.

The pseudoviscosity method is the sort of relaxation methods. It is based on use the non stationary algorithm to find the stationary solution as the limit of non stationary physical process. Normally it is formulated as the combination of Maxwell’s solver for the field problems, and “particle-in-cell” model for the particle dynamics. This method is extremely useful to detect the instability regimes for the almost stationary problems, but it is very inefficient for the true stable problems comparing with the other methods mentioned above.

The “pipe-current” method is the most popular method to simulate the stationary optics of high-current relativistic beams. It includes the set of equations for self-consistent problem: field equation (Poisson’s equation), motion equation (Lorentz equation), and continuity equation for the charge and current conservation law. This method has slightly different formulations for laminar and non laminar flows of charged particles.

The aberration approach is a version of more general perturbation theory applying to the light and charge particle optics. The general idea of this method is based on the expansion of the solution for trajectories on the set of small parameters of the problem, which gives the main advantages of high accuracy and reduces the computation time on many orders comparing the “pipe-current” method. Main disadvantage of this approach is that it is applicable for narrow enough beams only.

The principal ray method remove the limitation of the aberration approach, as it combine all positive features of the “pipe-current” and aberration methods in terms of the accuracy and efficiency of the solution. It is applicable for stationary and non stationary, self-consistent and weak current optics also.

The analysis of mathematical models is provided with the examples of numerical design carried out with use the computer codes implemented by the author.

### REFERENCES

- [1] *Astrelin V.T., Ivanov V.Ya.* The code for simulation of high-current beams of relativistic particles //Autometria. – 1980. - №3 .- PP.92-99.
- [2] *Ivanov V.Ya.* //Computer Aided Design of Physical Electronic Devices (in 2 volumes). – Institute of Mathematics of RAS Publishing, 1986.
- [3] *V. Ivanov.* //Proc. 2nd Int. Conf. on Computations in Electromagnetism. Nottingham, May 13-15, 1994. UK.
- [4] *V. Ivanov, K. Ko, A. Krasnykh, L. Ives, G. Miram.* 3-D method for the design of multi or sheet beam RF sources. //SLAC-PUB-9366.
- [5] *Ivanov V., Brezhnev V.* New formulation of the synthesis problem in electron optics. //Nucl.Instrum.Meth.A, - V.519. – 2004. – PP.117-132.
- [6] *Ivanov V.* LFSC – Linac Feedback Simulation Code //User’s Guide. Fermilab-TM-2409-CD, 2008.
- [7] *Ivanov V.* Green’s Function Technique in Forming of Intensive Beams // Int. J. of Modern Physics A. - Vol.24. -, No.5. -2000. – PP. 869-878.
- [8] *Ivanov V., Insepov Z., Antipov S.* Gain and Time Resolution Simulations in Saturated MCP Pores // NIM A, 52549. – 2010 PP. 02291-6.
- [9] *Insepov Z., Ivanov V., Jokela S. J. Veryovkin I. et al.,* Comparison of Secondary Electron Emission Simulation to Experiment, NIM A, 52549. - 2010.

## THE ANGLE DEPENDENCE OF A ION FLOW PARAMETERS IN A ELECTRON BEAM – PLASMA CLOUD ACCELERATION PROCESS.<sup>1</sup>

*I.L. MUZYUKIN\**, *D. VOLZHANINOV\*\**

\* *Institute of Electrophysics, Russian Academy of Sciences, Ural Branch, 106 Amundsena st., Ekaterinburg, 620016, Russia, plasmon@mail.ru*

\*\* *Ural Federal University 620002, 19 Mira street, Ekaterinburg, Russia*

It has been reported [1] that plasma acceleration by a electron beam results in a ion energy spectra that coincides with energy ion spectra of a pulsed vacuum discharges. Thus, one can assume that acceleration of plasma by electron beam is the basic plasma acceleration mechanism in a different types of a vacuum discharges . This work is devoted to examination the process of a plasma cloud expansion in a vacuum under different angles to electron beam direction.

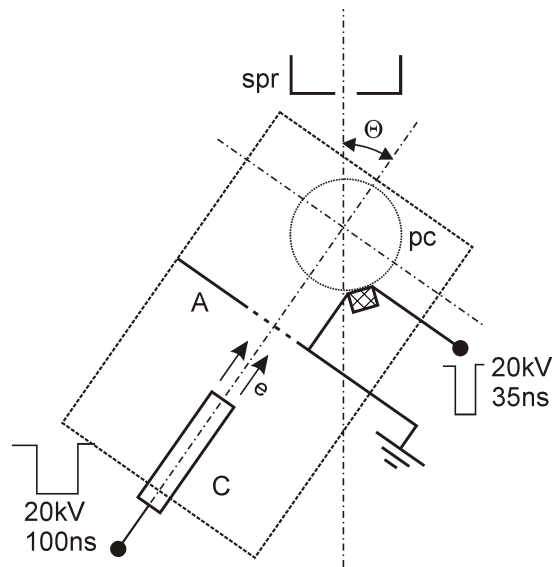


Fig. 1. Experimental setup C-Cathode, A-Anode, pc- plasma cloud, spr-Tomson spectrometer

Experimental setup is presented at Fig.1 It was revealed that electrons and ions of a plasma cloud are being accelerated in a wide space angle (+- 60 degrees). Energies of a charged particles decrease with angle growth. Space angle of hydrogen ions expansion is larger than 60 degrees. Space angle of heavy ions expansion is less than 45 degrees.

### REFERENCES

- [1] *I.L. Muzyukin // Discharges and Electrical Insulation in Vacuum (ISDEIV), 2012, Page(s): 619 - 622,- 1657*

<sup>1</sup> This work was supported in part by the Russian Fundamental Research Foundation under Awards 14-02-00575, 14-08-01137, 13-08-00619, 12-08-00310 and in part by Presidium UB RAS Project 12-P-2-1027

## INVESTIGATION OF PLASMA BUNCHES GENERATED BY PULSED SURFACE FLASHOVER IN VACUUM<sup>1</sup>

*P.A. MOROZOV, R.V. EMLIN, I.F. PUNANOV, K.A. KHRUSHCHEV*

*Institute of Electrophysics UB RAS, 106 Amundsena street, Yekaterinburg, 620016, Russia, lfd@iep.uran.ru, +7(343)267-88-26*

Pulsed surface vacuum flashover has been investigated for quite a long time and still attracts researchers attentions. In spite of the fact that a big number of works devoted to this complex phenomenon have been published, there are many problems to solve. A lot of problems arise in practical applications, especially in such spheres as pulsed plasma thrusters [1] and vacuum switches [2].

In this work the parameters of plasma bunches, that are generated during surface flashover on fluoroplastic were investigated in vacuum down to  $6 - 4 \cdot 10^{-4}$  mm of Hg. Pulsed generators having different output energy were used. Voltage under no load made 120-140 kV, rise times were 40-50 ns. Energy stored in the output stage of the generator was up to 5 J.

It has been shown that the generated bunch of particles propagated at a constant speed. The average velocity of the bunch slightly depends on pulse energy. The average velocities from 60 to 100 km/s were detected. The maximum average velocity is limited by 200 km/s. Plasma density (ion concentration) in the bunch depends on polarity of voltage pulse, discharge gap, and electrode geometry. Dependence of the shape of ion current signal on interelectrode distance and electrode geometry is considered. The energy of ions in the bunch of particles corresponds to thermal acceleration.

### REFERENCES

- [1] *W.J. Guman, D.M. Nathanson // Journal of Spacecraft and Rockets. 1970 Vol 7. No 4. PP. 409-415*
- [2] *S.M. Hu, X.L. Yao, J.L. Chen // IEEE Transactions on Plasma Science. 2012. Vol. 40. PP. 778-781*

---

<sup>1</sup> This work was supported by the program of the Presidium of the Ural Branch of the Russian Academy of Sciences.

## ENERGY TRANSFER IN A BLUMLEIN PULSE FORMING LINE OPERATING IN BIPOLAR PULSE FORMATION MODE<sup>1</sup>

*A.I. PUSHKAREV<sup>A</sup>, Y.I. ISAKOVA, I.P. KHAYLOV*

*Tomsk Polytechnic University 2a Lenin Ave., Tomsk, 634028, Russia, <sup>a</sup> e-mail: aipush@mail.ru*

The paper presents the results of a study on the energy transfer efficiency in a water Blumlein line terminated with either resistive load or an ion diode with self-magnetic field. The experiments have been conducted using the TEMP-4M pulsed ion accelerator configured to operate in double pulse mode. The accelerator consists of the Marx generator, double transmission line (Blumlein) and vacuum ion diode with self-magnetic insulation of electrons. The generator configured in double-pulse mode forms two pulses of opposite polarity: the first pulse is of negative polarity (300-600 ns, 100-150 kV), and this is followed by a second pulse of positive polarity (150 ns, 250-300 kV) [1]. The sources of the energy loss in Blumlein are found to be due to the leak current in water (used as dielectric medium) during charging of the Blumlein and in spark gaps during triggering. The total energy accumulated in the Blumlein is that transferred from Marx to Blumlein less the resistive losses. These losses (current leak in water, loss in spark gaps, etc.) amounts to 10 %.

The energy transfer efficiency from Blumlein to the resistive load or without the load (short circuit mode) was analyzed. Figure shows the data on the energy transfer in the diode connection when Blumlein is terminated with a resistive load.

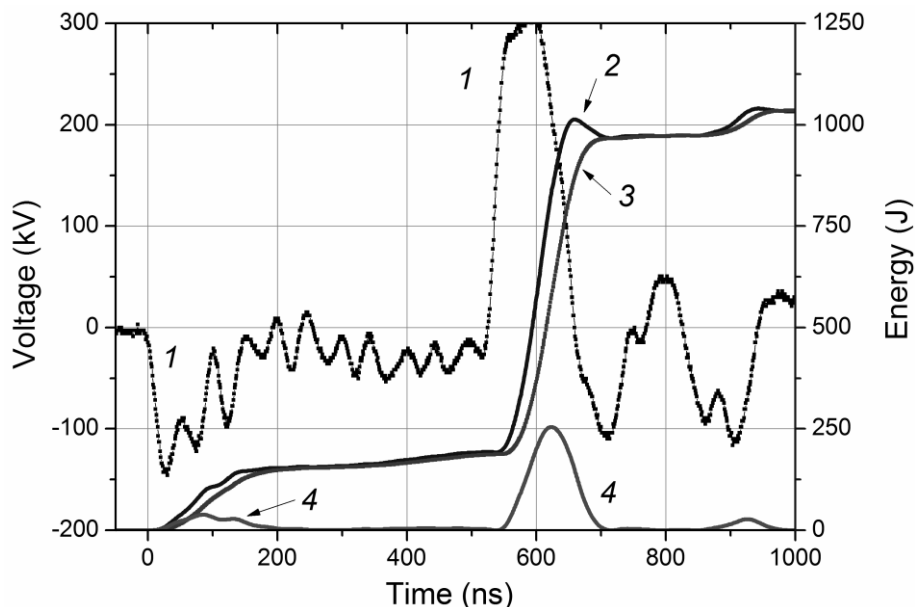


Fig. Waveforms of voltage at the output of Blumlein (1) and change in the energy transferred from Blumlein to the load (2), resistive losses of energy (3) and the energy stored in the inductance of the diode connection (4) of the accelerator

We found that out of 250 J of energy accumulated in the load inductance during the second voltage pulse 210 J (84%) is delivered to the load and the rest is returned in Blumlein. It was shown that 90% of the energy stored in Blumlein is delivered to the diode, and 90% of that is transferred to the diode during the ion beam generating pulse. The efficiency of energy transfer from Blumlein to the load is independent on the energy stored in Blumlein.

### REFERENCES

- [1] *Pushkarev A.I., Isakova Yu.I.* Surface & Coatings Technology.- 2013.- v. 228 S382–S384.

<sup>1</sup> This work was supported by The Ministry of education and science of the Russian Federation, project #2159

**ELECTRON ACCELERATOR WITH A MULTI-APERTURED PLASMA EMITTER<sup>1</sup>**

*M.S. VOROBYOV, N.N. KOVAL, S.A. SULAKSHIN, V.V. SHUGUROV*

*High Current Electronics Institute SD RAS, 2/3 Akademichesky av., Tomsk, 634050, Russia  
e-mail: vorobyovms@yandex.ru, phone: +7(3822)492683*

Emission properties of a multi-aperture plasma cathode and electron beam output from high-accelerating gap into the atmosphere are investigated. Electron-emitting plasma is generated by low pressure arc discharge in the anode chamber with dimensions  $(200 \times 150 \times 800)$  mm<sup>3</sup>, one side of which is blocked by a fine-wire grid. Special stainless foil mask is located on this grid. Mask separates emission surface 344 of the cell 12 mm in diameter, which are emission structures of the plasma emitter. Under a constant accelerating voltage applied between the emitter and the anode, which performs the role of the foil support grid exit window of the accelerator, with an area of these emission structures takes electron emission. In the support grid has the same number of holes as an emission structure mask, but the larger diameter of 15 mm. Holes alignment in the emission structure mask and support grid with a plane-parallel coaxial geometry achievement accelerating gap allows to minimize a beam losses on the support grid.

Thus, the electron beam total section  $(750 \times 150)$  mm<sup>2</sup> is a superposition of elementary beams formed by separate emission structures, the plasma boundary is stabilized fine-metal mesh. In experiments with an accelerating voltage of 180 kV and an emission current of 15 A and a pulse duration of 35 μs into the atmosphere was extracted 70 % emission current. Such a mechanism for extraction and transportation of the electron beam, not only increases the accelerator efficiency, reducing the loss of the beam on the support grid of the output foil window, but also increases the average power of the outputted electron beam, which reaches 2.5 kW in the experiments. Further increase of the average beam power was limited power supplies. Designed electron accelerator was used for radiation-induced vulcanization of natural rubber latex.

<sup>1</sup> This work was supported by RFBR projects № 14-08-00997-a and RAS Presidium program number 12 project 8.

## RESEARCH OF TRANSFER EFFICIENCY OF LOW-ENERGY HIGH-CURRENT ELECTRON BEAM IN PLASMA CHANNEL IN EXTERNAL MAGNETIC FIELD<sup>1</sup>

*V.P.GRIGORIEV, E.S. VAGIN*

*\*National Research Tomsk Polytechnic University, 634050, Russian Federation, Tomsk, Lenin Avenue, 30,  
[grig@am.tpu.ru](mailto:grig@am.tpu.ru).*

Effective high current (5-20 kA) and low energy (tens of keV) electrons beam transfer is possible only with almost complete charging neutralization. It is also necessary to use quite high current neutralization for elimination beam self-pinching effect.

The research is based on the self-consistent mathematical model that takes into account beam and plasma particles dynamic, current and charge neutralization of electron beam and examines the transfer of electron beam into a chamber with low-pressure plasma in magnetic field. A numerical study was conducted with using particle in cell (PIC) method.

The study was performed at various parameters of the system: the rise time and the magnitude of the beam current, gas pressure and plasma density and geometry of the system. Regularities of local virtual cathode field generated by the beam in the plasma channel, as well as ranges of parameters that let transfer beam with minimal losses, depending on the external magnetic field were determined through a series of numerical studies.

In addition, the assessment of the impact of the plasma ion mobility during the transition period and during steady beam was performed.

### REFERENCES

- [1] V.P.Grigoriev, T.V.Koval,, V.R.Kuhta, P.Rahadjo, K Uemura Transport and focusing of a low-energy electron beam in low-pressure ionized argon // *Journal of Technical Physics* – 2008. – 78, 1.
- [2] C.Birdsall, B.Langdon // *Plasma physics, via computer simulation* – Energoatomizdat, 1985.
- [3] V.P. Grigoriev, E.S.Vagin, V.V.Ofitserov, Macroparticles model of charge neutralization of the electron beam at injection in low-pressure plasma // *Bulletin of the Tomsk Polytechnic University* – 2010. – 316, 2.
- [4] N.N. Koval, S.V. Grigoryev, V.N. Devyatkov, A.D. Teresov, P.M. Schanin Effect of Intensified Emission During the Generation of a Submillisecond Low-Energy Electron Beam in a Plasma-Cathode Diode // *IEEE Trans. Plasma Science* – 2009. – Vol. 37, no 10, pp. 1890–1896.
- [5] M.U.Kreindel, E.A.Litvinova, G.E.Ozur, D.I.Proskurovsky, Non-stationary processes in an initial stage of formation of a high-current electronic beam in the plasma-filled diode // *Plasma Physics Reports* – 1991. – 17, 12.
- [6] D.S.Nazarov, G.E.Ozur, D.I.Proskurovsky, Generation if low-energy high-current electron beam in a gun with plasma anode // *Bulletin of higher education institutions. Physics* – 1994. – 37, 3.

<sup>1</sup> This work was supported by RFBR (Grants Nos. 13-08-98066 p\_сибирь\_a, 12-08-00251-a).



## NUMERICAL SIMULATION OF THE SECONDARY PLASMA SURFACE IN THE ION BEAM FORMATION<sup>1</sup>

*V.T. ASTRELIN\*\*\*, V.I. DAVYDENKO\*\*\*, A.V. KOLMOGOROV \**

*\*Budker Institute of Nuclear Physics SB RAS, Lavrentiev av. 11, Novosibirsk, 630090, Russia, [Astrelin@inp.nsk.su](mailto:Astrelin@inp.nsk.su), (383)329 49 24  
\*\*Novosibirsk State University, Pirogova str. 2, 630090, Russia*

A numerical simulation of the power proton source developed in BINP SB RAS was performed by the code POISSON-2 [1], modified to solve problems of modeling high current accelerators with plasma emitters [2]. The code allows solve the two-dimensional stationary tasks of electron and ion optics, including multiflow systems with external and self-consistent electric and magnetic fields. A shape of plasma surfaces was calculated in the “thin boundary” approximation from the equilibrium of a plasma pressure and electric field on the boundary.

Proton beam in the source is formed by three-electrode multislit ion optical system. Computer simulation was carried out for a single slit cell in the approximation of a two-dimensional plane-parallel geometry. A plasma flux from a neutralizer falls onto grounded grid. The second grid with applied potential  $-1$  kV is aimed to stop and break off the entering plasma flow, blocking the electron current from the plasma. Protons are emitted from gas-discharge plasma through apertures of emission grid being under applied potential of 20 kV.

Parameters of the proton emitting plasma are as the following. The plasma density is  $n \sim 10^{12}$  cm<sup>-3</sup>, the electron temperature is  $T_e \sim 8$  eV, ions one is  $T_i \sim 2$  eV, directed ions energy  $\varepsilon_{0i} \sim 20$  eV, the plasma potential  $\phi \sim +20$  V. Evaluation of plasma parameters, neutralizing the protons, is characterized by the following values. The plasma density is  $n \sim 10^{10}$  cm<sup>-3</sup>, electron and ion temperatures  $T_e \sim T_i \sim 2$  eV, the plasma potential  $\phi \sim +10$  eV. The electric field at the plasma boundary must be  $\sim 0.2$  kV/cm for equilibrium, electron current density is  $\sim 1.2$  A/cm<sup>2</sup> and the ion one is  $\sim 0.028$  A/cm<sup>2</sup>.

The external magnetic field is absent in the system. As for self magnetic field of currents, it is taken into account, as it may be important in the calculation of electron beams. Collisions and elementary processes in the plasma and gas are not included to the model. Plasma regions in the simulation are considered as equipotential with complete neutralization of the space charges.

The result of this simulation shows that neutralizing plasma stream reaches a saddle point of potential  $Y \sim 1$  cm and can not be stopped by electric field that is close to zero here. But if the potential of the second grid is chosen as  $U = -2$  kV, the plasma flow stops in a point  $Y \sim 1.2$  cm (Fig.1). In this case electrons of the plasma are returned and its ions fall onto second electrode.

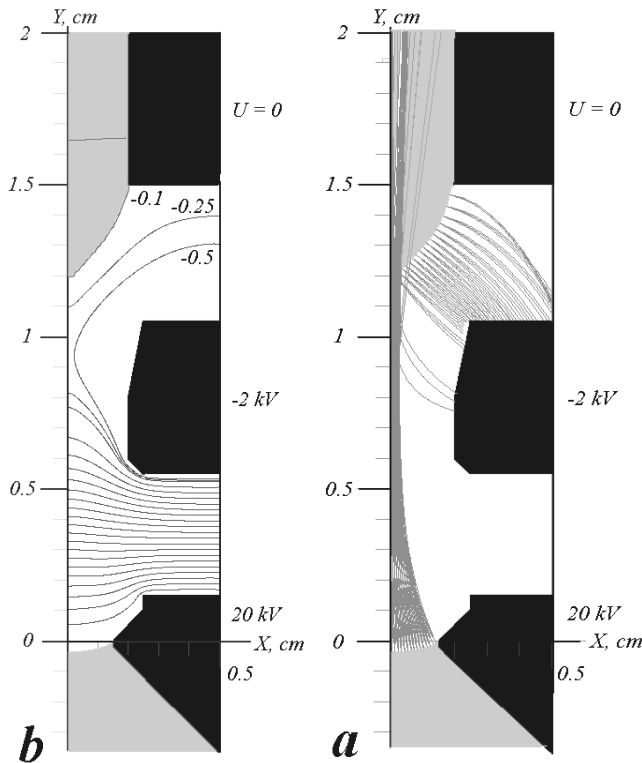


Fig.1. Particle trajectories (a) and distribution of potential (b) in the gun cell; electrodes are dark, plasmas are grey

### REFERENCES

- [1] *V.T. Astrelin, V.Ya. Ivanov. Avtometriya, 1980, v.3, p.92-99 (in Russian).*
- [2] *V. Astrelin, A. Burdakov, G. Derevyankin, et al. Proc. 15th Int. Symp. on High Current Electronics: Tomsk, 2008, p.11-15.*
- [3] *V.T. Astrelin, I.E. Karpov. Proceedings of the 4th International Kreyndel Workshop "Plasma Emission Electronics", Ulan-Ude, 2012, p.74-80 (in Russian).*
- [4] *V.T. Astrelin, I.E. Karpov. Proceedings of the 4th International Kreyndel Workshop "Plasma Emission Electronics", Ulan-Ude, 2012, p.88-90 (in Russian).*

<sup>1</sup> This work was supported by the RF Ministry of Education and Science, Grant 14.B37.21.0750, RFBR Grant No. 13-08-01064 and SB RAS Program (interdisciplinary integration Project №104)

## QUANTITATIVE X-RAY DIAGNOSTICS FOR MEASURING OF THE ELECTRON BEAM CURRENT DENSITY DISTRIBUTION ON A METAL TARGET

*V.V. KURKUCHEKOV\**, *I.A. IVANOV\*\**, *I.V. KANDAUROV\*\**, *YU.A. TRUNEV\*\**

*\*Novosibirsk State University, 2 Pirogova St., Novosibirsk, 630090, Russian Federation,  
kurkuchekov.victor@gmail.com, +7-923-130-8385*

*\*\*Budker Institute of Nuclear Physics of SB RAS, 11 Lavrentieva Prosp., Novosibirsk, 630090, Russian Federation*

For a number of electron beams applications (e.g. surface treatment of materials) the information about the beam current density distribution upon a target is of important value. In this paper, we present the results of experiments with X-ray pinhole camera diagnostics designed to measure in a single shot the electron beam current density distribution on a metal target.

The beam was generated in a source with arc plasma emitter and multiaperture electron optical system [1]. The main beam parameters were as follows: energy of electrons up to 100 keV, beam current up to 120 A, pulse duration of 0.1 - 0.3 ms and initial beam diameter of 5 - 8 cm. The beam was formed and transported in an axial magnetic field onto the plane molybdenum collector placed at 1.5 m from the source at the angle of 45 degrees to the beam direction. A beam spot X-ray image projected through a pinhole onto a conversion screen with gadolinium oxysulfide luminophore. The visible light from the conversion screen is registered by SDU-286 CCD-camera with SONY ICX285AL image sensor (1392 x 1032 square pixel). Due to a long luminophore afterglow, the registered signal was integrated over entire beam period. In image processing, each pixel output signal value is interpreted to be proportional to the local density of the beam electrons falling on the target. Linearity of the diagnostics at a given accelerating voltage was verified in a wide range of the beam parameters (pulse duration, beam current and beam spot size on the target). The spatial resolution was evaluated in special test experiments and was found not worse than 1.5 mm.

### REFERENCE

- [1] *V. V. Kurkuchekov et al. // Fusion Science and Technology. – 2013. – Volume 63. – Pages 292-294.*

## PLASMA CHANNEL FORMATION IN INERT GASES HE AND AR BY A LOW-ENERGY ELECTRON BEAM<sup>1</sup>

*I.L. ZVIGINTSEV, V.P. GRIGORIEV*

*TPU, Sovetskaya 84/3, Tomsk, 634034, Russia, zvigintsev@yandex.ru, +7(906)9503162  
TPU, Sovetskaya 84/3, Tomsk, 634034, Russia*

For efficient use of low-energy electron beams for technological purposes there is a need of their transportation to a target. For this purpose plasma channel pre-created by external sources is used or the beam is injected into a neutral gas creating plasma channel independently.

In this work the question of plasma channel formation by a low-energy electron beam is considered when filling a drift tube with argon or helium with gas pressure range 0.02..0.2 Pa. Investigations are carried out on the basis of a mathematical model [1, 2] including ionization processes, current and charge neutralization when passing high-current electron beam in inert gases of low pressure in the absence and in the presence of an external magnetic field  $B_z$ . In addition, the model is supplemented by a diffusion equation that allows determining influence of plasma diffusion on the plasma channel parameters.

Research of plasma channel parameters is performed for electron beams with experimental current pulse [3] (fig. 1). The plasma channel parameters relations on the system geometry, the external magnetic field, gas pressure and gas type are determined on the basis of numerical calculations. The influence of diffusion on the radial profile of the plasma density and the radius of the plasma channel depending on an external magnetic field and a total current field is investigated.

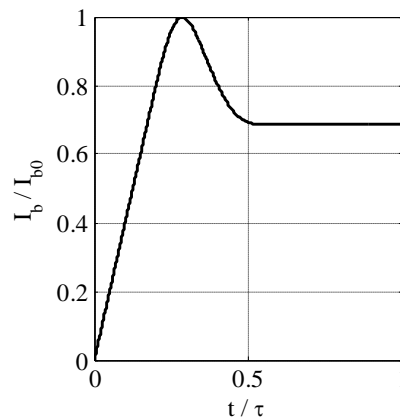


Fig. 1. Profile of experimental current pulse [3]

### REFERENCES

- [1] *V.P. Grigoriev and I.L. Zvigintsev* // Bulletin of the Tomsk Polytechnic University – 2011 – vol. 314 – № 5, pp. 40-43.
- [2] *V.P. Grigoriev and I.L. Zvigintsev* // Russian Physics Journal – 2012 – vol. 55 – № 10-3, pp. 460-462.
- [3] *G.E. Ozur, A.V. Batrakov, K.V. Karlik and L.A. Zyulkova* // Russian Physics Journal – 2013 – vol. 56 – № 7-2, pp. 37-41.

<sup>1</sup> This work was supported by RFBR (Grants Nos. 13-08-98066 r\_seberia\_a and 12-08-00251-a).

**HARD X-RAY SOURCES BASED ON OF HIGH-CURRENT PINCH DIODES**

V.K. PETIN, A.A. CHERTOV, A.V. LAVRINOVICH

*Institute of High Current Electronics  
Siberian Branch of Russian Academy of Sciences  
Tomsk, Russia, tel. 83822491520, [pvk1955@mail.ru](mailto:pvk1955@mail.ru)*

A number of hard X-ray sources based on high current pinch diodes are described. Pinch diodes have a voltage of 0.5-1.3 MV and currents from hundreds of kA to 1.5 MA. An area of the irradiated sources is varied in a wide range from tens to hundreds of cm<sup>2</sup>. Radiation pulse duration at half maximum (FWHM) is 50-60 ns. The optimal diode designs for hard X-ray output are described. The experimental spatial distribution of radiation is compared with the calculations. Calculations were performed for radiation sources of varying sizes. In the calculations takes into account the angular dependence of the radiation intensity.

## EFFECT OF ELECTRON EXTRACTION FROM A GRID PLASMA CATHODE ON THE GENERATION OF EMISSION PLASMA <sup>1</sup>

*V.N. DEVYATKOV\**, *N.N. KOVAL\*\**

*\*Institute of High Current Electronics SB RAS, 2/3 Akademicheskoy Ave., Tomsk, 634055, Russia, E-mail: vlad@opee.hcei.tsc.ru, Phone: +7(3822) 491-713*

*\*\* National Research Tomsk State University, 36 Lenin Ave., Tomsk, 634050, Russia*

The report presents research results on the electron emission from a plasma cathode with grid stabilization of the emission plasma boundary [1]. The effect of increase in the current of the main arc discharge generating the emission plasma is described. The increase in discharge current occurs when accelerating voltage is applied to the plasma cathode and electrons are extracted from the plasma through the fine metal grid stabilizing the emission plasma boundary. The electron emission from the arc discharge plasma changes the plasma parameters [2]. The change in the plasma potential and near-anode potential fall within the beam current pulse causes a change in the voltage across the gap between arc discharge cathode 1 and grid emission electrode 2 (Fig.1a). Figure 1b shows the pressure dependence of this voltage ( $U_d$ ) within 75  $\mu$ s after the beginning of the discharge current pulse of duration 200  $\mu$ s. The voltage  $U_d$  reveals a change not only in its value but also in its polarity due to switching of the electron component of the arc discharge current from the grid electrode to the acceleration gap. The experimentally detected change in the voltage  $\Delta U_d$  (no less than 160 V) is brought into the power supply circuit (PS), with a consequent increase in the discharge current  $I_d$  of the plasma cathode and in the emission current  $I_b$  due to the energy of the source powering the acceleration gap. The discharge current increases from  $I_d=150$  A to  $I_d=200$  A at an accelerating voltage of  $U_b=10$  kV. The thus arising positive feedback defines the possibility of uncontrollable changes in the parameters of emission current pulses formed by the plasma cathode and increases the probability of breakdown of the acceleration gap.

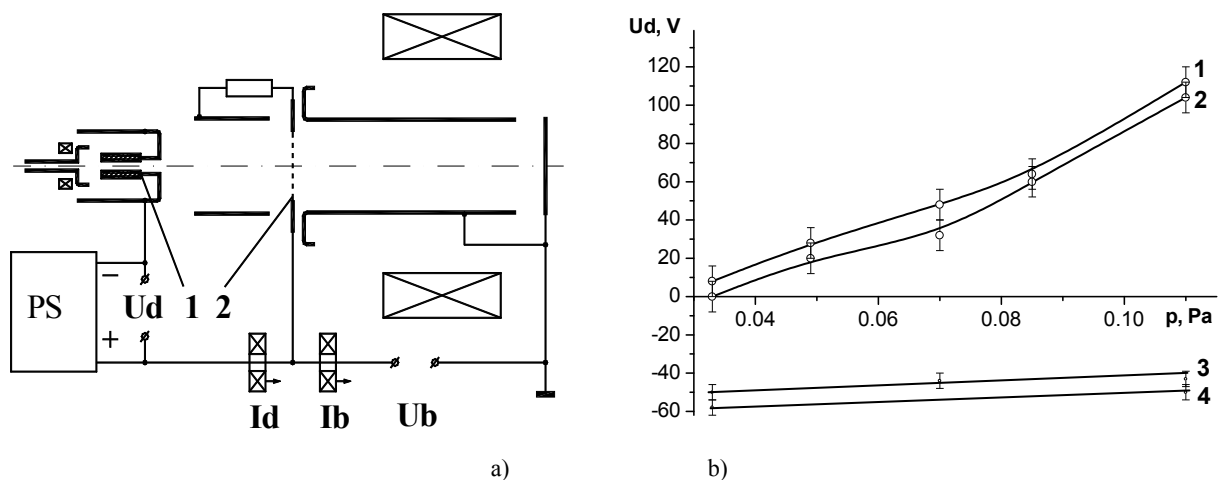


Fig. 1. Schematic of the electron source (a); pressure dependence of the voltage,  $U_d=f(p)$  (b): 1,2 –  $U_b=10$  kV; 3,4 –  $U_b=0$ ; 1,4 –  $I_d=250$  A; 2,3 –  $I_d=160$  A.

The effect of additional induced voltage in the power supply circuit of the discharge gap should be taken into account in designing power supply circuits for the plasma cathode. The additional voltage in the discharge circuit can lead to overloads of the PS elements. Moreover, the use of PS protective circuits can even further amplify the effect of increase in discharge and emission currents both with PS circuits based on storage capacitance and ballast resistance and with those based on switched inductive store.

### REFERENCES

- [1] *S.V.Grigoirev, V.N.Devyatkov, N.N.Koval, and A.D.Teresov.* // In Proc. 9th Intern. Conf. on Modification of Materials with Particle Beams and Plasma Flows: Tomsk: 2008, pp. 19-22.
- [2] *N.N.Koval, E.M.Oks, Yu.S.Protasov, N.N.Semashko* // Emission electronics, Moscow, MGTU, 2009, 596 p.

<sup>1</sup> This work was partly supported by program of the Presidium of the Russian Academy of Sciences No. 12 and RFBR project No.13-08-98108.

## INVESTIGATION OF PLASMA EMITTER BASED ON REFLECTIVE DISCHARGE WITH THE CATHODE SPOT FOR INTENSE PULSED SUBMILLISECOND ELECTRON BEAM

*S.V. GRIGORIEV, P.V. MOSKVIN*

*HCEI SB RAS, 2/3 Akademichesky Avenue, Tomsk, 634055, Russia, grigoriev@opee.hcei.tsc.ru, +7(3822)491300*

This paper describes the investigation of the electron emitter based on reflective discharge with the cathode spot to generate intense submillisecond low energy electron beam. Cathode plasma generated in a cylindrical discharge cell length 82 mm, diameter 84 mm. Cathode -emitter has a cylindrical magnesium insert. To facilitate ignition of the cathode spot to create an additional discharge. Output window of discharge system performed in the cathode - reflector has a diameter of 40 mm and overlapped with the cell grid  $0.3 \times 0.3 \text{ mm}^2$ . Operating argon gas fed through the emitter, the pressure in the chamber ranged from  $1.4 \cdot 10^{-2} \text{ Pa}$  to  $3 \cdot 10^{-2} \text{ Pa}$ . Axial magnetic field was 100 mT, electron energy of 25 keV and pulse duration of the beam current up to 200  $\mu\text{s}$ .

A distinctive feature is the presence of the represented emitter by positive feedback between the discharge current and accelerating voltage. Feedback allows you to obtain current in the accelerating gap fold excess (up to 6 times), discharge current (current to the anode of the discharge cell). In addition, there is an increasing of the beam current due to ion-electron emission from the surface of the emission electrode [1]. Current in the accelerating gap in the presented experiments reached 250 A.

In the experiments was obtained by a high recovery rate of electrons from the plasma emitter based on reflective discharge. It is 0.8. This is 15% higher than for a standard plasma emitter with the same geometry.

The connection of emission grid and cathode of discharge with a high negative potential of the accelerating voltage leads to increased current originally created by the cathode spot (40-50 A) due to the accelerating voltage power supply. Dense cathode spot plasma closes the accelerating gap of cathode discharge, while in the emission electrode location with a "rare" gas-discharge plasma accelerating gap is formed.

In low pressure ( $1.4 \cdot 10^{-2} \text{ Pa}$ ) detected beam current termination effect until the termination of the discharge current. With increasing current in the discharge cell from the anode 30 to 100 A current pulse in the accelerating gap is reduced from 200 to 70  $\mu\text{s}$ . As the magnetic field in the discharge cell beam pulse duration is slightly reduced. However, the acceleration voltage is not affected by the pulse duration.

At elevated ( $3 \cdot 10^{-2} \text{ Pa}$ ) pressure current pulse duration in the accelerating gap can exceed the pulse duration of the anode current discharge cell due to the relaxation of the plasma in the discharge cell emitter.

The electron beam generated by the electron source based on this emitter successfully used for the surface modification of titanium alloys.

### REFERENCES

- [1] *N.N. Koval, S.V. Grigoryev, V.N. Devyatkov, A.D. Teresov, P.M. Schanin // IEEE Trans. Plasma Sci. – 2009. Vol. 37, № 10. Pages 1890–1896.*

## MULTIARCS PLASMA EMITTER FOR SUBMILLICECOND ELECTRON BEAM WITH ENERGY UP TO 100 KEV AND CURRENT LEVEL UP TO 1KA

*M.S. VOROBYOV, S.V. GRIGORIEV, S.A. SULAKSHIN, P.V. MOSKVIN*

*HCEI SB RAS, 2/3 Akademicheskoy Avenue, Tomsk, 634055, Russia, grigoriev@opee.hcei.tsc.ru, +7(3822)491300*

The results of the experiment and the results of experiments made estimates of the main parameters of the electron diode with grid plasma cathode and anode plasma with open moving boundary plasma at an electron beam generation with submillisecond pulse duration ( $\sim 100 \mu\text{s}$ ) accelerating voltage up to 70 kV and beam current up to 1 kA.

The need for such an electron beam due to task of the additional heating the plasma formed by a relativistic electron beam in order to keep its temperature within milliseconds in research on controlled thermonuclear fusion at the GOL -3 equipment [1].

Grid plasma cathode (emitter) of the investigated electron source the based on multiarcs discharge with distributed emission centers [2]. Stable operation of the emitter grid stabilization achieved emission cathode plasma boundary. The anode plasma is created by the electron beam generated and transported in low-pressure gas (3 - 20 mPa) in a longitudinal magnetic field. The accelerating gap between the boundaries of the cathode and anode plasma, in this case, is set consistently with the parameters of the electron beam.

Investigation has been performed at 100  $\mu\text{s}$  pulse duration. At the same time, electron source based on represented multiarcs emitter has no principal - physical constraints on the pulse duration of the generated electron beam.

During the investigation achieved stable operation of the electron source at the electron beam with a current of 1 kA. Thus the total current of all 6- arc plasma emitter sources was 1.4 kA, the voltage on the accelerating gap of up to 70 kV. The diameter of the emitting surface of the plasma cathode 130 mm. Beam transported over a distance of 750 mm in an axial magnetic field of 30 mT to a water-cooled copper collector. According to preliminary estimates, up to 30% of the beam current is the current of secondary electrons produced by the ion-electron emission from the emission electrode surface.

It is shown that for small (200 A) discharge current multiarcs emitter, since the pressure of 30 mPa, the share of the current of secondary electrons than extracted from the plasma, even at a low voltage - 25 kV. Increasing the electron beam current by increasing the discharge current in the emitter leads to an increase in the concentration of the anode plasma. Consequently, increasing the ion current density on the electrode and the emission secondary electron current. A positive feedback, which investigated the emitter does not lead to a destabilizing effect on the work of the emitter and the electron source in general.

### REFERENCES

- [1] *V. Astrelin, A. Burdakov, G. Derevyankin, V. Ivanov, I. Kandaurov, S. Sinitsky, and Yu. Trunev // Numerical Simulation of Diodes with Plasma Electrodes. 15th International Symposium on High Current Electronics. Tomsk Publishing house of the IAO SB RAS. - 2008. - P. 11-15.*
- [2] *MS Vorobyov, VV Denisov, VN Devyatkov, SA Gamerman, NN Koval, VV Shugurov, SA Sulakshin, VV Yakovlev // The multiarc plasma cathode electron source. Proceedings of the 25th International Symposium on Discharges and Electrical Insulation in Vacuum Tomsk, Russia, September 2-7. – 2012. - Vol. 2. - P. 537-540.*

## ELECTRON SOURCE WITH GRID PLASMA EMITTER FOR GENERATING SUBMILLISECOND DURATION INTENSE BEAM<sup>1</sup>

*M.S. VOROBYOV, V.N. DEVYATKOV, N.N. KOVAL, S.A. SULAKSHIN, P.M. SCHANIN*

*High Current Electronics Institute SD RAS, 2/3 Akademichesky av., Tomsk, 634050, Russia  
e-mail: vorobyovms@yandex.ru, phone: +7(3822)492683*

In this paper an electron source with plasma emitter based on arc discharge system with six cathodes and a common cylindrical hollow anode is described (Fig. 1). At simultaneous ignition of vacuum arc discharges the hollow anode is filled of dense low-temperature plasma. An emission boundary of this plasma is stabilized a fine-grained metal grid with area of 150 cm<sup>2</sup>. The amplitude of the arc current from each cathode is (100 - 300) A. Under the influence of a constant accelerating voltage up to 90 kV which applied between a plasma emitter and grounded accelerating electrode, combined with the drift tube, electrons are extracted from the plasma and accelerated. At working pressure 0.04 Pa, an electron beam with a maximum amplitude of the current up to 1 kA and pulse duration at half-height of 100 μs, which is transported to the collector in a longitudinal magnetic field of 35 mT at a distance of 80 cm. Limiting parameters of the electron beam is a total energy of the beam at the level of about 4 kJ. Above this energy an electrical breakdown of the accelerating gap is occurred. The main reason for the breakdown of the gap is significant outgassing from the collector and the drift tube under the influence of an intense electron beam.

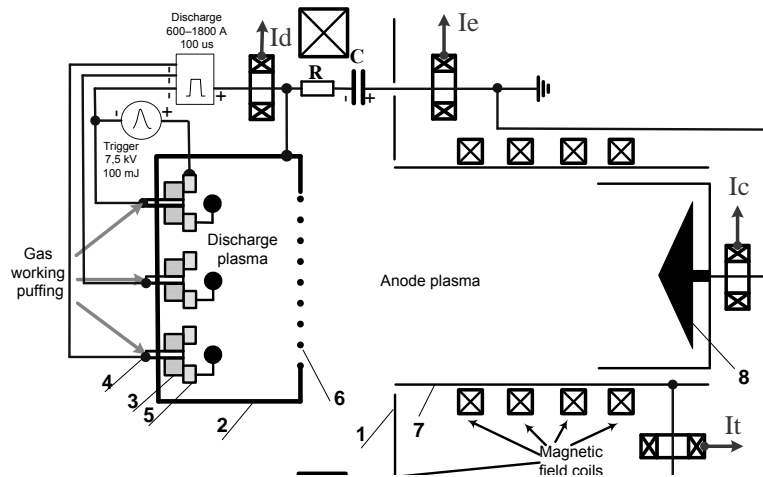


Fig.1. Scheme of the electron source with multiple arc plasma emitter: 1 – vacuum chamber; 2 - plasma emitter; 3 – insulator; 4 – cathode; 5 - ignition electrode; 6 – emission grid; 7 – drift tube; 8 – collector.

<sup>1</sup> This work was supported by RAS Presidium program number 12 project 8.



## THE REVIEW OF RECENT RESULTS ON LOW-ENERGY, HIGH-CURRENT ELECTRON BEAMS PRODUCTION<sup>1</sup>

G.E. OZUR

*\*Institute of High Current Electronics, SB RAS, 2/3 Akademicheskii Ave., Tomsk, 634055, Russia,  
E-mail: ozur@lve.hcei.tsc.ru, phone: +7-3822-492052*

The report represents a review on production of wide-area (tens of square centimeters), low-energy (20-40 keV), high-current (10-30 kA) electron beams (LEHCEBs) obtained within last three years. Such beams are of great interest for material surface treatment: increasing the corrosion resistance of metals and alloys, smoothing (polishing) of the surface, improvement the electric strength of vacuum insulation and so on [1-3].

To produce LEHCEBs, electron guns with plasma anode and explosive-emission cathode are generally used [3]. Plasma-filled diodes surpass the vacuum ones at all points: cathode emission and lifetime, current density and total beam current onto the target, uniformity of the energy density distribution via cross section. To manufacture an additional system for plasma anode formation is not complicated problem, so taking into account the above mentioned advantages, it looks fully justified.

In the report, different physical aspects are considered: (i) formation of the plasma anode with the use of hybrid discharge [4], (ii) transformation of the circular beam into a rectangular one [5], (iii) beam focusing and its energy density redistribution with the use of ferromagnetic inserts placed behind the target [6]. The last is also important from the point of view of the treatment of magnetic materials. All these efforts are directed, first of all, to improve the uniformity of the beam energy density distribution. Some non-stationary effects influencing on the beam current density in a double layer between the cathode and anode plasmas are also considered [7].

### REFERENCES

- [1] *Proskurovsky D.I., Ivanov Yu.F., Rotshtein V.P. et al // Journal of Vacuum Science & Technology. – 1998. – V. A16(4). – P. 2480-2488.*
- [2] *Uno Y., Okada A., Uemura K. et al // Precision Engineering. – 2005. – V. 29. – P. 449-455.*
- [3] *Ozur G.E., Proskurovsky D.I., Rotshtein V.P., and Markov A.B. // Laser & Particle Beams – 2003. – V. 21. – P.157-174.*
- [4] *Kiziridi P.P., Ozur G.E., Zjulkova L.A. Batrakov A.V. // Izv. vuzov. Fizika. - 2012. - V. 55, Issue 6/2. - P. 42-48.*
- [5] *Ozur G.E., Karlik K.V., Grigor'ev V. P., Koval' T. V., and Le Huy Dung // Zhurnal Tekhnicheskoi Fiziki, 2011, Vol. 81, No. 9, pp. 100–104.*
- [6] *Ozur G.E., Batrakov A.V., Karlik K.V., Zjulkova L.A. // Izv. vuzov. Fizika. - 2013. - V. 56, Issue 7/2. - P. 37-41.*
- [7] *Ozur G.E. // Fizika Plazmy, 2014, Vol. 40, No. 3, pp. 305–308.*

<sup>1</sup> This work was supported by Russian Foundation for Basic Research (grants ## 12-08-00213 and 13-08-98066) and Russian State Foundation for Scientific Research (project II.14.2.1 # 01201373605).

## NEW APPROACH IN THE ABERRATION THEORY FOR SOLVING OF 3D ELECTRON OPTICS PROBLEMS

V.YA. IVANOV

*ICT RAS, 6 Lavrentiev prosp., Novosibirsk, 630090, Russia, vivanov.48@mail.ru, +7(913)486-9002*

The new approach to solve the electron optics problems in three dimensions is presented. It is based on the principal ray method suggested by G. Grinberg [1] in 1948. His ideas extremely enlarged the application area for mathematical model in electron optics of three-dimensional beams of arbitrary shapes. Here aberration expansion is provided in the vicinity of an arbitrary-shape beam axis in curvilinear coordinate system, and in that way it is applicable as for narrow beams (classic aberration theory) as for a wide beam represented by small set of principal rays. Such approach can substantially reduce the amount of computations comparing the integration method for the Lorentz trajectories [2], and save the precision accuracy needed for the image optic devices.

The perspective Grinberg's approach were not realized before for full three-dimensional electron optic systems, probably because of the complexity of its mathematical apparatus. Here we present the first version of such computer code "OPTICS-3", and some results of numerical simulations with this code.

### REFERENCES

- [1] *Grinberg G.A. // Selected Questions of Mathematical Theory of electric and magnetic phenomena.- Moscow-Keningrad: USSR Academy of Science Publishing. - 1948.*
- [2] *Ivanov V.Ya. //Computer Aided Design of Physical Electronic Devices (in 2 volumes). – Institute of Mathematics of RAS Publishing. - 1986.*

## SURFACE MODIFICATION OF A DISPERSION-HARDENING 67KN5B ALLOY BY ION AND ELECTRON BEAMS <sup>1</sup>

*B.K. RAKHADILOV\**, *M.K. SKAKOV\**, *D.B. ZARVA\**, *A.V. GUL'KIN\**

*\* National Nuclear Center of the Republic of Kazakhstan, st.Krasnoarmeyskaya, 2 buil.54 B, Kurchatov, 071100, Kazakhstan, [bor1988@mail.ru](mailto:bor1988@mail.ru), 87756686239*

At present time, the processing effects by energy concentrated streams on structure and properties of metals and alloys are intensive researching. During processed by the concentrated streams of energy at the same time, radiation, thermal and shock-mechanical impacts performed [1]. Developing processes of structure restructuring in conditions far from thermodynamic equilibrium states, and provide the surface layers with a unique set of physical and mechanical properties [2]. Therefore the study of the mechanisms and features of a structural-phase state and microhardness changes of a dispersion-hardening alloy 67KN5B when the impact of ion and electron beams is a great scientific and practical interest. Therefore clarify the general regularities of phase transformations in the investigated alloy and the development of new, progressive methods of processing materials to improve their practically important properties. In connection with the above, the purpose of this work is to investigate the influence of electron irradiation and ion implantation on structural-phase state and microhardness of 67KN5B dispersion-hardening alloy.

To conduct irradiation, ion and electron beams produced flat alloy samples 67KN5B with dimensions 20x20x0,5 mm, after pre-processing: hardening 950<sup>0</sup>C (10 min) and rolling on 90%. Before irradiation samples were electrolytically polished. The introduction of nitrogen ions with 100 keV energy and 1×10<sup>17</sup>, 2×10<sup>17</sup>, 5×10<sup>17</sup> ion/sm<sup>2</sup> doses was conducted in a vacuum (10<sup>-4</sup> Pa) at 2 μA/sm<sup>2</sup> current density on the MKSR-99 ionic implanter. Continuous electronic irradiation was performed on the ELV-4 accelerator. The electrons energy on the surface of samples under irradiation was 1.3 MeV and beam current density - 10 μA/sm<sup>2</sup>. Samples have been exposed to 0,28 x 10<sup>19</sup> e<sup>-</sup>/sm<sup>2</sup> dose. In the course of irradiation temperature of the samples did not exceed 100<sup>0</sup>C. Study of the phase composition and crystal structure of alloy samples carried out by X-ray diffraction analysis on the diffractometer X'pert Pro at CuK<sub>α</sub>-radiation. The surface morphology was studied on a scanning electron microscope JSM-6390LV equipped with an attachment energy dispersive analysis. Microhardness of the samples surface layers before and after the process measured by the method of pressing-diamond indenter on the PMT-3 device with three loads of 20, 50 and 100 grams and 10 s time loads.

Analysis of the images obtained by scanning electron microscopy showed that in the process result to nitrogen ions in the sample surface are formed drop-shaped particles sized up to 0.5 μm, small blisters and pores. It is specified that under ion irradiation occurs spatial redistribution of alloying elements in the alloy. Energy dispersive X-ray analysis showed that the drop-shaped particles contains a larger number of niobium compared to the main material. It is assumed that these particles are the fine on the basis of niobium nitrides. However, X-ray study did not detect any new nitride phases, probably, due to their low concentration and the formation low depth. It is established that the ion implantation leads to an increase in the microhardness between 10 and 50%, depending on the irradiation dose. Microhardness reaches a maximum 5×10<sup>17</sup> ion/sm<sup>2</sup>dose. It is assumed that the increase in the microhardness of irradiation is connected with the intensive formation of radiation defects and drop-particles of new phase.

Electron-microscopic studies have established that as a result of electron irradiation occurs a change of surface morphology of the alloy samples. The surface becomes heterogeneous and has developed relief. As a result of electron irradiation on the surface of the sample alloy 67KN5B were found pores and fine inclusion size of 0.1-0.5 μm, which enriched niobium. It is assumed that these fine inclusions are formed as a result of surface segregation of niobium. It was determined that the alloy's surface microhardness after electron irradiation had increased almost in 2 times. The increase in microhardness alloy irradiated by the changes of structural-phase state of the surface layers with the formation of fine inclusions and radiation defects during the processing of the electron beam.

### REFERENCES

- [1] *Kurzina I.A. [and other] // Nanocrystalline the intermetallic and nitride patterns, formed by ion-ray process. □ Tomsk: Izd-vo NTL, 2008.*
- [2] *Kadyrzhanov K. [and other] // Ion-beam and ion-plasma modification of materials. M: MSU Publishing house, 2005.*

## TRANSITION OF LOW-CURRENT DISCHARGE WITH SELF-HEATED HOLLOW CATHODE INTO HIGH-CURRENT PULSE MODE<sup>1</sup>

*A.I. MENSHAKOV, N.V. GAVRILOV, A.I. LIPCHAK*

*Institute of Electrophysics UB RAS, 106 Amundsen St., Yekaterinburg, 620016, Russia,  
E-mail: aim@iep.uran.ru, phone (343)2678829*

The transition of direct current discharge (5 - 15 A) with self-heated hollow cathode from a titanium nitride (8 mm in diameter) in nitrogen flow ( $1-10 \text{ cm}^3 \text{ s}^{-1}$ ) into high-current pulse mode as a result of application of high voltage pulse (up to 1 kV, 0.1-1 ms) was studied. It was determined that high-current mode appearance is preceded by transition mode of glow discharge, characterized by step-like rise of current till 10-50 A, constant values of operating current and voltage, equal to applied voltage, and inverse relation between the mode duration (40-160  $\mu\text{s}$ ) and power dissipated in this phase of discharge (Fig. 1). Then the discharge during  $\sim 5-100 \mu\text{s}$  is transformed to high-current mode with current up to 300 A and reduced voltage (200 – 300 V), where current depends on the current of the d.c. discharge, values of pulse voltage and nitrogen flow. The pulse heating of cathode surface in transition mode and gas conditions in cathode hollow were estimated. The conditions of discharge development during the period of high-voltage application are very similar to that taking place in devices based on High Power Impulse Magnetron Sputtering (HIPIMS) [1]. The role of magnetic field concentrating the discharge near cathode is in this case played by electrostatic trap being formed in cathode hollow. Application of high-voltage pulse increases the energy of electrons emitted by thermoionic cathode which fact brings on enhancement of ionization processes in the volume and transformation of the discharge to the dense glow mode with mainly ion current on the cathode. At this stage the power  $\sim 10^4 \text{ W/cm}^2$  enough for intensive ion sputtering and additional heating of cathode surface layer is dissipated at the cathode surface. Traces of burn-off are visually observed at the surface of outlet edge of the cathode. Spectroscopic measurements of plasma composition and temperature of the cathode inner surface were made. Current amplitude and pulse duration are limited by transition of the discharge to arc mode. Thus, in this article high power impulse mode of discharge in hollow self-heated cathode was realized, and here, unlike HIPIMS [1] and superdense glow discharge [2] low-voltage high-current mode of discharge (300 A, 250 V, 200  $\mu\text{s}$ ) is achieved without magnetic field application.



Fig.1. Characteristic oscillograms of the discharge parameters (100 V/div, 50 A/div, 50  $\mu\text{s}$ /div)

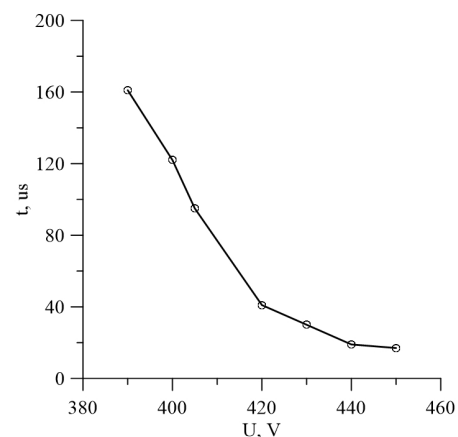


Fig.2. The dependence of pulse transition phase duration on the amplitude of voltage applied

### REFERENCES

- [1] *André Anders* // Surface & Coatings Technology. 2011. – No. 205. – Pages 1–9.  
[2] *Abramovich L. Yu., Klarfeld B. N., Nastich Yu. N.* // Zhurnal tekhnicheskoi fiziki. - 1969. - V. 39. – No. 7. – P. 1251 - 1255.

<sup>1</sup> This work was partially supported by RFBR, research project No. 14-08-00249-a and by Scholarship of the President of the Russian Federation, project No. CII-4355.2013.1.

**VARIOUS MECHANISMS OF GENERATION OF PLASMA AT LOW PRESSURES<sup>1</sup>***S.P. NIKULIN\***\*Institute of Electrophysics, Ural Division of RAS, Amundsena 106, Ekaterinburg, 620016, Russia,  
nikulin@iep.uran.ru, +(343)2678829*

Various mechanisms of generation of plasma in low-pressure discharge systems are discussed. The use of classical Langmuir model, in which formation of plasma is connected with capture of electrons in a potential hump, often leads not only to quantitative, but also to a qualitative divergence with results of experiments. It is shown that in certain cases the divergence can be eliminated, using such mechanisms as accumulation of ions in a potential hole and mutual compensation of charges of two streams of particles.

---

<sup>1</sup> This work was supported by RFFI, N12-08-00516-a

## INVESTIGATIONS ON GENERATION OF A NANOSECOND PULSE ELECTRON BEAM

*PONOMAREV D.V., KHOLODNAYA G.E., REMNEV G.E., KAYKANOV M.I., SAZONOV R.V*

*National Research Tomsk Polytechnic University,  
Lenin ave. 30, Tomsk, 634050, Russia, ponomarev8105@mail.ru, +7(3822)418540*

Radiation technologies are increasingly used in many fields of science and engineering, such as radiation sterilization of medical instruments, semiconductor radiation doping, ion implantation, radiation treatment of electronic products, application of ionizing radiation in environmental protection, food radiation treatment, etc.

The application of the electron accelerators, which generate submicrosecond electron beams with a current amplitude of up to a few kA [1] is promising.

The paper presents the findings of investigation on the generation of a nanosecond pulse electron beam using the TEA-500 accelerator [2] using different explosive emission cathodes. The main parameters of the accelerator are as follows: accelerating voltage of 350 to 500 kV; electron beam current of 6 kA to 11 kA; half-amplitude pulse duration of 60 ns; pulse energy of up to 120 J; pulse duration rate of up to 5 pulses per second. In our investigations we used a diode with an explosion-emission blade metal-dielectric cathode (MD-cathode) [3]. We used a 0.5-mm foil glass fiber laminate as an emitting edge of the cathode (Fig. 1). The effective diameter of the cathode was 62 mm, the height of MD-blades was 10 mm, a number of the blades was 11 pieces. The amplitude of the accelerating gap varied within 12 to 22 mm. The application of metal-dielectrics enabled to initiate an explosive electron emission in triple points of the emitting edge of the cathode, i.e. it increases the stability of the parameters of the electron beam for a large number of pulses

To restrict the impact of the edge effect on the electron beam generation, the shield was used in the construction of the cathode. The application of the screen in the proposed geometry reduces the electron emission from the peripheral part of the cathode, i.e. we can change the diode impedance at constant values of the cathode-anode gap by varying the location of the screen. Consequently, the parameters of the generated nanosecond pulse electron beam are changed. The data obtained are represented in the paper.

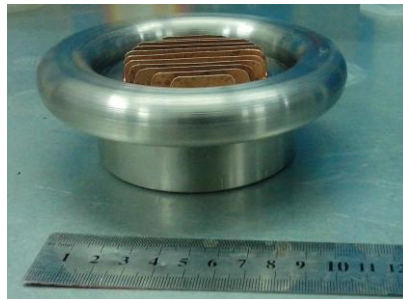


Fig. 1. The blade MD-cathode of the pulsed electron accelerator TEA-500

### REFERENCES

- [1] Bugaev S.P., Litvinov E.A., Mesyats G.A. and Proskurovski D.I. // *Usp. Fiz. Nauk.* – 1975. – V. 115. – No. 1., pp. 101-117.
- [2] Remnev G.E., Furman E.G., Pushkarev A.I., Karpuzov S.B., Kondratyev N.A., and Goncharov D.V. // *Prib. Tekh. Eksp.* – 2004. – No. 3. – pp. 130-134
- [3] Gunin A.V. Landl B.F., Korovin S.D., Mesyats G.A., and Rostov V.V. // Explosive-emission cathode with a long lifetime for high-power microwave radiation // *Pis'ma Zh. Tekh. Fiz.* – 1999. – V. 25. – No. 25. – pp. 84-94

## ON NEGATIVE ANODE VOLTAGE DROP OF HIGH-CURRENT VACUUM ARC<sup>1</sup>

*D.L. SHMELEV\**, *S.A. BARENGOLTS\*\**

\* *Institute of Electrophysics, Russian Academy of Science, Ekaterinburg, 620016, Russia, Shmelev@iep.uran.ru*

\*\* *Prokhorov General Physics Institute, Russian Academy of Sciences, 119991, Moscow, Russia*

The present paper is devoted to numerical simulation of the near-anode plasma layers of diffuse high current vacuum arcs as found in certain types of vacuum interrupters with an axial magnetic field. Recent theoretical results obtained by Ya. I. Londer and K. N. Ulyanov ([1], [2]) have shown that the anode voltage drop remains negative at any value of the ratio  $V_0/V_{th}$ , where  $V_0$  is the drift velocity of electrons and  $V_{th}$  is the thermal velocity of electrons. The present paper describes some results of numerical PIC simulation of near-anode plasma sheath. The comparison of the numerical results with the results of Ya. I. Londer and K. N. Ulyanov was performed (Fig. 1). It was found that for the completely ionized near-anode plasma the anode voltage drop really remains negative when the value  $V_0/V_{th}$  varies in the range 0-1. The values of negative voltage drop obtained from the simulation noticeably differ from those found in [1], [2]. It was found in addition that the average chaotic kinetic energy transferred by electrons from the plasma to the anode increases monotonously from  $2Te$  to  $\sim 2.4Te$  with  $V_0/V_{th}$  increase. The obtained results should be taken into consideration in the models developing for the simulation of the high-current vacuum arcs.

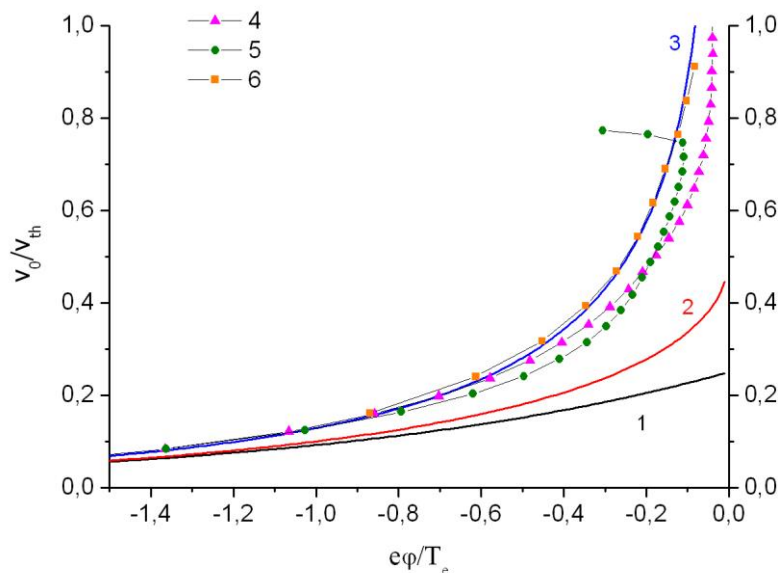


Fig. 1. Electron velocity  $V_0/V_{th}$  as function of near-anode voltage drop  $e\phi/T_e$ . 1.- Tonks-Langmuir law; 2.- analytical formula from [3]; 3.- analytical formula from [1], [2]; 4.- numerical result  $n=10^{14} \text{ cm}^{-3}$ ,  $T_e=4 \text{ eV}$ , coulomb collision; 5.- numerical result  $n=10^{15} \text{ cm}^{-3}$ ,  $T_e=4 \text{ eV}$ , coulomb collision (strong ion-sound instability develops at the end); 6.- numerical result  $n=10^{14} \text{ cm}^{-3}$ ,  $T_e=4 \text{ eV}$ , no coulomb collision;

### REFERENCES

- [1] Ya. I Londer, K. N. Ulyanov // IEEE Trans. Plasma Sci.–2013 – 41. – 2002–2006.
- [2] Ya. I Londer, K. N. Ulyanov // Plasma Phys. Rep.–2013 – 39. – 849-856.
- [3] R. L. Boxman, S. Goldsmith // J. Appl. Phys.–1983 – 54. – 592–602.

<sup>1</sup> This work was supported by the Russian Fundamental Research Foundation under Awards 12-08-00310, 13-08-00619, 14-08-01137, 14-02-00575

## HYBRID COMPUTATIONAL MODEL OF DIFFUSE HIGH-CURRENT VACUUM ARC <sup>1</sup>

*D.L. SHMELEV, I.V. UIMANOV*

*Institute of Electrophysics, Russian Academy of Science, Ekaterinburg, 620016, Russia, Shmelev@iep.uran.ru*

The present paper is devoted to the developing of a new numerical model for simulation of diffuse high current vacuum arcs (HCVA) as found in certain types of vacuum interrupters with an axial magnetic field. Most of the developed models for simulation of HCVA use the MHD approach ([1] for example). This is a good approach for the constricted columnar arc and for the diffuse-columnar arc. However, in case of diffuse HCVA with average current density below  $500 \text{ A/cm}^2$  the applicability of the MHD approach is questionable. One of the possible solutions of the problem is the developing of some kind of the hybrid model, which combines the MHD with the kinetic approach. The first attempt to develop the hybrid model for HCVA was made by Ya.I. Londer and K.N. Ulyanov [2]. This model treats the electron subsystem with the help of simplified MHD approach, while the ions subsystem is treated with the help of so-called current tube method (specific kind of PIC method). However, the model [2] can be applied only in case of very short interelectrode gap.

The present paper describes a newly developed hybrid model of HCVA. This is a nonstationary 2D axial symmetry model. The model assumes quasineutrality. The electron subsystem is described with the help of MHD approach. The ion subsystem is described with the help of PIC method taking into account the ion-ion coulomb collisions. The model allows to simulate: the supersonic/subsonic transition in HCVA, near-cathode mixing zone, and HCVA with multiply separate columns (Fig. 1).

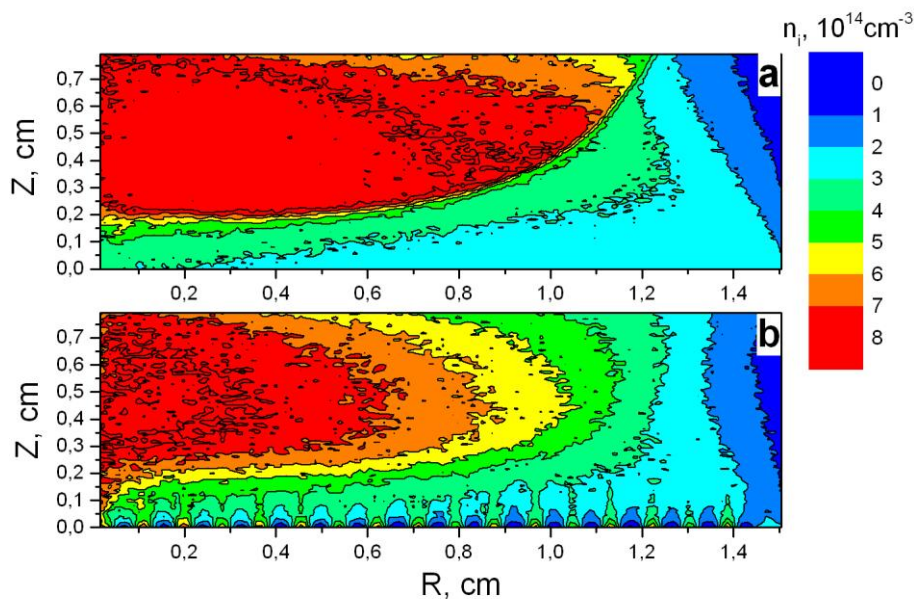


Fig. 1. An example of the simulation. Quasistationary ion density ( $10^{14} \text{ cm}^{-3}$ ) distribution, total current - 3.5 kA, AMF - 0.02 T. a) calculation with homogeneous distribution of the current and the ion flux at the cathode; b) calculation with cathode boundary conditions mimicking the cathode group spots.

### REFERENCES

- [1] *E. Schade, D.L. Shmelev // IEEE Trans. Plasma Sci.-2003 – 31. – 890–901.*
- [2] *Ya.I. Londer, K.N. Ulyanov // IEEE Trans. Plasma Sci.-2013 – 41. – 1996–2001.*

<sup>1</sup> This work was supported by the Russian Fundamental Research Foundation under Awards 12-08-00310, 13-08-00619, 14-08-01137, 14-02-00575



## FOCUSING AND TRANSPORT OF MODERATE ENERGY ELECTRON BEAMS WITH GAS-DISCHARGE PLASMA LENS <sup>1</sup>

A. GONCHAROV\*, V. GUSHENETS\*\*, A. DOBROVOLSKIY\*, I. LITOVKO\*\*\*, E. OKS\*\*, \*\*\*\*

\*Institute of Physics, National Academy of Sciences, 46 Prospect Nauky, Kiev, 03028, Ukraine

\*\*Institute of High Current Electronics, RAS, 2/3 Akademicheskyy, Tomsk, 634055, [gvi@opee.hcei.tsc.ru](mailto:gvi@opee.hcei.tsc.ru), +7(3822)491933

\*\*\*Institute for Nuclear Research, National Academy of Sciences, 47 Prospekt Nauky, Kiev, 03680, Ukraine

\*\*\*\*Tomsk State University of Control Systems and Radioelectronics, 40 Lenina Prospect, Tomsk, 634050, Russia

This paper presents the experimental and theoretical studies for wide aperture (diameter 6 cm), moderate energy (up to 40 keV) and high current (up to 100 Amps) pulsed electron beam focusing and transport through original plasma-optical device based on a configuration of high current plasma lens. The plasma lens is a toroidal plasma source like an anode layer thrusters with closed drift electrons that move in the  $E \times B$  field. The source of electrons is an electron plasma emission from hollow-anode vacuum arc discharge. The electrons are extracted and accelerated in a diode-type optical system between the grid emission surface of electron source and the gridless accelerating electrode formed by plasma inside the lens. In case of high-current mode the plasma lens operates in plasma mode to create transparent for electron beam plasma accelerating electrode and compensate space charge of the propagating electron beam. The lens magnetic field in this case uses for effective focusing beam. The operational characteristics of the electron source and plasma lens are experimentally measured and discussed. The space-charge field and the beam electron trajectories are numerically calculated for the lens used in the experiments.

<sup>1</sup> This work was supported in part by RFBR and SFBR of Ukraine under the program of joint Russian-Ukrainian research projects (RFBR Grant № 13-08-90416 and SFBR Grant № F53.2/013).

## ENERGY DENSITY REDISTRIBUTION OF LOW-ENERGY, HIGH-CURRENT ELECTRON BEAM WITH THE USE OF FERROMAGNETIC INSERTS<sup>1</sup>

*P.P. KIZIRIDI, G.E. OZUR*

*Institute of High-Current Electronics, SB RAS, Tomsk, Russia, kiziridi\_pavel@mail.ru*

Low-energy (20-40 keV), high-current (10-30 kA) electron beams (LEHCEBs) are of great interest for material surface treatment and have already found rather wide use in practice [1, 2]. To produce LEHCEBs, electron guns with explosive-emission cathode and plasma anode based on high-current reflective (Penning) discharge and are generally used. Investigations and experience on exploitation of such guns have shown that the uniformity of beam energy density distribution in cross section left much to be desired because the beam being even uniform in the injection plate acquires a maximum of energy density in the central part after transportation through a plasma channel [3].

To improve the beam uniformity, we suggest to redistribute the beam energy density using the "passive focusing". This method is concluded in placing of the hollow cylindrical ferromagnetic inserts (concentrators) which constrict the guide magnetic field lines [4]. Varying the sizes and magnetic permittivity of the inserts it possible both to focus and to redistribute beam energy density since it is proportional to the density of magnetic flux. It should be noted that external solenoid coils allows one to focus (or defocus) the beam only; any redistribution is impossible with such technique.

In the paper, the results of study of energy density distribution of LEHCEBs transported through a plasma channel in a guide magnetic field are presented. A stainless steel foil 200  $\mu\text{m}$  in thickness with backside coated by black dull paint served as the beam collector. The beam energy density distribution was measured with the use of thermal imager **TESTO 875-1**. For this purpose, the ferromagnetic insert was get out to the top by an electromagnet during the pause (about 1 s) between the beam pulse and fixing of the thermal image. The results of measurements are in good agreement with calculations [5] (Fig. 1). The data obtained are of great importance for the treatment of the parts made of magnetic materials.

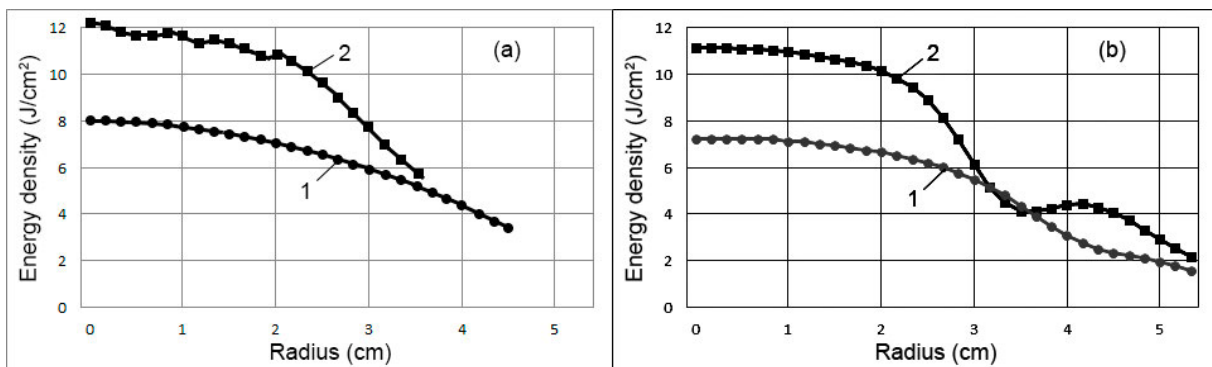


Fig. 1. Calculated (a) and experimental (b) energy density distribution via the beam radius: without a concentrator (curves 1) and with the use of a concentrator (curves 2). Beam pulse duration is 3  $\mu\text{s}$

### REFERENCES

- [1] Proskurovsky D.I., Ivanov Yu.F., Rotshtein V.P. et al // Journal of Vacuum Science & Technology. – 1998. – V. A16(4). – P. 2480-2488.
- [2] Uno Y., Okada A., Uemura K. et al // Precision Engineering. – 2005. – V. 29. – P. 449-455.
- [3] Ozur G.E., Proskurovsky D.I., Rotshtein V.P., and Markov A.B. // Laser & Particle Beams – 2003. – V. 21. – P.157-174.
- [4] Ozur G.E., Batrakov A.V., Karlik K.V., Zjulkova L.A. // Izv. vuzov. Fizika. - 2013. - V. 56, Issue 7/2. - P. 37-41.
- [5] Koval T.V., Le Hu Dung // Izv. Tomsk Polytech. Univ. - 2013. - V. 323. - Issue 2. - P. 127-131.

<sup>1</sup> This work was supported by Russian Foundation for Basic Research (grants ## 12-08-00213 and 13-08-98066) and Russian State Foundation for Scientific Research (project II.14.2.1 # 01201373605).

## A THEORETICAL STUDY OF AN INFLUENCE OF ELECTRIC FIELDS ON PROFILES OF ATOMIC SPECTRAL LINES

*E.V. KORYUKINA*

*National Research Tomsk State University, Lenin avenue 36, Tomsk, 634050, Russia, evk@phys.tsu.ru, (3822)417154*

In the study of processes taking place in plasma, a problem of the formation of spectral line profiles is very topical. An electric field is one of important factors influencing on the shape of a spectral line. The electric field can be both an external one and internal plasma microfield. An action of the electric field leads to shifts and splitting of spectral lines and also to spectral line broadening and asymmetry of spectral line profiles. If a width of a spectral line is so great that it does not allow us to register splitting this line into several components, the presence of the Stark effect can be revealed owing to spectral line shifts, their broadening, and an asymmetry of spectral line profiles. In this case, the quantity of the Stark components, their exact positions and the shape of spectral lines can be determined on based on theoretical calculations. Thereby, in order to reveal the mechanisms of the formation of emission spectral lines, one needs an exact and reliable theoretical method.

A theoretical approach based on diagonalization of the energy matrix of an atom in the electric field [1] allows us to calculate emission spectra of atoms in alternating electric fields of a circular polarization (electric fields of such polarization are often observed in plasma). The proposed method is correct in a wide range of changes in the strength and frequency of the electric field. In order to detect splitting a spectral line into components, determine the positions of the Stark component maxima and compute the shape of their profiles, the derivative spectra technique is applied. This technique was developed in [2].

In the present work, the formation mechanisms for the profiles of the  $2^1P_1-3^1D_2$  и  $2^3P_1-3^3D_2$  spectral lines for emission spectrum of helium are considered. These lines were observed in an experimental investigation of atomic emission spectrum of helium in peripheral regions of a current sheet plasma [3]. In a work [3], theoretical calculations of the positions and profiles for the observed spectral lines were carried out. The authors have concluded from their calculation results that a circularly polarized electric field of the strength  $F=105-120$  kV/cm and frequency  $\omega \sim 10^3$  MHz arises in plasma, and just this field is the reason for splitting spectral lines into the Stark components and an anomalous broadening of the singlet line.

In order to examine the correctness and reliability of our theoretical approach, we performed calculations of the emission spectral lines considered in [3] by our method of the energy matrix diagonalization. The calculations in the framework of our theoretical approach have allowed us to determine the positions and profiles of both spectral lines from [3] and ascertain the formation mechanisms of these spectral lines in the electric field. It was shown that the singlet  $2^1P_1-3^1D_2$  spectral line splits into three Stark components in the electric field; the Stark components of the  $2^1P_1-3^1D_2$  spectral line are shifted to the IR region, whereas the Stark components of the  $2^3P_1-3^3D_2$  spectral line are shifted to the UV region. In addition, a distance between the Stark components was calculated. Finally, it was found that an anomalous broadening of the singlet spectral line is specified by a strong interaction of the  $^1P_1$  и  $^1D_2$  states in the electric field. The triplet spectral line is considerably narrower than the singlet one due to the fact that the  $^3P_1$  and  $^3D_2$  states interact quite weakly in the electric field.

Our calculation results are in an excellent agreement with experimental data and their theoretical estimations of [3]. It confirms an efficiency of our theoretical approach as a reliable instrument for an identification of atomic emission spectra in the electric fields, in solution of problems of plasma spectroscopy and for plasma diagnostics.

### REFERENCES

- [1] *E.V. Koryukina // J. Phys. D: Appl. Phys. – 2005. – Vol. 38. – № 17. 3296–3303.*
- [2] *E.V. Koryukina, G. Revalde // Russ. Phys. J. – 2006. – Vol. 49. – № 4. 435–441.*
- [3] *A. G. Frank, V. P. Gavrilenko, N. P. Kyrie, E. Oks // J. Phys. B: Atom., Mol. and Opt. Phys. – 2006. – Vol. 39. – № 24. 5119–5129.*

## REGULARITIES IN THE BEHAVIOR OF TRANSITION PROBABILITIES IN THE EMISSION SPECTRUM OF ARGON IN AN ALTERNATING ELECTRIC FIELD

*E.V. KORYUKINA\**, *V.I. KORYUKIN\*\**

\*National Research Tomsk State University, Lenin avenue 36, Tomsk, 634050, Russia, evk@phys.tsu.ru, (3822)52-98-52

\*\*Siberian State Medical University, Moskowski Trakt 2, Tomsk, 634050, Russia

In the present work, an influence of an external electric field on the behavior of transition probabilities in the atomic emission spectrum of argon was investigated, and dependences of these probabilities on the frequency and strength of the electric field were found. The Ar atom under the effect of circularly polarized electric field (electric fields of such polarization are generated in high-frequency electrodeless lamps, spin LEDs and under laser excitation) was chosen as subject for study, because this rare gas is widely used either an excited medium or buffer gas in different excitation sources.

Transition probabilities  $A(JM \rightarrow J'M')$  between the Stark states were calculated by the method of the energy matrix diagonalization [1]. This method, free from limitations of perturbation theory, is valid in a wide range of frequency and strength of the electric field. In the framework of this method, regularities in the behavior of transition probabilities under changes in the electric field strength  $F$  and frequency  $\omega$  were investigated.

On based on our computations, a number of regularities was revealed.

**The  $F$ -dependence.** In the study of the dependence of transition probabilities on the electric field strength, the following regularities were found:

- 1) At a weak interaction of the Stark states, the  $M \rightarrow M'$  transitions are either equiprobable or pairwise equiprobable, strong state interactions leads to the nonequiprobability of all  $M \rightarrow M'$  transitions;
- 2) The behavior of transition probabilities  $A(JM \rightarrow J'M')$  with  $J \leq J'$  and  $J > J'$  is differed, a namely: for the  $J \leq J'$  transitions, probabilities of all transitions drastically diminish with the electric field switching on, and then they practically do not depend on the electric field strength. On the contrary, for the  $J > J'$  transitions, one of all probabilities slowly decreases with an increase in the electric field strength, whereas the rest ones demonstrate the same behavior as probabilities in the  $J \leq J'$  case;
- 3) Switching on the electric field leads to the  $M$ -ordered distribution of transition probabilities.

**The  $\omega$ -dependence.** In the study of the dependence of transition probabilities on the electric field frequency, the following regularities were found:

- 1) At a weak interaction of the Stark states, the  $M \rightarrow M'$  transitions are either equiprobable or pairwise equiprobable, and their probabilities do not depend on the electric field frequency;
- 2) In case of strong energy state interactions, all of the  $M \rightarrow M'$  transitions are unequiprobable at low electric field frequencies, and an increase in the electric field frequency leads to the pairwise equiprobability of the transitions.

On based on the calculation results, it was shown that transition probabilities between the energy levels  $A(J \rightarrow J')$  have a polynomial dependence on the electric field strength of the form

$$A(J \rightarrow J') = a_0 + a_1 F + a_2 F^2 + \dots + a_m F^m, \quad (1)$$

where a degree of the polynomial increases with the electric field frequency ( $m=3$  at  $\omega=100$  MHz,  $m=4$  at  $\omega \sim 10^5 - 10^6$  MHz, and  $m=5$  at  $\omega \sim 10^7$  MHz).

The obtained theoretical results allow us to explain the processes taking place in plasma, clarify the mechanism of filling of the Stark states and reasons for changes in spectral line intensities. Transition probabilities can be used as input data for calculations of lifetimes, spectral line intensities, and for solution of the population density balance equations. In addition, the calculation results are very useful for plasma diagnostics, and, finally, revealed regularities can be used for construction of new devices.

### REFERENCES

- [1] E.V. Koryukina // J. Phys. D: Appl. Phys. – 2005. – Vol. 38. – № 17. 3296–3303.

## MODEL OF A WEDGE-ELECTRODE CORONA DISCHARGE UNDER SATURATION<sup>1</sup>

G.S. BOLTACHEV\*, N.M. ZUBAREV\*\*, O.V. ZUBAREVA\*

\*Institute of Electrophysics, UB, RAS, ul. Amundsena 106, Yekaterinburg, 620016, Russia, olga@iep.uran.ru,+7(343)2678776

\*\*Lebedev Physics Institute, RAS, Leninskii pr. 53, Moscow, 119991, Russia

It is known [1, 2] that a corona discharge is initiated in a strongly nonuniform electric field near an electrode with a small radius of curvature. Neutrals are ionized by electron avalanches in a narrow ionization zone near an active electrode. The space charge of ions moving from this zone toward a counter electrode hinders ionization processes, screening the field at the corona electrode.

In this work, we construct an analytical model of a steady-state unipolar corona discharge from an ideal wedge-shaped electrode under the conditions of space-charge-limited current. It is assumed that the ionization zone is linear: a corona discharge is initiated only at the edge of the wedge (see Fig. 1).

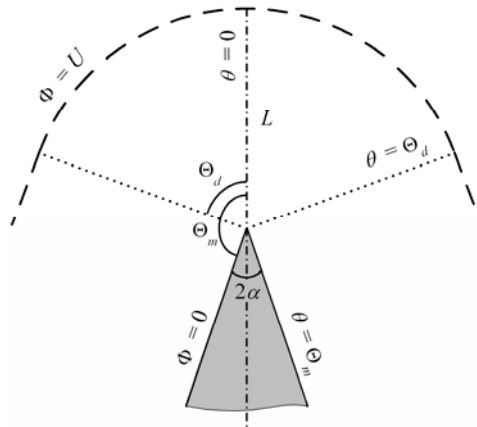


Fig. 1. Geometry of the problem. The corona electrode is represented by the wedge with half-angle  $\alpha$ .

As a rule, the outer zone of the corona discharge from cusps can be divided into two regions: the drift space with a space charge and the peripheral part, where the charge is absent. We managed to find exact solutions to the problem by sewing together a cylindrically symmetric solution for the field potential in the drift space and a plane symmetric solution at the periphery [3]:

$$\Phi = \begin{cases} UL^{-1}r, & 0 \leq |\theta| < \Theta_d, \\ UL^{-1}r \sin(\alpha + \theta), & \Theta_d \leq |\theta| \leq \Theta_m, \end{cases} \quad \rho = \begin{cases} -\varepsilon UL^{-1}r^{-1}, & 0 \leq |\theta| \leq \Theta_d, \\ 0, & \Theta_d \leq |\theta| \leq \Theta_m, \end{cases}$$

where  $\Phi$  is the electric field potential,  $\rho$  is the charge density,  $\varepsilon$  is the absolute permittivity of the medium,  $L$  is the interelectrode distance,  $U$  is the applied potential difference,  $r$  is the distance to the edge of the wedge,  $\theta$  is the polar angle,  $\alpha$  is half-angle of the wedge,  $\Theta_m \equiv 2\pi - \alpha$ , and  $\Theta_d = \pi - \alpha$  is the apex angle of the drift space.

According to the solutions, the saturation current of the corona discharge is expressed as

$$I = (\pi - 2\alpha)\mu\varepsilon L^2 U^2,$$

where  $\mu$  is the charge carrier mobility.

### REFERENCES

- [1] N. A. Kaptsov // Electrical Phenomena in Gas and Vacuum. – OGIZ, Moscow-Leningrad, 1947.
- [2] Yu. P. Raizer // Gas Discharge Physics. – Springer, Berlin, 1991.
- [3] G. Sh. Boltachev, N. M. Zubarev, and O.V. Zubareva // Tech. Phys. – 2014. – V. 59. – P. 365-371.

<sup>1</sup> This work was supported by the Russian Foundation for Basic Research (grant no 14-08-00235 and 13-08-96010\_r\_ural) and by the Presidium of the Russian Academy of Sciences in the framework of the program 29P.

## INVESTIGATION OF THE PARAMETERS OF THE ION FLUX FROM THE VACUUM DISCHARGE PLASMA IN THE DOUBLE-PULSE DISCHARGE ARRANGEMENT<sup>1</sup>

*YU.A. ZEMSKOV, I.L. MUZUKIN, I.V. UIMANOV*

*Institute of Electrophysics, Russian Academy of Sciences, Ural Branch, 106 Amundsena st., Ekaterinburg, 620016, Russia, zemskov@iep.uran.ru*

Mass-charge spectra and energy distributions of anomalous accelerated ions were obtained in the double-pulse setup. Where the plasma cloud of the 30 kV vacuum flashover interacted with the plasma flare of the 300 kV vacuum spark discharge. And the spark discharge was ignited using the delay line.

Voltage pulse source consisted of the Marx generator with the stored energy about 45 J and two transmission line based generators with a simultaneous triggering. Voltage pulse from one of the lines ignited the discharge in the first electrode gap (with a flashover), and the second triggered the Marx generator. The Marx generator was connected to the generator line with the interposition of a delay line with the time parameter up to 150 ns.

Plasma source was composed of two discharge gaps with the common anode. The anode was a tungsten disk with a 3 mm aperture. The first gap cathode was a copper disk with a 3 mm aperture. The teflon insulator was interposed between the electrodes of the first gap. The insulator had the cylindrical bore, that was coaxial with the apertures of the cathode and the anode. Thus the flashover was initiated in the gap when the 20 - 40 kV, 100 ns voltage pulse was applied to the cathode. The second gap cathode was an aluminum needle. In the second gap the vacuum spark discharge was initiated when the 300 - 400 kV voltage pulse from the Marx generator was applied to the needle cathode. The current was measured in the anode circuit with a coaxial low-inductance resistive shunt whose nominal resistance was 1  $\Omega$ . Ions and electrons traveling toward the copper cathode could enter the spectrometer via the cathode aperture. Quantitative analysis of the energy distributions and charge states of the plasma species was performed by modified method of Thomson parabolas with automated recording and processing of spectrograms. The signals of particles were registered in the single-pulse mode. Given the persistence of the phosphor screen, the integral signal of the pair of pulses in both gaps was recorded in one frame. Waveforms of a current in the anode circuit were taken for every captured frame. Thus it was possible to consider these particle spectrograms together with the respective waveforms, and consequently with the character of the discharge behavior.

Mass-charge spectra and energy distributions of the ions were obtained via the Thomson spectrometer with a different delay time of the second pulse. Therefore they were obtained in different conditions of the interaction of the flashover plasma cloud with the plasma flare of the 300 kV vacuum spark discharge.

<sup>1</sup> This work was supported in part by the Russian Fundamental Research Foundation under Awards 14-02-00575, 14-08-01137, 13-08-00619, 12-08-00310 and in part by Presidium UB RAS Project 12-P-2-1027

## HYDRODYNAMICS OF THE CRATER FORMATION ON THE CATHODE SURFACE IN A VACUUM ARC<sup>1</sup>

G. A. MESYATS\* AND I. V. UIMANOV\*\*

\*P.N. Lebedev Physical Institute, RAS, Moscow 119991, Russia

\*\*Institute of Electrophysics, UB RAS, Ekaterinburg 620016, Russia  
+7(343)267-87-68, uimanov@iep.uran.ru

There is much evidence that the elemental damage marks left by a vacuum arc on the cathode surface are microcraters. A microcrater is formed as a result of displacement of molten cathode metal from an explosive emission center (ecton) under the action of the pressure of the cathode spot plasma [1]. The extrusion of the molten metal from the crater results in the formation of microjets, which afterwards break into microdrops. These processes are most pronounced at low (near-threshold) discharge currents. It is supposed [2-4] that the hydrodynamic processes occurring on the cathode play a key part in self-sustained operation of a vacuum arc. This is due to that the formation of liquid-metal jets and their subsequent explosion give rise to new explosive emission centers that ensure the operation of the cathode spot and of the discharge as a whole. In [4], the hydrodynamics of the molten metal was considered by analogy with the classical problem of a liquid drop impact on a solid surface. Based on this analogy, the conditions are analyzed under which the liquid will change its regular behavior (spreading over the cathode surface) into a singular behavior (formation of microjets and droplets). It is shown that the conditions realized in vacuum arc cathode spots at near-threshold currents are close to the threshold conditions for splashing of the molten metal. This gives grounds to relate the existence of a threshold arc current to the existence of a splashing threshold for liquid metal.

In the present work, we simulate immediately the behavior of the molten metal during the crater formation and the initial stage of formation of liquid-metal jets, performing a self-consistent calculation of the molten metal area. To do this, a 2D axially symmetric hydrodynamic model has been developed which includes Navier–Stokes equations for an incompressible viscous fluid with a free surface and a heat conduction equation taking into account convective heat transfer. With the numerical model developed, we have investigated the space and time characteristics of the crater formation process depending on pressure and heat flux on the cathode surface. For a copper cathode, it has been shown that at a pressure of  $\sim 10^8$  Pa exerted on the free molten metal surface by the cathode spot plasma and a heat flux density of  $\sim 10^{12}$  W/m<sup>2</sup> at the cathode surface, micrometer-size craters are formed within several tens of nanoseconds. As this takes place, liquid-metal jets start forming on crater rims and propagating with a velocity of  $10^2$ – $10^3$  m/s in a direction making a small angle with the cathode surface.

### REFERENCES

- [1] G. A. Mesyats // Cathode Phenomena in a Vacuum Discharge: The Breakdown, the Spark, and the Arc, Nauka, Moscow. 2000.
- [2] G. A. Mesyats // J. Nucl. Mater. – 1984. – 128/129. – 618.
- [3] G. A. Mesyats // JETP Lett. – 1994. – 60. – 527.
- [4] G. A. Mesyats and N. M. Zubarev // J. Appl. Phys. – 2013. – 113. – 203301.

<sup>1</sup> This work was supported in part by the Russian Fundamental Research Foundation under Awards 14-02-00575, 14-08-01137, 13-08-00619, 12-08-00310 and in part by Presidium UB RAS Project 12-P-2-1027.

**PREEXPLOSION PROCESSES ON THE CATHODE IN VACUUM ARC CATHODE SPOT<sup>1</sup>**

*S. A. BARENGOLTS\**, *D. L. SHMELEV\*\**, *I. V. UIMANOV\*\**

*\*Prokhorov General Physics Institute, RA S, Mosco 119991w, Russia*

*\*\*Institute of Electrophysics, UB RAS, Ekaterinburg 620016, Rissia  
+7(343)267-87-68, uimanov@iep.uran.ru*

The mechanism of explosive center initiation on a cathode surface is one of the key points of the vacuum arc theory [1]. There is a strong opinion that explosive center (ecton) initiation is provided by the explosion of the solid or liquid (molten metal) microprotrusion. Microprotrusion heating by the plasma action was quite intensively studied previously (see [2]–[5], for example and for further references). In [2], a numerical 2-D non-stationary hydrodynamical model is developed to study the ignition of new explosive center beneath the plasma of a vacuum arc cathode spot. The obtained results show that taking into account the ion impact heating and the electric field of the space charge zone near the cathode surface ensure the "triggering" heat flux power, which is necessary for the development of the Joule heating of the microprotrusion followed by its explosion at reasonable values of the ion current and of the geometric parameters of the microprotrusion. The similar approach was used in [3, 4]. In [5], a numerical 1-D kinetic spherically symmetric model of heating of microprotrusion on the cathode under dense plasma is developed. The kinetic model is a model of 1D3V PIC/DSMC type. The calculations reveal a new mechanism of thermal runaway developing. It is assumed that this thermal runaway leads to the initiation of the explosive emission center. The heating of the metal surface by the flux of backward plasma electrons and the lowering of the cathode voltage drop due to current density growth play the main roles in this process.

In the present work, a 2-D axially symmetric hydrodynamic nonstationary model of the initiation of explosion center on cathode under dense plasma has been developed. The model includes cathode and cathode spot plasma region of vacuum arc. The surrounding plasma parameters are fixed on the boundary placed at a certain distance from the cathode microprotrusion surface. The applied voltage drop is also fixed on the same boundary. The further evolutions of the plasma, current, and cathode temperature are calculated self-consistently taking into account the influence of the plasma generated during the process. The model takes into account evaporation and thermo-field electron emission from the cathode. The developed model takes into account various mechanisms [2]–[5] of thermal runaway developing in the cathode microprotrusion within the framework of one numerical experiment. The model has allowed to study the efficiency of the different mechanisms in depend of time and plasma parameters.

## REFERENCES

- [1] *G. A. Mesyats* // Cathode Phenomena in a Vacuum Discharge: The Breakdown, the Spark, and the Arc, Nauka, Moscow. 2000.
- [2] *I. V. Uimanov* // IEEE Trans. Plasma Sci. – 2003. – 31. – № 5. pp. 822–826.
- [3] *S. A. Barengolts, G. A. Mesyats, and M. M. Tsvetoukh* // J. Exp. Theoretical Phys. – 2008. – 107 – № 6. pp. 1039–1048.
- [4] *S. A. Barengolts, G. A. Mesyats, and M. M. Tsvetoukh* // IEEE Trans. Plasma Sci. – 2011. – 39. – № 9. pp. 1900–1904.
- [5] *D. L. Shmelev and S. A. Barengolts* // IEEE Trans. Plasma Sci. – 2013. – 41. – № 8. pp. 1959–1963.

<sup>1</sup> This work was supported in part by the Russian Fundamental Research Foundation under Awards 14-02-00575, 14-08-01137, 13-08-00619, 12-08-00310 and in part by Presidium UB RAS Project 12-P-2-1027.



## THE INFLUENCE OF PRELIMINARY HIGH POWER ION TREATMENT OF WC-CO HARD ALLOY ON THE STRUCTURE, ADHESION AND TRIBOLOGICAL PROPERTIES OF DEPOSITED DIAMOND COATINGS

*V.V. UGLOV\**, *G.E. REMNEV\*\**, *S.A. LINNIK\*\**, *A.K. KULESHOV\**, *D.P. RUSALSKY\**

\* *Belarussian state university, pr. Nezavisimosti, 4, Minsk, 220030, Belarus, uglov@bsu.by, +375172095134*

\*\* *Tomsk polytechnic university, pr.Lenina, 30, Tomsk, 634050, Russia*

The synthesis of diamond coatings on WC-Co hard alloy using vapor deposition is of great interest nowadays as it allows increase of wear-resistance and application area of WC-Co instruments. However there are problems with structure imperfection and adhesion strength of such coatings. They are resulted from intensive cobalt diffusion to the surface and difference of thermal expansion coefficients of diamond and hard alloy. The chemical etching or transition layer forming is used for these problems solving. The perspective method using high power ion beam (HPIB) is considered in present work. HPIB can form alloyed transition layer which is depleted of cobalt and has dispersed carbide microstructure [1]. This allows changing of structure state, mechanical stresses, adhesion and tribological properties of deposited diamond coating on hard alloy.

The regimes of preliminary HPIB treatment by carbon and hydrogen ions with energy of 320 keV were as follows: ion current density of 50 A/cm<sup>2</sup>, pulse duration of  $9 \cdot 10^{-2}$  μs, pulses number of 3 and 100. The subsequent diamond coating deposition was performed using abnormal plasma glow discharge. The detailed description of installation and reactor as well as regimes of diamond coating deposition is presented in paper [2].

The investigations have shown that the improvement of adhesion of diamond coating with hard alloy is revealed after HPIB treatment with 100 pulses. At the same time the alloyed transition layer with the thickness of 0,1-0,3 μm forms in the surface layer of alloy and the mean roughness of alloy surface increases after HPIB treatment. The diamond coating deposited on modified layer has no evident texture. The degree of compressive mechanical stresses all along the surface is more uniform and has higher value on average comparing with the diamond coating deposited on untreated alloy. The diamond coating deposited on untreated alloy has low adhesion strength of 18 N. After HPIB treatment the tearing off of coating was not detected even at 110 N. The friction coefficient of such a coating was lower by 20% on average. The main reason of changing of adhesion and tribological properties of diamond coating on WC-Co alloy after HPIB treatment with 100 pulses is formation of more uniform and high dispersion microstructure.

### REFERENCES

- [1] *V.V. Uglov, G.E. Remnev, A.K. Kuleshov, V.M. Astashinski, M.S. Saltyrnakov // Poroshkovaja metallurgija i funkcional'nye pokrytija. – 2011. – № 3. P. 63–68 (in Russian).*
- [2] *S.A. Linnik, A.V. Gaydaychuk // Diamond and related materials. – 2013. – № 32. P. 43.*

## ASSESSMENT OF THERMODYNAMIC PARAMETERS OF SHOK WAVE PLASMA GAS

*O.V. VASILEVA, YU.N. ISAEV*

*Tomsk Polytechnic University*

Work is devoted to the solution of the one-dimensional equation of a hydraulic gas dynamics for the coaxial device - magneto plasma accelerator by means of Lax-Wendroff modified algorithm with an optimum choice of parameter of regularization – artificial viscosity. Replacement of the differential equations in private derivatives is made by final differences. Optimum parameter of regularization – artificial viscosity in the environment of MathCAD is added, using the exact known decision – a task Soda. The developed algorithm of calculation of thermodynamic parameters in a braking point is approved. On the basis of the offered algorithm in the environment of MathCAD thermodynamic parameters of a shock wave in front of the plasma piston are calculated at its departure from the coaxial magneto plasma accelerator. When modeling overwhelming unstable high-frequency fluctuations that allows to narrow area of heterogeneity are considered and to allocate only smooth decisions. Results of calculation of gas dynamic parameters in a point of braking coincide with literary data.

For single-dimensional non-steady gas-dynamic equations used tasks of conservation of mass, momentum and energy, written in divergence form:

$$\begin{cases} \frac{\partial \rho}{\partial t} + \frac{\partial(u\rho)}{\partial x} = 0 \\ \frac{\partial(u\rho)}{\partial t} + \frac{\partial(\rho u^2 + p)}{\partial x} = 0 \\ \frac{\partial(\rho(\varepsilon + \rho u^2 / 2))}{\partial t} + \frac{\partial(u(\rho\varepsilon + \rho u^2 / 2 + p))}{\partial x} = 0 \end{cases} \quad (1)$$

Here  $\rho$  – gas density;  $p$  – gas pressure;  $u$  – speed of propagation of the gas;  $\varepsilon$  – internal energy of the gas;  $t, x$  – time and coordinate.

In the calculation of the thermodynamic parameters the unperturbed environment was considered as one atom gas: constant of polytrop –  $\gamma = 5/3$ , pressure –  $p_1 = 105$  Pa, air-density –  $\rho_1 = 1.2$  kg/m<sup>3</sup>, the air temperature – 15°C,  $t = T_1 = 273.15 + 15 = 288.15$  K, the speed of sound, the unperturbed environments –  $c = 340$  m/s. On the charts shows changes in the thermodynamic parameters of shock wave velocity, pressure, density and temperature, directly in front of a plasma piston.

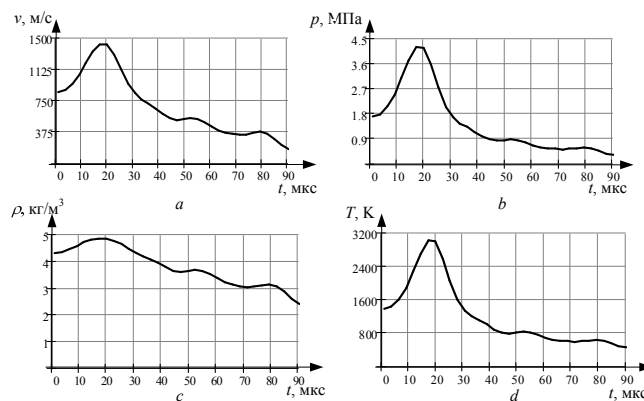


Fig. 1. Dynamics of change of thermodynamic parameters: a) the speed of the shock wave; b) pressure; c) in density); d) temperature

**REFLECTOMETRY OF ELECTRON DIODE WITH EXPLOSIVE EMISSION CATHODE**

*S.A. SHUNAILOV\**, *K.A. SHARYPOV\**, *V.G. SHPAK\**, *M.R. ULMASKULOV\**, *M.I. YALANDIN\**, *V.V. ROSTOV\*\**,  
*M.D. KOLOMIETS\*\*\**

*\* Institute of Electrophysics UB RAS, 106, Amundsen Street, Ekaterinburg, 620016, Russia, ssh@iep.uran.ru*

*\*\* High Current Electronics Institute SB RAS, 2/3, Akademicheskii Avenue, Tomsk, 634055, Russia*

*\*\*\* Ural Federal University, Ekaterinburg, 620002, Russia*

The results on the use of low-distorting reflectometry technique for studying the dynamic impedance of the magnetically isolated coaxial diode (MICD) are presented. MICD has a configuration typical for relativistic BWO of 8 mm wavelength range.

With time release no worse than 50 ps the changes in MICD current rise time was studied within five times peaking of accelerating voltage front (up to  $\sim 200$  ps). The data obtained were compared with beam current measurements by means of a collector sensor. It is shown that the leading fast section of the beam current pulse front has  $dI/dt > 10$  kA/ns. Here the local peak is achieved, where the current is significantly higher than the starting BWO current, and the voltage at the cathode at this point already provides acceleration of electrons to energies corresponding to the band of Cherenkov synchronism. Displacement of the formation of non-stationary BWO emission peak was recorded in the above-mentioned experimental conditions, while the changes of the beam rise time.

The experiments on exact binding of high-current beam emission to the front of the accelerating pulse are carried out with emitting edge radius variation of the tubular cathode, and also in the dependence of the dispersion of used graphite. The features of the MICD impedance dynamics in different magnetic fields are stated.

## POLISHING EFFECT OF METAL CATHODES WITH AGING BY SUBNANOSECOND VOLTAGE PULSES

*S.A. SHUNAILOV\**, *K.A. SHARYPOV\**, *M.R. ULMASKULOV\**, *M.I. YALANDIN\**, *V.V. ROSTOV\*\**, *M.D. KOLOMIETS\*\*\**

\* *Institute of Electrophysics UB RAS, 106, Amundsen Street, Ekaterinburg, 620016, Russia, ssh@iep.uran.ru*

\*\* *High Current Electronics Institute SB RAS, 2/3, Akademicheskii Avenue, Tomsk, 634055, Russia*

\*\*\* *Ural Federal University, Ekaterinburg, 620002, Russia*

With the use of dynamic time-domain reflectometry (DTDR) we studied a polishing effect when aging steel cathode by voltage pulses with amplitudes up to -400 kV and the rise time  $< 1$  ns (at the level of 0.1-0.9). DTDR method [1] allows one to match voltage (electrical field) at the cathode and vacuum diode current within an accuracy not worse than 50 ps, that is, to calculate the dynamic impedance of such non-linear load. Configuration of electrodes was typical for the vacuum magnetically isolated coaxial diode (MICD). External longitudinal magnetic field was as high as 2.3 T. Preliminary, semi-toroidal cathode's emissive edge with curvature radius of 1.2 mm was finished mechanically. The task was to determine the values of macroscopic electric field and the time delay of explosive electron emission (EEE) sufficient for the MICD idle operation.

With a gradual rise of electric field at the cathode (approximately, by the law of  $\cos(\omega t)-1$  to the maximum value of 1.3 MV/cm within  $\sim 2$  ns, the idle mode was observed in this time interval even for non-aged cathode. When increase the voltage amplitude, a 50-pulse cathode aging led to a similar EEE delay, while the field was already as high as 2.5 MV/cm. Dynamics of the delay growth varies substantially in the case of application the voltage pulse with a rapid increase in the beginning section of the front. While in a 500 ps the voltage on the fronts of both smoothly rising and sharpened pulse is approximately the same, the fast front initiates emission of hundreds of amps already at approx. 200 ps. For the sharpened voltage front, the cathode aging by equivalent number of pulses does not permit to get idle regime. The burst at the fast section of the current front retains, and EEE delay is less pronounced during the aging process. For noted cases, the impedance of MICD becomes approximately equal ( $\sim 150$  Ohm in a 2.5 ns) after aging by  $N=50$  pulses.

The data obtained on subnanosecond dynamics of a polishing effect for steel cathode at limited number of aging pulses are important for the development and optimization of electrode systems in miniature MICDs, electron and x-ray cold-cathode vacuum tubes operating in the range of pulse duration about nanosecond and shorter.

### REFERENCES

- [1] *K. A. Sharypov, et al., Time-domain reflectometry of high-voltage nonlinear loads with picosecond resolution, Rev. Sci. Instr. Vol. 84, Issue 5, pp. 055110(1-8), May, 2013.*

## KINEMATIC EFFECTS AT ELECTRON BEAM FRONT WITH VARIATION OF INITIATION CONDITIONS FOR EXPLOSIVE EMISSIVE CATHODE

*S.A. SHUNAILOV\**, *K.A. SHARYPOV\**, *M.R. ULMASKULOV\**, *M.I. YALANDIN\**, *V.V. ROSTOV\*\**

\* *Institute of Electrophysics UB RAS, 106, Amundsen Street, Ekaterinburg, 620016, Russia, ssh@iep.uran.ru*

\*\* *High Current Electronics Institute SB RAS, 2/3, Akademicheskii Avenue, Tomsk, 634055, Russia*

In the report we demonstrate the influence of advanced field emission initiation at the stage of voltage pre-pulse on transition of cold graphite cathode to explosive electron emission regime. Adjustable accelerating pulse was applied to the cathode in the experiments. The voltage amplitude was up to -300 kV and the rate of voltage rise attained  $\sim 1$  MV/ns. Consistent choice of the advance time of field emission initiation (i.e., pre-pulse duration), pre-pulse amplitude and the slope of main voltage pulse creates conditions for kinematic sharpening of e-beam front or for the formation of leading current burst during a free drift motion of accelerated electrons in a strong longitudinal magnetic field.

The measurements were carried out by collector-type beam current probe which could be displaced along drift vacuum chamber. Transient characteristic of this sensor had a fundamental constraint which not allows one the observation of real amplitude for the formed picosecond current burst. Time-domain calibration measurements and analysis of the bandwidth limitations of registration instruments showed that actual amplitude of the current spike with "visible" rise time as short as  $\sim 50$  ps could be underestimated by at least 1.5 times, and was higher than 0.5 kA. Earlier, the capabilities on formation of current bursts at the beam front were noted many times in the numerical models where PIC-code KARAT was used. However, in the real experiments with high-current electron beam these kiloampere-range, ultra-short bursts were detected for the first time.

## CELL PROLIFERATION IN THE MOUSE HIPPOCAMPUS AND HYPOTHALAMUS AFTER EXPOSURE TO NANOSECOND REPETITIVELY-PULSED X-RAYS

KHODANOVICH M.YU.<sup>1</sup>, NEMIROVICH-DANCHENKO N.M.<sup>1</sup>, KEREYA A.V.<sup>1,2</sup>, BOLSHAKOV M.A.<sup>1,2</sup>, KUTENKOV O.P.<sup>2</sup>, KRUTENKOVA E.P.<sup>1</sup>, KUDABAEVA M.S.<sup>1</sup>, PAN E.S.<sup>1</sup>, SEMJONOVA YU.N.<sup>1</sup>

<sup>1</sup>Tomsk State University, 36 Lenina ave, Tomsk, 634050, Russia, khodanovich@mail.tsu.ru, +73822529616

<sup>2</sup>Institute of High-Current Electronics SD RAS, 2/3 Akademichesky Ave., Tomsk, 634055, Russia

The studies of recent decades directly showed the ability of the adult brain to proliferate in special brain areas, such as dentate gyrus of hippocampus and subventricular zone of lateral ventricles. Also such zones are probably exist in hypothalamus. The phenomena of cell proliferation in the brain and, in particular, the formation of new neurons was named neurogenesis. Radiation is known as factor that stops cell proliferation and so X-rays irradiation is widely used for preventing or deceleration of neurogenesis even in low doses, beginning from 0.5 Gy [1]. However, some studies shows the difference between pulsed [2-4] and non-pulsed [5] X-ray impact on cancer cells, liver, and blood cells. We present the pilot study aimed to clear the effect of nanosecond repetitively pulsed X-rays on cell proliferation in mouse brain.

C57B1/6 adult mice of 8 males (25–30 g) were derived from Research Institute of Pharmacology of RAMS (Tomsk). For local exposure of brain to irradiation a mouse body (except head) was placed into leaden screen. The animal head was irradiated by 4000 impulses with frequency 13 Hz during 10 days. Every day a mouse was irradiated with a dose of 0.1 Gy during a trial (cumulative dose for 10 days was 1 Gy). As source of pulse-periodic X-rays irradiation the proton accelerator «Sinus 150» (Russia, impulse duration 4 nsec, accelerating voltage 300 kV, photon's energy spectra with maximum of 100 keV). Irradiated and sham-irradiated animals were used in the experiment. Three hours after irradiation or sham-irradiation the animals received bromodeoxiuridin in dose of 200 mg/kg for the evaluation of proliferation level in dentate gyrus of hippocampus. In 24 hours the animals were euthanized, the brain was frozen in liquid nitrogen steam. Therefore, the frozen brain sections (10 μm) were received, in which the number of newborn cells in dentate gyrus and hypothalamus was evaluated by immunohistochemical staining.

We revealed no significant differences between cell proliferation of irradiated and sham-irradiated animals both in hippocampus and hypothalamus (Fig. 1), despite relatively high cumulative dose of 1 Gy, probably, due to impulse mode of irradiation.

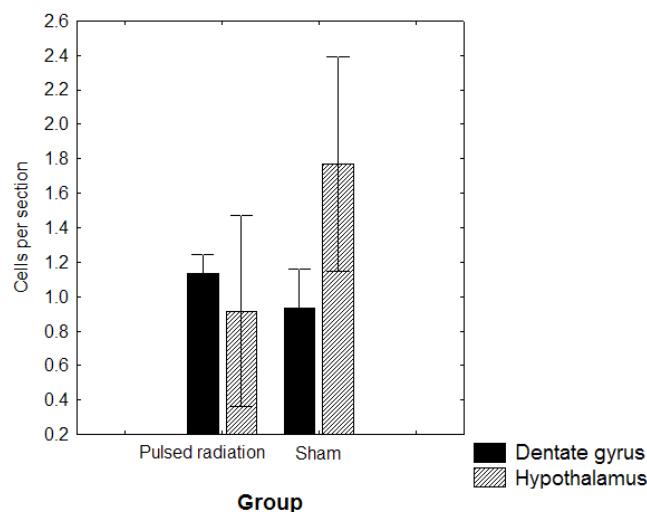


Fig. 1. No differences between cell proliferation of irradiated and sham-irradiated animals both in hippocampus and hypothalamus.

### REFERENCES

- [1] Rola R. et al. // Radiat Res. – 2008. – 169(6). – 626-632.
- [2] Litvyakov N.V. et al. // Siberian Journal of Oncology. 2006. № 1 (17). C. 24–31.
- [3] Zharkova L.P. et al. // TSU Vestnik Journal. Biology. – 2010. – 333. – 161–163.
- [4] Knyazeva I.R. et al. // Bulletin of Siberian Medicine. – 2009. – 1. – 24–30.
- [5] Martin C. et al. // Cellular and molecular biology. – 2001. – 47(3) – 459–65.

## NANOSECOND REPETITIVELY-PULSED X-RAYS AFFECT C-FOS EXPRESSION AND BEHAVIOR IN MICE

*KHODANOVICH M.YU.<sup>1</sup>, NEMIROVICH-DANCHENKO N.M.<sup>1</sup>, KEREYA A.V.<sup>1,2</sup>, BOLSHAKOV M.A.<sup>1,2</sup>, KUTENKOV O.P.<sup>2</sup>, KRUTENKOVA E.P.<sup>1</sup>, KUDABAEVA M.S.<sup>1</sup>, PAN E.S.<sup>1</sup>, SEMJONOVA YU.N.<sup>1</sup>*

<sup>1</sup>*Tomsk State University, 36 Lenina ave, Tomsk, 634050, Russia, khodanovich@mail.tsu.ru, +73822529616*

<sup>2</sup>*Institute of High-Current Electronics SD RAS, 2/3 Akademichesky Ave., Tomsk, 634055, Russia*

It is well known the negative effect of high doses (20-60 Gy) of radiation to central nervous system. However, some studies showed that even extremely low doses (1 Gy or less) of radiation, especially produced in the pulse mode, impact on the bioelectrical activity of neurons [1]. Modern methods of immunochemical staining allow to detect the changes in the neuronal activity of different brain areas using labeling of c-fos proteins which are produced by immediate early genes [2]. Our previous studies showed significant effect of repetitively-pulsed X-rays in low doses (0.2 and 1 Gy) to animal behavior and fat tissue [3]. Present study aimed to estimate the changes of the neuronal activity after nanosecond repetitively-pulsed X-rays in low dose (1 Gy).

The work was performed in 8 inbred male mice (m=25–30 g) breeding from Research Institute of Pharmacology of RAMS (Tomsk), using all ethic rules. For local exposure of brain to irradiation a mouse body (except head) was placed into leaden screen. The animal head was irradiated by 4000 impulses with frequency 13 Hz during 10 days. Every day a mouse was irradiated with a dose of 0.1 Gy during a trial (cumulative dose for 10 days was 1 Gy). As source of pulse-periodic X-rays irradiation the proton accelerator «Sinus 150» (Russia, impulse duration 4 nsec, accelerating voltage 300 kV, photon's energy spectra with maximum of 100 keV). Irradiated and sham-irradiated animals were used in the experiment. In 24 hours the animals were euthanized, the brain was frozen in liquid nitrogen steam. Therefore, the frozen brain sections (10 μm) were received, in which the level of c-fos proteins was evaluated by immunohistochemical staining in motor cortex, reticular formation, hypothalamus. The level of neuronal activation in above brain areas was estimated as a part of activated, i.o. expressed c-fos proteins, neurons from general neuron's number in area of 500×500 μm.

We revealed the significant impact of irradiation to the number of c-fos expressed cells in all explored brain structures ( $F(1, 39)=9,7800$ ,  $p=0.00333$ ). Irradiated animals had significantly higher level of c-fos expression in motor cortex and hypothalamus ( $p \leq 0.001$ ), and lower level in reticular formation ( $p < 0.05$ ), compared to sham-irradiated animals (Fig. 1).

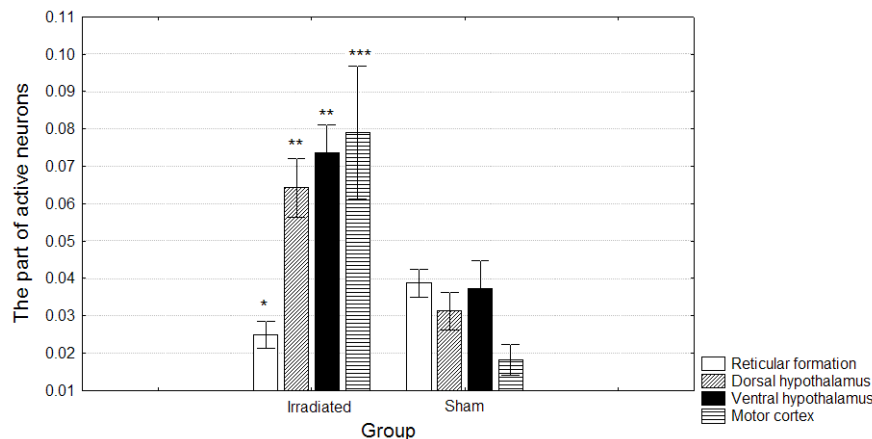


Fig. 1. Significant impact of nanosecond repetitively-pulsed X-rays radiation in dose of 1 Gy to neuronal activation in motor cortex, hypothalamus, and reticular formation (\* –  $p < 0.05$ , \*\* –  $p < 0.01$ , \*\*\* –  $p < 0.001$ ).

Revealed changes of neuronal activation correlates with the decrease behavior activity received in previous studies where the same dose of radiation and frequency were used.

### REFERENCES

- [1] Peymer S.I., Dudkin A.O., Sverdlov A.G. // Reports of the USSR Academy. – 1985. – 284(6). – 1481–1484.
- [2] McKenna J.T. et al. // Brain Research Bulletin. – 2009. – 80. – 382–388.
- [3] Kereya A.V. et al. // TSU Vestnik Journal. – 2014. – 379. – 209–213.

**APPLICATION OF A PLASMA ANODE FOR IMPROVING AN OPERATION STABILITY OF THE ELECTRON SOURCE WITH A BEAM EXTRACTION INTO THE ATMOSPHERE***E.N. ABDULLIN**Institute of High Current Electronics SB RAS, 2/3, Akademicheskoy ave., Tomsk, 634055, Russia  
E-mail: abdullin@lhfe.hcei.tsc.ru, phone: 8-3822-491913*

The experiments were carried out to obtain a large cross-section electron beam in the electron source with an explosive emission multi-point cathode and plasma anode and the electron beam extraction into the atmosphere through a foil window. Pre-filling of the interelectrode gap with artificially created plasma allows increasing the electric field strength at the points that facilitates the initiation of explosive emission and increases the reliability of the electron source operation. A regulation of the time delay of the accelerating voltage pulse supply to the interelectrode gap relative the turn-on time of plasma sources and current value of plasma sources allows controlling the beam current value. At the accelerating voltage of 200-250 kV in the diode with a plasma anode, the electron beam with current of 0.5-0.8 kA, duration of 1-2  $\mu$ s, cross-section of up to 200 cm<sup>2</sup>, and energy of 50 J/pulse was produced.



## GENERATION OF MICROSECOND ELECTRON BEAMS WITH THE ELECTRON ENERGY OF 100 KEV IN THE VACUUM DIODE WITH A PLASMA ANODE<sup>1</sup>

*E.N. ABDULLIN, R.N. GLAZKOV, M.V. NOVIKOV*

*Institute of High Current Electronics SB RAS, 2/3, Akademichesky ave., Tomsk, 634055, Russia  
E-mail: abdullin@lhfe.hcei.tsc.ru, phone: 8-3822-491913*

Technological applications of high-power electron beams are based on the thermal effect of the beams on the work pieces. The use of the plasma anode is the effective way to increase the current density and the energy density of the electron beams generated in the electron sources with explosive-emission cathodes that allows extending their technological capabilities.

Modern electron sources with a plasma anode allows generating the electron beams with the current density of up to 200-500 A/cm<sup>2</sup> and the energy density on the irradiated surface of up to 20 J/cm<sup>2</sup>. However, they are characterized by relatively low electron energies (~ 10-40 keV) and short duration of the electron current (~ 2-5 μs). The interest in the generation of the electron beams of high electron energy equal to 100 keV and more is caused by the large depth of penetration of the electrons into the irradiated material and, therefore, by the large thickness of the treated layer and by the wide range of application of such beams.

The paper presents the experimental results on the increase in the duration of the electron beams generated in the vacuum diode with a plasma anode at the accelerating voltages of 100 kV. To increase the duration of the beams, the restriction of the cathode plasma propagation into the interelectrode gap, the adjusting of the anode plasma concentration and the time of filling the gap with the aforementioned plasma, as well as the imposition of the external longitudinal magnetic field on the interelectrode gap were used. The mode of the diode operation with quasi-constant impedance in the course of 5-8 μs is realized. The electron beams with the electron energy of up to 130 keV, beam current of 1-2 kA, pulse length of up to 15-18 μs, energy of 1 kJ, and cross-section area of 30-40 cm<sup>2</sup> have been obtained. The possibility of using the electron beams for melting the near-surface layers of metals like stainless steel, Cu, Ti, and Ta has been demonstrated.

---

<sup>1</sup> This work was supported by RFBR, Grant No. 14-08-00707

## PLASMA-CATHODE ELECTRON SOURCE BASED ON A MULTI-ARC LOW-PRESSURE PULSED DISCHARGE IN A LONGITUDINAL MAGNETIC FIELD<sup>1</sup>

*V.N. DEVYATKOV\**, *N.N. KOVAL\*\**

\**Institute of High Current Electronics SB RAS, 2/3 Akademicheskoy Ave., Tomsk, 634055, Russia, E-mail: vlad@opee.hcei.tsc.ru, Phone: +7(3822) 491-713*

\*\**National Research Tomsk Polytechnic University, 30 Lenin Avenue, Tomsk, 634050, Russia*

The report presents a plasma-cathode electron source based on low-pressure pulsed arc discharges with grid stabilization of the emission plasma boundary. The main peculiarity of the source is the generation of an electron beam in a strong longitudinal magnetic field. Schematic of the source is shown in Fig. 1. Magnesium cathodes 2 are mounted on current leads 1 with insulation 10 in case 3. Emission electrode 4 of outer diameter 10.6 cm has output window 5 of dimensions  $1.6 \times 6.4$  cm covered with a metal grid. Grounded electrode 7 (a diaphragm of inner diameter 8 cm) is located 1 cm away from electrode 4. Collector 8 is spaced by 22 cm from emission grid 5. Electrodes 6 are used to provide better current density distribution over the beam cross-section. Electrodes 9 placed at floating potential and cylindrical electrode 11 are 7.5 cm in diameter. The longitudinal magnetic field is produced by solenoid 12.

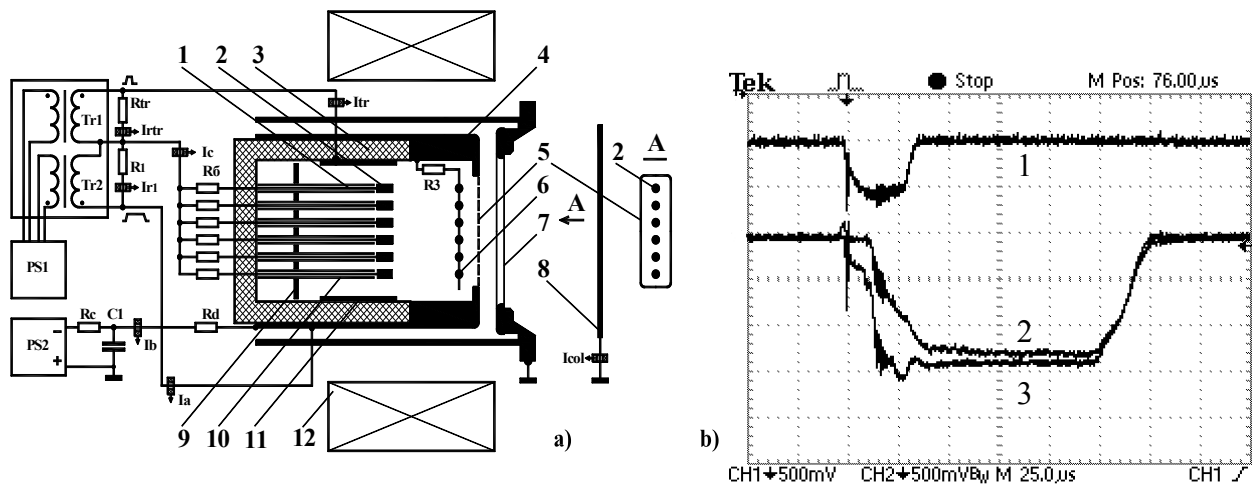


Fig. 1. Schematic of the electron source (a) and waveforms (b) for  $I_{tr}$  (1),  $I_a$  (2),  $I_b$  (3).  $p=0.13$  Pa,  $B=0.12$  T,  $U_{ps2}=5$  kV. 10A/div, 25  $\mu$ s/div.

The main arc discharges (powered from Tr2) are initiated by a discharge in crossed electric and magnetic fields [1] (powered from Tr1). The discharges are ignited in the range of air pressures  $p = 0.05$ – $0.5$  Pa. At  $p > 0.1$  Pa, a magnetic field of 0.05 T is sufficient to initiate the discharges. At lower pressures ( $p < 0.05$  Pa), a stronger magnetic field ( $B \geq 0.12$  T) is required. The electron source ensures the formation of an electron beam with an amplitude of up to  $I_b = 30$ – $40$  A at a pulse duration of 100  $\mu$ s, pressure of 0.13 Pa, accelerating voltage of 1–10 kV, and magnetic field of 0.12 T.

The electron source was developed as an alternative to the electron source with a hot cathode and its parameters were optimized for ionization of hypersonic air flow at a strong ( $B \geq 0.1$  T) magnetic field [2,3].

### REFERENCES

- [1] *A.G.Nikolaev and G.Yu.Yushkov, E.M.Oks, R.A.MacGill, M.R.Dickinson, and I.G.Brown // Rev. Sci. Instrum., Vol. 67, No. 9, September pp.3095-3098 (1996).*
- [2] *V.N.Devyatkov, N.N.Koval, V.P.Fomichev, A.B.Shevchenko // Proc. 10th Intern. Conf. on Modification of Materials with Particle Beams and Plasma Flows, Toms, 2010, pp.575-578.*
- [3] *T.A Korotaeva, V.P.Fomichev, A.P.Shashkin, M.A.Yadrenkin // Journal of Techn. Physics, Vol. 81, No.39, pp.10-17(2011).*

<sup>1</sup> This work was partially supported by Integration Project No. 104 of the Siberian Branch of the Russian Academy of Sciences and RFBR project No. 12-08-00251-a

## ANNULAR ELECTRON BEAM WITH VIRTUAL CATHODE IN COAXIAL DIODE WITH MAGNETIC INSULATION<sup>1</sup>

A. A. GRISHKOV\*, I. K. KURKAN\*\*\*, I. V. PEGEL\*\*\*

\* Institute of High Current Electronics SB RAS, 2/3 Akademicheskoy Ave., Tomsk, 634055, Russia, [ikk@lfe.hcei.tsc.ru](mailto:ikk@lfe.hcei.tsc.ru)

\*\* National Research Tomsk Polytechnic University, 30 Lenin Ave., Tomsk, 634050, Russia

The accumulation of electron charge during the transport of tubular high-current electron beam in a coaxial diode with magnetic insulation in the case of electron counter streams due to the formation of a virtual cathode was studied. Accumulation of electrons in these flows is accompanied by an increase in their relative energy spread and a simultaneous decrease in the maximum kinetic energy. The accumulation of electrons was described analytically and confirmed by numerical calculations. Theoretical studies based on the proven method of conservation laws z-component of the momentum of the field and particles were carried out [1]. Known theory was extended to the case of high-current electron tubular beam transporting in a uniform cylindrical channel with a spread of electron beam kinetic energy. Computer modeling was performed using PIC-codes KARAT[2] and OOPIC Pro[3] based on the method of large particles.

Using computer simulation conditions were chosen and experiments were performed on a high-current electron accelerator SINUS-7 in a wide range of parameters: the voltage at the cathode 350-800 kV, the magnetic field 8-24 kOe; while the current in the diode is changed within 2.0-12 kA. The voltage pulse duration (FWHM) was about 50 ns. Experimental dependence of the beam potential in the coaxial diode with magnetic insulation on the time was obtained. As predicted by theoretic model and computer simulation it shows decreasing of beam potential during the voltage pulse as a charge accumulates in the space between real cathode and virtual one. Studies and further development of the theory of transport of the electron beam with a virtual cathode is essential for understanding the physical effects in systems with high-current tubular electron beams. Obtained results can be designated for such areas as the generation of high-power microwave radiation in vircators, collective acceleration of ions moving virtual cathode in cylindrical channels and the generation of electron string ion sources.

### REFERENCES

- [1] A.A. Grishkov, I.V. Pegel // *Plasma Physics Reports*, - 2013, - Vol. 39, - No. 11, pp. 936–946.
- [2] V.P. Tarakanov // *User's manual for code Karat*. – Berkley Research Associate. Inc, Springfield, VA, 1992.
- [3] Verboncoeur J. P., Langdon A. B., Gladd N. T. // *Computer Physics Communications*. – 1995. –87. 199.

<sup>1</sup> This work was supported by RFBR grant 12-08-31447-mol-a.

FOIL-LESS PLASMA-FILLED DIODE FOR HPM GENERATOR<sup>1</sup>A.A. ELTCHANINOV\*, B.M. KOVALTCHUK\*, I.K. KURKAN\*\*\* , A.A. ZHERLITSYN\*\* Institute of High Current Electronics SB RAS, 2/3 Akademichesky Ave., Tomsk, 634055, Russia, [ikk@lfe.hcei.tsc.ru](mailto:ikk@lfe.hcei.tsc.ru)

\*\* National Research Tomsk Polytechnic University, 30 Lenin Ave., Tomsk, 634050, Russia

Plasma-filled diode regarded as perspective source of electron beam feeding HPM generator of GW power level, comparing to conventional explosive emission vacuum diode. Electron beam generation occurs in plasma double layer, where plasma boundary plays as an anode. It allows canceling the usage of anode foils or grids in HPM generators with the virtual cathode (vircator), which could limit its life time to few shots. There is no need for special treatment of a cathode surface to enhance emission such as velvet coating, blades or needles, etc., as preliminary generated plasma is a source of electrons. The presence of ions in the e-beam drift space could raise the limiting current for a drift space, but it could affect to microwave generation also.

Sectioned plasma-filled diode with beam current of about 100 kA, electron beam energy of about 0.5 MV and beam current density of 1-10 kA/cm<sup>2</sup> was realized. Cylindrical transport channel with the diameter of 200 mm and the length of about 30 cm was attached to the diode. Beam current measurements in a drift space were performed. Computer simulations of electron beam transport with the presence of ions were carried out with the 2.5D axisymmetric version of PIC-code KARAT. Obtained results would help optimizing electrodynamic system of HPM generator subjected to the presence of ions.

---

<sup>1</sup> This work was supported by by RFBR, grant No. 14-08-01123 -a

## RECONSTRUCTION OF THE ELECTRON BEAM SPECTRUM FROM AN ATTENUATION CURVE FOR VACUUM AND GAS DIODES<sup>1</sup>

*M.S. VOROBYOV\**, *E.KH. BAKSHT\**, *N.N. KOVAL'\**, *A.V. KOZYREV\*\*\**, *V.F. TARASENKO\*\*\**

\**Institute of High Current Electronics, Akademichesky Ave. 2/3, Tomsk, Russia, 634055, VFT@loi.hcei.tsc.ru, 49-16-85*

\*\**National Research Tomsk State University, Tomsk, 36 Lenina Avenue, 634050, Russia*

One of the parameters that carry important information on the mechanism of the generation of electrons in vacuum and gas diodes and applications of electron beams is the e-beam energy distribution. A magnetic and flight-time spectrometers use for this task.

The main objectives of this work are to study the feasibility of reconstruction of the electron beam spectrum from an attenuation curve.

The spectra of a microsecond and subnanosecond electron beam generated in the vacuum and gas diodes during the voltage pulses were reconstructed and analyzed. The electron energy distributions were calculated using the program than was created Kozyrev and Kozhevnikov [1].

Experiments on measurement of energy spectrum of electron beam from vacuum diode were performed on the electron accelerator DUET with pulsed plasma cathode [2]. Experiments on measurement of energy spectrum of electron beam from gas diode were performed with a SLEP-150 generator [3]. This generator was specially developed for obtaining electrons in gas diodes. The housing of the P-43 peaking spark gap served as the inner electrode of the high-voltage forming coaxial line. This allowed us to reduce the length of the forming line and obtain a voltage pulse in the transmission line with amplitude of ~140 kV in the incident wave and FWHM duration of ~1 ns. The voltage-pulse rise time was determined by the peaking spark gap and amounted to ~300 ps.

Figure 1(left) show experimental attenuation curves (points) for vacuum diode of accelerator DUET with voltage pulse 130 kV. Figures 1(right) depict the corresponding spectra of fast electrons reconstructed by the regularization method. The curve in Figures 1(left) show attenuation curves, which were calculated after the reconstruction of the corresponding spectrum (Figure 1(right)).

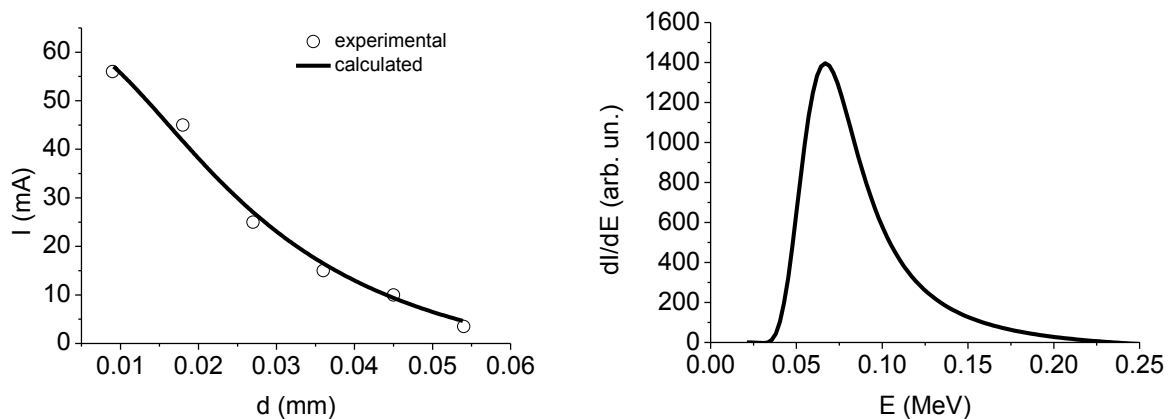


Fig. 1. Absorption curve (left diagram) and energy distribution (right diagram).

Same results were obtained with gas diode and SLEP-150 generator. Our results confirm that the electron energy distributions can be calculated using the program [1], than was created on minimum a priori assumptions by regularization of an ill-posed problem—a Fredholm integral equation.

### REFERENCES

- [1] *Baksht E.H., Burachenko A.G., Kozhevnikov V.Yu., Kozyrev A.V., Kostyrya I.D., Tarasenko V.F. J. Phys. D: Appl. Phys. - 2010. - Vol. 43. - 305201.*
- [2] *Koval N.N., Kreindel Yu. E., Tolkachev V.S., Schanin P.M. IEEE Trans. Electr. Insul. - 1985. - Vol. EI-20. No. 4. - P. 735-737.*
- [3] *Kostyrya I.D., Rybka D.V., Tarasenko V.F. Instruments and Experimental Techniques. - 2012. - Vol. 55. - No. 1. - P. 72-77.*

<sup>1</sup> The work is performed in the framework of the State task for HCEI SB RAS, project #9.5.2 and RAS Presidium program number 12 project 8.

## A THERMODYNAMICAL DESCRIPTION OF THE METAL SOLID AND LIQUID STATES, AND THE "CRYSTAL-LIQUID" AND "LIQUID-VAPOUR" PHASE TRANSITIONS AT THE INTENSIVE PULSE ENERGY INPUT<sup>1</sup>

*N.B. VOLKOV, E.A. CHINGINA*

*Institute of Electrophysics UB RAS, Amundsen Street, 106, Yekaterinburg, 620016, Russia, nbv@iep.uran.ru, +7(343)2678660*

The objective of the present paper is establishment of the phenomenological model of solid and liquid states of metal, allowing us to receive wide-band expressions for thermodynamic functions of metal at high energy densities, including through "crystal-liquid" and "liquid-vapor" phase transitions. To describe solid metal thermodynamic functions we use our earlier suggested phenomenological model [1, 2]. The model takes into account anharmonicity of lattice vibration. The small number ( $\leq 5$ ) of the model free parameters values are defined under the requirement of exact description of metal and its thermodynamic functions behavior at normal conditions, and also satisfying to theoretical asymptotes within the range of quantum-statistical matter model applicability.

Here we suggest that a liquid metal can be represented as "mixture" of clusters, where atoms oscillate with mean frequency  $\omega_E(V)$ , and bubbles with gaseous disorder. Free energy of the mixture can be formularized to:

$$F_L(V, T) = (1 - C_b) \left( F_*(V, T) - \frac{3}{MA} \left( \frac{T_E}{2} + T \ln \left( 1 - \exp \left( -\frac{T_E}{T} \right) \right) \right) + T \right) - C_b \left( \frac{3a_1}{mV^{m/3}} + \frac{T}{MA} \ln \left( \left( \frac{MAT}{2\pi\hbar^2} \right)^{3/2} \nu(V) \right) + \frac{T}{MA} \right) + F_e(V, T), \quad (1)$$

where  $M, A$  - atomic mass unit and atomic weight;  $C_b$  - bubbles concentration;  $T_E = \hbar\omega_E$  - zero oscillations energy (temperature);  $T$  - temperature in energy units;  $\nu = V - a_2(Z - \tilde{z})$  - free volume;  $Z, \tilde{z}$  - nucleus charge and current atomic (ion) charge;  $F_e$  - conductivity electrons, following Fermi statistics, gas free energy;

$$F_*(V, T) = -T(MA)^{-1} \sum_{\lambda=1}^{N_\lambda} \exp \left( -MA\varphi_{eq} K_\lambda (2T)^{-1} \right) - \quad (2)$$

- free energy structure part, defined by first coordination sphere [3] configurations ( $N_\lambda, K_\lambda, \varphi_{eq}$  - number of configurations, first coordination number in  $\lambda$  configuration and interaction potential value, corresponding to equilibrium configuration);  $a_1, a_2, m$  - model free parameters, defined under request of terms precise fulfillment in triple point, and also on melting curves (at normal conditions) and saturated vapors. Bubbles concentration is defined by solving the non-linear equation, accounting the threshold character of critical-size bubbles generation by homogeneous nucleation [4] and non-linear character of their interaction. During the formularization "liquid-vapor" phase transition kinetics, surface tension and matter stability in near-critical region features were also taken into account. Depending on temperature variation velocity the free energy can have several local minimums, each having a corresponding "frozen" shot-range order structure, existing for a long period. The free energy minimum at slow temperature variation has a corresponding thermodynamic equilibrium state of matter, when each volume and temperature value has its own corresponding equilibrium  $C_b$  value. At the "liquid-vapor" phase transition critical point it equals to 1/2, which is equivalent of an infinite liquid or gaseous percolating cluster [5] equiprobable existence in the critical point.

Thermodynamic functions for liquid and solid Cu were acquired. Shock-wave adiabatic curves had been built and were compared to the experimental results. Qualitative and quantitative agreement between the presented model and experimental data is shown.

<sup>1</sup> This work was supported by the RFBR (projects No. 13-08-00266-a and No. 14-08-31024-mol\_a) and FASO within the Presidium of Russian Academy of Sciences fundamental research program (UB RAS project No. 12-P-1005, state registration No. 01201266835).

## REFERENCES

- [1] *N. B. Volkov, E.A. Chingina // Physics of the pulse discharges: Proceedings of the XVI International Conference (19-22 August 2013, Nikolayev, Ukraine). - Nikolayev: KP "Mykolaivska drukarnya", 2013. P. 55-58.*
- [2] *N.B. Volkov, E.A. Chingina // Russian Physics Journal. – 2013. – V. 55 – № 10/3. P. 438-442.*
- [3] *N.B. Volkov // Nonlinear dynamics of current-carrying plasma-like media. /Doctoral thesis. - Yekaterinburg: IEP UB RAS, 1999.*
- [4] *V.P. Skripov // Metastable liquids. - New York: J. Wiley, 1974.*
- [5] *J.M. Ziman // Models of disorder: The theoretical physics of homogenously disorder systems. - Cambridge: Cambridge University Press, 1979.*

## EXPERIMENTAL AND NUMERICAL STUDY OF METALLIC ELECTRODE PARAMETERS DURING POWER TRANSMISSION BY SUBMICROSECOND CURRENT PULSE WITH LINEAR DENSITY ABOVE 1 MA/CM VIA MAGNETICALLY INSULATED TRANSMISSION LINES<sup>1</sup>

*S.I.TKACHENKO\** \*\*, *E.V.GRABOVSKII*\*\*\*, *P.V.SASOROV*\*\*\*\*, *G.M.OLEINIK*\*\*\*, *V.V.ALEKSANDROV*\*\*\*,  
*YU.G.KALININ*\*\*\*\*, *O.G.OLHOVSKAYA*\*\*\*\*, *K.V.KHISHCHENKO*\*\* , *P.R.LEVASHOV*\*\*

\**Moscow Institute of Physics and Technology, Dolgoprudny, Moscow Region, Russia*

\*\**Joint Institute for High Temperatures, RAS, Moscow, Russia*

\*\*\**State Research Center of Russian Federation, Troitsk Institute for Innovation and Fusion Research, Russia, Moscow*

\*\*\*\**Keldysh Institute of Applied Mathematics, RAS, Moscow, Russia*

\*\*\*\*\**Russian Research Centre "Kurchatov Institute", Moscow, Russia*

The possibility of power transfer by submicrosecond current pulse with linear density ( $I_l$ ) above 1 MA/cm via magnetically insulated transmission lines (MITL) was analyzed. Coaxial electrode system (CES) is used as output MITL section for transfer electromagnetic pulses from the pulse generator to the load. Similar problem was studied in [1] at much lower currents.

It is shown the electrodes are exposed to extreme stresses during the electrical energy transmission in current pulse with linear density above 1 MA/cm across the electrodes. Numerical data on the dynamics of the spatial distribution of temperature, pressure and density in the electrodes made of aluminum (Al), tungsten (W) and stainless steel (SS), during the current pulse and after its completion was obtained (see Fig. 1). The numerical results are compared with experimental data. The parameters of the plasma layers on the electrode surface of MITL ( $I_l \sim 3$  MA/cm) were also calculated.

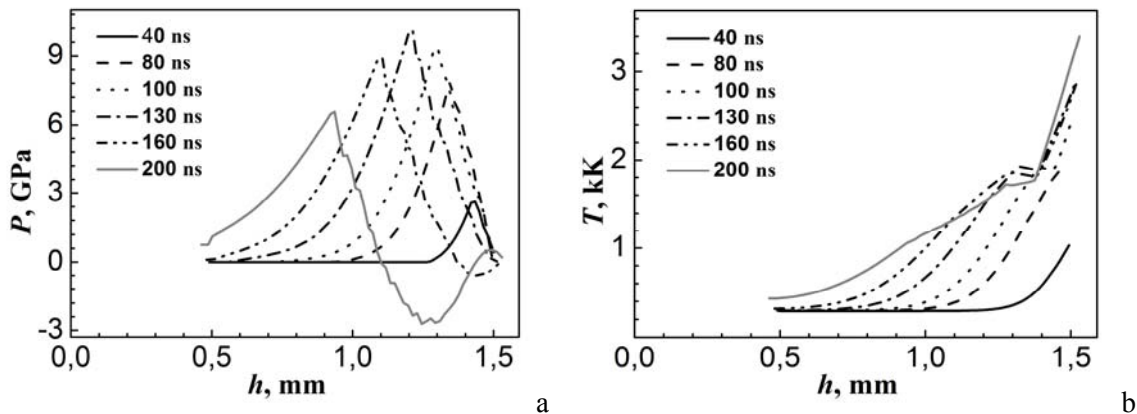


Fig. 1. Dependences of pressure (a) and temperature (b) through the electrode depth in different moments ( $I_l = 1$  MA/cm, - the linear density of current;  $D = 3$  mm - the outer electrode diameter;  $h_0 = 1$  mm - the electrode thickness)

### REFERENCES

- [1] *E. V. Grabovskii, et. al. // Plasma Physics Reports. - 2006. - V. 32. - pp. 718-728.*

<sup>1</sup> This work was partially supported by State Corporation Rosatom under the state contract on 16.05.2013 № H.4x.44.90.13.1108, and the Russian Foundation for Basic Research project nos. 14-0100678.



## EXPERIMENTAL RESEARCH OF X-PINCH NECK FORMATION<sup>1</sup>

*A.P. ARTYOMOV, S.A. CHAIKOVSKY, A.V. FEDUNIN, N.A. LABETSKAYA, V.I. ORESHKIN*

*Institute of High Current Electronics SB RAS, 2/3, Akademichesky ave., Tomsk, 634033, Russia  
Phone: 8(382-2) 492-133, e-mail: aap545@gmail.com*

The work is devoted to description of the results of the experiment where in the X-pinch dynamics were registered using four frame visible fast camera HSFC-Pro with the frame duration of 3 ns. The experiments were aimed on experimental verification of the whole X-pinch radiation pulse formation process beginning from the wire explosion through the wire expansion till the X-pinch “hot spot” implosion.

The experiments have been performed on the low scale pulsed power generator (250 kA, 180 ns) designed especially for X-pinch researches in HCEI, Tomsk. The X-pinches made of 2 or 4 molybdenum fine wires and of 4 tungsten wires with the different diameters were used in the experiment.

Fig.1 illustrates typical frames of the X-pinch made of 2 molybdenum wires with diameter of 25 microns. The line on the pictures indicates the initial position of wire cross-point that is denoted by  $Z_0$ . The cathode on the pictures is situated on the bottom. On the first picture on the Fig.1 the plasma jets are clearly visible which spreads to the cathode and anode side. The jets become noticeable at the first 10 ns of the process that approximately corresponds to electrical explosion of the X-pinch wires. The anode side jet reaches the velocity of  $10^7$  cm/s and has approximately 1.5 times higher than the cathode side jet. Such high jet velocity hardly corresponds to the plasma temperature attained at the wire explosion. Hence, these jets probably are developed due to implosion of the light plasma layer stripped by magnetic forces from the wire surface with possible velocity increasing due to cumulative effects at the X-pinch axis.

It have been registered that evolution of the X-pinch made of 4 wires is accompanied always by radial jets flowing from the initial wire cross-point. Two wires X-pinches do not show the same dynamics in the most of the shots. For molybdenum X-pinches the neck is formed as a rule higher than  $Z_0$  point (closer to the anode) and the “hot spot” is situated 200-400 microns higher than point  $Z_0$ . At this region the plasma diameter gradually increases in time but sharply falls down at 10-15 ns before X-ray pulse. Just before X-ray pulse on the plasma neck with length of 300 microns a lower scale constriction develops forming the “hot spot”. The fourth frame in the Fig.1 corresponds to the time of the X-ray pulse generation.

It have been also confirmed that anode side plasma jet could take some part of the X-pinch wires current because of evident pinching of the jet in the near anode region. This circumstance should be taken into the account at the theoretical modeling of the X-pinch dynamics.

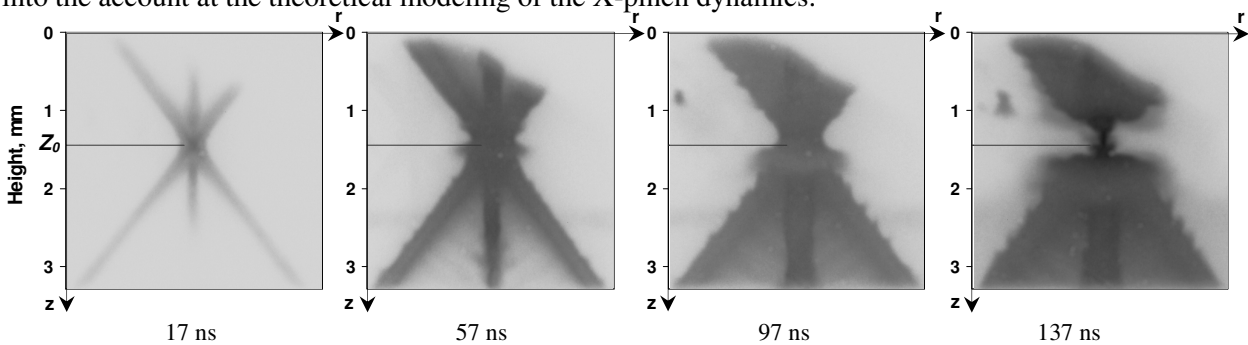


Fig. 1. Typical optical frames of the X-pinch made of 2 molybdenum wires with diameter of 25 microns.  $X_0$  – the initial position of the cross point of X-pinch wires.

<sup>1</sup> This work was supported in part by the RAS Presidium under the programs “Fundamental problems of pulsed high current electronics” and by the Russian Foundation for Basic Research (Grant #12-08-00868-a).

## STUDY OF THE IMPLOSION OF MG AND BI METAL-PUFF Z -PINCHES<sup>1</sup>

A.G. ROUSSKIKH<sup>\*</sup>, A.S. ZHIGALIN<sup>\*</sup>, R.B. BAKSHT<sup>\*\*</sup>, N.A. LABETSKAYA<sup>\*</sup>, S.A. CHAIKOVASKII<sup>\*</sup>, V. I. ORESHKIN<sup>\*</sup>

<sup>\*</sup> *Institute of High Current Electronics, Siberian Division, 634055 Tomsk, Russia.*

<sup>\*\*</sup> *Tel Aviv University, Laboratory of electric discharges and plasmas, Tel Aviv, Israel.*

The implosion of Mg and Bi metal-puff Z pinches was studied experimentally at a current of 450 kA with rise time of 450 ns. In a metal-puff Z pinch [1-3], the plasma shell is produced due to evaporation of the electrode material during the operation of a vacuum arc. In the experiment to be discussed, a single-shell and a shell-on-jet pinch load with magnesium and bismuth electrodes were used. Two-dimensional, 3-ns gated, visible-light images were recorded at different times during the implosion. At the experiments the pinch radiation was recorded by the XRD, a pinhole camera, and a nickel bolometer. Experiments with Mg metal-puff shell demonstrated that when the shell was formed by a collimated plasma flow with small radial divergence, Rayleigh–Taylor (RT) instability typical of gas-puff implosions was detected. The RT instability was completely suppressed in a mode where the initial mass distribution of the Mg shell approached a tailored density profile [4]. An energy analysis shows that a considerable portion of the energy that provides the radiation yield is produced due to the work  $pdV$ .

### REFERENCES

- [1] A.G. Rousskikh, A.S. Zhigalin, V.I. Oreshkin, S.A. Chaikovsky, N.A. Labetskaya, and R.B. Baksht // *Phys. Plasmas*. – 2011. – Volume **18**. – p.092707.
- [2] A.G. Rousskikh, R.B. Baksht, A.S. Zhigalin, V.I. Oreshkin, S.A. Chaikovsky, and N.A. Labetskaya // *Plasma Phys. Rep.* – 2012. – Volume **38**. – p.651.
- [3] R.B. Baksht, A.G. Rousskikh, A.S. Zhigalin, and V.I. Oreshkin // *IEEE Trans. Plasma Sci.* –2013. – Volume **41**. – p.182.
- [4] A.L. Velikovich, F.L. Cohran, and J. Davis // *Phys. Rev. Lett.* – 1996 – Volume **77**. – p.853.

<sup>1</sup> The work was supported in part by the Russian Foundation for Basic Researches under Grants # 14-02-00382-a.

**EXPERIMENTAL RESEARCH OF THE FINE FOILS EXPLOSION DYNAMICS<sup>1</sup>**

*A.S. ZHIGALIN, A.G. ROUSSKIKH, V.I. ORESHKIN, S.A. CHAIKOVSKY\*, V.V. KUZNETSOV\*\**

*\*Institute of High Current Electronics SB RAS, 2/3 Academichesky ave., Tomsk, 634055, Russia,  
E-mail: Zhigalin@ovpe2.hcei.tsc.ru*

*\*\*Kutateladze Institute of Thermophysics SB RAS, 1 Akad. Lavrent'eva ave., Novosibirsk, 630090, Russia*

The present work is devoted to studying of substances properties at high specific deposit energy using double-frame pulsed backlighting system [1]. The high specific deposit energy was reached at electrical conductor explosion (ECE). Fast mode of ECE was investigated. Fine foils of aluminum, cooper, titanium and nickel were used as conductors.

Experiments were carried out on the experimental complex consisting of three current generators. The first generator *WEG-1* [2] provided explosion of the fine conductors. This generator represents RLC-contour, with capacity 70 nF, which was charged to voltage 10 to 30 kV. High-resistance divider measured voltage only on the subcircuit where the exploding conductor was assembled.

The current derivative was measured with an inductive loop. The investigated conductor was mounted in special holder and the foil contacts with the electrodes were soldered.

Two other generators - radiographs *XPG-1* and *G<sub>2</sub>* with X-pinch load were used as diagnostics [3]. When the generators were operated with a low inductance load, there current pulse amplitude was up to 300 kA at the pulse rise time of 180 ns. Four crossed tungsten wires with diameter of 13 μm were used as a load. Using of x-pinch radiation the spatial image of exploded foil was registered. The image was registered on a film located behind the filter. The X-ray pulse power from X-pinches were registered using vacuum X-ray diodes that were located behind of 7 μm aluminum foil filters.

The measurement of the current flowing through a conductor and voltage on the exploded conductor has allowed to determine the energy deposited in the conductor, delay time of the bubbles formation relative to the moment of current-cutoff and the time dependence of the vapor bubbles quantity.

## REFERENCES

- [1] *Artyomov, A. P., Fedyunin, A. V., Chaikovsky, S. A., Zhigalin, A. S., Oreshkin, V. I., Ratakhin, N. A., & Rousskikh, A. G. // A double-frame nanosecond soft X-ray backlighting system based on X-pinches. – Instruments and Experimental techniques, 2013. – № 56(1). Pages 66-71.*
- [2] *Rousskikh, A. G., Oreshkin, V. I., Chaikovsky, S. A .et al. // Physics of Plasmas. – 2008. V. 15. P. 102706*
- [3] *Ratakhin N.A., Fedushchak V.F., Erfort A.A., Zharova N.V., Zhidkova N.A., Chaikovskii S.A., Oreshkin V.I. // Russian Physics Journal. 2007. V. 50. № 2. P. 193.*

<sup>1</sup> This work was supported in part by the RAS Presidium under the programs "Fundamental problems of pulsed high current electronics" and by the Russian Foundation for Basic Research (Grant #12-08-00868-a)

## NEUTRON EMISSION FROM DEUTERIUM GAS-PUFFS AT THE CURRENT LEVEL ABOVE 2 MA<sup>1</sup>

*A.V. SHISHLOV\**, *R.K. CHERDIZOV\**, *F.I. FURSOV\**, *V.A. KOKSHENEV\**,  
*B.M. KOVALCHUK\**, *N.E. KURMAEV\**, *A.YU. LABETSKY\**, *N.A. RATAKHIN\**,  
*D. KLIR\*\**, *J. CIKHARDT\*\**, *J. KRAVARIK\*\**, *P. KUBES\*\**, *K. REZAC\*\**, *O. SILA\*\**,  
*H. ORCIKOVA\*\*\**, *K. TUREK\*\*\**,  
*G.N. DUDKIN\*\*\*\**, *B.A. NECHAEV\*\*\*\**, *V.N. PADALKO\*\*\*\**

\* *Institute of High Current Electronics SB RAS, 2/3 Akademichesky Ave., Tomsk, 634055, Russia, E-mail: [ash@ovpe2.hcei.tsc.ru](mailto:ash@ovpe2.hcei.tsc.ru),  
Phone: +7 (3822) 492-133*

\*\**Czech Technical University in Prague, Faculty of Electrical Engineering, Technika 2, Prague, 16627, Czech Republic*

\*\*\**Nuclear Physics Institute, Academy of Science of Czech Republic, Na Truhlance 39, Prague, 18086, Czech Republic*

\*\*\*\**National Research Tomsk Polytechnic University, 30 Lenina Ave., Tomsk, 634050, Russia*

The experiments with deuterium gas-puffs were carried out on the GIT-12 generator (Tomsk, Russia). The generator operated in a direct drive mode without a plasma opening switch at 50 kV charging voltage (4.7 MA, 1.7  $\mu$ s). A new multi-shell load configuration, a deuterium gas-puff surrounded by a plasma shell, was used in the experiments. The plasma shell consisting of hydrogen and carbon ions was formed at the diameter of 350 mm by 48 plasma guns triggered 1.7-1.9  $\mu$ s before the onset of the generator current. The double-shell deuterium gas-puff was created by fast electromagnetic valve. Outer and inner nozzle diameters were 80 and 30 mm, respectively. The total mass of deuterium gas-puff was varied from 50 to 120  $\mu$ g/cm providing the implosion time in the interval from 600 to 750 ns at the peak implosion current 2.3-3 MA.

Z-pinch diagnostics included a four-frame time-gated x-ray pinhole camera, an optical streak camera, four B-dot probes, x-ray diodes, photoconducting detectors, and voltage and current probes. Neutron time-of-flight diagnostics was realized with the help of four radial and one axial detectors based on fast plastic scintillator and photomultiplier tube combination located at the distances from 170 to 2579 cm from the pinch. Neutron yields were measured by a silver activation detector, by TasTrak CR-39 detectors filtered by 4 mm of lead, and by five bubble detectors (BD-PNDs) placed at different distances and angles. Fast ions were detected by two stacks of CR-39 detectors located axially and radially at the distance of 19 cm and 58 cm, respectively.

In the experiments, the peak neutron yield from DD reactions reached  $Y_n = (2.9 \pm 0.3) \times 10^{12}$  at the deuterium gas-puff mass of about 100  $\mu$ g/cm and the peak implosion current of 2.7 MA. In comparison with our previous experiments with triple-shell deuterium gas-puff, the neutron yield increased by an order of magnitude. In the high yield shots, the neutrons with energies up to 15 and 22 MeV were registered by the TOF detectors in the radial and axial directions, respectively. A stack of CR-39 detectors registered up to 51 MeV deuterons (or up to 38 MeV protons) on the z-pinch axis. The observed neutron spectra can be explained by a suprathermal distribution of deuterons with the high energy tail  $f(E_d) \propto E_d^{-1.8}$ . The experimental data suggest that the high neutron yields were caused not only by higher energies of deuterons but also by their magnetization inside plasmas. The reached neutron yield of  $(2.9 \pm 0.3) \times 10^{12}$  neutrons means that the scaling law of deuterium z-pinch  $Y_n \propto I^4$  was extended to 3 MA currents.

<sup>1</sup> This work was supported by the IHCE SB RAS State Task No. 13.1.4, by the RFBR (Project No. 13-08-00479-a), by the Program for Basic Research of the Presidium of RAS "Fundamental problems of pulsed high-current electronics", by the MES RF (Project No. 2.1704.2011), by the GACR (Grant No. P205/12/0454), by the MSMT (Project Nos. LH 13283 and LG 13029), and by the IAEA (Grant No. RC 17088).

### 3D MHD SIMULATION OF CAPILLARY DISCHARGE FOR THE BELLA PROJECT<sup>1</sup>

*G.A. BAGDASAROV\**, *P.V. SASOROV\**, *O.G. OLKHOVSKAYA\**, *S. S. BULANOV\*\**, *C. G. R. GEDDES\*\*\**, *H.-S. MAO\*\*\**,

*C. B. SCHROEDER\*\*\**, *E. ESAREY\*\*\** and *W. P. LEEMANS\*\*\**

\*KIAM RAS, Miuskaya sq., 4, Moscow, 125047, Russia, gennadiy3.14@gmail.com, +7 499 978-13-14

\*\*University of California, Berkeley, California 94720, USA

\*\*\*Lawrence Berkeley National Laboratory, Berkeley, California 94720, USA

The project BELLA (LBNL, USA) is aimed to create an experimental facility for further advancing the development of laser-driven electron acceleration [1]. BELLA's unique attribute is the ability to use laser light to accelerate an electron beam up to 10 GeV level in a comparatively short distance of approximately one meter. The acceleration takes place during the propagation of a high power femtosecond laser pulse in the plasma formed in a capillary discharge. This capillary plasma forms a plasma channel able to guide the laser pulse, which in its turn forms a plasma wake wave that accelerates the injected electrons.

To achieve a good coupling of a laser pulse with the capillary wave guide it is necessary to have a tool for the simulation of a 3D electron distribution inside the capillary, near the open ends of the capillary as well as near the channels supplying neutral hydrogen into the capillary.

We use the MARPLE3D code [2] to perform such simulations. MARPLE3D is an Eulerian numerical tool designed for simulations of radiative magnetohydrodynamic (MHD) problems related to experiments with magnetically driven high energy density plasmas. Here we discuss two types of numerically investigated problems.

First, we simulate the 3D process of the capillary filling with a cold hydrogen before the discharge is fired through the side supply channels. The main goal of this simulation is to get a spatial distribution of the filling gas in the region near the open ends of the capillary. The real geometry is used for this and the next stage simulations, including the insulators, the supplying channels as well as the electrodes.

Our second, the main stage, is the 3D MHD simulation of the capillary discharge. Its main goal is obtaining a time-dependent spatial distribution of an electron density near the open ends of the capillary as well as inside the capillary. The simulation of the 1<sup>st</sup> stage determines the initial hydrogen density distribution for the capillary discharge simulation.

Main results of the simulations of two types will be presented at the conference.

#### REFERENCES

- [1] *W. P. Leemans et al.* // AIP Conf. Proc. – 2010 – 3. p. 1299.
- [2] *V. A. Gasilov et al.* // IOS Press, Series “Advances in parallel Computing” – 2012 – 22. pp. 235-242.

<sup>1</sup> This work was supported by the Office of Science of the US DOE under Contract No. DE-AC02-05CH11231 and by the RFBR, grant № 14-01-31154.

## CONVERGING SHOCK WAVES GENERATED BY UNDERWATER ELECTRICAL EXPLOSION OF SPHERICAL WIRE ARRAY

*O. ANTONOV, S. EFIMOV, M. KOZLOV, V. T. GUROVICH, Y. E. KRASIK*

*Physics Department, Technion, Haifa 32000, Israel; fnkrasik@physics.technion.ac.il; 972-4-8293559*

The results of experimental studies of a converging shock wave generated by underwater electrical explosion of a spherical wire array are reported. Two high-current generators, sub-microsecond ( $\sim 350$  ns rise time and  $\sim 550$  kA current amplitude) and microsecond ( $\sim 1.1$   $\mu$ s rise time and  $\sim 300$  kA current amplitude) timescale were used for wire array explosion. In the latter case, addition energy was transferred to the water flow by the imploding wire array due to the global pressure of the discharge current. In experiments, power and spectrum of self-light emission from an optical fiber, deformation of a copper tube and visible spectroscopy were measured to estimate the symmetry of the convergence. The results obtained were compared to the results of one dimensional hydrodynamic simulation, coupled with equation of states of water. The comparison showed that the shock wave keeps its uniformity along the major part of the convergence towards the implosion origin. The latter allows one to consider generation of water in extreme conditions ( $\sim 6 \cdot 10^{12}$  Pa,  $\sim 17$  eV,  $\sim 8$  g/cm<sup>3</sup>) [1,2] in the vicinity of the implosion origin.

The results of two-dimensional hydrodynamic simulations of the dynamics and stability of azimuthal non-uniformities in converging shock waves generated by an underwater explosion of a cylindrical wire array and their effect on the cumulation of energy in the vicinity of the converging axis will be presented as well [3]. It has been shown that in spite of the fact that such non-uniformities are always weakly unstable, for a broad range of experimentally relevant regimes these non-uniformities remain small and do not significantly affect the cumulation of energy. Only the non-uniformities with wavelengths comparable to the distance from the axis of convergence exhibit substantial growth that considerably attenuates the energy cumulation.

### REFERENCES

- [1] *O. Antonov, L. Gilburd, S. Efimov, G. Bazalitski, V. Tz. Gurovich, and Ya. E. Krasik*//Phys. Plasma – 2012 – 19 – №.102702-5.
- [2] *O. Antonov, S. Efimov, D. Yanuka, M. Kozlov, V. Tz. Gurovich, and Ya. E. Krasik*// Appl. Phys. Lett.– 2013 – 102–№.124104-6.
- [3] *M. Kozlov, V. Tz. Gurovich, and Ya. E. Krasik* // Phys. of Plasmas – 2013 – 20 – №.112701-6.

**MAGNETIC PROBE DIAGNOSTICS IN POWERFUL HIGH PRESSURE DISCHARGE<sup>1</sup>**

*M.E. PINCHUK*\* \*\*, *A.V. BUDIN*\*, *V.V. LEONT'EV*\*, *A.G. LEKS*\*,  
*A.A. BOGOMAZ*\*, *PH.G. RUTBERG*\*, *A.A. POZUBENKOV*\*

\**Institute for Electrophysics and Electric Power of Russian Academy of Sciences (IEE RAS),  
Dvortsovaya nab., 18, St.-Petersburg, 191186, Russia, [pinchme@mail.ru](mailto:pinchme@mail.ru), +7-812-315-17-57*

\*\**St.-Petersburg State Polytechnic University  
Polytechnicheskaya ul., 29, St.-Petersburg, 195251, Russia, [pinchme@mail.ru](mailto:pinchme@mail.ru)*

Experiments with magnetic probe diagnostics in gas discharge with current amplitude up to 1.2 MA, current rise rate  $\sim 10^{10}$  A/s, and at initial pressure up to 30 MPa were carried out. Previous experiment data with current up to 0.5 MA and energy input up to 100 kJ had been presented in [1]. Discharge was initiated by copper wire explosion. Discharge chamber was designed with axisymmetric geometry. Capacity of energy storage was changed. It was 1.2, 2.4 or 4.8 mF. Charging voltage was varied from 1 kV to 15 kV. Energy input was up to 300 kJ. The original construction of magnetic probe, working in condition of high current high pressure discharge with extreme heat and shock load, had been designed and created. Operation testing of magnetic probe under this parameters had been performed. Measurements of current density distribution had been carried out. According to the experiments the current channel radius was reduced with increasing initial gas density. The discharge channel was localized around the axis of discharge chamber. The channel radius was not exceeding 10 mm for investigated pressure and current ranges.

## REFERENCES

- [1] *M.E. Pinchuk, A.V. Budin, V.V. Leont'ev, A.G. Leks, A.A. Bogomaz, Ph.G. Rutberg, A.A. Pozubekov // Physics of Extreme States of Matter, IPSP RAS, Chernogolovka, 2014, pp. 189-192.*

<sup>1</sup> The work is partially supported by Russian Foundation for Basic Research (grant 12-08-01062-a).

## THERMODYNAMIC PROPERTIES AND PHASE CHANGES OF REFRACTORY METALS UNDER PULSED POWER INFLUENCES

*K.V. KHISHCHENKO*

*Joint Institute for High Temperatures RAS, Moscow, Izhorskaya st. 13 Bd.2, 125412, Russia, konst@ihed.ras.ru*

The adequacy of description of the thermodynamic properties and phase changes of materials is important for simulations of processes in condensed media under pulsed power influences, specifically such as an electrical explosion of conductors [1]. In this work, a semiempirical equations-of-state model with taking into account polymorphic phase transformations, melting and evaporation is proposed. Multiphase equations of state for three refractory metals (hafnium, tantalum and tungsten) are presented. As distinct from the previously obtained equations of state for the metals [2], a new form of expressions of the individual terms of the thermodynamic potential Helmholtz free energy is developed. It takes greater account of the thermal contribution of atoms in the liquid phase as well as the melting effect. A critical analysis of calculated results is made in comparison with available data from experiments with shock wave loading, isentropic release and high current pulsed heating.

### REFERENCES

- [1] *Lebedev S.V. and Savvatimskiy // A.I. Sov. Phys. Uspekhi, v. 27, pp. 749-771 (1984).*
- [2] *Fortov V.E., Khishchenko K.V., Levashov P.R. and Lomonosov I.V. // Nucl. Instr. Meth. Phys. Res. A, v. 415, pp. 604-608 (1998).*



## BASIC PHENOMENA IN PLASMA OPENING SWITCHES

*S.V. LOGINOV*

*Institute of High Current Electronics SB RAS, 2/3 Akademicheskoy ave., Tomsk, 634055, Russia, loginov@oit.hcei.tsc.ru*

The plasma opening switches (POSs) have been proven to be efficient for interruption of nanosecond megaampere current pulses and energy delivery to a load with substantial pulse compression [1]. This stimulates the research to increase the energy characteristics of generators with an inductive energy store and a plasma opening switch. The concept of power enhancement is pursued through creation of megajoule facilities with megaampere current and microsecond rise time. However, the attempts to use the successful experience of nanosecond POSs in the microsecond range fail to live up to expectations. At the same primary store energy and current, a tenfold increase in the conduction time of a microsecond switch compared to that of a nanosecond switch involves a proportional increase in the time of energy delivery to the load and hence a decrease in pulse power. This negative tendency requires comprehensive studies to elucidate the dynamics of the processes occurring in plasma opening switches.

The report summarizes the up-to-date understanding of the POS operation. Sections 1 and 2 discuss the mechanism of current flow and cutoff in nanosecond and microsecond switches [2, 3].

Section 3 proposes a technique to determine the parameters of a microsecond switch. Given the quantity  $\dot{I}$  (the rate of rise of the conduction current), the parameters of a microsecond POS with plasma aggregation can be determined reasoning from three conditions. The first condition,  $j_{mp}(t_0) \geq j_{sat}$ , requires that the current density at the downstream plasma edge in the magnetic piston plane be higher than the saturation current density. This condition defines the least possible plasma density  $n_m$  at which erosion can begin. The second condition,  $j(t^*) \leq j_{sat}$ , defines the cathode radius  $r_{cm}$  at which no erosion occurs up to the point in time  $t^*$ , when the current channel width compares with the diffusion depth. The third condition,  $l = \eta_{sh} a t_0^2 / 2$  ( $a$  is the piston acceleration,  $\eta_{sh} \approx 1.16$ ) defines the plasma length that provides the desired duration of the conduction phase.

Section 4 generalizes the switch voltage scaling arising on current interruption. In switches with low-density plasma, the conduction current  $I_c \propto n$  and the voltage depends linearly on  $I_c$ . With higher plasma density,  $I_c \propto n^{1/4}$  and the voltage is inversely proportional to  $I_c$ . The change in the scaling is due to a different mechanism of magnetic field penetration. The onset of rarefied plasma erosion occurs almost at the beginning of the current pulse, whereas the increase in plasma density precludes the erosion throughout the conduction phase and reduces the plasma dynamics to aggregation. As a result, the conditions for erosion can be attained only when the current channel reaches the downstream plasma edge and the plasma length decreases to a value insufficient for bipolar current flow. The inversely proportional dependence  $U_s(I_c)$  suggests that the tasks to increase the conduction time and to attain high resistance on current cutoff are contradictory. This is a logical consequence of the necessity for increasing the plasma density to provide the desired current with a microsecond rise time.

Section 5 is concluding remarks: this report gives a rational approach to clarify the mechanisms of current flow and cutoff in nanosecond and microsecond plasma opening switches. In the approach, there is no need to appeal to artificial solutions like, for example, convective magnetic field transport by electron flows against immobile ions [4]. It is also unreasonable to assume that the current during the conduction phase increases uniformly lengthwise the plasma and that the ion extraction on opening of the switch is amplified throughout the initial plasma length [5]. Such artificial solutions and assumptions ignore an important problem of magnetic field transport through fully ionized plasma.

### REFERENCES

- [1] Weber B.W., Comisso R.J., Goodrich P.J., et al. // IEEE Trans. Plasma Sci. – 1991. – Vol. 19. – № 5. – pp. 757–766.
- [2] Loginov S.V. // Phys. Plasmas. – 2011. – Vol. 18. – № 10. – p. 102104 (6 pp.).
- [3] Loginov S.V. // J. Plasma Phys. – 2013. – Vol. 79. – № 3. – pp. 321–326.
- [4] Kingsep A.S., Mokhov Yu.V., Chukbar K.V. // Sov. J. Plasma Phys. – 1984. – Vol. 10. – № 4. – pp. 495–498.
- [5] Ottinger P.F., Goldstein, S.A., Meger R.A. // J. Appl. Phys. – 1984. – Vol. 56. – № 3. – pp. 774–784.

## TOWARDS UNDERSTANDING OF ELECTRODYNAMIC PROCESSES OF PLASMA CHANNEL FORMATION DURING THE ELECTROMAGNETIC PULSE WITH PICOSECOND FRONT PROPAGATION ALONG THE COAXIAL LINE CONTAINING AN OPEN-ENDED OR MICROWIRE-ENCLOSED GAP<sup>1</sup>

*N.B. VOLKOV\**, *S.V. BARAKHVESTOV\**, *K.A. NAGAYEV\**, *S. I. TKACHENKO\*\**

*\*Institute of Electrophysics UB RAS, Amundsen Street, 106, Yekaterinburg, 620106, Russia, nbv@iep.uran.ru, +7(343)2678660*

*\*\*Moscow Institute of Physics and Technology, Institutsky pereulok, 9, Dolgoprudny MR, 141700, Russia*

The objective of the present paper is experimental investigation of the electrodynamic processes role in formation of the plasma channel during the electromagnetic pulse (EMP) having picosecond front propagation along the coaxial line containing in the central core the 5–15 mm long gap, being either open-ended or enclosed with microwires of Cu ( $d = 20\text{--}300\ \mu\text{m}$ ), W ( $d = 24.5\text{--}100\ \mu\text{m}$ ), amorphous alloy FeSiB ( $d = 100\ \mu\text{m}$ ) and carbon (fiber bunch of total diameter  $d = 100\ \mu\text{m}$ ). For the electromagnetic pulse formation we used the high-voltage pulse generator (HVPG) RADAN-220 (self-surge impedance  $Z_w = 50\ \Omega$  and energy  $w = 1\ \text{J}$ ), that was discharged to the 15 cm long and 10 cm in diameter inhomogeneous coaxial line. The HVPG charging voltage was  $U_0 = 220\ \text{kV}$ , EMP front duration  $\tau_f = 200\text{--}500\ \text{ps}$  (voltage-rise-rate  $\sim 1\ \text{MV/ns}$ ). Pressure in the line varied from  $10^{-4}$  to 760 Torr. The voltage at the chamber input was measured via the capacitance divider placed into the vacuum oil. The current at the end of the line was measured via the coaxial shunt, having  $R_{sh} = 0.4\ \Omega$  resistance and 5 GHz bandwidth. For the transversal currents, caused by the volume charge variations and charged particles flows from the discharge channel, measurements the Faraday cup, staying unscreened or being shielded with 1 cm thick organic glass plate, was used. Signals from shunt, divider and Faraday cup were logged via the Tektronix digital oscilloscopes with bandwidths of 0.5, 1 and 4 GHz. Also the discharge channel self-glowing integral images were taken via DSLR cameras Canon 450D and Canon 5D Mark II, and its space-time characteristics were investigated via streak-cameras AGAT SF-3M and Cordin-173 and coaxial photodiode PEC-22SPU-M. The integral spectrum and its continuous streak were obtained via MS 257 spectrograph and Cordin-173streak-camera correspondingly.

On both the experimental and the computer simulations basis it was shown that wave electrodynamic processes act the essential part in plasma channel formation during the high-voltage source with  $\sim 1\ \text{MV/ns}$  voltage-rise-rate discharge to the coaxial line containing an inter-electrode gap, being either open-ended or enclosed with microwires of various materials. We established that the current first half-wave, registered with oscilloscopes with various bandwidths, has qualitative and quantitative characteristics that are almost independent of the microwires material or diameter. The transversal current was measured via the Faraday cup staying unscreened or being shielded with the organic glass plate. It was established that during the first 50 ns the current is defined by both voltage temporal evolution and plasma channel volume charge variations; and at times greater than 500 ns – by the particles flows from the plasma. Charged particles from the plasma channel, generated during the HVPG discharge to the coaxial line containing open-ended air gap, flows absence was registered. The transversal current curves, acquired in experiments with either open-ended or wire-enclosed air gap for both unscreened and shielded faraday cup, comparison shows that current acquired at later times is defined by flows of charged particles from the expanding plasma, as a result of electrical explosion either of entire micron diameter conductor or just of its surface layer.

<sup>1</sup> This work was supported by the RFBR (projects No. 13-08-00266-a and No. 14-08-31024-mol\_a) and FASO within the Presidium of Russian Academy of Sciences fundamental research program (UB RAS project No. 12-P-1005, state registration No. 01201266835).

**NEUTRON PRODUCTION IN DEUTERIUM GAS-PUFF LINER IMPLOSIONS***S.A.SOROKIN*

*Institute of High Current Electronics SB RAS, 2/3 Akademichesky Ave., Tomsk 634055, Russia,  
E-mail: s.sorokin@rambler.ru, Phone: +7(382-2) 492322*

Experiments with deuterium gas-puff liner implosions have been performed on the MIG generator (1 MV, 1.5 MA, 80 ns). Single shell and double shell liners with different initial radii were imploded to generate DD fusion neutrons. A helical current return was used in some of shots to stabilize the liner implosions. The neutron yield was not raised by changing the implosion velocity from  $6 \cdot 10^7$  cm/s to  $1 \cdot 10^8$  cm/s, but it was increased from  $(1-5) \cdot 10^9$  for the single shell shots to  $(1-3) \cdot 10^{10}$  for the double shell shots. The neutron yields of  $(1-3) \cdot 10^{10}$  with a straight current return and  $(2-5) \cdot 10^9$  with a helical current return were measured. The results of the experiments reconfirm that the neutrons produced in deuterium liner implosions have not thermonuclear origin, but are generated by a beam-target mechanism in constrictions formed as a result of  $m=0$  instability developing.

## EXPERIMENTS ON THE COMPRESSION OF METAL-PUFF Z-PINCHES ON GENERATOR MIG WITH CURRENT LEVEL UP TO 2.3 MA<sup>1</sup>

*A.G. ROUSSKIKH\**, *A.S. ZHIGALIN\**, *R.B. BAKSHT\*\**, *N.A. LABETSKAYA\**, *S.A. CHAIKOVASKII\**, *V. I. ORESHKIN\**, *YU.A. SUKOVATICIN\**, *E.N. VOLKOV\**

\* *Institute of High Current Electronics, Siberian Division, 634055 Tomsk, Russia.*

\*\* *Tel Aviv University, Laboratory of electric discharges and plasmas, Tel Aviv, Israel.*

Two experimental test sets on the compression of metal-puff Z-pinches [1-3] were carried out on generator MIG at  $I \approx 2.3$  MA and  $t \approx 80$  ns. The first set has been devoted to the study of the Al metal-puff Z-pinches. The second set was devoted to the study of the Bi metal-puff Z-pinches. The main objective of these experiments is the optimization of the plasma shell formation assemblies from the point of view a radiation yield. Namely, we varied a collimator configuration via which forms the plasma shell, the amplitude and rise time of the plasma gun current, and the initial diameter of the plasma shell. To measure the K-shell Al radiation power, a pinhole camera and Diamond Radiation Detector (DRD) filtered with 18- $\mu$ m-thick polypropylene film and were used. We recorded also the integrated energy radiation (nickel bolometer) and the integrated radiation power (XRD with Al and Cu cathodes). The metal puffs were produced by plasma guns powered by a capacitive power supply with quarter period rise time  $T_{\text{gun}}/4 = 7 - 10$   $\mu$ s. The amplitude of current  $I_g$  carried by the plasma guns was 40 - 55 kA. The time  $t_{\text{del}}$  between the operation of the plasma guns and the operation of the MIG generator was controlled by using a delay generator;  $t_{\text{del}} = 9 - 12$   $\mu$ s. Based on the analysis of the results and comparison of experimental data with simulation the recommendations on metal-puff Z-pinches optimization were given.

### REFERENCES

- [1] A.G. Rousskikh, A.S. Zhigalin, V.I. Oreshkin, S.A. Chaikovsky, N.A. Labetskaya, and R.B. Baksht // *Phys. Plasmas*. – 2011. – Volume **18**. – p.092707.
- [2] A.G. Rousskikh, R.B. Baksht, A.S. Zhigalin, V.I. Oreshkin, S.A. Chaikovsky, and N.A. Labetskaya // *Plasma Phys. Rep.* – 2012. – Volume **38**. – p.651.
- [3] R.B. Baksht, A.G. Rousskikh, A.S. Zhigalin, and V.I. Oreshkin // *IEEE Trans. Plasma Sci.* –2013. – Volume **41**. – p.182.

<sup>1</sup> The work was supported in part by the Russian Foundation for Basic Researches under Grants # 14-02-00382-a.

## PRELIMINARY RESULTS FOR THE USE OF COUNTER PLASMA JETS FOR CREATION OF QUASISPHERICAL LINER<sup>1</sup>

A.G. ROUSSKIKH<sup>\*</sup>, A.S. ZHIGALIN<sup>\*</sup>, R.B. BAKSHT<sup>\*\*</sup>, N.A. LABETSKAYA<sup>\*</sup>, S.A. CHAIKOVASKII<sup>\*</sup>, V. I. ORESHKIN<sup>\*</sup>

<sup>\*</sup> *Institute of High Current Electronics, Siberian Division, 634055 Tomsk, Russia.*

<sup>\*\*</sup> *Tel Aviv University, Laboratory of electric discharges and plasmas, Tel Aviv, Israel.*

Implosion of quasispherical liner is one of direction of the fast Z pinch study [1]. We carried out the experiments to create a quasispherical liner based on metal-puff technology. For this goal we used two counter metal plasma jets. We used the system of the vacuum arcs located at the two opposite electrodes (ground and high-voltage electrodes). Profiling plasma flow radially was performed due to: a) the selection of the geometry and shape of the collimator of the plasma source and its location relative to the axis of the system, b) the selection of a ratio of the liner length to the initial radius of the expanding plasma. The amplitude of current carried by the vacuum arcs varied in the range 40-100 kA. Rise time of the arc current varied within 0.5 - 6 microseconds. Experimental study of the spatial distribution of the density in the central part of the electrode gap is presented. To determine the distribution of matter in the colliding plasma flows, we used X-ray radiograph based on X-pinch. In this experiment, we measured also the current (by a Rogowski coil), the voltage V (by active voltage divider), and the current derivative (by B-dot probe). Based on the analysis of the results, the recommendations on creation of a quasispherical liner based on metal-puff technology were made.

### REFERENCES

- [1] V.V. Aleksandrov, G.S. Volkov, E.V. Grabovski, A.N. Gribov, A.N. Gritsuk, Ya.N. Laukhin, K.N. Mitrofanov, G.M. Oleinik, P.V. Sasorov, I.N. Frolov // *Plasma Physics Reports*. – April 2012. – Volume 38. – Issue 4. – pp 315-337.

<sup>1</sup> The work was supported in part by the Russian Foundation for Basic Researches under Grants # 14-02-00382-a.

## INVESTIGATION OF FOIL MATERIAL INFLUENCE ON UNIFORMITY OF ELECTRICAL EXPLOSION

*A.V. PAVLENKO, A.N. GRIGORIEV, E.I. KARNAUKHOV*

*\*RFNC - Institute of Technical Physics, 13 Vasilieva street, Snizhinsk, 456776, Russia, alex\_nick@mail.ru*

Temporal waveforms of pressure amplitude in central and peripheral regions of a flat electrically exploded foil (copper M1, aluminum AD1M, brass L63, nickel alloy 80NCS, titanium VT1-00 and lead) have been measured. The measurements were performed using quartz pressure sensors arranged on the free surface of a dielectric substrate glued to the foil.

The coefficient of pressure heterogeneity and difference in explosion time for different foil material were defined. It is shown, the foil electrical resistivity is an important parameter that influence on foil explosion uniformity and difference in time of explosion. In addition to foil resistivity, the input specific energy, size and thickness of a foil also affects on foil explosion uniformity and difference in time of explosion.

## MECHANISM OF THE CURRENT QUENCHING IN HIGH-CURRENT LOW-PRESSURE PULSED GLOW DISCHARGE<sup>1</sup>

*N.V. LANDL\**, *YU.D. KOROLEV\*\*\**, *O.B FRANTS\**, *I.A. SHEMYAKIN\**, *V.G. GEYMAN\**

*\*Institute of High Current Electronics, Akademicheskoy Ave. 2/3, Tomsk, 634055, Russia, [landl@lnp.hcei.tsc.ru](mailto:landl@lnp.hcei.tsc.ru)*

*\*\*National Research Tomsk Polytechnic University, Lenin Ave., 30, Tomsk, 634050, Russian Federation*

The quenching of a pulsed current is characteristic of variety types of low pressure and vacuum discharges. The effect was observed in many experiments where the discharges in pseudospark switches, in hydrogen thyratrons, in plasma-filled diodes and the like were investigated [1-3]. For the conditions of the current quenching the current waveform has not a smooth shape but at a certain instant of time, a sharp decrease in current and the inductive voltage kick at the gap are observed.

It is understandable that a sharp decrease in current appears in a situation when a certain discharge region is not able to pass a current that is requested by external electric circuit. In other words, a bottleneck with an enhanced resistance abruptly appears in gas-discharge gap. Depending on a type of discharge, different physical mechanisms for interpretation of the current quenching have been proposed [2-4]. As applied to the discharge in thyratrons and pseudospark switches at least two alternative approaches are used.

One approach is based on the supposition that the hollow cathode region (or grid-anode region in the thyratron) is not able to carry an extremely high current density [2]. The other types of interpretation appeal to magnetic compression of the plasma column as a physical reason of quenching. According to this approach the plasma column can be compressed so fast and to such a small diameter that the inductive of the column starts suppressing the rise in the discharge current [4]. However, in [5] we had demonstrated that, in the pseudospark discharge, the phenomenon of magnetic compression of the plasma column could not be responsible for the quenching. One of the arguments in support of this conclusion was observation of an electron beam at the discharge axis during the development of the quenching process.

On the other hand, the experimental data [5] definitely show that during the process of current quenching the visible double electric layer between the negative glow and positive column plasma becomes noticeable at the short-exposition frames. In the regimes when the quenching is expressed most distinctively, length of the double electric layer becomes comparable with a gap distance, i.e. the positive column region practically disappears. The results of observation with temporal and spatial resolution allow us to conclude that the positive column region rather than the bore hole area is responsible for current quenching phenomenon.

The subject of this paper relates to the high-current low-pressure pulsed glow discharges with hollow cathode or the pseudospark discharge. The mechanism of the current passage at the high-current stages is considered. The discharge is treated as a self-organizing system that is able to rearrange itself to provide the current requested by external electric circuit. The principal discharge regions are the hollow-cathode plasma, the positive column plasma and the double electric layer that separates these plasma regions. In the model, the so-called generalized secondary emission coefficient [6] is used.

According to the model, the current quenching effect is determined by the processes in positive column plasma. Starting from a certain critical current a growth in positive column plasma density is not able to follow up the current rise in external circuit. Then the negative potential barrier near the anode is destroyed, and the region between hollow-cathode plasma and anode turns into a vacuum diode with ion neutralization. Resistance of this part of the gap is sharply enhanced and the external current decreases abruptly.

### REFERENCES

- [1] *Y.D. Korolev and K. Frank // IEEE Trans. Plasma Sci. 1999. – Vol. 25. – No. 5. – pp. 1525-1537.*
- [2] *T. Mehr, R. Tkotz, J. Stenzenberger, G. Hintz, J. Christiansen, P. Felsner, K. Frank, and M. Stetter // J. Appl. Phys. – 1995. – Vol. 79. – No. 2. – pp. 625-630.*
- [3] *M. Stetter, P. Felsner et.al // IEEE Trans. Plasma Sci. – 1995. – Vol. 23. – No. 3. – pp. 283-293*
- [4] *K. Bergmann, G. Schriever, O. Rosier, M. Muller, W. Neff, R. Lebert // Appl. Optics. – 1999. – Vol. 65 – pp. 5413 – 5417.*
- [5] *Yu. D. Korolev, O. B. Frants, V. G. Geyman, N. V. Landl, R. V. Ivashov, I. A. Shemyakin, R. E. Bischoff, K. Frank, and I. J. Petzenhauser // IEEE Trans. Plasma Sci. – 2005. – Vol. 29. – No. 5. – pp. 1648-1653*
- [6] *Y. D. Korolev, O. B. Frants, N. V. Landl, I. A. Shemyakin, and V. G. Geyman // IEEE Trans. Plasma Sci. – 2013. – Vol. 41. – No. 8. – pp. 2087–2096*

<sup>1</sup> This work was supported by the Russian Foundation for Basic Research under Grant 12-08-00360

## A LASER-INDUCED DISCHARGE THROUGH A VACUUM DIODE <sup>1</sup>

A. BOLDAREV\*, V. GASILOV\*, A. KRUKOVSKI\*, V. NOVIKOV\*, I. TSYGVINTSEV\*,  
O. OLKHOVSKAYA\*, I. ROMANOV\*\*

\* *Keldysh Institute of Applied Mathematics, Ac. Sci., Miusskaya sq., 4, 125047, Moscow, Russian Federation,*  
[vgasilov@keldysh.ru](mailto:vgasilov@keldysh.ru), +7(499)9723855

\*\* *Lebedev Physical Institute, Ac. Sci., Moscow, Russian Federation, Leninsky av., 53-4, 119333, Moscow, Russian Federation,*  
[laser.plasma@gmail.com](mailto:laser.plasma@gmail.com), +7(499)1326847

Studying the structure of microscopic pinches occurring in vacuum sparks is important in view of the development of new intense EUV radiation sources and ion sources with applications to nano-lithography, materials science, nuclear physics etc. To construct devices for new technologies it is important to know such source properties as its emissivity dependence on initial conditions of a spark ignition, the discharge chamber geometry, the foreplasma and the actual discharge plasma features. To date, laser-induced discharges have been experimentally investigated for a driver energy up to 25 J, current amplitude up to 27 kA, and the current rise rate about  $10^{11}$  A/s. In the experiments the laser pulse energy and power flux were varied in a rather wide range. It was found that the time required for a vacuum diode filling with a laser-produced plasmas was determined by a laser power acted on a cathode surface. The electric current characteristics depended on a mass amount of the cathode material ablated by the laser.

It was also found that there exist two regimes of a pinch development which are promising respecting its practical use:

- mode of a pinch forming at the forefront time of the current evolution (while the discharge is initiated by a low-level laser energy deposition), the pinch forming is followed by a beam of multiply charged ions generated at the cathode. This mode has the potential to be used for a deep ion implantation;
- mode of a pinch forming at the maximum current time (while the discharge is initiated by a high-level laser energy deposition). It is characterized by intensive light generation (e.g. a 13.5 nm wavelength radiation in the case of the tin cathode). This mode can be used for a design of new EUV radiation sources for lithographic systems.

Further studies of plasma properties corresponding to these modes can be successfully implemented only with a support of computer simulations which should be preceded by laboratory experiments.

In our presentation we discuss a mathematical model and a numerical analysis technique developed for simulations of processes occurring in a vacuum diode where an electrical current is induced by a laser pulse effect on a cathode surface. The model is 2D with respect to spatial variables. It describes the laser plasma "plume" forming, as well as magneto-hydrodynamic effects (pinching, etc.) caused by the electric current passage through the plasma. We also consider the results of the first computational experiments done via the developed model. Adjustment of the mathematical model with respect to known experimental data will make realistic a predictive modeling which will help to specify laser pulse parameters as well as the diode construction needed for various applications.

<sup>1</sup> The study was supported by RFBR under the grants No. 12-02-00708 and by the Mathematical department of RAS (The program of fundamental research, project N 3-3.6)



## MEASUREMENTS OF THE PLASMA PARAMETERS OF THE PSEUDOSPARK DISCHARGE<sup>1</sup>

*L.A. SHEMYAKIN\**, *Y.D. KOROLEV\**, *O.B. FRANTS\**, *N.V. LANDL\**

\* *Institute of High Current Electronics, Tomsk, 634055, Academichesky Ave, 2/3, Russian Federation, shemyakin@lnp.hcei.tsc.ru*

At present the pseudospark discharges are widely used in the high current switches with hollow cold cathode, installations for electrons and ions beams and EUV emission generations [1-3]. One of way investigation of this discharge deals with measurement of the plasma parameters as electron density and electron temperature [4]. This report focuses on a more detailed investigation of this issue. Most of experimental information is obtained due to spectroscopic luminosity investigations in the different discharge regions with high temporal and spatial resolution. The main attention is concentrated on the stages of dense and superdense glow discharges.

The discharge is initiated in a chamber which construction and electric circuit is shown schematically in Fig. 1. The general dimensions of the chamber are as follows: main gap space  $d = 4$  mm, thickness of the cathode and anode plate  $h = 4$  mm, diameter of the cathode aperture  $d_c = 3$  mm, diameter of the anode aperture  $d_a = 5$  mm. The main electrodes 1 and 2 were made of copper. The discharge is initiated in hydrogen at pressure  $p \approx (15 - 45)$  Pa. The main capacitor bank  $C_0 = 1.25$   $\mu$ F and the impedance of the electric circuit was approximately equal  $0.5$   $\Omega$ . The initial voltage on the gap,  $V_0$ , was about  $(1 - 2)$  kV. In this case the maximum value of current was approximately  $1.5$  kA. A static breakdown in the discharge chamber was investigated.

With use of lens 6, plasma image was reflected sharply to input slit of the optical multichannel analyzer or monochromator 7. Spatial scanning was realized by shift of the lens 6. The spectral range of the optical tract was  $300 - 830$  nm. There were a temporal resolution  $\Delta t = 2$  ns in the experiments. Usually two variants to register emission plasma were used. The emission of the cathode hole 3 (bore hole plasma) and the discharge column plasma 4 were recorded.

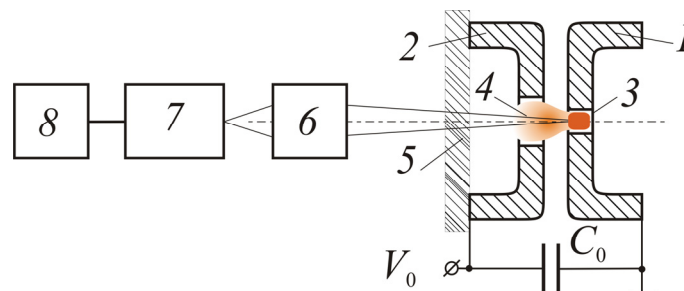


Fig. 1. Experimental setup: 1 – cathode, 2 – anode, 3 – bore hole plasma, 4 – discharge column plasma, 5 – quartz window, 6 – lens, 7 – optical multichannel analyzer or monochromator with photomultiplier, 8 – registration adaptor.

In the experiments there were a electron temperature  $T_e$  and electron density  $n_e$  measurement. The electron density was measured from  $H_\alpha$  and  $H_\beta$  Ballmer series hydrogen lines profile. In the stages of dense and superdense glow discharges and for different discharge areas the value of the electron density was  $n_e \approx 5 \cdot 10^{14} - 5 \cdot 10^{16}$   $\text{cm}^{-3}$ .

The electron temperature measurement was based on method of relative intensity of ion spectral lines to atom lines copper which appears in plasma spectra emission. For measurement the lines CuI 515,32 nm, CuI 521,82 nm and CuII 490,97 nm, CuII 493,16 nm were used. The correction of the  $T_e$  for nonequilibrium plasma of the pseudospark discharge was done. It was obtained, that during the stages of dense and superdense glow discharges the electron temperature of the column and bore hole plasma was  $(0,6 - 1,1)$  eV.

### REFERENCES

- [1] Frank K. and Christiansen J. // IEEE Trans. On Plasma Sci. – October 1989. – vol. 17 – no. 5 – P. 748.
- [2] Bochkov V.D., Dyagilev V, Ushich V. et. all. / IEEE Trans. On Plasma Sci. – Oct. – 2001. – Vol. 29 – No. 5 – P. 802.
- [3] Bergmann K., Schriever G., Rosier O. et all. // Appl. Optics. – 1999. – vol. 65 – PP. 5413 – 5417.
- [4] Hartmann W. and Lins G. // IEEE Trans. On Plasma Sci. – 1993. – vol. 21 – no. 5 – PP. 506 – 510.

<sup>1</sup> This work was supported by Russian Foundation for Basic Research under Grant 12-024-00360

**DYNAMICS OF LARGE-SCALE INSTABILITIES IN CONDUCTORS ELECTRICALLY EXPLODED IN STRONG MAGNETIC FIELDS***I.M. DATSKO, C.A. CHAIKOVSKY, N.A. LABETSKAYA, V.I. ORESHKIN**Institute of High Current Electronics SB RAS, 2/3 Akademichesky Avenue, Tomsk, 634055, Russia*

Interest in the electrical explosion of conductors (EEC) is related to various applications, such as generation of superstrong magnetic fields, implosion of heavy metal liners, transmission of energy using vacuum transmission lines, etc. The current flow in an electrically exploded conductor can occur in three modes: a mode of uniform current distribution, a skin-effect mode, and a transient mode. The basic phenomena characteristic of EEC occurring in the skin current mode are a shock wave (SW) and a nonlinear magnetic diffusion wave (NMDW) propagating in the conductor, formation of low-temperature plasma at the conductor surface, and thermal instabilities. The nonlinear diffusion of the electromagnetic field into the conductor features anomalously high speed compared to conventional diffusion.

The growth of large-scale instabilities during the propagation of a nonlinear magnetic diffusion wave through a conductor was studied experimentally. The experiment was carried out with the MIG terawatt pulsed power generator at a peak current of up to 2.5 MA with 100 ns rise time. The diagnostic complex of the MIG consisted of Rogowski coils, magnetic probes, voltage dividers, vacuum x-ray diodes (XRD), and an HSFC Pro four-frame optical camera capable of shooting pictures with a minimum exposure time of 3 ns. The generator loads were cylindrical aluminum conductors 3 mm in diameter each consisting of a solid rod of diameter 3 mm and a hollow tube of the same diameter and wall thickness 250  $\mu\text{m}$ . With this diameter, the electric field strength at the conductor surface does not surpass the value at which plasma generation begins (and, hence, the temperature dependence of conductivity changes) throughout the pulse duration.

It was observed that instabilities with a wavelength of 150  $\mu\text{m}$  developed on the surface of the conductor hollow part within 160 ns after the onset of current flow, whereas the surface of the solid rod remained almost unperturbed. A set of equations describing the propagation of an NMDW through a conductor similar to that used in the experiment and the growth of thermal instabilities in the conductor was solved numerically. The solution has shown that in the hollow conductor, as the NMDW front arrives at the conductor internal boundary, a reflected NMDW is generated that propagates outward and reaches the external boundary within 160 ns, i.e. noticeably earlier than it reaches the solid part of the conductor. Thus, the growth of instabilities is evidently associated with the propagation of NMDW; hence, the development of thermal instabilities is the most probable stratification mechanism for exploding conductors of this type. It should be noted that in an exploded aluminum conductor of the same structure but smaller (2 mm) in diameter, when the surface field strength became greater than that at which plasma generation began, instabilities occurred and developed simultaneously over the hollow and the solid part of the conductor.

## RESEARCH OF DEPENDENCE OF IMPLOSION PARAMETERS FROM TYPES OF CONFIGURATIONS IN EXPERIMENTS WITH DEUTERIUM GASS PUFF ON A GIT-12 GENERATOR<sup>1</sup>

R.K.CHERDIZOV\*, F.I. FURSOV\*, V.A. KOKSHENEV\*, N.E. KURMAEV\*, A.YU. LABETSKY\*, A.V. SHISHLOV\*,  
D. KLIR\*\*, J. CIKHARDT\*\*, J. KRAVARIK\*\*, P. KUBES\*\*, K. REZAC\*\*, O. SILA\*\*

\* Institute of High Current Electronics SB RAS, 2/3 Akademichesky Ave., Tomsk, 634055, Russia  
E-mail: rustam.k.cherdizov@gmail.com

\*\*Czech Technical University in Prague, Faculty of Electrical Engineering, Technicka 2, 16627 Prague 6, Czech Republic

This article is devoted to research of changing parameters of implosion depending from types of gas-puff. The results of experiments with gas-puff for different types of configurations (triple deuterium shell configuration, deuterium gas-puff with outer plasma shell, deuterium gas-puff with outer neon shell) are presented. Experiments were carry out on the GIT-12 generator in 2012-2013. The dependence of the rate of compression of the pinch from the maximum current and mass of gas-puff for different configurations are researched. Another results was considered too. This experiments allowed compose a certain statistics of parameters from configuration and optimized load parameters.

---

<sup>1</sup> This work was supported by the IHCE SB RAS State Task No. 13.1.4, by the RFBR (Project No. 13-08-00479-a), by the Program for Basic Research of the Presidium of RAS "Fundamental problems of pulsed high-current electronics", by the GACR (Grant No. P205/12/0454), by the MSMT (Project Nos. LH 13283 and LG 13029), and by the IAEA (Grant No. RC 17088).

**DIFFUSION OF THE FAST RISING STRONG MAGNETIC FIELDS INTO THE CONDUCTOR<sup>1</sup>***N.A. LABETSKAYA, V.I. ORESHKIN, C.A. CHAIKOVSKY, I.M. DATSKO, N.I. KUSKOVA\*, A.D. RUD\*\***Institute of High Current Electronics SB RAS, 2/3 Akademichesky Avenue, Tomsk, 634055, Russia**\*Institute of Pulse Processes and Technologies of NAS of Ukraine, 43a Zhovtnevy Avenue, Mykolayiv, 54018, Ukraine**\*\*G.V. Kurdyumov Institute for Metal Physics of NAS of Ukraine, 36 Academician Vernadsky blvd., Kiev, 03680 Ukraine*

The processes of nonlinear diffusion of the magnetic field into a conductor and a plasma formation on the surface of a conductor in fast rising strong magnetic fields are very important for the efficiency of electromagnetic energy transport by the vacuum transmission line of pulsed power generators [1, 2] with a current amplitude of 50 MA and a rise time of 100÷200 ns.

An experimental study of nonlinear diffusion of the magnetic field into a conductor with the growth rate of the magnetic field up to  $3.5 \cdot 10^9$  T/s was carried out on MIG generator (current amplitude up to 2.5 MA, the current rise time  $\sim 100$  ns). Thin-walled metallic tubes with an external diameter of 3 mm were used as a load of the current generator. The wall thickness of the tubes was varied in the course of the experiments.

The velocity of nonlinear magnetic field diffusion was determined by measuring the instant, when the nonlinear diffusion wave reaches the inner surface of the tube. The experiments showed that at the growth rate of the magnetic field of  $(1 \div 3.5) \cdot 10^9$  T/s the wave front velocity of nonlinear magnetic field diffusion was  $(0.15 \div 0.5) \cdot 10^6$  cm/s.

## REFERENCES

- [1] W.A. Stygar, M.E. Cuneo, D.I. Headley, H.C. Ives, R.J. Leeper, M.G. Mazarakis, C.L. Olson, J.L. Porter, T.C. Wagoner, J.R. Woodworth // Phys.Rev. ST Accel. Beams. – 2007. – V.10. – P. 03040.
- [2] A.A. Kim, M.G. Mazarakis., V.A. Sinebryukhov B.M. Kovalchuk, V.A. Visir, S.N. Volkov, F. Bayol, A.N. Bastrikov, V.G. Durakov, S.V. Frolov, V.M. Alexeenko, D.H. McDaniel, W.E. Fowler, K. LeChien, C. Olson, W.A. Stygar, K.W. Struve, J. Porter, R.M. Gilgenbach // Phys.Rev. ST Accel. Beams. – 2009. – V.12. – P. 050402.

<sup>1</sup> This work was partially supported by the joint project of SB RAS - NAS of Ukraine (№ 03-09-12)

## ELECTRODE EROSION IN HIGH CURRENT HIGH PRESSURE ARCS

M.E. PINCHUK\* \*\*, O.M. STEPANOVA\*\*\*, N.K. KURAKINA\*, A.A. BOGOMAZ\*

\**Institute for Electrophysics and Electric Power of Russian Academy of Sciences (IEE RAS), Dvortsovaya nab., 18, St.-Petersburg, 191186, Russia, [pinchme@mail.ru](mailto:pinchme@mail.ru), +7-812-315-17-57*

\*\**St.-Petersburg State Polytechnic University*

*Polytechnicheskaya ul., 29, St.-Petersburg, 195251, Russia, [pinchme@mail.ru](mailto:pinchme@mail.ru)*

\*\*\**St.-Petersburg State University, Physical Faculty,*

*Ulyanovskaya, 3, St.Petersburg, 198504, Russia, [o.m.stepanova@spbu.ru](mailto:o.m.stepanova@spbu.ru)*

In the report, erosion data of electrode made from steel, tungsten and copper are presented for high current arcs with current amplitude of 10 kA–2 MA, discharge duration of 50–500  $\mu$ s at the initial gas pressure of 1 kPa–40 MPa. The specific erosion value achieves above  $10^{-2}$  g/C in such discharges. Wide ranges of discharge current and discharge duration provide the heat flux to the electrode from  $\sim 10^4$  to  $\sim 10^9$  W/cm<sup>2</sup>. Thus, it allows us to study the phenomenon of erosion associated with heat fluxes of specified values. Heat flux more than  $10^6$  W/cm<sup>2</sup> exposed to the electrode within about 50 microseconds exceeds the critical value corresponding to intense electrode evaporation, and it is an intense erosion jet formation condition. Electrode plasma jets play a major role in erosion processes in the arcs [1].

Erosion by symmetrical material ejections from the whole electrode butt-end surface was detected [2]. In the work, main mechanisms of electrode erosion have been discussed. The electrode jets influence on erosion. The amount of substance ejected from the electrode surface has been estimated. The experimental data and data from [3-5] have been compared with the data calculated by a simple model of electrode heat erosion.

### REFERENCES

- [1] A.A. Bogomaz, A.V. Budin, V.A. Kolikov, M.E. Pinchuk, A.A. Pozubenkov, Ph.G. Rutberg // Zh. Tekh. Fiz., 2002, v 72, n 1, pp 28-35 [Tech. Phys., 2002, v 47, pp 26-33].
- [2] A.A. Bogomaz, A.V. Budin, V.A. Kolikov, M.E. Pinchuk, A.A. Pozubenkov, Ph.G. Rutberg // Doklady Akademii Nauk, v 388, n 1, pp 37–40 [Doklady Physics, 2003, v 48, n 1, pp 1-4].
- [3] G.V. Butkevich, G.S. Belkin, N.A. Vedeshnikov, M.A. Znavoronkov, *Electric erosion high current contacts and electrodes, Moscow: Energy, 1978 (in Russian) [Electricheskaya erosiya sil'notochnih kontaktov I elektrodov, Moskva: Energiya, 1978]*
- [4] A. V. Budin, V. A. Kolikov and Ph. G. Rutberg // Zh. Tekhn. Phys., 2007, v 77, n 8, pp 49-53 [Technical Physics, 2007, v 52, n 8, pp 1011-1015].
- [5] M.E. Pinchuk, A.A. Bogomaz, A.V. Budin, S.Yu. Losev, A.A. Pozubenkov, Ph.G. Rutberg / 9<sup>th</sup> CMM Proceedings, Tomsk, Russia, September 21-26, 2008, pp. 713-716.

## HYBRID X-PINCH ON A SMALL SCALE GENERATOR KING<sup>1</sup>

*I.N.TILIKIN, T.A.SHELKOVENKO, S.A. CHAIKOVSKY, V.B. ZORIN,*

*V.M.ROMANOVA, A.R.MINGALEEV, S.N.MISHIN S.A.PIKUZ*

*\*P. N. Lebedev Physical Institute, 53 Leninskiy Pr., Moscow 119991, Russia*

A small-scale soft x-ray generator KING was developed at the Institute of High Current Electronics. The generator consists of a base unit, control system, vacuum system, air-drying system, and diagnostic equipment. The base unit includes a 1000-nF fast capacitor bank and a vacuum chamber with a load unit. The bank charge voltage is 30–50 kV. Current through load has about 180kA and rise time 200 ns with charge voltage 40kV. Generator KING was designed to work with different types of X-pinch as a load to produce radiation source that could be used for point projection radiography [1].

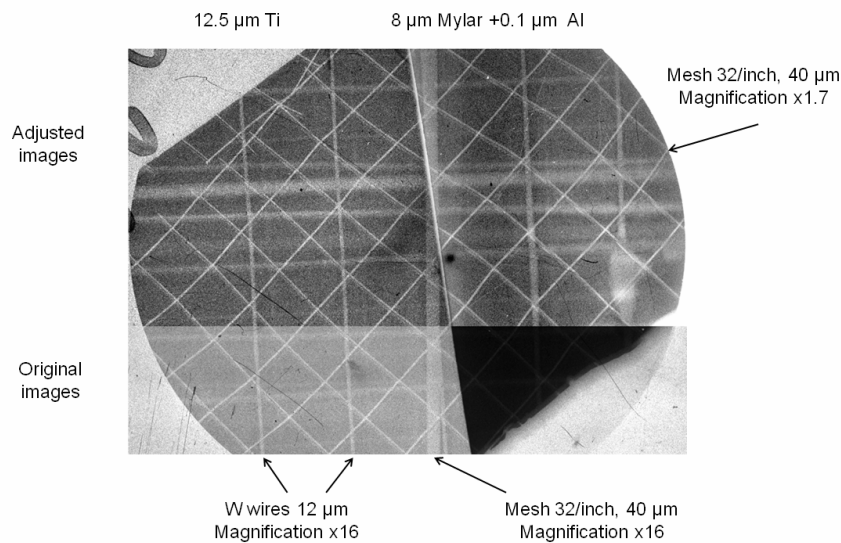


Fig. 1. Radiograph image of a test-object obtained in radiation of hybrid X pinch with Ag wire 25 microns diameter.

Hybrid X-pinch as a load was investigated on generator KING. It consists of two solid conic W electrodes with thin wire between electrodes [2]. Experiments showed that only Cu and Ag as wire materials could be used in hybrid X-pinches. Wire diameter should be 20-25 $\mu$ m and gap between electrodes around 2mm. As a diagnostics were installed PCD and Si-diode behind different filters for determination of radiation energy and timing of radiated pulses for different photon energy. Step wedge and pinhole camera were also used for detection of radiation in various photon energy. Radiograph imaging of test objects (small meshes with known period and wire diameters, W wires with known diameter) was used for determining of number of sources, intensity of each source and the source size. Spectrometer with convex CsAp crystal was used for measurement of the hybrid X pinch plasma parameters.

Experiments have showed that hybrid X-pinches could produce radiation source with size in scale of 1 micrometer with intense continuum radiation – hot spots. The hot spots could be used for point projection radiography and other applications (Fig.1). The hybrid X pinches have simpler configuration and less hard x-ray compare to standard multiwire X pinches, so using of the hybrid X-pinches could be more preferable for many applications.

### REFERENCES

- [1] Artyomov A. P., M. G. Bykova, S. A. Chaikovskiy et al. // Izvestiya vuzov. Physics. 2012. V.55. № 10/3, p.26-29.
- [2] T.A. Shelkovenko, S.A. Pikuz, S.N. Mishin et al. //Plasma Physics Reports, 2012, V 38, p.359-381

<sup>1</sup> This work was supported by RFBR grant 14-02-01206

## FORMATION OF SOLITONS UNDER CYCLOTRON RESONANCE INTERACTION OF SUPERRADIANCE PULSES AND CW SIGNALS WITH RECTILINEAR ELECTRON BEAMS<sup>1</sup>

*N.S. GINZBURG\**, *I.V. ZOTOVA\**, *A.S. SERGEEV\**, *E.R. KOCHAROVSKAYA\**, *V.YU. ZASLAVSKY\**

*A.G. SADYKOVA\*\**, *S.A. SHUNAILOV\*\**, *M.I. YALANDIN\*\**

\**Institute of Applied Physics RAS, 46 Ul'yanov St., N.Novgorod, 603950, Russia, ginzburg@appl.sci-nnov.ru, +78314164816*

\*\**Institute of Electrophysics, 106 Amundsen St., Ekaterinburg, 620016, Russia*

Development of short powerful electromagnetic pulse generator based on superradiance stimulates studies for further transformation of such pulses. These X and Ka bands pulses possess gigawatt power level and duration of 10-15 RF periods [1]. In this paper based on analogy to well known effect of self-induced transparency [2] of optical pulse propagating through passive (without inversion) two-level media we describe possibility of electromagnetic pulse self-compression under condition of cyclotron resonance absorption with counter propagating initially rectilinear electron beams. Actually in a certain area of parameters the initial electromagnetic pulse transforms into a soliton with amplitude and duration defined by its velocity. Similar to optics [2], the soliton formation can be accompanied by significant compression of initial electromagnetic pulse. Under the same condition the incident stationary signal can split into sequence of solitons with stable parameters. This effect can be used for modulations of intense CW radiation.

PIC-simulations of indicated effects were carried out with parameters close to planning experiments based on two synchronized high current accelerators RADAN. It was assumed that the signal is supplied to the interaction space from the collector side. Formation of soliton for the case of pulse input signal is shown in (Fig.1a). For the optimal case this process accompanied by essential compression of the input pulse. Fig.1b demonstrates the process of amplitude modulation of stationary input signal or a relatively long pulse under cyclotron resonance condition.

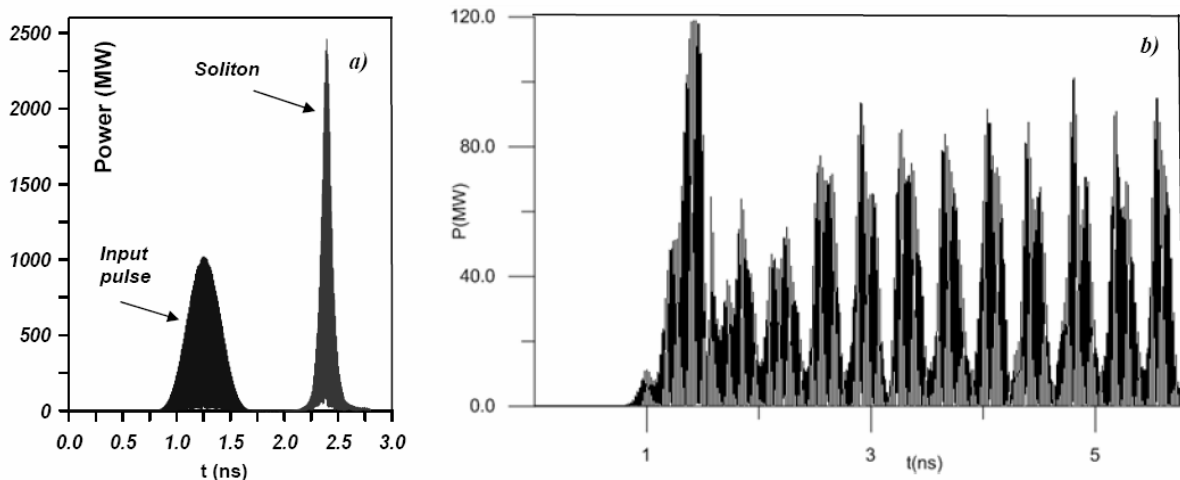


Fig. 1. (a) Formation of soliton accompanied by self-compression of input superradiance pulse. (b) Amplitude modulation of CW input signal with transformation into sequence of solitons.

### REFERENCES

- [1] *S.D. Korovin, A.A. Eltchaninov, V.V. Rostov, V.G. Shpak, M.I. Yalandin, N.S. Ginzburg, A.S. Sergeev, I.V. Zotova // Phys.Rev.E. – 2006. – V.74. – №1. 016501.*
- [2] *S.L. McCall, E.L. Hahn // Phys.Rev. – 1969. – V.183. – P.457–485016501.*

<sup>1</sup> This work was supported by Russian Fond of Fundamental Researches, grant 12-08-00628-a

## HALF-HORN AND STRIP-LINE ANTENNAS FOR MEASUREMENTS OF PULSES OF HIGH POWER ULTRA-WIDEBAND RADIATION

*V.M. FEDOROV, V.Y. OSTASHEV, V.P. TARAKANOV, A.V. UL'YNOV*

*Institute for High Energy Densities of JIHT of RAS,  
Izhorskaya 13/2, Moscow, 127412, Russia, +7(495)485-7944, [vmfedorov@ihed.ras.ru](mailto:vmfedorov@ihed.ras.ru)*

Abstract – Results of creation and diagnostics of the E-field sensors of the half-horn and strip-line antennas for electromagnetic traveling waves of high power pulses with ultra-wideband (UWB) frequency spectrum are presented in this article. The spectrum of the electromagnetic high power radiation occupies a frequency range out of 100 MHz up to 10 GHz. A creation of the effective high power pulse radiators is supposed reliable measurement of parameters of the radiators and the computer electromagnetic modeling of theirs. We use computer simulation of full electromagnetic numerical 3-D code of “KARAT” which allows calculate non stationary processing in real electro-dynamic systems. The  $E(t)$  electric fields in electromagnetic traveling waves (EMTW) were measured by different sensors. New E-field sensor of two-wire type has dielectric stalk with high  $\epsilon=16$  and small cross-section near  $1.5 \times 1.5 \text{ mm}^2$  and 40cm length. The sensor of electrical data were  $T_f=30\text{ps}$  time resolution and up to  $T_t=7\text{ns}$  pulse duration without distortions. Sensor tests were provided by experimentally with the TEM cell and computer simulation of full electromagnetic numerical 3-D code of “KARAT”. We have investigated the “classical” measurement antenna of a half-horn type. Pulsed resolution for the half-horn antennas are relatively narrow ( $T_t/T_f \ll 100$ ). The half-horn antennas have high dependence of the sensitivity for angle variation of wave fall directions in plane  $E$ -field.



## INFLUENCE OF THE DIFFRACTION REFLECTOR GEOMETRY ON THE MODE COMPOSITION IN THE AZIMUTHALLY NONUNIFORM MULTIWAVE CHERENKOV GENERATOR

*M. P. DEICHULY, V. I. KOSHELEV*

*Institute of High Current Electronics SB RAS, 2/3 Akademichesky Ave., Tomsk 634055, Russia  
E-mail: [koshelev@lhfe.hcei.tsc.ru](mailto:koshelev@lhfe.hcei.tsc.ru)*

In the paper [1] it is shown that the diffraction reflector used in the azimuthally nonuniform multiwave Cherenkov generator (MWCG) strongly effects the microwave radiation parameters. The position of the reflector relative to the slow-wave structure of MWCG is of great influence. At the same time, the influence of the diffraction reflector geometry on the generator operation has not been studied in detail.

The paper presents the numerical studies of the dependence of reflecting and transforming characteristics of the diffraction reflector on its geometrical parameters. It is shown that detuning of the upper frequency boundary of the non-transparency band in the reflector structure from the operating frequency of the generator has a strong influence on the transformation of modes in reflection. The results of calculations allow choosing the optimum geometry of the diffraction reflector in the azimuthally nonuniform MWCG for production of a linearly polarized wave beam.

### REFERENCES

- [1] *Deichuly M. P. and Koshelev V. I. // J. Commun. Technol. Electron. – 2013. – Vol. 58. - No. 8. P. 829-841.*

## ULTRAWIDEBAND RADIATORS SIMULATION IN HOMOGENEOUS LOSSY MEDIA<sup>1</sup>

*M. YU. ZORKALTSEVA, V. I. KOSHELEV, A. A. PETKUN*

*Institute of High Current Electronics SB RAS, Akademichesky Avenue 2/3, Tomsk, 634055, Russia,  
E-mail: fear2029@sibmail.com*

The paper presents a three-dimensional computer program based on the finite-difference time-domain method allowing simulating ultrawideband pulse radiation and obtaining antenna characteristics in the time and frequency domains. The program contains the libraries of the object-oriented modules written in Delphi. The program allows visualizing the distribution of the electromagnetic fields generated during simulation, getting the time dependences of the electromagnetic field components at any point in the computational domain, and saving them for post-processing. By means of the program one can analyze the spectra of the radiated and reflected pulses, plot the field hodograph curves at fixed points, get the diagrams of the field profiles in the set cross-section, and transform the fields to the far zone. To set the geometries of ultrawideband radiators, a separate program has been developed which allows specifying the cell arrays of metal objects [1].

Numerical simulation of ultrawideband radiators in a linear homogeneous medium has been carried out by means of the software developed. The geometry of the problem presented a three-dimensional parallelepiped filled with a medium which has permittivity  $\epsilon$  and conductivity  $\sigma$ . Fig. 1 shows the geometry of this problem. A hard source in the form of the resistive element, a soft source, and a one-dimensional virtual transmission line were used as the excitation sources for the antenna. In order to truncate the computational domain and to minimize reflections from the boundaries, the uniaxial perfectly matched layer was used. To determine the fields at large distances from the antenna, two independent algorithms for near-field to far-field transformation were used. One of them is based on Huygens principle, which requires the calculation of the electric  $\mathbf{J}_s(\mathbf{r}, t)$  and magnetic  $\mathbf{M}_s(\mathbf{r}, t)$  currents on a closed surface involving primary and secondary sources of the field. Another algorithm is based on the Kirhhoff integral representation and has a number of advantages compared with the Huygens principle. Firstly, the algorithm allows obtaining fields at any set distance from the radiator both in the near- and far-field zones. Secondly, to calculate any of the field components in the given direction out of Huygens surface, it is necessary to integrate the expression including the same field component that allows avoiding interpolation errors. In addition, all the field components can be computed independently from each other.

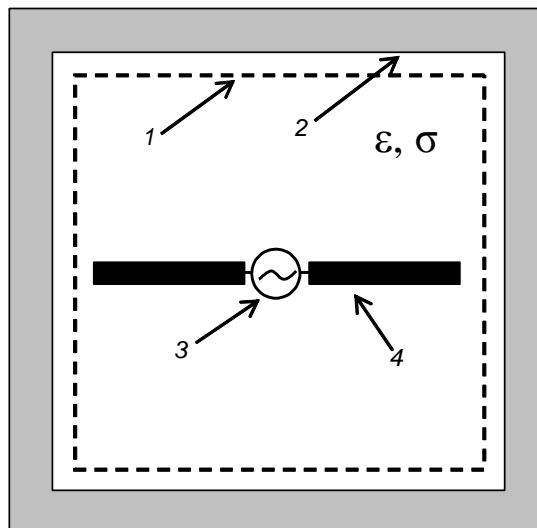


Fig. 1. Geometry of the problem for simulation of the radiators in a medium: 1 – Huygens surface, 2 – perfectly matched absorbing layer, 3 – excitation source for the antenna, 4 – transmitting antenna.

### REFERENCES

- [1] *Zorkaltseva M.Yu., Koshelev V.I., Petkun A.A.* // Russ. Phys. J. – 2013. – Vol. 56. – No. 8/2. P. 149-153.

<sup>1</sup> This work was supported by Russian Foundation for Basic Research, project № 13-08-98069-p\_Siberia\_a.

## PLASMA IN A RESONANT MICROWAVE PULSE COMPRESSOR: OBSERVATION, CHARACTERIZATION, AND INFLUENCE ON RADIATION EXTRACTION<sup>1</sup>

*A. SHLAPAKOVSKI\**, *L. BEILIN\**, *M. DONSKOY\**, *E. SCHAMILOGLU\*\**, *Y.E. KRASIK\**

*\*Physics Department, Technion, Haifa, 32000, Israel, shl@physics.technion.ac.il, (972) 4-829-5934*

*\*\*Department of Electrical and Computer Engineering, University of New Mexico, Albuquerque NM, 87131, USA*

Presently, mostly advanced microwave pulse compressors providing both high output power (hundreds of megawatt) and high power gain (20 dB and above) are resonant compressors with plasma interference switches [1]. Nevertheless, in spite of significant progress in their development, there is no clear understanding of processes that govern the plasma formation under a strong RF electric field in pressurized gases and ultimately determine a compressor's output power. As a result, the output power in existing high-gain compressors is significantly reduced compared to the power of the traveling wave component of RF field accumulated in a resonant cavity, and the output pulse waveform is far from rectangular one as it would be with ideal switching.

In this work, the nanosecond-scale evolution of the plasma formed in the switch of the S-band compressor was studied experimentally, and the influence of plasma dynamics on the compressor output pulse peak power and waveform was investigated in numerical simulations. The compressor comprised a cavity filled with dry air at up to  $3 \cdot 10^5$  Pa pressure and an H-plane waveguide tee as an interference switch; it generated output pulses of  $\sim 8$  ns duration and up to 7.4 MW peak power in 2.766 GHz frequency. The plasma discharge in the switch was triggered by a Surelite laser. The plasma was observed using fast-frame (2 ns) optical imaging with a 4QuikE intensified camera. The plasma has the form of filaments expanding along the RF electric field. From the imaging data, the typical size of the plasma and the velocity of its expansion were determined and the plasma density and effective collision frequency were estimated. In addition, spectroscopic measurements of the emitted light were carried out to obtain the nanosecond dynamics of the plasma density.

Numerical simulations of the microwave energy release from the compressor were performed using the 3-D version of the code MAGIC [2]. Gas ionization, plasma evolution and interaction with RF fields were simulated using different approaches provided by MAGIC: particle-in-cell approach accounting for electron-neutral collisions, gas conductivity model based on the concept of mobility, and hybrid modeling. The dependences of the microwave output pulse peak power and waveform on parameters that can be controlled in experiments, such as the external ionization rate, RF field amplitude, and background gas pressure, were investigated. It was shown that for a given input power and external ionization rate, there is an optimal pressure maximizing output power; the efficiency of power extraction, however, decreases with increasing pressure. The rise of the output power in time correlates with the rise of the plasma density; in addition, the output power rises with the expansion of the volume occupied by the plasma as a result of electron diffusion. Simulations of the radiation extraction from the cavity after the appearance of a plasma filament with the expansion velocity taken from the imaging data show a good agreement of the microwave output pulse waveform with those obtained in the experiments. In addition, the effect of self-breakdown with a minor output was demonstrated in simulations of the compressor charging with an initial background electron density.

### REFERENCES

- [1] S. Novikov, Yu. Yushkov, S. Artemenko, etc. // 16th Int. Pulsed Power Conf. – June 17-22, 2007. – Vol. 2. – pp. 1822-1825.
- [2] B. Goplen, L. Ludeking, D. Smithe, and G. Warren // Comput. Phys. Commun. – 1995. – Vol. 87. – No. 1/2, pp. 54-86.

<sup>1</sup> This work was partially supported by the Technion grant #20003813 and BSF grant #1009212.

## RADIATION OF HIGH-POWER ULTRAWIDEBAND PULSES BY A CYLINDRICAL SPIRAL ANTENNA<sup>1</sup>

*Yu.A. ANDREEV, A.M. EFREMOV, V.I. KOSHELEV, B.M. KOVALCHUK, A.A. PETKUN, K.N. SUKHUSHIN,  
M.Yu. ZORKALTCEVA*

*Institute of High Current Electronics SB RAS,  
2/3, Akademichesky ave., Tomsk, 634055, Russia, E-mail: andreev@lhfe.hcei.tsc.ru, 8-3822-49-19-00*

A source of high-power ultrawideband (UWB) radiation pulses with elliptical polarization has been created. The source consists of a SINUS-160 monopolar pulse generator, a bipolar pulse former, and a transmitting spiral antenna in a dielectric container. To increase the electric strength, the dielectric container made of glass fibre was filled with SF<sub>6</sub>-gas up to gauge pressure of 2 atm.

Characteristics of the antenna were studied in the experiments as well as simulated using a program based on the FDTD method. On the basis of the computer calculations, a cylindrical equidistant spiral antenna with the number of turns  $N = 4$  has been chosen. The average radius of the spiral antenna  $r = 95$  mm, the screen diameter  $D = 600$  mm, and the turn-to-turn distance was 134 mm. To increase the electric strength of the antenna and to reduce its wave impedance, the spiral turns were made of an 18 mm-diameter thick copper tube. Fig. 1 presents a comparison of waveforms of radiated pulses at the antenna axis at a 3 m distance from it screen.

In the source of high-power UWB radiation, a spiral antenna was excited by a 2 ns high-voltage bipolar pulse. The source operated at a pulse repetition frequency of 100 Hz. The energy efficiency of the radiator was 0.8 at the radiation ellipticity at the antenna axis equal to 0.75. The effective potential of the source of radiation reached 300 kV at the voltage amplitudes of the bipolar pulse generator equal to 190/+200 kV.

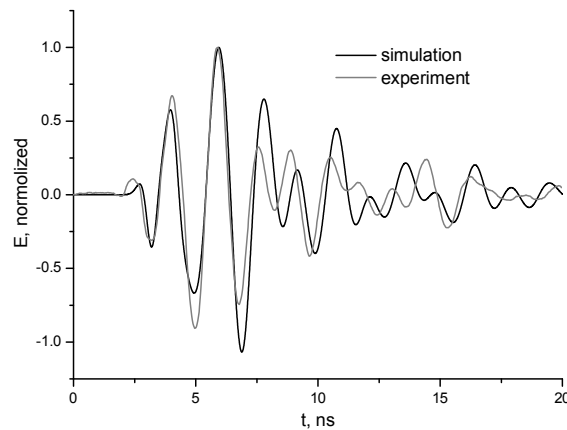


Fig. 1. Experimental and calculated waveforms of radiated pulses in the direction of the axis of the spiral antenna.

<sup>1</sup> This work was supported by the Program for basic research of the Presidium of RAS "Fundamental problems of pulsed high-current electronics".

## EXPERIMENTAL STUDY OF A FREQUENCY TUNABLE COAXIAL BWO WITH MODULATING REFLECTOR<sup>1</sup>

R. V. TSYGANKOV, A.I. KLIMOV, I.V. PEGEL, V.V. ROSTOV, E.M. TOTMENINOV

Institute of High Current Electronics, Siberian Branch, Russian Academy of Sciences, 2/3 Akademicheskoy Ave., Tomsk, 634055, Russia, tsygankov@lfe.hcei.tsc.ru, (3822)49-26-52

The report presents the results of studies of a coaxial relativistic backward wave oscillator (BWO) with a modulating reflector which is a radial inhomogeneity on the cross-sectionally uniform coaxial line. The oscillation mode with an efficiency of electron beam power conversion to electromagnetic radiation higher than 40% (with a power of ~300 MW) at a frequency of 1.2 GHz was calculated using the PIC code KARAT. The calculations demonstrated the possibility of mechanical frequency tuning within a band more than 10% by varying the drift section length between the reflector and slow wave structure (SWS) of the oscillator. Experiments were performed on the SINUS-7 high-current accelerator at a current pulse duration of ~50 ns. In the experiments, stable oscillation was obtained at an operating TEM wave with a frequency of 1.23 GHz, peak power of 290 MW, and efficiency of electron beam-to-radiation power conversion of ~30% at a microwave pulse duration of 30 ns. To suppress asymmetric spurious modes, longitudinal slits in the inner conductor of the line were used. The mechanical frequency tuning at half power level was estimated to be ~7% (Fig. 1).

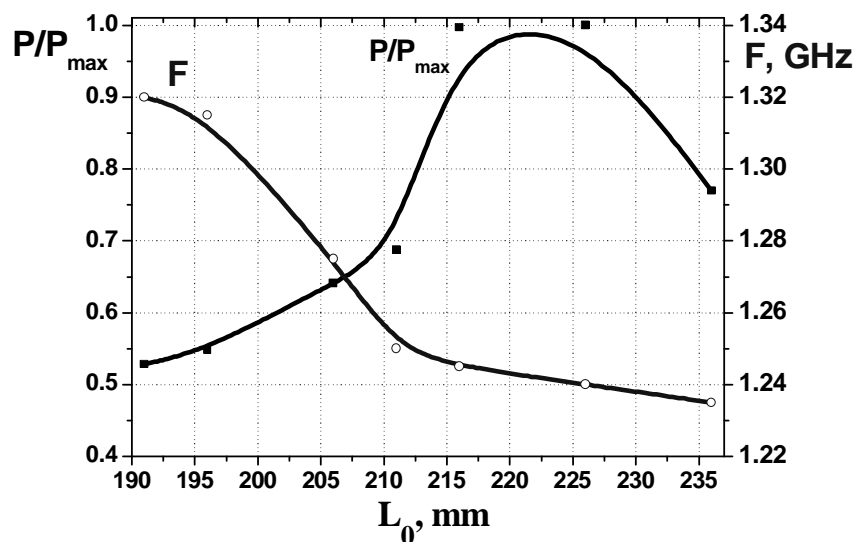


Fig. 1. Experimental dependence of normalized power  $P/P_{max}$  and frequency  $f$  on drift section length between the reflector and slow wave structure  $L_0$ .

### REFERENCES

- [1] V.P. Tarakanov // User's Manual for Code KARAT, Springfield: BRA, 1992.
- [2] E.M. Totmeninov, A.I. Klimov, V.Yu. Konev, I.V. Pegel, V.V. Rostov, R. V. Tsygankov, V.P. Tarakanov // Technical physics letters, 2014, vol. 40, issue 4

<sup>1</sup> This work was supported by Russian Foundation for Basic Research project number 14-08-00003\_a.

## **KLYSTRODE-LIKE MULTI-GW MICROWAVE OSCILLATORS WITH SELECTIVE CAVITIES AND $TM_{02}$ IRRADIATED MODES**

*J.C. JU, W. LI, H.W. YANG, J. ZHANG*

*College of Optoelectronic Science and Engineering, National University of Defense Technology, Changsha 410073, P. R. China,*

*[zhangjun\\_nudt@126.com](mailto:zhangjun_nudt@126.com), 86+84573765*

*A.A. ELCHANINOV, R.V. TSYGANKOV, A.V. GUNIN, V.V. ROSTOV*

*Institute of High Current Electronics SB RAS, Russian Federation, Tomsk*

As it's known, the sectioning of oversize slow wave structures can be used not only for the efficiency enhancement, but also for the mode selection. In this work, the clustering technique of sections with average diameter  $D \approx 2.5\lambda$  is considered. The main couple of counter-propagating waves is a  $TM_{02}$  waves with low reemission in  $TM_{01}$  waves. Particle-In-Cell simulations show the X-band oscillator efficiency of 43% (at 720 kV, 14 kA) and 41% (at 600 kV, 10 kA) for the Ku-band oscillator at central frequency 15 GHz.

## OVERSIZED RESONANT SLOW WAVE STRUCTURE FOR A MULTIGIGAWATT CHERENKOV OSCILLATOR

*R. V. TSYGANKOV, V. V. ROSTOV, A. A. ELCHANINOV*

*Institute of High Current Electronics, Siberian Branch, Russian Academy of Sciences, 2/3 Akademicheskoy Ave., Tomsk, 634055,  
Russia, tsygankov@lfe.hcei.tsc.ru,  
(3822)49-26-52*

The concept of a new Cherenkov oscillator with an oversized (with a mean diameter to wave length ratio of 2.4) resonant slow wave structure and operating  $TM_{02}$  mode was developed. The slow wave structure (SWS) consists of two like sections with a phase jump which provides mode selection near the  $\pi$ -mode with different longitudinal and transverse field structures. As shown by numerical optimization of the SWS geometry, the phase jump in the central part of the structure allows suppressing the electron beam coupling with modes matched at the edges of SWS with the  $TM_{01}$  wave. The operating mode of the low-Q resonator is converted mainly to  $TM_{02}$  waves running leftward and rightward. The diode unit with a cup-shaped cathode and an “adapter” acts as a quasi-optical reflector. The “adapter” consists of two grooves and provides a reduced level of the radial component of the electric field near the wall.

The wave propagating toward the cathode is reflected from it with a coefficient of up to 98% in the “cold” system and induces modulation of the emission current. The diffraction loss of the operating wave in the interelectrode gap for a frequency band of  $\sim 10\%$  is minimized by using an “adapter. The modulation depth of the electron current from the cathode, according to the PIC calculations<sup>1</sup>, reaches  $\sim 50\%$ . The chosen system requires tuning of the feedback phase, for example, by shift of the slow wave structure. The rated oscillating mode with the  $TM_{02}$  wave at 10 GHz corresponds to a peak power higher than 4 GW and efficiency of electron beam-to-radiation power conversion of 43% at a transient time of less than 10 ns. It is expected to perform experiment on the SINUS-7 high-current accelerator at a voltage of  $\approx 750$  kV and average beam current of  $\approx 14$  kA.

### REFERENCES

- [1] V.P. Tarakanov // User's Manual for Code KARAT, Springfield: BRA, 1992.

**BEHAVIORAL AND METABOLIC RESPONSES OF LABORATORY MICE AFTER EXPOSURE THE BRAIN TO NANOSECOND REPETITIVE PULSED MICROWAVES OF**

KEREYA A.V.<sup>1,2</sup>, BOLSHAKOV M.A.<sup>1,2</sup>, ZAMOSHCHINA T.A.<sup>2,3</sup>, KNYAZEVA I.R.<sup>1,3</sup>, KUTENKOV O.P.<sup>1</sup>, SEMJONOVA YU.N.<sup>2</sup>

<sup>1</sup>*Institute of High-Current Electronics SD RAS, Academic avenue, 2/3, Tomsk, 634055, Russia,  
E-mail: kereya21@mail.ru, tel: +7 3822 493191,*

<sup>2</sup>*National research Tomsk state university, Str. Lenin, 36, Tomsk, 634050, Russia*

<sup>3</sup>*Siberian state medical university, Moscow highway, 2, Tomsk, 634050, Russia*

Earlier it was shown that exposure to nanosecond repetitive pulsed microwaves (RPM) on epididymal adipose tissue of mice changed its mass. Recently, there is evidence that adipose tissue is in the center of a network of endocrine signaling systems which cooperate with neuroendocrine regulators [1]. Thus, adipose tissue response to the impact of RPM may provide a change of the state of the whole organism, including the brain. On the other side effects on the brain through the hormone systems may affect adipose tissue condition, other internal organs, as well as behavioral components of mice.

Therefore, the purpose of this study was to investigate behavioral and metabolic parameters of mice after irradiated by a nanosecond RPM on the brain.

The experiments were performed in compliance with all ethical norms and rules on 40 white outbred male mice weighing 25-30 g S57B1/6 line obtained from the nursery Institute of Pharmacology Center of SD RAMS. Laboratory generators based on the MI-505 magnetron served as RPM sources. The head of the animal was subjected to daily (within 10 days) 4000 nanosecond pulses RPM (100 ns pulse duration) with a pulse repetition frequency 6, 8, 13, 16 and 22 pulse per second (pps), peak power density (pPPM) 1500 W/cm<sup>2</sup>. The mouse body was covered with radioabsorbing materials for local irradiation of the brain. The experiment involved the irradiated and sham-irradiated animals. The behavioral components were assessed (horizontal, vertical components of motor activity, mink activity, grooming and defecation) according to the «open field» procedure immediately before and after the irradiation of mice, as well as the weight of organs (liver, spleen and epididymal fat) and hormone content in blood serum. Experiments have shown that the influence of nanosecond repetitive pulsed microwaves may have a significant effect on some of the behavioral responses of irradiated mice. After 10 days of irradiation the behavioral activity in all irradiated groups changed relative to the sham-irradiated group of mice, except the exposed at 8 pps. In the last case, the behavior of irradiated animals did not differ from the behavior of the control mice. The other frequencies caused activation of the passive-defensive behavior component or / and the weakening of the active-search components. The most significant changes were observed after exposure to the frequency 22 pps.

Except for changing behavioral responses, impacts of all frequencies accompanied by a reduction of the relative food consumption at a constant weight of epididymal adipose tissue. However, there was a statistically significant decrease in the relative weight gain of the animal while reducing the weight of the liver in comparison with the indicators in the sham-irradiated group after irradiation at 8 pps. This may be due to the impact of RPM on the brain developing depression in animals (activation of passive-defense components in the oppression of the active-search), compensation is induced release of glycogen from the liver and, therefore, there is a intensification of carbohydrate energy metabolism. It follows that the brain irradiation by nanosecond repetitive pulsed microwaves can affect the body in two ways: changes in behavioral activity and in metabolic processes, and after exposure at 8 pps effect controlled by different physiological systems.

## REFERENCES

- [1] *M. E. Frigolet E., V. Vela, N. Torres, A.R. Tovar // Archives of Medical Research. – 2008. – Vol. 39. – Issue 8. P. 715-728.*



## HIGH POWER MICROWAVE COUPLER

*A.I. KLIMOV, E.M. TOTMENINOV*

*Institute of High Current Electronics SB RAS, 2/3 Akademichesky Ave., Tomsk, 634055, Russia,  
E-mail: klimov@lfe.hcei.tsc.ru, Phone/Fax: +7-3822-491-991*

The loop directional coupler is a well-known device that has been built in circular waveguide with a  $TM_{01}$  mode [1]. The coupler can be connected to a high-power microwave (HPM) oscillator between its vacuum output and transmitting horn antenna, thus allowing measurements of HPM pulses.

The paper describes a coupler consisting of a circular waveguide section connected to a side structure with a 50- $\Omega$  strip line as a coupling loop. The aperture that couples the waveguide and the side structure is a round hole of proper diameter which ensures a desired coupling coefficient. Inside the cylindrical case of the structure, there is a plexiglass window which isolates the vacuum units of the device from those exposed to atmosphere. One end of the strip line is matched by a 50- $\Omega$  resistor and the other end is connected to a 50- $\Omega$  coaxial line terminated with a 50- $\Omega$   $N$ -type female connector.

A  $TM_{01}$  mode propagating in the circular waveguide has field components  $E_z$ ,  $E_r$ , and  $H_\phi$ ,  $E_z$  is zero at the waveguide, so the only field components which couple to the strip line are  $E_r$  and  $H_\phi$ . These field components leak through hole and excite currents on the strip line. The line acts as a capacitive voltage divider coupling to the passing electric field  $E_r$ , and so give rise to currents in both arms of the strip line in the same direction. The strip line also couples inductively to the time rate of change of the magnetic field  $dH_\phi/dt$  which excites currents in both arms of the strip line in opposite directions.

This device is intrinsically a “backward” coupler. Microwave power flowing forward in the main circular waveguide is coupled to the strip line and flows in the reverse direction. But with very strong field components  $E_z$  and  $E_r$  at a microwave power of several gigawatts, the coupling aperture can be shielded with a screen of thin wires soldered in the  $\phi$ -direction to avoid a microwave discharge, so only  $H_\phi$  can leak through the hole. In this case, the coupler is not directional, but yet it provides a possibility to observe the microwave power propagating in both directions in the main guide. For example, it is possible to observe the power reflected from the transmitting antenna.

Similar couplers with different coupling coefficients were used for measuring the characteristics of microwave pulses produced by HPM backward wave oscillators (BWOs). For example, the coupler used in the experiments on an S-band superradiant BWO [2] had a coupling coefficient of 57.7–63.3 dB at 3.2–4.1 GHz and its directivity was 5 dB. The coupler was calibrated using an Agilent 8719ET network analyzer and a  $TEM$ - $TM_{01}$  mode converter. In the calibration, the dummy load of the main circular waveguide was a BWO transmitting antenna, a vacuum calorimeter, or a suitable plastic bottle filled with ethanol. The swept frequency measurement revealed certain resonances of the coupling response over the bandwidth. However, as shown by comparison of the measurement results for different loads, these resonances depended mainly on peculiarities of the measuring circuit, rather than on properties of the coupler. The difference in linearized frequency dependencies of the coupling coefficient for different loads was no more than  $\pm 0.6$  dB. The characteristics of HPM pulses measured with the coupler [2] were a peak power of up to 1 GW, carrier frequency of 3.7 GHz, and pulse duration of 2.5–3 ns.

The experience of using couplers in different HPM experiments demonstrated that the coupling depended strongly on the purity of the pulse spectrum. A small amount of high-frequency parasitic modes could drastically affect the measurement results.

### REFERENCES

- [1] Earley L.M., Ballard W.P., Warton C.B. // IEEE Trans. Nucl. Sci. – 1985. – Vol. NS-32. – No 5. – PP. 2921–2923.
- [2] Afanasyev K.V., Bykov N.M., Gubanov V.P., et al. // Radioph. Quant. Electron. – 2006. – Vol. 49. – No 10. – PP. 754–759.

## EXPLOSIVE EMISSION CARBONE FIBER CATHODE FOR HIGH POWER MICROWAVE SOURCE<sup>1</sup>

*E. M. TOTMENINOV\**, *I. V. PEGEL\**, *O. P. KUTENKOV\**

\* *Institute of High Current Electronics, Siberian Branch, Russian Academy of Sciences  
2/3 Akademichesky Ave., Tomsk 634055, Russia, e-mail totm@lfe.hcei.tsc.ru  
ph. +7(3822)491-641, fax +7(3822)492-410*

The current characteristics and life time of the explosive emission cathode (Fig. 1) manufactured from a carbon fiber was investigated in repetition rate regime of high power microwave source at high voltage (diode voltage of 250 kV) modulating pulse duration of 5 ns. It was shown that the cathode life time can be as long as  $3.6 \cdot 10^6$  pulses. Measured value of the fiber material losing was of  $2.4 \cdot 10^{-4}$  gr/C. Changing of the carbon fibers state was observed caused by deposition of carbon from the cathode plasma. 7 %-efficiency of microwave generation was obtained using the cathode in the experiment with relativistic microwave oscillator without guiding magnetic field [1] driving by nanosecond accelerator “SINUS-7” at the carrier frequency of 4 GHz (Fig. 2). This efficiency was very similar to the efficiency of 8 % obtained with the oscillator using the velvet cathode at as low electric field strength as 200 kV/cm in the diode gap at the diode voltage of 560 kV. In the same conditions the microwave peak power was about 200 MW in the both cases.



Fig. 1. Fiber carbon cathode (left) and focusing electrode (right)

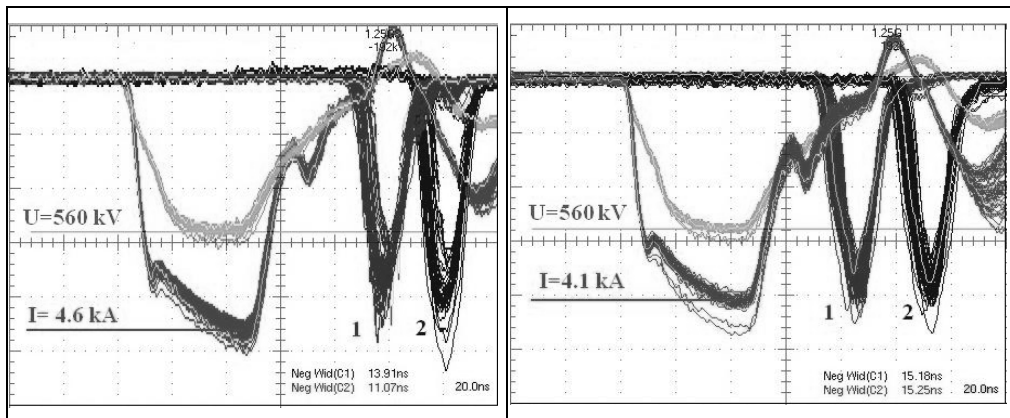


Fig. 2. Waveforms of diode voltage (U) beam current (I) and detected microwave signal from receiving antenna (1) and strip-line coupler (2) for velvet (left) and fiber carbon (right) cathode for batch (50 pulses) regime operation with repetition rate 20 Hz.

### REFERENCES

- [1] *Totmeninov E. M., Klimov A. I., Rostov V. V. // IEEE Transactions on Plasma Science. – 2010. –V. 38. –No. 10 (Part 2). pp. 2944—2947.*

<sup>1</sup> This work was supported by the Russian Foundation for Basic Research, project no. № 12-08-00659-a.

## CASCADE SWITCHES OF MICROWAVE RESONANT COMPRESSORS

*S.N. ARTEMENKO, V.A. AVGUSTINOVICH, S.A.GOREV, S.A.NOVIKOV, YU.G.YUSHKOV*

*Tomsk Polytechnic University, 30 Lenina str., Tomsk, 634050, Russia,  
E-mail: snartemenko@mail.ru, phone: +7 3822 417451*

A microwave switch of a resonant compressor is an element that affects the operation process substantially. The switch must be able to disrupt the standing wave pattern of a cavity very fast but should not low the electric strength of the compressor that is has to withstand high values of electric field strength during cavity excitation time of several microseconds. So the limiting output power of a compressor is determined by the switch design and its operation. The switching element is usually located in the area of maximum electric field strength of a standing wave [1] and the desire to put it in the area of lower field strength but keeping the same efficiency of operation is quite understood.

Presumably the cascade switch might provide the required way of operation. The studied cascade switches were of two designs. The first one was formed by waveguide tees connected in series where the direct input arm of a next tee is connected to a side arm of a preceding tee. This design is shown in Fig. 1a. the second design involves the waveguide tees connected in series only by their direct arms so making the direct output arm of a preceding tee the input arm of the next one.

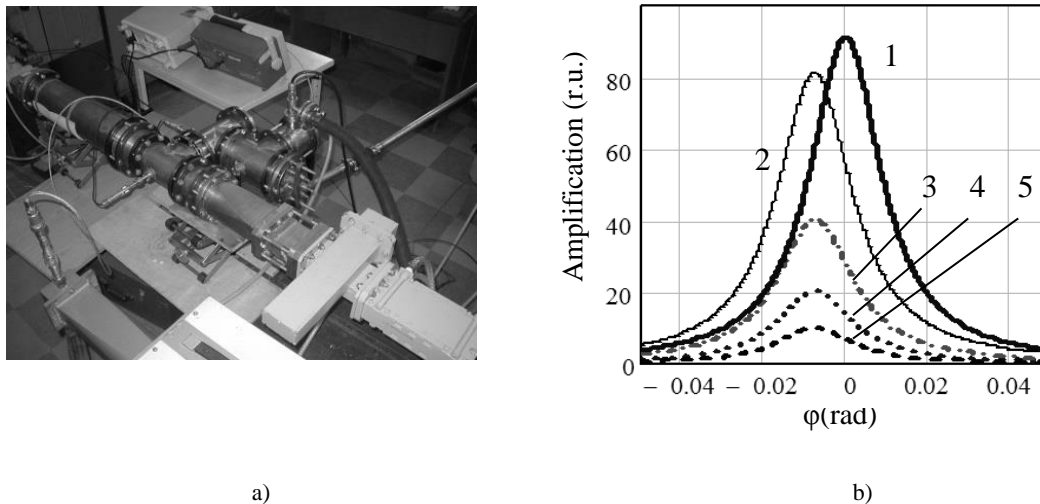


Fig. 1. a) External view of the storage cavity with the cascade switch. b) Power amplification calculated values for different sections of the X-band compressor plotted against the phase shift along the connecting common arm of the tees: 1- for the cavity with traditionally single output tee, 2- in the cavity with the cascade switch, 3- in the side arm of the first tee, 4- in the connecting arm of the tees, 5- in the last side arm with gaseous switch.

The electric field strength of the compressor of the first design was calculated relatively the power of an exciting microwave pulse. The plots of field strength values in terms of amplification for different parts of the storage cavity and the switch as functions of the electric length of the common connecting tee arm are presented in Fig. 1b.

It was shown that the considerable decrease of the switched power value and the increase of the output power and stability of the output pulse parameters can be provided by both designs at definite conditions. The cascade switches may be designed on the basis of oversized waveguides as well.

### REFERENCES

- [1] V.A.Avgustinovich, S.N.Artemenko, V.L.Kaminsky, S.A.Novikov, Yu.G.Yushkov //Instruments and Experimental Techniques. – 2007. – v.50. – №2. p.237 - 240.

**CRYOELECTRON RESONANT COMPRESSOR OF MICROWAVE PULSES<sup>1</sup>***S.N. ARTEMENKO, G.M.SAMOYLENKO**Tomsk Polytechnic University, 30 Lenin str., Tomsk, 634050, Russia, [sgm@tpu.ru](mailto:sgm@tpu.ru), 3822-417451*

Calculations of main parameters of the cooled version of a resonant microwave compressor are carried out. It was shown cooling down to the liquid nitrogen temperature increase the energy parameters Of common copper resonant microwave compression system sufficiently. Results of the experimental study of the S-band microwave compressor cooled down to 77K are presented.

The process of electromagnetic wave transmission through film made of the high temperature superconductor (HTSC) is analyzed. The phenomenon of fast transition of thin HTSC films in superconducting state into the normal state (S/N transition) is shown as a possible basis for the microwave energy switching in cooled compressors.

The version of the microwave compressor design including the cooled copper microwave cavity with the HTSC film switch is considered.

---

<sup>1</sup> This work was a part of the State Program "Nauka"

## OVERSIZED INTERFERENCE SWITCHES OF RESONANT MICROWAVE COMPRESSORS<sup>1</sup>

*S.A.NOVIKOV, V.A.AVGUSTINOVICH, S.N.ARTEMENKO, V.L.KAMINSKY, YU.G.YUSHKOV*

*Tomsk Polytechnic University, 30 Lenina str., Tomsk, 634050, Russian Federation.  
E-mail: nsa@tpu.ru, phone: +7 3822 417451*

Waveguide T- junctions are used as interference switches with either oversized [1] or single mode cavities [2]. The main requirement is the principal operational mode of a tee does not get transformed into higher modes and so this justifies the usage of single mode waveguides in interference switches of this type. Switching in a single mode waveguide can provide fast energy extraction but the area of switching element location has low electrical strength due to limited dimensions of the waveguide cross section.

A few new designs were considered in the work and it was shown in general that the cross section dimensions can be increased relatively to working frequency beyond the cutoff limits for higher modes if special symmetry of a device construction is maintained or a design provides suppression of higher modes. For example Fig.1 presents the interference tee switch with partitioned input rectangular waveguide arm. Each section operates at  $H_{10}$  mode but the combined radiation into the side arm allows usage of  $H_{01}$  mode with the electrical field strength parallel to bigger wall of the waveguide. This switch has higher electrical strength and the corresponding compressor has higher limiting output power.

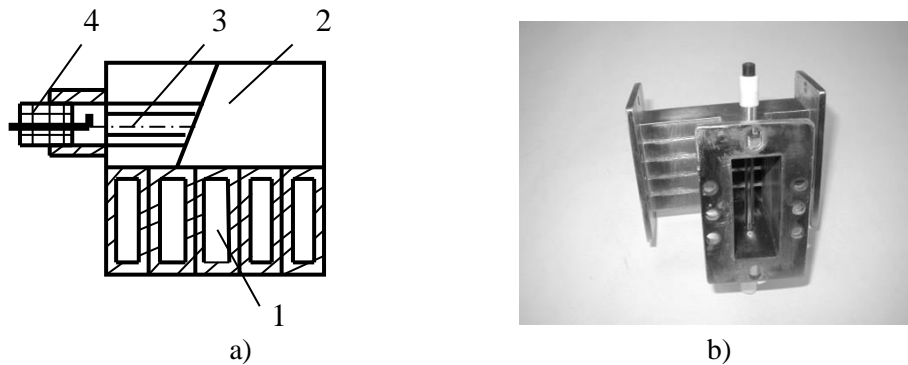


Fig. 1. a) Schematic of the oversized interference switch: 1- partitioned input direct arm of the tee, 2- oversized side arm with  $H_{01}$  – working mode, 3- dielectric discharge tube, 4- triggering switch; b) external view of the oversized interference switch.

Other types of switches made of oversized rectangular and circular waveguides were experimentally tested. Their high switching efficiency was exhibited at X- band and S- band experiments.

### REFERENCES

- [1] *R.A.Alvarez, D.L.Birx, E.J.Lauer, D.J.Scalapino* // Particle Accelerators. – 1981. – №11. p.125-130.
- [2] *V.A.Avgustinovich, S.N.Artemenko, V.L.Kaminsky, S.A.Novikov, Yu.G.Yushkov* // Instruments and Experimental Techniques.- 2007.- v.50. -№ 2. p.125-130.

<sup>1</sup> This work was performed as a part of State Program “Nauka”

## CONTROLLED ENERGY EXTRACTION FROM RESONANT CAVITY<sup>1</sup>

*S.A.GOREV, V.A.AVGUSTINOVICH, S.N.ARTEMENKO, S.A.NOVIKOV, YU.G.YUSHKOV*

*Tomsk Polytechnic University, 30 Lenina str., Tomsk, 634050, Russian Federation.*

*E-mail: nsa@tpu.ru, phone: +7 3822 417451*

The microwave compressor included the interference switch made of rectangular waveguides operating at  $H_{01}$  mode and so being oversized. The energy extraction process is controlled by variation of dimensions of single mode switches connected to the main oversized switch.

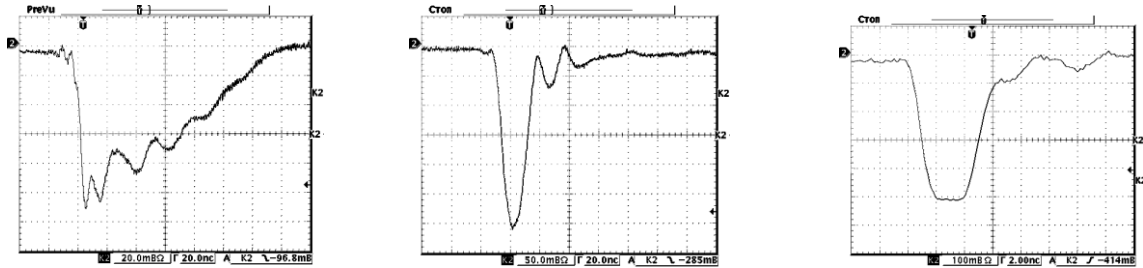


Fig. 1. Examples of formed microwave pulse envelopes. Time sweep rates are 20 ns/div, 20 ns/div and 2 ns/div correspondingly.

The output pulse width could be varied within the range boundary values related by the ratio equal to 10 approximately. The output pulse power was of tens kilowatts to several megawatts and output pulse envelopes showed the short nanosecond rise time. They are exhibited in Fig. 1.

<sup>1</sup> This work was performed as a part of State Program "Nauka"

**MODIFICATION OF THE FREQUENCY SPECTRUM OF ULTRA-WIDEBAND RADIATOR**

V.M. FEDOROV, V.Ye. OSTASHEV, A.V. UL'YNOV

*Associated Institute for High Temperature of RAS  
13/19, Izhorskaya ave., Moscow, 127412, Russia  
Phone: +7(495)485-7944, E-mail: [vmfedorov@ihed.ras.ru](mailto:vmfedorov@ihed.ras.ru)*

**Abstract** –Investigation of ways of modification of the ultra-wideband (UWB) radiation frequency spectrum is presented in this article. Two ways of modification of frequency spectrum of radiation for the directed pulse radiator are analyzed by an calculations. At first, UWB spectrum is modified under the fixed time shift between the radiation pulses generated by the elements of active antenna array, at second – due to mismatch of the wave impedance of components of antenna-feeder tract. Energy spectrums of the radiation directed along antenna axis are presented for the real view of unipolar pulse of antenna excitation. These spectrums are comparing with the spectrum of active array which radiates in coherent mode. This comparison is executed with antennas of equal area and at equality of the average electric power of antennas excitation. It is shown that amplitude of density of linear spectrum of radiation for the radiator with mismatched impedance of antenna-feeder tract exceeds the amplitude of the coherent radiation spectrum significantly. The possibility of control of frequency distribution of UWB radiation energy does UWB radiator the flexible tool in electromagnetic compatibility study, allowing reveal the spectral areas of criticality for electronic devices under the act of powerful electromagnetic pulses.

**SWITCHING OF STORAGE AND EXTRACTING MODES IN SUPERCONDUCTING RESONANT MICROWAVE COMPRESSORS WITH INTERFERENCE SWITCH<sup>1</sup>***S.N. ARTEMENKO, G.M. SAMOYLENKO**Tomsk Polytechnic University, 30, Lenin str., Tomsk, 634050, Russia, [sgm@tpu.ru](mailto:sgm@tpu.ru), 3822-417451*

The microwave switch on the basic of the waveguide H-tee designed as a cavity with variable parameters attached to one of the tee arms is considered. The superconducting version of a compressor with the switch of that type is analyzed.

It is shown there is possibility of fast-rate energy extraction by controlling the Q-factor or resonant frequency of the switching cavity.

High efficiency of the interference switch operation at energy storing is proved. The estimation of superconducting compression system parameters at the Q-factor value equal about  $5 \cdot 10^8$  is made.

It is shown that the amplification of the system in the range 40-60dB is quite possible at the output microwave pulse width 5-10ns. Some designs of the system are considered

---

<sup>1</sup> This work was a part of the State Program "Nauka"



## S-BAND VACUUM MICROWAVE CALORIMETER

*A.I. KLIMOV, A.A. ELTCHANINOV, V.V. ROSTOV*

*Institute of High Current Electronics SB RAS, 2/3, Akademichesky Ave., Tomsk, 634055, Russia,  
E-mail: klimov@lfe.hcei.tsc.ru, Phone/Fax: +7-3822-491-991*

The energy of high power microwave (HPM) pulses [1] is one of the most important characteristics of HPM sources. This characteristic is measured with microwave calorimeters. A microwave calorimeter, when used together with a microwave antenna or with a coupler and a detector, allows reliable measurements of pulse peak power. There are different calorimeter designs in which the dummy load is either connected to the vacuum output of an HPM source [2] or located outside its vacuum volume immediately upstream of the aperture of a transmitting horn antenna [3]. Microwave calorimeters can be designed for narrow-band or wide-band operation.

This paper reports on the design of a wide-band vacuum calorimeter the dummy load of which utilizes ethanol as a reaction mass and describes peculiarities of measuring the energy of HPM pulses with the calorimeter. The dummy load of the calorimeter comprises series-connected cylindrical and conical waveguides with a long ethanol-filled glass tube in the inside. The tube has two internal coils double-wound like “dreadlocks” and immersed in ethanol. One of the coils is made of thin copper wire and is used as a thermistor for measuring the increase in ethanol temperature. The other coil is made of manganin and is used for calibration of the calorimeter. The resistance of the thermistor and calibration coil at a temperature of 23° C is 92 and 12 Ohm, respectively. The coils are fixed to a long wooden frame inside the glass tube. There is also a capacitor battery with a switch for calibration of the calorimeter. The total capacitance of the battery is 0.1 F. The capacitor battery is charged to a maximum voltage of 45 V with a rectifier. When charged to a certain voltage, the battery can be discharged via the switch onto the calibration coil and the portion of energy inputted to ethanol can be correlated with the increase in thermistor resistance. The microwave power delivered to the dummy load and transported along the waveguides is absorbed in ethanol. The absorbed microwave energy is determined from the increment in thermistor resistance due to the increase in ethanol temperature, and the increase in thermistor resistance is measured with an ohmmeter.

The microwave power reflection coefficient from the dummy load of the calorimeter reaches 16 % within a band of 3.2–4.1 GHz. This gives a maximum systematic measurement error (underestimate) of microwave pulse energy. The random calibration error for the calorimeter is  $\pm 4\%$ .

The calorimeter was used for measuring the energy of HPM pulses in an S-band superradiant relativistic backward wave oscillator [2] which operated in the repetitive pulsed mode and produced microwave pulses with a carrier frequency of 3.7 GHz, peak power of up to 1 GW, and duration of 2.5–3 ns. The experimental measurements of microwave pulse energy showed the necessity of taking into account the difference in temporal dynamics between the energy distributions in the ethanol volume in calibration and microwave energy measurement. The calibration results could actually be applied to determine the microwave energy only within 70 or even 80 s after the microwave pulse or calibration pulse. Furthermore, this required a pause for the dummy load of the calorimeter to cool down and to recover its initial state. One more result obtained in the experiments concerned the probability of a microwave discharge on the surface of the glass tube used in the dummy load. The discharge could arise near the junction point of the circular and conical waveguides at a microwave peak power of about 1 GW. Therefore, the measurement results could be distorted or the glass tube could even be damaged. This means that the measured microwave power must be limited and the shape of the waveguides needs further optimization to provide more uniform microwave power absorption along the glass tube of the dummy load, to decrease the electric field strength, and thus to preclude the initiation of microwave discharge.

### REFERENCES

- [1] Benford J., Swegle J.A., Shamiloglu E. // High power microwaves. – Oxford: Taylor & Francis, 2007.
- [2] Afanasyev K.V., Bykov N.M., Gubanov V.P., et al. // Radioph. Quant. Electron. – 2006. – V. 49. – № 10. – PP. 754–759.
- [3] Klimov A.I., Vykhodtsev P.V., Elchaninov A.A., et al. // In Proc. of the 15th SHCE. Tomsk, Russia: IHCE SB RAS, 2008. – PP. 422–424.

## OUTPUT OF MICROWAVE ENERGY FROM THE RESONATOR MANAGED TRANSFORMATION MODE OSCILLATIONS

*V.S. IGUMNOV, V.A. AVGUSTINOVICH, S.N. ARTEMENKO, YU.G. YUSHKOV*

*National Research Tomsk Polytechnic University, 30 Lenina ave., Tomsk, 634050, Russia, vladislavigumnov@yahoo.com, +79138492895*

Presented the results of theoretical and experimental researches of formation of microwave pulses with adjustable power, duration, repetition rate and the shape of the envelope at energy outputting managed transformation of the resonator mode oscillations on the window between the resonator and waveguide stub. Changing the pulse parameters is carried tunable elements interspecies coupling. Demonstrated the possibility of formation of a series of subnanosecond microwave pulses at a fractional output power and nanosecond pulses of different duration for a single complete withdrawal of high-frequency energy from the compressor cavity. Shape of the pulses is calculated by the following recurrence relations between the amplitudes of the waves in the system:

$$b_2 \left( i \frac{T_1}{10} \right) = \varepsilon b_2 \left( -T_1 + i \frac{T_1}{10} \right) - \kappa b_2 \left( -\frac{22}{20} T_1 + i \frac{T_1}{10} \right) - \xi b_4 \left( -\frac{13}{20} T_1 + i \frac{T_1}{10} \right) \quad (1)$$

Eq.1 for the wave amplitude in the cavity.

$$b_4 \left( i \frac{T_1}{10} \right) = \gamma_0 b_2 \left( -\frac{11}{20} T_1 + i \frac{T_1}{10} \right) + \delta b_4 \left( -\frac{1}{10} T_1 + i \frac{T_1}{10} \right) \quad (2)$$

Eq. 2 for the wave amplitude in the waveguide stub.

$$d_2 \left( i \frac{T_1}{10} \right) = \mu b_2 \left( -\frac{1}{2} T_1 + i \frac{T_1}{10} \right) + \nu b_2 \left( -\frac{12}{20} T_1 + i \frac{T_1}{10} \right) + \chi b_4 \left( -\frac{3}{20} T_1 + i \frac{T_1}{10} \right) \quad (3)$$

Eq. 3 for the wave at the system output.

Where

$$\varepsilon = 0.5\sqrt{1-k^2}e^{-\alpha}, \kappa = -0.5\sqrt{1-k^2}\sqrt{1-h^2}e^{-\alpha-\beta}, \xi = -j2^{-0.5}h\sqrt{1-k^2}e^{-0.5(\alpha+\beta)-\gamma-j\varphi}, \mu = 0.5e^{-0.5\alpha}, \\ \nu = 0.5\sqrt{1-h^2}e^{-0.5\alpha-\beta}, \chi = -j2^{-0.5}he^{-0.5\beta-\gamma-j\varphi}, \gamma_0 = j2^{-0.5}he^{-0.5(\alpha+\beta)}, \delta = \sqrt{1-h^2}e^{-\gamma-j\varphi}.$$

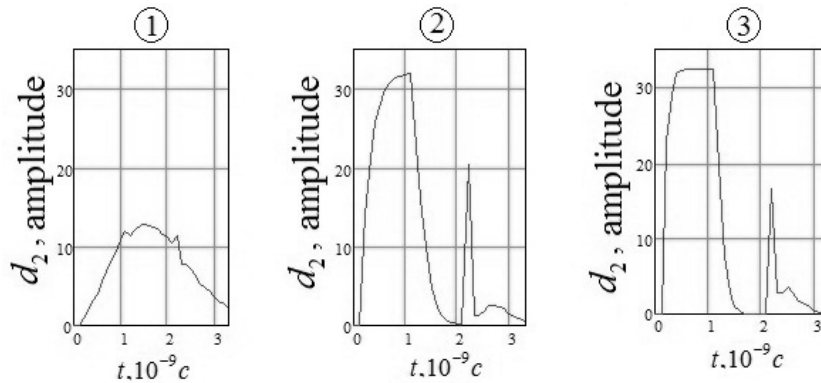


Fig.1. Calculated of the output microwave pulses at different values of interspecies coupling parameter  $h$  :

1)  $h = 0.4$ ; 2)  $h = 0.8$ ; 3)  $h = 0.9$ .

### REFERENCES

- [1] V.A. Avgustinovich, S.N. Artemenko, V.S. Igumnov, S.A. Novikov, Yu.G. Yushkov // *Electromagnetic waves and electronic systems*, 2011, Vol.16, № 7, pp. 43-45
- [2] V.S. Igumnov, V.A. Avgustinovich, S.N. Artemenko, S.A. Novikov, Yu.G. Yushkov, *Formation of Pulses with Controlled Parameters in a Resonance Microwave Compressor Employing Oscillation Mode Transformation // Technical Physics Letters*, 2013, Vol.39, №9, P.755-757

## ELECTROMAGNETIC WAVES OF TEM-TYPE IN PLASMA WAVEGUIDES WITH MULTIPLY CONNECTED CROSS SECTION IN THE EXTERNAL MAGNETIC FIELD

*I.N. KARTASHOV\**, *M.V. KUZELEV\*\**

\**Lomonosov Moscow State University (Faculty of Physics), 1-2 Leninskiye Gory, Moscow, 119991, Russia, kartashov@ph-elec.phys.msu.ru, +7(916)5787069*

\*\**Lomonosov Moscow State University (Faculty of Physics), 1-2 Leninskiye Gory, Moscow, 119991, Russia*

Electromagnetic waves in plasma waveguides with a multiply connected cross section in an external magnetic field are investigated. Existence of a quasi-TEM modes in a finite magnetic field which transform into true TEM mode within infinitely strong and zero magnetic field is shown. Results of the solution of the dispersion equation for a coaxial cylindrical plasma waveguide with an internal radius  $R_1 = 1$  cm and external radius  $R_2 = 2$  cm are presented on Fig.1. Low-frequency TEM mode has phase velocity less than a speed of light and can be excited by a straight electron beam. Frequency of this wave actually is defined by the value of a magnetic field (electronic cyclotron frequency).

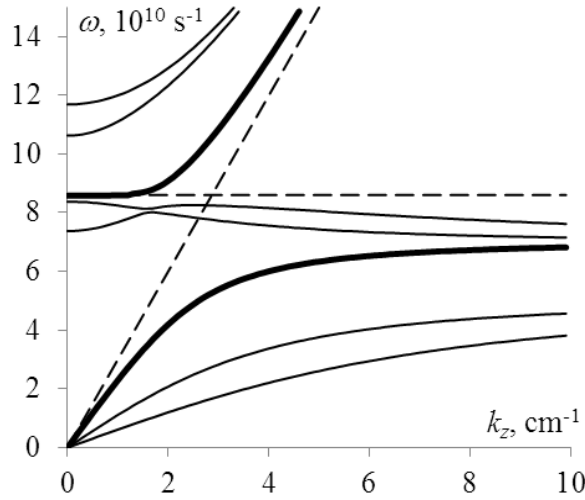


Fig. 1. Dispersion curves of waves of a coaxial plasma waveguide (plasma frequency  $\omega_{Le} = 5 \times 10^{10} \text{ s}^{-1}$ ) in a magnetic field (electron cyclotron frequency  $\Omega_e = 7 \times 10^{10} \text{ s}^{-1}$ ). Bold curves – TEM-modes, normal curves – electromagnetic modes  $E_{01}$  and  $B_{01}$ , high- and low-frequency Langmuir modes  $E_{01}$  and  $E_{02}$ , dashed curves – lines  $\omega = k_z c$  and  $\omega = (\omega_{Le}^2 + \Omega_e^2)^{1/2}$ .

Possibility of excitation of this wave by an electron beam moving with velocity  $u$  ( $\gamma$  – Lorentz factor,  $\omega_b$  – plasma frequency of the e-beam) is considered. The dispersion equation describing excitation of TEM mode in a coaxial plasma waveguide by an e-beam is

$$\omega^2 \left( 1 - \frac{\omega_{Le}^2}{\omega^2 - \Omega_e^2} \right) - k_z^2 c^2 = \frac{\omega_b^2 \gamma^{-1} (\omega - k_z u)^2}{(\omega - k_z u)^2 - \Omega_e^2 / \gamma^2}. \quad (1)$$

The left part of equation (1) determines the frequency of TEM mode, the right part describes excitation (radiation) of this wave by an e-beam. The strongest interaction of an e-beam and plasma takes place under condition  $\omega(k_z) = k_z u \pm \Omega_e / \gamma$  (a condition of a Doppler resonance). Using the assumption of the small density of electron beam we find an increment of beam-plasma instability

$$\delta\omega = \frac{1}{2} i \omega_b \gamma^{-1} \sqrt{\frac{\Omega_e}{\omega_0} \left( 1 + \frac{\omega_{Le}^2 \Omega_e^2}{(\omega_0^2 - \Omega_e^2)^2} \right)^{-1}}. \quad (2)$$

## A NEW COAXIAL HIGH POWER MICROWAVE SOURCE BASED ON DUAL BEAMS

YANGMEI LI\*, XIAOPING ZHANG

\*College of Optoelectronic Science and Engineering, National University of Defense Technology, Changsha 410073, China, sunberry1211@hotmail.com, +86 13875851674

In order to promote the output capability of the high power microwave sources (HPMs), that is, to acquire a higher peak power and an average power ( $>100\text{GW}$ ), two conditions must be satisfied. First, a high input electric power is supposed to be injected into the HPMs. Then the beam-wave conversion efficiency of the HPMs ought to be high enough. It is known that the low impedance HPMs are advantageous to obtain a high electric power. However, the high impedance HPMs are prone to achieve a high beam-wave interaction efficiency. In addition, the traditional HPMs with a confining magnetic field usually operate in the state of middle-high impedance due to the limitation of the space limit current, which restricts this type of HPMs to a relatively low input electric power.

To settle the problems aforementioned, a novel HPM source is proposed and investigated by the use of particle-in-cell (PIC) simulation code. The structure is coaxial based on coaxial dual annular beams, which is similar to the dual-band relativistic backward wave oscillator with dual beams[1]. In this new HPM source, however, the biggest difference is that, although it includes two separated beam-wave interaction regions, the microwaves generated are of the same frequency. The structure proposed here is like a relativistic backward wave oscillator (RBWO) created by utilizing the inner conductor of a coaxial transit-time oscillator (TTO)[2]. The inner and outer beam-wave interaction regions are designed to couple with each other to control the frequency and phase of the output microwaves. PIC simulations demonstrate that, as the diode voltage shifts from 650kV to 750kV, the frequency of two output microwaves will change simultaneously while staying the same; the phase difference will level off with a fluctuation of  $\pm 4^\circ$  at one burst; the relative phase difference will change about  $30^\circ$  in this voltage range. The results imply that the frequency and phase locking are achieved. The inner and outer output power conversion efficiencies of this source are bigger than their corresponding conversion efficiency when only one of the dual beams interacts with the RF structure, which indicates that the proposed structure is promising to realize a higher power if two output powers are combined.

### REFERENCES

- [1] Ting Wang, Jiande Zhang, Baoliang Qian, Xiaoping Zhang, Yibing Cao, Qiang Zhang // *Physics of Plasmas*, 2011, 18(1):013107.
- [2] Yibing Cao, Juntao He, Jiande Zhang, Qiang Zhang, and Junpu Ling // *Physics of Plasmas*, 2012, 19(7): 072106.

## TWO-CHANNEL SETUP FOR EXPERIMENTS ON RESONANT INTERACTION OF POWERFUL MICROWAVE PULSE WITH RELATIVISTIC ELECTRON BEAM

*K.A. SHARYPOV\**, *V.G. SHPAK\**, *S.A. SHUNAILOV\**, *M.R. ULMASKULOV\**, *M.I. YALANDIN\**,

*N.S. GINZBURG\*\**, *I.V. ZOTOVA\*\**, *E.R. KOCHAROVSKAYA\*\**, *V.YU. ZASLAVSKY\*\**

\* *Institute of Electrophysics UB RAS, 106 Amundsen St., Ekaterinburg, 620016, Russia, [const@iep.uran.ru](mailto:const@iep.uran.ru), +7(343)2678794*

\*\* *Institute of Applied Physics RAS, 46 Ul'yanov St., N.Novgorod, GSP-120, Russia.*

To study the effects of time-amplitude compression and "stoppage" of ultra-short electromagnetic pulses in the condition of cyclotron-resonant interaction with a beam of relativistic electrons [1], the experimental setup based on two independent synchronized high current accelerators is required. We do not consider the use of a single powerful generator with sequential splitting of high-voltage pulse towards two accelerating channel because of the complexities in independent adjustment of parameters of the beam and radiation in the individual channels. The report describes two variants of relative position of independent synchronous channels. The first channel is used for the formation of incident microwave pulse in non-stationary Ka-band relativistic BWO with a peak power of up to 500 MW. The second channel serves as e-beam-to-wave cyclotron-resonant interaction space. Report describes peculiar features of the system for registration of incident microwave pulse and transformed one when counter-input method is applied ("hot" experiment). Variants of radiation registration in alternative method with external reflector which turn the radiation at 315 degrees are compared ("cold" measurements).

### REFERENCES

- [1] *N.S. Ginzburg, et al., The amplification, compression, and self-induced transparency effects for the ultrashort electromagnetic pulses propagating along quasi-stationary electron beams // Radiophysics and Quantum Electronics. – 2012. – Volume. 54 – № 8-9. Pages 532-547.*

**EXPERIMENTAL APPROACHES ON FAST VARIATION PHASING SYSTEM IN MULTICHANNEL PULSE-PERIODIC RELATIVISTIC BWO**

*K.A. SHARYPOV\**, *V.G. SHPAK\**, *S.A. SHUNAILOV\**, *M.R. ULMASKULOV\**, *M.I. YALANDIN\**,

*I.V. ROMANCHEKO\*\**, *V.V. ROSTOV\*\**

*\*Institute of Electrophysics UB RAS, 106 Amundsen St., Ekaterinburg, 620016, Russia, [const@iep.uran.ru](mailto:const@iep.uran.ru), +7(343)2678794*

*\*\*High Current Electronics Institute SB RAS, 2/3 Akademicheskii avenue, 634055, Tomsk, Russia.*

Relativistic BWO of centimeters and millimeters wavelengths with "warm" dc-solenoids can work at repetitions frequencies of tens-hundred hertz and more. The duration of a pulses package depends on the magnetic field value because of heat off-take problems. It is especially actual for Ka-band BWO where the working magnetic field makes up to 2 T even before a cyclotron resonance. To scan an integrated wave beam at coherent summation from several BWO radiations in a short (~1 s) packages mode, quick tuning of a front of accelerating pulses delay time in nonlinear transmitting ferrite lines is required. In a limit, the delay variation ~ 15 ps for change of generation phase on 180 degrees must be provided on an interval between sequential pulses. For planned experiment conditions at a repetition rate of 10 Hz this interval will be 100 ms.

The programmed DC power sources giving in superposed magnetization solenoids of ferrite lines demanded currents ~ 5 A are in the testing processes. Also two alternative variants with pulse controlling of an accelerating front delay are considered. In the first case the ferrite superposed magnetization system will be sectioned. There will be a site with the pulse solenoid after the DC-solenoid with the fixed field. In the second case – the solenoid will be pulse wholly. In both cases the variation of a superposed magnetization field is feasible as due to change of capacitor storage discharge current, and a method of control over a delay of the accelerator turning on concerning a field pulse. We assume to carry out tests on a fast and controlled variation of a ferrite line delay on the model of a relativistic BWO power supply system. Data on influence of the reflected high-voltage pulse on an initial state of ferrite in the conditions of a pulse superposed magnetization are supposed to be submitted also.

## POWER OF THE LED CLUSTER IN HOUSING AND COMMUNAL LIGHTNING DEVICES

R.H. TUKSHAITOV\*, AIHAITI YISIHAKFU\*, R.M NIGHMATULLIN\*\*

\* Kazan State Power Engineering University, 420066, Kazan, Krasnosel'skaya street, 51, Russia

\*\* Research Center for Power Engineering Problems KSC RAS, 420111, Kazan, Lobachevsky street, 2/31, Russia  
Tel. 8 927-143-04-15: e-mail: trh\_08@mail.ru

In recent years, LED clusters are becoming more common in use, namely LED clusters of the type  $A \times B$  [1, 2]. Their technical certificates declare maximum allowed current, the value of which is constantly increasing over the years. For example, for LEDs type XLamp XP-G White and XP-L White, produced by Cree, the maximum current intensity is, respectively, 1500 and 2000 mA at the body temperature of 85°C [3]. This information contains an element of uncertainty, since the permissible amperage and temperature are determined primarily by the characteristics of LED radiators that are typically not provided by LED manufacturers.

The absence of technical specifications of exemplary radiators (effective area, dimensions, weight, material, thermal conductivity) leads to the situation that the temperature of the LEDs' p-n junction of different manufacturers will vary, and will often exceed the maximum allowed temperature thus reducing the lifetime and causing erroneous reporting [4].

We investigated the maximum possibilities of the eight-watt light-emitting diode Edipower II VF44 produced by Edison Opto with the radiator of metal cards from the materials of different thermal conductivity (duralumin, brass, steel) having area from 50 cm<sup>2</sup> to 750 cm<sup>2</sup> and a thickness of from 1 mm to 6 mm. When increasing of the area of these metal cards up to 330 cm<sup>2</sup> and tweaking their forms, we achieved the increase of LED cluster's maximum power from 8W to 25-30W at the temperature of 60° and permissible value of the plate radiator area of 10-12 sm<sup>2</sup>/W. There are further opportunities for increasing the initial nominal power of the lightning devices, such as increasing the number of clusters on the card, area, design etc., however, there is no definite association between these factors and further research is required. While temperatures in LED soldering area is low, a significant increasing of current intensity can reallocate voltage drop between the electrodes and the crystal that can affect the luminous efficiency. However, an additional research for determining this decrease value is still required.

The possibility of increasing the power of low-power LEDs from 50 to 250 mW was also established in earlier work at a stand-alone mode of their operation [5], while their testing is currently successfully continued in duration of more than 13,000 hours.

Increasing the power of LED clusters used without reducing their light output allows to minimize the cost of lightning devices designed for Housing and Communal Services, and significantly accelerate their implementation [5, 6].

Therefore LED manufactures should always provide technical specification of used radiators and criteria of evaluation of maximum current intensity in order to eliminate the uncertainty of LED technical characteristics.

### REFERENCES

- [1] TUKSHAITOV R.H. // *Sat scientific . tr. "Problems and prospects of development of domestic lighting, electrical engineering and energy" Saransk: MGU, 2012. P. 3-7.*
- [2] ASHRYATOV A.A., KOKINOV A.M., MIKAEVA S.A. // *Natural and technical sciences. 2012. № 6. P. 338-353.*
- [3] MITCH SAEYERS // *Semi-conductor light engineering. 2013. № 2. P. 66-67.*
- [4] TUKSHAITOV R.H., Aihaiti Yisihakefu // *Power of Tatarstan. 2013. № 4. P.55-58.*
- [5] TUKSHAITOV R.H., MALYSHEV V.B. // *New approaches to the design and control of LED lights // current issues of education and science . Sat scientific papers based on the International Scientific and Practical Conference . Tambov, 2014 . P. 122-123 .*
- [6] ALKHAMS YASSER S. A., TUKSHAITOV R.H. // *Materialy the reports XVIII of the international scientific and technical conference of students and graduate students "radio electronics, electrical engineering and power engineering". T. 1. Moscow: MEI, 2012. P. 180.*

## SOURCE OF HIGH POWER NANOSECOND ELECTROMAGNETIC EMISSION IN TERMS OF X-BAND SELFHEATED PULSED MAGNETRON

*P.YU. CHUMERIN\**, *V.N. SLINKO\**, *A.V. PERESIPKIN\**, *N.I. SKRIPKIN\*\**, *V.P. GUBANOV\*\*\**,  
*O.B. KOVAL'CHUK\*\*\**, *A.S. STEPCHENKO\*\*\**

*\*National Research Tomsk Polytechnic University, Lenin Avenue, 30, Tomsk, 634050, Russia,*  
[chumerinpy@tpu.ru](mailto:chumerinpy@tpu.ru), tel/fax 3822-41-74-51

*\*\*Scientific and production complex Pluton, N. Syromiatnicheskaya st.,11, Moscow, 105120,*

*\*\*\*Institute of High-Current Electronics, Akademichesky Avenue, 2/3, Tomsk, 634055, Russia*

The report represents the results of the elaboration of the impulsive energy source of high power nanosecond electromagnetic emission with resonant microwave compression pulses at the output of the X-band selfheated pulsed magnetron which is produced by Scientific and production complex Pluton. Concept of electric power supply of the magnetron construction, assembly scheme and basic specification were reviewed. Design of the resonant compression system was described. Results of the emission characteristics and principle energy and weight and dimensional features were enumerated.



**RESEARCHING OF THE RESONANT MICROWAVE COMPRESSION WITH USING SERIAL P-I-N DIODES IN THE MECHANISM OF THE SWITCH**

*P.YU. CHUMERIN\**, *V.N. SLINKO\**, *A.S. PERESIPKIN\**

*\*National Research Tomsk Polytechnic University Lenin Avenue, 30, Tomsk, 634050, Russia,  
chumerinpy@tpu.ru, tel/fax 3822-41-74-51*

The report represents the results of the research resonant microwave compression with using serial p-i-n diodes in the mechanism of the switch. Principles of the construction resonant compression systems of the X – band with the level of the output power 10 – 1000 kW were reviewed. Enumerated results of the testing features microwave compressions.

## THE RESEARCH OF THE RESONANT MICROWAVE PULSES COMPRESSION OF THE GUNN OSCILLATOR

P.YU. CHUMERIN\*, V.N. SLINKO\*, A.S. PERESIPKIN\*, V.I. YURCHENKO\*\*, V.A. KOCHUMEEV\*\*

\*National Research Tomsk Polytechnic University Lenin Avenue, 30, Tomsk, 634050, Russia,  
chumerinpy@tpu.ru, tel/fax 3822-41-74-51

\*\*Federal Research Institute of Semiconductors Divices Krasnoarmeyskaya st., 99a, 634034, Russia.

The report reviews the results of the first researches which is shows the possibility of the creation sources of the electromagnetic emission where power level is one kilowatt in X – band, by compression of the energy of the microwave pulses at the output Gunn oscillator. Systems of compression with supply by some Gunn oscillator were described and enumerated results of the testing variable microwave pulses.

## INVESTIGATIONS OF AN X-BAND OVERMODED CERENKOV HIGH-POWER MICROWAVE GENERATOR WITHOUT AN EXTERNAL MAGNETIC FIELD

*LIMING GUO\**, ZHIQIANG LI, TING SHU

\* College of Optoelectronic Science and Engineering, National University of Defence Technology,  
China, 410073, guoling@163.com,

Generally, Cerenkov microwave oscillator needs an external guiding magnetic field to confine the electron beams. The system of external magnetic is bulky and heavy. So scientists focus on how to decrease the magnetic field for obtaining a relatively light magnetic field system or even got rid of it. Russian researchers have done some simulation and experimental studies on the S-band relativistic Cerenkov oscillator without a guiding magnetic field<sup>[1-3]</sup>. But as we know, without an external magnetic field, the radial dispersion of the electron beam drifting along the axis would reduce the energy exchange between the electron flow and the electromagnetic field.

In order to improve the working band, an X-band overmoded ( $D/\lambda = 2.5$ ) Cerenkov high-power microwave generator without an external magnetic field is presented in this paper. By adding a constraining part to the cathode which does not emitting electron beam, the radial spread of the annular relativistic electron beam (REB) passing through the slow wave structure (SWS) is lowered and the output microwave power is also increased. The simulation results give the support of the assumption. As the cathode has an effect of focusing the REB, we call the name “focusing cathode” to symbolise it.

The annular REB emitted from the focusing cathode is induced into the resonant cavity by an anode foil with an absorption rate of 20%. When drifting along the axis, the REB is constrained in the radial direction by the electrostatic force of the focusing cathode’s constraining part. After passing through the nonuniform SWS, the electron beam is collected by a taper collector. Through optimizing the SWS and the radius of the output waveguide, a microwave with the power of 1.3GW and frequency of 9.2GHz was obtained under the diode voltage of 560kV, and electron beam current of 10kA in the simulation. The power conversion efficiency was 28%.

### REFERENCES

- [1] Eugene M. Totmeninov, Alexei I. Klimov, and Vladislav V. Rostov // *IEEE Trans. Plasma Sci.* – 2009. – 37. – № 7.
- [2] Eugene M. Totmeninov, Alexei I. Klimov, and Vladislav V. Rostov // *IEEE Trans. Plasma Sci.* – 2010. – 38. – № 10.
- [3] Eugene M. Totmeninov, Sergei A. Kitsanov, and Pavel V. Vykhodtsev // *IEEE Trans. Plasma Sci.* – 2011. – 39. – № 4.

## THE INFLUENCE OF THE DRIFT TUBE LENGTH ON THE STRUCTURE OF THE RADIATION FIELD OF MULTIWAVE CHERENKOV GENERATOR

V.A. CHEREPENIN, V.N. KORNIENKO

Kotelnikov's Institute of Radioengineering and Electronics RAS, Mochovaya st. 11, Moscow, 125009, Russia, E-mail korn@cplire.ru  
phone +7(495)6297678

It is well known that the radiation field of multiwave cherenkov generator has a complicated transverse structure [1]. It depends on many parameters. In particular, it has been shown that the predominance of symmetric modes in radiation field may depend on the quality of matching of the wave impedance at the cathode end of the electrodynamic structure (ES) [2].

Our task was to investigate the dependence structure of the radiation field from the geometric distance between the two sections of MVCG. To solve this problem, we used the methods of computational experiment. Numerical algorithm was based on the computational scheme described in [3].

We have considered the device similar in its design to the MVCG described in [1]. Its ES contains two sections of waveguide with periodic inhomogeneities. These sections are separated by the drift tube. Left and right ends of ES have good wave impedance match. The main parameters used in the simulation had the following values. Diameter of ES is 14 cm. Period of the spatial inhomogeneity of the circular waveguide is equal to 1.5 cm. First section contains 26 periods, second one – 8. Electron beam has initial energy which is 1.8 MeV. The current of beam is 16 kA. Lead magnetic field is 18 kGs.

The results of numerical simulation are presented on Fig.1.

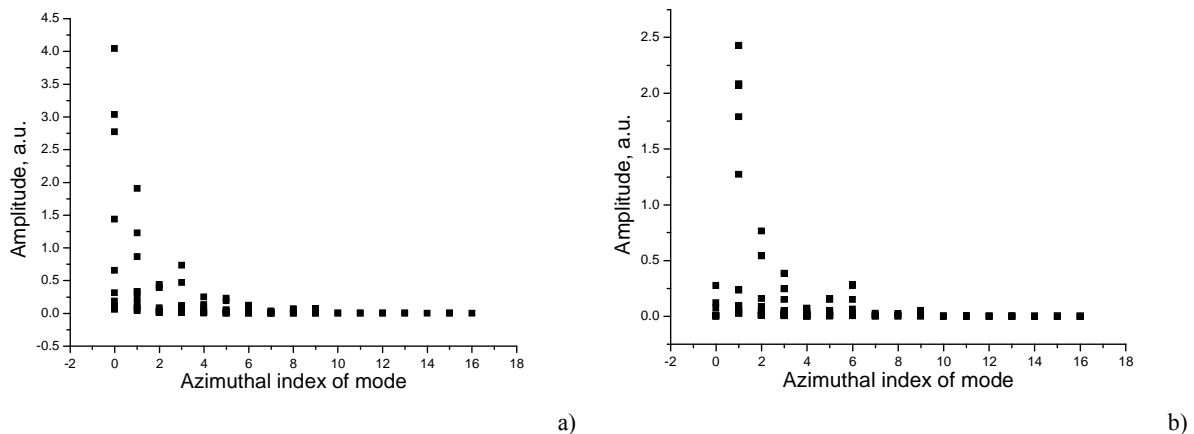


Fig. 1. *E*-mode amplitudes in the case when the length of the drift tube is 3.5 cm (a) and 4.5 cm (b)

As follows from the Fig.1, if the length of the drift tube is 3.5 cm, the axially symmetric modes are predominant. In case when the length is 4.5 cm, the *E*-mode with azimuthal index “1” has maximum amplitude.

Thus changing the length of the drift tube by an amount less than half the wavelength of radiation causes a significant change of the transverse structure of the radiation field.

### REFERENCES

- [1] S.P.Bugaev, V.I.Kanavets, V.I.Koshelev, V.A.Cherepenin. // Relativistic multiwave microwave oscillators. –Novosibirsk: Nauka, 1991.
- [2] V.A.Cherepenin, V.N.Kornienko // Izv.VUZov “PND”. – 2012. – V.20. - № 6. P.118-123.
- [3] Controlled Fusion. V.16 // Editor John Killeen. New York: Academic Press. 1976.

## INVESTIGATION OF GENERATION OF ELECTROMAGNETIC RADIATION IN A COAXIAL VIRCATOR WITH RADIALY DIVERGING BEAM

*T.V. KOVAL\**, *A.G. ZHERLITSYN\*\**, *G.G. KANAEV\*\**, *V.P.SHIYAN \*\**, *NGUYEN MAN' HUNG\**

*\*Institute of Cybernetics, Tomsk Polytechnic University, Lenin 30, Tomsk city, 634050, Russia, E-mail: tkoval@mail.ru*

*\*\*Institute of Physics and Technology, Tomsk Polytechnic University, Lenin 30, Tomsk city, 634050, Russia, E-mail: zherl@tpu.ru*

The paper presents the results of theoretical and experimental investigations of the generation of electromagnetic radiation in a coaxial vircator with radially symmetric diverging beam. The influence of the system geometry and beam parameters on the formation of a virtual cathode, radiation characteristics and mode structure. Theoretical studies were conducted using a numerical simulation method of large particles. The conditions of the main themes of the excitation wave in the resonance system with coaxial vircator diverging beam were defined. It is shown that with the help of the radiation pattern can determine the mode composition of the radiation beam and the degree of inhomogeneity.

The results of investigation of the excitation wave TEM in a coaxial vircator with its subsequent transformation into a wave of H10 rectangular waveguide are presented.

## PURIFICATION OF THE OUTPUT MODES OF OVERMODED RELATIVISTIC BACKWARD WAVE OSCILLATORS THROUGH MODE-COUPLED METHOD

*YUZHANG YUAN\**, JUN ZHAN, DIAN ZHANG

*\*College of Optoelectronic Science and Engineering, National University of Defense Technology, Changsha 410073, China, 1096437280@qq.com, +86 13739051841*

Because of the mode conversion effect at discontinuous position, successful suppression of mode competition in the beam-wave interaction process of an overmoded relativistic backward wave oscillator (RBWO) can not ensure the output modes purity. Optimizing the magnitude and the phase of the mode transmission coefficient in the device is significant for purifying the output modes. Based on that, a universal method of purifying the  $TM_{01}$  and  $TM_{02}$  mixed modes output through mode-coupled method by overmoded RBWO without decreasing the total output power is proposed in this paper. Through this method, the output  $TM_{01}$  and  $TM_{02}$  mixed modes with arbitrary power ratio can be purified into single  $TM_{01}$  mode.

### REFERENCES

- [1] Dian Zhang, Jun Zhang, Huihuang Zhong, Zhenxing Jin, and Yuzhang Yuan // *Physics of Plasmas* (1994-present) 21, 023115 (2014)
- [2] J. A. Nation // *Appl. Phys. Lett.* 17, 491 (1970).

## LONG TIME SYNCHRONIZATION OF RESONANT MICROWAVE COMPRESSORS BY LASER BEAM.

*M.S.ARTEEV, V.A. AVGUSTINOVICH, S.N. ARTEMENKO, V.L. KAMINSKY, S.A. NOVIKOV, YU.G. YUSHKOV.*

*PTI TPU, Lenina str.2 a, Tomsk, 634050, Russia, [arteev@tpu.ru](mailto:arteev@tpu.ru), (3822) – 417451.*

Resonant microwave compressors are fed by a single common source and have switches triggered by a laser beam. Conditions for obtaining the long operational time synchronization are studied experimentally. Possibility of the long operational time combining of output pulses in synchronism is ascertained and the synchronous operation of compressors strongly depends on identity degree of switching conditions that is the electric field strength in switching areas, insulating medium composition and rate of field amplitude variation in the storage cavities of compressors. Special conditions were created so the output pulse powers of 100 MW was reached by combining two pulses of 50 MW pulse power when the synchronous operation was held over 1,5 hours.

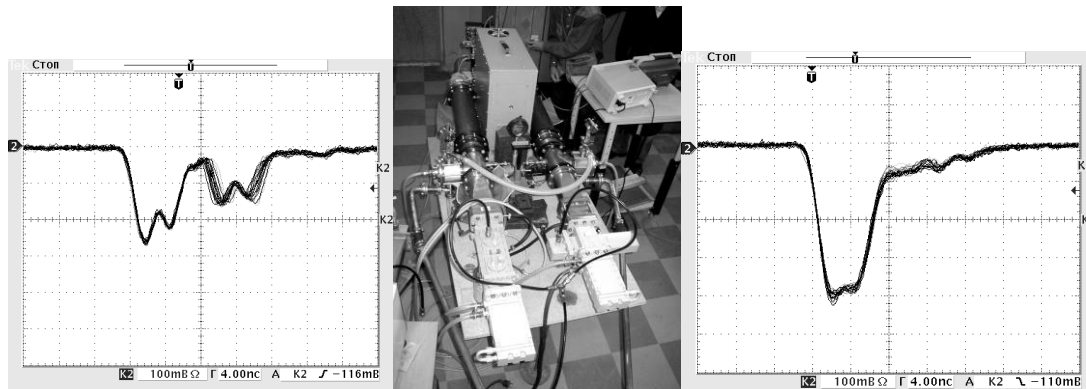


Fig.1. The external view of the experimental set including the laser and two synchronized microwave compressors. Oscillogramms of two separate pulses envelopes and the envelope of the total pulse observable over 1,5 hour.

## AMPLIFIER AND NOISE GENERATOR OF THE GHZ FREQUENCY BAND BASED ON THE PLASMA RELATIVISTIC MICROWAVE INSTALLATION

*I.E.IVANOV, P.S.STRELKOV, D.V. SHUMEIKO.*

*A.M. Prokhorov General Physics Institute of the Russian Academy of Sciences, 38 Vavilov Str., 119991 Moscow, +7, Russia,  
Phone:+7(499)135-2366,Fax:+7(499)135-0270, E-mail: iei@fpl.gpi.ru*

Injection of high-current relativistic electron beam into plasma waveguide produces a powerful microwave radiation with the possibility of "instantaneous" frequency tuning of the output radiation due to changes in the plasma density [1]. Such devices are called relativistic plasma microwave oscillators and amplifiers. The beam current is of  $\sim 2.5$  kA, electron energy is 500 keV. Output pulse duration of microwave radiation is equal to the duration of beam current pulse (500 ns), the average radiation power is 50 - 100 MW. The design of an amplifier differs from the one of an oscillator by the presence device of input microwave radiation (using a set of magnetrons at fixed frequencies) and using microwave absorber in the interaction space [2]. The microwave absorber allows you to create single passage mode system and get powerful output pulse at the frequency of the input radiation. The paper [2] shows the possibility of amplifying the external magnetron monochromatic signal to the level of the  $\sim 50$  MW with a gain of 30 dB. The major advantage of plasma systems is the possibility to amplify an input signal within a very wide bandwidth. If the input signal is absent, a intrinsic noise is amplified in the amplifier operating frequency band ( $\sim 2$  GHz). Thus, due to single passage mode gain (feedback cancellation) the installation moves to the generation of a noise pulse with a power of about 50 MW as in the case of amplification of the input monochromatic signal. Figure 1 a) shows the waveform of the electric field amplitude of the noise pulse with an energy of  $\sim 15.5$  J with direct recording high-speed oscilloscope (4 GHz). Microwave pulse consists of sequence uncorrelated trains lasting 3 - 5 ns, which corresponds approximately to the time of passage of wave to the length of the interaction space ( $\sim 70$  cm). Fig. 1 b) shows the Fourier spectrum of the noise signal obtained FFT-transformation of the signal (a).

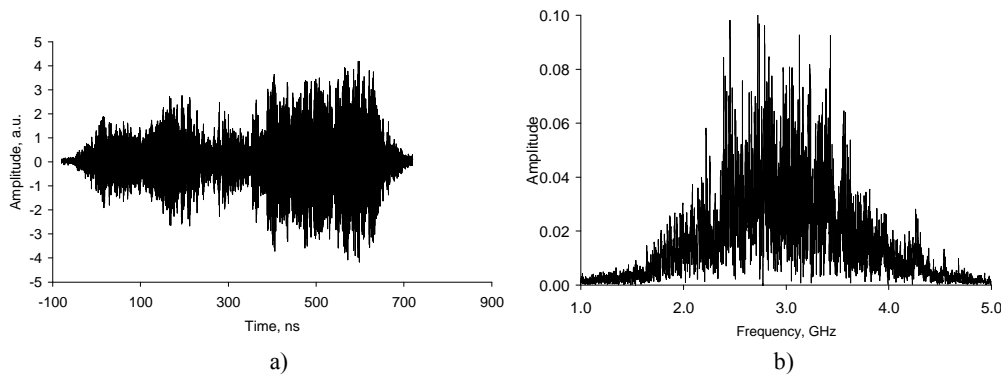


Fig. 1. Oscillogram of the radiation electric field (a) and b) is Fourier transform for signal (a).

### REFERENCES

- [1] *I.L.Bogdankevich, I.E.Ivanov, O.T.Loza, A.A.Rukhadze, P.S.Strelkov, V.P.Tarakanov, D.K.Ulyanov* // Plasma Phys. Reports. 2002, 28, 8, 690 – 698.  
[2] *P. S. Strelkov, I. E. Ivanov, and D. V. Shumeiko*// Plasma Physics Reports, 2012, 38, 6, 488 – 495.



## TWO-CHANNEL RF SOURCE BASED ON GYROMAGNETIC NONLINEAR TRANSMISSION LINES

*I.V. ROMANCHENKO, V.V. ROSTOV, V.YU. KONEV, A.V. GUNIN*

*Institute of High Current Electronics SB RAS, 2/3 Akademicheskii Avenue, Tomsk, 634055, Russia, E-mail: riv@lfe.hcei.tsc.ru, phone: (3822)491-391*

Recently we have demonstrated [1-2] that nonlinear transmission lines with bias saturated ferrites can be used for phase control of microwave pulses from two identical relativistic BWO in X-band and Ka-band. Picosecond stability of gyromagnetic NLTLs is more than enough to use themselves as oscillators in L-band for coherent power summation. In the report we present results of preliminary experiments with two gyromagnetic L-band NLTLs which are driven by split (2.0-2.5)-GW pulse from SINUS-200 high-voltage driver. The driver is equipped with a coaxial power divider and output transmitting lines with biased-saturated ferrites for controllable adjustment of the pulses delay. Two identical helix antennas are used for irradiation of rf pulses from NLTLs. General layout of the device is presented in Fig. 1.

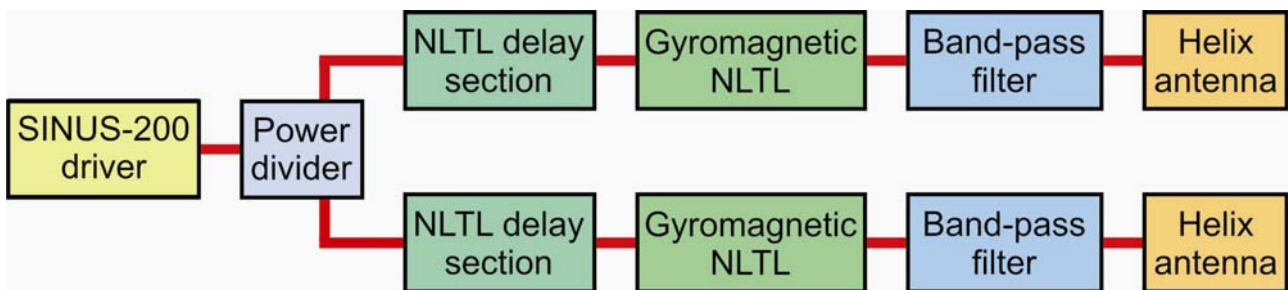


Fig. 1. Layout of two-channel RF source based on two gyromagnetic nonlinear transmission lines.

Signal measurements of the waveforms of RF pulses were carried out in a free space. The signal from individual NLTL's was detected and compared with integrated signal from both NLTLs. Near quadratic increase in the density of the power flux along the main radiation direction of the antenna system is proved. Stability of registered waveforms confirms the stable coherent superposition of the fields of two wave beams.

### REFERENCES

- [1] A. A. El'chaninov, et al. // Technical Physics. – 2011. – Volume 56. – № 1. – Pages 121–126.
- [2] K. A. Sharypov, et al. // Appl. Phys. Lett. – 2013. – Volume 103. – Pages 134103.

**INVESTIGATION ON CONDUCTION PROPERTIES OF HIGH CURRENT GAAS PCSS<sup>1</sup>***JIANG PING, LIU HONGWEI, YUAN JIANQIANG, LIU JINFENG, WANG LINGYUN, MA XUN, LI HONGTAO, XIE WEIPING**Key Laboratory of Pulsed Power, Institute of Fluid Physics, CAEP, P.O. Box 919-108, Mianyang 621900, China*

Abstract: Photoconductive semiconductor switches (PCSSs) show many potential applications for their advantages of high power capability, small volume, light-weight, high repetition rate, fast rise time, negligible time jitter, and perfect isolation. Thanks to non-linear working mode which makes laser diode as the trigger light source a possible solution and brings more flexibility, PCSSs with the mature material of GaAs crystal base have been widely investigated and show a good future. However, high current has always been a confliction referring to long working shots. This paper aims to find a balance between the high current and long working life. GaAs PCSSs with opposite electrodes are designed and tested. Triggering light energy is key parameter affecting the peak conduction current. Experiment reveals that higher current is obtained under larger energy, which peak value over 2.42kA has been acquired under 1.62mJ. Peak conduction current decreases by stages with the increase of working shots, which is 1.83kA after  $7 \times 10^5$  shots only 76% of the initial value. Resistance of the GaAs PCSS is found to vary with ambient conditions (light), bias voltage and working shots as well as bias voltage. Resistance under light is always lower than dark resistance, which is connected with the change of free electron number density. By the combined action of Negative differential effect, carrier mobility and electric field, dark resistance has a maximum value under certain voltage. With the increase of working shots, dark resistance is apt to become lower. Current filaments and the damage at the electrode ohm contact area are deemed to be the possible reasons leading to the performance degradation of the PCSS.

## REFERENCES

- [1] Liu Xisan // High pulsed power technology. – National Defense Industry Press, 2005.
- [2] William Charles Nunnally // IEEE transactions on plasma science. – 2005. – 33. – 4. 1262-1267.
- [3] Rahul Gunda, David S. Gleason, et al. // IEEE transactions on plasma science. – 2006. – 34. – 5. 1697-1701.
- [4] Ryutov D D, Derzon M S, Matzen M K // Reviews of Modern Physics. – 2000. – 72. – 1. 167-223.
- [5] Loubriel, G.M, Zutavern, F.J, et al // IEEE transactions on plasma science. – 1997. – 25. – 2. 124-130.
- [6] Zutavern F J, Armijo J C, et al // Proceedings of the 14th IEEE International Pulsed Power Conference. –2003. 591-594.
- [7] Steven F.Glover, Fred J.Zutavern, et al // IEEE Transactions on Plasma Science. – 2010. – 38. – 10. 2701-2707.
- [8] M.J. Cich, R. Kaplar, et al // IEEE. – 2007. 236-239.
- [9] T.A. Saiz, et al // IEEE International Pulsed Power and Plasma Science Conference. – 2007.
- [10] Liu Hongwei, Yuan Jianqiang, et al // High Power Laser and Particle Beams. – 2010. – 4. 795-798.
- [11] Loubriel, G.M; Zutavern, et al // IEEE Transactions on Plasma Science. – 1998. – 26. 1393-1402.

<sup>1</sup> This work was supported by a grant from Sichuan province leaders in academic and technical training project funding, as well as by a grant from the development of science and technology fund of china academy of engineering physics (2013B0402061). Tel: 86-0816-2484120. E-mail: jiangping303@126.com

## EXPERIMENT STUDY OF CONICAL MAGNETICALLY INSULATED TRANSMISSION LINE ON A 10-STAGE LINEAR TRANSFORMER DRIVER<sup>1</sup>

*GUO FAN, ZOU WENKANG, CHEN LIN, XIE WEIPING*

*Key Laboratory of Pulsed Power, Institute of Fluid Physics, CAEP, P.O. Box 919-108, Mianyang 621900, China, 394560789@qq.com, +86 13981127789*

Power flow in a conical magnetically insulated transmission line(MITL) has been studied on a 10-stage linear transformer driver(LTD) which had been constructed. This LTD generator is a magnetically insulated inductive voltage adder and composes 10 identical stages, each of which can give 100 kV/100 kA pulse on a matched load. The current transport efficiency has been studied when the conical MITL operated at both line limited region and load limited region. The experiment results show that the anode current can be efficiently transported in a conical MITL, but the cathode current has unavoidable loss current in both line limited region and load limited region.

### REFERENCES

- [1] *J. P. VanDevender*. Journal of Applied Physics, **50**(6), (1979) ,p3928-3934.
- [2] *P. F. Ottinger, J. W. Schumer*. Physics of Plasmas, **13**, 063109 (2006).
- [3] *D.V. Rose, D. R. Welch, E. A. Madrid, et al*. Physical review special topics-accelerator and beams, **13**, 010402 (2010).

---

<sup>1</sup> This work was supported by the Science Foundation of China Academy of Engineering Physics, China (Grant No.2013B0402060).

## A NOVEL MULTI-OUTPUT PULSED POWER SYSTEM AND ITS POWER SYNTHESIS

*YUE ZHAO\*\*\*, LIN CHEN\*\*, LIANGJI ZHOU \*\**

*\*China Academy of Engineering Physics, Mianshan Road, Mianyang, 621900, China, zy820314001@163.com, 08608162484120*

*\*\*University of Science and Technology of China, Huangshan Road, Hefei, 425900, China*

This paper describes a novel multi-output pulsed power system using a Transmission-Line-Transformer (TLT) based multiple-switch technology, which consists of 36 40nF 120kV high voltage capacitors, 36 low inductance high-pressure gas spark switches and 216 150kV 75Ω coaxial cables. The multiple switches are interconnected in series via a transmission line transformer (TLT), in such a way that the breakdown of all switches can be synchronized automatically by overvoltage, like in a Marx generator, and only one fifth or a quarter of all switches requires external synchronization trigger.

To gain insight into the principles and characteristics of this technology, an equivalent circuit model was developed. The simulation shows that when capacitors are charged to 120kV the 75Ω matched load can get a overdamped sinusoidal pulse, with a peaking voltage as high as 90kV, a pulse width approximately 300ns, and a risetime no more than 30ns. It was found that the closing of the first switch will overcharge the other switch, which subsequently forces the following to close. During this process, the discharging of capacitors is prevented due to the high secondary mode impedance of the TLT. When the closing process is finished and all switches are closed, the energy storage capacitors discharge simultaneously into the load(s) via the TLT. An interesting feature of this topology is that the voltage on any part of whole configuration will not exceed the capacitors charged voltage, which is unlike in a Marx generator.

To demonstrate this technology, a one ninth prototype system was developed. The prototype has four high-pressure gas spark switches, four 40nF 100kV polypropylene film pulse capacitors and 24 75Ω 100kV high voltage coaxial cables. There are several modes to synthesize the output side power, the TLT can be put in series for high-voltage generation, or in parallel to produce a large current pulse, or can be used to drive independent loads. The high voltage pulses even can be feed-in a induction voltage adder via high voltage coaxial cables, it is convenience to add a voltage as high as several megavoltage. The prototype was tested and the experiment showed an 80kV peak overdamped sinusoidal pulse voltage with 30ns risetime in load.

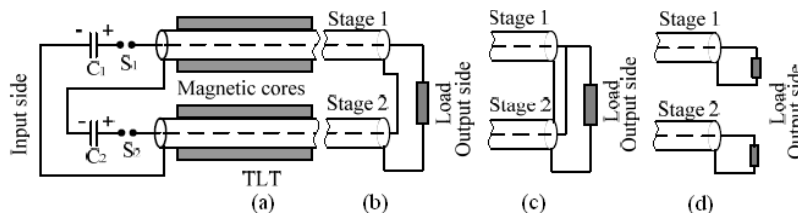


Fig. 1. (a) Schematic TLT structure; (b) With a series output; (c) With a parallel output; (d) With independent loads;

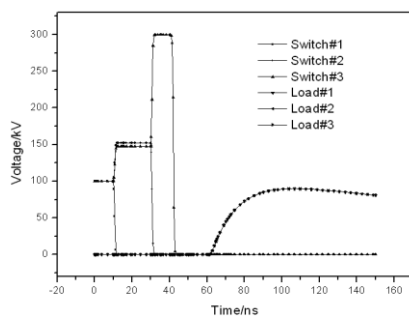


Fig.2. Switch and load voltages

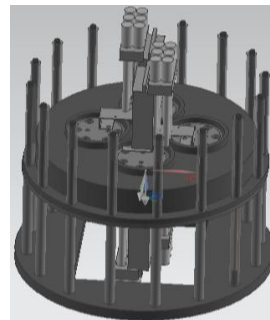


Fig.3. 3D schematic structure of TLT prototype

### REFERENCES

- [1]Z. Liu, A. J. M. Pemen, R. T. W. J. van Hoppe, G. J. J. Winands, E. J. M. van Heesch//IEEE Transactions on Dielectrics and Electrical Insulation, Vol. 16, pp.928-925,(2009).
- [2]Z. Liu, A. J. M. Pemen, E. J. M. van Heesch, K. Yan, G. J. J. Winands, D. B. Pawlok //11th International Conference on Electrostatic, 2012, pp:704-708.
- [3]K. Yan, H. W. M. Smulders, P. A. A. F. Wouters, S. Kapora, S. A. Nair, E. J. M. van Heesch, P. C. T. van der Laan, and A. J. M. Pemen. Journal of Electrostatics, Vol.58, 221-228,(2003).
- [4]Z. Liu, K. Yan, A. J. M. Pemen, G. J. J. Winands, and E. J. M. Van Heesch. Review of Scientific Instruments, Vol. 76, 2005.
- [5]K. Yan, E. J. M. van Heesch, S. A. Nair, and A. J. M. Pemen. Journal of Electro- statics, Vol.57, pp:29-33,(2003).

## SUPERFAST HIGH VOLTAGE THYRISTOR SWITCH

*A.I. GUSEV, S.K. LYUBUTIN, S.N. RUKIN, S.N. TSYRANOV*

*Institute of Electrophysics UB RAS, 106 Amundsen Str., Ekaterinburg, 620016, Russia, E-mail: rugin@iep.uran.ru*

A possibility of fast subnanosecond triggering of commercial low-frequency thyristors has been investigated. In experiments low  $dI/dt$  (200-400 A/mks) tablet thyristors having a silicon wafer of 32 to 40 mm in diameter and 2 kV DC operating voltage were used. For the thyristor triggering a fast subnanosecond pulse was applied across its main electrodes. During the switching process the voltage across 2 kV DC thyristor increased from 2 to 6 kV in about 600-800 ps, and then dropped to 50-100 V in about 300-400 ps. Under such conditions the thyristor closing process occurred due to initiation and propagation of fast ionization front across the semiconductor structure.

A stack of 6 thyristors connected in series operated at 12-kV charging voltage and switched 2-mkF capacitor bank into resistive load of 0.17 Ohm. At total circuit inductance of 110 nH the following discharge parameters were obtained: a peak current was ~29 kA,  $dI/dt$  was up to 100 kA/mks, FWHM was ~1 mks, and a peak power in the load attained 150 MW.

The paper will discuss the experimental circuitry and results obtained. The results of numerical simulations of the thyristor switching process will also be given.

**24 KV/75 KA HIGH CURRENT PROTECTION INDUCTOR ON 1 mH**

*A.V. KHARLOV, B.M. KOVALCHUK, E.V. KUMPYAK, G.V. SMORUDOV, N.V. TSOY*

*Institute of High Current Electronics, Tomsk, Russia, (7)-382-2492673, akharlov@lef.hcei.tsc.ru*

High voltage, high current inductors are required for many high pulsed power systems, incorporating capacitor banks. Those inductors simultaneously serve both as a pulse shaping and protection element in R-L-C circuits. A 25 kV/70 kA protection inductor on inductance of 1 mH with low stray field was designed, manufactured and tested. It was designed as a quasi-toroidal system, consisting of 4 coils (with 0.25 mH inductance each) evenly distributed in the perimeter of a square. The structure of coils was optimized to withstand a huge electromagnetic force produced by the 70 kA current. The 0.25 mH coil is made as multy-layer solenoid (6 layers) from cupper wire ( $6 \times 4 \text{ mm}^2$  net cross-section in copper) with fiberglass insulation. Layers are connected in parallel in order to decrease active resistance of the coil. This 0.25 mH inductor was tested at 70 kA peak current with a pulse length of  $\sim 20 \text{ ms}$ , which corresponds to the action integral  $\sim 32 \cdot 10^6 \text{ A}^2\text{s}$ . In this report, we present design of these inductors, describe the test bed, and present the test results.

## MODERNIZATION ON THL-100 A HYBRID FEMTOSECOND LASER SYSTEM<sup>1</sup>

V.F. LOSEV\* \*\*, E.N. ABDULLIN\*, S.V. ALEKSEEV\*, M.V. IVANOV\*, N.G. IVANOV\*, G.A. MESYATS\*\*\*, YU.N. PANCHENKO\*, AND N.A. RATAKHIN\*

\*Institute of High Current Electronics SB RAS, 2/3 Akademicheskoy Ave.,  
Tomsk, 634055, Russia, losev@ogl.hcei.tsc.ru (3822)491891

\*\*Tomsk Polytechnic University, 30 Lenin Ave., 634034 Tomsk, Russia

\*\*\*P.N. Lebedev Physical Institute of Russian Academy of Sciences, Leninsky Prospekt, 53, 119991 Moscow, Russia

This paper reports the modernization results of THL-100 multi-terawatt hybrid laser system of visible range [1, 2]. Also the laser system consists of a two basic parts - Start-480M titanium-sapphire starting complex and photochemical XeF(C-A) amplifier with a 24-cm aperture – both parts were improved. The purpose of upgrade was the increase of output laser system power. For it the energy of a starting complex was increased at 4 times by the use of additional titanium-sapphire amplifier which is pumped by second harmonic (532 nm) of Nd:laser with 0.7 J energy and 10 ns pulse duration. Also the dimensions of a grating compressor and prism stretcher were increased to ensure the optimal radiation intensity. In addition the quality of laser beam of a starting complex was improved by means of using of the spatial filters. To decrease the nonlinear effects in XeF(C-A) amplifier the thickness its input window of was decreased with 40 mm to 3 mm. The plane-parallel plate of output window was changed on wedge with 1 degree angle to decrease the interference effects of output laser beam. The femtosecond laser beam was amplified in the XeF(C-A) amplifier. The 32 round mirrors used in a multipass optical scheme (33 passes) of the XeF(C-A) amplifier have been replaced with new. The mirrors reflectance was 99.7 %. A photo of the XeF(C-A) amplifier is shown in Fig. 1.



Fig. 1. General view of the XeF(C-A) amplifier.

The laser beam parameters of the titanium-sapphire starting complex and photochemical XeF(C-A) amplifier after modernization will be reported on the conference.

### REFERENCES

- [1] Alexeev S.V., Ivanov N. G., Kovalchuk B.M., Losev V.F. Mesyats G.A., Mikheev L.D., Panchenko Yu.N., Ratakhin N.A., and Yastremsky A.G. // Atmospheric and Oceanic Optics. – 2012. – 25. – 221-225.
- [2] S.V. Alekseev, A.I. Aristov, N.G. Ivanov, B.M. Kovalchuk, V.F. Losev, G.A. Mesyats, L.D. Mikheev, Yu.N. Panchenko, and N.A. Ratakhin // Laser and Particle Beams. – 2013. – 31. – 17-21.

<sup>1</sup> This work was supported by RFBR (projects No. 13-08-00068, 13-08-98038-r\_sibir\_a, 14-08-00511)

## **GENERATION OF GIGAWATT PULSES WITH SUBNANOSECOND RISE TIME BY SEMICONDUCTOR SWITCHES**

*A.I. GUSEV, S.K. LYUBUTIN, M.S. PEDOS, B.G. SLOVIKOVSKY, S.P. TIMOSHENKOV, S.N. RUKIN, S.N. TSYRANOV*

*Institute of Electrophysics UB RAS, 106 Amundsen Str., Ekaterinburg, 620016, Russia, E-mail: rugin@iep.uran.ru*

A process of high-power current switching by Si semiconductor diodes has been experimentally implemented and theoretically studied. In the experiments in 50-Ohm oil-filled coaxial transmission lines with outer diameters of 50 to 100 mm, we have obtained 300 to 450-kV output pulses (up to 4 GW peak power) having a 300 to 400-ps rise time. All-solid-state SOS-driver with output voltage of 500 kV was used as a charging source forming an initial pulse with a few ns rise time. The pulse was sharpened further in the transmission line by series connected diodes, which switching process is based on the formation and propagation of a fast impact ionization front in the base of the diode.

The paper will discuss the experimental circuitry, design of the semiconductor switches, and the results obtained. The results of numerical simulations of the sharpeners switching process will also be given.



**TOROIDAL CORE PULSE TRANSFORMER WITH AN OUTPUT VOLTAGE OF 1.2 MV**

*A.V. LAVRINOVICH, A.A. KACHALCOV, and V.K. PETIN*

*Institute of High Current Electronics  
Siberian Branch of Russian Academy of Sciences  
Tomsk, Russia, tel. 83822491520, lavrinovich86@yandex.ru*

A sufficiently rather compact pulse transformer with a closed toroidal core was manufactured for charging a forming line up to 1.2 MV in 600–700 ns. The pulse transformer is a metal container of overall diameter 930 mm and length 626 mm. In the container, there is a closed toroidal core wound with a transformer steel strip 50  $\mu\text{m}$  thick and a secondary transformer winding. The primary winding has a single turn onto which two parallel-connected capacitors are discharged. The turn is formed by six high-voltage bushings and transformer container. Two parallel-connected secondary windings (each with 20 turns) are made of duralumin strip 8 mm thick profiled across its width to provide the same space between the turns. One end of the secondary winding is grounded and the other is connected with the forming line via a spring contact. For stabilization of the parameters of formed pulses, magnetization reversal of the core is used.

The transformer was tested at a voltage of 1.15 MV with no breakdown in more than 100 shots.

The problem in testing the toroidal core pulse transformer was in providing electrical insulation of its elements at a voltage across the secondary turn of 1.15 MV and duration of the applied voltage pulse of 600–700 ns.

## INFLUENCE OF THE SECONDARY ELECTRON EMISSION ON THE BREAKDOWN FORMATION TIME IN THE SWITCHES BASED ON THE OPEN DISCHARGE

P.A. BOKHAN, P.P. GUGIN, M. A. LAVRUKHIN, D. E. ZAKREVSKY

A. V. Rzhanov Institute of Semiconductor Physics SB RAS, Novosibirsk, Russia, [lavrukhin@isp.nsc.ru](mailto:lavrukhin@isp.nsc.ru)

The report is devoted to the study of a new type of the high-voltage subnanosecond switches (kivotrons) based on the open discharge [1]. These devices are gas switches with a small recovery time of the dielectric strength and a high peaking degree (~ 100) which allows them to produce pulses with subnanosecond wavefronts at frequencies up to 100 kHz, using as the primary sources generator with a voltage rise time of ~ 40 ns.

Results of experimental studies of the kivotrons with cathodes having a high coefficient of secondary electron emission are presented. With using such materials it is possible to significantly reduce the switching time and increase the peaking degree, which reduces the requirements for primary generators. The mechanism of accelerating the formation of the breakdown due to the secondary electron emission is discussed.

### REFERENCES

[1] Bokhan P.A. et al. // *Phys. Plasmas*. 2013. Vol. 20. № 3. P. 033507.

## APPLICABILITY EVALUATION OF HIGH VOLTAGE DISCHARGE TO DEMOLITION THE NUCLEAR DEBRIS

*K. UEMURA\**, *N. YAZAWA\*\**, *K. YANO\*\*\**, *V. KUKHTA\**

*\*ITAC Ltd. Shinmaywa 1-1, Takarazuka, 665-0052, Japan, [kensuke\\_uemura@itac-j.co.jp](mailto:kensuke_uemura@itac-j.co.jp), +81-90-3087-495*

*\*\*Hitachi General Electric Nuclear Energy Co., Ltd. 3-1-1 Saiwai-cho, Hitachi City, Ibaraki-ken, 317-0073, Japan*

*\*\*\*Japan Atomic Energy Agency, 4-49, Muramatsu, Tokai-mura, Naka-gun, Ibaraki-ken, 319-1184, Japan*

On the semi-nuclear debris samples consisted with the solid solution of (Zr, U)O<sub>2</sub> having the known 3 crystal structures of Cubic, Tetragonal and Monolithic, the characteristics of Porosity, Hardness and Electric Conductivity were measured, that are referred to the applicability evaluation for high voltage discharge demolition of nuclear debris. The measured characteristics were evaluated against the case histories of non-electro conductive materials demolition in Russia, Japan and Germany. The measured resistance of the said solid solution was the magnitude 10<sup>3</sup> ohm · cm or over and the value indicates the possibility to apply the high voltage discharge for the demolition of nuclear debris in case of damaged Fukushima Nuclear Power Plant.

**EXAMINATION OF TWO VARIANTS OF MPOS/LCD CONCATENATION IN THE EXPERIMENTS WITH DOUBLE GAS PUFFS ON THE GIT-12 GENERATOR**

V.A. KOKSHENEV, A.YU. LABETSKY, A.V. SHISHLOV, N.E. KURMAEV, F.I. FURSOV,  
R.K. CHERDIZOV

*Institute of High Current Electronics SB RAS, 2/3 Akademichesky Ave., Tomsk, 634055, Russia  
E-mail: [vak@oit.hcei.tsc.ru](mailto:vak@oit.hcei.tsc.ru)*

This paper is devoted to the development of devices forming fast-rising current pulses in a strongly radiating load. Two variants of the elements concatenation in a scheme consisting of the current generator (CG), the microsecond plasma opening switch (MPOS), the load current doubler (LCD) and a gas-puff load (GP) were investigated: **CG+MPOS+LCD+GP** (variant #1) and **CG+LCD+MPOS+GP** (variant #2). The experiments were carried out on the GIT-12 current generator. The double-shell **neon** gas puffs were used as a load. In the first operating mode (**CG+MPOS+LCD+GP**), the current in a load with the initial inductance of 9.5 nH reached the value of 4 MA and the current rise time was about 300 ns. In the second mode (**CG+LCD+MPOS+GP**), the switched current was up to 4.5 MA and the current rise time was ~100 ns. Usage of the current doubling circuit in combination with the plasma-dynamic switch allows increasing the rate of growth and the amplitude of current in the radiating load. The obtained in test experiments K-shell radiation yield of ~10 kJ/cm and a terawatt-level power allow expecting improvement of radiation characteristics of a last scheme in case of the load optimization.

## SANDIA-HIGH CURRENT ELECTRONIC INSTITUTE (HCEI) COLLABORATION IN FAST LTD DEVELOPMENT<sup>1</sup>

*M. G. MAZARAKIS, B. BUI, S. R. CORDOVA, M. E. CUNEO, R. J. FOCIA, W. A. FOWLER, F. R. GRUNER, B. T. HUTSEL, M. D. JOHNSTON, M. L. KIEFER, J. LECKBEE, F. W. LONG, D. J. LUCERO, D. H. MCDANIEL, G. R. MCKEE, J. MCKENNEE, T. D. MULVILLE, D. S. NIELSEN, B. V. OLIVER, J. L. PORTER, S. A. ROZNOWSKI, M. E. SAVAGE, B. STOLTZFUS, W. E. STRUVE, W. A. STYGAR, P. E. WAKELAND, T. J. WEBB, D. ZISKA*

*Sandia National Laboratory, PO Box 5800, Albuquerque N. M. 87185, mgmazar@sandia.gov*

Following the impressive operational success of the first slow (~1 microsecond) LTD in Gramat, France, that was invented, designed and built by the team at HCEI headed by Boris Kovalchuk (B. M. Kovalchuk, *et al.*, Fast primary storage device utilizing a linear pulse transformer. Russian Physics Journal, 1997, vol. 40, No. 12, pp. 1142-1153), Dillon McDaniel of Sandia asked the inventors if they could apply this technology for the production of fast ~100 ns pulses for Z-pinch research. The inventors accepted the challenge, and a number of communications (unfortunately unpublished) were exchanged between Sandia and HCEI on how the fast LTDs could be used for this research.

The idea of the fast (~100 nanosecond) LTD was suggested in 1998 a meeting in Gramat, France. (A. A. Kim, not published), the premise of that suggestion was to assemble a number of identical sections (today called bricks) consisting of small capacitors, positioning them evenly around the axis of a circular cavity, and triggering them simultaneously connected in parallel to a common load. The first published theoretical analytical study of such fast LTD,s was presented in the 1999 Pulsed Power Conference in Monterey, California (M. G. Mazarakis *et al.*, A compact, high-voltage e-beam pulser. In Proc. 12<sup>th</sup> Pulsed Power Conf., Monterey, California, p. 412). This paper attracted a lot of interest in the pulsed power community, resulting in a large number of requests for copies. Following that, a strong collaboration started between Sandia and HCEI which culminated in the production of 10 of the largest to-date 1 MA, 1 GW fast LTD cavities which compose now the Mykonos voltage adder at Sandia.

The different stages of the fast LTD development through the years and the up-to-date accomplishments will be presented. Although this technology has mushroomed around the globe, this paper will concentrate solely in the Sandia-HCEI collaboration.

<sup>1</sup> Sandia is a multiprogram laboratory managed and operated by Sandia Corporation, a wholly owned subsidiary of Lockheed Martin Company, for the United States Department of Energy's National Nuclear Security Administration under Contract No. DE-AC04-94AL85000.

## STABILITY OF THE PULSE SHAPE IN SQUARE PULSE LTD'S WITH 5<sup>TH</sup> HARMONICS<sup>1</sup>

*V.M. ALEXEENKO\**, *S.S. KONDRATIEV\**, *S.V. VASILIEV\**, *V.A. SYNEBRYUKHOV\**, *A.A.KIM\*\*\**,  
*M.G. MAZARAKIS\*\*\**, *J. LECKBEE\*\*\**, *M. L. KIEFER\*\*\**

*\*Institute of High Current Electronics SB of RAS, Academichesky Ave. 2/3, Tomsk 634055, Russia,  
alekseenko\_ym@mail.ru, (3822)493159*

*\*\*National Research Tomsk Polytechnic University, Lenin Ave. 30, Tomsk 634050, Russia*

*\*\*\*Sandia National Laboratories, P.O. Box 5800 Albuquerque, NM 87185, USA*

The Square Pulse LTD's produce the quasi-rectangular output pulse, the rise time and the top length of this pulse depend on the configuration of such LTD's. The rise time decreases, and the flat-top length increases with the number of higher harmonic bricks in the cavity [1]. However, increasing the number of the higher harmonic bricks affects the output pulse shape stability. This is mainly due to the time jitter of the spark gap switches of those bricks.

In this report we will present the simulated statistical variation of the output pulse shape produced by the Square Pulse LTD,s containing 1<sup>st</sup>, 3<sup>rd</sup> and 5<sup>th</sup> harmonic bricks. A number of different time jitters will be considered and their influence on the pulse stability will be discussed.

### REFERENCES

- [1] A.A. Kim, et.al., Square Pulse LTD with 5<sup>th</sup> harmonic bricks. In Proc.PPPS-2013, June 16-21, 2013, San Francisco, California, USA, to be published

<sup>1</sup> This work was supported by Sandia NL, USA, under the contract #1370056.

## ENERGY COUPLING BETWEEN THE LC-CIRCUIT AND THE DYNAMIC Z-PINCH LOAD: ANALYTICAL APPROXIMATION<sup>1</sup>

*A.A.KIM\*\*\*, V.I. ORESHKIN\**

*\*Institute of High Current Electronics SB of RAS, Academichesky Ave. 2/3, Tomsk 634055, Russia, kim@oit.hcei.tsc.ru, (3822)492751*

*\*\*National Research Tomsk Polytechnic University, Lenin Ave. 30, Tomsk 634050, Russia*

The problem of energy coupling between the LC-circuit and the dynamic Z-pinch load is important for the designing the efficient Z-pinch drivers based on LTD technology. This problem was independently solved parametrically in [1,2], but for better understanding and visualization of the solution it is useful also to investigate this problem analytically, derive an approximate analytical solution and determine its accuracy.

In the report we will present such an analytical solution for the case

$$\frac{\Delta L_{\max}}{L_G + L_0} < 1, \quad (1)$$

where  $\Delta L_{\max}$  is the peak variation of the Z-pinch inductance,  $L_G$  the inductance of the LC-circuit, and  $L_0$  the initial inductance of the Z-pinch. The restrictions of the Eq. 1 will be discussed, and the comparison between the analytical and parametrical solutions will be presented.

### REFERENCES

- [1] *J. Katzenstein* // Journal of Applied Physics. – 1981. – Volume 52. – № 2. Pages 676-680.
- [2] *V.I. Oreshkin* // Technical Physics Letters. – 2013. – Volume 39. – Issue 8. Pages 669-672.

<sup>1</sup> This work was supported in part by INPC CAEP, China, under the contract №12JC02701RU.

## POWER FLOW IN THE POS-TO-LOAD TRANSITION REGION

*S.V. LOGINOV*

*Institute of High Current Electronics SB RAS, 2/3 Akademicheskoy ave., Tomsk, 634055, Russia, loginov@oit.hcei.tsc.ru*

The creation of terawatt plasma radiation sources has long been pursued through developing and verifying the pulse compression technology with an intermediate inductive store and a plasma opening switch (POS). The POS is attractive for its very simple design being a vacuum coaxial segment filled with fully ionized plasma. During the conduction phase, the switch separates the load from the energy store; at a certain current, the switch resistance increases sharply, thus providing fast energy transfer to the load.

The development of POSs requires solving three interrelated problems. The first problem is to determine the mechanism of magnetic field transport through a plasma bridge [1]. This process defines the switch conduction time and hence the inductor stored energy. The second problem is to ascertain the causes for current interruption and the factors responsible for the rate of energy delivery to a load [2]. This problem is critical for prospects of the technology. Experiments show that energy transfer occurs when a switch-to-load transition region of rarefied plasma exists. For this reason, the second and third problems go hand and hand and consist in providing minimum energy loss. Substantiated solutions of the above problems are in great demand because they can uncover capabilities of the technology used in designing megaampere setups with microsecond current rise times.

The chief cause for low-efficiency energy transfer from an inductive energy store to a short-circuit load is insufficient switch resistance on current interruption. Additionally, the efficiency is lowered due to the presence of a switch-to-load transition region of rarefied plasma. This region can be formed even in preliminary plasma injection due to plasma stream reflection from the switch electrodes. However, a decisive factor for the formation of the region is the multicomponent ionic composition of the plasma bridge. The axial electric polarization field separates the ions by hydrogen-carbon plasma aggregation, and the hydrogen ions thus take the lead over the carbon ions in their motion to the load. As a result the current channel, when passed through the region of initially injected plasma, enters the region of rarefied hydrogen plasma. If the current channel, in this case, reaches the state necessary for plasma erosion, the transition region will fail to stop this process. To do this requires that the plasma density in the channel is an order of magnitude higher than that in the transition region. Subject to this proviso, the decrease in saturation current with a decrease in channel width, due to magnetic insulation of electrons, exceeds its increase induced by the increase in density in rarefied plasma aggregation. However, the transition region severely impedes the energy transfer to the load because this region provides conditions for passage of magnetized electron flow which is escaped from the erosion gap on opening of the switch.

Uncontrollable formation of the transition region is a typical process for microsecond megaampere switches which complicates matching an energy store and a load. The spatial plasma distribution thus depends largely on the embodiment of the transition region, and its optimization, as a rule, is made experimentally. This report provides analysis of the GIT-4 experiments aimed at defining the capabilities of POSs for energy transfer to a load of inductance comparable to the inductance of the energy store vacuum section. The analysis is performed using the substantiated technique [3] which allows quantitative estimation of the POS efficiency. Section 2 describes tested versions of the transition region. Section 3 presents experimental results, their discussion, and generalization. Section 4 gives concluding remarks on the possibilities of POS application for effective energy transfer to a load. Under the same conditions with a conduction current of  $\sim 1$  MA and POS voltage of  $\sim 1$  MV, the energy transferred to the load depends strongly on the transmission line design. The transition region of rarefied plasma severely impedes the energy transfer to a load. The intense electron flow in this switch-to-load transition region results in additional plasma production on the cross-sectional irregularities of the load. This can eventually lead to cutoff of the load from the energy store.

### REFERENCES

- [1] *Loginov S.V. // Phys. Plasmas. – 2011. – Vol. 18. – № 10. – p. 102104 (6 pp.).*
- [2] *Loginov S.V. // J. Plasma Phys. – 2013. – Vol. 79. – № 3. – pp. 321–326.*
- [3] *Loginov S.V. // IEEE Trans. Plasma Sci. – 2011. – Vol. 39. – № 12. – pp. 3386–3390.*



## A HIGH-VOLTAGE IGBT-BASED SWITCH<sup>1</sup>

*A.V. PONOMAREV, A.I. GUSEV, M.S. PEDOS, Y.I. MAMONTOV*

*Institute of Electrophysics, Ural Branch, Russian Academy of Sciences,  
Ekaterinburg, Russia, e-mail: apon@iep.uran.ru*

The high-voltage IGBT-based switch has been developed and experimentally studied. Blocking voltage reaches 20-kV while the maximum pulse current is up to 350 A. The switch can be used for unipolar or dumping harmonic oscillation pulses formation.

Within this paper the electrical circuit diagram and parameters of the switch operations as well as examples of application are described.

---

<sup>1</sup> This work was partially supported by RFBR, research project No. 13-08-00255-a.

## STUDIES OF DEPENDENCE OF CATHODE PLASMA JET VELOCITY ON DESIGN OF ELECTRODE ARRAY IN A LOW INDUCTANCE VACUUM SPARK

BEKLEMISHCHEV A.V., GORBUNOV S.P., PAPERNY V.L. \*, SEMENOV D.B.

\*Irkutsk St. University, 1, K.Marx Str., Irkutsk, 664003, Russia, [paperny@math.isu.runnet.ru](mailto:paperny@math.isu.runnet.ru), +7(3952)521242

Ion velocity of a plasma jet is important parameter for many applications i.e. pulsed plasma thrusters, vacuum switches and so on. This work presents results of experimental studies of the process of ion acceleration in a low inductance vacuum spark. Measurements of the ion velocity were made by time-of-flight (TOF) method at different interelectrode gap and different shape of the anode. A low-inductance capacitor 2  $\mu\text{F}$  is loaded up to a voltage at the range  $U_0 = 300 - 1400$  V. The discharge is run between the Cu cylinder cathode of 1mm diameter and a grounded anode at the different distances apart from the cathode. There are two shape of the anode: annular anode with inner diameter 3mm and plane grid anode with 50% geometrical transparency. The discharge is ignited by a high voltage breakdown on the end surface of the ceramic tube between the igniter metallic ring and the cathode. The discharge current is measured by a Rogovsky coil directly in the cathode circuit. All experiments were made in a vacuum chamber that is pumped by the oil-free pump down to a pressure of  $(6-9) \times 10^{-4}$  Pa. The time-of-flight measurements the cathode plasma flow velocity are performed as follows. The plasma is generated at the front face of the cathode, expands through the anode and entered a drift tube connected to the chamber. After passing the tube the cathode ions are registered with a collector biased of a negative potential of  $(-400)\text{V}$ . The collector is placed at the distances  $L = 0.3$  m apart from the anode. We studied in the experiments the dependence of the ion velocity from the discharge voltage (current) at different interelectrode gap  $l$  and different shape of the anode. The results of TOF measurements are presented in fig.1. One can see from the figure that, first, the ion velocity  $V$  of the plasma jet was increased with rising discharge voltage (current). Namely, with annular anode, the velocity of ions increases from  $V=3 \cdot 10^4$  m/s at  $U_0=300\text{V}$  up to  $V=11 \cdot 10^4$  m/s at  $U_0=1400\text{V}$  at the interelectrode gap  $l=3\text{mm}$ . Second, the ion velocity increases with decreasing interelectrode gap at the same discharge voltage in experiments with annular anode. So, at the discharge voltage  $U_0=600\text{V}$  the ion velocity was about  $V=3 \cdot 10^4$  m/s at  $l=9\text{mm}$  and  $V=5 \cdot 10^4$  m/s at  $l=3\text{mm}$ . Third, the velocity of the ions of plasma jet depended on anode shape i.e. with the annular anode it is greater then that with plane grid anode at the same initial voltage and same interelectrode gap. This results us permit to enhance the plasma jet velocity by optimization of interelectrode gap and the shape of the anode.

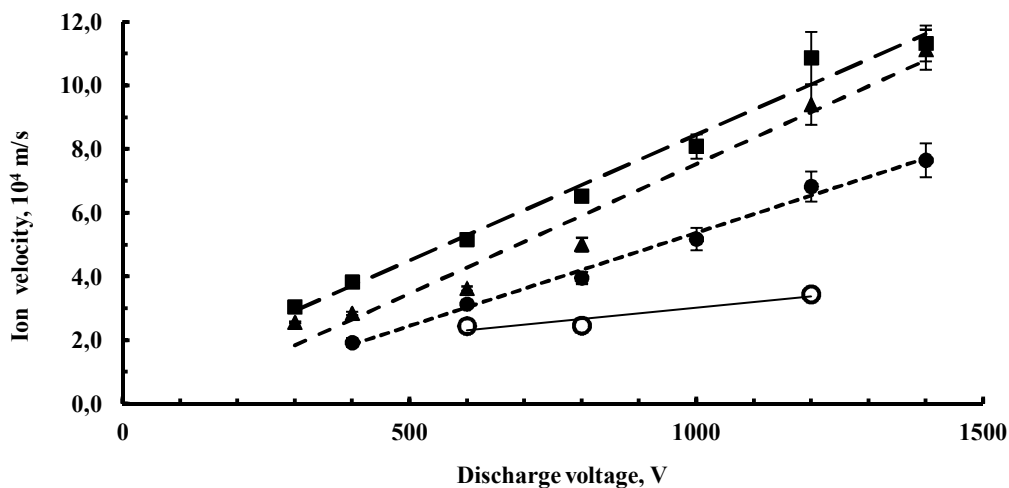


Fig.1 Dependence of ion velocity on discharge voltage with annular anode at the interelectrode gap of 9mm (●), 6mm (▲), 3mm (■) and with plane grid anode for the interelectrode gap 9mm (○).

## OPTIMIZATION OF THE VACUUM INSULATOR STACK OF THE MIG PULSED POWER GENERATOR

G.KHAMZAKHAN\*, S. A. CHAIKOVSKY\*\*

\*Tomsk Polytechnic University, 30, Lenin Avenue, Tomsk, 634050, Russia, goha\_respect@mail.ru

\*\* Institute of High Current Electronics SB RAS, 2/3, Akademichesky ave., Tomsk, 634055, Russia

The multi-purpose pulsed power installation MIG intends for generation of the voltage pulses up to 6 MV at the e-beam load and the current pulses up to 2.5 MA with rising time of 100 ns at the inductive loads like Z-pinch. The peak electrical power of the MIG pulse can attain 2.5 TW. The MIG generator currently operates by the following scheme: line pulse transformer – water pulse-forming lines – vacuum transmission line – load. A capacitor bank capable of storing about 400 kJ of total energy is used as an energy store. A line pulse transformer with an in-series capacitance of 190 nF transfers part of the energy stored in the capacitor bank into the first pulse-forming line whose electrical length and impedance are, respectively, 75 ns and 1.3  $\Omega$ . After operation of a single-channel water spark gap, part of the energy is transferred into the second pulse-forming line (26 ns, 0.65  $\Omega$ ). As a nine-channel water spark gap operates, up to 120 kJ of energy, with a power of 1.2–1.4 TW, is supplied through a 0.65- $\Omega$  transmission line to a cone vacuum transmission line with a load placed on the axis. The water transmission line is separated from the vacuum line by an insulator stack. The MIG generator is relatively compact among machines of this power level. The dimensions (length, width, height) of the pulse transformer with a primary energy store are 5.5×3.2×2.7 m<sup>3</sup>. The length and diameter of the transmission lines are, respectively, 6 m and 2.3 m.

The insulator stack consists of the five polyethylene rings with diameter of 900 mm separated by stainless steel grading rings. The total insulator width is 155 mm. The polyethylene rings are made with 45° inclining on the vacuum surface. In course of the MIG exploitation the insulator is exposed to the voltage pulses with amplitude 700 – 1500 kV and 50–60 ns FWHM.

Some malfunctions at the insulator operation were detected. The most pronounced were the vacuum surface flashing before the current maximum and deep discharge traces at the water surface of the two polyethylene rings placed closer to the ground. The vacuum surface flashing resulted in lowering of the load current but did not damaged the polyethylene rings. The breakdown along the water surface produced so significant intrusion in the ring body that their lifetime were limited by 10-20 shots.

This work was stimulated by the aforesaid points and has a purpose to understand the malfunction reasons and get some recommendation on improvement of the insulator performance. On the first stage the electrostatic simulations of the electric field distribution of the existing insulator design were performed. It was shown that voltage is not evenly divided among the rings. The highest average electric field at the first ring (from the water line) was calculated to be approximately three times of that at the fifth ring. At the second stage a wide set of the calculations were performed to find out the ways of the uniform grading of the voltage and improve the conditions at the triple junction. On the base of the simulation the modified design of the insulator stack was developed that features the uniform voltage grading and approximately 1.5 reduction of the peak electrical field along the vacuum surface due to anode side  $d/4$  plug at the grading rings ( $d$  – the polyethylene ring thickness). This design seems to be more reliable and could be fabricated with minor expenses.

## FINITE ELEMENT ANALYSIS FOR STRESS, TEMPERATURE AND MAGNETIC FIELDS OF A 70 KA INDUCTOR

*A.V. KHARLOV*

*Institute of High Current Electronics, Tomsk, Russia, (7)-382-2492673, akharlov@lef.hcei.tsc.ru*

The protection inductor serves for limiting the peak current in order to protect the high energy capacitor bank in case of a short circuit. Because of the high current and strong magnetic field, the Lorentz force in the protection inductor is large. This report describes numerical simulation of the inductance and the optimization of the stresses in the protection inductor. A finite element analysis with the ELCUT software is used to calculate the magnetic field, temperature rise and stresses in the protection inductor. A 2D static finite element analysis model of the inductor has been built for calculating the stresses in the copper coils and fiberglass body as well as the static inductance. Furthermore, a harmonic finite element analysis model has been built to analyse effects such as the influence of eddy currents in the copper wires and induced current in the stainless steel flanges on the stress and inductance. Eddy currents cause an uneven distribution of stresses and reduce the inductance. The typical maximum stresses in our design are 100 MPa in the copper coils and 140 MPa in the fiberglass body tubes; these are both below the yield strength of these materials. Simulations results are compared with the experimental tests and good agreement is observed.

## IMPROVEMENT OF XEF(C-A) AMPLIFIER PARAMETERS OF THL-100 TERAWATT LASER SYSTEM<sup>1</sup>

E.N. ABDULLIN\*, N.G. IVANOV\*, V.F. LOSEV\*, \*\*

\*Institute of High Current Electronics SB RAS, 2/3 Akademicheskoy Ave.,  
Tomsk, 634055, Russia, [IVANOV.NG@sibmail.com](mailto:IVANOV.NG@sibmail.com), (3822)491891

\*\*Tomsk Polytechnic University, 30 Lenin Ave., 634034 Tomsk, Russia

Generation of over-intensity light fields is the actual task for both fundamental research and for many practical applications. Thanks to the advent of stretching technology and a subsequent pulse compression presently the petawatt power level was realized. In recent for high-power radiation in the visible spectrum region the hybrid laser systems combining a gas and a solid active media are used [1]. So, in 2012 the achievement of 14 TW power level on THL-100 laser system was reported about [2].

In this paper we report the modification results of the gas booster of the THL-100 laser system in order to increase its output power. Figure 1 illustrates the principle of the active medium pumping. The electron beam injected through a titanium foils with six sides into the gas cell excites a Xe. VUV radiation (172 nm) of Xe penetrates into the laser cell through the CaF<sub>2</sub> window and one creates an active medium. In the original electron accelerator design the return conductor in a vacuum diode\* consisted of a two plates shown in the figure 1.

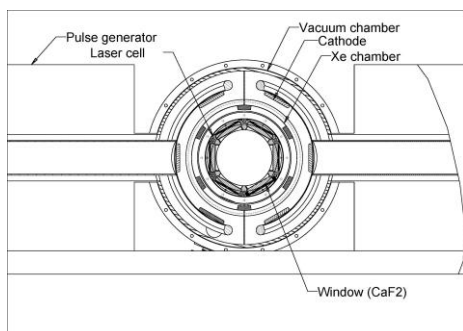


Fig. 1. Cross section schematic diagram

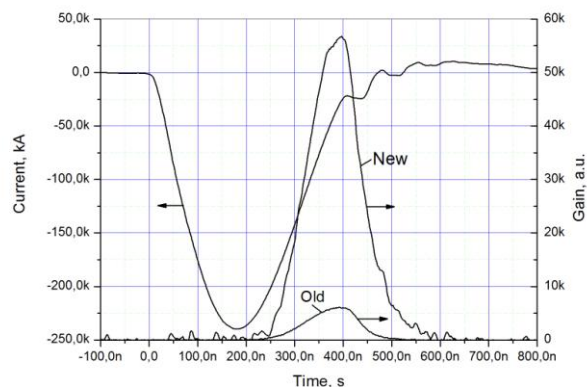


Fig. 2. Diode current and small signal

According to our studies in this case substantial proportion of the electrons energy was lost due to the high magnetic field intensity at the edges of the electron beam. To eliminate this drawback it was suggested to introduce the additional conductors in the form of rods which connect the edges of the gas cell with the outer wall of the vacuum chamber.

Our further measurements showed that in the new design the injection efficiency of electron beam into the gas cell was higher on 1.3 times. The electron energy injected into gas cell was 9.5 kJ, it corresponds to 50% of the total energy of vacuum diode. Measurement of the VUV radiation energy injected into the laser cell shown 30% increase as well. Measurement of a small signal gain carried out on 33 passes through the active medium shown its increasing on the order of magnitude in compare with the old accelerator design (Fig. 2).

### REFERENCES

- [1] Mikheev L.D. // *Laser and Particle Beams*. – 1992. – **10**. 473–478.
- [2] Alexeev S.V., Ivanov N.G., Kovalchuk B.M., Losev V.F., Mesyats G.A., Mikheev L.D., Panchenko Yu.N., Ratakhin N.A., and Yastremsky A.G. // *Atmospheric and Oceanic Optics*. – 2012. – **25**. 221–225.

<sup>1</sup> This work was supported by RFBR (Grants № 13-08-98038, № 13-08-00068, № 14-08-00511)

## NUMERICAL SIMULATION AND ANALYSIS OF ENERGY LOSS IN A NANOSECOND SPARK GAP SWITCH

*I.V.LAVRINOVICH, V.I.ORESHKIN*

*Institute of High Current Electronics SB RAS, 2/3 Akademichesky ave., Tomsk 634033, Russia*

*Phone: 8(382-2) 492-335, e-mail:lavrivan@mail.ru*

A system of differential equations for the *RLC* circuit of a capacitor-switch assembly was derived being supplemented with an equation for the spark resistance of the switch in accordance with the Braginsky model. The parameters that affect the solutions of equations for the circuit with parallel or series connection of several capacitor-switch assemblies to a common inductive load were determined. Based on numerical solution of the system of equations, a dependence of the energy  $E_H$  released in the spark within the first half-period on the discharge circuit and switch parameters was found.

**EFFECT OF THE DISCHARGE CIRCUIT AND SPARK GAP PARAMETERS ON ENERGY LOSS  
IN AN HCEICAP 80-0.25 CAPACITOR-SWITCH ASSEMBLY OPERATING ONTO A LOW-  
IMPEDANCE LOAD**

*I.V.LAVRINOVICH*

*Institute of High Current Electronics SB RAS, 2/3 Akademichesky ave., Tomsk 634033, Russia  
Phone: 8(382-2) 492-335, e-mail:lavrivan@mail.ru*

The report presents the results of tests of a capacitor-switch assembly operating onto a low-impedance load. The parameters varied in the tests were the operating pressure, main gap in the switch, and load impedance. Based on the obtained experimental data, dependences of the energy loss in switching on the varied parameters were constructed. Comparative analysis of the experimental and numerical simulation data was performed.

## HIGH-VOLTAGE FRONT SHARPENING AND WAVEFORM MODIFICATION BY FERRITE LINES

*M.R. ULMASKULOV, S.A. SHUNAILOV*

*Institute of Electrophysics UB RAS, 106, Amundsen Street, Ekaterinburg, 620016, Russia, marat@iep.uran.ru*

The paper presents experimental results on formation of high-voltage short pulses with high-frequency modulation of the top by biased ferrite coaxial line. The line represents a classic oil coaxial waveguide with ferrite rings arranged between the central and outer electrodes. A short pulse no longer than two periods of high-frequency modulation was used. Thus, the ferrite line allows to get rapidly damped modulation of pulse top. As a result the pulse (-200kV, 1.5ns) was transformed into a three peak pulse (FWHM of each ~300ps). But the voltage of the first peak was increased up to ~ 280kV.

Experiments using spiral coaxial oil line with a ferrite core were conducted as well. A central conductor in this line was a hollow triple spiral with an inner ferrite core. An important difference of such line is that the pulse forms longitudinal field in ferrite. External bias field having a longitudinal direction and a comparable value can effectively shift the magnetization of the ferrite core. It can be changed both strength and field direction for this. The outer electrode of the coaxial line is a closed loop for the pulse longitudinal magnetic component where part of the energy is converted for short-circuit current. This makes a difference in the ferrite magnetization. As a result the voltage pulses (-130÷140 kV) with a sharpened front from ~2 ns to ~ 0.5 ns and pulses of irregular shape (front of 0.7-1 ns) with controlled prepulse can be formed.



**IN-PHASED OPERATION OF MULTI-CHANNEL KA-BAND BWOS**

M.R. ULMASKULOV\*, V.G. SHPAK\*, M.S. PEDOS\*, I.V. ROMANCHEKO\*\*, V.V. ROSTOV\*\*, S.N. RUKIN\*, K.A. SHARYPOV\*, S.A. SHUNAILOV\*, M.I. YALANDIN\*

\* Institute of Electrophysics UB RAS, 106, Amundsen Street, Ekaterinburg, 620016, Russia, marat@iep.uran.ru

\*\* High Current Electronics Institute SB RAS, 2/3, Akademicheskii Avenue, Tomsk, 634055, Russia

We investigate in-phased multi-channel HPM auto-oscillators without electrodynamic coupling, namely, relativistic Ka-band BWOs. Explosive emission cathodes of the e-beam injectors were powered by stable splitting voltage pulses produced by an all-solid-state modulator, type S500. In two-channel version of the device, a coherent summation of the fields of wave beams from superradiance BWOs each capable of producing over 700 MW of power has been demonstrated [1]. The voltage fronts were shortened to 300 ps in controlled delay shock-excited ferrite lines. The standard deviation of the phase difference between the microwave pulses was less than 2% of the RF period. These results established the ground of the further experiment with four-channel HPM system which is in preparatory stage now. Enhancement of the modulator output voltage to the level of -500 kV@ 50 Ohm will allow attaining the voltage amplitude of -200 kV in each of the four parallel feeding channels, as it was done in two-channel option of the device. In this case, due to coherent summation of the fields, a 16-fold rise of the radiation power density could be attained in the main direction of antenna system arranged in the form of 2-D array (125x125 mm). This parameter will be equivalent for a would-be single HPM device with output power of 700 MW x 16 > 10 GW. For two-channel version, similar parameter of 700 MW x 4 ~ 3 GW has been obtained to date

## REFERENCES

- [1] K. A. Sharypov, et al., *Coherent summation of Ka-band microwave beams produced by sub-gigawatt superradiance backward wave oscillators*, *Appl. Phys. Lett.*, 2013, Vol. 103, p.134103.

## DEPENDENCE OF THE BREAKDOWN VOLTAGES OF SUBNANOSECOND GAS DIODES FROM THE GAS PRESSURE AND THE DEGREE OF THE DISCHARGE GAP OVERVOLTAGE<sup>1</sup>

*S.N. IVANOV, K.A. SHARYPOV, V.G. SHPAK*

*Institute of Electrophysics, Amundsena Str. 106, Ekaterinburg, 620016, Russia, E-mail: stivan@jep.uran.ru, Phone: +7(343)2678824*

In this paper the data on the breakdown voltages ( $U_{br}$ ) of gas diodes depending on the gas pressure ( $p$ ) and the degree of the discharge gap overvoltage were obtained in subnanosecond range. The experiments were carried out in a uniform electric field. Nitrogen was used as the test gas in all experiments. The pressure was changed within from atmospheric to 40 atm. Experiment started under minimum width of the discharge gap  $d = 0.25$  mm. Then  $d$  increased with step of 0.1 - 0.2 mm under fixed pressure of the gas until the discharge gap stopped to breakdown. Received data were built in coordinates  $U_{br}(pd)$  (fig.1).

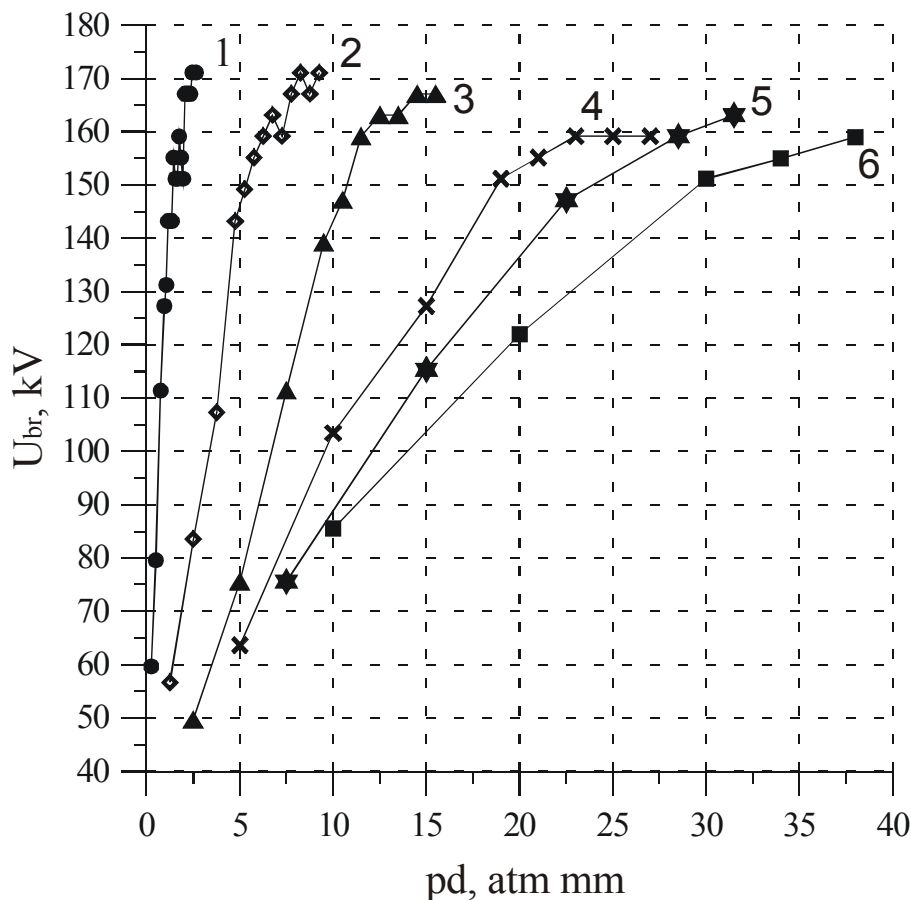


Fig. 1. Dependence of the breakdown voltages from product of the pressure to the cathode-anode distance (Paschen's curve). Nitrogen pressure for curves: 1 – 1 atm; 2 – 5 atm; 3 – 10 atm; 4 – 20 atm; 5 – 30 atm; 6 – 40 atm.

It is shown that in subnanosecond range the law of similarity is violated. Under the constant value of the product of the pressure to the cathode-anode distance the breakdown voltages of subnanosecond gas gap essentially depends on pressure of the gas in the gap.

<sup>1</sup> This work was supported by the Russian Fund for Basic Research (grant 12-08-00282-a).

## THE MEASURING OF THE BREAKDOWN FORMATION TIME OF SUBNANOSECOND DISCHARGE IN NITROGEN AT HIGH PRESSURES<sup>1</sup>

*S.N. IVANOV, K.A. SHARYPOV, V.G. SHPAK*

*Institute of Electrophysics, Amundsena Str. 106, Ekaterinburg, 620016, Russia, E-mail: stivan@jep.uran.ru, Phone: +7(343)2678824*

In this paper the experimental results of registration of the breakdown formation time ( $t_{\text{form}}$ ) in gas diodes with different width of the discharge gap are given. The experiments were carried out in a uniform electric field. Pure nitrogen (99.996%) was used as the test gas in all experiments. This is the mostly used gas in high-pressure gas dischargers. The voltage pulse, with the amplitude of  $102 \pm 2$  kV, full width at half maximum (FWHM) of about 380-400 ps, and the front of about 250 ps at the level of 0.1-0.9 from amplitude was applied to the studied gas gap. In this case the voltage rise rate at the pulse front was up to  $3.3 \times 10^{14}$  V/s. During all experiments, described in this paper, the parameters of voltage pulse have not changed. The dependences of the breakdown formation time (fig. 1) for different pressures of nitrogen and the degree of the discharge gap overvoltage were obtained.

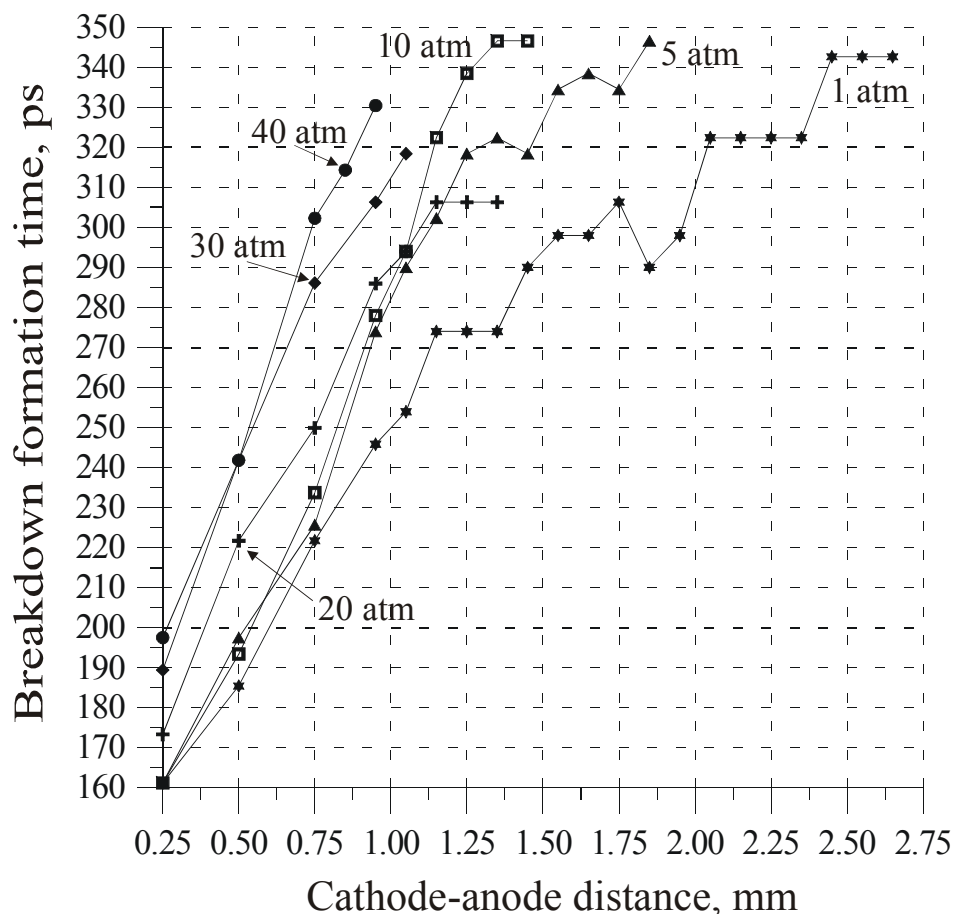


Fig. 1. The dependence of the breakdown formation time from cathode-anode distance for different pressures of nitrogen.

It is seen that  $t_{\text{form}}$  in the discharge gap with invariable gap increases the pressure when increase. At that increase constitutes around (40-50)% when the pressure increase at 40 times.

<sup>1</sup> This work was supported by the Russian Fund for Basic Research (grant 12-08-00282-a).

**LOW-VOLTAGE HIGH-CURRENT DISCHARGE INITIATION IN A VACUUM DIODE<sup>1</sup>**

*A.A. ZHERLITCYN, B.M. KOVALCHUK, N.N. PEDIN*

*Institute of High Current Electronics, 2/3, Akademichesky av., 634055 Tomsk, Russia, andzh@oit.hcei.tsc.ru*

Preliminary creation of ion flow in a vacuum diode before applying the voltage pulse allows removing the beam current limitation by own space charge, reducing the diode impedance, and increasing the beam power. The sources based on the surface dielectric breakdown are most widely used to create a plasma flow. Plasma extends as a result of hydrodynamic expansion with a velocity of  $\sim 10^6$  cm/s determined by the plasma temperature (units of eV). Besides this, the ions with the velocities exceeding the thermal velocity are recorded. It is evident that this flow can be used for ion compensation of the electron beam charge in high-current relativistic diodes. This paper presents the results of oscillographic study of the ion flow propagation from a capillary plasma gun in combination with single-frame photography of plasma glow with a resolution up to 3 ns. Ignition of a high-current low-voltage discharge with the current of 100 kA in the absence of complete filling of the diode gap with plasma is demonstrated. The situation in which plasma fills only a part of the diode gap prior to ignition of high-current discharge is favorable for the realization of the current cutoff with a high rate.

---

<sup>1</sup> This work was supported by by RFBR, grant No. 14-08-01123 -a

## PLASMA-FILLED DIODE POWER INCREASE DUE TO THE GROWTH OF THE CURRENT RISE RATE<sup>1</sup>

*A.A. ZHERLITCYN, B.M. KOVALCHUK, N.N. PEDIN*

*Institute of High Current Electronics, 2/3, Akademichesky av., 634055 Tomsk, Russia, andzh@oit.hcei.tsc.ru*

The characteristics of the plasma-filled diode when changing the current rise rate by 2 times were obtained. The rise rate was varied by changing the inductance of the secondary coil vacuum line of the linear transformer used as a pulsed power driver. The possibility of increasing the current amplitude by increasing its rise rate was demonstrated at fixed initial conditions. So, increase in the current rise rate by 2 times resulted in the rise of the current amplitude from 100 to 185 kA, transmitted charge from 6 to 10 mC while retaining the low-resistance phase duration of 100 ns. At the current amplitude rise by more than 1.5 times, the diode impedance rise rate in a high-resistance phase was retained at the level of 0.5  $\Omega/\text{ns}$  which allowed increasing the diode power by 1.6 times from 100 to 160 GW. The diode voltage remained at the level of approximately 1 MV due to the fast current drop in a high-resistance phase. Conservation of the resistance rise rate allows forecasting the growth of the diode voltage proportional to the current in case of increasing the current rise rate without reducing the inductance.

---

<sup>1</sup> This work was supported by by RFBR, grant No. 13-08-00109 -a

## SIMPLE CLADDING TECHNIQUE FOR CONSTRUCTING CVD<sup>1</sup>

*K. HOJATZADEH* \*

\*IRAN Electronic and Communication Research Center, Kargar Ave., Tehran, 1439955471, Iran, K.Hojatzadeh@yandex.ru , +98-021-84978833

Many pulsed power experiments often necessitate the accurate measurement of high transient voltages with very short rise times. Capacitive Voltage Divider (CVD) is an accurate and reliable voltage measurement technique in ultra wideband systems. The ultimate goal in capacitive voltage monitoring is a simple design, with good high frequency response, convenient attenuation ratio and longtime constant measurement capability. Design and construction of a self-integration CVD with flat frequency response, enough attenuation ratio and time window is extremely valuable for use in capturing sub nanosecond pulses. We propose a new and simple design for CVDs with flat frequency response up to 2.5 GHz, having enough division ratios more than 70 dB and integration times greater than 5 ns. Also it is capable of handling 50 kV transient pulses through the RG-218 Cable in 50  $\Omega$  loading. Due to their simple and low-cost construction structure they can be widely used and scaled in many sub nanosecond application. The simulation of the CVD with full wave FDTD codes and commercial circuit analysis programs shows good agreement with the experimental results.

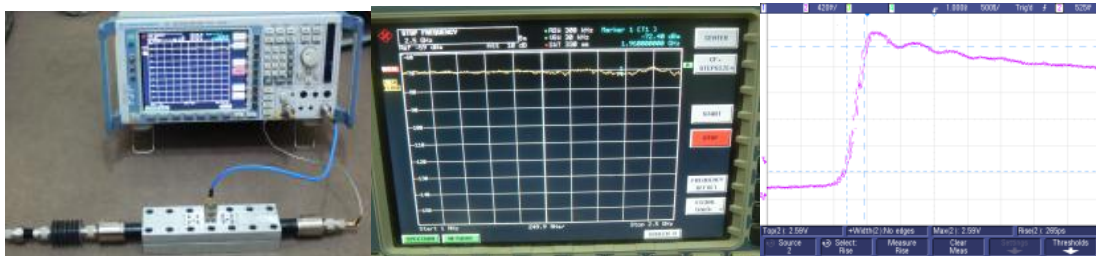


Fig. 1. The Umbrella CVD, Time and frequency domain calibration.

We calibrate the sensor in both time and frequency domain to ensure of its capabilities. We use a Piece of RG-218 cable as a test bed which is incorporated with a purposed CVD. We extract the attenuation factor and frequency response of the CVD with using a 10 kHz to 30 GHZ ROHDE&SCHWARZ spectrum analyzer which works in network analyzer mode with 3 GHz frequency response and 100 dB dynamic ranges. The time domain response of CVD extracted using various home-made high voltage pulsers up to 50 kV/ 265 ps rise time Pulser. The results of time domain and frequency domain of the CVD are in good agreement and shows that the CVD will providing a powerful measurement tool especially in high voltage short transition times.

### REFERENCES

- [1] P.Choi, M. Favre., "A fast capacitive voltage monitor for low impedance pulse lines " *Proc Tenth IEEE Pulsed Power Conf., Albuquerque, NM*, pp. 880 - 885 vol.2,1995
- [2] Df.R. Cooper, E.Y. Chu, and R.M. Ness, "An innovative fast-response, co-axial, capacitive high voltage probe", *Proc 7th IEEE Pulsed Power Conf., Monterey, CA*, p.390, 1989

<sup>1</sup> This work was supported by Iran Electronic and Communication Research Center

**DIAGNOSTICS OF SUB-NANOSECOND HIGH VOLTAGE PULSES**

*N.M. BYKOV\**, *I.K. KURKAN\*\**, *A.S. STEPCHENKO\**

*\* Institute of High Current Electronics SB RAS, 2/3 Akademichesky Ave., Tomsk, 634055, Russia, [ikk@lfe.hcei.tsc.ru](mailto:ikk@lfe.hcei.tsc.ru)*

*\*\* National Research Tomsk Polytechnic University, 30 Lenin Ave., Tomsk, 634050, Russia*

The usage of probes such as capacitive voltage divider, D-dot and current loop in sub-nanosecond time scale is under review. Sensors of different types were tested with the pulses of different characteristic time – from 20 ns to 0.2 ns in the research of sub-nanosecond gas gap breakdown. The experiments approved acceptable measurement accuracy of differentiating sensors (D-dot and current loop) in sub-nanosecond time scale.

Theoretical estimates for amplitude distortions of measurements were obtained for pulses with characteristic times shorter than electric length of capacitive divider. Benefits of capacitive dividers whose arms are filled with dielectric materials of close properties were shown. In this case the dividing coefficients varied little from tens to tenths of nanoseconds that allows direct recording of wideband waveforms with minimal distortions.

## LONG LIFE-TIME, CORONA STABILIZED GAS SWITCHES FOR REPETITIVELY OPERATED MARX GENERATORS

*E.G. KRASTELEV*

*Joint Institute of High Temperatures Russian Academy of Sciences, Izhorskaya st. 13 Bd.2, Moscow, 125412, Russia,  
ekrastelev@yandex.ru, +7 (916) 795-6495*

A long life-time corona-stabilized self-breaking two-electrode and triggered three-electrode gas switches for voltage up to 100 kV (bipolar charging up to  $\pm 50$  kV) were developed for Marx generators, operating in pulse-periodic mode with repetition rate up to a few tens of hertz.

All switches include two main electrodes of toroidal geometry. In addition to them three-electrode switches have a trigger disk electrode with a central hole which is located midway between the main electrodes. In contrast to traditional design of so called "distortion field" switches with a thin trigger disk electrode used in Marx generators operating in single pulse mode, the middle electrode is made in form of a thick disk for effective heat removal from the discharge zone and increasing of a life-time limited by erosion. Toroidal electrodes provide a long life-time due to large area of the working part of the surface. In order to reduce erosion and increase the life-time a copper-tungsten (70 % W + 30 % Cu) composite material is used for working parts of the electrodes.

High dynamic characteristics of the switches are achieved by pre-ionization of the working gas (dry air, N<sub>2</sub>) with help of an additional corona discharge. The pulsed corona is generated by an additional corona needle that is installed inside a cavity of one of the main toroidal electrode. The gas pre-ionization provides high stability of pulsed breakdown voltage of self-breaking switches and a low breakdown time delay of the triggered three-electrode switches in the absence of the "distortion field" effect.

The effective protection of the surface of the insulating body from the dust arising from the electrodes erosion was achieved by blowing the working gas from inlet holes at the end flanges and throwing it out along the axial channel in the electrode holders. Furthermore, this scheme provides quick recovery of electric properties of the gas by the removal of the discharge products from areas with high electric field along the shortest path through the main electrodes.

The design of several models of the switches developed for Marx generators with stored energy from 40 J up to 1 kJ and repetition rate up to 25 Hz as well as results of their tests will be presented.



## COMPLEX OF THE ELECTROPHYSICAL EQUIPMENT FOR ELECTROPULSE TECHNOLOGIES

*I.V. ERMILOV*

*Highway Entuziastov 11A, building 3, apt. 197, Moscow, 111024, Russia*

*E-mail: [rustgr2@yandex.ru](mailto:rustgr2@yandex.ru), tel. +7 (495) 361-95-47*

Company JSC "Russian Technology Group 2" has developed a complex of the electrophysical equipment for electropulse technologies. Pulse capacitors are designed with the specific energy up to 300J/kg with minimum inductance up to 10nH, with usual and coaxial conclusions, with a frequency up to 1Hz (monopulse) and up to 500Hz (frequent). Capacitors have 3 gabarits, but by the request of the customer the housing can be with other dimensions. Total developed about 220 types of capacitors with voltage of 3 to 200kV and a capacity of 10nF up to 300 $\mu$ F. [1]

For charging capacitor have developed compact high voltage chargers type IVN. Maximum voltage chargers varies from 10 to 50kV. Infinitely adjustable voltage produced at the same time from 100V to a maximum value. Provides for both local and remote control of the power supply. Maximum power of IVN-1, IVN- 2, IVN-3, IVN-5 is 1kW. Source IVN- 6 has a maximum power of 8 kW. Produced also a traditional source of IVN-4 with a voltage up to 50 kV and output power up to 50kW. [2]

A series of spark gap in ceramic-metal case of type RGU have developed for discharge capacitors. Produces 18 types of spark gap with voltage from 5 to 100kV and a current of 20 to 100 kA. Recently was developed a powerful spark gap with a voltage of 150kV and a current up to 150kA. [3]

Control device of spark gap have voltage of signal 7 -10V and the current of control of 0,1-0,2A.

In some cases, for very large currents is advisable to use the system «crow-bar», that is to say the diode unit, which is established parallel to the battery of capacitor. A series diode units has developed with voltages from 5 to 50 kV and currents up to 100 kA with a duration 100 $\mu$ s. [2]

### REFERENCE

- [1]. *I.V. ERMILOV*//Electricity.2006, № 9, pp73-79
- [2]. *I.V. ERMILOV*//Magnetic pulse treatment materials. International Scientific conference. Samara, 2007, pp80-90
- [3]. *I.V. ERMILOV, Y.B. Smakovskii, V.L. Laptev*//Instruments and Experiment Techniques, 2003, vol.46, №1, pp45-47

## HIGH-POWER GENERATOR OF QUASI-RECTANGULAR PULSES

V.A. KOKSHENEV

*Institute of High Current Electronics SB RAS, 2/3 Akademicheskoy Ave., Tomsk, 634055, Russia  
E-mail: yak@oit.hcei.tsc.ru*

We consider a method of forming the powerful rectangular pulse on the active load without usage of the additional stage of energy compression in the form of traditional forming line. The method is based on the operation of the Marx generator, placed within a conductive screen, in an intermediate inductive storage mode. The analysis of such scheme is made. It is shown that inductance  $L_S$  and capacitance relative to conductive screen  $C_S$ , distributed on the stages of the Marx generator, form the forming line (Fig. 1). The energy in the forming line is stored in the inductive elements using current interrupter. As a result, almost rectangular shape pulse with a duration of  $\tau \cong 2N \cdot (L_S \cdot C_S)^{1/2}$  is formed on the active load, where  $L_S$  is the inductance of a stage, which consists of the inductance of the stage arrester, the induction of the storage capacitor  $C_0$  and the induction of their connections;  $C_S$  is the capacity of a stage relative to conductive screen ( $C_S \ll C_0$ ), and  $N$  is the number of stages of the Marx generator. In the matching mode ( $R_L = \rho_{FL} = (L_S/C_S)^{1/2}$ ) for the ideal opening switch the load voltage multiplication factor  $K_U = U_L/U_g = (C_0/C_S)^{1/2}/2N$ .

The results of calculations and test experiments for the Marx generator, placed inside a conducting screen, with current interrupter based on electrically exploded conductors (EEC) are shown. Scheme parameters are:  $C_0 = 0.4 \mu\text{F}$ ,  $N = 33$ ,  $L_S \cong 0.42 \mu\text{H}$ ,  $C_S \cong 44 \text{ nF}$ . For the stage charging voltage of  $U_0 = 60 \text{ kV}$  the output voltage is  $U_g = 2 \text{ MV}$ . EEC-opening switch was made out of 3 m long copper wires with a diameter of 30 or 60 microns, exploded in the air. In the matching mode (on the active load of  $R_L = \rho_{FL} = (L_S/C_S)^{1/2} \cong 100 \Omega$ ) the pulse with the amplitude of  $U_L = 2.5 \text{ MV}$  and the pulse duration of  $\tau = 290 \text{ ns}$  was obtained. For the load resistance of  $R_L \cong 2 \text{ k}\Omega \gg \rho_{FL}$  the voltage was  $U_L \cong 4.5 \text{ MV}$ .

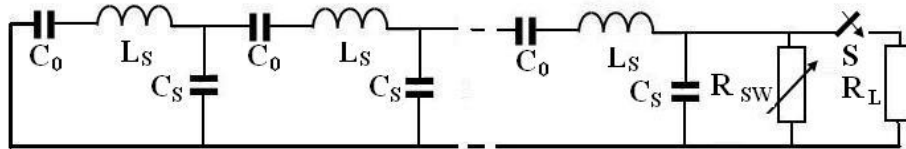


Fig. 1. Equivalent circuit of generator:  $R_{SW}$  – opening switch,  $S$  – separating switch.

## STUDY ON THE VELOCITY OF THE SINGLE-STAGE COIL ELECTROMAGNETIC LAUNCHERS

XUZHE XU, YAOHONG SUN, PING YAN

*Institute of Electrical Engineering Chinese Academy of Sciences, No.6 Zhongguancun Beiertiao, Beijing, 100190, China,  
Key Laboratory of Power Electronics and Electric Drive, Chinese Academy of Sciences, Beijing, China*

*xz xu@mail.iee.ac.cn, 8610-82547119*

In this paper, the force of the armature in the single-stage helical coil electromagnetic launcher is described by simulation and theoretical analysis. On the conditions of different Ampere-turns, the forward acceleration forces and the interaction time of armature and coil will change obviously. Before the force of the armature becomes the deceleration force, shut off or reduce the pulse current of the coil, the exit velocity will reach the maximum value. The velocity of the armature is calculated by using the stress test in the experiment. Place a piece of pressure sensitive film in the certain distance from the exit of the helical coil, the armature will hit the pressure sensitive film while the coil obtains the high pulse current. Measure the impact pressure, convert it into the dynamic energy values, and the exit velocity of the armature can be calculated. Experimental results shown that the exit velocity of the armature can be significantly improved by controlling the pulse width of the discharge current.

## DEVELOPMENT OF FREQUENCY-TUNED HIGH VOLTAGE AC POWER SUPPLY FOR DBD APPLICATION

*YINGHUI GAO\**, *RONGYAO FU\**, *KUN LIU\**, *XUEKE CHE\*\**, *TAO SHAO\**, *YAOHONG SUN\**, *PING YAN\**

\* *Institute of Electrical Engineering, Chinese Academy of Sciences, Zhongguancun Beiertiao 6, Beijing, 100190, China, Key Laboratory of Power Electronics and Electric Drive, Chinese Academy of Sciences, Beijing, China*

[gyh@mail.iee.ac.cn](mailto:gyh@mail.iee.ac.cn), 8610-82547119

\*\* *Equipment Academy, Beijing, 101416, [chedk@163.com](mailto:chedk@163.com), 8610-66368440*

High frequency high voltage AC power supply is widely used in discharge plasma research and the industrial applications. A frequency-tuned and voltage-tuned AC power supply used in the research of flow control by dielectric barrier discharge is introduced in this paper. The output voltage, output frequency and the matching relation between the power supply and the DBD load will influence the effect of dielectric barrier discharge. The power supply which the output frequency and the output voltage can be regulated was developed, and can be operated in the burst mode to realize the flow control.

The power supply adopts the series resonant topology. Five frequency ranges were divided from 1 kHz to 50 kHz, and five resonant points exist. The output voltage including its frequency and amplitude and the burst operation mode were controlled by the control system. The output power is 2kW, and the output voltage is 30kV. Figure 1 shows the waveforms of the output voltage and the output current with DBD load.

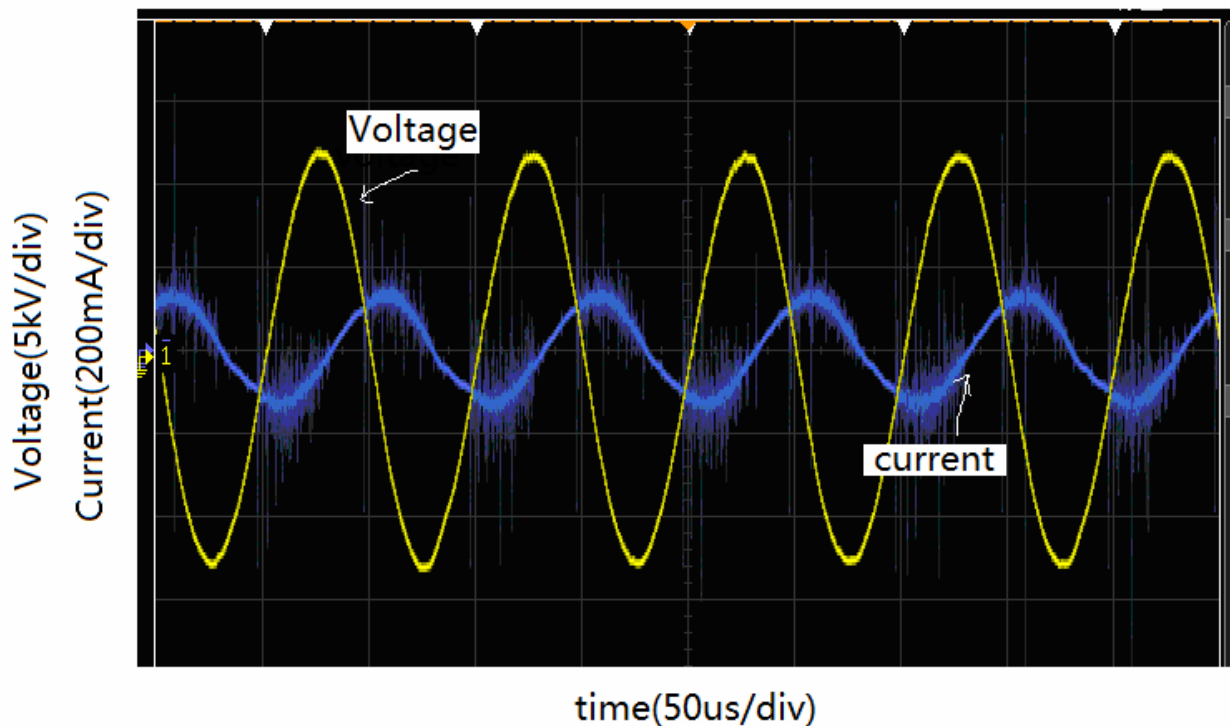


Fig. 1. Waveforms of the output voltage and the output current

## SUPERSHORT AVALANCHE ELECTRON BEAMS IN SF<sub>6</sub><sup>1</sup>

*V.F. TARASENKO, D.V. BELOPLOTOV, M.I. LOMAEV, D.A. SOROKIN*

*Institute of High Current Electronics, Akademicheskoy Ave. 2/3, Tomsk, Russia, 634055  
VFT@loi.hcei.tsc.ru, +7-3822-491685*

In recent years, there has been a lot of research progress achieved on generation of runaway electrons (RAEs) in laboratory gas discharges at increased pressure (see, e.g., the reviews [1, 2]). Most attention in the field in the last decade was focused on the parameters and properties of RAEs in atmospheric air and on the mechanism of their generation. New experimental data were obtained due to the development of measuring equipment and technologies.

The objective of the study is the peculiarities of a supershort avalanche electron beam (SAEB) generation in SF<sub>6</sub> and, for comparison, in air and other gases under the same experimental conditions. The paper also reports on the measurements of the ionization wave front velocity in the gap at a time resolution up to 10 ps. The present study continues the research of SAEB in SF<sub>6</sub>, than was published in [3].

Experiments were performed on the setup (see Fig. 1) with nanosecond generator.

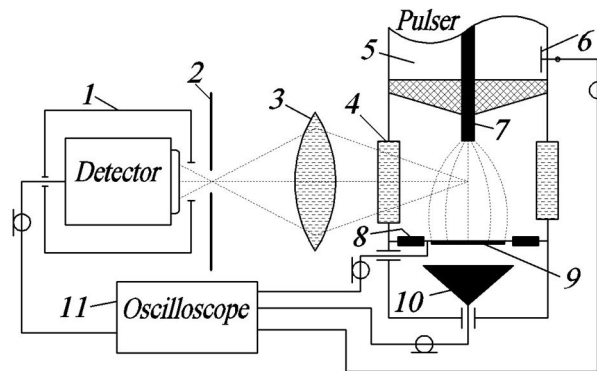


Fig. 1. Block-diagram of experimental setup: 1 – photodetector PD025 in metal box; 2 – screen with slit; 3 – lens; 4 – side window; 5 – transmission line of RADAN-220 generator; 6 – capacitive voltage divider; 7 – high voltage electrode; 8 – current shunt; 9 – ground electrode made of thin foil; 10 – collector; 11 – oscilloscope.

From our studies, the following conclusions could be drawn:

The SAEB amplitude for SF<sub>6</sub> at pressures of 0.05–0.1 MPa is much lower than that for air and nitrogen and is commensurable with the SAEB amplitude for krypton. This is due to the increase of electron energy which is lost in excitation and ionization in heavy gases. The attachment of electrons plays a small role in SAEB generation, resulting in almost the same SAEB amplitudes in air and nitrogen.

At a pressure of 0.1 MPa and the same voltage across the gap, the energy of RAEs generated in SF<sub>6</sub> is lower than that in air.

The diffuse discharge in SF<sub>6</sub> and SF<sub>6</sub>-nitrogen mixture is formed not only at negative polarity but also at positive polarity of the electrode with small curvature radius.

The obtained data confirm the generation mechanism of most of the RAEs between the ionization wave front and the plane anode. The SAEB width is substantially influenced by the ionization wave front velocity. The ionization wave velocity decreases with the increase of the pressure in SF<sub>6</sub>, nitrogen, and air. Comparing with the ionization wave velocity in air and nitrogen, the velocity is lower in SF<sub>6</sub>, so the SAEB width for SF<sub>6</sub> is longer than that for air and nitrogen.

### REFERENCES

- [1] Tarasenko V.F., Baksh E.KH., Burachenko A.G., Kostyrya I.D., Lomaev M.I., Rybka D.V. // Plasma Dev. Oper. - 2008. – Vol. 16. - 267-298.
- [2] Levko D., Krasik YA.E., Tarasenko V.F. // Internat. Rev. Phys. – 2012. - Vol. 6. - 165-195.
- [3] Baksh E.KH., Burachenko A.G., Erofeev M.V., Lomaev M.I., Rybka D.V., Sorokin D.A., Tarasenko V.F. // Laser Phys.- 2008. – Vol. 18. - 732-737.

<sup>1</sup> The work is performed in the framework of the State task for HCEI SB RAS, project №13.1.3.

## RUN-AWAY ELECTRON PREIONIZED DIFFUSE DISCHARGE AS EFFICIENT SOURCE OF LASER RADIATION<sup>1</sup>

*A.N. PANCHENKO, M.I. LOMAEV, N.A. PANCHENKO, V.F. TARASENKO, A.I. SUSLOV*

*Institute of High Current Electronics SB RAS, Academicheskoy av., 2/3, Tomsk, 634055, Russia,  
e-mail: [alexei@loi.hcei.tsc.ru](mailto:alexei@loi.hcei.tsc.ru), phone: +7 3822 492392*

It was shown that runaway-electron-preionized volume (diffuse) discharge (REP DD) can be used as an excitation source of active gas mixtures at elevated pressures and can produce laser emission in the IR [1], visible [2] and UV [3, 4] spectral ranges. In those works, runaway electrons and laser radiation were generated in the same discharge gap.

In the report, results of application of the REP DD for excitation of different active gas mixtures are presented. It was shown that the REP DD allows to obtain stimulated radiation in the IR, visible and UV spectral ranges at atomic transitions of neon (585.3 nm), argon (750.3 nm) and fluorine (712.8 and 731.1 nm), and at molecular transitions of N<sub>2</sub> (337.1 nm), XeF\* (351 and 353 nm), HF (2.8-3.2 μm) and DF (3.8-4.2 μm).

Kinetic model of the REP DD in mixtures of nitrogen with SF<sub>6</sub> is developed allowing to predict the radiation parameters of nitrogen laser at 337.1 nm. Calculated voltage and current of the REP DD are shown in Fig.1.

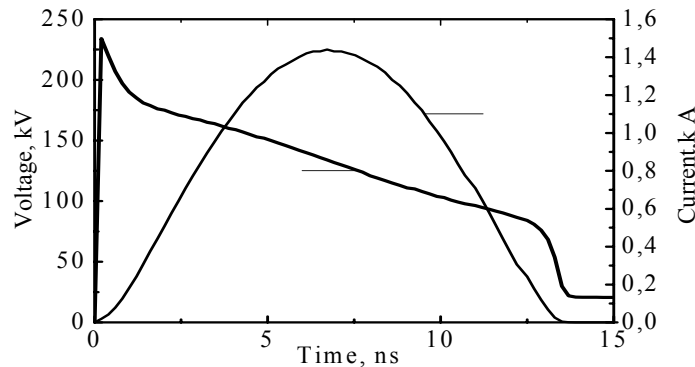


Fig. 1. Calculated waveforms of the REP DD current and voltage across the laser gap in N<sub>2</sub>-SF<sub>6</sub> mixture

The investigations conducted show the promising prospects of REP DD employment for exciting a series of gas lasers. Generation was obtained on molecules N<sub>2</sub>, HF, and DF with the efficiency close to the limiting value. It was established that the REP DD is most efficient for pumping lasers with the mixtures comprising electro-negative gas SF<sub>6</sub>. The addition of SF<sub>6</sub> increases the breakdown voltage in the gaps with electrodes having the shape of blades and makes the pump power higher.

Under REP DD pumping the generation at transitions of helium, neon, argon, and molecules XeF\* was obtained in the mixtures of inert gases with NF<sub>3</sub> also in visible and UV spectral ranges. However, in those mixtures the generation efficiency was comparatively low, seemingly, due to the loss of discharge uniformity at increased contents of NF<sub>3</sub> in the mixture.

### REFERENCES

- [1] Alekseev S.B., Gubanov V.P., Kostyrya I.D., Orlovskii V.M., Skakun V.M., Tarasenko V.F. // *Quantum Electron.* – 2004. – Volume 34. – № 11. – Pages 1007–1010.
- [2] Tarasenko V.F., Bakshat E.Kh., Burachenko A.G., Rybka D.V., Lomaev M.I., Tel'minov A.E. // *Izv. Vyssh. Uchebn. Zaved., Ser.Fiz.* – 2011. – Volume 54. – № 5/2. – Pages 5–9.
- [3] Bakshat E.Kh., Tarasenko V.F., Burachenko A.G. // *Quantum Electron.* – 2009. – Volume 39. – № 12– Pages 1007–1111.
- [4] Vil'tovskii P.O., Lomaev M.I., Panchenko A.N., Panchenko N.A., Tarasenko V.F., Rybka D.V. // *Quantum Electron.* – 2013. – Volume 41. – № 7. – Pages 605–609.

<sup>1</sup> This work was supported by the Russian Foundation for Basic Research, grant No. 14-08-00074

**IONIZATION WAVE SPEED DURING BREAKDOWN OF DISCHARGE GAP «POINT-PLANE»<sup>1</sup>***D.V. BELOPLOTOV\*<sup>\*\*</sup>, M.I. LOMAEV\*, D.A. SOROKIN\*, V.F. TARASENKO\*<sup>\*\*</sup>**\*Institute of High Current Electronics, 2/3 Akademicheskoy Avenue, Tomsk, 634055, Russia, VFT@loi.hcei.tsc.ru, +7-3822-491685**\*\*National Research Tomsk State University, Tomsk, 36 Lenina Avenue, 634050, Russia*

The breakdown in a gases gap with non-uniform electric field is implemented by ionization wave, which propagate from a potential electrode with small radius of curvature to a grounded electrode [1-3]. Speed of ionization wave is depended by different conditions and takes the value of ~0.1-20 cm/ns [1, 4-6].

In this experiment the temporal pulse shape of nitrogen radiation was detected from different areas of the discharge gap with  $d = 13$  mm filled with  $N_2$  and mixture of gases  $SF_6:N_2$  (0.975:0.025).

Time delay between appearance of radiation from the potential electrode area and from the grounded electrode area was observed. Dependents of delay by gases, pressure and a polarity of high voltage pulses of generator RADAN-220 is shown in Fig. 1.

Fig. 1. Delay between appearance of radiation from the potential electrode area and from the grounded electrode area vs pressure in  $N_2$  for positive (1) and negative (2) polarity, and in  $SF_6:N_2$  (0.975:0.025) for positive (3) and (4) negative polarity.

Importantly, the radiation from the potential electrode area occurs simultaneously irrespective of gases, pressure and polarity of the potential electrode. Maximal delay was obtained in  $SF_6:N_2$  (0.975:0.025) at pressure of 0.25 MPa with negative polarity of the potential electrode. For  $N_2$  at a pressure of 0.3 MPa with negative polarity, the delay of the anode signal with respect to the cathode signal was ~ 280 ps ( $v \sim 4.6$  cm/ns), and with positive polarity, it was ~ 210 ps ( $v \sim 6.2$  cm/ns). The minimum delay of the anode signal with respect to the cathode signal, which could be determined on this setup, was ~90 ps ( $v \sim 14.4$  cm/ns) for  $N_2$  at a pressure 0.1 MPa and negative voltage pulse polarity.

## REFERENCES

- [1] Vasilyak L. M., Vetchinin S. P., and Polyakov D. N. // Technical Physics Letters. – 1999. – T. 25. – №. 9. – C. 749-751.
- [2] Pancheshnyi S.V., Nudnova M.M., and Starikovskii A.Yu. // Physical Review E. - 2005. - Vol. 71. - 016407
- [3] Wang D., Jikuya M., Yoshiga S., Namihira T., Katsuki S., and Akiyama H. // IEEE Trans. Plasma Sci. - 2010. - Vol. 35. - No. 4. - 1098-1103.
- [4] Pai D., Stancu G.D., Lacoste D.A., and Laux C.O. // Plasma Sources Sci. Technol. - 2009. - Vol. 18. - 045030.
- [5] Tarasenko V. F. // Plasma Phys. Rep. – 2011. – Vol. 37. - 409-421.
- [6] Shao T, Tarasenko V.F, Chen Zhang C., Burachenko A.G., Rybka D.V., Kostyrya I.D., Lomaev M.I., Baksh E.Kh., and Yan P. // Review of Scientific Instruments. - 2013. - Vol. 84. - 053506.

<sup>1</sup> This work was supported by RFBR №12-08-00105-a.

## REDUCING THE COMPLEXITY OF MONTE CARLO MODELING OF ELECTRON AVALANCHES IN GASES<sup>1</sup>

*G.Z. LOTOVA\**

*\*ICMMG SB RAS, pr.Academika Lavrentieva 6, Novosibirsk, 630090, Russia, lot@osmf.sbcc.ru, +7(383)3287721*

We consider the problem of gas discharge simulation in a uniform electric field. All programs using Monte Carlo method [1] for modeling electron avalanches are based on the algorithm that neglects the own electric field of electrons. This algorithm is very time-consuming. The aim of this work is to reduce the complexity of Monte Carlo algorithms and increase the computation accuracy of functionals. We study the behavior of basic functionals at a fixed time: the number of electrons in avalanche, the average energy, the average coordinates, the diffusion coefficient, the drift velocity, and the first Townsend coefficient [2]. The results of this work can be also used for testing the Monte Carlo programs.

We simulate the free path of electrons by use of the piecewise linear approximation [3] for each small time step  $\Delta t$ . Usually, at the end of step the collision is modeled with the probability  $P = 1 - \exp(-\sigma N \Delta l)$ . Here  $\sigma$  is the total microscopic cross-section,  $N$  is the density of gas molecules,  $\Delta l$  is the path length. We propose to use a different formula for the probability, so that the complexity is reduced and the accuracy increases. We also derive the optimal value for the time step  $\Delta t$ . This value depends on the maximum allowable relative error of resulting functionals.

Earlier it was shown that the diffusion approximation does not work well if the ratio  $E/p$  is greater than 300 V/(cm · Torr). Here  $E$  is the electric field,  $p$  is the gas pressure. For this regime we propose new accurate methods for finding the diffusion coefficient and the first Townsend coefficient. In particular, we find the optimal step length of particle density histograms (or of the frequency polygons), which is necessary for calculating the diffusion radius.

### REFERENCES

- [1] *Ermakov S.M., Mikhailov G.A. // Course of statistical modeling. – Moscow, Nauka, 1976 (in russian).*
- [2] *Korolev Yu.D., Mesyats G.A. // Physics of pulsed discharge in gases. – Moscow, Nauka, 1991 (in russian).*
- [3] *Akkerman A.F. // Modeling of trajectories of the charged particles in a matter. – Moscow, Energoatomizdat, 1991 (in russian).*

<sup>1</sup> This work was supported by integration projects of SB RAS № 47, 126; RFBR grants № 13-01-00746, 12-01-00727, 12-01-00034, 13-01-00441, 12-05-00169 and grant for Scientific Schools HIII-5111.2014.1.



## X-RAY PARAMETERS AT THE FORMATION OF CORONA DISCHARGE <sup>1</sup>

*D.V. RYBKA, A.G. BURACHENKO, I.D. KOSTYRYA, V.F. TARASENKO\**

\* *Institute of High Current Electronics, Siberian Branch, 2/3 Akademichesky Ave., Tomsk, 634055 Russia, [RDm@loi.hcei.tsc.ru](mailto:RDm@loi.hcei.tsc.ru) 8-(382-2)-492-392*

Interest in studying of spark, diffuse and corona discharges in air at atmospheric pressure and other gases at various parameters of voltage pulses applied to the electrode with a small radius of curvature, unabated now [1, 2]. Under conditions of high electric field at the cathode, X-rays and runaway electron beams are recorded in these discharges. In paper [3], by using voltage pulses of nanosecond duration, runaway electron beam with FWHM duration of  $\sim 100$  ps was obtained simultaneously in diffuse and corona discharge. In this paper, we adhere to the following view of the terminology: we call «diffuse discharge» such a shape in which the plasma radiation fills the entire gap from the cathode to the anode, and corona - one in which the radiation is concentrated only near of the electrode with a small radius of curvature. In the case of corona discharge, the runaway electron beam recorded at a considerable distance from the brightly glowing region of the corona discharge. However, the amplitude of the beam current in diffuse discharge was three orders of magnitude more than the corona discharge.

This paper presents the results of experimental studies of the amplitude-time characteristics of X-rays in a repetitively pulsed nanosecond discharge in nitrogen. It is shown that with increasing pressure there is a transition from a diffuse discharge form to corona (Fig. 1 a-c), accompanied by increasing of the X-ray pulse duration (Fig. 1d).

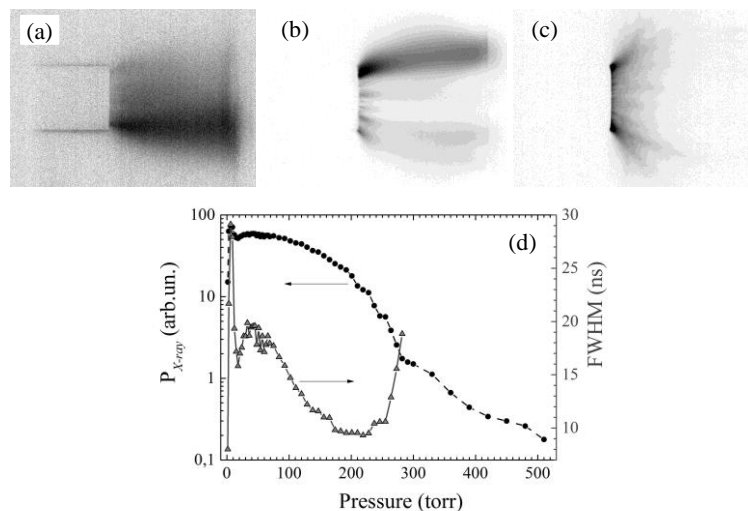


Fig. 1. Photos of the discharge at different pressures of nitrogen: a) 42 torr; b) 300 torr; c) 675 torr; d) dependence of the X-ray pulse amplitude and duration at half-maximum on the nitrogen pressure.

### REFERENCES

- [1] *Tardiveau P, Moreau N, Bentaleb S, Postel C, and Pasquiers S // J. Phys. D: Appl. Phys. – 2009. – 42. 175202.*
- [2] *Dwyer J R, Saleh Z, Rassoul H K, Concha D, Rahman M, Cooray V, Jerauld J, Uman M A, and Rakov V A // J. Geophys. Res. – 2008. – 113. D23207.*
- [3] *Kozyrev A.V., Kozhevnikov V.Yu., Kostyrya I.D., Rybka D.V., Tarasenko V.F., Shitz D.V. // Atmospheric and oceanic optics. – 2011. – V. 24. – № 11. Pages 1009-1017 [in Russian].*

<sup>1</sup> This work was supported by RFBR grant number 12-08-00081\_a.

## MEASUREMENT OF RUNAWAY ELECTRONS PREIONIZED DIFFUSE DISCHARGE PLASMA PARAMETERS BY OPTICAL EMISSION SPECTROSCOPY METHODES<sup>1</sup>

*M.I. LOMAEV*\*,\*\*, *D.A. SOROKIN*\*, *T.I. BANOKINA*\*\*\*, *V.F. TARASENKO*\*,\*\*\*

\**Institute of High Current Electronics, 2/3 Akademicheskoy Avenue, Tomsk, 634055, Russia, Lomaev@loi.hcei.tsc.ru, 49-23-92*

\*\**Tomsk State University of Control Systems and Radioelectronics, Tomsk, 40 Lenina Avenue, 634050, Russia*

\*\*\**National Research Tomsk State University, Tomsk, 36 Lenina Avenue, 634050, Russia*

Currently runaway electron diffuse discharge (REP DD) draws much attention [1-4]. The interest to this subject now is due to the both some fundamentals discharge formation's problems and the potential possibility of practical applications of low temperature REP DD plasma. REP DD is characterized by the generation of runaway electron beam and X-ray in gas discharge volume that provides the formation of diffuse discharge at high pressure, very short (fractions – ones of nanosecond) duration of discharge formation stage, high level of specific excitation power (up to 1 GW/cm<sup>3</sup>). It is explained to impede considerably a study and technical realization of REP DD.

Many published papers devoted to REP DD are deal with a runaway electron beam's generation, its time-amplitude characteristics, time behavior and amplitude of a voltage and discharge current pulses. Prospects of these discharges' practical application are associated mainly with the possibility of forming of a low temperature dense plasma at elevated pressure of different gases and their mixtures.

The measurements of electrons density  $N_e$ , electron  $T_e$  and gas  $T_g$  temperatures and enhanced electric field  $E/N$  of REP DD plasma is important from both fundamental and practical points of view. Firstly, the knowledge of these parameters is important at creation and verification of REP DD's theoretical model. Secondly, it is necessary to characterize the main properties of REP DD's plasma used in practical applications.

The subject of this study was to carry out the measurements of  $N_e$ ,  $T_e$ ,  $T_g$  and  $E/N$  in the plasma of REP DD formed in helium and nitrogen at elevated pressures.

The measurements were carried out in helium at pressure of 1 – 6 atm and nitrogen at atmospheric pressure at both single pulse and pulse-periodic modes. A single pulse and pulse-periodic modes of REP DD were realized by use of high-voltage pulses with rate of voltage increasing of about  $5 \cdot 10^{14}$  V/s and  $2 \cdot 10^{13}$  V/s, respectively. In the both cases, the gas discharge gaps with sharply nonuniform distribution of electric field strength were used. The values of  $N_e$  were calculated with the well-known method based on a measurement of the Stark broadening of atomic spectral lines [5]. Since the state of REP DD plasma is nonequilibrium, the values of  $T_e$  and  $E/N$  were determined with the method based on the radiation-collisional plasma model [6, 7]. The values of  $T_g$  were calculated with the use of rotational distribution in emission spectrum of nitrogen.

The maximum  $N_e$  value in helium at pressure of 1 atm achieved of  $\sim 5.4 \cdot 10^{15}$  cm<sup>-3</sup>. The plasma of REP DD in nitrogen at pressure of 1 atm and pulse repetition rate of 2 kHz is characterized as follows:  $N_e \sim 4 \cdot 10^{14}$  cm<sup>-3</sup>,  $T_e \sim 2$  eV, and  $E/N \sim 270$  Td,  $T_g \sim 1250$  °K. The dynamics of  $T_e$  and  $E/N$  values in REP DD plasma of nitrogen was determined, as well.

### REFERENCES

- [1] *L. P. Babich // High-Energy Phenomena in Electric Discharges in Dense Gases: Theory, Experiment and Natural Phenomena, ISTS Science and Technology Series, Vol. 2, Arlington, Virginia: Futurepast, 353, 2003.*
- [2] *D. S. Levko, Y. E. Krasik, V. F. Tarasenko // International Review of Physics. – 2012. – 6. - No. 2. 165-195.*
- [3] *G. A. Mesyats, M. I. Yalandin, A. G. Reutova, K. A. Sharypov, V. G. Shpak, and S. A. Shunailov // Plasma Physics Reports. – 2012. – 38. - No. 1. 29–45.*
- [4] *T. Shao, V. F. Tarasenko, Ch. Zhang, A. G. Burachenko, D. V. Rybka, I. D. Kostyrya, M. I. Lomaev, E. Kh. Baksht and P. Yan // Review of Scientific Instruments. – 2013. – 84. 053506.*
- [5] *H. R. Griem // Spectral line broadening by plasmas, Academic Press, New York and London, 408, 1974.*
- [6] *N. Britum, M. Gaillard, A. Ricard, Y. M. Kim, K. S. Kim and J. G. Han // J. Phys. D: Appl. Phys. – 2007. – 40. 1022–1029.*
- [7] *P. Paris, M. Aints, M. Laan and F. Valk // J. Phys. D: Appl. Phys. – 2004. – 37. 1179–1184.*

<sup>1</sup> The work is performed in the framework of the State task for HCEI SB RAS, project №13.1.3.

## EXPERIMENTAL AND NUMERICAL STUDY OF THE NANOSECOND HIGH-VOLTAGE DISCHARGE FORMATION IN SHARPLY-NONUNIFORM ELECTRIC FIELD<sup>1</sup>

*E.KH. BAKSHT, S.YA. BELOMYTTSEV, A.G. BURACHENKO, A.A. GRISHKOV, V.A. SHKLYAEV, V.F. TARASENKO*

*Institute of High-Current Electronics SB RAS, 2/3, Akademichesky Ave., Tomsk, 634055, Russia,  
beh@loi.hcei.tsc.ru, +73822492392*

In recent years, the interest in the nanosecond high-voltage gas discharges has increased significantly. However, the question concerning the physical processes taking place in the diode during the formation of the high voltage (>100 kV) nanosecond discharge (including pressure below atmospheric) has not been resolved to the end to date. Due to the short duration of the stage of the discharge formation (hundreds of picoseconds), numerical simulation is the best method for solving this problem.

In this paper, we propose an experimental study and numerical modeling of processes in a gas-filled diode at high (>100 kV) voltage.

During the experiments, the current and voltage waveforms in the gas-filled diode at different pressures in the region of units-tens of Torr were obtained.

To check the results of the experiments and their physical interpretation, the computer simulation was conducted. During the work, we used the two-dimensional axisymmetric PIC KARAT [1] and XOOPIC [2] codes (in some cases, three-dimensional calculations were made using the KARAT code as well).

At the same initial conditions, discrepancies in the results of axisymmetric calculations were negligibly small. The results of simulation are in good agreement with the data obtained in the course of the experiments and allow reconstructing the dynamics of the processes in the studied conditions on a qualitative level.

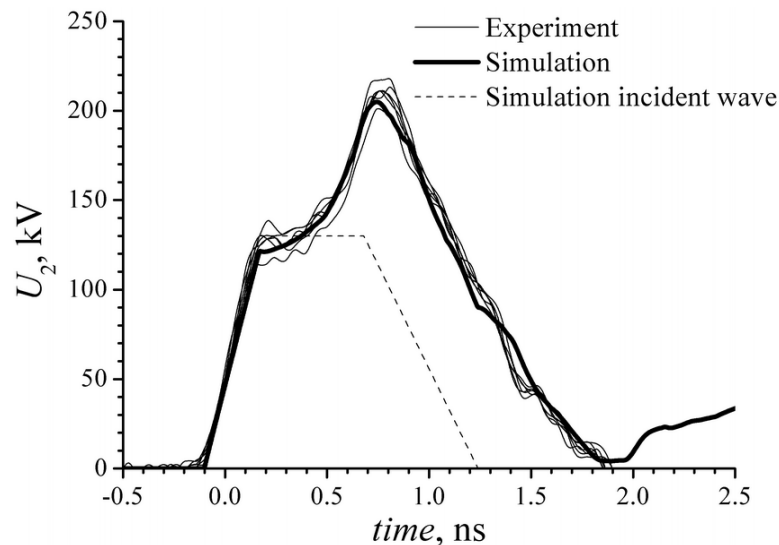


Fig. 1. Comparison of voltage waveforms from the capacitive divider, located in a transmission line at a distance of 50 mm from the diode, obtained during the experiment (thin curves), with calculated waveforms obtained by numerical simulation (thick curve).

### REFERENCES

- [1] V.P. Tarakanov // *User's manual for code Karat*. –Berkley Research Associate. Inc, Springfield, VA, 1992.
- [2] J.P. Verboncoeur, A.B. Langdon, N.T. Gladd // *Comput. Phys. Commun.* – 1995. – 87. – №1. pp. 199-211.

<sup>1</sup> This work was supported by the grant of RFBR No14-02-00136

**EXPERIMENTAL INVESTIGATION OF NANOSECONDS DISCHARGE INITIAL STAGE IN AIR OF ATMOSPHERIC PRESSURE**

*A.A. TRENKIN, V.I. KARELIN, Yu.M. SHIBITOV*

*State Corporation on Atomic Energy "Rosatom" Federal State Unitary Entity "Russian Federal Nuclear Center – All-Russian Scientific and Research Institute of Experimental Physics", 37 Mira Ave., Sarov, 607190, Russia, E-mail: trenkin@ntc.vniief.ru, phone: (83130)27252*

The paper presents investigation results of initial stage of nanosecond discharge in the air of atmospheric pressure. Spatial characteristics of the discharge were studied by photographing its luminescence and autograph method. The discharge images and photos of the current channels prints on electrodes surface are obtained. The discussion results of obtained experimental data are presented.

**SIMULATION OF AN AVALANCHE OF RUNAWAY ELECTRONS FORMED  
IN AN ATMOSPHERIC PRESSURE AIR DISCHARGE**

*E.V. ORESHKIN\**, *S.A. BARENGOLTS\**, *S.A. CHAIKOVSKY\**, \*\*, *V.I. ORESHKIN\*\**

*\*P. N. Lebedev Physical Institute, RAS, Moscow*

*\*\*Institute of High Current Electronics, SB, RAS, Tomsk, E-mail: oreshkinev@scalpnet.ru*

A numerical simulation of a beam of runaway electrons formed from an individual emission zone on a cathode has been performed for discharges in air of atmospheric pressure. The model is based on solving numerically two-dimensional equations of motion for the electrons and allows one to describe the dynamics of the fast electrons injected from the surface of the emission zone. In calculations it was supposed that the electric field at the surface of the emission zone is enhanced due to which conditions are realized for the electrons injected from the surface to switch into the mode of continuous acceleration. It is shown that the formation of a runaway electron beam in a highly overvolted discharge is largely associated with avalanche-type processes and that the number of electrons of an avalanche reaches 50% of the total number of runaway electrons.

## PULSE-PERIODIC GENERATION OF SUPERSHORT AVALANCHE ELECTRON BEAMS AND X-RAY EMISSION<sup>1</sup>

*A.G. BURACHENKO, E.H. BAKSHT, M.V. EROFEEV, V.F. TARASENKO*

*Institute of High Current Electronics, Akademicheskoy Ave. 2/3, Tomsk, Russia, 634055  
BAG@loi.hcei.tsc.ru, +7-3822-492392*

The aim of the present work was to study the supershort avalanche electron beam (SAEB) parameters and the X-ray exposure dose in the pulse-periodic mode of the discharge at different durations of the voltage pulse front. Information obtained in this study can be used to create pulse-periodic electron accelerators and X-ray sources with a subnanosecond pulse duration, as well as to better understand the formation mechanism of a diffuse discharge at elevated pressures. The second aim of this work was to detect an SAEB at pulse repetition frequencies of higher than 1 kHz. This work continues studies [1, 2], where an SAEB was obtained at voltages of tens of kilovolts, a helium pressure of ~100 Torr, and a pulse repetition frequency of 1 kHz.

The experiments were carried out in the discharge chamber, to which voltage pulses with an amplitude of up to 35 kV and a repetition frequency of up to 3.5 kHz were supplied from an NPG-15/2000N generator [3] via a 3-m-long cable. The FWHM of the voltage pulse at a matched load (75 Ω) was ~6 ns, the front duration at a level of 0.3-0.9 being ~2.5 ns. In some experiments, sharpening spark gap was installed between the generator and the discharge chamber, due to which the duration of the voltage pulse front was reduced to ~0.3 ns. In most experiments, the discharge gap length was 12 mm and 6-mm-diameter stainless-steel tubular cathode.

It is shown that, in the pulse-periodic mode of a diffuse discharge, gas heating in the discharge gap results in a several fold increase in the SAEB amplitude (the number of electrons in the beam), see Fig. 1.

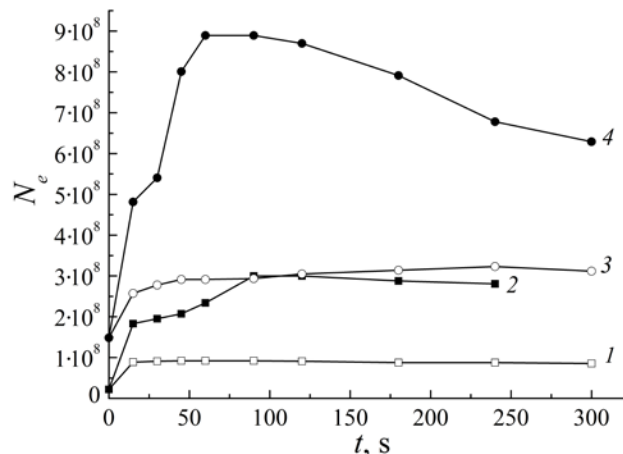


Fig. 1. Number of SAEB electrons as a function of time for the generator voltage of 25 kV and repetition frequencies of 60 (1) and 2000 (2) Hz and for the generator voltage of 35 kV and repetition frequencies of 60 (3) and 500 (4) Hz.

At a generator voltage of 25 kV, nitrogen pressure of 90 Torr, and pulse repetition frequency of 3.5 kHz, a runaway electron beam was detected behind the anode foil. It is found that, when the front duration of the voltage pulse at a nitrogen pressure of 90 Torr decreases from 2.5 to 0.3 ns, the X-ray exposure dose in the pulse-periodic mode increases by more than one order of magnitude and the number of SAEB electrons also increases. It is shown that, in the pulse-periodic mode, the full width at half-maximum of the SAEB is larger and the decrease rate of the gap voltage is lower than those in the single-pulse mode.

### REFERENCES

- [1] Erofeev M. V., Baksht E.Kh., Tarasenko V.F., & Shut'ko, Y. V. // *Technical Physics*. – 2013. – T. 58. – №. 2. – 200-206.
- [2] Shao T., Tarasenko V.F., Zhang C., Baksh E.K., Zhang D., Erofeev M.V., & Yan P. // *J. of Applied Physics*. – 2013. – T. 113. – №. 9. – 093301.
- [3] Korotkov S.V., Aristov Y.V., Kozlov A.K., Korotkov D.A., Lyublinsky A.G., & Spichkin G.L. // *Instruments and Experimental Techniques*. – 2012. – T. 55. – №. 5. – 605-607.

<sup>1</sup> The work is performed in the framework of the State task for HCEI SB RAS, project №13.1.3.

**DISCHARGES WITH RUNAWAY ELECTRONS: SIMULATIONS AND EXPERIMENTS**

S. YATOM\*, D. LEVKO\*, V. VEKSELMAN\*, S. TSKHAI\*\*, V. T. GUROVICH\*, Y. E. KRASIK\*

\*Physics Department, Technion. Haifa 3200, Israel; finkrasik@physics.technion.ac.il; 972-4-8283559

\*\*Lebedev Physics Institute, Russian Academy of Sciences, 117924 Moscow, Russia

Runaway electrons (RAE) play a crucial role in the initiation of high-voltage (HV) electrical discharges in pressurized gases. In this report the results of Particle-in-Cell (PIC) numerical modeling [1] and experimental research [2-5] of such type of the discharge will be presented. PIC simulations considers in detail the process of field-emitted electron acceleration in the vicinity of the cathode leading to the appearance of RAE. It is possible also that RAE are generated as a result of the acceleration of electrons emitted from the anode side of the virtual cathode formed in the cathode-anode gap due to the space charge of electrons emitted from the cathode and electrons generated by the gas ionization. In addition, PIC simulations allow the study of the process of termination of RAE generation, which occurs because of the shielding of the field emission by the space charge of generated electrons or/and due to the transition of field emission into the explosive emission. The dependencies of the potential and space-charge of electron and ion distributions in the cathode-anode gap, electron energy and velocity distribution for different types and pressures of gases, and the form and amplitude of the applied voltage will be presented and analyzed.

The properties of high-energy RAE generated during a ns time scale discharge in an air filled diode (150kV, 5ns/1ns duration HV pulse) at pressures up to  $3 \cdot 10^5$  Pa were studied using x-ray absorption spectroscopy. Energy distribution functions for RAE produced in PIC simulation were used to create the x-ray attenuation curves via a computer-assisted technique simulating the generation of x-ray by energetic electrons. The simulated attenuation curves showed good agreement with experimental results

Time- and space-resolved visible-emission spectroscopy measurements were applied to study plasma parameters in electrical discharges in He and hydrogen gas at pressure of  $10^3$  Pa. The plasma evolution during the discharge was investigated by applying line-shape analysis of several He I and  $H_\alpha$  spectral transitions, with the Stark, opacity, resonance and van de Waals effects accounted for. The analysis shows that the discharge plasma is not in equilibrium and that significant electric fields of several kV/cm are present in the plasma during the discharge. Regions of plasma with significantly different electron densities are identified and a qualitative model of the plasma formation and evolution is proposed.

Experimental results of a study of the electric field in a plasma channel produced during ns discharge at a  $H_2$  gas pressure of  $(2-3) \cdot 10^5$  Pa by the coherent anti-Stokes scattering method will be reported as well. It was shown that this type of gas discharge is characterized by the presence of an electric field in the plasma channel with root-mean-square intensities of up to 30 kV/cm. Using polarization measurements, it was found that the direction of the electric field is along the cathode-anode axis.

## REFERENCES

- [1] D. Levko, Ya. E. Krasik and V. Tarasenko// Intern. Rev. Phys. – 2012 – 6 – №.165-195.
- [2] S. Yatom, J. Z. Gleizer, D. Levko, V. Vekselman, V. Gurovich, E. Hupf, Y. Hadas and Ya. E. Krasik, EuroPhysics Lett. – 2011 – 96 – №.65001-4.
- [3] S. Yatom, D. Levko, J. Z. Gleizer, V. Vekselman and Ya. E. Krasik// Appl. Phys. Lett. – 2012 – 100 – №.024101-3 (2012).
- [4] S. Yatom, E. Stambulchik, V. Vekselman, and Ya. E. Krasik// Phys. Rev. E. – 2013 – 88 – №. 013107-11.
- [5] S. Yatom, S. Tskhai, and Ya. E. Krasik// Phys. Rev. Let. – 2013 – 111 – №.255001-4.

## GENERATION OF RUNAWAY ELECTRON BEAMS IN NANOSECOND-PULSE DISCHARGES<sup>1</sup>

T. SHAO\*, C. ZHANG\*, H. MA\*, W. YANG\*, Y. SUN

\*Institute of Electrical Engineering, Chinese Academy of Sciences, Beijing, 100190, China, st@mail.iee.ac.cn

In the past years, there has been increasing interest in nanosecond diffuse discharges in an inhomogeneous electric field. These discharges are initiated at increased pressures due to the generation of runaway electrons. In this paper, two collectors are made for measuring runaway electron beams (REBs) in nanosecond-pulse discharges. These collectors are used to measure the REBs in discharges sustained by a VPG-30-200 nanosecond-pulse generator with a pulse width of 3~5 ns and a rise time of 1.2~1.6 ns. One of collectors is optimal designed in order to improve the impedance matching characteristics and obtain better waveforms of REBs.

Experimental results show that REBs can be effectively measured by the collectors, and the optimized collector has shorter time resolution and higher amplitude of the REBs. When the applied voltage is 80 kV, REBs can be measured with an amplitude of 160 mA and full width at half maximum of less than 1 ns. Experimental results with pulse sequences prove that the collectors have excellent reliability, and both the transient response and time resolution are stable. Furthermore, REBs in different gas types (air, nitrogen, helium and sulfur hexafluoride (SF<sub>6</sub>)) are studied by using the optimized collector. Results show that the amplitudes of the REBs in SF<sub>6</sub> are smaller than those in air, nitrogen and helium. In addition, the energy spectrum of the runaway electron is estimated by measuring the REBs behind aluminum foils with different thicknesses.

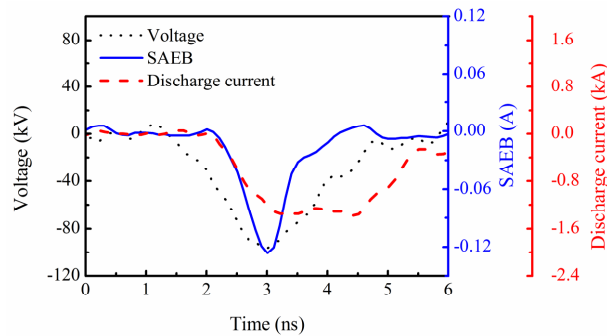


Fig. 1. Waveforms of voltage pulse, discharge current and SAEB behind foil at pressures of SF<sub>6</sub> 200 Pa. VPG-30-200 generator, d = 12 mm.

### REFERENCES

- [1] Zhang C, Tarasenko V F, Shao T, Baksht E K, Burachenko A G, Yan P, Kostyray I D // Laser and Particle Beams – 2013.–31. – № 2. 353-364.
- [2] Shao T, Tarasenko V F, Zhang C, Baksht E K, Zhang D, Erofeev M V, Ren C, Shutko Y V, Yan P // Journal of Applied Physics – 2013.–113. – № 9. 093301.
- [3] Alekseev S B, Lomaev M I, Rybka D V, Tarasenko V F, Shao T, Zhang C, Yan Ping // High Voltage Engineering – 2013.–39. – № 9. 2112-2118.

<sup>1</sup> This work was supported by the National Natural Science Foundation of China under Grants 51222701, 51207154, 51211120183, and the National Basic Research Program of China under Grant 2014CB239505



## CONDITIONS FOR STREAMER-TO-DIFFUSE DISCHARGE TRANSITION IN ATMOSPHERIC PRESSURE AIR GAPS<sup>1</sup>

*P. TARDIVEAU*

*Paris-Sud University, CNRS, LPGP, rue Henri Becquerel, Orsay, 91400, France, [pierre.tardiveau@u-psud.fr](mailto:pierre.tardiveau@u-psud.fr), +33169157250*

Under moderate overvoltages, non-thermal plasmas develop in centimeter air gaps as multi-channel structures referred as well-known streamer discharges. When voltage rising edge is strongly shortened down to a few nanoseconds and amplitude increased over several tens of kilovolts, this classical physics seems not to operate anymore and new macroscopic behaviors appear [1]. The change of the discharge morphology into a diffuse and large structure suggests processes yet underestimated in non uniform electric field configurations, such as runaway electrons generation and X-rays emission [2]. Under very strong overvoltages, higher than 400 %, the physics of streamers and the models which are used to describe it show their limit. The electric fields become so high that the hypothesis of local field equilibrium, usually admitted for electrons, must be reconsidered and one must take into account the existence of electrons and radiations of very high energies.

Within the experimental studies presented here, effects of pressure on diffuse discharges created in a tip-to-plane configuration are considered. Transition into a multi-channel structure is analyzed with respect to the overvoltage intensity and the inter-electrode distance. Between 1 and 3 bar, a good agreement with well-known pressure similarity rules is shown in air gaps, considering the size  $D_{\max}$  of the gap under which the development of the discharge is completely diffuse from its start at the tip to its junction to the cathode plane (Fig. 1).

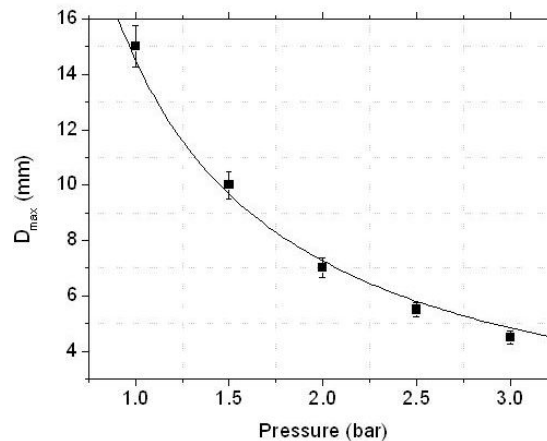


Fig. 1. Pressure evolution of the maximal gap length for which the discharge remains completely diffuse (positive high voltage tip-to-plane configuration).

Effects of small fractions of propane or heptane in air are studied as well. Filamentary structures appear as soon as a few percents of hydrocarbons are added. A possible explanation is related to X-rays emission considered to justify the diffuse property of the discharge. Hydrocarbons may modify the electron energy distribution function and reduce its high energy part. Fewer electrons would be accelerated to high energies and therefore, lower intensity X-radiations would be produced at the tip, much shortly absorbed than it is in atmospheric air.

Finally, it is shown that air discharges studied under extreme non-uniform electric fields at atmospheric pressure show some similarities with externally pre-ionized discharges at lower pressures, which have proved their efficiency to create homogeneous volumes of plasma since a long time.

### REFERENCES

- [1] *P. Tardiveau, N. Moreau, S. Bentaleb, C. Postel, S. Pasquiers // J. Phys. D: Appl. Phys.- 2009.- 42.- 175202.*
- [2] *T. Shao, C. Zhang, Z. Niu, P. Yan, V.F. Tarasenko, E.Kh. Bakshat, A.G. Burahenko, Y.V. Shutko // App. Phys. Letters. - 2011. - 98. - 021503.*

<sup>1</sup> This work was supported by the National Agency of Research (ANR) under contract no ANR-05-BLAN-0181.

## WIDE-APERTURE X-RAY RADIATION SOURCES, BASED ON ATMOSPHERIC PRESSURE DISCHARGES

S.N. BURANOV, V.V. GOROKHOV, V.I. KARELIN, P.B. REPIN

*State Corporation on Atomic Energy "Rosatom" Federal State Unitary Entity "Russian Federal Nuclear Center – All-Russian Scientific and Research Institute of Experimental Physics", 37 Mira Ave., Sarov, 607190, Russia,  
E-mail: [karelin@ntc.vniief.ru](mailto:karelin@ntc.vniief.ru), phone: (83130)45477*

Investigation results of X-Ray radiation sources, based on high-voltage diffusive discharges are presented in the paper. The discharge was formed in three-electrode systems, having apertures of mesh anodes up to  $2.9 \times 0.9 \text{ m}^2$ . The discharge length was 50-100 ns, voltage up to 1 MV at a rise time of 10-20 ns. The experiments were carried out in the air and  $\text{CO}_2\text{-N}_2\text{-He}$  media of atmospheric pressure. It was found out that the discharge is a source of high-energy electrons and x-ray radiation. Average energy of the electrons was 20-30 keV, maximum energy –100-150 keV. X-Ray radiation pulse length was 10-30 ns, effective quanta energy – 8-18 keV. Absorbed dose of 60-300 Roentgen was recorded in the gaps up to 40 cm. Physical model of high-energy electrons is presented in the paper.

## **GENERATING HIGH ENERGY ELECTRONS IN HIGH-VOLTAGE PULSED DISCHARGES IN AIR, DEVELOPING IN REGIME OF CURRENT CHANNELS MICROSTRUCTURING**

*A.A. TRENKIN, V.I. KARELIN*

*State Corporation on Atomic Energy "Rosatom" Federal State Unitary Entity "Russian Federal Nuclear Center – All-Russian Scientific and Research Institute of Experimental Physics", 37 Mira Ave., Sarov, 607190, Russia, E-mail: trenkin@ntc.vniief.ru, phone: (83130)27252*

Research results of spatial characteristics of laboratory nanosecond gas discharges in air of atmospheric pressure are presented in the paper. It is experimentally established that autographs of the discharges on the electrodes surface form clusters (up to 1000 and more) of microchannels of 1...30  $\mu\text{m}$  diameters and, in some cases, the discharges are accompanied by fluxes of high-energy electrons and X-ray radiation. The fractal dimension of a lightning discharge is determined. It is established that, with respect to the fractal dimension and, hence, the character of spatial structure organization, the lightning discharge is analogous to high-voltage discharges of other types, including streamer corona, surface, nanosecond diffuse, spark, and streamer-free discharges. Dynamic of electron transport in current channels fractal branching systems is considered. Obtained results allow explaining generation of high energy electrons in high-voltage discharges, developing in a regime of the current channels microstructuring.

## NANOSECOND-PULSE BREAKDOWN WITH THE INVERSION OF EFFECT POLARITY<sup>1</sup>

*V.F. TARASENKO, D.V. BELOPLOTOV, M.I. LOMAEV, D.A. SOROKIN*

*Institute of High Current Electronics, Akademicheskoy Ave. 2/3, Tomsk, Russia, 634055  
VFT@loi.hcei.tsc.ru, +7-3822-491685*

The objective of the present work is to study the breakdown in SF<sub>6</sub> and nitrogen in an inhomogeneous electric field and to clarify why the inversion of polarity effect did occur and did not occur.

On Setup, the discharge voltage, current through the gap, runaway electron (RAE) beam current downstream of foil (a supershort avalanche electron beam, SAEB), and radiation from different regions of the gap were measured, respectively. The voltage pulse produced by the RADAN-220 generator was applied to a tubular electrode of small curvature radius via a short transmission line. This high voltage electrode was made of stainless steel foil of 100 μm thickness rolled up into a tube of 6 mm diameter. The ground electrode was a plane and was located 13 mm away from the end face of the high voltage electrode. The optical radiation from different discharge regions was extracted through a side window and was transmitted by a lens to a photodiode placed in a metal box. The DSA 72504D (25 GHz, 100 GS/s) oscilloscope and a high-speed PD025 photodiode (Photek LNS20 cathode, transient response rise time of ~ 80 ps) were used for measuring the ionization wave velocity. Typical waveforms of the voltage, discharge current, SAEB (at negative voltage pulse polarity), and radiation from the gap region near the tubular electrode at a nitrogen pressure of 0.2 MPa for negative polarity are shown in Figs. 1.

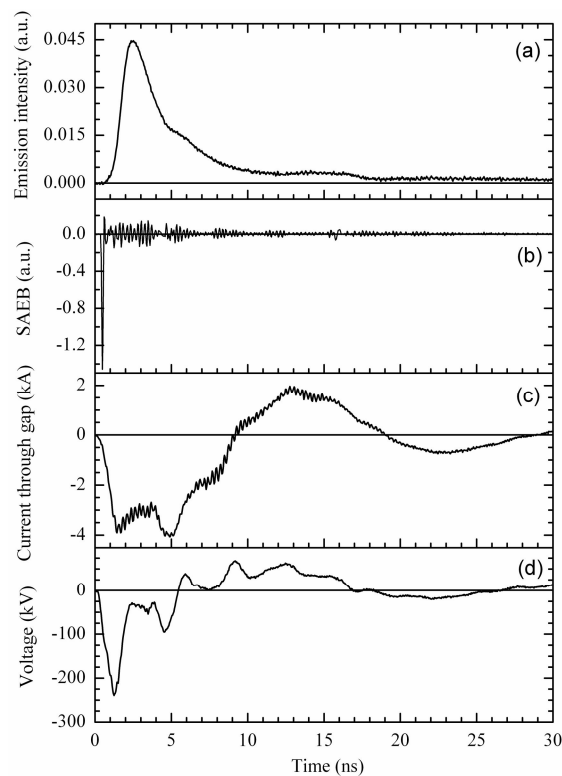


Fig. 1. Waveforms of emission intensity near tube electrode with negative polarity of RADAN-220 generator (a), runaway electron beam behind foil (SAEB) (b), current through gap (c), and voltage pulses (d). Pressure of nitrogen: 0.2 MPa.

The breakdown characteristics of gas gaps in an inhomogeneous electric field at subnanosecond voltage pulse rise times are studied. It is shown that at a voltage pulse rise time of ~0.5 ns, the inversion of polarity effect takes place not only in electronegative gases such as SF<sub>6</sub>, but also occurs in electropositive nitrogen. The inversion of polarity effect is related to a delay of electron emission from the plane cathode on arrival of the ionization wave front anode to the cathode. It is found that with a voltage pulse rise time of ~0.5 ns, the inversion of polarity effect occurs at SF<sub>6</sub> and SF<sub>6</sub>-N<sub>2</sub> pressures of 0.25 MPa and lower.

<sup>1</sup> The work is performed in the framework of the State task for HCEI SB RAS, project №13.1.3.

## DECREASING OF THE DIVERGENCE OF RUNAWAY ELECTRON BEAM GENERATED IN ATMOSPHERIC PRESSURE GAS MEDIA CONTAINING THE HOT CHANNEL<sup>1</sup>

V.V. LISENKOV\*, V.A. SHKLYAEV\*\*

\*Institute of Electrophysics UD RAS, Amundsena Street, 106, Ekaterinburg, 620016, Russia,  
lisenkov@iep.uran.ru., +7-343-2678779

\*\*Institute of High Current Electronics SD RAS, Academichesky Avenue, 2/3, Tomsk, 634055, Russia

In our paper [1] we presented the results of numerical research of high-effective runaway electron (RAE) beam generation in atmospheric pressure gas media containing the hot channel. In this paper we investigated the ability of decreasing of RAE beam divergence with a help of external magnetic field or dielectric tube.

We used the well-known XOOPIC package [2]. This package is based on the method of large particles, which is used to simulate the motion of charged particles in external and internal electromagnetic fields. Elastic and inelastic electron collisions are simulated by the Monte Carlo method. The dynamics of the electromagnetic field in both the diode and input line is calculated based on the Maxwell equations. The package uses a two-dimensional axisymmetric approximation.

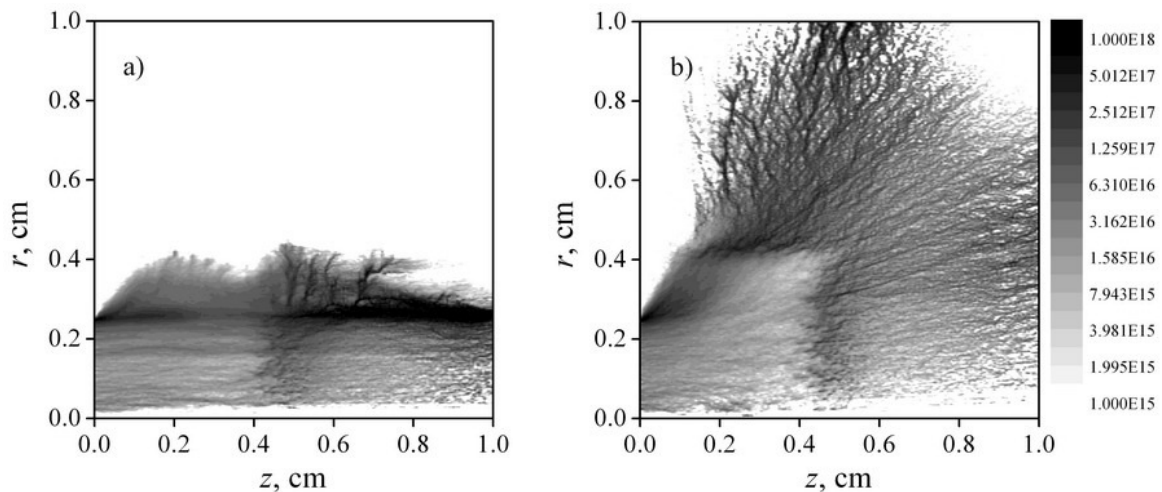


Fig. 1. Phase portraits of electrons in coordinates  $(z, r)$  with (a) and without (b) external magnetic field.

Figure 1 shows the phase portraits electrons in coordinates radius  $(r)$  -  $z$ -axis with (a) and without (b) external magnetic field of 1 T. Due to the presence of this field runaway electrons move almost along the axis  $z$ , slightly going outside the radius of the hot channel, where there generated. Ionizing gas, the fast electrons initiate the formation of plasma channel within the radius of hot channel (Fig. 1 a).

In the absence of a magnetic field (Fig. 1 b) runaway electrons immediately begin to diverge in the radial direction producing almost homogeneous bulk preionization. As a result, the diffuse discharge occupies almost whole volume between the electrodes.

It's interesting, that magnetic field has no significant effect on the amplitude, duration, and the dynamics of the energy spectrum of RAE beam. Most likely, this is due to the fact that the external magnetic field does not change the dynamics of the plasma and the electric field inside the hot region, where the electrons mostly transfer into runaway mode.

Using the dielectric tube results in same effect then magnetic field.

### REFERENCES

- [1] V.V. Lisenkov, V.A. Shklyayev // Technical Physics Letters. – 2013. – 39. – 732-735.
- [2] J. P. Verboncoeur, A. B. Langdon, and N. T. Gladd // Comput. Phys. Commun. – 1995. – 87. – 199.

<sup>1</sup> This study was supported by the Russian Foundation for Basic Research (projects 12-08-00229-a and 13-08-01314-a) and integration project No. 107 "High- and low-pressure gas discharges and new electrophysical devices on their basis" with collaborative participation of IEP UD RAS and IHCE SD RAS.

## CALCULATION OF ELECTRODE SHAPE FROM GIVEN ELECTRIC FIELD DISTRIBUTION USING FINITE ELEMENT METHOD<sup>1</sup>

*D.S. FARAFONOV\**, *V.A. SHKLYAEV\*\**

*\*OAO "NPC Polus", 56 'B' Kirova Avenue, Tomsk, 634050, Russia*

*\*\*Institute of High Current Electronics, 2/3 Academichesky Avenue, Tomsk, 634055, Russia*

In some application in pulse power it is necessary to provide physical fields with specified space distribution. In particular, gas discharge research requires a special distribution of electric field along the anode-cathode gap. These problems are inverse problems and their solutions are more complex than solutions of forward problems.

The subject of this article is solution of inverse problem for Laplace's equation using finite element method. This problem is calculation of the cathode shape which corresponds to given electric field distribution. In this article the problem is considered in quasistatistical approximation.

Field distribution is set in some domain (domain A) and in another one (domain B) must be surface of the cathode to find. Due to finite-element discretization domain A becomes a set of vertices A. Vector of desired potentials in set A is  $V_0$ . Set of broken line  $L_i$ , which lie in domain B and consist of boundaries between finite elements we call permissible lines. Each permissible line has not self-crossings. Each permissible line represents some cathode surface shape. Let all vertices of permissible line  $L_i$  have potential  $U_0$ . For each line  $L_i$  potentials is calculated and vector of potentials in set A is  $V_i$ . Line  $L_k$  is solution of the problem if vector  $V_k$  is closer to vector  $V_0$  than each other vector  $V_i$ :

$$|V_k - V_0| \rightarrow \min . \quad (1)$$

Problem of finding line  $L_k$  corresponding equation (1) is a combinatorial problem. Each line  $L_i$  corresponds to vertex of some graph G and each edge of this graph corresponds to transformation between two vertices. If we have initial shape of electrode  $L_0$  we need an algorithm to find the solution  $L_k$ .

Some algorithms to find approximate solution are developed. These algorithms based on transformations of electrode shape. These algorithms tested on some examples and some shapes of electrode are calculated. Algorithms use fast realization of finite element method based on Kron's method of tearing.

### REFERENCES

- [1] *P.P. Silvester, R.L.Ferrary* // Finite Elements For Electrical Engineers. - Moscow, 1986.
- [2] *G. Kron* // Diakoptics; The Piecewise Solution Of Large-Scale Systems. - Moscow, 1972.

<sup>1</sup> This work was supported by Russian Foundation for Basic Research, grant №. 13-08-01314

## SPACE-TIME DISTRIBUTION OF NITROGEN RADIATION IN BREAKDOWN OF DISCHARGE GAP WITH NON-UNIFORM ELECTRIC FIELD<sup>1</sup>

*D.V. BELOPLOTOV\*\*\*, M.I. LOMAEV\*, D.A. SOROKIN\*, V.F. TARASENKO\*\*\**

*\*Institute of High Current Electronics, 2/3 Akademicheskoy Avenue, Tomsk, 634055, Russia, VFT@loi.hcei.tsc.ru, 49-16-85*

*\*\*National Research Tomsk State University, Tomsk, 36 Lenina Avenue, 634050, Russia*

The space-time distribution of radiation intensity of the discharge plasma in nitrogen and other gases was obtained by optical methods. Distance between electrodes of the discharge gap was  $d = 13$  mm. The pressure was changed from 0.1 up to 0.7 MPa. Non-uniform electric field was provided by geometry of electrodes («tube-plane», «knife-knife» and «knife-plane»). The nanosecond high-voltage pulses from generator RADAN-220 applied across the discharge gap.

It was found, that the breakdown of part of the discharge gap in nitrogen at pressure of 0.7 MPa is implemented by ionization wave. The other part of discharge gap ionized simultaneously in entire volume. It is confirmed by distribution of nitrogen radiation along discharge gap (Fig. 1a, 1b) and by distribution of rate of intensity rise (Fig. 1c, 1d).

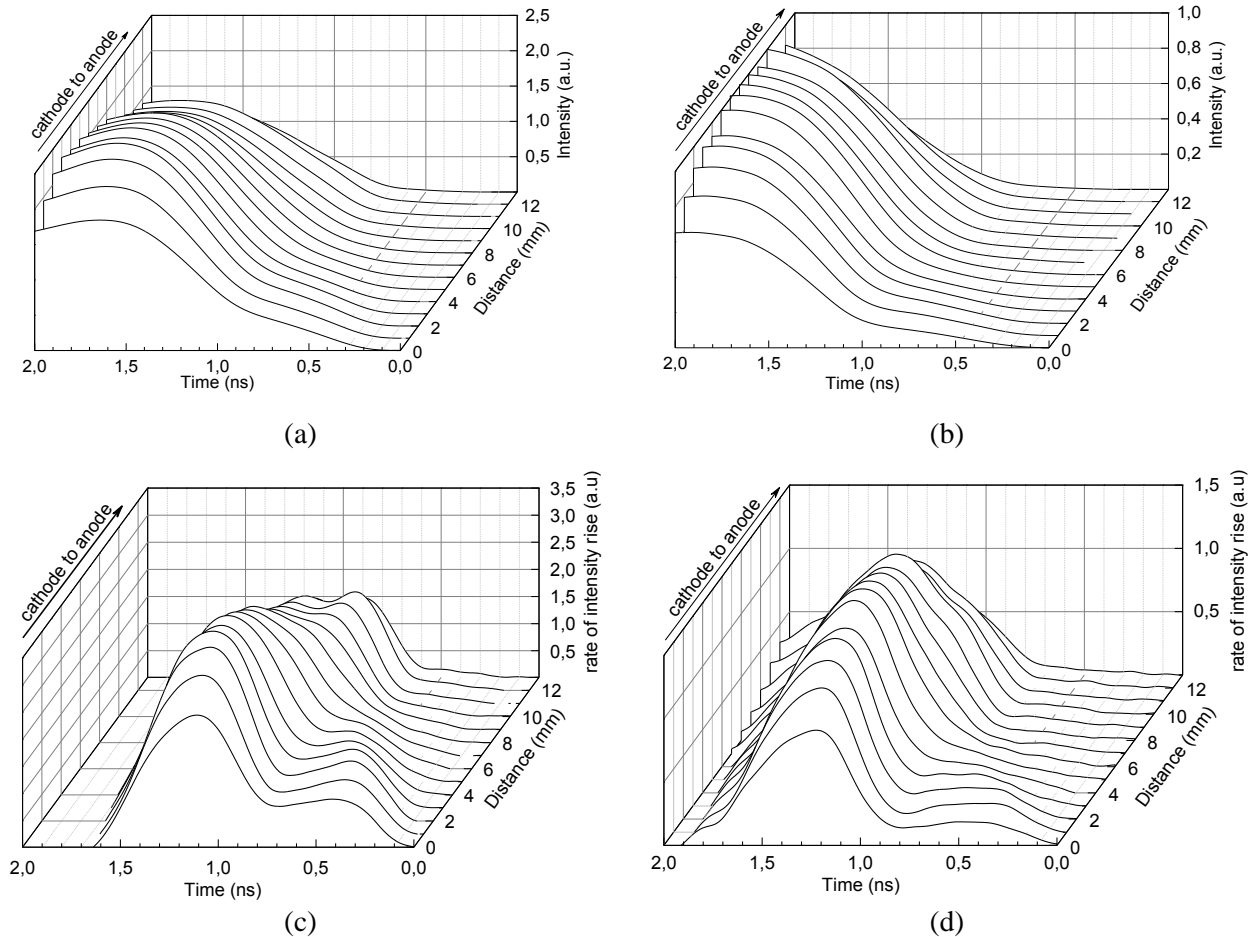


Fig. 1. Distributions of intensity and rate of intensity rise along discharge gap with «tube-plane» configuration of electrodes (a), (c) respectively and with «knife-knife» configuration of electrodes (b), (d) respectively in nitrogen at pressure of 0.7 MPa

The supershort avalanche electron beam (SAEB) [1] was recorded in nitrogen and other gases under the same experimental conditions.

### REFERENCES

- [1] Tarasenko V.F., Baksh E.Kh, Burachenko A.G., Kostyrya I.D., Lomaev M.I., Rybka D.V. // Plasma Dev. Oper. - 2008. – Vol. 16. - 267-298.

<sup>1</sup> The work is performed in the framework of the State task for HCEI SB RAS, project №13.1.3.

## RUNAWAY ELECTRONS DURING BREAKDOWN UNDER VOLTAGE PULSES WITH RISE TIME 0.6 MICROSECOND<sup>1</sup>

*I.D. KOSTYRYA, V.F. TARASENKO*

*Institute of High Current Electronics, Akademicheskoy Ave. 2/3, Tomsk, Russia, 634055  
VFT@loi.hcei.tsc.ru, +7-3822-491685*

The beams of runaway electrons and X-rays during the discharges in the air of the atmospheric pressure are registered in many scientific groups, see reviews [1, 2] and references therein. In these experiments the nanosecond voltage pulses with and subnanosecond rise times were used.

X-rays on the flat part of the voltage pulse of microsecond duration was obtained in [3]. The X-ray pulse duration under these conditions was approximately equal to the duration of voltage pulse. With rise time of voltage pulses 0.8 and 4  $\mu\text{m}$  the beam of runaway electrons was reported in [4].

In this paper we investigated the generation of runaway electrons and X-rays in the air at atmospheric pressure with rise time of voltage pulses 0.6  $\mu\text{m}$ .

Experimental setup was established on the basis of the generator SLEP-100, in which first capacitor (9 nF) was connected with pulse transformer. The secondary winding of pulse transformer was connected with the cathode of gas diode. A cathode was made from stainless steel in the form of a cone with a base diameter 6 mm or from steel ball. The anode was made from grid, which was located before Al or copper foil or photo film RF-2 in the black paper.

The new data on generation of runaway electrons and X-rays with long rise time of voltage pulses were obtained. Oscilloscope traces of the voltage pulse and runaway electron current are shown in the Figure 1.

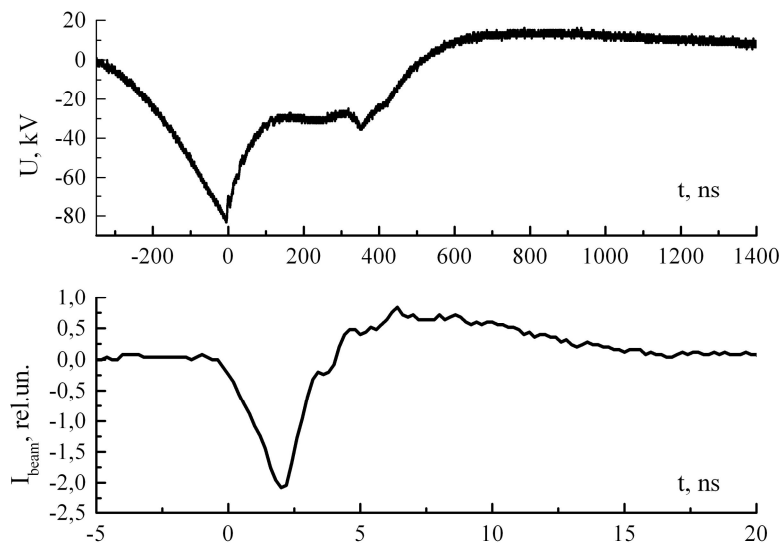


Fig. 1. Figure signature: Times new roman, 9 pt, the first line indent – 0 pt, centered; the interval before – 6 pt, after – 6 pt. (style “Congress2014 Figure caption”)

The runaway electron beam was record using the collector. Also the runaway electrons and X-rays were registered with the scintillator and FEU-100, and on film RF-2. The pulse duration from collector was shorter than from FEU-100.

### REFERENCES

- [1] *Tarassenko V.F., Bakshat E.KH, Burachenko A.G., Kostyrya I.D., Lomaev M.I., Rybka D.V. // Plasma Dev. Oper. - 2008. – Vol. 16. - 267-298.*
- [2] *Levko D., Krasik YA.E., Tarassenko V.F. // Internat. Rev. Phys. – 2012. - Vol. 6. - 165-195.*
- [3] *Bosamykin V.S., Karelin V.I. Pavlovskii. A.I., Repin V.I. //Pis' ma Zh. Tekh. Fiz. – 1980. – T. 6. – 885-888.*
- [4] *Loiko T.V. // Sov. Phys. Tech. Phys. – 1980. – T. 25. – №. 2. – 232-234.*

<sup>1</sup> The work is performed in the framework of the State task for HCEI SB RAS, project №13.1.3.



## GENERATION OF RUNAWAY ELECTRON BEAMS IN GAS DIODE WITH DIELECTRIC FILMS<sup>1</sup>

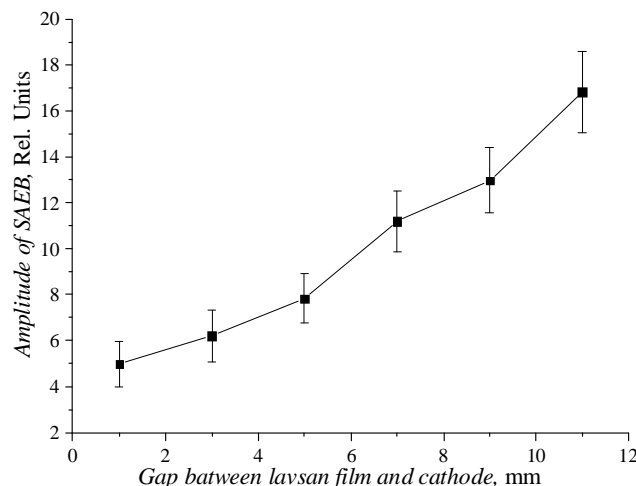
*I.D. KOSTYRYA, V.F. TARASENKO*

*Institute of High Current Electronics, Akademicheskoy Ave. 2/3, Tomsk, Russia, 634055  
VFT@loi.hcei.tsc.ru, +7-3822-491685*

Runaway electrons (RAE) beam generation by nanosecond discharges in atmospheric pressure air experimentally studied over 40 years. However, the results of the many experimental and theoretical works on generating beams of RAE at elevated pressures were not consistent. This calls for further experimental and theoretical studies of different modes of generation of RAE in gases at high pressure. One such issue is the influence of dielectric films in the gas diode on the amplitude of the current of RAE. So in the papers [1, 2] it was alleged that when placed in a bit between two films of dielectric allows to considerably increase the amplitude of the RAE current. On the other hand in the work [3] registered reduction of amplitude of RAE current with dielectric films in gas diode. In [4, 5] registered a major impact dynamic capacitive current on signal from the collector behind the anode, which was made from the mesh.

The purpose of this paper to study the influence of dielectric thin films placed in the gas diode on generation of supershort avalanches electron beam (SAEB) in atmospheric pressure air.

Experiments were conducted using a generator SLEP-150, as well as gas diode with tubular cathode and anode from metal foil or mesh. The dependence of amplitude SAEB of location of 50  $\mu\text{m}$  thick lavsan film in the gap is shown in figure.



Found that the number of electrons for anode foil smoothly increases as you move from the film 50  $\mu\text{m}$  thick by lavsan the cathode to the anode. Demonstrates that when you install the lavsan film at a distance 3 mm from the cathode and increase its thickness from 50 up to 100  $\mu\text{m}$  number of electrons for stamping reduced about 4 times. While installing lavsan films at a distance of 1 and 11 mm from the cathode, increasing its thickness from 50 up to 100  $\mu\text{m}$ , leads to a reduction in the number of electrons for the foil no more than 20%. Increase in amplitude SAEB with dielectric films in gas diode in the experiments was not recorded.

### REFERENCES

- [1] *Korolev V.S., Maltsev A.N. // Izv. VUZOV Phys. (Russ. Phys. J.). – 1993. – T. 6. – №. 1. – C. 67-70.*
- [2] *Maltsev A.N. // IEEE Transactions on Plasma Science. - 2006. -V. 34. - No. 4. - P. 1166-1174.*
- [3] *Mesyats G.A., Shpak V.G., Shunailov S.A., Yalandin M.I. // Technical Physics Letters. – 2008. – T. 34. – №. 2. – C. 169-173.*
- [4] *Kostyrya I. D., Tarasenko V. F. // Technical physics. – 2006. – T. 51. – №. 11. – C. 1512-1516.*
- [5] *Shao T., Tarasenko V.F., Zhang C., Burachenko A.G., Rybka D.V., Kostyrya I.D., Yan P. // Review of Scientific Instruments. – 2013. – T. 84. – №. 5. – C. 053506-053506-7.*

<sup>1</sup> The work is performed in the framework of the State task for HCEI SB RAS, project №13.1.3.

**AIR GAP BREAKDOWN ON RUNAWAY ELECTRONS**

*A.G. SADYKOVA\**, *S.A. SHUNAILOV\**, *M.I. YALANDIN \**, *A.V. GUREVICH\*\**, *K.P. ZYBIN\*\**, *A.F. SADYKOV\*\*\**,  
*M.D. KOLOMIETS\*\*\*\**

\* *Institute of Electrophysics UB RAS, 106 Amundsen Str., Ekaterinburg, 620016, Russia, anuta@iep.uran.ru, +7(343)2678824*

\*\* *P.N. Lebedev Physical Institute RAS, 53 Leninskij Prospekt, 119991, Moscow, Russia*

\*\*\* *Institute of Metal Physics UB RAS, 18 Sofia Kovalevskaya Str., Ekaterinburg, 620219, Russia*

\*\*\*\* *Ural Federal University, 19 Mira Str., Ekaterinburg, 620002, Russia*

Air breakdown on runaway electrons was investigated experimentally when the macroscopic electric field approximates to the critical value ( $E_c$ ) for runaway of above-thermal electrons not only at the cathode but throughout the discharge gap. In this limit spatial and temporal increment of an avalanche of runaway electrons is sharply reduced at high values of the specific electric field ( $E/p$ ). The complexity of the experiment was to provide and prove the existence of a strong field  $E > E_c$  at the time interval that is sufficient for the development of avalanche gain of almost all free electrons. It was proved. As a result the electron current in tens of amperes was observed behind the anode grid in a relatively small paraxial sector. The extrapolation of the divergent electron flow to the front sector and taking into account the energy threshold for the detected particles ( $> 2$  keV) allow us to conclude about the nature of the observed high-current electron avalanche growing less than 100 ps. Interest in study of this regime based on the fact that according to theoretical concepts similar effect takes place in an electric field of high-altitude lightning leader tips and results in generation of intense electron beams producing terrestrial gamma flashes.

## FORMATION OF DIFFUSE AND SPARK DISCHARGES IN NONUNIFORM ELECTRIC FIELD IN PULSE REPETITION MODE<sup>1</sup>

*E.H. BAKSHT, A.G. BURACHENKO, M.V. EROFEEV, V.F. TARASENKO*

*Institute of High-Current Electronics SB RAS, 2/3, Academicheskoy Ave., Tomsk, 634055, Russia,  
beh@loi.hcei.tsc.ru, +73822492392*

The goal of the paper is to study the initial stages of the diffuse and spark discharge formation in the nonuniform electric field at the elevated pressures of nitrogen, air and argon in a pulse-periodic mode by means of a CCD camera. The experiments were carried out in the conditions of generation of runaway electron beams and X-rays at the voltage pulse rise time of  $\sim 2$  ns and pulse repetition rate of 400 Hz.

In the work, a FPG-60 high-voltage, pulse-periodic generator and discharge chamber were used. The high-voltage generator allowed forming at a high-resistance load (1-10 kOhm) the negative-polarity voltage pulses of the amplitude up to 60 kV, voltage rise time of  $\sim 2$  ns and FWHM of 4-5 ns. In the experiments, the amplitude of the incident voltage wave was usually 10-15 kV. A sharp-edged cathode made in the form of a cone (No1) with an apex angle of  $30^\circ$  or a 6-mm-diameter tube (No2) with a wall thickness of 100  $\mu\text{m}$  and a flat anode were used. The voltage across the gap was measured with a capacitive divider and the discharge current – with a shunt connecting the anode with the chamber case. The interelectrode gap was typically 2 mm. The discharge was photographed with a HSFC-PRO four-channel CCD-camera.

The studies of a nanosecond discharge in air, nitrogen, and argon at elevated pressures have shown that at a pulse repetition frequency of 400 Hz and negative-polarity of the electrode with a small radius of curvature, the formation of the diffuse discharge takes no more than 1 ns, see Fig. 1.

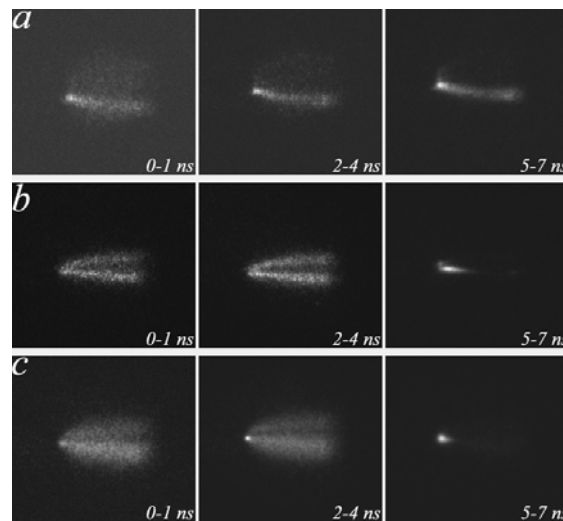


Fig. 1. Photos of discharge glow in argon (a), air (b) and nitrogen (c) during one pulse. Cathode No1, pressure - 0.1 MPa, interelectrode gap - 2 mm.

Under conditions of the above-described experiment, cathode spots in argon, air, and nitrogen can be formed during the time interval of  $\leq 1$  ns, see also [1]. After the bright spots appear on the cathode, the spark leaders' propagation begins. Under the conditions of these experiments, at low pressures of nitrogen, air, and argon, a supershort avalanche electron beam (SAEB) [2] was recorded behind a thin-foil anode. At a pressure of 0.1 MPa and less, the X-ray autographs were obtained on the Kodak RAR film 2497.

### REFERENCES

- [1] Tarasenko V.F., Baksht E.Kh., Burachenko A.G., Erofeev M.V. // High Voltage Engineering. - 2013. - Vol. 39. - No. 9. – 2105-2111.
- [2] Tarasenko V.F., Baksht E.KH., Burachenko A.G., Kostyrya I.D., Lomaev M.I., Rybka D.V. // Plasma Dev. Oper. - 2008. – Vol. 16. - 267-298.

<sup>1</sup> The work was supported by the grant of RFBR No12-08-00105\_a.

## **DIELECTRIC FILMS AND WATER MODIFICATION IN DIFFUSE BARRIER DISCHARGE, FORMED BY PREDIONIZATION FAST ELECTRONS AT AN PULSE SHORT RISE-TIME OF VOLTAGE.<sup>1</sup>**

*V.M.ORLOVSKII, V.A.PANARIN, M.A.SHULEPOV*

*Institute of High Current Electronics SB RAS, Academic Ave. 2/3*

*Tomsk, 634055, Russia*

*E-mail: [orlovskii@loi.hcei.tsc.ru](mailto:orlovskii@loi.hcei.tsc.ru)*

Diffuse discharge formation by voltage pulses with short rise-time (less than 1 ns) and nanosecond duration without an additional source of preionization when water or thin dielectric films are placed on the anode. It is shown that the diffuse discharge is formed due to avalanche reproduction of a charge initiated by run-away electrons and then supported by the secondary breakdowns, propagated on channels of ionized gas. When a dielectric film (polyethylene, lavsan, etc) or water placing multiple diffuse discharge action modifies the substance. The Fourier analysis of IR absorption spectra showed differences in the spectra of irradiated and not treated object for a polyethylene film. Changes in the polyethylene film absorption after 120 discharge pulses in air is observed for a valency symmetric band on  $2861\text{ cm}^{-1}$  (change  $\sim 25\%$ ) and the deformation bands at  $725\text{ cm}^{-1}$  (change  $\sim 8\%$ ),  $1465\text{ cm}^{-1}$  (change  $\sim 5\%$ ). The changes are suggested to be due to formation of superoxide groups formed in the process of oxidation of the polyethylene chain. Thus, the increase in adhesion and interaction susceptibility in gases is possible. Research IR absorption spectra of water shown availability of frequencies of a valency symmetric band  $\nu_1$ , a valency asymmetric band  $\nu_3$  and overtones of a deformation band  $2\nu_2$  in a range  $3700 - 3100\text{ cm}^{-1}$  without obviously expressed peaks, deformation band  $\nu_2$  with a maximum at  $1649,8\text{ cm}^{-1}$  and composite torsion and deformation bands  $\nu_L + \nu_2$  with a maximum at  $2134\text{ cm}^{-1}$ . After 120 diffuse discharge pulses in air absorption of water was changed in the follows way: band  $\nu_L + \nu_2$  completely disappeared, while other bands remained without change. Probably this result is caused by transformation of water molecules in clusters.

Thus, the volume diffuse discharge in molecular and atomic gases can be used for modification of dielectrics and waters.

---

<sup>1</sup> This work was supported by the framework of the State task for HCEI SB RAS, project #9.5.2.

**FORMATION OF THE HARMONIC HIGH-FREQUENCY OSCILLATIONS IN THE DISCHARGERS BASED ON THE PHOTOELECTRON OPEN DISCHARGE.**

*P. A. BOKHAN, P. P. GUGIN, M. A. LAVRUKHIN, AND DM. E. ZAKREVSKY*

*A.V. Rzhanov Institute of Semiconductor Physics, Siberian Branch of the Russian Academy of Sciences,  
Lavrent'ev Ave. 13, Novosibirsk 630090, Russia*

In the planar and cylindrical constructions based on the photoelectron open discharge (POD) it is possible to achieve conditions under which the majority of the runaway electrons reaches the opposite accelerating gap. With further increase of the accelerating potential they can gain much more energy than losing it in the drift space and thus perform few oscillations between the accelerating gaps. In the absence of a drift space this process becomes more evident, especially under the conditions in which the energy gained by the electrons allows them to make several oscillations during the decreasing of the acceleration potential. Thus, an increase of the voltage in the POD based constructions leads to the formation of high-frequency harmonic current oscillations in the construction with frequencies from hundreds of MHz to GHz.

Period of these oscillations depends on the pressure of the gas mixture and parasitic parameters of the discharge constriction and their intensity depends on value of the storage capacitor and self-capacitance of the discharge construction and on the value of the applied voltage. This oscillatory process has a systematic nature. The report discusses the physical causes of these oscillations and their approximate mathematical model. Several examples of the practical applications of this effect are described.

## MEASURING TECHNIQUE OF CURRENT PULSES OF PICOSECOND DURATION IN REAL TIME MODE<sup>1</sup>

*D.V. RYBKA, E.V. BALZOVSKII, V.F. TARASENKO\**

*\* Institute of High Current Electronics, Siberian Branch, 2/3 Akademicheskoy Ave., Tomsk, 634055 Russia, RDm@loi.hcei.tsc.ru 8-(382-2)-492-392*

Progress of oscilloscope methods for the study of ultrafast processes in a gas discharge caused by occurrence of modern digital real-time oscilloscopes with bandwidth of 30 GHz or more, and a sampling rate of more than 80 GS/sec [1-3]. These measuring instruments are primarily oriented to solve problems of microelectronics, computer technology, digital communication channels and so on, and make the work of engineers much easier in the development and verification of compliance signals of high-speed serial data transmission.

At the same time, the use of digital real-time oscilloscopes with wide bandwidth makes it possible to record a temporary shape and amplitude values of the single electrical signals registered by the current (voltage) sensors at research of prebreakdown phenomena in gas discharge physics [4, 5]. When bandwidth analog input paths of oscilloscope is about ~ 30 GHz, registration of temporary waveform features with a time resolution of 10 picoseconds becomes possible. However, the question arises about the reliability of the data while working in the area of the upper limit of the bandwidth of the recording device. Therefore interesting to compare the waveforms recorded by different oscilloscopes with close values of bandwidth.

This paper presents the results of experimental studies of the amplitude characteristics and determination of the temporal shape of the current pulse of runaway electrons, generated in a high electric field at the cathode when high voltage pulses of nanosecond duration applying for a discharge gap, see fig.1. We used digital real-time oscilloscopes with a bandwidth of 500 MHz to 30 GHz (Table 1):

Table 1.

Manufacturer:	Model	Bandwidth	Sample rate	Rise time
Tektronix	TDS3054B	500 MHz	5 GS/s	0.7 ns
Tektronix	DPO70604	6 GHz	25 GS/s	65 ps
Tektronix	TDS6154C	15 GHz	40 GS/s	28 ps
Tektronix	MSO72004C	20 GHz	100 GS/s	18 ps
Tektronix	DSA72504D	25 GHz	100 GS/s	16 ps
LeCroy	WaveMaster 830Zi	30 GHz	80 GS/s	15.5 ps

Fig.1. Pulses from voltage divider (a) and current collector (b) recoded by LeCroy WaveMaster 830Zi oscilloscope. Discharge gap with a flat anode and a tubular cathode with small radius of curvature was 12 mm. Air at atmospheric pressure was in the gas diode.

### REFERENCES

- [1] <http://www.agilent.com>
- [2] <http://www.lecroy.com>
- [3] <http://www.tektronix.com>
- [4] E.Kh. Baksht, E.V. Balzovskii, A.I. Klimov, I.K. Kurkan, M.I. Lomaev, D.V. Rybka, and V.F. Tarasenko // Instruments and Experimental Techniques. – 2007. – Vol. 50. – No. 6. pp. 811-814.
- [5] V.F. Tarasenko, D.V. Rybka, A.G. Burachenko, M.I. Lomaev, and E.V. Balzovsky // Rev. Sci. Instrum. – 2012. 83. 086106.

<sup>1</sup> The work is performed in the framework of the State task for HCEI SB RAS, project #13.1.3.

## RESEARCH ON CHARACTERISTICS OF LOW-PRESSURE GAS DISCHARGE IN HOLLOW CATHODE

KOVAL T.V., LOPATINT I.V., OGORODNIKOV A.S., NGUYEN BAO HUNG

National Research Tomsk Polytechnic University, Lenin 30, Tomsk city, 634050, Russia, lnhh27@gmail.com, +79528877165

This work describes experimental and theoretical research on the generation of low-temperature plasma in a glow discharge with a large area hollow cathode. Discharge characteristics are studied in a self-contained and non-self-contained regimes of burning with a gas pressure of 0,2-1,5 Pa (argon, nitrogen). The experimental and theoretical dependences of burning intensity, plasma concentration and plasma temperature from the gas pressure and anode area were obtained. It is experimentally and numerically shown that in a self-contained glow discharge the high homogeneity of plasma is reached with concentration up to  $10^{17}\text{m}^{-3}$  and plasma temperature reaches 1V. The effect of processed parts located inside the hollow cathode on plasma concentration is researched theoretically, using numeric modeling. It is shown that by using the current of an auxiliary discharge, it is possible to control the concentration of plasma even in the presence of processed parts.

### REFERENCES

- [1] *Nikulin S.P.* // Russian Physics Journal. – 2001. – V. 44. – No. – 9. – PP. 969–976.
- [2] *Yu.D.Korolev and Klaus Frank* //IEEE Trans. Plasma Sci. 1999. – V. 27. – No. – 5. – PP. 1525–1537.
- [3] *Hagelaar G.J.M., Pitchford L.C.* //Plasma Sources Sci. Technol. 2005. – V. 14. – PP. 722–733.
- [4] *Lakhtin Yu. M.* // Theory and technology of nitriding. – M.: Metallurgy, 1991.

## SIMULATION OF HIGH PRESSURE NANOSECOND GAS DISCHARGE IN COAXIAL GAP<sup>1</sup>

*A.V. KOZYREV\**, *V.YU.KOZHEVNIKOV\**, *N.M. DMITRIEVA\*\**

\**Institute of High Current Electronics, pr. Akademichesky, 2/3, Tomsk, 634055, Russia, [kozyrev@to.hcei.tsc.ru](mailto:kozyrev@to.hcei.tsc.ru)*

\*\**National Research Tomsk State University, pr. Lenina, 36, Tomsk, 634030, Russia*

This work was stimulated by experiments with fast electrons in a pulsed corona discharge, in particular, by paper [1].

The coaxial geometry of the discharge gap was selected as the simplest example of a one-dimensional and non-uniform problem at the same situation.

To simulate the corona used "minimal" theoretical model, which consists of two continuity equations for the concentrations of ions and electrons, including the function of the impact ionization source, as well as the Poisson equation for the calculation of the electric field. In the model singly charged ion and electron flows are described in the drift-diffusion approximation. So we research only short time discharges (1 ns and shorter) it was supposed ions were motionless during all stages.

For the numerical solution of partial differential equations Method-Of-Line was used. In coaxial geometry, the electric field near the cathode is essentially uniform, so non-uniform computational grid was chosen, and cell sizes decreased exponentially from the anode to the cathode.

Electrical voltage pulse  $U(t) = U_0 \sin^2(\pi/T)$  is applied to the coaxial gas-filled gap (inner electrode - cathode of radius  $r_1 = 0.5$  mm, outer electrode - anode of radius  $r_2 = 4$  cm  $\gg r_1$ ), gas (air) at a pressure of  $p = 760$  Torr,  $T = 1$  ns. The typical results of simulating is shown in Fig.1.

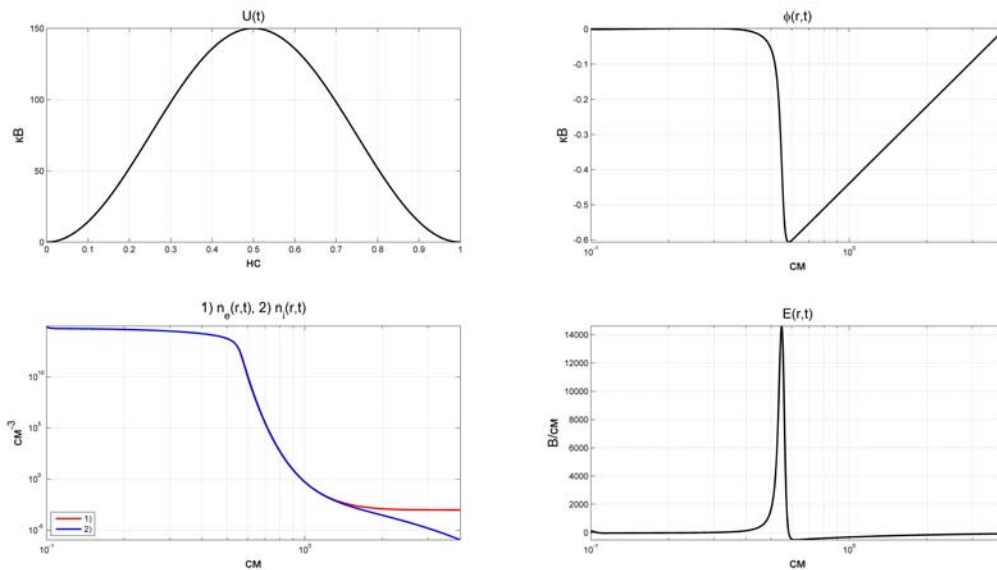


Fig. 1. A preset time dependence of the voltage drop on the gap (left top), and calculated space distributions of ions and electrons (left bottom), electrical potential (right top), electric field strength (right bottom) at the end of voltage pulse.

Fast generation of near-cathode plasma is accompanied by a significant increasing of electrons concentration up to  $\sim 10^{10}$  cm<sup>-3</sup>, then there is the screening of the electric field near the cathode. The ionization wave (it is a sharp gradient of plasma concentration) expands from the cathode to the anode. This wave front has a velocity of about  $\sim (2-3) \cdot 10^9$  cm/s.

Fast electrons in a nonuniform (coaxial) discharge geometry can be generated in the volume of the gap at the front of the ionization wave.

### REFERENCES

- [1] *Tao Shao, V. F. Tarasenko, etc. // New J. Phys. – 2011. – 13. – 113035.*

<sup>1</sup> This work was supported by Russian Fund of Basic Researches (project 12-08-00081\_a)



**RESEARCH PULSE-PERIODIC SOURCE UV-RADIATION BASED ON DIFFUSE DISCHARGE INITIATED BY RUN-AWAY ELECTRON BEAM<sup>1</sup>**

*A.G. BURACHENKO, E.H. BAKSHT, M.I. LOMAEV, A.N. PANCHENKO, V.F. TARASENKO*

*Institute of High Current Electronics, Akademichesky Ave. 2/3, Tomsk, Russia, 634055  
BAG@loi.hcei.tsc.ru, +7-3822-492392*

In recent years, high-voltage nanosecond discharges having no additional sources of preionization have been widely studied. In [1], this discharge mode was suggested to be called REP DD (volume discharge initiated by an avalanche electron beam). It was shown that using the REP DD results in creation of effective lasers [2, 3] and sources of UV and VUV radiation with high pulse power [4]. However, in the lasers and sources of spontaneous radiation excited by REP DD, a single-pulse mode was commonly used [2]. Researches of the sources of spontaneous UV radiation in a pulse-periodic mode at a specific power of REP DD excitation exceeding  $\geq 1$  MW/cm<sup>3</sup>, pulse repetition rate of  $\geq 1$  kHz, and interelectrode gaps of  $\geq 0.5$  cm have not been carried out previously. This paper presents the results of the study of radiative characteristics of the REP DD plasma when the discharge is excited in a pulse-periodic mode.

In the experiments, a four-channel FPG-60 oscillator was used to generate a REP DD [5]. The oscillator formed an incident-wave voltage pulse of up to 30 kV with FWHM of  $\sim 4$  ns, and a front edge of  $\sim 2.5$  with a frequency up to 2 kHz. To investigate the parameters of the discharge and radiation in a more wide range of experimental conditions, two discharge chambers differing in their design were applied. The cathodes with a small radius of curvature were used. To study the radiation of the REP DD plasma, a HSFC-PRO CCD camera, a EPP2000C-25 StellarNet-Inc and a HR4000 Ocean Optics B.V. spectrometers as well as a Photek PD025 Solar Blind high-speed photodiode and a FEC-22 SPU coaxial photocell were used.

An extensive pulse-periodic source of spontaneous radiation with the pulse repetition rate of up to 2 kHz was created and its characteristics were studied. Laser UV radiation was obtained at the wavelength of 337.1 nm.

## REFERENCES

1. Tarasenko V.F., Orlovsky V.M., Shunailov S.A. // Rus. Phys. Journ.2003. N 3. P. 94.
2. Baksht E.Kh., Burachenko A.G., Tarasenko V.F. Quantum electronics, 39, 1107 (2009).
3. Viltovsky P.O., Lomaev M.I., Panchenko A.N., etc. Quantum electronics, 43, 605 (2013).
4. Baksht E.Kh., Lomaev M.I., Rybka D.V., Tarasenko V.F. Quantum electronics, 36, 576 (2006).
5. Efanov V.M., Efanov M.V., Komashko A.V. et al. Ultra-Wideband, Short Pulse. Electromagnetics 9, Part 5 (2010).

<sup>1</sup> The work is performed in the framework of the State task for HCEI SB RAS, project №13.1.3.

## OPTIMUM BEAM ENERGY FOR GENERATION OF RUNAWAY ELECTRON AVALANCHES IN LABORATORY CONDITIONS<sup>1</sup>

*V.A. SHKLYAEV, V.V. RYZHOV*

*Institute of high current electronics SB RAS, 2/3 Akademichesky av., Tomsk, 634055, Russian Federation,*

*E-mail: shklyaev@to.hcei.tsc.ru, (3822)491-471*

*National Research Tomsk polytechnic university, Lenina av.30, Tomsk, Russian Federation, 634050*

Analytical data are presented to show that for the primary electrons moving in gas at a pressure  $p$  and external electric field  $E$  (lower than the critical field  $E_{cr}$ ), there exists an optimum energy  $\varepsilon_0$  at which the maximum number of secondary electrons with energy  $\varepsilon_c$  sufficient for runaway is generated in the gas.

An electron moving in gas in an external electric field gains energy from the field and expends it in inelastic collisions with neutral gas particles. This electron, having an initial energy  $\varepsilon_0$  higher than a certain value  $\varepsilon_c$ , is continuously accelerated in the field with a strength of even lower than the critical strength  $E_{cr}$  (required for electrons with zero initial energy to pass to continuous acceleration). Part of the electron energy is lost in inelastic collisions with neutral gas particles, including its loss in ionization. The secondary electrons arising in ionization have an energy of no more than  $(\varepsilon_0 - I)/2$ , where  $I$  is the ionization potential. If the energy of a secondary electron is higher than  $\varepsilon_c$ , this electron passes to the mode of continuous acceleration, otherwise all of its initial energy is expended in inelastic collisions and the electron becomes "thermal" (its energy is  $\sim 1-5$  eV). If the energy of a primary electron is less than  $2\varepsilon_c + I$ , there will be no secondary electrons capable of passing to continuous acceleration. On the contrary, if its energy is much higher than  $2\varepsilon_c + I$  (e.g., 1 MeV), the primary electron is able to travel large distances without a single collision, including ionization collision. Thus, the probability of a secondary electron capable of passing to continuous acceleration in a bounded space (experimental setup) and hence the probability of runaway electron avalanches is low. It can be concluded that there exists an optimum energy of the primary electron  $\varepsilon_0$  at which ionization results in the maximum number of electrons having an energy higher than  $\varepsilon_c$  and capable of passing to continuous acceleration. It is shown that the energy of the primary electron should thus be about  $4\varepsilon_c$ .

For all these conditions to be met, the electrode configuration in a discharge gap is required to be such that it can provide the formation of a runaway electron beam with an energy of  $\sim 4\varepsilon_c$  near the cathode and its injection into a field region of strength lower than the critical one.

<sup>1</sup> This study was supported by the Russian Foundation for Basic Research project 13-08-01314-a and integration project No. 107 "High- and low-pressure gas discharges and new electrophysical devices on their basis" with collaborative participation of IEP UD RAS and IHCE SD RAS.

**ANTITUMOR EFFECTS OF PULSED X-RAY RADIATION**

*M.A. BULDAKOV\**, *O.P. KUTENKOV\*\**, *M.A. BOLSHAKOV\*\*\**, *V.V. ROSTOV\*\**, *N.V. CHERDYNTSEVA\**

\*Cancer Research Institute, SB RAMS, Tomsk, Russia, 634050, buldakov@oncology.tomsk.ru

\*\*Institute of high-current electronic SB RAS, Tomsk, Russia

\*\*\*Tomsk State University, Tomsk, Russia

*Purpose/Objective.* Main radiotherapy problem of cancer treatment is absence efficacy of low doses of radiation and side-effect as a result of high doses applying. It related with the biological sensitivity and reaction of tumor cells on radiation. Biological effects could be increased by using pulse-modulated radiation. Previously we observed that application of nanosecond pulses of X-ray radiation with determinate pulse repetition frequency allowed significantly increase sensitivity of tumor cells even when low doses applied. The source of low-dose repetitively pulsed X-ray radiation was first developed and created at the Institute of high-current electronics (Russia).

*Material/methods.* "Sinus-150" as a generator of pulse periodic X-ray was applied. A high-voltage pulse had a half-height duration of 4 ns and amplitude of 260 kV. The calculated photon energy spectrum had a maximum at 90 keV, and most of the quantum flux was the 60-200 keV range. Solid-type of Lewis lung carcinoma was prepared by intramuscularly transplantation of  $3 \times 10^6$  cells into the hind limb of C57BL/6 female mice. Mice were exposed to local irradiation (5 fractions) up to total doses 0.1, 0.2, 0.5, or 1 Gy. Tumor volumes were measured with calipers and a volume calculated  $(L+W+W/2)$ . The metastases of the lung were counted using a stereoscopic microscope.

*Results.* Tumor weight and size on day 19th after tumor injection displayed the significant decrease after low-dose pulsed X-ray irradiation. Highest inhibition of tumor growth observed in group with absorbed dose 0.2 Gy (50 % compare to control group). Irradiation with the doses 0.5 and 1 Gy didn't provide high antitumor effects. To estimate the antimetastatic activity of pulsed X-ray the number of colonies in lung (MII) and the area of each colony (MGI) were analyzed. Highest inhibition of metastasis observed in group irradiated with 0.2 Gy. Colony formation decreased almost by 98% (MII) and cell number reduced at 68 % (MGI). Irradiation of mice with other doses produced almost equal effects. Both MII and MGI after 0.1, 0.5 and 1 Gy irradiation didn't exceed 60 %.

*Conclusion.* Pulse regime of X-ray radiation provides antitumor efficacy up to 50 % and antimetastatic action up to 60 – 90 %. Same effects of non-pulsed X-ray radiation could be achieved when the absorbed dose exceed 10 – 20 Gy.

## ELECTRICAL DISCHARGE PHENOMENA APPLICATION FOR SOLID FOSSIL FUELS IN-SITU CONVERSION

*A.A. BUKHARKIN\**, *V.V. LOPATIN\**, *S.M. MARTEMYANOV\**, *I.A. KORYASHOV\**

*\*Tomsk Polytechnic University, Lenin av., Tomsk, 634050, Russia, amplexor@ya.ru, +7 913 886 22 06*

In last five years attention to in-situ solid fossil fuels processing significantly grown up for a number of apparent reasons. Underground pyrolytic conversion of oil shale and brown coal into gas fuel and synthetic oil using of electrophysical bed heating is very efficient technology for this aims.

Application of high voltage to oil shale initiates partial discharges (PD) with following treeing like in insulating dielectrics [1]. Critical PDs [1] and treeing with high propagation rate are occurred under low electrical intensity  $\sim 10^2$  V/cm due to oil shale high porosity, heterogeneity and anisotropy. Completed discharge is occurred, as a result of these phenomena.

Carbonization initiated around plasma channel on treeing stage and extended during all time electromagnetic action. Carbonized rock electrical resistance is decreased by 8÷10 degrees to  $10\div 10^3$  ohm·cm, and shale and coal could be heated by Joule heat in carbonized volume and discharge plasma. High-current supply needs for this heating stage. Also, high-voltage supply with steep-grade characteristic can be used for PDs and treeing initiating and heating carbonized rock with low resistance.

Thus, these phenomena allows to in-situ processing in order to produce flammable gas and synthetic oil from inferior solid fossil fuels by pyrolytic conversion. Computations show that ratio between energy derived from gas flaming and energy for shale conversion more than fifty. Therefore, oil shale conversion by electrical discharge phenomena application can be very efficient as needs a little energy.

### REFERENCES

- [1] *Kuchinsky G.S.* // Partial discharges in high voltage construction [in Russian]. – L: Energy, 1979, 224p.

## ACCELERATOR URT-1M-300 FOR MOBILE INSTALLATION<sup>1</sup>

*S.YU.SOKOVNIN<sup>1,2</sup>, M.E.BALEZIN<sup>1</sup> S.V.SCHERBININ<sup>1,2</sup>*

<sup>1</sup>*Institute of Electrophysics, Ural Branch of Russian Academy of Sciences, Ekaterinburg, Russia sokovnin@iep.uran.ru*

<sup>2</sup>*Ural Federal University, Ekaterinburg, Russia*

The electron accelerator URT-1M-300 for mobile installation was created for radiation disinfecting of clothes, footwear, documents and personal belongings from pathogenic microorganisms in field conditions to correct drawbacks that were found the URT-1M electron accelerator operation (the accelerating voltage up to 1 MV, repetition rate up to 300 pps, electron beam size 400x100mm, the pulse width about 100 ns).

Accelerator configuration was changed that allowed to reduce significantly by 20% tank volume with oil where is placed the system of formation high-voltage pulses, thus the average power of the accelerator is increased by 6 times at the expense of increase in pulses repetition rate [1].

Was created the system of the computerized monitoring parameters (output parameters and thermal mode) and remote control of the accelerator (charge voltage, pulse repetition rate), its elements and auxiliary systems (heat of the thyatron, vacuum system), the remote control panel is connected to the installation by the fiber-optical channel, what lightens the work for service personnel.

For receiving an electron beam of big width (to 400 mm) was used the metaldielectric cathode from several elements cathode to make not more than ~15 % non-uniformity distribution of beam current density on the outlet foil. For X-rays radiation mode generator was created the multilayered anode consisting of the tantalic convector, an aluminum framework and a thin layer of cooling water (2mm).

The accelerator can be used for the radiation technologies in layers by thickness up to 0.3 g/cm<sup>2</sup>.

### REFERENCES

- [1] *S.Yu.Sokovnin, M.E.Balesin, S.V.Tscherbinin// Accelerator URT-1M for radiation technologies//PTE,2013,№4, p.47-50.*

<sup>1</sup> This work was supported by the Ural Branch of the Russian Academy of Sciences (projects 13-08-96056 p\_ypa1\_a, 12-M-23-2007 and 12-T-3-1009)

**20-CM GUIDED DISCHARGE PRODUCED BY COMPACT MARX GENERATOR SIMULTANEOUSLY TRIGGERED WITH FEMTOSECOND LASER FILAMENTS.**

*L. ARANTCHOUK\**, *A. HOUARD\*\**, *G. POINT\*\**, *Y. BRELE\*\**, *J. LAROUC\**,  
*J. CARBONNE\*\**, *Y.-B. ANDRE\*\**, *A. MYSYROWICZ\*\**

\* *Laboratoire de Physique des Plasmas UMR7648 - Ecole Polytechnique, CNRS - 91128 Palaiseau, France*

\*\* *Laboratoire d'Optique Appliquée - ENSTA ParisTech, Ecole Polytechnique, CNRS - 91761 Palaiseau, France*

A compact 180-kV Marx generator is triggered simultaneously with a guided discharge in atmospheric air by femtosecond laser filaments. High voltage pulse of 180 kV with a runtime  $\leq 20$  ns and temporal jitter  $\leq 1$  ns could be produced with a charging voltage higher than 70% of self-breakdown. We determined that the Marx performance in terms of jitter and delay start to degrade when the laser input is lower the 50 GW. The guided discharge with a length as long as 21 cm can be achieved in this way.

The delay between the discharge and the Marx pulse is mostly dependent on the ratio  $E_{\text{disch}} = \text{Marx output voltage} / \text{discharge length}$ . The best discharge characteristics were observed using a geometry where the laser beam enters from the output generator side and with a positive voltage polarity.

## MARX GENERATOR BASED MOBILE COMPLEX FOR LIGHTNING CURRENT TESTS OF GROUNDING SYSTEMS

*Y.A. BYKOV\**, *V.P. SMIRNOV\**, *E.V. GRABOVSKIY\*\**, *G.M. OLEYNIK\*\**, *A.N. GRIBOV\*\**, *E.M. BAZELYAN\*\*\**

*\*Joint Institute for high temperatures RAS, 13 Izhorskaya street, Moscow, 125412, Russia, [Yrka.2@mail.ru](mailto:Yrka.2@mail.ru), 8(916)2664168*

*\*\*RF SSC Troitsk Institute for innovation and fusion research, 12 Pushkovih street, Moscow, 142190, Russia*

*\*\*\*Krzhozhanovsky power engineering institute (ENIN), 19 Leninsky prospect, Moscow, 119991, Russia*

A mobile complex for tests of lightning protection systems is developed and constructed. It is designed for open air measurements of the conductivity of ground together with electrodes of grounding protection systems at current levels close to currents of lightning discharges. The test complex is based on application of a Marx generator as a source of high-voltage and high-current pulses with the next parameters: the stored energy of the Marx generator – more than 4 MJ, the total output voltage – 2.4 MV. This set of parameters provides the possibility of measurements of the ground resistivity from 10 up to 100 Ohm at the current levels up to 50 kA.

The first full-scale open air tests were done at voltage levels up to 2 MV. Results of measurements as well as the main parameters of the Marx generator and the design of the basic elements will be presented and discussed.

## MAGNETIC PULSED WELDING OF STAINLESS STEEL AND OXIDE DISPERSION-STRENGTHENED STEEL TUBES WITH END PLUGS<sup>1</sup>

V.I. KRUTIKOV\*, S.N. PARANIN\*, V.V. IVANOV\*, D.S. KOLEUKH\*, A.V. SPIRIN\*, J.-G. LEE\*\*, M.-K. LEE\*\*, C.-K. RHEE\*\*

\* Institute of Electrophysics of the Ural Branch of Russian Academy of Sciences (IEP), 106 Amundsen str., Yekaterinburg, 620016, Russian Federation, [krutikov@iep.uran.ru](mailto:krutikov@iep.uran.ru), +7(343)2678827

\*\* Korea Atomic Energy Research Institute (KAERI), Daejeon, Republic of Korea

The results on magnetic pulsed welding of tubes to end plugs are presented in the paper. The welded materials are: corrosion-resistant chromium steel AISI 410 tubes with the same steel end plugs and 9 Cr oxide-dispersion strengthened (ODS) steel tubes with Grade 91 ferritic-martensitic steel end plugs. AISI 410 finds its application in aircraft engines [1], as a wear resistant clad material on components such as continuous caster rolls [2], as a material for steam turbine blades [3]. Grade 91 ferritic-martensitic and ODS steels are used in boiler industry. The conventional liquid state welding makes AISI 410 and Grade 91 steels susceptible to cracking [1,4]. The liquid state welding of ODS steels is also unacceptable because of the dispersed oxide particles disordering.

Magnetic pulsed welding of metals [5] proved effective in the welding of aluminum and copper alloys and mild steels. The welding geometry (Fig. 1a) was similar to the one suggested in [6,7]. Under the action of applied pulsed magnetic field, the fixture was compressed to yield a solid-state joint (weld seam). Copper driver was used to compress the tube effectively.

Parameters of the pulse generator: charging voltage  $U_0$  up to 25 kV, capacity of energy storage  $C = 425$  or  $210 \mu\text{F}$ , period duration of pulsed current  $T = 27$  and  $20 \mu\text{s}$ , respectively (Fig. 1b). Inductor represented one turn coil made out of hardened steel and had the effective volume of 8.8 mm in diameter and 12 mm long. The outer diameter of steel tube was 7 mm, its wall thickness was 0.6 mm. Copper driver was 8 mm in outer diameter at a wall thickness of 0.5 mm.

In experiments, we explored the weld quality as a function of  $U_0$ ,  $C$ , and plug cone angle  $\alpha$ .

The optimum welding conditions were found. For achieving the required magnetic field amplitude (40 T at the period length of 20–27  $\mu\text{s}$ ), the current amplitude of 700–750 kA was applied at the one-turn coil with the working length of 12 mm. The weld seam had a characteristic wavy structure (Fig. 1c). The joint thickness did not exceed  $10 \mu\text{m}$ .

The leakage test showed a good helium tightness at the level of  $1 \times 10^{-9} \text{ mbar} \cdot \text{l} \cdot \text{s}^{-1}$ .

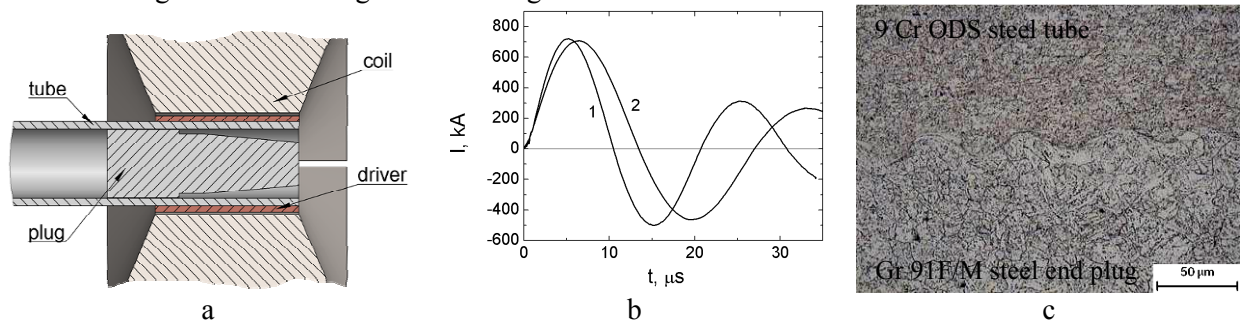


Fig. 1. a – schematic diagram of magnetic pulsed welding experiment, b – typical current wave-forms at different circuit parameters ( $C[\mu\text{F}]/U_0[\text{kV}]$ ): 1 – 210/13, 2 – 425/8.5, c – photomicrograph of the weld seam of 9 Cr ODS steel to Grade 91 steel.

### REFERENCES

- [1] A.G. Olabi, M.S.J. Hashmi // Journal of Materials Processing Technology. – 1998. – 77. – pp 216 – 225.
- [2] Ramesh Puli, E. Nandha Kumar and G.D. Janaki Ram // Transactions of the Indian Institute of Metals. – 2011. – 64. – 41-45.
- [3] A.K. Bhaduri, T.P.S. Gill, S.K. Albert, K. Shanmugam, D.R. Iyer // Nuclear Engineering and Design. – 2001. – 206. – 249-259.
- [4] A.G. Olabi, M.S.J. Hashmi // Journal of Materials Processing Technology. – 1996. – 56. – № . 88-97
- [5] A.A. Dudin // Magnitno-impulsnaya svarka metallov (Magnetic Pulsed Welding of Metals) – M.: Metallurgiya 1979.
- [6] W.F. Brown, J. Bandas, N.T. Olson // Welding Journal. – 1978. – 6. – № . 22-26
- [7] J. McGinley // Proceedings of the 17th International Conference on Nuclear Engineering (ICONE17). Brussels, Belgium, 2009

<sup>1</sup> This work is based on the results of the Joint Research Project between KAERI in Korea and IEP in Russia (Agreement № 13/13) supported by KAERI R&D Program. This work is also supported by Russian Foundation for Basic Research (project № 13-08-00883-a) and Ural Branch of the Russian Academy of Sciences (project № 12-Y-2-1029)



COMPARATIVE ASSESSMENT OF REPETITIVE PULSED X-RAY RADIATION EFFICIENCY ON FUNCTIONAL ACTIVITY OF MICE LIVER MITOCHONDRIA<sup>1</sup>*I.R. KNYAZEVA<sup>1,2</sup>, V.V. IVANOV<sup>2</sup>*<sup>1</sup>*Institute of High-Current Electronics, Siberian Division, Russian Academy of Sciences, Tomsk, 634055 Russia;*<sup>2</sup>*Siberian State Medical University, Tomsk, 634050 Russia, 8(3822)529364, e-mail: knyazeva\_irekle@mail.ru*

Emergence of sources of the nanosecond repetitive pulsed X-ray, generating impulses lasting from units to tens nanoseconds, created need for studying biological effect of this type of radiations. These radiations have a high intensity due to short pulse duration, and accumulated values of the absorbed dose are relatively small. Earlier we have shown that repetitive pulsed X-rays can produce a variety of biological effects in which mitochondria may play an important role. Besides, it changes the oxidative modification of lipids and proteins [1] and have an influence on the level of reactive oxygen species (ROS) in mice hepatocytes [2].

In present work we have analyzed the functional activity of mitochondria, mitochondria's level of ROS generation and activity antioxidant enzymes of mitochondria after exposure of the pulsed X-ray (8 - 25 pps pulse repetition rate;  $0.3-1.8 \times 10^{-6}$  Gy/pulse dose, total dose  $1.2-7.2 \times 10^{-3}$  Gy) was investigated. The X-ray source was a Sinus-150 accelerator (pulse duration 4 ns, photon energy 90–120 keV) [3]. It was found that short-time irradiation changes the oxygen consumption rate of mitochondria in different metabolic states, mitochondria's level of ROS generation and the activity of antioxidant enzymes of mice liver mitochondria. The greatest change was observed in the activity of metal-containing enzymes: superoxide dismutase and glutathione peroxidase. The irradiation effect depended on the pulse repetition frequency, radiation intensity, and dose.

The analysis of own and few reported data allows to conclude that mechanisms of biological effect of repetitive pulsed X-ray are nonspecific. Therefore the assessment of orientation and comparison the influence of pulse periodic mode efficiency to continuous radiation is of interest. The report will contain the comparative analysis of pulse biological efficiency, repetitive modes of X-ray influence.

## REFERENCES

- [1] M.A. Bolshakov, V.V. Rostov, M.S. Korovin, et al., // Biophysics. – 2005. – V.50 (1). – P. 104-109.  
[2] L. P. Zharkova, I. R. Knyazeva, V.V. Ivanov, et al. // Tomsk State Univ. Bulletin. – 2010. – V.333. – P. 161-163.  
[3] K.P. Artemov, A.A. Elchaninov, O.P. Kutenkov, et al. // Instrum. Exp. Tech. – 2004. – V.5. – P. 67–68.

<sup>1</sup> The work was supported by the analytical target program “Development of scientific potential of higher school” (projects No. № 2.1.1/2777 and 2.1.1/13778).

## ELECTROEROSION GENERATOR OF AEROSOL METAL AND OXIDE NANOPARTICLES<sup>1</sup>

*I.V. BEKETOV, A.V. BAGAZEEV, E.I. AZARKEVICH, V.V. IVANOV, A.I. MEDVEDEV, D.S. PORTNOV,  
A.M. MURZAKAEV*

*Institute of Electrophysics UB RAS, 106, Amundsen str., Ekaterinburg, Russia, 620016, [beketov@iep.uran.ru](mailto:beketov@iep.uran.ru), 8(343)267-88-19*

In connection with the development of nanotechnology and their introduction into industrial production it is necessary to develop generators to obtain aerosols, consisting of nanoparticles with the required concentration and necessary average size. Such the devices can be used for the calibration of the analyzers of aerosols, testing of gas filters of thin clearing, carrying out measurements in clean rooms and for other applications. One of the perspective types of generators suitable for the solution of this task is pulsed erosion accelerator of plasma, in which nanoparticles of material are formed by the erosion of electrodes and are derived from the accelerator channel with high speeds.

This work is a continuation of the works on creation of aerosol generator [1]. To generate aerosol flows of metal and oxide nanoparticles the installation on the basis of the plasma accelerator of coaxial type has been developed and tested. The power supply to the accelerator was realized from the current pulse generator with a variable capacitive storage of 0.1-0.4  $\mu\text{F}$ . Charging voltage of the capacitor bank was varied from 10 to 20 kV, and the frequency from 0.1 to 1.1 Hz. Synthesis of oxide or metal aerosol particles was held in the air flow at atmospheric pressure or in inert gas (Ar, N<sub>2</sub>) respectively. The conditions of production of aerosols of Ti, Cu, Al and Fe and their oxides have been investigated. The dependences of the average particle size and the concentration of aerosols from the discharge energy and pulse repetition frequency have been obtained. As well the influence of duration of the discharge pulse on the parameters of the produced aerosols is shown. The produced aerosol nanoparticles were analyzed by TEM, XRD and EDX. Measurements of the concentration and the particle size distribution was performed by the diffusion aerosol spectrometer DAS 2702 ("AeroNanoTech", LTD) connected to the gas system of the installation. In the energy range of the capacitive store from 10 to 80 J, and at changing of the discharge pulses repetition rate frequency from 0.1 to 1.1 Hz the average size of aerosol particles varies from 25 to 90 nm, and their concentration from 2 to  $5 \cdot 10^6 \text{ cm}^{-3}$ . For all tested materials the particle size distribution is normal logarithmic with GSD of approximately 2 in the whole range of energies and frequencies. The Increasing power of the capacitive store and the discharge pulses frequency lead to a monotonic increase in the average particle size and concentration of the aerosol. The experimental dependences of the aerosol concentration from the energy of the store for the tested metals showed that the highest aerosol concentration and respectively the highest erosion had been observed when using copper electrodes. And the tested metals form a number on reduction of erosion resistance: Ti, Fe, Al, Cu. The electron microscopy the oxide aerosols particles obtained in at different conditions has showed that the particles were agglomerates consisting of spherical primary particles from 2 to 10 nm. Increasing of the power of the capacitor storage increases the average size of the primary particles. At producing of metal aerosols the average size of primary particles is 15-25 nm depending on the synthesis conditions. The X-ray analysis showed that the oxide aerosols contained amorphous nanoparticles. The process of the synthesis of aerosols has good handling and reproducibility.

### REFERENCES

- [1] I. V. Beketov, A. V. Bagazeev, A. I. Medvedev, V. V. Ivanov, A. P. Safronov, O. R. Timoshenkova // 3<sup>rd</sup> International congress on radiation physics, high current electronics and modification of materials. - Tomsk, Russia. - 17-21 September, 2012. - TPU. - p. 252-253.

<sup>1</sup> The authors acknowledge financial support of RFBR grant 12-08-01155-a

**MULTI-BOREHOLE ELECTRO-BLAST FOR CONCRETE MONOLITH SPLITTING OFF<sup>1</sup>***A.S. YUDIN, N.S. KUZNETSOVA, V.V. LOPATIN**Tomsk Polytechnic University, Lenina av, 30 Tomsk, 634028, Russia, tevn@hvd.tpu.ru, 8(3822)606-172*

The method of monolith splitting off and fracture of oversized concrete lumps by pulsed electrical discharge is presented. The pulsed power generator with stored energy up to 63 kJ and electro-explosive polyethylene cartridge with wire for discharge initiation [1] are described. The experimental data of multi-borehole and step by step monolith splitting off with using of the polyethylene cartridge are given. The simultaneous initiation of discharge in two boreholes with 30 cm spacing, transferred energy in each borehole ~23 kJ and sequential initiation of discharge with transferred energy in one borehole ~47 kJ are investigated. The concrete splitting off with dimensions of 300×300×300 mm by the four boreholes and the total energy ~100 kJ take place. It is shown that multi-borehole initiation of the electrical discharge leads to the cracks formation in predefined direction and to the directional solid splitting off. The experimental results shown that the multi-borehole electro-blast method in comparison with step-by step one has advantage in consumed energy .

## REFERENCES

- [1] Kuznetsova N. S. , Lopatin V. V . , Burkin V. V., Golovanevsky V. A. , Zhgun D. V. , Ivanov N. A. Theoretical and experimental investigation of electro discharge destruction of non-conducting materials // IEEE International Pulsed Power Conference: Digest of Technical Papers, Chicago, June 19-23, 2011. - Chicago: University of Missouri, 2011 - pp. 267-273.

---

<sup>1</sup> This work was supported by Government, science task № 2367, and RFBR, research project No 14-08-01088/14

### **300 KV, NANOSECOND PULSED POWER GENERATOR WITH A GLYCERIN INSULATED PEAKING CAPACITOR FOR FINE DISINTEGRATION OF QUARTZ**

*E.G. KRASTELEV, A.A. SEDIN, V.I. TUGUSHEV*

*Joint Institute of High Temperatures Russian Academy of Sciences, Izhorskaya st. 13 Bd.2, Moscow, 125412, Russia,  
ekrastelev@yandex.ru, +7 (916) 795-6495*

Pulsed power generator is designed for application in production of fine grains of mineral quartz and it also may be used for selective fragmentation of other nonconductive minerals. The main parameters of the generator are the next: amplitude of the output voltage – up to 300 kV, output impedance is about 10 Ohm, half of period of the discharge current –  $\approx 70$  ns, current amplitude – up to 25 kA. The generator is developed for repetitive mode of operation with a pulse repetition rate up to 16 pps.

The ns-pulsed power generator consists of a 320 kV Marx generator, high voltage glycerin insulated coaxial peaking capacitor and an output gas switch followed by discharge chamber.

The Marx generator is assembled of 4 pairs of bipolar charged up to  $\pm 40$  kV capacitors 20 nF each switched by 4 long life-time corona stabilized three-electrode gas switches. The maximum stored energy is about 130 J. All elements of the Marx generator are assembled in a rectangular-shape tank filed by transformer oil.

The HV coaxial capacitor is installed vertically outside of the Marx generator tank. It is connected to the coaxial output of the Marx generator by a short oil-filled coaxial line. An additional flat coil made of copper tube is installed inside of the Marx generator tank and connected in series with the HV capacitor. It serves for the adjusting of the charging time of the HV capacitor to an optimal value of about 2.5 – 3  $\mu$ s. An output gas switch and a discharge chamber are installed at the top of the coaxial capacitor. The output switch operates in a self-breakdown mode in a pressurized to 2,5–3 atm circulating N<sub>2</sub>. A new design of the switch with the gas pre-ionization by an additional pulsed corona discharge provides a stable operation at voltage levels close to the peak capacitor voltage.

The generator was constructed several years ago. Since that it is used as a laboratory installation for selective fragmentation of minerals and as a test bench for development of a new electro-discharge technology of pure quartz production.

The main characteristics of the generator as well as the design of the key systems will be presented.

## CHARACTERISTICS OF DEPOSITION OF SILICEOUS COATINGS FROM ABLATION PLASMA FORMED USING A HIGH-INTENSIVE ION BEAM

*SAZONOV R.V., KHOLODNAYA G.E., PONOMAREV D.V., REMNEV G.E.*

*National Research Tomsk Polytechnic University  
Lenin Avenue, 30, Tomsk, 634050, Russia, E-mail: sazonr@mail.ru, phone+7(3822)418540*

The durability of the conventional materials used in industrial power engineering in high-temperature corrosive medium is low. The reserves on increasing the long high-temperature durability and resistance to the chemical and abrasive wear with different steels on the basis of iron with alloy additives used in heat and power engineering are almost exhausted. It causes the demand for the study of the possibilities for the application of innovative high-temperature, corrosion-resistant materials and high technologies for manufacturing the articles on their basis. Nowadays the most promising material is the siliceous coatings, which enable to produce the specified combination of the properties, such as high specific strength and modulus of elasticity, high-temperature strength, wear resistance, high thermal conductivity and heat-reflection properties, radiation strength, etc. [1].

In the present paper, we showed the results of the investigations on the characteristics of the formation of silicon dioxide thin films from ablation plasma formed using a high-intensive ion beam (HIIB) under the action of silicon dioxide on the nanosized pressed powder. In our investigations, we used the SiO<sub>2</sub> particles (the average size of the particles was 40-60 nm) produced in the plasma chemical reactor from the gas phase under the nanosecond pulse electron beam [2]. Also we used the particles of two types of SiO<sub>2</sub> (the first type – the particles with an average size of 10-15nm; the second type – the silicon dioxide particles with an average size of 25-90 nm) produced by combustion of silicon tetrachloride in the air plasma. The source of HIIB was the modernized TEMP-4M pulsed ion accelerator [3] based on the diode with a magnetic self-isolation [4]. The density of the ion beam energy on the target was 4 J/ cm<sup>2</sup>.

The methods of analysis used in the paper made it possible to measure the relation of the chemical composition and crystal structure of the target and the substrate. In the paper, we also analyzed the results and discussed the possibilities of the change of the crystal structure of the target and the deposited coating using the ablation method.

### REFERENCES

- [1] *Lebedeva Yu.E., Popovich N.V., and Orlova L.A. // Proceedings of VIAM. – 2013. – Access mode: <http://viam-works.ru>.*
- [2] *Remnev G. E. and Pushkarev A. I. // High Energy Chemistry. – 2006. – Volume 38. – № 5. P. 348-349.*
- [3] *Pushkarev A.I. and Isakova Yu.I. // Surface & Coatings Technology. – 2013. – Volume 228. P. S382-S384.*
- [4] *Remnev G. E. et al. // Vacuum. – 1991. – Volume 42. – №1/2. P. 159-162.*

## CHARACTERISTICS OF PROPAGATION OF A NANOSECOND PULSE ELECTRON BEAM UNDER FOREVACUUM PRESSURES

*KHOLODNAYA G.E., SAZONOV R.V., PONOMAREV D.V., REMNEV G.E.*

*National Research Tomsk Polytechnic University*

*Lenin Avenue, 30, Tomsk, 634050, Russia, E-mail: galina\_holodnaya@mail.ru, phone+7(3822)418540*

Nowadays most of the experimental results on the propagation of the electron beams are obtained in the axially symmetric drift spaces using the metal and dielectric drift tubes with a diameter compared to the lateral dimension of the electron beam [1-3]. Besides, many experiments on the electron beam transport in different gases (in the self-focusing mode at the L distance on the order of several betatron lengths [4-5]) show that the most effective propagation of the electron beam occurs under low pressures  $p \sim 1$  Torr. Under the pressures below 1 Torr, the effective propagation of the electron beam is prevented by the processes related to the characteristic feature of magnitude of the current (magnetic) compensation, beam space charge neutralization, and beam-plasma instabilities, changing the conditions for propagation of the pulse electron beams (resistive fire-hose instability, lateral instability, etc.) [5].

In the present paper, the investigations on the characteristics of the propagation of a nanosecond pulse electron beam under forevacuum pressures using a cut-off calorimeter and a Faraday cup are presented. The experimental investigations are performed on the laboratory stand, which consists of the TEA-500 accelerator and a plasma chemical reactor. The major parameters of the accelerator are as follows: to 350-400 keV electron energy; 9-11 kA ejected electron current; 60 ns half-amplitude pulse duration; to 5 pps pulse repetition rate; and to 120 J pulse energy [6]. The stability of the operation of the accelerator was checked using Rogowski coil and a capacitor voltage divider. The spread of the accelerating voltage and the beam current in the diode did not exceed 5%. In the experiments using the Faraday cup as a quantitative evaluation of the propagation of a nanosecond pulse electron beam, the total charge of the electron beam at the distance under study was chosen. The ejected energy of the beam which reached the collector at the distance under study was registered using the cut-off calorimeter.

### REFERENCES

- [1] *Rudakov L.I., Smirnov V.P., and Spector A.M. // Pis'ma Zh. Tekh. Fiz. – 1972. – Volume 15. – № 9. P.540-543.*
- [2] *Khodataev K.V. // Pis'ma Zh. Tekh. Fiz.. – 1973. – Volume 18. – №3. P.184-186.*
- [3] *Ryabchikov A.I., Stepanov I.B., and Eremin S.E. // The Bulletin of Tomsk Polytechnic University. – 2010. – Volume 316. – № 4. C. 90-93.*
- [4] *Jordan S., Ben-Amar Baranga A., Benford G. et al // Phys. Fluids. – 1985. – Volume 28. – № 2. P. 366-382.*
- [5] *Gladyshev M.V. and Nikulin M.G. // Zh. Tekh. Fiz.. – 1997. – Volume 67. – № 67. P. 94-98.*
- [6] *Remnev G.E., Furman E.G., Pushkarev A.I., Karpuzov S.B., Kondrat'ev N.A., Goncharov D.V. // Instr. Exp, Tech.. – 2004. – Volume 47. – № 3. P. 394-398.*

## MOBILE INSTALLATION FOR RADIATION DISINFECTING

*BALESIN M.E.<sup>1</sup>, BOREYSHO A.S.<sup>2</sup>, EVDOKIMOV I.M.<sup>2</sup>, SAENKO M.YU.<sup>2</sup>, SOKOVNIN S.YU.<sup>1,4</sup>, TSCHERBAKOV M.G.<sup>3</sup>, SCHERBININ S.V.<sup>1,4</sup>.*

<sup>1</sup>*Institute of Electrophysics, Ural Branch of Russian Academy of Sciences, Ekaterinburg, Russia sokovnin@iep.uran.ru*

<sup>2</sup>*LLC "Research and Production Enterprise "Laser Systems"*

<sup>3</sup>*Military base 47051*

<sup>4</sup>*Ural Federal University, Ekaterinburg, Russia*

Mobile installation is intended for radiation disinfecting of clothes, footwear, documents and personal belongings from pathogenic microorganisms in field conditions (with a contamination density -  $1 \cdot 10^5$ , CFU/cm<sup>2</sup>), and also for disinfection of bank notes on paper basis, mailings, sterilization of products medical appointment, disinfecting of medical waste.

Installation provides absorbed dose level in mode of electronic and X-rays radiation: at mode of sterilization and sporocidal mode - from 25 to 30 kGy, and at bactericidal mode - 6 kGy. Installation productivity on disinfecting in mode of X-rays radiation makes: 240 kg/h on sporocidal mode and 800 kg/h on bactericidal mode, and in mode on disinfecting of mailings (envelopes) by electron irradiation make not less than 3200 pieces/hours.

Installation is created on the basis of four upgraded electron accelerators URT-1M [1] which are established to provide geometry of two side irradiation mode. The URT-1M-300 accelerator has the following parameters: the accelerating voltage -up to 900kV, the pulse width about 100 ns, repetition rate up to 300 pps, the size of electrons beam 400×100 mm.

Installation is equipped with quickly replaced cartridges (500\*300\*70mm) for processed products in the mode of X-rays radiation and the metal line for work in mode of electron irradiation.

Built-in biological protection and ventilation for removal ozone provides possibility of safe work for service personnel.

Accelerators and auxiliary systems of installation have the built-in computerized monitoring system and communication at that the remote control console is connected with installation by the fiber-optical channel.

Installation is placed on the automobile chassis of the cross-country ability, incorporates survival facilities. Power supply can be carried out both from an industrial network, and from the mobile diesel of the power plant which is a part of installation.

### REFERENCES

[1] *S.Yu.Sokovnin, M.E.Balesin, S.V.Tscherbinin// Accelerator URT-1M for radiation technologies//PTE,2013,№4, p.47-50.*

## FEATURES OF LASER RADIATION GAIN IN THE GAS AMPLIFIER OF THE THL-100<sup>1</sup> LASER SYSTEM

*A.G.YASTREMSKII\**, *N.G. IVANOV\**, *V.F. LOSEV\*\**, *YU.N. PANCHENKO\**

*Institute of High Current Electronics SB RAS, 2/3, Akademichesky ave., Tomsk, 634055, Russia*

*\*\*Tomsk Polytechnic University, 30 Lenin Ave., 634034 Tomsk, Russia*

*E- mail: ayastremskii@yandex.ru*

The purpose of this paper is experimental and theoretical study of the influence of the pumping energy, proportion of mixture, shape of the pumping pulse, location of the mirrors on amplification characteristics of modified THL-100 laser system

Laser radiation of Sapphire 488 HP continuous laser with  $\lambda=488$  nm wavelength and average power of 25 mW was used in the experimental investigations. A numerical code has been developed to simulate the characteristics of amplifier. The base of the code is a model, detailed description of which was given in [1]

Results of experimental measurements and numerical simulations of the effect a pressure of the buffer gas  $N_2$  and  $XeF_2$  on the gain characteristics at the energy of pumping radiation  $E = 210$  J and 240 J are presented in the paper. Experimentally and theoretically was showed that at pressure  $XeF_2$   $P = 0.2$  torr, maximum gain— $(5 - 6) \cdot 10^4$  may be achieved at a pressure of  $N_2 = 0.5$  atm and at a pumping energy  $E = 240$  J, and the gain  $2 \cdot 10^4$  may be achieved at a pumping energy  $E = 210$  J. With increasing and decreasing pressure of  $N_2$  the gain is decreases. The results of numerical simulation and experimental measurements of dependence the maximum gain dependence vs  $N_2$  pressure are shown in Figure 1.

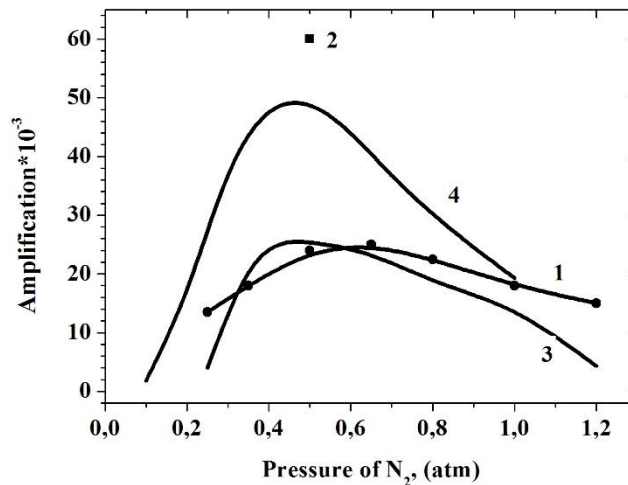


Fig.1 Dependence of the gain on the pressure of  $N_2$ . 1,3 - experiment and calculation results for pump energy -210 J, 2, 4 - experiment and calculation for  $E = 240$  J

It is shown that at constant pumping energy the gain of laser radiation depends weakly on the shape of the pump pulse. The results of numerical studies dependence of the gain from the distance of mirrors to the outer edge of the gas amplifier are shown in the work. In the paper the possibility of operation of the amplifier in a generator mode is discussed. Analyses of simulation results shows that in our conditions it is possible to obtain an annular laser radiation with energies up to 7 J.

### REFERENCES

- [1] *S.V. Alekseev, A.I. Aristov, Ya.V. Grudtsyn, et al.*// Quantum Electronics. – 2013. –V.43.– № 3. PP. 190 – 200 .

<sup>1</sup> This work was supported by RFBR under Project No 14-08-00511



## DETERMINATION OF RELATIVE BIOLOGICAL EFFECTIVENESS OF PULSED X-RAYS IN COMPARISON WITH THE STANDARD GAMMA RADIATION ON HUMAN PERIPHERAL BLOOD LYMPHOCYTES IN THE RANGE OF THERAPEUTIC DOSES<sup>1</sup>

A.A. BELENKO<sup>\*</sup>, K.A. KRAVCHENKO<sup>\*</sup>, O.P. KUTENKOV<sup>\*\*</sup>, S.A. VASILYEV<sup>\*\*\*</sup>, A.S. URAZOVA<sup>\*</sup>, I.N. LEBEDEV<sup>\*\*\*</sup>,  
M.A. BOL'SHAKOV<sup>\*\*</sup>, V.V. ROSTOV<sup>\*\*</sup>

<sup>\*</sup> Tomsk State University, Tomsk, 634050 Russia; e-mail: greyden@sibmail.com

<sup>\*\*</sup> Institute of High Current Electronics, Siberian Branch of Russian Academy of Science, Tomsk, 634055 Russia

<sup>\*\*\*</sup> Institute of Medical Genetics, Siberian Branch of Russian Academy of Medical Science, Tomsk, 634050 Russia

Relative biological effectiveness is one of the most important factors affecting any biological effects of ionizing radiation. In a number of studies of low dose pulsed X-rays specific effects were shown that was not observed using continuous irradiation (Bol'shakov, 2007; Buldakov, 2011, Vasilyev, 2012, 2013). In the Institute of High Current Electronics custom high-power electric pulse generator Sinus-150 was developed generating nanosecond pulsed X-rays. The aim of this study was to determine the relative biological effectiveness of pulsed X-rays in compare with standard <sup>60</sup>Co gamma rays.

Human peripheral blood lymphocytes were obtained from three healthy individuals. Cells were irradiated by pulsed X-rays using linear accelerator Sinus-150 (current intensity 4 kA, peak energy 90-100 keV, pulse length 4 ns) with various total doses (0.5-2 Gy) and with pulse repetition frequency from 8 to 25 pulses per second (pps). In parallel, cells from the same donors were exposed to <sup>60</sup>Co gamma rays using gamma-therapeutic device Theratron Equinox (Cancer Research Institute, SB RAMS). Mean dose rate remained constant throughout the experiment and was 13.67 mGy/s. Radiation induced  $\gamma$ H2AX nuclear foci visualized by fluorescence microscopy were used as a marker of radiation induced DNA double strand breaks. Cells were incubated *in vitro* for 30 min, 2 h, 4 h and 18 h after irradiation.

There were no significant differences of the level of radiation-induced  $\gamma$ H2AX foci between pulsed X-rays and gamma-rays at 30 minutes after irradiation. Significantly higher effect was shown only at several time points after exposure to pulsed X-rays with a pulse repetition frequency of 25 pps: 0.5 Gy and 1 Gy after 2 hours (p=0.01 and p=0.009, respectively), 2 Gy after 4 hours (p=0.006) and 1 Gy after 18 hours (p=0,018). However, pulse repetition frequency had no significant effect on the level of  $\gamma$ H2AX foci after irradiation by pulsed X-rays (p=0.37, ANOVA).

Thus, comparison of gamma – radiation and pulsed X-rays in the range of high doses revealed no significant differences in the level of radiation-induced DNA double-strand breaks. Perhaps, these results are determined by undercount of radiation – induced foci: as they occur in big amounts, they overlap. On the other hand, previously detected pulsed X-rays effects can be presented only in a range of low doses.

<sup>1</sup> This work was supported by RFBR grant 12-04-00893

## INFLUENCE OF THE ELECTRODES EROSION ON ARC DYNAMICS IN HIGH CURRENT RAILGUNS

*A.V. KHARLOV*

*Institute of High Current Electronics, Tomsk, Russia, (7)-382-2492673, akharlov@lef.hcei.tsc.ru*

A simple and effective model has been developed to study the behavior of a high-velocity plasma arc motion in linear rail geometry in high pressure gas for high current and high charge transfer pulses. Such approach can be employed also for simulation of many types of plasma accelerators, magnetically driven arcs and plasma-driven electromagnetic launchers. Arc motion in a rail gap channel in general can be described as moving current contour under action of accelerating magnetic force and aerodynamic drag of the medium, which acts on the rear plasma bridge surface. The plasma channel forms bridge between the rails, and is accelerated along the electrodes due to  $\mathbf{j} \times \mathbf{B}$  force exerted by the discharge current  $I(t)$ . Self-consistent treatment of plasma motion and electrodes heating has been employed. Stainless steel (Cr/Ni/Ti 18/10/0.6÷0.8), copper, and tungsten have been considered here as the electrode materials, because these materials are widely used for manufacturing of electrodes. Good agreement with the experiment is observed in considered range of parameters.

## EFFECT OF ELECTRO DISCHARGE PARAMETERS ON THE DESTRUCTIVE ACTION OF PLASMA CHANNEL IN SOLID MEDIA<sup>1</sup>

*N.S. KUZNETSOVA, V.V. LOPATIN, A.S.YUDIN*

*National Research Tomsk Polytechnic University, Lenin Avenue, Tomsk, 634050, Russian Federation,  
tevn@hvd.tpu.ru, (3822)606172*

The research data of concrete fracturing and splitting off of the free surface by borehole electro-blast with the discharge initiation by the wire explosion have been presented. The method is based on the initiation of a capillary discharge by the exploding wire inside the solid dielectric material [1]. The effectiveness of splitting off and fracturing of concrete depending on different combinations of the shock wave transfer media (gel, water and polyethylene) was determined. It is shown that the long mode of electrical energy release ( $T_{0.5} = 36 \mu\text{s}$ ) is more effective in comparison with the short one ( $T_{0.5} = 18 \mu\text{s}$ ) for the concrete splitting off. The combined usage of capillary discharge in the polyethylene and in the gel leads to the most effective fracturing of the solid material. With the pulse amplitudes of 13 kV and wire length of 100 mm concrete pieces of 15×15×30 cm could be split off. Specific energy deposition of  $\sim 50 \text{ kJ/cm}^3$  leads to the pressure build-up of  $\sim 2.4 \cdot 10^9 \text{ Pa}$  in the plasma channel of capillary discharge. Under the action of pressure the highly conductive plasma channel expands and generates the shock wave, causing the mechanical stress formation in solid. The generator energy conversion into the plasma channel and into the wave of mechanical stresses in concrete has been considered. The dynamics of shock-wave propagation is investigated in condensed media polyethylene (gel)–concrete depending on discharge circuit parameters.

### REFERENCES

- [1] *Kuznetsova N. S. , Lopatin V. V. , Burkin V. V. , Golovanevsky V. A. , Zhgun D. V. , Ivanov N. A. // IEEE International Pulsed Power Conference. 2011. P. 267-273.*

<sup>1</sup> This work was supported by a Russian Government, project № 2367 and RFBR, research project No 14-08-01088/14

## GENERATION OF NEUTRONS DURING A NANOSECOND HIGH-VOLTAGE

### DISCHARGE IN LOW PRESSURE DEUTERIUM<sup>1</sup>

*M.I. LOMAEV*<sup>\*,\*\*\*</sup>, *B.A. NECHAEV*<sup>\*\*</sup>, *V.N. PADALKO*<sup>\*\*</sup>, *G.N. DUDKIN*<sup>\*\*</sup>,  
*D.A. SOROKIN*<sup>\*</sup>, *V.F. TARASENKO*<sup>\*,\*\*\*\*</sup>, *E.N. SCHUVALOV*<sup>\*\*</sup>

<sup>\*</sup>*Institute of High Current Electronics, 2/3 Akademichesky Avenue, Tomsk, 634055, Russia, Lomaev@loi.hcei.tsc.ru, 49-23-92*

<sup>\*\*</sup>*National Research Tomsk Polytechnic University, Tomsk, 30 Lenina Avenue, 634050, Russia*

<sup>\*\*\*</sup>*Tomsk State University of Control Systems and Radioelectronics, Tomsk, 40 Lenina Avenue, 634050, Russia*

<sup>\*\*\*\*</sup>*National Research Tomsk State University, Tomsk, 36 Lenina Avenue, 634050, Russia*

To create short duration pulsed sources of neutrons applied in nuclear physic the high-power ultra-short pulsed lasers [1, 2] and high-voltage discharges in low-pressure deuterium with metal cathodes saturated with deuterium or tritium [3, 4] are used. The neutron generation with deuterated cathodes was highly unstable [3] and the maximum neutron yield amounted to only  $\sim 10^3$  per pulse at a deuterium pressure of 1–2 Torr. In the case of tritium rich cathodes, a greater cross section for the D-T reaction allowed the neutron yield of  $\sim 2 \times 10^4$  per pulse to be obtained at a deuterium pressure of  $\sim 3$  Torr. Later the stable neutron generation was obtained due to D-D reaction in high-voltage nanosecond discharge in low-pressure deuterium at use of deuterated cathodes [5]. The study and creation of short duration sources of neutrons are very important from the standpoint of their practical applications, in particular, for calibrations of system registrations of experimental setups, used to carry out the investigations in the field of nuclear physic.

The subject of the present paper is to carry out the comparative measurements of a neutron yield at high-voltage discharges in low-pressure deuterium with metal anodes made from stainless steel and estimation of the neutrons' pulse duration as well.

The high-voltage pulser RADAN-220 (voltage pulse parameters: rise time  $\sim 0.5$  ns, duration on a matched load  $\sim 2$  ns, amplitude of voltage pulse up to 350 kV) was used to deuterium's excitation at pressure of 0.1 – 5 torr. A metallic plate coated by a layer of deuterated zirconium was used as a grounded cathode. 6 mm diameter tube made from stainless steel or 8 mm diameter tube composed from 0.2 mm diameter tungsten wires performed the function of potential anode. The optimal value of interelectrode length was found to be of  $\sim 5$  mm. The comparative results of a neutron yield at use both stainless steel and tungsten wires anode are presented in the Table 1.

Table 1.

Number of series	Number of shots	Neutrons number in series	Average neutrons number per shot	Maximal neutrons number per shot	Maximal neutrons yield from cathode per shot	Type of anode
1	50	589	11.8 $\pm$ 3.9	18	3100	Stainless steel
2	20	489	24.5 $\pm$ 11	70	12000	Tungsten wires

The value of the neutrons' pulse duration estimated on the base of a dispersion of neutrons' registration time was found to be about 1.5 ns.

#### REFERENCES

- [1] *K.W. Ledingham, P. McKenna, P.R. Singhal // Science. - 2003. - 300. 1107-1111.*
- [2] *A. Macchi // Appl. Phys. B. - 2006. - 82. 337-240.*
- [3] *L.P. Babich, T.V. Loiko // Dokl. Akad. Nauk USSR. – 1990. – 313. – No. 4. 846-849. (in Russian).*
- [4] *V.Ya. Averchenkov, L.P. Babich, T.V. Loiko, N.G. Pavlovskaya, S.P. Pushov // Technical Physics. – 1995. – 65. – No. 5. 156-167. (in Russian).*
- [5] *M.I. Lomaev, B.A. Nechaev, V.N. Padalko, S.I. Kuznetsov, D.A. Sorokin, V.F. Tarasenko, and A.P. Yalovets // Technical Physics. – 2012. – 57. - No. 1. 124–130.*

<sup>1</sup> The work is performed in the framework of the State task for HCEI SB RAS, project №13.1.3.

## SPLASHING OF ELECTRODES MATERIAL AT THE HIGH-VOLTAGE NANOSECOND DISCHARGE IN DEUTERIUM, HYDROGEN, HELIUM AND ARGON<sup>1</sup>

*M.I. LOMAEV*<sup>\*\*\*</sup>, *B.A. NECHAEV*<sup>\*\*</sup>, *V.N. PADALKO*<sup>\*\*</sup>, *G.N. DUDKIN*<sup>\*\*</sup>,  
*D.A. SOROKIN*<sup>\*</sup>, *V.F. TARASENKO*<sup>\*\*\*\*</sup>, *E.N. SCHUVALOV*<sup>\*\*</sup>

<sup>\*</sup>*Institute of High Current Electronics, 2/3 Akademicheskoy Avenue, Tomsk, 634055, Russia, Lomaev@loi.hcei.tsc.ru, 49-23-92*

<sup>\*\*</sup>*National Research Tomsk Polytechnic University, Tomsk, 30 Lenina Avenue, 634050, Russia*

<sup>\*\*\*</sup>*Tomsk State University of Control Systems and Radioelectronics, Tomsk, 40 Lenina Avenue, 634050, Russia*

<sup>\*\*\*\*</sup>*National Research Tomsk State University, Tomsk, 36 Lenina Avenue, 634050, Russia*

It is known, that due to the effect on the tungsten or zirconium target of the plasma flow with an energy value between the melting and boiling thresholds of the tungsten, a target material splashing is occurred and tracks of the flying material drops are observed [1]. An electrode material splashing is occurred during the formation of the vacuum arc discharge in the gap with cathode made of liquid metal. In this case, tracks of the flyaway material is observed [2].

The subject of the present paper is to study the appearance of luminous tracks observed in the gas discharge gap due to splashing of an electrodes material at the high-voltage nanosecond discharge in deuterium, hydrogen, helium and argon.

The high-voltage pulser RADAN-220 (voltage pulse parameters: rise time ~ 0.5 ns, duration on a matched load ~ 2 ns, amplitude of voltage pulse up to 350 kV) was used to deuterium, hydrogen, helium and argon excitation at pressure of 1 – 60 torr. A metallic plate coated by a layer of deuterated zirconium was used as a grounded electrode. 6 mm diameter tube made from stainless steel or 8 mm diameter tube composed from 0.2 mm diameter tungsten wires performed the function of potential electrode (Figure 1).

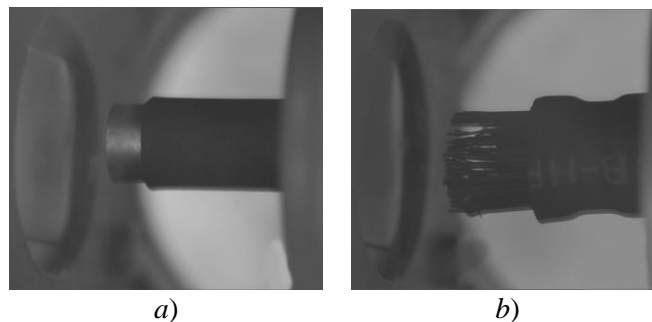


Fig. 1. Plate grounded (left) and potential stainless steel tube (a) and tungsten wires tube (b) electrodes.

The splashing of the tungsten wires and deuterated zirconium electrodes' material observed in all gases under study at pressure of 1 – 60 torr at both positive and negative polarity of potential electrode. On the Figure 2 the typical photos of luminous tracks and discharge glowing in deuterium are presented.

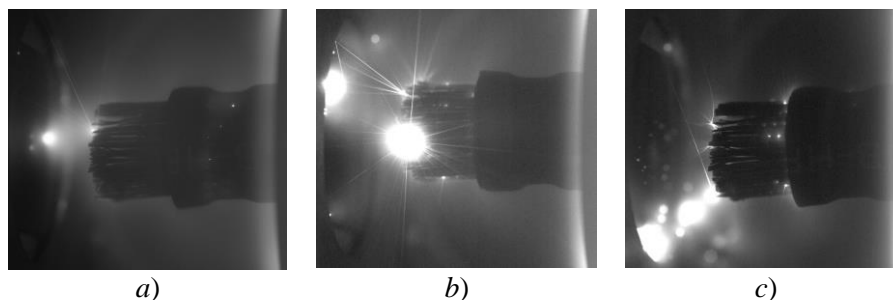


Fig. 2. Photos of discharge gap at high voltage nanosecond discharge in deuterium at pressure of: 1 torr (a), 3 torr (b), 15 torr (c). The polarity of the potential tungsten wires tube electrode is positive. Gap distance is 5 mm.

### REFERENCES

- [1] *Klimov N.S., Podkovyrov V.L., Zhitluhin A.M. et al. // VANT. Ser. Thermonuclear Fusion. - 2009. - No. 2. 52-61. (in Russian).*  
[2] *Popov S.A., Proskurovsky D.I., Batrakov A.V. // IEEE Trans. Plasma Sci. - 1999. - 27. - No. 4. 851-857.*

<sup>1</sup> The work is performed in the framework of the State task for HCEI SB RAS, project №13.1.3.

## RADIATION SOURCES IN THE UV SPECTRAL RANGE<sup>1</sup>

YU.N. PANCHENKO\*, A.V. PUCHIKIN\* AND V.F. LOSEV\*\*,\*\*

\* Institute of High Current Electronics SB RAS, 2/3 Akademicheskoy Ave.,  
Tomsk, 634055, Russia, ypanchenko@sibmail.com (3822)491891

\*\*Tomsk Polytechnic University, 30 Lenin Ave., 634034 Tomsk, Russia

This article describes the results of experimental studies in formation of volumetric and multi-channel diffuse discharge in inert gases at atmospheric pressure containing additives of CO, CO<sub>2</sub>, CCl<sub>4</sub>.

Found the possibility of forming the plasma which has high intensity radiation in the ultraviolet range of the spectrum. The output radiation has intense spectral line at 247.8 nm due to the transition <sup>1</sup>P<sup>0</sup> – <sup>1</sup>S excited carbon atom C I. The presence of excited carbon atom C(<sup>1</sup>P<sup>0</sup>) was achieved via dissociative reaction of CO with excited atom of He\* or Ne\*.

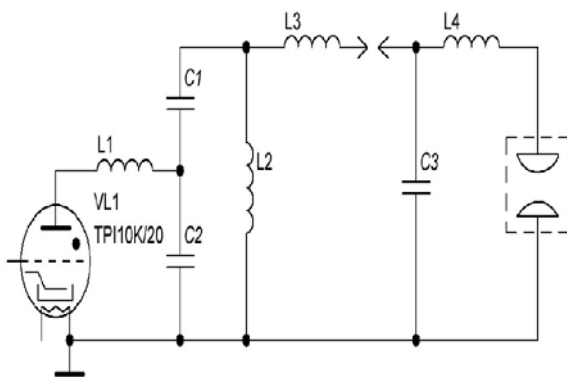


Fig.1. Schematic diagram of excitation circuit. C1= 80 nF, C2= 40 nF, C3= 22 nF, L1= 20 nH, L2= 0.15 mH, L3= 150 nH, L4 = 3 nH

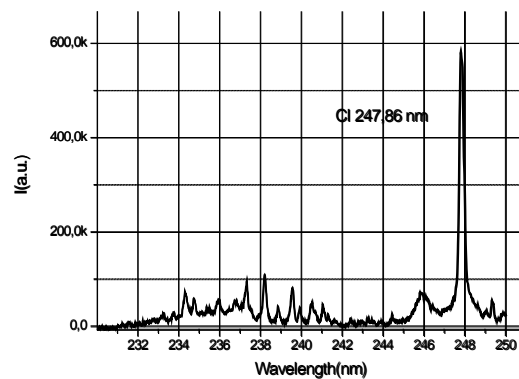


Fig. 2. The spectral distribution of discharge plasma radiation intensity in the UV range. Composition of the gas mixture of CO:Ne-50:500 mbar, P = 0.55 bar. U<sub>0</sub> = 18 kV.

Generated plasma was pumped with generator based on a LC- inverter Fig. 1. Preionization of the discharge gap was carried out by UV - radiation that occurs at triggering spark gaps installed in the second loop of the circuit. Storage capacitors C1 and C2 and discharge capacitor C3 had the values of 80, 40 and 22 nF respectively. Thyatron TPI1-10k/20 was used as the commutator. The inductance of the first L2 and the second L3 discharge contours were 130 and 4 nH respectively. The length of the electrodes was 500 mm, the electrode gap - 18 mm. Electrodes were of cylindrical shape work surface with the radius of 6 mm.

In the course of the experiments were defined the optimal conditions of discharge excitation in CO and CO<sub>2</sub> (10-50 mbar) and Ne or He (500 mbar), allowing to obtain an efficient source of UV radiation. Figure 2 shows the spectral distribution of the radiation intensity of discharge plasma in the UV range. Most of the radiation energy was registered during the time interval of 5-10 ms after the breakdown of the discharge period.

### REFERENCES

- [1] C. K. N. Patel, R. A. McFarlane, and W. L. Faust // Physical Review.- 1964.- 133.- № 5A.- P. A1244-A1249.
- [2] R. W. Waynant // Appl. Phys. Lett. – 1973. – 22. – № 8. P. 419-420.

<sup>1</sup> This work was supported by RFBR (projects No 13-08-98024-r\_sibir\_a) and by grants in the framework of the RAS SD integration project (No. 9).

## INFLUENCE OF CURRENT MODULATION ON VOLUME DISCHARGE HOMOGENEITY AND EFFICIENCY OF A WIDE-APERTURE XeCl-LASER<sup>1</sup>

*I.N. KONOVALOV, A.N. PANCHENKO, V.F. TARASENKO*

*\*Institute of High Current Electronics SB RAS, Akademicheskoy av., 2/3, Tomsk, 634055, Russia, E-mail: [ivan@lgl.hcei.tsc.ru](mailto:ivan@lgl.hcei.tsc.ru),  
Phone +7 3822 491644*

Efficiency of XeCl-laser excitation and uniformity of the output power distribution over the beam aperture is primarily determined by uniformity of volume electric discharge in the laser active volume. Stability of the volume discharge depends on initial phenomena occurring in the process of discharge gap breakdown and active media formation. Therewith during volume discharge existence formation of micro- and macroinhomogeneity can occur in the discharge bulk.

Homogeneity of the volume discharge is achieved using two-circuit pulsed generator, which provides discharge current of the primary capacitor with high-frequency modulation due to oscillatory discharge of the peaking capacitor.

In the present report it was shown that current-voltage and spatial characteristics of volume discharge in XeCl- laser differ significantly in the excitation modes with energy input from capacitive and inductive energy storages. During discharge of a capacitor increase of the volume discharge current density leads to decrease of electric field in the plasma. In an oscillation excitation mode when energy stored in the inductance of the discharge circuit is deposited into the active medium increase of the volume discharge current density is accompanied with linear increase of the electric field in the plasma. In the case of pumping of the active medium from capacitive energy storage the volume discharge and laser spot widths are ~ 2 times higher as compared with those obtained under pumping from the inductive energy storage, specific input power is comparable.

Thereby a periodic change of the current density distribution in the active volume with different conductivity is observed in the case of high-frequency modulation of the volume discharge current in the wide-aperture XeCl-laser. This excitation method in contrast to a quasi-stationary pumping regime has strong effect on the plasma-chemical processes dynamics and aligns current density in the discharge bulk preventing development of micro- and macroinhomogeneities in the discharge plasma.

<sup>1</sup> This work was supported by Grant of President of Russian Federation, Scientific School-1305.2014.2.

DISCHARGE-PUMPED KrF LASER <sup>1</sup>

YU.I. BYCHKOV, YU.N. PANCHENKO, A.V. PAVLINSKY, A.V. PUCHIKIN, A.G. YASTREMSKII, S.A. YAMPOLSKAYA.\*

\*Institute of High Current Electronics SB RAS, 2/3 Akademicheskoy ave., Tomsk, 634055, Russia, E-mail: [s\\_yampolskaya@yahoo.com](mailto:s_yampolskaya@yahoo.com), phone: 8 (3822) 49-17-52

Electric discharge KrF excimer lasers ( $\lambda = 248$  nm) are widely applied in various fields of physics, medicine, microelectronics, photochemistry and biology. Many applications require radiation pulses of short duration and high power. Experiments show, that for the excimer laser with a pulse duration on the FWHM 20 – 30 ns, is typical that lasing begins near the current maximum and main energy is produced on a pumping decline. For these conditions, the amount of laser energy will be increases with decreasing delay time from start of the pumping to start of laser generation. Moreover, a necessary condition to obtain lasing is a preservation of the uniformity of the discharge after the current maximum.

The report presents the results of experimental and numerical investigations of KrF laser with a pulse duration at the half maximum  $\sim 30$  ns [1]. Calculations were performed using 0D (approximation of homogeneous discharge) [2] and 2D models of KrF laser (discharge is not uniform in width). In the two-dimensional model used real electrode profile, the same as in the experiment. In Fig. 1a showing the experimental and calculated time dependences of the discharge current and the measured laser power. It is seen, that there is a good agreement between experimental and calculated results as 0D well as 2D models.

Based on 0D model, the analysis of the kinetic processes in the active medium was performed. It was shown, that the long time lasing delay in KrF laser is necessary for creation of inversion.

2D model was used to study the behavior of the inhomogeneous pumping discharge and lasing in such circumstances. In Fig. 1b are presented electron density distributions across the width of the discharge at different times. These results indicate that after the maximum of the current, width of the discharge strongly decreases. Nevertheless, the discharge on the second half cycle of current can produce up to 20 % of the whole laser energy.

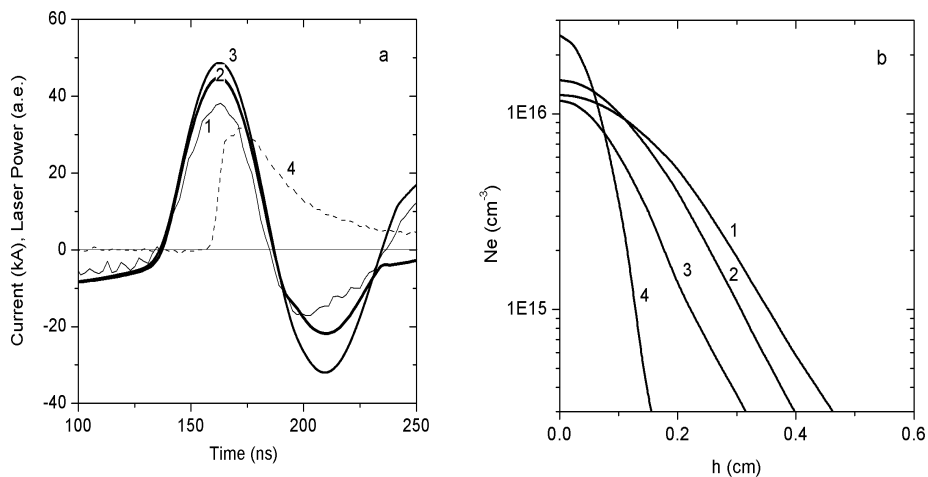


Fig. 1. Current: experiment – 1, 0D model – 2, 2D model – 3, Experimental laser power – 4 – (a); Distributions of electron density for times: 150 ns – 1, 170 ns – 2, 180 ns – 3, 220 ns – 4.

## REFERENCES

- 1] Yu.N. Panchenko, M.V. Andreev, V.V. Dudarev, N.G. Ivanov, V.F. Losev, A.V. Pavlinsky, A.V. Puchikin // Russian Physics Journal. – 2012. – V. 55. – № 10. 303–307.
- 2] A.G. Yastremsky, Yu.I. Bychkov, S.A. Yampolskaya // in Proc. Of 16<sup>th</sup> International Symposium on High Current Electronics. – Tomsk. – 2008. – P. 589–592.



## CONTROL AND FORMATION OF THE OUTPUT RADIATION INTENSITY PROFILE IN AN EXCIMER LASER<sup>1</sup>

M.V. ANDREEV, YU.N. PANCHENKO, A.V. PAVLINSKY

<sup>1</sup> Institute of High-Current Electronics of the Siberian Branch of the Russian Academy of Sciences,  
2/3 Akademicheskoy Ave, Tomsk, 634055, Russia

Many scientific and practical research require stable performance of the laser radiation used. This paper describes a technique for measuring and control the profile of output radiation based on the analysis of the transverse intensity distribution of the output radiation for an excimer laser.

In the developed method when processing the received image of the beam we initially apply "filtering" (by transforming original bitmap to binary form and removing digital noise), and then determine the transverse dimension of the laser beam. For filtering we used Otsu method [1]. From our perspective, this is one of the most effective methods for calculating binarization threshold for halftone images compared to the methods of Burns [2] and the lower limit method. When analyzing the fingerprint image of the laser beam Figure 1(a) by Otsu method binarization threshold is 85, 104 for Burns, and 125 for the lower limit method. The area treated is reduced relative to the original beam (80 binarization threshold) 2%, 23 % and 33 %, respectively. Figure 1 (b) shows the image of the output beam from the misaligned cavity.

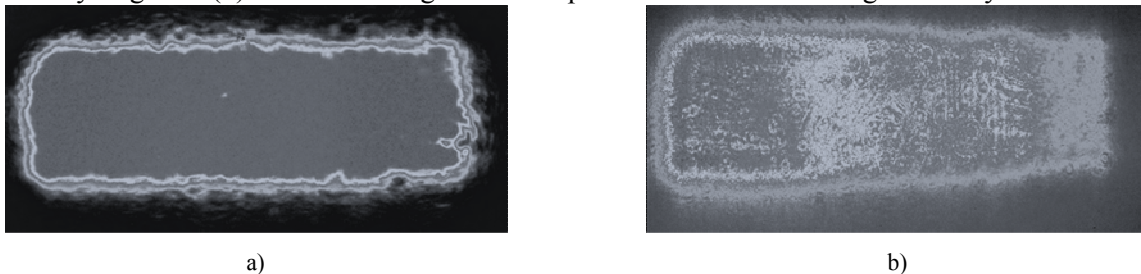


fig 1 a) intensity distribution of laser beam in case aligned out mirror b) intensity distribution of laser beam in case misaligned out mirror

Then, using an adaptive medial filter (AMF), we remove part of the pixelated noise ("salt and pepper") that can appear after the transformation of the source bitmap into binary form. And also we determine the center of mass ( $M_x$ ,  $M_y$ ) of image. For adjustment of the output mirror of the cavity in addition to the moment of mass of points center coordinates, it is necessary to constantly control the intensity and of the laser beam.

On the base of the proposed processing method we have implemented a system for aligning the output cavity mirror of a pulsed laser with the accuracy of output beam positioning of.

### REFERENCES

- [1] Linda G. Shapiro and George C. Stockman // Computer Vision.– pp 279– 325, New Jersey, Prentice-Hall S.V.
- [2] D. Darian Muresan, Thomas W. Parks Adaptive principal components and image denoising. // IEEE ICIP 2003
- [3] Szymon Graboski, Wojciech Bienieck A two-pass median-like filter for impulse noise removal in multi-channel images. // KOSYR.– 2003.– pp. 195-200.

<sup>1</sup>This work was supported by RFBR (projects No 13-08-98024-r\_sibir\_a) and by grants in the framework of the RAS SD integration project (No. 9).

**APPLICATION OF HIGH – POWER NANOSECOND MICROWAVE PULSES IN A NON-EQUILIBRIUM PLASMA CHEMISTRY.**

M.S.ARTEEV

*PTI TPU, Lenina str.2 a, Tomsk, 634050, Russia, [arteev@tpu.ru](mailto:arteev@tpu.ru), (3822) – 417451.*

The paper discusses the features of gas discharges initiated by powerful microwave nanosecond pulses. Plasma produced in such discharges, in a wide range of pressures as a homogeneous both in the longitudinal and transverse directions and is characterized by a high degree of the non-equilibrium and efficiency using of microwave pulses – more than 80% energy deposited into a gas accumulated in excited and ionized states of molecules (atoms) of the gas. These make them challenging powerful nanosecond microwave pulses to improve efficiency and performance of gas – phase plasma chemical reactors. As an example given some experimental results of studies on the preparation of chemically pure silicon when exposed to microwave pulses with the power  $\sim 10^7$  W and duration 5 ns on the mixture  $\text{SiF}_4 - \text{Ar}$ .

## STUDY OF PHYSICOCHEMICAL PROCESSES ACCOMPANYING AIR PURIFICATION FROM STYRENE VAPOR BY PULSED ELECTRON BEAM<sup>1</sup>

*I.E. FILATOV, YU.S. SURKOV, S.A. NIKIFOROV*

*Institute of Electrophysics of the Ural Branch of the Russian Academy of Sciences, 106 Amundsen st., Ekaterinburg, 620016, Russia  
[fil@iep.uran.ru](mailto:fil@iep.uran.ru), +7(3432678828)*

Styrene is a one of the most important industrial air pollutant. One of the most effective methods of cleaning the air from its vapors is electron beam processing [1]. Most of the works explore the effectiveness of air purification from styrene, but do not touch the end products of its transformation. Meanwhile, some of the end products have the potential toxicity. In this work the technique of a comprehensive study of the final products of volatile organic compounds (VOCs) transformation of in the air treated by an electron beam or other method of non-thermal plasma generation is proposed. The method is demonstrated on example of the styrene vapor conversion. The basis of the experimental setup is a portable electron accelerator RADAN [2] with following parameters: energy of electrons – 180 keV, beam current – 500A, pulse duration – 3 ns, pulse repetition rate – 10 s<sup>-1</sup>. This accelerator is complemented with several specially designed reaction chambers (cells). One of them allows you to explore the energy parameters of air purification system and contains of styrene vapor analysis system on a base of GLC. Part of the final products has reduced volatility and therefore accumulates on the walls of the reaction chamber. To collect these products another special miniature cells [3,4] was been developed, in which the final products are collected in a tube filled with adsorbent. Further analysis of the final products is carried out by GLC / MS method. Assignment of specific compounds of the chromatographic peaks is based on a comparison of the mass spectra with mass spectra database.

It has been shown, that most of the final products are products of styrene partial oxidation. One of the products is benzaldehyde, which was detected by the standard GLC procedure. A number of other products of incomplete styrene oxidation also founded. The mechanisms of styrene oxidation in the plasma generated by electron beam are discussed. Investigation of the products showed that the main mechanisms held with the participation of reactive oxygen species. Investigation of the products showed that the main mechanisms held with the participation of reactive forms of oxygen.

The proposed method allows to evaluate the possibilities and drawbacks of the methods of air cleaning air from toxic VOCs by electron beam and other methods of none-thermal plasma generation. This information will be useful for the development of new combined air purification methods.

### REFERENCES

- [1] *Yu. N. Novoselov, I. E. Filatov // Technical Physics.-2003.-Vol. 48.- № 1. P 1594-1597.*
- [2] *G.A. Mesyats, V.G. Shpak, M.I. Yalandin. and S.A. Shunailov // Radiat. Phys. Chem.-1995.-Vol. 46.-№ 4-6, P. 498.*
- [3] *Yu. N. Novoselov, I. E. Filatov // Technical Physics Letters.-209.-Vo. 35.-№ 5.- P. 412-414.*
- [4] *I.E. Filatov, E.V. Kolman //Izvestia Vuzov. Fizika.-2014.- 239-242. Vol.57.-№ 3/2. – P. 239-242.*

<sup>1</sup> This work was supported by RFBR project № 13-08-00975a

## PRODUCTS OF CS<sub>2</sub> DECOMPOSITION IN AIR UNDER THE INFLUENCE OF STREAMER CORONA<sup>1</sup>

*I.E. FILATOV, D.L. KUZNETSOV, V.V. UVARIN, YU.S. SURKOV, S.A. NIKIFOROV, G.G. UGODNIKOV*

*Institute of Electrophysics, Ural Division of the Russian Academy of Sciences,  
106 Amundsen str., Ekaterinburg, 620016, Russian Federation, E-mail: [fil@iep.uran.ru](mailto:fil@iep.uran.ru), Phone: (343)2678828*

Carbon disulfide CS<sub>2</sub> is a toxic component being contained in exhaust gases from cellophane and viscose production. Alternative to conventional technologies are electrophysical methods of CS<sub>2</sub> conversion, for example, the use of DC corona discharge [1], electron beam and non-self-sustained discharge [2].

The report presents the results of investigation of CS<sub>2</sub> decomposition in air under the influence of streamer corona. The installation [3] was used with the following parameters: high voltage 150-170 kV, streamer corona discharge current amplitude 100-300 A, pulse duration 15-30 ns, pulse repetition rate 1-10 Hz. Air mixture containing 50-10000 ppm CS<sub>2</sub> was processed. A quantitative composition of mixture before and after processing was determined by a method of gas chromatography.

Main products of CS<sub>2</sub> decomposition are SO<sub>2</sub>, COS and CO<sub>2</sub>. When CS<sub>2</sub> was almost totally converted, further processing led to decomposition of SO<sub>2</sub> and COS with a formation of H<sub>2</sub>SO<sub>4</sub> and CO<sub>2</sub>. It can be seen (Fig. 1) that CS<sub>2</sub> concentration decreased from 10000 ppm to 650 ppm after 30000 streamer corona shots with energy expenditures to remove one CS<sub>2</sub> molecule 8 eV/molecule. In this case energy efficiency of CS<sub>2</sub> removal is 360 g·kWh<sup>-1</sup>.

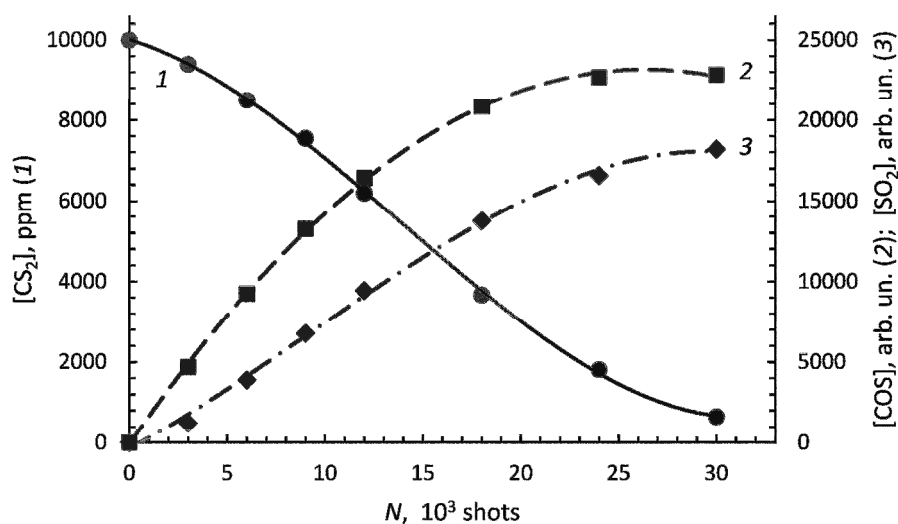


Fig. 1. Dependencies of CS<sub>2</sub> concentration (1) and main products of its decomposition – carbonyl sulfide COS (2) and sulfur dioxide SO<sub>2</sub> (3) – on the number of streamer corona shots *N*

With initial 3000 ppm CS<sub>2</sub> its concentration decreases to 50 ppm after 12000 shots with energy expenditures 11 eV/molecule and energy efficiency 260 g·kWh<sup>-1</sup>. The obtained energy efficiency of CS<sub>2</sub> decomposition is worse than with the use of pulsed electron beam [2] but better than with the use of DC corona discharge [1]. We believe that the mechanism of CS<sub>2</sub> decomposition in streamer corona discharge is the same as with the use of electron beam.

Thus, main products of CS<sub>2</sub> decomposition and energy efficiency of the use of streamer corona discharge are determined. The advantages of the streamer corona method in comparison with electron-beam one are less complexity, lower costs, higher reliability and safeness.

### REFERENCES

- [1] X. Yan, Y. Sun, T. Zhu, X. Fan // Journal of Hazardous Materials. – 2013 – 261. P. 669-674.
- [2] Y.N. Novoselov, A.I. Suslov, D.L. Kuznetsov // Rus. Technical Physics. – 2003 – 48 – № 6. P. 780-786.
- [3] Kuznetsov D.L., Filatov I.E., Surkov Yu.S. // Izvestiya Vuzov. Fizika. – 2012 – 55 – № 10/3. P. 236-240.

<sup>1</sup> This work is supported by RFBR (project No 12-08-00130-a)

**THE FRAGMENTATION OF POLYSILICON BAR BY USING PULSED POWER TECHNOLOGY***YAOHONG SUN, RONGYAO FU, YINGHUI GAO, PING YAN*

*Institute of Electrical Engineering Chinese Academy of Sciences, No.6 Zhongguancun Beiertiao, Beijing, 100190, China,  
Key Laboratory of Power Electronics and Electric Drive, Chinese Academy of Sciences, Beijing, China  
yhsun@mail.iee.ac.cn,8610-82547119*

Usually, the fragmentation of poly-silicon bar was treated by hand (using a hammer) or by mechanical machine. Due to the high labor intensity, large noise, dust and metal pollution, it is hard to be manufactured on a large scale. Also, because of the large size of the poly-silicon bar with a maximum diameter of 180 mm and a length of 2.8m), the electro-dynamic fragmentation machine was not suitable for this application. The electro-hydraulic method was adopted in our experiments. This method utilized the shock wave effect generated by pulsed discharge underwater. A pulsed power supply with a stored energy of 8kJ was used, which mainly consisted of a high voltage charging supply, energy storage capacitors, a discharging switch and a coaxial discharging electrode. Two types of samples with a diameter of 75 mm and 160 mm respectively were used. The distance between the discharging electrode and the poly-silicon bar is approximately 10 mm. Experimental results shown that 3-6 kJ /single shot could be enough for the fragmentation of the poly-silicon bar.

## REFERENCES

- [1] *Mueller. G, etc // Pulsed Power Conference (PPC), 2011 IEEE. P. 46-102.*
- [2] *Jud. Hammon , etc // Pulsed Power Conference (PPC),2001 IEEE. P. 1142-1145.*
- [3] *T.H.G.G.Weise , M.J.Loffler.// Pulsed Power Conference, 1993 IEEE. P. 19-22.*
- [4] *M. Hamelin, etc // Pulsed Power Conference ,1993 IEEE. P. 11-15*



**12<sup>th</sup> International Conference  
on Modification of Materials  
with Particle Beams and Plasma Flows**



**Co-Chairmen:**

Nikolai Koval Institute of High Current Electronics, Tomsk, Russia  
 Valery Krivobokov Institute of Physics and Technology, TPU, Tomsk, Russia

**International Advisory Committee:**

Andre Anders Lawrence Berkeley National Laboratories, USA  
 Ian Brown Lawrence Berkeley National Laboratories, USA  
 Massimiliano Bestetti Politecnico di Milano, Italy, Milan  
 Oleg Dolmatov Institute of Physics and Technology, TPU, Tomsk, Russia  
 Vladimir Engelko D.V. Efremov Scientific Research Institute of Electrophysical Apparatus, St. Petersburg, Russia  
 Igor Garkusha National Science Center Kharkov Institute of Physics and Technology, Kharkov, Ukraine  
 Nikolai Gavrilov Institute of Electrophysics UB RAS, Ekaterinburg, Russia  
 Kairat Kadyrzhanov L.N. Gumilyov Eurasian National University, Astana, Kazakhstan  
 Alexander Korotaev National Research Tomsk State University, Tomsk, Russia  
 Eduard Kozlov Tomsk State University of Architecture and Building, Tomsk, Russia  
 Alexander Ryabchikov Institute of Physics and Technology, TPU, Tomsk, Russia  
 Georgy Mladenov Institute of Electronics, Sofia, Bulgaria  
 Jindrich Musil University of West Bohemia, Plzen, Czech Republic  
 Timothy Renk Sandia National Laboratories, Albuquerque, New Mexico, USA  
 Vladimir Rotshtein Tomsk State Pedagogical University, Russia  
 Petr Schanin Institute of High Current Electronics, Tomsk, Russia  
 Alexander Semenov Institute of Physical Material Science SB RAS, Ulan-Ude, Russia  
 Yuriy Sharkeev Institute of Strength Physics and Materials Science SB RAS, Tomsk, Russia  
 Vyacheslav Shulov Moscow Aviation Institute (National Research University), Moscow, Russia  
 Yang Si-Ze Institute of Physics, Chinese Academy of Sciences, Beijing, China  
 Anatoly Smyslov Ufa State Aviation Technical University, Russia  
 Kensuke Uemura ITAC Ltd., Niigata, Japan  
 Vladimir Uglov Belarusian State University, Minsk, Republic of Belarus  
 Alexander Yalovets South Ural State University, Chelyabinsk, Russia  
 Georgi Yushkov Institute of High Current Electronics SB RAS, Tomsk, Russia

**Sessions:**

Beam and plasma sources  
 Fundamentals of modification processes  
 Modification of material properties  
 Coatings deposition  
 Nanoscience and nanotechnology



## GENERATION OF LOW-TEMPERATURE PLASMA OF LOW-PRESSURE ARC DISCHARGES FOR SYNTHESIS OF WEAR-RESISTANT NITRIDE COATINGS<sup>1</sup>

*O.V. KRYSINA\*, N.N. KOVAL\*, I.V. LOPATIN\*, V.V. SHUGUROV\**

*\*Institute of high current electronics SB RAS, 2/3 Akademichesky ave., Tomsk, 634055, Russia,  
[krygina\\_82@mail.ru](mailto:krygina_82@mail.ru), +7(3822)49-17-13*

The parameters of mixed gas-metal plasma were measured and analyzed. The results were compared with those of independent gas and metal plasmas. The influence of ion-plasma assistance on the element composition of coatings based on titanium nitride is shown, specifically in regard to the influence of parameters of non-self-sustained arc discharge based on a combined filament and hollow cathode ("PINK").

It was revealed that the concentration of gas-metal plasma is approximately equal to the sum of the gas and metal plasma concentrations, which were measured independently under arc discharges with the same characteristics. It was experimentally shown that the increase of the arc current of "PINK" led to an increase of the plasma concentration at constant gas pressure. In simultaneous work with gas and metal plasma sources, the growth of the arc current of "PINK" with a constant arc current of the evaporator leads to similar growth of the mixed gas-metal plasma. This fact indicates that we can change the arc current of "PINK" (at constant gas pressure) during coating deposition, which allows us to easily control the density of the gas ion current to the substrate, and thereby change the stoichiometry of the growing coating. This allows for simplification of the deposition technology for multilayer and gradient coatings, and also for improvement of the repetition of the deposition process for these types of coatings.

The concentration of elements in TiN type coatings was measured by Auger spectrometry. Varying parameter was arc current of plasma source "PINK" ( $I_p=0\div 100$  A). Other parameters of deposition mode were similar ( $I_d=100$  A;  $p_{N_2}=0,3$  Pa;  $t=5$  min;  $U_b=U_n$ ). After deposition of TiN coatings from metal plasma in atmosphere of molecular nitrogen with ratio of Ti:N is approximately equal to 1:1. The ratio of Ti:N for coating deposited with ion-plasma assistance at comparative low arc current of "PINK" (20 A) is approximately equal to 1:1 too. At subsequent increase of arc current of "PINK", i.e. at increase of percentage of charged particles of nitrogen (plasma concentration), simultaneous increase of nitrogen concentration and decrease of Ti concentration in TiN coating occur. At ratio of arc currents of evaporator and "PNK" 1:1 the concentration of titanium in coating became in two times lower, than nitrogen concentration. For accurate explanation that the complex investigation of phase-structural state and fine structure of obtained coatings (particularly, measurement of lattice parameter of main phase  $\delta$ -TiN) is necessary. Possible explanations of the effect are following: 1) penetration of nitrogen to lattice of TiN, which leads to increase of lattice parameter; 2) formation of other phases of  $Ti_xN_y$ . This is consequence of change of coating synthesis conditions, particularly parameters such as deposition rate at significant change of arc current of "PINK"; temperature of substrate during coating deposition at high current of "PINK", etc.

Based on obtained results the current of "PINK" has to equal 5-20% of total current on substrate for deposition of monophase TiN coating with stoichiometric composition.

Similar dependence of nitrogen concentration on arc current of "PINK" was observed at deposition of multicomponent Ti-Al-N coatings.

<sup>1</sup> This work was supported by Project SB RAS II.9.5.1 "Research foundations of development of electrophysical equipment for obtaining and properties modification of nanostructured layers and coatings" and by the Russian Foundation for Basic Research (grant No. 13-08-98108-r\_sibir-a).

## UNBALANCE MAGNETRON PLASMA SOURCE FOR ION MASS-SEPARATOR<sup>1</sup>

*V.L. PAPERNY,\* V.I. KRASOV\*, N.V. ASTRAKCHANTSEV\*\*, N.V. LEBEDEV\*\**

*\*Irkutsk St. University, 1, K.Marx Str., Irkutsk, 664003, Russia, [paperny@math.isu.rumet.ru](mailto:paperny@math.isu.rumet.ru), +7(3952)521242*

*\*\* Irkutsk St. Technical University, 83, Lermontov Str., Irkutsk, 664070, Russia*

Recent experiments showed that vacuum arc plasma source supplied with a transport system based on a curved magnetic field has a significant mass-separation property [1]. The report presents the results of the preliminary studies characteristics of an unbalanced magnetron plasma source supplied with the transport system. The magnetron source has 50 mm diameter cathode manufactured of a stainless steel with 60 mT maximum value of the magnetic field in the vicinity of the cathode. The discharge was fed with a LC-pulse line resulting in current pulse of 700 microsecond duration and up to 50 A peak value. The line was charged initially up to – 800 V voltage. To initiate the pulsed discharge, the auxiliary duty low-current (100 mA) steady-state magnetron discharge was sustained. The working vessel was evacuated down to the  $2 \times 10^{-3}$  Pa, then the working gas, argon, was introduced up to the pressure of  $2 \times 10^{-3}$  Pa. The guiding magnetic field of the transport system was formed with a set of magnetic solenoids, so that three of them were co-axial both to each other and to the magnetron axis. Due to the specific design of the device, the cathode axis was shifted relative to the common axis of the solenoids. As a result, the magnetic field lines passing through the cathode surface were deflected and at the exit of the transport system, where the parameters of the cathode jet were measured, the field lines were directed almost perpendicular to their initial direction. The magnetic induction near the cathode was about 20 mT, while at the exit plane, it was of 2 – 3 mT. The ion energy distribution at the exit of the transport system was measured by means of a retarded field analyzer (RFA) that was located at 90 degrees to the initial direction of the plasma flow. The ion energy distribution was determined by measuring the dependence of the ion collector current  $I_c$  on the potential  $V_r$  applied to the retarding grid and subsequent numerical differentiation of the dependence obtained. It was found that the shape of the ion energy distribution obtained under these experimental conditions differs substantially from the routine distribution observed earlier in plasma of a pulsed high current magnetron. Namely, the distribution had a double-humped shape so that there presented the fast and slow ion components in the plasma flow. The directed energy of the fast ion component was close to 50 eV and the directed energy of the slow component was of 10 eV. Note that energy of the fast component exceeded substantially the ion energy in the magnetron discharges plasma observed earlier. We suppose that the result obtained is due to arising of an acceleration mechanism in the plasma flow through action of the inhomogeneous magnetic field.

### REFERENCES

- [1] *V L Paperny, V I Krasov, N V Lebedev and N V Astrakchantsev// Plasma Sources Sci. Technol. –2011. – V.20 –035005.*

<sup>1</sup> This work was supported by the RFBR, project № 14-02-00943

## ELECTRIC AND THERMAL CHARACTERISTICS OF STEAM PLASMA GENERATOR

*A.S. ANSHAKOV<sup>1,2</sup>, S.I. RADKO<sup>2</sup>, E.K. URBAKH<sup>1</sup>, A.E. URBAKH<sup>1</sup>, V.A. FALEEV<sup>1</sup>*

<sup>1</sup>*Kutateladze Institute of Thermophysics SB RAS, Lavrentyev ave. 1, Novosibirsk, 630090, Russia, anshakov@itp.nsc.ru, (383)330-80-92*

<sup>2</sup>*Novosibirsk State Technical University, Marks ave. 20, Novosibirsk, 630092, Russia*

The steam plasma generators, workable today, use the thermoemission or thermochemical electrodes as the cathodes. The thermocathodes of tungsten require the oxygen-free media: the so-called shielding gases (argon, nitrogen). In this case steam plasma contains the admixtures of foreign gases.

To eliminate this effect and simplify the construction scheme of the plasmatron, the design of steam plasma generator with copper tubular electrodes was suggested. To exclude droplet formation on the water cooled surfaces of a discharge chamber, we use the system of indirect cooling of the outer surface of electrodes. The thickness of a steel shell ring with low heat conductivity to a copper electrode, required for maintaining the temperature of working electrode surface of above 100°C, was calculated. The steam temperature at the vortex chamber outlet of plasmatron is 250-300°C.

The voltage-current and voltage-consumption characteristics of an arc discharge, and heat fluxes to electrodes were studied experimentally, and thermal efficiency and enthalpy of steam plasma were determined. The voltage-current characteristics in steam are descending and in comparison with air they are located higher. According to estimates, electric field strength is 18-20 V/cm, this means that the arc glows in the atmosphere of hydrogen and oxygen.

The plasmatron power is 60-100 kW, thermal efficiency is 60-65%, specific erosion of electrodes is about 10<sup>-9</sup> kg/C.

## ELECTRON BEAM CHARACTERISTICS FOR SUB-NANOSECOND PULSE INTERACTION WITH METAL TARGETS<sup>1</sup>

*K.A. NAGAYEV\**, *S.V. BARAKHVOSTOV\**, *I.L. MUZYUKIN\**, *I.S. TURMYSHEV\**, *V.P. TARAKANOV\*\**, *U.A. ZEMSKOV\**,  
*E.A. CHINGINA\**, *N.B. VOLKOV\**

*\*Institute of Electrophysics UB RAS, 106 Amundsen st., Yekaterinburg, 620016, Russia, [kanagayev@iep.uran.ru](mailto:kanagayev@iep.uran.ru), +7(343)2678776*

*\*\*Joint Institute of High Temperatures RAS, 13 Bd.2 Izhorskaya st., Moscow, 125412, Russia*

The matter physical properties modification is one of the intense electron beams applications area, for this reason the ultra-fast processes at high energy densities investigation is a task of great interest. If metal is taken to be quantum plasma, then a sub-nanosecond duration pulse impact can lead to generation of strongly non-equilibrium states of metal, in particular that would be ion-sound and Langmuir turbulence, resulting into lasting relaxation to the equilibrium state.

In order to investigate the mechanisms of excitation and relaxation the EXCITOR experimental setup was built. It generates an electron beam lasting for about 500 ps and with electrons energy of about 100 – 200 keV. The basic element is the compact high-voltage generator RADAN-300 having the doubled formation line. The nanosecond pulse from the generator, when passing through the special converter, is refined to 115 kV and shortened to 500 ps. The vacuum diode is a coaxial line with samarium or graphite emitter tip. For the anode 20 μm Cu foil and steel mesh with 40x40 μm cell were used.

Here we report about integral energy spectrum characteristics, and also about the beam current, acquired on the experimental setup via the Thompson spectrometer and the Faraday cup respectively. In our experiments we had revealed that the integral energy spectrum has Gaussian shape and its peak is close to 105, 110, 130 keV for the inter-electrode distance being 1, 2 and 5 mm correspondingly. Particles with energies within the range from 50 to 200 keV were observed in the spectra. The beam spectrum acquired with anode mesh is quiet similar to the one acquired with solid anode. The obtained experimental data match qualitatively and quantitatively the electron beam formation numerical simulations using KARAT electromagnetic code, where the computational domain was close to the real vacuum chamber geometry, and the experimental voltage pulse from the vacuum diode input was taken to be the boundary conditions. The experimental particles energies values also are in good agreement with the calculated ones.

Further work is aimed at mechanisms of excitation and relaxation of highly non-equilibrium states of metals investigations, using interferometric measurement system for acquiring both modulus and phase of laser beam absorption ratio.

<sup>1</sup> The work is carried out under the partial financial support of the RFBR (project No.13-08-00266-a, project No.14-08-31024-mol\_a) and FASO within the Presidium of Russian Academy of Sciences fundamental research program (UB RAS project No.12-P-1005, state registration No.01201266835).

## ON THE FOCUSED BEAM PARAMETERS OF AN ELECTRON GUN WITH A PLASMA EMITTER

*S. KORNILOV\**, *N. REMPE\**, *A. BENIYASH\*\**

*\*Elion Ltd., 74 Vershinin str., Tomsk, 634045, Russia, mail@elion-tomsk.ru, +73822414859*

*\*\*Institute of Materials Science, Leibniz University of Hannover, D-30823 Garbsen, Germany*

The report presents the measurement results of the focused beam brightness in the electron gun with plasma emitter. The beam brightness was approximately  $10^{10}$  A·m<sup>-2</sup>·sr<sup>-1</sup> under the beam power up to 4 kW and an electron energy of 60 keV at the focal distance of 0.5 m.

Qualitative assessment of the beam parameters was performed by welding test pieces.

The results describing the possibility in principle of using the guns with a plasma emitter in nonvacuum technological devices are presented.

## **ELECTRON BEAM CURRENT DENSITY DISTRIBUTION OF THE PULSED FORE-VACUUM PLASMA SOURCE BASED ON ARC DISCHARGE**

*A.V. KAZAKOV, A.V. MEDOVNIK, V.A. BURDOVITSIN, E.M. OKS*

*Tomsk State University of Control Systems and Radioelectronics, 40 Lenin street, Tomsk, 634050, Russia,  
mail: [Kazakov89@sibmail.com](mailto:Kazakov89@sibmail.com), phone: (3822) 41-33-69*

The paper presents results of investigation radial electron beam current density distribution of the broad beam pulsed plasma electron source. This electron source is based on high current arc with cathode spot and it operates at fore-vacuum pressure range (4-15 Pa). With accelerating voltage 5-12 kV and pulse duration 100-300  $\mu$ s, electron beam current value was as high as 80 A. There was found a strong influence of emission plasma density distribution on electron beam uniformity. To smooth out density of the emission plasma a special redistributing electrode was located inside the hollow anode of the arc discharge unit. Special features of formation uniform beam at fore-vacuum pressure are described and discussed.

## PULSED NON-SELF SUSTAINED GLOW DISCHARGE WITH LARGE HOLLOW CATHODE<sup>1</sup>

*V.V. DENISOV, YU.H. AKHMADEEV, V.V. YAKOVLEV, I.V. LOPATIN, P.M. SCHANIN, S.S. KOVALSKIY, N.N. KOVAL*

*Institute of High Current Electronics SB RAS, 2/3, Akademichesky ave., Tomsk, 634055, Russia,  
Phone: +7(3822) 492-683, E-mail: [volodyadenisov@yandex.ru](mailto:volodyadenisov@yandex.ru)*

Processes for surface modification of materials using low pressure discharges plasma improved over a hundred years, but their abilities are not fully understood. During the last two decades has been made a significant leap in the development of this area and the application of plasma for the production of coatings and surfaces with desired properties and especially with the use of pulsed discharges which have been actively used in plasma technology.[1] Pulsed discharges have the following advantages over stationary discharges: the ability to work at high power levels (one or two orders of magnitude higher than for the stationary discharge), the ability to control time of active plasma state by changing the duty cycle of the discharge pulse, the ability to minimize the inhomogeneity of the plasma from the center to the borders (typical for stationary discharges), resulting in a more uniform plasma in the processing and deposition of thin films on a substrate [2].

Increased pulse power along with the ability to change parameters such as frequency and duration of pulses allow to realize more flexible and sometimes not yet achieved effects in surface modification and deposition of thin films. Described features are common for many types of discharges including self-sustained arc discharge [1], high-current pulsed magnetron discharge, pulsed glow discharge. In [3-4] shows the high potential of a stationary non-self-sustained glow discharge with a hollow cathode for generating of plasma in large volumes for technological applications.

In the work the study of the regularities of formation and burning of non-self-sustained pulsed glow discharge with hollow cathode on experimental stand described in [3] was carried out. To burn the main discharge power supply with an output voltage up to 350 V, output pulse current up to 500 A, the maximum average output power of 30 kW, a pulse repetition rate up to 1 kHz and the ability to change the duty cycle of 1 to 100 % was used. Inflow of the working gas (argon or nitrogen) into the working chamber is realized through an electron source on the basis of plasma generator with integrated cold hollow cathode [5], which was placed on the chamber door. To obtain the current-voltage characteristics of the discharge the values of current and voltage at time points corresponding to the discharge current saturation state were measured. For getting of non-self-sustained parameters of the plasma of pulse glow discharge with a hollow cathode was used cylindrical Langmuir probe. In the work were performed probe measurements, including determining of the radial distribution of the main plasma parameters (concentration and the plasma potential and electron temperature) and their change depending on the ratio of the area of the anode and cathode.

### REFERENCES

- [1] *A. Anders* // Surface and Coatings Technology.- 2004.- №183.- p. 301–311.
- [2] *H. Conrads, M. Schmidt* // Plasma Sources Sci. Technol. – 2000. - №9.- p. 441–454.
- [3] *Lopatin I.V., Akhmadeev Yu.H., Koval N.N., Schanin P.M.* // Prib. i Teh. Eksp. – 2011. – № 1. – p. 151-156.
- [4] *Lopatin I.V., Akhmadeev Yu.H., Koval N.N., Kovalskiy S.S., Schanin P.M., Yakovlev V.V.* // in: Proc. of Xth International Conference on Modification of Materials with Particle Beams and Plasma Flows, Tomsk, Russia, September 20 -24, 2010: Proceedings. – Tomsk: Publishing house of the IAO SB RAS, 2010. P. 35-38.
- [5] *L.G. Vintizenko, S.V. Grogoriev, N.N. Koval et al* // Izv. VUZov. Fizika. – 2001. – V.9. – p. 28-35

<sup>1</sup> This work was supported by the RFBR grant (projects No. 14-08-00997-a) and SB RAS presidium project No. 24.

## ELECTROSTATIC TRAP EFFECT IN GLOW DISCHARGES

A.S. METEL

Moscow state university "STANKIN", Vadkovsky per. 1, Moscow, 127055, Russia, a.metel@stankin.ru

Possibility of the plasma generation by means of the glow discharge at the gas pressure 0.01 – 0.1 Pa without any use of magnetic field for the first time was demonstrated in [1]. Electrons were electrostatically confined inside a large hollow cathode with a variable area  $S_0$  of its output orifice, the inner volume of the cathode  $V$  reaching 0.02 m<sup>3</sup>. The anode was located outside the cathode and for this reason the aperture of electron escape out of the cathode was equal to  $S_0$ . It was experimentally shown in [1], that the lowest working pressure  $p^{\text{ex}}$ , at which the discharge expires, is directly proportional to  $S_0$ .

In addition it was found that at  $S_0 < S^* = (\pi/e)^{1/2}(2m/M)^{1/2}S \approx (2m/M)^{1/2}S$ , where  $e$  is the Naperian base,  $m$  and  $M$  are the electron mass and the ion mass, and  $S$  is the cathode surface area, a stationary double layer is always observed in discharge near the cathode orifice. The anode plasma of the double layer decays at the gas pressure appreciably exceeding  $p^{\text{ex}}$  for the cases when the double layer does not exist at  $S_0 > S^*$ . Decay of the anode plasma results in the discharge extinction, and to avoid it the anode should be positioned inside the electrostatic trap. As an example of electrostatic trap with an inner anode the Fig. 1 presents a multi-rod cathode of the plasma emitter generator of a broad electron beam gun [2].

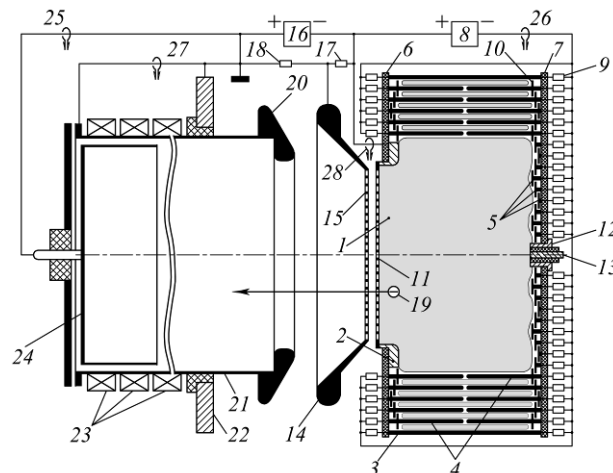


Fig. 1. The discharge scheme: 1 – plasma, 2 – anode, 3 – outer cathode rods, 4 – inner rods, 5 – cathode discs, 6 and 7 – dielectric flanges, 8 – discharge power supply, 9 – resistors, 11 – emissive grid, 12 and 13 – igniting electrodes

The trap consists of 204 external 3 and 780 inner cathode rods 4 isolated from each other and connected to the discharge power supply 8 through individual resistors 9 with the 430-Ω resistance. The gaps between the inner rods are filled with plasma 1 confined by the external rods 3 and cathode discs 5 and 10. Current limitation in the circuits of the rods prevents from glow-to-arc transitions at the pulse width  $\tau \sim 5$  ms of the glow discharge current up to 1 kA.

When the mean ionization length  $\lambda_N$  of emitted by the cathode electrons exceeds the trap width  $a = 4V/S$ , where  $V$  is the trap volume and  $S$  is the area of the cathode and anode surface [1], and their energy relaxation length  $\Lambda = (eU_c/W)\lambda_N$ , where  $U_c$  is the cathode fall of potential and  $W$  is the gas ionization cost, is lower than the trap length  $L = 4V/S_a$ , where  $S_a$  is the anode surface,  $U_c$  is independent of the pressure  $p$ .

In this middle pressure range due to multiplication of fast electrons in the cathode sheath [3, 4]  $U_c$  diminishes about 2 times from its maximum  $W/e\gamma$ , where  $\gamma$  is coefficient of ion-induced electron emission, with the discharge current reduction. At  $\Lambda > L$  the cathode fall  $U_c$  rises from hundreds to thousands of volts and  $p$  tends to the discharge extinction pressure  $p^{\text{ex}}$ , at which the ionization length  $\lambda_N$  of electrons with energy equal to the energy of electrons emitted by the cathode in the middle pressure range is equal to  $L$ .

## REFERENCES

- [1] Metel A.S. // Sov. Phys. Tech. Phys. – 1984. – V. 29. – No 2. – P. 141–147.
- [2] Metel A.S., Melnik Yu.A. // Instrum. Exp. Tech. – 2013. – V. 56. – No 3. – P. 317–324.
- [3] Metel A.S., Nastyukha A.I. // Radiophys. Quantum Electron. – 1976. – V. 19. – No. 12. – P. 1307–1311.
- [4] Metel A.S. // Sov. Phys. Tech. Phys. – 1985. – V. 30. – No 10. – P. 1133–1136.



## BROAD BEAMS OF HIGH-ENERGY REACTIVE GAS MOLECULES

*A.S. METEL, V.P. BOLBUKOV, M.A. VOLOSOVA, S.N. GRIGORIEV, YU.A. MELNIK*

*Moscow state university "STANKIN", Vadkovsky per. 1, Moscow, 127055, Russia, a.metel@stankin.ru*

A new method is proposed for production of broad beams of high-energy neutral atoms and molecules of reactive gases for the surface modification of products made of dielectric materials.

Instead of the ion plasma emitter generation at a potential of about 100 kV, extraction of the ions from the emitter and their acceleration using a multi-grid system followed by neutralization of the positive space charge of the broad ion beam by electrons, conversion of the ion beam into the fast neutral molecule beam and separation of residual ions from the beam using a magnetic field [1], it is now possible to produce the fast molecule beams due to the ions acceleration and charge exchange collisions in the sheath between a plasma emitter and a grid under a high negative potential [2].

The emitter potential may be close to and even equal to the potential of the grounded vacuum chamber, which makes the emitter generation much easier. Volume of a separate gas discharge chamber (GDC) mounted on a flange of the vacuum chamber as well as the vacuum chamber itself can be filled with a uniform plasma using the glow discharge with electrostatic confinement of electrons [3]. When in the center of the vacuum chamber a high-transparency grid is placed and a high-voltage pulse is applied to the grid, ions from the plasma emitter many times oscillate through the grid and due to collisions with the gas molecules turn into fast neutral molecules thus forming two beams propagating in opposite directions. Energy of the molecules in those beams is distributed continuously from zero to the value corresponding to the high-voltage pulse amplitude.

When the grid is composed of parallel flat plates, the charge exchange due to collisions with the gas molecules is amplified by charge exchange due to reflections from the plates [4].

If the high voltage is applied to a hollow cylinder with two flat grids at the ends of the cylinder the charge exchange collisions of ions accelerated in the sheath between the plasma and the grid can occur inside the cylinder. When the distance between those grids appreciably exceeds the sheath width then beams of homoenergetic fast neutral atoms and molecules can be produced.

To transform ions from the plasma emitter inside a GDC into a beam of fast neutral molecules, there is between the GDC and the vacuum chamber an isolated from the chamber holder of emissive grids, and the high voltage is applied to the holder. The ions oscillate through the grid between the plasma emitter inside the GDC and a secondary plasma inside the vacuum chamber produced due to injection into the chamber of fast molecules [5]. As the density of the secondary plasma is by an order of magnitude lower, equivalent current of the fast molecules into the chamber is by an order of magnitude higher than into the GDC.

### REFERENCES

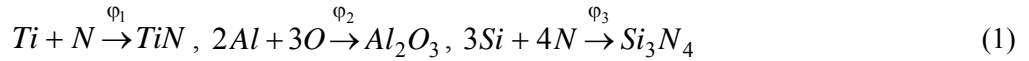
- [1] *Gabovich M.D., Pleshvtsev N.V., Semashko N.N.* // Ion and Atomic Beams for Controlled Nucl. Fusion and Technology. – Energoatomizdat, Moscow, 1986 [in Russian].
- [2] *Metel A.S.* // Plasma Phys. Rep. – 2012. – V. 38. – No 3. – P. 254–262.
- [3] *Metel A.S., Grigoriev S.N., Melnik Yu.A., Panin V.V.* // Plasma Phys. Rep. – 2009. – V. 35. – No 12. – P. 1058–1067.
- [4] *Ranjan A., Donnelly V.M., Economou D.J.* // J. Vac. Sci. and Technol. A. – 2006. – V. 24. – No 5. – P. 1839–1846.
- [5] *Metel A.S., Melnik Yu.A., Panin V.V.* // Plasma Physics Reports. – 2011. – V. 37. – No 4. – P. 357–365.

## THE MODEL OF MICROSTRUCTURE FORMATION DURING MAGNETRON SPUTTERIN

*M.A. MIKOLAYCHUK\**, *A.G. KNYAZEVA\**

*\*Institute of Strength Physics and Materials Science, pr. Akademicheskii 2/4, Tomsk, 634021, Russia,  
mihail@mikolaichuk.com, +79234290599*

In this problem we consider a coating generating on the specimen under magnetron sputtering. Plasma has equal compound in the all parts of considerable domain (Ti, Ni, Al, O<sub>2</sub>, Si). We consider a few chemical reactions which lead to coating generating:



Mass changing rate could be defined as

$$\frac{d}{dt} \int_V \rho_i dV = \int_V \frac{\partial \rho_i}{\partial t} dV \quad (2)$$

Where  $i$  is component number,  $\rho_i$  is component density. In the general this integral equals to sum of mater coming through the surface of the volume and generating because of chemical reactions. But due to high rates of the sputtering process, diffusion between to elementary volume is absent. Then

$$\int_V \frac{\partial \rho_i}{\partial t} dV = \sum_{n=1}^3 \int_V \mu_i \nu_{in} \varphi_n dV \quad (3)$$

where  $\mu$  is molar mass,  $\nu_{in}$  is stoichiometric coefficient,  $\varphi_n$  is a rate of the chemical reaction number  $n$ . For the system of reactions (1) rates could be defined as

$$\varphi_1 = k_1 C_{Ti} C_N, \quad \varphi_2 = k_2 C_{Al}^2 C_O^3, \quad \varphi_3 = k_3 C_{Si}^3 C_N^4,$$

Consider a unit area of the real sample, broken down into  $N \times N \times N$  elementary volumes. We suppose that the same plasma composition is present in each of these volumes. At the initial time in a unit area there are randomly distributed nucleation centers. In our model nucleation center is an element in which there is a nonzero concentration of one of the products at initial time. Assuming that the compounds are not soluble in each other, we assume that further in this element can be formed only "nucleated" compound. Reagents that do not take part in the formation of this compound will remain unbound.

We supposed that, by analogy with the method of cellular automata, the state of the elementary volumes depends on the state of its neighbors. It means that compound should be generated in a specific volume element in dependence on the value of the average concentration of the reaction products in the neighboring volumes.

On the other hand, the reaction will proceed more intense around the larger reactant unreacted. To estimate this quantity, we introduce the parameter  $\eta$  –neighbors empty elements containing only reagents. The parameter  $\eta$  is equal to 1 when all neighbors are not occupied and assumes a 0 value, if there are no empty elements around. Summarize that, according to equations (3) and total derivative definition we could formulate ordinary differential equations system

$$\begin{aligned} \frac{dC_{Ti}}{dt} &= -w\eta\mu_{Ti}\varphi_1, & \frac{dC_N}{dt} &= -w\eta\mu_N[\varphi_1 + 4\varphi_3], & \frac{dC_{Al}}{dt} &= -w\eta\mu_{Al}2\varphi_2, & \frac{dC_O}{dt} &= -w\eta\mu_O3\varphi_2, \\ \frac{dC_{Si}}{dt} &= -w\eta\mu_{Si}3\varphi_3, & \frac{dC_{TiN}}{dt} &= w\eta\mu_{TiN}\varphi_1, & \frac{dC_{Al_2O_3}}{dt} &= w\eta\mu_{Al_2O_3}\varphi_2, & \frac{dC_{Si_3N_4}}{dt} &= w\eta\mu_{Si_3N_4}\varphi_3. \end{aligned}$$

At initial time, the concentration of all components of the system are given. In general, the concentration of the products is equal to zero, and the concentration of the reactants depend upon the composition of the plasma. For simplicity, we assume that at all points of the computational domain, the plasma composition is the same. Thus appearance of nuclei at the initial time, will be treated as the presence of elementary volumes with a nonzero concentration of one of the reaction products.

The problem solved numerically. Each ordinary differential equation solved with Runge-Kutta method.

## INVESTIGATION OF STATIONARY NON-SELF-SUSTAINED GLOW DISCHARGE WITH A LARGE AREA HOLLOW CATHODE

*YU.H. AKHMADEEV, V.V. DENISOV, I.V. LOPATIN, P.M. SCHANIN, S.S KOVALSKY*

*Institute of High Current Electronics, 2/3 Akademichesky Avenue, Tomsk,  
634055, Russia, ahmadeev@opee.hcei.tsc.ru, 8(3822)491-713*

Problems of energy efficiency and environmental engineering industries which are used or required technology surface treatment products are closely related to scientific problem to establish the regularities of forming of dense homogeneous discharge plasma in large volumes. Identifying such regularities for specific ion-plasma systems can simultaneously receive important scientific advance in this industry and demonstrate promising engineering solutions obtained for a large number of production tasks.

This paper presents the results of research of a stationary non-self-sustained glow discharge with a hollow cathode with about 2 m<sup>2</sup> area. Discharge is ignited and operated in high-current (up to 140 A) form at low (0.4-1 Pa) pressures due to injection of electrons from the plasma of cold hollow cathode arc discharge.

The principal possibility of creating of dense homogeneous discharge plasma in large (0.2 m<sup>3</sup>) vacuum volumes at low pressures have been demonstrated and obtained its basic parameters. It is shown that increasing the current from 20 A to 140 A leads to change in the discharge voltage from 50 V to 150 V. That is considerably lower than discharge voltage of the self-sustained glow discharge in the same electrode system.

## PULSED NON-SELF-SUSTAINED ARC DISCHARGE WITH FILAMENT CATHODE AND HOLLOW CATHODE<sup>1</sup>

*V.V. DENISOV, V.V. YAKOVLEV, S.S. KOVALSKIY, N.N. KOVAL*

*Institute of High Current Electronics SB RAS, 2/3, Akademicheskoy ave., Tomsk, 634055, Russia,  
Phone: +7(3822) 492-683, E-mail: [volodyadenisov@yandex.ru](mailto:volodyadenisov@yandex.ru)*

Low-temperature plasma generated by different types of stationary and pulsed discharges has been widely used in various fields of science and technology. Technological performances of using the plasma processing are determined mainly by such plasma parameters as temperature and electron concentration. Relatively high concentrations are typical for RF plasma discharge ( $\sim 10^{13} \text{ cm}^{-3}$ ), but such systems are still quite expensive and the plasma production in large volumes with good uniformity also has certain difficulties. Recently, for generation of highly non-equilibrium plasma was developed the method of high power pulsed magnetron sputtering (HIPIMS) [1]. At the same time in the literature there are practically no data on the characteristics and processes of formation of non-self-sustained pulsed arc and glow discharges which have their own features due to the presence of an auxiliary source of electrons. Studies [2, 3] show the high potential of non-self-sustained stationary discharges for plasma formation in high volumes for technological applications. Pulsed burning of non-self-sustained discharge allow to achieve several times higher power in pulsed mode than in the steady state, so that the advantages of pulsed discharges are inherent for non-self-sustained discharges. Pulsed discharge regimes with electron oscillation which includes non-self-sustained arc discharges with a hollow cathode provokes particular interest. It is due to the possibility of obtaining a high pulse power by increasing the number of ionizations conducted by injected into the main discharge electrons at close to the maximum gas ionization cross section. The number of ionization conducted by oscillating electrons inside the hollow cathode in this case will depend on the energy of injected in the main discharge electrons. Energy of the injected electrons in the main discharge depends on the pulsed discharge burning voltage.

In the work the study of the regularities of formation and burning of low pressure non-self-sustained pulsed arc discharge in plasma source with filament cathode and hollow cathode "PINK" was carried out.[4] For the burning of discharge between the anode (the camera) and a hollow cathode pulse voltage was applied with the amplitude (20-200)V and with current up to 500A, with pulse frequency up to 1 kHz for different values of filament cathode current which provides electron emission for the main discharge burning. To obtain the current-voltage characteristics of the discharge the values of current and voltage at time points corresponding to the discharge current saturation state were measured. For getting of plasma parameters of pulsed plasma non-self-sustained discharge with filament cathode and hollow cathode was used cylindrical Langmuir probe.

### REFERENCES (STYLE "CONGRESS2014 TITLE REFERENCES")

- [1] *Authors A.Anders, J. Andersson, A. Ehiasarian // J. Appl. Phys.-2007. – 102. – p. 113303.*
- [2] *Lopatin I.V., Akhmadeev Yu.H., Koval N.N., Schanin P.M. // Prib. i Teh. Eksp. – 2011. – № 1. – p. 151-156.*
- [3] *Lopatin I.V., Akhmadeev Yu.H., Koval N.N., Kovalskiy S.S., Schanin P.M., Yakovlev V.V.// in: Proc. of Xth International Conference on Modification of Materials with Particle Beams and Plasma Flows, Tomsk, Russia, September 20 -24, 2010: Proceedings. – Tomsk: Publishing house of the IAO SB RAS, 2010. P. 35-38.*
- [4] *L.G. Vintizenko, S.V. Grogoriev, N.N. Koval et al // Izv. VUZov. Fizika. – 2001. – V.9. – p. 28-35*

<sup>1</sup> This work was supported by the RFBR grant (projects No. 14-08-00997-a) and SB RAS presidium project No. 24.

## A SOURCE OF METAL VAPOR AND PULSED BEAMS OF HIGH-ENERGY GAS MOLECULES

*A.S. METEL, V.P. BOLBUKOV, M.A. VOLOSOVA, S.N. GRIGORIEV, YU.A. MELNIK*

*Moscow state university "STANKIN", Vadkovsky per. 1, Moscow, 127055, Russia, a.metel@stankin.ru*

Application to a substrate during the sputter deposition process of negative high-voltage pulses results in production of nc-Ti<sub>2</sub>N/nc-TiN nanocomposite tough and superhard (HV 5000) fracture tough coatings. Mixing of the substrate and coating materials through bombardment by 50-keV ions results in adequate compressive stress of the coating and interface width exceeding 1 μm [1, 2], which ensures a good adhesion and allows deposition of 100-μm-thick coatings.

It is impossible to apply high-voltage pulses to dielectric substrates and coatings. Hence, the above method cannot be used for improvement of the dielectric materials. To synthesize dielectric coatings with the same superb properties on complex-shaped dielectric products a source of broad pulsed beams of high-energy molecules has been developed the molecule trajectories coinciding with those of metal atoms [3, 4].

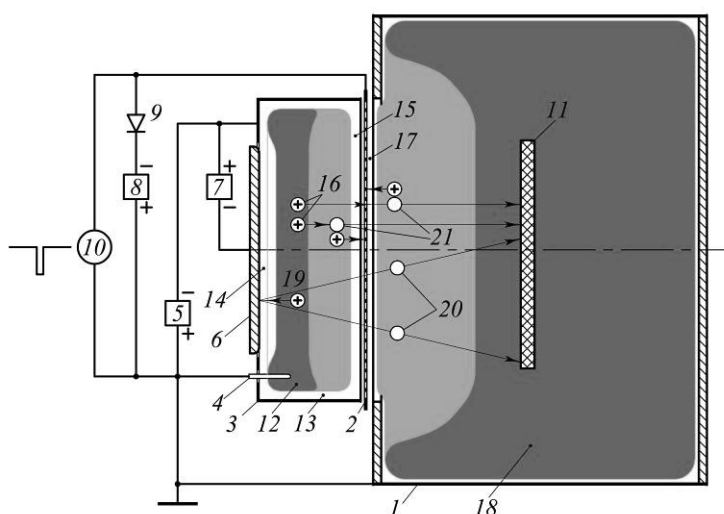


Fig. 1. Scheme of the source. 1 – vacuum chamber, 2 – emissive grid, 3 – hollow cathode, 4 – anode, 5, 7 and 8 – DC power supplies, 6 – target, 9 – diode, 10 – high-voltage pulse generator, 11 – dielectric product, 12 – plasma emitter, 13, 14, 15 and 17 – space charge sheaths, 16, 19 – ions, 20 – metal atoms, 21 – fast neutral atoms and molecules

The source is equipped with generator of negative high-voltage pulses 10, and its anode 4 is connected to grounded chamber 1. Hence, plasma emitter 12 and secondary plasma 18 in the chamber are equipotential. At the pressure of 0.4 Pa and negative potential of the grid 1 keV the charge exchange length 40 mm of argon ions 16 exceeds the width of sheaths 15 and 17 near grid 2, which practically excludes generation of fast neutral atoms and molecules in the sheaths. Atoms 20 sputtered by 2-keV-ions 19 deposit on dielectric product 11 without bombardment by fast molecules.

When a 40-kV pulse is applied to the grid 3, the total width of sheaths 15 and 17 grows up and several times exceeds the charge exchange length. After ions 16 have passed the way between boundaries of plasma emitter 12 and secondary plasma 18 produced due to injection into the chamber of fast molecules [5, 6], almost all of them are transformed into fast atoms and molecules 21 [7] bombarding the coating. Hence, the source creates for synthesis of dielectric coatings the same physical conditions as in [1, 2].

### REFERENCES

- [1] Ruset C., Grigore E. // Surf. Coat. Technol. – 2002. – V. 156. – P. 159–161.
- [2] Grigore E., Ruset C., Short K.T., Hoefl D., Dong H., Li X.Y., Bell T. // Surf. Coat. Technol. – 2005. – V. 200. – P. 744–747.
- [3] Grigoriev S.N., Melnik Yu.A., Metel A.S. // Instrum. Exp. Tech. – 2013. – V. 56. – No 3. – P. 358–364.
- [4] Metel A., Bolbukov V., Volosova M., Grigoriev S., Melnik Yu. // Surf. Coat. Technol. – 2013. – V. 225. – P. 34–39.
- [5] Metel A.S., Melnik Yu.A., Panin V.V. // Plasma Physics Reports. – 2011. – V. 37. – No 4. – P. 357–365.
- [6] Metel A., Grigoriev S., Melnik Yu., Panin V., Prudnikov V. // Jpn. J. Appl. Phys. – 2011. – V. 50. – No 8. – P. 08JG04/1–4.
- [7] Metel A.S. // Plasma Phys. Rep. – 2012. – V. 38. – No 3. – P. 254–262.

## CURRENT-VOLTAGE CHARACTERISTICS OF A NEGATIVE BIASED COLLECTOR IN PLASMA GENERATED BY ELECTRON SOURCE WITH A PLASMA EMITTER<sup>1</sup>

*O.A. BUREYEV, N.V. GAVRILOV*

*Institute of Electrophysics, Ural Division of the Russian Academy of Science, 106 Amundsen St., Ekaterinburg, 620016, Russia,  
E-mail: bureyev@iep.uran.ru, Phone: (343)2678829*

Current-voltage characteristics of a negative biased collector placed in the plasma produced by a broad (50 cm<sup>2</sup>) electron beam with an energy of 0.1-1 keV and beam current of 1-2 A were obtained, for the collector negative bias potential varied in the range of 0.1-1 kV. Beam was injected into a cylindrical cavity which was under accelerating potential, the distance between the electron source and the collector was 10 cm, the pressure of argon was varied in a range of  $3 \cdot 10^{-2}$  -  $3 \cdot 10^{-1}$  Pa, the material of the collector - molybdenum, stainless steel, titanium, pyrolytic graphite. The obtained characteristics generally are nonmonotonic and have from one to three values of the floating potential.

As is known, current in the circuit of a negative biased collector in a nonequilibrium plasma containing the fast electron flux determined by a combination of primary and secondary streams of species [1]:

$$I = I_i(1+\gamma) - I_{el}(1-\sigma), \quad (1)$$

where  $I_{el}$  – current of fast electrons,  $\sigma$  – S.E.E. coefficient,  $I_i$  – ions saturation current from the plasma,  $\gamma$  – coefficient of ion-electron emission. Correspondingly, the main factors affecting the current-voltage characteristics of the collector are the energy of fast electrons, the gas pressure, collector material and its surface state. A feature of the research is broad range of the gas pressure, wherein the plasma electron source is able to stably operate, and the consequent significant change in degree of momentum relaxation of the electron beam and in the ions saturation current from the plasma. Another feature is the dependence of electron emission properties of such type of the electron beam source on the gas pressure and the accelerating voltage.

Dependences of the ion part of the current on the collector potential for different values of electron beam energy obtained by extrapolating the results of measuring the current from decaying plasma in pulsed electron beam generation mode (900  $\mu$ s, 1 kHz). At  $U_{bias} < U_e$  the ion current is slightly different from the ions saturation current at cutoff of fast electrons. Collector current-voltage characteristics shown in Fig. 1.

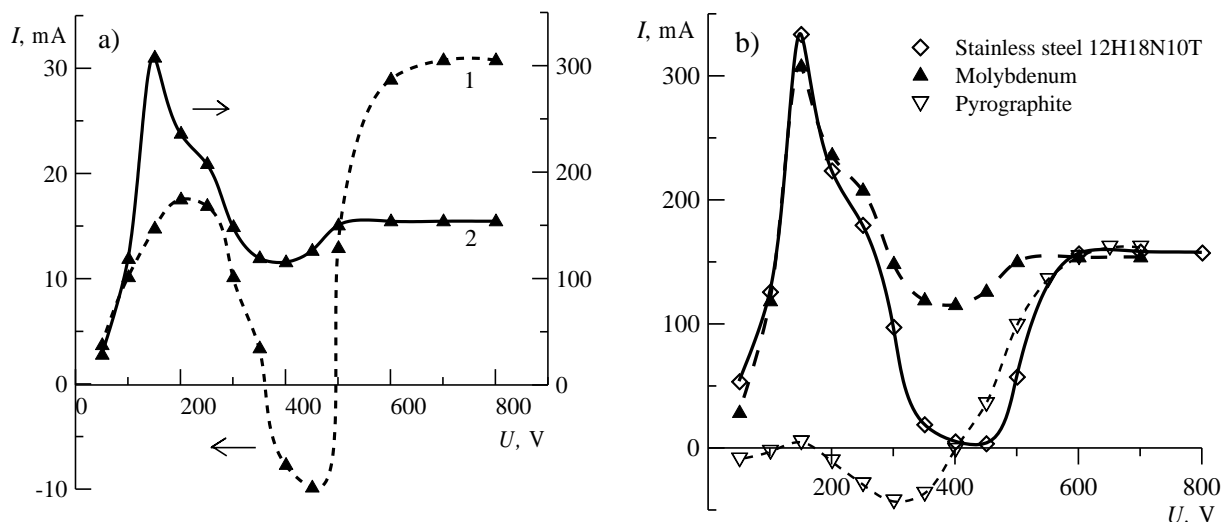


Fig. 1.  $I$ - $U$  characteristics of the collector: (a) molybdenum collector, 1 –  $P = 6.7 \cdot 10^{-2}$  Pa, 2 –  $P = 2.7 \cdot 10^{-1}$  Pa; (b) three different collector materials with  $P = 2.7 \cdot 10^{-1}$  Pa, beam energy 500 eV.

### REFERENCES

- [1] C.-H. Nam, N. Hershkowitz, M.H. Cho, T. Intrator, and D. Diebold // *J. Appl. Phys.* 63, 5674 (1988).

<sup>1</sup> This work was supported by the program of basic research of the Presidium of RAS (project No 12-P-2-1046).

## PLASMA AND ION SOURCE OF BORON BASED ON PLANAR MAGNETRON DISCHARGE<sup>1</sup>

*A.V. VIZIR, \*V. I. GUSHENETS, \* E. M. OKS\*\*\*, K.P.SAVKIN\*, A.S. BUGAEV\*, G. YU. YUSHKOV\**

*\*High Current Electronics Institute SD RAS, 2/3 Akademicheskoy av., Tomsk, 634050, Russia,*

*\*\*State University of Control Systems and Radioelectronics, 40 Lenina av., Tomsk, 634050, Russia*

*e-mail: [vizir@opee.hcei.tsc.ru](mailto:vizir@opee.hcei.tsc.ru), phone: +7(3822)491776*

A planar magnetron sputtering device with thermally isolated solid target made from boron has been designed and demonstrated. The magnetron is intended to use for generation of boron ion beams and plasmas. Boron has low electrical conductivity at room temperature, which increases with temperature; therefore, high target temperature is required for high-current discharge operation. The target is well insulated thermally. It was heated preliminary by an initial low-current (2-50 mA), high-voltage (up to 2000 V) DC magnetron discharge mode. An initial discharge power of 4 W was adequate to start heating of the target, and after several minutes, the target temperature reaches the required value (more than 300 degrees of Celsius), after that a transition of the discharge to low-voltage (500 V) mode is observed. Applying high current pulses (10-30 A, 100-300 microseconds) over the DC heating discharge results in a self-sputtering operational mode of the magnetron discharge. Ion beam was extracted from the discharge plasma. Beam mass-to-charge composition was measured with a time-of-flight system. The maximum boron ion fraction in the beam is 99%, and the mean boron ion fraction, time-integrated over the whole pulse length, is about 95%. At the same time, with low-current DC mode of the discharge, the ion fraction of boron does not exceed 5%. This kind of boron ion and plasma source could be competitive to conventional Freeman-type boron ion and plasma sources that utilize compounds such as BF<sub>3</sub>, and could be useful for beamline and plasma immersion implantation in semiconductor industry applications and other fields.

### REFERENCES

- [1] *J. H. Freeman // Nucl. Instrum. Methods. - 1963. - Vol. 22. - p. 306.*
- [2] *A. S. Perel, W. K. Loizides, and W. E. Reynolds // Rev. Sci. Instrum. - 2002. - Vol. 73. - p. 877.*
- [3] *J. M. Williams, C. C. Klepper, D. J. Chivers, R. C. Hazelton, and J. J. Moschella // J. Vac. Sci. Technol. - 2008. - B 26 - p. 368.*
- [4] *A. Anders, J. Andersson, and A. Ehasarian // J. Appl. Phys. - 2007. - Vol. 102. - p. 113303.*
- [5] *A. Anders, J. Andersson, and A. Ehasarian // J. Appl. Phys. - 2008. - Vol. 103. - p. 039901.*
- [6] *J. Andersson and A. Anders // J. Appl. Phys. - 2008. - Vol. 92. - p. 221503.*
- [7] *J. Andersson and A. Anders // Phys. Rev. Lett. - 2009. - Vol. 102. - p. 045003.*
- [8] *A. Anders, E.M. Oks // J. Appl. Phys. - 2009. - Vol. 106. - p. 023306.*
- [9] *E.M. Oks, A. Anders // J. Appl. Phys. - 2009. - Vol. 105. - p. 093304.*
- [10] *V. I. Gushenets, A. Hershcovitch, T.V. Kulevoy, E. M. Oks, K. P. Savkin, A. V. Vizir, and G. Yu. Yushkov // Rev. Sci. Instrum. - 2010. - Vol. 81. - p. 02B303-3.*
- [11] *A.V. Vizir, E.M. Oks, I.G. Brown // IEEE Trans. Plasma Sci. - 1998. Vol. 26(4). - p.1353-1356.*
- [12] *I. G. Brown and J. C. Kelly // Journal of Applied Physics. - 1988. Vol. 63(1). - p. 254*
- [13] *G. Yu. Yushkov and A. Anders // IEEE Transactions on Plasma Science. - 2010. - Vol. 38(11). - p. 3028 - 3034.*

<sup>1</sup> This work was supported by Russian Foundation for Basic Research under grant # RFBR 13-08-00185a.

## PLASMA TREATMENT OF SILICATE MELT OBTAINING<sup>1</sup>

*G.G. VOLOKITIN, N.K. SKRIPNIKOVA, O.G. VOLOKITIN, V.V. SHEKHOVTSOV*

*\*Tomsk state university of architecture and building, Russia, 2, Solyanaya, 634003, Tomsk, Russia, vgg-tomsk@mail.ru, +7-913-829-36-03*

### **Introduction.**

The plasma technologies used for receiving high-temperature silicate melts, allow achieving high temperatures, providing transition of initial silicate materials to the melted condition. Today considerable experience on producing high-temperature melts from ashes waste by plasma technology [1-2] is saved up. The silicate module of such waste is much higher, than at the raw materials (basalt) which are traditionally used for receiving silicate melts in mineral fibers production. Researches in this field assumes that it is possible to use as raw materials for high-temperature silicate melts production, waste of enrichment various ores, such as feldspar wastes of molybdenum ores enrichment, the chemical composition of such waste allows to utilize them by processing in silicate melt with use of energy of low-temperature plasma.

Feldspar wastes of molybdenum ores enrichment makes from 90 to 99%. The huge number of this waste accumulates in dumps of mining productions [3-5]. Chemical composition of studied raw materials are characterized by the maintenance of SiO<sub>2</sub> (62 %) which similar to the content of silicon dioxide in technical glasses and can be used for receiving silicate melts in mineral fibers production [6-7]. For production of qualitative mineral fiber it is necessary to achieve uniformity of melt on a chemical composition. Using traditional technologies in high-temperature melts production is interfaced to long temperature impact on raw materials that leads to increase energy consumption.

### **Conclusions.**

It is established that the studied feldspar wastes of molybdenum ores enrichment can be used for receiving mineral fibers by production of heat-insulating materials [5-6]. Thus energy of low-temperature plasma allows receiving melts uniform in a chemical composition from feldspar wastes of molybdenum ores enrichment that positively influences quality of mineral fiber. It is established that the received cooled fusion from feldspar wastes of molybdenum ores enrichment is in a vitreous condition and is characterized by lack of crystal phases. It is characterized by low crystallization ability and the high module of acidity that assumes high thermal and chemical stability of mineral fiber on its basis [9].

### REFERENCES

- [1] A.A. Nikiforov, E.A. Malov, N.K. Skripnikova, O.G. Volokitin, Research of plasma technology silicate refractory melts receiving. Thermophysics and aeromechanics. (2009) 159–163.
- [2] O.G. Volokitin, Research of physical characteristics of silicate melt stream in the conditions of additional heating, Vestnik TGASU. (2010) 117–120.
- [3] S. Yoshizawa, M. Tanaka, A.V. Shekdar, Global Trends in Waste Generation. Global Symposium on Recycling: “Waste Treatment and Clean Technology”. (2004) 1541–1552.
- [4] G.R. Butkevich Problems of involvement of mining production wastes in economic activity // Building materials (2013) 62–66.
- [5] L. Barbieri, T. Manfredini, I. Queralt, M. Romero, Vitrification of fly ash from thermal power station. Glass Technology (1997) 165–170.
- [6] V.I. Vereschagin, A.E. Buruchenko, I.V. Kaschuk, Possibilities of use of secondary raw materials for receiving construction ceramics, Building materials. (2000) 20-22.
- [7] A.D. Shiltsina, V.I. Vereschagin, Use of feldspar raw materials of Khakassia for receiving ceramic tiles, Glass and Ceramics. (1999) 7-9.
- [8] ML Ovecog, Microstructural characterization and physical properties of a slag-based glass-ceramic crystallized at 950 and 1100 C. Journal of the European Ceramic Society (1998) 161–168.
- [9] O.G. Volokitin, N.K. Skripnikova, G.G. Volokitin, V.I. Vereschagin, V.V. Shehovcov, Mineral fibre, produced in device of low temperature plasma from burning products of coal and oil shales. Building materials (2013) 17-22.

<sup>1</sup> This work was supported by Council on grants of the Russian Federation President MK-2330.2013.8



**GENERATION OF HIGH CHARGE STATES METAL ION BEAMS  
BY VACUUM ARC ION SOURCES FOR SURFACE MODIFICATION<sup>1</sup>***V.P. FROLOVA<sup>1</sup>, A.G. NIKOLAEV<sup>1</sup>, K.P. SAVKIN<sup>1</sup>, G.YU. YUSHKOV, E.M. OKS<sup>1,2</sup>**<sup>1</sup>Institute of High Current Electronics SB RAS, 2/3 Akademicheskoy Ave.,**Tomsk, 634055, Russia, nik@opee.hcei.tsc.ru, +7 (3822) 491-776**<sup>2</sup>Tomsk State University of Control Systems and Radioelectronics, 40 Lenin Ave., Tomsk, 634050, Russia*

High charged metal ion beams find many applications in fundamental nuclear and atomic physics as well as in applied science such as an ion beam surface modification. Metal ions produced by vacuum arc are often multiply charged, typically involving charges states 1+ to 3+, and in rare instances 4+ and 5+. A number of different techniques have been used for increasing the ion charge states of vacuum arc in ion sources. These approaches include use of a strong magnetic field at the cathode region, application of additional short-time arc current pulses or even a “train of spikes”, and additional ionization by means of an electron beam injected into the arc plasma. For all of these approaches the mean ion charge states can be increased, but by no greater than a factor of about 2, so ion beams included ion charge state up to 7+. Higher ion charge states up to 10+ have been obtained by two different other methods. The first one heating of plasma confined in magnetic trap by powerful gyrotron and the second one is generation in high current vacuum arcs when the power dissipated in the arc gap reached ~10 MW for a few microseconds. For technological applications the second method which can be realized by simple technique seems more preferable. Here a combination of strong magnetic field in cathode area and short high current pulse of arc for high charge metal ion beams are proposed. It can be allow reaching more high charged states of metal ion that was done before. Design of new ion source and some preliminary results for high charge metal ion beams generation are discussed.

---

<sup>1</sup> This work was supported by RFBR under grant numbers RFBR-14-08-00031 A.

## CONDITION FOR BURNING CESIUM PLASMA LAYER ARC WITH EXTERNAL IONIZATION

V. P. ZIMIN

*National Research Tomsk Polytechnic University Avenue Lenin, 30, Tomsk, 634050, Russia, zimin@tpu.ru, 8-3822-426100*

Efficiency cesium plasma discharge depends on various types of energy losses which are significantly affected by the temperature of electrons. Ionization processes in the volume the cesium arc caused by stepwise ionization is exponentially dependent on the electron temperature [1]. External ionization affects the condition of burning arc, changing the temperature of the electrons. The report focuses on the study of conditions of burning cesium arc with external ionization in the thermionic diode.

Analyzes the boundary value problem of diffusion of the plasma density, which describes the processes in the low voltage arc discharge in cesium thermionic diode. The system of differential equations boundary value problem is written with respect to the plasma density and ion current density. Boundary conditions boundary-value problem for jumps of potentials recorded at the plasma – electrodes that inhibit plasma electrons [2, 3] and take into account external local ionization near the electrodes. Volume generation function positive singly charged ions Cs considers stepwise ionization [1] and external ionization source, uniformly distributed in the electrode gap.

Analysis of boundary-value problem in a general setting is performed on the phase plane plasma density – ion current. A specific of the mathematical problem is the presence of a singular point of the center, which affects the shape of the plasma density distribution in the gap.

A transcendental equation for the conditions of arcing in Cs considering external ionization

$$\sqrt{k_2 k_3} - \frac{\arctg \left[ -\frac{(J_{i0} + \psi_0 + k_1/k_2) \sqrt{k_2}}{(n_0 + \psi/k_3)} \right] + \arctg \left[ -\frac{(J_{id} + \psi_d + k_1/k_2) \sqrt{k_2}}{(n_d + \psi/k_3)} \right]}{d} = 0$$

where  $k_1, k_2, k_3$  – the coefficients of the boundary value problem of differential equations describing the transport and ionization processes in the plasma and electron temperature dependent;  $J_{i0}, J_{id}$  – ion current density at the emitter and collector;  $n_0, n_d$  – the plasma density at the emitter and collector;  $\psi_0, \psi_d$  – external ionization source at the emitter and collector;  $\psi$  – the source in the external ionization electrode gap;  $d$  – the gap between electrodes of the diode.

Solution of the equation allows to obtain the value of the electron temperature at which the arc burns.

Dividing the phase portrait of the distribution of the plasma parameters on the segments, we can write a similar equation for the plasma layer.

Plasma density distribution (phase portraits of solutions of differential equations) and the condition change the form of the arc in the case of negligible value stepwise ionization in the gap. In this case the solution of the problem does not depend on the electron temperature and is totally dependent on external sources of ionization values at the electrodes and the plasma volume.

### REFERENCES

- [1] *Bakshat F.G., Djuzhev G.A., Marcinkovskij A.M. and al. Thermionic converters and low-temperature plasma. – Moscow, Nauka, 1973.*
- [2] *V.P. Zimin // Bulletin of the Tomsk Polytechnic University.– 2013.– Volume 322.– № 2.– P. 11–15.*
- [3] *V.P. Zimin // Bulletin of the Tomsk Polytechnic University.– 2013.– Volume 323.– № 2.– P. 158–163.*

## GENERATION OF PHOSPHORUS POLYATOMIC IONS IN PLASMA OF A LOW-PRESSURE DISCHARGE WITH FILAMENT CATHODE<sup>1</sup>

*V.I. GUSHENETS\**, *E.M. OKS\*\**, *A.S. BUGAEV\**

*\*Institute of High Current Electronics, RAS, 2/3 Akademicheskoy, Tomsk, 634055, gvi@opee.hcei.tsc.ru, +7(3822)491933*

*\*\*Tomsk State University of Control Systems and Radioelectronics, 40 Lenina Prospekt, Tomsk, 634050, Russia*

The paper presents latest results of experimental investigations on the phosphorus molecular ions production in the plasma of ion source with directly heated cathode and emission slit size  $2.5 \times 40 \text{ mm}^2$ . Phosphorus is one of the doping materials much used in semiconductor technology. In the vapor phase up to a temperature of  $800^\circ\text{C}$ , the phosphorus is found in the form of its most stable compound - tetra atomic molecules [1]. A source of phosphorus vapor as a plasma-forming medium is phosphine - a gaseous compound of phosphorus with hydrogen ( $\text{PH}_3$ ). At a temperature of  $500^\circ\text{C}$ , phosphine begins to decompose into phosphorus  $\text{P}_4$  and molecular hydrogen. The ion source is equipped a dissociator that splits phosphine molecule(s) into hydrogen and molecular phosphorous components before they are delivered to a discharge chamber. The decomposition of phosphine into  $\text{P}_4$  and molecular hydrogen in the dissociator makes it possible to completely exclude the presence of toxic phosphorous-hydrogen compounds at the output of the ion source and simultaneously increases the fraction of molecular  $\text{P}_4$  and  $\text{P}_2$  ions generated by the ion source. Experimental data are presented the influence of the discharge chamber temperatures and temperature of the dissociator heater as well as the influence of other operating parameters on the mass-charge state of the ion beam. Maximum currents of  $\text{P}_4$  and  $\text{P}_2$  separated ion beam reached values of  $290 \mu\text{A}$  and  $470 \mu\text{A}$  respectively for  $1.8 \text{ mA}$  total ion emission (Fig. 1).

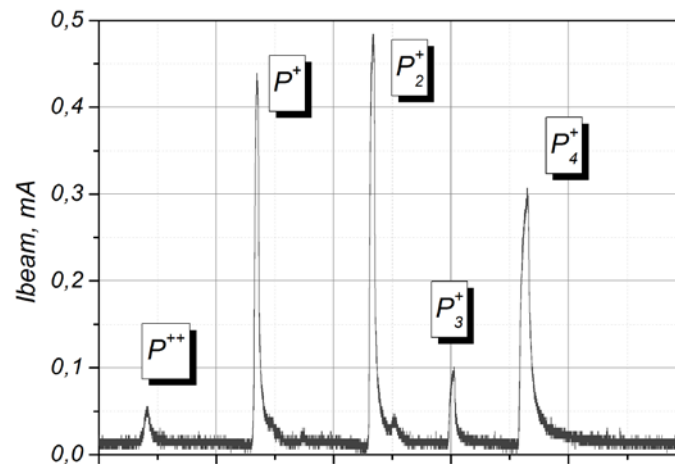


Fig. 1. Mass-charge state of the phosphorus ion beam for some operating parameters: accelerating voltage – 14 kV, discharge current – 140 mA, emission current – 1.8 mA.

### REFERENCES

- [1] *J. D. Carette and L. Kerwin // Can. J. Phys. – 1961. – 39. – 1300–1319.*
- [2] *J. N. Baillargeon, K. Y. Cheng, S. L. Jackson, and G. E. Stillman // J. Appl. Phys. – 1991. – 69. – 8025–8030.*

<sup>1</sup> This work was supported by Russian Foundation for Basic Research Grant No. 12-08-00183-a.

## COMPUTER SIMULATION OF MAGNETRON DISCHARGE

*D.V. KORZHENKO, S.N. YANIN*

*Tomsk Polytechnic University, Lenin av., 30, Tomsk, 634050, Russia, dman@tpu.ru, +7-913-854-8924*

Magnetron sputtering deposition is a widely used technique for obtaining of metal and compound thin films. Development of new magnetrons for optimization of thin layer's uniformity or target's utilization ratio is costly when done by experimental attempts only [1]. Computer simulations help to decrease development time and cost for such optimization.

Computer model of the electrical discharge in the crossed electrical and magnetic fields (magnetron discharge) based on the particle-in-cell and Monte-Carlo methods [2] was developed. This model considers electrons' motion in the magnetic field along target's surface and electrons' drift towards the anode and ionization process of the operating gas. Also model considers motion of the secondary, tertiary etc electrons, which were born during the motion of the primary electron. Ions which were born during electrons' motion bombard the target's surface thus result ion-electron emission. Results for the value of the dark cathode space, area of the intensive atom ionization were gained. These results agree well with known experimental and calculated data [3]. Calculated self-consistent redistribution of the electric field during the discharge corresponds well with experiment.

### REFERENCES

- [1] S. Kadlec // *Surface & Coatings Technology*. – 2007. – 202. – № .895-903.
- [2] C.H. Shon, J. K. Lee // *Applied Surface Science*. – 2002. – 192. – № .258-269.
- [3] A. Bogaerts, K. De Bleecker, I. Kolev, M. Madani // *Surface & Coatings Technology*. – 2005. – 200. – № .62-67.

## BIPOLAR POWER SUPPLY FOR REACTIVE MAGNETRON SPUTTERING<sup>1</sup>

*V.O.OSKIRKO, A.A.SOLOVIEV, A.P.PAVLOV, I.V.IONOV, N.S.SOCHUGOV<sup>†</sup>*

*Institute of High Current Electronics, 2/3 Akademicheskii Ave., Tomsk, 634055, Russia, oskirkovo@gmail.com, 8(3822)491651*

In the present work a 10 kW bipolar power supply for magnetron sputtering systems and substrate biasing was fabricated. The developed circuit design allowed increasing the output pulses frequency up to 100 kHz and positive pulses length up to 10  $\mu$ s. This allowed considerably reducing the number of arcs during the reactive sputtering processes. Figure 1.a shows the output current and voltage pulses of asymmetrical shape feeding a magnetron sputtering system.

The arc energy was regulated due to the power supply by adjusting the time delay from the arc detection moment. Minimal response time of an arc suppression system was less than 1  $\mu$ s and the arc energy was only several milijoules. Figure 1.b shows the output current and voltage pulses of the power supply during an arc and response of the arc suppression system.

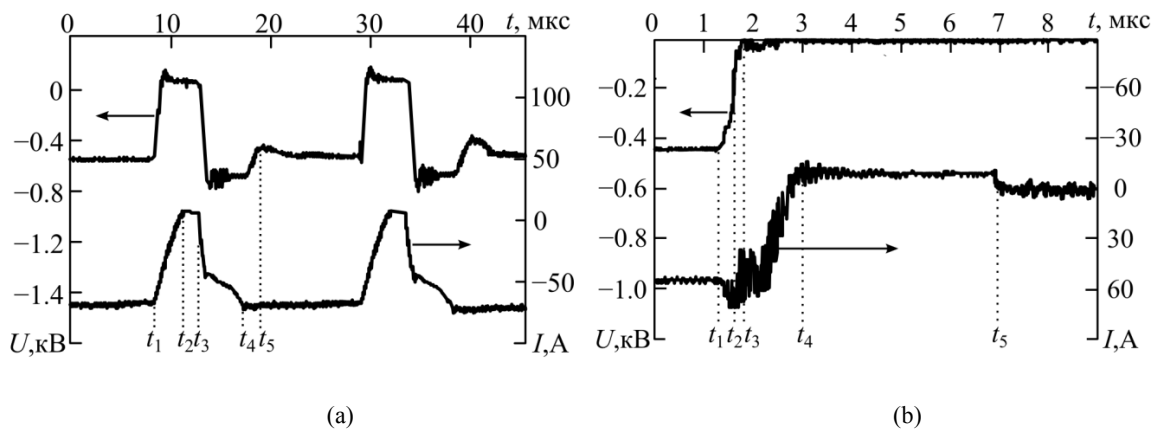


Fig. 1. a. The output current and voltage pulses of the power supply feeding a magnetron sputtering system, b. The output current and voltage pulses of the power supply during an arc

The power supply was used for YSZ (yttria-stabilized zirconia) films deposition, which were an electrolyte for solid oxide fuel cells. The deposition rate and stability of the sputtering process were considerably increased due to asymmetrical mid-frequency bipolar pulses. Therefore, there are prerequisites for the use of such power supply on an industrial scale.

<sup>†</sup> This work was supported by the state assignment of Institute of High Current Electronics SB RAS and by Russian Foundation for Basic Research grant no. 14-08-31679 mol\_a

## MODERNIZATION OF ION-PLASMA MODULES FOR APPLICATION OF NANOSTRUCTURED CARBON COATINGS

*S.A. TRIFONOV<sup>1</sup>, V.T. BARCHENCO<sup>1</sup>, A.A. LISEKOV<sup>2</sup>, G.A. NIKOLAYCHUK<sup>3</sup>*

<sup>1</sup>*Saint Petersburg Electrotechnical University "LETI", Saint-Petersburg, Russia, [s.trifonov.89@rambler.ru](mailto:s.trifonov.89@rambler.ru), +79516701237*

<sup>2</sup>*Institute of Problems of Mechanical Engineering (IPME) Russian Academy of Sciences (RAS), Saint-Petersburg, Russia*

<sup>3</sup>*Ferrite Domen Co., Saint-Petersburg, Russia,*

Thin carbon films in the amorphous state ( $\alpha$ -C) containing bound hydrogen, are called hydrogenated films ( $\alpha$ -C: H). The films are submit material with variable optical, electrical and mechanical properties during production process. This gives up great possibilities for application of these films in various devices [1]. In particular, nanostructured films of amorphous hydrogenated carbon with ferromagnetic nanoparticles are promising structures to formation of radio- absorbing materials (RAM) [2, 3].

Among the above-mentioned technologies for producing carbon films in many ways stands out the ion-plasma technology based on magnetron sputtering systems. Flow of plasma evaporated particles is generated in highly non-equilibrium conditions. This fact defines a very weak effect of temperature on the parameters of the sputtering process. This circumstance allows flexible regulation of the process parameters of the films and affects their physical and chemical properties and performance characteristics.

To improve the quality and performance of products before the film formation process the substrate material must be subjected to finishing treatment to activate the surface and remove the water vapor and residual gases from the surface.

In the basic installation finish ion cleaning occurred in the glow discharge in argon at pressures in the range of 2 - 5 Pa. The energy of the ions bombarding the surface, determined by the automatic offset, which is formed to ensure the vanishing of the charge brought in from the plasma to isolated or dielectric surface. In the absence of a magnetic field near the surface the magnitude of the potential difference in the boundary layer is approximately  $7kT_e$  ( $k$  - Boltzmann constant,  $T_e$  - the electron temperature) and for the conditions under consideration is in the range of 20 - 30 V. These energies of ions are close to the critical potential of sputtering, so cleaning conditions in the considered system are far from optimal.

To improve the quality of the finish ion cleaning was developed plasma source of fast neutrals on the basis of non-self glow, construction similar to that described in [4].

The main difference of the developed module is the fact that the energy disjoint-charge of the ions is less than 30 eV, which eliminates the appearance of the charge embedded in the surface layers of the structure and reduces heating of treated surface.

### REFERENCES

- [1] *Nikolaichuk G.A., Yakovlev S.V., Trifonov S.A. and others // Hydrogenized carbon sputtered Ultra wide band multilayer radio-absorbing coatings with 3d-metal magnetic nanoparticles The 18th International Crimean Conference "Microwave & Telecommunication Technology" - 2008,- 2. 579-580.*
- [2] *Nikolaychuk G A, Petrov V V, Yakovlev S V and others // Radio-absorbing materials on the base of nanostructures (Nanotekhnika)- 2009 - 1 (17) 41-44*
- [3] *Yakovlev S. V., Ivanov V. P., Nikolaichuk G. A. // Complex dielectric permittivity measurement of thin-film radio-absorbing materials in 300 MHz to 40 GHz frequency range using the resonator method Proceedings of the XVII International Conference "Magnetism, near and far spin-spin interaction." – 2009 – S. 57-58*
- [4] *Barchenko V. T., Bystrov Y. A., Kolgin E. A., ed. Bystrov Y. A.// Ion-plasma technologies in electronic production (St. Petersburg Branch: Energoatomizdat) - 2001*

## MASS -CHARGED COMPOSITION OF BEAM PLASMA GENERATED BY FORE-VACUUM PLASMA ELECTRON SOURCE <sup>1</sup>

YU.G.YUSHKOV\*, D.B. ZOLOTUKHIN\*, E.M.OKS\*\*\*, K.P.SAVKIN\*\*, A.V. TYNKOV\*\*\*

\*Tomsk State University of Control Systems and Radioelectronics, Tomsk, 40 Lenin ave., 634050, Russia

\*\*Institute of High Current Electronics SB RAS, Tomsk, 2/3 Akademichesky ave., 634055, Russia

In this paper the results of experimental investigation of mass and charge composition of gas discharge plasmas are presented. The discharge was initiated by electron beam [1] which interacted with metal collector in noble gases (argon or helium) and in residual atmosphere of vacuum chamber at pressures of  $10^{-2}$  –  $10^{-1}$  torr. The inverted time-of-flight spectrometer [2], designed by us was used for research in the beam plasma produced by a fore-vacuum plasma electron source, allows one to determine the mass-charge state of the generated beam plasma.

It was shown that the ion beam extracted from the electron beam plasma contains a small fraction of the collector material ions. Thus, we have demonstrated the possibility of metal ions generation using electron beams at these pressures.

### REFERENCES

- [1] A.A. Zenin, A.S. Klimov, V.A. Burdovitsin, E.M. Oks // *Pis'ma Zh. Tekh. Fiz.* – 2013. – Volume 39(10). – Pages 9-14.
- [2] Gushenets, V.I.; Burachevsky, Yu.A.; Vizir, A.V.; Oks, E.M.; Savkin, K.P.; Tynkov, A.V.; Yushkov, G.Yu. // *Rev. Sci. Instrum.* - 2014. - Volume 85(2). - Pages 02A738-3.

---

<sup>1</sup> This work was supported by RFBR under the grant number RFBR-14-08-31090

## **SPECIAL FEATURES OF RIBBON ELECTRON BEAM FORMATION BY PLASMA SOURCE UNDER HIGHER PRESSURE<sup>1</sup>**

*A.S. KLIMOV, V.A. BURDOVITSIN, E.M. OKS*

*Tomsk State University of Control Systems and Radioelectronics, 40 Lenin ave., Tomsk, 634050, Russia, E-mail:  
[klimov@main.tusur.ru](mailto:klimov@main.tusur.ru), phone: 8-905-990-52-41*

The features of ribbon electron beam generation based on hollow cathode discharge at pressures of 5-40 Pa are presented. Geometry of the accelerating gap has designed. It let to focus the ribbon electron beam and to transport it on a distance of several tens of centimeters in the absence of axial magnetic field. It is shown that the use of special construction of the emission electrode lets to increase the working pressure of ribbon electron beam source up to 30 Pa in the air and up 50 Pa in a helium atmosphere.

---

<sup>1</sup> This work was supported by Russian Foundation for Basic Research, grant №. 14-08-00047



## EXTRACTING ELECTRONS AND IONS OUT OF REFLEX-DISCHARGE WITH A HOLLOW CATHODE BY ALTERNATING ELECTRIC FIELD

V.YA. MARTENS, M.M. MAKOVSKY, I.V. NIKITIN

North Caucasus Federal University, 2, Kulakov Blvd, Stavropol, 355029, Russia  
Phone: +78652 94-40-71, +78652 73-53-89; E-mail: [vmartens@yandex.ru](mailto:vmartens@yandex.ru)

Research of reflex-discharge with a hollow cathode [1] has shown the possibility of effective extraction out of it, through the hole in a cathode, both electrons and ions at an appropriate polarities DC accelerating electric field. However, in some practically important cases is interesting the simultaneous or seesaw extraction of electrons and ions out of discharge. For example, in the synthesis of dielectric or semiconductor films by ion plating onto a substrate there is an accumulation of the positive charge of the ions on the growing surface, which impedes further growth of the film. This charge can be compensated by electrons extracted from the same discharge. In this study was investigated extracting electrons and ions out of reflex-discharge with a hollow cathode by supplying on the acceleration gap alternating sine wave voltages with frequency of 50 Hz. It should be appreciated, that voltage current characteristic of the accelerating gap such source charged particles nonlinear and asymmetric relatively the coordinate axes [1]. According to theory of non-linear electric circuits this leads to distortion of the laws of variation over time of current and voltage of the accelerating gap.

Schematic of the experimental device is plotted in Fig. 1, and current and voltage oscillograms of the accelerating gap are plotted in Fig. 2. The peculiarity of investigated source of charged particles is that the plasma potential on the axis of reflex-discharge of approximately on 300 V higher than the potential of the cathode. This accelerating voltage for ions provided by a DC voltage source 6, and it is added to the accelerating voltage  $U_{ac}$  of AC source 7. This explains a significant amount of ions arriving at the collector at  $U_{ac} = 0$ . This also explains the fact that at positive potentials of collector relative to the cathode, not exceeding 300 V, to the collector receives simultaneously ions and electrons, and at voltages up to about 200 V ions prevail, and at higher voltages - electrons.

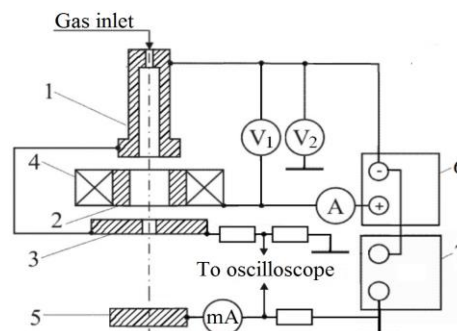


Fig. 1. Schematic of the experimental device: 1 - hollow cathode, 2 - anode, 3 - cathode-reflector with a hole diameter of 5 mm, 4 - magnet 5 - collector, 6 - DC source, 7 - AC source.

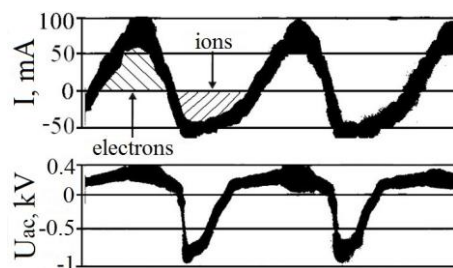


Fig. 2. Oscillograms of the current and voltage of accelerating gap, the air pressure of 15 mPa, discharge current with hollow cathode of 0,1 A, discharge voltage 350 - 420 V.

### REFERENCES

- [1] V.Ya. Martens // Technical Physics. – 2002. – Vol. 47. – № 11. Pp. 1389 – 1396.

## EXTENSION OF PULSED INDUCTIVELY-COUPLED PLASMA IN VACUUM

A.I. KUZMICHEV, S.A. MAIKUT, D.V. TKACHENKO, L.YU. TSYBULSKIY

NTUU "Kiev Polytechnical Institute", KPI-2230, 37 pr. Pobedy, Kiev, 03056, Ukraine

E-mail: A.Kuzmichev@edd.ntu-kpi.kiev.ua, phone: 38 044 4549503

Induction vapor and gas ionizers are often used in the art of physical vapor deposition (PVD) of coatings in order to generate so called inductively-coupled plasma. Plasma species are employed for evaporation by heating or sputtering of raw coating materials, for ion-kinetic assistance of forming the desired coating microstructures and providing chemical reactions for synthesis of complex coating compositions, for thermal effect on the substrates and cleaning the substrates prior to coating deposition. In recent years, pulse modes of plasma generation and ion impact on coating growth are of great interest because pulse modes expand the ranges of possible operation parameters, substrate materials and coatings.

After the excitation of current oscillations in the inductor, the plasma is generated inside the inductor coil and moves towards the vacuum chamber walls and the substrate. Accordingly, the substrate ion current has the form of a pulse whose the face front is shifted in time relatively to the inductor current pulse. Fig. 1 depicts the example of dependences of the velocity of Al vapor plasma boundary movement in the substrate direction on the inductor current oscillation frequency  $f$  for two inductor voltage pulse amplitude values. Experimental curves were obtained by measuring the ion current pulse delays on Langmuir probes located at different distances from the inductor. The velocity is  $(0,5 - 2,5) \times 10^4$  m/s. It can be assumed that the delay time of the ion current pulse is inversely proportional to the average velocity of the plasma boundary.

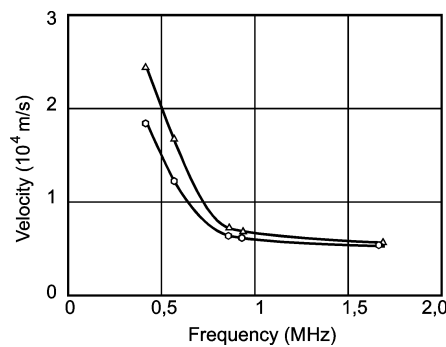


Fig. 1. Dependence of Al plasma boundary velocity on inductor current frequency: inductor voltage amplitude – 2.5 kV (lower curve) and 3.5 kV (upper curve)

In this paper we also solve the mathematical problem on the plasma motion in the pulsed electromagnetic field of the inductor of conical shape in order to identify the characteristics of the plasma movement. The problem is solved in the hydrodynamic approximation. The following expression is obtained for the plasma boundary velocity  $V$ :

$$V \approx \frac{\mu_0 e^2 \sin 2\Theta U^2}{32\pi m M R^2 L (2\pi f)^2} \frac{v}{v^2 + (2\pi f)^2},$$

where  $e$ ,  $m$  – electron charge and mass,  $M$  – ion mass,  $\mu_0$  – magnetic constant,  $R$  – average inductor radius,  $L$  – inductor inductance,  $2\Theta$  – vertex angle of the cone,  $v$  – particle collision frequency. From the physical point of view, the plasma motion is due to the action of the radial component of the inductor magnetic field. When  $v \gg 2\pi f$ , the extension plasma velocity  $V$  is directly proportional to the square of the inductor voltage amplitude and inversely proportional to the inductor current frequency. This is correlates with the experiments.

It is possible to calculate the probable Al ion energy  $\varepsilon$  of the directed motion within the plasma flow. When the velocity is  $0.5 \times 10^4$  m/s, the energy  $\varepsilon$  is 3.5 eV; then at  $1.0 \times 10^4$  m/s  $\varepsilon$  is 14 eV and at  $2.5 \times 10^4$  m/s  $\varepsilon$  is 87.5 eV.

Thus, when the pulsed mode of inductor power supply is used, not only the generation of the ions of depositing material and working gas but also their acceleration towards the substrate can be obtained. This allows simplifying the coating apparatus with ion assisting.

## FAST NEUTRALS SOURCE WITH LOW OPERATING PRESSURE

V.T. BARCHENKO, N.A. BABINOV

*Saint Petersburg Electrotechnical University «LETI», Prof. Popova str. 5, 197376,  
SPb, RU, E-mail: [vtbarchenko@yandex.ru](mailto:vtbarchenko@yandex.ru)*

Using a fast neutrals beam is an efficient method of dielectric processing such as etching, cleaning or activation of surface. Since in nowadays many technological processes can be performed in one working volume at the same time and some of them may require sufficiently low pressure in the working volume creation a fast neutrals source with low operating pressure is an important problem.

In the most of existing fast neutrals sources ions are generating in the plasma then accelerated in the electrical field and neutralized by the resonance recharge. This system works well when the pressure is high enough but has two major drawbacks.

Firstly, the span length needed for efficient neutralization of the ion beam is inversely proportional to the pressure in the span area. Therefore the lower the pressure the longer needed span length. If the pressure is lower than 1 Pa the length required is too long.

Secondly, no matter how long the span length is, some of the ions from the beam will fly through the span length without neutralization. In some cases these high energy ions can significantly impair the processed surface.

To avoid these drawbacks the three-electrode system was proposed. The fast neutrals source consists of laminar cathode, grounded anode in the form of the frame and additional box shaped cathode at the floating potential. The plasma concentrates between the main and additional cathodes, two of them the hollow cathode effect through which the pressure at which the discharge can be maintained is significantly reduced.

In this system of fast neutrals source the neutralization in the reflection from the metallic surface is the main way of neutralization. Ions are extracted from the plasma, accelerated in the cathode potential drop and neutralized by the reflection from the plates of laminar cathode. Since efficiency of this way of neutralization does not depend on pressure, the operation pressure of fast neutrals source is limited only by discharge maintaining pressure. Since efficiency of neutralization increases with atomic mass of metal increasing, the cathode should be made from the metal with high atomic mass such as molybdenum.

The important distinction of this fast neutrals source system is that ions are neutralized at the bottom of the potential well made by cathode. Even though some of the ions do not neutralized at the cathode, they are inhibited in the cathode electric field and cannot leave cathode potential well with energy greater than thermal. Thus only neutral fast particles can reach processed surface with great energy and the damage that may be caused by fast ions is completely eliminated.

In addition to using the hollow cathode effect another method to reduce operation pressure of the fast neutrals source was applied. Since the laminar cathode creates significant resistance to the flow of gas it is possible to create a pressure difference between the internal and external volumes of the fast neutrals source. The gas is inserted to the volume formed by main and additional cathodes. If the pumping speed is high enough, the internal and external pressures may differ several times. In created fast neutrals source the pressures differed by 2.5 times. Thus, since the fast neutrals source operation pressure is limited only by discharge maintaining pressure the minimal operating pressure is reduced by 2.5 times only due to the use of this effect.

The experimental model of the fast neutrals source was created. While the pressure is higher than 3 Pa discharge voltage is lower than 1000 V. But with a further reduction of the pressure the discharge voltage starts to rise and at the pressure of 1 Pa is greater than 3000 V. For the further reduction of the source operating pressure necessary to increase the size of the source or the pumping speed of the vacuum pump.

## THE INTERRELATION OF ENERGY PARAMETERS AND GAS CONVECTION RATE IN CAPACITIVE DISCHARGE EXCILAMPS<sup>1</sup>

*E.A. SOSNIN\**, *A.A. PIKULEV \*\**, *V.A. PANARIN\**, *V.F. TARASENKO\**

\* *Institute of High Current Electronics SB RAS, 2/3 Akademicheskii ave., Tomsk, Russian Federation, 634055, badik@loi.hcei.tsc.ru, 83822900207*

\*\* *All-Russia Scientific Research Institute of Experimental Physics, Russian Federal Nuclear Centre, 37 Mira Ave, Sarov, Nizhny Novgorod region, 8313028424*

The study object is to obtain the influence of gas convection on radiation intensity capacitive discharge excilamps. Such lamps are a subclass of modern discharge sources of radiation [1].

The experimental setup (fig. 1) allowed to change gas convection rate in excilamp bulb by varying of input energy into gas discharge (active side A) and pressure. The bulb was filled by mixtures of Xe:Cl<sub>2</sub> = (400-50):1 and pressure  $p < 90$  Torr. During operation the radiant excittance and pressure jump values has been registered. It is enough to calculate thermal convection calculation.

For this purpose the Navier–Stokes equation for cylindrical tube in cylindrical coordinates ( $l, r, \varphi$ ) [1] has been solved:

$$\frac{\Delta p}{l} + \rho g(\mathbf{e}, \mathbf{k}) = \frac{\mu}{r} \frac{d}{dr} \left\{ r \frac{du}{dr} \right\},$$

where  $\Delta p$  – difference of pressure on element length  $l$ ;  $u = u(r)$  – radial distribution of gas speed;  $g$  – free fall acceleration;  $\mathbf{k}$  – unit vector of a vertical axis (0z);  $(\mathbf{e}, \mathbf{k})$  – scalar product of unit vectors  $\mathbf{e}$  and  $\mathbf{k}$ ;  $\rho$  – gas density;  $\mu$  – coefficient of dynamic viscosity.

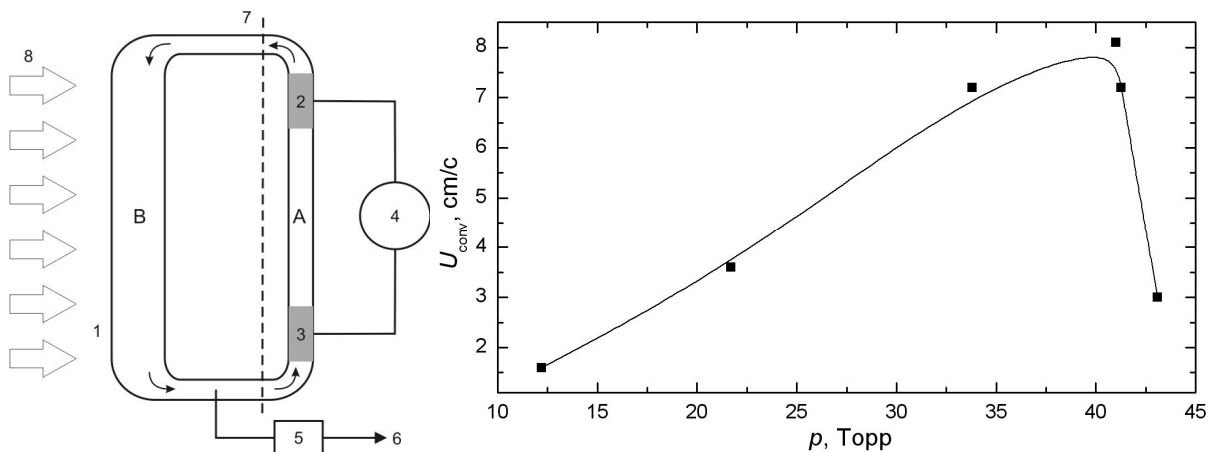


Fig. 1. The experimental setup (left) and calculated convection rate in active side A (right) in Xe/Cl<sub>2</sub>=200/1 mixture: 1 – bulb; 2, 3 – electrodes; 4 – power supply; 5 – pressure transducer; 6 – to gas mixture preparation block; 7 – partition; 8 – air-flow. A – active size of bulb, where capacitive discharge have place; B – buffer size of bulb

The calculation of convection results values are shown in a fig. 1. The comparison with radiant excittance values under different mixture pressures is revealed, that the radiation intensity values correlates with convection rate. It means that the convection could be a marker of radiation efficiency of capacitive discharge excilamps.

### REFERENCES

- [1] *E.A. Sosnin, V.F. Tarasenko, M.I. Lomaev // UV and VUV excilamps. – Saarbrücken, Deutschland / Germany: LAP LAMBERT Academic Publishing, 2012.*
- [2] *L.D. Landau, E.M. Lifshits // Theoretical physics. Vol. VI. Hydrodynamics. – Moscow, Nauka, 1988.*

<sup>1</sup> The work was supported by RFBR (project No. 12-08-00020-a).

**STUDY OF PARAMETERS AND CONTINUOUS SERVICE DURATION OF TECHNOLOGICAL VOLUMETRIC GAS-DISCHARGE PLASMA GENERATOR WITH THERMIONIC CATHODE***D.P. BORISOV, A.D. KOROTAEV, V.M. KUZNETSOV**Tomsk State University, 36, Lenin ave., Tomsk, 634050, Russia, [borengin@mail.ru](mailto:borengin@mail.ru), 8-913-885-82-45*

Characteristics and design features of electrode systems for source of gas-discharge plasmas produced in an arc discharge in gas sustained by electron emission from a hot cathode and advanced technological vacuum-plasma generator relying on them are presented.

The main results of the paper are provided in an experimental study of continuous service time thermionic cathode filament and of the plasma generator with thermionic cathode on parameters such as their operating current and the discharge voltage and the filament heating power. It has been shown that increasing the burning voltage from 28 to 60 V significantly reduces the period of continuous service filament thermionic cathode and of the plasma generator.

Conclusion of this paper is that increasing the concentration of the discharge plasma in the vacuum chamber volume appropriately to achieve an increase in the discharge current plasma generator that is not as critical impact on the lifetime of the filament as a plasma generator discharge voltage.

High values of the parameters and advantageous properties of the plasmas generated by the proposed sources in large vacuum volumes are obtained.

## AUTOMATED LANGMUIR PROBE MEASUREMENT SYSTEM FOR INVESTIGATION OF PLASMA PARAMETERS OF LOW-PRESSURE DISCHARGE<sup>1</sup>

S.S.KOVASLKIY\*., V.V. DENISOV\*, N.N. KOVAL\*., I.V. LOPATIN\*.

\*Institute of High-Current Electronics, RAS, 4 Akademicheskoy Ave., Tomsk 634055, Russia, [skov@sibmail.com](mailto:skov@sibmail.com), +7-905-089-84-67

\*\*National Research Tomsk State University, 36, Lenina Ave., Tomsk, 634050 Russia

Due to the dynamic development of technologies based on the use of plasma generated by low-pressure discharge, important question is the developing of automated measurements systems intended for operational research of stationary and pulsed plasma of low-pressure discharges, as well as for control and optimize low-temperature plasma based processes.

To solve such problems is well established traditional method of electrical probes. This method allows to measure the basic parameters of plasma such as electron temperature, concentration of charged particles, plasma potential, and directional velocity of charged particles. In some cases the probe measurements allow to find a particle velocity distribution function. Modern theories of probe measurements allow studying stationary, RF and microwave discharges in the pressure range from a few tenths of Pascal to atmospheric pressure.

In this paper describes an automated Langmuir probe measurement system established for rapid measurements of key parameters of the plasma of the low-pressure discharges. The system can be used with single or double electric probe, and also provides the ability to synchronize time of measurements with the power source of the discharge, which is important for measuring the plasma generated by low-pressure pulsed discharges.

The system automatically measures the instantaneous values of current and voltage at the probe tip, the maximum amplitude of the signal is  $\pm 300$  mA and  $\pm 300$  V with an accuracy of  $\pm 0,1\%$  for each of the channels. Waveform of the signal on the probe is a bipolar sawtooth with an amplitude of  $\pm 10$  to  $\pm 300$  V (10 V discrete adjustment) and a frequency of 1 to 100 Hz (1 Hz discrete adjustment). Registration time of one probe characteristic in different experiments can be varied from 10 ms to 100 s.

This system is used to study the non-self sustained glow discharge in the stationary and pulsed modes for a wide range of operating parameters. The results of these measurements are necessary for optimization of surface nitriding of materials and products.

### REFERENCES

- [1] Lopatin I.V., Schanin P.M., Akhmadeev Y.H., Kovalsky S.S., Koval N.N. // Plasma Physics Reports. – 2012 – Vol. 38 – № 7. pp. 585-589.
- [2] Lopatin I.V., Koval N.N., Kovalsky S.S., Schanin P.M. // Izv. VUZov. Fizika. – 2012 – Vol. 55 - № 12-2. pp. 206-210.

<sup>1</sup> This work was supported by the RFBR grant (projects No. 14-08-00997-a) and SB RAS interdepartmental project No. 107

## STUDY OF INFLUENCE OF THE LOW-TEMPERATURE HYDROGEN PLASMA PARAMETERS ON THE HYDROGEN SATURATION EFFICIENCY OF METALS

V.S. SYPCHENKO, N.N. NIKITENKOV, YU.I. TYURIN, O.V. VILHIVSKAYA, T.I. SIGFUSSON

Tomsk Polytechnic University, Lenin str. 30, Tomsk, 634050 Russia, sypchenko@tpu.ru, 89528998948

Interaction of molecular hydrogen with metals is studied over the last century. Interaction of low energy hydrogen atoms with metals is also considerable interest from the point of view of fundamental research as well as in connection with the operation of large tokomaks. Amount of experimental data in the field of the hydrogen materials science and in hydrides chemistry due to the complexity and specific features of the experiment in activated atmospheres is little. Saturation of materials from hydrogen plasma (HP) is one of the easiest ways to saturation. This method enables to saturate the material to a high concentration and high-purity hydrogen with a suitable choice of parameters and the method for producing plasma.

The purpose of the present work is study the influence of the high-frequency discharge power in hydrogen plasma on hydrogen accumulation in the titanium. The installation for hydrogen saturation of metals and semiconductors from high-frequency (HF) HP has been developed and created for study of processes of hydrogen penetration and state in material.

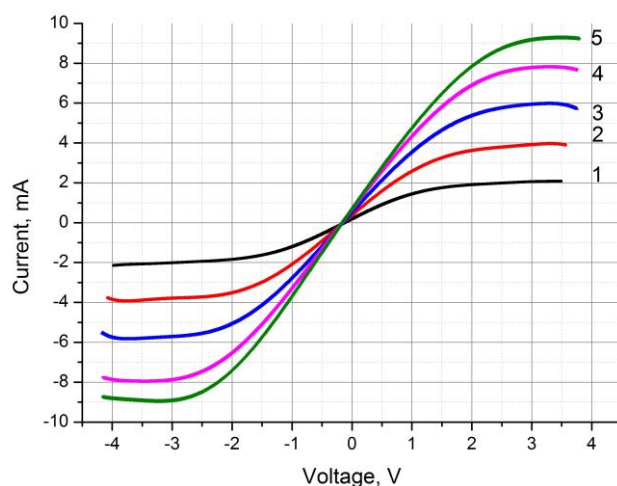


Fig. 1 Voltage-current characteristics HP gained by Langmuir's probe at different absorbed HF powers of the discharge, W: 1 - 50, 2 - 100, 3 - 150, 4 - 200, 5 - 250.

Saturation of titanium samples by a size of  $10 \times 5 \times 0,1$  mm happened at following parameters: pressure  $P = 27$  Pa, temperature on the sample surface was  $T = 773$  K, the time exposure  $t = 2$  h; powers of the discharge (the absorbed power of the generator) from 50 to 250 W with a step of 50 W.

A double Langmuir's probe was used for plasma examination. It allows to measure (indirect) concentration, temperature and medial velocity of electrons, a potential and an electric field in plasma, and also to size up a plasma ionization degree. The voltage-current characteristics gained in-process are shown in the figure 1.

The peculiarities of absorption and hydrogen state in saturated samples were explored by a thermo-stimulated gas release method. Weight concentration of hydrogen after saturation was measured by the RHEN-602 hydrogen analyzer. The treating of experimental results was made in software package OriginLab 8.6.

The experiment results allow drawing following deductions:

1. The electrons energy decrease while the electrons concentration and ionization degree increase at increase of power of the HF discharge.
2. The efficiency of saturation of titanium samples increases at growth of the absorbed HF radiation power.
3. The optimum absorbed HF power for effective saturation is 200 W.

## CONDITIONS FOR THE EXISTENCE OF HIGH-CURRENT LOW-PRESSURE DISCHARGE FORMS IN CIRCULATION CYLINDRICAL MAGNETRON

V.T.BARCHENKO\*, N.V. KRUTOVICH\*, S.YU.UDOVICHENKO\*\*

\*Popov s. 5, Saint-Petersburg, 197376, Russia

\*\*Semakov s. 10, Tyumen, 625003, Russia

The most promising sources of charged particle beams, designed to modify the surface properties of materials are low-pressure glow discharges magnetron and a hollow cylindrical cathode [1-3]. The possibility of using bit system type inverted magnetron tube to produce beams of charged particles is shown in [4,5]. Experimental studies of this system in terms of the generation of electron and ion beams as in pulsed and continuous modes of operation [6].

In [7] presented a physical model of a high-current glow discharge with a cylindrical hollow cathode, and in [8] - a model of direct discharge in a cylindrical magnetron. In the inverted magnetron cathode where as we develop the cylinder with additional edges [9], and is coaxial anode rod can be more efficient generation of fast electrons and correspondingly high intensity gas ionization compared with direct magnetron. This leads to an increase of the discharge current at constant gas pressure and to increase the emissivity of the discharge gap.

In this paper, we maintain a high-current discharge conditions in inverted cylindrical magnetron. In this magnetron, a minimum value of the magnetic field, which still allows the existence of the discharge, is greater than in a planar magnetron, and is not much different from the corresponding values in the direct magnetron.

Just as in the direct magnetron, with decreasing values of the magnetic field increases the minimum gas pressure required for maintaining the discharge in the form of High inverted magnetron.

Comparison of analytical results obtained by simulation with the same experimental data for direct magnetron [8] showed that in the first case, the minimum gas pressure twice. This does not contradict the measurements made in [6], where at a pressure of 10<sup>-3</sup> Torr inverted magnetron discharge exists in the form of low-current with a current of less than 1 A and a voltage of several kV burning. With an increase in pressure increases the intensity of the ionization occurs and an abrupt transition to a high-current discharge, which is accompanied by a decrease in the discharge of several hundred volts.

### REFERENCES

- [1] Veresov LP Veresov OL, MI Dzkuya and other. Research cold cathodes of plasma sources, generating hydrogen ion beams // TF. 2001.T.71. Issue 10. P.50 - 53.
- [2] Veresov LP Veresov OL Ion source with cold cathode magnetron plasma and magnetic compression // Zh.TF 2003.T.73. Issue 10. P.122.
- [3] Litvinov PA // Problems of Atomic Science and Technology. Ser. Nuclear physics research. 1997. MY. 4.5 (31,32). T.11. P.48-50.
- [4] Oks EM, Chagin AA // TF 1988. T.58. Number 6. S.1191
- [5] Oks EM, Chagin AA, PP Schanin // TF. 1989. V.59. Number 10. P.188
- [6] Barchenko VT Krupovich NV, Udovichenko S.Yu. Modeling of high-current glow CVC hollow cathode discharge excited in terms of the left branch of the Paschen curve // Math. ETU "LETI". 2012. № .1. P.18-23.
- [7] Barchenko VT Krupovich NV, Udovichenko S.Yu Conditions of burning high current low-pressure discharge in a cylindrical magnetron // Math. ETU "LETI". 2013.
- [8] Barchenko VT, Golubev VP, Potsar AA, GV Tarvid // AS Number 866610. With a priority date of 11/16/79 .. 1991. pp. 18-23



## DEVELOPMENT AND EXPERIMENTAL CHARACTERIZATION OF AN ELECTRON BEAM SOURCE BASED ON A PLASMA EMITTER AND MULTIPLE APERTURE ELECTRON OPTICAL SYSTEM

*I.V. KANDAUROV\**, *V.T. ASTRELIN\**, *YU.A. TRUNEV\**, *V.V. KURKUCHEKOV\*\**

*\*Budker Institute of Nuclear Physics of SB RAS, Lavrentieva 11, Novosibirsk, 630090, Russia, i.v.kandaurov@inp.nsk.su*

*\*\*Novosibirsk State University, Pirogova 2, Novosibirsk, 630090, Russia*

We report on our continued development of a powerful, long pulse electron beam source based on a plasma emitter and multiaperture electron optical system. The source is designed for studying the beam-plasma interaction in linear plasma devices and physical modelling of extreme thermal loads on metal surfaces. The plasma emitter is produced by a cold-cathode arc discharge in low pressure hydrogen. The electrons are extracted from the discharge plasma and accelerated in a diode electron optical system with plane molybdenum electrodes performed as hexagonal «grids» with multiple round apertures. A more detailed description of the beam source and its operation can be found in our previous publications [1].

The recent upgrades were aimed at rising of the beam current and improvement of radial distribution of the beam current density. The number of emission apertures was increased from 241 up to 499. The diameter of multiaperture structure increased from 82 mm to 118 mm, accordingly. Also, the plasma emitter was modified in terms of its geometry and magnetic field configuration. As a result, in some experimental regimes the total beam current increases more than twice up to 280 A at the pulse length of 0.2 ms and the diode voltage of about 80 kV. With a lower beam current of 150 A the pulse duration can be lengthened up to 1 ms. Two-dimensional beam current density distribution at the metal target was measured with an X-ray pinhole camera at different regimes of plasma emitter operation. The results of the measurements and discussion are provided.

### REFERENCES

- [1] *V. V. Kurkuchekov et al // Fusion Science and Technology. – 2013. – Volume 63. – № 1T. Pages 292-294.*

## E-BEAM INSTALLATION "SOLO-M" FOR SURFACE MODIFICATION METALLIC AND CERMET MATERIALS

*S.V. GRIGORIEV, V.N. DEVYATKOV, A.V. MIKOV, P.V. MOSKVIN, A.D. TERESOV*

*HCEI SB RAS, 2/3 Akademicheskoy Avenue, Tomsk, 634055, Russia, grigoriev@opee.hcei.tsc.ru, +7(3822)491300*

The description and main characteristics of the vacuum electron-beam installation created for the surface treatment (modification) of metallic and cermet materials, as well as for research on extreme effects on materials and structures like coating-substrate.

The main element of the installation is an electron plasma cathode source which generates a pulsed electron beam diameter of 1 to 5 cm, with the necessary energy density on the substrate. Electron beam currents up to 250 A, the energy density up to  $100 \text{ J/cm}^2$ , adjustable pulse duration (20-200)  $\mu\text{s}$  and a pulse repetition rate of single pulses up to 10 Hz is formed in a gas-filled diode with a plasma cathode at an accelerating voltage of 25 kV up to and transported longitudinally pulsed magnetic field at a distance of 40 cm in the region of its interaction with the solid.

The beam incident on the surface to be treated, produces ultrafast heating (within a pulse duration of  $\sim 10^{-4}$  s) to the melting temperature of the substrate material. With super-quick cooling by conduction in the surface layer of the substrate from a few to a few tens of micrometers formed the fine structure of the improved material. Cleaned surface, annealed fusible impurities in steel hardening structure is formed, increases surface hardness. Furthermore, in the liquid phase under vacuum through the surface tension of the surface relief occurs burnishing (polishing). In the case of impact of the beam on the surface of the coating-substrate structure is an intensive mixing of the coating material to the backing material in a liquid phase, which allows to obtain products at the surface of the functional layer with improved properties (for example surface wear and corrosion resistant alloy layers). By using such a beam may melt the surface of various materials, including hard and refractory, such as Mo, W, WC-Co, etc. without changing the dimensions of the product.

Required space of treatment (maximum  $20 \times 20$  cm) is achieved by scanning products in two coordinates X, Y. Electron source consists of a discharge cell, using the main and auxiliary (trigger) discharges, emission grid, accelerating electrode and the drift tube. As the beam collector used a sample of material processed or product. Modulation of the beam current is carried by a main discharge. Accelerating voltage of 25 kV is provided to DC-power source.

Installation structurally composed of three units connected in the in-line module. The central unit includes an electron gun, the vacuum chamber with a vacuum system and the system diagnostics. Left block and the right block include a computer control system installation and power supply system of the electron gun.

**SIMULATION OF DISCHARGES IN  $E \times H$ -FIELDS WITH A SELF-HEATED CATHODE**

*L.A. ZYUL'KOVA*\*, A.V. KOZYREV\*

\*Institute of High Current Electronics SB RAS, 2/3 Akademicheskii Av., Tomsk, 634055, Russia,  
kozyrev@to.hcei.tsc.ru, [lorik@lve.hcei.tsc.ru](mailto:lorik@lve.hcei.tsc.ru), (7-382-2)-49-15-44, (7-382-2)-49-16-95

**Abstract** – Discharges in crossed  $E \times H$ -fields with a self-heated cathode are investigated. A model of the discharges are presented. Results of simulation of the discharges are discussed.

## INVESTIGATION OF THE ELECTRICAL DISCHARGE IN THE SALINE SOLUTIONS IN A VICINITY OF THE THRESHOLD VOLTAGES<sup>1</sup>

*Y. D. KOROLEV\*\*\*, I. A. SHEMYAKIN\*, R. V. IVASHOV\*, V. S. KASYANOV\*,  
N. V. LANDL\*, Y. SUN\*\*\*, T. SHAO\*\*\*, Y. GAO\*\*\**

\* *Institute of High Current Electronics, Academichesky Ave., 2/3, Tomsk, 634055, Russian Federation, [korolev@inp.hcei.tsc.ru](mailto:korolev@inp.hcei.tsc.ru)*

\*\* *National Research Tomsk Polytechnic University, Lenin Ave., 30, Tomsk, 634050, Russian Federation*

\*\*\* *Institute of Electrical Engineering Chinese Academy of Sciences, #6, Zhongguancun Beiertiao, Beijing, P. R., 100190, China*

Last time a considerable interest has been generated in the direction that is associated with the pulsed electrical discharges in electrolyte or discharges in the saline solutions. The discharges are widely used in the so-called plasma scalpels in surgery, installations for underwater sound waves generation, water switches and so on [1, 2].

It was shown [3], that there is the characteristic feature of the discharges in the saline solutions. In the initial stage, due to an enhanced current density, the gas microcavities arise at a surface of active electrode. The cavities have a form of microbubbles, conglomerate of microbubbles, and vapor layers. An increase in a voltage at the gap to threshold values leads to the appearing a gas discharge plasma in the microcavities. The discharge current flows from the active electrode to other electrode via the volume of saline solution. This report is focused on investigation of gas discharge processes formation and identification of its forms. The main attention is concentrated on the optical and spectral investigations.

The experimental setup is shown schematically in Fig. 1. The coaxial electrode system is used. The system consists of active and grounded electrodes 1, 3 and ceramic insulator 2. Diameter of the inner electrode is about 0,5 mm. The main electrode 1 is made of titanium. The voltage from the pulsed generator *PG* is applied to the electrodes through the transmitting cable of the length *l*. In the experiments the negative-polarity and bipolar rectangular pulses are used. The pulse duration and pulse repetition rate were 10–40  $\mu$ s and 0,1–100 kHz correspondingly. The voltage of the generator was change from 100 V to 400 V. The value of the current was 2 A in maximum.

The integrated emission spectra and temporal behavior of spectral lines were recorded. The spectrometer USB2000+ and photomultiplier PMT (Fig. 1) were used. The spectral range of the optical tract was 300–830 nm. There was a temporal resolution about 2 ns.

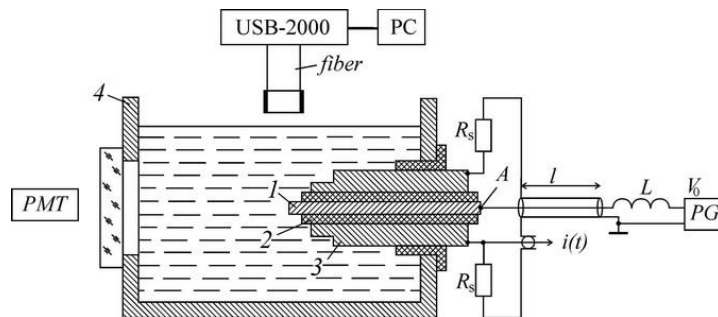


Fig. 1. Experimental setup: 1 – active electrode, 2 – ceramic insulator, 3 – grounded electrode, 4 – chamber.

A set of experimental data to describe the mechanism of the gas discharge formation in the cavities has been obtained. It is shown that the discharge process is a non steady-state character, and the forms of discharge burning were determined by the polarity of the applied voltage to the active electrode. A sparks in the cavities are mainly observed at negative voltage polarity. Using a voltage of positive polarity leads to a glow discharge.

### REFERENCES

- [1] *K. R. Stalder, J. Woloszko, I. G. Brown, C. D. Smith // Appl. Phys. Lett. – 2001. – Vol. 79. – No. 27. – PP. 4503–4505.*
- [2] *Y. H. Sun, Y. X. Zhou, M. J. Jin, Q. Liu, and P. Yan // Journal of Electrostatics. – 2005. – Vol. 63. – PP. 969–975.*
- [3] *R. V. Ivashov, V. G. Geyman, Y. D. Korolev // Russian Physics Journal. – 2012. – Vol. 55 – No. 12/3 – P. 113.*

<sup>1</sup> This work was supported by the Russian Foundation for Basic Research under Grant 14-08-91153

## COMPARATIVE ANALYSIS OF MATERIAL SURFACE FORMATION PROCESSES UNDER THE ACTION OF DIFFERENT TYPES OF INTENSE ENERGY FLOWS TREATMENT<sup>1</sup>

*A.YA. LEYVY, V.M. ASTASHYNSKI\*, N.N. CHERENDA\*\*, V.V. UGLOV\*\*, A.P. YALOVETS*

*South-Ural State University, Physical Department, Lenina 76, Chelyabinsk 454080, Russia, e-mail: [leyvy@mail.ru](mailto:leyvy@mail.ru)*

*\*A.V. Lykov Heat and Mass Transfer Institute of the National Academy of sciences of Belarus,*

*P. Brovka str., Minsk, 220072, Belarus, e-mail: [ast@hmti.ac.by](mailto:ast@hmti.ac.by)*

*\*\*Belarusian State University, 4, Nezavisimosti ave., Minsk, 220030, Belarus E-mail: [Cherenda@bsu.by](mailto:Cherenda@bsu.by)*

Treatment of materials under the action of intense energy flows is the prospective technique of surface properties modification. Plasma treatment can be used for enhancement of strength properties, increase of coating adhesion, alloying of material surface layer.

Earlier it was shown [1, 2] that surface dynamics under the action of charged particles flows is determined by the balance of surface tension forces, viscosity as well as forces appeared due to substance expansion during heating. It is also necessary to take into account the pressure of flow on the surface in case of plasma flows treatment.

Formation of surface relief under the action of compression plasma flows (CPP) was investigated in Ref. [3]. It was shown that CPP treatment resulted in formation of two different surface regions (central part and periphery). Central part is the area where interaction with surface of plasma flow perpendicularly directed to the surface takes place. This area absorbs maximum energy of the flow. Periphery area is formed due to plasma spread along the surface and development of Kelvin-Helmholtz instability. It was shown that treatment with the energy absorbed by the surface 10-15 J/cm<sup>2</sup> per pulse subcritical treatment regime is observed (without ablation). Smoothing of surface relief in central part should be observed in this case [1] However, the experimental data [3] show an increase in roughness during processing plasma flows.

Comparative analysis of material surface formation processes under the action of different types of intense energy flows treatment: electron and ion beams, plasma flows is carried out in this work. The mechanisms of surface relief formation in central part of target are investigated.

### REFERENCES

- [1] V. S. Krasnikov, A. Ya. Leivi, A. E. Maier, and A. P. Yalovets // Tech. Phys.- 52, 431, 2007
- [2] N. B. Volkov, A. E. Maier, K. A. Talala, and A. P. Yalovets// Tech. Phys. Lett. **32**, 424, 2006
- [3] Astashynski V.M., Leyvi A.Y., Talala K.A., Uglov V.V., Cherenda N.N., Yalovets A.P. // Journal of Surface Investigation 7 (5) (2013), pp. 1005-1012

<sup>1</sup> This work was supported in part by the Ministry of Education and Science of the Russian Federation (contract no. 1030 (2014105-G3) for support of research at the South Ural State University).

## NUMERICAL MODELING OF PHYSICAL PROCESSES AND STRUCTURAL CHANGES IN METALS UNDER INTENSIVE IRRADIATION WITH USE OF CRS CODE: DISLOCATIONS, TWINNING, EVAPORATION AND STRESS WAVES<sup>1</sup>

*A.E. MAYER\**, *E.N. BORODIN\*\**, *V.S. KRASNIKOV\*\*\**, *P.N. MAYER\**

\*Chelyabinsk State University, Br. Kashirinikh str., 129, Chelyabinsk, 454001, Russia, mayer@csu.ru, +7(351)7997161

\*\*Institute of Problems of Mechanical Engineering RAS, V.O. Bolshoj pr. 61, 199178, St. Petersburg, Russia

\*\*\*South-Ural State University, Lenina av., 76, Chelyabinsk, 454080, Russia

Here we present the CRS computer program which is intended to calculate the dynamical deformation of metals under intensive loading including the irradiation by high-current electron and powerful ion beams. The incorporated mathematical models allow one not only to calculate stresses and deformations, but the structural changes induced by loading as well. For example, the dislocation density, volume fraction of twins in the solid part of metal and drop size in the ablated material can be estimated by simulation with CRS.

The CRS numerically solves the equations system, which consists of continua mechanics equations, supplemented by equations of dynamics and kinetics of various structural defects: dislocations, grain boundaries, twins, micro-cracks and vapor bubbles. The dislocation plasticity model [1,2], the grain boundary sliding model [3,4], the mechanical twinning model [5], the spall fracture model [6,7] and the nonequilibrium evaporation model [8,9] are incorporated in CRS. Transport and energy release of fast electrons are calculated according to [10], the energy release function of ions can be taken from the BETAIN code [11]. The wide range equations of state [12,13] are used for spherical part of stresses.

Some simulation results of the joint evolution of structural defects in the irradiated metal are presented. Elastic-plastic properties of metal determined by dislocations, twins and grain boundaries significantly influence on the stress fields generated by the intensive irradiation. Nonequilibrium character of metal evaporation in the energy release zone leads to a metastable state of overheated metal melt there, which leads to formation of essential tensile wave following the stress wave in the solid part of the irradiated metal. The CRS code can be a useful tool in theoretical estimation and interpretation of experiments in the field of materials modification by intensive energy fluxes.

### REFERENCES

- [1] Krasnikov V.S., Mayer A.E., Yalovets A.P. // International Journal of Plasticity. – 2011. – 27. – № 8. 1294-1308.
- [2] Krasnikov V.S., Mayer A.E. // Surface and Coatings Technology. – 2012. – 212. – 79-87.
- [3] Borodin E.N., Mayer A.E. // Materials Science and Engineering: A. – 2012. – 532. – 245-248.
- [4] Borodin E.N., Mayer A.E. // Physics of the Solid State. – 2012. – 54. – № 4. – 808-815.
- [5] Borodin E.N., Atroshenko S.A., Mayer A.E. // Technical Physics. – 2014. – in press.
- [6] Mayer A.E., Krasnikov V.S. // Engineering Fracture Mechanics. – 2011. – 78. – № 6. – 1306-1316.
- [7] Mayer A.E., Khishchenko K.V., Levashov P.R., Mayer P.N. // Journal of Applied Physics. – 2013. – 113. – № 19 – 193508.
- [8] Mayer P.N., Mayer A.E. // Technical Physics Letters. – 2012. – 38. – № 6. – P. 559-561.
- [9] Dudorov A.E., Mayer P.N., Mayer A.E. // Vestn. Chelyabinsk State University. Physics. – 2012. – № 14 (256). – P. 53-61.
- [10] Evdokimov, O.B., Yalovets, A.P. // Nuclear Science and Engineering. – 1974. – 55. – 67-75.
- [11] Yalovets A.P., Mayer A.E. // Proc. 6-th Int. Conf. CMM-2002. Tomsk. – 2002. – 297-299.
- [12] Fortov V.E., Khishchenko K.V., Levashov P.R., Lomonosov I.V. // Nuclear Instruments and Methods in Physics Research A. – 1998. – 415. – № 3. – 604-608.
- [13] Kolgatin S.N., Khachaturov'yants A.V. // Teplofizika Vysokikh Temperatur. – 1982. – 20. № 3. – 90-94.

<sup>1</sup> This work was supported by the Grant of the President of Russian Federation (MD-286.2014.1) and the Russian Foundation for Basic Research (Grant No. 14-01-31454)

## UNFILTERED ALUMINIUM VACUUM ARC PLASMA APPLICATION FOR INTERMETALLIC LAYERS FORMATION USING HIGH-FREQUENCY SHORT-PULSE PLASMA IMMERSION ION IMPLANTATION METHOD<sup>1</sup>

*D.O. SIVIN, A.I. RYABCHIKOV, A.I. BUMAGINA*

*National research Tomsk Polytechnic University, Lenina 2, bldg. 4, Tomsk, 634050, Russia,  
E-mail: sivin@tpu.ru, phone (3822) 70-17-77 ext. 2515*

The objective of this work was to investigate a possibility of unfiltered DC aluminium vacuum arc plasma application for plasma immersion aluminium ion implantation. It is shown experimentally that the number density of aluminium macroparticles (MPs) on the substrate surface is decreased dynamically by 3 orders when the ion-plasma substrate treatment time is increased from 15 s to 3 min at the bias potential – 2 kV (Fig. 1).

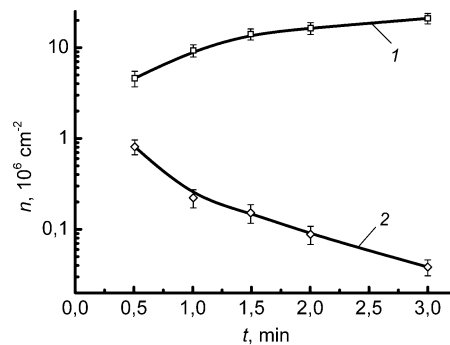


Fig. 1. Dependence of MP number surface density (n) on the substrate on deposition time (t): (1) – at anode potential on the substrate  $\varphi_b = 0$  V; (2) – at repetitively-pulsed bias potential  $f=10^5$  p.p.s.,  $\varphi_b = -2$  kV,  $\tau = 7$   $\mu$ s.

An enhancement of aluminium MP ion sputtering on the heated substrate surface take place because of aluminium drops flattening to a very thin film. Evaporation of large MPs on heated substrate surface influences on significant decrease of aluminium MPs number density. Experimental results indirectly indicate that the effect of evaporation of the small MPs during their movement in the sheath also takes place.

It was shown that at high intensity low energy plasma immersion implantation of aluminium ions in titanium and nickel substrates a deep layer (several  $\mu$ m) of aluminium dopants with concentration in the range of (12–35) at % can be formed (Fig. 2).

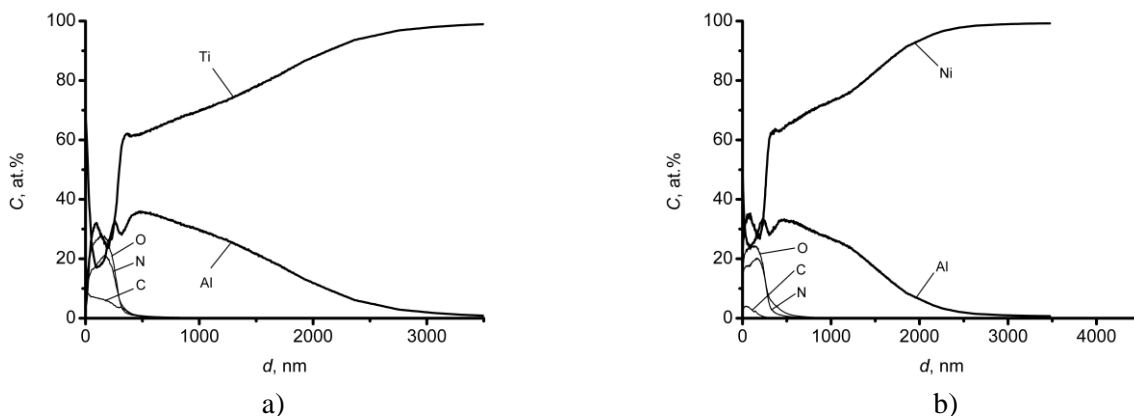


Fig. 2. AUGER dopant depth profiles in the titanium (a) and nickel (b) samples after 6 min of processing time at high-frequency short-pulsed negative bias ( $\varphi_b = -2$  kV,  $f=10^5$  p.p.s.,  $\tau = 7$   $\mu$ s).

<sup>1</sup> This work was supported by Ministry of Education and Science of the Russian Federation, assignment «Science».

## THE EFFECT OF IRRADIATING REGIMES WITH INTENSE PULSED ELECTRON BEAMS ON CRATER CREATION TAKING PLACE ON THE SURFACE OF TARGETS FROM NICKEL ALLOYS

*V.A. SHULOV\**, *A.N. GROMOV\*\**, *D.A. TERYAEV\**, *O.A. BYTZENKO\**, *V.I. ENGELKO\*\*\**

*\*Moscow Aviation Institute, 4 Volokolamskoye shosse, A-80, GSP-3, Moscow 125993, Russia, Tel.: (499) 1584424, Fax: (499) 1582977, E-mail: shulovva@mail.ru*

*\*\*Chernyshev Machine Building Enterprise, 7 Vishnevaya Street, A-80, GSP-3, Moscow 123362, Russia, Tel.: (495) 4914988, Fax: (495) 4915652, E-mail: teryaev\_a@avia500.ru*

*\*\*\*Efremov Institute of Electro-physical Apparatus, 1 Sovietsky Avenue, Metallostroy, St. Peterburg 189631, Russia; Tel.: (812) 4627845, Fax: (812)4639812, E-mail: engelko@niiefa.spb.ru*

Crater creation phenomenon on the surface of turbine blades with NiCrAlY resistant coating during irradiation with intense pulsed electron beams was investigated with the use of scanning electron microscopy and optical metallography. It is shown that the use of intense pulsed electron beam as well as high power pulsed ion beam leads to creation of craters on the surface of vacuum-plasma NiCrAlY coatings but among numerous types of craters formed under the action of high power pulsed ion beams here only round-shaped craters with the concavity in the centre and microdrops with light-vapor components of coatings are created.



## ION TRAJECTORIES CALCULATION FOR NEGATIVELY BIASED NEEDLE ELECTRODE IN THE VOLUME DISCHARGE PLASMA.

*A.G. REMNEV\**, *K. UEMURA\**, *A.V KOZYREV\*\**, *V.V. LOPATIN\*\*\**,

*\*ITAC Ltd., Shinmaywa 1-1, Takarazuka 665-0052, Japan, aleksey\_remnev@itac-j.co.jp, +81-90-6347-0791*

*\*\* Institute of High Current Electronics, Akademichesky Avenue 2/3, Tomsk, 634055, Russia*

*\*\*\* Institute of High Technology Physics, Lenin Avenue 2a, Tomsk, 634050, Russia*

Previously we have reported a method of ion-plasma sharpening of medical needle [1, 2]. The needles were orderly placed in two-dimensional array and underwent bias ion sputtering in the plasma of hot filament hollow cathode plasma generator. Argon was used as the plasma forming gas. Addition of purified air allowed achieving of smoother surface and sharper cutting edges of the needle [3].

Besides the sharpening, an unexpected distinctive needle shape was observed as the result of ion-plasma sputtering treatment [2]. In order to understand the mechanism of such shape modification the ion fluence distribution needs to be evaluated.

The ion trajectories were calculated for the simplified 2D model. The plasma sheath from which the ions are extracted with Bohm velocity is generally of complex shape, dictated by the plasma density and the voltage drop across the plasma sheath. However we can consider two particular cases: [i] the plasma density is relatively high and the voltage is relatively low, so the plasma leaks into the gaps between the needles; [ii] the plasma density is relatively low and the voltage is relatively high, so the double layer is getting large and the ion emission surface become planar. In the present study only second case was investigated. Space charge in the plasma sheath is neglected.

Complex topology of the electrode system, even for the simplified model, doesn't allow calculating of the electric field distribution analytically, so it was simulated with finite element analysis (FEA) method [Fig. 1a]. The resulting piecewise function  $E(x,y)$  was then used for the ion trajectories calculation. The trajectories were calculated in the Maple mathematics software [Fig. 1b].

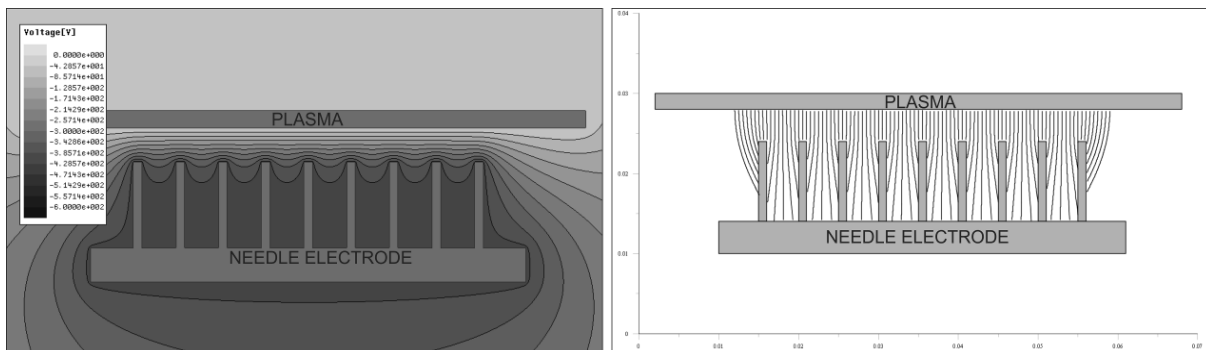


Fig. 1. left – FEA of electric field distribution, right – calculated trajectories of the ions. Plasma sheath – 4mm, pitch between needles – 5mm, starting ion velocity – 0 m/s.

FEA model and generated Maple code allows varying of some of the starting conditions of the trajectories computation, such as width of the plasma sheath, pitch between the needles, initial velocity of the ions.

Distribution of the ion fluence along the needle surface and angles of the ion incidence can be obtained from the simulation. Experimental and theoretical results are compared and discussed.

- [1] A. G. Remnev, K.V. Shalnov, V.R. Kukhta, K. Uemura // Digest of Micro and Nano fabrication Conference (MNC). 2011.
- [2] A.G. Remnev, K.V. Shalnov, K. Uemura, K. Nagato // ISPlasma2012 proceedings. – 2012. 78.
- [3] O. Alghuraira, A.G. Remnev, K. Nagato, S. Ikeshima, O. Yasunoria, K. Uemura, M. Nakao // Procedia CIRP. – 2013. – 5. 53-56.

## MELTING OF THIN METAL FILM ON DIELECTRIC SUBSTRATE UNDER THE ACTION HIGH POWER ION BEAM NANOSECOND DURATION<sup>1</sup>

*V.S. KOVIVCHAK, T.V. PANOVA, R.B. BURLAKOV, E.V. KNYAZEVA*

*Omsk State University, pr. Mira, 55a, Omsk, 644077, Russia, [kvs@univer.omsk.su](mailto:kvs@univer.omsk.su), +7(3812)224972*

High power ion beam (HPIB) treatment of various machine parts with thin film coating has drawn great attention from many researchers in engineering for applications such as increase in erosion and corrosion resistance, reduction of friction coefficient and formation of metal nanoparticles [1, 2]. The short duration ion beam and the high current density of this beam can induce heating, melting, and vaporization of metals on a time scale of nanoseconds to microseconds. In order to seek the optimal process conditions in HPIB treatment of thin metallic films, better understanding of the physical process is needed for process design and control in an industrial environment.

In this work, HPIB melting of aluminum and chrome thin films deposited on a glass and glass-ceramic substrates is studied at various current density of ion beam to better understand the basic mechanisms involved in the melting and solidification processes. Maximum thickness of the films was 0,15  $\mu\text{m}$  and 2  $\mu\text{m}$  for chromium and aluminum, respectively.

Irradiation was performed on a Temp accelerator by a proton-carbon (30%  $\text{H}^+$  and 70%  $\text{C}^+$ ) beam with an average energy of 300 keV, a duration of 60 ns, in the current density range of 20– 150  $\text{A}/\text{cm}^2$  with a variation in the number of irradiation pulses from 1 to 10. Substrate surfaces were analyzed using a JEOL (JSM-6610LV) scanning electron microscopy with X-ray microanalysis (Inca Energy 350).

The action HPIB on these films leads to a change in surface morphology of film. It is depends on the current density and the number of irradiation pulses. Discontinuity of Al film is formed at low beam current density of HPIB ( $\sim 30 \text{ A}/\text{cm}^2$ ). Increasing the current density leads to the formation of network-like structure on the surface substrate. The transformation of this structure into arrays of aluminum particles of different shapes and sizes was observed at high current densities ( $> 100 \text{ A}/\text{cm}^2$ ). SEM images of surface aluminum film ( $h=1,9 \mu\text{m}$ ) shown in Fig. 1 at various beam current density. Average size metal particles on glass substrate is 1,1  $\mu\text{m}$  for chrome film ( $h=0,08 \mu\text{m}$ ) and 23  $\mu\text{m}$  for aluminum film ( $h=1,9 \mu\text{m}$ ) at HPIB irradiation with current density 100  $\text{A}/\text{cm}^2$ . Possible mechanism of formation surface morphology in system “thin metal film – dielectric substrate” under the action of the HPIB were discussed taking into account the energy loss of carbon and hydrogen ions in chrome and aluminum thin films.

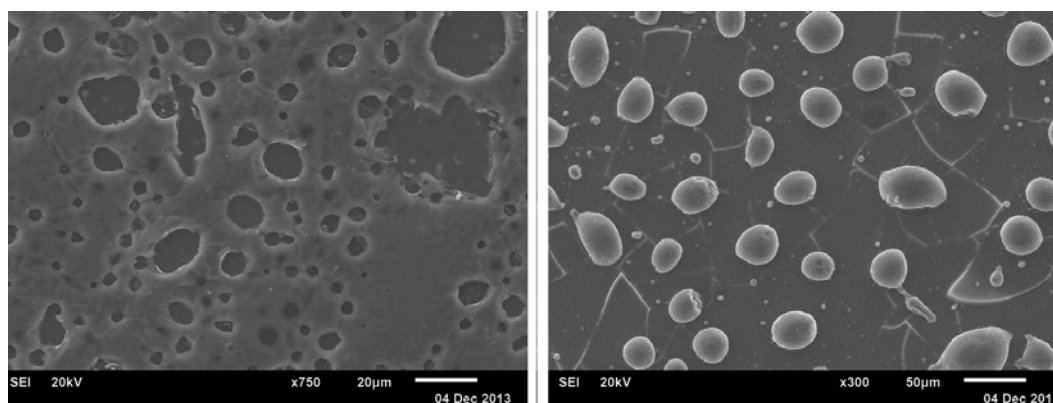


Fig. 1. Al film on glass substrate after HPIB irradiation with a current density: 50  $\text{A}/\text{cm}^2$ , 1 pulse (left); 150  $\text{A}/\text{cm}^2$ , 1 pulse (right)

### REFERENCES

- [1] V.S. Kovivchak, R.B. Burlakov, T.V. Panova, N.A. Davletkil'deev // Technical Physics Letters. - 2008. - V. 34. - № 4. - P. 358-360.
- [2] V.S. Kovivchak, V.I. Dubovik, R.B. Burlakov // Journal of Surface Investigation. – 2009. - V. 3.- № 2. – P. 268-270.

<sup>1</sup> This work was supported by RFBR and Government of Omsk region in the context of the research project 13-08-98141 r\_siberia\_a

## THE ANALYSIS OF POSSIBILITIES OF THE MAGNETRON SPUTTERING SYSTEMS FOR HIGH-RATE DEPOSITION OF FUNCTIONAL COATINGS

*G.A. BLEYKHER, V.P. KRIVOBOKOV, A.V. YURYEVA*

*Tomsk Polytechnic University, Lenina av. 2A, Tomsk, 634028, Russia, [bga@tpu.ru](mailto:bga@tpu.ru)*

Currently, the magnetron sputtering systems (MSS) are commonly used for the deposition of nanostructured modifying thin coatings on the surface of materials. They have gained considerable popularity due to the fact that they provide good quality and a great variety of functional properties of the deposited coatings. However, the achieved productivity of technological processes using them often does not meet the needs of industrial production. In particular, for DC MSS applied to metal it is 1..10 nm/s, and in the preparation of complex coating composition - even less. Therefore, we need new ways (through the inclusion of additional mechanisms) of increasing the growth rate of coatings while ensuring their operational properties.

Deposition rate is primarily determined by the rate of atoms emission from the target surface (or erosion rate). Its increase only by collisional sputtering, now generally used, exhausted itself. It is necessary to include a mechanism of evaporation. Due to the fact that the evaporation rate is nonlinear (almost exponentially) increases with increasing temperature of the surface it is possible to achieve a very high intensity of atoms remove from the target surface. Thus, one way to increase the growth rate of the coatings is the creation of conditions when the evaporation will occur.

Evaporation mechanism can be run by different methods. For example, it is realized when using the magnetron sputtering systems with liquid-phase targets. The target substance is melted due to the fact that its heat insulation is created from the remaining elements of the cathode assembly and a magnet system, which must be cooled during operation in MSS. The thermal energy released in the target by the plasma remains in it. Under certain conditions, it is sufficient to melt the target material and to create the intense evaporation at the surface.

The another possible way to create evaporation is increase the current density of the MSS plasma ions bombarding the target surface and carrying most of the energy transferred into the discharge. It can be realized when using the high-current pulsed magnetron systems, and using the assisting ion beam whose action enhances the ionization processes in the magnetron diode plasma.

The objective of the work, the results of which are presented in this article, is to analyze the possibilities of different kinds of MSS (high-current pulsed MSS and MSS with liquid-phase targets) to create evaporation at the target surface. The solution to this problem is satisfied by calculation. To do this, the mathematical models of heat and erosion processes on the cathode assembly based on the thermal conductivity equations with phase transitions are developed. The data on regularities of the target surface erosion in the event of phase transitions and the parameters of MSS, which ensure the best performance and energy efficiency of erosive material extraction, are obtained. It is shown that the inclusion of evaporation increases the target surface erosion yield and the coating growth rate at least an order of magnitude compared to MSS modes in which the collision sputtering takes place only.

The experimental studies of the growth rate of metallic coatings using MSS with liquid-phase targets were carried out. The calculated results and experimental data are in good agreement. This testifies to the correctness of formulated physical ideas and obtained regularities.

## EFFECT OF PULSED PLASMA FLOWS TREATMENT ON THE MICROSTRUCTURE OF CHROMIUM FERRITIC-MARTENSITIC STEEL EK181

*P.S. DZHUMAEV\**, *O.V. EMELYANOVA\**, *V.L. YAKUSHIN\**, *B.A. KALIN\**, *M.G. GANCHENKOVA\**, *A.T. KHEIN\**,  
*M.V. LEONT'EVA-SMIRNOVA\*\**, *R.Z. VALIEV\*\*\**, *N.A. ENIKEEV\*\*\**

*\*National Research Nuclear University MEPhI (Moscow Engineering Physics Institute), Kashirskoe shosse, 31, Moscow, 115409, Russia, PSDzhumaev@mephi.ru*

*\*\*JSC A.A. Bochvar All-Russian Scientific Research Institute for Inorganic Materials, Rogova st., 5a, Moscow, 123098, Russia*

*\*\*\*Ufa State Aviation Technical University, ul. K.Marksa, 12, Ufa, 450000, Russia*

The ferritic-martensitic steels are considered as prospective materials for the fuel element claddings of the fast breeder reactors. This work presents the results of an experimental study of the pulsed plasma flows treatment effects on the microstructure and the strengthening of the chromium ferritic-martensitic steel EK 181 (16Cr12W2VTaB) surface layers. The samples used for the investigation were made in three initial states: hot-rolled and annealed, traditional heat treatment (hardening from 1100°C, tempering at 720 °C for 3 h), and nanostructured by severe plastic deformation processing (SPD).

Modification of the samples surface was made by high-temperature nitrogen pulsed plasma flows (HTPPF) with a specific energy ( $Q$ ) of an incident flow changing in the range of 17–28 J/cm<sup>2</sup> with a pulse duration of 20 μs. The number of irradiation pulses was up to 8. The microstructure of the initial samples and samples treated by plasma flows was investigated by optical and scanning electron microscopy. The microhardness of the samples surface layers was measured using Vickers method with indenter load of 0.5 N.

It has been found that the treatment of EK181 steel samples by nitrogen plasma flows with a specific power of ~ 1.0 MW/cm<sup>2</sup> (the number of pulses  $N = 3$ ) leads to the surface melting. An increase in the specific power of the plasma flows results in an intensive melting of the surface layers accompanied with formation of a rough relief when solidify. The heating and subsequent high-speed cooling of the surface layers make it possible to fix a non-equilibrium martensitic structure with formation of cellular nanostructure. Characteristic mean size of grain of the cellular structure is 140 - 150 nm, and the depth of the modified layer ranges from 3 to 10 microns depending on the pulsed plasma flows specific energy.

It has been shown that these microstructural changes lead to the surface hardening up to 1.20–2.4 times. The degree of microhardness increase depends on the initial state and the plasma treatment conditions ( $Q$  and  $N$ ).

It is revealed that independent of the samples fabrication technology and their heat treatment, HTPPF processing allows to create the gradient materials with the similar two dimensional nanostructured surface layers.

## THE LIQUID-PHASE MASS TRANSFER IN THE TARGET DURING PROCESSING PLASMA FLOWS<sup>1</sup>

*A.YA. LEVY, A.P. YALOVETS*

*South-Ural State University, Physical Department, Lenina 76, Chelyabinsk 454080, Russia, e-mail: [levy@mail.ru](mailto:levy@mail.ru)*

The treatment by intensive plasma flows is one of the most important material processing problem which is widely used to improve physical and chemical surface properties. It results in material hardening, roughness reducing, improving adhesion and mass transfer of substances for systems with covering; and also it is used for metal alloying.

Most of processing modes correspond to the case where solid near-surface layers of a target become liquid. Mass transfer mechanisms of a substance during processing plasma flows, such as diffusion and thermocapillary convection are thoroughly investigated.

A simple evaluation of a role that thermal diffusion plays in this experiment, demonstrates that within the period of a melt's lifetime (a few tens of microseconds), the depth of penetration for the coating's atoms due to diffusion does not exceed 1  $\mu\text{m}$ .

Due to exposure to intense energy, the substance is heated and experiences acceleration; it contributes to creation of conditions necessary for development of RTI. When the exposure is over, the medium moves without acceleration; at this stage RMI develops and exists up to the moment of crystallization. We suggest that such joint action of both RTI and RMI under the influence of intense energy flows shall be called, in short, Taylor-type instability.

This study investigates the role that development of Taylor-type instability and thermocapillary convection plays in processes of liquid-phase mass transfer during processing plasma flows

---

<sup>1</sup> This work was supported in part by the Ministry of Education and Science of the Russian Federation (contract no. 1030 (2014105-G3) for support of research at the South Ural State University).

## STRUCTURAL CHANGES INTO SURFACE LAYERS OF PARTS FROM TITANIUM ALLOY VT9 DURING IRRADIATION WITH INTENSE PULSED ELECTRON BEAMS

*V.A. SHULOV\**, *D.A. TERYAEV\**, *A.N. GROMOV\*\**, *O.A. BYTZENKO\*\**, *G.G. SHIRVANYANZ\**, *V.I. ENGELKO\*\*\**

*\*Moscow Aviation Institute, 4 Volokolamskoye shosse, A-80, GSP-3, , Moscow 125993, Russia, Tel.: (499) 1584424, Fax: (499) 1582977, E-mail: shulovva@mail.Ru*

*\*\*Chernyshev Machine Building Enterprise, 7 Vishnevaya Street, A-80, GSP-7, Moscow 123362, Russia, Tel.: (495) 4914988, Fax: (495) 4915652, E-mail: teryaev\_a@avia500.ru*

*\*\*\*Efremov Institute of Electro-physical Apparatus, 1 Sovietsky Avenue, Metallostroy, St. Peterburg 189631, Russia; Tel.: (812) 4627845, Fax:(812)4639812, E-mail: engelko@niefa.spb.ru*

The present paper reviews the experimental results dedicated to the effect of irradiating conditions with intense pulsed electron beams on physical and chemical state of the surface layer of gas turbine engine blades from VT9 refractory  $\alpha+\beta$ -titanium alloy. The main attention was concentrated in the results of structural investigations carried out by transmission electron microscopy.

## MODELING OF RESIDUAL STRESS AND STRAIN FIELDS IN HOMOGENEOUS AND CONTAINING INCLUSIONS TARGETS WITH A FLAT OR PERTURBED SURFACE<sup>1</sup>

*V.S. KRASNIKOV\**, *A.P. YALOVETS\*\**, *S.V. KASHUKOV\*\**

*\*South-Ural State University, Lenina av., 76, Chelyabinsk, 454080, Russia, vas.krasnikov@gmail.com, +7(351)2679023*

*\*\* South-Ural State University, Lenina av., 76, Chelyabinsk, 454080, Russia*

In this work we study residual stress and plastic deformation fields forming during treatment by charged particles beams. The motivation of this investigation is the dependence of the target performance on residual stresses and structural transformations during after beam processing. Several studies have ascertained a decrease of target surface strength after radiation treatment [1, 2], the authors attribute this undesirable effect to the formation of residual tensile stresses. Contribution to the final state of the surface makes target surface microrelief, in [1, 2] showed that the presence on the irradiated surface microcraters causes additional deformation of the underlying material, and their presence on the surface leads to a significant reduction in performance of target [3] .

Simulation of residual stress fields and plastic deformation is carried out in a two-dimensional cylindrical formulation. The mathematical model includes the equations of continuum mechanics combined with empirical model plasticity by Zerilli-Armstrong, which takes into account the strain hardening and thermal softening of the target material. The study of additional stresses generated near microcraters is carried out. Since the majority of processed targets are heterogeneous structure, the particular interest is the modeling of the inclusion with different properties.

### REFERENCES

- [1] *Rotshtein V.P., Ivanov Y.F., Markov A.B., Proskurovsky D.I., Karlik K.V., Oskomov K.V., Uglov B.V., Kuleshov A.K., Novitskaya M.V., Dub S.N. // Surface Coating Technologies – 2006. – 200. – 6378.*
- [2] *Zhang K.M, Zou J.X., Grosdidier T., Dong C. // Vacuum – 2011. – 86. - 1273.*
- [3] *Zhang Z., Yang S., Lv P., Li Y., Wang X., Hou X., Guan Q. // Applied Surface Science – 2014. – 294. – 9..*

<sup>1</sup> This work was supported by the South-Ural State University (National Research University) in frames of state assignments No. 1030 of the Ministry of Education and Science of Russia (No. 2014105-GZ).

## MODELING OF POWDER MEDIUM EVOLUTION DURING ELECTRON AND LASER SYNERGING<sup>1</sup>

*V.V. POGORELKO, A.P. YALOVETS*

*South-Ural State University, 76, Lenin av., Chelyabinsk, 454080, Russia, yalovets.alex@rambler.ru*

In recent years the technology of volumetric products laser and electronic synthesis are intensively developing [1, 2]. These technologies will speed up process and reduce the cost of functional products manufacturing. One of the most perspective applications is a method of selective laser sintering. There are large temperature gradients ( $10^3$ - $10^4$  K/m), high heating and cooling rates ( $10^3$ - $10^6$  K/s), as well as plasma-chemical phenomena in case of laser irradiation during selective laser sintering. Under these conditions classical approaches and models used in powder metallurgy cease adequately describe the observed phenomena [1].

In this paper we have developed and implemented new continuum model of heating and cooling for ultradispersed medium in time of laser or corpuscular irradiation. The basis of this model is the assumption that pressure in the system remains constant and equal to pressure of ambient inert gas used for sintering. This model takes into account melting and crystallization processes, relaxation of medium to external pressure, movement of the under the force of gravity and action of capillary forces. The wide-range equation of state is used to describe condensed phase. The system of equations is written for 2D cylindrical geometry and includes continuity equation for components (solid phase, melt and inert gas), equation for internal energy and equation of motion for melt.

Numerical studies of the formation of temperature fields in ultradispersed medium and dynamics of the volume fraction of condensed phase in the process of heating and cooling were performed. It is shown that the movement of melt under the force of gravity is the determining factor in the formation of phase composition (condensed phase and gas pore). The role of capillary forces manifests at the boundary of melt and solid phase. This role is an intensive filling of pores by melt.

### REFERENCES

- [1] *I.V. Shishkovsky* // Laser synthesis of functionally graded mesostructures and volumetric products. – M.: FIZMATLIT, 2009.
- [2] *S.F. Gnyusov, S.Yu. Tarasov* // Surf. Coat. Technol. – 2013. – Vol. 232. – P.775-783.

<sup>1</sup> This work was supported in part by the Russian Foundation for Basic Research (project no. 130800037- a) and by the Ministry of Education and Science of the Russian Federation (contract no. 1030 (2014105-G3) for support of research at the South Ural State University).



## MACROPARTICLES NUMBER DENSITY DECREASING ON THE SAMPLE, IMMERSED IN VACUUM ARC TITANIUM PLASMA, AT REPETITIVELY PULSED BIASING<sup>1</sup>

*D.O. SIVIN, A.I. RYABCHIKOV, A.I. BUMAGINA, O.S. TUPIKOVA*

*National research Tomsk Polytechnic University, Lenina 2, bldg. 4, Tomsk, 634050, Russia,  
E-mail: sivin@tpu.ru, phone (3822) 70-17-77 ext. 2515*

We have studied the features of the Ti microparticles (MPs) accumulation on a substrate immersed in a DC vacuum arc plasma with a high frequency short pulse negative bias. The influence of several factors including processing time, the parameters of bias potential, and substrate characteristics was defined. It was found that the MP accumulation on a repetitively biased substrate was uneven over time. A deposition of MPs to substrate were significantly decreased after 1 min of processing at bias parameters  $f=10^5$  p.p.s.,  $\varphi_b = -2$  kV and  $\tau = 7$   $\mu$ s. It was experimentally shown that DC vacuum arc plasma without pre-filtering of MPs can be used for high frequency short pulse plasma immersion metal ion implantation.

---

<sup>1</sup> This work was supported by Ministry of Education and Science of the Russian Federation, assignment «Science».

**MECHANISMS OF MACROPARTICLES NUMBER DENSITY DECREASING ON A SUBSTRATE IMMERSSED IN VACUUM ARC PLASMA AT REPETITIVELY PULSED BIASING<sup>1</sup>**

*A.I. RYABCHIKOV, D.O. SIVIN, A.I. BUMAGINA, P.S. ANANIN, S.V. DEKTYAREV*

*National research Tomsk Polytechnic University, Lenina 2, bldg. 4, Tomsk, 634050, Russia,  
E-mail: [bai@tpu.ru](mailto:bai@tpu.ru), phone (3822) 70-17-77 ext. 2362*

The objective of this investigation was to study the physical mechanisms of macroparticles (MPs) number density decreasing on a substrate immersed in vacuum arc plasma. It was found that the negative repetitively pulsed biasing of a substrate immersed in vacuum arc plasma significantly reduce the MPs content on surface. Several different physical mechanisms of the MPs decreasing on the negatively biased substrate have been identified. It was established that up to 10% of negatively charged in plasma MPs are repulsed from the sheath electric field. Almost the reducing of MPs density by 20 % takes a place due to ion sputtering after 2 min of processing. It was found that enhanced ion sputtering, MPs evaporation on substrate surface and even evaporation of MPs in a sheath can take place depending on the cathode material and the irradiation parameters.

<sup>1</sup> This work was supported by Ministry of Education and Science of the Russian Federation, assignment «Science».

## INVESTIGATION OF POSSIBILITIES OF MICROPARTICLES CONTENT DECREASING ON SUBSTRATE IMMERSSED IN VACUUM ARC PLASMA<sup>1</sup>

*A.I. RYABCHIKOV, D.O. SIVIN, A.I. BUMAGINA*

*National research Tomsk Polytechnic University, Lenina 2, bldg. 4, Tomsk, 634050, Russia,*

*E-mail: [bai@tpu.ru](mailto:bai@tpu.ru), phone (3822) 70-17-77 ext. 2362*

The result of experimental study of macroparticles (MPs) accumulation on negatively biased substrate immersed in DC vacuum arc titanium plasma are presented. It was found that the negative high frequency short pulse biasing of substrate with respect to the adjacent plasma significantly reduces the MPs content on substrate surface. It was shown that the decreasing of MPs surface number density on a negatively biased substrate is defined by the pulse duration, pulse amplitude and processing time. The surface density of MPs with the size less than 1.5  $\mu\text{m}$  was decreased in 1500 fold at the bias pulse repetition rate  $10^5$  pulse per second (p.p.s.), bias potential  $-2$  kV, pulse duration 8  $\mu\text{s}$  and processing time 9–18 min. The total MPs surface density in these cases was decreased in 67fold.

---

<sup>1</sup> This work was supported by Ministry of Education and Science of the Russian Federation, assignment «Science».

**INFLUENCE OF SUBSTRATE CHARACTERISTICS AND NEGATIVE BIAS PARAMETERS TO THE RATE OF VACUUM ARC MACROPARTICLES ACCUMULATION<sup>1</sup>***A.I. RYABCHIKOV, D.O. SIVIN, A.I. BUMAGINA**National research Tomsk Polytechnic University, Lenina 2, bldg. 4, Tomsk, 634050, Russia,  
E-mail: [ralex@tpu.ru](mailto:ralex@tpu.ru), phone (3822) 70-17-77 ext. 2361*

Several regularities of the metal macroparticles (MP) accumulation on the surface of a substrate immersed in vacuum arc metal plasma at high-frequency ( $10^5$  pulse per second (p.p.s.), short-pulsed ( $7 \mu\text{s}$ ) negative bias potential with an amplitude from 1 to 3.2 kV has been investigated. It was shown that the substrate temperature and the surface morphology play a very important role in macroparticle number density control on the substrate immersed in vacuum arc plasma. A possibility to change the metal particle number density on substrate in the range from  $10^5 \text{ cm}^{-2}$  to  $10^7 \text{ cm}^{-2}$  depending on low energy high-frequency short-pulse negative bias parameters and substrate surface morphology characteristics has been demonstrated. The application of high-frequency short-pulse plasma immersion ion implantation or coating deposition method for the dielectric coating formation with metal particle inclusions is also discussed.

<sup>1</sup> This work was supported by Ministry of Education and Science of the Russian Federation, assignment «Science».

## FORMATION OF THE SURFACE MORPHOLOGY OF COOPER ALLOYS UNDER THE ACTION OF A HIGH POWER ION BEAM NANOSECOND DURATION<sup>1</sup>

*V.S. KOVIVCHAK, T.V. PANOVA, K.A. MICHAILOV*

*Omsk State University, pr. Mira, 55a, Omsk, 644077, Russia, [kvs@univer.omsk.su](mailto:kvs@univer.omsk.su), +7(3812)224972*

Most modern alloys used in industry consist of components with different volatilities. Studying the effect of volatile components on the formation of the surface morphology of alloys and the change in the composition under the action of a high power ion beam (HPIB) is of scientific and applied interest. It was shown earlier that the presence of highly volatile impurities in an alloy (metal) can favor the formation of craters on the surface upon intense ion beam action [1–3]. However, the role of highly volatile components (in a wide concentration range) and the homogeneity of their volume distribution in the formation of the surface relief upon HPIB action have been barely studied to date. Such studies should be better performed on copper alloys, i.e., alloys with a low melting temperature containing components with distinctly different volatilities.

Copper-based alloys were chosen as the objects of the study, these included: brass LS 59-1 (37.35–42.2% Zn, 0.8–1.9% Pb), brass L 63 (34.22 - 37.5% Zn, 0.07% Pb), bronze BrOS 10-10 (9–11% Sn, 8–11% Pb), bronze VB23NC (3-4% Zn, 18-22% Pb, 3-4% Ni, 3-4% Sb), bronze BrAJ 9-4 (8–10% Al, 2–4% Fe) and Cu-Al alloy (46% Al) with easily fusible and highly volatile components in their composition, e.g., Zn, Pb, Sn, and Sb. Irradiation was performed on a Temp accelerator by a proton–carbon (30% H<sup>+</sup> and 70% C<sup>+</sup>) beam with an average energy of 300 keV, a duration of 60 ns, in the current density range of 20– 150 A/cm<sup>2</sup> with a variation in the number of irradiation pulses from 1 to 5. The surface of the irradiated copper alloys was studied by means of scanning electron microscopy and X-ray microanalysis.

Since lead is not completely soluble in liquid copper, copper alloys with lead after solidification contain lead inclusions. The typical initial surface of brass LS 59-1 is shown in Fig. 1 (left). The irradiation of brass LS 59-1 to a single HPIB pulse with a  $j = 50$  A/cm<sup>2</sup> leads to intense melting, evaporation and ejection of lead from its surface inclusions with the formation of craters with a flat bottom and a deep hole at its center, Fig. 1 (right). Thereby, the formation of the morphology, first of all craters, on the surface of copper alloys containing elements with different volatilities under HPIB action depends not only on the vapor pressure during evaporation of the most volatile component and their concentrations, but also on the homogeneity of the distribution of these element over volume. The volatile elements localized in the surface layer with a thickness less than the projected path of beam ions most strongly affect the surface roughness under HPIB irradiation.

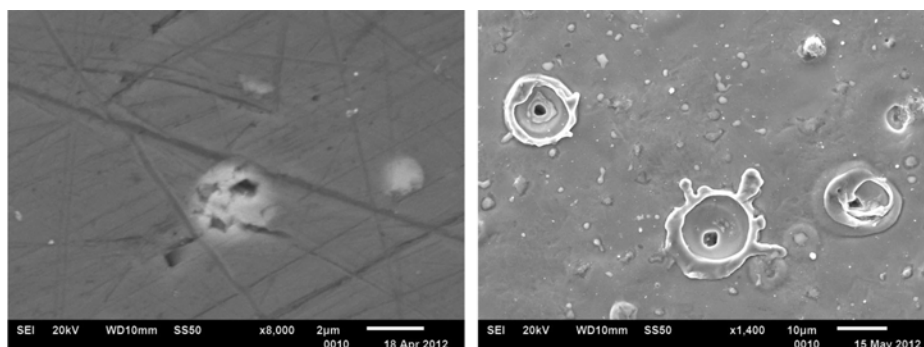


Fig. 1. Surface of brass LS 59-1: initial (left) and after HPIB irradiation with a current density of 50 A/cm<sup>2</sup>, 1 pulse (right)

### REFERENCES

- [1] V. A. Shulov, G. E. Remnev, N. A. Nochovnaya et al.// *Poverkhnost, Fiz. Khim. Mekh.* – 1994. - No. 7. P. 117-123.
- [2] T.J. Renk, P.P. Provencio, S.V. Pracad et al.// *Proc. IEEE.* – 2004. – 92. – P. 1057-1065.
- [3] V. S. Kovivchak, T. V. Panova, V. I. Blinov, and R. B. Burlakov//*Poverkhnost*. – 2006. No. 4. – P. 69-71.

<sup>1</sup> This work was supported by RFBR and Government of Omsk region in the context of the research project 12-08-98042\_r\_siberia\_a

## LOCALLY NONEQUILIBRIUM MODEL OF NONLINEAR HEAT CONDUCTION IN METALLIC SYSTEMS UNDER CONCENTRATED ENERGY FLUX IRRADIATION<sup>1</sup>

G. A. VERSHININ, G.I. GERING, T.V. PANOVA

Dostoevsky Omsk State University, pr.Mira, 55a, 644077, Omsk, Russia, [vershininga@omsu.ru](mailto:vershininga@omsu.ru), ph: +79136403877

High-speed solidification of binary alloys after exposure to high-power pulsed streams of charged particles or laser radiation when in a short period of time a large amount of energy is injected into the surface layer of the material is characterized by ultra-high temperature gradients and velocities of the interface [1]. In this situation the heat and mass transfer during both melting and crystallization occur under apparently in a locally non-equilibrium conditions, which have a decisive influence on the formation of the microstructure and properties of the resultant solid phase, determined mainly by the temperature and the impurity concentration gradients near the solidification front from the liquid phase [2]. In this paper to determine these gradients are used the generalized transport equations taking into account the spatial - temporal nonlocality [3] and the temperature dependence of thermal properties of the medium. We solve one-dimensional boundary value problems for locally nonequilibrium description of the propagation of temperature and heat flow in a flat layer filled with volume absorption of heat. Thermal conductivity, volumetric heat capacity, relaxation times of the temperature gradient and heat flux vector presents a power functions of temperature during the heating process [4]. A difference scheme is used for finding a numerical solution to the problem. Results of calculations of temperature fields in the layer at different moments of time with the certain values of the problem parameters are given. Using theoretical inferences and data of performed numerical calculations, the nonlinear effect of spatial localization of thermal perturbations is established.

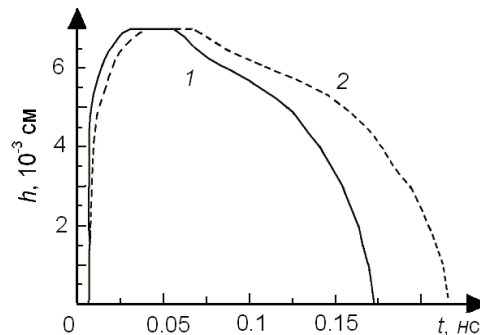


Fig.1. Depth of the melt, depending on the time of observation. Curve 1 - the prediction of the linear theory, 2 - nonlinear.

The modeling results for the depth of the melt in the alloy steel a sample under laser beam irradiation at  $3 \cdot 10^{11} \text{ W / cm}^2$  intensity are presented in the figure. While the maximum depth of the melt in both cases almost identical, the times of the substance in liquid state is different.

### REFERENCES

- [1] *Herlach D.M.* // Mater. Sci. Eng. – 1994. – V. R12. – PP. 177-183.
- [2] *Galenko P., Sobolev S.* // Phys. Rev. Lett. A.– 1997. – V. 55. - № 1. – PP. 343-352.
- [3] *Vershinin G.A., Gering G.I., Afonkina E.A.* // Poverkhnost'. Rentgenovskie, Sinkhrotronnye i Neitronnye Issledovaniya. - 2012. - No. 3. - PP. 14-16.
- [4] *Tzou D.Y., Chiu K.S.* // Int. J. Heat Mass Transfer. – 2001. – V. 44. – PP. 1725-1734.

<sup>1</sup> Work carried out with the financial support of the Ministry of Education and Science of the Russian Federation within the state assignment for scientific research in high schools on the years 2014-2016. Project number 2139.

## ABOUT THE NATURE OF PERCOLATION CONDUCTIVITY OF ARTIFICIAL POLICRISTALLINE GRAPHITE

*E.I. ZHMURIKOV*

*Budker Institute of Nuclear Physics, 690090, Novosibirsk, SB RAS*

*E-mail: [evg.zhmurikov@gmail.com](mailto:evg.zhmurikov@gmail.com)*

In this paper the author considers the nature of the energy barriers that come up at the edge of the graphene planes of carbon composite crystal phases. In particular, if a carbon atom is located at the edge of the base plane, then some of its valence bonds are torn. This leads to an electron configuration change in this atoms and must be accompanied by disappearance of the  $\pi$ -electron states in the electron spectrum near the Fermi level and formation of an energy gap similar to the band gap in diamond [1]. The conductivity of carbon composites, which has of percolation nature, is realized via an infinite conducting cluster with a notorious excess over the percolation threshold. The energy barriers that arise from the anisotropy of conductivity on the crystallite boundaries may add some resistance to the overall conductivity of the sample. In this case, the temperature dependence of the conductivity is determined by the temperature dependence of the conductivity of the crystallites [2]; the overall temperature dependence of the conductivity of the polycrystalline graphite sample is shown in Fig. 1

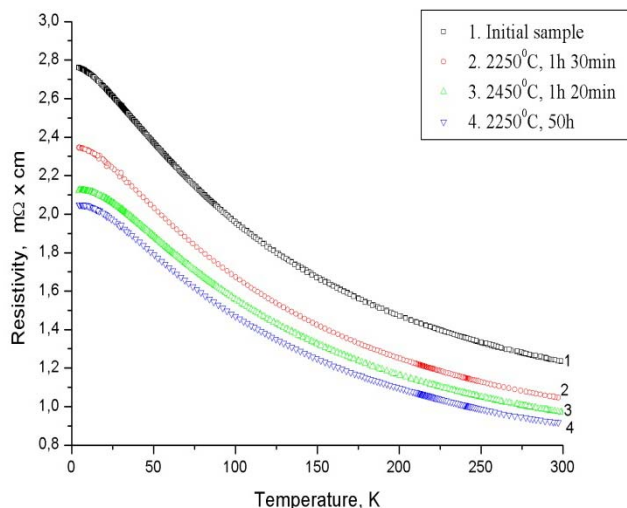


Fig. 1. Temperature dependence of specific electrical resistivity for annealing and non- annealing MPG-7 samples [3].

From X-ray analysis and magnetoresistance measurements at low temperatures it was supposed [3] that intense defect generation in MPG-7 carbon composite sample by heated to high temperatures begins at the borders of the crystallites borders, while the crystallite itself does not change up to a temperature causing the destruction of the sample. Indeed, it is reason to suppose that the crystal itself improves its crystal structure to some extent.

The observed changes in the temperature dependence (Fig. 1) can be explained from the most general percolation theory ideas, stating that the electrical resistance after thermal treatment of composites increases, if the percolation systems is below the percolation threshold and decreases if the percolation systems is above the threshold [4]. This property is a characteristic feature of percolation systems.

### REFERENCES

- [1] Volkov A.P., Obrazcov A.N., Pavlovsky I. Yu, *at al.* // *J. of Surface Investigation*, 1999, №5-6, p.161-166.
- [2] Kotosonov A.S. // *Ph.St.Sol.*, 1989, V. 31, N.8, p.146.
- [3] Zhmurikov E. I., Romanenko A. I., Anikeeva O.B. *at al.* // *High-temperature Effects on the Electrical Properties and Macrostructure of Carbon Composites* // *Inorganic Materials*, 2006, V. 42, N 6, pp. 609-616
- [4] *Gantmacher V.F. Electrons in disordered solids – A4*, M: Fizmatlit, 2003, 176p.

## MORPHOLOGY, STRUCTURE AND OPTICAL PROPERTIES OF THE TITANIUM DIOXIDE FILMS SYNTHESIZED ON AIR AND IN AN ATMOSPHERE OF OXYGEN<sup>1</sup>

V.M. IEVLEV\*\*\*, S.B.KUSHCHEV\*\*\*, A.N. LATYSHEV\*, L.Y. LEONOVA\*, O.V. OVCHINNIKOV\*, A.S.KOTKO\*,  
E.V. POPOVA\*

\*Voronezh State University, Universitetskaya pl.1, Voronezh, 394006 Russia; e-mail: opt@phys.vsu.ru; tel.:(473)2-208-780

\*\*Moscow State University, Leninskie gory 1, Moscow, 119991, Russia;

\*\*\* Voronezh State Technical University, Moskovskii pr. 14, Voronezh, 394026, Russia

Unique chemical and physical, in particular optical, properties the titan dioxide [1] can be used for development of radiators on the basis of homojunction TiO<sub>2</sub>(n)/TiO<sub>2</sub>(p). Now there is no general approach to the decision of this problem, and there are only separate works [2].

Synthesis thin TiO<sub>2</sub> films carried out two methods. The first method consist in magnetron high-frequency dispersion of a target of the titan and condensation films on not warmed up substrate in the environment of air, argon + air or argon + oxygen and the subsequent annealing in vacuum 10<sup>-3</sup> Pa at T = 970 K. The second method represented electron beam evaporation and condensation Ti-layers on a substrate at T = 870 - 1470 K in vacuum 10<sup>-4</sup> Pa and their subsequent oxidation in an atmosphere of oxygen or air at temperature 970 K. The cleanliness of targets not less than 99.98 %. As a substrate applied synthetic mica which surface prepared splitting on air on a plane (001). Thickness of films measured on MarSurf M400. It made 100 ± 10 nanometers. The alloying of Ti-layers made by vacuum condensation Ni together with Ti at the rate of 1 - 4 % Ni.

Structure and orientation of films investigated by methods of diffraction fast electrons and appearing through electronic microscopy on microscopes EMB-100BR and Tecnai G2 20F S-T. Absorption spectra of thin films in visible and near UV areas investigated on one-beam spectrophotometer Shimadzu UV-mini-1240 in spectral area of 300-1950 nm. Spectra of a luminescence registered in spectral area 400 - 860 nm by means of optical monochromator MDR-23 to which target crack it was connected photomultiplier tube R928P, working in a mode of the account of photons. The sample placed in vacuum optical cryostat in which reached pressure 10<sup>-4</sup> Pa, and cooled up to temperature 77 K. The control of excitation and registration light stream impulses of photomultiplier carried out by means of a computer through the block of interface. A luminescence was excited by nitric laser LGI-21 with length of the wave 337 nm and capacity on of 3 kW, duration of an impulse of 8 ns and frequency of following of impulses of 100 Hz. The spectra of photo depolarization measured also in optical cryostat at temperature 77 K by means of high-resistance electrometer.

As a result of the lead researches following results are received.

1. The titanium dioxide thin films synthesized of various structures: anatase, anatase + brookite + rutile, brookite + rutile. Partial shares of crystal updatings depend on conditions of the film formation. Conditions of formation single-phase focused films are found. In all cases the films had nanocrystal structure with the size of grains from 10 up to 25 nanometers.

2. The absorption spectra of samples of complex phase structure represent additive addition парциальных spectra of each phase.

3. The nickel and nitrogen alloying of samples leads to displacement of absorption bands and their red borders in the short-wave and long-wave parties, accordingly.

4. The luminescence in near infra-red area (825 nm) is defined by oxygen vacancies. The samples which were oxidized on air at heats had the greatest intensity of a luminescence in this area. The green bands are defined by the defects localized on a surface.

5. The titanium dioxide films have a wide spectrum of impurity electronic states in the forbidden zone.

The received experimental data allow to predict an opportunity of use the titanium dioxide thin films in optoelectronic system.

### REFERENCES

- [1] Hashimoto K., Irie H., Fujishima A. // *Japanese Journal of Applied Physics.* – 2005 - V.44 - № 12. P. 8269–8285.  
[2] Pascual J., Camassel J., Mathieu H. // *Phys. Rev. B.* – 1978 - V. 18 - №10. P. 5606 – 5614.

<sup>1</sup> This work was supported by RFFI (11-03-12140-ofi-m-2011) and project of Minobrnauki «Carrying out of research works».



## **RADIATION-THERMAL EFFECTS IN NI-TI ALLOY AT SUCCESSIVE IMPACT OF KRYPTON IONS AND ANNEALING**

*V.P. POLTAVTSEVA, V.I. ANTONYUK, S.B. KISLITSIN*

*\*Institute of Nuclear Physics, Ibragimov str. 1, Almaty, 050032, Republic of Kazakhstan, [poltavtseva@inp.kz](mailto:poltavtseva@inp.kz), +7(727)3866839*

The paper presents the experimental study of the patterns of the structural-phase state changing, hardening/softening and temperature intervals of martensitic transitions in Ni-Ti alloy with the shape memory effect under sequential impact of krypton ions with the energy of 280 keV and 1.75 MeV/a.m.u. and post-radiation annealing in the range of temperatures ( $100 \pm 300$ )°C. It was found that the additional post-radiation annealing results in repeated formation of martensite phase B19', responsible for the shape memory effect in the region of the Ni-Ti alloy modified with high-energy ions of krypton, and the temperature of its formation decreases with the growth of implantation fluence. The effect of radiation-thermal hardening was established, stipulated by the ordering of radiation defect structures (phases), while the degree and the temperature of maximum hardening also increase with the growth of implantation fluence and the softening observed at higher temperatures, is connected with their annealing. It was revealed that there is a rise of the temperature interval of martensitic transformation observed due to temperature increase at its beginning and end, the appearance of temperature interval between the beginning and the end of reverse transformation and the structural hysteresis of electrical resistivity. It is shown that the growth of implantation fluence reduces the probability of R- phase nanoscale particles formation.

The obtained preliminary results indicate the prospects in terms of development of radiation technologies in order to produce Ni-Ti based radiation-resistant alloys through the consistent application of implantation of high-energy heavy ions of krypton and post-radiation annealing.

## THE STRUCTURAL-PHASE STATES OF NEAR-SURFACE LAYERS IN NiTi ALLOY CAUSED BY HIGH-CURRENT ELECTRON BEAM TREATMENTS<sup>1</sup>

*M.G. OSTAPENKO*\* \*\*, *L.L. MEISNER*\* \*\*\*, *A.A. LOTKOV*\*, *E.YU. GUDIMOVA*\* \*\*, *M.A. ZAKHAROVA*\*\*\*

\*ISPMS SB RAS, pr-t Akademicheskij, Tomsk, 634021, Russia, [artifakt@ispms.tsc.ru](mailto:artifakt@ispms.tsc.ru), +7(3822)286819

\*\*NR TPU, pr-t Lenina, Tomsk, 634050, Russia

\*\*\*NR TSU, pr-t Lenina, Tomsk, 634036, Russia

The interaction of intense-pulsed energetic beams such as ion, electron and laser beams with materials and its application in industry have attracted much attention over the past few decades [1-2]. Among these pulsed beam techniques, low energy high-current pulsed electron beam is a relatively new technique developed for the surface modification of metallic materials [3]. The interaction of the pulsed electron beam with the material can introduce very fast heating, melting and possible evaporation in the surface layer of the material that are followed by a very fast cooling process due to the heat conduction toward the cold substrate. These non-equilibrium processes can easily change the structural-phase state in the surface layers. The structural-phase state modifications produce considerable changes in the basic functional properties of the alloys [4]. Therefore, the aim of our work is to study the structural-phase states of near-surface layers in NiTi alloy after electron beam treatment with surface melting.

The investigated  $\text{Ti}_{49.5}\text{Ni}_{50.5}$  (further – TiNi) alloy was prepared from iodides Ti and Ni of grade NO using six-fold arc remelting. The initial NiTi specimens at room temperature were in the two-phase state: a main phase with B2 structure, lattice parameter  $a_{B2}^0 = 3.0132 \pm 0.0005 \text{ \AA}$  and a small  $\text{Ti}_2\text{Ni}$  phase amount (<5 vol. %). Electron beam treatment was conducted at the IHCE SB RAS (Tomsk, Russia). The NiTi specimens were subjected to pulsed (pulse duration  $\tau = 150 \text{ \mu s}$ , number of pulses  $N = 5$ ) surface irradiation by a low-energy ( $U = 15 \text{ kV}$ ) high-current ( $I = 70 \text{ A}$ ) electron beam of energy densities:  $E_1 = 15 \text{ J/cm}^2$ ,  $E_2 = 20 \text{ J/cm}^2$  and  $E_3 = 30 \text{ J/cm}^2$ . XRD analysis of structural phase states in NiTi near-surface layers was performed on the equipment of the Shared Use Center “Nanotech” of ISPMS SB RAS (Tomsk, Russia) on a DRON-7 diffractometer (Burevestnik, Russia) in Co- $K_\alpha$  radiation.

It was found that increasing the power density of the electron beam from the  $E_1 = 15 \text{ J/cm}^2$  to  $E_3 = 30 \text{ J/cm}^2$  leads to an increase of the volume fraction of the martensite phase in B19' surface layer (thickness of not less than 10 microns) from 5 vol.% to about 80 vol.%, respectively. However, on the diffraction patterns taken in asymmetric Bragg diffraction geometry for the irradiated NiTi specimens with energy density in the beam  $E_1 = 15 \text{ J/cm}^2$  and  $E_2 = 20 \text{ J/cm}^2$  it was shown that decreasing the glancing angle decreases the intensity of the B19' peaks, and at the least glancing angle ( $\alpha = 3^\circ$ ), their intensity is close to zero. This means that no martensite phase is present in the new modified layer. In contrast, in samples treated with pulsed electron beams at energy density in the beam  $E_3 = 30 \text{ J/cm}^2$ , the surface layer to the depth of penetration of X-ray beam is in the martensitic state.

Analysis of changes in the lattice parameters of B2 phase on in-depth distribution from the irradiated surface TiNi samples showed that the dissolution phase  $\text{Ti}_2\text{Ni}$  the surface layer leads to a change in the ratio of Ti and Ni in the B2 phase formed by solidification of the molten layer. Formed in the main phase B2 of the modified layer enriched with titanium as compared with its original content in the B2 phase prior to irradiation. On the top surface, the Ti content can reach about 51 at.%. The increased Ti content in the surface layer also favors the martensitic transformation by increasing the  $M_s$  temperature in this layer, but the martensitic transformation was not triggered in the top surface melted zone. It could be considered that the subsurface layer had significantly deformed while the melted zone was not yet solidified.

### REFERENCES (STYLE “CONGRESS2014 TITLE REFERENCES”)

- [1] Pogrebnjak A.D., Ladysev V.S., Pogrebnjak N.A., Michaliov A.D., Shablya V.T., Valyaev A.N., Valyaev A.A., Loboda V.B. // Vacuum. – 2000. – Vol. 58. – P. 45–52.
- [2] Rotshtein V.P., Ivanov Yu.F., Markov A.B. Review in book: Materials surface processing by directed energy techniques ed Pauleau Y (Amsterdam: Elsevier).–2006.–P. 205-240.
- [3] Zhang, K. M., Yang, D. Z., Zou, J. X., Grosdidier, T., & Dong, C. // Surface and Coatings Technology. – 2006. – V. 201(6). – P. 3096-3102.
- [4] Zou J. X., Zhang K. M., Hao S. Z., Dong C., Grosdidier T. // Thin Solid Films. – 2010. – V. 519(4). – P. 1404-1415.

<sup>1</sup> The work was performed under Program of SB RAS No. III.23.2 (project No. III.23.2.1), supported by the Ministry of Education and Science of the Russian Federation (state contract No. 16.522.11.2019) and by the grant of President of the Russian Federation (Scholarship of the President of the Russian Federation SP-236.2012.4)

## INVESTIGATION OF NiTi GRADIENT SURFACE LAYERS WITH CHANGING ATOMIC CRYSTAL STRUCTURE FORMED AS A RESULT OF ELECTRON-BEAM IMPACTS<sup>1</sup>

V.O. SEMIN\*, A.A. NEYMAN\*\*, L. L. MEYSNER\*\*

\*Tomsk State University, Lenin str., 30, Tomsk, 634050, Russia, werder1@sibmail.com

\*\*Institute of Strength Physics and Materials Science of Siberian Branch Russian Academy of Sciences Russia, pr. Akademicheskii, 2/4, Tomsk, 634021, Russia, nasa@ispms.tsc.ru

At present, NiTi as Shape Memory Alloys are known to be widely practically used as very perspective functional alloys for applying in various branches of industry, especially in medicine. Its unusual behavior is associated with thermoelastic martensitic deformation occurs under certain conditions. But opportunities in making NiTi for biomedical applications are inferred different types of treatments. Therefore a lot of techniques are directed on improving biocompatibility NiTi implants by means of transforming structure in surface layers. One of the effective methods of modifying chemical and phase composition, crystalline structure of alloys is low energy high current electron beam (LEHCEB).

The purpose of present work is to investigate the influence of LEHCEB in regime of pulse melting on the structural-phase conditions and gradient structure in the surface layers of the alloy based on NiTi.

Surface treatment was carried out with LEHCEB by means of experimental equipment «SOLO» (Institute of High Current Electronics SB RAS) in the mode: the electron beam density  $10 \text{ G/cm}^2$ , 10 pulses, the single pulse duration  $50 \mu\text{s}$ .

Surface modification is based on two modification factors: temperature wave and wave of stress. It causes very fast heating, melting and subsequent quenching with high velocity of moving the front of crystallization (up to  $10^9 \text{ K/c}$ ). Such combine heat and stress waves treatment allows forming structure gradient with specific distribution of elements (Ti, Ni, C, O) in depth from the surface. To perform cross section investigations, the specimens were cut in the direction of beam axis and polished mechanically. Transmission electron microscopy (JEM 2100 JEOL, Japan CCU «Nanotech» ISPMS SB RAS (SUC TRC SB RAS)) was carried out by the thin foil method preparing method of ion etching (Fig. 1).

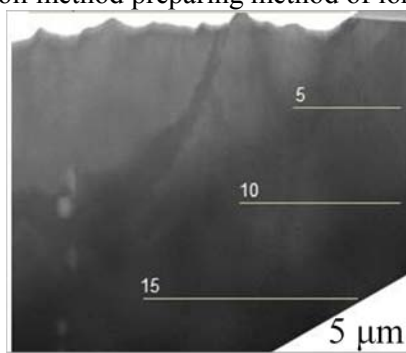


Fig. 1. Bright field image of foil NiTi after LEHCEB treatment.

Experimental procedure of layer-by-layer analyses was as follows. Microdiffraction patterns were obtained with small step from the surface up to the depth ( $30 \mu\text{m}$ ) including melting zone, heat affected zone and untreated layers. Decoding of microdiffractions obtaining from treated and untreated samples was conducting with specific computer program «MicroDif» using programming code of MathCad. The program designed comprise crystallographic data for all specific in Ni-Ti system phases. It becomes possible to determine indexes of crystallographic planes and directions and accurately calculate lattice parameters.

Transmission electron microscopy results shown that after electron beam treatment crystalline structure changed dramatically. Subsurface layers formed from the melt are characterized by one phase condition based on B2 structure having significant distortion of crystalline lattice. The value of lattice distortion reaches  $\sim 5\%$  near the surface (up to  $8 \mu\text{m}$ ) and decreases to initial value on the depth of  $20 \mu\text{m}$ . The surface layers of material upon melting and recrystallization to a depth of several microns characterized by the columnar structure of nano-sized scale, oriented perpendicular to the exposed surface of the sample.

## DIFFRACTION COMPLEX INVESTIGATION OF SILICONE COATINGS AND MODIFIED SURFACE LAYERS OF TITANIUM NICKEL

*S.N. MEISNER, A.I. LOTKOV, L.L. MEISNER, A.V. TVERDOKHLEBOVA*

*Institute of Strength Physics and Materials Science, 2/4, pr. Akademicheskii, Tomsk, 634021, Russia*

The paper presents the investigation results of the structure and the physico-mechanical properties of silicon coatings with a submicron thickness on the near-surface layers of a NiTi substrate. The coatings were produced by the different magnetron deposition regimes.

The interface layers between the coating and NiTi substrate were found using Auger-electron spectroscopy. The interface layers contain a high concentration of impurity elements such as oxygen and carbon. The thickness of the interface layers and the concentration of oxygen and carbon could be varied by changing the deposition parameters.

The X-ray structure analysis using the Grazing Incidence Diffraction Method showed that, under the coatings, the near-surface layer of the NiTi substrate was characterized, as a rule, by a three-phase condition: a high-temperature phase with a B2 structure, a martensite phase B19' and a Ti<sub>2</sub>Ni phase (fig. 1). The B2 and Ti<sub>2</sub>Ni phases were present in the samples before the sputtering, whereas the B19' phase was formed after magnetron sputtering. The martensite phase indicates the presence of elastic stress fields induced by the magnetron deposition.

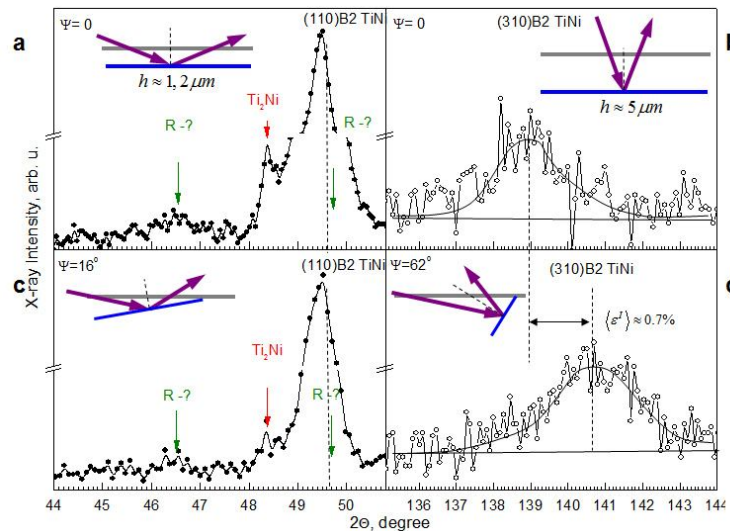


Fig. 1. Fragments of X-ray diffraction patterns for the TiNi specimens with Si coatings sputtered by the direct current and pulse magnetron deposition regimes: (a), (b) - Bragg diffraction geometry, (c), (d) - asymmetric diffraction scheme ( $\alpha = 8^\circ$ ), Co-K $\alpha$  radiation.

The crystal lattice strain ( $\epsilon''$ ) was estimated using the approximation method. It was found that in the samples with the silicon coatings deposited by the pulse magnetron method these strains were 2-3 times greater than those in the samples with direct current sputtering. It should be noted that the values  $\epsilon''$  are also large and change from 0.1% to 0.9%. Taking into account that the size of the coherent-scattering region in the near-surface layers of the NiTi substrate  $D > 100$  nm, we can make a conclusion that these strains caused by the surface treatment are not associated with the crystalline grain size.

Analysis of the strain values associated with the stresses showed that in the near-surface layer of the NiTi substrate the crystal lattice of the B2 phase underwent a tensile stress perpendicular to the sample plane and a compressive stress in the planes that were parallel to the surface. The mean levels of both stresses were 0.6% - 1%.

The microstructure changes of the near-surface layers in the modified NiTi substrate by the electron backscattered diffraction (EBSD) method showed that as a result of the coating deposition refining of the interface layer of the NiTi substrate occurred. In the near-surface layer of the TiNi substrate low-angle boundary is observed. Those findings conform with the X-ray structure analysis datas on the presence of the significant elastic stresses in the TiNi substrate layer adjoining the coating. Probably a partial removal of the elastic stresses occurs with the formation of the low-angle boundaries in those layers.

## STRESSES IN INTERFACE BETWEEN COATING AND SUBSTRATE INDUCED BY THERMAL DIFFUSION AT EXTERNAL HEATING<sup>1</sup>

*M.V. CHEPAK-GIZBREKHT\**, *A.G. KNYAZEVA\*\**

*Tomsk Polytechnic University, 30, Lenin ave., Tomsk, 634050, Russia*

*\*mv2016@mail.ru, \*\*anna-knyazeva@mail.ru*

The processes of thermal material treating are accompanied by modification of structure and properties as a result of thermo activated processes. At that, fast heating, which is typical for electron-beam and ion-plasma treatment processes, leads to the appearance of new effects concerned with the processes, which may be neglected at slow heating. One of them is thermo diffusion. This effect is studied enough for gases and liquids and, for example, it is used to separate mixtures. For solid materials the influence of thermo diffusion is taken into account in directional monocrystal crystallization processes. Recently, this effect has been neglected, because diffusion processes (tempering and annealing) were conducted in the similar to stationary conditions. However, in high speed temperature treatment conditions the neglect of thermo diffusion is not allowed.

On the other hand, fast heating, which is accompanied by a mass transfer process, is the reason for stresses and deformations in a treatment zone. It changes, in its turn, not only physical, but mechanical properties, too.

The investigation of this effect experimentally is difficult because of its high speed passing. Therefore, the main information about the role of thermo diffusion can give mathematical modeling. As far as the phenomenon is poorly investigated for solid materials and the conditions of particle flow treatment, it is necessary to conduct a purposeful research of the conditions, when it is developed strikingly. For this purpose we need to make the formulation of special physical models, corresponding to treatment conditions.

One of those models is the fast heating of a coated material. We suppose that the diffusant impurity is contained only in coating. The heating of the plate with coating is happening evenly. The heating and diffusion zone for the observation period is much less than the plate thickness. Lateral surfaces of the plate are isolated, so heat fluxes are equal to zero. In these conditions it is possible to accept the problem as one-dimensional. The functions of concentration and temperature on the time and coordinates are found [1].

In this paper we consider the equilibrium problem of the elastic plate with coating; as far as we assume that the temperature is far from materials melting temperature. Thermal diffusion role in the formation of stresses and deformations can be investigated in the following way. Using the correlations from thermo elasticity theory [2], we can write the ratio between the components of stresses and deformations, which depend not only on temperature, but also on concentration. Whereas, the solutions for bodies with a canonical form are found, they can be used for our problem, having summarized in the case of a double-layer plate with thermo diffusion.

The problem is solved analytically precisely by Laplace integral transform method.

A received solution allows revealing the following: at particular ratio of thermo diffusion coefficients near the bound "coating-substrate" the amplitude of stresses is increasing, the sign of stresses may change, and maxima and minima are arising near the bound. All of these factors (stresses remain in material after treatment because of irreversible processes) influence directly on adhesive properties.

On the basis of the found dependencies it is possible to make a forecast about the influence of mechanical and thermo physical material properties ratio on the amount of residual stresses and the depth of diffusion zones.

### REFERENCES

- [1] *A.G. Knyazeva, M.V. Chepak-Gizbrekht // Russian Physics Journal. – 2013. Vol. 56. – № 12/2.*
- [2] *Bruno A. Boley, Jerome H. Weiner // Theory of thermal stresses. – Word-Publishing Inc., 1964.*

<sup>1</sup> This work was supported by Russian Foundation for Basic Research, grant number 13–08–98058

## EVOLUTION OF STRUCTURE AND PHASE COMPOSITION OF TITANIUM ALLOYED WITH MOLYBDENUM, CROMIUM AND ZIRCONIUM AFTER COMPRESSION PLASMA FLOWS IMPACT AND HIGH TEMPERATURE INFLUENCE

*V.I. SHYMANSKI\*, N.N. CHERENDA\*, V.V. UGLOV\*, V.M. ASTASHYNSKI\*\*, A.M. KUZMITSKI\*\**

*\* Belarusian State University, Minsk, Belarus, e-mail: [shymanskiv@mail.ru](mailto:shymanskiv@mail.ru), [uglov@bsu.by](mailto:uglov@bsu.by) 220030, Nezavisimosty ave., 4*

*\*\* A.V.Luikov Heat and Mass Transfer of the National Academy of Science of Belarus, Minsk, Belarus, e-mail: [ast@hmti.ac.by](mailto:ast@hmti.ac.by) 220072, P. Brovka Str., 15*

Producing of the surface layers alloyed with different elements in materials is a promising way for improving its physical and mechanical properties. Ion implantation can be considered as a classical approach for this purpose. Nowadays the influence of plasma flows or beams of charged particles on a metal is more effective method for surface modification. In these cases alloying of the surface layer is a result of atoms penetration from the atmosphere gas or previously deposited metal thin coating. The latter allows to produce alloys with different metallic components with controlled its concentration. The multicomponent alloying is possible in the case of high energy density combined with long pulse duration of impacting flow.

Titanium is a widespread material but its application depends on its physical and mechanical properties that are achieved by its alloying with other metals. In the present work the surface layers in titanium were alloyed with Mo, Cr and Zr atoms by means of compression plasma flows impact on the Mo/Cr/Ti, Cr/Mo/Ti and Mo/Zr/Ti systems. The Mo, Cr and Zr coatings with the thickness about 1 micrometer were formed during arc-vacuum deposition. The compression plasma flows were generated by a magneto-plasma compressor compact geometry in the residual (400 Pa) nitrogen atmosphere. The energy density absorbed by the surface layer of impacted material was changed from 13 to 35 J/cm<sup>2</sup> that allowed to form the surface layers with different elemental compositions. After the plasma impact the samples were undergone to high-temperature annealing in vacuum as well as in air at 100 – 500 °C.

The described above influence by compression plasma flows allowed to form the surface layers in the titanium substrate alloyed with the atoms from the coating deposited previously. The research of spatial distribution of the alloying elements showed their deep penetration (up to 20 micrometers) and the uniform distribution along the melted layer, rising of absorbed energy density resulting in increase of alloyed layer and decrease of the alloying elements concentration. Since Mo, Cr and Zr atoms possess different limit of dissolubility in the lattice of titanium change of their concentration provided the different ratio of low-temperature ( $\alpha$ ) and high-temperature ( $\beta$ ) phases of titanium in the surface layer. The high-temperature annealing following to the plasma influence results in decomposition of the solid solutions  $\beta$ -Ti(Mo,Cr) and  $\beta$ -Ti(Mo,Zr) formed during solidification of the surface melted layer. X-ray diffraction analysis allowed to find the enhancement of the thermal stability of the multicomponents solid solutions compared to the  $\beta$ -Ti(Mo),  $\beta$ -Ti(Cr) and  $\beta$ -Ti(Zr) as a result of different diffusion mobility of the dissolved atoms. Formation of the solid solution based on the titanium crystal lattice as well as the surface nitride layer prevents the bulk material from the intense oxidation during high-temperature annealing in air.

**SURFACE ALLOYING OF COPPER USING A QUASISTATIONARY PLASMA ACCELERATOR**

*N.N. CHERENDA\**, *A.P. LASKOVNEV\*\**, *A.V. BASALAI\*\**, *V.V. UGLOV\**, *V.M. ASTASHYNSKI\*\*\**, *A.M. KUZMITSKI\*\*\**

*\* Belarusian State University, Nezavisimosti ave., 4, Minsk, 220030, Belarus,  
e-mail: Cherenda@bsu.by, +375172265834*

*\*\* State Scientific Institution "The Physical Technical Institute of the National Academy  
of sciences of Belarus", Kuprevich str., 10, Minsk, 220141, Belarus*

*\*\*\* A.V.Lykov Heat and Mass Transfer Institute of the National Academy of sciences of Belarus,  
P.Brovka str., Minsk, 220072, Belarus*

Compression plasma flows generated in quasi-stationary plasma accelerators are characterized by comparatively long lifetime, high temperature and high velocity of plasma particles. These main characteristics allow us to use effectively compression plasma flows for "coating/substrate" system mixing with subsequent formation of deep layers (tens of micrometers) containing atoms of both the coating and the substrate. A high-cooling speed of the surface layer provides formation of metastable phases. This approach was used to form different types of alloys in the surface layer of copper. Titanium, zirconium and chromium were chosen as alloying elements. Chromium forms mechanical mixture with copper while zirconium and titanium form intermetallides and solid solutions in copper with a different solid solubility limit according to the binary phase diagrams. Copper possesses high heat conductivity in contrast to other metals resulting in a very high cooling speed. Thus, one can expect a substantial difference between phase composition formed by plasma impact and equilibrium phase composition.

Treatment of copper M1 by compression plasma flows was carried out with the energy absorbed by the surface in the range of 14-23 J/cm<sup>2</sup> per pulse to obtain different concentrations of alloying elements in the surface layer. The investigations conducted earlier showed that the increase of absorbed energy resulted in the alloying element concentration decrease. Nitrogen was used as a plasma forming gas. The number of pulses varied in the range of 1-6, which influenced homogeneity and the concentration of alloying elements. A number of techniques including X-ray diffraction, Rutherford backscattering spectrometry, scanning electron microscopy, optical microscopy, energy dispersive X-ray microanalysis etc. were used for characterization of the surface layer.

The findings showed that phase composition of the alloyed layer correlated with the type of equilibrium phase diagram. Insoluble elements (Cr-Cu) form a mechanical mixture with dispersed structure. Zirconium possessing a low solid solubility limit leads to formation of Cu<sub>5</sub>Zr intermetallide and Cu(Zr) oversaturated solid solution. The increase of the solid solubility limit results in formation of a highly oversaturated solid solution. This effect was observed in case of titanium atoms alloying. The following annealing leads to decomposition of the metastable supersaturated solid solution with precipitation of fine-dispersed Cu<sub>4</sub>Ti intermetallides. The formation of alloying elements nitrides due to the interaction of surface atoms with a plasma forming gas was found. The type of alloying element influences strongly microstructure of the alloyed layer, copper grains size and texture. The mechanisms of the observed structural changes are discussed.

High heat conductivity of copper in contrast to other elements results in a short time of melt existence and a short time of liquid mixing by convection whirls. Thus, strong nonuniformity of alloying elements distribution is observed. The increase of the number of pulses up to 6 leads to more uniform distribution.

The structure and phase composition changes resulted in the improvement of copper surface layer mechanical properties. For instance alloying by titanium atoms allows increasing the surface layer microhardness 1.5 times and decreasing the friction coefficient 2.5 times.

The findings showed that compression plasma flows could be effectively used for predictable formation of a number of alloys in the surface layer of copper with enhanced properties by means of "coating/copper" system treatment.

## STRUCTURAL AND MORFOLOGICAL FEATURES OF TINI SURFACE LAYERS FORMED WITH HIGH CURRENT PULSED ELECTRON BEAM<sup>1</sup>

A.A. NEYMAN\*, V.O. SEMIN\*, L.L. MEYSNER\*, A.I. LOTKOV\*, N.N. KOVAL\*\*, A.D. TEREŠOV\*\*

\*Institute of Strength Physics and Materials Science of Siberian Branch Russian Academy of Sciences,  
pr. Akademicheskii, 2/4, Tomsk, 634021, Russia, nasa@ispms.tsc.ru, (3822)28699

\*\*Institute of High Current Electronics of Siberian Branch Russian Academy of Sciences,  
pr. Akademicheskii, 2/3, Tomsk, 634055, Russia

At the moment attention is given to the surface of alloys based on nickel titanium is associated with its use in medicine. Known that impact of low-energy high-current electron beams can change the chemical and phase composition, grains and defect structure both in the zone of direct impact as well as in the deeper areas of the material. Being formed surface layer structure strongly depends on the electron-beam impact parameters.

The purpose of the work is to determine the regularities of structure and morphology formation in the based on NiTi alloy surface layers due to electron-beam impacts in the pulsed melting mode.

Surface modification of NiTi (Ti<sub>49.5</sub>Ni<sub>50.5</sub>) samples performed on a high-current low-energy electron beam plant «SOLO» (IHCE SB RAS, Tomsk, Russia) in two regimes. First regime is: beam energy density  $E=10 \text{ J/cm}^2$ , 10 pulses, pulse duration 50 ms. Second regime is:  $E=30 \text{ J/cm}^2$ , 5 pulses, pulse duration 50 ms.

Studies were conducted using X-ray diffraction, optical, scanning and transmission electron microscopy methods. It was found that various treatments have led to formation of completely different structural states in NiTi surface layers. In the samples with the first regime impact superficial layer is like a single crystal structure, oriented normally to the plane of the modified surface (Fig. 1a,b). There is a clear boundary between dislocation structures of the remelted and underlying layers (Fig. 1b). The analysis of electron diffraction pattern showed that the structure of these layers belongs to the B2 phase.

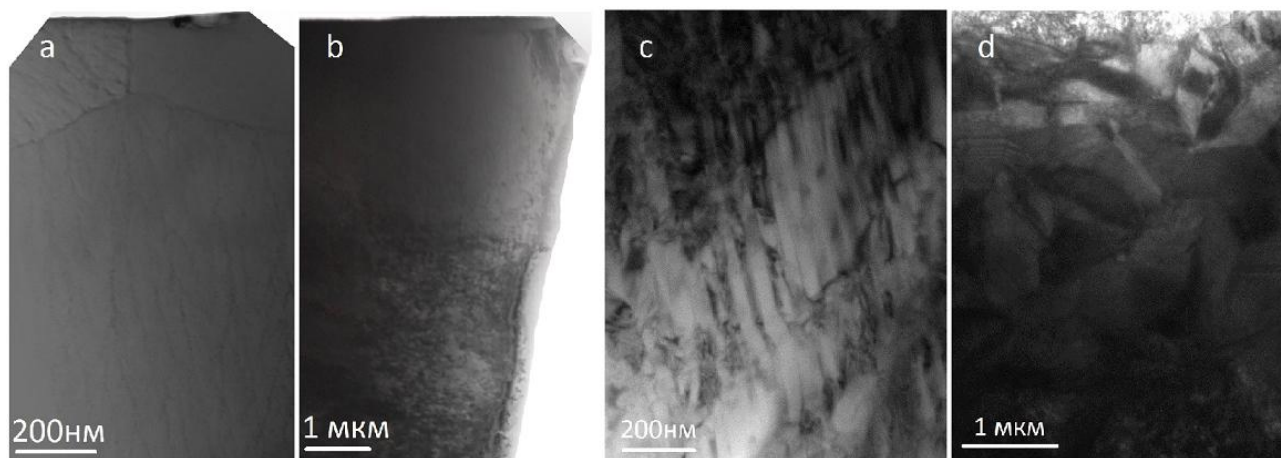


Fig. 1. Bright field images in the areas of direct electron beam impact in the NiTi samples.  
a, b – first and c, d - second regime impact.

In the sample with the second regime impact, a more complex and multi-layered morphological picture is observed. Surface layer deep into 30 microns is characterized by a martensitic R and B19' structures although electron beam melted depth not exceed 15 microns. The top layer has a fine crystalline morphology randomly oriented mixed martensitic lamellae (Fig. 1c). As we move deeper into the material crystallites become larger and their orientation acquires several specific directions lamellae (Fig. 1d). It can be assumed that this accommodative martensite, which originated in the field of elastic stresses in the heat affected zone which explains the crystallites orientation.

Further study is expected to be carried out to determine the volume fraction of martensite phases and their influence on the deformation behavior of the material.

<sup>1</sup> This work was supported by SB RAS project № III.23.2.1 (in the parts of research by methods XRD and SEM) and by RFBR grant 14-08-31602\_mol\_a (in the part of TEM and sample preparation).



## IMPROVING THE EXPLOITATION PROPERTIES OF TITANIUM ALLOY BY HIGH DENSITY PLASMA

*K.N. RAMAZANOV, V.V. BUDILOV, I.S RAMAZANOV*

*Ufa State Aviation Technical University, K. Marx str.12, Ufa, 450000, RF, ramazanovkn@gmail.com, +7(347)2730763*

Titanium alloys are used in the aviation industry to make critical products such as helicopter rotor head, shafts, gears, compressor parts of turbine engine, wheels and low-pressure and high-pressure compressor vanes. However, there are negative properties that limit using of titanium alloys as a structural material: low surface hardness and low wear resistance [1].

The ion nitriding process is an effective method of titanium alloys surface hardening. However, it takes a long time, so high density plasma is used to intensify the process. The hollow cathode effect (HCE) is an efficient way to increase plasma density [2].

The aim of presented work is to study the influence of the ion nitriding using HCE on the microstructure, phase composition, surface layer hardness of VT-6 titanium alloy.

Analysis of obtained volt-ampere characteristics showed that under the HCE discharge current several times higher than without the HCE occurrence at the same discharge voltage. Found that generation of charged particles increases due to oscillating electrons in cathode hollow formed by part surface and screen.

Microhardness test of nitrided samples showed that surface microhardness increased to 2.5 times in case of use of the HCE, and to 2 times without HCE. Found that microhardness growth occurs due to titanium nitrides and alloying elements nitrides formation on the samples surface.

Microscopic examination of nitrided samples of VT-6 showed presence of nitride layer and diffusion zone. Found that ion nitriding using HCE leads to thicker nitrided case comparing to nitriding without HCE occurrence. So, nitride layer and diffusion zone thicknesses of samples nitride with HCE was 20...25  $\mu\text{m}$  and 60...80  $\mu\text{m}$  respectively, according to 17  $\mu\text{m}$  and 19  $\mu\text{m}$  for case without HCE.

X-ray diffraction analysis of nitride samples showed decreasing of  $\alpha$ -phase and increasing of  $\beta$ -phase amounts due to approaching the temperature of  $\alpha \rightarrow \beta$  polymorph transformation. Level of this transition in case of using HCE was higher comparing to conventional ion nitriding. Process had led to titanium nitrides formation of various stoichiometry ( $TiN$ ,  $Ti_2N$ ).

From analysis of obtained data revealed the ion nitriding with HCE leads to mechanical characteristics improvement. Therefore, it is an effective way to better the operational properties of parts of VT-6 titanium alloy.

### REFERENCES

- [1] *Chechulin B. B., Ushkov S., Razuvaeva I. H., Goldfane V.N. // Titanium alloys in mechanical engineering, Leningrad, «Mashinostroenie», 1977, 247p.*
- [2] *V.V. Budilov, R.D. Agzamov, K.N. Ramazanov // Metal Science and Heat Treatment. 2007, Volume 49, Issue 7-8, pp 358-361.*

## **RADIATION GRAFT POLYMERIZATION OF POLYMETHYLMETHACRYLATE ON POLYMER FILMS**

*M.A. REZVOVA, V.D. ZHEVNYAK, K. UEMURA, V. PAK*

*Kemerovo State University, Krasnaya St. 6, Kemerovo, E-mail: rezvovamasha@rambler.ru, phone: +79130796140*

The testing of different methods of radiation graft polymerization of polymethylmethacrylate on the films of polymeric materials was conducted in order to increase their strength. The problem of hardening investigated polymeric materials is associated with finding ways to improve the performance of products based on them, namely products used in medicine for the introduction into the human body. As the objects of study were selected polyamide, polyethylene terephthalate film and the film of low density polyethylene. Polymethylmethacrylate – biologically inert polymer, allowed for use in medical products, was used for graft. Three methods of graft polymerization were studied: the method of crosslinking of polymer blends, the peroxide method and direct method of vaccination from a monomer solution of different concentrations. Radiation graft polymerization was carried out under the action of  $\gamma$  - radiation  $\text{Co}^{60}$  on installing MPX- $\gamma$ -20 with a radiation dose rate of 2.2 kGr/h. The conditions of the processes were chosen, the radiation yield of grafted polymer was defined, the strength properties of the modified materials were investigated.

## NEW BINARY MOLYBDATES: SYNTHESIS, STRUCTURE, PROPERTIES<sup>1</sup>

*O.D. CHIMITOVA\**, *B.G. BAZAROV\**, *A.E. SARAPULOVA\*\**, *A. KOMAREK\*\*\**, *D. MIKHAILOVA\*\**,

*S.G. DORZHIEVA\**, *H. EHRENBERG\*\*\**, *J.G. BAZAROVA\**

\*Baikal Institute of Nature Management SB, RAS, Sakh'yanovoi street 6, Ulan-Ude, 670047, *chimitova\_od@mail.ru*, 8(3012)433362

\*\*Max Planck Institute for Chemical Physics of Solids, Nötnitzer Straße 40, D-01187 Dresden, Germany

\*\*\*Karlsruhe Institute of Technology (KIT), Institute for Applied Materials (IAM), Hermann-von-Helmholtz-Platz 1, D-76344 Eggenstein-Leopoldshafen, Germany

The present work is devoted to synthesis of complex molybdenum oxides as possible functional materials such as electrolytes, catalysts and ion battery materials [1]. It is known that  $AR(MoO_4)_2$  compounds with A - heavy alkali metal, and R- magnetic cations like  $Fe^{3+}$  or  $Cr^{3+}$  belongs to the group of magnetic solids [2]. These compounds exhibit various physical properties due to a polymorphism of their structures [3]. In the present work the phase formation in the  $A-Fe^{II,III}-Mo-O$  system (A= Rb, Cs) at elevated temperatures was studied.

During the investigation of the  $Rb(Cs)-Fe^{II,III}-Mo-O$  system new crystalline phases were found:  $A_2Fe_2(MoO_4)_3$ ,  $Cs_4Fe(MoO_4)_3$  and  $AFe_5(MoO_4)_7$  (A=Rb, Cs). Single crystals of the  $AFe_5(MoO_4)_7$  composition were synthesized by a slowly cooling from 1073 K down to room temperature in an inert atmosphere. A monoclinic unit cell with  $a = 6.8987(4)$  Å,  $b = 21.2912(12)$  Å,  $c = 8.6833(5)$  Å and  $\beta = 102.190(2)^\circ$  was determined by single-crystal X-ray diffraction. The data were collected with a Bruker D8 VENTURE diffractometer using monochromatized Mo-K $\alpha$  radiation at room temperature. The structure was solved and refined in the space group P21/m. It consists of separate  $FeO_6$  octahedra and zigzag  $Fe_4O_{18}$ -units of edge-sharing  $FeO_6$ -octahedra (Fig. 1), which are connected through corners with  $MoO_4$ -tetrahedra. Rubidium atoms occupy channels in the structure along the a-axis. From a structural point of view, a high ionic conductivity of Rb ions at elevated temperature may be expected for this phase.

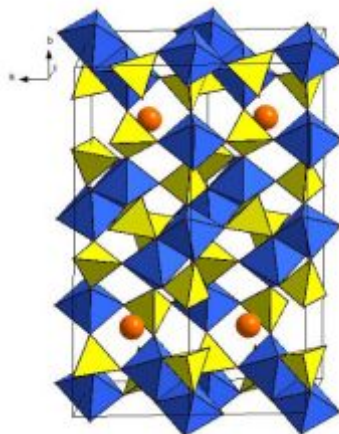


Figure 1. Crystal structure of  $RbFe_5(MoO_4)_7$ .

Blue octahedra are  $FeO_6$ -units,  $MoO_4$ -tetrahedra are yellow, Rb-ions are orange spheres.

For  $CsFe_5(MoO_4)_7$  with  $Fe^{+2.6}$ , there are three different Fe sites in the structure: two 4 f and one 2 e. Based on charge neutrality, a simple ionic model of localized electrons would suggest the existence of  $Fe^{3+}$  on one 4 f and the 2 e site and  $Fe^{2+}$  on the other 4 f site. Determination of the antiferromagnetic structure of  $CsFe_5(MoO_4)_7$  from neutron powder diffraction revealed the smallest magnetic moment of  $1.6 \mu_B$  for Fe on the 2 e site in comparison to  $2.6$  and  $3.5 \mu_B$  for Fe on 4f sites. Complex molybdates of an alkaline metal and  $Fe^{II}$  with  $Mo_yO_x$  clusters and a metallic Mo-Mo bond seem to be stable only for a small alkaline element. All attempts to obtain Cs, Fe molybdates with  $Fe^{2+}$  and Mo in an oxidation state lower than +6.

### REFERENCES

- [1] Kenisarin, M.M. // Renewable sustainable energy Rev. – 2010. – Vol. 14. – 955-970.
- [2] Isupov, V.A. // *Ferroelectrics* – 2005, - Vol. 321. 63-90 Authors // Journal. – Year. – Volume. – №. Pages.
- [3] Inami T., Ajiro Y., Goto T. // *J. Phys. Soc. Japan*. – 1996. – Vol. 65, 2374–2376.
- [4] T. Namsaraeva, B. Bazarov, D. Mikhailova, N. Kuratieva, et.al. // *Eur. J. Inorg. Chem.* -2011, 2832–2841

<sup>1</sup> This work was partially supported by SB RAS (Grant 28.13), Grant of the Presidium RAS № 8, Grant of the RF President «MK-6247.2013.2»

## STRUCTURAL-PHASE CONDITIONS OF THE “TA-COATING/NITIT-SUBSTRATE” SURFACE LAYERS MELTED WITH LOW-ENERGY HIGH-CURRENT ELECTRON BEAM<sup>1</sup>

*E.YU. GUDIMOVA\*\*\*, L.L. MEISNER\*\*\*, A.I. LOTKOV\*, M.G. OSTAPENKO\**

*\*Institute of Strength Physics and Materials Science of Siberian Branch Russian Academy of Sciences, 2/4, pr. Akademicheskii, Tomsk, 634021, Russia, [egu@ispms.tsc.ru](mailto:egu@ispms.tsc.ru), (3822)286-819*

*\*\*National Research Tomsk State University, 36, pr. Lenina, Tomsk, 634050, Russia*

TiNi-based alloys widely applied in various fields of medicine on account of its unique properties, such as shape memory effect and superelasticity [1]. Using of these alloys for cardiovascular surgery requires increased radiopacity, biocompatibility and corrosion resistance [2]. The solution to this problem is possible by using an integrated approach, which includes magnetron sputtering deposition of radiopacity coatings and subsequent electron beam treatment. This surface modification makes it possible to form surface layers with new physical properties due to changes in structural-phase conditions and preserve original properties in the material bulk. The purpose of the work is structural-phase conditions of the “Ta-coating/ NiTi-substrate” surface layers melted with low-energy high-current electron beam.

The initial samples (TiNi) were in the two-phase state: main phase B2 (bcc structure, lattice parameter  $a_{B2}^0 = 3.0188 \pm 0.0005 \text{ \AA}$ ) and small amount (<5 vol %) of the intermetallic  $Ti_2Ni$  phase. Modification of the surface samples was conducted in IHCE SB RAS (Tomsk). Magnetron sputtering deposition of tantalum coatings on surface TiNi (further – Ta/TiNi) was conducted with the following parameters: voltage  $U = 270 \text{ B}$ , target current (Ta)  $I = 2.5 \text{ A}$ , growth rate of the deposited layer of  $v = 10 \text{ \mu m/h}$ . The working chamber prior to the deposition of coatings was filled with Ar under pressure  $P_{Ar} = 0.3 \text{ Pa}$ . The thickness of coatings composed 500 nm. Further treatment of samples Ta/NiTi carried out low-energy ( $U = 15 \text{ kV}$ ) high-current ( $I = 70 \text{ A}$ ) electron beam under high vacuum ( $\sim 10^{-6} \text{ Pa}$ ), at energy density  $E = 20 \text{ J/cm}^2$ , duration pulse  $\tau = 150 \text{ \mu s}$  and a quantity of pulses  $n = 5$ . Investigation of the structure parameters have been studied by the methods of X-ray diffraction (XRD) analysis on the DRON-7 diffractometer using a symmetrical and asymmetric ( $\alpha = 3^\circ, 6^\circ, 12^\circ$ ) schemes in Co-K $\alpha$  radiation (shared use center «Nanotech» ISPMS SB RAS, Tomsk).

XRD patterns of samples Ta/NiTi irradiated by electron beams showed the presence of phases B2, B19' and a small amount of  $\alpha$ - Ta (~5 vol. %). It was found [3] that the  $Ni_{50}Ti_{45}Ta_5$  alloy possesses high temperature shape memory effect and at room temperature is in the martensitic state. The volume fraction of martensitic phase B19' increases with decreasing thickness of the analyzed layer (decreasing angle  $\alpha$ ). It is apparent that this phase is localized in the surface region of the sample. The separation by the approximation method of the contributions to the physical broadening of the X-ray reflections showed that sizes  $D$  the regions of coherent scattering B2-phase in the surface layers Ta/NiTi after electron beam treatment does not change relatively values in the initial sample  $D \geq 100 \text{ nm}$ , and microstrain and stress second kinds are  $\epsilon^{II} = 0,003$ ,  $\sigma^{II} = E/337$ , respectively. It should be noted, that the lattice parameter of B2 phase decreased to  $a_{B2} = 3.0144 \pm 0.0005 \text{ \AA}$ . Most likely this is due to a change in the surface layers chemical composition by mixing the coating and substrate. Thus, the pulsed electron beam treatment of surface layers of NiTi alloy with tantalum coatings leads to the formation of surface alloy based on NiTi, doped Ta.

### REFERENCES

- [1] *Otsuka K., Ren X. // Progress in Materials Science. – 2005 – V.50 – 511–678 pp*
- [2] *Ratner B.D., Hoffman A.S. // Biomaterials science: an introduction to materials in medicine. Edited by B.D. Ratner et.al., 2-nd edition, Elsevier Academic Press, 2004, 201 – 218 pp*
- [3] *Gong C.W., Wang Y.N., Yang D.Z. // Journal of Alloys and Compounds, - 2006. - 61-65 pp*

<sup>1</sup> The work was performed under Program of SB RAS (project No. III.23.2.1) and by the grant of Russian Foundation for Basic Sciences (№ 14-08-31602\_mol\_a)

## MODIFICATION OF THE NEAR-SURFACE LAYERS OF STEEL AND COPPER PLATES UNDER THE ACTION OF DISCHARGE PLASMA<sup>1</sup>

*M.V. EROFEEV\*·\*\**, *M.A. SHULEPOV\**, *V.F. TARASENKO\*·\*\**, *K.V. OSKOMOV\**

*\*Institute of High Current Electronics, Academicheskyy Ave. 2/3, Tomsk, 634055, Russia, mve@loi.hcei.tsc.ru*

*\*\*Tomsk Polytechnic University, Lenin Ave. 30, Tomsk, 634050, Russia*

Electric discharges of different types as well as electron beams are now widely used for the modification of near-surface layers of various materials [1]. As is known [2], a volume discharge can be generated using inhomogeneous electric field in air at atmospheric pressure. For this purpose, high-voltage (~100 kV) pulses of nanosecond duration are applied to a gasfilled interelectrode gap. A specific feature of such discharges is the accompanying X-ray emission and the formation of the supershort avalanches electron beams (SAEBs) [3-5]. A runaway electron preionized diffuse discharge (REP DD) is easily realized in various gases and at different pressures. At the REP DD, the anode is influenced by the plasma of a dense nanosecond discharge with the specific input power up to hundreds of megawatt per a cubic centimeter, by the SAEB. This allows forecasting the REP DD application for modification of metal surfaces in different technological processes as well as for the dielectric surface modification at a definite anode design [6-9].

Surface of steel and copper plates were treated by plasma of a REP DD in air, CO<sub>2</sub> and nitrogen at atmospheric pressure in a periodic pulse regime at frequencies of 1 Hz (RADAN-220) and 500 Hz (NPG-15/2000N). The experiments were performed using a gap with the plane anode and cathode with a small radius of curvature. A distance from a flat anode to a tubular cathode could be varied within 7–16 mm.

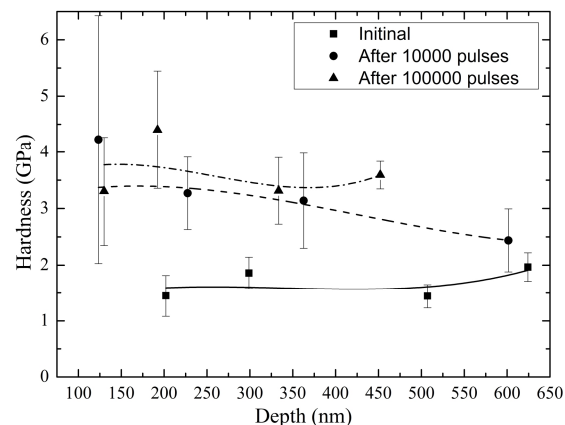


Fig. 1. The hardness of the surface layer of steel specimens before and after treated in nitrogen. NPG-15/2000N pulser

It is established that the surface layer of the discharge-treated the steel and copper plates is cleaned from carbon contaminations. The investigations performed have shown that when all specimens are treated with REP DDs, oxidation of the surface layer is observed too. Hardness and elastic modulus of the samples were measured by Berkovic diamond indenter on the system of NanoTest 600. We analyzed load-unload curves by Oliver-Pharr method [10] at 2, 5, 10 and 20 mN loads. It has been found that the treatment of a copper and steel surface by this type of discharge increases the hardness of the surface layers (see Fig. 1 for steel plate). This increases the hardness of a thin surface layer after 10<sup>5</sup> pulses is by a factor up to 3.

### REFERENCES

- [1] *A. N. Didenko, Yu. Sharkeev, et al // Long-Range Effects in Ion-Implanted Metallic Materials. – NTL Publishers, Tomsk, 2004.*
- [2] *L. V. Tarasova, L. N. Khudyakova // Sov. Tech. Phys. – 1969. – 14. 1148–1151.*
- [3] *V. F. Tarasenko, E. Kh. Bakst, A. G. Burachenko, I. D. Kostyrya, et al // Plasma Devices Oper. – 2008. – 16. 267–298.*
- [4] *E. Kh. Bakst, A. G. Burachenko, I. D. Kostyrya, M. I. Lomaev, et al // J. Phys. D: Appl. Phys. – 2009. – 42. 185201.*
- [5] *V. F. Tarasenko // Plasma Physics Reports. – 2011. – 37. 409–421.*
- [6] *M. A. Shulepov, V. F. Tarasenko, I. M. Goncharenko, N. N. Koval', et al // Technical Physics Letters. – 2008. – 34. 296–299.*
- [7] *V. F. Tarasenko, M. A. Shulepov // High-Power Laser Ablation VII Proc. SPIE Conf. 7005. – 2008 70051N.*
- [8] *M. A. Shulepov, Y. K. Akhmadeev, V. F. Tarasenko, Y. A. Kolubaeva, et al // Russian Physics Journal. – 2011. – 53. 1290–1294.*
- [9] *A. V. Voitsekhovskii, D. V. Grigor'ev, A. G. Korotaev, et al // Russian Physics Journal. – 2011. – 54. 1152–1155.*
- [10] *W. Oliver, J. Pharr // J. Mater. Res. – 1992. – 7. 1564–1572.*

<sup>1</sup>This work was supported by the framework of the State task for HCEI SB RAS, project #9.5.2.

## COMPARATIVE EXPERIMENTS ON ION BOMBARDMENT AND MECHANICAL SHOCK LOADING OF Al-Cu-Mg ALLOYS

V.V. Ovchinnikov\*, N.V. Gushchina\*, L.I. Kaigorodova\*\*  
A.N. Grigoriev\*\*\*, A.V. Pavlenko\*\*, V.V. Plokhoi\*\*\*

\*Institute of Electrophysics, UB RAS, Amundsena Str. 106, Yekaterinburg, 620016, Russia, viae05@rambler.ru, (343)267-87-74

\*\*Institute of Metal Physics, UB RAS, S.Kovalevskoi Str. 18, Yekaterinburg, 620041, Russia

\*\*\*Russian Federal Nuclear Center, Zababakhin Institute of Technical Physics (RFNC-VNIITF), Chelyabinsk region, Snezhinsk, Vasiliev Str. 13, 456770, Russia

We have performed comparative experiments in order to confirm the hypothesis that dynamic long-range effects under the particle irradiation of condensed matter, presumably connected with the emission and propagation of post-cascade shock waves in material [1], have not a thermal but a shock-wave nature. The experiments have included ion-beam exposure and mechanical shock loading of the samples of Al-Cu-Mg alloy using a special shock testing machine at VNIITF Russian Federal Nuclear Center.

Cold-worked samples 3 mm thick of aluminum alloys VD1 and D16 were irradiated with continuous Ar<sup>+</sup> ion beams on an ILM-1 ion beam implanter equipped with a PULSAR-1M ion source based on a glow discharge with a hollow cold cathode that was developed at the Institute of Electrophysics, UB RAS [2]. The ion energy was varied from 20 to 40 keV; the ion current density, which was uniform over the beam cross section, was from 50 to 400  $\mu\text{A}/\text{cm}^2$ ; and the level of irradiation corresponding to fluence value from  $10^{15}$  to  $7.5 \cdot 10^{17} \text{ cm}^{-2}$ .

In the course of irradiation, the sample temperature was controlled with the help of a chromel-alumel thermocouple welded to an identical test sample. At low irradiating fluence ( $10^{15}$ – $10^{16} \text{ cm}^{-2}$ ), the samples were heated by a beam to temperatures from 40 to 130 °C; at higher doses ( $\geq 10^{17} \text{ cm}^{-2}$ ), to a temperature of 400 °C and below.

In addition, similar samples of cold-worked aluminum alloys were subjected to mechanical shock loading at the speed of a striker of about 400 m/s. The heating temperature of the samples in the inelastic interaction process did not exceed 300 °C, as in the case of the low-fluence ion irradiation ( $D < 10^{17} \text{ cm}^{-2}$ ).

Electron microscopy showed cellular dislocation structure in the initial cold-worked state of the alloys VD1 and D16. The cell boundaries presented dense dislocation tangles.

The shock loading of the VD1 and D16 alloy samples resulted in the transformation of the cellular structure into a subgrain one. In addition, the shock loading effected on the composition of the products' of solid solution decomposition in the alloys. For example, particles of a metastable phase S'(Al<sub>2</sub>CuMg) were revealed to form in the cold-worked alloy VD1 under shock loading. In the alloy D16, a phase, the composition of which is close to Al<sub>5</sub>Cu<sub>6</sub>Mg<sub>2</sub>, is observed after shock loading instead of a metastable phase  $\theta''$  that is observed in the deformed sample.

Similar structural and phase changes occur throughout the entire volume of the samples of the alloys after ion irradiation to fluences of  $10^{15}$ – $5 \cdot 10^{16} \text{ cm}^{-2}$ .

Summarizing, it was found that the microstructure change processes in the alloys VD1 and D16 under mechanical shock loading are similar to the effect of accelerated cold (at abnormally low temperatures) radiation annealing that we observed in cold-worked aluminum alloys under irradiation with Ar<sup>+</sup> ion beams ( $E = 20$ – $40 \text{ keV}$ ) [3, 4]. This result confirms the possible role of shock-wave processes in the course of structural and phase transformations initiated in the initial stage of irradiation, which have not been considered in the classical of the solid-state radiation physics until recently.

### REFERENCES

- [1] Ovchinnikov V.V. // Physics-Uspokhi. 51. P. 955–964 (2008).
- [2] Gavrilov N.V., Nikulin S.P., and Radkovskiy G.V. // Pribory i tekhnika eksperimenta. 1, 93 (1996).
- [3] Ovchinnikov V.V., Gushchina N.V., Makhin'ko F.F., et al. // Phys. Met. Metallography, 105, 4, p. 375–382 (2008).
- [4] Ovchinnikov V.V., Gavrilov N.V., Gushchina N.V., et al. // Russian Metallurgy (Metally), 3, 207 (2010).

## FORMATION OF HIGHLY ELECTROCONDUCTIVE SURFACE ALLOYS WITH A LOW-ENERGY HIGH-CURRENT ELECTRON BEAM

*E.V. YAKOVLEV, A.B. MARKOV*

*Institute of High Current Electronics, 2/3 Akademicheskoy Avenue, Tomsk, 634055, Russia, yakovev@lve.hcei.tsc.ru, +7 3822 491571*

It is well-known that deposition of coatings and irradiation of materials by concentrated energy fluxes in particular by low-energy high-current electron beams (LEHCEB) of microsecond duration are effective methods of surface modification [1]. Formation of surface alloys by a thin film deposition followed by a LEHCEB mixing with the substrate combines all advantages of these methods.

The paper is devoted to the formation of silver-brass surface alloy with a LEHCEB. Formation of the surface alloy was carried out with the electron-beam machine "RITM-SP" [2-3]. Formation of the silver-brass surface alloy is the result of several iterations of thin silver film deposition onto brass substrate and its subsequent mixing by a LEHCEB irradiation. The number of iterations is specified to provide the required thickness of the coating and its properties. The benefit of the above described technique is that the surface alloying is performed in a single vacuum cycle.

The changes in morphology and topography were observed by scanning electron microscopy (SEM), atomic force microscopy (AFM) and optical profilometry. Chemical composition of the surface layer and in-depth elements distribution in samples with the silver-brass surface alloy were investigated by energy dispersive X-ray (EDX) microanalysis.

The research shows that the parameters of LEHCEB while mixing of the film (silver)–substrate (brass) system has a great influence on the structure and properties of formed silver-brass surface alloy. In particular, Fig 1 shows intricate microstructure that can be observed in some treatment modes. The size of the columns formed is of diameter of about 100  $\mu\text{m}$  and of height of about 40  $\mu\text{m}$ . The size increases with an increase of energy density of LEHCEB. The element composition of the columns is characterized by a reduced copper content than that in other areas of the sample surface.

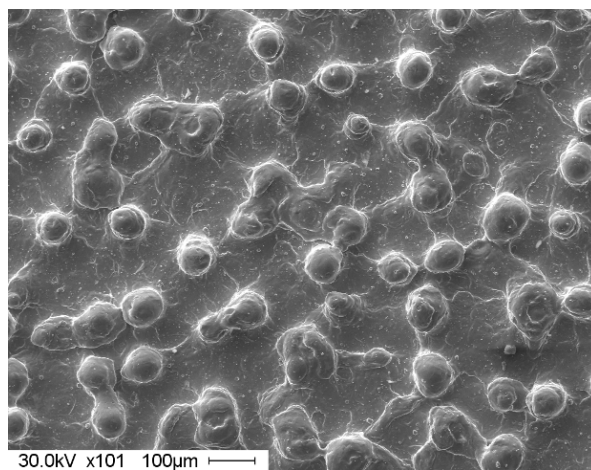


Fig. 1. SEM images of the surface sample after formation of the silver-brass surface alloy.

### REFERENCES

- [1] *D. I. Proskurovsky, V. P. Rotshtein, G. E. Ozur, A. B. Markov, D. S. Nazarov, V. A. Shulov, Yu. F. Ivanov, and R. G. Buchheit, // J. Vac. Sci. Technol. A. 1998. - Vol. 16. - P. 2480-2488.*
- [2] *A.B. Markov, E.V. Yakovlev, V.I. Petrov // IEEE Transactions Plasma Science. -2013. - Vol. 41. - № 8. - P. 2177-2182.*
- [3] *Markov A. B., Mikov A. V., Ozur G. E., Padei A. G. // Instruments and Experimental Techniques. – 2011. – Vol. 54. – № 6. – P. 862-866.*

## STRUCTURE AND PROPERTIES OF SURFACE Al-Si-Ti-Cu ALLOY, SYNTHESIZED ON SILUMIN BY MELTING OF (Ti-Cu) FILM/(Al-Si) SUBSTRATE SYSTEM<sup>1</sup>

*Yu.F. IVANOV\*\*\*, O.V. KRYSINA\*, E.A. PETRIKOVA\*, A.D. TERESOV\**

*\*Institute of High-Current Electronics of the Siberian Branch of the Russian Academy of Sciences, 2/3 Akademicheskoy Avenue, Tomsk, 634055, Russia, E-mail: [yufi55@mail.ru](mailto:yufi55@mail.ru), 8(3822)49-17-13*

*\*\* National Research Tomsk Polytechnic University, Lenin Avenue, 30, Tomsk, 634050, Russia*

Surface alloys of Al-Si-Ti-Cu composition with submicro- and nanosized structure were formed by means of melting film/substrate systems by high-intensity pulse electron beam with submillisecond pulse duration on “SOLO” setup (Fig. 1). It is showed that element concentration of surface layer with thickness of  $\approx 5 \mu\text{m}$  changes in range of (7...10) wt. % Si; (3...17) wt. % Ti and (2...6) wt. % Cu (the rest of composition - Al) versus the mode of electron-beam treatment.

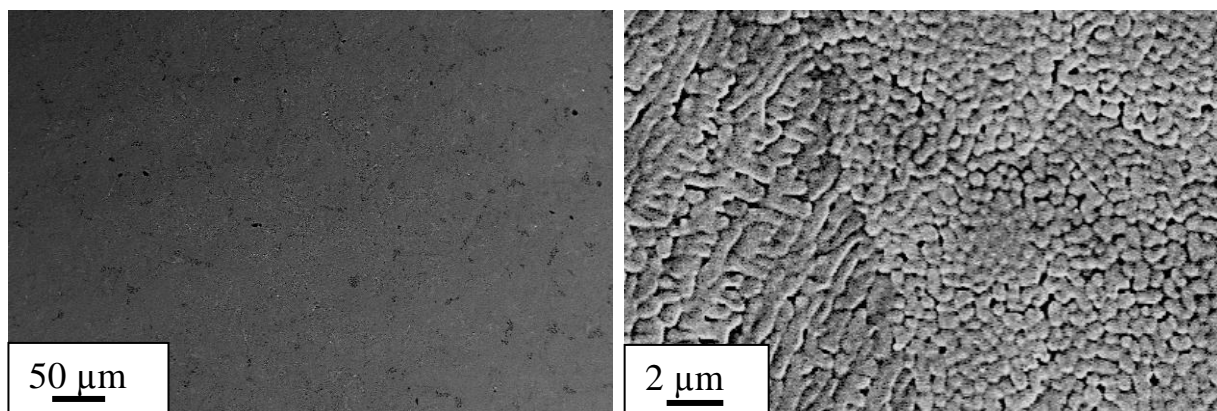


Fig. 1. SEM images of surface Al-Si-Ti-Cu alloy structure formed after irradiation of film (Ti-Cu)/substrate (Al-Si) system by high-intensity electron beam

The formation of multiphase structure of surface layer with thickness of  $\sim 10 \mu\text{m}$  was revealed by methods of X-ray analysis in Bragg-Brentano configuration at investigation of surface Al-Si-Ti-Cu alloys. Its qualitative and quantitative composition depends on element composition of system and on mode of electron-beam treatment. There is solid solution based on aluminum, silicon and titanium aluminide  $\text{Al}_3\text{Ti}$  in (TiCu)/(AlSi) system. Volume concentration of  $\text{Al}_3\text{Ti}$  is maximal at following irradiation mode:  $15 \text{ J/cm}^2$ ,  $100 \mu\text{s}$ , 20 pulses, 0,3 Hz.

Hardness, wear-resistance and friction coefficient of film/substrate system were researched in initial state and after electron-beam treatment. It is showed that the formation of surface alloys is attended by multiple increase of hardness (in  $\approx 5$  times) and wear-resistance (in  $\approx 26$  times), and decrease of friction coefficient of material (in  $\approx 1,4$  time).

The research of hardening and tribological characteristics of surface alloys synthesized at electron-beam treatment of film (TiCu)/substrate (AlSi) system allows revealing the formation of multilayers structure and too thin surface layer with high hardness (higher in 40 times compared with initial state), intermediate layer with hardness closed to that of initial material and transitional layer with hardness in  $\approx 2$  times higher compared with initial state.

<sup>1</sup> This work was supported by RFBR projects № 13-08-00416-a



## THE METALS AND ALLOYS SURFACE NITRIDING IN DC AND PULSED MODES OF NON-SELF-SUSTAINED GLOW DISCHARGE WITH A LARGE AREA HOLLOW CATHODE

*I.V. LOPATIN, YU.H AKHMADEEV, V.V. DENISOV*

*Institute of High Current Electronics, 2/3 Akademichesky Avenue, Tomsk, 634055, lopatin@opee.hcei.tsc.ru, +7 (3822) 491713*

Metal and alloy surfaces ion-plasma nitriding in the bulk discharges plasma without hydrogen and hydrogen-containing gases adding, under conditions of treated surface ion cleaning during nitriding process, recently gaining ground in science and industry. Wherein, the problem of large parts treatment uniformity without displacing and rotating mechanisms using during nitriding process is actual. In order to solve this problem, a nitriding method in a large area hollow cathode glow discharge plasma we propose. Discharge voltage decreasing and the plasma concentration increasing by the using of non-self-sustained discharge operation mode is achieved. The subject of investigation is if a certain constant current density of ions with a given energy (DC discharge regime) maintaining is enough. On the other hand, if implementation of a pulsed discharge regime is expedient. In this case, the average ion current density is the same, and its peak value exceeds the average of 2 or more times. Setting such parameters as the average ion current density and fixed ion energy should ensure the maintenance of the required workpiece temperature.

In this paper, the investigation of titanium alloy VT1-0 and steel 40X samples nitrided in non-self-sustained large area hollow cathode glow discharge (main discharge) plasma in constant or pulsed modes results are compared. The sample temperature, exposure time and ion energy (discharge voltage) have been keeping the same. In the first case, the main discharge current was constant up to 150 A. The ion current density on the treated surface was constant up to 6 mA/cm<sup>2</sup>. In the second case, the main discharge was operates in a pulsed mode with a frequency of 1 kHz, discharge current up to 450 A and an ion current density up to 18 mA/cm<sup>2</sup>. The main discharge current amplitude at a predetermined discharge voltage by an auxiliary discharge current have been regulating. The desired sample temperature by adjusting the duty ratio of the main discharge current pulses have been maintaining. An analysis of the obtained modified layers have been held.

## ATMOSPHERIC PRESSURE PLASMA JET DRIVEN BY DIELECTRIC BARRIER DISCHARGE<sup>1</sup>

*M.V. EROFEEV\*·\*\**, *V.F. TARASENKO\*·\*\**

\**Institute of High Current Electronics, Academichesky Ave. 2/3, Tomsk, 634055, Russia, mve@loi.hcei.tsc.ru*

\*\**Tomsk Polytechnic University, Lenin Ave. 30, Tomsk, 634050, Russia*

In recent years, low temperature plasma and their jets have found wide area of applications in surface and material processing, biomedical engineering, and medicine [1-5]. Atmospheric pressure plasma jet usually has temperature below 150 °C, generates a high concentration flow of reactive chemical species that can etch and deposit surfaces of various materials, including those with thermally sensitive substrates. In this work, the cold plasma jet has been achieved in He, Kr, Ar and Ar-N<sub>2</sub> at atmosphere pressure in a 0.5 millimeter capillary quartz DBD system driven by a one-polar pulsed power generator with a voltage amplitude of –6 kV and frequency of 69 kHz. The pin of high voltage tungsten electrode was 8 mm away from the opening of the quartz capillary. The gas flowing velocity varied from 0.2 to 1 m<sup>3</sup>/h for all gases.

The length of the plasma jet was measured visually. As was shown, that as the gases flowing velocity were increased from 0.2 to 0.5 m<sup>3</sup>/h, the length of the plasma jet increased linearly up to 3 cm for He, 2 cm for Kr and Ar, and up to 1 cm for Ar-N<sub>2</sub> mixture (fig. 1). In pure N<sub>2</sub>, in such excitation condition, there was no discharge at all. At a flow rate in excess of 5 m<sup>3</sup>/h, the plasma jets length decreased, and, in the case of He, reached 1.5 cm at 8 m<sup>3</sup>/h.

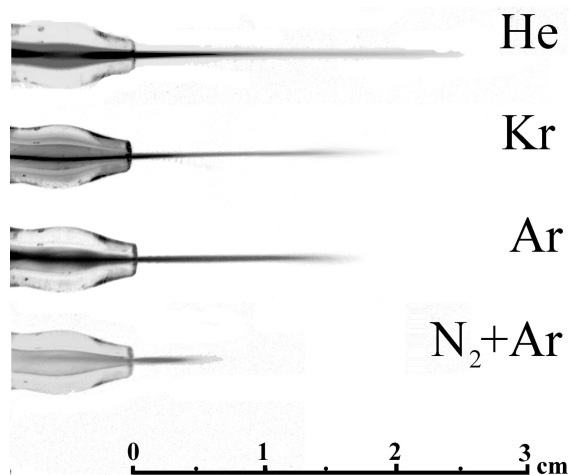


Fig. 1. Photographs of the He, Kr, Ar and Ar-N<sub>2</sub> plasma jets at the same gas velocity of 0.5 m<sup>3</sup>/h. The exposure time is 1/13 s

The emission spectra were dominated by the presence of excited nitrogen species due to the opening to ambient air. It contained excited nitrogen molecules (2nd positive system) in a range of 300–390 nm and ionized nitrogen molecules in a range of 390–480 nm. Additionally, the bands of NO at 220–280 nm were detected.

### REFERENCES

- [1] Z. Cao, J. L. Walsh, M.G. Kong, // *Appl. Phys. Let.* – 2009. – 94(2). 021501.
- [2] M. Laroussi // *IEEE Trans. Plasma Sci.* – 2009. – 37(6). 714–725.
- [3] M. Kong, G. Kroesen, G. Morfill, T. Nosenko, T. Shimizu, J. Dijk, J. Zimmermann // *New J. Phys.* – 2009. – 11. 115012.
- [4] Fridman, G. et al. // *Plasma Process. Polym.* – 2008. – 5(6). 503–533.
- [5] M. V. Erofeev, I. E. Kieft, E. A. Sosnin, E. Stoffels // *IEEE Trans. Plasma Sci.* – 2006. – 34. 1359–1364.

<sup>1</sup>This work was supported by the framework of the State task for HCEI SB RAS, project #13.1.3.

**PLASMON DISPERSION ENGINEERING IN GASE VIA AI-DOPING**

*D.M. LUBENKO<sup>1</sup>, YU.M. ANDREEV<sup>2,3</sup>, K.A. KOKH<sup>4,5</sup>, G.V. LANSKII<sup>2,3</sup>, V.F. LOSEV<sup>1,6</sup>, V.A. SVETLICHNYI<sup>3</sup>*

*<sup>1</sup>Gas Lasers Laboratory, High Current Electronic Institute of SB RAS, 2/3 Akademicheskii Ave., Tomsk 634055, Russia*

*<sup>2</sup>Laboratory of Geosphere-Biosphere Interactions, Institute of Monitoring of Climatic and Ecological Systems SB RAS, 10/3, Akademicheskii Ave., Tomsk, 634055, Russia*

*<sup>3</sup>Laboratory of Advanced Materials and Technologies, Siberian Physical-Technical Institute of Tomsk State University, 1, Novosobornaya Sq., Tomsk, 634050, Russia*

*<sup>4</sup>Laboratory of Crystal Growth, Institute of Geology and Mineralogy SB RAS, 3 Koptyug Ave., Novosibirsk 630090, Russia*

*<sup>5</sup>Novosibirsk State University, 2, Pirogov Str., Novosibirsk 630090, Russia*

*<sup>6</sup>Tomsk Polytechnic University, 30 Lenin Ave., 634034 Tomsk, Russia*

Phase matching is among most important ways in the achievement of high laser frequency conversion efficiency in nonlinear crystals. Common choices in the phase matching control are: 1. angular positioning, 2. crystal temperature regulation, 3. heavily doping or so called growing of solid solution crystals composition. In all above mentioned cases phase matching control is attained by variation of dispersion properties for o- and e-waves that are proportionally changing all over the transparency range. Here we propose control of THz range dispersion properties independently on UV-visible and mid-IR dispersions. In accordance with the considered method THz dispersions are governed by regulation of plasma input in dielectric function  $\tilde{\epsilon}(\omega)$ :

$$\tilde{\epsilon}(\omega) = \epsilon(\infty) + \sum_{j=1}^J \frac{S_j \omega_{TOj}^2}{\omega_{TOj}^2 - \omega^2 - i\Gamma_j \omega} - \frac{\omega_p^2}{\omega(\omega + i\langle\tau\rangle^{-1})}, \tag{1}$$

where  $S_j$  is the strength of the oscillator,  $\omega_{TOj}$  is the frequency of the transverse optical phonon,  $\Gamma_j$  the phonon relaxation rate,  $\omega_p$  is the plasma frequency, and  $\langle\tau\rangle$  is the average momentum relaxation time for free electron. The third term is the contribution from plasma. Thus, ordinary wave dispersion can be written as  $n(\omega) = \text{Re}[\epsilon(\omega)]^{1/2}$ . From relation (1) it comes that  $n(\omega)$  response in doped GaSe crystals depends on the relative position of transverse optical phonons and plasma frequency, phonons and average momentum relaxation times, strength of phonon oscillators and plasma frequency, that is depends on free electron density. Plasma frequency  $\omega_p$  can be estimated by

$$\omega_p = \sqrt{\frac{Nq^2}{m\epsilon_0}}, \tag{2}$$

where  $N$  is the density of free electrons;  $q$  and  $m$  are electron charge and efficient mass, respectively. It was found that Al-doping in GaSe results in more than four orders of the magnitude lower conductivity that makes relation  $\omega_p \gg \omega_{E(TO)}$  undoubtedly valid. In this case the input of the most intensive and low intensity phonon modes and all lower intensity phonons in the dielectric response can be neglected and the input will be governed by relation

$$\epsilon(\omega) = \epsilon_\infty - \frac{\omega_p^2}{\omega(\omega + i\langle\tau\rangle^{-1})} \quad \text{or} \quad \epsilon(\omega) = \epsilon_\infty - \frac{\omega_p^2}{\omega^2} \tag{3}$$

because collisions between free electrons at low density are negligible ( $\tau \approx \infty$ ) and they can be considered as moving freely. Thus, through control of Al cocentration on the growth stage,  $\omega_p$  was keeping under the control. In other words dispersion properties of plasma and it input in the o-wave dielectric response in THz range were under the control independently on the other range dispersions. Finally, plasma density control by control of the Al concentration lets some one to control phase matching and THz birefringence. Other details will be delivered.

## RADIATION EFFECTS IN NANOCRYSTALLINE TiZrAl(Si)N FILMS IRRADIATED BY He IONS

*V.V.UGLOV\**, *G.ABADIAS\*\**, *S.V.ZLOTSKI\**, *A.Y. ROVBUT\**, *S.S. LESHKEVICH*, *I.A.SALADUKHIN\**

*\*Belarusian State University, Minsk, Belarus*

*\*University of Poitiers, Poitiers, France*

Addition of Al and Si atoms to the Ti-Zr-N alloy with different their concentrations can significantly modify its structure and phase composition. Al being a soluble impurity, it can be embedded into the crystal lattice of the (Ti,Zr)N solid solution and promote the formation of a nanocrystalline structure. Si being an insoluble impurity, it allows to create a nanocomposite structure. Decrease of the grain size to nanoscale greatly increases the area of the grain boundaries which can effectively absorb of radiation defects.

In this work the radiation processes in He ion irradiation (40 keV He, doses  $2 \cdot 10^{16} \text{ cm}^{-2}$  and  $5 \cdot 10^{16} \text{ cm}^{-2}$ ) in thin (400 nm) TiZrAl(Si)N films deposited using reactive unbalanced magnetron sputtering method (deposition temperature 600°C) were investigated. For (Ti,Zr)<sub>1-x</sub>Si<sub>x</sub>N films it was found that the increase of Si content results in the transformation of the structure from nanocrystalline ( $x \leq 6.2$  at.%) to nanocomposite ( $6.2 < x \leq 13$  at.%) and then to amorphous ( $x \geq 14.8$  at.%) state. The phase composition of the films changes from two-phase (crystalline c-TiZrN + amorphous a-SiN) to the amorphous a-TiZrSiN system. All (Ti,Zr)<sub>1-x</sub>Al<sub>x</sub>N ( $11 < x \leq 23$  at.%) films are single-phase systems consisting of nanocrystalline substitution c-(Ti,Zr,Al)N solid solution with (111) preferred orientation.

It was found that He ion irradiation of (Ti,Zr)<sub>1-x</sub>Si<sub>x</sub>N films does not change the phase composition and structure. The macro-stress (increase in the lattice parameter of the solid solution c-TiZrN) and microstress (broadening of the diffraction lines of the solid solution c-TiZrN) growth with the increase of He dose that is result of radiation-induced defects formation in the grains of the solid solution.

The irradiation of the TiZrAlN films by He ions leads to radiation-induced recrystallization. The most intense process of grain growth was found for (Ti,Zr)<sub>1-x</sub>Al<sub>x</sub>N ( $x = 10.5$  at.%) films. Along with the announced process the irradiation leads to increase of the Al atoms mobility and formation two solid solutions c-(Ti,Zr,Al)N with different Al contents. It was found that the irradiation by He ions influences on the thermal stability of the phase composition after following vacuum annealing in the temperature range 600-1000° C. The annealing of uneradicated (Ti,Zr)<sub>1-x</sub>Si<sub>x</sub>N films does not change in the phase composition of the films. But the relaxation of internal stresses decreases the lattice parameter of the c-TiZrN solid solution.

In the case of He irradiated (Ti,Zr)<sub>1-x</sub>Si<sub>x</sub>N films the phase composition stability was revealed after the annealing at 800°C. The annealing at 1000°C changes the elemental and phase composition of the (Ti,Zr)<sub>1-x</sub>Si<sub>x</sub>N films and results in partly spinodal decomposition of the c-TiZrN solid solution, TiN and ZrN nitrides and a solid solution phase of c-TiZrN depleted in zirconium being formed.

The (Ti,Zr)<sub>1-x</sub>Al<sub>x</sub>N ( $x = 10.5$  at.%) films after vacuum annealing at 1000°C remained as the single-phase systems. More intense Al diffusion towards the grain boundaries of (Ti,Zr)<sub>1-x</sub>Al<sub>x</sub>N ( $x = 20.3$  and  $23.2$  at.%) films at temperatures of 900-1000°C leads to the formation of both (Ti,Zr)N and (Ti,Zr,Al)N solid solutions.

It was shown that Al concentration influences on the thermal stability of irradiated (Ti,Zr,Al)N solid solution. The single-phase system of irradiated (Ti,Zr)<sub>1-x</sub>Al<sub>x</sub>N ( $x = 10.5$  at.%) films is stable after vacuum annealing at 1000°C. He ions implantation into (Ti,Zr)<sub>1-x</sub>Al<sub>x</sub>N ( $x = 20.3$  and  $23.2$  at.%) films leads to the thermal stability improvement of the (Ti,Zr,Al)N solid solution.

The influence of radiation-induced defects on the phase composition and thermal stability of the solid solutions are discussed.

## INTERMETALLIC FREE ALUMINUM SURFACE TREATMENT WITH SOLO ELECTRON BEAM IRRADIATION

P. RAHARJO\*, K. MURAKAMI\*\*, K. UEMURA\*, M. OKANO \*\*

\*ITAC Ltd. Shinmaywa 1-1, Takarazuka, 665-0052, Japan, kensuke\_uemura@itac-j.co.jp, +81-90-3087-4959

\*\* Industrial Technology Center of Okayama Prefecture, Okayama, Japan

Getting the mirror polished surface of aluminum A-series with pre-treatment with extrusion following the mechanical treatment and with post-treatment of anodizing was said impossible with the generation of the intermetallic compounds (IMC) through the pre-treatments.

IMC could be detected with the cosmetic inspection to be called as the defects of orange peels [1]. Against the post treatment of anodizing, the depth of IMC free zone from the top surface should be over than 50microns. To overcome the tasks, we developed the novel treatment technology using SOLO electron beam (EB) irradiation [2] to evaporate top surface zone with pre-treatment of chemical etching. The optimum EB irradiation parameters were selected on the energy Joule per cm<sup>2</sup>, repetition of irradiation Hz, scanning speed, repeating the characterization of the cross section with SEM, TEM and etc. Thus we could attain also to determine the nature of IMC depending of A-series alloy of A1050 and A6063 (AISI).

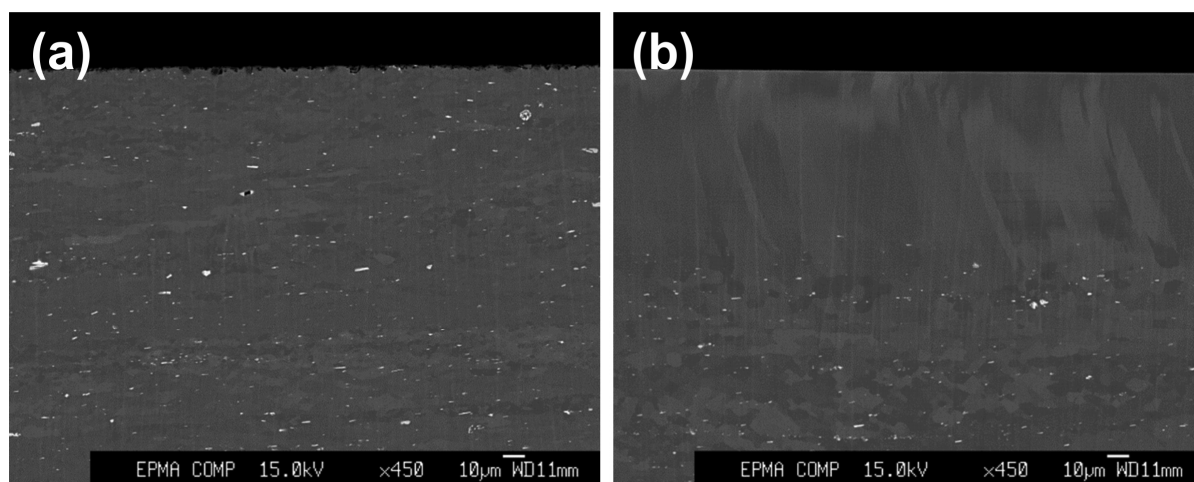


Fig. 1 Field Emission EPMA backscattered electron images of A1050 cross section from the top surface (a) before EB irradiation and (b) after EB irradiation. (a) exhibits much of IMC, and (b) exhibits IMC free zone with the depth of 73 microns from the top surface.

### REFERENCES

- [1] P.S. Lee, H.R. Piehler, B.L. Adams, G. Jarvis, H. Hampel, A.D. Rollett // Journal of Materials Processing Technology. – 1998. – 80-81. – 1. 315-319.
- [2] Uglov V.V., Kuleshov A.K., Soldatenko E.A., Koval N.N., Ivanov Yu.F., Teresov A.D. // Surface & Coatings Technology. – 2012. – 206. 2972–2976.

## MODIFICATION OF THE FUEL CLADDINGS SURFACE WITH A WIDE RANGE SPECTRUM ION BEAM

*N.V. VOLKOV, B.A. KALIN, R.A. VALIKOV, A.S. YASHIN, R.SH. YAPPAROV*

*National research nuclear university MEPhI, Kashirskoe sh., 31, Moscow, 115409, Russia, [nvvolkov@mail.ru](mailto:nvvolkov@mail.ru), +7(903)507-61-98*

Corrosion, erosion, destruction and deterioration resistance of fuel claddings are determined by the structural phase condition (SPC) of subsurface layers of zirconium alloys, which could be significantly modified by radiation-beam technology (RBT).

With the aim to corrosion reduction and finish treatment (mechanical polishing) replacement, experiments to identify the influence of different ion-treatment modes (cleaning, polishing) of radial  $\text{Ar}^+$  and  $\text{Ar}^+ + \text{He}^+$  beams with wide-range energy spectrum on the claddings condition and corrosion properties were performed.

Experiments were performed on the tubes from E110 alloy, 500 mm length ( $\varnothing 9,15$ ). Cleaning mode was defined from 1-2 mkm sputtering layer thickness, and polishing – from the relief alignment maximum and circular technological scratches removal. Then samples were tested in autoclaves (350 °C, 16,5 MPa) up to 3000 h.

Surface condition analysis has shown, that surface roughness decreases from 1,2-1,8 mkm to 0,3-0,5 mkm after ion polishing, and friction coefficient decreases up to 0,3 after outer surface alloying, for example, aluminum atoms, by ion mixing method.

As a result of corrosion tests has been found, that ion polishing generally decreases the oxide film thickness, which especially evident at large time autoclave tests. In the linear approximation, oxide film grow rate reduction after ion-beam treatment from magnitude 0,0004 mkm/h, typical for the samples in state condition (after mechanical polishing), to 0,0002 mkm/h for the samples after ion cleaning and 0,00015 mkm/h for the samples after ion polishing, has shown.

It has been found, that the main factor, decreasing claddings and fuel rod treatment rate, - is probability of the claddings overheating (temperature should not exceed 100–150 °C), due to the limited thermal conductivity of the product.

## AN ELECTRON BEAM TREATMENT ON WEAR RESISTANCE OF THE VT1-0 TITANIUM<sup>1</sup>

N.V. GIRSOVA\*, B.P. GRITSENKO\*\*\*\*, Y.F. IVANOV\*\*\*\*, K.V. KRUKOVSKIY\*, A.D. TERESOV\*\*, N.N. KOVAL\*\*

\*Institute of Strength Physics and Materials Science, SB RAS, 2/4, Academicheskii Ave, Tomsk, 634021 Russia,  
gritsenko@ispms.tsc.ru, 8-9138841797

\*\*Institute of High Current Electronics SB RAS, 2/3, Academicheskii Ave, Tomsk, 634021 Russia,

\*\*\*National Research Tomsk Polytechnic University, Tomsk, 634050, av. Lenin, 30, Tomsk, Russia

Analysis of the wear resistance studies of titanium and its alloys has shown that traditional methods of increasing of the wear resistance are ineffective [1]. In this connection investigations of the electron beam treatment effect as a function of the structure and tribological properties of technically pure VT1-0 titanium are interesting. The purpose of this work is to identify the correlation between the structures of the surface layer under different treatments further formation of the secondary structures and wear resistance.

Samples of technically pure VT1-0 titanium used with initial structure and after treatment by a high-intensity electronic beam with the short duration of effect in residual atmosphere of argon at pressure  $\sim 10^{-2}$  Pa [2]. The modes of electron beam processings are resulted in table 1.

Table 1. Parameters of the electron beam used for sample processing

Mode	Duration of impulses, mcs	Number of pulses	Pulse frequency in Hz	Electron energy, keV	The energy density of the electron beam J/cm <sup>2</sup>
1	50	3	0,3	18	10
2	50	3	0,3	18	15
3	50	3	0,3	18	25

The elemental, phase composition and defect substructure of the samples was investigated using a transmission electron microscope JEM-2100 and EM-125K in CCU "NANOTECH" ISPMS SB RAS. Improvement of the wear resistance is reached when there are the conditions for the formation of secondary structures in a kind of island formations [3]. The maximum increase of wear resistance is observed in the samples irradiated with the beam energy density of 25 J/cm<sup>2</sup>.

The studies showed that the structural-phase state of the surface layer of these samples (with a maximum value of the wear resistance) is characterized by the formation of lamellar microstructures on the basis of the  $\alpha$ -Ti, the allocation of uniformly distributed fine oxycarbide phase, and absence of the layers of the  $\beta$ -Ti on grain boundaries.

It is possible to believe that such structure-phase state of the surface layer of the sample leads to the formation of the secondary structures on friction surfaces, and, as consequence to essential increase of the wear resistance of a material.

### REFERENCES

- [1] D.N. Garkuov // Tribotekhnika wear and bezyznosnosnoct - Moscow. MSHA, 2001.
- [2] N.N. Koval, Y.F. Ivanov // Izvestiya Vuzov. Phisica.- 2008.- № 5.- pp. 60-70.
- [3] B.P. Gritsenko, Y.F. Ivanov, N.N. Koval, K.V. Krukovskii, N.V. Girsova, A.D. Teresov, I.V. Ratochka I.V. Mishin // Friction and Wear.- 2012.- T. 33.- № 3.- pp. 236-241.<sup>1</sup>

<sup>1</sup> This work was supported by integrated project under a contract from the 01.07.2013 № 02.G25.31.0099 under the Government of Russian Federation, Ministry of Education and Science

**ELECTRON-ION-PLASMA ALLOYING OF SILUMIN WITH TITANIUM<sup>1</sup>**

*E.A. PETRIKOVA\**, *YU.F. IVANOV\*\*\**, *E.A. BUDOVSKIH\*\*\**, *A.D. TERESOV\**

\* *Institute of High Current Electronics SB RAS, 2/3 Akademichesky Ave, Tomsk, 634055, Russia, elizmarkova@yahoo.com, +79234239926*

\*\**National Research Tomsk Polytechnic University, Tomsk, 634050, Lenin Avenue, 30, Tomsk, Russia*

\*\*\**Siberian State Industrial University, Kirov str 42 Novokuznetsk, 654000 Russia*

Aluminum alloys, primarily silumins, have found wide application in aircraft, automobile, and motor industries. The use of silumins as structural materials is governed by their excellent castability, high mechanical strength and corrosion resistance, and relatively small specific weight. It is due to these properties that silumins rank among candidate materials to replace stainless steel in various constructions. An obvious shortcoming of silumins is their low strength characteristics which considerably narrows the application range of these materials [1, 2]. Recently technology development of the hardening of silumins associated with the development of combined processes including sequentially several ways to modify the material [3].

Electro-explosive alloying and pulsed electron beam treatment are widely used in industries for surface modification [1, 2]. The first one leads to alloying of surface layer of thickness up to ~100µm but exhibits the rough surface. Another one modifies a thin layer but has an ability to smooth the surface. The aim of the work was to combine these two types of treatment to obtain a thick alloyed layer with smooth surface. Moreover we compared this method of surface modification with combined treatment including vacuum arc deposition a Ti coating followed by electron-beam.

The structure and phase composition of the silumin before and after treatment by electron beam were investigated by scanning electron microscopy (SEM – 515 “Philips”) and transmission electron microscope (EM - 125). The elemental composition of the samples was studied by scanning electron microscope SEM – 515 “Philips” with EDAX microanalyzer Genesis. The microhardness measurements were carried out using the PMT-3 microhardness tester at normal load of 0.5 N.

The modes of treatment leading to a dramatic improvement of microhardness and wear-resistance of modified material have been determined.

## REFERENCES

- [1] *Belov N.A., Savchenko S.V., Hvan A.V. // Phase composition and the structure of silumin. – M.: MISIS, 2008.*
- [2] *Stroganov G.B., Rotenberg V.A., Gershman G.B. // Alloys of Aluminum with Silicon. - M.: Metallurgy, 1977.*
- [3] *Laskovnev A.P., Ivanov Yu.F., Petrikova E.A. and others // Modification of the structure and properties of the eutectic silumin by electron-ion-plasma treatment. – Belarusian navuka, Minsk, 2013.*

<sup>1</sup> This work was supported by RFBR grant (project №. 13-08-00416).



## FORMATION OF GRADIENT LAYERS OF THE TI-NB ALLOY SYSTEM BY ELECTRON-BEAM SURFACING

YU.P. SHARKEEV<sup>1</sup>, I.A. GLUKHOV<sup>1</sup>, A.YU. EROSHENKO<sup>1</sup>, M.G. GOLKOVSKI<sup>2</sup>, V.A. BATAEV<sup>3</sup>, S.V. FORTUNA<sup>1</sup>

<sup>1</sup>*Institute of Strength Physics and Materials Science of the Siberian Branch of the Russian Academy of Sciences, 2/4 Akademicheskii prospect, Tomsk, 634021, Russia, e-mail: gia@ispms.tsc.ru, tel.: +7 (3822)286-809*

<sup>2</sup>*Budker Institute of Nuclear Physics, 11 Academician Lavrentiev prospect, Novosibirsk, 630090, Russia*

<sup>3</sup>*Novosibirsk State Technical University, 20 Karl Marx prospect, Novosibirsk, 630073, Russia*

Presently a promising direction for the medical materials science is the application of biocompatible titanium alloys with a low elastic modulus, for example, Ti-Nb and Ti-Nb-Zr alloy systems. The alloying of titanium with zirconium and niobium ensures the elastic modulus reduction to 55–80 GPa, which is comparable with the elastic modulus of bone tissue [1, 2]. Titanium-niobium alloys can be produced by different methods: variations of electric arc processing in metallurgical furnaces, powder metallurgy techniques, including powder compaction and sintering, and high-energy electron-beam surfacing. Gradient titanium–niobium layers can also be formed by electron-beam deposition of powders of certain chemical composition on the metal substrate.

The paper employs a high-energy powder metallurgy method, namely, electron-beam surfacing, to form Ti-Nb layers gradient in composition on the titanium surface [3]. The energy source is an electron beam emitted to atmosphere with an electron energy of 1.4 MeV and penetrating deep into powder layers. Multiple surfacing provides Ti-Nb layers of the thickness 3 mm and more on titanium substrate. The alloying material is represented by a mixture of Nb (48 mass. %) and Ti (12 mass. %) powders and the flux by a mixture of fluorides CaF<sub>2</sub> (27 mass. %) and LiF (13 mass. %). The investigation was performed on specimens after single, double and triple surfacing.

The investigations show that the method of high-energy electron beam powder metallurgy affords the formation of Ti-Nb alloys with the predicted elemental composition and microstructure as well as with high mechanical properties on the titanium substrate. By varying the number of electron-beam treatments from one to three, the total thickness of a deposited Ti-Nb layer increases from 1.5 to 3 mm and the niobium concentration increases from 18 to 41 at.%. Deposited layers reveal the presence of  $\alpha'$ ,  $\alpha''$  - phases. The increase of surfacing number leads to  $\beta$ -phase formation. The amount of the latter grows with each treatment. The microhardness of Ti-Nb alloys is equal to 3200-3400 MPa.

### REFERENCES

- [1] XU Li-juan, XIAO Shu-long, TIAN Jing, CHEN Yu-yong, HUANG Yu-dong. Microstructure and dry wear properties of Ti-Nb alloys for dental prostheses // *Trans. Nonferrous Met. Soc. China* – 2009 – No. 19 – P. 639-644.
- [2] Mitsuo Niinomi, Masaaki Nakai, Junko Hieda. Development of new metallic alloys for biomedical application // *Acta Biomaterialia* – 2012 – No. 8 – P. 3888-3903.
- [3] Golkovski M.G., Bataev I.A., Bataev A.A., Ruktuev A.A., Zhuravina T.V., Kuksanov N.K., Salimov R.A., Bataev V.A. Atmospheric electron-beam surface alloying of titanium with tantalum // *Material Science & Engineering A* – 2013 – No. 578 – P. 310-317.

## **EFFECT OF ION-PLASMA MODIFYING TREATMENT ON THE MECHANICAL AND TRIBOLOGICAL PROPERTIES OF TITANIUM ALLOYS VT6 WITH COARS AND ULTRAFINE STRUCTURE**

*V.M. SAVOSTIKOV\*, A.I. POTEKAEV\*, A.N. TABACHENKO\*, E.F. DUDAREV\*, I.A. SHULEPOV\*\**

*\*Siberian Physical-Technical Institute of Tomsk State University, 1, Novosobornaya Sq., Tomsk, 634050, Russia, svm.53@mail.ru, +7(382 2) 53-35-77*

*\*\*Tomsk Polytechnic University, 30, Lenin av., Tomsk, 634050, Russia*

In this paper we studied the effect of ion-plasma doping surface layer and magnetron deposition of coating Ti-C-Mo-S on the surface hardness, tensile strength and elongation at break of coarse and ultrafine titanium alloys VT6. Carried out comparative studies of tribological properties (friction coefficient and wear resistance) of this alloy in different structural states and deposited coated Ti-C-Mo-S. It has been established that ion-plasma doping a surface layer or coating deposition at a substrate temperature of 350-400 ° C does not lower the tensile strength and elongation at break of ultrafine alloy VT6. Tribological coating Ti-C-Mo-S reduces friction coefficient of ultrafine alloy VT6 by 8.8 times and increased wear resistance by 400 times.

## SYNTHESIS OF ALUMINUM OXIDE AND ZIRCONIUM DIOXIDE WITH COMBINATION OF SPRAY DRYER METHOD AND REVERSE PRECIPITATION METHOD

*A.E. ILELA, G.V. LYAMINA\**

*\*Department of Nanomaterials and Nanotechnology,  
Tomsk Polytechnic University, Lenina Avenue, 30, Tomsk, 6, 34050, Russian Federation,  
alfaedison@mail.ru, phone: 89131035945.*

Due to the unique combination of properties (high mechanical strength, hardness, wear-resistance, fireproofness, thermal conduction, chemical inertness), aluminum and zirconium oxides ceramics is broadly applied in modern equipment [1]. Spray dryer method and reverse precipitation method are the methods for production of nanopowders. In this work we offer to use the system of Nano Spray Dryer B-90 for synthesis of aluminum oxide and zirconium dioxide. The innovative piezo crystal driven spray head generates a mist of fine droplets with very narrow size distribution. In this work some aqueous-alcoholic solutions of aluminum sulphate and zirconium oxychloride are used. After the drying the formed powders are annealed and tested by X-ray Phase Analysis and Scanning Electron Microscopy. Also we use the powders synthesized by the chemical deposition for the comparison of the properties. It is shown that formed powders of  $\text{Al}_2\text{O}_3$  and  $\text{ZrO}_2$  have a particle size of less than 100 nm and a granule range from 0.5 to 5  $\mu\text{m}$  [2]. Nano Spray Dryer B-90 allows receiving more pure products.

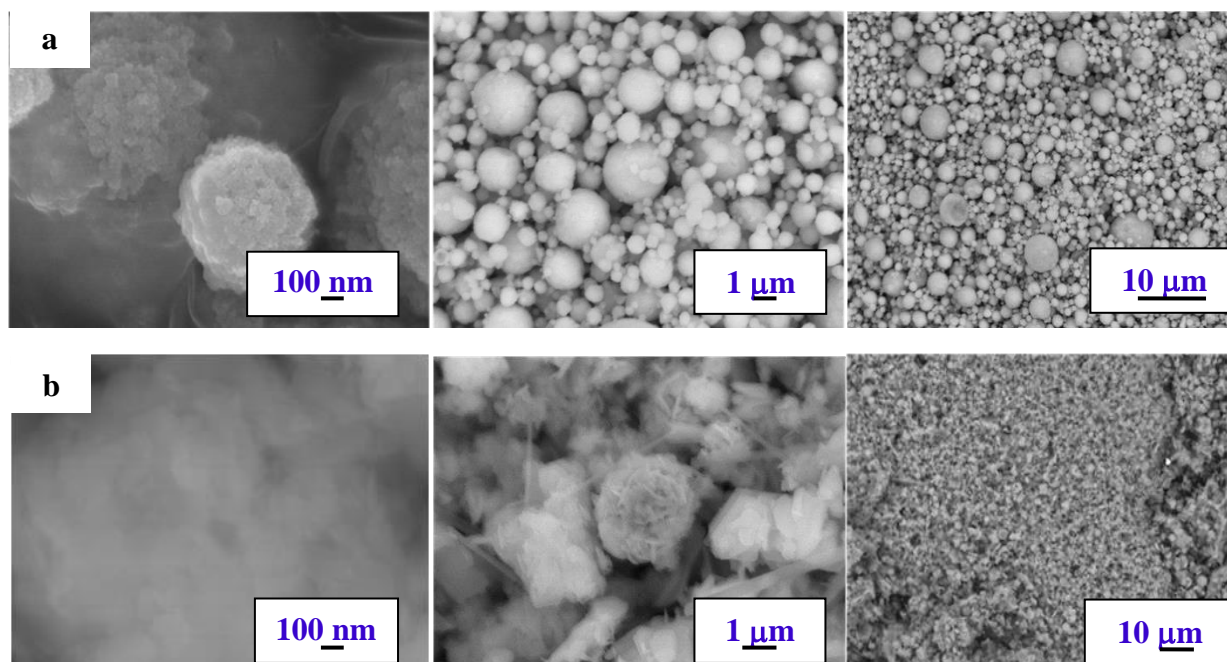


Fig.1 – SEM images of the nanopowders (a) aluminum oxide and (b) zirconium dioxide obtained by spray drying of the sol formed by the reverse precipitation method

As a result of this work, it was shown that the installation of nano spray drying have significant prospects for development and application of obtained nanopowders. Based on the experimental data it is possible to develop the methods of synthesis of nanoscale aluminum and zirconium oxides from the solutions with more complex composition.

### REFERENCES

- [1] Marcinauskas L. *Deposition of alumina coatings from nanopowders by plasma spraying* // Material Science. – 2010. – Vol.16 – No.1. – P. 47–51.
- [2] A. E. Ilela, G. V. Lyamina, V. N. Demcenko. Aluminum oxide and zirconium oxide nanopowders synthesis by chemical precipitation and spray drying methods / Proceedings of the 18th International Scientific and Practical Conference of Students, Post-graduates and Young Scientists XVIII Modern Technique and Technologies, Tomsk, 2012. – P. 244 – 245.

## CLEANING OF GAAS SURFACE BY THE TREATMENT IN ATOMIC HYDROGEN FLOW AND ULTRAVIOLET IRRADIATION

*E.V. EROFEEV\**, *I.V. FEDIN\*\**, *A.I. KAZIMIROV\*\**, *V.A. KAGADEI\*\*\**

\*Research & Production Company "Micran", 47 Vershinina st., Tomsk, 634045  
Russia, [erofeev@micran.ru](mailto:erofeev@micran.ru), +79138876039

\*\*Tomsk State University of Control Systems and Radioelectronics, 40 Lenina Prospect,  
Tomsk, 634050, Russia

\*\*\*Institute of High Current Electronics SB RAS, 2/3 Akademichesky Ave.,  
Tomsk, 634055, Russia

Rather fast demagnification of IC elements typical sizes and nanoelectronics development do stimulate elaboration of new technologies allowing formation of atomically clean and smooth monocrystalline surface of semiconductors wafers presenting minimum introduced charges and defects. Treatments of semiconductor structures by kinetic-energy-enhanced neutral reactive particles beams is considered to be one of such perspective technologies and surface cleaning of semiconductor materials by atomic hydrogen (AH) flow is today one of demanded methods of surface preparation [1]. The disadvantage of this method is a high diffusivity of atomic hydrogen into the thin layers of semiconductor. It can increase the number of defects in semiconductor. It is possible to assume that the additional ultraviolet irradiation during atomic hydrogen treatment can solve the above-named problem and limit the atomic hydrogen penetration into semiconductor.

The work purpose is investigation the influence of *in situ* ultraviolet and atomic hydrogen treatment of GaAs surface on its electrical parameters and morphology.

In experiments *i*-GaAs (100) substrate was used. The TLM patterns was fabricated by the AuGeNi ohmic contacts and lift off method. The samples were treated in a flow of atomic hydrogen with a flow density of  $j = 10^{16}$  at·cm<sup>2</sup>·s<sup>-1</sup> during  $t = 5-30$  min at room temperature or were additionally treated in ultraviolet irradiation ( $\lambda = 222$  nm). The sheet resistance of GaAs surface was measured by the TLM method. The surface morphology of treated samples was investigated with scanning electron microscopy (SEM).

That have been shown, the atomic hydrogen treatment of GaAs surface increase the sheet resistance. It can be caused by the atomic hydrogen penetration into GaAs during surface cleaning. Additional ultraviolet irradiation during AH treatment reduce the sheet resistance increase (fig. 1). So there are less penetrated atomic hydrogen in GaAs after the treatment during the same time. But the morphology of atomic hydrogen and UV treated surface is more rough. It can be caused by GaAs etching mechanism. The mechanisms responsible for discovered phenomenon has been discussed.

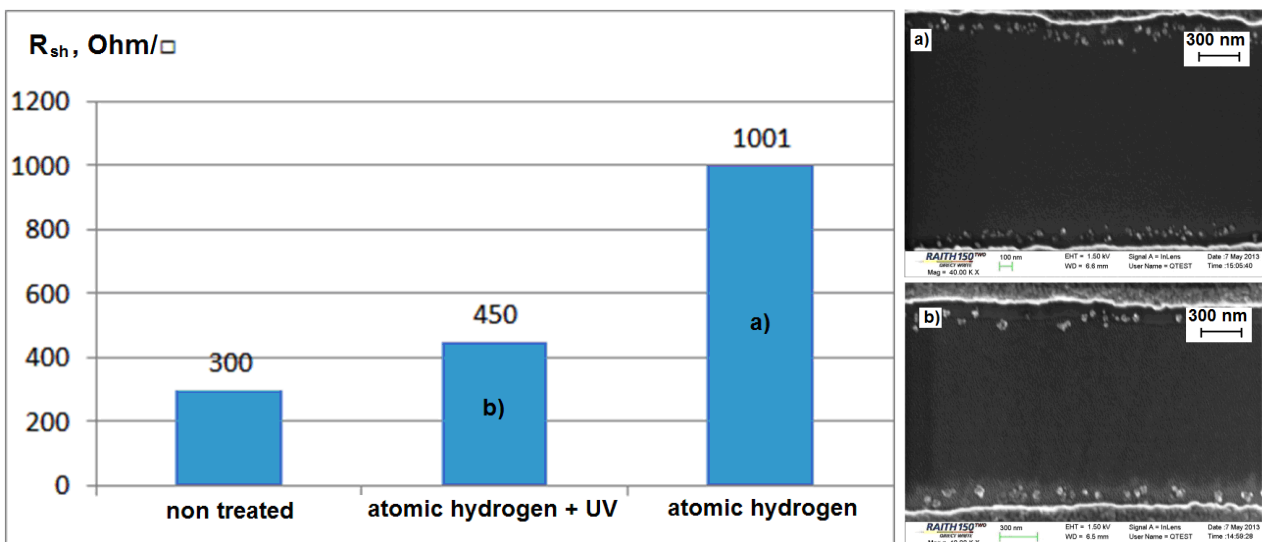


Fig. 1. Sheet resistance of n-i-GaAs after different surface treatments (left) and SEM surface morphology (right)

### REFERENCES

- [1] Sugaya T., Kawabe M. / Low-Temperature Cleaning of GaAs Substrate by Atomic Hydrogen Irradiation // Jpn. J. Appl. Phys. – 1991. – V.30. – №3A. – P. 402 – 404.

**SELF-ORGANIZED BIMODAL STRUCTURE OF THE CuCr-CONTACT ALLOYS**

*V. DURAKOV\**, *S. GNYUSOV\*\**, *B. DAMPILON\*\**

\* *Institute of Strength Physics and Materials Science Siberian Branch of Russian Academy of Sciences, 2/4, pr. Akademicheskii, Tomsk, 634021, Russian Federation, E-mail: [electron@ispms.tsc.ru](mailto:electron@ispms.tsc.ru), 8(3822)286913*

\*\* *National Research Tomsk Polytechnic University, Lenin Avenue, 30, Tomsk, 634050, Russian Federation*

CuCr-alloys containing 20-50 wt.% chromium are recognized the contact material and are therefore widely used for a vacuum circuit breakers in medium voltage class due to their high breaking capacity, resistance to breakdown in vacuum, high electrical and thermal conductivity. During the training of vacuum circuit breakers with short-circuit currents melts contact surfaces, which alters the structure of the contact material. Crystallization under nonequilibrium conditions contributes to the formation of bimodal structure consisting of primary chromium precipitates dendritic morphology and secondary chromic phases spherical form released from the supersaturated solid solution by dynamic aging. This structure is more favorable for the vacuum circuit breakers that allow us to call the process of crystallization under nonequilibrium conditions by self-organizing structure of the contact metal.

The method of electron-beam cladding forms the structure of the contact alloy under conditions close to the work of the vacuum circuit breaker at the maximum currents and does not require additional treatment in the form of training contacts short-circuit currents.

## INCREASE IN REFLECTIVITY FILMS OF THE ALUMINUM FILMS IN THE UV RANGE BY MEANS OF CHANGE OF MICRO STRESS IN THE COATING

*S.P. UMNOV, O.KH. ASAINOV*

*Tomsk Polytechnic University, 30 Lenina Avenue, 634050 Tomsk, Russia,  
[usp@tpu.ru](mailto:usp@tpu.ru), (3822)41-79-56*

Thin Aluminum films were prepared using the method of medium frequency (MF) magnetron sputtering with and without argon ion beam assistance. The influence of argon ion beam on the reflectivity in the UV range and the structure of aluminum films was studied. The reflectivity of these films was measured by a spectrophotometer. The structure of the films was studied by transmission electron microscopy (TEM), X-ray diffractometry (XRD) and atomic-force microscope (AFM). The study has shown that the films deposited with the assistance of the argon ion beam have more significant microstresses associated with an increase of crystallites microstructure defects as compared to the films deposited without ion assistance. Comparison of the measured reflectivity of aluminum films deposited without and with the assistance of the ion beam has shown that the films characterized by a higher level of microstructure defects have increased reflectivity in the UV range. The studies suggest that the defects of thin aluminum films crystal structure influence its optical properties.

## **INVESTIGATION OF THE SURFACE PROPERTIES OF STEEL 52100 AFTER TREATMENT BY PULSED CONCENTRATED ENERGY FLUXES**

*V.V. DEMIDENKO, S.K. PAVLOV, M.V. ZHURAVLEV, G.E. REMNEV*

*High-Technology Physics Institute of National Research Tomsk Polytechnic University, 634050, Tomsk, Russia, phone: +7(3822)41-91-58, e-mail: dvv@tpu.ru*

This paper is dedicated to investigation of the surface of structural steel 52100 applied to manufacturing of details where high hardness and wear resistance, in particular rings of bearings, is required. Surface properties make significant influence on operation life of finished articles. In this connection, possibility of deriving of essentially different morphology and relief by modifying treatment such as high-power ion beam (HPIB) and pulsed spark discharge (PSD) is considered. The comparative results of influence HPIB and PSD on surface morphology, a roughness and mechanical parameters (microhardness, friction factor) are presented. It is shown that the surface treated by HPIB with energy density of 1.5-3.5 J/cm<sup>2</sup> becomes a wavy relief with the presence of characteristic morphological objects such as micro-craters. PSD treatment with energy per pulse of 0.075-0.3 J leads to formation of a regular needle relief. Both treatment methods allow to vary a roughness in the set limits and to receive well-developed surface. A decrease in friction factor for the steel surface treated by HPIB by 37 %, for treated by PSD by 84 % compared with initial surface is established.

## INVESTIGATION OF ACTIVE LAYERS OF THE METHANOL AND ETHANOL OXIDATION ELECTROCATALYSTS PREPARED USING ION BEAM ASSISTED DEPOSITION TECHNIQUE<sup>1</sup>

V.V. POPLAVSKY, A.V. DOROZHKO, V.G. MATYS

Belarusian State University of Technology, Sverdlov St, Minsk, 220050, Belarus,  
e-mail: vasily.poplav@tut.by , phone +375296757142

Active layers of the methanol and ethanol oxidation electrocatalysts were prepared by ion beam assisted deposition (IBAD) of catalytic (Pt, Ir) and activating (Ni, Sn, RE, et al.) metals onto valve metal (Al, Ti, Ta) and carbon (AVCarb<sup>®</sup> Carbon Fiber Paper P50 (Ballard Material Products Inc.)) supports. The deposition method is characterized by the use of deposited-metal ions as assisting ions. The deposition of metal and the mixing of precipitable layer with substrate by accelerating ions of the same metal were carried out of neutral fraction of vapor and ionized plasma of vacuum pulsed electric arc, respectively. For acceleration of the assisting metal ions the voltage of 10 or 20 kV was used.

Investigation of the composition and microstructure of layers was carried out by RBS, SEM, EPMA, EBSD and XPS methods. It has been established that the obtained catalytic layers are characterized by amorphous atomic structure and contain atoms of the deposited metals, substrate material, as well as impurities of oxygen, carbon and hydrogen; their thickness reaches ~30–100 nm. According to RBS-data (Fig. 1) the content of platinum atoms in the layers is  $\sim 2 \times 10^{16} \text{ cm}^{-2}$ , concentration of platinum atoms in the deposition maximum equals about a few at.%.

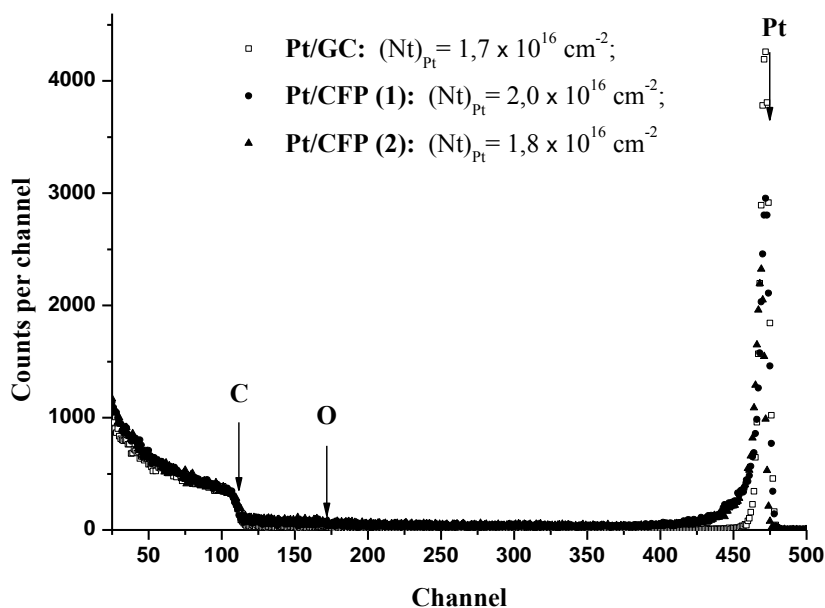


Fig. 1. RBS spectra of <sup>4</sup>He ions ( $E_0 = 1.5 \text{ MeV}$ ) scattered from the glassy carbon (GC) and AVCarb<sup>®</sup> Carbon Fiber Paper (CFP) supports surfaces with a layers prepared by platinum deposition

The activity of electrocatalysts in the processes of electrochemical oxidation of methanol and ethanol, which form the basis for the principle of operation of low temperature fuel cells (DMFC and DEFC), is significantly higher than the activity of a platinum electrode. The content of platinum in the prepared layers is less than  $\sim 0.01 \text{ mg/cm}^2$ , whereas the platinum content in electrocatalysts for DMFC and DEFC, which are used at present, is  $\sim 1\text{--}5 \text{ mg/cm}^2$ . In comparison with the traditional methods of the deposited catalysts preparation, the proposed one-stage IBAD method appears to be promising and often more preferable. It allows of the introduction of microamounts of a doping impurity in the near-surface layer of a substrate under non equilibrium conditions and of the formation of cohesive catalytic layers at ultra-low platinum consumption.

<sup>1</sup> This work was supported by Belarusian State scientific program of energy efficiency



## CORROSIVE CHARACTERISTICS OF ALUMINUM AND STEELS SUBSTRATES WITH LAYERS PREPARED BY ION BEAM ASSISTED DEPOSITION OF ZINC AND WITH COATINGS PRODUCED BY ELECTROLYTIC ZINCING<sup>1</sup>

*V.V. POPLAVSKY, V.G. MATYS*

*Belarusian State University of Technology, Sverdlov St, Minsk, 220050, Belarus,  
e-mail: vasily.poplav@tut.by, phone +375296757142*

Ion beam assisted and galvanic deposition of zinc onto pure aluminum, aluminum alloy, carbon steel and stainless steel substrates has been carry out. The ion beam assisted deposition (IBAD) method is characterized by the use of deposited-metal ions as assisting ions. The deposition of metal and the mixing of precipitable layer with substrate by accelerating ions of the same metal were carried out of neutral fraction of vapor and ionized plasma of vacuum pulsed electric arc, respectively. For acceleration of the assisting metal ions the voltage of 10 kV was used. Investigation of the composition and microstructure of layers prepared by IBAD was carried out by RBS, SEM and EPMA methods. It has been established that the obtained layers contain the atoms of deposited zinc, substrates material components, as well as impurities of oxygen and carbon; their thickness reaches ~30–100 nm. According to RBS-data the content of zinc atoms in the layers is  $\sim 2 \times 10^{16} \text{ cm}^{-2}$ . Electrolytic zincing of substrates was performed from the solution containing ZnO, NaOH and brightener. The received coatings were subject to passivation in Cr(III) containing solution. The thickness of coatings amounts to 12  $\mu\text{m}$ . Corrosion tests of samples with the investigated layers and coatings were carried out by an electrochemical method of quasipotentiostatic current-potential plots. 3% NaCl solution was used as the corrosion environment. Comparison of the obtained results demonstrated superior stability to electrochemical corrosion of all investigated materials with layers prepared by vacuum one-stage ion beam assisted deposition (Fig. 1).

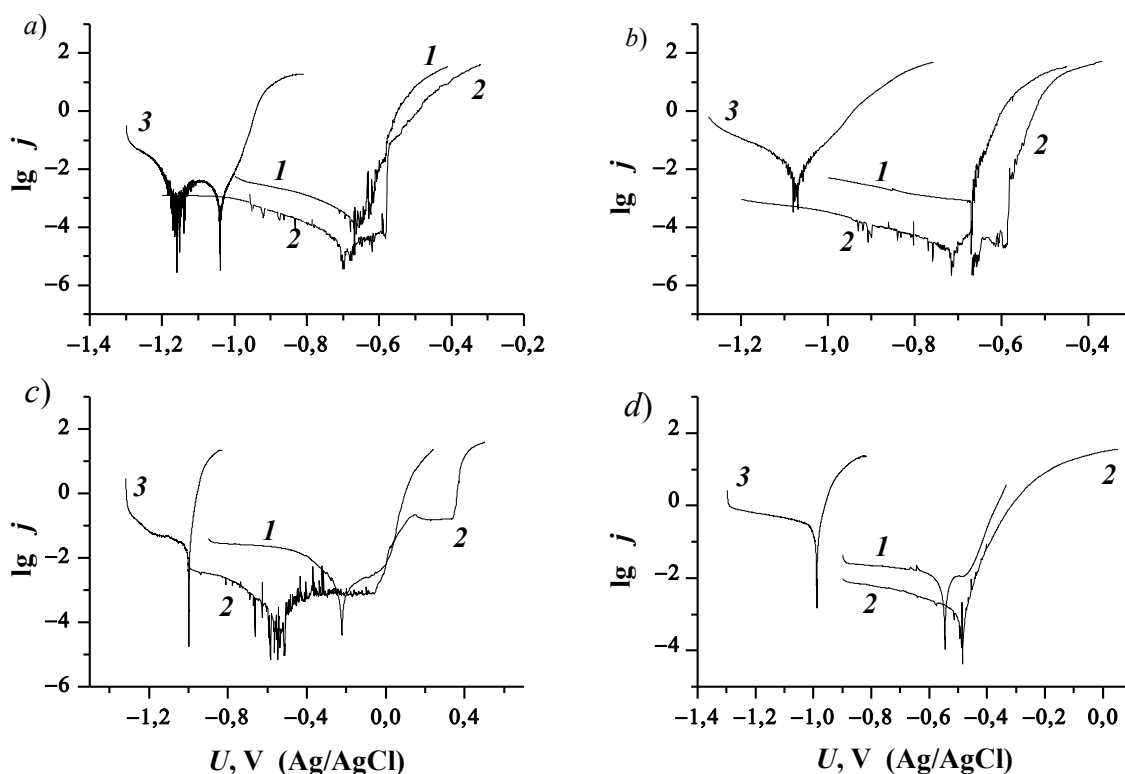


Fig. 1. Current-potential plots of aluminum (a), aluminum alloy (b), stainless steel (c) and carbon steel (d) with layers prepared by ion beam assisted deposition of zinc (2) and with coatings produced by electrolytic zincing (3); 1 – uncoated materials

<sup>1</sup> This work was supported by Belarusian State scientific program of galvanic technology

## SURFACE RESISTANCE OF CERAMIC AND POLYMERIC INSULATORS AFTER COMBINED METAL AND GAS ION IMPLANTATION<sup>1</sup>

*K.P.SAVKIN\**, *A.S.BUGAEV\**, *A.G.NIKOLAEV\**, *E.M.OKS\*\*\**, *M.V.SHANDRIKOV\**, *A.V.TYNKOV\*\*\**, AND *G.YU.YUSHKOV\**

\* *Institute of High Current Electronics SB RAS, 2/3 Akademicheskoy ave., Tomsk, Russia, 634055, +73822491776*

\*\* *Tomsk State University of Control Systems and Radioelectronics, 40 Lenin ave., Tomsk, Russia, 634050*

Implantation of metal ions in the surface of the dielectric is an effective tool for the synthesis of the surface layers, consisting of a composite of target material and implanted impurity. The result of the implantation process is the modification of the mechanical, optical and electrical properties of the dielectric surface, while retaining original properties throughout its volume [1]. Effects resulting from the implantation of metal and gas ions in solid dielectrics continue to be an actual matter of many investigations [2]. The most obvious phenomenon related with the modification of the electrical properties of the dielectric material is the reduction of the surface resistance with increasing implantation dose [3]. It was found that as a result of the implantation of the metal atoms, the surface layers formed a so-called matrix of conductivity, consisting of single islands or crossing clusters, which are formed by atoms of the implanted species.

Conduction electrons are transported through the surface layer under the influence of an external electric field, and, as a result of tunneling, pass directly via conducting channels, and also, as a result of combining of both types of conductivity [4].

In our previous work, we made implantation of platinum ions for increasing of electrical conductivity of glass ceramic rods. We have shown the increasing of the dielectric strength of insulating areas of by enabling surface charge bleeding-off through the layers with surface resistance about several tens GOhm/square [5].

In presented work we investigated the sheet resistance of the flat alumina and polymeric samples after combined metal and gas high energy ion implantation with mean energies several tens keV, as a function of exposure dose. Electrical breakdown strength of treated ceramic was investigated as a function of surface conductivity. It was shown that, after the creation of a weak conducting layer on the surface of the ceramic with sheet resistance about several units  $10^9$  Ohm/sq insulator, the electric field strength of the flashover can be increased by more than 25%.

### REFERENCES

- [1] *A.L. Stepanov and I.B. Khaibullin. // Rev. Adv. Mater. Sci. – 2005. – Volume 9. – Pages 109-129.*
- [2] *F. Liu, M.R. Dickinson, R.A. MacGill, A. Anders, O.R. Monteiro, I.G. Brown, L. Phillips, G. Biallas, T. Siggins // Surf. & Coat. Tech. - 1998. - Volume 103-104. - Pages 46-51.*
- [3] *Pichugin V.F., Frangulian T.S., Kryuchkov Yu.Yu., Feodorov A.N., Riabchikov A.I. // Nucl. Instr. & Meth. B - 1993. - Volume 80-81. - Pages 1203-1206.*
- [4] *M. C. Cattani, M. C. Salvadori, F. S. Teixeira. // arXiv:0903.3587v1 - 2009.*
- [5] *A. Nikolaev, E.M. Oks, K. Savkin, G. Yu. Yushkov, D.J. Brenner, G. Johnson, G. Randers-Pehrson, I.G. Brown, and R.A. MacGill. // Surf. & Coat. Tech. – 2007 - Volume. 201 - Pages 8120–8122.*

<sup>1</sup> This work was supported by RFBR and Tomsk Region Government under the joint grant number RFBR-13-08-98121-r\_Siberia\_a

## EFFECT OF A PULSED ELECTRON BEAM IRRADIATION ON THE STRUCTURAL AND PHASE STATE AND HYDROGEN DEGASSING OF ZR-1NB ALLOY<sup>1</sup>

*E.N. STEPANOVA\**, *G.P. GRABOVETSKAYA\*\**, *I.P. MISHIN\*\**, *A.D. TERESOV\*\*\**

\* *National Research Tomsk Polytechnic University, 30, Lenin Avenue, Tomsk, 634050, Russia, enstepanova@tpu.ru*

\*\* *Institute of Strength Physics and Materials Science of Siberian Branch of Russian Academy of Sciences, 2/4, Akademichesky Avenue, Tomsk, 634021, Russia*

\*\*\* *Institute of High Current Electronics of Siberian Branch of Russian Academy of Sciences, 2/3, Akademichesky Avenue, Tomsk, 634055, Russia*

Comparative studies of the annealing and pulsed electron beam irradiation influence on the evolution of the structural and phase state and hydrogen degassing of an ultrafine-grained zirconium Zr-1Nb-0.22H (hereinafter, the hydrogen concentration is indicated in mass %) alloy were performed.

Ultrafine-grained structure with an average size of grain-subgrain structure elements of  $\sim 0,45 \mu\text{m}$  was obtained in alloy by the method comprising preliminary hydrogenation to the concentration of 0.22 %, quenching from the ( $\alpha + \beta$ ) region and a single uniaxial compression by 70–75 % at 873 K.

By the method of X-ray diffraction analysis the ultrafine-grained Zr-1Nb-0,22H alloy is found to contain such secondary phases as Nb(Zr) and  $\text{Zr}_\beta$  besides main  $\text{Zr}_\alpha$  phase. Secondary phases in the form of rounded shape particles, the dimensions of which vary from a few nanometers to tens micrometers, are located at grain boundaries of the main  $\text{Zr}_\alpha$  phase. Hydrogen is present in the alloy in the solid solution in  $\text{Zr}_\alpha$  and  $\text{Zr}_\beta$  phases as well as in the form of  $\text{ZrH}_{0,86}$  and  $\text{ZrH}_{2,225}$  hydrides.

Hydrogen concentration in the Zr-1Nb-H alloy is found to remain higher than concentrations corresponding technical standards for this alloy (0,002–0,001 %) for all used annealing modes in dynamic vacuum at the temperature range of (773–853) K. The highest hydrogen degassing (residual concentration of 0,00873 %) is observed as a result of annealing at 853 K for 1 h. After degassing remaining hydrogen is present in the alloy in the form of  $\text{ZrH}_{0,86}$  and  $\text{ZrH}_{2,225}$  hydrides precipitates.

Using of pulsed electron beam irradiation for the hydrogen degassing of ultrafine-grained Zr-1Nb-0,22H alloy decreases the temperature of active hydrogen degassing for (50–100) K and reduces the time of degassing in comparison with annealing in dynamic vacuum. In this case hydrogen concentration in the alloy decreases both in irradiated and non-irradiated parts of the sample. The values of residual hydrogen concentration in the Zr-1Nb-0,22H alloy after degassing by a pulsed electron beam irradiation depends on the mode of sample irradiation. The most effective mode of pulsed electron beam exposure in the terms of hydrogen concentration reducing to a values corresponding to the technical standards for this alloy is an irradiation at 803 K for 30 min. The hydrogen concentration in this case is reduced to 0.00187 % (in the irradiated) and 0.00572 % (in the non-irradiated part of the sample), which approximately corresponds to the technical standards for a given alloy.

Studying of the Zr-1Nb-H alloy structure is shown that using above mentioned regimes of vacuum annealing and the pulsed electron beam irradiation results in growth of grain-subgrain ultrafine-grained structure elements. During annealing at 773 K for 2 h the average size of grain-subgrain structure elements of the alloy increases from 0.45 to  $\sim 0.7 \mu\text{m}$ . When the annealing temperature rises up to 853 K the average size of grain-subgrain structure elements of the Zr-1Nb-H alloy grows to  $\sim 1.3 \mu\text{m}$  in 1 hour. Using of pulsed electron beam irradiation for hydrogen degassing leads to a further increase in the growth rate of the elements of an ultrafine-grained grain-subgrain structure. Thus, at a temperature of 853 K the average size of grain-subgrain structure elements of the Zr-1Nb-0,22H alloy rises to  $1.2 \mu\text{m}$  for  $\sim 30$  min.

<sup>1</sup>This work was supported by RFBR project №13-02-98007 r\_sibir\_a

## INFLUENCE OF COMPRESSIVE PLASMA FLOWS TREATMENT PARAMETERS ON STRUCTURE AND MICROHARDNESS OF THE Zr COATING/T15K6 HARD ALLOY SYSTEM

E.A. KRUTSILINA\*, V.V. UGLOV\*, A.K. KULESHOV\*, V.M. ASTASHYNSKI\*\*, A.M. KUZMITSKI\*\*

\*Belarusian State University, Nezavisimosty av., 4, 220030 Minsk, Belarus, e-mail: uglov@bsu.by, tel. +375172095512

\*\*A.V. Luikov Heat and Mass Transfer Institute of the National Academy of Sciences of Belarus,

P. Brovka str., 15, 220072 Minsk, Belarus

Irradiation of the “coating/substrate” systems by compressive plasma flows (CPF) is known to provide uniform distribution of alloying element throughout the melted layer as well as its diffusive saturation with plasma forming gas [1, 2]. The penetration of additional elements to the surface layer gives an opportunity to change initial structure and phase composition of the surface layers and to influence on their mechanical properties. In this study the samples of T15K6 hard alloy with Zr coating were irradiated by 1 and 5 pulses of CPF at operating voltage at the capacitor bank of 3.5 kV and nitrogen pressure (p) 3 and 10 Torr. According to [3] dissolution of zirconium in titanium carbide with solid solution formation provides increase of fracture toughness and compressive stress approximately in 1,3 and 1,5 times correspondingly. Zirconium is also characterized by high chemical affinity to nitrogen and carbon, so the formation of zirconium nitride, carbide and carbonitride phases in surface layer is possible. Usually formation of these phases changes mechanical properties of the material.

After one pulse of CPF treatment at p=3 Torr the intensities of WC, (Ti,W)C and Zr diffraction lines decrease significantly comparing with ones in the initial state. In the surface layer ZrN and W phases are formed. Five pulse of CPF influence leads to the formation of (Ti,Zr,W)C multielement solid solution. Besides, weak reflexes from W and TiN or TiC.2N.8 phases at the diffraction pattern.

One pulse of CPF treatment at p=10 Torr results in formation of significant amount of ZrN phase, hence pure Zr is also found. In addition to the mentioned phases the strong diffraction peaks of (Ti,W)C and WC carbides as well as a weak W diffraction lines are observed at the diffraction pattern. After five pulses of CPF influence the amount of ZrN phase also rises, the diffraction lines of W become more intensive, and the intensities of (Ti,W)C and WC diffraction reflexes decrease. Alloying of (Ti,W)C solid solution with zirconium after these CPF regimes is not found.

Phase composition analysis of the surface after CPF treatment allows concluding that increase of nitrogen pressure to 10 Torr at constant values of pulse number causes decrease of CPF energy. Therefore the highest temperature on the surface as well as thickness of heat effected zone is decreased, too. At the same time the surface concentration of nitrogen increases resulting in formation of ZrN nitride amount. The formation of W phase occurs in the result of WC decomposition occurring at temperature above 1200 °C. WC carbide is known to be thermodynamically less stable phase than (Ti,W)C solid solution.

For the sample treated by one pulse of CPF at p=10 Torr layer-by-layer analysis was carried out by X-ray diffraction in the grazing incidence geometry at incidence angles ( $\alpha$ ) of 2, 3, 5 and 10°. At  $\alpha=2^\circ$ , which corresponds to the X-ray penetration depth of 0,5  $\mu\text{m}$ , the intensive diffraction lines of WN or  $\beta$ -W<sub>2</sub>N phases are found. Zr, ZrN, WC<sub>1-x</sub> phases, (Ti,W)C, WC initial carbides and Co also present at the diffraction pattern. At  $\alpha=3^\circ$  (the penetration depth of 0,8  $\mu\text{m}$ ) number and the intensities of the diffraction lines of Zr, ZrN, (Ti,W)C and WC increase but the intensities of WN or  $\beta$ -W<sub>2</sub>N decrease. Further increase of  $\alpha$  to 5 and 10° (the penetration depth of 1,2 and 2,2  $\mu\text{m}$  correspondingly) results in significant decrease of the WN or  $\beta$ -W<sub>2</sub>N lines intensities and appearance of the W diffraction reflexes.

CPF irradiation of the Zr/hard alloy system causes changes of the microhardness values with depth from the surface. Microhardness increases at depth of 0,5  $\mu\text{m}$  up to 5 and 3 times as compared with initial microhardness of the Zr/hard alloy system and hard alloy. Formation of additional dispersed nitride and carbide phases is one of the reasons of microhardness increase.

### REFERENCES

- [1] V.V. Uglov, N. N. Cherenda, V.M. Anishchik, A.K. Stalmashonak, V.M. Astashynski, and A.A. Mishchuk // Vacuum. – 2007. – 81. – P. 1341.
- [2] V.V. Uglov, N.N. Cherenda, V.M. Anishchik, A.K. Stalmashonak, A.G. Kononov, Yu.A. Petuhov, V.M. Astashynski, and A.M. Kuzmitski // Journal of High Temperature Material Processes. – 2007. - 11. – P. 383.
- [3] X. Zhang, N. Liu, C. Rong, and J. Zhou // Ceramics International. - 2009. – 35. – P. 1187.

**HYDROGEN UPON NON-POLAR SURFACES OF ZNO: AB INITIO STUDY**

A. USSEINOV\*, E.A. KOTOMIN\*\*, YU.F. ZHUKOVSKII\*\*, J. PURANS\*\*, A. AKILBEKOV\*, A.K. DAULETBKOVA\*

\*L.N. Gumilyov Eurasian National University, Munaitpasov 5, 010000 Astana, Kazakhstan, useinov\_85@mail.ru, 8(7172) 70-95-00

\*\*Institute of Solid State Physics, Kengaraga 8, LV1063 Riga, Latvia

Understanding of the atomic and electronic structure of defective/doped ZnO is of great importance for improving performance of electrodes in optoelectronic devices based on transparent conducting oxides, e.g., light-emitting diode (LED). Particular interest in this case is connected with clarification of a role of hydrogen impurities penetrating into ZnO thin films from plasma.

We report results of *ab initio* modeling of atomic hydrogen adsorption onto the two nonpolar  $(10\bar{1}0)$  and  $(11\bar{2}0)$  surfaces of ZnO positioned into two sites: *i*) atop surface O atom; *ii*) atop surface Zn atom. Our calculations of the corresponding 2D supercells have been performed using the hybrid DFT method (using PBE0 exchange-correlation functional) within the formalism of linear combination of atomic orbitals (LCAO) as incorporated into the CRYSTAL-2009 computer code [1]. This approach allows us to obtain very accurate calculations of the optical gap and defect level positions therein. The defect-induced electronic charge redistribution, lattice distortion, adsorption energy as well as the density of electronic states (DOS) and band structure have been calculated for both  $(10\bar{1}0)$  and  $(11\bar{2}0)$  surfaces of ZnO.

As a result, we have shown that energetically favorable position of hydrogen atom on both surfaces is atop the surface oxygen with similarly adsorption energies, whereas hydrogen locations atop the surface Zn is unstable. It should be noted also that hydrogen incorporation induces the defect states, which contribute below and within the surface conduction band. Thus, it is characterized as a shallow donor. Analysis of the charge redistribution has shown that hydrogen atom forms strong chemical bond with surface oxygen atom, unlike that in bulk. Based on our calculations, we have shown that hydrogen adsorption leads to decrease of both  $(10\bar{1}0)$  and  $(11\bar{2}0)$  surface relaxations and reduces the surface energy, in consistence with results of other DFT calculations [2].

## REFERENCES

- [1] Dovesi R, Saunders V R, Roetti R, Orlando R, Zicovich-Wilson C M, Pascale F, Civalleri B, Doll K, Harrison N M, Bush I J, D'Arco P and Llunell M // CRYSTAL09 User's Manual, University of Torino, Torino, Italy. – 2009.
- [2] Siao Y I, Liu P L and Wu Y T // Appl. Phys. Express. – 2011. – Vol. 4. – p. 125601

## STRUCTURE AND TRIBOLOGICAL PROPERTIES OF COPPER ALLOYED WITH ZIRCONIUM ATOMS UNDER THE INFLUENCE OF COMPRESSION PLASMA FLOWS

A.P. LASKOVNEV\*, N.N. CHERENDA\*\*, A.V. BASALAI\*, V.V. UGLOV\*\*, V.M. ASTASHYNSKI\*\*\*, A.M. KUZMITSKI\*\*\*

\* State Scientific Institution "The Physical Technical Institute of the National Academy of sciences of Belarus", Kuprevich str., 10, Minsk, 220141, Belarus,  
e-mail: Anna.basalay@mail.ru, +375172634970

\*\*Belarusian State University, Nezavisimosti ave., 4, Minsk, 220030, Belarus,

\*\*\* A.V. Lykov Heat and Mass Transfer Institute of the National Academy of sciences of Belarus,  
P.Brovka str., Minsk, 220072, Belarus

Cu–Zr alloys have many applications in electrical and welding industries due to their high strength, high electrical and thermal conductivity [1]. These alloys can be synthesized in the surface layer of copper under the influence of concentrated energy flows which allow injecting high energy into a material in a relatively short period of time. Such energy flows, e.g. compression plasma flows [2], are widely used for enhancement of surface layer properties. The investigation of structure and phase composition as well as tribological properties of copper surface layers alloyed with zirconium atoms under the influence of compression plasma flows was the main aim of this work.

Surface layer alloying was carried out by compression plasma flows impact on copper preliminary coated by zirconium. Zirconium was deposited on the copper samples by means of the cathodic vacuum-arc deposition technique. The thickness of the coating was about 2 micrometers. Treatment of the formed «zirconium coating-copper» system samples was carried out by three pulses of compression plasma flows in nitrogen atmosphere (the residual pressure was 400 Pa). The absorbed energy density changed from 14 to 23 J/cm<sup>2</sup> per pulse.

Treatment of the «zirconium coating-copper» system by compression plasma flows leads to formation of a zirconium alloyed layer. Its thickness is about 40 μm (at the absorbed energy density of 23 J/cm<sup>2</sup>). The growth of the energy absorbed results in the increase of the alloyed layer thickness.

According to the results of X-rays spectral analysis the concentration of zirconium varies from 4,4 to 7,7 at % depending on the absorbed energy density. The formation of Cu<sub>5</sub>Zr intermetallide and ZrN nitride was observed by X-rays diffraction.

The change of phase composition results in modification of the microhardness and friction coefficient. The microhardness increase up to 2.4 GPa (3 times in comparison with untreated copper) was found after compression plasma flows treatment at 23 J/cm<sup>2</sup>, which can be explained by intermetallide and surface nitride formation. Tribological tests showed that the minimal friction coefficient (0.15) was observed after treatment at the absorbed energy density of 23 J/cm<sup>2</sup>.

Thus, alloying by compression plasma flows is an efficient method to obtain hardened surface layers. In particular copper alloying with zirconium under the influence of compression plasma flows provides 3 times microhardness increase and 1.7 times friction coefficient decrease.

### REFERENCES

- [1] M. Azimi, G.H. Akbari // Journal of Alloys and Compounds. – 2011. – 509. – № 1. 27-32.
- [2] N. N. Cherenda, V.V. Uglov, V.I. Shymansky, V.M. Astashynski, A.M. Kuzmitski // Journal of optoelectronics and advanced materials. – 2010. – 12. – № 3. 749-753.

## METHANE-HYDROGEN MIXTURES PRODUCTION FROM HYDROCARBON GAS USING MICROWAVE PLASMA.

*A.G. ZHERLITSYN, K.S. LAZAR, V.P. SHEJAN*

*National Research Tomsk Polytechnic University, Lenin Avenue 30, Tomsk, 634050, Russian Federation, klazar@mail.ru, + 79528824610*

In the advanced concept of “green” high-effective energy technologies, special emphasis is placed on the production of methane-hydrogen mixtures (MHM), containing from 20% to 48% of hydrogen. The application of this product as methane-hydrogen fuel (MHF) at gas-turbine power plants (GTPP), for example, reduces  $\text{NO}_x$ , CO and  $\text{CO}_2$  emissions, increases the efficiency of GTPP, and shortens the consumption of hydrocarbon gas.

This work presents research results of MHM production from hydrocarbon gas using microwave plasma under atmospheric pressure. Research results were obtained by using a plasma-chemical reactor (Fig. 1).

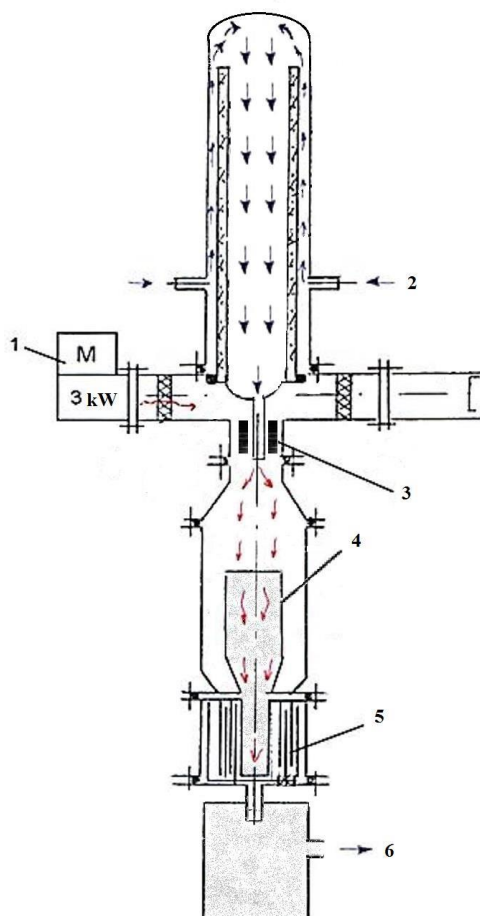


Fig. 1. Scheme of plasma-chemical reactor: 1 – magnetron, 2 – gas input, 3 – flash chamber, 4 – agglomerate, 5 – separator, 6 – methane-hydrogen mixture.

The research has shown that in the result of hydrocarbon gas conversion (95-97% of methane) in microwave plasma the MHM is produced containing from 30% to 50% of hydrogen. Such a mixture may be referred to MHF.

It also has been estimated that from 1 m<sup>3</sup> of hydrocarbon gas up to 1.5 m<sup>3</sup> of MHM is produced.

## SPECIAL FEATURES OF BEAM PLASMA GENERATED INSIDE A GLASS TUBE BY FORE-VACUUM PLASMA ELECTRON SOURCE

*D.B. ZOLOTUKHIN\**, *V.A. BURDOVITSIN\**, *E.M. OKS\*\**

\*Tomsk State University of Control Systems and Radioelectronics, 40, Lenin ave., Tomsk, 634050, Russia, [ZolotukhinDen@gmail.com](mailto:ZolotukhinDen@gmail.com), +7-953-922-23-02

\*\*Institute of High Current Electronics SB RAS, 2/3, Akademichesky ave., Tomsk, 634055, Russia

Electron beams generated by fore-vacuum plasma electron sources [1] have been employed successfully for electron beam welding of ceramic to metal, modification the surface properties of non-conductive materials [2] or just to produce beam-plasma for various applications. [3]. Generation of the beam plasma in inner hollow of dielectric tubes looks attractive both for plasma chemistry and sterilization technologies. The purpose of this paper is to demonstrate such possibility with glass tube as well as to present some special features and parameters of this plasma.

Schematic view of the experimental set-up is shown in Fig. 1.

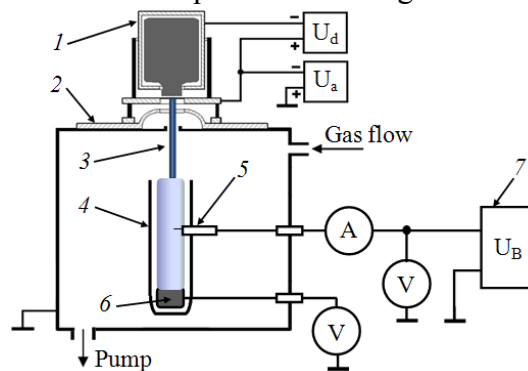


Fig.1: Experimental set-up: 1 – fore-vacuum plasma electron source, 2 – vacuum chamber, 3 – electron beam, 4 – glass tube, 5 – Langmuir probe, 6 – collector, 7 – the source of bias voltage  $U_B$ .  $U_d$ ,  $U_a$  – the sources of discharge and accelerating voltages, respectively.

During the experiments, the beam plasma parameters (density and electron temperature) were measured. The measurements confirm that it is possible to produce the beam plasma inside the glass tube. It is found that the beam-produced plasma parameters inside the tube have higher values compared with beam plasma parameters in case of absence of the tube at the same experimental conditions.

### REFERENCES

- [1] *Burdovitsin V.A., Oks E.M.* // Laser and particle beams. – 2008. – 26. – PP. 619–635.
- [2] *A.K. Goreev, V.A. Burdovitsin, A.S. Klimov, E. M. Oks* // New materials processing technologies. – 2012. – 3. – PP.446-449.
- [3] *E. H. Lock, R. F. Fernsler and S G Walton* // Plasma Sources Sci. Technol. – 2008. – 17. – P. 025009.



**STABILITY OF THE ELECTRICAL BREAKDOWN CHANNEL IN IONIC CRYSTALS***V.D. KULIKOV**Tomsk Agricultural Institute, 634050, Tomsk, Russia, e-mail: [vdkulikov@rambler.ru](mailto:vdkulikov@rambler.ru)*

The analysis of the factors determining the transverse dimensions of the front channel breakdown and radial stability in alkali-halide crystals in the framework of the mechanism of generation of charge carriers through the cascade of Auger transitions was made. Transverse dimensions determined by the diameter of the front zone of tunnel junctions in the positive electrode. Radial stability associated with the implementation of resonant and Auger transitions on the border of the front channel and the constant speed of its surface. Theoretically rate stability achieved a fixed value of the product of electric field strength on the square of the plasma conductivity breakdown channel around all of the front of channel breakdown.

## ENHANCEMENT OF THE PERFORMANCE OF CUTTING TOOLS BY THE IRRADIATION IN GLOW-DISCHARGE PLASMA

*U. SHAMIANKOU, V. ABIDZINA, M. BELAYA, A. SHAMIANKOVA*

*\*Belarusian-Russian University, Mira Av. 43, Mogilev, 212005, Belarus  
E-mail: obidina@tut.by, phone: +375-296-466821*

There are too many methods to enhance the performance of cutting tools and treatment in glow-discharge plasma is among of these methods. Improving wear resistance of cutting tools made of high-speed, tool steel and hard alloy has been very important recently. Efficiency of metal processing has been reducing due to low index of tool wear resistance. Therefore the aim of this work is to study the influence of the glow-discharge on the structure and operating properties of the above-mentioned steel and alloy.

The inserts made of WC-Co, TiC-Ni-Mo and GIALLOY PA CO-Cr alloys were chosen as objects for the investigation. The inserts as well as samples of high-speed and tool steels were exposed to glow-discharge by ions of residual gases of the vacuum. Discharge capacity was varied from 0.2 to 0.9 kW/m<sup>2</sup>. During the irradiation the temperature in the chamber did not exceed 320K. Before and after the irradiation in glow-discharge plasma samples were studied using metallographic analysis, X-ray diffraction, Vickers microhardness test and atomic force microscopy.

Using metallographic analysis and studying microhardness along the depth of the samples made of high-speed and tool steel, we concluded that the depth of the modified layer was in the range from 10 to 30 microns and depended mostly on power density of the discharge. After the irradiation we observed the appearance of texture, changes in phase structure of the samples as well as rearrangement of the dislocation structure that corresponded to highly deformed state.

The irradiation of the samples in glow-discharge plasma led also to an increase in microhardness up to 5 times. Performed tests under production conditions showed that the modification of the working surface of the tool led to an increase in their operating properties in 3 - 5 times.

After the irradiation the inserts made of WC-Co hard alloy had a set of structure and phase changes taking place in surface layer up to 250 microns. The sizes of grains both WC and Co were changed, grain aggregations were formed and unsharp interphase boundary WC – Co was observed.

The irradiation of the inserts made of TiC-Ni-Mo hard alloy in glow-discharge plasma led to structure changes along the depth up to 100 microns. During the irradiation TiC redistribution along the depth of the sample was observed as well as Ni redistribution along the grain boundary of the solid phase.

Thus, treatment of hard alloys in the glow discharge plasma ensures the formation of unique structural phase transitions in their surface layers, as well as the large scale structure modification. The irradiation of high-speed and tool steels in glow-discharge plasma leads to significant improvement in their operating properties and may be one of new widely-used advanced hardening technologies.

## **SIMULATION OF ELECTRON-BEAM SURFACING OF COATINGS WITH FEB AND FETI MODIFYING PARTICLES WITH TAKING INTO ACCOUNT PHYSICAL-CHEMICAL TRANSFORMATIONS**

*O.N. KRYUKOVA\*, A.G.KNYAZEVA\*\**

*\* Institute of Strength Physics and Materials Science, Akademicheskii Avenue, 2/4, Tomsk, 634021, Russia, okruk@ispms.tsc.ru, (3822) 286-831*

*\*\* National Research Tomsk Polytechnic University, Lenin Avenue, 30, 634050, Tomsk*

Powder metallurgy methods combined with the use of concentrated energy fluxes have special capabilities for obtaining of materials and compositions with given (improved) properties. For example, electron-beam treatment can significantly improve the performance of the parts coated by conventional methods. As a result of electron beam heating, the structure of the coating and basics changes, the hardness and wear resistance the coating material increases.

The properties of the melt are greatly influenced by a complex modification and microalloying. For coatings produced with the electron beam processing, modification not only leads to refinement of the structure, but also to restrain of the coagulation of secondary phases in the coating process. In the case of FeB and FeTi particles, the electron beam treatment is accompanied by physical and chemical transformations.

Physicochemical processes under nonequilibrium conditions of high-energy processing are nonequilibrium, and evaluation of composition, based only on the equilibrium phase diagrams without analysis of dynamics of the process can lead to the wrong conclusion about the structure and composition of processed layers.

To determine the completeness of the reaction under nonequilibrium conditions and to predict the composition of weld metal it is necessary to include in consideration of reaction kinetics, i.e., the rate and duration of the interaction of the metal with the environment. Having the state diagram of a complex system, we can select possible compounds that form during reactions, and write the kinetic equations in addition to the energy balance equation. As a result of the numerical realization of the model we can obtain the phase and chemical composition of the coating under nonequilibrium conditions, which is one of the important characteristics of the coating formed during electron beam treatment.

In this paper we propose the model of the electron-beam coating with FeB and FeTi modifying particles with taking into account physicochemical transformations. The dissolution process is described on the basis of formal-kinetic approach. The processes of melting and crystallization is described in the framework of the two-phase zone. The result of the numerical solution is the phase and chemical composition of the produced coating, the size of the heat affected zone and the molten pool, depending on the parameters characterizing the surfacing mode.

The described model allows us to give recommendations for process optimization.

## SINGULARITIES AND REGULARITIES OF PHASE FORMATION IN Zr-Y-O System

A.A. KLOPOTOV\*\*\*, O.S. TOLKACHEV\*\*\*, Y.F. IVANOV\*\*\*\*, O.G. VOLOKITIN\*

\*Tomsk state university of architecture and building, Tomsk, 634002, Russian Federation [klopotovaa@tsuab.ru](mailto:klopotovaa@tsuab.ru), 89059910837

\*\*Tomsk State University, Tomsk, 634050, Russian Federation

\*\*\*National research Tomsk Polytechnic University

\*\*\*\*Institute of High-Current Electronics of the Siberian Branch of the Russian Academy of Sciences, Tomsk, Russian Federation

Ceramics on the zirconium oxide basis (substantially yttrium stabilized ceramics) occupies a special place among the promising ceramics materials and it is used in different industries. It possesses good characteristics of mechanical property, such as ultimate flexural strength is up to 2,5 GPa, high fracture strength, acid and thermal stability, corrosion-proof and wear resistant, coefficient of friction and very low coefficient of friction with metals. The aim of the present work is to make a thermodynamic analysis of phase formation processes in Zr-Y-O system.

Based on  $ZrO_2-YO_{1,5}$  the researching compounds include zirconium, which is belong to transition metal group and characterized by 2 electrons at unfilled 4d-shells and by 2 electrons at the outer 5s-shell.

From the one side it is recommended to name yttrium as rare-earth metal, from the other side, because of electron on the unfilled 4d-shell it has features of transition metal. Herewith among the rare-earth metals yttrium got a special place, because of its Y atoms hasn't f-electrons. Y atoms are characterized by one electrons at unfilled 4d-shell and by 2 electrons at the outer 5s-shell (electron configuration Y:  $[Kr]4d^25s^1$ ). The special features of yttrium are based on its involving not only in interatomic bonds of outer shell s-electrons, but in the interatomic bonds of inner 4-levels electrons. Yttrium has an electronegativity value ( $\chi=1,2\div 1,3$ ), which is close to the same value of zirconium. So yttrium is also has ability to form compounds both with electropositive and electronegative elements. Zr and Y are considerably differ from each other by atomic radius values ( $R_Y = 0,1801$  nm and  $R_{Zr} = 0,1602$  nm). The third component of the  $ZrO_2-YO_{1,5}$  is oxygen, which is considerably differ from Zr and Y by its chemical properties. This can be described by differences in these elements atom's structure. The mixed valence of oxygen's atom, lightness of other element electron attachment, and also its ability to lose the own electrons in the reactions provide the ability to form the oxygen solid solution in Zr and Y matrixes and to form the number of suboxides.

The fulfilled analysis of the literature let us to reveal the following features, which describe the specificity of zirconium and yttrium interaction with oxygen.

First, there is the formation of solid solutions, the maximum solubility of oxygen can vary from thousandths and hundredths to tens of atomic percent. In  $\alpha-Zr$  solubility of oxygen reaches 29 at.%. In  $\alpha-Zr$  dissolved oxygen to about 10.4 at.%. Yttrium oxygen solubility also depends on the crystal modification: in  $\beta-Y$  is 30.4 at.%. % O, in  $\beta-Y$   $\square$  15,9% at.% O [1].

Secondly, oxygen with transition metals can produce compounds with an ordered structure formed from solid solutions in the metal-oxygen formed mainly of variable composition – from suboxides to peroxide compounds. This phenomenon is well manifested in the Zr and Y [2].

Thirdly, there is a great variety of different phases and polymorphic transformations at different temperatures and pressures. In systems Zr-O and Y-O is due to the different nature of the chemical bond in the compounds. Typically metallic bond that exists in solid metal with oxygen in the individual phases and compounds begins to shift into a covalent and ionic with a gradual transition from one compound to another. It is also possible manifestation and intermediate types of bonds (covalent combination with metallic, covalent and ionic, etc.).

All these features allow you to explain the huge variety of phases formed in the system Zr-Y-O and may explain the unique combination of properties of ceramics based on zirconium dioxide.

### REFERENCES

- [1] Phase Diagrams of Binary Metallic Systems / Ed. Lyakisheva N.P. M.: Machinery, T. 1-3 (1996-2000)  
 [2] T.P. Chernyaeva, A.I. Stukalov, V.M. Gritsina. Oxygen in zirconium. [in Russian], Kharkov. (1999).

## REGULARITIES OF NANOSTRUCTURED ELECTRON-BEAM HARDENING OF METAL-CERAMIC (HARD) ALLOYS SURFACE LAYER<sup>1</sup>

*Yu.F. IVANOV\*\*\*, A.D. TERESOV\*, Yu.A. DENISOVA\*, V.E. OVCHARENKO\*\*\*, A.V. BELYI\*\*\*\**

*\*Institute of High Current Electronics SB RAS, Tomsk, 634055, Russia, E-mail: yufi55@mail.ru, phone:8(3822)491713*

*\*\*National Research Tomsk Polytechnic University, Tomsk, 634050, Russia*

*\*\*\*Institute of Strength Physics and Materials Science SB RAS, 634021, Tomsk, Russia*

*\*\*\*\*Physico-technical Institute NAS Belarus', 220141, Minsk, Belarus*

Objective: To analyze the regularities of the surface layer hardening of a metal-ceramic (hard) VK8 alloy (8 wt.% Co - 92 wt.% WC), subjected to high-intensity pulsed electron beam processing, providing of surface layers hardening of hard alloys from molten state at a cooling rate  $\sim 10^6$  K/s and allows to form the surface layer multiphase structure of nano-size and submicrocrystalline-size range, with improved physical and mechanical properties.

Modification of hard alloy was performed by high intensity (up to  $100 \text{ J/cm}^2$ ) submillisecond (20 ... 200  $\mu\text{s}$ ) pulse (up to  $10 \text{ s}^{-1}$ ) electron beam irradiation of its surface on the "Solo" setup (Institute of High Current Electronics SB RAS, Tomsk). Research carried out by scanning and transmission electron microscopy and X-ray analysis. Properties of the surface layer were studied by determining the microhardness.

Numerical methods for the linear heat equation shows that the main influence on the temperature profile of the metal-ceramic surface layer warm when it is irradiated with a single pulse renders the change of the energy density of the electron beam: increasing the energy density of the electron beam from 10 to  $40 \text{ J/cm}^2$  leads to an increase in the heating temperature of the irradiated surface from 1500 K to 4000 K.

The studies of the phase composition and structure in the surface layer of the metal-ceramic (solid) VK8 alloy treated with high-intensity pulsed electron beam were done. It has been shown that high-speed heat treatment of hard alloy by pulsed electron beam leads to the formation of a multilayer structure. Identified (as a result of the analysis of the fracture surface and transverse section of VK8 hard alloy) surface layer, thermal influence layer and the transition layer, blending into the bulk material. Investigations of the structure of each identified layer were performed. Phase analysis of an electron beam modified surface layer of VK8 hard alloy was carried out. It has been established that high-speed heat treatment of hard alloy accompanied by formation of the new carbide phases -  $\text{W}_2\text{C}$ ,  $\beta\text{-WC}$  and graphite in the surface layer. Relative content of  $\text{W}_2\text{C}$  tungsten carbide increases with the increasing of electron beam energy density; at an energy density of  $40 \text{ J/cm}^2$  and more this carbide becomes predominant phase of the material surface layer. Performed electron microscopic analysis (transmission electron diffraction microscopy) of VK8 hard alloy surface layer subjected to pulsed electron beam treatment. The fact of submicron-nanocrystalline structure formation is confirmed (Fig. 6). Formation of the following phases:  $\text{Co}_6\text{W}_6\text{C}$ ,  $\text{Co}_7\text{W}_6$ ,  $\text{Co}_3\text{W}$  identified in addition to the phases detected by X-ray analysis. The lack of diffraction peaks of given phases on X-ray phase data indicates a small amount of such phases in the material surface layer.

Hard alloy electron beam irradiation regimes, leading to an increase in the microhardness of the surface layer at 1.5 times were revealed. Based on these results it is concluded that the increase in hardness of a metal-ceramic material due to the formation in the surface layer of a multilayer multiphase multimodal structure of submicron and nano-sized range.

<sup>1</sup> This work was supported by project of Foundation for Basic Research of National Academy of Sciences of Belarus and Siberian Branch of the Russian Academy of Sciences №5

## **APPLICATION OF INTENSE PULSED ELECTRON BEAMS FOR REPAIR AND PROPERTY RECOVERY OF TURBINE BLADES WITH PERFORATE HOLES**

A.N. GROMOV\*, V. A. SHULOV\*\*, O. A. BYTSENKO\*\*, D. A. TERYAEV\*\*, A. D. TERYAEV\*\*, V. I. ENGELKO\*\*\*

\**Chernyshev Machine Building Enterprise, 7 Vishnevaya Street, A-80, GSP-7, Moscow 123362, Russia, Tel.: (495) 4914988, Fax: (495) 4915652, E-mail: teryaev\_a@avia500.ru*

\*\**Moscow Aviation Institute, 4 Volokolamskoye shosse, A-80, GSP-3, , Moscow 125993, Russia, Tel.: (499) 1584424, Fax: (499) 1582977, E-mail: shulovva@mail.ru*

\*\*\**Efremov Institute of Electro-physical Apparatus, 1 Sovietsky Avenue, Metallostroy, St. Peterburg 189631, Russia; Tel.: (812) 4627845, Fax:(812)4639812, E-mail: engelko@niefa.spb.ru*

It is shown that intense pulsed electron beam of microsecond duration is a high effective instrument for modification and repair of turbine blades with perforate holes without the decrease of fatigue strength.

## STUDY OF HYDROGEN ACCUMULATION IN PALLADIUM, SILVER AND SILVER-PALLADIUM ALLOY

N.N. NIKITENKOV\*, Yu. I. TYURIN\*, V.S. SYPCHENKO\*, I.V. DUSHKIN\*, A.N. NIKITENKOV\*, O.V. VILKHIVSKAYA\*, I. SIGFUSSON\*\*

\*National Research Tomsk Polytechnic University, 30, Lenin ave., Tomsk, 634050, Russia,  
E-mai: Nikitenkov@tpu.ru, phone:+79138526482

\*\*University of Iceland, Innovation Centre, Keldnaholt, IS 112, Reykjavik, Iceland

It is known that palladium is widely used for solving a wide range of problems in hydrogen energetics. However there is a deficiency of palladium which seriously impedes its use, particularly, for the membrane manufacture (e.g., in membrane reactors for the production of ultra-pure hydrogen [1-5]). The deficiency is that the alternate heating and cooling of palladium in a hydrogen atmosphere makes it gradually brittle and deformed. At the same time, some of palladium-silver alloys are able to work in an atmosphere of hydrogen without losing their mechanical strength for a long time [4].

The results presented below are development of the research [6].

The aim of the research presented in this article is to clarify the influence of silver on the capture of hydrogen by palladium-silver alloy. First of all, it is necessary to examine the efficiency of hydrogen capture by palladium, silver and palladium-silver alloy (in this case  $\text{Pd}_{60}\text{Ag}_{40}$ ) by different saturation methods: electrolytic, plasma, and Sieverts's (from the gas phase).

Hydrogen penetration into palladium, silver, and palladium-silver alloy ( $\text{Pd}_{60}\text{Ag}_{40}$ ) was studied by the thermo-stimulated gas release (TSGR) method at three methods of saturation of samples:

- 1) from the plasma of high-frequency discharge (HFD),
- 2) from electrolyte (in an electrolytic cell at use of studied samples as cathodes),
- 3) from the gas phase at elevated temperature and pressure (Sieverts's method).

Researches are made by TSGR and X-ray phase analysis (XPA) methods.

The presence of silver in the alloy of palladium-silver leads to the following features:

1. The capture of hydrogen by Pd and  $\text{Pd}_{60}\text{Ag}_{40}$  samples depends on the method of saturation. In that case when hydrogen saturation from electrolytic and plasma in both samples is being trapped in the same type of traps (not significantly different in binding energy). While the saturation by Sieverts method takes place, traps formed are characteristic for each type of the samples.
2. In electrolytic and plasma saturation in palladium and palladium-silver alloy, the main type of trap is the binding of hydrogen in palladium hydride.
3. Alloying palladium with silver does not lead to a deterioration of sorption capacity of the alloy  $\text{Pd}_{60}\text{Ag}_{40}$  compared to Pd.

## REFERENCES

- [1] G.S. Buranov, N.R. Roshan, N.B. Kol'chugina, and other: *Alternative Energy and Ecology*. Vol 7– 39 (2006), p. 36.
- [2] G.F. Tereshchenko, N.V. Orekhova and M.M. Yermilova: *Critical Technologies. Membranes.*, Vol 1 – 33 (2007), p. 4.
- [3] V.A. Kirillov, V.D. Meshcheryakov, O.F. Brizitskii and V.Ya. Terent'ev: *Theoretical Foundations of Chemical Engineering*. (2010), p. 243.
- [4] V.M. Gryaznov, V.S. Smirnov, *Problems and methods of modern science*. (1999), p. 22.
- [5] E.E. McLeary, J.C. Jansen and F. Kapteijn: *Microp. & Mesop. Mat.* (2006) 198.
- [6] V.S. Sypchenko, N.N. Nikitenkov, T.I. Sigfusson, Yu.I. Tyurin, E.N. Kudryavtseva, A.M. Khashkhash, I.P. Chernov and V.D. Khoruzhii: *Bull. Russ. Acad. Scien. Physics*. Vol 76(6) (2012) 712.

## ENERGY EXCHANGE IN METAL-HYDROGEN SYSTEMS UNDER RADIATION EXPOSURE

*Yu.I. TYURIN* \*, *V.D. KHORUZHII* \*, *Yu.A. SIVOV* \*, *I.P. CHERNOV* \*, *I.N. SIGFUSSON* \*\*

\* *National Research Tomsk Polytechnic University, Tomsk, 634050 Russia*  
[tyurin@tpu.ru](mailto:tyurin@tpu.ru), +79138507475

\*\* *Innovation Centre of Iceland, Keldnaholt, IS112, Reykjavik, Iceland*

Investigations of nonequilibrium thermally processes of diffusion and desorption of hydrogen (deuterium) from saturated with H and D atoms metals and alloys (palladium, titanium, stainless steel, etc.) in atomic, molecular, and ionized states were performed while the specimen exposure to the electron beam and X-ray quanta in the subthreshold range. It was revealed that actively absorbing the irradiation energy, the hydrogen subsystem of  $MeH_x$  alloys of transits to excited state. Since the frequency of collective oscillations of the hydrogen subsystem is outside the phonon spectrum of the metal crystalline lattice, its relaxation is hindered. It was found that the hydrogen subsystem, preserving for a long time the supplied energy on the time scale of electronic relaxation in metals, is able to stimulate processes of rapid diffusion, nonequilibrium hydrogen escape under irradiation. This indicates manifestation of collective properties by the internal hydrogen metal atmosphere and is represented in a number of nonlinear effects, in particular, in the dependences of the release rate, diffusion coefficients, energy of hydrogen (deuterium) atoms on the density and energy of the exciting electron beam, or X-ray quanta.

Contrary to the known models of electron-stimulated desorption [1, 2], which normally use electron energies from 0.5 to several keV, in the present work we consider not only the processes of hydrogen molecule formation and detachment from metal surfaces, but also processes stimulating hydrogen diffusion from the bulk of the specimen, because the energies lie in keV region. At such energies, the depth of electron penetration into metals is several micrometers. The considered model of radiation-stimulated gas release is, probably, the first attempt to describe jointly the electron-stimulated diffusion and desorption of hydrogen (deuterium).

Moreover, this study discusses mechanisms of migration of hydrogen under ionizing radiation. It was obtained that in these conditions, one of the reasons that hydrogen displacement from localization sites becomes thermally nonequilibrium due to the long-life nonequilibrium vibrational excitations energy  $\hbar\omega$  of the hydrogen subsystem but not the thermal energy  $kT$ . The nonequilibrium ( $\hbar\omega / kT$ ) and the lifetime of the excited hydrogen subsystem in metals can be sufficient for stimulation of nonequilibrium diffusion and release of hydrogen and deuterium from metals under irradiation. One more cause of the nonequilibrium hydrogen (deuterium) escape into vacuum under irradiation from a metal saturated with H and D atoms is effective lowering of the potential barrier for  $H^+$  and  $D^+$  release from bulk of metal onto the surface and their neutralization, and also acceleration of the recombination of H and D atoms into molecules and the nonequilibrium molecule desorption under electron beam exposure. A manifestation of this effect is release of all H and D atoms from the entire metal volume under irradiating only a local surface region with an area much smaller than that of the entire sample.

### REFERENCES

- [1] *K. Oura, V.G. Lifshits, A.A. Saranin, et. al. // Introduction to the Physics of Surfaces, Moscow: Nauka, 2006, p. 490.*  
 [2] *D. Wudraf, T. Delchar // Modern Techniques of Surface Science, Moscow: Mir, 1989, p. 568.*



**DESIGNING OF WEAR-RESISTANT CHROME-VANADIUM WHITE IRON COATING:****PART 1. VACUUM ELECTRON-BEAM HARDFACING**

*B.V. DAMPILON\*\**, *V.G. DURAKOV\*\**, *S.F. GNUSOV\*\**, *A.I. ZIGANSHIN\*\**, *A.M. TOLSTOKULAKOV\**

*\*National Research Tomsk Polytechnic University, 30 Lenina av., Tomsk, 634050, Russia, [dampilon@ispms.tsc.ru](mailto:dampilon@ispms.tsc.ru)*

*\*\*Institute of Strength Physics and Materials Science, 2/4 Akademicheskii av., Tomsk, 634021, Russia*

The results of research of structure and abrasive wear resistance of the eutectic chrome-vanadium white iron coating after electron-beam welding and subsequent aging are presented in the paper. The results showed that the obtained coating consist of complex eutectic carbides  $M_7C_3$ ,  $V_2C$  and metastable austenite matrix. Subsequent aging of samples with coating at a temperature of  $1100^\circ\text{C}$  leads to intensive precipitation of secondary fine carbides  $M_7C_3$  and  $MC$  from the metastable austenite matrix of coating.



Fig. 1. Microstructure of chrome-vanadium white iron coating after aging.

After aging the matrix is undergoing  $\gamma \rightarrow \alpha$  transformation and has mainly martensite structure (90%) and retained austenite (10%). As a result of ageing increases twice the abrasive wear resistance and the hardness of the coating.

## DESIGNING OF WEAR-RESISTANT CHROME-VANADIUM WHITE IRON COATING: PART 2. MULTIPOINT IMPULSE ELECTRON-BEAM PROCESSING

*B.V. DAMPILON<sup>\*\*</sup>, V.G. DURAKOV<sup>\*\*</sup>, S.F. GNUSOV<sup>\*\*</sup>, A.I. ZIGANSHIN<sup>\*\*</sup>, N.Y. KRYLOVA<sup>\*</sup>*

*<sup>\*</sup>National Research Tomsk Polytechnic University, 30 Lenina av., Tomsk, 634050, Russia, [dampilon@ispms.tsc.ru](mailto:dampilon@ispms.tsc.ru)*

*<sup>\*\*</sup>Institute of Strength Physics and Materials Science, 2/4 Akademicheskii av., Tomsk, 634021, Russia*

The results of structure formation research of eutectic chrome-vanadium cast iron coating after multipoint pulsed electron-beam processing and aging are presented in the paper. The modified zones structure is characterized by significant content of the austenitic matrix and the eutectic colonies in the form of small isolated rounded inclusions. Eutectic colonies have a shape of a fan with the leading carbide phase VC. Significant amount of fine-dispersed carbides  $\text{Cr}_7\text{C}_3$  precipitated from the matrix is observed after aging in the 900-1100°C temperature range. After aging the matrix is undergoing  $\gamma \rightarrow \alpha$  transformation and has mainly martensite structure. Aging makes the modified zones significantly harder and leads to increasing of wear-resistance of the coating.

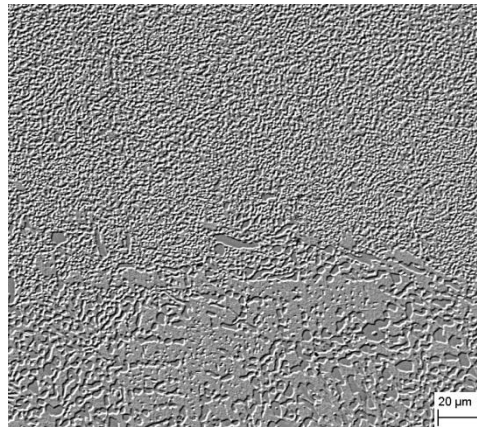


Fig. 1. Microstructure of modified zone of chrome-vanadium white iron coating after aging.

## ACTION OF DISCHARGE INITIATED BY RUNAWAY ELECTRON BEAM ON STEEL: COMPOSITION, STRUCTURE AND PROPERTIES<sup>1</sup>

*M.A. SHULEPOV, M.V. EROFEEV, YU.F. IVANOV, K.V. OSKOMOV, V.F. TARASENKO*  
*Institute of High-Current Electronics of the Siberian Branch of the Russian Academy of Sciences,*  
*2/3 Akademicheskoy Ave, Tomsk, 634055, Russia*

Study on the impact of the runaway electron preionized diffuse discharge (REP DD) on various materials is relevant and interesting task. This allows to describe a scope of applicability of this type of discharge in science and industry.

Here are the results of studies of the impact REP DD on the steel St3ps (this is analogous of the German steel RSt 37-2 or USA steel A 570).

In these experiments, for the formation of REP DD used discharge chamber and four-channel generator FPG-60 [1]. The impact was carried out under a nitrogen atmosphere at normal pressure. The amplitude of the incident wave in the transmission line voltage (cable impedance 75 Ohm) could be adjusted up to 30 kV. The cathode was installed in parallel 100 stainless steel needles, with diameter of 0,7 mm, which was attached to the conductor in two rows. The anode was a strip of the material under study. Electrode gap was ~ 7mm. There were two series of experiments, which was made  $10^5$  and  $10^6$  of discharge pulses on the sample surface

After exposure to discharge on steel St3ps observed a threefold increase in the hardness of the surface of samples (Fig. 1.a). Changes of the structure in the surface layers were investigated by transmission electron diffraction microscopy of thin foils (Fig. 1.b).

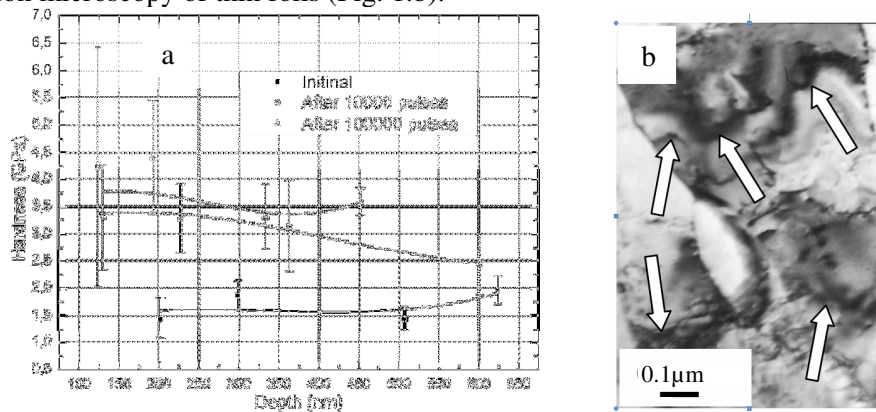


Fig.1. The effects of REP DD on the surface of the steel St3ps: a. - surface hardness of steel samples, b. - the appearance in the steel structure of bending extinction contours (indicated by arrows).

Chemical composition studies of the samples showed that the resulting discharge effects on the steel, the total carbon content in the surface layers of St3ps decreased by 15%, and the oxygen concentration increased to 1.9 times compared to the original sample.

Studies revealed changes in the structure of steel the appearance in the steel structure of bending extinction contours in the surface layer of the samples after influence the discharge This clearly indicates on existence of the internal stress fields. The sources of these fields (stress concentrators) are boundary of grains, fragments, bandpass substructures. Physical reason for the appearance of bending contours is the incompatibility of plastic deformation of steel volumes.

Thus, the changes detected in samples of steel St3ps, the exposed REP DD indicate a strengthening effect of this type of discharge for steel.

### REFERENCES

- [1] Efanov V.M., Efanov M.V., Komashko A.V. et al. *Ultra-Wideband, Short Pulse // Electromagnetics.-2010.- № 9.-Part 5*

<sup>1</sup> This work was supported by the framework of the State task for HCEI SB RAS, project #9.5.2.

## CORROSION RESISTANCE IMPROVEMENT OF 12% CR FERRITIC-MARTENSITIC STEEL BY PULSED PLASMA TREATMENT

V.L. YAKUSHIN\*, P. S. DZHUMAEV\*, B.A. KALIN\*, A.T. KHEIN\*, M. V. LEONT'EVA-SMIRNOVA\*\*,  
I.A. NAUMENKO\*\*, V.I. POL'SKII\*

\* National Research Nuclear University MEPhI (Moscow Engineering Physics Institute), Kashirskoe sh., 31, Moscow, 115409, Russia, VLYakushin@mephi.ru

\*\* JSC A.A. Bochvar All-Russian Scientific Research Institute for Inorganic Materials, Rogova st., 5a, Moscow, 123098, Russia

An important problem of modern reactor materials is the development of radiation- and corrosion-resistant steels and alloys for the core components of nuclear reactors. 12% Cr ferritic-martensitic steels are considered as a promising fuel element cladding material for new generation fast breeder reactors with liquid metal coolant. One of the promising methods for modifying the microstructure of the surface layers of steels to improve their corrosion resistance is the use of concentrated energy fluxes, in particular their treatment by high-temperature pulsed gas plasma flows (HTTPF).

The experimental results of the investigations on the corrosion resistance improvement by HTTPF treatment (including the liquid phase surface alloying method) of 12% Cr ferritic-martensitic steels (EP823 (16Cr12MoWSiVNbB) and EP900 (16Cr12MoWSiNbVCeNB)) in flowing liquid lead conditions are presented.

The surface alloying technique involved deposition of thin (0,4–0,8  $\mu\text{m}$ ) homogeneous layers of alloying elements (Al or Cr) on the outer surface of the tube and liquid-phase surface mixing of the coating and base material surface layers under HTTPF action.

Processing of chromium steels fuel cladding tubes using nitrogen pulsed plasma flows ( $\sim 20$  ms) with a specific power  $q \sim 1 \text{ MW/cm}^2$  ( $N \geq 2$ ), leads to the surface melting. At the same time hardening creates a two-dimensional nanocrystalline structure in the surface layers. The mean grain size of cellular structure is about 100 nm. Increasing the plasma flows specific density leads to more intensive melting of the surface layers and to formation of a rough relief after solidification. In this relatively "hard" processing modes ( $q \geq 4 \text{ MW/cm}^2$ ), formation of micro-cracks on the surface was observed. Pulsed nitrogen plasma modification of the microstructure of the surface layers of fuel cladding tubes leads to an increase in their microhardness up to 50 % depending on the processing conditions.

Study of the microstructure and elemental composition showed that the most deep, defect-free surface-doped layers of fuel cladding tubes with a high content of alloying elements, particularly aluminum or chromium, were observed in pulsed plasma processing of samples with an energy density of the incident flux  $Q = 21 \text{ J/cm}^2$ , and the number of radiation pulses  $N = 3$ . It was established that the alloying elements are distributed homogeneously in depth of the surface layer with a thickness of more than 10 times higher than the thickness of the previously applied coating.

Corrosion tests were carried out in a dynamic liquid lead loop with an increased and controlled oxygen content ( $C_{\text{O}} = (1-4) \cdot 10^{-6} \text{ wt\%}$ ) at the temperature of 620-650°C and the test duration of 1000 - 5000 h. SEM investigations of the surface and cross-section of samples after corrosion tests have shown that the surface alloying significantly increases the corrosion resistance of the steel. The enrichment of grain boundaries with alloying elements and their uniform distribution in the grains will significantly reduce the time required for the formation of the fine, stable, dense protective oxide layer on the steel surface, and thus lead to increased corrosion resistance of the steel.

## RESIDUAL STRESS STATE IN OXIDE DISPERSIVE STEEL DUE TO IRRADIATION BY SWIFT HEAVY IONS

V.V. UGLOV\*, V.A. SKURATOV\*\*, S.V. ZLOTSKI\*

\*Belarusian State University, Minsk, Belarus, e-mail: uglov@bsu.by 220030, Nezavisimosty ave., 4

\*\*FLNR, JINR, Dubna, Russia, e-mail:skuratov@jinr.ru 141980 Joliot-Curie Str., 6

Being considered as promising candidate materials for future reactors, oxide dispersion strengthened (ODS) steels are subject of extensive irradiation testing with various radiation sources. The dispersion of nano-sized oxides associated with the ferritic matrix confers very good creep strength at high temperature and resistance to radiation swelling at high dose [1-3]. The ferritic ODS steels have superior void swelling resistance by virtue of the inherently favorable interaction between point defects. Besides, the dispersoids also act as trapping sites for irradiation induced point defects thereby enhancing the swelling resistance. In addition, the dispersed oxide particles impede the movement of dislocations providing the required high temperature creep resistance, which is otherwise low in ferritic steels.

Performance of this material in nuclear reactor can be modeled by means of irradiation by swift Bi ions, that are typical nuclear fusion products. Radiation damage results in microstructure alternation leading to formation of micro and macro stresses that influence the material performance. The residual stress state of ferrite matrix of the steel was investigated by various XRD methodics and dependence on the irradiation dose was analyzed.

In this paper we present the results of study of residual stress of Fe-15Cr-2W-0.2Ti-0.35Y<sub>2</sub>O<sub>3</sub> ODS (KP123) steel irradiated with 700 MeV Bi ions.

It was found that the microstructures of unirradiated K123-ODS steel is consist of elongated grains (size about 0.5 μm) and dense oxide nanoparticles were observed. The oxide nanoparticle sizes in K123-ODS are typically ranging from 1-2 nm to 25 nm. Diffraction peaks of steel are belong to doped ferrite α-Fe (C, Me)- a solid solution of carbon and alloying elements (Me = Cr, W, Ti).

XRD stress analysis was performed on unirradiated and ion-irradiated samples using the sin<sup>2</sup>ψ method. In the present case, measurements were carried out on (110) and (211)-oriented α-Fe(Me) crystallites. The analysis were obtained at three rotation angles φ (0°, 45°, 90°). By the linear approximation the curves for the stress tensor of unirradiated and irradiated Bi ODS steel were calculated.

For calculations the values of the elastic constants were used for α-Fe ( $\nu^{110} = \nu^{211} = 0.28$  and  $E^{110} = E^{211} = 220$  GPa) and the lattice parameter was determined as  $a_0 = (a_{\phi\psi} + a_{\phi+180\psi})/2$  at  $\psi=0$ . The results are shown in the Table 1.

Table 1. The stress tensor of unirradiated and irradiated by Bi ions ODS steel.

	$\sigma_{11}$ [GPa]	$\sigma_{12}$ [GPa]	$\sigma_{13}$ [GPa]	$\sigma_{22}$ [GPa]	$\sigma_{23}$ [GPa]	$\sigma_{33}$ [GPa]
Unirradiated	-1,41±0.06	-0,005±0.002	-0,0019±0.0006	-1,46±0.06	0,0019±0.0006	-0,80±0.02
$6.15 \times 10^{12}$ [cm <sup>-2</sup> ]	-1,37±0.05	-0,03±0.01	0,017±0.005	-1,38±0.05	-0,017±0.005	-0,78±0.02

It was found that the unirradiated sample of ODS steel KP-123 has a compressive stress ( $\sigma_{11} = -1,41$  GPa,  $\sigma_{22} = -1,46$  GPa,  $\sigma_{33} = -0,80$  GPa), which is due, apparently, to the introduction of nanoscale phase Y<sub>2</sub>O<sub>3</sub>.

Irradiation with high-energy ions (dose of  $6.15 \cdot 10^{12}$  Bi/cm<sup>2</sup>) does not change the level of compressive stresses in the ferrite matrix, which is apparently due to the low dose ion irradiation.

### REFERENCES

- [1] S. Ukai, S. Mizuta, M. Fujiwara, T. Okuda, T. Kobayashi // J. Nucl. Sci. Technol. –2002. –V.239. –P.778–788.
- [2] A. Alamo, V. Lambard, X. Averty, M.-H. Mathon // J. Nucl. Mater. –2004. –V.329–333. –P.333–337.
- [3] Y. de Carlan, J.-L. Bechade, P. Dubuisson, J.-L. Seran, P. Billot, A. Bougault, T. Cozzika, S. Doriot, D. Hamon, J. Henry, M. Ratti, N. Lochet, D. Nunes, P. Olier, T. Leblond, M.-H. Mathon // J. Nucl. Mater. –2009. –V.386–388. –P.430–432.

## APPLICATION OF GLOW-DISCHARGE AND CONSTANT MAGNETIC FIELD FOR HARD ALLOY MODIFICATION

*V. ABIDZINA, U. SHAMIANKOU, F. TRUHACHEV, M. BELAYA, A. SHAMIANKOVA, A. SERYKAU*

*Belarusian-Russian University, Mira Av. 43, Mogilev, 212005, Belarus  
E-mail: obidina@tut.by, phone: +375-296-466821*

Surface hardening by glow-discharge is an effective but not very productive method. The efficiency of the treatment is known to depend on diffusion processes intensity. Increasing glow-discharge temperature in the cathode region up to 0.2-0.3 value of the melting temperature of processed materials leads to diffusion processes acceleration and greater material modification.

The abovementioned temperature is reached within 15 – 20 minutes depending on the dimensions and mass parameters of a workpiece treated by glow-discharge plasma. The application of glow-discharge and magnetic field with the magnetic induction of 0.2-0.3 T increases the temperature and heating rate of the processed surfaces due to higher ion current density by increasing the generation of charged particles. This leads to an increase in the intensity of the ion bombardment and significant increase in the rate of material hardening, thereby reducing processing time.

After the irradiation of WC-Co, WC-TiC-Co and TiC-Ni-Mo hard alloys we obtain the results mentioned below.

Glow-discharge treatment increases the microhardness of WC-Co hard alloy on average by 8 – 12 %, WC-TiC-Co hard alloy on average by 10 – 12 % and TiC-Ni-Mo hard alloy on average by 10 – 15 %.

The application of glow-discharge and constant magnetic field increases the microhardness of WC-Co and WC-TiC-Co hard alloys on average by 10 – 15 % and TiC-Ni-Mo hard alloy on average by 15 – 20 %. Moreover, the processing time by the first and second methods of treatment was about 30 and 22 minutes correspondingly.

Thus, the application of the magnetic field reduces the processing time on average by 35%, which indicates greater effectiveness of this method.

## RADIATION ANNEALING OF THE ALLOY 1424 (Al–Mg–Li–Zn) WITH POWERFUL BEAMS OF ACCELERATED IONS

*F.F. Mahinko\**, *V.V. Ovchinnikov\**, *S.M. Mozharovsky\**, *N.V. Gushchina\**, *L.I. Kaigorodova\*\**

\**Institute of Electrophysics, UB RAS, Amundsena Str. 106, Yekaterinburg, 620016, Russia, viae05@rambler.ru, (343)267-87-74*

\*\**Institute of Metal Physics, UB RAS, S.Kovalevskoi Str. 18, Yekaterinburg, 620041, Russia*

Our work suggests the results of the investigation of the influence of Ar<sup>+</sup> ion irradiation on the microstructure, phase composition, and mechanical properties of the cold-worked alloy 1441. The alloy 1424, which has been developed at the Federal State Unitary Enterprise "All-Russian Research Institute of Aviation Materials" (Moscow), refers to the third generation alloys and has several advantages compared with other aluminum-lithium alloys. At the same time here are serious problems in cold working of this alloy. To recover its plasticity, metallurgists usually use complicated technological operations, including saltpeter quenching by a card method, because of the inefficiency of a coil annealing in a furnace. Consequently, it is an actual attempt to use cold radiation annealing for recovering the plasticity of the alloy 1424; this phenomenon was observed in aluminum alloys in [1, 2]. In the future, this method will enable the implementation of cold coiled rolling of hard-deformable aluminum alloys.

The samples of the alloy 1424 were irradiated with continuous Ar<sup>+</sup> ion beams on an ILM-1 ion beam implanter equipped with a PULSAR-1M technological ion source based on a low-pressure glow discharge with a hollow cold cathode [2], generating gas ion beams with circular cross sections ( $S \sim 100 \text{ cm}^2$ ,  $E = 5\text{--}50 \text{ keV}$ ,  $j = 10\text{--}500 \text{ }\mu\text{A/cm}^2$ ).

Cold-worked 1441 alloy plates 7.3 mm thick were irradiated from one side with argon ions at the energy of 40 keV and the ion current density of  $200 \text{ }\mu\text{A/cm}^2$ . As the fluence increases from  $5 \cdot 10^{16} \text{ cm}^{-2}$  to  $3.7 \cdot 10^{17}$  (and, respectively, irradiation time from  $\sim 40 \text{ s}$  to 5 min), the tensile strength  $\sigma_u$  steadily decreases from 471 to 392 MPa. The plasticity of the alloy in this case grows from 4.7 to 13.7%. First, the yield strength  $\sigma_{0.2}$  increases from 351 to 414 MPa, but then returns to its initial value and then decreases to 264 MPa. The maximum softening in combination with the maximum elongation occurs at the fluence  $F = 4.5 \cdot 10^{17} \text{ cm}^{-2}$ :  $\sigma_u = 389 \text{ MPa}$ ,  $\sigma_{0.2} = 181 \text{ MPa}$ ,  $\delta = 20.8 \%$ . Only the yield strength is reduced (as compared with the previous fluence), but the tensile strength remains almost the same and is 389 MPa.

A two-fold increase in the ion current density to  $400 \text{ }\mu\text{A/cm}^2$  resulted in the decrease in the irradiation time to 2 min, which is required to accumulate a fluence of  $3 \cdot 10^{17} \text{ cm}^{-2}$ , providing almost the same softening level:  $\sigma_u = 390 \text{ MPa}$ ,  $\sigma_{0.2} = 181 \text{ MPa}$ ,  $\delta = 17.8 \%$ . As a result of short-term radiation, we obtained a level of properties of the alloy that satisfies the regulated requirements and makes further cold rolling possible. As a result, the use of intermediate annealing operations allowed us to roll the alloy to a thickness of 1 mm.

Metallographic examination has shown that irradiation promotes recrystallization processes over the entire thickness of the samples. The process of recrystallization manifests itself, depending on the mode of radiation, either through the broadening of the deformation bands, or through the formation of both equiaxial and elongated grains with sizes of 2-6 microns inside initial grains, which form chains parallel to surfaces of the sheet.

Electron microscopy data indicate that the irradiation decreases the density of grain boundary precipitates and refines intermetallic compounds Al<sub>6</sub>Mn. All that leads to an increase in the plasticity of the alloy. Irradiation also provokes the formation of fine particles of a metastable  $\delta$ -phase (Al<sub>3</sub>Li)  $\sim 10\text{--}15 \text{ nm}$  in diameters; but the volume density of the particles is so small that it does not affect the cold rolling of the alloy by 20-30%.

### REFERENCES

- [1] Ovchinnikov V.V., Gavrilov N.V., Gushchina N.V., et al. // Russian Metallurgy (Metally), 3, 207 (2010).  
 [2] Gavrilov N.V., Nikulin S.P., and Radkovskiy G.V. // Pribory i tekhnika eksperimenta. 1, 93 (1996).

## FEATURES OF ELECTRON-BEAM TREATMENT OF LOW-ALLOYED AND GREY CAST IRON SCH20

V.D. OCHIROV, D.E.DASHEEV, N.N. SMIRNYAGINA

*Institute of Physical Materials Science SB RAS, Sakhyanovoy Street, 6, Ulan-Ude, 670047, Russia, [smirnyagina09@mail.ru](mailto:smirnyagina09@mail.ru), 83012433845*

In this work, we studied the effects of electron heating on the properties of cast iron (grey SCH-20 and low-alloyed) and the conditions of education, structure and properties of boride layers were investigated. The main process forming the structure of iron is the process of graphitization (carbon sequestration in the structural-free form), as it determines not only the number, form and distribution of graphite in the structure, but the metal base (matrix) of cast iron.

Saturation of the surface cast iron boron was carried out in order to increase their surface hardness, wear resistance, corrosion resistance, heat resistance, etc. In the paper discussed the features of boriding of cast iron by electron beam processing of samples with daubs based on amorphous boron.

Microhardness measurements found significant diffusion of atoms of boron through the layer. A decrease in microhardness observed with  $HV = 730 \pm 5 \text{ kg/mm}^2$  to  $HV = 520 \pm 5 \text{ kg/mm}^2$  at a depth of boride layer to 200 microns. Microhardness of the metal matrix at a depth of 1200 microns is  $HV = 250 \pm 3 \text{ kg/mm}^2$ . Layers held firmly, do not split off at an appreciable deformation of the samples, and not crumble in the manufacture of thin sections.



## STRUCTURE AND PHYSICAL PROPERTIES OF $\text{CsCrTi}_{0.5}(\text{MoO}_4)_3$ <sup>1</sup>

*S.G. DORZHIEVA, J.G. BAZAROVA, B.G. BAZAROV*

\* *Baikal Institute of Nature Management, Siberian Branch, Russian Academy of Sciences, Sakh'yanova Street 6, 670047 Ulan-Ude, Russia, sdorzhh@binm.bscnet.ru, 8(3012)433362*

In the present work of  $\text{CsCrTi}_{0.5}(\text{MoO}_4)_3$  molybdate was synthesized as single phase samples. Thermal behaviour of the crystal structure, thermal conductivity, dielectric permittivity and electronic conductivity were studied.

According to the X-ray powder diffraction measurements,  $\text{CsCrTi}_{0.5}(\text{MoO}_4)_3$  crystallizes in the  $R\bar{3}$  space group. The diffraction pattern of  $\text{CsCrTi}_{0.5}(\text{MoO}_4)_3$  is presented in Fig. 1. Structure parameters and some interatomic distances are refined. The average interatomic distances (Cr,Ti)-O of 1.96 Å in (Cr,Ti)O<sub>6</sub>-octahedra, Mo-O of 1.78 Å in MoO<sub>4</sub>-tetrahedra and Cs-O of 3.34 Å in CsO<sub>12</sub>-polyhedra are in excellent agreement with the literature data.

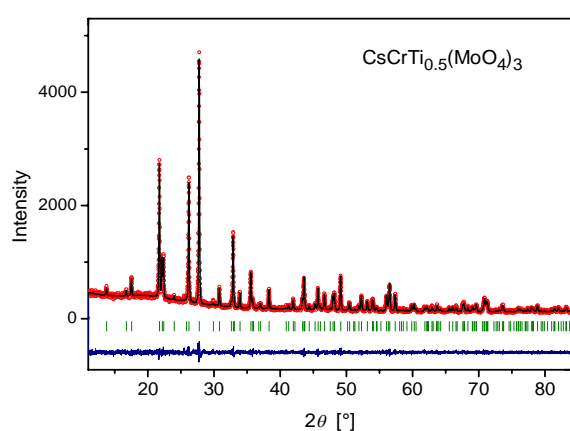


Fig. 1. Measured and calculated powder diffraction pattern for  $\text{CsCrTi}_{0.5}(\text{MoO}_4)_3$  together with the difference curve (Cu-K $\alpha_1$  radiation).

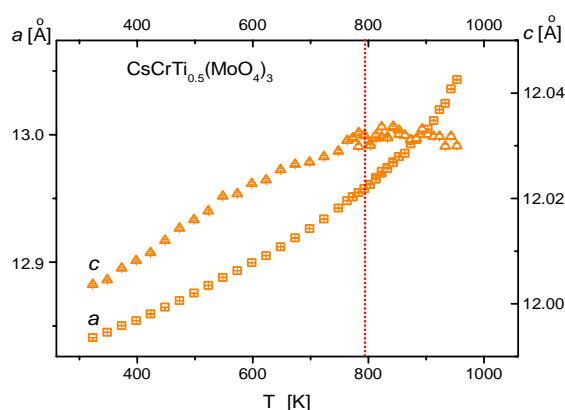


Fig. 2. Temperature evolution of lattice parameters of  $\text{CsCrTi}_{0.5}(\text{MoO}_4)_3$ .

The DSC-curves of  $\text{CsCrTi}_{0.5}(\text{MoO}_4)_3$  show a reversible endothermic signal at temperatures above 700 K during first and second heating. According to the XRD analysis after DSC measurements this compound remained single-phase sample. Estimated standard enthalpy of these thermal effects corresponds to about 6.2 kJ/mole.

In order to clarify the nature of the observed thermal effects structural studies at elevated temperatures were performed using synchrotron powder diffraction. The thermal expansion behavior show anomalies at the temperatures, at which DSC signals are visible. For  $\text{CsCrTi}_{0.5}(\text{MoO}_4)_3$  the thermal expansion along the  $c$  axis in the high-temperature region is practically zero, whereas along the  $a$  direction it is larger than at low temperatures. The average Cs-O and (Cr,Ti)-O distances increase with increasing temperature whereas the average Mo-O distance slightly decreases. The temperature dependence of the isotropic thermal displacement parameter of Cs ions in  $\text{CsCrTi}_{0.5}(\text{MoO}_4)_3$  is monotonous without any kink in the whole temperature range indicating no drastic increasing the Cs<sup>+</sup> mobility in the high-temperature range.

Temperature dependence of thermal conductivity shows a complicated behavior. In the low-temperature region up to 550 K a decreasing the thermal conductivity was observed while in the high-temperature region above 700 K a drastic increasing was measured.

Temperature dependences of the electronic conductivity show sharp increasing from 10<sup>-5</sup> to 10<sup>-2</sup> S/cm at the temperatures above 750 K. Temperature dependence  $\epsilon(T)$  for  $\text{CsCrTi}_{0.5}(\text{MoO}_4)_3$ , measured at 1MHz from room temperature to 860 K, has a well defined maximum at about 805 K, which is most likely due to a transition into a piezoelectric state. This temperature corresponds to the change in the thermal expansion coefficients along the  $a$ - and  $c$ -axes. The endothermic signal at 820 K should also relate to the sharp increase of the dielectric constant.

<sup>1</sup> This work was supported by a Grant of the RF President «MK-6247.2013.2», SB RAS (Grant 28.13), Grant of the Presidium RAS № 8.

## PLASMA-ELECTROLYTIC MODIFICATION OF HIGH-SPEED STEEL SURFACE LAYERS

B.K. RAKHADILOV, M.K. SKAKOV\*

\* National Nuclear Center of the Republic of Kazakhstan, st. Krasnoarmeyskaya, 2 buil.54 B, Kurchatov, 071100, Kazakhstan, [bor1988@mail.ru](mailto:bor1988@mail.ru), 87756686239

In today's engineering attention is at the development of surface hardening technology. It is known that the surface condition largely determines the level of strength and operational properties of products. The surface of the product is experiencing increased wear and contact load. Technology of surface hardening based on modifying impact on the metal surface energy or physic-chemical methods, which radically changes its structure and properties. Modification of the influence of high-energy is an effective means of improvement of physic-mechanical and operational properties of high-speed steels surfaces [1]. One of the modern methods of high-energy modification, which helps to significantly reduce the overall processing time and significantly improve wear-resistance of structural and tool steels, is plasma-electrolytic modification [2]. Plasma-electrolytic modification is significant changes of structural-phase state and accordingly material properties in the thin surface layers due to the physical impacts of ions of low-temperature plasmas and electric discharge.

In this regard, the purpose of this work is to study the influence of electrolytic-plasma nitriding on the phase-structural States and tribological properties of surface layers of R9, R6M5, R18 high-speed steels.

For electrolytic-plasma nitriding used samples from R6M5, R18 and R9 steels with dimensions  $10 \times 30 \times 30 \text{ mm}^3$  and after standard thermal processing for these steels. Electrolytic-plasma nitriding of the samples was conducted in the electrolyte from an aqueous solution containing 20% urea 10% sodium carbonate at  $T=550^\circ\text{C}$  in within 7 minutes. Tribological tests on the sliding friction conducted on high-temperature THT-S-BE-0000 tribometer according to «Ball – Disk» scheme. Testing of the samples, abrasive wear was carried out on pilot plant for testing the abrasive wear of the friction of not rigidly fixed abrasive particles in the scheme «Rotatory roll – Flat surface» in accordance with State Standard 23.208-79, which coincides with the American standard ASTM S 6568. Metallographic investigations were carried out on an optical microscope «ALTAMI-MET-1M». Microstructure of steel investigated on the scanning electron microscope JSM-6390LV. Study of the phase composition and crystal structure of specimens were carried out by X-ray diffraction analysis on the D8 ADVANCE diffractometer in  $\text{CuK}\alpha$ -radiation.

Determined that after electrolytic-plasma nitriding fine inclusions with average size  $\sim 0.1 \mu\text{m}$  are formed on high-speed steels surfaces. It is assumed that these fine inclusions are fine nitrides of alloying elements. It is established that on R9, R6M5, R18 steels surfaces after electrolytic-plasma nitriding at the temperature is  $550^\circ\text{C}$  formed nitrated layer consisting of the diffusion layer with  $\text{Fe}_4\text{N}$  ( $\gamma'$ -phase) monophasic nitride. It was found that after electrolytic-plasma nitriding increases the resistance of high-speed steels to abrasive wear. Relative wear-resistance of high-speed steels samples after nitriding is increased by  $\sim 30\%$  as compared with the initial samples. Determined that the wear intensity of the nitrated samples of R9, R6M5, R18 high-speed steels is reduced by 77%, 81% and 83%, respectively, indicating a significant increase of high-speed steels wear-resistance after electrolytic-plasma nitriding. Increase of wear-resistance after electrolytic-plasma nitriding, mainly due to the formation on the surface of a diffusion layer of nitrogen martensite with  $\text{Fe}_4\text{N}$  ( $\gamma'$ -phase) monophasic nitride. A significant increase of high-speed steels wear-resistance after electrolytic-plasma nitriding shows the prospects of using this method for improving the performance of cutting tools.

### REFERENCES

- [1] Vereshhaka A.S. // Rabotosposobnost' rezhushhego instrumenta s iznosostojkimi pokrytijami. – M.: Mashinostroenie, 1993.  
Suminov I.V., Belkin P.N. i dr. // Mir materialov i tehnologij. V 2-h tomah, Tom 1. – M. izd. Tehnosfera, 2011.

### FRAGMENTED STRUCTURE AND ORIENTATION RELATIONSHIPS BETWEEN DIFFERENT FRAGMENTS IN TINI SURFACE LAYER AFTER ION IMPLANTATION<sup>1</sup>

*A.V. TVERDOKHLEBOVA, L.L. MEISNER, S.N. MEISNER*

*Institute of Strength Physics and Materials Science of Siberian Branch Russian Academy of Sciences, 2/4, pr. Akademicheskii, Tomsk, 634021, Russia, a@vtverd.ru, +7 (3822) 286996*

By the electron backscatter diffraction method there were investigated changes in the microstructure of the surface layer of NiTi after pulse impacts on the alloy surface by medium energy silicon ion beams. It was found that the surface layer is characterized with the presence of the martensitic phase B19' within the B2 fragmented grain structure with the high concentration of phase and interphase boundaries, the linear fragment sizes exceeding 1 micron, grain fragmentation is inhomogeneous and depends on the crystallographic orientation of the initial grain. Internal structure of the one grain is fragmented by almost 1/3 of its volume, and in the other grain any significant structural changes is not observed. The most heavily fragmented structure was observed in grains, which crystallographic orientation was close to the direction  $\langle 111 \rangle$ , relative to the ion impact direction. The angles misorientation of the fragments was analyzed relative to the each other and initial crystallographic orientation of B2 structure (Fig. 1).

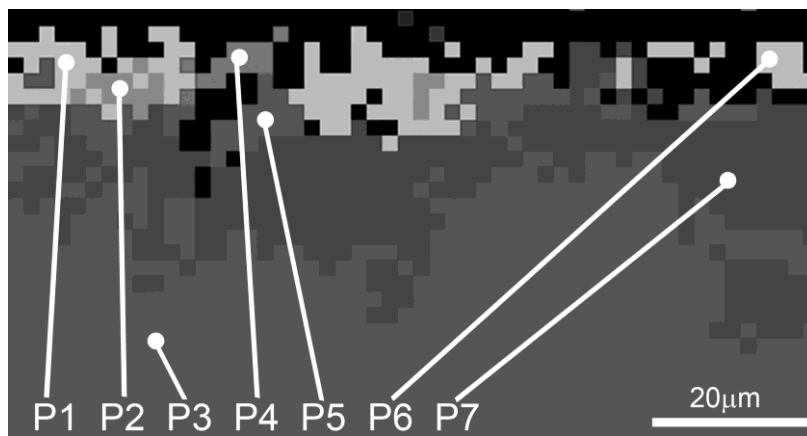


Fig. 1. The Euler angles misorientation map for the subgrain structure.

Rotation matrices were constructed for Euler angles obtained from the experiment. Based on these matrices the axis and angle of rotation to transform one fragment to another were calculated. Thus calculations have shown that there are special type boundaries between subgrains formed after irradiation impact (Tab. 1, 2).

Table 1. The Euler angles and crystallographic orientation relative to the impact direction  $\vec{z}$  of fragments.

	P1	P2	P3	P4	P5	P6	P7
$\phi_1; \Phi; \phi_2$	137.3;143.5;265.3	137.3;143.5;265.3	142.9;53.5;43.2	142.9;53.5;43.2	145.5;32;84.2	110.1;146.3;267.4	21.1;53.4;46.6
$\vec{z}$	$\langle \bar{2}, 0, \bar{3} \rangle$	$\langle 1, 2, \bar{1} \rangle$	$\langle 1, 1, 1 \rangle$	$\langle \bar{1}, 0, 2 \rangle$	$\langle 1, 0, 2 \rangle$	$\langle \bar{1}, 0, \bar{2} \rangle$	$\langle 1, 1, 1 \rangle$

Table 2. The axis  $\langle h, k, l \rangle$  and angle  $\theta$  of rotation to transform one fragment to another.  $\Sigma$  is the ratio of the size of the coincident site lattices unit cell to the standard unit cell.

	P3↔P7	P3↔P5	P3↔P4	P5↔P6	P7↔P1	P7↔P2
$\langle h, k, l \rangle$	$\langle \bar{1}, \bar{1}, \bar{1} \rangle$	$\langle 0, 1, 2 \rangle$	$\langle 0, 1, 2 \rangle$	$\langle 3, \bar{1}, \bar{2} \rangle$	$\langle 0, 2, \bar{1} \rangle$	$\langle 1, 1, 0 \rangle$
$\theta$	120°	48°	180°	180°	154°	147°
$\Sigma$	7	15	15	19	15	13a

<sup>1</sup> This work was supported by SB RAS project № III.23.2.1

**RADIATION SYNTHESIS AND PROPERTIES OF THE COPOLYMER BASED ON N-VINYLPYRROLIDONE AND METHACRYLIC ESTER IN THE PRESENCE OF SYNTHETIC ION EXCHANGERS.**

*V.M. LE, V.D. ZHEVNYAK, V. PAK*

*Kemerovo State University, Krasnaya St. 6, Kemerovo, E-mail: ya808@yandex.ru, phone: +79095139931*

This work is devoted to the study of processes of radiation copolymerization N - vinylpyrrolidone (N-VP) and methyl methacrylate (MMA) in the presence of synthetic ion-exchangers. As the crosslinking agent is used diethylene glycol divinyl ether (DVEDEG). The optimum ratio of the monomers and the absorbed radiation dose were determined. It is shown that in the dose range 25-45 kGr parameters do not change the three-dimensional grid.

The kinetics of equilibrium swelling of the copolymer N-VP and MMA, depending on the type of the ion-exchanger and its quantitative content, was studied. The values of diffusion coefficients and water absorption. The determining factors of radiation copolymerization are the concentration crosslinking component and the absorbed dose from the analysis of these data.

## MICROSTRUCTURE OF LAYERS IN MULTILAYER THERMAL BARRIER COATINGS ON THE BASIS OF ZrYO / SiAlN<sup>1</sup>

*M. V. FEDORISCHEVA, V.P. SERGEEV, M.P. KALASHNIKOV, V.V. NEYFELD*

*Institute of Strength Physics and Materials Science, SB RAS, 2/4Academicheskii Ave, Tomsk, 634021 Russia, [fmw@ispms.tsc.ru](mailto:fmw@ispms.tsc.ru), +79627763406*

Thermal barrier coatings on the basis of the Si-Al-N and Zr-Y-O systems are used in the production of gas turbine engines to protect units from heat: combustion chambers, impellers, blades and nozzle turbine, etc. [1,2]. Nanostructured multilayer coatings are special interest. They provide the minimum amplitude of modulation of normal and tangents stresses on all interfaces of multilayered coatings.

The nanocrystalline structures have no dislocations, so the structural states with high curvature-torsion of the crystalline lattice are formed. This characteristic of the material have an important role in all types of structural - phase transitions in solids.

The paper deals with the results of electron-microscopic study of the curvature-torsion of the crystal lattice of the elastic stress state in the layer of the Zr - Y - O in multilayer coatings of the Zr YO / Si Al N. Estimates of the curvature-torsion of the crystal lattice allows us to estimate the level of local internal stresses, which lead to a significant improvement in the mechanical properties of nanomaterials.

The fine structure of the multilayer coatings was investigated by TEM on the JEM-2100 device. A foil prepared by «cross-section» method using installation ION SLISER-EM-09100IS. The curvature-torsion of a crystal lattice and internal local stresses were estimated using TEM method using the techniques described in [9,10].

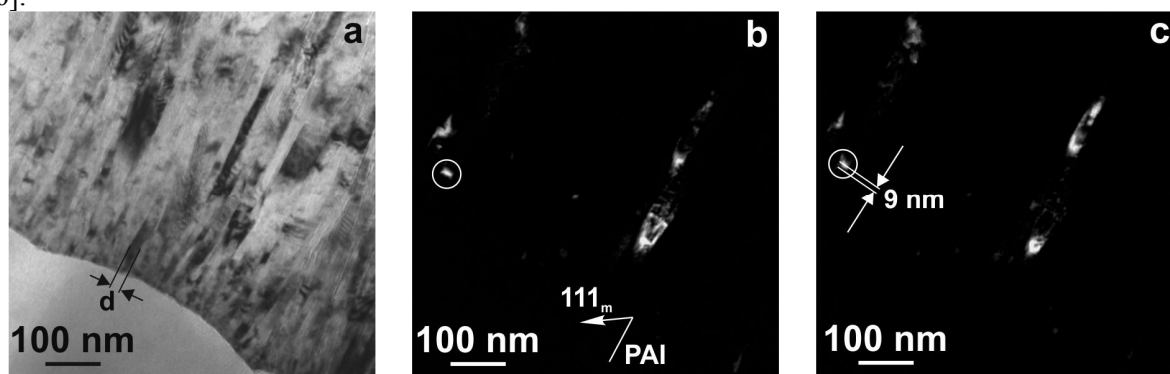


Fig. 1. TEM image of the microstructure of the ZrYO/SiAlN multilayer coating. Bright-field image of the Zr-Y-O layer at the boundary with a layer of Si-Al-N, the cross-section of the grain size is shown by arrows (a); dark-field image of the extinction bending contour (b) and angle inclination of goniometry is one degree (c).

It was established that layers on the basis of the Zr-Y-O in a multilayer coating Zr Y O / Si Al N have a columnar structure. The cross grain size is 80 nm, the height of the column is about 1000 nm. In this case it value corresponds to the thickness of the deposited layer. It was shown that the structure of all layers on the basis of Zr-Y-O in the multilayer coating is not depend on the position of the coating layer. The curvature - torsion of the crystal lattice and the internal elastic stresses depend on the cross grain size of the layer of Zr-Y-O. The larger cross-section grains size in the layer, the smaller the curvature-torsion of the crystalline lattice and internal elastic stresses. Such dependencies are caused by the structure of nanograins, which are formed in the coating.

### REFERENCES

- [1] *W. Ma and H. Dong // Thermal barrier coatings. – Woodhead Publishing Limited, 2011.*
- [2] *Korotaev, D.P. Borisov, V.Yu. Moshkov, S.V. Ovchinnikov, Yu.P. Pinzhin, A.N. Tyumentsev // Physical Mesomechanics.- 2009.-12.- p.269 - 279.*
- [3] *E.V. Kozlov, A.N. Zhdanov, N.A. Koneva // Physical Mesomechanics.- 2006.- 9.- P. 75 – 85.*

<sup>1</sup> This work was supported by Russian Academy of Sciences, Siberian Branch, project № III.23.1.1.

## THE REGULARITIES OF WEAR OF TITANIUM NICKELIDE MODIFIED BY THE METHOD OF HIGH-DOSE ION IMPLANTATION AND ELECTRIC-SPARK ALLOYING

*K.V. KRUKOVSKIY, O.A. KASHIN, A.I. LOTKOV*

*Institute of Strength Physics and Materials Science of Siberian Branch Russian Academy of Sciences, 2/4, pr. Akademicheskii, Tomsk, 634021, Russia, kvk@ispms.tsc.ru, (3822)286-936*

Titanium nickelide along with unique properties such as shape memory effect and superelasticity effect has high corrosion resistance and wear resistance [1, 2]. This led to the use of this alloy in medicine and astronautics. Despite the high wear resistance, components, working in space technology should work reliably for a long time without the possibility of maintenance, so the additional increase in wear resistance is important.

This paper presents the study of wear regularities of titanium nickelide with coarse-grained structure modified by the methods of high-dose ion implantation and spark alloying of molybdenum. Ion implantation was carried out on the device DIANA 2. Accelerating voltage under implantation was 60 kV, the pulse repetition frequency of 50 Hz, 200 ms duration, fluence was  $5 \times 10^{17}$  ions/cm<sup>2</sup>. Electric-spark alloying (ESA) was performed with the device «SE - 5.01», voltage was  $V = 59$  V, the capacitance  $C = 85$  uF. Testing of the samples was carried out in a "pin on disk" in the boundary lubrication. Counterbody was made of hardened bearing steel. Test load was 25 N, 100 N, 250 N, sliding speed of 3 m/s.

In sliding titanium nickelide with coarse-grained structure on the graph of dependence of the sample weight loss from the path of friction observed the initial stage of a high rate of wear and stage a constant low wear rate, which is characteristic for normal wear. At the initial stage of the test sample material is transferred to the counterbody and on the counterface is formed layer of the transferred material, the same mechanism has been observed in [3]. At the stage with low wear rate the layer which was formed on counterbody disappears almost entirely. The morphology of friction surface of samples in a scanning microscope using backscattered electron detector showed that the surface has areas with differing contrast of the base material, which occupy approximately 50% of the contact area, according to microprobe analysis revealed them to iron. Surface contact patch has traces of adhesion gripes, but not typical for adhesive wear.

In sliding titanium nickelide the implanted molybdenum, as in the case of initial titanium nickelide on the graph of the weight loss of samples from the sliding path observed the initial stage with a high wear rate and stage with constant low wear rate, which is characteristic for normal wear. However, the wear rate decreased by 10 times.

Layer thickness at ESA is  $10 \div 50$  microns. Furthermore, as a result of the ESA the material surface has a surface roughness, which can also be controlled by adjusting the process parameters. When tested titanium nickelide modified by ESA molybdenum, in the investigated conditions is practically not observed wear even after increasing the load up to 250 N.

### REFERENCES

- [1]. L.G. Korshunov, V.G. Pushin, N.L. Chernenko // The Physics of Metals and Metallography. – 2011. Volume 112. № 3. Pages 308-319.
- [2]. G D F. Gao, H.M. Wang // Materials characterization. – 2008. Volume 59. Pages 134–135.
- [3]. B.P. Gritsenko, Y.F. Ivanov, N.N. Koval', K.V. Krukovskii, N.V. Girsova, A.D. Teresov, I.V. Ratochka, I.P. Mishin // Journal of friction and wear. – 2012 Volume 33. № 3. Pages 184-189.

## PULSED ION BEAM EFFECT ON THE TITANIUM AND ZIRCONIUM ALLOYS

*I.P. CHERNOV, E.V. BEREZNEEVA, P.A. BELOGLAZOVA, N.S. PUSHILINA, G.E. REMNEV*

*National Research Tomsk Polytechnic University, Lenina 30, Tomsk 634050, Russia, tpu.chernov@gmail.com*

Titanium alloys because of low density, good biocompatibility and high corrosion resistance are widely used in medical, aerospace and chemical technique. In turn, zirconium alloys are important constructional materials of nuclear reactors. They have a low thermal neutron capture cross section, high corrosion resistance and strength characteristics. However, Ti, Zr alloys are hydride-forming, the penetration of hydrogen into the bulk material leads to a decrease of plasticity, formation of cracks and, as a consequence, the subsequent destruction. Therefore, the protection against the penetration of hydrogen in titanium and zirconium alloys is an important problem. Promising ways protective coatings are pulse beam methods which are actively being developed. Such effects can increase the wear resistance, strength, corrosion resistance [1,2].

In the report discusses the results of studying the surface properties titanium VT1- 0 and zirconium Zr1% Nb alloys irradiated by pulsed beams of carbon ions with an energy of 200 keV, pulse  $\tau = 80$  ns, energy density of  $1.5 \text{ J/cm}^2$ . In the process of irradiation the surface layer is formed with modified structure - phase state, feature layer is grain refinement to 0.15 - 0.8 microns ( grain size of non-irradiated alloys  $\sim 7$  microns). The modified surface layers possess higher hardness (40%) and durability (30%) compared with the original zirconium alloy. It is very important that they are an effective barrier against the penetration of hydrogen into the bulk material. The penetration of hydrogen in alloy bulk is 2 - 3.0 times lower. In addition, the degradation of mechanical properties of alloys modified by pulsed beams under the influence of hydrogen is much slower than that of the original alloy.

Observed significant changes in the microstructure of irradiated alloys due to high rates of heating and cooling the material in the effect a pulsed beam, as well as the formation of carbides in the modified layer.

### REFERENCES

- [1] *I.P. Chernov, S.V. Ivanova, N.S. Pushilina, N.N. Koval et.al. //Technical Physics. - 2012 - Vol. 57 - №. 3 - p. 392-398*
- [2] *Pushilina N. S., Chernova E. V., Lider A. M., Ivanova S. V. //Technical Physics. - 2013 - Vol. 58 - №. 9. - p. 1280-1283*

## FORMATION OF CARBON STEEL - STAINLESS STEEL SURFACE ALLOY ON CARBON STEEL SUBSTRATE<sup>1</sup>

*V.I. PETROV, A.B. MARKOV, E.V. YAKOVLEV*

*Institute of High Current Electronics, 2/3 Akademichesky Avenue, Tomsk, 634055, Russia, petrov@lve.hcei.tsc.ru, +7 3822 491571*

Carbon steels are widely used in industry due to its mechanical properties, high weld and cutting ability. Despite additional treatment area of applications of carbon steels is limited by its low corrosion resistance and hazardous chemicals like arsenic (As) which present in carbon steels. Properties of carbon steels can be modified and field of its applications can be enlarged using coatings. There are a lot of methods for coating carbon steels studied, but surface alloys haven't been used for this task previously.

Most important properties of coating are porosity and adhesion. High adhesion and low porosity leads to high efficiency of coating during lifetime of device. Non-porous coatings which can't be removed from the surface have a great interest both for science and industry. The surface alloy is a new type of coating which correspond to this parameters. Formation of surface alloys is performed using deposition of films by means of magnetron sputtering followed by a low energy high current electron beam liquid-phase mixing of the film and the top layer of substrate in a single vacuum cycle.

Carbon steel A 414 Grade A were chosen as a substrate and stainless steel type 12X18H10T (AISI 321) were used for deposition due to its availability and high corrosion resistance of stainless steel. Facility «RITM-SP» used for formation of surface alloys described in [1]. Optimal conditions of treatment and deposition were determined. Initial and treated by electron beam samples and samples with surface alloys of 2.5, 5, 7.5 and 10  $\mu\text{m}$  thick were investigated.

Morphology of the surface of samples and cross section were explored by scanning electron microscopy (SEM). Distributions of the chemicals on the surface of samples and in-depth elements distribution in the sample with 10  $\mu\text{m}$  surface alloy were investigated using EDXA. The microindentation hardness testing of surface layers were studied using a diamond Vickers indenter at peak load 0.5 N. To observe grain structure of cross section it has been etched by 2%  $\text{HNO}_3$  alcoholic solution and ferrichloride water solution.

Treatment of carbon steel by electron beam leads to smoothing and homogenization of its surface. Roughness of treated sample is 1.7 times lower than initial and microhardness is 1.15 times higher, but formation of surface alloys allows to smooth samples more effectively. Roughness of a sample with formed 10  $\mu\text{m}$  thick surface alloy 2 times lower than the roughness of treated sample, and 3.4 times lower than the roughness of initial sample. At the same time microhardness of samples with formed surface alloys 1.8 times higher than the microhardness of virgin sample, and it's more than 1.5 higher than microhardness of treated sample. Chemical composition on the surface of samples with formed surface alloys is equal to the chemical composition of deposited material for all thicknesses. Non-porous layer of stainless 10  $\mu\text{m}$  thick and also non-porous transitional layer 4  $\mu\text{m}$  thick are observed at the cross section of the sample with 10  $\mu\text{m}$  thick surface alloy. Presence of rather thick transitional layer argues to the high adhesion of surface alloy.

### REFERENCES

- [1] *Markov A. B., Mikov A. V., Ozur G. E., Padei A. G.* // Instruments and Experimental Techniques. – 2011. – Vol. 54. – № 6. – P. 862-866.

<sup>1</sup> This work was supported by the SB RAS project for basic research, code "II.14.2.1", title "Explosive-emission processes in vacuum discharge and development of fundamental bases of their application in technologies", Gov. Reg. No. 01201373605.



## TRANSPORT CHARGE OF GALLIUM ARSENIDE FILMS SYNTHESIZED ON POLYCRYSTALLINE SILICON BY IONICS ABLATION

A.V. KABYSHEV, F.V. KONUSOV, G.E. REMNEV, S.K. PAVLOV

Tomsk Polytechnic University, Lenin ave. 30, Tomsk, 634050, Russia, E-mail: konusoev@hvd.tpu.ru

GaAs is prospective material for electronics. Integration of perspective semiconductors GaAs and Si is important in optoelectronic aims but restrains by problems of defectiveness and materials compatibility. Electrical characteristics and transport charge mechanism in GaAs films, produced by epitaxy methods and by subsequent processing are change in wide ranges from dielectric to semiconductors. The unique properties of the amorphous–microcrystalline films, produced by different pulsed methods – from RF–plasma, flash evaporation, co–evaporation of elements and lasers deposition allows to use its for buffer layers production with differ lattice parameters, heterojunctions, antireflecting coatings in the devices. Advantage of pulsed methods is the possibility of passivation directly during growth and conjunction of heterogeneous materials. A films deposition from the plasma created by power ions bunch allows to realize the high velocity deposition and to form the films on considerable squares and on different substrates. Energetic characteristics and mechanisms of transport charge of its films were not studied.

In this work the electrical and photoelectrical characteristics of GaAs films, deposited on the polycrystalline silicon by pulsed ionics ablation with using of accelerator «TEMP» ( $U=200$  kV;  $j=180-230$  A/cm<sup>2</sup>,  $t_p\sim 60$  ns,  $n_{imp}\sim 100$ ,  $P=10^{-2}$  Pa,  $v_d\leq 1$  mm/s) and its change after thermal vacuum annealing ( $T_{an}=300-900$  K,  $P<10^{-2}$  Pa). Surface and volume dark conduction  $\sigma$ , photoconduction  $\Delta\sigma_{ph}=\sigma_{ph}-\sigma$  ( $\sigma_{ph}$ –conduction at illumination  $h\nu=1.5-4.0$  eV), photosensitivity  $K=\Delta\sigma_{ph}/\sigma$  were measured at  $T=300-500$  K and peculiarities of conduction mechanisms were investigated.

GaAs films, deposited on Si by ionics ablation on the parameters are not inferior to films, produced by alternative pulse and epitaxial methods, and surpass the GaAs films, deposited on Al<sub>2</sub>O<sub>3</sub>. Conduction and photoconduction of GaAs films deposited on Si has a mixed type and implemented by activation and hopping mechanisms with participation of localized near a Fermi level defects states. Two stages of annealing  $T_{an}=300-600$  and  $600-1200$  K were established. These stages were characterized by an optimal ratio between the values of conduction and photoconduction, the activation energies and density of localized states, and also the peculiarities of the transport charge mechanisms. After annealing at  $300-600$  K change of characteristics of hopping and activation components of conduction was caused by redistribution of the charge carriers between shallow and more deep levels, created by donors and acceptors defects. After annealing at  $600-1000$  K density of localized states, causing hopping conduction, stabilized at a level  $N(E_F)=(5-10)\cdot 10^{16}$   $\text{cm}^{-3}$ . The formed parameter of surface dark and photoconduction, correlation between them and the dominant conduction mechanism were due to charge exchange processes, annihilation of unstable defects and joints them into clusters.

## MODIFICATION OF ZIRCONIA CERAMICS BY TREATING THE SURFACE OF POWERFUL PULSED ION BEAMS

I.P. VASIL'EV\*, S.A. GHYNGAZOV\*, T.S. FRANGULYAN\*, A.V. CHERNYAVSKI\*

\* Tomsk Polytechnic University, Lenin str., 30, Tomsk, 634050, Russia, E-mail: [ghyngazov@tpu.ru](mailto:ghyngazov@tpu.ru), phone +7 (3822) 563864

The modifying effects of powerful pulsed beam (PPB) of accelerated carbon ions on subsurface layers zirconium ceramics composition (mol%)  $97\text{ZrO}_2\text{-}3\text{Y}_2\text{O}_3$  were investigated. The ion beam had the following parameters: the energy of the accelerated ions is  $E = 200$  keV, current pulse duration equal  $\tau_{\text{и}} = 100$  ns, pulse current density  $j_i = 40$  and  $150$  A/cm<sup>2</sup>. The total number of pulses was  $N = 100$  and  $300$ . At current densities  $j_i = 40$  and  $150$  A/cm<sup>2</sup> during the pulse  $2,5 \cdot 10^{13}$  and  $9,4 \cdot 10^{13}$  cm<sup>-2</sup> ions C<sup>+</sup> are implanted in the sample, respectively. The structural-phase state, elemental composition and mechanical properties of subsurface ceramic layers modified by ion beam were investigated. By scanning electron microscopy revealed that the ceramic processing by powerful pulsed beam of accelerated ions of C<sup>+</sup> leads to melting of the surface layer whose depth is  $3 \mu\text{m}$ . It was found that microstructure of treated layer is differ from that of the bulk material. In this area the grains are elongated towards the surface. The size of the grains in the longitudinal direction on average 4 times larger than in the transverse direction. According X-ray diffractometry data the carbon ions implantation in the surface layer of ceramics in an amount of  $3,1 \cdot 10^{19}$ – $3,6 \cdot 10^{20}$  cm<sup>-3</sup> is not accompanied by the formation of new impurity phases. When processing ceramics by ion PPB with  $W_i = 3$  J/cm<sup>2</sup> (fluence  $f \geq 9,4 \cdot 10^{15}$  cm<sup>-2</sup>) the formation of zirconia cubic phases up to 30 wt. % is observed. Processing of ceramics by PPB causes significant reduction in the size of coherent-scattering region X-rays (CSR) phases present in the material. The CSR size of grain c-ZrO<sub>2</sub> phase was 15-20 nm. Based on analysis of the elemental composition irradiated surface layers by SIMS method and their electrical conductivity a conclusion was drawn that the main cause of the cubic phase stabilization in zirconia is the formation non-stoichiometric oxygen vacancies with high concentrations under ion treatment. It was found that action of ion beam on ceramics leads to a magnitude reduction of such mechanical characteristics as microhardness, nanohardness and Young's modulus. This fact indicates that the plasticity of the modified layer compared to its initial state is increased.

## EFFECT OF ION IMPLANTATION ON THE ANTIBACTERIAL PROPERTIES OF MATERIALS MEDICAL IMPLANTS<sup>1</sup>

*A.G. NIKOLAEV<sup>1</sup>, E.M. OKS<sup>1,2</sup>, A. OZTARHAN<sup>3</sup>, E. SOKULLU<sup>4</sup>, G.YU. YUSHKOV<sup>1</sup>, V.P. FROLOVA<sup>1</sup>*

*<sup>1</sup>Institute of High Current Electronics SB RAS, 2/3 Akademichesky Ave.,  
Tomsk, 634055, Russia, nik@opee.hcei.tsc.ru, +7 (3822) 491-776*

*<sup>2</sup>Tomsk State University of Control Systems and Radioelectronics, 40 Lenin Ave., Tomsk, 634050, Russia*

*<sup>3</sup>Izmir University, Uckuyular, Izmir, 35350, Turkey*

*<sup>4</sup>Izmir Katip Celebi University, Cigli Main Campus, Izmir, 35620, Turkey*

Experiments on ion implantation of biomedical implants for modification of their surface antibacterial properties are presented. Using ion source Mevva-V.Ru [1] as implanter it is providing generation of ion beams of almost all elements of the periodic table at accelerating voltages up to 60 kV, with doses up to the surface unit  $1E17$  ions / sq cm. In studies of the antibacterial properties of biomedical implants a culture L929 - fibroblast-like cells of the connective tissue of the mouse, very traditional for immunological studies was used.

Based on measurements involving techniques of Rutherford backscattering protons was measured penetration depth of the ions in the surface layer of implanted samples. Parameters were selected ion implantation, in which the change of antibacterial properties of the implant material is not accompanied by a deterioration of its surface characteristics. The effect of implantation of silver ions on the antibacterial properties of materials for biomedical implants are discussed.

### REFERENCES

- [1] *A.G. Nikolaev, E.M. Oks, K.P. Savkin, G.Yu. Yushkov, and I.G. Brown // Review of Scientific Instruments. – 2012. – V. 83 – № 2. P. 02A501.*

<sup>1</sup> This work was supported by TUBITAK and RFBR under the joint Turkish-Russian research program, grant numbers are TUBITAK No 212M047 and RFBR-13-08-91370 CT\_a, correspondently.

## THE INFLUENCE OF A DIFFUSION DISCHARGE IN THE AIR AT ATMOSPHERIC PRESSURE ON THE ELECTRO-PHYSICAL PROPERTIES OF NARROW-GAP SEMICONDUCTORS CDHGTE

A.V. VOITSEKHOVSII\*, D.V. GRIGORYEV\*, A.G. KOROTAEV\*, A.P. KOKHANENKO\*, I.V. ROMANOV\*, V.F. TARASENKO\*\*, M.A. SHULEPOV\*\*

\*National Research Tomsk State University, Lenin av. 36, Tomsk, 634045, Russia, 745-denn@elefot.tsu.ru, (83822)413517

\*\*High-Current Electronics Institute, 2/3 Akademicheskoy Avenue, Tomsk, 634055, Russia, VFT@loi.hcei.tsc.ru, (83822)491685

Nowadays various discharges and electron beams are widely used for modification of near-surface layers of materials [1]. Feature of these discharges is the combined effect of a dense nanosecond-discharge plasma with the power density of energy contribution of hundreds of megawatts per cubic centimeter, a supershort electron beam with a wide energy spectrum and optical radiation of different spectral ranges of the plasma discharge. The aim of this work is to study the effect of a nanosecond volume discharge in air at atmospheric pressure on the electro-physical properties of epitaxial film grown by molecular beam epitaxy.

For tests, three series of specimens epitaxial CdHgTe films p-type conductivity ( $p = 1 \div 2.5 \times 10^{16} \text{ cm}^{-3}$ ,  $\mu_p = 300 \div 500 \text{ cm}^2 \text{ V}^{-1} \text{ s}^{-1}$ ), grown by molecular beam epitaxy at the Institute for Semiconductor Physics of the Siberian Branch of the Russian Academy of Sciences (Novosibirsk) were prepared. The as-grown specimens were located in a gas diode on a copper anode. Use was made of a Radan-220 generator as a pulse-voltage source forming voltage pulses with the amplitude  $\sim 230 \text{ kV}$  (open-circuit voltage), high-amplitude pulse duration  $\sim 2 \text{ ns}$  (at a matched load), and rise time  $\sim 0.5 \text{ ns}$ . The specimens were irradiated in the pulsed-periodic mode at the pulse repetition rate  $1 \text{ Hz}$ . The action was realized through 100–1200 pulses for a series of specimens irradiated in air.

The electrophysical parameters of the CdHgTe specimens before and after irradiation were found from the Hall-effect measurements using the Van-der-Pauw method. The measurement were performed at a direct current through the specimen ( $I = 1 \text{ mA}$ ) for two directions of the current and two directions of the constant magnetic field.

Analysis of the results of measurements of the electro-physical parameters of the CdHgTe epitaxial-film specimens subjected to pulses of a nanosecond volume discharge reveals that upon irradiation by 100–1200 pulses all the specimens exhibit an increase in conductivity. The specimens irradiated by 100 – 400 pulses, however, exhibit a decrease in the Hall coefficient. In so doing, the field dependence of the Hall coefficient is characterized by a shift of the inversion point of the Hall coefficient sign to the region of higher magnetic fields from 0.17 T to 0.28 T.

An increase in the number of volume-discharge pulses up to 600 results in the inversion of the Hall-coefficient sign in the range more than 0.2 T. A still further increase in the number of pulses exposure leads to a decrease in the value of the Hall coefficient. It has been suggested that, on or near the surface of the film formed by a layer of highly conductive n-type, whose parameters are such that the measured field dependence of the Hall coefficient corresponds to the n-type conductivity. Also the lack of relaxation of electrical parameters of irradiated specimens within 3 months is noted.

Thus, our experimental data show that the action of pulses of nanosecond volume discharge in air at atmospheric pressure leads to changes in the electrophysical properties of CdHgTe epitaxial films due to formation of a near-surface high-conductivity layer of the n-type conduction. The preliminary results show that it is possible to use such actions in the development of technologies for the controlled change of the properties of CdHgTe narrow-band solid solutions and production of structures whose structure is heterogeneous with respect to conduction.

### REFERENCES

- [1] M. A. Shulepov, V. F. Tarasenko, I. M. Goncharenko, et al. // *Technical Physics Letters*. – 2008. – Volume. 8 – № 7. Pages. 51.

## PHASE AND STRUCTURE TRANSFORMATIONS IN DOPED BARIUM CERATE AT HEAVY ION IRRADIATION

I.V. KHROMUSHIN<sup>1</sup>, T. I. AKSENOVA<sup>1</sup>, T. TUSEYEV<sup>1</sup>, K.K. MUNASBAEVA<sup>1</sup>,

YU.V. ERMOLAEV<sup>2</sup>, V.N. ERMOLAEV<sup>2</sup>, A.S. SEITOV<sup>2</sup>

<sup>1</sup>Institute of Nuclear Physics, Ibragimov str.1, Almaty, 050032, Kazakhstan, [aksenova@inp.kz](mailto:aksenova@inp.kz), +7 727 3866841

<sup>2</sup> – Kazakh National Technical University, 22, Satpayev str., Almaty, Kazakhstan

Recently it was noticed that proton conducting properties of barium cerates can be improved by different kind of irradiation of the materials. It is supposed that irradiation of the perovskite proton conductors with the ABO<sub>3</sub> structure stimulates formation of the additional oxygen vacancies and increases in concentration and mobility of charge carriers, improving proton conducting properties of cerates. It is extremely important to obtain a lot of elementary knowledge concerning the radiation induced effects on some physical properties for the perovskite-type ceramics [1-3].

The effects of oxygen, neon, argon, krypton ion irradiation on structure and properties of the doped barium cerates BaCe<sub>0.85</sub>Nd<sub>0.15</sub>O<sub>2.925</sub> were studied.

The samples of ceramic barium cerate in the form of 10x5x1 mm sized plates were preliminary annealed in air at 650°C for 7 hours. Heavy ion irradiation was performed on the DC-60 accelerator at the Institute of Nuclear Physics of the Republic of Kazakhstan. Irradiation characteristics are shown in Table 1. Ion ranges and vacancy yield were calculated using the SRIM – 2013 program.

Table 1- Ion energies, calculated ranges and vacancy yield

High energies				Low energies			
Ion type	Energy of ions, [MeV]	Ion ranges, [μm]	Yield, Vacancies/ion	Ion type	Energy of ions, [keV]	Ion ranges [μm]	Yield, Vacancies/ion
O	28	13.0	1740	O	40	0.080	243
Ne	35	12.7	2700	Ne	40	0.065	320
Ar	70	13.2	8100	Ar	100	0.080	800
Kr	147	15.3	31000	Kr	260	0.108	2500

Surface relief and structure of the irradiated barium cerates were investigated by x-ray analysis, scanning electron and atomic force microscopies. It is appeared that both structure and surface relief depend on the type and energies of the ions. So, blistering was observed on the surface of the material after irradiation by low energy Ne ions, whereas no blistering was observed after irradiation with Ar and Kr ions.

In case of high energy ion irradiation of barium cerates the solid phase structural transformation of the material surface took place. At high energy ion irradiation by Ne, Ar, Kr ions the cerate surface undergoes the following stages of the spherulite growth - nucleation, growth (view of cauliflower), formation of spherulitic crust, correspondingly. It is necessary to notice that such structures were not found on the samples irradiated by the oxygen ions.

The difference in surface structure evolution of the cerates at irradiation by oxygen and noble gas ions was explained by defect oversaturation in the last case because of stable “noble gas – vacancy” complex formation as a result of low gas solubility in the ceramic. High stability of these complexes was confirmed by gas thermodesorption study where no rare gas release from the samples was found up to 1000°C.

At irradiation of samples by the oxygen ions an equilibrium defect concentration must be lower because of high oxygen solubility in the oxide lattice and no spherulite like structures are formed.

It was shown that modification of the A - sublattice of the oxide during irradiation takes place and high stable Ba - deficient phase and BaO are formed.

Analysis of the data received has shown that the high energy heavy ions are able to change the properties of the cerates to the distances exceeding the ion ranges in many times in these materials.

### REFERENCES

- [1] Jae-Hwan Kim, Bun Tsuchiya, Shinji Nagata, Tasuo Shikama. // Solid State Ionics. - 2008. - 179.- pp.1182-1186.
- [2] I.V. Khromushin, T. I. Aksenova, T. Tuseyev, K.K. Munasbaeva, Yu.V. Ermolaev, V.N. Ermolaev, A.S. Seitov // *Advance Materials Research*. – 2013.- 781-784.- pp. 357-361.
- [3] Bun Tsuchiya, A.Morono, E.R. Hodgson, S.Nagata, T. Shikama // Solid State Ionics. - 2008. - 179.- pp.909-912.

## OSSEOINTEGRATION AND ELASTIC PROPERTIES OF POROUS TITANIUM – DIAMOND-LIKE CARBON – BONE TISSUE COMPOSITE<sup>1</sup>

A.P.RUBSHTEIN\*, A.B.VLADIMIROV\*, E.B.MAKAROVA\*\*, S.A.PLOTNIKOV\*

\*Institute of Metal Physics Ural Branch of Russian Academy of Sciences, 18 S.Kovalevskaya St., Ekaterinburg, 620990, Russia,  
A.Vladimirov@imp.uran.ru

\*\*V.D. Chaklin Ural Scientific & Research Institute of Traumatology and Orthopaedics,  
7 Bankovskiy per., Ekaterinburg, 620014, Russia

Porous titanium implants were produced by compacting spongy titanium granules with subsequent vacuum sintering. On the implant surface the diamond-like carbon (DLC) films were deposited using PVD technique to improve biocompatibility. The mechanical properties (compression tests) of porous titanium have been determined. Experiments on animals have been performed using implants with 30, 40 and 50 % porosity. Studying of osseointegration shows that DLC deposition promotes formation of mature bone tissue at the periimplant area. By 6 months, the bone tissue ingrows the implant to full depth and its composition in the peripheral pores approximates that of compact bone tissue. A direct dependence is observed between the average values of conventional yield strength of porous titanium – diamond-like carbon - bone tissue composite and the volume of intergrown bone tissue.

<sup>1</sup> This work was supported by Russian Basic Research Foundation (Project 13-02-96031-r\_ural\_a) and Presidium of Russian Academy of Sciences under the program "Basic Sciences to Medicine" (Project 12-II-2-1012).

## MODELING OF HEAT TRANSFER, STRUCTURAL FEATURES AND MECHANICAL PROPERTIES OF BORIDE LAYERS ON CARBON STEELS, FORMED UNDER THE INFLUENCE OF THE ELECTRON BEAM<sup>1</sup>

*D.E.DASHEEV\**, *I.N. BADMAEVA\**, *A.E. POLUKONOVA\**, *N.N. SMIRNYAGINA\**, *A.S. MILONOV\**, *V.M. KHALTANOVA\*\**

\* *Institute of Physical Materials Science SB RAS, Sakhyanovoy Street, 6, Ulan-Ude, 670047, Russia, [smirnyagina09@mail.ru](mailto:smirnyagina09@mail.ru), 83012433845*

\*\* *Buryat State University, Smolin Street, 24a, Ulan-Ude, 670000, Russia*

The aim of the work is the calculation and analysis of thermal fields in the zone of influence of powerful electron beams for steel 3. We used the following methods: calculation of temperature fields and graphics distribution of temperature fields produced by mathematical environment Maple (13.0). Impact of electron beam was carried out using a powerful electron-beam installation with axial gun on thermionic cathodes. Pulsed electron beam was performed using electron-beam installation SOLO.

The electron beam is considered as a volumetric heat source.

The temperature at the point with coordinates  $x, y, z$ :

$$T(x, y, z, \tau) = \frac{q_0}{(4\pi a)^{\frac{3}{2}} c \rho} \int_{-\infty}^{\infty} dx' \int_{-\infty}^{\infty} dy' \int_{-\infty}^{\infty} dz' \int_0^{\tau} G(x', y', z', \tau) d\tau, \quad (1)$$

where  $G$  is the Green's function of this problem. Maximum temperature ranges from at  $z = h, r = 0$ . The temperature at this point:

$$T(x, y, z, \tau) = \frac{q_0}{16c\rho\kappa_1 a^{\frac{3}{2}} \sqrt{\kappa_2}} \times \int_0^{\tau} \operatorname{erfc} \left[ \frac{h\sqrt{\kappa_2} \left(1 + \frac{\tau_1}{\tau}\right)}{\sqrt{1 + \frac{\tau_1}{\tau}}} \right] \times 10^{(\tau+\tau_0)\sqrt{\tau+\tau_1}} d\tau \quad (2)$$

$c\rho$  – volumetric heat capacity,  $\text{kal}/\text{sm}^3 \times \text{grad}$ ;

$\kappa_1$  – coefficient of concentration of source on surface,  $\text{sm}^{-2}$ ;

$\kappa_2$  – coefficient of concentration of source in volume,  $\text{sm}^{-2}$ ;

$a$  – coefficient of thermal diffusivity,  $\text{sm}^2/\text{s}$ ;

$h$  – depth position of maximum of energy release;

$\tau$  – present time;

$x, y, z$  – current position.

The report discusses the thermal field in the center of the cylindrical sample steel 3 of 15 mm diameter with the impact of the electron beam (20 keV) having a diameter of 1.0 mm within 1-300 seconds. Different input modes of the electron beam analyzed, which take into account the scanning rate (0-80 Hz) and sawtooth character of movement of the beam on the surface.

<sup>1</sup> This work was supported by the Russian Foundation for Basic Research, project no: 12-08-31496

## THE FORMATION OF NiCrBSi COATINGS WITH INCREASED WEAR RESISTANCE BY GAS POWDER LASER CLADDING<sup>1</sup>

*N.N. SOBOLEVA, A.V. MAKAROV, I. YU. MALYGINA, A.L. OSINTSEVA*

*Institute of Engineering science of Ural Branch of the RAS, 34, Komsomolskaya Str., Yekaterinburg, 620049, Russian Federation, natashasoboleva@list.ru, +7(343)3753578*

Coatings deposition by laser cladding is the modern effective method of hardening, wear resistance increase and reconstruction of worn-out machinery surface. Nickel-based hardfacing alloys have become increasingly popular in recent years owing to their excellent performance under conditions of abrasion, corrosion and elevated temperature [1, 2, 3].

The formation speciality investigation of NiCrBSi coatings with increased abrasive wear resistance and high-temperature stability by gas powder laser cladding and additional heat treatment or deformation processing has been carried out.

The possibilities of strengthening and improving abrasive wear resistance of NiCrBSi coating formed by gas powder laser cladding by means of increase in chrome, carbon and boron content have been established.

NiCrBSi–TiC composite coatings have been formed by addition 15 and 25 wt. % percent TiC titanium carbide particles to deposit powder PG-SR2 (0,48% C; 14,8% Cr; 2,6% Fe; 2,9% Si; 2,1% B; Ni – base). It was allowed to achieve strengthening and increasing abrasive wear resistance upon wear over fixed corundum abrasive owing to microcutting process limitation by coarse high-strength TiC particles.

The hardness and wear resistance increase effect of Ni-based coatings obtained by laser cladding and additional high-temperature (1000-1075 °C) annealing has been discovered. It was arisen from formation of high-strength carbide and boride particles (Cr<sub>7</sub>C<sub>3</sub>, Cr<sub>23</sub>C<sub>6</sub>, CrB) frame. The thermal stability of the coatings has been investigated. It has been found that the structure and properties of these coatings after the high-temperature annealing was stable up to temperature of annealing. The new combined method of producing wear resistance Ni-based coatings with advanced high-temperature stability (gas powder laser cladding and additional optimized annealing at 1000-1075 °C temperature) has been developed [4].

The influence of the technological parameters of frictional treatment (indenter material, cutting-coolant technological environment, loading and friction coefficient) on phase composition, surface roughness and microhardness of PG-SR2 NiCrBSi gas powder laser clad coating surface has been investigated. The effective hardening of PG-SR2 coating surface by frictional treatment using boron nitride indenter in air and hard-alloy indenter in argon under conditions of relatively large friction coefficient in "indenter-coating" pair at the same time providing both favourable stress state of surface layer and high-grade surface roughness has been determined. It has been shown that frictional treatment promotes the increase of coating surface wear resistance upon wear over fixed corundum abrasive as well as under conditions of adhesive wear process (dry sliding friction).

### REFERENCES

- [1] *K.Gurumoorthy, M.Kamaraj, R.K.Prasad, R.A.Sambasiva, S.Venugopal // Mater. Sci. and Eng. A., 456, 11-19 (2007).*
- [2] *C.Navas, R.Colaco, J.DeDamborenea, R.Vilar // Surf. Coat. Technol., 200, 6854-6862 (2006).*
- [3] *B.Cai, Y.-f.Tan, L.He, H.Tan, L.Gao. // Trans. Nonferrous Met. Soc. China, 13, 1681-1688 (2013).*
- [4] *A.V.Makarov, N.N.Soboleva, I.Yu.Malygina, A.L.Osintseva // Patent RU 2492980 C1, 2013.*

<sup>1</sup> This work was supported in part by the project no. 12-P-1-1027 (according to the Program of the Presidium of the Russian Academy of Sciences no. 25); the project no. 12-T-1-1010 (according to the Program of the Division of Power Engineering, Machine Building, Mechanics, and Control Processes (OEMMPU) of the Russian Academy of Sciences no. 13) and the project of young researchers of the Ural Branch of the Russian Academy of Sciences no. 14-1-NP-139.



## USING OF THE EFFECT OF THE HOLLOW CATHODE FOR LOCAL ION NITRIDING OF MACHINE PARTS

*K.N. RAMAZANOV, V.V. BUDILOV, U.G. KHUSAINOV, I.V. ZOLOTOV*

*Ufa State Aviation Technical University, K. Marx str.12, Ufa, 450000, RF, ramazanovkn@gmail.com, +7(347)2730763*

It is well known that destruction of machine part originates on surface and surface layer of the material [1]. On operating, surface of the part undergoes higher loads than its core. It is notable that loads generally influence only separated areas of part surface. In such cases, only enough to harden the work surface of the part. Therefore, one of the priorities in modern engineering is the development of effective local nitriding methods.

Review of the literature showed that ion nitriding is one of the most common methods of structural-phase modification, the use of which in the industrialized world is constantly expanding. As practice shows, using of nitriding is particularly effective for machine parts that operates in wear conditions [2].

The aim of presented work is to study the influence of local ion nitriding with hollow cathode effect (HCE) [3] on microstructure, phase composition, surface microhardness, microhardness profile through the diffusion layer of 16KhNVFMB-Sh steel.

The microstructure analysis of nitrated layer showed presence of dark diffusion zone that had different thickness on exposed surface and areas covered by screen. Nitrated layer is an  $\alpha$ -phase nitrogen ferrite that has body-centered cubic structure. Lattice perion depends on nitrogen content. Crossing from nitrated layer to core is smooth, which is one of the main requirements to the microstructure of the nitrated steel.

The thickness of diffusion layer under screened surface is up to 4 times greater comparing to same under uncovered area and was 80...85  $\mu\text{m}$ . That allows concluding that using the screen leads to local growth of hardened layer thickness. Found that the HCE occurrence produces conducive conditions for sorption processes that ensure high concentration of diffusing component on the cathode surface.

Microhardness test showed screened surface microhardness growth approximately up to 2 times compared to original microhardness. Microhardness drop through the diffusion layer can be linked to decreasing of dissolved nitrogen concentration in  $\alpha$ -phase.

To determine the growth rate of the nitrated layer, the influence of processing time on diffusion zone thickness was studied. The results showed that ion nitriding process significantly accelerated t short-time exposures up to 4 hours. Exposure for 12 hours led to diffusion process saturating; in this case nitride layer depth was up to 100  $\mu\text{m}$ . Thus, studies demonstrate the effectiveness of the local ion nitriding of steel 16Kh3NVFMB-Sh using HCE.

### REFERENCES

- [1] *V. M. Zinchenko*, Surface engineering gears methods of chemical-thermal treatment. Moscow: Publishing House of the MSTU N.E. Bauman, 2001.
- [2] *S. A. Gerasimov, L. I. Kuksenova, V. G. Lapteva*, Structure and wear resistance of nitrated structural steels and alloys. Moscow: Publishing House of the MSTU N.E. Bauman, 2012.
- [3] *V.V. Budilov, R.D. Agzamov, K.N. Ramazanov* // Metal Science and Heat Treatment. 2007, Volume 49, Issue 7-8, pp 358-361.

## **EFFECT OF POWER MODE ON RESISTANCE IR-LEDS TO THE FAST-NEUTRON IRRADIATION**

*A.V.GRADOBOEV, V.V.SEDNEV*

*National Research Tomsk Polytechnic University, 30, Lenin Avenue, Tomsk, 634050, Russia,  
E-mail gradoboev1@mail.ru, phone +7-913-866-84-05*

Radiation exposure leads to the degradation of the parameters of semiconductor structures and various semiconductor devices fabricated on their basis. The main aim of research - to study the influence power mode on resistance IR-LEDs based on double heterostructures AlGaAs to irradiation by fast neutrons. The studies found that resistance to radiation LEDs under irradiation by fast neutrons in the active power mode (transmission operating current) substantially exceeds the resistance to irradiation in passive power mode supply (without missing operating current). The observed difference in radiation resistance can not be explained by thermal annealing of radiation defects. Possible mechanisms of radiation LEDs resistance with increasing irradiation in active power mode.

**EFFECT OF ELECTRIC FIELD BUILT OF PN-JUNCTION ON IR-LEDS RESISTANCE UNDER IRRADIATION BY GAMMA-RAYS**

*A.V.GRADOBOEV, V.V.SEDNEV*

*National Research Tomsk Polytechnic University, 30, Lenin Avenue, Tomsk, 634050, Russia,  
E-mail gradoboev1@mail.ru, phone +7-913-866-84-05*

It is known that the rate of radiation defects in the Schottky barrier of diodes of GaAs and InP embedded depends on the availability of an electric field. The main aim of research - to study the influence of the built-in electric field at the pn-junction resistance IR-LEDs based on double heterostructures AlGaAs under irradiation by gamma-rays. The studies found that the rate of introduction of defects in the presence of an electric field built pn-junction or a reverse bias is less noticeable defects in the rate of introduction of the neutral region where no electric field. Possible ways of improving the radiation resistance of infrared LEDs is observed.

## TITANIUM SURFACES DURING FORMATION OF SILICIDES AND BORIDES INITIATED BY HIGH-ENERGY TREATMENT. MODIFICATION OF STRUCTURE AND PROPERTIES

A.A. KLOPOTOV\*\*\* YU.F. IVANOV\*\*\*\* A.I. POTEKAEV\*\*, O.G. VOLOKITIN\*, V.D. KLOPOTOV\*\*\*\*

\*State University of Architecture and Building, Tomsk, 634002, Russia, [klopotovaa@tsuab.ru](mailto:klopotovaa@tsuab.ru), 89059910837

\*\*National Research Tomsk State University, Tomsk, 634050, Russia

\*\*\*Institute of High-Current Electronics of the Siberian Branch of the Russian Academy of Sciences, Tomsk, 634055, Russia

\*\*\*\*National Research Tomsk Polytechnic University, Tomsk, 634050, Russia

Titanium and its alloys have been extensively used as structural materials in many industrial applications. The major merits making titanium and its alloys promising materials is their high strength-to-density ratio in a wide range of operating temperatures and corrosion resistance. It is due to these properties that they are thought of as materials of choice for aerospace engineering (e.g., manufacture of engine parts and propulsion nozzles, and aerospace coating deposition), chemical industry and medicine [1]. Among the disadvantages of titanium and its alloys are their comparatively low heat resistance, relatively low elasticity modulus, and poor tribological performance [2]. Surface properties of a machine part are generally of the uttermost importance. Thus, formation of composite surface layers from these alloys could become a promising practical application.

An analysis of the literature data shows that transition-metal silicides, similarly to borides, in terms of their physical-mechanical properties, have to be classified as metallic compounds exhibiting high electric conductivity, whose temperature dependences of thermopower in binary compounds with metals are similar to those of metal-metal pairs [3]. Titanium silicides and borides cannot be referred to interstitial alloys, since they do not satisfy the Hägg rule and considerably exceed the critical Hägg ratio, 0.59. As a result, in binary systems, Ti-Si, substitution for silicon ions gives rise to formation of metallic structures with the ratio  $R_{Si}:R_{Me} > 0.9$ , the content of silicon in silicides being up to 50 at.%. In the cases of a higher content of silicon, substitution of metal atoms for silicon results in the formation of complex crystalline structures and an increased role of the covalent bonding between the atoms.

A TEM-based microdiffraction analysis offers a more detailed examination of the material phase composition and allows identifying the phases whose content is only a few fractions of a percent. For instance, the second phases, identified using indexing of the XRD patterns obtained from the surface layer of the technical-grade VT1-0 titanium subjected to plasma doping formed by the EWE of graphitized carbon fiber pre-charged with  $TiB_2$  powder, are the following: titanium carbide, TiC, and titanium borides of a variety of compositions, TiB,  $TiB_2$ ,  $Ti_2B_5$  and  $Ti_3B_4$ . An investigation of the second-phase morphology demonstrated that titanium carbide particles are predominantly globular, with their size varying from 50 to 150 nm. The titanium boride (TiB) particles are also globular and their size ranges from 50 to 100 nm. Titanium boride particles of other compositions ( $TiB_2$ ,  $Ti_2B_5$  and  $Ti_3B_4$ ) are much finer and their size ranges from 5 to 15 nm. Typically, these boride particles are found on dislocations, cell boundaries, fragments and subgrains.

We have performed an analysis of the diagrams of the binary (Ti-Si, Ti-B, Si-B) and ternary (Ti-Si-B) phase states and revealed a possibility for a wide range of metastable compounds to be formed as a result of nonequilibrium conditions created by processing of the material under study with high-density energy flows. Using the methods of XRD and TEM-based diffractometry, we have performed examination of the phase composition of the surface layer made from the technically pure VT1-0 titanium specimens subjected to concentrated energy flows (irradiation with plasma generated by EWE of conducting materials and with high-intensity, pulsed, sub-millisecond electron beams) and detected the formation of titanium silicide and boride particles of nano- and submicron size ranges.

### REFERENCES

- [1] I.J. Polmear, *Light Alloys: From Traditional Alloys to Nanocrystals*, Butterworth-Heinemann (2005).
- [2] V.I. Muraviev, P.V. Bakhmanov, B.I. Dolotov et al., *Ensuring Security of Structures Made from Titanium Alloys (Ed. V. I. Muraviev) [in Russian]*, Moscow, Ecom (2009).
- [3] G.V. Samsonov and Ya.S. Umanskii, *Solid Compounds of Heat-Resistant Metals [in Russian]*, Moscow, Metallurgiya (1957).

## USING OF NON-STEADY STATE LOW-CURRENT PLASMATRON FOR DIELECTRIC SURFACE ADHESION INCREASING<sup>1</sup>

*I.A. SHEMYAKIN\**, *Y.D. KOROLEV\**, *O.B. FRANTS\**, *N.V. LANDL\**, *V.S. KASYANOV\**, *A.V. BOLOTOV\**, *V.G. GEIMAN\**

\* *Institute of High Current Electronics, Tomsk, 634055, Academichesky Ave, 2/3, Russian Federation, shemyakin@inp.hcei.tsc.ru*

It is known that one way to improve the surface adhesion of polymers based on modified surfaces by the action of a non-equilibrium gas discharge plasma. Such discharges as a CD discharge, barrier, corona, etc. [1–3] let you modify a large area the flat surface. When treating a complex surface of small area, the efficiency usage of such discharges falls. It was shown [4] that the use of a discharge triggers in a low-level non-stationary plasmatron, improves adhesion surface polypropylene sleeves needles for medical syringes. This report focuses on a more detailed investigation of this issue.

The discharge was initiated in electrode system of the classical coaxial plasmatron in the gas fluent at atmospheric pressure. The following gases such as air and nitrogen were used in the experiments. Gas flows were of 0.2–1.0 g/s when the average current was about 0,2 A and the average gas input power was about 100 W. Emission spectra from different regions of the plasma torch of the plasmatron were recorded. The analysis of reactions in the plasma was carried out, and the mechanisms leading to adhesion increased was discussed.

A plasma torch used for surface modification of polypropylene sleeves medical syringe needles. A technique allowing to place the samples into different areas of the plasma torch with spatial and temporal resolution of at least 0.1 mm and 0.1 s was presented. A way to monitor changes in surface adhesion based on the measurement of the detachment force needle from the sleeve  $F_d$  has been described.

The set of experimental data on the influence of the geometry of the plasma torch nozzle, the flow rate and the type of gas, as well as the exposure time on detachment force  $F_d$  is shown. It has been shown the substantially increasing of the surface adhesion when using air and nitrogen on exposure times of about 1 s (Fig. 1). The analysis of the possibility of using no-steady-state low-current plasma torch in manufacturing needles for medical syringes done.

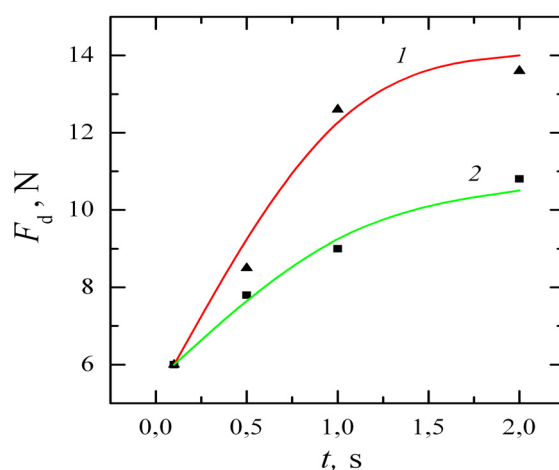


Fig. 1. Dependence of a detachment force versus the exposure time. Long nozzle, gas flow 0,8 g/s, 1 - air, 2 - nitrogen.

### REFERENCES

- [1] *M. Noeske, J. Degenhardt, S. Strudthoff, and U. Lommatzsch* // *Int. J. Adhesion and Adhesives*. – Apr. 2004. – vol. 24 – no. 2. – P. 171.
- [2] *S. Kropke, Y. S. Akishev, and A. Hollander*. // *Surface Coating Tech.* – Jul. 2001. – vol. 142. – P. 512..
- [3] *Nguen K.H., Ananev V.V.* // *Izv. Vyzov. Publisher and polygraph problems*. – 2009. – no. 6. – P.23.
- [4] *Shemyakin I.A., Korolev Y.D., Frants O.B.et.all...* // *Russian Physics Journal*. – 2012. – vol.55 – no. 12/3 – P. 113.

<sup>1</sup> This work was supported by Russian Foundation for Basic Research under Grant 13-08-98110

## FORMATION OF WAVE-GUIDE LAYERS IN LITHIUM NIOBATE WITH THE USE OF COPPER IMPLANTATION AND DIFFUSION<sup>1</sup>

*L.N. ORLIKOV, S.I. ARESTOV, K.M. MAMBETOVA*

*Tomsk University of Control Systems and Radioelectronics, 40 Lenin Ave, Tomsk, 634050, Russia, e-mail: oln4@yandex.ru*

The implantation of copper into Lithium Niobate in the prohibited crystal zone lets form a definite energetic level for optic transits. This paper examines conditions of optic wave-guided layers formation on Niobate Lithium due to the method of implantation copper ions with the next diffusion.

Researches include the evaluation of the gas extraction mechanism from the crystal, the ion purification-process of the crystal by the Hall's source, the process of implantation, the thermal forming process of copper scum in the inert atmosphere, the diffusion process and crystal annealing.

To increase a film adhesion the gas emission mechanism (from near-surface layers or volume) was estimated. For this purpose the crystal raying is made in the low-energy plasma, and the monochromator DMR 2 recorded the intensity of the oxygen lines under different discharge rates. The crystals with the minimal gas extraction were chosen when the intensity of the oxygen lines was minimal and almost did not change while alternating a discharge rate.

The crystal purification was carried out by the gaseous-ion source of Hall's type in which the current density and the form of the ionic flux were operated due to a potential gradient on the central electrode.

During the implantation as a source of speeding up ions the ionic source of pulse-batch action "Diana" with dielectric surface discharge was used. The process of implantation was carried out under accelerating potential 20 kV. The amount of implantation measured was  $3 \cdot 10^{17}$  ion/cm<sup>2</sup>. The calculated film thickness under the amount of implantation  $3 \cdot 10^{17}$  ion/cm<sup>2</sup> is 50 nm.

After the process of implantation the formation of copper scum having thickness 0.5 mkm on Niobate Lithium was carried out due to the vacuum evaporation or by means of the magnetron. Then the diffusion under the temperature 1050 K was conducted.

Two beams (non-object and signal) with the length 532 nm, obtained on the beam splitting cube, were cut into the waveguide layer on the Bragg angle. The reading of the photorefractive hologram was carried out by the radiation of injector laser diode on the wave length of 655 nm.

### Results.

The photoinduced absorption of the non-object beam and transfer of the optical power from the non-object beam into the signal one and vice versa were found out.

The biggest alteration of the diffraction pattern is observed due to the maximal impurity-dopant incorporation of crystal with the use of copper. Calculations show that perhaps changes of diffraction efficiency are connected with the magnitude variation of the crystal spatial field.

The availability to use ion sources for adding of measured impurity of copper and other metals during the formation of optic transits in the prohibited crystal zone was shown.

The combination methodic of diffusion and implantation technologies is perspective in order to create light-controlled active optic wave-guided layers, solid sources of electrons and X radiation.

<sup>1</sup>This work was supported within the task of Ministry of Education and Science of the Russian Federation No № 2014/225 (project №2491), and the Russian Foundation for Fundamental Research – Belarusian Republican Foundation for Fundamental Research Grant (projects № 12-02-90038 Bel\_a and № F12-R-222 )

## STRUCTURE AND PROPERTIES OF THE SURFACE ALLOY Ti – Y, FORMED BY THE COMBINED METHOD JOINING THE ELECTRIC EXPLOSION ALLOYING AND THE ELECTRON – BEAM TREATMENT<sup>1</sup>

*Yu.F. IVANOV<sup>\*,\*\*</sup>, K.V. SOSNIN<sup>\*\*\*</sup>, V.E. GROMOV<sup>\*\*\*</sup>, N.N. MOROZOVA<sup>\*\*</sup>, A.D. TERESOV<sup>\*</sup>*

*\*Institute of High – Current Electronics of the Siberian Branch of the Russian Academy of Sciences, 2/3 Academicheskoy Avenue, Tomsk, 634055, Russia, E – mail: [yufi55@mail.ru](mailto:yufi55@mail.ru), 8(3822)49-17-13*

*\*\*National Research Tomsk Polytechnic University, Lenin Avenue, 30, Tomsk, 634050, Russia*

*\*\*\*Siberian State Industrial University, Kirov str 42 Novokuznetsk, 654000 Russia*

In connection with the latest achievements in the development of the technology of ultra – high speed solidification of metallic melts, being realized, in particular, under high energy pulsed methods of effect, a distinctly pronounced interest to alloying components, earlier being considered to be unpromising due to their small solubility in a solid state, was formed. For titanium they are rare – earth elements the alloying by which can make possible to create the heat resistant alloys with thermally stable dispersion hardening.

The goal of this paper is to develop the surface alloy Ti – Y formation method, to study its structure and properties. The base material is a titanium alloy BT6; and alloying was done by plasma being formed under electric explosion of titanium foil of mass 100 mg, on the surface of which yttrium powder of mass 400 mg was located. A surface alloy thus formed was subjected to additional thermal treatment by intensive electron beam, varying the energy density of electron beam.

By methods of optical and scanning microscopy a formation of the surface alloyed layer of (20... 30)  $\mu\text{m}$  nets, under which a zone of thermal effect of 40  $\mu\text{m}$  thickness is located, is revealed. Volume fraction of  $\alpha\text{-Y}$  in the alloyed layer (according to the results of X-ray phase analysis) varies within 55% to 73% (a remainder is  $\alpha\text{-Ti}$ ) and depends on the energy density of electron beam. A structure of the grain type is formed on the surface of irradiation at a small volume fraction of  $\alpha\text{-Y}$  (55%). The elongated interlayers of  $\alpha\text{-Y}$  (Fig. 1,a) are noted on the grain boundaries, a two – phase ( $\alpha\text{-Ti} + \alpha\text{-Y}$ ) structure of cellular crystallization with cell size of 0,5  $\mu\text{m}$  (Fig. 1,b) – in grain volume. A structure of lamellar eutectic with a relatively small grain size (10 - 20)  $\mu\text{m}$  (Fig 1,c) are noted on the surface (volume fraction of  $\alpha\text{-Y}$  73%).

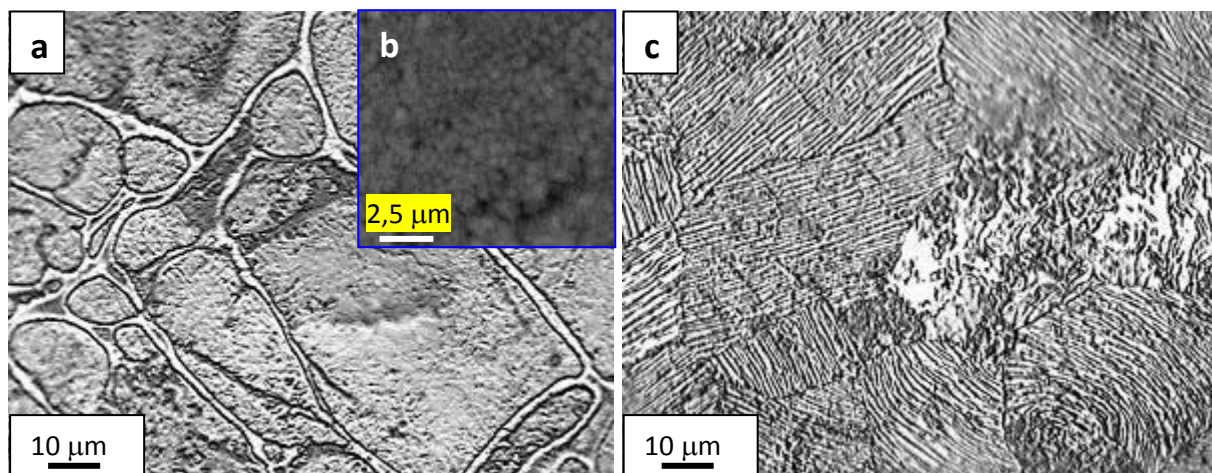


Fig. 1 Structure of a surface alloy Ti-Y, being formed in electric explosion alloying and the subsequent electron beam treatment: images (a) and (c) are obtained by the methods of optical microscopy, (b) – by methods of scanning microscopy.

Tribological properties of surface alloys Ti – Y were defined at dry friction according to the disk – ball scheme on high temperature tribometer THT –S-AX, CSEM, Switzerland. It was determined that formation of lamellar eutectic results in multiple decrease (compared to alloy BT6) of friction coefficient (more than a factor of 7) and speed of wear (more than a factor of 3).

<sup>1</sup> This work is done in the frameworks of the project FNI SDRAS № 11.9.5.2.

## THE PLASMA-IMMERSION ION IMPLANTATION OF TITANIUM IN STAINLESS STEEL AND ALUMINIUM IN TITANIUM

I.A. SHULEPOV, A.I. BUMAGINA, D.O. SIVIN, A.N. SUTYGINA, N.N. NIKITENKOV, O.V. VILHIVSKAYA, A.K. BOZHENKO, I.N. KHIMICH

Tomsk Polytechnic University, Lenin str. 30, Tomsk, 634050 Russia, nikitenkov@tpu.ru, 89138536482

One of the methods of improving the materials operational properties is a plasma-immersion ionic implantation. The purpose of this report is study a modification of passive hardness of a X18H10T steel at implantation of the titanium, and at aluminum implantation in titanium by a plasma-immersion ion implantation method.

Before implantation samples were exposed to the ion refining in argon plasma at pressure  $\sim 1$  Pa. Processing time was 15 minutes. The implantation conditions: a pulse length of an short-pulsing high-frequency potential of bias -  $7 \mu s$ , frequency of impulses -  $10^5$  Hz, amplitude of a potential of bias - 2 kV. Processing time for steel varied from 0.5 to 3 and for titanium from 0.5 to 6 minutes.

The initial and modified samples are taken for research of passive hardness. The passive hardness and friction coefficient are determined with a friction gauge «High Temperature Tribometer». The measuring results of a friction coefficients are presented in tables 1 and 2.

Table 1

Friction coefficient dependence on processing time of titanium samples

Processing time, min	Friction coefficient
initial	0.490
0.5	0.469
0.75	0.481
1	0.472
1.5	0.512
2	0.677
3	0.489
6	0.497

Table 2

Friction coefficient dependence on processing time of steel samples

Processing time, min	Friction coefficient
initial	0.437
0.5	0.506
1	0.490
1.5	0.494
2	0.236
3	0.168

Squares of a track of wear have been determined with use of three-dimensional roughness indicator "Micro Measure 3D Station". 9 values of a track squares have been determined for each sample and a medial arithmetical value is deduced. The results are presented in table 3.

Table 3

Mean value the track squares dependence on time of implantation

$S_{\text{treck}}, \mu m^2$	Processing time, min							
	0.5	1	1.5	2	3	initial		
	126	667	747	53	49	605		
$S_{\text{treck}}, \mu m^2$	Processing time, min							
	0.5	0.75	1	1.5	2	3	6	initial
	4126	3752	4002	6705	10338	5309	6313	7952

The depth distributions of an element composition in nearsurface layers after implantation were explored also.

### Conclusion

With the help of the plasma-immersion ion implantation is possible increase of passive hardness and decrease of a friction coefficient for the titanium modified by aluminum, and for X18H10T steel modified by titanium.



## FORMATION OF BIOCOMPATIBLE LAYERS ON THE IMPLANT SURFACE USING VACUUM ARC DEPOSITION AND SUBSEQUENT PULSED ELECTRON-BEAM TREATMENT<sup>1</sup>

*A.D. TERESOV, V.V. SHUGUROV, YU.F. IVANOV, YU.A. DENISOVA, E.A. PETRIKOVA, YU.H. AKHMADEEV, N.N. KOVAL*

*Institute of High Current Electronics SB RAS, 2/3 Akademichesky Ave, Tomsk, 634055, Russia, tad514@sibmail.com, +79234039163*

Currently the great experience of mixing of the materials surface layers using powerful ion [1, 2], pulsed electron beams [3, 4] and compression plasma flows [5] has accumulated.

Radiation, thermal and shock mechanical stress are carried out at the same time during treatment by the concentrated streams of energy. Developing restructuring processes taking place in conditions far from thermodynamic equilibrium and allow to obtaining surface layers with a unique set of structural and physico-mechanical properties [5].

It has not yet determined what type of surface, the level of nano/macro/micro structure of the implant surface is optimal for bone remodeling and protection against bacteria [6, 7]. Through targeted surface modification techniques it is possible to enhance biointegration of the implants materials significantly and make them to solve unusual problems.

It is widely known that zirconium and its alloys have a good bioinertness for body tissue and is used for manufacturing of orthopedic implants. However, the high cost of zirconium makes looking for other cheaper ways to manufacture implants. In this paper we propose to use a coating of zirconium (Zr, 1% Nb) a thickness of up to 2  $\mu\text{m}$  to improve the biocompatibility of the metallic implants surface. To improve adhesion of zirconium coating with metal substrate and to create a uniform microstructure on the material surface is proposed to use pulsed electron beam with submillisecond pulse duration.

VT1-0 titanium alloy, 12H18N10T stainless steel and CoCrMo alloy (Wironit) are used as initial materials in the form of flat specimens of dimensions 10x10x4 mm. Zr coating deposition was carried out by vacuum arc method at «TRIO» setup. Deposited film thickness was varied in the range of 0.5-2  $\mu\text{m}$ . The thus-obtained samples were irradiated by a pulsed electron beam at «SOLO» setup. During the irradiation energy density was varied in the range of 10-25  $\text{J}/\text{cm}^2$ , pulse duration of 150  $\mu\text{s}$  and the pulse number of 3.

Investigations of specimens surface using scanning electron microscopy, elemental analysis, profilometry and tribological investigations showed that for all materials there is a significant increase in the adhesive properties of the coating compared with untreated specimens due to mixing of a coating material and the substrate material to a thickness of up to 10  $\mu\text{m}$ , the thickness of the modified layer depends on the initial thickness of the coating and the energy density. Furthermore, it was shown that a homogeneous grain structure was formed in the surface of the irradiated specimens, where the crystallite size ranges of 1-2  $\mu\text{m}$ .

### REFERENCES

- [1] *V.I. Boyko, A.N. Valyaev, A.D. Pogrebnyak // Uspekhi Fizicheskikh Nauk. – 1999. – № 169. P. 1243-1271.*
- [2] *T.V. Panova, V.S. Kovivchak, K.O. Sharifulin // Izvestiya Vuzov. Fizika. – 2011. – № 1/3. P 165-168.*
- [3] *A.B. Markov, V.P. Rotshtein, Yu.F. Ivanov, D.I. Proskurovsky, K.V. Karlik, I.A. Shulepov // Surf. Coat. Technol. – 2004. – V. 180–181. P. 382–386.*
- [4] *N.N. Koval, S.V. Grigoryev, V.N. Devyatkov, A.D. Teresov, P.M. Schanin // IEEE Trans. Plasma Sci. – 2009. – V. 37. – № 10. P. 1890-1896.*
- [5] *V.V. Uglov, N.T. Kvasov, Yu.A. Petukhou, N.N. Koval, Yu.F. Ivanov, A.D. Teresov, V.M. Astashinski, A.M. Kuzmitski // Proceeding of VI International Conference Plasma Physics and Plasma Technology, Minsk, Belarus, September 28 – October 2. – 2009. P. 433-436.*
- [6] *K. Anselme, P. Davidson, A.M. Popa, M. Giazon, M. Liley, L. Ploux // Acta Biomater. – 2010. – V. 6. – № 10. P. 3824-3846.*
- [7] *F. Variola, J.B. Brunski, G. Orsini, P. Tambasco de Oliveira, R. Wazen, A. Nanci // Nanoscale. – 2011. – № 3. P. 335-353.*

<sup>1</sup> This work was supported by the RFBR grant (projects No. 12-08-00597-a) and SB RAS interdepartmental project No. 10.

## **SURFACE MODIFICATION OF 65G STEEL BY ELECTROSPARK ALLOYING AND ELECTRON-BEAM INFLUENCE METHODS<sup>1</sup>**

*YU.A. DENISOVA\**, *YU.F. IVANOV\**, *E.A. PETRIKOVA\**, *E.A. KOLUBAEV\*\**, *A.D. TERESOV\**, *V.V. SHUGUROV\**

*\*Institute of High Current Electronics SB RAS, 2/3 Akademicheskoy ave., Tomsk, 634055, Russia, e-mail: [yulija@opee.hcei.tsc.ru](mailto:yulija@opee.hcei.tsc.ru),  
Tel. +7(3822)491713*

*\*\*Institute of Strength Physics and Materials Science SB RAS, 2/4 Akademicheskoy ave., Tomsk, 634021, Russia*

Electrospark alloying is an effective method of working surfaces hardening of the tools, machines details and mechanisms. This method allows to obtain coatings with high adhesion to the basis material and having enhanced performance characteristics. The shortcoming of this materials treatment method is formation of high-relief surface with pores and cracks. Decreasing of roughness after electrospark alloying can be achieved by electron-beam treatment of the modified surface. During the work regularities and mechanisms of formation of structural and phase state in the surface layer of 65G steel in the conditions of ultrahigh speeds of heating and cooling at surfaces electrospark alloying (hard alloy WC8) and its subsequent pulsed electron-beam treatment have been revealed. Researches of evolution of element and phase composition, defective substructure of structural steel surface layer depending on parameters of the electron-beam treatment were carried out. The mechanical (microhardness) and tribological (wear resistance, friction coefficient) characteristics of the modified layers of structural steel were defined.

<sup>1</sup> This work was supported by the RFBR grant (projects No. 14-08-31706 мол\_a)

## NUMERICAL SIMULATION OF PHYSICAL AND CHEMICAL PROCESSES AT LASER SINTERING OF METAL POWDERS<sup>1</sup>

*S.N. SOROKOVA\**

*\*National Research Tomsk Polytechnic University, avenue Lenina, Tomsk, 634063, Russia, E-mail: s\_sorokova@tpu.ru, (3822)421480*

Laser sintering powders is one of new technologies for producing surface coatings of powder (including nanostructured) materials. In this method, the powder material is sintered by laser radiation. To use this method, thermoplastic finely dispersed powders with the good viscosity and solidifies rapidly, for example, polymers, waxes, nylon, ceramic or metal powders with the fusible binder additive. Heating velocity by laser irradiation provides opportunities for studies of the thermal, kinetic, rheological and mechanical processes. The literature devoted to both theoretical and experimental research of laser sintering are investigated structural changes, melting, volume change, shrinkage, porosity change, etc. (Merzhanov A.G., Stelmach L.S., Stolin A.M., Avvakumov E.G., Knyazev A.G., Pobol I.L., Pribitkov G.A., Shishkovsky I.V., etc.). But in known models clearly is not taken into account the interaction between of the thermal and non-thermal phenomena. About necessity a joint study of the direct and inverse effects referred to in the works Boldyrev V.V., Boldyreva E.V., Lyakhov N.Z., Knyazeva A.G., etc.

In this paper, on the example of the model system investigated regimes of laser sintering. The behavior of powder medium is described by analogy with a viscous compressible liquid taking into account to thermal stress and concentration. Absorption of laser radiation penetration into the material is considered in the form of volumetric heat source in the heat equation for the powder medium according to the law close to the Bouguer law for optically homogeneous media. For the numerical realization of the model has been developed special numerical algorithm and computer program. The influence of various characteristics of the laser exposure (frequency, duration, etc.) on the dynamics of coating synthesis is investigated in detail.

<sup>1</sup> This work was supported by RFBR № 13-03-01179-a

## MODIFICATION OF THE Co AND Ni-BASED POWDER ALLOYS COATINGS PROPERTIES BY ADDED IRRADIATION

*D.L. ALONTSEVA*

*East-Kazakhstan State Technical University, Ust-Kamenogorsk, 69 Protozanov St., 070004, Kazakhstan, tel.+7-3272-540-586, dalontseva@mail.ru*

The protective powder Ni and Co based coatings produced by a plasma detonation method designed for the protection of surfaces of industrial products working at high temperatures and in corrosive environments (cylinder liners, cervical shaft gas turbine engine compressor stators, the details of construction of pipelines, etc). To homogenize the structure of powder coatings produced by plasma detonation additional treatment by plasma jet or electron beam is applied [1].

This report presents new results of transmission and scanning electron microscopy, X-ray diffraction and atomic force microscopy investigation of the structure-phase compositions of thick (150  $\mu\text{m}$ ) coatings on the base of Ni and Co deposited by plasma-detonation on steel substrates. The coatings wear resistance, corrosion, microhardness tests were performed. Based on a series of experimental studies of the structure and properties of such coatings before and after additional irradiation by electron beam or plasma jet [2-4], we concluded that it is necessary to simulate the temperature distribution during irradiation to justify the choice of such irradiation parameters as power density and the speed of the source. Comparing the experimental data with the temperature profile calculations we can offer the best modes of radiation that do not cause excessive heating of a coating, but at the same time lead to changes in the phase composition (formation of strengthening nanoparticles).

The aims of this research:

- 1) Developing a model of coating composition on the basis of the experimental data analysis;
- 2) Estimation of temperature distribution in a two-layer metal sample exposed to a DC pulse plasma jet or DC e-beam depending on added irradiation rates
- 3) Establishing structure-phase and mechanical differences in the coatings before and after added treatment by irradiation.

The model of structure for plasma-detonation coatings was developed. Computer simulation of temperature distribution in depth from the surface of coatings under direct current pulse plasma jet and direct current low-energy electron beam irradiation was done, and certain parameters for additional treatment by irradiation were proposed. The irradiation was carried out according to design conditions.

It was found that the exposure of coatings to irradiation according to the recommended modes leads to the evolution of the structural-phase state of coatings and substantial improvement of performance properties of modified surfaces. It was established that the roughness of the modified coatings decreased by 2 times, the wear resistance of modified surfaces increases by 3 times, the microhardness increases by an average of 25%. The mechanism of coating improvement after additional treatment by DC e-beam or by DC pulse plasma jet was identified. In general the structure-phase changes are represented by the increase of nanosized intermetallic phase volume concentration and the increase of the width of the diffuse zone in the coating layer contacting the substrate.

### REFERENCES

- [1] *Misaelides P., Hatzidimitou A., Noli F. et al.*// Surface and Coatings Technology.- 2004. - Vol.180-181. P. 290 – 296.
- [2] *Alontseva D.L., Russakova A.V. et al.*// Materials Science (Medžiagotyra). - 2013.-- Vol. 19. - №3. P.277-282.
- [3] *Alontseva D., Russakova A.*//Advanced Materials Research. -2013. - Vol. 702. P. 94-99.
- [4] *Alontseva D., Krasavin A. et al.*// Acta Physica Polonica A. - Vol. 123. - № 5. P.867-870.

## MODIFICATION OF COATING (ZrN) / SUBSTRATE (AlSi) SYSTEM BY A PULSED ELECTRON BEAM<sup>1</sup>

*E.A. PETRIKOVA\**, *YU.F. IVANOV\*\*\**, *A.D. TERESOV\**, *A.V. TKACHENKO\*\**, *O.V. KRYSINA\**

\* *Institute of High Current Electronics SB RAS, 2/3 Akademichesky Ave, Tomsk, 634055, Russia, [elizmarkova@yahoo.com](mailto:elizmarkova@yahoo.com), +79234239926*

\*\**National Research Tomsk Polytechnic University, Tomsk, 634050, Lenin Avenue, 30, Tomsk, Russia*

Coatings with unique strength and tribological properties have been formed on eutectic silumin by electron - ion - plasma treatment and the regularities of their creation have been revealed. Results showing a multiple increase in the physical, mechanical and tribological characteristics of silumin (microhardness, wear resistance, fatigue life, corrosion resistance, Young's modulus, friction coefficient) are presented and the physical mechanisms of this phenomenon are opened.

Superhard ZrN coatings (thickness of a coating of 1  $\mu\text{m}$ ) were synthesized on the surface of silumin eutectic composition (Al-12Si-2Cu-1Mg-0, 5Mn-1Ni-0,1Ti, at. %) at the cathode of zirconium alloy E110 evaporation in nitrogen atmosphere. Coatings deposition have been carried out on the automatic ion- plasma "TRIO" plant with arc evaporator and plasma source based on a combined filament and hollow cathode «PINK». The coating / substrate system is formed in two ways: (1) coating was deposited on the polished surface of silumin samples; (2) coating was deposited on the surface of silumin pretreated by a pulsed electron beam on the «SOLO» setup (20  $\text{J}/\text{cm}^2$ , 150  $\mu\text{s}$ ; 1-5 pulses, 0.3 Hz). Additional alloying coating to a substrate have been carried out by a pulsed electron beam irradiating of the coating / substrate system on the «SOLO» to improve the adhesion strength.

<sup>1</sup> This work was supported by RFBR grant (projects № 13-08-98084\_r-a-Siberia).

## EFFECT OF CROSSED ELECTRIC AND MAGNETIC FIELDS ON ION NITRIDING IN A GLOW DISCHARGE.

R.K. VAFIN, K.N. RAMAZANOV

Ufa State Aviation Technical University, K. Marx str.12, Ufa, 450000, RF, vafinrk@mail.ru, +7(347)2730763

The aim of this work is to study the electrophysical characteristics of a glow discharge in crossed electric and magnetic fields, as well as an assessment of its impact on the structural-phase composition and mechanical properties of tool steels R6M5 and H12.

Visual picture glow discharge in crossed electric and magnetic fields corresponds to the usual definition [1,2] and is characterized glow toroidal shape, located near the cathode, and the drift region is almost dark. Fig. 1 is a photograph of the glow of the cathode region of a glow discharge in a magnetic field at a pressure of 80 Pa.

Glow and the positive column region of the negative glow discharge purple, orange cathode layer, an anode layer pink. After gas injection during the first 3-5 minutes of the positive column is divided into separate layers separated by dark spaces, so-called strata. At a working gas pressure of 80 Pa, the bright glow of the plasma torus-shaped almost "lies" to the cathode Fig 1., by reducing the mean free path of the charged particles.

Fig. 2 shows the volt-ampere characteristics of the discharge, resulting in different pressures in the chamber Ar. With decreasing pressure volt-ampere characteristics shifted to higher operating voltages, by reducing the concentration of charged particles. Increase the residence time of electrons in the plasma glow discharge cathode placed in a magnetic field shifts the volt-ampere characteristics up (Fig. 2). Volt ampere characteristics of the discharge in crossed electric and magnetic fields, in contrast to the traditional scheme has a steeper rise, indicating that the ionization efficiency.



Fig. 2. Photo cathode region of a glow discharge in a magnetic field at a pressure of 80 Pa

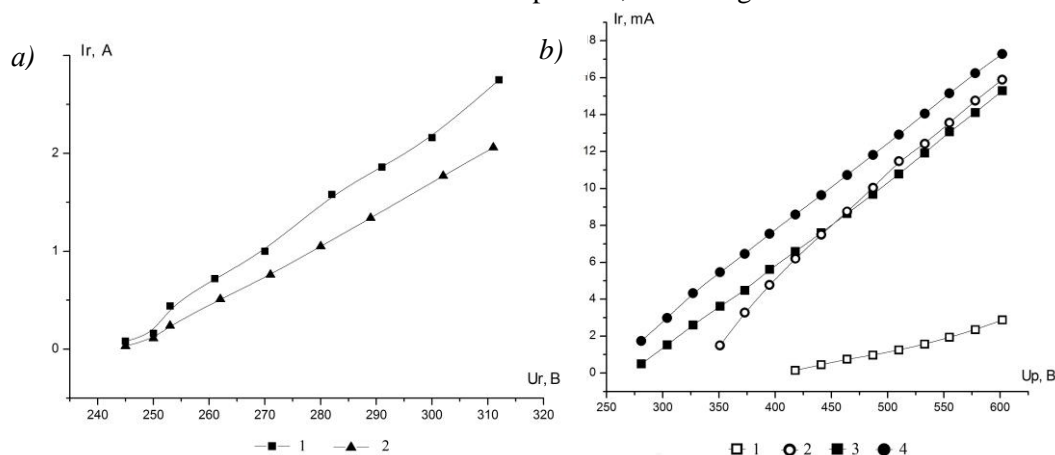


Fig. 2. Volt-ampere characteristics of a glow discharge in Ar at different pressures:

a - 100 Pa (1 - a magnetic field; 2 - no magnetic field)

b - 5 Pa (1 - without a magnetic field, 2 - a magnetic field) and 15 Pa (3 - without a magnetic field, 4 - magnetic field)

### REFERENCES

- [1] AA Soloviev, NS Sochugov, KV Oskomov, SV Rabotkin Investigation of plasma unbalanced magnetron sputtering system // Plasma Physics. – 2009. – T35. – №5 . P. 443-452.
- [2] OV Kibalnikova, AM Mikhailov, YV Seryanov, AV Baskakov, Effect of magnetic field on the nitriding steels of Fe-Ni-Cr // Physics and chemistry of materials processing. – 2002. – №2 . P. 86-89.

## STRUCTURAL CONVERSION OF SURFACE LAYER Mg BY THE ACTION HIGH POWER BEAM IONS OF CARBON

*E.V. GOLOSOV\**, *M.V. ZHIDKOV\**, *Y.R. KOLOBOV\**, \*\*\*\*,  
*A.E. LIGACHEV\*\**, *G.V. POTYOMKIN\*\*\**, *G.E. REMNEV\*\*\**, *M.Y. SMOLJAKOVA\*\*\**

*\*Belgorod State University, Belgorod*

*\*\*Institute of the general physics A.M. Prokhorov RAS, 119991, Moscow, Vavilova s., 38, e-mail: carbin@yandex.ru*

*\*\*\*Tomsk Polytechnic University, Tomsk*

*\*\*\*\*Institute of the structural macrokinetic and problem materials RAS, Moscow*

The paper presents the results of a study for morphogenesis of the juvenile surface Mg by the action short pulse beam ions of carbon. Samples with the size of  $30 \times 15 \times 5 \text{ mm}^2$  made from Mg for SEM microscopy and electron probe microanalysis were used. Before the irradiation all samples were polished to high luster on the glazing machine LaboroPol-5. The irradiation of samples Mg was carried on the installation TEMP-4 by energy of ions 250 keV and residual pressure in the working chamber  $P \sim 3 \cdot 10^{-4} \text{ Pa}$ . The flows ions with power surface density in the (0,5 – 2,5)  $\text{J}/\text{sm}^2$  range and the doses  $D = 100, 1, 3$  pulses range was used. Investigation the state of the irradiation surface and element analysis of the surface layer of the modified specimens has been performed on the QUANTA 3D with attachment EDAX.

On the fig.1 shown results observations of morphogenesis of the juvenile surface Mg specimens in dependence from (depending on versus) power surface density flow ions of carbon. Concentration of craters on the surface and content of carbon in the surface layer were increased.

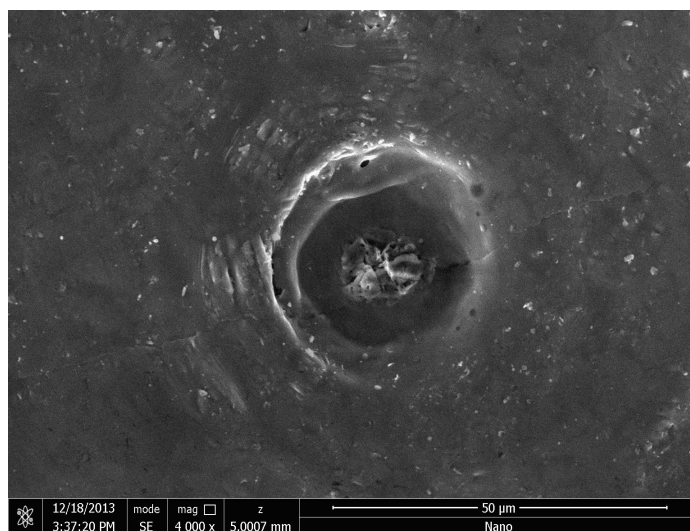


Fig.1 The juvenile film with craters on the surface

## THE PROPERTIES SURFACE OF STEEL 12X18H10T BY PULSE ION BEAM OF CARBON TREATED

*E.V. GOLOSOV\**, *M.V. ZHIDKOV\**, *Y.R. KOLOBOV\**, \*\*\*\*,  
*A.E. LIGACHEV\*\**, *G.V. POTYOMKIN\*\*\**, *G.E. REMNEV\*\*\**, *M.Y. SMOLJAKOVA\*\*\**

*\*Belgorod State University, Belgorod*

*\*\*Institute of the general physics A.M. Prokhorov RAS, 119991, Moscow, Vavilova s., 38, e-mail: carbin@yandex.ru*

*\*\*\*Tomsk Polytechnic University, Tomsk*

*\*\*\*\*Institute of the structural macrokinetic and problem materials RAS, Moscow*

The paper presents the results of a study for restructuring and physical-chemical conversions by the action pulse beam ions of  $H^+$  и  $C^+$  of accelerator TEMP-4. The samples with diameter 6 mm of made from stick strain of 12X18H10T before the irradiation were polished to high luster on the glazing machine LaboroPol-5. The irradiation of samples was carried by energy of ions 250 keV and residual pressure in the working chamber  $P \sim 3 \cdot 10^{-4}$  Pa. The flows ions with power surface density in the (0,5 – 2,5)  $J/cm^2$  range and the doses  $D = 100, 1, 3$  pulses range was used.

The topography of surface and structural- phases state layers all samples on the QUANTA 3D with attachment EDAX were investigated.

On the fig.1 shown of surface treated samples.

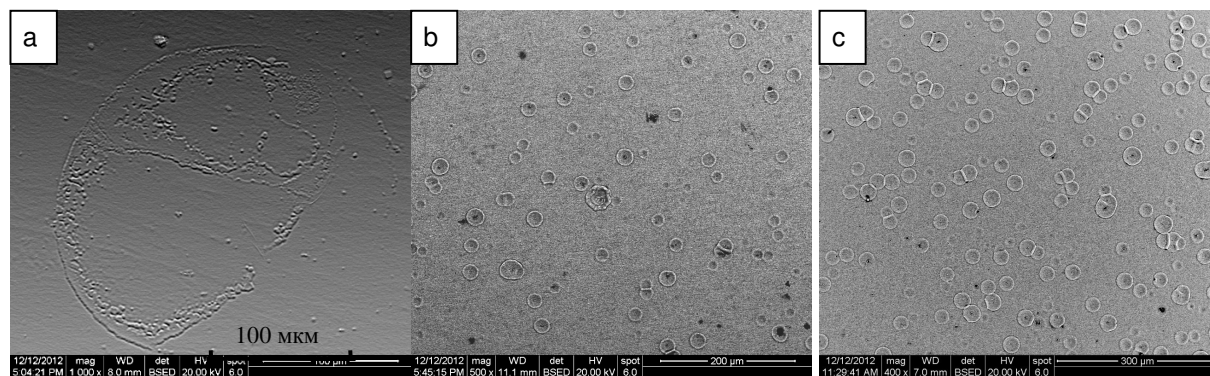


Fig.1 The surface stainless modified ion beam with power surface density in the (0,5 – 2,5)  $J/cm^2$  range.

The results of investigations structural-phases state of stainless 12X18H10T shown significant evolution structure of surface and surface layers by action intense ion beam with short duration pulse. In this case defect-free grain structure pattern and probability of nucleation and expansion fatigue crack essential decreased.

### REFERENCES

- [1] *A.D. Korotaev, A.N. Tsyumentsev, Yu.P. Pinzhin, G.E. Remnev // FMM, 1996, T.81, B.5, C118-127*
- [2] *V.A. Shulov, G.E. Remnev, Nochovnaj at all // Poverchnost. Fizika, chimiaj, mehanika. 1994, №7, c.117-128*



## COMBINED SURFACE TREATMENT OF HARD ALLOY CUTTING TOOL

*S.V. FEDOROV, A.A. OKUNKOVA, YE MIN SOE*

*MSTU "STANKIN", Vadkovskiy per. 3A, 127055, RF, [av288291@akado.ru](mailto:av288291@akado.ru), 499 972 95 61*

The development of face-hardening technology for metals and alloys is connected with the development of combined processes. These processes include consecutive several methods of material modification for the reason to produce a combination of the properties, which are not available by usage of each of these technologies separated.

The presented work based on the surface modification of replaceable hard alloy cutting insert for increasing of their exploitation properties while consecutive usage two of surface technologies : preliminary micro alloying by low-energy high-current electron beam and wear-resistant vacuum-arc coating [1,2].

The cutting tool surface coating by thin layer of IV – V group carbide former (in this case Nb, Hf, Ti) before electron beam treatment gives multiple-phase carbide structure by usage of micro alloying. With a coating for wear-resistant complex special properties could be achieved by two-component nitride (TiAl)N which is capable of heightened thermal stability.

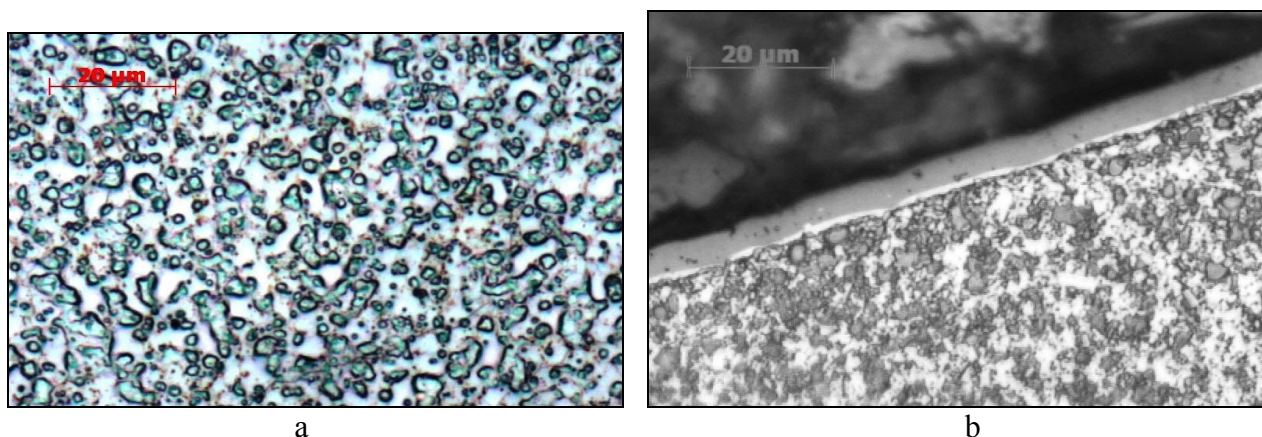


Fig. 1 a) Cutting insert surface of hard-alloy VK6OM (K05 by ISO) after micro alloying by the alloy NbHfTi, b) Cutting insert cross-section of hard-alloy VK6OM after combined surface treatment.

The sufficiently deep modified layer (several micrometres) (Fig.1) is achieved as a result of multiple electron beam impact and repeating of coating operations by alloying layer. Experiments show that the best results for the cutting tool wear-resistance is caused by less intensive chemical interaction formed while micro alloying of carbides with treated material. Critical temperatures for hardened cutting tool achieves while high cutting speeds.

### REFERENCES

- [1] Patent of RF on the invention N 2501865  
 [2] S.V. Fedorov, M.D. Pavlov, A.A. Okunkova, // Journal of Friction and Wear, 2013, Vol. 34, No. 3, pp. 190–198.

## THE EFFECT OF ELECTRON BEAM INJECTION (100 eV) ON THE CHARACTERISTICS OF TiN COATINGS DEPOSITED BY REACTIVE MAGNETRON SPUTTERING<sup>1</sup>

A.S. KAMENETSKIKH\*, N.V. GAVRILOV\*, A.V. CHUKIN\*\*

\* Institute of Electrophysics of the UB of RAS, 106 Amundsen St., Yekaterinburg, 620016, Russia, E-mail: alx@iep.uran.ru

\*\* Ural Federal University, Institute of Physics and Technology, 51 Lenin St., Yekaterinburg, 620000, Russia

TiN coatings on specimens of steel AISI 430 and hard alloy T15K6 were deposited by magnetron sputtering of Ti in Ar/N<sub>2</sub> mixture ionized by a broad (50 cm<sup>2</sup>) beam of low-energy (~100 eV) electrons. A balanced magnetron with target Ø 80 mm in diameter operating in pulse periodic mode (50 kHz, 10 µs, the current amplitude 2 A) and an electron source with grid plasma cathode [1, 2] were used in the experiments. The current of electron emission was regulated by varying the discharge current in the range of 0 - 8 A. Negative bias (50 kHz, 10 µs) with amplitude 100 V was applied between the specimens and earthed walls of vacuum chamber.

It was shown that electron beam injection brings on the fact that maximum of dependence of coatings' nanohardness on the magnitude of N<sub>2</sub> flow shifts to lower values (Fig.1). The effect of electron beam on coatings' characteristics is caused by a change in mass composition and charge state of gas-discharge plasma particles and intensification of the processes of generation of active particles that forms the coating. The results of element analysis show that the increase of discharge current of the electron source till 8 A at constant N<sub>2</sub> flow 2 ml/min results in the growth of N/Ti concentrations ratio in the coating from 0,78 to 1,05.

The structure and phase state of the coatings was studied by XRD method. It was shown that electron beam injection at discharge current 1 A leads to reduction of average value of grain size till 7 nm. The discharge current increase from 1 to 8 A was accompanied with grain size growth till 11 nm. Characteristic grain size for the mode without electron beam injection was ~25 nm. The dependences of texture coefficients (111), (200) and (220) on discharge current (Fig. 2) are non-monotonous. The analysis of literature data and results of our experiments show that along with the change of elastic deformation energy there is another dominating factor that determines preferential orientation of TiN coating crystallites. As authors think the enhanced concentration of atomic nitrogen in electron beam plasma may be such factor.

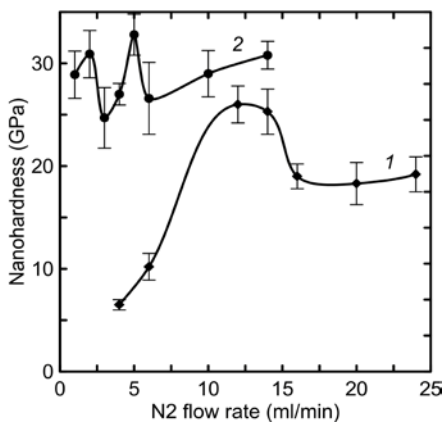


Fig. 1. Dependences of coatings' nanohardness on N<sub>2</sub> flow rate. Discharge current of the electron source: 1 - 0; 2 - 5 A.

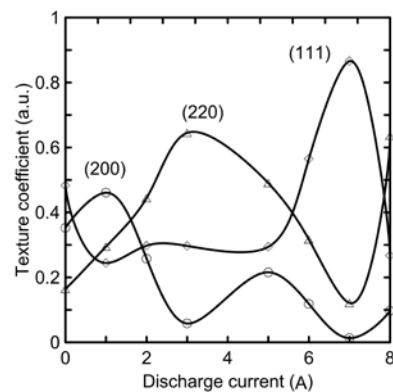


Fig. 2. Dependences of texture coefficients on the discharge current of electron source. N<sub>2</sub> flow 2 ml/min.

### REFERENCES

- [1] Gavrilov N.V., Emlin D.R., Kamenetskikh A.S. // *Izvestia Vuzov. Fizika*. - 2007. - V.50. - № 9. P. 149-153
- [2] N.V. Gavrilov, A.I. Men'shakov // *Instruments and Experimental Techniques*. - 2011, - V.54, № 5. P. 732-739

<sup>1</sup> This work was partially supported by the Programs of Basic Researches of the Presidium RAS (project 12-II-2-1046) and UB RAS (project 12-II-2-2012).

## FORMATION'S FEATURES OF SUPERHARD BORIDE LAYERS $MeB_2$ ON CARBON STEELS UNDER THE INFLUENCE OF POWERFUL ELECTRON BEAMS IN A VACUUM<sup>1</sup>

*D.E.DASHEEV\**, *N.N. SMIRNYAGINA\**, *Z.M. KHALTAROV\**, *V.M. KHALTANOVA\*\**

*\*Institute of Physical Materials Science SB RAS, Sakhyanovoy Street, 6, Ulan-Ude, 670047, Russia, fokter@mail.ru, 89246524544*

*\*\*Buryat State University, Smolin Street, 24a, Ulan-Ude, 670000, Russia*

Formation of borides layers of iron, titanium and zirconium carbon steels investigated. The new method is applied for obtain superhard borides under the influence of powerful electron beam in a vacuum. This method uses the self-propagating high-temperature synthesis (SHS), and its products are fused to the surface of carbon steel under the influence of powerful electron beam. Thermodynamically was shown that the synthesis of borides in high vacuum at temperatures of 900-1000 possible to directly on the steel surface without melting of this surface [1]. Reaction of formation of borides and carbides of transition metals are exothermic. Under certain conditions, it is possible to undertake a process of self-propagating high-temperature synthesis (SHS), which is characterized by high values of the activation energy. It has been proposed to use electron beam as initiator SHS process and a heat source for the electron beam welding SHS products. In this paper, we used the stoichiometric reactionary daubs based on metals oxide, boron and carbon.

In the process of surfacing of SHS products, there is partial melting of the surface in a narrow zone (5-7 microns) with a small volume of melt, at crystallization of which the formation layers occurs. Crystallization occurs in the conditions of a small volume of the melt and leads to the formation of dendritic structure.

Studies have shown that the use of electronic heating allows to reduce friability and to increase ductility of superhard layers. Microhardness layers reaches 2500-3000 MPa.

### REFERENCES

- [1] *Smirnyagina N.N., Tsyrenzhapov B.B., Milonov A.S. Phase equilibria in the systems  $Me-B-C-O$  ( $Me = Ti, Zr u V$ ) // RUSSIAN JOURNAL OF PHYSICAL CHEMISTRY A. – 2006. – Vol. 80. – № 11. P. - 2081-2086.*

<sup>1</sup> This work was supported by the Russian Foundation for Basic Research, project no: 12-08-31496 and 14-08-31412.

## **FORMATION FEATURES OF THE TRANSITION METALS BORIDES NANOSTRUCTURE LAYERS FORMED BY AN ELECTRON-BEAM SURFACING OF SHS PRODUCTS IN VACUUM AND THEIR STRENGTH PROPERTIES<sup>1</sup>**

*A.S. MILONOV, D.E. DASHEEV, A.D. DORZHIEV, N.N. SMIRNYAGINA*

*Institute of Physical Materials Science SB RAS, Sakhyanovoy Street, 6, Ulan-Ude, 670047, Russia, terwer81@mail.ru, 89085938616*

Conditions of formation, structure and wear properties of borides layers on a surface of cutting plates from instrumental steels R18 and U8A was investigated, it have been formed at electron beam processing in a vacuum. Electron beams are used as the initiator and heating source of self-propagating high temperature synthesis (SHS) of refractory borides. At the electron beam boriding of instrumental steels R18 and U8A the layer was formed as a result of the deep profusion that has spotted its structure. It is established that at directional crystallization the main axis the ruled dendrites is oriented in a heat removal direction. The structure of dendrites (the chain separate globules) evidences about intermittent character of their formation. It is established that formation boride layer in the thickness 8-10 microns on a surface of cutting plates from instrumental steels R18 and U8A, allows to increment resistances of cutters almost in 1,5 times (for a handled steel 12H18N10T). More substantial increase of resistance of cutters is related to increase of a thickness boride layer. At electron beam boriding the thickness boride layer can reach 300 microns, however temperature of processing thus makes 1100-1200°C. Time of processing of 2-3 minutes. Proceeding from it, electron beam boriding can be recommended not as final, and as the intermediate operation of processing of the cutting tool, for example, before a heat treatment.

<sup>1</sup> This work was supported by the Russian Foundation for Basic Research, project No. 12-08-98036-r\_sibir\_a

## STRAIN AND FRACTURE OF SINGLE-LAYER AND GRADIENT-LAYERED NANOSTRUCTURED COATINGS BASED ON TITANIUM NITRIDE<sup>1</sup>

*S.V. OVCHINNIKOV\**, *A.D. KOROTAEV\*\**, *YU.P. PINZHIN\**

\* *Institute of Strength Physics and Material Science, Siberian Division, RAS, 2/4 Akademicheskoy Ave., Tomsk, 634021, Russia, [ovm@spti.tsu.ru](mailto:ovm@spti.tsu.ru), +73822531569*

\*\* *National Research Tomsk State University, 36 Lenin Ave., Tomsk, 634050*

A combination of strength and ductility required for the synthesis of wear resistant coatings can be determined based on the results of studies of the microstructure and the mechanisms of modifications at the specific mechanical loading, in particular, on the basis of the indentation, scratch and tribological testing. Received to date, see for example [1, 2], the relevant data are qualitative in nature, and their interpretation is related to the mechanics of crack propagation in brittle materials, whereas the synthesis capabilities ensure the formation of multicomponent and nanocomposite systems, fracture toughness which can adjust the ratio of the volume fractions and adhesion phases with different properties.

In this regard this work presents results of studying the microstructure changes in the areas of deformation and fracture of single-layer and gradient-layered, including hetero- and nanostructured coatings of Ti-Al-Si-Cu-N obtained using electron microscopy dark-field analysis method of bending-torsion of the crystal lattice. Depositions of coatings were performed by magnetron sputtering targets of Ti, Al-Si alloy and Cu. A change in power during the synthesis contributed to the formation coatings with variable elemental and phase compositions by their thickness.

For single-phase single-layer coatings found significant (tens%) reduction in thickness below the top of the indenter at a constant form of the substrate, indicating at the plastic deformation of the coating, which at the microscopic level is expressed in the growth of density and values of the misorientation and nonequilibrium state of small and high angle boundaries of columnar crystals. The effects of macroscopic deformation and failure of such coatings in scratch-testing due to the ratio of hardness of the substrate and coating, their adhesive and cohesive strength, expressed in the localization of deformation and fracture in the coating on the hard alloy and the significant effects of the soft substrate at the macro and micro heterogeneous nature of the coating deformation were determined. It was found that in areas of coating failure can be observed sharp inhomogeneity of the structural state at distances of up to 1-2  $\mu\text{m}$ .

The formation of thin (20-30 nm) bands of localization of deformation in gradient-layered nanocrystalline coatings with increasing size (3-4 times) nanocrystals in the bands was show. Preferential regions of development of these bands are zones of deformation and fracture of the substrate (underlayer) and surface stress concentrators (example, the top of indentation). It is established that the interface layer structure deflects radial cracks from the direction of the boundaries of the columnar crystals. Preferential inhibition of these and inclined cracks observed in nanocrystalline layer due to intensive branching. Factors contributing to the strength (fracture toughness) coatings at the transition from single-layer to the gradient-layered coatings are: hardening of the surface layer by transformation it into a nanocrystalline state; branching fine cracks in the surface layer, gradient-layered structure with extended interfaces, inhibiting the spread of cracks deeper material, development of localized deformation bands in the gradient-layered nanocrystalline coatings with a high copper content.

### REFERENCES

- [1] *Xie Z.H., Hoffman M., Munroe P., Singh R. // J. Mater. Research. - 2007. - V. 22. N 8. - P. 2312-2318.*
- [2] *Verma N., Cadambi S., Jayaram V., Biswas S.K. // Acta Materialia. - 2012. -V. 60. - P. 3063-3073.*

<sup>1</sup> This work was supported by grant RFBR № 13-08-00502

## SOLID-PHASE TRANSFORMATIONS GRAPHITE - AMORPHOUS CARBON - CRYSTAL CARBYNES BY CHARGED PARTICLES BEAMS<sup>1</sup>

*A.P.SEMENOV, I.A.SEMENOVA, N.N.SMIRNYAGINA*

*Ulan-Ude, 670047, Russia, semenov@ipms.bscnet.ru, 8(3012)433184*

The solid-phase transformation of graphite to carbyne by intense electron beam sets a high content of carbon phases with sp hybridization of the valence electrons is considered. Two stages of the process are identified [1]. In the first stage microns thick carbon coating is deposited by sputtering of the graphite by ion beam of argon with an energy of 4 keV and at a pressure of  $6,6 \cdot 10^{-3}$  Pa. In the second step the thermodynamic heating of the coating is carried out at a pressure of  $2 \cdot 10^{-3}$  Pa by the beam of electrons with an energy of 20 keV and a duration of 1-2 s. The process of the direct solid-phase transformation of graphite into carbyne and crystallization of the hexagonal carbyne is provided at 1500-1600 K.

Fig. 1 and 2 show the infrared absorption spectra and the Raman spectrum of the carbon coating after the electron beam treatment. Absorption bands at 810, 1040, 1920, 2300  $\text{cm}^{-1}$  and there is a "failure" in 1300-1600  $\text{cm}^{-1}$  are presented in the spectrum of Fig. 1.

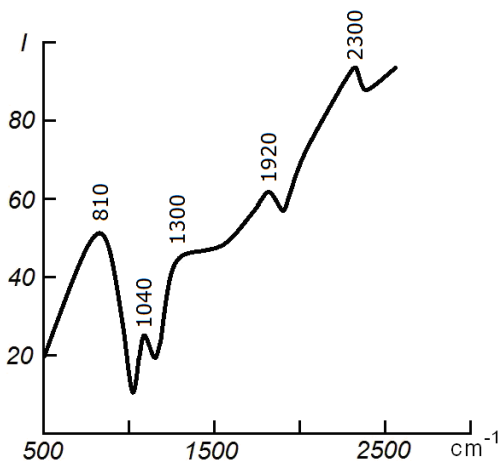


Fig.1. The infrared absorption spectra of carbyne

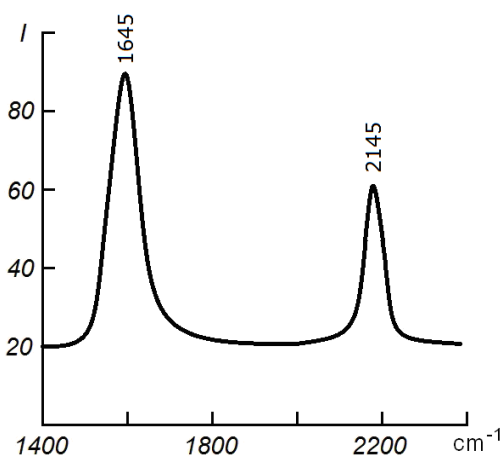


Fig.2. The Raman spectrum of the carbyne

These data confirm the results of X-ray analysis and indicate the formation of carbyne [2]. Carbyne is present in polyynes and cumulene forms. Polyynes have a linear chain  $\text{—C}\equiv\text{C—C}\equiv\text{C—}$  linked by the curved elements  $\text{—C}\equiv\text{C—}$  (the interatomic distance  $\text{—C}\equiv\text{C—}$  0,1207 nm,  $\text{—C—C—C—}$  0,1379 nm, the angle at the bridging C atom with the chain direction  $60^\circ < \alpha_p < 65^\circ$ ) and cumulenes have linear chains  $\text{=C=C=C=C=}$  ( $\text{C=C}$  0,1282 nm), connected by the curved elements of  $\text{C—C=C—}$  ( $23^\circ < \alpha_c < 25^\circ$ ). Polyynes structure of atomic carbon chains is determined by the stretching bands of the triple bonds  $\text{—C}\equiv\text{C—}$  at 2100-2300  $\text{cm}^{-1}$  (very strong), and the deformation vibrations at 800  $\text{cm}^{-1}$ . Cumulene structure is expressed by the absorption bands at 1950  $\text{cm}^{-1}$  (very strong) and 1070  $\text{cm}^{-1}$  (medium intensity). Absorption band at 1600  $\text{cm}^{-1}$  is associated with the fundamental absorption band for the cumulene carbyne (regular zigzags with linear fragments of 4 carbon atoms).

The Raman spectra in Fig. 2 shows two lines in 1645 and 2145  $\text{cm}^{-1}$  corresponding to the stretching vibrations of the cumulene bonds  $\text{=C=C=C=C=}$  of the carbon chains.

### REFERENCES

- [1] *Semenov A.P.* // Sputter ion beams: production and application. - BSC SB RAS, 1999.
- [2] *Semenov A.P., Smirnyagina N.N.* // Inorganic materials. - 1998. - V.34. - N8. - P.982-985.

<sup>1</sup> This work was supported by RFBR (project № 12-08-98000-p\_siberia\_a) and Basic Research Program SB RAS (project № II.9.3.1).

## INVESTIGATION OF TIN-CU COMPOSITE LAYERS PROPERTIES RECEIVED IN A VACUUM INSTALLATION OF DUAL ACTION BY MAGNETRON SPUTTERING AND ARC EVAPORATION

*D.B-D. TSYRENOV\**, A.P. SEMENOV\*, N.N. SMIRNYAGINA\*

\* *Institute of Physical Materials Science SB RAS, Sakhyanovoy Street, 6, Ulan-Ude, 670047, Russia, dmitriyza@mail.ru, 89148388358*

The main electro physical and technological parameters of the plasma generator, which implements a hybrid technology of formation of functional composite TiN-Cu coverings have been studied. The feature of this technology is the possibility of coordinated work of vacuum arc evaporator and planar magnetron. Possibility of the combination of different growth processes (evaporation in the arc vacuum category, accompanied by ionic bombing, and magnetron dispersion) in one installation opens new receptions of coverings cultivation. This combination gives us the following advantages: the possibility to apply coverings on details of a difficult geometrical form, high speeds of sedimentation, evaporate d's particles high coefficient of ionization, plasma-chemical sedimentation, low temperature of the substrate, a small degree of film impurity with extraneous gas inclusions.

The composition, structure and mechanical properties of the composite TiN-Cu layers on fused silica substrates are discussed in the report.

NANOCOMPOSITE COATINGS WITH AN AMORPHOUS MATRIX <sup>1</sup>

KOROTAEV A. D.

National Research Tomsk State University, 634036, Tomsk, pr. Lenina, 36, Russia  
Institute of Strength Physics and Materials Science SB RAS, Tomsk, Russia

Siberian Physical-Technical Institute of Tomsk State University, Tomsk, Russia, [korotaev@phys.tsu.ru](mailto:korotaev@phys.tsu.ru), +73822530394

High-strength, hard ( $H_{\mu} > 20 \div 25$  GPa) and superhard ( $H_{\mu} \geq 40$  GPa) nanocomposite and amorphous (DLC type) PVD coatings are generally characterized by high internal stresses and low cohesive (fracture toughness) and adhesive strength. Depending on the fracture mechanism, the coatings are classified into those exhibiting high resistance to formation of nucleation microcracks and low resistance to crack propagation and those showing high resistance to propagation of microcracks (nanostructured and nanocomposite materials). Unfortunately, both types have low fracture toughness.

The paper presents a review of current methods for improving cohesive strength of the coatings made from amorphous carbon (DNG/AM type materials) and superhard nanocomposite coatings, given their comparatively high hardness ( $H_{\mu} > 15 \div 20$  GPa), wear resistance and low friction coefficient ( $\mu \leq 0.2$ ).

A team of TSU and ISPMS research workers proposed a new approach to synthesizing the above-described coatings using multi-elemental compositions and the physical principles of selecting their components.

The main idea of their synthesis is thought to be self-organization of their microstructure during simultaneous nucleation of the growth islands of a number of mutually insoluble or slow-soluble phases.

The method for predicting the composition of an alloy consists in the selections of elements ensuring the following:

- Multiphase nature of coatings with little difference in the phase-formation heat;
- Possibility of relaxation of internal stress concentrators at the phase boundaries and formation of nanocrystalline high-plasticity phases;
- Decrease in grain-boundary sliding by the developed system of phase boundaries;
- Decrease in the elasticity modulus, with high hardness being retained, and minimum difference with the substrate (product) elasticity modulus.

The efficiency of the proposed principles of coating formation is investigated using superhard coatings of the Ti-Al-Si-Cr-Ni-Cu-C-O-N and Al-Cr-Si-Ti-Cu-O-N systems based on an amorphous matrix and amorphous carbon.

The coatings were formed by the method of magnetron sputtering combined with ion-plasma treatment using independent gas-ion sources of the PINK type and multi-elemental magnetron cathodes in the SPRUT and LEGEND facilities.

The characteristic features of phase-structure and elastic-stressed states of the coatings were examined by the methods of X-ray structural analysis, focused-beam and transmission electron microscopy in conjunction with the energy dispersive analysis.

The mechanical and tribological properties of the coatings were performed via measuring their micro- and nanohardness and friction and wear coefficients under ball-on-disk testing conditions.

The paper discusses the results of investigations, which support the proposed approach to designing multi-elemental nanocomposite coatings, and principles for selecting their compositions.

<sup>1</sup> This work was supported by grant RFBR № 13-02-9802



**LASER-OPTICAL DIAGNOSTIC OF DISPERSED PHASE PARAMETERS APPLIED TO ADDITIVE TECHNOLOGY OF SURFACE MODIFICATION BY HIGH-DENSE ENERGY SOURCE<sup>1</sup>**

**A.A.MICHALCHENKO\***, V.I. NALIVAICO\*\*, E.V. KARTAEV\*, V.I. KUZMIN\*, **D.V. SERGACHEV\***, G.A. PINAEV\*\*\*

\*Khristianovich institute of theoretical and applied mechanics, SB RAS, institutskaya str. 4/1, Novosibirsk, 630090, Russia, dsergachev@itam.nsc.ru, +7(923)147-71-12

\*\*Institute of automation and electrometry, SB RAS, ac. Koptug ave., Novosibirsk, 630090, Russia

\*\*\*Institute of laser physics, SB RAS, ac. Lavrentyev ave., Novosibirsk, 630090, Russia

Development of additive laser and plasma technologies surfaces recovery of machine parts and mechanisms leads to create new methods or adapt existing ones of control and diagnostics of critical process parameters affecting the quality of the product. These critical process parameters in dust-laden high-dense energy jet are temperature and velocity of the applied in-flight particles before hitting the substrate.

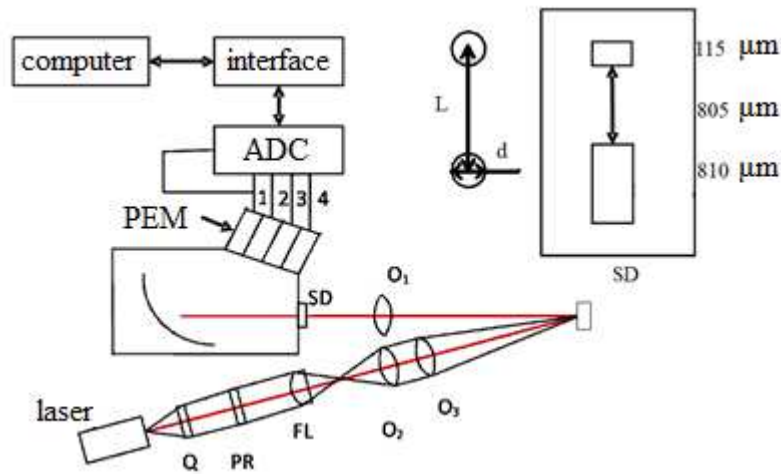


Fig. 1. Optical scheme of diagnostics system.

To monitor particles properties laser-optical measurement system has been created by combining the existing methods of solid phase parameter registration, which are based on spectrometer [1], and laser optical system. As shown in fig. 1 scheme of the device includes two independent time-of-flight methods of measuring particle velocity: passive method, which is based on the own radiation of the heated particles in the gas stream and active one, using a laser beam scattering effect. The radiation source was a single-mode YAG-laser ( $\lambda = 532 \text{ nm}$ ). The laser beam is spatially separated by a quarter-wave plate Q and PR Wollaston prism into two beams with orthogonal linear polarizations. Mask of receiving slit of the spectrometer using the receiver lens  $O_1$  was posed with laser constrictions formed by the optical system FL,  $O_2$ ,  $O_3$  so that image of laser constriction and image of mask were overlaid. Light passing through the lens  $O_1$  and mask SD, was divided by wavelength and detecting individual PEMs. PEM signals are then digitized by the ADC. Temperature measurements has been carried out in the assumption of a gray body at three wavelengths ( $\lambda_1 = 616 \text{ nm}$ ,  $\lambda_2 = 700 \text{ nm}$ ,  $\lambda_3 = 532 \text{ nm}$ ). Launch of the registration system has been initiated by passing particle through first laser constriction. The latter gave an advantage over the existing analogues in the world to measure the local melting index of particles.

The measurements of the velocity and temperature of particles in plasma spraying processes and coaxial laser cladding have been carried out. First, the method of three-color pyrometer for measuring the temperature of the condensed phase in the gas stream during laser cladding was applied.

REFERENCES

[1] Nalivaiko V.I., Chubakov P.A., Pokrovsky A.N., Mikhilchenko A.A., Kuz'min V.I., Kartaev E.V. // J. Thermophysics and Aeromechanics – 2007. – Volume 4. – № 2, pp. 247-256.

<sup>1</sup> This work was supported by RFBR, project 14-02-00732

## CHROMIUM OXYCARBIDE COATING WITH PVD AND NON STAEEDY PLASMA, AND ITS APPLICATIONS

*T.KADO\**, *K. UEMURA\*\**, *V. KUKHTA\*\**, *K. SHALNOV\*\**, *T.TSUCHIYA\*\**

*\* Former National Institute of Advanced Industrial Science and Technology (AIST), Kure, Hiroshima, Japan,*

*\*\*ITAC Ltd. Shinmaywa 1-1, Takarazuka, 665-0052, Japan, kensuke\_uemura@itac-j.co.jp, +81-90-3087-495*

Two coating processes of chromium oxy-carbide ( $\text{CrO}_x\text{C}_y$ ) were developed. The former one is with reactive sputtering process with starting materials of Cr,  $\text{CO}_2$  and  $\text{CH}_4$  in the vacuum chamber. The coating with metallic miller surface shows the relatively high hardness and ultra-high corrosion resistance even in the severe surrounding that chrome plating could not be sustained. This also shows the sterilization effect against Escherichia Coli to extend the possible application in the different field from anti-corrosion, abrasion resistance and other mechanical applications.

The later process is under development to coat chromium oxy-carbide with non-steady plasma in the air with the starting material of chromium carbide. Coating in the air predicts that the application can be extended dramatically for the abrasive and corrosion resistances.

## MAGNETRON DEPOSITION OF PROTECTIVE COATINGS ON BASE OF Si-AL-N ON GLASSES OF WINDOWS OF SPACE VEHICLES

*V.P. SERGEEV\**, *M.P. KALASHNIKOV\**, *A.V. VORONOV\**, *I.A. BOZHKO\**, *E.V. RIBALKO\**, *YU.F. KHRISTENKO\*\**

*\*Institute of Strength Physics and Materials Science SB RAS, 2/4, Akadmicheskii av., Tomsk, 634021, Russia, [vsereg@mail.tomsknet.ru](mailto:vsereg@mail.tomsknet.ru), 73822491481*

*\*\* Scientific research institute of applied mathematics and mechanics of Tomsk state university, 30, Lenin av., Tomsk, 634050, Russia*

Collisions of space vehicles (SV) with meteoroids a natural origin and products of anthropogenous pollution of space concern to number of the major factors causing damage and fracture SV. To the greatest degree various optical devices suffer from shocks of micrometeoroids: window glasses, solar cells, etc. Shock of a high-speed microparticle, without dependence from its origin, causes mechanical and plasma processes at which on a surface the crater is formed, the shock wave is spread, microcracks arise. To one of expedients of the solution of this problem can become deposition over glass of high hard refractory coatings with high coefficient of elastic restitution and a low the temperature of the linear expansion coefficient, transparent in visible field of a spectrum.

The purposes of article are:

- studying of method of pinch of shock resistance in conditions high-speed (3 - 5 km/s) bombardment by iron microparticles of the quartz glasses used in windows of space vehicles, by means of a deposition on them of coatings,
- investigation of opportunities of production of the transparent protective coatings on the basis of nitrides of silicon and aluminum with method of pulsing magnetron sputtering of composite targets,
- determination a structurally-phase state and the optical-mechanical properties at which there is the most essential pinch of shock resistance of glasses with coatings on the basis of Si-Al-N.

By methods of a X-ray diffraction analysis and transparent electronic microscopy (TEM) of the high resolution it is ascertained, that Si-Al-N coatings of thickness ~10 microns are transparent at relations Si:Al 1:4 and 4:1. Thus the Al-poor coatings have the amorphous nature, and the Al-rich coatings - nanocrystalline multiphase structure. On basis method of the TEM dark-field images the medial size of grains of crystalline coatings 5 - 12 nanometers is certain. A glasses with an amorphous coatings maintain the transmittance quantity of visible light the within the limits of the observational error whereas it decreases for 6 % with nanocrystalline coatings.

Deposition of coatings raises microhardness, an elastic modulus and coefficient of elastic restitution of the superficial stratum of a quartz glass. The greatest magnification of these properties, accordingly, in 3.4, 3.5 and 1.7 times is observed at a deposition of the nanocrystalline coatings.

Trials of the observational samples for shock resistance spent by means of MPX23/8 light gas gun in the scientific research institute of applied mathematics and mechanics of Tomsk state university. For carrying out of statistically significant trials of the observational samples the special jiggling - a subject table which was located in the vacuum chamber has been designed. This table provided simultaneous arrangement of four initial glasses and four glasses with coatings in strictly certain standings concerning a gun trunk.

As particles for bombardment of the observational samples microparticles of a classified iron powder with the medial size  $56.3 \pm 8.2 \mu$ , with the shape of particles of close to spherical have been chosen. The lump of a portion of a powder for each shot was a stationary value  $60.0 \pm 0.1$  mg, thus their velocities of a throwing made 3-5 km/s.

It is ascertained, that on glasses with coatings a surface density of formed craters under the same requirements of trial it is essential below, than on glasses without coatings. Thus more effective depression up to  $3.9 \cdot 10^6 \text{ m}^{-2}$  is observed at deposition on a glass of Si-Al-N crystalline coatings against value  $10.8 \cdot 10^6 \text{ m}^{-2}$  on glasses without coatings.

## CHARACTERIZATION OF TITANIUM-ZIRCONIUM SURFACE ALLOYS PRODUCED BY MAGNETRON SPUTTERING DEPOSITION AND LEHCEB TREATMENT

*M. BESTETTI\**, *M.F. BRUNELLA\**, *A.B. MARKOV\*\**, *E.V. YAKOVLEV\*\**

\*Politecnico di Milano, Via Mancinelli 7, Milano, 20131, Italy, [massimiliano.bestetti@polimi.it](mailto:massimiliano.bestetti@polimi.it), +39 0223993166

\*\* Institute of High Current Electronics RAS, 2/3, Akademicheskoy Ave., Tomsk 634055, Russia

The formation of surface alloys by combining the magnetron sputtering deposition of thin metal layers onto a metal substrate, followed by treatment with low-energy high-current electron beams (LEHCEB) is a very interesting technique [1].

The present work describes the possibility of using the combined technique PVD + LEHCEB for producing Ti-Zr surface alloys on titanium substrates. Zirconium thin films of different thicknesses were deposited by magnetron sputtering deposition onto Ti grade I substrates. Then, the alloying procedure was carried out by LEHCEB treatment by controlling the number of pulses.

The structure of Ti-Zr surface was assessed by X-ray diffraction (XRD) and the elemental depth profiles were determined by glow discharge optical emission spectroscopy (GDOES). The changes in morphology and composition were observed by scanning electron microscopy (SEM) and the mechanical properties were evaluated by means of microindentations experiments. Ti-Zr surface alloys of thickness in the range between 2 and 4 micrometers were obtained as a function of the number of EB pulses. The number of pulses has also an effect on the morphology and homogeneity of the surface alloys as observed by SEM and EDS. The alloys are characterized by a composition gradient: the concentration of zirconium from the surface decreases (from 43 to 20 at.%) going into the bulk of the sample. Correspondingly, a significant increase in the film microhardness was measured. The analysis of the crystalline structure by X-ray diffraction allowed to identify a distorted cubic-like crystal structure in the produced films.

Corrosion behavior of Ti-Zr alloys was also investigated and a ranking was found by electrochemical potentiodynamic measurements in 1M H<sub>2</sub>SO<sub>4</sub> at room temperature. Preliminary results, that must be confirmed, showed that a higher content of zirconium in the surface alloys seems to correspond to a lower corrosion current density.

### REFERENCES

- [1] *A.V. Batrakov, A.B. Markov, G.E. Ozur, D.I. Proskurovsky, and V.P. Rotshtein*, Surface alloying of metallic substrates with pre-deposited films through a pulsed electron-beam mixing // *Eur. Phys. J. Appl. Phys.*, 43 (2008) 283–288

## PROPERTIES OF ZrO<sub>2</sub> AND TiO<sub>2</sub> COATINGS ON ZIRCONIUM ALLOYS

*N.S. PUSHILINA\**, *E.V. BEREZNEEVA\**, *I.P. CHERNOV\**, *N.N. KOVAL\*·\*\**, *O.V. KRISINA\*\**, *V.N. KUDIYAROV\**,  
*V.V. SHUGUROV\*\**

*\*National Research Tomsk Polytechnic University, Lenin ave. 30, Tomsk, 634050, Russia, [tpu.chernov@gmail.com](mailto:tpu.chernov@gmail.com)*

*\*\*Institute of High Current Electronics SB RAS, 2/3 Akademichesky Avenue, Tomsk, 634055, Russia*

Zirconium alloys are important constructional materials of nuclear reactors. They have a low thermal neutron capture cross section, high corrosion resistance and strength characteristics. However, Zr alloys are hydride-forming, the penetration of hydrogen into the bulk material leads to a decrease of plasticity, formation of cracks and, as a consequence, the subsequent destruction. Therefore, the protection against the penetration of hydrogen in titanium and zirconium alloys is an important problem. Promising ways protective coatings are pulse beam methods which are actively being developed. Such effects can increase the wear resistance, strength and corrosion resistance.

The report discusses the results of studies on the structure, physical and mechanical properties and penetration of hydrogen in volume Zr1%Nb alloy coated ZrO<sub>2</sub> and TiO<sub>2</sub>, deposited by vacuum arc plasma-assisted method. Coatings have high wear resistance, hardness and good adhesion to zirconium alloy. It has been established that a high hardness, wear resistance and better adhesion to the substrate belongs to coating of zirconium oxide (ZrO<sub>2</sub>). Resistance tests on hydrogen at a temperature of 400°C showed that the ZrO<sub>2</sub> coating reduces the rate of hydrogen sorption into Zr1%Nb alloy in a ~2.4 times, TiO<sub>2</sub> coating does not affect the absorption of hydrogen.

## INFLUENCE OF MICROARC OXIDATION PARAMETERS ON THE ROUGHNESS AND WETTABILITY OF THE CALCIUM PHOSPHATE COATINGS DEPOSITED ON THE NANOSTRUCTURED TITANIUM

*E.G. KOMAROVA, YU.P. SHARKEEV, E.V. LEGOSTAEVA, V.V. CHEBODAEVA*

*Institute of Strength Physics and Materials Science of SB RAS, 2/4, Akademicheskii ave., Tomsk, 634021, Russia,*

*E-mail: katerina@ispms.tsc.ru, phone: +7 (3822) 286-809*

The titanium and its alloys have been widely used as dental, orthopedic and traumatologic implant materials because of their excellent mechanical properties, chemical stability, and biocompatibility. To improve the biocompatibility of titanium-based implants, various physical and chemical treatments have been performed. The treatments modify the structure, composition, and chemical properties of the titanium surface [1]. The microarc oxidation (MAO) is a relatively convenient and effective technique to deposit the calcium phosphate (CaP) biocoatings on the titanium surface with complex geometric form. This technique can introduce various elements into the coatings and produce functional coatings with a porous structure. Over the years of time in Lab. of Physics of Nanostructured Biocomposites of ISPMS of SB RAS the novel biocomposite material on the base of the bulk nanostructured titanium and the CaP coatings have been developed to create the dental implants with given rough surface and high biocompatibility [2]. The physical and mechanical properties of coatings, such as a roughness and adhesion strength to a substrate are important role. One of the most important properties of implants is the wettability, because cell adhesion occurs much better on the hydrophilic surfaces. In the most cases the wettability depends on the roughness of the surface and its chemical composition.

The paper presents the MAO as a method of deposition of the CaP coatings at the various voltage 150 ÷ 400 V for obtaining the surface with different roughness that effect on the coating wettability. In order to form the CaP coatings on the nanostructured titanium surface the technique Micro-Arc 3.0 was developed and the aqueous solutions of phosphoric acid with calcium carbonate and hydroxyapatite were patented [3].

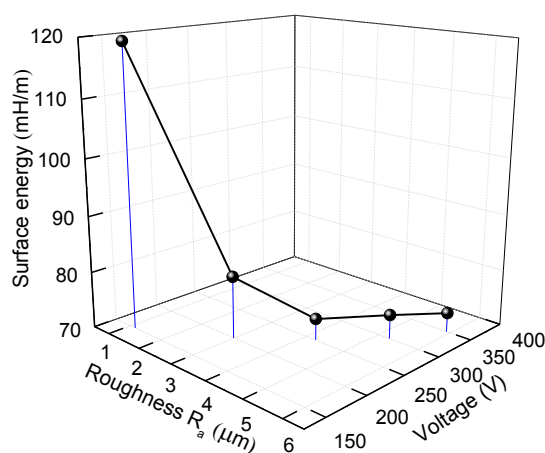


Fig. 1. The dependence of the surface energy of the CaP coatings on the surface roughness ( $R_a$ ) and the voltage of the MAO process

The investigation of the properties of the CaP coatings show that the increasing of the voltage from 150 to 400 V leads to the linear increasing of roughness value ( $R_a$ ) from 1 to 8  $\mu\text{m}$  and the linear decreasing of the contact angles with water and glycerol from 35 to 5° and from 70 to 15°, consequently. In this case, the surface energy decreases according to the hyperbolic law from 120 to 73 mH/m. This is due to the increasing of the surface roughness of the CaP coatings (fig.1). For the CaP coatings the critical value of the surface energy corresponds to the value of the water surface tension when the roughness value is higher than 4  $\mu\text{m}$ . The CaP coatings obtained by the MAO method have high hydrophilicity due to rough topography and chemical composition containing the calcium and phosphate phases.

### REFERENCES

- [1] Yu.P. Sharkeev, E.V. Legostaeva, A.Yu. Eroshenko, I.A. Khlusov, O.A. Kashin // Composite Interfaces. – 2009. – Vol.16. P.535-546.
- [2] E.V. Legostaeva, K.S. Kulyashova, E.G. Komarova, M. Epple, Yu.P. Sharkeev, I.A. Khlusov // Materials Science and Engineering Technologies. – 2013. – Vol. 44. – No. 2-3. P. 188-197.
- [3] G.A. Shashkina, Yu.P. Sharkeev, Yu.R. Kolobov, A.V. Karlov. Calcium-phosphate coatings on titanium and titanium implants and method its deposited. Russian Patent No. 2291918. 2007.

**COMPLEMENTARY ELECTROCHROMIC DEVICE WITH PMMA GEL ELECTROLYTE***A.N. ZAKHAROV, P.S.GALKIN\*, N.F. KOVSHAROV, A.A.SOLOVIEV**Institut of High Current Electronics SB RAS, 2/3 Akademichesky Ave, Tomsk, 634055, Russia, zare17@yandex, (3822)491651  
\*Nikolaev Institute of Inorganic Chemistry SB RAS, 3 Acad. Lavrentiev Ave, Novosibirsk, 630090, Russia*

In this study, the design of complementary electrochromic devices (ECD) with two reversible redox electrodes, operating in series is presented. A complementary electrochromic device consists of three major components: electrochromic working electrode, electrochromic counter-electrode, and electrolyte. Thin-film electrochromic layers are coated on the optically transparent electrodes (glass coated with fluorine-doped tin oxide). The electrochromic films in ECD are thin films of tungsten trioxide ( $\text{WO}_3$ ) and Prussian blue [iron (III) hexacyanoferrate (II)]. The following of gel electrolyte (mass ratio) was used: 12% PMMA, 38% propylene carbonate, 38% ethylene carbonate, 12%  $\text{LiClO}_4$ . Tungsten oxide films with thickness 400-800 nm were deposited on the glass substrates by DC magnetron sputtering. Prussian blue films on the glass substrates were electrochemically deposited.

The optical transmittance change between maximum and minimum transmittance of the ECD is shown in Fig.1.

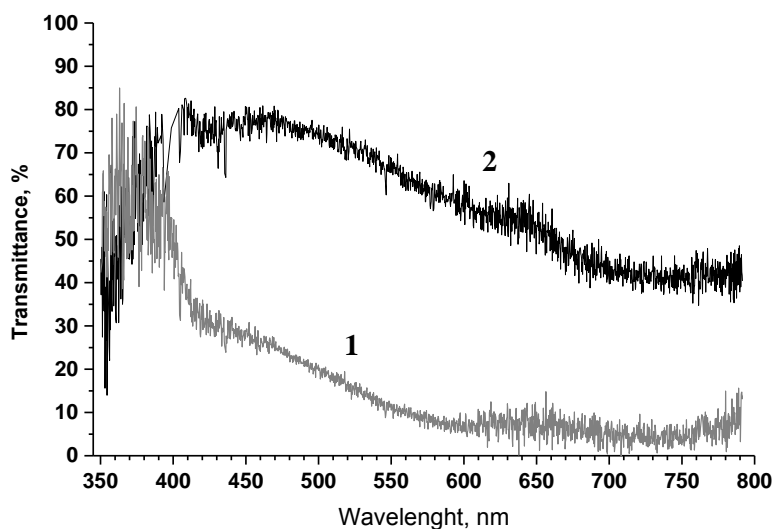


Fig. 1. Transmittance spectra of the ECD in fully colored (1) and bleached (2) state between 350 and 800 nm

## HEAT SAVING COVERING MATERIAL FOR GREENHOUSES

*S.V.RABOTKIN, A.A. SOLOVIEV, N.F. KOVSHAROV, M.M. PUGOVKIN, N.S. SOCHUGOV<sup>†</sup>*

*Institute of High Current Electronics, 2/3 Akademicheskii Ave., Tomsk, 634055, Russia, rabotkin@yandex.ru, 8(3822)491651*

A heat saving covering material based on a polyethylene film with a multilayered coating was fabricated. It allows reducing the heating costs for greenhouses.

A technique of low-e heat saving ZnO:Ga/Ag/ZnO:Ga coatings deposition on a polyethylene film was developed. The coatings have a transmittance of 77-78 % in the visible range of spectrum and reflectance of 91 % in the infrared range of spectrum.

It was first proposed to use ZnO:Ga as a dielectric layer in the oxide-metal-oxide structure, which was deposited by magnetron sputtering of a ceramic ZnO:Ga<sub>2</sub>O<sub>3</sub> cathode in the argon atmosphere. The layer considerably increases the resistance of the coating to atmospheric conditions. Also, the polyethylene film pretreatment by oxygen ion beam generated by an ion source with an anode layer was first proposed. The pretreatment increases considerably the adherence of the multilayered low-e coating to a substrate. A metal functional layer was deposited by high current magnetron sputtering, which allows increasing a transmittance of the coating.

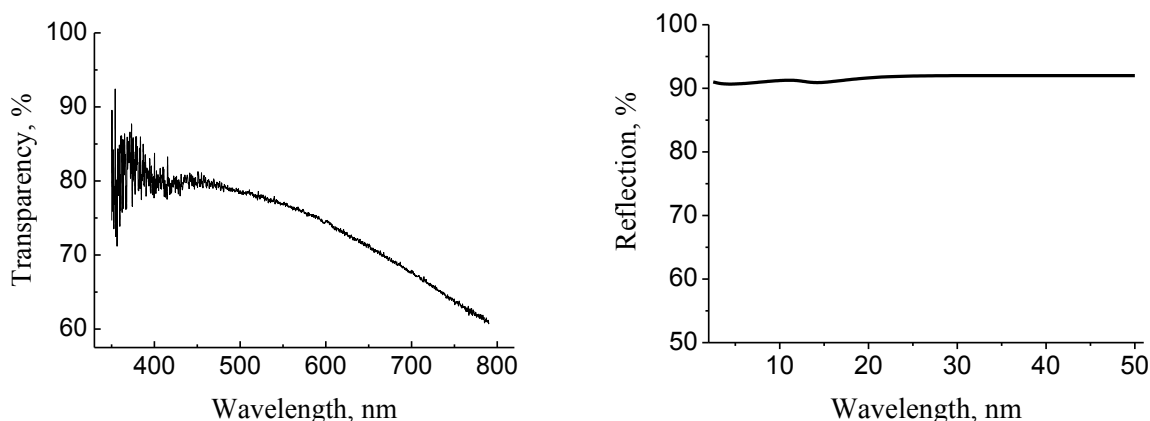


Fig. 1. Low-e coating spectra in the visible (left) and infrared (right) range

A full-scale test of greenhouse models have shown that the polyethylene film with a multilayered low-e coating used as a greenhouse covering material allows decreasing heating costs for greenhouses in winter twice as much.

The studies of the greenhouse models showed that cucumber hybrids "Marinda" and "Courage" grow better in the greenhouses with the heat-cover material, so it is an effective method of increasing yields. Yield in the greenhouse with the heat saving covering material is 13-35% higher than with polyethylene film.



## THE IMPACT OF ELECTRON BEAM PASS NUMBER ON COMPOSITE COATINGS STRUCTURE AND PROPERTIES<sup>1</sup>

S.F. GNYUSOV\*, A.A. IGNATOV\*, V.G. DURAKOV\*\*

\*Tomsk polytechnic university, Lenina Avenue 30, Tomsk city, 634050, Russia, gnyusov@rambler.ru, +79528806615

\*\* Institute of Strength Physics and Materials Science of Siberian Branch Russian Academy of Sciences, Akademicheskii avenue 2/4, Tomsk, 634021, Russia

Technological conditions of electron beam surfacing (EBS) are related with some features. The melting, crystallization and following cooling of surfaced metal take place in very nonequilibrium conditions because of high power density of electron beam and processes of strong local overheating. The temperature in local overheating area can considerably exceed the metal melting temperature value. It leads to intensification of diffusing processes, hard phases dissolving and oversaturated solution formation. High cooling velocities of surfaced metal can form new nonequilibrium structures. In addition the surfacing by 4...5 e-beam passes is needed for forming the hardened layer with thickness of 3...4 mm. It can greatly affect the alteration of early surfaced layer structure and phase composition.

In this work the impact of e-beam pass number on phase-structure state, element composition and mechanical characteristics of coating on the basis of M2 steel and M2+20%WC and on substrate heat-affected zone is observed.

The coating microstructure examination, transversal section hardness measurements and X-ray analysis are carried out.

The powders of M2 steel and M2+20%WC as surfacing materials for electron-beam surfacing in a vacuum were used.

The microstructural analysis of M2 coating against the E-beam pass number shows that the coating microstructure formed by one pass is presented by columnar crystals that are typical for melted metal. This structure disappears with much equiaxial grains formation by recrystallization processes progress. It takes place by increasing of E-beam pass number and correspondingly much specimen heating. The material layer of 100...150 mm thickness with austenite-martensitic structure is formed in transition zone "coating-substrate" as a result of substrate melting by first pass.

The combined analysis of microstructure and X-ray data shows that martensite volume fraction is changed as a curve line with minimum against E-beam pass number. The quantity of retained austenite doesn't exceed 15% for four passes. The most quantity of martensite and disperse carbide extractions after three E-beam passes is observed. The multi-modal distribution of reinforcement particle sizes formed in a hardened layer carbide subsystem is presented by fine-grain precipitations of eutectic carbide M<sub>6</sub>C with grain size  $d_1 = 3.8 \mu\text{m}$ , submicrocrystalline precipitations of grain size  $d_2 = 0.65 \mu\text{m}$  (VC) and secondary M<sub>6</sub>C carbides of  $d_3 < 0.25 \mu\text{m}$ . The greatest  $\mu$ -hardness value is obtained by three E-beam passes (8000 MPa) and then this value brings down to 6500 MPa. The change of heat-affected zone width is non-linear. It is practically stable for small pass number (1 – 2), then dramatic grows by 3-4 passes and stay stable by multipass surfacing once more.

The microstructural analysis of M2+20%WC coating against the E-beam pass number shows that martensite quantity grows with increasing of E-beam pass number from 1 to 4. According to X-ray data retained austenite quantity decreased from 88% to 67%. The needled martensite extracts inside the austenitic grains in transition zone from substrate to surface for all specimen. The quantity of this martensite doesn't exceed 30%. The width of transition zone with austenite-martensitic structure is about 100...150  $\mu\text{m}$ .

## THE FORMATION OF SLIDING WEAR RESISTANT COMPOSITE COATINGS ON THE BASIS OF HIGH SPEED STEEL<sup>1</sup>

S.F. GNYUSOV\*, A.A. IGNATOV\*, V.G. DURAKOV\*\*

\*Tomsk polytechnic university, Lenina Avenue 30, Tomsk city, 634050, Russia, gnyusov@rambler.ru, +79528806615

\*\* Institute of Strength Physics and Materials Science of Siberian Branch Russian Academy of Sciences, Akademicheskii avenue 2/4, Tomsk, 634021, Russia

The modern structural materials should have special tribological properties for working in extreme wear conditions. The heavy-loaded friction units work in such conditions by high linear velocities and high applied loadings. As a rule this processes can be accompanied by forced lubricant deficiency. The striking example of this friction unit is heavy-loaded gear shafts whose structural feature is that the bearing journals are the inner races of needle bearing. At the given conditions this bearing journals fail pending one month by continuous running. The formation of uniform multi-modal distribution of reinforced phases in austenitic-martensitic matrix by electron-beam surfacing (EBS) in vacuum was observed in previous studies [1]. Thus the assumption that it is possible to create the coating with enhanced sliding wear resistance by EBS is made.

In this work the investigation of sliding process against steel counterpar and phase-structural state alteration of composite coatings on the basis of M2 steel obtained by EBS is observed. The conditions of sliding wear: sliding velocities range is 1.2 – 3.6 mps, loadings are 20 – 100 N and temperature is up to 200°C.

The sliding test is carried out by friction machine “CMT-20” according to “wheel – two plane blocks” with step-by-step rise of velocity and loading and without lubricant. The counterpart is the wheel manufactured from quenched 52100 steel (HRC 63...65) with diameter of 62 mm and width of 15 mm.

The structure of surfaces coatings before and after wear test is researched by optical, scanning electron and ion-electron microscopes. The research of chemical composition is carried out by X-ray spectrum analysis. The roughness is measured by scanning interferometer.

Two areas of extremely gross wear by sliding velocities 2.4 and 3.6 mps and loadings of 60 and 100 N respectively are established for sliding pair M2 – 52100. Two areas of steady-state wear are observed by load range 20...40 N and 60...80 N.

The significant reduction of wear intensity (in 2...3 times) for friction pair M2+20%WC – 52100 as compared with M2 coating is established. It is caused by simultaneous increase of carbide phase volume fraction and residual matrix austenite both. The wear intensity of composite coating linear grows with loading increase at sliding velocities 2.4 and 3.6 mps. It mostly depends on oxidative wear development. The oxide layer areas begin to form at 20 N.

### REFERENCES

- [1] S.F. Gnyusov, A.A. Ignatov, V.G. Durakov //LTPJ. – 2010.

<sup>1</sup>This work is carried out with financial support of State Tasks of NIR TPU No. 862

## THE FORMATION OF WEAR RESISTANT COATINGS FOR HEAVY LOADED PARTS AS BEARING JOURNALS OF GEAR SHAFT<sup>1</sup>

S.F. GNYUSOV\*, A.A. IGNATOV\*, V.G. DURAKOV\*\*

\*Tomsk polytechnic university, Lenina Avenue 30, Tomsk city, 634050, Russia, gnyusov@rambler.ru, +79528806615

\*\* Institute of Strength Physics and Materials Science of Siberian Branch Russian Academy of Sciences, Akademicheskiiy avenue 2/4, Tomsk, 634021, Russia

The modern structural materials working in extreme wear conditions should have special tribological properties. Specifically, there is a problem of heavy-loaded reduction unit fail cause of intense wear of nitrated bearing journal for needle bearing. At the given conditions this parts fail pending one month by continuous running. The structural feature of this reduction unit is that the bearing journals are the inner races of needle bearing.

The formation of uniform multi-modal distribution of reinforced phases in austenitic-martensitic matrix by electron-beam surfacing (EBS) in vacuum was observed in previous studies [1, 2]. In addition carried wear tests show that these coatings demonstrate excellent abrasive and sliding wear resistance. The full-scale wear test was carried out after successful small-scale test.

The investigation of full-scale wear test of gear shaft bearing journal coatings aimed for needle bearing fit and analysis of phase-structural state of base metal heat-affected zone is observed.

Gear shafts of heavy loaded reduction units of Tomskneftehim Ltd are made of J24056 steel.

The powder of M2 steel with dispersibility of 50...350  $\mu\text{m}$  as surfacing material for EBS in a vacuum was used. The structure of surface coating after annual full-scale test is researched by optical, scanning electron microscopes. The research of chemical composition is carried out by X-ray spectrum analysis. The  $\mu$ -hardness values of coating and base metal near the coating are measured. The roughness is measured by contactless profilometer.

According to profilometry data the wear of rolling surface doesn't exceed about 4  $\mu\text{m}$ . The roughness (Ra) for race groove surface is 0.207  $\mu\text{m}$ , for total coating surface – Ra=0,244 $\pm$ 0,304  $\mu\text{m}$ . The coating formed by EBS is presented by martensitic-austenitic matrix reinforced by carbides. The multimodal size distribution of reinforce particles is formed in carbide subsystem. The initial ferrite-pearlite structure of J24056 steel has evident streaking of structural components that is partially succeeded after final heat treatment (normalization) and following EBS. The surfaced coating has hardness value about 600...800 HV. This thickness hardness alteration is caused by weld bed overlay technology that provides the partial thermocycling and the alteration of retained austenite and secondary carbides quantity.

### REFERENCES

- [1] S.F. Gnyusov, A.A. Ignatov, V.G. Durakov // The impact of electron beam pass number on phase-structural state and wear resistance of coatings on the basis M2 steel, LTPJ, 2010
- [2] S.F. Gnyusov, A.A. Ignatov, V.G. Durakov // The wear features of composite coating on the basis of M2 steel in pair with 52100 steel in the wide range of sliding velocities and loadings, TPU News, 2013

<sup>1</sup> This work is carried out with financial support of State Tasks of NIR TPU No. 862

## DEPOSITION DIOXIDE TITANIUM THIN FILMS BY MEANS OF DUAL MAGNETRON: OPTICAL AND PHOTOCATALYTIC PROPERTIES

*D.V. SIDELEV, Y.N. YURJEV*

*Department of Hydrogen Energetic and Plasma Engineering, Tomsk Polytechnic University, Lenin avenue 30, Tomsk, 634050, Russian Federation, [Dimas167@tpu.ru](mailto:Dimas167@tpu.ru), +7-983-238-71-79*

The research of photocatalysis is a one of the most perspective scientific field of thin films and coatings. It is assumed that dioxide titanium ( $\text{TiO}_2$ ) thin films have a great potential to application as a photocatalytic material [1]. Furthermore,  $\text{TiO}_2$  thin films exhibit high antireflective properties and are applied in low-e coatings, etc [2]. In this case, the aim of work is a research of optical and photocatalytic properties of  $\text{TiO}_2$  thin films, which were deposited by dual magnetron sputtering system (dual MS).

Thin films deposition was carried out by ion-plasma installation «Yashma» using the dual magnetron with Ti target (99.5 %) in a wide range of changes in flow ratio Ar and  $\text{O}_2$ . The thickness of samples was 50 nm and controlled by quartz thickness gauge «Micron-5». The substrate was a glass and monocrystalline Si. Preliminarily, samples were subjected to ion pre-treatment. The research of optical properties was performed by spectrophotometer SF-2000 and ellipsometry method. The determination of photocatalytic activity was occurred by decomposition of methylene blue [3].

The research of deposition mode with changes in the magnetic field configuration of dual MS was performed. There was a slight increase of deposition rate in the case of «closed» configuration. Regularities between optical and photocatalytic properties for transition and oxide deposition modes were defined.

### REFERENCES

- [1] *Tayade R.J., Surolia P.K., Kulkarni R.G., Jasr R.V.* // Science and Technology of Advanced Materials. – 2007. – № 8. – p. 455-462.
- [2] *Szczyrbowski J., Briiuer G., Teschner G., Zmelty A.* // Journal of Non-Crystalline Solids. – 1997. – № 218. – p. 25-29.
- [3] *Zeman P., Takabayashi S.* // Surface and Coatings Technology. – 2002. –№ 153. – p. 93-99.

## THE FEATURES OF FORMATION AND CHARACTERISTICS OF SINGLE- AND MULTILAYER Ti-Al-N COATINGS PREPARED BY VACUUM ARC PLASMA-ASSISTED DEPOSITION<sup>1</sup>

*O.V. KRYSINA\**, *N.N. KOVAL\**, *V.V. SHUGUROV\**, *A.A. KALUSHEVICH\**

*\*Institute of high current electronics SB RAS, 2/3 Akademichesky ave., Tomsk, 634055, Russia,  
[krysina\\_82@mail.ru](mailto:krysina_82@mail.ru), +7(3822)49-17-13*

The deposition of wear-resistant ion-plasma coatings is one of effective methods of improvement of service characteristics and life time of details, instruments and products. Multicomponent coatings of Ti-Al-N system are widely used as wear-resistant coatings with low friction coefficient and unique properties. In spite of numerous papers of that subject the investigations on synthesis and its optimization and also coating research are carrying out and remain actual problem.

In the work researches of Ti-Al-N coating deposition by vacuum arc method with plasma assistance and characteristics of obtained coatings are showed. The experimental works of ion-plasma coating deposition were carried out on automated set-up "QUINTA", and its detailed description is elsewhere [1]. Synthesis of Ti-Al-N system coatings was carried out by follow modes: (1) at generating several metal plasma flows (using Ti and Al single-element cathodes) in the presence of nitrogen reactive gas and (2) at evaporating sintered powder cathodes containing additional element (Al).

In addition, besides monolayer Ti-Al-N coatings the mulatilayer Ti-Al-N/TiN coatings were deposited. Total thickness of obtained coatings was about 3-5  $\mu\text{m}$ . Comparative analysis of physical and mechanical properties, phase-structural state and elemental composition of Ti-Al-N coatings deposited under different conditions of formation was carried out.

### REFERENCES

- [1] *Shugurov V.V., A.A. Kalushevich, N.N. Koval, V.V. Denisov, V.V. Yakovlev. Automated vacuum ion-plasma installation // Izv. vuzov. Physica. - 2012. - № 12/3. - pp. 118-122.*

<sup>1</sup> This work was supported by Project SB RAS II.9.5.1 "Research foundations of development of electrophysical equipment for obtaining and properties modification of nanostructured layers and coatings" and by the Russian Foundation for Basic Research (grant No. 13-08-98108-r\_sibir-a).

## OXIDATION RESISTANCE OF ION-PLASMA NITRIDE COATINGS DEPOSITED BY VACUUM ARC PLASMA-ASSISTED METHOD<sup>1</sup>

*O.V. KRYSINA\**, *N.N. KOVAL\**, *S. DOYLE\*\**

*\*Institute of high current electronics SB RAS, 2/3 Akademichesky ave., Tomsk, 634055, Russia,*

*[krygina\\_82@mail.ru](mailto:krygina_82@mail.ru), +7(3822)49-17-13*

*\*\*Karlsruhe institute of technology, ANKA Synchrotron Radiation Facility, Hermann-von-Helmholtz-Platz 1, 76344 Eggenstein-Leopoldshafen, Germany*

Wear-resistant multicomponent coatings on the basis of titanium nitride are used for improvement of physicomechanical properties and for increase of service characteristics of various details, tool and articles. These coatings (i.e., Ti-Cu-N, Ti-Al-N, Ti-Si-N, Ti-Al-Si-N) possess high hardness, high corrosion and wear resistances, and etc. It is necessary to note that the existence of nanocrystalline structure ( $d \leq 100$  nm) provides the significant increase of the main properties. As the working surface of the majority of tools, device details and articles heats up in open air during their using, one of important criteria of a certain type of coating is the oxidation resistance at increased temperature. One of the main characteristics for wear-resistant multicomponent nanocrystalline coatings is oxidation resistance at high temperature, because usually real details with coatings undergo high-temperature heating on open air during using.

Besides, the multicomponent coatings produced by ion-plasma methods at intensive ion bombardment, are often in a tension. Therefore decrease of the main properties due to relaxation of residual stresses is observed during time. In order to confirm the fact of the high physicomechanical characteristics existence proved by stable coating structure, it is necessary to carry out the tests of coating thermal stability.

The investigation of coatings based on TiN (Ti-Al-N, Ti-Si-N, Ti-Cu-N) synthesized by vacuum arc method on resistance to oxidation were carried out after annealing of the coated samples in open air up to  $\approx 1000^\circ\text{C}$ . After cooling they were investigated by methods of optical microscopy, micro- and nanoindentation, profilometry, SEM, x-ray analysis and etc.

<sup>1</sup> This work was supported by the Russian Foundation for Basic Research (grant No. 13-08-98108-r\_sibir-a).

## THE EFFECT OF MAGNETRON DISCHARGE OPERATION MODES ON TIN COATINGS CHARACTERISTICS<sup>1</sup>

*A.S. MAMAEV, O.A. BUREYEV*

*Institute of Electrophysics, 106 Amundsen St, Yekaterinburg, Russia, asm@iep.uran.ru, +7(343)2678829*

The effect of titanium target sputtering modes on microhardness and adhesion of the coatings to the substrate was studied. TiN coatings were deposited to the substrate surface (ЭП637А steel) by reactive magnetron sputtering of titanium target in three modes: No. 1 – low-power pulses magnetron sputtering with ion assistance; No. 2 – high-power pulses magnetron sputtering, and No. 3 – mixed magnetron sputtering mode using pulses of high and low power. Average discharge power was the same in all three modes and equaled 800 W.

The process of coating deposition included three stages: ion cleaning of the substrate surface from impurity, deposition of Ti sublayer (~ 100 nm thick) and deposition TiN coating (1 – 5 μm). The distance between magnetron target and the substrate was made 10 cm. The adhesion Ti sublayer was deposited at the same mode of magnetron sputtering as TiN coating itself, but in Ar environment only. Gas mixtures containing Ar and N<sub>2</sub> in relations from 30/1 to 30/10 were used to deposit TiN coatings by reactive magnetron sputtering of Ti target at the gas pressure equaled 0,5 Pa. The maximum coatings microhardness were achieved by means of adjustment of the value of nitrogen flow rate to the chamber in each mode.

At the first mode the pulses frequency was made  $f = 50$  kHz, the pulse duration  $\tau = 10$  μs, the current amplitude  $I = 3$  A. The negative bias voltage  $U_b = 75$  V ( $f = 50$  kHz) was applied to the substrate and the gas mixture was ionized additionally by a broad (80 mm in dia.) low-energy electron beam (~100 eV). The average ion current density at the substrate surface  $j_m$  was 3,4 mA/cm<sup>2</sup>, the specimen temperature  $T = 300^\circ\text{C}$ , the speed of coating deposition  $v = 1,25$  μm/h.

The mode No. 2 parameters were as follows:  $f = 1$  kHz,  $\tau = 80$  μs,  $I = 30$  A,  $U_b = 0$  V, the ion current density at one impulse  $j_i = 1,3$  mA/cm<sup>2</sup>,  $T = 190^\circ\text{C}$ ,  $v = 1,2$  μm/h.

At the mode No. 3 two magnetron devices were operated simultaneously: the first – at the mode No. 1 (2 A, 50 kHz, 10 μs), and the second – at the mode No. 2 (100 A, 200 Hz, 30 μs),  $U_b = 75$  V,  $j_m = 0,06$  mA/cm<sup>2</sup>,  $j_i = 10$  mA/cm<sup>2</sup>,  $T = 160^\circ\text{C}$ ,  $v = 2,1$  μm/h.

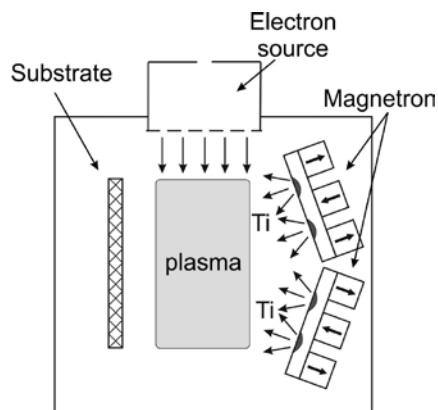


Fig. 1. Schematic diagram of the gas-discharge device

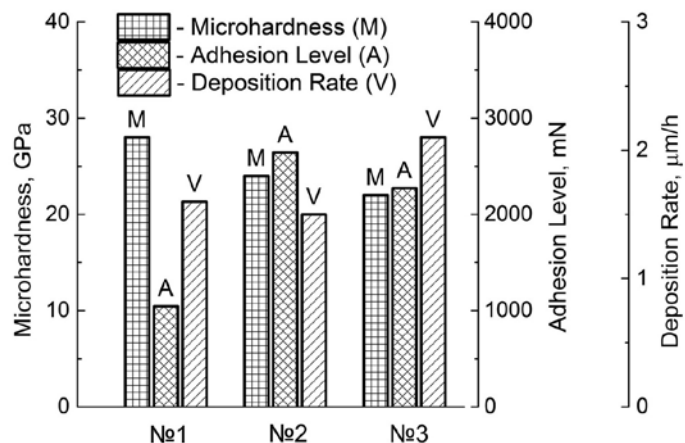


Fig. 2. Dependence of the microhardness, the adhesion and the coating deposition speed on the magnetron operation mode

Coatings with the highest value of microhardness were obtained at the mode No. 1, but such coatings have the lowest adhesion to the substrate. At the mode No. 2 the coatings adhesion was two times higher than it was at the mode No. 1. The 3-rd mode provides a high speed (~ 2 μm/h) of the coating deposition with a high coating hardness (~ 22 GPa) and an improved adhesion to the substrate ( $L_{kp} \sim 2273$  mN). That fact allows to consider this 3-rd mode to be optimum for deposition of TiN coatings to ЭП637А steel.

<sup>1</sup> This work was partially supported by the Program of Basic Researches of UB RAS (project 12-И-2-2012).

## INVESTIGATION OF COPPER-ALUMINUM CONTACT PAIR SURFACE OBTAINED BY PLASMODYNAMIC METHOD<sup>1</sup>

*YU. L. KOLGANOVA, A. A. SIVKOV, A.S. SAIGASH, I.I. SHANENKOV*

*National Research Tomsk Polytechnic University, Lenina av., 30, 634050, Tomsk, Russia, julia\_kolganova@mail.ru, 89059906700*

In the electrical energy industry base materials for conductive elements are copper and aluminum. However, when it's necessary to join them together, the loss of electricity increases due to the additional contact resistance. Using a coaxial magneto plasma accelerator it is possible to combine aluminum and copper in the contact pair [1]. The obtained copper coating on an aluminum substrate has such advantages as a high quality and a low specific transition contact resistance.

In figure 1 shows obtained sample by plasmodynamic method. For a complete analysis, samples were examined with the three-dimensional non-contact profilometer - Micro Measure 3D Station to study the surface structure of the contact pair copper-aluminum with different resistance values. The scanning area was 2x2 mm and the scanning pitch was 8 microns. The results of this analysis are profilograms, which were used to construct 3D images of the surface and identify parameters of the roughness profile and other data.

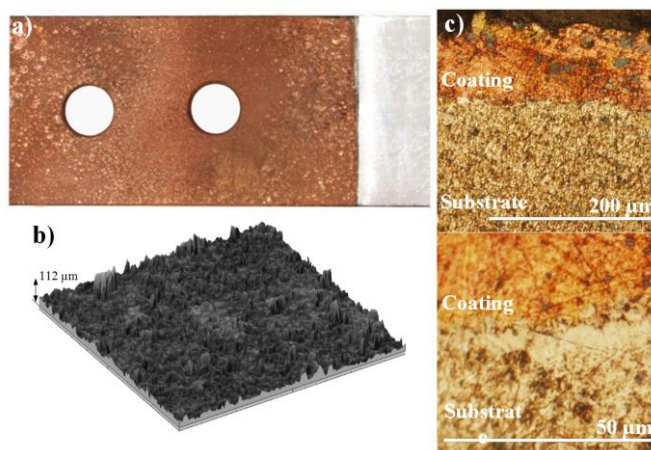


Fig. 1. Sample contact pair copper-aluminum with copper coating a) Obtained aluminum tip with copper coating b) 3D-model surface sample c) Optical micrographs of the cross-sectional slice

The profile of the obtained sample with the lowest specific transition resistance has the most uniform surface and contains projections and hollows, the height and depth of which in average are less than 10  $\mu\text{m}$ . The analyzed sample surface with a large resistance value in comparison with the low resistance sample has more uneven profile. The profile of this sample consists of clearly seen peaks with average height of 30  $\mu\text{m}$  and maximum height of 190  $\mu\text{m}$ . The arithmetic mean profile roughness ( $R_a$ ) of the sample with the lowest resistance is 5,4  $\mu\text{m}$  and for a contact pair with the highest resistance is 15,5  $\mu\text{m}$ . Using the obtained data revealed the experimental dependence of the transition contact resistance from the average surface roughness of samples was revealed. The graph shows that with increasing of sample profile roughness the transitional contact resistance increases. In theory, this is explained as follows: due to decrease of roughness the contact area increases and, therefore, the specific transitional contact resistance decreases.

### REFERENCES

- [1] Sivkov A.A., Saigash A.S. Kolganova Yu. L. // *Izvestiya Vyzov. Fizika.* – 2012. – 55. – № 12-3. Pages 139-141.

<sup>1</sup> This work was supported by RFBR research project No. 14-08-31122



**BIAS-ASSISTED MAGNETRON SPUTTERING OF YTTRIA-STABILISED ZIRCONIA<sup>1</sup>**

*A. A. SOLOVYEV\**, *S. V. RABOTKIN\*\**, *I. V. IONOV\*\**, *A. N. KOVALCHUK\**, *A. V. SHIPILOVA\*\**

\* *Tomsk polytechnic university, Lenin Ave. 30, Tomsk, 634050, Russia, andrewsol@mail.ru, (3822) 491-651*

\*\* *Institute of High Current Electronics SB RAS, 2/3 Akademicheskii Ave., Tomsk, 634055, Russia*

The morphology of yttria-stabilised zirconia (YSZ) layers deposited by reactive magnetron sputtering was studied with regard to their application as thin electrolytes for solid oxide fuel cells (SOFC). A thin layer of YSZ was deposited on the top of a porous anode Ni-YSZ layer for SOFC. The effect of bias potential applied to the substrate (DC, pulsed and bipolar-pulsed) and temperature of the substrate on the layer morphology and gas-tightness was investigated. It was shown that use of bias allows changing the layer growth morphology and promoting the growth of dense and less columnar films. The use of substrate heating allows increasing a coating adhesion to the anode layer. The preferential crystallographic orientation of the sputter deposited thin layers has been investigated.

<sup>1</sup> This work was performed under the State target for Institute of High Current Electronics SB RAS and RFBR grant № 14-08-31164 mol\_a.

## WEAR RESISTANCE OF NANOCOMPOSITE FILMS WITH DIAMOND-LIKE CARBON COMPONENT<sup>1</sup>

*A.B.VLADIMIROV, S.A.PLOTNIKOV, A.P.RUBSHTEIN*

*Institute of Metal Physics, Ural Division RAS, 18 S.Kovalevskay St., Ekaterinburg, 620990, Russia,  
phone: +7(343)-378-38-35, email: A.Vladimirov@imp.uran.ru*

Abrasive wear resistance of nanocomposite films with carbon diamond-like component has been studied. The nanocomposite film consists from TiC and hard diamond-like carbon layers. Thickness of each layer is not more than 100 nm. Carbon layers were deposited by impulse arc sputtering of graphite target (first process) or by decomposition of a hydrocarbon in glow-discharge plasma (second process). The concentration of carbon in nanocomposite films depends on frequency of pulses (first process) or pressure of acetylene in work chamber (second process).

The wear resistance test of nanocomposite films was carried out in jet of abrasive particles falling perpendicularly on sample surface. Diameter of particles is about 100  $\mu\text{m}$ , velocity - 10 m/s. It was established that wear resistance of nanocomposite films rise with increase of carbon concentration. Obtained films are perspective for improve of wear resistance of cutting tools.

<sup>1</sup> This work was supported by Presidium of Ural Division RAS (projects No 02-T-2-1008 and №12-И-2-2012)

## GRADIENT-LAYERED COATING OF TI-AL-SI-N, TI-AL-SI-CU-N - CONDITIONS OF FORMATION AND STRUCTURE <sup>1</sup>

*S.V. OVCHINNIKOV\**, *A.D. KOROTAEV\*\**, *YU.P. PINZHIN\**, *V.A. SLABODCHIKOV\*\**

\* *Institute of Strength Physics and Material Science, Siberian Division, RAS, 2/4 Akademicheskoy Ave., Tomsk, 634021, Russia, [ovm@spti.tsu.ru](mailto:ovm@spti.tsu.ru), +73822531569*

\*\* *National Research Tomsk State University, 36 Lenin Ave., Tomsk, 634050*

One promising area of creation of functional coatings is the synthesis of adaptive gradient and gradient-layered on elemental, phase composition and structure states on the basis of experimentally studied conditions and mechanisms of their formation. In this regard this work presents results of the study changes in microstructure, elemental and phase composition in the gradient-layered, including heterophase, nanostructured systems of Ti-Al-Si-N, Ti-Al-Si-Cu-N obtained using electron microscopy dark field analysis method of bending-torsion of the crystal lattice, nano-beam diffraction and X-ray microanalysis. Depositions of coatings were performed by magnetron sputtering targets of Ti, Al-Si alloy and Cu. A change in power during the synthesis contributed to the formation coatings with variable elemental and phase compositions by their thickness.

It was shown for the system Ti-Al-Si-N that the concentration of poorly soluble (insoluble) impurities affects the change of the structural parameters - the value of the lattice parameter of titanium nitride, dimensions coherent scattering regions, curves-torsion of the crystal lattice. The concentration of the dopant (Al, Si), corresponding to the transition of the coating structure from the submicrocrystalline to the nanocrystalline state was found. The structure of the transition zone from submicron to nanocrystalline region was determined. This transition is accomplished by increasing the density of longitudinal along the growth direction of low-angle grain boundaries, fragmentation of the nanocolumn structure by cross boundaries and the rise of the disorientation at them with increasing silicon concentration under growth coating.

Deposition of the gradient-layered coating with high concentrations of Al and Si (15 and 9 at.%) and increasing the Cu concentration at surface of the coating up to 11 at. % causes formation nanograin structure away from the nitrated sublayer with the crystal size in the range from 2-3 to 7 nm. The increasing of copper concentration is accompanied by a slight decrease in the average crystal size (from 5 to 4 nm), the increasing in bending-torsion of the crystal lattice and elastic stresses in the individual crystals from  $\sim E/50$  to  $\sim E/30$  (average value,  $E$  - Young's modulus). The regularities of the structure formation of homogeneous and gradient-layered compositions of system Ti-Al-Si-Cu-N depending on the type and concentration of the impurity are: transition coating in the nanocrystalline state in excess of the critical value of the silicon concentration in the narrow (2.5-3 at.%) concentration range, the growth degree of local distortions of the crystal lattice by increasing the concentration of copper in the entire investigated range of its concentrations (up to 11 at.%), while maintaining the nanocrystalline state.

It was shown that ion activation energy of the coatings growth change in the range to 300 eV determines the selective sputtering of the alloying elements with a depletion silicon in coating, changing size of the grain in the submicrocrystalline columnar structure and sharper, as compared to coating of Ti-Al-Si-N, a transition in a nanocrystalline structure with boundaries between layers of different composition. We discuss possible causal regard element composition, lattice parameters and grain structure of the coating on the basis of these data.

<sup>1</sup> This work was supported by grant RFBR № 13-08-00502

## DLC COATINGS DEPOSITION BY MAGNETRON DISCHARGE PLASMA

*Y.N. YURJEV, D.A. ZAITCEV, D.V. SIDELEV, O.S. TUPIKOVA*

*\*Tomsk Polytechnic University, Lenin avenue 30, Tomsk, 634050, Russian Federation, yurjev@tpu.ru, +7-923-424-42-13*

Functional carbon-based coatings are widely used in many branches of science and technology due to their wide range of unique properties [1, 2]. The use of magnetron discharge such as a tool of thin films deposition has a set of advantages as compared with traditional methods of deposition of carbon-based films: deposition on a large-scale substrate, a slight thermal action on a substrate, absence of drop fraction and etc.

DLC coatings were deposited by means of ion-plasma installation «Yashma-5» with a dual magnetron sputtering system (dual MS). The film thickness was 1  $\mu\text{m}$ . The DLC coatings deposition was due to sputtering of graphite targets in Ar plasma. Two configurations of dual MS with different magnetic fields (B field) were reviewed: closed B field and mirror B field configurations [3].

It was shown that the properties of coatings depend on Ar pressure in a vacuum chamber and magnetic field configuration of dual MS. The rise of Ar pressure resulted in an increase of deposition rate, which is associated with electrical discharge parameters and maximum power of supply. The coating hardness decreased with rising work pressure in the case of mirror B field configuration (Fig. 1). When closed B field configuration was used, that regularity is a non-linear. There is a maximum of hardness at 0.13 Pa.

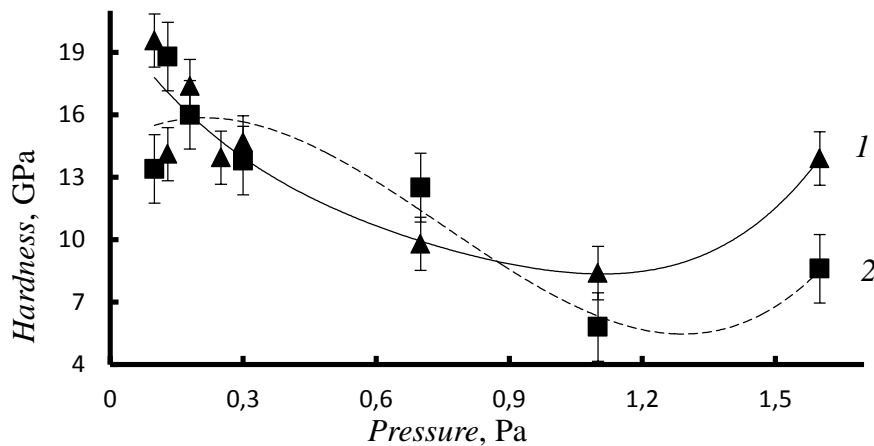


Fig. 1. The dependence between coatings hardness and work pressure: 1 - mirror B field; 2 - closed B field.

### REFERENCES

- [1] Gutierrez C.A., Meng E. // *J. Micromech. Microeng.* – 2010. – № 20. – 095028. – p. 1-12.
- [2] Wojciechowski K.T., Zybala R., Mania R., Morgiel J. // *Journal of Achievements in Materials and Manufacturing Engineering.* – 2009. – v. 37. – № 2. – p. 726-729.
- [3] Musil J., Baroch P. // *IEEE Transactions on Plasma Science.* – 2005. – v. 33. – № 2. – p. 338-339.

## MATHEMATICAL MODELING OF ION IMPLANTATION PROCESS WITH ACCOUNT THE VACANCIES GENERATION

*E.S. PARFENOVA\**, *A.G. KNYAZEVA*

*TPU, Lenina Avenue, 30, Tomsk, 634050, Russia*

*\*[Linasergg@mail.ru](mailto:Linasergg@mail.ru), 8 (3822) 41-91-51*

The ion implantation is one of the most perspective methods of surface treatment of metals. The main advantages are the high reproducibility and the possibility of introducing impurities in any material. The friction coefficient, wear resistance, hardness and other characteristics are improved after processing. The general subjects of energy effects study are redistribution of atoms in the surface layers of metals, the mass transfer processes and changes of the surface properties. It is necessary to know the defect structure is formed after implantation and ion distribution for greater efficiency. The simplest radiation defects are vacancies and interstitials (Frenkel pair). Many researchers associate these phenomena with the "long-range effect".

Among the discoverers of "long-range effect" can be noted P.V. Pavlov and D.I. Tetelbaum, D.C. Sud and G. Dirnli, V.S. Hmelevskaya, V.N. Chernikov and A.P. Zakharov, M.I. Guseva, V.M. Anishchik and V.V. Uglov, Y.A. Perlovich, A.N. Didenko and A.E. Ligachev, S.A.B. Bol and L.M. Matt [1]. In [2] it is shown that excess of atoms (introduced and own) in interstitial positions and the presence of vacancies are generated owing to radiation in the area over mileage of ions leads to a specific spatial distribution of point defects. Removal of impurity and defect structures out of the implanted layer is connected, on the one hand, with the generation of elastic waves arising at the time of ions introduction in the solid and, on the other hand, with static stresses in the implanted layer are induced by ion implantation [3]. That is why it is important to consider such wave processes in the construction of mathematical models of surface treatment process. But investigators pay attention to various processes of this treatment in the construction of mathematical models and do not consider the possible mutual influence of different phenomena.

The introduction of impurities by the vacancy mechanism is much simpler, and ions expend less energy. That is why the admixture can propagate on distances much greater than the thickness of the surface-alloyed layer. Besides a tension has significant influence on the distribution of the implanted impurity in the surface of the target. These stresses arise when ion impact on the surface of the metal. In work [4] is shown that taking into account stresses leads to qualitative changes in the profile of the impurity concentration.

In this paper the process of co-propagating waves of impurity concentration and waves of mechanical stresses is considered, also the influence of generated vacancies is studied. The detailed validation of the model is provided.

### REFERENCES

- [1] *Didenko A.N., Sharkeev Yu.P., Kozlov E.V. // Effekty dalnodeystviya v ionno-implantirovannykh metallicheskikh materialakh. – Tomsk, Izd-vo NTL, 2004.*
- [2] *Sugakov V.I. // Yadernaya fizika i energetika. – 2009. – V.10. – №4. 395-402.*
- [3] *Aparina N.P., Guseva M.I., Kolbasov B.N., Korshunov S.N., Mansurova A.N., Martynenko Yu.V. // Voprosy atomnoy nauki i tekhniki – Termoyadernyy sintez. – 2007. – №3 . 18-27.*
- [4] *Demidov V.N., Knyazeva A.G., Ilina E.S. // Izv. Vuzov. Fizika. – 2012. – №5/2 . 34-42.*

## ANALYSIS OF THE FORMATION PROFILES OF IMPLANTED IONS DEPENDING ON THE STRUCTURAL STATE OF THE TARGET AND THE IMPLANTATION MODES

V.T. BARCHENKO, T.S. PAVLENKO

*Saint Petersburg Electrotechnical University «LETI», Prof. Popova str. 5, 197376,  
SPb, RU, E-mail: [vtbarchenko@yandex.ru](mailto:vtbarchenko@yandex.ru)*

Application of modified ion beams nanocrystalline and fine-grained materials makes it necessary for prediction of their mechanical properties and, as a consequence, the development of universal theoretical models for predictions. Experimental studies titanium specimens with different grain sizes, of the modified aluminum ion beams have revealed the benefits of nanocrystalline modified samples compared with a coarse their analogs.

Regularities of the mass transfer in metallic materials under irradiation of pulse-periodic particle beams vacuum-arc ion sources «Diana-2» and «MEVVA-5.RU» is analyzed. In the papers [1-2] presented the concentration profiles of aluminum ions in a structured titanium after ion beam implantation at source «Diana-2» and «MEVVA-5.RU».

Measured by Auger-electron spectroscopy of the concentration profiles of aluminum in titanium are characterized by a broad peaks of implanted ions, the position and form of which depend on the structure of the target. High-dose ion implantation ( $10^{17} \div 10^{18}$  ions/cm<sup>2</sup>) carried by the ion beam vacuum arc sources. In describing the observed regularities of mass transfer takes into account the energy uniform beam, since in used sources generated ions in different charge states. Accordingly, the actual task is to identify the observed regularities of mass transfer in the experiments. As targets used titanium samples with grain sizes of 0.1, 1.4, 15, 38 microns at the ion beam irradiation source «Diana-2», and samples of titanium with a grain size 175 nm when irradiated with an ion beam source «MEVVA-5.RU».

By modeling revealed that the formation of concentration profiles of implanted ions occurs mainly by two mechanisms: originally an impurity is distributed statistically, with increasing fluence, and accordingly, the concentration of defects generated by ion beam structures begin to contribute to the thermal and radiation- induced diffusion, surface sputtering processes samples with different degrees of intensity.

### REFERENCES

- [1] T.V. Vahni, G.A. Vershinin, T.S. Grekova, B.P. Gritsenko, I.A. Kurzina, Y.P. Sharkeev // Abstracts XXXIX International Conference on Physics of Charged Particles with Crystals. - M.: University Book, 2009. - P. 149.
- [2] G.A. Vershinin, T.V. Vahni, A.I. Suslov, I.A. Kurzina, Y.P. Sharkeev // Abstracts XLII International Conference on Physics of Charged Particles with Crystals. - M.: University Book, 2012. - P. 173.

**ACCURACY AND ROUGHNESS OF TIN COATINGS DEPOSITED BY VACUUM ARC PLASMA**

V. V. BUDILOV, K. N. RAMAZANOV, V. V. POSTNOV, I. I. YAGAFAROV, B. F. USMANOV

Ufa State Aviation Technical University, K. Marx str.12, Ufa, 450000, RF, ramazanovkn@gmail.com, +7(347)2730763

Coating deposition by vacuum arc plasma is effective way of part running ability enhancement. Coating thickness and roughness depend on both preprocess machining surface condition and deposition conditions [1,2,3,4]. Achievable surface roughness of coated by vacuum arc plasma deposition high (5-6) level of accuracy parts with 0.1...0.8  $\mu\text{m}$  surface average roughness strongly depends on deposition conditions [5]. Thereby assurance of given arithmetic average roughness and coating thickness values when hardening high precision parts is an actual problem.

TiN coatings were deposited on 13Kh11N2V2MF-Sh; 30KhGSNA; ZhS6K; VT-18; 38KhA; KhN68VMTYuK-VD substrates. Surface average roughness and TiN coating thickness measurements were done. Coating thickness and surface roughness were studied as a function of substrate surface inclination and distance from plasma flow. Experiments were carried out on substrates with different types of preprocess machining. The influence of coating thickness, deposition conditions, and deposited materials on coated surface roughness were studied.

It was established that surface roughness increase with increasing of coating thickness and arc current values and decrease with reactive gas pressure increasing. Substrate temperature and negative voltage bias values according to experimental data are roughness neutral. The impact of substrate surface inclination and distance from plasma flow on coating thickness and surface average roughness was revealed. The coating deposited by vacuum arc plasma thickness distribution law was assigned.

## REFERENCES

- [1] V. V. Budilov, N. N. Koval, R. M. Kireev, K. N. Ramazanov. // Integrated methods of engineering structural material treatment by glow and vacuum arc discharges. – Moscow. Mashinostroenie, 2013.
- [2] Ch. Chokwatvikul, S. Larpiattaworn, S. Surinphong, Ch. Busabok, P. Termsuksawad // Journal of Metals, Materials and Minerals. – 2011. – Vol.21. – No.1 . 115-119.
- [3] B. Straumal, W. Gust, N. Vershinin, R. Dimitriou, E. Rabkin // Surface and Coatings Technology. – 2000. – 125 . 157–160.
- [4] M. Ali, E. Hamzah, I.A. Qazi, M.R.M. Toff // Current Applied Physics. – 2010. – Vol.10. – Issue 2 . 471–474.
- [5] V.V. Budilov, R.M. Kireev, I.I. Yagafarov // Russian Aeronautics. – 2012. – Vol. 55. – Issue 2 . 203-207.

**ELECTRODEPOSITION OF ZINC ALLOYS IN THE PRESENCE OF X-RAY RADIATION FIELD***V.M. ANISHCHIK\*, N.G. VALKO\*\***\*Belarusian State University, 4, Pr. Nezavisimosty, Minsk, 220030, Belarus**\*\*Yanka Kupala State University of Grodno, 22, Ozheshko Street, 230023, Belarus**Phone+375297841915, e-mail: N.Valko@grsu.by*

The results of the experimental research the effect of the X-ray irradiation on the growth processes, on the formation of structure, phase composition, and the physical-mechanical properties of binary and ternary alloys of zinc from the sulfate electrolytes to the low-carbon steel are presented in this work.

The experimental dates indicate that the effect of X-ray irradiation during a process on the electrolyte for electrodepositing Zn-Ni, Zn-Co, Zn-Fe, Zn-Ni-Co has a positive effect [1-2]. It is established the increasing speed of electrodeposition as a result the intensifying diffusion in an electrolyte in the X-ray irradiation [3]. The effect of the X-ray irradiation on the electrodeposition of Zn-Ni, Zn-Co, Zn-Fe, Zn-Ni-Co coatings also promotes to formation of compact and nonporous alloys. It is observed the dependence of the rate of deposition from electrolysis mode and irradiating by the method of complete factor experiment. The statistical models worked out of the electrodeposition of binary alloys of zinc in the X-rays field. The coefficients analyses in the regression equations as the factors affecting to the current output, leads to the conclusion that the action of X-rays irradiation on the electrodeposition of alloys of zinc leads to expand an operating density range and reduce the dependence of the rate of mass deposition on the cathode from temperatures factor. Using the developed model can adequately define the optimal modes of electrolytic deposition of zinc alloys coatings in the x-rays irradiation to obtain high-quality coatings with the maximum current output of the metal.

It is discovered, that the microhardness of the alloys of zinc with iron group metals, formed in the X-Ray irradiation conditions is above, and the coefficient of friction is considerably lower than in the models, precipitate with the same conditions but without the irradiation.

## REFERENCES

- [1] *Anishchik V., Val'ko N., Vojna V // Journal of surface investigation, X-ray, synchrotron and neutron techniques.-2010:- Vol 4 .- № 1.- 2010 p. 142-145.*
- [2] *Vako N //Physics of the solid state.-2013.-Vol.55.- № 11.-P.2196.*
- [3] *Ershov, B., Kelm M., Janata E. // Radiat. Phys. Chem.- 2000.-Vol. 59. - P. 309-312.*



## FORMATION OF COMPOSITE NI-TI AND FE-TI COATINGS WITH ADJUSTABLE RATIO OF COMPONENTS FOR PHOTOCATALYTIC APPLICATION<sup>1</sup>

K.P.SAVKIN\*, M.V.SHANDRIKOV\*, A.V.TYUNKOV\*\*

\*Institute of High Current Electronics SB RAS, Akademichesky ave. 2/3., Tomsk, 634055, Russia,  
shandrikov@opee.hcei.tsc.ru, (3822)491-776

\*\* Tomsk State University of Control System and Radioelectronics, Lenina ave. 40, Tomsk, 634050, Russia

Titanium dioxide is used as material for photocatalytic sterilization in medical and food industries [1]. At the same time the band gap of titanium dioxide is 3.2 eV. This leads to the fact that the initiation of the oxidation processes on the surface of the coating is possible only in the ultraviolet spectrum of sunlight. The shift in the absorption of titanium oxide to the visible region is possible by adding an impurity metals such as Ni, Cu, V, Cr, Pt and other [2,3].

In our study the formation of composite Ni-Ti and Fe-Ti coatings with adjustable ratio of components for photocatalytic application was realised. The results of microroughness, phase and components of such coatings are presented. The coatings were obtained by means of BTIBD method with use of plasma generator with external injection and sputtering metal targets [4].

Our results demonstrate that the proposed approach allows a precision control of the percentage of components coatings by precision control the bias voltage on the sections of the targets (fig.1). The heterogeneity of proportions of the components in the coating does not exceed  $\pm 2\%$ . The heterogeneity of the samples with linear dimensions of 30x30 cm<sup>2</sup> does not exceed 15%.

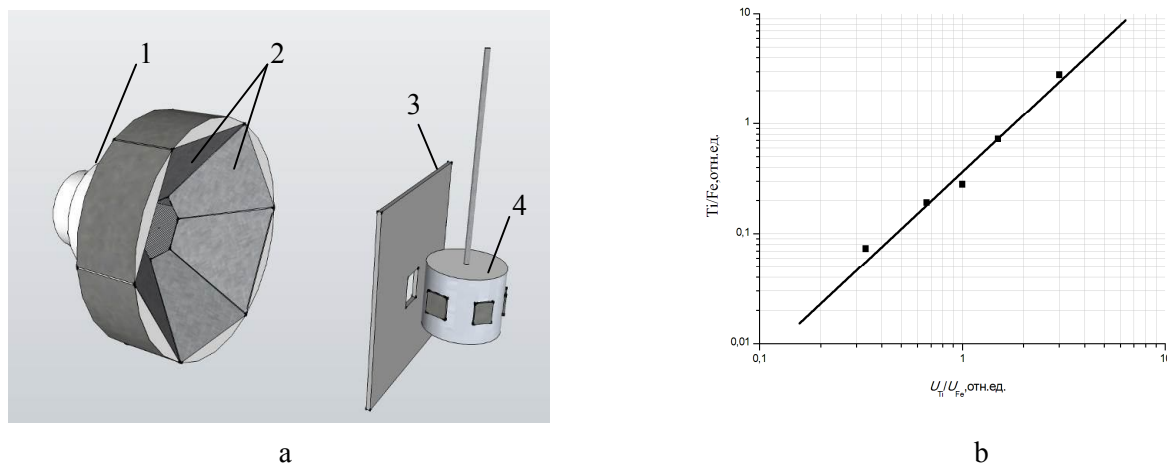


Fig. 1 The experimental setup: 1 – gaseous discharge plasma gun with electron injection, 2 - sputtering targets, 3 – shield, 4 - rotary sample holder (a) and the percentage composition of Fe-Ti coating versus the bias potential of targets (b).

### REFERENCES

- [1] Kim B., Kim D., Cho D., Cho S. // Chemosphere. – 2003. – V.52. – P.277-281.
- [2] D.H. Kim, K.S. Lee, Y.S. Chung, and S.J. Kim. // J.Am.Ceram.Soc. – 2006. – V.89. – P.515.
- [3] S. Klosek and D. Raftery.// J.Phys.Chem. – 2001. – B.105. – P. 2815.
- [4] A.S.Klimov, A.V.Medovnik, A.V.Tyunkov, K.P.Savkin, M.V.Shandrikov and A.V.Vizir // Rev. Sci. Instrum. – 2013. – V.84. – P. 013307.

<sup>1</sup> This study was supported by the Russian Foundation for Basic Research, project no. 12-08-00151-a

## CALCIUM PHOSPHATE COATINGS PREPARED BY RF-MAGNETRON SPUTTERING DEPOSITION: CHALLENGES AND PROSPECTS

*V.F.PICHUGIN*

\*Tomsk Polytechnic University, Lenin Av.30, Tomsk, 634050, RF, [pichugin@tpu.ru](mailto:pichugin@tpu.ru) (382)2564158

The problem of biocompatibility improvements of materials interacting with organism is a modern trend in medical materials science. Bioinert metal implants when applied clinically may cause complications because their artificial surface interferes with bone tissue. Biocomposites "implant + coating" combine high mechanical properties of implant and a good biocompatibility of the coating.

The method of RF-magnetron sputtering is an effective way to modify the surface of metal implants, to produce ultrathin ( $h < 1 \mu\text{m}$ ) biocompatible calcium phosphate (CaP) coatings. This method provides coatings that are uniform in thickness and in composition and that exhibit high performances.

We have fulfilled integrated studies of physical, mechanical, physicochemical and biomedical characteristics of the coatings based on hydroxyapatite and produced by rf-magnetron sputtering. These coatings were deposited by sputtering of targets made from stoichiometric or silicon-substituted hydroxyapatite [1, 2].

1. Calcium phosphate coatings deposited by rf-magnetron sputtering are uniform and dense without visible defects (pores and microcracks). The main elements of the relief of the coating surface are domed islands "grains". The average grain size is (10-100) nm and depends on the modes of deposition.

2. The coating consists of two phases - the crystalline and amorphous, wherein the crystalline phase has the structure of hydroxyapatite. The coating has amorphous structure at a power density of rf discharge  $0.05 \text{ W/cm}^2$  and predominantly crystalline at a power density of  $0.50 \text{ W/cm}^2$ .

3. The presence of silicon in the coatings deposited by sputtering of a target of silicon-containing hydroxyapatite was confirmed by the data of energy dispersive X-ray spectroscopy, however, the question on the position of silicon ions in the coating structure remains opened. This suggests that ions of silicon are located in the structure of the amorphous regions of the coating.

4. Silicon-substituted calcium phosphate coatings have the same physical and mechanical properties as the coating prepared from stoichiometric hydroxyapatite.

5. The ratio of the elements in the coatings in particular Ca/P depends on the power density absorbed by the substrate, bias voltage and the deposition time.

6. rf-magnetron sputtering allows preparing the pure or silicate-containing hydroxyapatite-based coatings with the different structure, morphology, stoichiometry and thickness by variation of the negative bias voltage.

7. rf - magnetron calcium phosphate coatings have high biocompatibility and do not cause of active local and systemic reactions.

8. The magnetron hydroxyapatite-based coatings with roughness of 8-th grade and above are bioinert and do not possess the osteoconductive and osteoinductive properties.

9. The surface structuring enhances osteogenic properties of the magnetron coatings *in vitro* and *in vivo*. The functional activity of the stromal cells depends on the dimensions of 3D niches for them on the surface of the coating. Calcium phosphate coating stimulates the secretory activity of osteoblasts in the range of roughness  $R_a = (0,5-5,5) \mu\text{m}$ .

10. Insertion of silicate - ions in the structure of the coating does not exert any significant effect on their osteogenic activity.

**The problems to be solved:** develop a model of the technological processes and get her analytical description; on the base of the analytical model develop the methods of selection and control of the modes of coating deposition; develop physically correct model and analytical description of the processes of the control of deposited coatings properties; determine the limits of applicability of this method for the formation of biocompatible coatings; develop the requirements for the composition and characteristics of a technological complex for industrial manufacturing of the coatings.

### REFERENCES

- [1] V.F. Pichugin, R.A. Surmenev a, E.V. Shesterikov, et al.// Surface and Coatings Technology 202 (2008) 3913–3920  
 [2] V.F. Pichugin,, M.A. Surmeneva (Ryabtseva) et al.//Journal of Surface Investigation. X-ray, Synchrotron and Neutron Techniques. 2011. Vol. 5 №. 5 p. 863-869

## STRUCTURE TRANSFORMATIONS ON THE SURFACE OF THE Al-Cr, Al-Cr-Si POWDER CATHODES SUBJECTED TO VACUUM ARC HEATING

G.A. PRIBYTKOV, V.V. KOZHOVA, A.P. SAVITSKII

Institute of Strength Physics and Materials Science, Akademichesky ave., 2/4, Tomsk, 634021, Russia,  
Phone: (3822) 286-962, E-mail: gapribytkov@mail.ru

It is known that the surface of vacuum arc cathodes is heated up to high temperatures exceeding the melting point of the cathode material. The surface melting leads to an increased content of drops in the arc erosion products. An intensity of drops generation is the greater the lower is a melting temperature of the cathode material [1].

It is known that in the surface layer of cathodes consisting of a compacted mixture of aluminum and 50 at.% titanium powders the titanium aluminides are formed as a result of the vacuum arc heating [2].  $Ti_3Al$  and  $TiAl$  aluminides have melting points in the range of 1475 - 1447 °C, which multiply exceeds the aluminum melting point (660 °C). Thus, the formation of refractory compounds on the working surface of the cathodes can reduce formation of the drops and improve a quality of the deposited coatings.

We studied the structure and phase composition of the surface layer on the Al-30 at.% Cr and Al-25 at.% Cr-10 at.% Si cathodes modified by vacuum arc action. On the cross-sectional metallographic patterns a continuous layer up to 80 microns thick can be seen. A sharp border separates the layer from virgin cathode material, having a composite structure of chromium and silicon particles imbedded into the aluminum matrix (fig 1b, c).

According to XRD analysis the modified layer is composed of binary and ternary intermetallic compounds depending on the elemental composition of the cathode. Modified layer originate from a continuous film of the melt formed on the cathode surface as a result of vacuum arc heating. Melting-crystallization origin of the modified layer is confirmed by the slightly waving smoothed relief on the cathode surface (fig 1a). There is a cracks net covering the surface. The cracking had occurred during the cooling process due to the difference of the thermal expansion coefficients of the underlying initial cathode material and brittle intermetallic layer on the cathode surface.

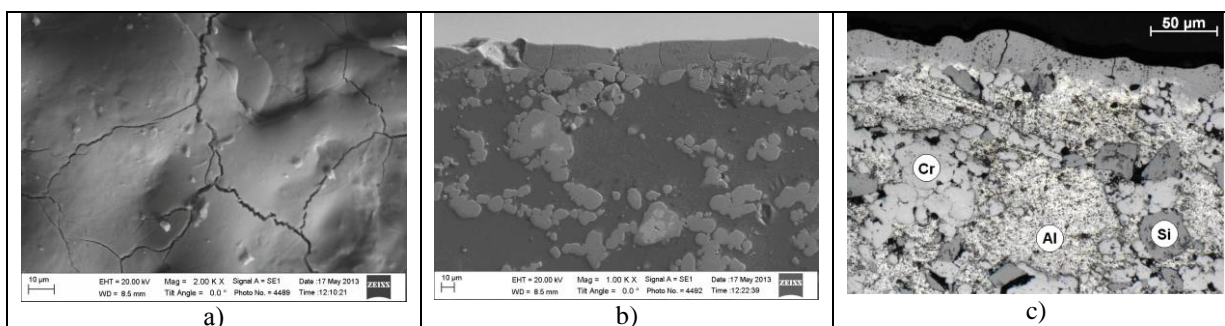


Fig. 1. Image of the outer surface (a) and a cross section (b, c) of the modified layer.  
The elemental composition of the cathodes (at.%):  $Al_{70}Cr_{30}$  (a, b);  $Al_{65}Cr_{25}Si_{10}$  (c).

EDX analysis has detected a depletion of modified layer with aluminum and silicon. The possible reason of the depletion is a selective evaporation of the light elements from the liquid metal bath.

We propose two possible reasons of surface melting of Al-Cr, Al-Cr-Si cathodes consisting of the blend of elemental powders. One of them is a large aluminum content in powder blend. Another one is lower melting point of chromium aluminides as compared with titanium aluminides.

### REFERENCES

- [1] A.W. Nurnberg, D.Y. Fang, U.H. Bauder. Temperature dependence of the erosion of Al and TiC by vacuum arcs in a magnetic field. *Journal of Nuclear Materials*. 1981, vol. 103-104, p. 305-308.
- [2] G.A. Pribytkov, I.A. Andreeva, B.B. Korzhova. Structure transformations on the surface of Al-Ti cathodes under action of the vacuum arc. *Physics and chemistry of materials processing*. 2011, №1, p. 36-44.

## A STRUCTURE AND PROPERTIES OF THE COATINGS DEPOSITED AT VACUUM-ARC EVAPORATION OF Al-Cr, Al-Cr-Si POWDER CATHODES IN VARIOUS GASEOUS MEDIA

*G.A. PRIBYTKOV, V.V. KORZHOVA, A.P.SAVITSKII*

*Institute of Strength Physics and Materials Science, Akademichesky ave., 2/4, Tomsk, 634021, Russia,  
Phone:(3822) 286-962, E-mail:gapribyt@mail.ru*

Multi-component nitride coatings on aluminum and chromium base are considered the most promising among coatings for cutting tools. According to many publications tool life with AlCrN, AlCrTiN, AlCrSiN coatings significantly superior than that of the tools with TiAlN coating [1-3]. The tools durability is provided by higher thermal stability, resistance to oxidation, when heated in air to 800-1000<sup>0</sup>C and a smaller friction coefficient against steel of AlCrN base coatings. In recent years, many studies of nitride coatings additionally doped with carbon or oxygen which are introduced by sputtering targets containing non-metallic components or through the gas phase were published [4, 5]. These coatings may be attributed to complex carbonitrides, carboxides or oxynitrides depending on the composition.

This paper presents the results of a study of the coatings deposited on 12X18H10T stainless steel substrates by vacuum-arc evaporation of the hot-compacted Al-Cr and Al-Cr-Si powder cathodes in vacuum, argon, nitrogen, carbon dioxide and in N<sub>2</sub>+12 vol. % C<sub>2</sub>H<sub>2</sub> mixtures. The technology regimes of the cathode evaporation were as follows: arc current – 100 A, process durability – 90 minutes, negative bias voltage on the substrate 60-170 V. The microstructure, phase and elemental composition of the coatings were investigated by SEM, X-ray diffraction and EDX spectroscopy methods.

The deposited coatings are of 8-15 μm. thickness and have dense, slightly lamellar structure independent of the gaseous media and cathode composition. The content of non-metal elements in the coatings depends on the gaseous media. A specific feature of the whole investigated coatings is high (up to 21 at. %) carbon content. The carbon content in the coating deposited in carbon dioxide media is lower than in the coatings deposited in argon and close to that in the coating deposited in vacuum media. So we can assume that the basic source of carbon in the investigated coatings is vacuum oil vapor consisting of hydrocarbon molecules.

At X-ray diffraction analysis revealed a few weak, broadened reflections from the coatings, deposited in carbon and oxygen containing media. The reason is a partial or complete amorphisation of the coatings, similar to reported in [4, 5]. The coatings deposited in argon, vacuum and nitrogen media consist of crystalline phases.

A great scientific and practical interest is an effect of a change of the elemental composition in the coating as compared to that in the evaporated cathode. A conventional reason of changes in the elemental composition of the coating is the selective sputtering effect from the growing coating surface induced by ion bombardment [6-8]. An intensity of selective sputtering governs by the energy of bombarding ions that depends on ion mass and electric charge, bias voltage and a pressure in vacuum chamber. So the most pronounced selective sputtering effect resulting in the coating depletion with aluminum and silicon is observed for the coatings deposited in argon media. As a result of heavy argon ions bombardment a content of Al and Si in the coating in total reduces to 29 – 33% compared to their content in the cathode.

### REFERENCES

- [1] *K. Yamamoto, T. Sato, K. Takahara, K. Hanaguri // Surf. Coat. Technol., 174, 620 (2003).*
- [2] *K.Ichijo, H.Hasegawa, T.Suzuki // Surf. Coat. Technol. 201, 5477 (2007).*
- [3] *Li Chen, Yong Du, S.Q. Wang, Jia Li // Int. J. of Refractory Metals & Hard Mater. 25, 400 (2007).*
- [4] *Sung-Kyu Ahn, Se-Hun Kwon, Kwang-Ho Kim // Trans. Nonferrous Met. Soc. China 21, 78 (2011).*
- [5] *Xiaoying Li, Wenwen Wu, Hanshan Dong // Surf. Coat. Technol. 205, 3251 (2011).*
- [6] *Shulaev V.M., Andreev A.A., Stolbovoi V.A., Pribytkov G.A., Gurskih A.V., Korosteleva E.N., Korjova V.V. Physical engineering of surface 6, 105 (2008).*
- [7] *Pribytkov G.A., Gurskih A.V., Shulaev V.M., Andreev A.A., Korjova V.V. Fizika i khimija obrabotki materialov 6, 34 (2009).*
- [8] *Luchaninov A.A., Strel'nitskii V.E. // Physical engineering of surface 10, 4 (2012).*

### SURFACE TENSION OF DEPOSITED COATINGS<sup>1</sup>

*S.A. GUCHENKO, V.M. YUROV, V.CH. LAURYNAS, O.N. ZAVATSKIY*

*Karaganda State University of the name of academician E.A. Buketov, 28 University Street, Karaganda, 100028, Kazakhstan, [exciton@list.ru](mailto:exciton@list.ru), 8(7212)78-61-78*

Coating properties (mechanical, tribological, etc.), as well as thin films are determined, primarily, their surface energy  $\omega$  or surface tension  $\sigma$ .

We have recently proposed methods for experimental determination of the surface tension of the deposited coatings. The first method involves the measurement of surface tension by determining the dependence of the microhardness of the thickness of the deposited coating. Microhardness of the deposited coating on the thickness of the formula:

$$\mu = \mu_0 \cdot \left(1 - \frac{d}{h}\right), \tag{1}$$

where  $\mu$  - microhardness of the deposited coating;  $\mu_0$  - «thick» sample;  $h$  - thickness of the deposited coating. The parameter  $d$  is related to the surface tension  $\sigma$  formula:

$$d = \frac{2\sigma v}{RT}, \tag{2}$$

where  $v$  - is the molar volume of the deposited coating;  $R$  - universal gas constant,  $T$  - temperature (K) at which the measurement is made. In the coordinates of  $\mu \sim 1/h$  ( $h$  - reverse the thickness of the deposited coating) turns direct, the slope of which determines  $d$ , and by the formula (2) is calculated as the surface tension of the deposited coating ( $\sigma$ ). As an example, consider the definition of the surface tension of titanium nitride coatings. The coating thickness was determined by an oblique thin sections using a metallographic microscope. The results are shown in Fig. 1.

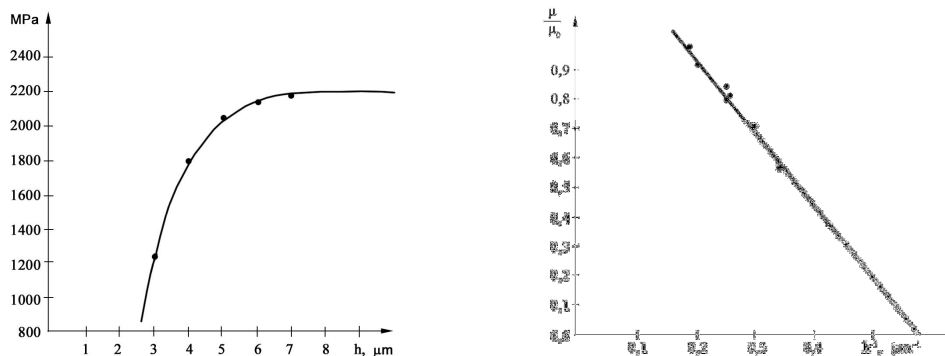


Fig. 1. Microhardness of the thickness (a) and backward thickness (b) a titanium nitride coatings

In the coordinates  $\mu/\mu_0 \sim 1/h$  experimental curve rectified by giving the value  $h = 1,3 \mu\text{m}$ . Titanium nitride  $v = 11,44 \text{ cm}^3/\text{mol}$ . and from (2) for the surface tension obtained:  $\sigma = 0,474 \text{ N / m}$ . The second method measures the dependence of the electrical conductivity of the coating thickness. Experimental dependence of the electrical conductivity of the deposited coating  $\Omega$  of its thickness  $h$  is described by a formula similar to (1). Conductivity nitride titanium coatings determined contactless method.

In the coordinates  $\Omega \sim 1/h$  experimental curve rectified in accordance with (1), giving a value of  $d = 1,4 \mu\text{m}$  and from (2) for the surface tension obtained:  $\sigma = 0,479 \text{ N / m}$ . This value substantially coincides with the result obtained from the microhardness of the coating thickness. The proposed methods are unique and allow you to define the most important characteristic of the deposited coating - surface tension, which determines the performance of the coated materials and products made of them, allows purposefully create new structural materials.

<sup>1</sup>This work was supported under the Program: 101 Ministry of Education and Science of the Republic of Kazakhstan "Grant funding for research". Priority: The intellectual potential of the country. By priority of Fundamental research in the natural sciences

## NUMERICAL JUSTIFICATION OF THE METHOD OF ACOUSTIC DIFFERENTIATION OF NANOPARTICLES BY THE SIZES. CURRENT STATE OF METHODS OF DIVISION OF DISPERSE MATERIALS

*S. V. KALASHNIKOV\**, *A. V. NOMOYEV\*\**

*\* Laboratory of physics of nanosystems of BSU, Smolina st., 24a, Ulan-Ude, 670000, Russia; betch\_kail@mail.ru; +79246580873*

*\*\* Laboratory of physics of nanosystems of BSU, Smolina st., 24a, Ulan-Ude, 670000, Russia*

In recent years strengthening of interest to positioning micro and nanoparticles on surfaces, to their use for modifying of known materials and creation of the new is observed.

Modern methods of division of particles are based on density and size difference (the size - selective sedimentation, Brownian diffusion and use of a vibration segregation), on a difference of superficial properties (a highly effective liquid chromatography), on a charge difference depending on the size (gel electrophoresis), on a difference of a dielectric constant in connection with the size of particles, and as on an acoustic impedance (ultrasonic division).

As for acoustic division, it is a new and perspective method, however use of this way for nanodimensional systems is still insufficiently studied. The first mentions of use of microfigures of Chladni for division of nanodisperse materials contain in [1]. Encouraging results on division of nanopowder of dioxide of silicon by an acoustic method are received in [2].

Classical way of visualization of standing fluctuations – putting any powder (usually sand) on a surface of the plate making cross fluctuations under the influence of, for example, bow of a violin. Thus powder forms the picture known under the name of figures of Chladni which were open for them in 1787. And now became standard school experiment [3]. Is much less known that very small powder accumulates in the antinodes surface fluctuations.

Formation of figures on a flexible plate – the main example of influence of two forces – forces of Newton and Stokes's strength: Newtonian forces tend to form Chladni's classical figures while Stokes's strengths tend to form Chladni's return figures.

Property of figures of Chladni spatially to divide particles into two fractions, various by the size, and is used in an acoustic method of division of particles. The main results of direct numerical modeling (are taken from [4]) are given in this article.

Results of modeling are the following. If modeling is executed with gold particles, their movement Newtonian forces operate. Because of fluctuations of a plate of a particle start jumping up and consecutive jumps tend to increase kinetic energy of particles. However in nodal lines at a plate zero speed and collisions with it reduce kinetic energy of particles. As a result, since all 80000 particles which have been uniformly distributed on a plate in modelled system, within several seconds the majority of them accumulated in nodal lines, forming Chladni's standard figures.

Now we reduce density of particles to 20 kg/m<sup>3</sup>, holding constant diameter. It leads to Stokes's strength, which almost in thirty times more, than the gravitational force operating on a particle. These easy particles move in antinodes and form Chladni's forming division of particles by the sizes the inverse figures as the mass of particles depends on their size.

### REFERENCES

- [1] *Acikalin T., Bietsch A., Dorrestijn M., Gerber Ch., Hegner M., Meyer E., Raman A.* Chladni Figures Revisited Based on Nanomechanics. // *Physical review.* – 2007. – №98.
- [2] *Kalashnikov S., Lygdenov V., Nomoev A., Romanov N.* The division of nanoparticles of silicon dioxide in size method figures Chladni // *Actual problems of the Humanities and natural Sciences.* – 2012. – №8. (43). – C. 21-28.
- [3] *Stockmann H.-J.* Ein Nomade der Wissenschaft // *Physik Journal.* – 2006. – № 5, 47.
- [4] *Van Gerner H.J.* Newton vs stokes: competing forces in granular matter. – Enschede, 2009.

## NOVEL NANOCARBON CATHODES FOR EXPLOSIVE ELECTRON EMISSION<sup>1</sup>

V. BARYSHEVSKY\*, N. BELOUS\*, A. GURINOVICH\*, E. GURNEVICH\*, P. KUZHIR\*, \*\*, S. MAKSIMENKO\*, \*\*, P. MOLCHANOV\*, M. SHUBA\*, V. ARKHIPOV\*\*\*, A. GUSELNIKOV\*\*\*, A. OKOTRUB\*\*\*, T. KAPLAS\*\*\*\* and Y. SVIRKO\*\*\*\*

\*Research Institute for Nuclear Problems, Belarusian State University, Bobruiskaya Str. 11 Minsk, 220030, Belarus, [polina.kuzhir@gmail.com](mailto:polina.kuzhir@gmail.com), +375297501835

\*\*National Research Tomsk State University, 36, Lenina Avenue, Tomsk, 634050, Russia

\*\*\*Nikolaev Institute of Inorganic Chemistry, SB RAS, 3 Acad. Lavrentiev av., 630090 Novosibirsk, Russia, [spectrum@niic.nsc.ru](mailto:spectrum@niic.nsc.ru), + 7383 330 53 52

\*\*\*\*Institute of Photonics, University of Eastern Finland, P.O. Box 111, Joensuu FI-80101, Finland; [yuri.svirko@uef.fi](mailto:yuri.svirko@uef.fi), +358504422540

We report on the properties of explosive emission cathodes with working surface made of pyrolytic carbon (PyC) films ( Fig.1a,b), and of aligned multi-walled carbon nanotubes (MWCNT, Fig.1c,d). For cathodes with diameter of 50 mm, we observed the current density as high as  $300\text{A}/\text{cm}^2$  under applied voltage below 400 kV for both types of covering nanomaterials. The Raman measurements reveal that the nanometrically thin PyC film survives after 7 shots (see Fig. 1a,b), whereas MWCNTs remain structurally the same after 21 shoots (see Fig.1e). In order to study the cathode degradation we compared optical microscope images of the cathode before and after shots. We observed that the pre-deposited PyC and MWCNT-array cathode prevent copper evaporation and oxidation (see insets into Fig.1a,b). This property ensures a higher explosion emission stability of the nanocarbon/Cu-cathodes in comparison with conventional graphitic ones. Nanocarbon/Cu cathodes are expected to be most promising for applications that require electric field strengths from 50 to 60 kV/cm.

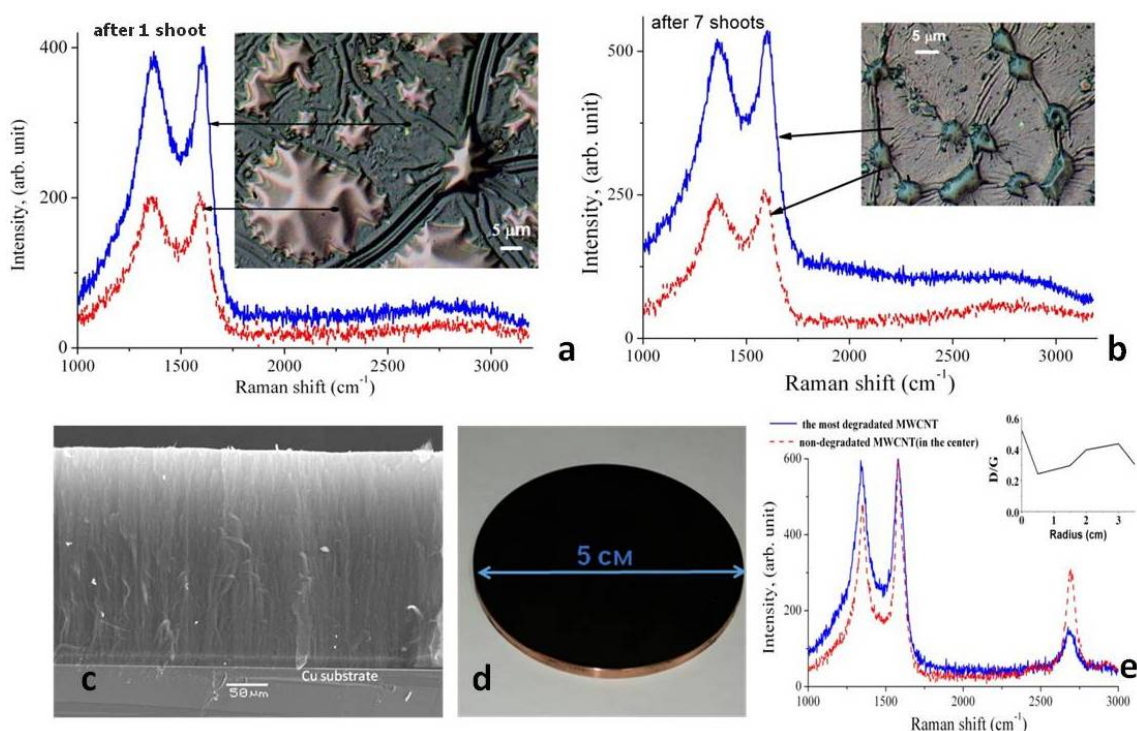


Fig. 1. (a), (b) Raman spectra of PyC pre-deposited on Cu substrate after one (a) and seven (b) shoots. Insets are optical high resolution images of PyC/Cu cathode, after 1 and 7 shoots correspondently. (c) High resolution SEM image of MWCNT array grown on the Cu substrate. (d) Photographic image of MWCNT/Cu cathode. (e) Raman spectra of MWCNT after 1 and 21 shoots.

### REFERENCES

- [1] T. Kaplas and Y. Svirko // J. Nanophotonics . – 2012. – Volume 6. – 061703.
- [2] A. V. Okotrub, L. G. Bulusheva, A. G. Kudashov, V. V. Belavin, and S. V. Komogortsev // Nanotechnol. Russ. – 2008. – Volume 3. – 191.

<sup>1</sup> This work was supported by the Finnish Technology and Innovation Agency (TEKES) and the EU FP7 projects CACOMEL FP7-247007

## INTERACTION OF NANOPARTICLES AND POLYMER DISPERCED LIQUID CRYSTALS

*N.A. ROMANOV<sup>1</sup>, A.V. NOMOEV<sup>1</sup>*

<sup>1</sup> *Laboratory of physics of nanosystems of BSU, Smolina st., 24a, Ulan-Ude, 670000, Russia*

*[Nromanov@mail.ru](mailto:Nromanov@mail.ru), 89676212383*

Now in the research centers intensive researches on development of flexible screens and creation of displays, microdisplay equipment, modulators, etc. on the basis of the liquid crystals (LC) encapsulated in polymer with use of flexible basic surfaces are conducted. The Polymer dispersed liquid crystals (PDLC) are the composite film materials containing drops of spontaneously focused anisotropic liquid crystals. Under the influence of electric field the anisotropic LC containing in PDLC, change the orientation that leads to change of their optical properties. Along with positive properties in comparison with the pure liquid crystals, the displays which were applied in traditional LC, PDLC are characterized by the raised level of the operating field necessary for reorientation of molecules of LC in drops, and change of time of a response of LC on an electric impulse. Therefore researches on decrease in an operating field and improvement of dynamic characteristics of PDLC are important PDLC for practical use in future technologies. Development of new liquid crystals and polymeric matrixes with the improved characteristics - difficult and long process therefore search of the new approaches consisting in development of composite materials on the basis of commercially available liquid crystals and polymeric matrixes is conducted.

We considered a special case of introduction in PDLC of particles of silver plated by silicon (Si (Ag)). It had noticeable impact on a critical field of reorientation of molecules of liquid crystals and response times. For the samples containing particles of Ag, time of a response of inclusion of 260 microsec (mcs), and relaxation time 16 millisecond (ms). In the samples containing particles of Si (Ag), these times are respectively equal 80mcs and 25mcs.

Also experiments with Ta-Si particles were made. [1] In case of NLC addition Ti nanoparticles with concentration from 0,1 Mas. % to 1.0 Mas. the % with sizes of 100 nanometers, this time decreases twice from 15 ms to 7.5 ms. Authors of this work offer two mechanisms of interaction of nanoparticles of the titan with NLC molecules. The first mechanism is explained by lack of electric field in a carrying-out metal particle and as a result increase in density of electric field round it that does NLC molecules by faster. The second mechanism is based on suppression of effect of an shielding of the electric field arising owing to availability of ionized impurity in NLC. Adsorption round nanoparticles of the titan in lack of electric field leads to their neutralization that gives reduction of time of an optical response. [2] ]

In our work the addition of NLC occurs yanus-like nanoparticles therefore to two mechanisms the third is added. Its essence consists in the following. Janus particles the liofilnost therefore they are attached is inherent (are adsorbed) by only one party to NLC molecule. As the nanoparticle on the to the sizes much more the cross size of a molecule of NLC and intermolecular distance, from the opposite side of a molecule of an attachment doesn't occur. Molecules to a nanoparticle are generally attached through some layers of molecules only to one party of a nanoparticle. As a result of action of electric field there is the additional rotating moment of force caused by existence of the dipolar moment at a yanus-like nanoparticle, bringing to faster turn of molecules, both attached to it, and being close. This described mechanism leads to reduction of time of an optical response and it is obvious, to reduction of tension of operation. The experimental fact of increase in time of a relaxation with 16 to 25 ms at a addition particles of Ag/Si confirms existence of the offered mechanism: more inertial particles with the attached molecules after switching off of electric field more slowly pass in an initial state.

Introduction in structure of polymeric and liquid crystal composition of small-sized metal or carbon particles is one of the most perspective ways of change of properties of a composite. The entered particles influence physical properties of LC thanks to their interaction at molecular level. In particular, dielectric anisotropy of LC that provides achievement of the highest density of electric energy when giving an operating field increases.

### REFERENCES

- [1] *A. Romanov [etc.]//Mechanism of formation of yanus-like nanoparticles TaSi2@Si. N Young scientist. - 2012 . No. 8. — P. 9-11.*  
 [2] *Yong-Seok Ha, Hyung-Jun Kim, Hong-Gyu Park, and Dae-Shik Seo // Enhancement of electro-optic properties in liquid crystal devices via titanium nanoparticle doping / "Homeotropic alignment of liquid crystals on a nano-patterned polyimide surface using nanoimprint lithography," Soft Matter. – 2011. №7(12), P. 5610–5614.*



## MICROWAVE PLASMA ETCHING OF CARBON NANOTUBE ARRAYS

*D.V. GORODETSKIY, O.V. POLYAKOV, M.A. KANYGIN, L.G. BULUSHEVA, A.V. OKOTRUB*  
*Nikolaev Institute of Inorganic Chemistry SB RAS, 3, Acad. Lavrentiev Ave., Novosibirsk, 630090, Russia*  
*gordim2005@yandex.ru, 8(923)113-01-97*

The unique properties of carbon nanotubes (CNTs) make them applicable with respect to all the major nanotechnologies. However, there are many problems of using CNTs in devices. The treatment of individual tubes represents one of the main difficulties preventing the use of CNTs in many applications. Therefore, there is a strong need to develop a novel technique in order to preset different target properties of nanotubes after the growth via modifying thereof.

The arrays of vertically aligned CNTs were obtained in a flow-through gas-phase chemical reactor, in the course the thermal decomposition a reaction mixture at the surface of silicon substrates. For the experiment, the furnace was heated to a temperature of 800°C. The reaction mixture that represented a 2% ferrocene ( $\text{Fe}(\text{C}_5\text{H}_5)_2$ ) solution in toluene ( $\text{C}_6\text{H}_5\text{CH}_3$ ) was fed into the zone of synthesis in the form of an aerosol.

The CNT arrays on Si substrate were treated by means of a microwave hydrogen plasma discharge with an operating frequency of 2.45 GHz and a maximum input microwave power equal to 5 kW. The samples obtained were examined with the use of scanning electron microscopy, transmission electron microscopy and Raman spectroscopy. A correlation between the etching rate and the power of microwave discharge was revealed. It has been found, that the plasma power equal to 600 W results in the destruction of outer layers of the CNT array under investigation, whereas the plasma treatment at a higher power (about 4500W) additionally leads to opening the tips of the tubes. The field emission (FE) properties of these modified structures were measured. As a result, the FE threshold of plasma-treated samples is better as compared to initial CNT arrays.

## SYMMETRIC GRADIENT THEORY OF MICROSTRUCTURE-DEPENDENT BEAMS<sup>1</sup>

*S.A. LURIE \**

*\*Institute of Applied Mechanics, Russian Academy of Sciences, Moscow 125040, Leningradskii pr.7, building 1, Russia  
and  
Institute for Problems in Mechanics RAS, Moscow, 119526, Pr. Vernadskogo, 101-1, Russia*

We will show first that without loss of generality, the large number of independent material coefficients of strain gradient elasticity may be reduced considerably by using an additional, order-of-differentiation symmetry condition. We demonstrate that in strain gradient elasticity, this symmetry condition is essential both for avoiding the appearance of energetically insignificant material coefficients and also for the validity of free variation formulations commonly employed when deriving the field equations of strain gradient elasticity. Based on this symmetry condition, we derive the minimal symmetry admissible theory of isotropic strain gradient elasticity with a total of only four independent material coefficients. The generalized continuum model with adhesion interaction is also introduced. The strain gradient's framework and Lagrange's variational formalism are used for a natural incorporation of the adhesion terms which makes it particularly useful for studying the size dependent elastic responses of composite media and structured materials, in particular those with the submicron and nanoscale microstructures. The adhesion theory, which generalizes the continuum adhesion model of Young-Laplace media, is used where in general case, four physical parameters are defined [1-3].

We elaborate the microstructure-dependent theory of beams that can be very interesting and stimulating for both theoretical and engineering applications. We use accurate qualitative analysis and show that a non-classical theory of beams can be constructed by using a simple completely symmetric gradient theory, which in principle provides the same order of solutions where in the equilibrium equations and boundary conditions, the stress components with additional order of smallness are exhibited. This leads to asymptotically consistent model of non-classical theory of microstructure-dependent beams. At the same time, we only use the kinematic relations based on the Timoshenko's theory and no additional assumptions are used except the correctness requirements associated with the fundamental principle of symmetry. Thus, it is proven that in this case, consistent variational formulation leads to a refined theory of microstructure-dependent beams, which are different from the other theories developed in the works of Ma H.M. (2008), Gao X.L (2010), and Reddy J.N. (2011).

The new proposed model contains one material length scale parameter and in general case, two additional length scale parameters linked to the surface energy. Unlike the classical Timoshenko beam's theory, this model able to capture the size effect when both bending and axial deformations are considered. It is shown that by using the correct models that satisfy the symmetry principle, one can make a substantial correction to simulate the results of deformations for very thin beam structures. Similar trends are observed for the free vibration problem, where it is shown that the natural frequency predicted by the new model is higher than that by the classical model, with the difference between them being significantly large only for very thin beams. However, this effect is only associated with scale parameter related to surface properties and not with length scale effect. It is worthy to note that this new beam's theory gives results that are remarkably consistent with the available experimental data for all frequency range with appropriate choice of parameters.

### REFERENCES

- [1] S. Lurie, D. Volkov-Bogorodsky, V. Zubov, N. Tuchkova// *Comp. Mater. Sc.* 2009, 10(1), 709-714
- [2] P. Belov, S.Lurie, // *J. of Composite Materials and Structures*, 2007, 14(3), 519-536
- [3] S. Lurie, N. Tuchkova// *Composites and nanostructures*, 2009, 2(2), c. 25-43.

<sup>1</sup> This work was supported by a grants RFBR 12-01-00273 and 13-01-00872.

## SYNTHESIS OF SILICA NANOWIRES FROM FREE JET ACTIVATED BY ELECTRON BEAM PLASMA<sup>1</sup>

*S.YA. KHMEL\**

\* *Institute of Thermophysics SB RAS, Lavrentiev ave., 1, Novosibirsk, 630090, Russia, khmel@itp.nsc.ru, +7(383) 335 66 76*

Silica nanowires were synthesized from mixture monosilane with hydrogen by gas-jet electron beam plasma CVD method for the first time. The synthesis was carried out on silicon substrate with micrometer-sized particles of Sn catalyst. Oriented arrays of silica nanowires bunches (“microropes”) were synthesized in the area corresponding of the mixture jet axis [1]. Every particle of catalyst produces bunch (“micropipe”) of silica nanowires with diameter about 15 nm. It seems that the synthesis proceeds by the vapor–liquid–solid mechanism, and several nanowires grow synchronously from the surface of one catalyst particle. These silica nanowires were produced with growth rate about 25 nm/s and at low temperature about 330 °C which are compatible with low-cost substrates.

Fig. 1 shows low-magnification SEM image of high-density oriented arrays of silica nanowire bunches (“microropes”) which were synthesized in the area corresponding of the mixture jet axis. The bar in Fig. 1 indicates less than 1.5 microns catalyst particles from which bunches (“microropes”) of nanowires originate. Also SEM observations show that diameter of these bunches is proportionate to catalyst particles size.

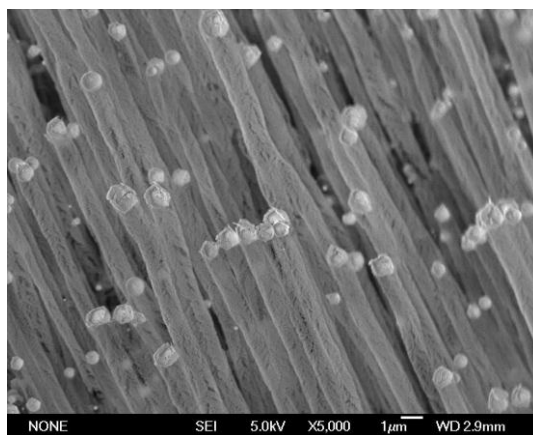


Fig. 1. SEM image of high-density oriented arrays of silica nanowires bunches (“microropes”) in the area corresponding to the mixture jet axis

SEM observations show that this method provides different morphology of the nanowires and catalyst. Oriented arrays of silica nanowires bunches (“microropes”) were synthesized in the area corresponding to the mixture jet axis. Cocoons-like, bamboo-like, and jellyfish-like morphology was observed in the area corresponding to periphery of the jet [2].

Possible growth model has been suggested in order to explain the results. Probably there was realized vapor-liquid-solid (VLS) growth mechanism, the catalyst-on-bottom (COB) mode, where multiple nanowires grow simultaneously from the surface of one catalyst drop. Nonuniform heating of the catalyst particles due to directed plasma flow leads to the preferential growth of nanowires on one side of the particles. So we have self-organizing bottom–up process of synthesis of oriented arrays of silica nanowire “microropes” at enough low temperature and high growth rate

### REFERENCES

- [1] E. A. Baranov, A. O. Zamchiy, and S. Ya. Khmel // *Technical Physics Letters*. – 2013. – V.39. – №.11. P.1023–1025.
- [2] A. Zamchiy, E. Baranov, S. Khmel // *Physica Status Solidi C*. – 2014. – in press.

<sup>1</sup> This work was supported by the Russian Foundation for Basic Research (grant no. 11-08-00740-a)

## UNIVERSAL VACUUM SETUP FOR RF-MAGNETRON DEPOSITION OF BIOACTIVE COATINGS: COMPONENTS AND FACILITIES<sup>1</sup>

*Y.U.P. SHARKEEV\**, *K.S. KULYASHOVA\**, *A.G. RAU\*\**, *YU.A. GLUSHKO\**, *V.YA. ROMANOV\*\**, *K.G. SALIMI\*\*\**

\* *Institute of Strength Physics and Materials Science (ISPMS SB RAS), pr. Akademicheskii, 2/4, Tomsk, Russia, root@ispms.tomsk.ru, 634021*

\*\* *TETA Ltd., st. Sovetskaya, 1/2, Tomsk, Loskutovo, Russia, rau@tetacom.ru, 634526*

\*\*\* *BMTechnology, 2-nd Kotlyakovskii per., 18, of. 224, Moscow, Russia, salami@bmte.ru, 115201*

RF-magnetron sputtering is one of the modern technologies that make possible to put thin calcium phosphate coatings on the surface of varied materials, including dielectric materials, such as ceramic. This method is used to form the nanostructured biocompatible calcium phosphate coatings in ISPMS of SB RAS. RF-magnetron sputtering setup (fig. 1) has been designed for forming the multicomponent, multilayered, and gradient biocoatings on the surface of ceramics and bioinert metals. It is equipped with varied options for clearing, activation, and passivation of surfaces by gas ion flows and for ionic mixing of the layer deposited with the substrate. The setup has been used to implement technologies of deposition of functional biocoatings of medical application on products shaped as revolution bodies, polyhedrons, and planes. It was completely automated, except for loading-unloading of specimens being treated. It was equipped with systems of protection against abnormal situations. The setup has adjustable software for implementation of different technological processes.



Fig. 1. Universal vacuum setup for RF-magnetron deposition of bioactive coatings on ceramic and bioinert metals.

The setup consists of the following main units. 1. Vacuum chamber with pure oil-free pumping (turbo molecular high-vacuum pump and spiral vacuum pump). It has the lower button arrangement of magnetrons and ion sources. 2. Two RF-magnetron plasma sources. 3. Ion gas source for surface clearing, activation and passivation. 4. Manipulator with the option of constant and periodic rotation of specimens in the treatment zone and their displacement from one treatment zone to another. 5. Ion implanter for ion mixing of coating with substrate. 6. System of gas supply and control. 7. Racks for pumps, automatics cooling and heating systems. 8. Rack with power supply sources for RF-magnetrons and ion sources. All working regimes are controlled with PC.

The structure of the RF-magnetron coatings put on different substrates and their physical, chemical and mechanical properties are discussed. It was found that the RF-magnetron calcium phosphate coatings have good biocompatibility. They are nontoxic and they enhance the proliferation process.

<sup>1</sup> This work was partially supported by the Russian program of fundamental research SB RAS (program III.23.2, project “Scientific foundations of forming composite materials and coatings with functionalized structure for biomedical applications”) and Russian state contract (Project No. 11411.1008700.13.002)

## BIOACTIVE CALCIUM PHOSPHATE COATINGS DEPOSITED BY RF-MAGNETRON METHOD: STRUCTURE AND PROPERTIES<sup>1</sup>

*K.S. KULYASHOVA\**, *YU.P. SHARKEEV\**, *A.A. MAMAEVA\*\**, *A.V. PANICHKIN\*\**, *R.K. AUBAKIROVA\*\**, *YU.A. GLUSHKO\**,  
*A.B. SAINOVA\**

\* *Institute of Strength Physics and Materials Science (ISPMS SB RAS), pr. Akademicheskii, 2/4, Tomsk, Russia,*  
*kseniya@ispms.tomsk.ru, 634021*

\*\**Center of Earth Sciences, Metallurgy and Ore Beneficiation, JSC, Shevchenko st., 29/133, Almaty, Republic of Kazakhstan, 050010*

Today many research groups give their attention to development of calcium phosphates coatings based on hydroxyapatite. The hydroxyapatite has attracted considerable attention because of its close resemblance to the chemical and mineral components of teeth and bones. As a result of this similarity hydroxyapatite has shown good biocompatibility with bone tissue. Different methods of coatings deposition are known as micro-arc oxidation, sol-gel method, plasma spraying et.al. Radio-frequency (RF) magnetron sputtering is one of the modern technologies that make possible to put thin calcium phosphate coatings on the surface of varied materials, including dielectric materials, such as ceramic. This method is used to form the nanostructured biocompatible calcium phosphate coatings in ISPMS of SB RAS.

Thin calcium phosphate coatings were prepared by RF-magnetron deposition on titanium substrates (VT1-0) at 100, 150, 200 and 250 W. The phase composition, surface morphology, structure, adhesive bond strengths and microhardness of calcium phosphate coatings and composite material “coating - titanium” were investigated by X-ray diffraction, scanning electron microscopy, infrared spectroscopy, mechanical scratch-test and microhardness test. Structure of coatings was studied before and after isothermal annealing at 700°C. The coating structure depends on the power of RF-discharge. Molecular bonds typical for hydroxyapatite are formed for annealed coatings. It was experimentally established that increasing of power of RF-discharge up to 250W provided a denser and thicker coating and promoted the formation of amorphous phase in the higher concentration that is greater than 20%. In this case the long-time strength of the coatings is determined by the ratio of the amorphous and crystalline phases. The adhesive bond strength of a calcium phosphate coating was achieved up to 100 MPa (the load on indenter up to 18.3 N). Experimentally established that the increase of the RF-discharge power leads to increasing of microhardness value from 2350 to 3200 MPa. Microhardness measurement also was carried out according to [1]. This technique allows to determine values of microhardness and to estimate contribution of calcium phosphate coatings to integral microhardness of composite material “coating - titanium”. Load on indenter was changed from 0.2 to 2.0 N. The indentation depth ( $h_k$ ) was determined experimentally. Microhardness of coatings was calculated according to

$$H_f = H_s + \frac{h(H_k - H_s)}{C \cdot t}, \quad (1)$$

where  $H_f$  is a microhardness of coating;  $H_k$  is a microhardness of composite “coating - titanium”;  $H_s$  is a microhardness of substrate;  $C$  is inversely value of  $t/h_k$ ,  $t$  is thickness of coating and it is equal to 0.8  $\mu\text{m}$ . Values of microhardness were determined as following.  $H_f$  is 2900 MPa,  $H_k$  is 3200 MPa,  $H_s$  is 1780 MPa.

### REFERENCES

- [1] *Manika I.P., Maniks Ya. E., Muktepavel F.O.* // The determination of microhardness of thin films and coatings. – Institute of physics of Academy Science of Latvian SSR, 1990.

<sup>1</sup> This work was partially supported by the Russian program of fundamental research SB RAS (program III.23.2, project “Scientific foundations of forming composite materials and coatings with functionalized structure for biomedical applications”).

## MODIFICATION OF CERAMICS B4C BY HIGH INTENSITY ELECTRON BEAM

*M.S. PETUKEVICH* \*, *M.P. KALASHNIKOV* \*, *Y.F. IVANOV* \*, \*\*, *A.D. TERESOV*, *O.L. KHASANOV*

\*National Research Tomsk Polytechnic University, Lenin Avenue, 30, Tomsk, 634050, Russia,

E-mail: petukevich@tpu.ru, phone: 8- (3822) 701777 -1 доб. 2263

\*\*Institute of High-Current Electronics of the Siberian Branch of the Russian Academy of Sciences, 2/3 Akademicheskoy Avenue, Tomsk, 634055, Russia

The boron carbide B<sub>4</sub>C (B<sub>13</sub>C<sub>2</sub>) is one of the most chemically resistant and solid substances. In this regard, its scope is vast; powder of boron carbide is used for manufacturing chemical glassware, abrasives and grinding materials, protective plates for bulletproof vests, etc. With high hardness (is second only after diamond and boron carbonitride CBN), boron carbide products are very difficult to grinding and polishing. One highly effective way of smoothing the surface of refractory materials is melting it by high intensity impulsed electron beam.

The aim of this work - identification and analysis of patterns of structural phase transitions occurring in the surface layer of ceramics based on boron carbide, melted by high intensity impulsed electron beam. The Sintering of Boron carbide powder was performed by method of spark plasma sintering (SPS). High-intensity electron beam irradiation was carried out on the "Solo". The disquisition of the starting powder of boron carbide, sintered ceramics in the initial state and the state after the electron beam irradiation was made by scanning and transmission electron microscopy. Was established that the powder in the initial state is nanoscale materials, single crystallites of which ranging between 20 nm to 40 nm (Figure 1a). There are dense ceramics with high strength of the grain boundaries was formed at optimum mode of sintering. The grain size are within a 10 microns, the pore size ~ 1 mm (Fig. 1b). The irradiation of ceramics by pulsed electron beam ((20 ... 40) J/cm<sup>2</sup>, 200 ms; 3 imp.) Is accompanied by melting of the surface layer thickness ~10 microns. The fracture of melted layer is non-porous and transcrySTALLINE, that says about high level of strength crystallite boundaries (Figure 1c). The melted layer is broken into fragments cracks sizes (40 ... 60) microns. In volume of fragments revealed a polycrystalline structure with a crystallite size ranging from 1 nm to 5 nm (Fig. 1d). In volume of fragments was revealed a polycrystalline structure with a crystallite size ranging from 1 nm to 5 nm (Fig. 1d). The crystallites are separated by thin (within 50 nm) layers of the second phase, which allows surely analyze their size and shape.

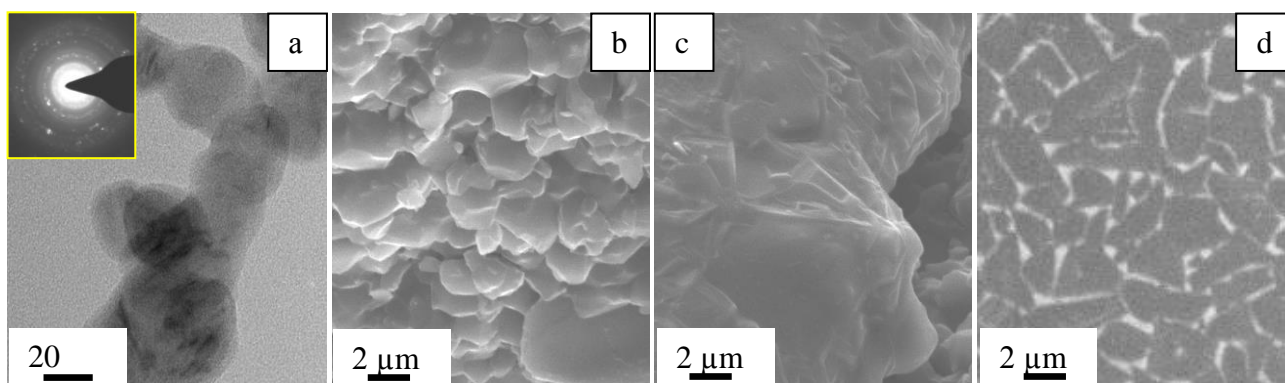


Fig. 1. Electron microscopic images of the original structure of boron carbide powder (a), the fracture surface of the sintered ceramics (b) and ceramics, electron beam irradiation (c), d - ceramic surface after irradiation with an electron beam, and - transmission electron microscopy, and b-r - Scanning electron microscopy.

Thus, irradiation of ceramics by pulsed electron beam in melting mode of the surface layer is accompanied by smoothing the surface layer and forming the structure with a non-porous high strength crystallite boundaries.

## USE COPPER CENTRAL ELECTRODE IN THE COAXIAL ACCELERATOR FOR IN CHARGE Ti-N-CU

A.A.SIVKOV, D.YU.GERASIMOV, A.A.EVDOKIMOV, A.I.USIKOV

National Research Tomsk Polytechnic University, Lenin ave 30, Tomsk, Russia, [kraamis@gmail.com](mailto:kraamis@gmail.com), 8-905-992-51-76

Technological progress poses materials science tasks of creating new materials with unique properties. These properties can have a ceramic obtained by pressing and sintering a super hard material powder of nanocrystalline structure [1]. For synthesis of material using coaxial magnetoplasma accelerator [2-5].

The introduction of copper in the composition of the charge occurs due to spark operated with material of the central electrode (CE) of the accelerator, which is made of copper.

By the first experiment, the central electrode was used with a flat end portion, and by the second experiment the end portion CE is formed as a cone. The solution provides more than 30 % increase in the specific surface erosion CE and operated copper. Thus, the use of CE with the end portion formed in a cone shape is more efficient in terms of using the energy supplied to the accelerator operated for electroerosion copper. It should be noted that the change in the geometry of CE has almost no effect on the amount of erosion wear electrode barrel  $\Delta m$ .

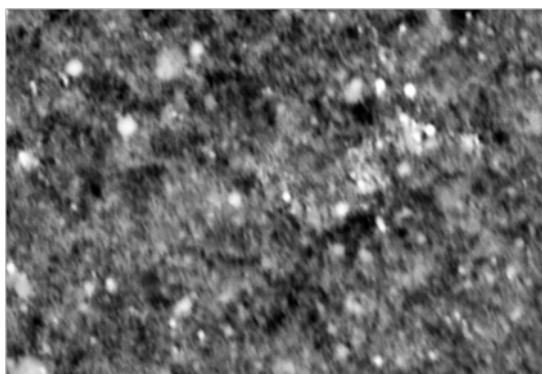


Fig. 1 - SEM-picture UDP-fraction composite product plasmodynamic synthesis of TiN-Cu

To determine the qualitative characteristics, dynamic synthesis product was subjected to analytical studies such as x-ray diffraction and scanning electron microscopy. Quantitative structure-phase analysis of the diffraction patterns was performed using full-profile analysis program Powder Cell 2.4 base and structural data PDF4+. Contents cTiN, cTi<sub>2</sub>CN and Cu was 60%, 30% and 10%, respectively.

XRD analysis showed that the main component of the obtained powder is titanium nitride. Also present in the sample and titanium carbonitride caused carbon impurity from the insulator CE. The fraction of copper present in the test sample in a small amount. In this small proportion of particles sizes up to ~ 500 nm. This demonstrates the bimodal size distribution.

**Conclusion.** In this paper the possibility of using copper KMPU central electrode for batch superhard material based on TiN-Cu. Experimentally shown that the use of a central electrode end portion formed in the shape of a cone is more efficient in terms of using energy supplied to the accelerator for spark operated copper. XRD analysis showed that the synthesis product is a dynamic mixture of nanosized nitride crystalline phases with a titanium carbonitride and a small content of nanosized copper particles. OCD show that the product is nanodispersed.

### REFERENCES

- [1] Akarachkin SA Technology of production of nanoceramics // Proc. Abstracts. The first scientific conference "Current state and prospects of development of technology and the production of ceramics" / NEVZ-Union - Novosibirsk, 2009 p. 250-253.
- [2] A utility model patent number 61856 Russian Federation. Coaxial magnetoplasma accelerator / Gerasimov DY, Saygash AS, AA Sivkov
- [3] Patent number 2442095 Russian Federation. 7F41V 6/00 H05H 11/00. Coaxial magnetoplasma accelerator / Sivkov AA Gerasimov DY, Evdokimov AA, Posted 10.02.2012 Bull. number 4
- [4] Patent number 2459394 RF H05H 5/03 Coaxial magnetoplasma accelerator / Evdokimov AA, Sivkov AA Gerasimov D.YU - Posted 20.08.2012 Bull. number 23
- [5] Sivkov AA Gerasimov DY, AS Tsybina Spark of fissile material in a coaxial magnetoplasma accelerator coating // Electrical Engineering. - 2005. - № 6. - S. 25-33.

## USING BIMETALLIC ELECTRODE COAXIAL ACCELERATOR FOR BATCH SUPERHARD MATERIAL TiN-Cu

A.A.SIVKOV, D.YU.GERASIMOV, A.A.EVDOKIMOV, A.I.USIKOV

National Research Tomsk Polytechnic University, Lenin ave 30, Tomsk, Russia, [kraamis@gmail.com](mailto:kraamis@gmail.com), 8-905-992-51-76

Introduction of certain additives in the ultrafine powder of highly rigid materials such as titanium nitride, for example, copper, is made to improve the physical and mechanical characteristics [1, 2]. Plasmodynamic method based on coaxial magnetoplasma accelerator (CMPA) [3] allows to obtain nanocomposite powder in a single process. This paper presents the results of investigations on the preparation of ultrafine powder compositions TiN-Cu using CMPA [4, 5].

Introduction of copper is achieved by installing a copper cylindrical sleeve at the beginning of the accelerating channel titanium barrel of CMPA using titanium central electrode. Electroerosion wear of surface AC significantly depends on the degree of shielding his trunk wall, which in turn is directly related to the transverse conductivity of the wall. Copper sleeve will increase the degree of screening, ie adversely affect the electroerosion wear. Analysis of the energy parameters of experiments with whole and cut sleeve showed their practical identity. However, reducing the degree of shielding volume AC copper sleeve due to its longitudinal section provided nearly double the spark of use copper. At the same time between titanium practically preserved. Thus, the use of a copper sleeve with longitudinal slits is more efficient in terms of use of electroerosion material.

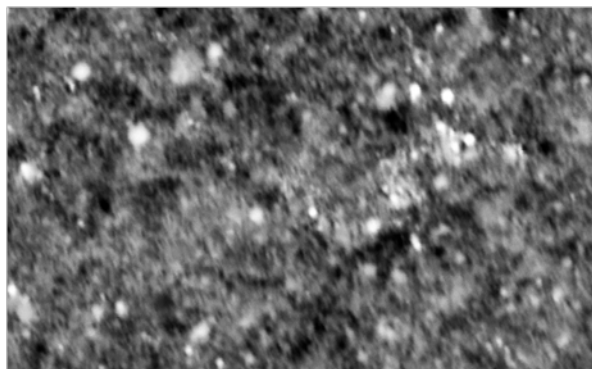


Fig 1. SEM-picture composite product plasmodynamic synthesis of cTiN-Cu.

To determine the qualitative characteristics, dynamic synthesis product was subjected to such analytical studies such as x-ray diffraction and scanning electron microscopy.

Fig. 1 shows a SEM-picture of a powdery product synthesis cTiN-Cu, obtained with a scanning electron microscope Hitachi TM3000. The picture shows the most luminous objects are particles of copper, the largest size is ~300 nm. From this, it can be assumed that the average particle size consistent with the size of the copper coherent scattering region current phase.

**Conclusion.** The possibility of using CMPA with bimetallic electrode - barrel charge for superhard powder material based on TiN-Cu. XRD analysis showed that the product of dynamic synthesis consists of two phases : cTiN and Cu. This method allows to control the ratio of mixture components in a wide range by varying the geometry of the copper sleeve, the interaction of electromagnetic energy and energy of process.

### REFERENCES

- [1] Abadias, G. Nanoscaled composite TiN/Cu multilayer thin films deposited by dual ion beam sputtering: growth and structural characterization / G. Abadias, Y.Y. Tse, A. Michel, C. Jaouen, M. Jaouen // *Thin Solid Films*, Volume 433, Issues 1–2, 2 June 2003, p. 166–173.
- [2] Andreasena, K.P. The structure and the corresponding mechanical properties of magnetron sputtered TiN–Cu nanocomposites / K.P. Andreasena, T. Jensen, J.H. Petersena, J. Chevalliera, J. Böttigera, N. Schellb // *Surface and Coatings Technology*, Volume 182, Issues 2–3, 22 April 2004, p. 268–275.
- [3] Patentr 2150652 Russian Federation. Coaxial accelerator. Sivkov AA 7F41V 6/00. Publ. 10.06.2000. Bull. 16.
- [4] Sivkov A.A., Gerasimov D.Y., Tsybina A.S. Eroding time between material in a coaxial accelerator magnetoplasma coating // *Electrical Engineering*. - 2005. - № 6. - S. 25-33
- [5] Sivkov A.A., Nailty E.P., Gerasimov D.Y. Direct dynamic synthesis of nanosized titanium nitride in high-speed pulsed plasma jet spark // *Superhard materials*. Kiev. - 2008. - № 5. - C. 33-39.



## ON POSSIBILITY OF PLASMADYNAMIC SYNTHESIS OF ULTRADISPERSED CRYSTALLINE PHASES IN SUPERSONIC PLASMA JET FLOWING INTO THE AIR ATMOSPHERE

*I.I. SHANENKOV\*, A. A. SIVKOV\*, A.YA. PAK\*, YU.L. KOLGANOVA\**

\* National Research Tomsk Polytechnic University, Lenina Avenue, 30, 634050, Tomsk, Russia, [Swordi@list.ru](mailto:Swordi@list.ru), ph.: 89069561366

For the last 25 years the synthesis of compounds in the carbon-nitrogen system has been become widely-spread [1]. It is connected with the fact that CN<sub>x</sub> materials with different stoichiometry may exhibit different properties and may be used in various fields of science and technology [2]. However, the introduction of nitrogen into the graphite framework is difficult task and requires high pressure and temperature.

Obtaining of various crystalline phases in the CN system, based on the method of direct plasmodynamic synthesis in the supersonic jet of the carbon electro discharged plasma, was described previously [3]. In addition to yield the desired phase of carbon nitride a lot of unbound carbon is in the synthesis product. So, it was proposed to use air as the gaseous environment to burn the surplus carbon in synthesis stage.

Such a way a series of experiments using ambient air was carried out. During the experiments no destructions in the system were. It is found that by varying the power supplied to the accelerator from the capacitive energy storage it is possible to influence on the synthesis product and increase the yield of carbon nitride phase. In the experiments the value of supplied energy was varied from 40 to 70 kJ.

To investigate the phase composition of obtained samples the X-ray diffractometry (XRD) analysis was carried out. According to calculated data by using both an air atmosphere and increasing of the input energy value the reducing of unbound graphite can be achieved. This fact can be connected with graphite combustion during the experiment.

XRD results are in a good accordance with data of the transmission electron microscopy (TEM). Morphological changes in the composition of the samples are clearly visible on TEM-images. This is also confirmed by electron diffraction images (SAED), which indicate a decrease in reflexes corresponding to the graphite phase.

Differential thermal analysis data confirm the results of XRD and TEM. Samples, synthesized at lower values of the input energy, are characterized by the highest content of unbound carbon. In the sample synthesized at the maximum supplied energy on the DTA curves exhibit two distinct maxima and this powder is characterized by the lowest content of unbound carbon in the graphite form and the highest content of CN<sub>x</sub> and W<sub>2</sub>C phases.

Thus the possibility of the plasmadynamic synthesis of ultradispersed crystalline phases in supersonic plasma jet flowing into the air atmosphere is shown. The phases of graphite, carbon nitride CN<sub>x</sub> and tungsten carbide W<sub>2</sub>C are mainly presented in the final synthesis products. By varying the energy parameters of capacitive energy storage it is possible to influence on the final product composition.

### REFERENCES

- [1] *G. Goglio, D. Foy, G. Demazeau // Materials Science and Engineering. – 2008. – Vol. 58. 195-227.*
- [2] *A. Sivkov, A. Pak, I. Shanenkov, Y. Kolganova, I. Prosvirin // Advanced materials research. – 2014. – Vol. 880. 36-41.*
- [3] *A.A. Sivkov, E.P. Naiden, A.Ya. Pak // Journal of superhard materials. – 2009. – Vol. 31. – №5 . 300-305.*

## COMPOSITE NANOPARTICLES SYNTHESIS

*E.CH. KHARTAEVA<sup>1</sup>, B.B. BALDANOV<sup>2</sup>, B.R. RADNAEV<sup>2</sup>, S.B. BATOROEV<sup>2</sup>*

<sup>1</sup>*Laboratory of radio sounding of natural media of IPMS SB RAS, Sakhyanovoy st. 6, Ulan-Ude, 670047, Russian Federation, [erzhena.har@mail.ru](mailto:erzhena.har@mail.ru), 89140533395*

<sup>2</sup>*Laboratory of physics of nanosystems of BSU, Smolina st., 24a, Ulan-Ude, 670000, Russian Federation*

A fundamentally new way of producing nanopowders has been worked out by the method of evaporation and vapor condensation in the stream of carrier gas [1]. Heating source material is electronic accelerator of continuous action of ELV- 6, developed in INP SB RAS [2]. A feature of the accelerator is a high electron energy (1.4 MeV), and the ability to manufacture the beam into the atmosphere. The electrons move at relativistic speeds, and their mean free path, for example in air, is up to 6 meters, which allows to vaporize materials at atmospheric pressure. The range of beam power varies from 0 to 100 kW (beam current up to 75 mA), the concentration of power reaches 5 MW per 1 cm<sup>2</sup> (when released to the atmosphere), allowing both to evaporate refractory substances under atmospheric conditions, and conduct the synthesis in the high temperature "gas" phase. Benefits are also high efficiency of the process due to the direct conversion of electrical energy into heat energy in the heated material, the heating rate is above 1000 degrees per second, and "chemical purity" of the electron beam. The evaporation of the source solidis made in the reactor, then a vapor is transported from the heating zone, and simultaneously diluted and cooled by the air (or other carrier gas). Further, in the appropriate elements of the installation the condensed and solidified nanoparticles are trapped and collected in powder form. Different types of reactors have been developed, in which the synthesis of nanoparticles was performed in air, argon, nitrogen, helium, xenon. With incomplete use of the accelerator power (less than 50%) the performance for nanopowders of some substances of several kilograms per hour was achieved.

The evaporation of the source solidis made in the reactor. Nanoparticles formed by evaporation are carried away entrained by air stream and pumped through the tubes of the heat exchanger (coalescent) for cooling, where they form agglomerates. In various elements of installation the capture of powder occurs with different average size dof the original particles and its subsequent discharge (from the cyclones and the filter). After a thin mechanical filtration the air does not contain any contaminants and is drawn "into the street". In general, the method used can be attributed to a condensation methods for preparing ultrafine powders of refractory substances. As compared to laser and plasma methods the described method has the advantage as due to penetrating of electrons to the material the energy is generated within the substances.

In producing of nanopowders of different substances there are some peculiarities especially in technology. Let's for example, consider the production of silicon nanopowder. There was a hole with the diameter of 5 mm for gas inlet into the chamber from which the narrow jet of gas was coming out directed onto the surface of the evaporated material in a graphite crucible which was placed inside a special water-cooled steel chamber. This design allowed to remove quickly the steam from the evaporation zone and contributed to mixing and cooling the obtained particles with the carrier gas. Since the penetration depth of the electron beam in silicon is a fraction of a millimeter, only its upper layer was converted into steam. Water-cooling of crucible's walls contributed to the formation of a thin layer of solid silicon, preventing the contact of liquid silicon with the walls. There were two cameras between the hole releasing the accelerator beam and the crucible that prevented the penetration of air into the evaporation zone. This system allows to save the carrier gas and conduct long-term experiments.

In the first experiments, the molten silicon (having a high reactivity) interacted with the walls of the stainless steel to form a molten ferrosilicon (FeSi), that eventually led to the destruction of the installation. Therefore, a graphite crucible was used of a small volume (internal diameter is 35 mm, depth is 50 mm), which was set in a chamber in 50 mm from the outlet of the electron beam. This distance provided a beam with the diameter of 6-7 mm, depending on the used gas (7 mm to argon and 6 mm for the nitrogen).

Thus, as a result of experiments with different materials nanoparticles of different compositions (core-shell, Janus-like, hole) were obtained.

### REFERENCES

- [1] *Bardakhanov S.P., Korchagin A.I., Kuksanov N.K., Lavrukhin A.V., Salimov R.A., Fadeev S.N., Cherepkov V.V.*// Producing of nanopowders by evaporating of the starting materials in the electron accelerator at atmospheric pressure. ASR.2006.T.409, № 3. Pp.320-323.  
 [2] *Akhiezer A.I., Berestetskii V.B.*// Quantum electrodynamics. 3rd ed.M., 1969.P 624.

# BORON CARBIDE NANOPOWDER SYNTHESIZED USING ELECTRODISCHARGED PLASMA

I.A. RAKHMATULLIN, A.A. SIVKOV, A.F. MAKAROVA

Tomsk polytechnic university, Lenin st. 30, Tomsk, Russia, 634000, [riam@tpu.ru](mailto:riam@tpu.ru), +79539220212

Coaxial magnetoplasma accelerator with graphitic electrodes generates short time ( $\leq 1$  ms) high current ( $\leq 150$  kA) electrodischarged plasma with supersonic speed (up to 8 km/s in vacuum) [1]. Placing a powder mixture of amorphous boron and carbon black at a ratio 4:1 into the electrodischarged gap allows to produce boron carbide nanopowder in the argon atmosphere.

Obtained grey powder product was researched by using XRD, HRTEM, TEM and SEM.

Using Spark Plasma Sintering (SPS) machine synthesized powder was used to produce ceramic. Density, hardness and crack resistance were measured for sintered ceramic. Measured results showed the hardness close to monocrystal and increasing of crack resistance up to  $7.0 \text{ MPa/m}^{1/2}$  that is higher than for ceramic sintered at the same conditions using powder with nanosized additives [2].

XRD pattern of synthesized product is shown at fig. 1. As it seen the product mostly consist of boron carbide with silicon carbide, boron oxide and graphite as impurities.

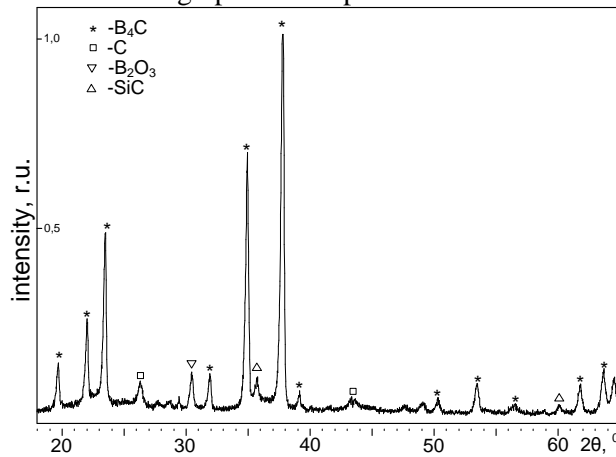


Fig. 1. Synthesized product XRD pattern

XRD pattern of sintered ceramic at fig. 2 shows that free carbon and boron oxide reacts until sintering with formation of boron carbide. As it could be seen small amount of free carbon still exist in bulk sample.

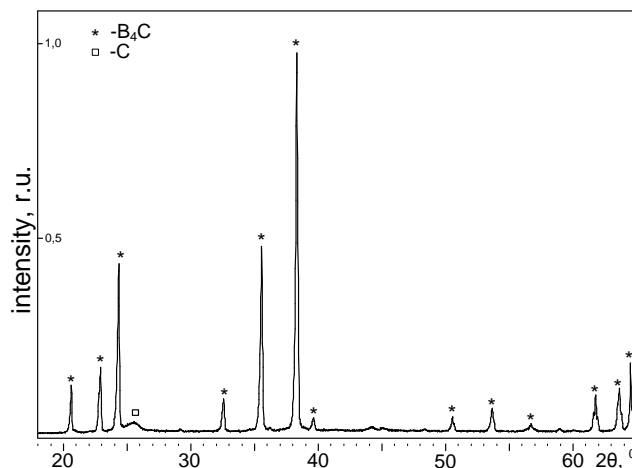


Fig. 2. Sintered ceramic XRD pattern

## REFERENCES

- [1] Patent RF # 2431947 H05H 11/00 F41B 6/00, published 20.10.2011.
- [2] Oleg L. Khasanov et al.//Advanced Materials Research. – 2013. – vol. 872. – pp. 45-51.

## REORIENTATION OF SINGLE $F_2$ -CENTERS IN LiF CRYSTAL

*S.V. BOICHENKO\**, *K. KÖNIG\**, *S.A. ZILOV\*\**, *V.P. DRESVYANSKIY\**,

*A.L. RAKEVICH\**, *A.V. KUZNETSOV\**, *A.V. BARTUL\**, *E.F. MARTYNOVICH\*\**

\*Irkutsk Filial of Institute of Laser Physics SB RAS, 130 a Lermontov st, Irkutsk, 664033, Russia, E-mail: filial@ilph.irk.ru

\*\*Institute of Applied Physics, Irkutsk State University, 20 Gagarin Blvd., Irkutsk 664003, Russia

Experiments on registration of fluorescence of single  $F_2$ -centers in LiF were carried out with laser fluorescent confocal microscope PicoQuant MicroTime 200. Picosecond semiconductor laser with wavelength 470 nm was used for excitation of color centers. Repetition rate of laser pulses was 5 and 10 MHz, duration of a pulse was about 60 ps, polarization was linear. Laser beam was directed normally on surface of the crystal (100). Vector of polarization was set in the two directions: along the axis [100] (orientation "0°"), or the axis [110] (orientation "45°"). The sample was a colored LiF crystal with spatial gradient of concentration of color centers. The area of the sample with low enough concentration was chosen to observe single centers.

Typical dependencies of fluorescence intensity on time for "0°" and "45°" orientations of the sample are shown at fig. 1.

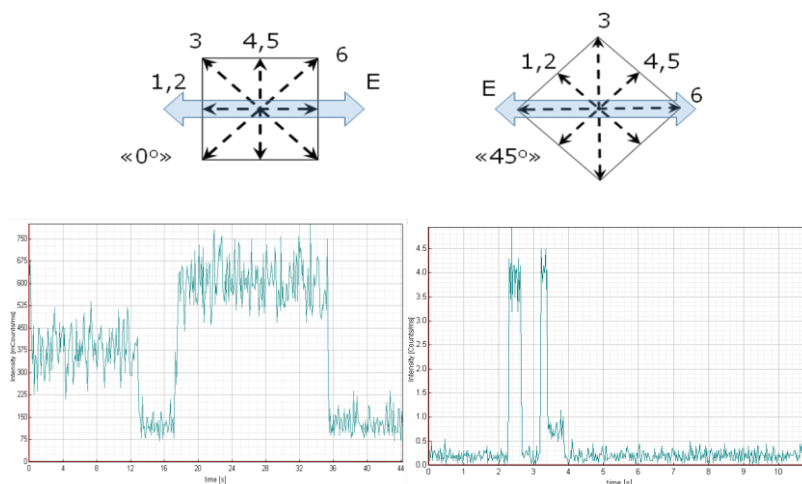


Fig. 1. Projections of linear oscillators on (100)-plane with different orientations of  $F_2$ -center (at the top). Typical dependencies of fluorescence intensity on time for "0°" and "45°" orientations of the sample (at the bottom).

$F_2$ -center is a pair of anion vacancies with trapped electrons in crystal lattice of LiF. Vacancies are placed along  $C_2$ -axis. Absorption (at 470 nm) and fluorescence (at 670 nm) of  $F_2$ -center are described by linear oscillator with orientation along one of the six possible  $C_2$ -axis. It is possible to calculate the ratio of intensities of fluorescence for different orientations of  $F_2$ -center for the cases of "0°" and "45°" orientations of the sample: for "0°"-orientation the ratio is  $I_{1,2}: I_{3,6}: I_{4,5}=1:2:0$  and for "45°" -orientation the ratio is  $I_6: I_{1,2,4,5}: I_3=8:1:0$ . This theoretical result is in good agreement with experiment.

This work was supported by Russian Foundation for Basic Research.

## ON THE POSSIBILITY OF DIRECT DYNAMIC SYNTHESIS OF NANODISPERSED CuO

*A.S.SAIGASH\**, A.A. SIVKOV, A.S. IVSHUTENKO

Tomsk Polytechnic University, 30, Lenin av., Tomsk, 634050, Russia, E-mail: [S\\_nast@mail.ru](mailto:S_nast@mail.ru) Phone: +8(3822) 56-36-82

The paper shows the possibility of direct dynamic synthesis of ultrafine copper oxide phases in hypervelocity jet electro plasma. Jet pulse is generated high-current coaxial magnetoplasma accelerator [1, 2]. The center electrode was made of copper accelerator rod and electrode shaft made from copper tubing. The chamber was filled technically pure nitrogen at atmospheric pressure. Selection of the resulting powdery product was conducted through several hours after deposition on the weighted fractions of the chamber wall at room temperature. Analytical studies of the resulting product made using: X-ray diffraction diffractometer Shimadzu XRD7000S ( $\text{CuK}_\alpha$ -radiation); scanning electron microscopy on a microscope Hitachi TM3000, transmission electron microscopy on a microscope Philips SM 30 and Philips SM12.

X-ray structural analysis of the phase composition (fig. 1), carried out using the full-profile analysis PowderCell 2.4 and structural data base PDF4+, showed that the main crystalline phase of the product (85%) is a copper oxide CuO with space group  $F4/m-3\ 2/m$  with a low content Cu<sub>2</sub>O (3.5%) and a copper Cu (8%). Using SEM revealed that the powder agglomerates is up to 40 microns in size. The agglomerates are composed of a plurality of nanoscale particles. With TEM, revealed that the average particle size of from 80 to 150 nm.

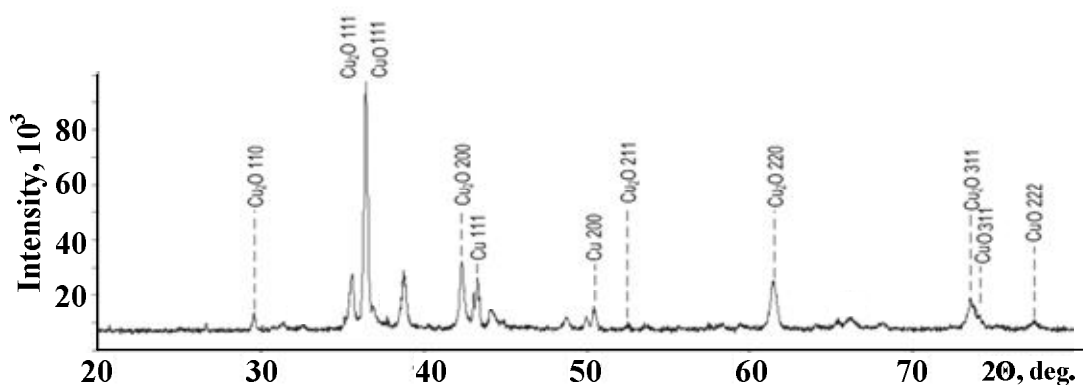


Fig. 1. XRD-spectrum of the powder

### REFERENCES

- [1] A.A. Sivkov, A. S. Saigash, Kolganova, Yu.L. Patent № 137433 RU, 2014
- [2] A.A. Sivkov, A. S. Saigash, A.Yu. Pak. A.A. Evdokimov // Nanotechnic -2009. - № 2(18), p. 38-44).

<sup>1</sup> This work was supported by RFBR, research project No. 14-08-31122 мол. а.”

## SPECTRAL CHARACTERISTICS OF THE NANOPHOSPHORS, RECEIVED ON THE BASIS OF $\text{Sr}_2\text{Gd}_8(\text{SiO}_4)_6\text{O}_2$ : EU POLYCRYSTALS<sup>1</sup>

*SOKOVNIN S.YU.<sup>2,3</sup>, ZUEV M.G.<sup>1,3</sup>, IL'VES V.G.<sup>2</sup>, BAKLANOVA I.V.<sup>1</sup>*

<sup>1</sup>*Institute of Solid State Chemistry, Ural Branch of Russian Academy of Sciences, Ekaterinburg, Russia*

<sup>2</sup>*Institute of Electrophysics, Ural Branch of Russian Academy of Sciences, Ekaterinburg, Russia sokovnin@iep.uran.ru*

<sup>3</sup>*Ural Federal University, Ekaterinburg, Russia*

By the method of evaporation by the pulse electron beam were received amorphous nanopowders (NP) on the basis of polycrystalline phosphors  $\text{Sr}_2\text{Gd}_8(\text{SiO}_4)_6\text{O}_2$ : Eu. NP were received by evaporation of ceramic targets with structure oxyapatites on air on the NANOBIM-2 installation. Voltage – 40 kV, frequency – 100 Hz, beam current – 0,5 – 0,6 A. Experiment time – 60 min. NP from the target of structure  $\text{Sr}_2\text{Gd}_{6.4}\text{Eu}_{1.6}\text{Si}_6\text{O}_{26.8}$  were on glass sedimented. Powders had white color. The assessment of the average size NP particles gives size ~ 5 nanometers. As a result of roasting at high temperatures NP crystallize in structure oxyapatites. Raman range of NP shows structure formation which has a little difference from the initial microsample. The lines arrangement in the NP range speaks of presence at it generally isolated  $\text{SiO}_4$  groups. At the same time emergence in the range of frequencies in the field of 600 – 700  $\text{cm}^{-1}$  attests to the fact that it is forming an insignificant concentration polymerized silicon - oxygen fragments.

The  $\text{Eu}^{3+}$  photoluminescence spectra of the samples in the polycrystalline and nanodimensional states were recorded. Two lines for transition  $^5\text{D}_0 \rightarrow ^7\text{F}_0$  indicate formation of two types optical centers created by  $\text{Eu}^{3+}$ . Essential distinction of data micro and nanophosphors consists in sharp strengthening of intensity transitions  $^5\text{D}_0 \rightarrow ^7\text{F}_2$  for NP (in ~ 10 times). It is caused, apparently, by reduction the nonradiatives losses of energy excitement due to weakening of electronic-vibration interaction ions  $\text{Eu}^{3+}$  with the immediate oxygen environment.

## CARBIDE NANOPARTICLES FORMATION IN THE SURFACE LAYERS OF METALS BY HIGH-INTENSE PULSED ION BEAMS

*V.I. SHYMANSKI\*, G.E. REMNEV\*\*, S.K. PAVLOV\*\*, V.V. UGLOV\**

*\* Belarusian State University, Minsk, Belarus, e-mail: [shymanskiv@mail.ru](mailto:shymanskiv@mail.ru), [uglov@bsu.by](mailto:uglov@bsu.by) 220030, Nezavisimosty ave., 4*

*\*\* High-Voltage Research Institute at of National Tomsk Polytechnic University, e-mail: [remnev@hyd.tpu.ru](mailto:remnev@hyd.tpu.ru), 2a Lenin Ave., Tomsk, 634028, Russia*

The synthesis of heterostructures presenting small particles embedded in a metal matrix is a new approach in the materials modification area. Formation of the particles with the crystal lattice differed from the matrix one is more affective way for producing a dispersed hardened layered in materials. Moreover such structures can posses the improved radiation stability. In the case of the metals with hexagonal (Ti) or body-centered (W) crystal lattice it can be achieved by producing the carbide or nitride particles with face-centered cubic crystal lattice.

In the present work the high-intense (power density more than  $10^7$  W/cm<sup>2</sup>) pulsed (pulse duration about 100 ns) beams (HIPB) of carbon ions with energy 200 – 250 keV were used for surface alloying of metals (Ti and W) with carbon to produce the carbide particles. To increase the dose of carbon ions the influence was carried out with a large number of pulses (100 – 500). By means of X-ray diffraction it was found that the particles of TiC and WC carbides were formed in the surface layers of titanium and tungsten. Mechanical tests shown the improving the hardness of the modified layers of the metals due to dispersed mechanism of hardening.

Another approach for mechanical properties improving consists of the HIPB influence on the copper samples. Carbon is practically non-dissolved in the crystal lattice of the copper. So the implanted carbon can form clusters as well as amorphous layer that is depends on the carbon ions dose, current density and number of pulses.

Combination of these two ways can be realize as HIPB influence on the “coating/substrate” system where the coating and the substrate are characterized by the different dissolubility of carbon. In the case of copper substrate and titanium (thickness about 100 – 200 nm) coating the impact of the ion beams with the energy density absorbed by the surface layer 0.2 – 1.0 J/cm<sup>2</sup> in the titanium coating TiC particles are formed. The consequent impact by the ion beams with energy density about 2 J/cm<sup>2</sup> on the modified system allows to melt the surface layer of the copper substrate and to embed the TiC particles in the surface layer. The result of such combined treatment by HIPB improves the mechanical properties (increase hardness and decrease friction coefficient) of the modified materials.

## THE PLASMADYNAMIC SYNTHESIS OF NANODISPERSED SILICON CARBIDE AND THE PRODUCT CHARACTERISTICS MANAGEMENT

*D.S. NIKITIN\**, *A.A. SIVKOV\*\**

\* *Tomsk Polytechnic University, Lenina Avenue, 30, Tomsk, Russia, 634050, dima\_n@sibmail.com, 8-913-813-64-06*

\*\* *Tomsk Polytechnic University, Lenina Avenue, 30, Tomsk, Russia, 634050, sivkovAA@mail.ru, 8-905-992-96-17*

Synthesis of silicon carbide is interested due to the presence of a wide range of his unique mechanical, thermal and electrical properties: superhardness, strength, thermal and corrosion resistance, radiation hardness, unique semiconductor characteristics [1]. The first successful synthesis of SiC was realized by Acheson in 1892 and the most of the SiC powders produced today is manufactured using the Acheson process. There are a great number of nano-SiC synthesis techniques: combustion synthesis (SHS and VCS), physical vapor transport (PVT), chemical vapour deposition (CVD), sol-gel, liquid phase sintering, mechanical alloying and plasmochemical synthesis [2]. But the unique mentioned properties of the produced SiC cannot be generally realized due to dependence on the synthesis methods. In this connection the development of new simple and productive methods for the direct synthesis of nanodispersed high-quality silicon carbide is an important problem. Synthesis method needs to have such advantages as lower energy requirement, simpler and cheaper equipment, higher product purity, and finer and well-sintered starting powders [2]. The paper presents the results of the plasmodynamic synthesis and the ability to control the synthesis process and change characteristics of the product.

The above method can be realized in a high-speed pulse jet of the dense Si-C plasma. The jet is generated by a pulse (~100  $\mu$ s) high-current (~100 A) coaxial magnetoplasma accelerator (CMPA) [3] with graphite electrodes. The fundamental possibility of silicon carbide synthesis by proposed method was shown in the paper [4]. An obvious development of this research work is a more detailed analysis of the product synthesis and the study of the influence of various factors, particularly the plasma jet energy, on the product formation and characteristics.

The synthesized product was analyzed by modern techniques: X-ray diffraction, transmission electron microscopy. According to micrographs size distributions of the particles were constructed. Resulting histograms are shown in Fig. 4. The results of statistical analysis of TEM-images is confirmed the tendency of the crystals growth when the energy level of the plasma shot increases.

Thus, the main result of the paper is a demonstration of the capabilities plasmodynamic synthesis of nanosized silicon carbide cubic system. Change the level of input energy can adjust in the system size distribution of the product synthesis.

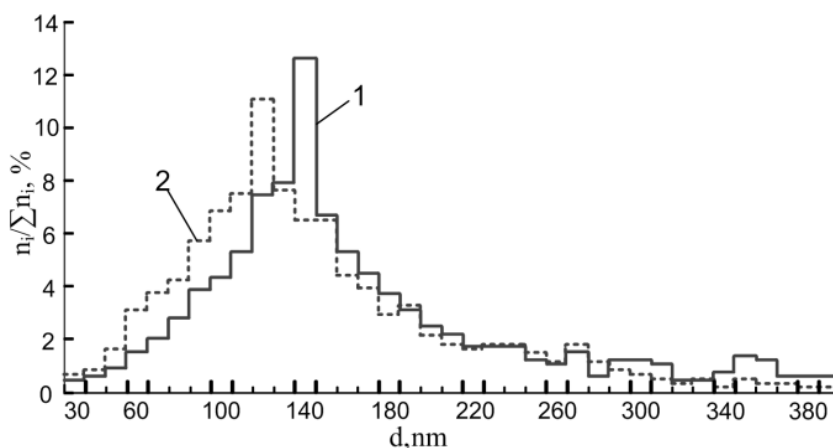


Fig. 1. Histograms of size distributions: 1 – Exp. 1; 2 – Exp. 2

### REFERENCES

- [1] *W.Wesch // Nucl. Instrum. Methods Phys. Res., Sect. B. – 1996. – V. 116. – P. 305–321.*
- [2] *R.Andrievski // Rev.Adv.Mater.Sci. – 2009. – V. 22. – P. 1-20.*
- [3] *A.A.Sivkov, A.Ya.Pak // Patent RU № 2431947, 2011.*
- [4] *A.A.Sivkov, D.S.Nikitin, A.Ya.Pak, and I.A.Rakhmatullin // Tech.Phys.Let. – 2013. – V. 39, No. 2. – P. 15-20.*



## ABILITY OBTAINING THE PHASE OF IRON OXIDE

*A.A.SIVKOV\**, *A.A.SVECHKANEVA\**

\* Tomsk Polytechnic University, Lenin ave, 30, Tomsk, 630050, Russia, svechkaneeva@mail.ru, +7(3822)563-682

Increased interest in nano-objects can be attributed to their unusual physical and chemical properties. Of special importance are magnetic properties allowing to distinguish more clearly multidimensional materials and nanomaterials.

Magnetic characteristics of the materials can be to some extent controlled by changing size, shape, composition and structure of nanoparticles. However, control fails when synthesizing nanoparticles similar in size and chemical composition, thus causing differences in their properties.

The purpose of the experiment is to obtain ultra-dispersed nanostructural iron oxide with a novel plasma-dynamic method. The material has a wide range of applications in electronics, medicine (targeted drug delivering, contrasting agents in magnetic resonance imaging, hyperthermia), magnetic storage media, radio absorptive materials.

This article describes a novel method for obtaining ultra-dispersed iron oxide powder by using coaxial magneto-plasma accelerator (CMPA). The obtained powder contains all main oxide phases: magnetite  $\text{Fe}_3\text{O}_4$ , maghemite  $\gamma\text{-Fe}_2\text{O}_3$ , hematite  $\alpha\text{-Fe}_2\text{O}_3$ ,  $\epsilon\text{-Fe}_2\text{O}_3$ . The powders exhibit high magnetic properties similar to compact iron oxide properties.

The stock-electrode is made of a steel pipe with a cylindrical acceleration channel (AC) diameter  $d_{ac} = 15$  mm and length  $\ell_{ac} = 220$  mm. The air atmosphere pressure  $P_0 = 1$  atm. in the chamber-reactor (CR).

The cylindrical channel in the central electrode insulator provides starting conditions for the formation of plasma structure with Z-pinch heavy-current discharge with the blowout plasma seal closed on the acceleration channel cylindrical surface. Discharge voltage and power ultimately increase with the current step-up and plasma acceleration to the AC edge. When plasma leaves the acceleration channel, voltage and power smoothly step-down proportionally to the current step-down.

Dispersity, chemical and phase composition of the powdered material are determined by the original components composition, process energetics, plasma speed and expansion velocity, cooling and hardening of the synthesized material drops. Therefore, the main advantage of the direct plasma-dynamic synthesis is that rising of the main components, material synthesis and dispersion are accomplished within one short-term CMPA operating cycle (up to  $10^{-3}$  M/s).

Of special interest is iron oxide  $\epsilon\text{-Fe}_2\text{O}_3$  phase content with 25-35 % mass percent.  $\epsilon\text{-Fe}_2\text{O}_3$  trimetric modification is metastable as distinct from the stable, easily synthesized in both macro-crystalline and nanoscale state, nature-occurring phases of magnetite, maghemite and hematite.

The given paper proves the feasibility of direct plasma-dynamic synthesis of ultra-dispersed hetero-phased iron oxide powders with a novel highly efficient method. The micro-atomized material, obtained with the plasma jet air discharge at normal pressure, exhibits highly magnetic properties due to high concentration of magnetite, maghemite and  $\epsilon\text{-Fe}_2\text{O}_3$  with the average particle size of about 50 nm. Formation and preserving a substantial amount of trimetric  $\epsilon\text{-Fe}_2\text{O}_3$  modification, metastable under standard conditions, is a unique characteristic of the powders obtained with plasma-dynamic synthesis. Magnetic nano-particles are widely used in different sciences (especially for biological applications) due to their particles narrow size distribution and stable reproducible characteristics.

The obtained experimental data illustrate the feasibility of nano-dispersed hetero-phased iron oxide powders synthesis with a highly-efficient, cost-effective method. It has been proved that hetero-phased iron oxide UDP exhibit high magnetic characteristics, similar to multidimensional materials characteristics. It suggests their wide applicability in engineering, biology, spintronics and medicine.

### REFERENCES

- [1] Gubin S.P., Koksharov Y.A., Jurkov G.U. *Magnetic nanoparticles: preparation, structure and properties // Uspehi himii. – 2005. – 74(6). – №.539-574.*
- [2] Osipov V.V., Platonov V.V., Ujmin M.A., Podkin A.V. // *Laser synthesis of nanopowders of magnetic iron oxides. – Journal Technical Physics. – 2012. – 82(4). – №.123-129.*
- [3] Sivkov A.A., Naiden E.P., Gerasimov D.Ju. *Direct dynamic synthesis of nanosized titanium nitride in high-speed pulsed electrical discharge plasma jet // Superhard materials. – 2008. – 5(175). – №.33-39.*

## SYNTHESIS OF NANOPARTICLES OF SPECIFIED SIZE AND OBTAINING TECHNOLOGY OF OPAL MATRICES

*G.A. KURALBAYEVA*<sup>\*</sup>, *A. K. KOPY SHEVA*<sup>1</sup>, *G.E. SATAEVA*<sup>2</sup>, *I.I. GANINA*<sup>3</sup>, *K.N. BAYMAGAMBETOV*<sup>4</sup>, *A.A. AMIROVA*<sup>5</sup>

*\*Kazakhstan, Astana, L.N. Gumilyov Eurasian National University, galiy.91@mail.ru, +77012799890*

In recent years, there's a growing interest in composite materials based on nanoporous opal matrices. Because, the physicochemical properties this materials caused by several reasons. First, the proximity of the size of the nanocrystal to the radius of delocalization of quasiparticles, which determines the size dependence of optical, luminescence properties of these materials. Second, the number of atoms on the crystal surface is comparable proportion of the total number of atoms in its entirety. These atoms provide a significant contribution to the thermodynamic characteristics and, in the case of nanoscale crystals, largely determine the structural phase transitions, the melting point of objects, etc. Third, own custom size of these crystals is close to the size of polyatomic molecules. This causes the kinetics of chemical processes on the surface.

During the implementation there was developed the technique for producing aqueous suspensions of nanoparticles SiO<sub>2</sub>. As a basis for the synthesis of such spheres as silicon dioxide we used method Stober. The dependence of polydispersity of these suspensions depending on synthesis conditions was achieved. It was found that polydispersity can be significantly reduced with additional preparation of the initial reagents.

It is known that the nucleation of silicon dioxide particles proceeds by adding ammonia to tetraethoxysilane Si (OC<sub>2</sub>H<sub>5</sub>)<sub>4</sub> (TEOS). Reducing the initial concentration of TEOS at the time of adding of ammonia promotes more even reaction well as the decrease of the dispersion of resulting suspension in half or twice. The value of dispersion of SiO<sub>2</sub>-size particles in the resulting suspension is from 5% to 10%.

As a result of research of porosity of opal matrix stacked with spherical particles of silicon dioxide with different diameters (70-250 nm), it was found that the particle density SiO<sub>2</sub>, obtained by cultivation of a multistage depends on their diameter and naturally decreases with its rise.

The technique was developed and spherical SiO<sub>2</sub> particles with different average sizes from 70 nm to 250 nm were synthesized.

There was shown the possibility of obtaining monodisperse SiO<sub>2</sub> particles of different sizes, with a regular spherical shape and the ability to control the surface morphology. Such particles may be used for the development of modern high-energy radiation detection systems, general-purpose fluorescent screens, the new lighting system, etc.

### REFERENCES

- [1] *Stober W., Fink A., Bohm E.* Controlled growth of monodisperse silica spheres in the micron size range // *J. Colloid Interface Sci.* – 1968. – Vol. 26, N 1. – P. 62–69.
- [2] *Xuan Li, Chen Zhang, Zhongjie Du, Hangquan Li.* Preparation of hydrophilic/hydrophobic porous materials // *Journal of Colloid and Interface Science.* – 2008. – Vol. 323. – P. 120-125

## FINE STRUCTURE OF ENERGY SPECTRA IN FIELD EMISSION PROCESS OF TUNGSTEN-ZIRCONIA HETEROSTRUCTURE<sup>1</sup>

I.S. TURMYSHEV, O.R. TIMOSHENKOVA, A.M. MURZAKAEV

*Institute of Electrophysics UB RAS, 106 Amundsen st., Ekaterinburg, 620016, Russia, ivatur@rambler.ru, +7(343)2678794*

Thermofield emission cathodes based on ZrO<sub>2</sub>/W heterostructures are widely used as a point electron source nowadays. At present issue results of simultaneous study of Volt-Ampere characteristics (VACH) and energy spectra of such cathodes are discussed just under field emission terms. Firstly, needle shaped tungsten cathodes were coated by thin (~ 10 nm) film of ZrO<sub>2</sub> by means of thermo-field diffusion methods under ultra high vacuum conditions. In this case the tungsten emitters were used as reference patterns and their characteristics were measured before the coating process. It is shown that VACH of coated emitters plotted in Fowler-Nordheim coordinates has non-linear character contrarily to “metallic” VACH.

Such behavior of VACH may be attributed to complicated energy spectra obtained during VACH measurement and complex electronic structure of thin film. There are two peaks on the spectra plot with 3-5 eV distance between them depending on emission voltage. It is shown that energy spectra of coated cathodes have a regular fine structure, and all metamorphoses of the energy spectra are connected with variation of amplitudes of fine structure peaks while the positions of the peaks are constant during emission process for fixed thickness of zirconia layer.

Considerable part of the work deals with computer modeling of the field processes which can lead to rising of the fine structure and such a way attempts to explain behavior of energy spectra. It was shown that at least two-threshold potential barrier can lead to energy spectrum fine structure appearance. Relying on experimental data and taking into account equal distance between fine structure peaks it was established that model potential barrier must have a parabolic valley between two extrema an exact shape of which should be established.

<sup>1</sup> This work was supported by the RFBR (project No. 13-08-00266-a, project No. 14-08-31024-mol\_a) and FASO within the Presidium of Russian Academy of Sciences fundamental research program (UB RAS project No. 12-P-1005, state registration No. 01201266835).

## STRUCTURAL TRANSFORMATIONS OF NANOGLOBULAR CARBON UNDER THE ACTION OF HIGH ENERGY PULSED BEAMS

YU.G. KRYAZHEV\*, M.V. TRENKIN\*, N.N. KOVAL\*\*, G.M. SEROPYAN\*\*\*, A.D. TERESOV\*\*, V.A. LIKHOLOBOV\*

*\*Institute of Hydrocarbon Processing, Omsk Scientific Center SB RAS, 54 Neftezhavodskaya str., Omsk, Russia, kriaghev@ihcp.ru*

*\*\*Institute of High Current Electronics SB RAS, 2/3 Akademichesky ave., Tomsk, 634055, Russia*

*\*\*\*F.M. Dostoevsky State University, 55a Mira ave., Omsk, 644077, Russia*

Synthesis of carbon nanoscale materials (CNM) is a priority in the world science. Nano-globular carbon (NGC) is the most available CNM (industrial carbon black). We developed the concept that under pulsed power influence it is possible the transformation of NGC to other types of CNM. Specificity of pulsed irradiation of NGC is alternated pulse heating (to temperatures of phase transitions) and subsequent rapid cooling of the particles, followed by dissociation of carbon-carbon bonds and the formation of energetically favorable structural modifications.

The fruitfulness of this approach is shown in examples of the impact on NGC by submillisecond pulse electron irradiation with an energy density of  $10\div 50$  J/cm<sup>2</sup> at a pulse width of 100  $\mu$ s and nanosecond laser pulses (wavelength of 1064 nm) with an energy density of 1200 to 6300 J/cm<sup>2</sup>. Samples of industrial carbon black with primary particle diameters of 10 to 500 nm were investigated. The structure of obtained products was determined by transmission electron microscopy. General laws of NGC transformations under the action of electron and laser pulsed radiations were established.

There is an ordering of the structure of spheroidal particles, which manifests in a decreasing of the distance between the graphene layers and increasing of their spatial extent. The structural ordering of the irradiated particles increases with the size of original globules and radiation energy density increasing.

Restructuring of NGC with the formation of two types of particle with the original morphology of nanocapsules and rose-like particles is take place.

Rose-like particles are the globules with diameter of 100-500 nm, on the cut of which is observed the rows of parallel spatially extended graphene layers with the distance between them of 0.345 nm characteristic for graphite. Nanocapsules are hollow spheres with a diameter of 10-30 nm with a shell consisting of 5-10 graphene layers with the distance between 0.355-0.365 nm.

## PLASMADYNAMIC SYNTHESIS OF YTTRIUM-BARIUM CUPRATES FOR HIGH-TEMPERATURE SUPERCONDUCTORS

*K.I. STEPANOV\*, A. A. SIVKOV\*, A.S. IVASHUTENKO\*, I.I. SHANENKOV\**

\* National Research Tomsk Polytechnic University, Lenina Av., 30, 634050, Tomsk, Russia, *Stepanov.k.i@mail.ru*, ph: 89138611061

In the modern world there is a necessity in use of a large number of the electric power. There are two ways of the solution of this problem: directly increasing number of generating capacities due to the construction of new power plants, or transition to superconducting modules [1]. Both ways take place to be, but, nevertheless, the second way is the most perspective. However, it rests against a creation problem the high-temperature superconductors.

The new approach connected with application of high-intensity influences is developed in high-temperature superconductivity (HTSC) laboratory (discharge plasma, magnetic-pulse pressing, dispergating of powders). The way of the plasmadynamic synthesis of charge mixture for high-temperature superconductors was developed with the use of the coaxial magnetoplasma accelerator of professor Sivkov [2]. The obtained charge mixture can be used for sintering in a bulk sample.

The essence of a method of the charge mixture obtaining consists in the following: initial components hydroxide of barium ( $\text{Ba}(\text{OH})_2$ ), nitrate yttrium ( $\text{Y}(\text{NO}_3)_3$ ) are loaded into the accelerator where the discharge is caught fire and due to interaction with an external magnetic field of the inductor the plasma flow is formed. The copper oxide ( $\text{CuO}$ ) turns out to be as the result of copper electric conductors explosion, and as an additional result of pure copper erosion from the walls of a copper-made accelerating channel. Such a way accumulated copper is oxidized to copper oxide. At the plasma flow development, the specified particles are dispergated due to colliding with camera walls.

A series of experiments connected with the charge mixture of yttrium-barium cuprates obtaining was carried out. Obtained samples without any special preparation were investigated by using a structural and phases analysis with the X-ray diffractometer Shimadzu XRD 7000. Also transmitting electron microscopy (TEM) was carried out. According to it the average size of particles are not more then 500 nm. It is in a good accordance with XRD data.

Obtained powders were sintered by using a double-sided magneto-pulse press. The pressed sample with a diameter of 10 mm was annealed to obtain a ceramic tablet.

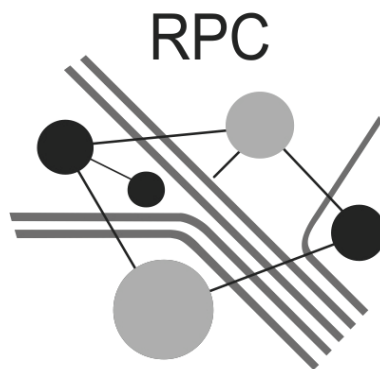
Thus, the possibility of the plasmadynamic synthesis of the yttrium-barium cuprates charge mixture in supersonic plasma jet is shown. Also by using magneto-pulse pressing and annealing it is possible to obtain the ceramic.

### REFERENCES

- [1] *P. De Gen // Superconductivity of metals and alloys. – M: ITS Media, 2012.*
- [2] *Stalemate. 2243474 Russian Federation. 7F41B 6/00. Coaxial accelerator / Yu. Gerasimov, A.A. Sivkov. Prior. 31.07.2003. Publishing 27.12.2004, Bulletin No. 36.*



**16<sup>th</sup> International Conference  
on Radiation Physics  
and Chemistry of Condensed Matter**



**Co-Chairmen:**

Vladimir Lopatin Institute of High-Technology Physics, TPU, Tomsk, Russia  
Viktor Lisitsyn Institute of High-Technology Physics, TPU, Tomsk, Russia

**International Advisory Committee:**

Gilles Damamme CEA – Centre du Ripault, France  
Hans-Joachim Fitting Rostock University, Germany  
Boris Kalin Moscow Institute of Physical Engineering, Russia  
Vsevolod Kortov Ekaterinburg State Technical University, Russia  
Evgenij Martynovitch Irkutsk State University, Russia  
Abdirash Akilbekov L.N. Gumilyov Eurasian National University, Kazakhstan  
Daniel Maiys CEA DAM, France  
Boris Grinev Institute for Scintillation Material of NAS, Ukraine  
Kurt Schwarz CSI Accelerator Center, Darmschtadt, Germany  
Yurij Zakharov Kemerovo State University, Russia  
Evgenij Kotomin Institute of Solid State Physics, Latvia  
Anatoly Kupchishin Al-Farabi Kazakh National University, Kazakhstan  
Aleksandr Lushchik Tartu University, Estonia  
Mustafa Kidibaev Bishkek, Institute of Physics, Kyrgyzstan  
Boris Shulgin Ekaterinburg State Technical University, Russia  
Aleksandr Nepomnyashchikh Institute of Geochemistry, Russia  
Ivan Neklyudov Kharkov Institute of Physics and Technology, Ukraine  
Oleg Tolbanov National Research Tomsk State University, Russia  
Yuri Tyurin Institute of Physics and Technology, TPU, Russia  
Sergei Chizhik National Academy of Sciences, Belarus  
Alexey Yakovlev Institute of High-Technology Physics, TPU, Tomsk, Russia

**Sessions:**

Elementary processes  
Nonlinear effects  
Surface phenomena  
Physical basis of radiation-related technologies  
Methods of testing



## THE ROLE OF DEEP CENTERS IN FORMATION OF LUMINESCENT AND DOSIMETRIC PROPERTIES OF WIDE-GAP MATERIALS

*S.V. NIKIFOROV, V.S. KORTOV*

*Ural Federal University, 19 Mira street, Ekaterinburg, 620002, Russian Federation, [s.v.nikiforov@urfu.ru](mailto:s.v.nikiforov@urfu.ru), +79126068140*

The mechanisms and features of thermoluminescence (TL) in different materials are studied due to the necessity of fundamental and applied problem solution. In the simple model of TL only two localized level are considered: trap and recombination center. The development of this model takes into account the competitive influence of deep trapping centers. The deep centers have an energy depth, which is more than ones of main trapping centers. The deep traps are stable thermally in usual range of TL registration (thermally disconnected deep traps).

The main features of deep trap influence on the luminescent properties of different wide-gap dielectrics (LiF, CaF<sub>2</sub>, SiO<sub>2</sub>, CaSO<sub>4</sub>:Dy, Al<sub>2</sub>O<sub>3</sub>) are discussed. The analysis of experimental results described in literature shows that the presence of deep traps is responsible for sensitization and desensitization effects, and also for the non-linearity of TL dose response. The filling of deep centers by charge carriers leads to the appearance of phototransferred thermoluminescence (PTTL). We carry out the complex experimental study of the features of deep traps' influence on luminescent and dosimetric properties of crystalline and nanostructured anion-defective aluminium oxide. The oxygen vacancies were created by thermochemical and radiation coloration. The presence of deep traps is confirmed by the investigation of high-temperature TL after UV-, beta-, X-ray and pulsed electron excitation. It was founded that the occupancy state of deep centers determines the TL sensitivity to radiation and its' dependence on heating rate, the shape of TL dosimetric peak, thermal quenching of luminescence, superlinearity of dose response, emission spectrum, the output and decay time of optically stimulated luminescence (OSL). The suppositions about the electron or hole nature of traps with different thermal depth are well founded.

The interactive trap system model (ITS) is the most universal model describing the TL mechanism in wide-gap materials at heating stage in the presence of deep traps. The essence of the model is the competitive capture of charge carriers by deep traps during the registration of the main TL peak. We established the main role of interactive mechanism of trap interaction in formation of luminescent properties of anion-defective Al<sub>2</sub>O<sub>3</sub> single crystals. The possibilities of the ITS model are extended for explanation of TL dose responses obtained at different heating rates, steps of dose variation and initial concentrations of charge carriers at localized states. On the base of new experimental results the ITS model was added by hole trapping centers. The supposition was made about the universality of interactive mechanism of interaction between traps with different nature in anion-defective Al<sub>2</sub>O<sub>3</sub>. The interpretation of the temperature dependence of the interaction efficiency of traps due to taking into account the process of thermal ionization of excited states of F-centers is proposed.

On the base of obtained results the methods of dosimetric properties improvement and widening the functional application of TL detectors on the base of crystalline Al<sub>2</sub>O<sub>3</sub> are elaborated. The possibility of use of PTTL and thermally assisted OSL in this material for high radiation doses registration (more than 10 Gy) is discussed.

## OPTICAL, EMISSION AND TIME-RESOLVED SPECTROSCOPIES OF THE THIN NANOSTRUCTURED LAYERS BASED ON ANION-DEFECTIVE GAMMA-ALUMINA<sup>1</sup>

*A.I. SURDO\* \*\*\*, M.I. VLASOV\*, V.G. IL'VES\*\*\*, I.I. MILMAN\*\*, V.A. PUSTOVAROV\*\*, A.I. SLESAREV\*\*, S.YU. SOKOVNIN\*\*\*, V.YU. YAKOVLEV\*\*\*\**

\* Institute of Industrial Ecology of UB RAS, S. Kovalevsky, 20, Ekaterinburg, 620219, Russia, surdo@ecko.uran.ru, 7(343)3743771

\*\* Ural Federal University, Mira, 19, Ekaterinburg, 620000, Russia

\*\*\* Institute of Electrophysics of UB RAS, Amundsen, 106, Ekaterinburg, 620016, Russia

\*\*\*\* Tomsk Polytechnical University, Lenin Ave., 30, Tomsk, 634034, Russia

Using technology of the target evaporation by pulsed electron beam amorphous-nanocrystalline alumina based thin nanostructured layers (TNL) with mass thickness varies from 3 to 15 mg/cm<sup>2</sup> were obtained [1]. Among nanostructures they have a record high and comparable with macrostructures yields of thermally stimulated and optically stimulated luminescence (TL and OSL). It was shown also [1] that the high luminescence yield show annealed up to 970 K samples that contain simultaneously maximum possible concentrations of Al<sub>2</sub>O<sub>3</sub>  $\gamma$ -phase and anion vacancies. At the same time it is known that F<sup>+</sup> and F centers (anion vacancies with one or two electrons respectively) are dominating one in anion-defective corundum ( $\alpha$ -Al<sub>2</sub>O<sub>3- $\delta$</sub> ). They cause unique dosimetry properties of the TL-OSL detectors based on  $\alpha$ -Al<sub>2</sub>O<sub>3- $\delta$</sub> . Therefore purpose of this work is to study luminescent properties of  $\gamma$ -Al<sub>2</sub>O<sub>3- $\delta$</sub>  TNL using synchrotron radiation, time-resolved luminescent spectroscopy, radioluminescence, optically and thermally stimulated exoelectron emission and to compare them with those in  $\alpha$ -Al<sub>2</sub>O<sub>3- $\delta$</sub>  in order to reveal analogies and establish the nature of the active centers in  $\gamma$ -Al<sub>2</sub>O<sub>3- $\delta$</sub> .

It is shown that luminescence with maximum at 2.75 eV dominates in photoluminescence spectra of the initial unirradiated samples. There are 4 bands with maxima around 3.9, 4.4, 5.3 and 6.2 eV observed in its excitation spectrum measured in the fast time gate. Similar time-resolved excitation spectrum of the F-center singlet-singlet luminescence with maxima at 4.8, 5.3, 5.9 and 6.4 can be observed in initial unirradiated  $\alpha$ -Al<sub>2</sub>O<sub>3- $\delta$</sub> . Given the conditions of TNL samples synthesis in reducing environment and possible proximity of electron structure of F-type defects in  $\gamma$ - and  $\alpha$ -Al<sub>2</sub>O<sub>3- $\delta$</sub>  it is supposed that it is also F centers in the initial unirradiated  $\gamma$ -Al<sub>2</sub>O<sub>3- $\delta$</sub>  that most intensively emit around 2.75 eV. It is found that the time-resolved spectra of the intrinsic center luminescence in the  $\gamma$ - and  $\alpha$ -Al<sub>2</sub>O<sub>3- $\delta$</sub>  samples under excitation around 6 eV are similar too. They have two bands. In  $\alpha$ -Al<sub>2</sub>O<sub>3- $\delta$</sub>  they are caused by F and F<sup>+</sup> centers that emit at 3.26 and 3.8 eV respectively. By analogy with  $\alpha$ -Al<sub>2</sub>O<sub>3- $\delta$</sub> , centers that emit around 3.85 eV in  $\gamma$ -Al<sub>2</sub>O<sub>3- $\delta$</sub>  can be attributed to F<sup>+</sup> centers. Moreover, their lifetime at excited state agree with that for F<sup>+</sup> centers in  $\alpha$ -Al<sub>2</sub>O<sub>3- $\delta$</sub>  and equal to 2 ns. Table 1 contains the main data obtained using synchrotron radiation in this study and in [2]. From a comparison of spectrum and kinetic parameters of the F and F<sup>+</sup> centers for  $\alpha$ -Al<sub>2</sub>O<sub>3</sub> and  $\gamma$ -Al<sub>2</sub>O<sub>3</sub> it follows that they are similar. Slight discrepancy may be caused by different structural and phase states of Al<sub>2</sub>O<sub>3</sub> ( $\gamma$ -phase is a cubic crystal system, while  $\alpha$ -phase is a trigonal system) and by dimension effects (single crystal and nanocrystal). In addition to the data obtained using synchrotron radiation spectra of TL, radioluminescence and optically and thermally stimulated exoelectron emission were studied.

Table 1. Parameters of singlet-singlet transitions in  $\alpha$ -Al<sub>2</sub>O<sub>3</sub> and  $\gamma$ -Al<sub>2</sub>O<sub>3</sub> at T=8K.

Active centers		$\alpha$ -Al <sub>2</sub> O <sub>3</sub>	$\gamma$ -Al <sub>2</sub> O <sub>3</sub>
F	h $\nu_{ex}$ , eV	4.8, 5.2, 5.9, 6.4	3.9, 4.4, 5.3, 6.2
	h $\nu_{em}$ , eV	3.26	2.75
	$\tau$ , ns	1.6	4.3
F <sup>+</sup>	h $\nu_{ex}$ , eV	4.8, 5.4, 5.9, 6.6	4.9, 5.2, 5.7, 6.4
	h $\nu_{em}$ , eV	3.80	3.85
	$\tau$ , ns	2.0	2.0

### REFERENCES

- [1] A.I. Surdo, I.I. Milman, M.I. Vlasov, V.G. Il'ves, S. Yu. Sokovnin // Technical Physics Letters. – 2013. – V. 39. – I. 1. – P. 5-8.  
 [2] A.I. Surdo // Russian Physics Journal. – 2011. – V. 54. – I. 1(3). – P. 277-283.

<sup>1</sup> This work was supported in part by the Ural Branch of RAS (projects № 12-U-2-032) and by RFFI (project № 14-02-31522).

## INFLUENCE OF THE PHOTOTRANSFER EFFECTS ON THE TL AND OSL YIELDS, KINETICS AND EMISSION SPECTRA IN TLD-500 DETECTORS<sup>1</sup>

*M.I. VLASOV\**, *A.I. SURDO\*\*\**, *I.I. MILMAN\*\**, *E.V. MOISEIKIN\*\**, *R.M. ABASHEV\**

\* *Institute of Industrial Ecology of UB RAS, S. Kovalevsky, 20, Ekaterinburg, 620219, Russia, maxim.vlsv@ya.ru, 7(343)3743771*

\*\* *Ural Federal University, Mira, 19, Ekaterinburg, 620000, Russia*

Anion-defective corundum ( $\alpha\text{-Al}_2\text{O}_{3.8}$ ) based TLD-500 detectors are widely used in dosimetry control and environmental monitoring [1]. For the estimation of the absorbed dose the yield of thermoluminescence (TL) in the area of the main dosimetry peak at 450 K or the yield of optically stimulated luminescence (OSL), usually under continuous stimulation, are measured [1]. Usage of the detectors suppose invariability of their dosimetry properties during operation. However, accumulated data indicates that TL and OSL yields of  $\alpha\text{-Al}_2\text{O}_{3.8}$  based detectors strongly depend on filling extent not only of the main dosimetry trap, responsible for the peak at 450 K, but also of the more deep trap depleted at 720 K [2]. Under optical stimulation in  $\alpha\text{-Al}_2\text{O}_{3.8}$  effect of charges phototransfer, i.e. transfer of charges, captured at the deep traps into shallow traps, is observed. Therefore, purpose of this work is to reveal in  $\alpha\text{-Al}_2\text{O}_{3.8}$  correlations between TL and OSL yields and charge carriers phototransfer under variable stimulation wavelength and controlled filling of the main and deep traps responsible for the TL peaks at 450 and 720 K respectively.

Under optical stimulation by blue light with  $\lambda=450\text{-}470$  nm correlation of the phototransfer effects with TL and OSL yields and kinetics in  $\alpha\text{-Al}_2\text{O}_{3.8}$  was established. It was obtained that intensity of the fast component of OSL decay curve is connected with extent of the main dosimetry trap filling. With its complete thermal emptying charge carriers phototransfer from the deep trap depleted around 720 K, to the main trap is observed, that is confirmed by OSL rise and appearance of phototransferred TL in the area of the main dosimetry peak. It was shown that the slow component of OSL decay is caused by consecutive phototransfer of charge carriers from the deep trap to the main one and then from the main trap to luminescence recombination centers. It is important that as the deep trap filling TL and OSL yields can increase up to 100 times. So, along with the slowly changing fast component the time decay constant of the slow component and its contribution into OSL light sum increase essentially.

It was found that under stimulation by green light with  $\lambda=520\text{-}525$  nm OSL yield correlates with extent of deep trap filling too: with complete filling it increases up to 100 times. However, in the kinetics there is no slow decay component. Charge carriers phototransfer from the deep trap to the main one is not observed and, as a consequence, extent of the deep trap filling remains constant. It is of the applied importance that OSL stimulation in  $\alpha\text{-Al}_2\text{O}_{3.8}$  by green light depletes predominantly main dosimetry trap, and sensitivity obtained as a result of deep trap filling persists after reading of data from the detector. Moreover, in the course of the results obtained with usage of blue and green stimulation lights, spectrum of optical depletion, that shows maximum around 400 nm, and peak degradation dependence on x-ray dose for the TL peak at 720 K were studied.

For dosimetry peak at 450 K dynamics of TL spectrum transformation and change in its kinetic parameters depending on the main trap filling method (ionizing radiation or phototransfer from the deep trap) and on the phototransfer duration were studied. It was found that in the spectrum of the TL peak at 450 K, formed as a result of phototransfer, luminescence of the  $\text{F}^+$  centers (330 nm) dominates. Weak luminescence of the F centers (420 nm) is observed only at its low-temperature part.

### REFERENCES

- [1] *Yukihara E.G., McKeever S.W.S. // Optically stimulated luminescence. Fundamentals and applications. – West Sussex: Wiley, 2011.*
- [2] *Surdo A.I., Milman I.I., Vlasov M.I. // Rad. Meas. – 2013. – V. 59. – P. 188-192.*

<sup>1</sup> This work was supported in part by the Ural Branch of RAS (projects № 12-U-2-032, № 14-2-NP-174) and RFFI (project № 14-02-31522).

**ELASTIC WAVES IN IRON CRYSTALLITES INDUCED BY IRRADIATION**

A.V. KORCHUGANOV\*, D. S. KRYZHEVICH\*\*, K. P. ZOLNIKOV\*\*

\**Institute of Strength Physics and Materials Science, Siberian Branch of Russian Academy of Sciences, 2/4, pr. Akademicheskii, Tomsk, 634021, Russia, alex.v.kor@gmail.com, +7 (3822) 28-69-73*

\*\**National Research Tomsk State University, 36, Lenina Avenue, Tomsk, 634050, Russia*

Generation of elastic waves due to formation and annihilation of Frenkel pair was first theoretically predicted by V. L. Indenbom and named “radiation shaking” [1]. In this work formation and propagation of elastic waves in iron crystallites caused by generation of atomic displacement cascades is investigated by means of molecular dynamics simulations. Atomic interactions are described by pair potential [2]. Simulated crystallites are shaped as cubes. Periodic boundary conditions are applied in all directions. Atomic displacement cascades are generated with primary knock-on atom energy from 15 eV to 100 keV. Temperature of specimens is varied between 10 and 300 K.

Velocities of elastic waves, caused by generation of atomic displacement cascades, and stress fields created by them have been assessed for different crystallite temperatures and crystallographic directions of primary knock-on atom’s momentum. Interaction between elastic waves and point defect clusters has been investigated. It has been shown that formation of Frenkel pair in material generates stress wave, which propagates distance of 25-35 lattice parameters. More actively elastic waves are generated on ballistic stage of atomic displacement cascade evolution and propagate with speed of sound in material. It has been found out that these waves can change structure of point defect clusters.

## REFERENCES

- [1] *Indenbom V.L. // Pis'ma v JTF. – 1979. – 5. – № 9. Pages 489-492.*
- [2] *Romanov V.A., Sivak A.B., Chernov V.M. // VANT. – 2006. – 66. – № 1. Pages 129-150.*

## DEFECT PROPERTIES OF LBAF SINGLE CRYSTALS<sup>1</sup>

*I.N. OGORODNIKOV\**, *V.A. PUSTOVAROV\**, *S.I. OMELKOV\*\**, *M. KIRM\*\**, *L.I. ISAENKO\*\*\**

\*Ural Federal University, 19 Mira Street, Ekaterinburg, 620002, Russia, *i.n.ogorodnikov@urfu.ru*, +7(343)3754711

\*\*Institute of Physics, University of Tartu, 142 Riia Street, Tartu, 51014, Estonia

\*\*\*Institute of Geology and Mineralogy SB RAS, 43 Russkaya Street, Novosibirsk, 630058, Russia

Fluoride crystals with the general formula  $\text{Li } M \text{ AlF}_6$  ( $M = \text{Ca, Sr, Ba}$ ) are traditionally used as optical laser materials operating in the ultraviolet (UV) and vacuum ultraviolet (VUV) spectral ranges [1]. Among them, the  $\text{LiCaAlF}_6$  and  $\text{LiSrAlF}_6$  crystalline systems have been studied in sufficient detail.

At the same time, the  $\text{LiBaAlF}_6$  (LBAF) system has been paid much less attention. We are aware of only a few research works on this system. Luminescent properties and self-trapped excitons in undoped LBAF crystals have been studied in [2]. From the luminescence optical spectroscopy data it follows that the experimental estimation of the LBAF energy bandgap is  $E_g \approx 12.1$  eV [2]. Crystallographic data for the real LBAF crystals were presented in [3]. At the same time, we are not aware of the research work on the LBAF electronic structure. However, any practical application of LBAF as a functional material in quantum optics requires knowledge of electronic structure not only for the rare-earth and transition dopants, but for the host crystal as well.

The paper presents the results of a study of undoped LBAF single crystals, carried out using the low-temperature ( $T=10$  K) far ultraviolet optical and luminescence spectroscopy with a time resolution. The spectroscopy is conducted upon excitation with synchrotron radiation in the energy range 3.7-40 eV and supported by the X-ray photoelectron spectroscopy at room temperature. Calculations of the spectra of the optical functions were made on the basis of the low-temperature ( $T=10$  K) reflection spectra recorded in the energy range of 3.7-40 eV. The bandgap of investigated compound was found at  $E_g = 12.3$  eV, the energy threshold for creation of the unrelaxed excitons at  $E_{n=1} = 11.6$  eV, and the low-energy fundamental absorption edge at 11.0 eV. The valence band of LBAF single crystal is formed by  $2p$ -states of fluorine. The second energy gap  $E_{g2} = 6-7$  eV separates these states from the upper core states consisting of filled  $5p$  Ba states. The subnanosecond photoluminescence emission band at 6.6 eV in LBAF single crystal is due to radiative valence-core transitions  $2p \text{ F}^- \rightarrow 5p \text{ Ba}^{2+}$ . Photoluminescence (PL) excitation (PLE) spectroscopy was carried out for both the excitonic and fast VUV emissions. A pulse cathodoluminescence (PCL) spectroscopy method (110 keV, 1 ns, 60 A/cm<sup>2</sup>) was used to characterize the fast VUV emission and proof its origination from the radiative valence-core transitions  $\text{F}^- \rightarrow 5p \text{ Ba}^{2+}$ . Our results leads to a conclusion that there is a partial overlap between the upper core level and the valence band of LBAF. In addition to this, the modeling of the PL excitation spectra was performed for excitonic luminescence. These spectra provide information on the location of the fundamental absorption edge of LBAF single crystals.

Photoluminescence and UV-VUV optical absorption spectroscopy studies have shown that as a result of electron beam irradiation there is a change in the optical and luminescent properties of single LBAF crystals.

The explanation for that lies in poor radiation stability of studied compound under electron beam. It was already shown [2], that under continuous irradiation by 10 keV electron beam the emission intensity quickly drops with time, and at lower temperatures this effect is much stronger. In the current experiment the electron energies are 10 times higher, leading to complete degradation of some PL components even under pulsed (ca. 2 pps) irradiation already at 78 K.

Based on the experimental and theoretical results on the electronic structure and optical luminescence spectroscopy of LBAF single crystals, the article discusses possible channels of defect formation, and the origin of the optical absorption bands in the UV and VUV spectral regions.

### REFERENCES

- [1] *M.J.Weber* Handbook of Lasers. – Boca Raton, FL: CRC Press, 2000.
- [2] *S.I.Omelkov, M.Kirm, E.Feldbach, V.A.Pustovarov, et al.* –2010. – J. Phys.: Condens. Matter. – 22. P.295504.
- [3] *A.A.Merkulov, L.I.Isaenko, S.I.Lobanov, D.Y.Naumov, N.V.Kuratieva* –2008. –Acta Crystallogr. – C64. P.i66.

<sup>1</sup> This work was partially supported by the Ministry of Education and Science of Russian Federation (grant No.14.A18.21.0076), Siberian Branch of Russian Academy of Sciences (Grant No.28), HASYLAB DESY (Project No.20110843), European Social Fund ('Mobilitas', MJD219 and MTT83), and Baltic Science Link project coordinated by the Swedish Research Council, VR.

## THE EFFECT OF TEMPERATURE AND IRRADIATION DOSE ON THE LUMINESCENCE PROPERTIES OF $\text{Eu}^{3+}$ DOPED PHOSPHATE GLASS

V. M. LYSITSIN\*, E. F. POLISADOVA\*, H. A. OTHMAN\*\*

\* Tomsk polytechnic university, 30 Lenin Avenue, Tomsk 634050, Russian Federation

\*\*Faculty of Science, Menoufiya University, Shebin El-Kom, Egypt

E-mail: hosamssl4@yahoo.com

Ions of europium are actively used as an activator for materials sensitive to ionizing radiation: scintillator, crystalline phosphors, and light radiation up-converters.  $\text{Eu}^{3+}$  ions have narrow emission band in the visible region, a long lifetime of the excited state, and high quantum yield [1,2]. The aim of this work is to study the influence of temperature and irradiation dose on spectrum and kinetics of luminescence phosphate glass doped  $\text{Eu}^{3+}$ .

A metaphosphate glass system of the composition  $50\text{P}_2\text{O}_5-20\text{Li}_2\text{O}-30\text{ZnO}:x\text{E}_2\text{O}_3$  (with  $x$  ranges from 0.5 to 5 wt %) was synthesized by the melt-quench technique. Time-resolved Cathode luminescence spectra revealed the f-f transitions characteristic of the  $\text{Eu}^{3+}$  ion. Emission intensities and decay times of the f-f transitions show dependence on the irradiation dose. An increase in the emission intensity of the  ${}^5\text{D}_0-{}^7\text{F}_j$  ( $J = 2, 4, 6$ ) transitions was observed.

The emission decay kinetics were fitted to double exponential model, where the decay times of the long time component decrease with increasing the electron irradiation density. The characteristics of the luminescence spectra and their dependence on temperature were investigated. While the luminescence decay times show almost no dependence on temperature, a shift to longer wavelength in the emission peak position corresponding to the  ${}^5\text{D}_0-{}^7\text{F}_2$  was observed at 15 oK.

Although, it could be noticed that in the emission spectra of materials with  $\text{Eu}^{3+}$  [3] peak at 614 nm is

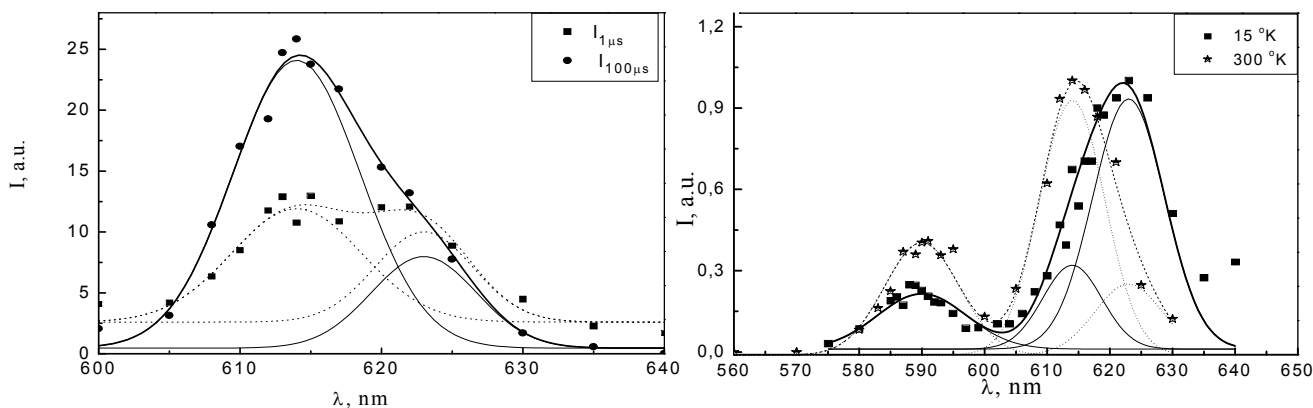


Fig. 1. Deconvolution of the emission peak of  $\text{Eu}^{3+}$  in spectral range 605-635 nm at  $T = 15$  and 300 K

somewhat distorted, not Gaussian, with a characteristic "shoulder" on its long-wavelength side, but with no further explanation.

Study of the time-resolved spectrum of europium doped samples after irradiation suggests the presence of two elementary gaussian components of the 614 nm peak.

### REFERENCES

- [1] C. Görler-Walrand, K. Binnimans in K.A. Gschneidner Jr., L. Eyring(Eds.) *Handbook on the Physics and Chemistry of Rare Earths*, vol. 25, Amsterdam (1998).
- [2] S. Surendra Babu, P. Babu at al. *J. of Luminescence*. 126, 109 (2007).
- [3] Nieuwpoort W. C. and Blasse // *Solid State Commun.* - 1966. - Volume. - 4. Pages227.

## P-D EXCITON ANNIHILATION IN SOLID STATE SOLUTIONS $\text{Ni}_x\text{Zn}_{1-x}\text{O}^1$

V.N. CHURMANOV\*, V.I. SOKOLOV\*\*, V.A. PUSTOVAROV\*, V.YU. IVANOV\*, N.B. GRUZDEV\*\*, P.S. SOKOLOV\*\*\*,  
A.N. BARANOV\*\*\*

\* Ural Federal University, Mira str. 19, Yekaterinburg, 620002, Russia, e-mail: chenov@olympus.ru, phone: +79126382765

\*\* Institute of Metal Physics UB RAS, S. Kovalevskaya str. 18, Yekaterinburg, 620990, Russia

\*\*\* Lomonosov Moscow State University, Moscow, 119991, Russia

Investigation of energy spectrum of 3d-transition metal oxides is actual problem of the condensed matter physics. Recently interesting results were achieved in connection with the observation of photoluminescence (PL) and photoluminescence excitation (PLE) spectra of  $\text{Ni}_x\text{Zn}_{1-x}\text{O}$  solid solutions. Narrow lines  $I_1$  and  $I_2$  were observed at the energies of 3.339 eV and 3.393 eV respectively [1,2]. In this paper the PL measurements were made on the samples of solid solutions  $\text{Ni}_x\text{Zn}_{1-x}\text{O}$  ( $x = 0.3$ , and  $0.6$ ) with rock salt crystal structure in the temperature region of (8 – 50) K. The measurements of PL spectra under soft X-ray excitation were made on a SUPERLUMI station (HASYLAB (DESY), Hamburg). The time-resolved PL spectra as well as the PL decay kinetics under XUV excitation have been measured on a BW3 beamline.

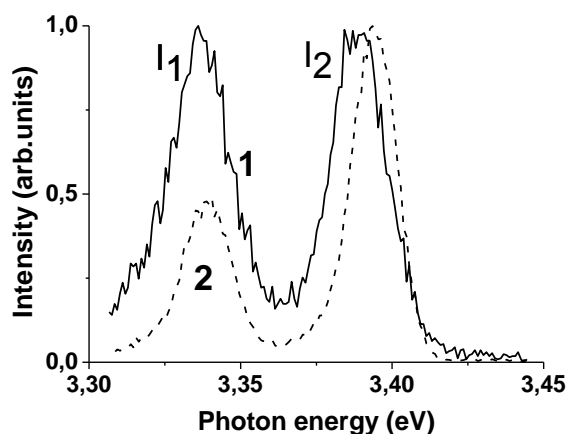


Figure 1. X-ray luminescence spectra (fast component) of  $\text{Ni}_{0.6}\text{Zn}_{0.4}\text{O}$  at temperatures 30 K (1) and 8 K (2). Excitation energy  $E_{\text{exc}}=130$  eV.

Fig. 1 represents narrow lines  $I_1$  and  $I_2$  at differ temperatures. It is well seen that the relation of maximal intensities of the lines changes with increasing of temperature. At 8 K the relation  $I_2/I_1$  is somewhat more than 2, at 30 K intensities become equal. The line  $I_2$  shifts towards low energies approximately by 7.5 meV. The shifting of this line is  $-0.35$  meV/K. The shifting of the line  $I_1$  is significantly less. The intensities decay with the time of 0,66 ns and 0,25 ns correspondingly. Such a fast radiative recombination is observed in  $\text{Ni}_x\text{Mg}_{1-x}\text{O}$  solid solutions where we expect only p-d charge transfer transitions. Taking into account the strong decreasing of the lines with temperature growing, similar to donor and acceptor excitons in II-VI compounds doped with 3d elements [3], shifting of the line  $I_2$  ( $-0.35$  meV/K) and the edge of p-d transitions at the temperature lowering from 300 K to 90 K received for thin films NiO on CaF2 substrate ( $-0.42$  meV/K) and on quartz substrate ( $-0.29$  meV/K) [4] we can assume that  $I_1$  and  $I_2$  lines arise due to p-d exciton annihilation. For the final conclusion a detailed investigation of the absorption edge in NiO at low temperatures is required by the methods of absorption and electroabsorption.

### REFERENCES

- [1] V. Sokolov, V. Pustovarov, V. Churmanov et al // Pis'ma v ZhETF. – 2012. – V.95, iss.10. – pp.595-600.
- [2] V. Sokolov, V. Pustovarov, V. Churmanov et al // Phys. Rev. B. – 2012. – V.86. – 115128.
- [3] V. Sokolov // Semiconductors. – 1994. – V.28. – pp. 329-343.
- [4] C.E. Rossi, W. Paul // J. Phys. Chem. Solids. – 1969. – V.30. – pp. 2295-2305.

<sup>1</sup> This work was partially supported by the Ural Branch of RAS (grant № 12-u-2-1030) and the Ministry of Education and Science of Russian Federation (the basic part of the government mandate). Also this research project has been supported by UrFU under the Framework Programme of development of UrFU through the «Young scientists UrFU» competition.

## RADIATIVE RELAXATION OF SOFT X-RAY PHOTONS IN COMPLEX OXIDES<sup>1</sup>

V.YU. IVANOV, V.A. PUSTOVAROV

\* Ural Federal University named after the first President of Russia B.N. Yeltsin, Mira street 19, Yekaterinburg, 620002, Russia, v.ivanov@urfu.ru, +7(343)3754711

The absorption of the X-ray photons in condensed matter is followed by the dissipation of the initial electronic excitation (EE) energy through several competitive tracks. The comparative study of the experimental manifestations of such tracks provides us with understanding the fundamental processes of the EE evolution. This work presents the comparative analysis of data obtained through two observation tracks of the exciting photon relaxation in the ultra-soft x-ray region (50-210 eV): x-ray fluorescence and photoluminescence in UV-VUV region. The goal of present research is to determine the participation of different crystal sublattices in EE evolution processes in the multi component wide-band gap oxide crystals.

This type of analysis has first been applied to the study of different tracks of EE relaxation in a binary beryllium oxide when excited near the K-edge of cation absorption [1,2]. The effect of resonant inelastic scattering of exciting photons was discovered in spectra of x-ray fluorescence. This is the evidence of the cation excitons relaxation through fast lattice distortions. It was determined that the energy loss associated to the processes of cation excitons relaxation is similar to the energy loss associated with the self-trapping of anion excitons excited in the vicinity of the fundamental absorption edge. Later on [3] the assumption was made that the relaxation of anion and cation excitons occurs in the same structural crystalline units of multi component oxide crystals. Therefore the observation of different tracks of the x-ray photons relaxation can be used to identify such units.

The present work summarizes the results of the study of different tracks of x-ray photons radiative relaxation in a number of multi component oxides.  $\text{Al}_2\text{BeO}_4$ ,  $\text{Be}_2\text{SiO}_4$ ,  $\text{Al}_3\text{Be}_2\text{Si}_6\text{O}_{18}$  crystals form a group of compounds characterized by similar cation radii but different in the symmetry of the cation-oxygen tetrahedral.  $\text{Y}_2\text{SiO}_5$ ,  $\text{Gd}_2\text{SiO}_5$ ,  $\text{La}_2\text{Be}_2\text{O}_5$  crystals form another group of compounds differ in cation radii in different crystal sublattices and characterized by the presence of d-states in the bottom of conduction band.

It is determined that for the crystals of the first group the fast relaxation of cation excitons appearing when the crystal absorbs the quantum with energies near the K- or L-edges of the crystal-forming cations of Al, Be and Si is observed only if the symmetry of the local crystalline unit nearing the cation is lowered. It is important to mention that the fast relaxation of the low energy anion excitons appearing in a crystal as a result of the initial excitation energy transfer (Auger process) occurs in the same local crystalline units. When the experiment is carried out with the crystals containing heavy cations the fast relaxation for neither cation nor anion excitons (nor the associated deformation of the crystal lattice) is observed near the light cations. The presence of d-states in the bottom of conduction band is most possible reason of this experimental fact. The excitons appearing in this process are characterized by a heavier (trapped) electronic component and that makes the following exciton relaxation energetically more efficient in comparison to the relaxation of excitons with the electronic component formed by the s- or p-orbitals of light cations.

### REFERENCES

- [1] V.Pustovarov, V. Ivanov, M. Kirm, A.Kikas, K.Kooser, T.Kõõmbre, A.Kruzhalov, E.Zinin // Journal Nuclear Inst. and Methods in Physics Research. – 2007. – A575. – № 1. 172–175.
- [2] T. Kaambre, A.Kikas, K.Kooser, V.Kisand, M.Kirm, A.Saar, E.Nommiste, V.Ivanov, V. Pustovarov, I. Martinson // Journal of Electron Spectroscopy and Related Phenomena. – 2007. – V.156–158. – P.299–302.
- [3] V.Ivanov, A.Kikas, T.Kõõmbre, M.Kirm, I.Kuusik and V. Pustovarov // IOP Conf. Series: Materials Science and Engineering. – 2010. V.15. - Art. No.012088.

<sup>1</sup> This work was partially supported by the Ministry of Education and Science of Russian Federation (the basic part of the government mandate)



## PULSED LUMINESCENCE OF LiF-Fe<sub>2</sub>O<sub>3</sub> CRYSTALS

*V.KOREPANOV\**, *P.PETIKAR\*\**, *A.KAMRIKOVA\*\*\**

*\*Tomsk Polytechnic University, Lenin Avenue 30, Tomsk. 634050, Russia, korepanov@tpu.ru, 89138416887*

*\*\* Tomsk Polytechnic University, Lenin Avenue 30, Tomsk. 634050, Russia*

*\*\*\* Tomsk Polytechnic University, Lenin Avenue 30, Tomsk. 634050, Russia*

Lithium fluoride doped with heavy metal oxides can be used as a scintillator in registration systems of astrophysical neutrinos and dark matter particles [1]. We have investigated the pulsed cathodoluminescence of LiF-Fe<sub>2</sub>O<sub>3</sub> crystal at 20...300 K within the time range of 10 ns to 10 ms. The luminescence was excited by means of a high-current nanosecond electron beam. The luminescence was registered using an MDR 204 monochromator, PMT 97, 83, and a Tektronix oscilloscope. The temporal resolution is 7 ns.

Two bands of pulsed cathodoluminescence with the maxima at 2.65 eV and 2.85 eV have been detected in the spectra of the activator luminescence of LiF-Fe<sub>2</sub>O<sub>3</sub>. The bands apparently belong to the two types of electron states of the luminescent center. The decay kinetics of the luminescence in each band is described by two exponentials with the decay times at 300 K:  $\tau_1 = 1,9 \mu\text{s}$  and  $\tau_2 = 74 \mu\text{s}$ , respectively.

The decrease in the crystal temperature leads to the change in the luminescence decay time  $\tau$ , flashed light sums  $S = I \cdot \tau$ , and the ratio of band intensities  $I$ . At temperatures below 200 K, the slow decay component in the luminescence spectra is not noticeable against the background of the fast one due to the significant decrease in the intensity  $I$ . At 20 K, therefore, both the bands are only represented by the fast luminescence decay component with  $\tau_1 = 3,3 \text{ ms}$ .

The temperature dependence analysis of  $\tau$ ,  $I$  and  $S$  in the fast luminescence component shows that abrupt changes in the parameter values of pulsed cathodoluminescence (Fig. 1) are related to temperature intervals of the creation and accumulation of structural defects in pure lithium fluoride:

Analysis of the fast component luminescence shows that abrupt changes in parameter values pulsed cathodoluminescence (Fig. 1) associated with temperature intervals of the formation and accumulation of structural defects in pure lithium fluoride: the destruction of the excitons and delocalization of H-centers (50 - 60 K), delocalization of  $V_k$ -centers (125 K), decrease in the formation of self-trapped excitons, and increase in the formation of color centers (100 - 120 K).

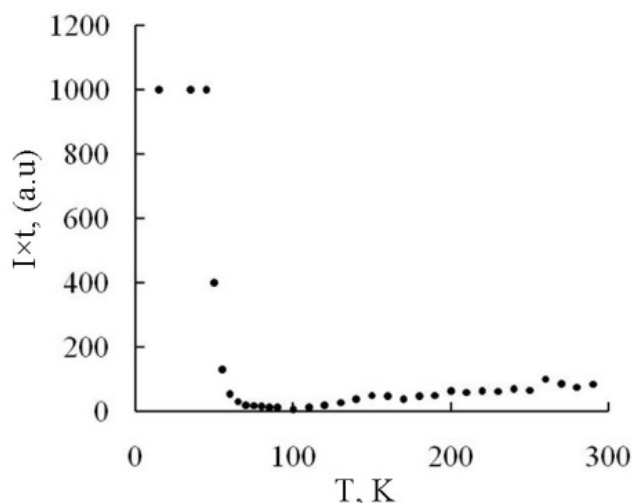


Fig. 1. Temperature dependence of  $S$  after exposure to the electron momentum

Therefore, the research findings allow us to experimentally determine how energy is transferred from the base of the LiF crystal center to the light - Fe<sub>2</sub>O<sub>3</sub> complex and to find out the reasons why there is a stage of the luminescence buildup in lithium fluoride crystals doped with heavy metal oxides.

### REFERENCES

[1] *D.Abdurashitov, A.Gektin, A.Nepomnyaschih, E.Radzhabov, N.Shiran // ISMART.- 2012, Dubna. –November 20.*

## CREATION OF REVERSIBLE AND IRREVERSIBLE RADIATION DEFECTS IN WIDE-GAP MATERIALS DOPED WITH DIFFERENT IMPURITIES<sup>1</sup>

A. LUSHCHIK\*, Ch. LUSHCHIK\*, T. KÄRNER\*, A. MAAROOS\*, A.I. POPOV\*\*, E. VASIL'CHENKO\*

\*Institute of Physics, University of Tartu, Riia 142, Tartu 51014, Estonia, [aleksandr.lushchik@ut.ee](mailto:aleksandr.lushchik@ut.ee), +372 7374619

\*\*Institute of Solid State Physics, University of Latvia, Kengaraga 8, Riga LV-1063, Latvia

Binary and complex wide-gap materials (WGMs,  $E_g > 5$  eV) doped with different impurities are widely used as detectors and dosimeters for photons, electrons, neutrons, light and heavy ions as well as media for the storage of radioactive waste, etc. The energy absorbed by WGMs during irradiation is transformed not only into luminescence of different types and heat but also into the formation of different structural radiation defects (RDs). According to long-standing investigations of the specific features of the creation and annealing processes of RDs, a part of radiation-induced damage can be annealed via a subsequent thermal heating – these are the so-called reversible radiation defects. However, a part of defects – irreversible RD – do not undergo a complete thermal annealing.

Contributions of different impurities to the creation of various RDs in WGMs of different types have been studied in Tartu and Riga for about a half of century. The changes of the characteristics of WGMs in the form of single crystals, ceramics or thin films caused by their irradiation with photons, electrons, neutrons,  $\alpha$ -particles and swift heavy ions (SHIs:  $^{197}\text{Au}$ ,  $^{238}\text{U}$ ,  $\sim 2$  GeV, GSI, Darmstadt) have been systematically investigated using a complex of highly sensitive methods of optical and thermoactivation spectroscopy (incl. synchrotron facilities in Moscow, Lund and Hamburg). It is worth noting that such SHIs spend more than 99.9% of their energy on ionization losses providing an extremely high density of electronic excitation within cylindrical ion tracks. Only a small part of SHIs energy is used in the end of ion path for the creation of RDs via elastic collisions with host atoms (the knock-out creation mechanism of RDs). Both reversible and irreversible RDs are formed at the periphery of ion tracks at fluences about  $\Phi = 10^{11}$  ions/cm<sup>2</sup>, while a sharp rise of the relative number of irreversible RDs is detected after irradiation with  $\Phi \geq 10^{12}$  ions/cm<sup>2</sup> when a considerable overlapping of neighbouring tracks takes place. The last fact agrees well with theoretical predictions of the collective creation of 3D defects under the dense irradiation of metal alloys predisposed to anharmonic interactions. These processes are realized in WGMs as well. Mixed WGMs with many atoms per unit cell exhibit increases radiation resistance due to the absence of crowdion-type displacement of interstitials that impedes the separation of defects within Frenkel pairs.

According to our experimental results, an introduction of luminescent impurities into WGMs with  $E_{\text{FD}} > E_g$  ( $E_{\text{FD}}$  – the threshold energy for the creation of a pair of Frenkel defects) decreases the efficiency of RDs creation via a solid-state analogue of the Franck-Hertz effect: there is a competition between the direct excitation of impurity centres by hot conduction electrons and defects creation at hot electron-hole recombination. However, in many metal oxides with  $E_{\text{FD}} > 3E_g$ , the situation is more complicated and the presence of various impurities just decreases the radiation resistance of a material.

Even the traces of calcium (important feature is the presence of  $3d^0$  states) cause a sharp increase of the creation efficiency of RDs, especially of irreversible ones in WGMs, which did not undergo specific procedures of a deep purification. According to recent theoretical calculations, complex metal oxides (in particular,  $\text{CaSO}_4$ ) possess a complex conduction band containing a d-subband about 1.5 eV above the bottom formed by s-states. A long-lived conduction d-electron participates in a slow hopping diffusion resulting in the appearance of a tunnel luminescence and increased recombination probability between a d-electron and a radiation-induced hole within the core electron shells of a metal oxide. The energy released at such recombination is sufficient for the creation and transformation of structural RDs.

Several possibilities of the increasing of radiation resistance of WGMs are discussed: synthesis of thin layers under additional doping with fluorine that decreases the surface contamination; the use of materials with complex multiatomic unit cells; the absence of complex impurity centres, which contain two-three spatially close heavy ions and, therefore, serve as seeds for the creation of radiation damage via collective creation mechanisms of irreversible RDs. The combination of high luminescence yield and high resistance against irradiation, needed for many applications, also depends on the density of electronic excitations formed during irradiation and the mechanical stresses (pre- and radiation-induced ones).

<sup>1</sup> This work was supported by Estonian Research Council – Institutional Research Funding IUT02-26.

## THERMOLUMINESCENT AND PHOTOLUMINESCENT SPECTROSCOPY OF Li<sub>6</sub>GdB<sub>3</sub>O<sub>9</sub>:Ce CRYSTAL-FIBERS

*D. O. VOSTROV, I. N. OGORODNIKOV, V. A. PUSTOVAROV, I. N. SEDUNOVA*

*Ural Federal University, Yekaterinburg, Russia, VostrovDO@yandex.ru*

The Ce-doped lithium lanthanide borates doped with rare-earth ions present a class of new scintillators. The Li<sub>6</sub>GdB<sub>3</sub>O<sub>9</sub>:Ce incorporate the popular neutron absorbing nuclei with high cross-sections (B, Li and Gd) and consequently it is considered as a potential material for thermal neutron detection. Synthesis of crystal-fiber samples is more technological process than the crystal growing. The investigation of luminescence characteristics of LGBO:Ce materials in bulk and powder forms was carried out early [1-2]. The present work is devoted to studying of thermoluminescence and photoluminescence spectroscopy in Li<sub>6</sub>GdB<sub>3</sub>O<sub>9</sub>:Ce fibers by X-ray and ultraviolet (UV) excitation.

Li<sub>6</sub>GdB<sub>3</sub>O<sub>9</sub>:Ce were produced *I. N. Sedunova* using micro pulling down method at Universite Lyon 1 (Lyon, France) at argon atmosphere. The steady-state X-ray-induced luminescence (XRL) spectra measured in the interval from 1.5 to 6.2 eV at the 90 and 300 K temperature. The thermoluminescence (TL) glow curves in spectral-integrated and in spectral-selective regime were measured at linear heating rate of 0.3 K/s over the temperature range from 90 to 500 K. The photoluminescence (PL) and PL excitation spectra measured in the interval from 1.4 to 6 eV at the 90 and 300 K.

XRL spectra is characterized by low-intensity broad band at 2.95 – 3.1 eV (400 – 420 nm) is attributed to the d → f transitions in Ce<sup>3+</sup> ions. At TL glow in spectral-integrated regime observed four peaks around 142.5, 199.5, 270.5 and 312.5 K. However for TL glow in spectral-selective regime not observing emission at 313 nm (3.97 eV) and 400 nm (4.00 eV). PL spectra is characterized by a broad band at 2.95 – 3.1 eV (400 – 420 nm) and a peak in the region 1.93 eV (643 nm). We discuss in the paper the peculiarities of electron excitations dynamics and recombination processes in fibers that explain the experimental data.

### REFERENCES

- [1] *J.B. Czirr, G.M. MacGillivray, R.R. MacGillivray, P.O. Seddon* // Nucl. Instr. and Methods in Phys. Res, 1999, A 424 (1), pp.15–19.
- [2] *I.N. Ogorodnikov, V.A. Pustovarov, S.I. Omelkov, A.V. Tolmachev, R.P. Yavetskiy* // Optics and Spectroscopy, 2007, 102 (1), pp.60–67.

## A DEFECT FORMATION IN ALKALI METAL SULFATE

*T.N. NURAKHMETOV, R.A. KUTERBEKOV, A.Zh. KAINARBAI, A.M. ZHUNUSBEKOV, K.Zh. BEKMYRZA, B.M. SADYKOVA, S. PAZYLBEK, D.H. DAURENBEKOV*

*Eurasian National University named after L.N. Gumileva, Kazhymukan 13, Astana, 010008, Kazakhstan,  
[kbekmyrza@yandex.kz](mailto:kbekmyrza@yandex.kz) +7 702 33 43 610*

Defect formation in alkali metal sulfate is carried by subthreshold mechanisms. Experimentally shown that x-ray, ultraviolet and Synchrotron radiation create electron and hole trapping centers in sulfates by similar way.

Based on the study of recombination luminescence which occurs when electrons and holes recombine with the hole and electron trapping centers we can judge about the mechanisms of generation of these defects. Almost all sulfates when irradiated by X-rays and ultraviolet radiation arise a short-waves (3.6-3.8 eV) and long-wavelength broad band with several maxima in the spectral range of 2 - 3.2 eV. Figure 1 shows the spectrum of x-ray irradiated crystal  $K_2SO_4$  at liquid nitrogen temperature (curve 1). The same figure (curve 2) shows the photoluminescence  $K_2SO_4$  crystal which excited by a photons with energy 6.0 - 6.2 eV at 300 K. Figure 1 shows that the X-ray and ultraviolet light are create the same emission spectra in the spectral region 3.65 - 3.7 eV, and 2.6-3.0 eV.

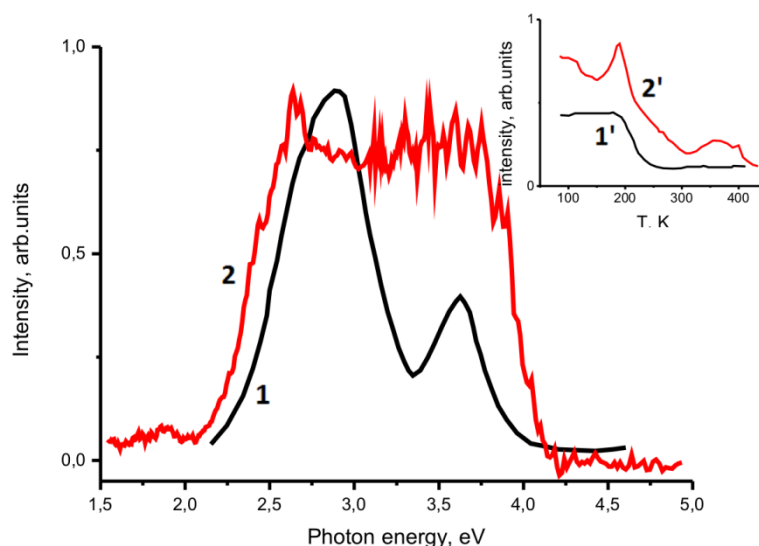


Fig. 1. X-ray spectra and photoluminescence spectra of the irradiated crystal  $K_2SO_4$  and their temperature dependence

Inset in the figure shows the temperature dependence of x-ray at 3.65 - 3.7 eV (curve 1') and 2.6-3.0 eV (curve 2') in  $K_2SO_4$  from liquid nitrogen temperature to 400K. It is seen that the emission of 3.65 eV at 200 K decreases exponentially, and the broad band emission of 2.6 - 3.0 eV in the same temperature range luminescence intensity increase and then decreases exponentially

It is assumed that the intrinsic radiation of 3.65 eV associated with the recombination of electrons with self-trapped hole. Radiation at 2.6 - 3.0 eV associated with recombination processes of electron-hole trapping centers which were created by irradiation. Increase of luminescence intensity in broad emission band in the temperature range (~200 K) may be related with delocalization of the electron and hole on the accumulated trapping centers during the phase transition.

We are discuss the mechanisms creating correlated electron and hole trapping centers responsible for the broad emission band recombination.

## CONFIGURATION OF SELF-TRAPPED EXCITON IN AL<sub>2</sub>O<sub>3</sub>

A.Y. KUZNETSOV, M.A. BOTOV, A.S. MAKAROV, A.B. SOBOLEV

Ural Federal University, Mira 19, Yekaterinburg, 620002, Russia, scibma@gmail.com, 375-47-11

An exciton is a quantum of electronic excitation energy traveling in the periodic structure of a crystal. In a wide range of solids including Al<sub>2</sub>O<sub>3</sub> crystal this bounded state of an electron and hole can undergo self-trapping and form a small molecule-like quasiparticle.

Presented work is devoted to theoretical investigation of possible configuration of self-trapped exciton (STE) in corundum crystal. Our study is based on *ab-initio* calculations performed in CRYSTAL09 program package using Hartree-Fock approximation and density functional theory. Atoms of crystal were described by their full-electron basis set (8-511-1 for Al and 8-411G for O) with optimized valence shells. Supercell for defect calculation contain 120 atoms. All calculations were made with full geometry relaxation of supercell.

As a first part of study we perform calculation of perfect Al<sub>2</sub>O<sub>3</sub> crystal. Basis sets was shown to be correct. After that STE modeling was carried out. Orientation of STE in crystal is close to be perpendicular to z-axis, i.e. it lies mainly in horizontal plane.

As far as electronic structure is concerned it is presented in density of states and charge density distributions (e.g. Fig.1 and Fig.2).

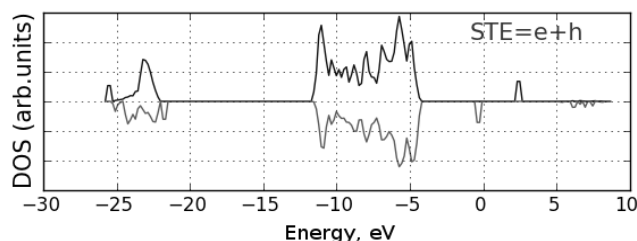


Fig. 1. Density of States chart for STE in Al<sub>2</sub>O<sub>3</sub> crystal calculated by B3LYP method in supercell with 120 atoms

Electron and hole levels are clearly observable. It should be noted that the hole density distribution differs from one calculation method to another. Hartree-Fock method localize hole predominantly at one oxygen while hybrid B3LYP method delocalize hole density between two near oxygen atoms in comparable proportions. Center of electron density and two hole-carrying oxygen atoms in the last case form not a line but rather some kind of triangle with obtuse angle value 147 degrees.

Two defect levels in band structure of material are showing up in luminescence spectrum also. Experimental STE luminescence bands are known to be 3.8 eV and 7.5 eV.

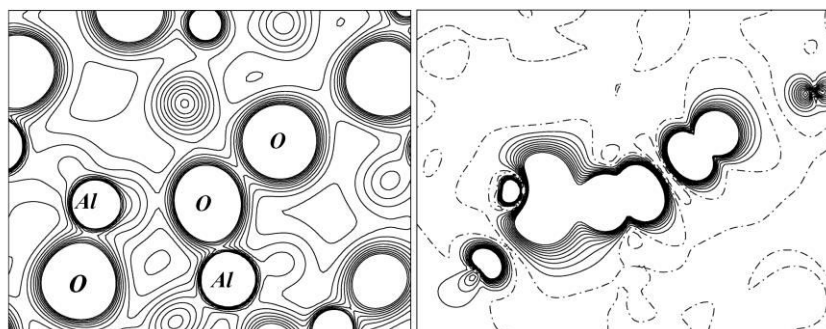


Fig. 2. Charge (left) and spin (right) density maps of STE (horizontal configuration). Slice represents an STE-plane (which contains electron density center and two oxygen atoms with hole localized on them). Presented maps covers data obtained by B3LYP method in supercell with 120 atoms in corundum crystal

Our calculations give band of luminescence close to 3.8 eV. Differences between all used methods of calculation do not exceed 0.2 eV.

## ON CHANNELING OF RELATIVISTIC ELECTRONS IN THE FIELD OF CROSSED LASER BEAMS

*E.N. FROLOV<sup>1,2</sup>, A.V. DIK<sup>1</sup>, S.B. DABAGOV<sup>1,3,4</sup>, K.P. ARTYOMOV<sup>5</sup>*

<sup>1</sup>LPI RAS, Leninsky pr., 53, Moscow, 119333, Russia, [frol.onn@gmail.com](mailto:frol.onn@gmail.com), +7 (985) 166 62 66

<sup>2</sup>NR TPU, Lenina st., 30, Tomsk, 634050, Russia

<sup>3</sup>LNF INFN, Via E. Fermi, 40, Frascati (RM), 00044, Italy

<sup>4</sup>NRNU MEPhI, Kashirskoye sh., 31, Moscow, 115409, Russia

<sup>5</sup>IHCE SB RAS, Akademicheskoy av., 2/3, Tomsk, 634055, Russia

As known channeling of charged particles in crystals takes place when relativistic charged particles enter a crystal aligned under some specific angle to its main directions and perform oscillations transverse to the motion direction in the averaged lattice potential [1, 2]. Great attention is paid to the phenomena of channeling since it provides beam shaping and steering techniques. Besides, channeled particles become a source of special kind of radiation known as channeling radiation [3]. Some studies have shown that channeling conditions could be realized not only in crystals and not only for charged particles, but also in other systems such as capillaries (neutral particles channeling) (see in [4] and Refs. in), plasma [5], nanotubes (see in [6] and Refs. in) [7] and laser fields [8, 9, 10].

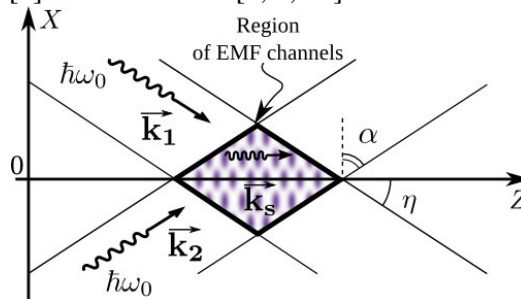


Fig. 1. General system geometry. The region, where the channels are formed, is outlined in the center. The peaks of transverse electrical component of the field propagating in the  $k_s$  direction are shown in color.

In this work we present new results on relativistic electron beam channeling in the field of crossed laser beams (Fig. 1). As we reported before [11, 12], relativistic charged particles in this field could be trapped in channels of the averaged potential:

$$U_{\text{eff}} = \frac{e^2 u_0^2 k^2 \left[ (1 + \cos^2 \alpha) \beta_0^2 - \cos(2\alpha) - 2\beta_0 \sin \alpha \right]}{8\gamma m \omega_0^2 (1 - \beta_0 \sin \alpha)^2 \cos^2 \alpha}, \quad (1)$$

where  $m$  and  $e$  stand for channeled particle's mass and charge,  $\gamma$  is particle Lorentz factor,  $\beta_0$  is particle longitudinal velocity normalized by the speed of light,  $u_0$  is the summarized longitudinal vector potential amplitude,  $\alpha$  is the angle shown on the Fig. 1,  $k$  is the wave vector absolute value and  $\omega_0$  is laser frequency.

This expression differs greatly from the conventional ponderomotive potential usually used for the description of such systems and has some peculiarities to be covered by our report together with the dynamics and radiation of electron bunches channeled in the potential.

### REFERENCES

- [1] D.S. Gemmel // Rev. Mod. Phys. – 1974. – 46 № 1. 129
- [2] J. Lindhard // K. Dan. Vidensk. Selsk. Mat.-Fys. Medd. – 1965. – 34 № 14
- [3] M.A. Kumakhov // Phys. Lett. A. – 1976 – 57. 17
- [4] S.B. Dabagov // Phys. Usp. – 2003. – 46. 1053
- [5] A.V. Dik, A.Z. Ligidov, and S.B. Dabagov // Nucl. Instr. Meth. B. – 2013. – 309. 210
- [6] S.B. Dabagov, and N.K. Zhevago // Riv. del Nuovo Cimento. – 2008. – 31 № 9. 491
- [7] A. Karabarbounis, S. Sarros, and Ch. Trikalinos // Nucl. Instr. Meth. B. – 2013. – 316. 160
- [8] M. Bertolotti, C. Sibilila, and Li Fuli // Trends in Quantum Electronics. – 1986. 155
- [9] A.V. Andreev, and S.A. Akhmanov // Zh. Eksp. Teor. Fiz. – 1990. – 99. 1668
- [10] M.V. Fedorov, K.B. Oganesyan, and A.M. Prokhorov // Appl. Phys. Lett. – 1988. – 53. 353
- [11] E.N. Frolov, A.V. Dik, and S.B. Dabagov // Nucl. Instr. Meth. B. – 2013. – 309. 157
- [12] E.N. Frolov, A.V. Dik, and S.B. Dabagov // J. Phys. Conf. Ser. – 2014. – (to be published)

## THE INFLUENCE OF OXYGEN-CONTAINING IMPURITIES ON THE EMISSION DECAY KINETICS IN CsI

*L. TREFILOVA\**, *V. YAKOVLEV\*\**, *N. OVCHARENKO\**, *A. GRIPPA\**, *A. MITICHKIN\**

*\*Institute for Scintillation Materials, 60 Lenin Avenue, Kharkov 61001, Ukraine, [laratrefilova@ukr.net](mailto:laratrefilova@ukr.net), +38(057)3410246*

*\*\*Tomsk Polytechnic University, 30 Lenin Avenue, Tomsk 634034, Russian Federation*

This paper ascertains whether any oxygen-containing impurities in CsI lattice increase the emission decay time at 310nm. CsI, CsI:Na, CsI:Eu crystals doped with oxygen-containing impurities Cs<sub>2</sub>O, WO<sub>3</sub>, Cs<sub>2</sub>WO<sub>4</sub>, Cs<sub>2</sub>SO<sub>4</sub>, Cs<sub>2</sub>CO<sub>3</sub>, CsIO<sub>3</sub> were exposed to an electron pulse beam. Na, Eu and W concentrations were chemically determined. The concentration of oxoanions was evaluated by their absorption coefficient. It was found that either under electron or two-photon excitations [1] the cathodoluminescence decay curves at 310 nm fit the sum of two exponents:

$$I = I_f \exp(-t/\tau_f) + I_s \exp(-t/\tau_s), \quad (1)$$

where  $I_f$  and  $I_s$  - intensities of fast and slow decay components at  $t=0$ ;  $\tau_f$  and  $\tau_s$  - time decay constants of fast and slow components.

It was also found that  $WO_4^{2-}$ ,  $SO_4^{2-}$ ,  $IO_3^-$ ,  $CO_3^{2-}$  oxoanions do not increase as thought by [2] but dramatically decrease the emission decay time especially in crystals containing  $CO_3^{2-}$  ions (Table 1).

Table 1. Fitting and experimental parameters of 310nm emission decay kinetics at T=295K

№	Crystal	$C_{cation}$ , (mass%)	Oxoanion absorption coefficient, $cm^{-1}$	Emission decay kinetics parameters in the region of $\lambda_{max}=310$ nm					
				$I_f$	$I_s$	$I_s/I_f$ , %	$\tau_f$ ns	$\tau_s$ ns	$\tau_{90\%}$ * ns
1	“pure” CsI	–	–	3.8	0.4	10.5	27	150	77
2	CsI:Cs <sub>2</sub> O	–	$CO_3^{2-}$ , $K_{880cm^{-1}} = 0.186cm^{-1}$	4.8	0.1	2.1	25	150	61.2
3	CsI:CsIO <sub>3</sub>	–	$IO_3^-$ , $K_{820cm^{-1}} = 0.24cm^{-1}$	3.9	0.11	2.6	25	150	65
4	CsI:WO <sub>3</sub>	0.014%W	–	3.3	0.35	10.6	25	150	77
5	CsI:Cs <sub>2</sub> WO <sub>4</sub>	0.04%W	$WO_4^{2-}$ , $K_{820cm^{-1}} = 0.24cm^{-1}$	4.1	0.35	8.5	25	150	68
6	CsI:Cs <sub>2</sub> SO <sub>4</sub>	–	$SO_4^{2-}$ , $K_{630cm^{-1}} = 0.15cm^{-1}$	3.2	0.35	9.1	25	120	68.4
7	CsI:Cs <sub>2</sub> CO <sub>3</sub>	–	$CO_3^{2-}$ , $K_{880cm^{-1}} = 0.73cm^{-1}$	4.4	0.03	0.7	21	120	47.6
8	CsI:EuI <sub>2</sub> ,Cs <sub>2</sub> CO <sub>3</sub>	0.04% Eu	$CO_3^{2-}$ , $K_{880cm^{-1}} = 0.024cm^{-1}$	5.7	0.15	2.6	25	120	51
9	CsI:EuI <sub>2</sub> ,Cs <sub>2</sub> CO <sub>3</sub>	0.039%Eu	–	3.55	0.4	11	23	150	75.6
10	CsI:NaI,Cs <sub>2</sub> CO <sub>3</sub>	0.002%Na	$CO_3^{2-}$ , $K_{880cm^{-1}} = 0.002cm^{-1}$	3.7	0.3	8.1	25	120	71
11	CsI:NaI,Cs <sub>2</sub> CO <sub>3</sub>	0.0028%Na	$CO_3^{2-}$ , $K_{880cm^{-1}} = 0.135cm^{-1}$	4.8	0.12	2.5	25	130	64.4

$\tau_{90\%}$ \* - time at which the emission intensity decreases by 90%

It was suggested that short- and long-living self-trapped excitons responsible for the fast and slow decay components arise in CsI lattice at 295K under an electron pulse. The oxoanions suppress the population of long-living state.

### REFERENCES

- [1] *H. Nishimura et al // Phys. Rev. B – 1995 – 51 – № 4, P. 2167.*  
 [2] *V.L. Cherginets et al // Kharkov University Bulletin, Chemical Series – 2012 – 1026 – №21 (44), P. 308-312.*

## DYNAMICAL DEFECTS IN IRRADIATED MATERIALS AND RADIATION STABILITY OF SOLIDS

*V.V. UGLOV\**, *N.T. KVASOV\**, *V.I. SHYMANSKI\**, *G.E. REMNEV\*\**

\* *Belarusian State University, Minsk, Belarus, e-mail: [shymanskiv@mail.ru](mailto:shymanskiv@mail.ru), [uglov@bsu.by](mailto:uglov@bsu.by) 220030, Nezavisimosty ave., 4*

\*\* *High-Voltage Research Institute at of National Tomsk Polytechnic University, e-mail: [remnev@hvd.tpu.ru](mailto:remnev@hvd.tpu.ru), 2a Lenin Ave., Tomsk, 634028, Russia*

Scattering cross-section  $\sigma$  and threshold displacement energy  $E_d$  are fundamental parameters used in radiation physics for description of the charged particles deceleration in the matter. These parameters define the radiation stability of the materials. It is evidence that the binding energy  $E_b$  is a part of the threshold displacement energy  $E_d$ . The correlation between theoretical, experimental and simulated results of  $E_d$ ,  $E_b$ , Young module ( $E$ ), melting point ( $T_m$ ) and sublimation energy ( $E_s$ ) determination for different materials is discussed.

The nature of another part of threshold displacement energy  $E_d$  is conditioned by the energy atom loss during its motion in the area of instability. In this area the energy of the atom is less than  $E_d$  and the Frenkel's defects are not generated. Thereupon the dynamical defects generated during the irradiation are considered as a pair of vacancy and knocked-on atom existing during a short period of time ( $10^{-12} - 10^{-11}$  s). The maximum moving-off the atom is characterized in this case by the radius of the area of instability  $R$ . Its motion can be described by the following equation:

$$\frac{d^2r}{dt^2} + \xi \frac{dr}{dt} + f(r) = 0 \quad (1)$$

where  $\xi$  – the coefficient characterizing the reaction of the matter on the moving atom ( $\xi=7.72 \cdot 10^{-44} N \cdot Z/m$ ),  $N$  – atoms concentration in the matrix,  $f(r)$  – the energy of the electrostatic interaction attributed to the atom mass  $m$ . The law of motion of the atom, the value of  $R$  and life time  $\tau$  of the dynamical defects for the considering materials were determined after the simulation. The following expression for threshold displacement energy was suggested:

$$E_d = E_b + A_e + mv\xi R, \quad (2)$$

where  $v$  – the average velocity of the atom in the area of instability,  $A_e$  – the work carrying out for overcoming the electrostatic forces.

In the work the possible ways of increase of radiation stability of solids and producing of nanostructured materials are discussed.



## SIMULATION OF SUBLINEAR DOSE DEPENDENCE OF THERMOLUMINESCENCE AS A RESULT OF COMPETITIVE INTERACTION OF TRAPPING CENTERS

*S.V. NIKIFOROV, V.S. KORTOV*

*Ural Federal University, 19 Mira street, Ekaterinburg, 620002, Russian Federation, [s.v.nikiforov@urfu.ru](mailto:s.v.nikiforov@urfu.ru), +79126068140*

Nonlinear dose dependences of thermoluminescent (TL) yield are observed in a number of materials (LiF, SiO<sub>2</sub>, Al<sub>2</sub>O<sub>3</sub>, CaSO<sub>4</sub>:Dy) which are applied as a radiation detectors in dosimetry, geological and archaeological dating [1-4]. Superlinearity of dose response corresponds to growth of the dose dependence slope with dose increase. The decrease of this slope corresponds to sublinearity [5]. Sublinearity is usually observed at high doses and is explained by occupancy saturation of trapping centers with growth of irradiation dose. It was established [6], that sublinear dose dependence can occur in the case of simple “one trap-one recombination center” model, even when the state of centers’ occupancy is far from saturation. The point of view exists that the sublinearity can be associated with the competition in capture of charge carriers between the traps of different nature [7]. The calculation of dose dependences in terms of the interactive trap system model shows that the competitive interaction between two electron traps leads to appearance of superlinearity [1,3]. The TL dose dependences in the case of competition between traps, which can capture of carriers of different signs, are not investigated.

This work deals with the analysis of the possibility of TL dose response sublinearity in terms of the kinetic model of competitive interaction between electron and hole traps.

The electron (N), hole (M) traps and recombination center (H) are taking into account in the model under study. During the irradiation of the crystal at room temperature free charge carriers are formed, which can capture on electron and hole traps. Further during heating electrons, which are released from trap N, can recombine with hole, captured on trap M, at the same time with the radiative recombination at center H. It is proposed that the traps M are stable thermally during TL measurements. The hole occupancy of trap M increases with dose D, the probability of electron and hole recombination on this trap grows. As a result the number of recombination acts on the luminescence center H decrease. It leads to decrease of TL output and therefore to sublinear dose dependence. The system of differential kinetic equations, describing the model under study for excitation and heating stages, is solved numerically by Gear method. The concentrations of electrons and holes in delocalized bands and captured on the traps are calculated. The TL glow curves for different irradiation doses are calculated too. It is established that the TL output goes sublinear at certain set of model parameters. It is shown that the model under study can be used for explanation of sublinearity of TL peaks from deep traps in anion-defective aluminium oxide single crystals. The TL output of these peaks, according our experiments, are proportional to  $D^{0.3}$ .

### REFERENCES

- [1] *Sunta, C.M., Kulkarni, E.M., Yoshimura, E.M., Mol, A.W., Piters, T.M. and Okuno, E.*// Phys. Stat. Sol. (b). – 1994. – Vol. 186. – P. 199-208.
- [2] *Chen R., Yang X.H., McKeever S.W.S.*//J. Phys. D: Appl. Phys. – 1988. –Vol .21 . – P. 1452-1457.
- [3] *Nikiforov S.V., Kortov V.S., Kazantseva M.G.*//Phys. Solid State. -2014. – Vol. 56. – P. 536-541.
- [4] *Lakshmanan A.R., Bhatt R.C., Supe S.J.*//J. Phys. D: Appl. Phys. – 1981. –Vol .14 . – P. 1683-1706.
- [5] *Chen R., McKeever S.W.S.*//Radiat. Meas. – 1994. –Vol. 23. - P. 667-673.
- [6] *Lawless J.L., Chen R., Pagonis V.*//Radiat. Meas. – 2009. –Vol. 44 . – P. 606-610.
- [7] *Rodine E.T., Land P.L.* //Phys. Rev. B. – 1971. –Vol. 4 . – P. 2701-2704.

## FEATURES OF TL PROPERTIES OF TLD-500 DETECTORS IRRADIATED IN PULSED RADIATION FIELDS<sup>1</sup>

R.M. ABASHEV\*, A.I. SURDO\*, I.I. MILMAN\*\*, E.V. MOISEYKIN\*\*, M.I. VLASOV\*

\* Institute of Industrial Ecology of UB RAS, S. Kovalevsky, 20, Ekaterinburg, 620219, Russia, abashevrm@mail.ru, 7(343)3743771

\*\* Ural Federal University, Mira, 19, Ekaterinburg, 620000, Russia

Extending application of pulse X-ray sources of nano- and subnanosecond duration in radiation control, medicine, when studying fast-proceeding physical and chemical processes requires an adequate choice of measurement means of the absorbed doses from the personnel. It is important to note that the use of electronic dosimeters is complicated because of strong electromagnetic interference from pulsed sources. Therefore, thermoluminescent accumulative detectors are most commonly applied for these purposes. Available data indicate to TL output dependence from commonly used detector materials on the basis of LiF, CaF<sub>2</sub>, Li<sub>2</sub>B<sub>4</sub>O<sub>7</sub> from dose rates in an impulse of X-rays [1]. Therefore, the purposes of this research is to study features of accumulation and thermoluminescence processes by TLD-500 detectors on the basis of the anion-defective corundum irradiated by pulsed X-ray and electron beams with micro- and nanosecond pulse duration.

Features of TL properties of TLD-500 detectors excited by pulsed X-ray and electronic radiation in dose range from 10<sup>-2</sup> to 50·10<sup>4</sup> Gy and dose rates from 10<sup>6</sup> to 10<sup>10</sup> Gy/s were studied. It was found that in contrast to the stationary X-radiation TL response of TLD-500 detectors strongly depends on pulse dose rate P<sub>p</sub>. When P<sub>p</sub> ≥ 1.8·10<sup>7</sup> Gy/s and X-ray irradiation dose D higher 0.8 Gy TL curves are modified, along with the main peak at 430 K the peak at 570 K becomes rather intensive. Its contribution in illuminated light sum increases with increase not only P<sub>p</sub>, but also D in range from 0.8 to 70 Gy.

It is stated that when D ≥ 20 Gy occurs redistribution of light sums on high-temperature TL peaks at 720 and 800 K, with the greatest sensitivity to radiation under the conditions described being for the TL peak at 800 K (fig. 1). The emission band at 300 nm corresponding to peak at 800 K is observed in spectrum of TL. For peak at 800 K dose dependence is linear in the dose range from 2 to 50 kGy.

It is also shown that the range of application of TLD-500 detectors can be significantly expanded as the dose range studied in work corresponds to areas of radiation technologies such as sterilization of medical products, processing of food, modification of polymeric products, etc. Since the pulse electronic radiation of low-energy creates in the surface layer of the irradiated object a dose commensurable with the dose received by means of the electronic accelerator, the above mentioned can be used for express sterilization of products surfaces in the place, without resorting to the centralized procedure by means of accelerators.

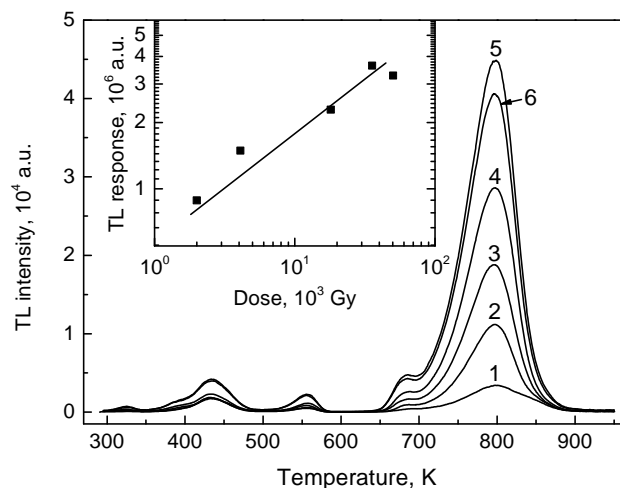


Fig. 1. TL curves of TLD-500 detectors irradiated by pulsed electron beam with P<sub>p</sub> ≈ 2.5·10<sup>10</sup> Gy/s and D: 1 – 0.5 kGy; 2 – 2 kGy; 3 – 4 kGy; 4 – 18 kGy, 5 – 36 kGy, 6 – 50 kGy. Dose dependence of peak at 800 K is shown on an insert.

### REFERENCES

- [1] [1] Gorbics S.G., Attix F.H. // *Health Physics*. – 1973. – Volume. – 25. Pages 499-506.

<sup>1</sup> This work was supported by Presidium of the Ural Branch of Russian Academy of Sciences (projects № 12-Y-2-032, № 14-2-III-174) and Russian Foundation for Basic Research (project № 14-02-31522)

## EFFECT OF DISLOCATION DENSITY ON EXCITON LUMINESCENCE INTENSITY OF GaN EPITAXIAL LAYERS

V.I. OLESHKO\*, S.G. GORINA\*, S.V. LAZAREV\*\*, V.V. LOPATIN\*

\* National Research Tomsk Polytechnic University, Lenin Avenue, 30, Tomsk, 634050, Russia,

E-mail: [oleshko@tpu.ru](mailto:oleshko@tpu.ru), +7 (3822) 701777 +1 +2293#

\*\* Karlsruhe Institute of Technology (KIT)/Synchrotron Facility ANKA, 76344 Eggenstein-Leopoldshafen, Germany

Group-III-nitrides are promising materials for creation of optoelectronic devices. Currently they are being used as a basis for many LEDs operating from UV to IR region. Gallium nitride (GaN) layers are usually being deposited on a foreign substrate such as sapphire ( $\text{Al}_2\text{O}_3$ ). Due to the difference of the lattice parameters direct deposition of gallium nitride on sapphire leads to formation of defective epitaxial layers with a dislocation density of about  $10^9 \text{ cm}^{-2}$ . Manufacturers constantly improve epitaxial growth technology and try to reduce the dislocation density, which is one of the main factors determining the radiation efficiency of GaN. Non-destructive methods of layers control are being used in the process of development of the quality gallium nitride layers producing technology. These are diffractometry and photoluminescence (PL).

The purpose of this work is to study the influence of dislocation density on the exciton luminescence intensity of GaN epitaxial layers.

We investigated GaN thin films with different dislocation densities grown on a sapphire substrate (001) by metal-organic vapor-phase epitaxy in an AIXTRON 200/RF-S horizontal flow reactor. On top of the substrate, an oxygen doped AlN nucleation layer (~20 nm) was deposited, followed by a 300 nm thick GaN layer. The GaN growth was then interrupted for the *in situ* deposition of a submonolayer-thick  $\text{SiN}_x$  mask, followed by GaN overgrowth. The dislocation density has been varied by tuning the  $\text{SiN}_x$  interlayer deposition time between 0 and 180 s. The total thickness of GaN film was  $1.8 \mu\text{m}$  for samples with the  $\text{SiN}_x$  layer and  $2.4 \mu\text{m}$  for the sample without it. The dislocation density in four samples was measured by diffractometry and reached  $(22.7; 8.5; 5.3; 2.9) \cdot 10^8 \text{ cm}^{-2}$ , respectively. PL of the samples was excited by a pulsed nitrogen laser ( $\lambda = 337.1 \text{ nm}$ ) with a pulse duration of ~ 4 ns at 300 K. PL spectra were measured using a fiber optic spectrometer AvaSpec-2048-2.

Measured PL spectra show that all the samples have spectrum dominated by peak at 363 nm (FWHM ~ 100 meV, decay time  $\tau \leq 15 \text{ ns}$ ). This peak belongs to GaN ( $E_g = 3.39 \text{ eV}$  at 300 K) and it is caused by recombination of excitons bound to defects [1]. Dependence of PL intensity on the dislocation density in the samples is shown in Fig. 1.

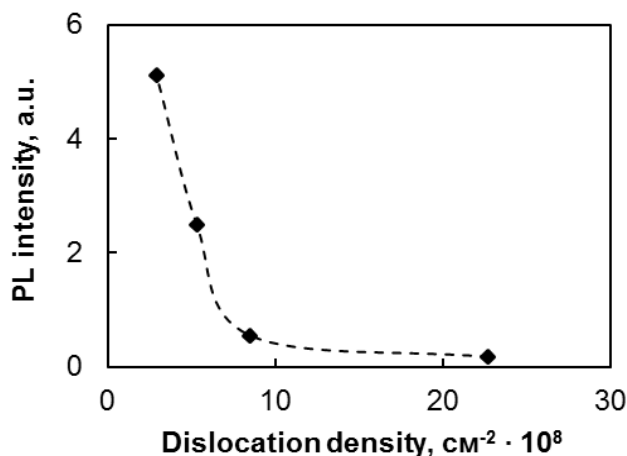


Fig. 1. Dependence of PL intensity on the dislocation density in GaN.

The results of this work demonstrate a high sensitivity of PL method to the total dislocation density in GaN epitaxial layers. Apparently, the dislocations are one of the main types of defects responsible for non-radiative recombination of excitons in epitaxial GaN.

### REFERENCES

- [1] Bunea G.E., Herzog W.D., Unlu M.S., Goldberg B.B., Molnar R.J. // *Appl. Phys. Lett.* – 1999. – V. 75. – № 6. P. 838-840.

## STUDY OF THE $D(p, \gamma)^3\text{He}$ REACTION AT ULTRALOW ENERGIES USING A ZIRCONIUM AND TITANIUM DEUTERIDE TARGETS

*V.M. BYSTRITSKY\**, *A.R. KRYLOV\**, *A.V. PHILIPPOV\**, *G.N. DUDKIN\*\**, *G.A. MESYATS\*\*\**, *B.A. NECHAEV\*\**,  
*V.N. PADALKO\*\**, *F.M. PEN'KOV\*\*\*\**, *YU.ZH. TULEUSHEV\*\*\*\**, *M. FILIPOWICZ\*\*\*\*\**, *VIT.M. BYSTRITSKII\*\*\*\*\**,  
*S. GAZI\*\*\*\*\**, *J. HURAN\*\*\*\*\**

*\*Joint Institute for Nuclear Research, Dubna, Moscow Region, Russia*

*\*\*National Scientific Research Tomsk Polytechnic University, Tomsk, Russia*

*\*\*\*Lebedev Physical Institute of the Russian Academy of Sciences, Moscow, Russia*

*\*\*\*\*Institute of Nuclear Physics, Almaty, Kazakhstan*

*\*\*\*\*\*AGH University of Science and Technology, Faculty of Energy and Fuels, Cracow, Poland*

*\*\*\*\*\*Trialpha Energy, Inc., Foothill Ranch, CA, USA*

*\*\*\*\*\*Institute of Electrical Engineering SAS, Bratislava, Slovakia*

### ABSTRACT

The article is devoted to the investigation of a pd-reaction ( $p + d \rightarrow {}^3\text{He} + \gamma(5.5 \text{ MeV})$ ) undergoing in titanium and zirconium deuterides in astrophysical collision energy region of protons and deuterons ranging from 5.3 to 10.5 keV. The experiments have been performed using the Hall NSR TPU (Tomsk, Russia) pulsed plasma accelerator. The number of accelerated protons in 10  $\mu\text{s}$  pulse was  $5 \cdot 10^{14}$  at a repetition rate of  $7 \cdot 10^{-2}$  Hz. Detection of 5.5 MeV gamma rays was carried out using eight detectors based on crystals of NaI(Tl) ( $100 \times 100 \times 400$  mm) placed around the TiD target. Dependences of the astrophysical  $S$ -factor  $s$  and the effective pd reaction cross sections on the proton-deuteron collision energy are measured. The result of pd-reaction study in zirconium deuteride agrees with the experimental data obtained by the LUNA collaboration with the target of gaseous deuterium. For the first time, the potential electronic screening of the interacting protons and deuterons in titanium deuteride has been measured.

## FORMATION OF DIAMAGNETIC PRODUCTS IN NITRATE-CONTAINING MATRICES UNDER THE ACTION OF LIGHT QUANTA WITH AN ENERGY OF 5.58 eV<sup>1</sup>

*M.B. MIKLIN\*, L.D. KRIGER\*, V.A. ANAN'EV\**

*\*Kemerovo State University, Krasnaya street, 6, Kemerovo, 650043, Russian Federation, miklin@kemsu.ru, 9039098094*

Photolysis of crystalline nitrates and nitrate -containing crystals by light with photon energy of 4.88 eV (254 nm) was studied in detail elsewhere. It is known that the quantum yields of the products, as well as the direction of the chemical breakdown of molecules and molecular ions can greatly depend on the energy of the acting radiation. The aim of this work is to study the composition and effectiveness of chemical degradation processes occurring electronically excited nitrate ions in different matrices under the action of light with energy 5.58 eV (222 nm) at 300 K.

Identification of products and determine their content were carried out methods of optical and infrared spectroscopy in solids and chemical analysis after dissolution of the irradiated samples. Photolysis was studied crystalline nitrates of alkali and alkaline earth metals, as well as ion-molecular crystals doped by nitrate ions. It is shown that the composition of the decomposition products of the nitrate ion is not essentially changed. It was shown existence of other (additional) channel decomposition, resulting in a substantial change in the quantum yields. Crystalline environment play an important role in the redistribution of efficiency of channel decomposition.

---

<sup>1</sup> This work was supported by gosudarstvennogo zadaniaya KemGU N2014/64

**PROCESSES OF CHEMICAL DEGRADATION OF ELECTRONICALLY EXCITED STATES OF DIFFERENT SYMMETRY AND ENERGY IN CRYSTALLINE NITRATES<sup>1</sup>**

*M.B. MIKLIN\*, L.D. KRIGER\*, V.A. ANAN'EV\**

*\*Kemerovo State University, Krasnaya street, 6, Kemerovo, 650043, Russian Federation, miklin@kemsu.ru, 9039098094*

Low-energy excited states of the nitrate ion have the symmetry (group D3h):  ${}^1A_1''$ ,  ${}^3E'$ ,  ${}^1E'$  and  ${}^2E'$  and arising from the transitions  $a_2'' \leftarrow a_2'$  ( $\lambda$  max  $\sim$  300 nm),  $a_2'' \leftarrow e''$  ( $\lambda$  max  $\sim$  250 nm),  $a_2'' \leftarrow e''$  ( $\lambda$  max  $\sim$  200 nm), and  $a_1' \leftarrow e'$  ( $\lambda$  max  $\sim$  185 nm), respectively [1]. These may lead to different chemical reactions, which depend on the symmetry of the excitations and of its energy. The aim of this paper is to explore ways of decomposition of nitrate ion in different crystal matrices depending on the symmetry energy and its electronically excited state.

Light sources used for photolysis: 1)  $\lambda = 172$  nm - xenon excilamp, 2)  $\lambda = 222$  nm – chlorine-krypton excilamp, 3)  $\lambda = 253.7$  nm - low pressure mercury lamp and 4)  $\lambda \geq 310$  nm - high pressure mercury lamp with a light filter. ESR, UV/Vis and IR spectroscopy was used for the registration of the photolysis products in solids.  $\text{NO}_2^-$  content in samples was determined by spectrophotometrically after dissolving the sample in water at pH 2. Determination of  $\text{ONOO}^-$  was performed iodometrically after dissolving the samples in an acetate buffer.

Photochemical decomposition of the nitrate to nitrite under the action of light with  $\lambda \geq 310$  nm is observed at temperatures above 400K only.

Irradiation of crystalline nitrates with light  $\lambda = 253.7$  nm or 222 nm causes in their optical and vibrational spectra of absorption bands characteristic of nitrite ions and peroxyxynitrite. Paramagnetic particles were not found in this case.

Photolysis of crystalline nitrates by light 172 nm at 300K ions leads to formation of nitrite and peroxyxynitrite. Formation paramagnetic products not been found. A similar effect at 77 showed that nitrates of sodium, potassium and cesium ions generated radical atomic oxygen  $\bullet\text{O}^-$ , and in rubidium nitrate additional radical  $\bullet\text{NO}_2$ .

Quantum yield of the photolysis products were increasing quite significantly with growth photon energy and depend on the free volume strongly. Symmetry of the excited state defines a set of products and changes channels their formation.

## REFERENCES

- [1] *Anan'ev V., Miklin M. // Optical Materials. - 2000. -V.14. -P. 303.*

<sup>1</sup> This work was supported by gosudarstvennogo zadaniaya KemGU N2014/64

## LUMINESCENT PROPERTIES AND MORPHOLOGY OF COMPOSITE MATERIALS $\text{ZnWO}_4$ <sup>1</sup>

*D.T. VALIEV\**, *E.F. POLISADOVA\**, *I. A. TUPITSYNA\*\**, *A. A. ZHOROV\**

\*National Research Tomsk Polytechnic University, Lenin Avenue, 30, Tomsk, 634050, Russia, [dtdamirka@gmail.com](mailto:dtdamirka@gmail.com)

\*\*Institute for Scintillation Materials, Lenin Avenue, 60, Kharkov 61001, Ukraine

For the solving problems radioecology, radio-medicine, astrophysics are requires the detection of weak flow of ionizing radiation. Increasing the sensitivity of the recording system is possible by increasing the solid angle of detection, and thus increasing the area of its input window [1]. In this connection the development of scintillation isotropic, homogeneous materials large area becomes relevant. Composite material in the form of scintillation nanocrystals distributed in a polymer matrix, are promising solutions to the objects identified problems [2]. Creating composite materials enables to reduce the requirements for crystal growth technologies in terms of their headroom. It is possible to grow smaller crystals used hydrothermal and sol-gel methods for the synthesis of scintillation materials. Composite materials are more homogeneous in the volume and the surface. In addition, the technology of composite scintillators allow to create multiple scintillation detectors for the detection of two types of radiation [3].

The test materials were prepared at the Institute for Scintillation Materials ISMA NAS Ukraine, Kharkov. The test samples were polymer films of thermal-resistant, low-molecular and organosilicic rubber film  $\text{ZnWO}_4$  and  $\text{ZnWO}_4:\text{Eu}^{3+}$  nanocrystals were prepared by microwave-hydrothermal synthesis with different pH of the solution. The europium was added in the form of an oxide. SEM surface morphology of the samples is studied (fig. 1). The characteristics of luminescence depending on the particle size and technology were studied.

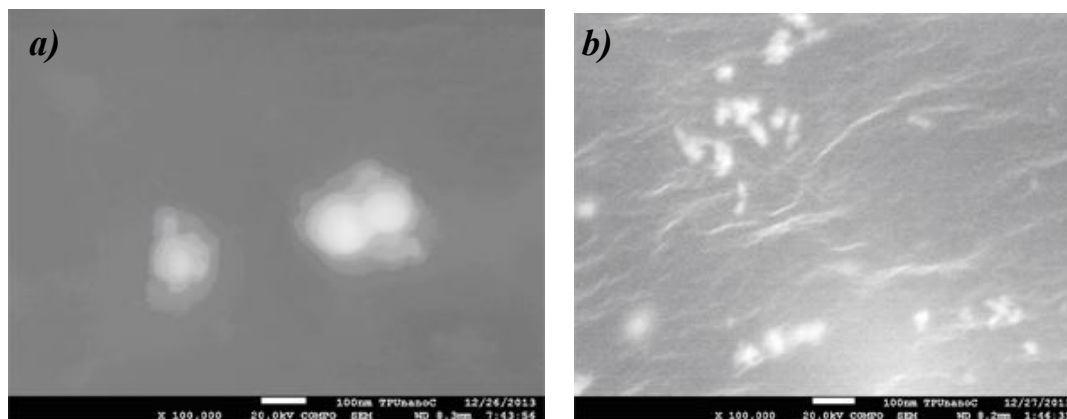


Fig. 1. Images of  $\text{ZnWO}_4$  samples with a grain (a) and rod (b) structure obtained by scanning electron microscopy

The spectrum was measured after exposure of a single pulse EB (“a spectrum per pulse”). After excitation by pulsed EB the integrated PCL spectra were recorded in the spectral range of 1.5– 4.0 eV by high-precision fiber optic spectrometer AvaSpec-2048 without time resolution.

It is shown that the size of the crystal particles and grains affects the luminescence properties in excitation by electron radiation. The questions on the influence of morphology on the luminescent properties of composite materials are discussed.

### REFERENCES

- [1] Nanotechnology Research Directions for Societal Needs in 2020 Retrospective and Outlook. *Editors:* Mihail C. Roco, Chad A. Mirkin, Mark C. Hersam 2010 p.548.
- [2] *Andryushchenko L.A., Grinev B.V., Goriletsky V.I. et al. // Semiconductor Electronics & Optoelectronics. (2001).-v.4.-pp. 126-130.*
- [3] *Budakovsky S.V., Galunov N.Z., Grinyov B.V. et al. // Rad. Measur. 2007. – v. 42 –, № 4-5, P. 565–568.*

<sup>1</sup> The work was supported by State assignment «Science» and State contract No 3.1329.2014.

Results by electron microscopy were obtained in the scientific and educational innovation center "Nanomaterials and Nanotechnology" TPU.

## RADIATIVE-OPTICAL PROPERTIES OF NONSTOICHIOMETRIC BeO CRYSTALS<sup>1</sup>

*M.D.PETRENKO\**, I.I.MILMAN, I.N.OGORODNIKOV, V.YU.IVANOV

\*Ural Federal University, Mira Street 19, Yekaterinburg, 620002, Russia, E-mail: m.d.petrenko@gmail.com,  
Phone: +7(343)3754711

Intentionally changing of stoichiometric composition in wide-band oxides by thermochemical or radiation treatment results in significant changing of their radiative-optical properties. [1,2] Besides, violation of stoichiometry can occur at crystal growth or at forming their in the crust. In [3] experimental manifestations of naturally produced anion-vacancies in natural BeO crystals (so-called bromellite) were registered for the first time. The purpose of this work is to compare radiative-optical properties of bromellite and similar defects in sintetic beryllium oxide samples with intentionally broken stoichiometry.

The natural BeO crystals from Malyshevskoe deposit near Yekaterinburg were studied in our work. The subjects of comparison were nominally pure single crystals of BeO grown from a solution in a sodium or lithium tungstate melt by V.A.Maslov, additively colored at the temperature near 1900°C and under the beryllium vapour pressure value ca.2.5 kPa. The concentration of produced anion vacancies (F-centers) were estimated in the order of magnitude of  $3 \times 10^{17} \text{ cm}^{-3}$ . Thermally stimulated luminescence (TL) of the samples were measured after exposing to X-ray irradiation. TL, X-rays induced luminescence (XRL) have been measured using standard methods.

The TL curves for bromellite, prestine and additively-colored samples are presented at Fig. 1. The shape of bromellite and additively colored BeO samples TL curves is more elementary as compared with prestine sample TL. There are curves with one dominating band with small shoulder in low-temperature zone. This allows us to assume that metamict in bromillite crystal and intentionally-induced non-stoichiometry are similar. The detailed comparative investigation of studied samples at different experiment conditions was performed for these objects.

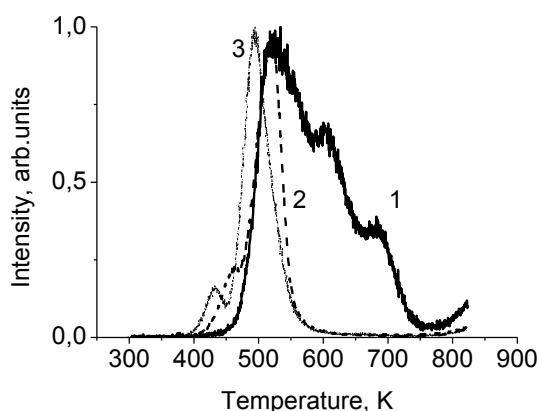


Fig. 1. TL curves for prestine (1), additively colored (2) and natural (3) samples of BeO crystal

The probable nature of metamict in bromellite based on the comparative results obtained is discussed.

### REFERENCES

- [1] R.S.Wilks // *Journal of Nuclear Materials* **26**, 137 (1968).
- [2] V.S.Kortov, I.I.Milman, S.V.Nikiforov, E.V.Moiseikin // *Fizika tverdogo tela* **48**, 421 (2006).
- [3] V.Yu.Ivanov, V.A.Pustovarov, A.V. Kruzhalov, E.I.Zinin // *Journal of Surface Investigation. X-ray, Synchrotron and Neutron Techniques* **4**, 671 (2009)

<sup>1</sup> This work was partially supported by the Ministry of Education and Science of Russian Federation (the basic part of the government mandate)



**PHOTOLYSIS OF CRYSTALLINE NITRATES OF ALKALI AND ALKALINE EARTH METALS WITH LIGHT OF THRESHOLD AND SUBTHRESHOLD ENERGY QUANTA.**

*A. O. GAVRILYK\**, *V. H. PAK\*\**

*\*Kemerovo State University, Krasnaya 6, Kemerovo, Russia, 89049660622, [gavrilyuck.a@yandex.ru](mailto:gavrilyuck.a@yandex.ru)*

*\*\*Kemerovo State University, Kemerovo, Russia, [v.h.pak@mail.ru](mailto:v.h.pak@mail.ru)*

Known radiolysis or photolysis ( $\lambda$  -254 nm) of crystalline nitrates at room temperature leads to the formation of oxygen ions and nitrite, peroksonitrat. Besides only formed in the radiolysis of paramagnetic centers (PC)  $\text{NO}_2$ ,  $\text{O}^-$ ,  $\text{O}_2^-$  and  $\text{O}_3^-$ . Photolysis of nitrates of alkali metals with light of 254 nm does not lead to the HRC and alkaline practically explored. Photolysis study high-energy light more fragmentary. In this paper, we have expanded the range used for the photolysis light, studied the formation of paramagnetic centers, and compared with the formation of the PC when irradiated with gamma radiation. [1]

The study of the EPR spectra in the photolysis of light 222 and 172 nm showed that irradiation of single crystals of potassium nitrate, sodium at 300 K by light with wavelength 172 nm, 222 nm, as well as 254 nm does not cause any of the EPR signals. Light with a wavelength of 172 nm at 77 K leads to anisotropic singlet lines with spectroscopic parameters relating to the radicals  $\text{O}^-$  and  $\text{O}_3^-$ .

Experimental data suggest that the formation of PC by the vacuum UV light is performed in several stages. At low photon energies (up to about 5.2 - 5.5 eV) may only peroksonitrat education and nitrite. Radical formation and  $\text{O}^-$ ,  $\text{NO}_2$  according to the correlation of electronic states is possible only from the triplet states, always with the vibrational levels higher than that required for dissociation with the formation of nitrite and oxygen atom.

And because the action of the vacuum ultraviolet light in all investigated crystalline nitrates oxygen radicals appear and, under certain conditions, and a radical  $\text{NO}_2$ . while, as by irradiation with gamma radiation mainly nitrogen radicals and only after a certain heating of the samples appear oxygen radicals, indicating different mechanism of formation upon exposure to different photon energies. [2]

**REFERENCES**

- [1] *Tagaya K* ESR Study of X-Irradiated  $\text{Sr}(\text{NO}_3)_2$  // Jap. J. Appl. Phys. - 1985 V. 24. №1. - P.75
- [2] *Bannov S. I, Micklin M. B.* Composition and properties of paramagnetic centers in irradiated barium nitrate // Chem. high. power lim. - 1997.- V.31. Number 4. Pp. - 264-266.

**CRYSTALLINE ALKALINE-EARTH NITRATES DECOMPOSITION UNDER RADIOLYSIS***V.A. ANANEV\*, L.D. KRIGER\*, M.B. MIKLIN\***\*Kemerovo State University, Krasnaya street 6, Kemerovo, 650043, Russia, eprlab@kemsu.ru, 83842588286*

The radiolysis of crystalline alkali nitrates has brought forth numerous experimental studies. Peroxynitrite, nitrite and oxygen were discovered as final products of samples decomposition. In contrast, one finds that often minor consideration is given to end-products formation under radiolysis of alkali-earth nitrates. The goal of the present paper is to study the composition of the end-products and their accumulation under radiolysis of crystalline alkali-earth nitrates.

The powders of barium, strontium, calcium, and magnesium nitrates were grown by slowly evaporating the corresponding salts of analytical reagent grade.

The samples were irradiated with  $^{60}\text{Co}$   $\gamma$ -rays at  $\sim 310$  K.

The optical reflectance spectra of the both irradiated and untreated samples were recorded by means of a "Shimadzu UV-2450" spectrophotometer. The spectra were registered at room temperature. The optical absorption spectra of untreated alkaline-earth nitrate crystals consist of two bands with maximum positions at  $\sim 270$ - $290$  nm (293, 284, 273, and 282 nm for  $\text{Mg}(\text{NO}_3)_2 \cdot 6\text{H}_2\text{O}$ ,  $\text{Ca}(\text{NO}_3)_2 \cdot 4\text{H}_2\text{O}$ ,  $\text{Sr}(\text{NO}_3)_2$ , and  $\text{Ba}(\text{NO}_3)_2$ , respectively) and  $< 230$  nm.

The contents of the end-products in solid samples were evaluated chemically from their concentrations in the solution obtained after dissolution of the irradiated samples. The analytical procedure for the determination of peroxynitrite and nitrite was described earlier [1]. The samples were analyzed in 30 min after irradiation.

Irradiation of the samples results in two new bands in the spectrum of each nitrate. The parameters of these bands are similar to the parameters of the spectra due to peroxynitrite and nitrite in  $\gamma$ -irradiated  $\text{RbNO}_3$  and  $\text{CsNO}_3$  crystals. The optical spectra of irradiated alkali-earth nitrates are stable at room temperature.

The increasing the absorbed dose leads to a decrease in the rate of peroxynitrite accumulation in studied nitrates. The radiation-chemical yield of peroxynitrite was calculated from the initial linear part of its accumulation curves. It increase in the series  $\text{Ca}(\text{NO}_3)_2 \cdot 4\text{H}_2\text{O}$  ( $0.093 (100 \text{ eV})^{-1}$ )  $<$   $\text{Ba}(\text{NO}_3)_2$  ( $0.042 (100 \text{ eV})^{-1}$ )  $<$   $\text{Sr}(\text{NO}_3)_2$  ( $0.011 (100 \text{ eV})^{-1}$ )  $<$   $\text{Mg}(\text{NO}_3)_2 \cdot 6\text{H}_2\text{O}$  ( $> 0.001 (100 \text{ eV})^{-1}$ ).

The accumulation of nitrite is linearly depends on absorbed dose in  $\text{Sr}(\text{NO}_3)_2$  and  $\text{Ba}(\text{NO}_3)_2$ . The calculated radiation-chemical yield of nitrite is equal to 0.37 and 1.49 ( $100 \text{ eV})^{-1}$  for  $\text{Sr}(\text{NO}_3)_2$  and  $\text{Ba}(\text{NO}_3)_2$ , respectively.

## REFERENCES

- [1] *L.D. Kriger, M.B. Miklin, E.P. Dyagileva, and V.A. Anan'ev // Russian J. Phys. Chem. A. 2013. - V. 87. - №2. - P.319-322.*

## THE IMPURITY ION INFLUENCE ON THE RECOMBINATION PROPERTIES OF POTASSIUM DIHYDROGEN PHOSPHATE CRYSTALS

*T. A. KOKETAI, B. S. TAGAYEVA, A. K. TUSSUPBEKOVA, G. I. MUSSINA, B. A. BAIZHIGITOVA*

*Karaganda State University named after E.A.Buketov, Universitetskaya str. 28, Karaganda 100028, Kazakhstan,  
aintus\_070482@mail.ru, phone +77004943861*

This paper studies the influence of the impurity ions of divalent copper on recombination properties of potassium dihydrogen phosphate (KDP) crystals.

Fig. 1 shows the absorption spectra of KDP-Cu(NO<sub>3</sub>)<sub>2</sub> crystal before (curve 1) and after (curve 2) irradiation with X-rays. Curve 2 represents the measurements after annealing at 140 K. In this case, the matrix may retain only radiation-induced absorption band with a maximum at 2.8 eV. Fig. 1 shows that the optical density in the absorption bands of divalent copper ions is decreased by irradiation.

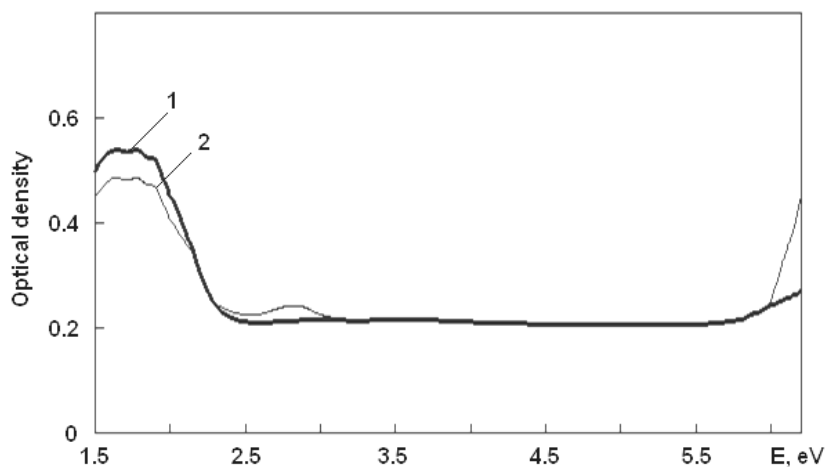


Fig. 1: Absorption spectra of KDP-Cu(NO<sub>3</sub>)<sub>2</sub> crystal

The measurements of the absorption spectra of irradiated crystals KDP-CuSO<sub>4</sub> did not reveal changes in the optical density of the impurity absorption bands.

These results show that after the activation of potassium dihydrogen phosphate crystals by CuSO<sub>4</sub> and Cu(NO<sub>3</sub>)<sub>2</sub> salts divalent copper ions enter into the crystal lattice differently [1]. Interstitial divalent copper ions are not directly involved in radiation-stimulated processes. Their effect is limited to the increase in thermal stability of some defects of the matrix and the formation of additional vacancies.

Hence, we propose that the divalent copper ions are the electron traps.

### REFERENCES

- [1] A. Otani, S. Makishima. *J. Phys. Soc. Jap.* – 1969. – Vol.26. – pp. 85-87.

## STUDY OF THE PROCESSES IN ACTIVATED AMMONIUM HALIDE CRYSTALS

T. A. KOKETAI, B. S. TAGAYEVA, A. IBRAYEVA

*Karaganda State University named after E.A.Buketov, Universitetskaya str. 28, Karaganda 100028, Kazakhstan,  
katkargu@mail.ru, phone +77212770379*

Ammonium halide crystals are the closest alkali halides analogue by the type of chemical bond and the structure of the crystal lattice spectral and luminescence researches of impurity luminescence centers in ammonium halide crystals [1] show the similarity of their properties in these systems.

We have studied the temperature dependence of the first maximum of the exciton absorption bands in the ammonium halide crystals. There is observed its long-wavelength shift within one crystal modification. There are small relative changes of the parameter which characterizes the exciton-phonon interaction in ammonium halide crystals phase transitions. Changes of the first maximum position of exciton absorption bands lie for the order-disorder transition within the band gap changes. Comparative analysis of changes in the parameter of the exciton-phonon interaction and the absorption bandwidth temperature dependence with the anomalous behavior of the peak position of this band does not give correlations. This suggests that the anomalous behavior of the exciton absorption bands maximum due to the band structure changes.

Previously it was found that if the electron-phonon interaction for the impurity center there are actual optical vibrations, then changes of their static parameters in phase transitions are insignificant, if there are actual acoustic vibrations, then changes are more substantial. For activator centers there is a correlation between the absorption bands behavior with the active vibrations frequencies [2].

This led to the conclusion that the properties of impurity centres in the phase transition play the main role of the changes in the crystal lattice parameters, which leads to changes in the phonon spectrum and the effective masses of the oscillators [1]. Differences in the behaviour of impurity centres and excitons are explained by the fact that next coordination spheres play the main role for the first ones, whereas the second ones are collective electronic excitations. Therefore, excitons properties depend on long-range order essentially and therefore on the band structure. Excitonic phase transitions affect the frequency of active modes which are relevant to the exciton-phonon interaction.

Previous studies have shown that in ammonium halide crystals doped with  $Tl^+$ ,  $Ga^+$ ,  $Cu^+$  and  $Ag^+$  ions at  $T=80$  K, there are the unrelaxed excitons migration and the transfer of their energy to impurity centers. Here two mechanisms of energy transfer from excitons impurity centers are low temperature and high temperature. The first one relates to unrelaxed excitons migration, the second one - with relaxed excitons hopping diffusion. There are received the results for  $Tl^+$  and  $Cu^+$  ions in ammonium iodide. Excitons are relevant for the interaction with acoustic vibrations. For the relaxed excitons manifested typical situation for impurity centers. Therefore, changes of the hopping diffusion activation energy are connected with force constants changes, i.e. they are determined by the structure of nearest coordination spheres.

Theoretically, the problem of scattering of excitons by impurity centers is not solved. We found that there is a correlation between the frequency difference which is topical for the excitons scattering, and vibration frequencies of impurities. This leads to the idea that the unrelaxed excitons are scattered by vibrations induced by impurities. Then it becomes clear why the excitons path length is different for different impurities.

### REFERENCES

- [1] Koketai T.A. Luminescence and phase transitions in ammonium halides crystals. - 1985. - 59(2). - pp. 337-341.
- [2] Koketai T.A. // Exciton energy transfer mechanisms to impurity centres in ammonium halides crystals. - 1984. - 6. - pp. 9-12.

## THE FORMATION OF DIPOLE DEFECTS IN KCl CRYSTALS AT LATTICE SYMMETRY LOWERING BY CATION-HOMOLOGS AND PLASTIC STRESS<sup>1</sup>

*K.Sh. SHUNKEYEV\**, *D.M. SERGEYEV\*\**, *Z.K. AIMAGANBETOVA\*\*\**, *A.A. BARMINA\**, *G.D. SERIKBAYEVA\**

\*Aktobe Regional State University named after K.Zhubanov, 34 Moldagulova avenue, Aktobe, 030000, Kazakhstan, shunkeev@rambler.ru, +77132547382

\*\*Military Institute of Air Defense Forces, 39 Moldagulova avenue, Aktobe, 030012, Kazakhstan

\*\*\*Al-Farabi Kazakh National University, 71 Al-Farabi avenue, Almaty, 050040, Kazakhstan

Recently due to the practical application of multifunctional materials in the micro- and nanoelectronics the intensive research is carried out on the formation of dipole defects in ionic dielectrics, which give input in the common ionic conductivity [1]. The results of our research on the creation of halogen radiation defects in alkali halide crystals are confirmed by the halogen aggregation process of different configuration –  $Cl_3^-$ ,  $Cl_5^-$  and  $Cl_7^-$  in NaCl crystal under superhigh pressures [2].

The current work used light cation-homolog (KCl-Na, KCl-Li) and plastic stress as external physical factors. They create dipole complexes –  $(Cl_3^-)_{aca} Na_i^+ Cl_i^-$ ,  $(Cl_3^-)_{aca} Li_i^+ Cl_i^-$  and divacancies  $(v_c^- v_a^+)$  in a crystal. KCl, KCl-Na, KCl-Li and KCl-Sr crystals are prepared on the basis of complex method developed in the Institute of Physics of Estonia Tartu University. The dipole currents were registered with the thermostimulated depolarization method in the region of low temperatures [3, 4]. The formation efficiency of  $Cl_3^-$ -centers was researched by the registration of optic absorption of deformed and X-rayed crystals in automatic mode on the spectrophotometer “Evolution -300”.

The following main patterns were established: The dipole complexes  $Li_i^+ v_c^-$ ,  $v_c^- Sr_c^+$  in KCl-Li, KCl-Sr crystals and divacancies  $(v_c^- v_a^+)$  are found in plastic stressed KCl crystal with typical depolarization temperature at 180K, 230K and 205K correspondingly. The absorption band is registered in the absorption spectrum; the band is typical for interstitial halogen atom –  $(Cl_i^-)$ , which is a part of  $(Cl_3^-)_{aca} Li_i^+ Cl_i^-$ ,  $(Cl_3^-)_{aca} Na_i^+ Cl_i^-$  - and  $(Cl_3^-)_{aca} Sr_c^+ Cl_i^-$ -centers in KCl-Li, KCl-Na and KCl-Sr.

Thus, the generation efficiency of  $(Cl_3^-)_{aca}$  - and  $(Cl_3^-)_{aca} M_i^+ Cl_i^-$ -centers in KCl crystal is interpreted with the energy expediency of lattice realignment at the interaction of movable interstitial halogen atoms between each other in the field of vacancy complexes  $Li_i^+ v_c^-$ ,  $v_c^- Sr_c^+$  and  $v_c^- v_a^+$ .

### REFERENCES

- [1] *M.D. Volnyanski, S.N. Plyaka, M.P. Trubitsin, A.H. Obaidat Yakhiya* // Physics of Solid State. – 2012. – Vol. 54. – № 3. – P. 471-475.
- [2] *W. Zhang, A. Oganov, A. Goncharov, Q. Zhu, S. Boulfelfel, A. Lyakhov, E. Stavrou, M. Somayaazulu, V. Prakapenka, Z. Konopkova* // Science. – 2013. – Vol. 342. – P. 1502-1505.
- [3] *K. Shunkeyev, E. Sarmukhanov, A. Bekeshev, Sh. Sagimbaeva, K. Bizhanova* // Journal of Physics: Conference Series. – 2012. – Vol. 400. – P. 052032.
- [4] *K. Shunkeyev, A. Barmina, K. Bizhanova, D. Sergeyev, S. Shunkeyev* // Izvestiya vuzov. – 2012. – Vol. 55. – № 11-3. – P. 209-212.

<sup>1</sup> This work was supported by the grant funding of Ministry of Education and Science of the Republic of Kazakhstan No 1955/GF3, 1332/GF-OT

## THE ASSEMBLY MECHANISMS OF ELECTRON-HOLE PAIRS IN KCl CRYSTAL AT LATTICE SYMMETRY LOWERING BY CATION-HOMOLOGS AND LOW TEMPERATURE UNIAXIAL STRESS<sup>1</sup>

*K.Sh. SHUNKEYEV\**, *N.N. ZHANTURINA\*\**, *Sh.Zh. SAGYMBAEVA\**, *S.K. SHUNKEYEV\**

*\*Aktobe Regional State University named after K. Zhubanov, 34 Moldagulova avenue, Aktobe, 030000, Kazakhstan, shunkeev@rambler.ru, +77132547382*

*\*\*Al-Farabi Kazakh National University, 71 Al-Farabi avenue, Almaty, 050040, Kazakhstan*

The effect of strengthening of intrinsic luminescence of alkali halide crystals (AHC) registered at 80K at the process of X-ray radiation after the low temperature uniaxial stress is hard to explain by the self-trapping of only free excitons [1,2]. This fact is based in two physical reasons:

First, this interpretation holds for AHC having sufficient free path length of free excitons before self-trapping (for example, for KI at 80 K -  $350a$ , where  $a$  – lattice constant). For KCl crystal at 80 K free path length of free excitons is about only  $2a$  [3]. This means that in KCl at 80K almost all the free exciton transits in self-trapped state.

Second, in AHC the X-ray quantum up to 90% creates electron-hole pairs, and not free excitons, as in the case of selective photoexcitation in the vacuum ultraviolet region of the spectrum corresponding to the creation of monohalogen excitons.

In this regard, it was specifically investigated the luminescence of KCl-Na, firstly, at the condition of the absence of free excitons in order to detect the effect of the assembly of electron-hole pairs, creating by X-ray radiation, secondly, by the lowering of lattice symmetry by the cation (Na), which is lighter than the main lattice cation (K).

In the spectra of X-ray luminescence of KCl crystal was registered the strengthening of self-trapped excitons luminescence in the field of sodium -  $e_s^0(Na)$  with a maximum at 2.8 eV in the temperature range  $80 \rightarrow 300K$ , when there is a complete quenching of the self-trapped exciton luminescence  $e_s^0$  in regular lattice sites.

The luminescence with a peak at 2.8 eV is registered:

- in the flash spectra of KCl-Na crystal at photoexcitation in the region of spectrum F'- absorption band after a preliminary X-ray irradiation at 80K.
- in the spectra of thermally stimulated luminescence in the temperature range 140-240K, which indicates about the contribution of the hole-recombination luminescence at the thermal destruction of  $V_k$  (Na) - center with electronic color centers.

By the linear part of the 2.8 eV luminescence rise in the temperature range  $140 \rightarrow 240K$  was estimated activation energy (60 meV), which is less than the energy of jump diffusion of  $V_k$  - centers in KCl (0.54 eV).

It is assumed that the activation energy of the 2.8 eV luminescence rise (60 meV) is associated with the presence of potential barrier for the assembly of self-trapped hole in the field of the sodium with an electron for the transition to the state of self-trapped exciton  $e_s^+(Na) + e^- \rightarrow e_s^0(Na)$ .

### REFERENCES

- [1] V. Babin, A. Elango, K. Kalder, A. Maaroos, K. Shunkeev, E. Vasilchenko, S. Zazubovich // Journal of Physics Condensed Matter. – 1999. – Vol.11. – P. 2303-2317.
- [2] A. Elango, Sh. Sagimbaeva, E. Sarmukhanov, T. Savikhina, K. Shunkeev // Radiation Measurements. – 2001. – Vol. 33. – P. 823-827.
- [3] Ch. Lushchik, A. Lushchik // Decay of Electronic Excitons with Defect Formation in Solids. –Moscow, Nauka, 1989.

<sup>1</sup> This work was supported by the grant funding of Ministry of Education and Science of the Republic of Kazakhstan No 1955/GF3, 1332/GF-OT

## INCREASE IN THE UMKLAPP VOLTAGE IN SUPERCONDUCTING TUNNEL JUNCTIONS WITH NON-MONOTONE JOSEPHSON CURRENT<sup>1</sup>

*K.Sh. SHUNKEYEV\**, *D.M. SERGEYEV\*\**, *Z.K. AIMAGANBETOVA\*\*\**, *N.N. ZHANTURINA\*\*\**

*\*Aktobe Regional State University named after K.Zhubanov, 34 Moldagulova avenue, Aktobe, 030000, Kazakhstan, serdau@rambler.ru, +77132547382*

*\*\*Military Institute of Air Defense Forces, 39 Moldagulova avenue, Aktobe, 030012, Kazakhstan*

*\*\*\*Al-Farabi Kazakh National University, 71 Al-Farabi avenue, Almaty, 050040, Kazakhstan*

It is known that in superconducting tunnel junctions (STJ) with nonmonotonic Josephson current a number of very interesting effects related to violation of the standard monotonic dependence of supercurrent creates. In this paper, we consider an increase in voltage of the umklapp in STJ. Usually view full of the current-voltage characteristics (CVC) of Josephson junction (JJ) depends on the type of transition and the magnitude of its capacity  $C$ , characterized by the MacCumber-Stewart parameter  $\beta = (\omega_c/\omega_p)^2 = 2\pi I_c R_n^2 C / \Phi_0$  (here  $\omega_c$  – a characteristic frequency,  $\omega_p$  – the plasma frequency,  $\Phi_0$  – the quantum of magnetic flux,  $I_c$  – critical current,  $R_n$  – normal resistance). When the external current  $I$  exceeds a critical value  $I_c$ , the resistive switching takes place. Switching on the resistive branch of CVC time  $\tau_R \approx \tau_n = R_n C$ . In the case of JJ with large  $C$  voltage fluctuations around the average value of  $\bar{V}$  are small. Consequently, in the resistive state the supercurrent is in the monotonous sinusoidal shape and its average value  $\bar{I}_s = 0$ . At the decrease in the capacity of JJ  $\bar{I}_s$  becomes different from zero, so the resistive branch of the CVC is not the same with  $I_N(\bar{V})$ .

In STJ of SIS-structure return umklapp to the superconducting branch of CVC to zero voltage ( $V=0$ ) occurs at the current increase through the TJ to a certain value  $I_d = V_d/R$ , according to the umklapp voltage

$$V_d = k_d V_p, \quad (1)$$

where

$$V_p = \hbar \omega_p / 2e = [\hbar I_c / 2eC]^{1/2} \quad (2)$$

– Josephson plasma voltage;  $\hbar$  - Planck's constant,  $e$  - an electron charge,  $k_d = 1,4 \div 3,5$ . Usually the return jump time  $\tau_d \leq \tau_R$  [1]. Value of  $V_d$  is a few tenths of a voltage of the energy gap  $V_g$ , i.e  $I_d \ll I_c$  and full branch of CVC becomes hysteresis. The reason of the decrease in  $V_d$  with the growth of  $C$  is in the fact that increasing capacity more effectively shunts the Josephson oscillations initiating imklapp to a zero voltage. And with the growth of  $C$  a decrease in the plasma frequency is observed. Hysteresis on the CVC of the SIS-structures does not completely disappear even when the  $C \rightarrow 0$ , when in JJ with direct conductivity, in which the dependence  $I_N(\bar{V})$  is close to linear, i.e at  $C \rightarrow 0$  CVC has no hysteresis. In [2,3] have been shown the increase in the plasma frequency  $\omega_p$  in STJ with nonmonotonic Josephson current. In such structures, due to the increase in  $\omega_p$  plasma voltage  $V_p$  also increases according to (2), which affects to the magnitude of the umklapp voltage (1) and will lead to a shift of the umklapp point from  $V_p/V_g$  (plasma voltage  $V_p$  normalized to the voltage of the energy gap  $V_g$ ) to  $V_p^*/V_g$ , where  $V_p^*$  - changed plasma voltage under the influence of non-monotonic Josephson current.

Thus, it is established that the nonmonotonic behavior of the Josephson current in superconducting TJ increases the umklapp voltage to the superconducting branch of CVC and narrows its hysteresis.

### REFERENCES

- [1] *K.K. Likharev // Dynamics of Josephson junctions and circuits. – Gordon and Breach, 1986.*
- [2] *D.M. Sergeyev // Solid State Phenomena. – 2013. – Vol. 200. – P. 272-275*
- [3] *D. Sergeyev, K. Shunkeyev, N. Zhanturina, S. Shunkeyev // IOP Conference Series: Materials Science and Engineering. – 2013. – Vol. 49. – P. 012049.*

<sup>1</sup> This work was supported by the grant funding of Ministry of Education and Science of the Republic of Kazakhstan No 1955/GF3, 1332/GF-OT

## OPTICAL AND LUMINECENCE PROPERTIES OF LITHIUM GADOLINIUM ORTHOBORATE CRYSTAL

*M.S. KISELEVA\**, *I.N. OGORODNIKOV\**, *I.N. SEDUNOVA\**, *D.O. VOSTROV\**, *V. YU. YAKOVLEV\*\**

\* Ural Federal University, Mira St., 19, Yekaterinburg, 620002 Russia, [kiseleva.marija@gmail.com](mailto:kiseleva.marija@gmail.com), +7(343)375-4711

\*\* Tomsk Polytechnic University, 30 Lenina Avenue, 634050, Tomsk, Russia

Present research is devoted to investigation of lithium gadolinium orthoborate  $\text{Li}_6\text{Gd}(\text{BO})_3$  (LGBO) crystal by means of pulse methods - radiolysis and cathode luminescence. The mathematical model of tunneling electron transfer was applied for interpretation of experimental data on transient optical absorption (TOA) and pulse cathodoluminescence (PCL).

The LGBO crystals are interesting objects for investigations from the practical point of view. In particular materials based on LGBO have properties for neutron detection. Continence of light stable isotopes  $^6\text{Li}$  and  $^{10}\text{B}$  in LGBO of allow use them for thermal neutron detection. The LGBO crystal also contains  $^{155,157}\text{Gd}$  which has high capture cross-section of slow neutrons with energy less then few keV.

There is monoclinic crystal system of LGBO crystals with center of symmetry (space group  $\text{P}2_1/\text{c}$ ). The boron–oxygen anionic group can be identified in the LGBO structure. A characteristic feature of the crystal is contrast between the purely covalent chemical bonds in this group and relatively weak ionic bonds of the lithium cation with the anionic group. The presence of the sublattice of weakly bound cations in combination with the stable anionic framework should have an effect on both the dynamics of electronic excitations and the specifics of radiation defect formation.

For interpretation of experimental results on TOA of LGBO crystals the model of tunneling electron transfer in terms of defect mobility was used [1]. Present model is based on numerical solving of Smoluchowsky equation for correlation function  $Y(r,t)$ , obtained results were used for calculation of non-stationary reaction rate  $K(t)$  and hence  $n(t)$ , The results of modeling for different temperatures was compared with TOA data for  $T=380\text{ K}$ ,  $340\text{ K}$ ,  $293\text{ K}$  (Fig. 1) [2]. The concentration of the defect is  $n$ , and initial defect concentration is  $n_0$ . It was assumed the measured induced optical absorption is proportional to actual defect concentration.

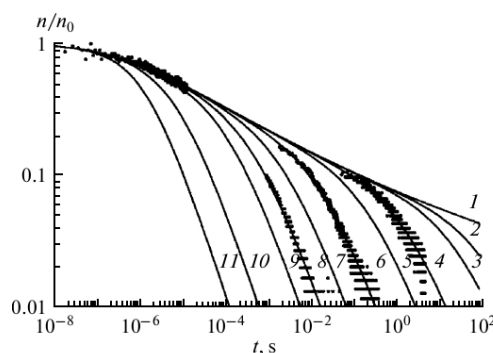


Fig. 1. Time dependences for defect concentration  $n(t)$  at temperatures of (1) 200, (2) 260, (3) 270, (4) 293, (5) 310, (6) 340, (7) 360, (8) 380, (9) 400, (10) 450, and (11) 500 K. The data points show the experimental results on the TOA decay kinetics in LGBO crystals at the 3.7 eV absorption band.

As can be seen from the graph used model describes experimental data very well. There are two characteristics stage of this kinetics. The initial part is controlled by electron tunneling process and analytical solution can be applied in case of immobile defects. The final part is controlled by diffusion process. Thermo stimulated shortening of the decay kinetics is observed with temperature increasing.

In present research we discuss formation mechanisms, nature of lattice defects and irradiative relaxation processes of electronic excitations under pulse electron beam for single-crystalline and crystal fiber LGBO samples.

### REFERENCES

- [1] *I.N. Ogorodnikov, M.S. Kiseleva // JETP. – 2012. – 141. – № 6. 1-12.*
- [2] *I.N. Ogorodnikov, M.S. Kiseleva, I.N. Sedunova // Khimiya Vysokikh Energii. – 2012. – 46. – № 3. 199-204.*



## NUMERICAL SIMULATION OF THZ SOURCE BASED ON COHERENT SMITH-PURCELL RADIATION GENERATED BY FEMTOSECOND MULTI-BUNCH ELECTRON TRAIN

*K.P. ARTYOMOV\*\*\*, L.G. SUKHIKH\**

*\*Institute of High Current Electronics, 2/3 Akademichesky Avenue, Tomsk, 634055, Russia,  
artyomov@to.hcei.tsc.ru, +7(3822)49-23-92*

*\*\*National Research Tomsk Polytechnic University, Tomsk, 30 Lenin Avenue, 634050, Russia*

Generation of coherent Smith-Purcell radiation in the THz region by femtosecond multi-bunched electron beam with 10 MeV energy was simulated for lamellar and echelette gratings. The simulation was carried out using particle-in-cell electromagnetic code KARAT [1]. Parameters of the gratings were optimized in order to maximize the radiation power. The echelette grating with blaze angle 30 degrees was found to be an optimal one for suppression of high order harmonics.

### REFERENCES

- [1] *V.P. Tarakanov* // User's Manual for Code KARAT – Springfield: BRA – 1992

## THE INFLUENCE OF OXYGEN ON THE FORMATION OF Eu CENTERS IN CsI:Eu CRYSTALS

N. OVCHARENKO\*, V. YAKOVLEV\*\*, L. TREFILOVA\*, V. ALEKSEEV\*, A. GRIPPA\*, E. KISIL\*\*\*

\*Institute for Scintillation Materials, 60 Lenin Avenue, Kharkov 61001, Ukraine, [ovcharenko@isma.kharkov.ua](mailto:ovcharenko@isma.kharkov.ua), +38(057)3410246

\*\*Tomsk Polytechnic University, 30 Lenin Avenue, Tomsk 634034, Russian Federation

\*\*\*Institute for Single Crystals, 60 Lenin Avenue, Kharkov 61001, Ukraine

Spectral-kinetic properties of defects caused by Eu ions in CsI lattice have been investigated. CsI:Eu crystals were grown by the Stockbarger technique in vacuum.  $\text{Eu}_2\text{O}_3$ ,  $\text{EuI}_2$  and  $\text{Cs}_2\text{CO}_3$  were used as dopants. The total concentration of  $\text{Eu}^{2+}$  and  $\text{Eu}^{3+}$  ions in the crystals was determined by voltammetry. It was found that Eu in crystals CsI:EuI<sub>2</sub>, CsI:Eu<sub>2</sub>O<sub>3</sub> grown in vacuum has the same oxidation level as in the dopants  $\text{EuI}_2$  and  $\text{Eu}_2\text{O}_3$ , respectively.  $\text{Eu}^{2+}$  ions enter the lattice with the cation vacancy which compensates their excess charge, and give rise to two broad bands in the range of 250-320 nm and 320-430 nm in the absorption spectrum. It was found that the emission spectrum of CsI:EuI<sub>2</sub> crystal exposed to N<sub>2</sub> laser pulse ( $\lambda=337$  nm) depends on the concentration of  $\text{Eu}^{2+}$  ions and at 295K fits one or two Gaussians out of the set of three Gaussians with parameters  $\lambda_{\text{max}}=450$  nm, FWHM=0.2 eV;  $\lambda_{\text{max}}=440$  nm, FWHM=0.2 eV;  $\lambda_{\text{max}}=456$  nm, FWHM=0.17 eV caused by monomer, dimer and trimer of  $\text{Eu}^{2+}-\text{v}_c^-$  dipoles, respectively. Unlike  $\text{Eu}^{2+}$ , the resonance transitions of  $\text{Eu}^{3+}$  ions escape detection in absorption spectra, but they give rise narrow bands with maxima at  $\lambda_{\text{max}} = 360, 379, 393, 464$  nm in the excitation spectrum of the red emission in the region of at  $\lambda_{\text{em}} = 615$  nm (Fig.1), caused by  $^5\text{D}_0 \rightarrow ^7\text{F}_2$  of  $\text{Eu}^{3+}$  ions.

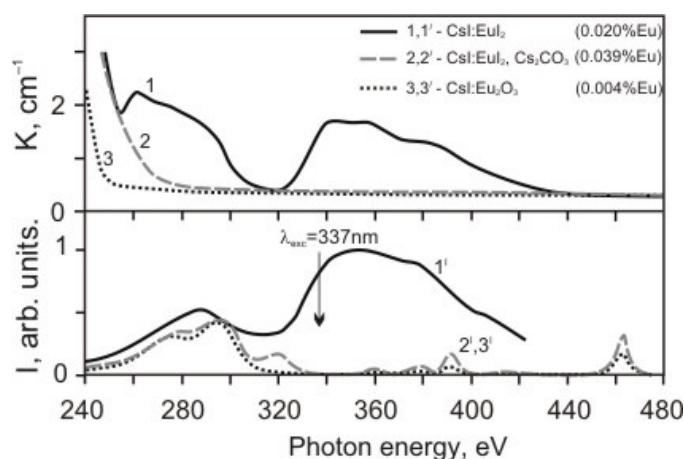


Fig. 1. Absorption (1-3) and excitation spectra (1',2') in the region of  $\lambda_{\text{lum}}=440$  nm (1') and  $\lambda_{\text{lum}}=615$  nm (3',2') for CsI:Eu crystals activated by  $\text{EuI}_2$  (1,2,1',2') and  $\text{Eu}_2\text{O}_3$  (3,3') with  $\text{Cs}_2\text{CO}_3$  additive (2,2'). T=295 K.

All  $\text{Eu}^{2+}$  ions oxidize giving rise  $\text{Eu}^{3+}$  ions in CsI:EuI<sub>2</sub> crystal growing with a high concentration of carbonate, therefore one can not excite the transitions proper for  $\text{Eu}^{2+}$  ions. It was found that only some of  $\text{Eu}^{2+}$  ions oxidize in CsI:EuI<sub>2</sub> crystal growing with a small amount of oxygen-containing impurities, and so there are both  $\text{Eu}^{2+}$  and  $\text{Eu}^{3+}$  ions in the lattice. One observes along with 440 nm band of  $\text{Eu}^{2+}-\text{v}_c^-$  dimers a long-wave band with  $\lambda_{\text{max}}=505$  nm (FWHM=0.29 eV) in the luminescence spectrum of such crystal excited 337 nm laser pulse. This band is regarded to be caused by  $^3P_1 \rightarrow ^1S_0$  transition in the interstitial oxygen  $\text{O}_i^{2-}$  ion with which  $\text{Eu}^{3+}$  ions enters the lattice to compensate its excess charge. The emission pulse in a band with  $\lambda_{\text{max}}=505$  nm has an exponential rise with time constant  $\tau = 60$  ns which coincides with a time constant of one out of two decay components ( $\tau_{1d} = 60$  ns и  $\tau_{2d} = 380$  ns) of 440 nm emission of  $\text{Eu}^{2+}-\text{v}_c^-$  dimers. The coincidence of the time constants testifies the resonance energy transfer from  $\text{Eu}^{2+}$  donor to  $\text{O}_i^{2-}$  acceptor in Eu center which is  $\text{Eu}^{2+}\text{v}_c^- \text{Eu}^{3+} \text{O}_i^{2-}$  mixed dimer consisting of  $\text{Eu}^{2+}$  and  $\text{Eu}^{3+}$  ions in cation positions, a cation vacancy and an interstitial oxygen  $\text{O}_i^{2-}$ .

## NUMERICAL COMPARISON OF TWO MODELS FOR LEAD AZIDE INITIATION

A.AOUFI\*, G. DAMAMME\*\*

\*Centre SMS, UMR CNRS 5307, Laboratoire Georges Friedel, EMSE, 158 cours Fauriel, 42027, France; [aoufi@emse.fr](mailto:aoufi@emse.fr).

\*\*CEA-GRAMAT, GRAMAT BP 80200 - 46500 GRAMAT, FRANCE.

The purpose of this work is to compare from a numerical point of view several coupled mathematical modeling related to the initiation of heavy metal azides available in the literature[1][2][3][4].

The initiation will be thermal laser energy deposit.

In the first model, a first order kinetics following an Arrhenius type law is used to compute the spatial and temporal evolution of the conversion rate of the exothermic reaction of  $(\text{Pb}(\text{N}_3))_2$ . A coupling with the heat equation is also taken into account. Several 1d/2d geometries and configurations are considered;

Spherical: in this case, a 1d modeling with and without inclusion of a metallic particle is considered. In the first case the influence of laser energy deposit is taken into account in the metallic inclusion.

Slab: in this case, a 1d modeling with and without a PMMA type confinement is considered.

Cylindrical: in this case a 2d extension of the previous modeling is considered. The effect of the radius of the energy deposit zone is considered for the determination of the initiation and propagation of the combustion front.

In the second model a coupling between a diffusion equation for electron/hole and the initial number of azide sites, the number of electron-holes pairs that are generated, the number of  $\text{N}_6^*$  groups formed and the number of azote molecules finally formed.

A numerical software implementing an implicit finite-volume scheme for the discretization of the coupled set of equations is used to investigate the behavior of these parabolic-type equations and to compare their results.

Several 1d/2d animations are presented and discussed.

### REFERENCES

- [1] Krieger V, Valensky A., *Vel'k V*, // 11<sup>th</sup> RCP, pp 44-46.
- [2] Tsipilev V, Morozova E. // *Condensed medium ignition by laser pulsed radiation of bandgap absorption spectral range, Russian Physics Journal*, 2009, Vol. 52, n 8/2, pp 32'-326.
- [3] Lisitsyn V.M., Oleshko V.I., Tsipilev V.P., Yakovlev A.N., To a question on the pre-explosive phenomena, thresholds and criteria of initiation heavy metals azides an external impulse// *Energetisckie kondensirovannye sistemy. Chernogolovka. M.-:Yanus-K-2006.*
- [4] Lisitsyn V.M., Oleshko V.I., Tsipilev V.P., Yakovlev A.N // About power thresholds, criteria, kinetics and mechanisms of ignition of explosives by laser pulsed electrons beams // *Physics. -2006 N°10.*

**COMPARISON OF TWO MODELS FOR LASER INITIATION OF HEAVY METAL AZIDE**

*G. DAMAMME\**, *A.AOUFI\*\**,

*\*\*CEA-GRAMAT, Gramat BP 80200 - 46500 Gramat, France ; gilles.damamme@cea.fr*

*\*Centre SMS, UMR CNRS 5307, Laboratoire Georges Friedel, EMSE, 158 cours Fauriel, 42027, France ; aoufi@emse.fr*

This work will compare two initiations modeling of heavy metal azides available in the literature [1], [2], [3] and their numerical results.

The initiation will be a laser energy deposit (focused or defocused). Several energy and time dependence of the energy deposit, will be considered.

In the first model, a heat diffusion equation and an Arrhenius chemical kinetic law are used to propagate the exothermic reaction of decomposition of  $\text{AgN}_3$  or of  $\text{Pb}(\text{N}_3)_2$  to form nitrogen molecule  $\text{N}_2$  and metal. The laser energy deposit is here a thermal process. Several 1d/2d geometries and configurations are considered (spherical, slab, cylindrical).

In the second model, no direct thermal effect is considered but an electron/hole mechanism and its indirect consequences. The transformation of  $\text{N}_3^-$  azide ions, into  $\text{N}_3^*$  neutral activated molecules is considered to be an electron-holes pairs formation, which can diffused, be recombined or conduct to the formation of  $\text{N}_6^*$  groups which finally will decomposed into azote  $\text{N}_2$  molecules. Different mechanisms of coupling between these chemical species (catalyze) are also taken into account. Energy laser deposit is, in that model, supposed to be taken place as an electron-hole pair creation. Several 1d/2d geometries and configuration will be considered.

Comparison of the two models, for the equation and the type of mechanisms as for the results on the reaction thresholds, will be made.

## REFERENCES

- [1] *V. Krieger, A. Valensky, V. Vel'k, 11<sup>th</sup> RCP, pp 44-46. V. Tsipilev and E. Morozova, condensed medium ignition by laser pulsed radiation of bandgap absorption spectral range, Russian Physics Journal, 2009, Vol. 52, n° 8/2 , ppp 324-326*
- [2] *Lisitsyn V. M. , Oleshko V. I., Tsipilev V. P. , Yakovlev A. N. To a question on the preexplosive phenomena, thresholds and criteria of initiation heavy metals azides an external impulse // in book : Energetiskie kondensirovannye sistemy. Chemogolovka. M. -: Yanus-K - 2006*
- [3] *Lisitsyn V. M. , Oleshko V. I., Tsipilev V. P. , Yakovlev A. N. About power thresholds, criteria, kinetics and mechanisms of ignition of explosives by laser pulsed electron beams // Physics. - 2006 - N°10*

**INFLUENCE OF THE THICKNESS AND ABSORPTION COEFFICIENT OF FILM ON IGNITION THRESHOLD OF PETN BY LASER PULSE**

*A.V. KHANEFT<sup>\*,\*\*</sup>, A.V. DOLGACHEV<sup>\*</sup>, A.S. ZVEREV<sup>\*</sup>, A.YU. MITROFANOV<sup>\*</sup>*

*\*Kemerovo State University, Krasnaya, 6, Kemerovo, 650043, Russia, [khaneft@kemsu.ru](mailto:khaneft@kemsu.ru), 83842583195*

*\*\*National Research Tomsk Polytechnic University, Tomsk, Russia*

In the simulation of ignition of energetic materials, when laser radiation is absorbed by inclusions, the distribution of light flux can be neglected. In the case of metal particles this is true, as the skin depth is small. However, in the case of inclusions consisting, for example, of metal oxides, it is necessary to take into account the distribution of light energy. In this paper a simulation of the ignition of PENT by the copper oxide film heated by laser radiation. The system of thermal conductivity equations was solved:

$$\rho_1 c_1 \frac{\partial T_1}{\partial t} = \lambda_1 \frac{\partial^2 T_1}{\partial z^2} + \alpha(1 - R_1) I_0(t) \exp(-\alpha z) \frac{[1 + R_2 \exp(2\alpha(z - h_1))]}{[1 - R_1 R_2 \exp(-2\alpha h_1)]}, \tag{1}$$

$$\rho_2 [c_2 + H_f \delta(T_2 - T_f)] \frac{\partial T_2}{\partial t} = \lambda_2 \frac{\partial^2 T_2}{\partial z^2} + \rho_2 Q Z \exp\left(-\frac{E}{RT_2}\right) \tag{2}$$

with initial and boundary conditions

$$T_1(z, 0) = T_2(z, 0) = T_0, \quad \frac{\partial T_1(0, t)}{\partial z} = \frac{\partial T_2(h_1 + h_2, t)}{\partial z} = 0, \quad \lambda_1 \frac{\partial T_1(h_1, t)}{\partial z} = \lambda_2 \frac{\partial T_2(h_1, t)}{\partial z}, \tag{3}$$

where  $h_1, T_1$  – the thickness and temperature of the oxide film;  $h_2, T_2$  – the thickness and temperature of PETN. Notation physicochemical variables in equations (1) and (2) are standard. Dependence of the intensity of the time was given in the form of a rectangular pulse.

Calculations have shown that ignition of PETN takes place near absorbing film. In this case dependences of the delay time and thus the critical energy density of laser pulse ( $W^* = t^* I_0 / \tau$ ) on the film thickness have the form of curves with a minimum (Fig.1).

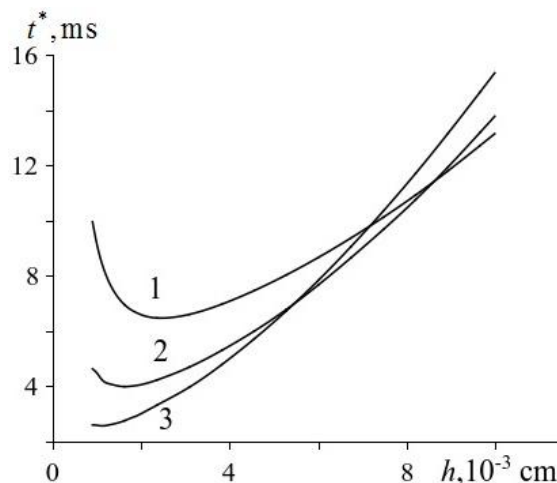


Fig. 1. Dependence of delay time on a thickness of film at  $\alpha = 150$  (1), 300 (2) and 600  $\text{cm}^{-1}$ .

Physics of the process is as follows. At  $h_1 < \alpha^{-1}$  it is necessary upload for more energy in a "thin" film. It is connected by that quantity of reserved heat in a film is proportional to its thickness. In case of a "thick" film ( $h_1 > \alpha^{-1}$ ) more energy is needed to heat the "cold" part of the film.

## PHOTOCHEMICAL AND THERMOCHEMICAL REGIMES OF LASER INITIATION OF PETN<sup>1</sup>

*A.S. ZVEREV\**, *A.G. KRECHETOV\**, *A.Y. MITROFANOV\**, *V.N. MOROZ\**, *N.V. POLEEVA\**

\**Kemerovo State University, Krasnaya 6, Kemerovo, 650043, Russia, [lira@kemsu.ru](mailto:lira@kemsu.ru), +73842588117*

We propose a method to identify the mechanism of thermal laser initiation, while the more efficient photochemical initiation mechanism. The basis of being offered the first approach is based on the following considerations are quite simple. To initiate the explosion photochemical mechanism must photocreation threshold (minimum) concentration of excited states –  $N_0$ , providing further development chain reaction [1]. If these are short-lived excited state, the threshold concentration is only created during the lifetime of this state –  $\tau$ , and a further increase in the duration of the pulse initiates –  $t$  is "useless". This was the situation we face in self- most diverse areas of physics, such as optics, semiconductors [2] for short-lived radionuclides activation analysis [3], etc.

For the case of PETN and  $\lambda = 1060$  nm, according to the duration of the pre processes [1],  $\tau$ , in any case, not more than a few microseconds, ie increasing the duration of the initiating pulse over  $t \sim 10$  ms will not lead to an increase in  $N$ , and hence the efficiency of the photochemical initiation.

If the characteristic length of the actual thermal processes that determine the efficiency of thermal initiation exceeds  $\tau$ , then this mechanism of initiation situation is may be the reverse: an increase in the pulse duration ( $t > \tau$ ) will increase by heating of, and hence the effectiveness of the thermal initiation mechanism.

This difference opens the possibility in principle of management contributions photochemical and thermal mechanisms in the initiation process by changing the duration and power of the initiating pulse.

Since the laser initiation of PETN at high powers initiating pulse (usually the first harmonic pulses in the nanosecond range neodymium lasers power of  $\sim 10^8$  W) have been studied [1, 4, 5], we focused on the initiation of pulses millisecond range, but significantly less power ( $\sim 10^3$  W).

Initiating source of fiber laser pulses served with a collimator YLS-150/1500-QCW IPG P30-001460 with a pulse duration of 20 ms and an average pulse power of about  $10^3$  watts.

The starting material for obtaining samples from the light-absorbing inclusions serve PETN suspension supplemented with carbon black in hexane. Obtained after drying blend was compressed into tablets.

Samples for the study were a tablet with a diameter of 3 mm and a thickness of 0.5 mm, pressed into a stainless steel mandrel at a pressure of 200 MPa. Density of the samples at the same time was  $1.7$  g/cm<sup>3</sup>.

It is shown that the threshold for thermochemical initiation of pure PETN with illumination of about  $10^4$  W/cm<sup>2</sup> than  $75$  J/cm<sup>2</sup> threshold same thermochemical initiation PETN with light-absorbing inclusions (0.1 wt% carbon black) drops to  $14$  J/cm<sup>2</sup>.

### REFERENCES

- [1] *Aluker E.D., Krechetov A.G., Mitrofanov A.Y., Nurmukhametov D.R., and Kuklja M.M.* // J. Phys. Chem. C. – 2011. Volume 115. – №14. P. 6893–6901.
- [2] *J. I. Pankove.* // Optical Processes in Semiconductors. – Engelwood Cliffs, 1971).
- [3] *C. Vandecasteele.* // Activation analysis with charged particles. – Ellis Horwood, Chichester, 1988).
- [4] *Aluker E.D., Aluker N.L., Belokurov G.M., et al.* // Energetic Materials: Chemistry, Hazards, and Environmental Aspects. – Novapublishers, 2010. P. 213–227.
- [5] *V. V. Danilenko* // Explosion: physics, engineering, technology. – Energoatomizdat, 2010 [in Russian].

<sup>1</sup> This work was supported by state assignment of Ministry of Education and Science of Russian Federation № 2014/64.

## FLUCTUATION MODEL OF PULSE PHOTOINITIATION OF ENERGETIC MATERIALS<sup>1</sup>

A.Y. MITROFANOV\*, N.N. ILYAKOVA\*, A.G. KRECHETOV\*, A.O. TERENTYEVA\*, A.S. ZVEREV\*

\*Kemerovo State University, Krasnaya 6, Kemerovo, 650043, Russia, [lira@kemsu.ru](mailto:lira@kemsu.ru), +73842588117

We propose a fluctuation model of the photochemical initiation of an explosive chain reaction in energetic materials. In accordance with the developed model, density fluctuations of photo-excited molecules serve as reaction nucleation sites due to the stochastic character of interactions between photons and energetic molecules. A further development of the reaction is determined by a competition of two processes. The first process is growth in size of the isolated reaction cell, leading to a micro-explosion and release of the material from the cell towards the sample surface. The second process is the overlap of reaction cells due to an increase in their size, leading to the formation of a continuous reaction zone and culminating in a macro-explosion, *i.e.*, explosion of the entire area, covering a large part of the volume of the sample. Schematically courses of development of reaction at low and at high levels of light irradiation are shown on fig. 1. At low energies, the reaction cell are not overlapping, thus forming cavities (fig. 1a). At high energies, overlapping leads to explosion of a sample (fig. 1b).

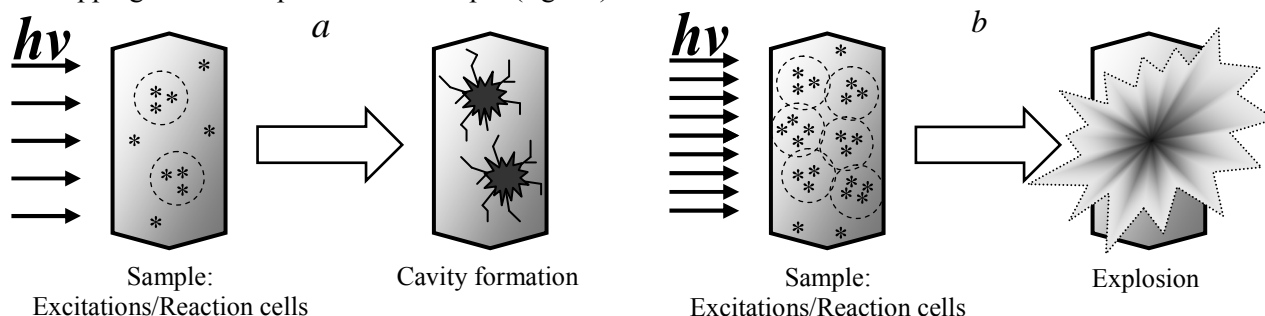


Fig. 1. Schematic description of photoinitiation process, including reaction cells formation and their growth.

Within the proposed analytical model, we derived expressions of the explosion probability and the duration of the induction period as a function of the initiation energy (exposure). An experimental verification of the model was performed by exploring the initiation of pentaerythritol tetranitrate (PETN) with the first harmonic of YAG: Nd laser excitation (1,064 nm, 10 ns), which has confirmed the adequacy of the model. This validation allowed us to make a few quantitative assessments and predictions. For example, there must be a few dozen optically excited molecules produced by the initial fluctuations for the explosive decomposition reaction to occur and the life-time of an isolated cell before the micro-explosion must be of the order of microseconds. The results of approximation of probability and induction period vs. initiation exposition are shown on fig. 2.

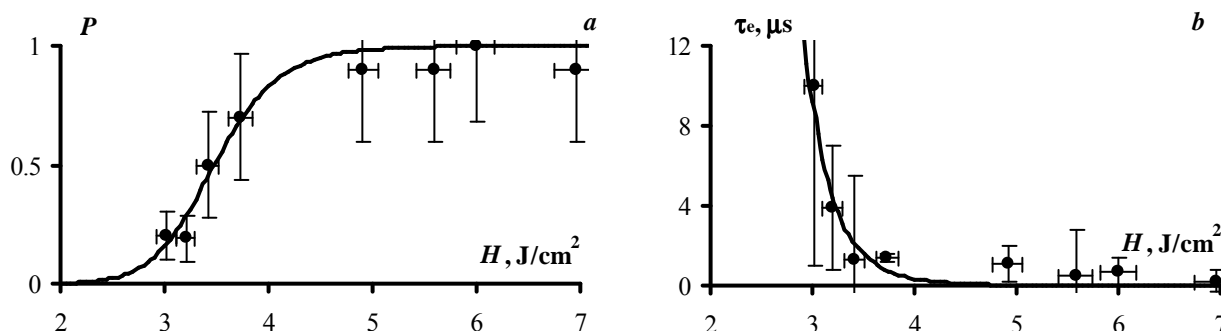


Fig. 2. The probability of explosion as a function of initiation exposure (a) and the duration of the induction period as a function of initiation exposure (b) (1064 nm, 10 ns) are obtained as an experimental result of initiation of at least ten PETN samples (dots) and as a result of approximating the obtained experimental data (solid line). The approximation parameters are the same for both dependencies.

<sup>1</sup> This work was supported by state assignment of Ministry of Education and Science of Russian Federation № 2014/64.

## MODEL OF THE PHOTOSTIMULATED FRAGMENTATION OF MOLECULES OF PETN ND:GLASS PULSE LASER INITIATION<sup>1</sup>

*A.G. KRECHETOV\**, *A.S. PASHPEKIN\**, *Y.P. SAKHARCHUK\**, *V.N. SHVAYKO\**, *A.V. TUPITSYN\**

\*Kemerovo State University, Krasnaya 6, Kemerovo, 650043, Russia, [lira@kemsu.ru](mailto:lira@kemsu.ru), +73842588117

A model of the photostimulated fragmentation of the PETN molecule irradiated by the first harmonic of a neodymium laser (1060 nm) is proposed. Photoexcitation at 1060 nm leads to the  $n \rightarrow \pi^*$  transition of the  $2p$  nonbonding electron of the oxygen to the  $\pi^*$  antibonding orbital, a transition that causes the rupture of the O–N bond and the formation of  $\text{NO}_2^*$  radicals, thereby ensuring a further development of explosive decomposition. In the case of a free molecule or a molecule located on the surface of a microcrystal, the process does not require any thermal activation. In the case of a molecule at a regular lattice site, an additional activation energy (0.4 eV) is needed to overcome the potential barrier associated with the passage of  $\text{NO}_2^*$  through a bottleneck between the nearest-neighbor molecules.

A schematic diagram is shown on fig. 1.

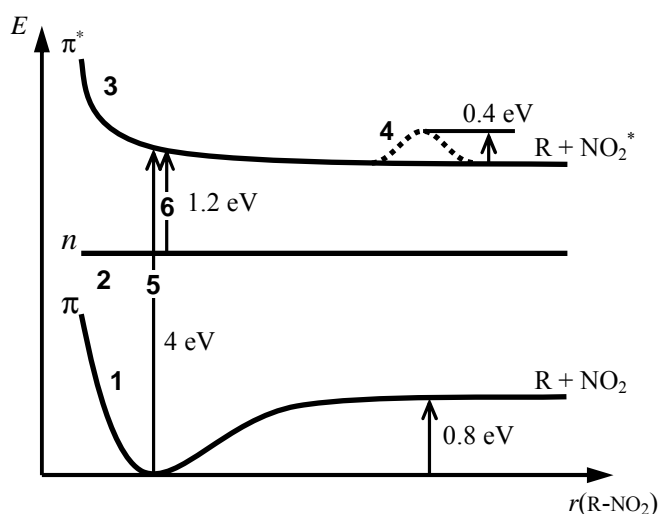


Fig. 1. Schematic diagram of the potential energy curves and optical transitions for the O—NO<sub>2</sub> bond in the PETN molecule ( $E$  is the energy,  $r$  is the distance between the radicals R, i.e.,  $\text{C}_3\text{H}_8\text{O}_{10}\text{N}_3$  and  $\text{NO}_2$ ): (1—3) potential energy curves for the bonding ( $\pi$ ), nonbonding ( $n$ ), and antibonding ( $\pi^*$ ) orbitals, respectively; (4) potential barrier associated with the passage of the  $\text{NO}_2$  radical through a bottleneck between neighboring molecules; (5, 6)  $\pi \rightarrow \pi^*$  (4 eV) and  $n \rightarrow \pi^*$  (1.2 eV) optical transitions, respectively.

<sup>1</sup> This work was supported by state assignment of Ministry of Education and Science of Russian Federation № 2014/64.



## THE FORMATION OF FRACTAL CLUSTERS IN DISORDERED MEDIA

*K. BAKTYBEKOV\**, *A. BARATOVA\*\**

\**U.M. Sultangazin Research Space Institute, Munaipassov, 3, Astana, 010008, Kazakhstan, + 7 701 773 12 21, bkazbek@mail.ru*

\*\**L.N. Gumilyov Eurasian National University, Kazhymukan, 13, Astana, 010008, Kazakhstan*

Research of bimolecular reactions reducing to energy transfer and to spatial division of interacting molecules in disordered media has an important significance in condensed media physics. Mainly, these studies have a theoretical character and don't explain the existence of the complex spatial structures-fractal clusters in disordered media.

In this work computer model generating of these structural distributions is presented. These structures are formed owing to nonlinear processes. Our computer program «Molecular clusters» generates assigned number of clusters of one sort of particles with assigned cluster's size. The second sort of particles was distributed accidentally on the surface. The distance between nearest molecules in coupled cluster is described by maximal distance at which effective energy transfer is possible. On the fig. the spatial structure of matrix with coupled distribution of donor molecules and accidental distribution of acceptor molecules is presented.

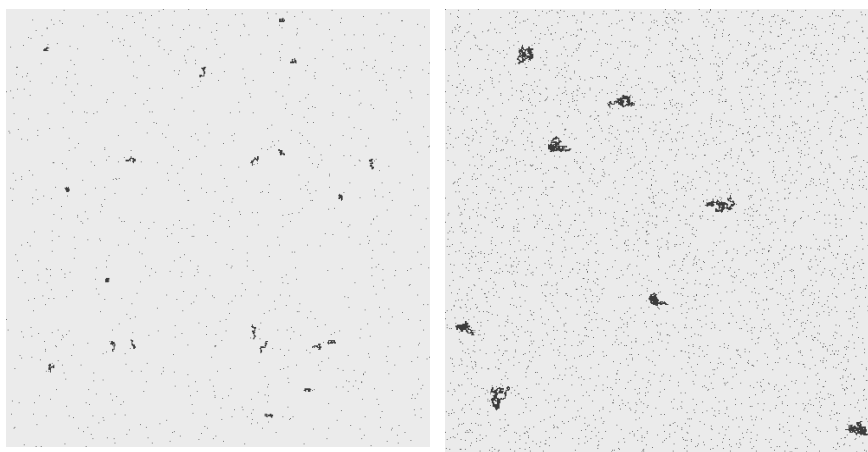


Fig. Spatial structure of matrix with coupled distribution of donor molecules and accidental distribution of acceptor molecules with different number of particles in cluster: a) 50 particles, b) 500 particles.

Structural and dynamical peculiarities of matrix at electron excitation energy transfer determine luminescence kinetics because probability of energy transfer depends on intermolecular distance, relative orientation and relative motion on interacting chromophores (donor and acceptor of electron excitation energy). Faster annihilation kinetics in matrix with chaotic distribution of reagents is observed. Microclusters formation on the surface reduces to excitations localization in the range of cluster, to annihilation kinetics decrease. We explained change of rate coefficient on the basis of model excitation trapping introduced by Kopelman [1]. Excitation trapping dependence on concentration of occupied points by donors molecules determines by clusters size distribution and average number of points in cluster. At concentration decrease average number of points in any cluster will tend to one. Trapping probability becomes proportional to traps concentration. Thus, reagents distribution in system will change from accidental when acceptor molecule very fast finds donor molecule and interacts with it to cluster at which with decrease of trap density trapping probability decreases and from cluster to uniform for which interaction kinetics is described by simple formally kinetic approaching. Conducted multifractal analysis of reagents distribution at different time pieces of kinetic dependences showed that clustering and regulation processes occur faster in higher degree of order matrices.

### REFERENCES

- [1] *J.Hoshen, R. Kopelman // Phys. Rev. B.– 1976. – Volume 14. – № .8. Pages 3438-3445.*

## THE MODERN VARIANT OF THE MICROCENTER HEAT EXPLOSION MODEL<sup>1</sup>

*A. V. KALENSKII, V. G. KRIGER, I. YU. ZYKOV, M. V. ANANYEVA*

*Kemerovo State University, Kemerovo, Russia, kriger@kemsu.ru*

The microcenter model of the energetic materials explosion initiation is based on the assumption that there are inclusions with radii about 100 nm strong absorbing laser irradiation in the sample's volume. The temperature of inclusion and in its neighborhood rises greatly during the laser pulse, which leads to a reaction zone formation. The cross section of the light absorption by the inclusion is thought to be equal its geometrical cross-section. It means that the absorption efficiency  $Q_{abs} = 1$ . This assumption needs to be proved because the inclusion's size is comparable with the light wave length and strong diffraction effects must take place.

For the formulation of the modern variant of microcenter model of the laser initiated heat explosion the dependence of absorption cross section on the inclusion's radius was made in terms of Mie theory. The simulation showed that - The dependence of  $Q_{abs}$  on  $r$  is a curve with a maximum. Its position and amplitude are determined by the light wave length, inclusion's and matrix's material. When the radius is small the absorption efficiency tends to zero in accordance with Rayleigh law, in the area of large radii  $Q_{abs}$  tends to a steady state with oscillations.- The absorption efficiency values are great for the materials with faint metal features.- The light wave length decreasing leads to diminishing of the radius value at which the maximum on the curve is observed and the maximum amplitude becomes higher as a rule.

The program for kinetic analysis of explosive decomposition of condensed energy material was made. Functions of this program are calculation: -dependence of absorption efficiency and dispersion efficiency on the inclusion's radius. -Space and time distribution of temperature in the system energetic material-metal, - the lowest values of the critical energy density.

The calculated absorption efficiencies were taken into account during the calculation of the maximum temperature of the inclusions' heating by the laser pulse. The kinetics of inclusions' heating in the energetic materials volume was simulated and the conditions of explosion initiation were obtained. The critical energy density and the inclusion radius corresponding to the minimal energy of initiation were calculated.

The theoretical calculations have shown the possibility of significant reduction of the critical energy density of explosive decomposition of cyclonite-aluminum compounds compared to pure compressed pills and single crystals of cyclonite.

<sup>1</sup> This work was supported by The Russian Foundation for Basic Research, project № 14-03-00534 A.

## CYCLONITE -ALUMINUM COMPOUNDS' SENSIVITY TO THE LAZER PULSE<sup>1</sup>

A. V. KALENSKII<sup>1</sup>, A. A. ZVECOV<sup>2</sup>, I. YU. ZYKOV<sup>1</sup>, A. P. NIKITIN<sup>2</sup>, B. P. ADUEV<sup>2</sup>

<sup>1</sup>*Kemerovo State University, Kemerovo, Russia, kriger@kemsu.ru*

<sup>2</sup>*Institute of coal chemistry and material science, Russia, lesinko-iuxm@yandex.ru*

The microcenter model of the energetic materials explosion initiation is based on the assumption that there are inclusions with radii about 100 nm strong absorbing laser irradiation in the sample's volume. The temperature of inclusion and in its neighborhood rises greatly during the laser pulse, which leads to a reaction zone formation and decomposition converts to self-acceleration mode

The recent experiments have shown that nano-sized inclusions in the energetic materials (including tertiary explosive) increase sensitivity to the laser effect.

In the modified microcenter model of the laser initiated heat explosion the dependence of absorption cross section on the inclusion's radius was made in terms of Mie theory. The calculations were made for the aluminum inclusions in cyclonite and for first and second harmonic of the neodymium laser.

The calculations and the experimental measurement of critical density of the laser pulse energy were made. It was made for cyclonite with nano-size aluminum inclusions for two wave-length (first 1064 nm and second 532 nm harmonic of the neodymium laser). The comparison of experimental and theoretical was conducted.

---

<sup>1</sup> This work was supported by The Russian Foundation for Basic Research, project № 14-03-00534 A.

## THE CRITICAL DENSITY OF INITIATION ENERGY FOR PETN-NIKEL AND RDX-NIKEL COMPOSITES<sup>1</sup>

A. V. KALENSKII<sup>1</sup>, I. YU. ZYKOV<sup>1</sup>, A.P. BOROVIKOVA<sup>1</sup>, A. P. NIKITIN<sup>2</sup>

<sup>1</sup>*Kemerovo State University, Kemerovo, Russia, kriger@kemsu.ru*

<sup>2</sup>*Institute of coal chemistry and material science, Russia, lesinko-iuxm@yandex.ru*

A creation of energetic materials which are selective sensitive for laser irradiation for capsule compositions of optic detonators has been ongoing for over two decades. An optic detonators on a base of such primary explosives as silver azide, lead azide, copper perchlorate, iron, cobalt have been work out. But there is lack of use such optic detonators – they have a high sensitive not only to laser pulse, but to a wide range of impacts of different nature (impact, friction, heat, radiation, etc.). Fundamentally new explosives synthesis and an introduction to existing ones photosensitive additives are currently the main directions of development of optical detonators.

Early it was shown that photosensitive additives must to decrease critical energy density of the explosives laser initiation. There is an assumption that photosensitive nanometal additives will increase sensitivity to tertiary explosives laser initiation. In this case it is necessary to calculate critical energy density of tertiary explosives' composites with metals.

The critical energy density was calculated in case of the modernized microcenter heat explosion model.

The laser absorption efficacy (for the first harmonic of a neodymium laser, 1064nm) for nickel inclusions in PETN and RDX depending on the inclusion's radius was calculated. The critical energy density of initiation of the tertiary explosive composites was determined and the critical radius of inclusions of nickel, at which the critical density is minimal, was calculated.

<sup>1</sup> This work was supported by The Russian Foundation for Basic Research, project № 14-03-00534 A.

## KINETICS AND MECHANISMS OF SOLID PHASE BRANCHED CHAIN REACTIONS IN THE ENERGY MATERIALS<sup>1</sup>

*V.G. KRIGER, A.V. KALENSKII, D.V. BALYKOV, P.G. ZHURAVLEV, M.V. ANAN'EVA, A.P. BOROVIKOVA*

*Kemerovo State University, Krasnaya st., 6, Kemerovo, 650043, Russian Federation, kriger@kemsu.ru, +7(3842)580591*

In this paper we study the kinetics and mechanisms of solid phase branched chain reactions initiated in energy materials (at the example of heavy metal azides) by means of external physical fields (electric field, electromagnetic radiation). Charge carriers and intrinsic defects of the crystal lattice are the active particles in a chain reaction model. We studied the influence of decomposition products - metallic nanoclusters - on the initiation and evolution of chain reaction regularities including after termination of external influence. We defined model kinetics parameters, criteria and conditions implementation for the stationary, oscillatory and explosive decomposition of heavy metal azides. The problem of heavy metal azides explosive decomposition initiation in the weak fields is discussed.

---

<sup>1</sup> This work was supported by The Russian Foundation for Basic Research, project № 14-03-00534 A.

## THE MODELING OF ORGANIC EXPLOSIVE INITIATION BY A SHORT ELECTRON PULSE

G.A. IVANOV\*, A.V. KHANEFT\*\*,\*\*

\*Kemerovo State University, Krasnaya, 6, Kemerovo, 650043, Russia, [khaneft@kemsu.ru](mailto:khaneft@kemsu.ru), 83842583195

\*\*National Research Tomsk Polytechnic University, Tomsk, Russia

The equation of heat conductivity taking into account fusion and the kinetic equation for chemical reaction of the first order are solved:

$$\rho[c + H_f \delta(T - T_f)] \frac{\partial T}{\partial t} = \lambda \frac{\partial^2 T}{\partial x^2} + \frac{\Lambda(x)}{R_{ef}} I(t) + \rho Q \frac{d\eta}{dt} \quad (1), \quad \frac{d\eta}{dt} = k_1(1 - \eta). \quad (2)$$

Here  $R_{ef}$  is the effective length of linear range of electrons;  $I(t)$  is the energy-flux density of the electron beam;  $\Lambda(x)$  is the density distribution of the absorbed energy of the electron beam along the crystal.

The criterion for initiation of explosives by an electron beam is determined:

$$\rho Q Z \exp\left(-\frac{E}{RT_m}\right) = \frac{\lambda \Delta T_m}{R_{ef}^2} \left( -\frac{1}{\Lambda_m} \frac{\partial^2 \Lambda_m}{\partial \xi^2} + \frac{4}{F(\gamma)} \frac{R_{ef}^2}{r_0^2} \right), \quad W^* = \rho R_{ef} (c \Delta T_m + H_f), \quad (3)$$

where  $\Delta T_m$  is the critical temperature at maximum absorption of the electron beam;  $W^*$  is the critical energy density of the pulse;  $r_0$  is the representative beam radius. The results of calculations, shown in fig. 1, indicate thermal mechanism of PETN initiation by the electron beam.

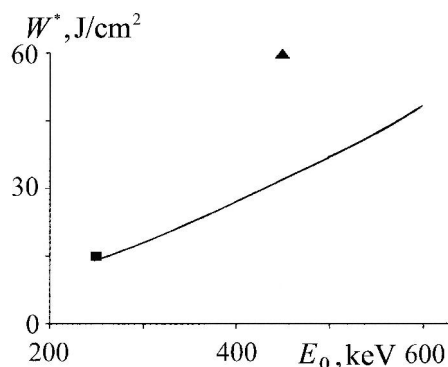


Fig. 1. The dependence of the critical energy density of PETN initiation on the initial energy of the electrons: the line is the calculation by the criterion (formula (3)); ■ is the experiment [1]; ▲ is the threshold energy of PETN detonation [2].

The pressure of the plasma, forming at PETN detonation in the energy release zone, is estimated by formula [3]:

$$P = (\gamma_{ef} - 1)w,$$

where  $\gamma_{ef} = 1,2$  is the plasma specific heat – to – solid specific heat ration;  $w$  is the volume density of absorbed energy. The volume density of energy for explosives is determined by:

$$w = \rho(Q - \Delta H_f) + W_D / \Delta z_1,$$

where  $\Delta z_1$  is the reaction zone thickness. If  $W_D = 60 \text{ J/cm}^2$ ,  $R_{ef} = 415,0 \cdot 10^{-4} \text{ cm}$  at  $E_0 = 450 \text{ keV}$  and  $\Delta z_1 \approx 76 \cdot 10^{-4} \text{ cm}$ , then  $P \approx 1,96 \text{ GPa}$ . The range of electrons in RDX, HMX and TATB is determined. The dependence of the sensitivity of explosives to the action of the electron pulse is defined.

### REFERENCES

- [1] B.P. Aduiev, G.M. Belokurov, S.S. Grechin, and E.V. Tupitcin. Tech. Phy. Lett. – 2004. – Vol. 30. –P. 660 – 664.
- [2] V.I. Oleshko, V.I. Korepanov, V.M. Lisitsyn, A.S. Skripin, V.P. Tsipilev // Pic'ma v JTF. – 2012. – Vol. 38. – No. 9. – P. 37-43.
- [3] S.S. Batsanov, B.A. Demidov, and L.I. Rudakov. JETP Letters. –1979. – Vol. 30. – P. 575 – 577.

## INFLUENCE OF THE SIZE OF THE NANOPARTICLES OF ALUMINUM AND NICKEL ON THE THRESHOLD OF THE LASER INITIATING BLAST PETN<sup>1</sup>

B.P. ADUEV, D.R. NURMUKHAMEDOV, A.A. ZVEKOV, A.P. NIKITIN, R.I. KOVALEV

\* Institute of Coal Chemistry and Material Science SB RAS, Sovetskii pr., 18, Kemerovo, 650000, Russia, lesinko-iuxm@yandex.rul, +7 (384 2) 36-37-66

In the present work was measuring thresholds of the explosive decomposition of PETN with inclusions of nickel and aluminium two sizes, measured absorption coefficients of these models of optical-acoustic method and a discussion of results, using [1]

The initiation was used as the source of the YAG: Nd<sup>3+</sup> laser, Q-modulated mode at the fundamental (1064 nm) with pulse width at half amplitude 14 ns. Samples of PETN with inclusions of nickel and aluminium were manufactured by pressing. Used samples of a diameter of 3 mm, thickness 1 mm, density  $\rho = 1.73 \pm 0.04 \text{ g/cm}^3$ .

Obtained probability of explosion PETN containing 0.1% by mass of the ultra-fine particles of nickel with particle sizes in the maxima distribution (270-300) nm (140-175) nm (first and second synthesis, respectively) and aluminum particles in the maxima distribution (100-120) nm (120-170) nm (first and second synthesis, respectively) depending on the energy density of the laser pulse initiator.

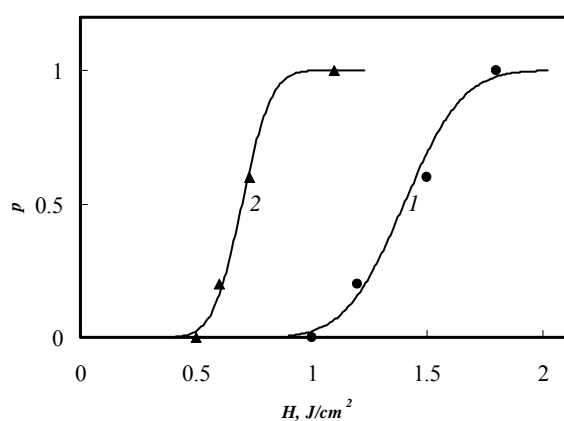


Fig. 1. Figure signature: Dependence of the probability of explosion of samples of laser pulse energy density. Indexes 1 and 2 in samples of PETN 0.1 masses. % nickel powder first and second synthesis, respectively.

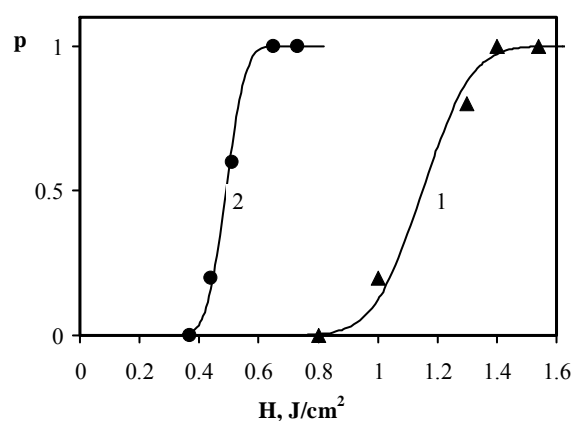


Fig. 2. Figure signature: Dependence of the probability of explosion of samples of laser pulse energy density. Indexes 1 and 2 in samples of PETN 0.1 masses. % of aluminum powder first and second synthesis, respectively.

The results are presented in Figures 1. and 2. Critical energy corresponding to the 50% probability of explosion for samples containing nickel the first synthesis was the  $H_{cr}(1) = 1.4 \text{ J/cm}^2$ , for samples of the second synthesis of the  $H_{cr}(2) = 0.7 \text{ J/cm}^2$ . For samples containing nanoparticles of aluminum: the first synthesis was the  $H_{cr}(1) = 1.15 \text{ J/cm}^2$ , for samples of the second synthesis of the  $H_{cr}(2) = 0.5 \text{ J/cm}^2$ .

The micro- hearth theory of laser ignition are calculated according to section of light absorption and the absorption coefficient  $K$  to the size of the inclusions. Results are consistent with the micro- hearth model of the initiation of the explosion.

Thus, the same conditions of the experiment found on  $H_{cr}$  to the size of the inclusions in PETN.

### REFERENCES

- [1] Kriger, V.G., Kalenskii, A.V., Zvekov, A.A., Zykov, I.Yu., Aduiev, B.P. // Combustion, Explosion and Shock Waves. – 2012. – 48, № 6. – C. 705-708.

<sup>1</sup> The work was partially supported by Russian Foundation for Basic Research (13-03-98032\_r\_sibir\_a).

## STUDY LIGHT SCATTERING AND ABSORPTION IN ALUMINUM NANOPARTICLES IN PETN<sup>1</sup>

B.P. ADUEV, D.R. NURMUKHAMEDOV, A.A. ZVEKOV, A.P. NIKITIN

\* Institute of Coal Chemistry and Material Science SB RAS, Sovetskii pr., 18, Kemerovo, 650000, Russia, lesinko-iuxm@yandex.rul, +7 (384 2) 36-37-66

The paper objective is to determine the scattering and absorption cross sections using the experimental results obtained with an integrating sphere.

The pressed pellets of pentaerythritol tetranitrate (PETN) contained aluminum nanoparticles were used as the experimental samples because they are perspective explosive materials for optic detonators. The size distribution of the nanoparticles showed the maximum at 100 – 120 nm. The aluminum oxide (Al<sub>2</sub>O<sub>3</sub>) content estimated with electron microscope JEOL JSM63901A equipped with a JEOL JED2400 feature for the element analysis was 24 wt%. The weighted amount of the mixture pressed into the pellets with the diameter  $3 \pm 0.01$  mm and  $0.13 \pm 0.01$  mm thicknesses. This procedure allowed us to obtain samples with density value of the monocrystal ( $1.73 \pm 0.03$  g/cm<sup>3</sup>). The pellets did not have any visible defects such as bubbles or cracks which were able to contribute to the scattering. The light wavelengths was 643 nm and 1064 nm.

An integrating photometric sphere was used to determine the reflectance and transmittance.

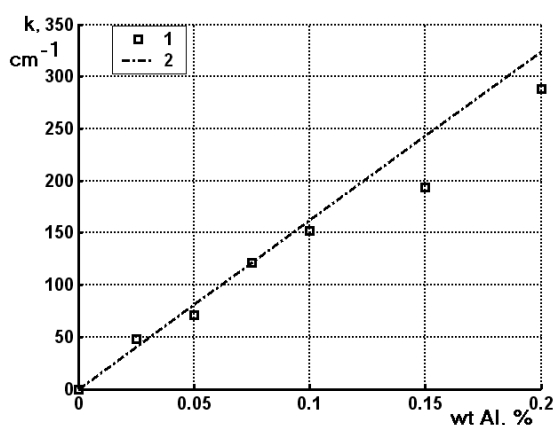


Fig. 1. Figure signature: The apparent absorption coefficient dependence on the aluminum weight percentage. 1 – experiment, 2 – calculation.

The fig. 1 presents the experimental (1) and calculated (2) apparent absorption coefficients dependent on the aluminum weight percentage. The experimental margins were estimated as

$$d^{-1} \ln[(1-R)/T]. \quad (1)$$

The theoretical ones were calculated as the energy distribution curve slope in the semilogarithmic coordinates. The experimental and calculated results agree well (figure 5). The Beer's type dependence of the apparent absorption coefficient on the aluminum concentration arises in terms of the both approaches (fig. 5).

The transmittance and sum of transmittance and reflectance of the petn pressed pellets containing aluminum nanoparticles at the light wavelength 643 nm were measured. The results were processed in terms of the Mie theory and radiative transfer theory. The absorbed energy distribution inside the sample was calculated. It was shown that the Beer's type law is applicable approximately. The apparent light absorption cross section determined, which takes into account both scattering and absorption, is bigger than the geometrical one. The obtained aluminum refractive index agrees well with the handbook's data.

<sup>1</sup> The work was partially supported by Russian Foundation for Basic Research (13-03-98032\_r\_sibir\_a). The authors thank prof. Viktor Yakovlev for the hired integrating sphere.



## NUMERICAL INVESTIGATION OF PARTIAL IGNITION AND PROPAGATION DURING TIC COMBUSTION SYNTHESIS IN 2D POLAR COORDINATES

*A. AOUI\**, *G. DAMAMME\*\**

*\*Centre SMS, UMR CNRS 5307, Laboratoire Georges Friedel, EMSE, 158 cours Fauriel, 42027, France; faoufi@emse.fr*

*\*\*CEA-GRAMAT, Gramat BP 80200 - 46500 Gramat*

Self-propagating High temperature Synthesis (SHS) process was discovered by Merzhanov [1] and uses the energy released by the exothermic reaction itself to ensure its self-propagation combustion synthesis inside the material after a localized heat supply has been performed for several seconds on the surface of the solid mixture. This paper analyzes the ignition and propagation of the combustion front in the case of a cylindrical sample of Titanium and carbide, where the height is significantly greater than its radius. The modelling is therefore two dimensional in space and is expressed in a polar coordinate system because of the geometry's symmetry. A one-step kinetics is used to describe the exothermic synthesis  $Ti+C \rightarrow TiC$  in the solid phase. The computation of the conversion rate and the temperature field takes into account the heat generated by the kinetics. Two cases are considered here:

1. The heat supply is uniform distributed on the exterior of the cylinder. The modelling is computed in a one-dimensional cylindrical coordinate system.
2. The heat supply is located on a part of the exterior of the cylinder. The key parameter is the angle of the sector on which the heat is supplied. A parametric study is done to analyze the behavior of the combustion wave as a function of the angle. The propagation pattern is stable because the Zeldovich number is below the critical threshold above which the propagation is unstable.

Our numerical software implements a fully implicit finite-volume method to discretize the coupled set of equations and is used to perform the parametric study. Animations showing the propagation pattern will be presented and discussed. In the case of a uniform heat supply of a Titanium carbide cylinder the induction time is computed numerically and its relation with the temperature of the furnace in which the cylinder is heated up is represented in Fig. 1. [2],[3].

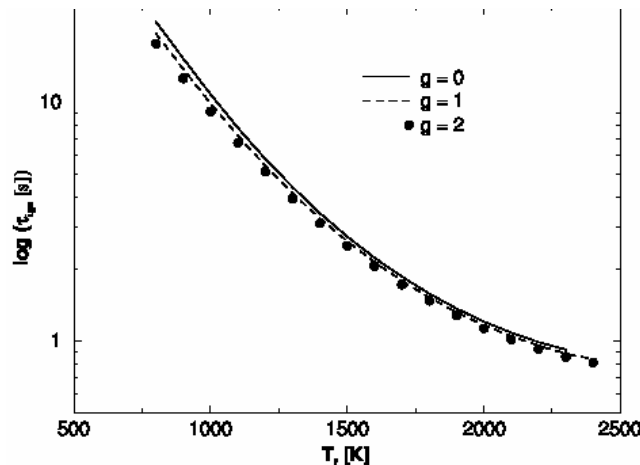


Fig. 1. Evolution of the logarithm of the induction time for slab geometry ( $g=0$ ), cylindrical geometry ( $g=1$ ) and spherical geometry ( $g=2$ ) as a function of the furnace temperature.

### REFERENCES

- [1] *A.G. Merzhanov // Solid flames: discoveries, concept, and horizons of cognition, Combustion Science and Technology.*
- [2] *A. Aoufi, G. Damamme // Applied Mathematics and Computation, Volume 176, Issue 1, 1 May 2006, Pages 99-116*
- [3] *A. Aoufi, G. Damamme // "Numerical Simulation - From Theory to Industry", book edited by Mykhaylo Andriychuk, ISBN 978-953-51-0749-1*

## SOLID-STATE ELECTRON-HOLE PLASMA IN SILVER AZIDE

*V.I. KRASHENININ\**, *E.G. GAZENAUER\**, *A.P. RODZEVICH\*\**, *L.V. KUZMINA\**

\*Kemerovo State University, Krasnaya Street, 6, Kemerovo, 650043, Russia, [specproc@kemsu.ru](mailto:specproc@kemsu.ru), 83842580605

\*\*Yurginskiy Technological Institute of the Tomsk Polytechnic University, Leningradskaya, 26, Yurga, 652050, Russia, [nimez@rambler.ru](mailto:nimez@rambler.ru), 83845162248

Nonequilibrium solid-state plasma is formed in semiconductors by electrons and holes which injected from the contacts or resulting from excitation by an external source [1]. In the present work shows the possible existence of electron-hole plasma, which manifested in the threadlike crystals of silver azide set of inherent her attributes: by the collective response of particles of plasma on external influence, registered current instability.

The objects of investigation - threadlike crystals of silver azide with an average sizes of 10 on  $10^{-1}$  mm<sup>2</sup> and a thickness of 0.03 mm. Initiation was carried out contact electric field by intensity - 300 V/cm, contact material – gallium; in these conditions the mode of monopolar injection of holes is carried out. The model of processes solid phase decompositions of threadlike crystals of silver azide includes: generation of nonequilibrium electrons and holes; the transfer of electron and hole to the surface of crystal in reactionary regions (RR) which formed by regional dislocations in surface region of a crystal, and also realization in RR of chain chemical reaction [2, 3].

The results of the experimental research shows, that electrons and holes which generated after energy effect drift in a noncontact electric field (intensity to  $10^{-4}$  V/m) a uniform package with the ambipolar mobility. The analysis of volts of the ampere dependences in studied system showed existence at the time of decomposition of current instabilities. Current-voltage characteristics of threadlike crystals of silver azide (Ag-AgN<sub>3</sub>-Ag) represented in a figure 1. In the beginning (figure 1 a), current falls exponentially, and then does not depend from time (the shaped line – a residual current according to which was under construction curve). At emergence of the superlinear site (voltage more than 70 V) nature of dependence of current from time sharply changes - at inclusion of tension there are current instabilities (figure 1 b).

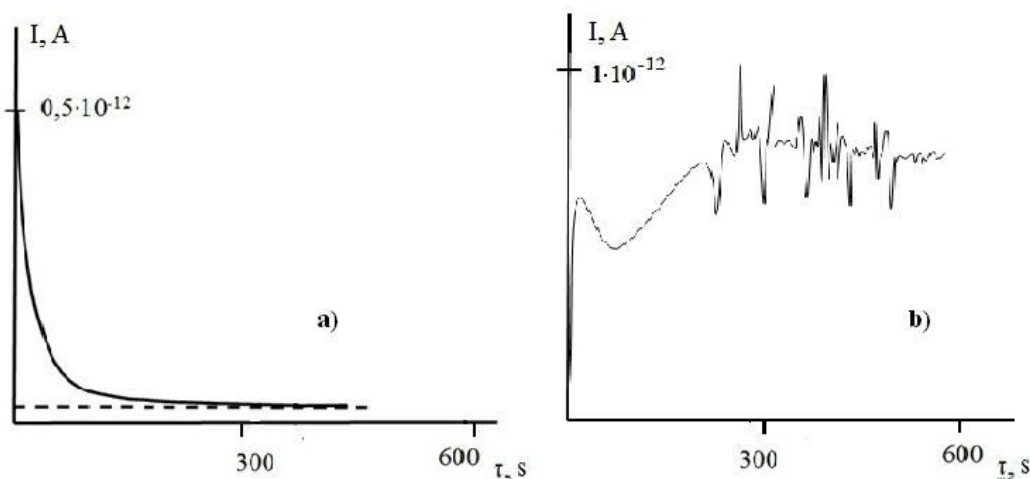


Fig. 1. Dependence of current from time in Ag-AgN<sub>3</sub> (threadlike crystals)-Ag system (interelectrode distance –  $10^{-3}$  m) with tension of electric field: a) 10 V; b) 80 V.

Besides, initiation of chemical reaction in a threadlike crystal of silver azide happens only in the presence of RR in a crystal. If RR in a crystal are absent, signs of decomposition is not observed at least, within 20 clocks.

Thus in silver azide during chemical reaction in reactionary areas (which formed by regional dislocations in surface region of a crystal) are generated not simply nonequilibrium electrons and holes, but solid-state electron-hole plasma.

### REFERENCES

- [1] *Pozhela Y.K.* // Plasma and current instability in semiconductors. M: Science, 1977. 367 p.
- [2] *Rodzevich A.P., Gazenaur E.G., Krashenin V.I.* // News of higher educational institutions. Physics. 2012. V. 55. No. 11-3. P. 87-91.
- [3] *Gazenaur E.G., Krashenin V.I., Kuzmina L.V.* // Materials science. 2011. No. 5. P. 2-6.

## INITIATION OF FURAZANOTETRAZINEDIOXIDE AND MIXES ON ITS BASIS BY HIGH-CURRENT ELECTRON BEAM

*V.I. OLESHKO\**, *V.E. ZARKO\*\**, *V.V. LYSYK\**, *V.P. TSIPILEY\**, *P. KALMYKOY\*\*\**

*\*Tomsk Polytechnic University, Lenin Avenue, 30, Tomsk, 634050, Russia,*

*E-mail: [oleshko@tpu.ru](mailto:oleshko@tpu.ru), +7 (3822) 701777 +1 +2293#*

*\*\*Institute of Chemical Kinetics and Combustion, Institutskaya St., 3, Novosibirsk, 630090, Russia*

*\*\*\*Federal Research & Production Center ALTAI, Biysk, Russia*

The endothermic substance furazanotetrazinedioxide ( $C_2N_6O_3$ , FTDO) with high enthalpy of formation (4200 kJ/kg) is of great interest as a perspective high-energy material [1]. However, its practical use is complicated due to the high sensitivity to the mechanical impact which is comparable to sensitivity of lead azide. For resolving this problem it is suggested to crystallize FTDO in a mix with dinitrodiazapentane ( $C_3H_8N_4O_4$ , DNP). Previously we obtained data on energy thresholds ( $H$ , J/cm<sup>2</sup>) for electron beam initiation of FTDO and mixes FTDO/DNP with the FTDO content of 49 and 65 weight % [2]. The process of pulsed radiative impact on explosives has some specific features. They allow more complete determination of mechanism of energy materials explosive conversion.

In the present work behavior and features of electron beam initiation of FTDO samples and FTDO/DNP mixes (with FTDO content of 75 and 80 weight %) are studied.

FTDO samples were pressed with a pressure of 400 MPa in the form of tablet with 3 mm diameter and 420–450  $\mu$ m thickness up to density of 1.44 g/cm<sup>3</sup>. Samples of FTDO/DNP mixes were prepared by crystallization of corresponding melt at the temperature of 20 C. Nanosecond pulse electron accelerator GIN-600 (average electron energy ~250 keV, maximal current ~3 kA, pulse duration at FWHM ~15 ns) was used as a source of excitation (initiation). The energy density  $H$  of electron beam ejected out of the vacuum chamber was varied in the range of 0.05–0.25 J/cm<sup>2</sup> by changing the distance between output foil of accelerator and sample. Upon irradiation of samples in a vacuum chamber the  $H$  value varied within the range of 0.05–60 J/cm<sup>2</sup> via changing the cathode-anode distance and using diaphragms. Kinetic characteristics of FTDO cathodoluminescence (CL) and gloving of explosive decomposition products were registered by measurement system based on grating monochromator MDR-23, PMT-84 and oscilloscope Tektronix DPO 3034 paired with PC. Resulting time resolution of measurement system was ~15 ns. Measurements were carried out at initial temperature of 300 K. Integral spectra of explosion were registered by means of a fiber-optical spectrometer AvaSpec 2048-2. Spectral range of measurements was 480–980 nm, spectral resolution ~1.5 nm.

It was revealed that irradiation of the FTDO samples by an electron beam with the value of energy density  $H \geq 0,09$  J/cm<sup>2</sup> leads to explosive decomposition of samples. Two peaks of gloving appear on a kinetic curve. The first short peak on the oscillogram represents CL of sample. The second long-time peak corresponds to gloving of explosive decomposition products arising with a delay  $t_{ind} \sim 1.0\text{--}1.2$   $\mu$ s after irradiation instant.

Increasing of electron beam energy density within the range of  $0,09 \leq H \leq 0,25$  J/cm<sup>2</sup> leads to monotonous reduction of the induction period from 1200 to 30 ns and simultaneous reduction of duration of explosive luminescence pulse. It was found that two types of luminescence are distinguished in spectra of explosion plasma of samples: line spectrum of atoms being a part of explosive material and a sample holder as well as continuous spectrum representing gloving of dense low-temperature plasma. Line and continuous spectra intensity ratio depends on a mass of explosive, sample holder material and conditions of plasma torch expansion (free expanding and interaction with an obstacle). It is established that the sensitivity of pure FTDO to the action of a pulse electronic beam is close to the sensitivity of heavy metals azides ( $AgN_3$ ,  $TiN_3$ ), and the sensitivity of FTDO/DNP mix is close to the sensitivity of pentaerythritol tetranitrate (PETN).

### REFERENCES

- [1] Kiselev V.G., Grican N.P., Zarko V.E et al // *Combust. Explos. Shock Waves*. – 2007. – V43. – № 5. 77–81.
- [2] Oleshko V.I., Zarko V.E., Lysyk V.V. et al // *Rus. Phys. Journal*. – 2013. – V56. – № 12/2. 63–68.

## CREATION OF DEFECTS IN CERAMICS LITHIUM FLUORIDE BY FEMTOSECOND LASER PULSES<sup>1</sup>

*V.P. DRESVYANSKIY\**, *S.V. ALEKSEEV\*\**, *V.F. LOSEV \*\**, *M.A. MOISEEVA\**, *E.F. MARTYNOVICH\**

*\*Irkutsk Branch of Institute of Laser Physics SB RAS, 130a Lermontov st, Irkutsk, 664033, Russia, E-mail: [filial@ilph.irk.ru](mailto:filial@ilph.irk.ru)*

*\*\*Institute of High Current Electronics SB RAS, 2/3 Akademichesky Avenue, Tomsk, 634055, Russia*

Experimentally investigated the interaction of optical ceramics based on lithium fluoride with femtosecond laser pulses near infrared. Studied the formation of luminescence centers in LiF ceramics by femtosecond laser pulses in a low external aperture focusing of the exciting radiation (950 nm, 50 fs, 6 mJ). Exciting laser pulses focused by a lens with a focal length of 425 mm, and the sample was placed at some distance in front of the location of the lens focus.

Research topology defect formation and photoluminescence of the irradiated laser samples were carried out on the highly sensitive scanning confocal fluorescence microscope with picosecond time resolution MicroTime 200 firms PicoQuant GmbH with spatially - selective time -correlated single photon counting. Microscope allows to register the longitudinal and transverse spatial distribution of concentrations of defects created by laser radiation, and build microscopic images inside the irradiated volume of the medium in the fluorescent emission at 10 nm scanning step with selection of images of the luminescence decay time.

Research optical absorption spectra of ceramic samples, initial and irradiated by intense femtosecond laser pulses in the filamentation mode. Spectra, kinetics and spatial distribution of the intensity of the photoluminescence excitation photoluminescence picosecond laser pulses also research in the spectral region of the absorption induced color centers from 370 to 640 nm.

Found that the optical ceramics under the action of femtosecond laser pulses is painted in self-focusing and multiple filamentation of laser radiation when its intensity is greatly increased. Disclosed the cause of higher spatial density filaments of femtosecond laser pulses in optical ceramics compared with the single crystal. It is a high internal in homogeneity ceramic samples compared to single crystals. It is known that the spatial heterogeneity of the environment or of the incident radiation favors multiple filamentation in self-focusing.

Shown that under the action of femtosecond laser radiation near-infrared optical ceramics based on wide band crystalline compounds are effectively LiF color centers that are typical of radiation colored single crystals. Luminescence centers created by laser radiation, color centers are characteristic of radiation colored single crystals. The mechanism of their creation involves highly nonlinear generation of electron-hole pairs in the passage of the filaments, their recombination to form anionic excitons decay of excitons into Frenkel defects, overcharging them, migration and aggregation.

<sup>1</sup> This work was supported by the Programme No. 13 of Presidium of RAS

## PERIODIC STRUCTURES OF LUMINESCENT CHANNEL INDUCED FEMTOSECOND LASER RADIATION IN CRYSTALS<sup>1</sup>

*S.A. ZILOV\*, V.P. DRESVYANSKIY\*, E.F. MARTYNOVICH\*\**

*\*Irkutsk Branch of Institute of Laser Physics SB RAS, 130 a Lermontov st, Irkutsk, 664033, Russia, E-mail: [filial@ilph.irk.ru](mailto:filial@ilph.irk.ru)*

*\*\*Institute of Applied Physics, Irkutsk State University, 20 Gagarin Blvd., Irkutsk 664003, Russia*

It is known that in crystals lithium fluoride, under the action of radiation femtosecond titanium sapphire laser to effectively create luminescent defect, in particular aggregates  $F_2$  and  $F_3^+$  color centers. A prerequisite for formation of color centers under the influence of the Ti: sapphire laser is focusing and subsequent laser filamentation accompanied by a sharp increase in its intensity. This ensures that the flow of highly nonlinear processes of absorption of laser radiation. We assume that the effectiveness of this interaction is largely determined by the relative orientation must elementary oscillators characterizing quantum systems that absorb radiation and the direction of polarization of the electric vector of the exciting laser radiation. To establish this fact, we carried out studies of the interaction of femtosecond radiation titanium sapphire laser (wavelength 950 nm, pulse duration of 50 fs, pulse repetition rate of 10 Hz, pulse energy of 6 mJ) with LiF crystals with artificially induced anisotropy.

For the experiments, samples were prepared in the form of crystals of size  $\sim$  parallelepiped 10x10x50 mm. Mechanical load to induce anisotropy was applied to the two opposite faces of the big box. Mechanical stress was applied in the first sample along the crystallographic axis  $C_4$ , in the second - along the  $C_2$  axis. The excitation radiation titanium sapphire laser was directed into the crystal normal to small faces of the parallelepiped, and the electric vector is oriented at an angle of  $\pi/4$  to the induced optical axis. The samples were irradiated for 180 s, in the low- aperture focusing, when the excitation light is focused by a lens with a focal length of 425 mm, and the sample was placed at a distance of 30 mm from the location of the focal lens.

Experiments showed that the sample after irradiation by femtosecond laser beam along the entire length of the samples formed luminescent channel consisting of a plurality of tracks left filaments of different lengths observed upon photo excitation at 450 nm. Evaluation of spectral and kinetic characteristics of the observed luminescence showed that the main types of luminescent defects in laser-induced aggregates are  $F_2$  and  $F_3^+$  color centers. In addition, the luminescence intensity of stress induced in the crystal of lithium fluoride centers becomes spatially periodic modulation with a period of about 3 mm. It should be noted that the periodic structure is observed in both the first and second samples with different orientations. Therefore the formation of a spatially periodic structure, cannot be explained by any anisotropic factor.

The authors suggest that the observed phenomenon is due to the fact that the probability of photo ionization (electron transition from the valence band to the conduction band) with linear polarization of the light more than the circular at the same Keldysh parameter (and , consequently, for the same value of the field strength) [1]. Developed on the basis of these assumptions, the mathematical model adequately describes the observed spatially periodic pattern of luminescence centers in anisotropic dielectrics.

### REFERENCES

- [1] *V.S. Popov*// Physics-Uspekh - 2004. - V.174. - №9. P. 921-951.

<sup>1</sup> This work was supported by the Programme No. 13 of Presidium of RAS

**A SOLID-CHAIN REACTION FOCUS OFFSET IN A NONCONTACT ELECTRIC FIELD<sup>1</sup>**

*V.G. KRIGER, A.V. KALENSKII, D.V. BALYKOV, P.G. ZHURAVLEV, M.V. ANAN'EVA, A.P. BOROVIKOVA*

*Kemerovo State University, Krasnaya st., 6, Kemerovo, 650043, Russian Federation, kriger@kemsu.ru, +7(3842)580591*

In this paper we study regularities of a solid-chain reaction focus offset in a noncontact electric field which is local initiated in a crystal by means of radiation or contact electric field. It is shown that a solid-chain reaction focus offsets with a mobility of electron carriers in accordance with experiment [1]. It is shown that: a reaction passes with oscillatory mode; bipolar drift mobility can change its sign depending on the sign of the currently dominant carrier concentration. We defined parameters of process passing including after external influence.

## REFERENCES

- [1] *V.Yu. Zakharov, V.I. Krashenin* // The slow decomposition of silver and lead azides. – Tomsk, NTL, 2006.

---

<sup>1</sup> This work was supported by The Russian Foundation for Basic Research, project № 14-03-00534 A.

## A METHOD OF INTRINSIC OPTICAL NONLINEARITY MEASUREMENT

*D.M. LUBENKO<sup>1</sup>, YU.M. ANDREEV<sup>2,3</sup>, G.V. LANSKII<sup>2,3</sup>, V.F. LOSEV<sup>1,4</sup>, V.A. SVETLICHNYI<sup>3</sup>*

<sup>1</sup>*Gas Lasers Laboratory, High Current Electronic Institute of SB RAS, 2/3 Akademicheskii Ave., Tomsk 634055, Russia*

<sup>2</sup>*Laboratory of Geosphere-Biosphere Interactions, Institute of Monitoring of Climatic and Ecological Systems SB RAS, 10/3, Akademicheskii Ave., Tomsk, 634055, Russia*

<sup>3</sup>*Laboratory of Advanced Materials and Technologies, Siberian Physical-Technical Institute of Tomsk State University, 1, Novosobornaya Sq., Tomsk, 634050, Russia*

<sup>4</sup>*Tomsk Polytechnic University, 30 Lenin Ave., 634034 Tomsk, Russia*

Efficiency of laser frequency conversion in a nonlinear crystal is proportional to the squared second order nonlinear susceptibility coefficient whose value can be decreased by weak optical quality. This (efficient) nonlinearity coefficient can be significantly restored by a post growth treatment or by a doping. So, there is an important practical interest to estimate its value by any fast, cheap and adequate measurement method after modification. Estimation of efficient nonlinearity by comparison of output signals of a THz generator under fs pulse pump is a hard task due to complicity of the estimation algorithm caused by extra wide band spectrum of fs pulse and unknown difference in the physical properties of the parent and modified crystals. However, we have designed a suitable algorithm to estimate and apply it to doped GaSe crystals used for THz generation under fs pump. Main idea of the proposed algorithm is as follows. On the one hand, THz wave amplitude  $E^{THz}$  is determined by well-known relation

$$E^{THz}(\omega) \sim d_{eff} \cdot F(\omega, \tau_p) \cdot G(\lambda, \omega, d, \theta), \quad (1)$$

where  $d_{eff} = |\bar{e}_{THz} \cdot \chi^{(2)} \cdot \bar{e}_2 \bar{e}_1|$  is efficient nonlinearity coefficient,  $F(\omega, \tau_p) = \omega \cdot e^{-\frac{(\tau_p \cdot \omega)}{2}}$  is determined by energetic and spectral properties of fs pump pulse,  $G(\lambda, \omega, d, \theta) = \frac{e^{-i d(\Delta k(\lambda, \omega, \theta)) - 1}}{i(\Delta k(\lambda, \omega, \theta) + i\alpha_{THz}(\omega))} e^{-\alpha_{opt}(\lambda) d}$  accounts phase mismatching (phase matching conditions). Let us consider

for determinacy phase matching condition for oo-e interaction that is  $k(\lambda, \omega, \theta) = \frac{(n_{gr.opt}(\lambda, \theta) - n_{THz}(\omega, \theta)) \cdot \omega}{c}$ , where  $\bar{e}_{THz}$ ,  $\bar{e}_2$ ,  $\bar{e}_1$  are unity orthonormal vectors of interacting waves,  $\tau_p$  is pulse duration;  $\alpha_{opt}(\lambda)$  and  $\alpha_{THz}(\omega)$  are absorption coefficients;  $d$  is a crystal thickness;  $n_{gr.opt}(\lambda, \theta)$  and  $n_{THz}(\omega, \theta)$  are group and phase refractive indices in visible and THz range, respectively;  $d_{eff} = d_{22} \cos \theta \sin 3\theta$  is efficient nonlinear coefficient that is hard to be determined. On the other hand, output signal is proportional to THz wave amplitude  $E^{THz}(\omega)$ , apparatus function of the detector  $A(\omega, \tau_p)$  that depends on pump pulse parameters and transfer function  $S(\omega)$  of the optical tract. So, in the common case output signal can be estimated by relation

$$E^{det.}(\omega) = K(\omega, \tau_p) \cdot d_{22} \cdot G(\lambda, \omega, d, \theta). \quad (2)$$

The multiplier  $K(\omega, \tau_p)$  in (2) accounts all parameters of the optical tract. Individual crystal properties are accounted by magnitudes of  $d_{22}$  and function  $G$  that is governed by dispersion, absorption and geometric properties of the crystal under the study. Thus, by accounting  $G_{doped}(\lambda, \omega, d, \theta)$  and  $G_{GaSe}(\lambda, \omega, d, \theta)$  and using relation (2) the ratio of efficient coefficients  $d_{22}^{doped} / d_{22}^{GaSe}$  can be estimated as

$$\frac{E_{doped}^{det.}(\omega)}{E_{GaSe}^{det.}(\omega)} = \frac{d_{22}^{doped} \cdot G_{doped}(\lambda, \omega, d, \theta)}{d_{22}^{GaSe} \cdot G_{GaSe}(\lambda, \omega, d, \theta)}. \quad (3)$$

Dispersion properties of pure and doped GaSe were measured by THz-TDS method and used in  $G$ -function estimations by designed software. For Ag-doped GaSe estimated  $d_{22} = 0.93 \pm 0.14$  that seems quite correct value and well in coincidence with published data. Other details will be reported.

## OPTICAL QUALITY CONTROL OUT OF THE MAXIMAL TRANSPARENCY RANGE

*D.M. LUBENKO<sup>1</sup>, YU.M. ANDREEV<sup>2,3</sup>, K.A. KOKH<sup>4,5</sup>, G.V. LANSKI<sup>2,3</sup>, V.F. LOSEV<sup>1,6</sup>, V.A. SVETLICHNYI<sup>3</sup>*

<sup>1</sup>*Gas Lasers Laboratory, High Current Electronic Institute of SB RAS, 2/3 Akademicheskii*

*Ave., Tomsk 634055, Russia*

<sup>2</sup>*Laboratory of Geosphere-Biosphere Interactions, Institute of Monitoring of Climatic and Ecological Systems SB RAS, 10/3, Akademicheskii Ave., Tomsk, 634055, Russia*

<sup>3</sup>*Laboratory of Advanced Materials and Technologies, Siberian Physical-Technical Institute of Tomsk State University, 1, Novosobornaya Sq., Tomsk, 634050, Russia*

<sup>4</sup>*Laboratory of Crystal Growth, Institute of Geology and Mineralogy SB RAS, 3 Koptuyug Ave., Novosibirsk 630090, Russia*

<sup>5</sup>*Novosibirsk State University, 2, Pirogov Str., Novosibirsk 630090, Russia*

<sup>6</sup>*Tomsk Polytechnic University, 30 Lenin Ave., 634034 Tomsk, Russia*

Optical properties of wide used nonlinear layered structure GaSe crystals are significantly improving by doping with isovalent elements. We found that direct search of optimal doping concentration by conventional absorption spectroscopy is inconsistent due to low optical losses of GaSe in the maximal transparency range (absorption coefficient  $\alpha \leq 0.1-0.2 \text{ cm}^{-1}$ ) and limited crystal lengths. To solve this problem, indirect technique for identification of optimal concentration through parameters of phonon or exciton absorption peaks was proposed that is demonstrated in Fig.1.

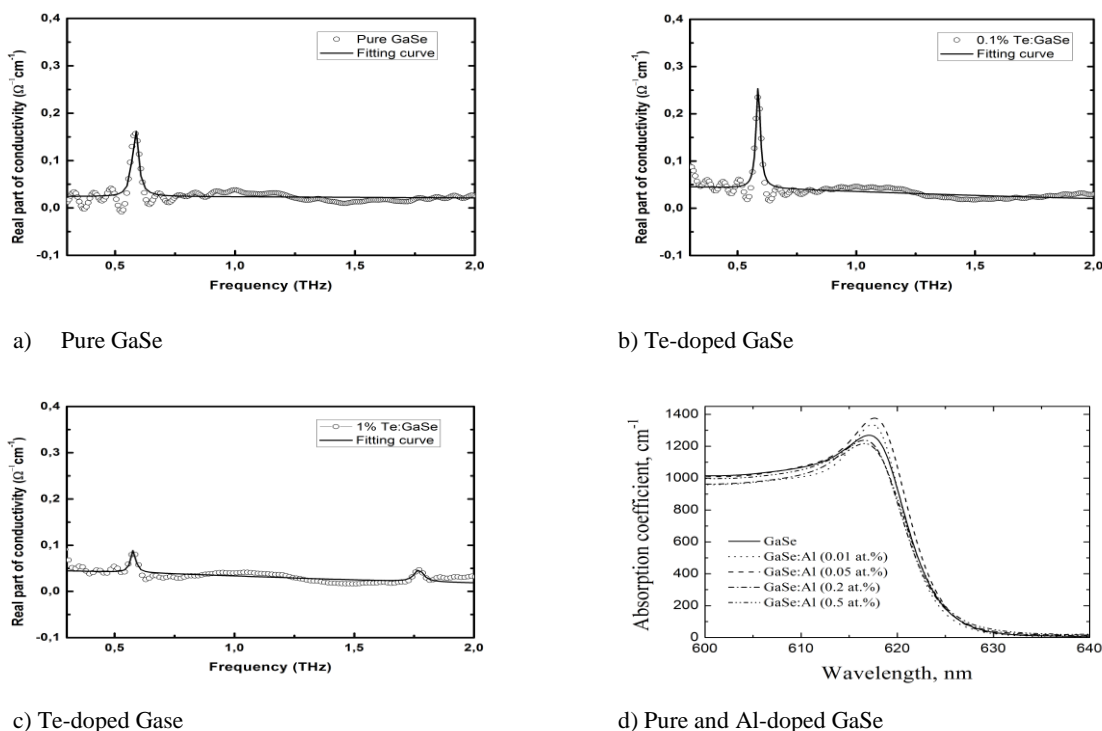


Fig.1. (a, b, c) Transformation of the phonon absorption peak at 0.59 THz and its spectral bandwidth versus Te-doping, so as of (d) exciton peak versus Al-doping.

Frequency conversion experiments have shown that maximal efficiencies are achieving when peak intensities are maximal and spectral bandwidths are minimal. In the second case optimal doping can be also identified from maximal gradient of the short-wave absorption edge and minimal absorption coefficient at its bottom. It seems that identification method designed can be applied to other doped optical crystals.



## REACTION INITIATION BY LASER IMPULSE IN THE ENERGETIC MATERIALS MIXTURE<sup>1</sup>

*A.G. KNYAZEVA\**, *V.E. ZARKO\*\**

*\*Tomsk Polytechnic University, Lenin street, 30, Tomsk, 634050, Russia, anna-knyazeva@mail.ru, 8-382-2-42-14-80*

*\*\*Institute of Chemical Kinetics and Combustion, Institutskaya, 3, Novosibirsk, 634090, Russia*

Chemical reaction initiation by laser radiation gets attention of scientists many years. It is stipulated by practices of laser employment and new physical effect which appear when new materials or new laser sources are developed. For example when short high intensive concentrated impulses are used the mechanism of energetic material initiation is determined by specific features of interrelation of laser radiation with substances of various structure, thermal physical, kinetic and mechanical properties. In the literature, the heat, chain and deformation mechanisms are discussed for reaction propagation from initial hot spot formed by laser radiation.

In this paper we discuss the model of reaction initiation in the mixture of energetic materials. The mathematical formulation of the problem takes into account the heating of the cylindrical specimen by concentrated laser radiation, the absorption of radiation in the volume, the source distribution along space coordinates; the heat capacity change near by melting temperature depending on composition of initial mixture; the ideas of theory of two-phase zone for melting description; chemical heat release and heat absorption due to the chemical reactions in substances containing in the mixture. The problem is solved numerically. The temperature and concentrations distributions have been constructed. During calculation we determine the melting zone size evolution, reaction time initiation.

Taking into account the pressure growth in the reaction zone due to temperature gradient and material properties change, we could reflect the pressure influence on the reaction rates. For this purpose we use the state equation in differential form containing material properties: thermal expansion coefficient; concentration expansion coefficients, bulk module. The appearing in the reaction zone pressure is found high quite and leads to the reaction acceleration.

Some preliminary results were published in [1]

### REFERENCES

- [1] *Knyazeva A.G., Zarko V.E. // Izv. Vuzov: Fizika (In Russian). – 1013. – 56. – № 7/2. – 8–13*

<sup>1</sup> This work was supported by RFFI, grant number is 12-03-13502

**ELECTROTHERMAL TREEING APPLICATION FOR JOUL HEATING OF OIL SHALE**

*S.M. MARTEMYANOV, V.V. LOPATIN, A.A. BUKHARKIN, I.A. KORYASHOV, A.A. IVANOV\**

*\*Tomsk polytechnic university, Lenin av., 30, Tomsk, 634050, Russia  
E-mail: sergmartemyanov@mail.ru, Tel.: +7(3822)701777 (2377)*

Partial discharges (PD) in the porous dielectrics are appeared under effect of high electric field intensity. PDs are not cause of material instant breakdown, but they are cause of accumulation of dielectric local damage. [1] Electrical treeing, which is represents tree-like structures formation, occurred due to increasing of PD concentrations and current pulse amplitude reduces the dielectric strength of materials and initiate breakdown. Treeing is most investigated in polymer dielectrics as a negative effect with following insulating parts failure. [2]

Dendrites are growth abnormally fast and having large dimensions in some types of layered solid fuels. Dendrite in the oil shale starts to grow on low intensity, and their propagation rate is considerably higher than in polymers. This effect could be applied for a plasma channel inducing and electric heating of oil shale in pyrolytic conversion technologies.

Partial discharges are the reason of dendrites formation in the oil shale as well as in other dielectrics. Presents of PDs is confirmed by typical for this phenomena oscillogram of current flowing through the rock. Distinguishing features of treeing in oil shale is effected by the influence of high temperatures around the plasma channel. Phase conversion with the formation of hydrogen and light hydrocarbons  $C_nH_{2n+2}$  causes formation of carbonization region with a resistivity of 10-100 Ohm·cm. In the oil shale this phenomena observed even at the stage of dendrites growth, so treeing could be called electrothermal in contrast to the electrical treeing occurring in the polymers.

## REFERENCES

- [1] *Kuchinsky G.S. // Partial discharges in high voltage construction [in Russian]. – L: Energy, 1979, 224p.*
- [2] *Dissado L.A., Fothergill J.C. // Electrical degradation and breakdown in polymers. – London: Peter Peregrinus Ltd., – 1992.*

## THE MODELING OF ORGANIC EXPLOSIVE INITIATION BY A SHORT LASER PULSE

V.A. DOLGACHEV\*, A.V. KHANEFT\*\*,\*\*

\*Kemerovo State University, Krasnaya, 6, Kemerovo, 650043, Russia, [khaneft@kemsu.ru](mailto:khaneft@kemsu.ru), 83842583195

\*\*National Research Tomsk Polytechnic University, Tomsk, Russia

The heat conduction equation in cylindrical coordinates taking into account melting and the multiple reflections of the light beam from the opposite sides of the sample with the respective initial and boundary conditions is solved:

$$\rho[c + H_f \delta(T - T_f)] \frac{\partial T}{\partial t} = \lambda \left( \frac{1}{r} \frac{\partial}{\partial r} \left( r \frac{\partial T}{\partial r} \right) + \frac{\partial^2 T}{\partial z^2} \right) + \alpha(1 - R_1) I_0(t) \exp\left(-\alpha z - \frac{r^2}{r_0^2}\right) \frac{[1 + R_2 \exp(2\alpha(z - L))]}{[1 - R_1 R_2 \exp(-2\alpha L)]} + \rho Q Z \exp\left(-\frac{E}{RT}\right). \quad (1)$$

Designations of physical and chemical values in the equation (1) are standard.

The criterion for the initiation of explosives with by a short laser pulse is obtained:

$$z_1 \rho Q Z \exp\left(-\frac{E}{RT_m}\right) = \lambda \frac{\Delta T_m}{F(\gamma)} \left\{ \alpha \operatorname{th} \left[ \alpha L - \frac{1}{2} \ln(A_2 F^2(\gamma)) \right] + \frac{4z_1}{r_0^2} \right\},$$

$$W^* = \frac{[1 - A_1 A_2 \exp(-2\alpha L)]}{[1 + A_1 \exp(-2\alpha L)]} \cdot \left[ \frac{c \rho \Delta T_m}{\alpha(1 - A_1)} + \frac{\rho H_f}{\alpha(1 - A_1)} \right], \quad E^* = \pi r_0^2. \quad (2)$$

where  $\Delta T_m = T_m - T_0$  is the critical temperature of the sample;  $T_0$  is the initial temperature of the sample;  $W^*$  is the critical energy density of the laser pulse;

$$F(\gamma) = (1 + \gamma)/(1 - \gamma T_0 / \Delta T_m), \quad z_1 = \alpha^{-1} \ln F(\gamma), \quad \gamma = RT_m / E.$$

The results of numerical calculations of equations (1) and (2) and the results of the experiment [1] are shown in Fig. 1. The results of numerical calculations are in good agreement with the experiment.

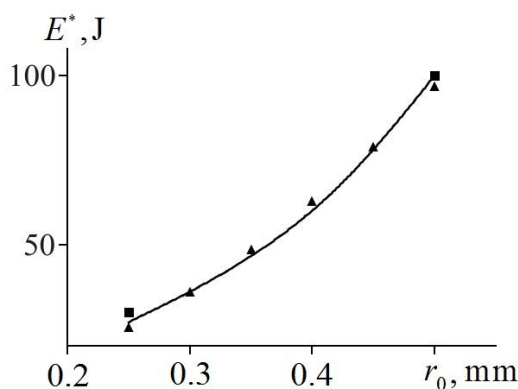


Fig. 1. The dependence of the threshold energy of initiation of PETN on the laser beam radius: line 1 is numerical calculation at  $\alpha = 0,065 \text{ cm}^{-1}$ , ■ is the experiment [1], ▲ is the calculation by the criterion.

The results of numerical calculations show that at the same absorption coefficients PETN is more sensitive but TATB is more heat-resistant.

### REFERENCES

- [1] A.I. Bykhalo, E.V. Zhuzhukalo, N.G. Koval'skii, A.N. Kolomiiskii, V.V. Korobov, A.D. Rozhkov, and A.I. Yudin // Combust., Expl., Shock Waves. – 1985. – Vol. 21. – No. 4. P. 481–483.

## THE INITIATION OF THE EXPLOSION IN THE COMPOSITE BASED ON RDX AND ALUMINIUM NANOPARTICLES IN A LASER ACTION

B.P. ADUEV, D.R. NURMUKHAMEDOV, I.Y. LISKOV, A.P. NIKITIN, N.V. NELUBINA, G.M. BELOKUROV

\* Institute of Coal Chemistry and Material Science SB RAS, Sovetskii pr., 18, Kemerovo, 650000, Russia, lesinko-iuxm@yandex.rul, +7 (384 2) 36-37-66

Decomposition of RDX explosive when exposed to high power laser and electronic pulses not systematically studied. There is work [1], indicating the possibility of explosive decomposition of RDX with additives of micron-sized aluminum when exposed to laser pulses.

This work was carried out for the first time, initiating the detonation of RDX with the addition of aluminum nanoparticles under the influence of the first and second harmonics of neodymium laser.

The initiation was used as the source of the YAG: Nd<sup>3+</sup> laser, Q-modulated mode at the fundamental (1064 nm) and the second harmonic (532 nm) with pulse width at half amplitude 14 ns. Samples of RDX with inclusions of aluminium produced by pressing. Used samples of a diameter of 3 mm, thickness 1 mm, density  $\rho = 1.78 \pm 0.03 \text{ g/cm}^3$ . The grains average size of the RDX powder was 4-5  $\mu\text{m}$  and 100-500  $\mu\text{m}$ .

Received the likelihood of detonation of RDX containing 0.1% by mass of the aluminum particles in the maximum distribution (100-120) nm depending on the energy density of the laser pulse initiator.

In the first of a series of experiments were carried out on the spot samples of pressed composition of RDX with the size of grains of 100-500  $\mu\text{m}$  and 0.1% aluminum nanoparticles. Experiments carried out with the first and second harmonics of the laser showed that under experimental conditions with maximum energy density 30 J/cm<sup>2</sup> and 15 J/cm<sup>2</sup>, respectively, initiating an explosion does not occur.

In the second series of experiments were carried out on the spot samples of pressed composition of RDX with the size of grains 4-5  $\mu\text{m}$  and 0.1% aluminum nanoparticles. In this case, identified an opportunity to initiate the explosion. The critical energy density corresponding to the 50% probability of explosion less than 7 J/cm<sup>2</sup> for the first and second harmonics of the laser.

Thus, it is shown that the source of the powder particle size RDX could have an impact on the fact of the explosion and this must be taken into account in further experimental and theoretical studies.

### REFERENCES

- [1] Ioffe V. B., Dolgolaptev A. V., Aleksandrov V. E., Obrazcov A. P. // Fizika gorenija i vzryva. – 1985. – T. 21. – № 3. – pp. 51-55.

## A STUDY OF OPTOACOUSTIC EFFECTS IN STRONGLY ABSORBING MEDIUM UNDER THE INFLUENCE OF NEODYMIUM LASER PULSE<sup>1</sup>

B.P. ADUEV, D.R. NURMUKHAMEDOV, A.P. NIKITIN, I.Y. LISKOV, R.I. KOVALEV

\* Institute of Coal Chemistry and Material Science SB RAS, Sovetskii pr., 18, Kemerovo, 650000, Russia, lesinko-iuxm@yandex.rul, +7 (384 2) 36-37-66

Pulsed optical radiation, thus being consumed by the sample, stimulates the elastic perturbations in the sample or its surrounding environments, as well as resurfacing of its surface. Registration and analysis of these disturbances can restore a variety of physical parameters of the studied environment and distribution [1].

In this paper using optoacoustic method (OA) [2] is the direct measurement of light intensity in a strongly absorbing medium on the example of the explosive PETN-based composition of mix and 0.03 per cent mass aluminum nanoparticles (100 nm). For measuring optical characteristics of absorbing medium pulse OA method on installation with direct registration of OA. For their arousal was used the second harmonic (532 nm) of neodymium laser, Q-modulated mode with pulse width at half amplitude 14 ns. Samples of PETN with inclusions of aluminium produced by pressing. Used samples of a diameter of 3 mm, thickness 1 mm, density  $\rho = 1.73 \pm 0.03 \text{ g/cm}^3$  for PETN.

In the dependences of the amplitude of the acoustic signal and the rate of absorption of the energy density of neodymium laser second harmonic. The results are presented in Figure 1.

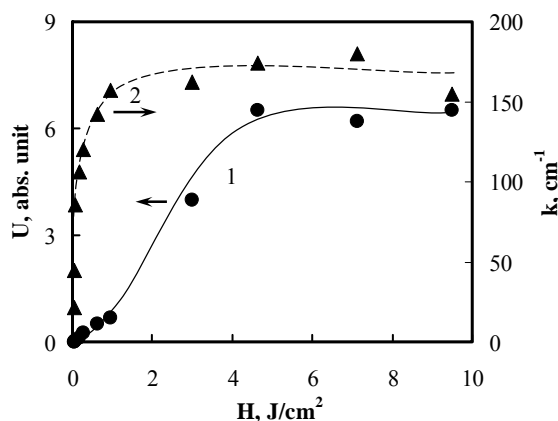


Fig. 1. Figure signature: Amplitude dependence of optoacoustic signal (1) and absorption factor (2) for the composition of the mix on the basis of PETN and 0.03 weight percent aluminum nanoparticles (100 nm) of the energy density of the second harmonic of a neodymium laser

A non-linear dependence of the amplitude of the optical-acoustic alarm (Fig. 1, curve 1) absorption factor (Fig. 1, curve 2) to spot the whole on the basis of PETN and 0.03 per cent mass aluminum nanoparticles (100 nm) of second harmonic energy density neodymium laser. This effect we associate with the heating of the nanoparticles. As the energy of the laser pulses increased heating of the nanoparticles, which leads to an increase in their electrical resistance. As a consequence, increases the rate of absorption and the amplitude of the acoustic signal. Satiety signals allegedly linked to the melting of inclusions.

Thus, it is demonstrated that the laser light in the studied samples is absorbed by the nanoparticles of aluminum with the formation of thermal elastic perturbations.

### REFERENCES

- [1] S V Egerev, L M Lyamshev, O V Puchenkov // Sov. Phys. Uspekhi. – 1990. – 33. – 9. – № 739–762.  
 [2] A A Karabutov, I M Pelivanov, N B Podymova, S E Skipetrov // Quantum electron. – 1999. – 29. – 12, № 1054–1059.

<sup>1</sup> The work was partially supported by Russian Foundation for Basic Research (13-03-98032\_r\_sibir\_a).

## SIMULATION OF STRESSED-STATE OF THE PLATE INVOKED BY CHANGING REGIME OF EXTERNAL HEATING AND SOLID-PHASE CHEMICAL CONVERSION<sup>1</sup>

Y.A. CHUMAKOV\*, A.G. KNYAZEVA\*\*

\*ISPMS SB RAS, pr. Akademicheskii, 2/4, Tomsk, 634055, Russia, yura014@ramble.ru

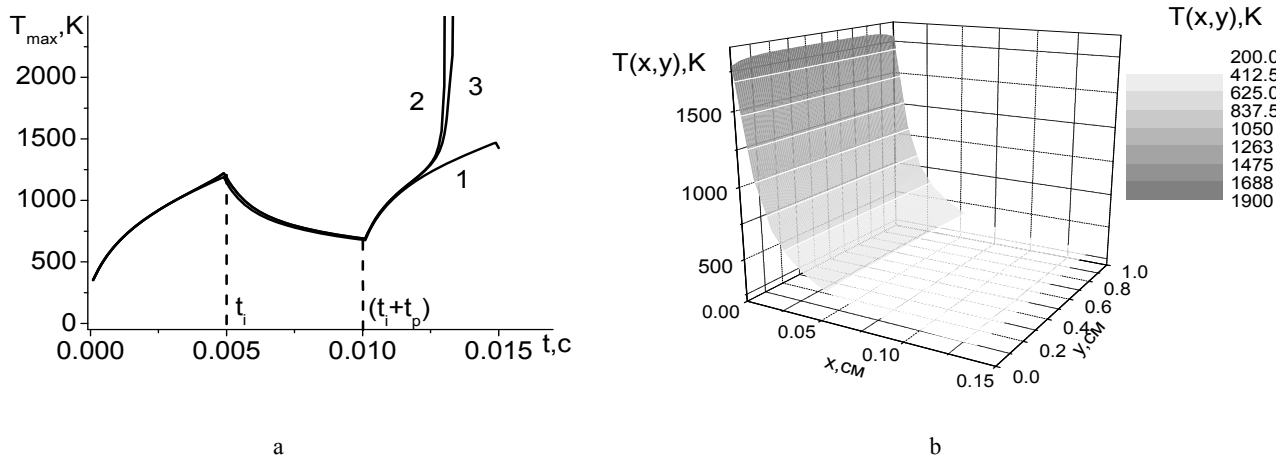
\*\*TPU, Lenin Avenue, 30, Tomsk, 634034, Russia

The different types of high-energy sources used in state-of-the-art technologies of surface treatment beside thermal regime conduct to mechanical stresses arising at the heating area. The stresses can result in generation and accumulation of damage and also ones lead to changing of chemical macrokinetics and phase transformation. The different conditions of treatment details fixation in the experiment lead to arising of many interesting phenomena.

The present work deals with investigation of influence strains-deformed state on regimes propagation of solid-phase exothermic chemical reaction. Coupled of deforms, temperature and concentration fields under external heating and uniaxial tension were included.

The stationary plate from reactive material is considered. The plate has length -  $L_x$ , width -  $L_y$ , height -  $L_z$ , and the condition  $L_z \ll L_x, L_z \ll L_y$  was included. The external loading direction is perpendicular chemical reaction spreading direction. The melting temperature is not reached. The exothermal reaction is assumed to describe summary schema  $A \rightarrow B$ . The form of rate reaction kinetic function is varied.

The second part of general problem is the mechanical equilibrium problem. In the this case is assumed the uniform loading along  $L_y$  is  $\sigma_{yy}=P$  at the  $x=0$  and  $x=L_x$ . The borders of plate at the  $y=0$  and  $y=L_y$  are free.



Pic. 1. Maximal temperature of plate (a) and temperature distribution at the moment  $t=0.015$  c (b);  $t_t=t_p=5 \cdot 10^{-3}$  c, number of impulse  $n=10$ ,  $q_0=10^7$  W/m<sup>2</sup>,  $P=1$  GPa, TiC. Curve number: 1. – without chemical reaction; 2. - one-step reaction.; 3. –take into account product inhibition kinetics ( $m_0=2$ ,  $n_0=0$ )

The minimal values of temperature, stresses and deforms was found to observe without chemical reaction (pic 1,a curve 1). In this case, deform and temperature fields are weakly affected by the assumption of coupled thermal and mechanic processes. Maximum values of temperature, stresses and deform was observed in the case of  $\varphi(\eta) = (1-\eta)$  without assumption of coupled processes (pic. 1, a, curves 2). Decreasing of temperature gradient and values stresses and deforms is caused by account of product inhibition kinetics. The assumption of coupled processes leads to arising of non-unidimensionality border effect, decreasing the value of temperature, stresses and deforms at the plate as the results of this processes significant energy mechanical dissipation, and increasing temperature gradient at the treatment border was observed.

<sup>1</sup> This work was supported by state project « Development of physical principle of metallic and composite material designing with multimodal internal structure» №01201350716, program III.23.2.

## THE ELECTRON-HOLE LIQUID EXCITATION IN THE DIAMOND UNDER THE ACTION OF PULSED UV LASER RADIATION<sup>1</sup>

*E.I. LIPATOV\**, *D.E. GENIN\**, *D.V. GRIGOR'EV\*\**, *V.F. TARASENKO\*\*\**, *S.M. AVDEEV\**, *A.G. BURACHENKO\**

*\*Institute of High Current Electronics SB RAS, 2/3, Akademichesky Avenue, Tomsk, 634055, Russian Federation, lipatov@loi.hcei.tsc.ru, phone: +7 3822 411685*

*\*\*Tomsk State University, 36, Lenina Avenue, Tomsk, 634050, Russian Federation*

The electron-hole liquid (EHL) is the condensed state of excitonic gas in semiconductors [1]. The EHL appears at the cryogenic temperature and at the high charge carrier density. It exists in the form of drops in time scale of tens nanoseconds – hundreds microseconds [2]. The size and the lifetime of EHL drops determines by thermodynamic equilibrium between the EHL evaporation and its condensation from the saturated gas of free excitons, and the process of carrier recombination in EHL drops also [3].

The diamond is the supermaterial with the highest hardness, thermoconductivity and voltage of electrical breakdown. EHL drops exist in a semiconductor at temperatures lower than the critical temperature. The diamond characterizes the very high critical temperature ( $T_c \sim 165$  K) [4]. Critical temperatures of traditional semiconductors (Si, Ge, GaAs et al.) are lower than 30 K [1-3]. The EHL in diamond may be observed in photo- and cathodoluminescence spectra like the wide structureless band (see Fig. 1.) with the maximum at  $\lambda \div 238$ -241 nm [5-8].

In the paper the spectral-kinetic parameters of radiative recombination of electron-hole plasma, excitonic gas and droplets of electron-hole liquid in the natural and synthetic diamond have been reported.

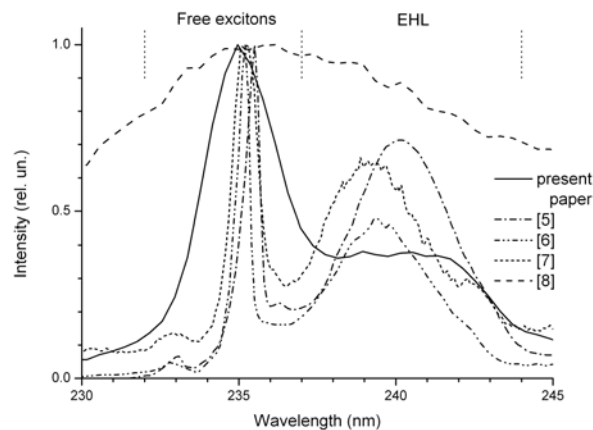


Fig. 1. Photoluminescence spectra of several diamond samples: present paper – synthetic CVD (chemical vapour deposited) diamond, temperature 90 K, laser 222 nm; [5] – synthetic HPHT (high-pressure high-temperature), 20 K, 219 nm; [6] – synthetic HPHT, 15 K, 202 nm; [7] – synthetic CVD, 30 K, 220 nm; [8] – natural of IIa type, 150 K, 222 nm.  
Note: the free exciton band appears in the spectral range of 232-237 nm, the EHL band – of 237-244 nm.

### REFERENCES

- [1] *Keldysh L.V.* // Proceedings of the Ninth International Conference on the Physics of Semiconductors. – Moscow: Nauka. – 1968. – P.1303.
- [2] *Keldysh L.V.* Electron-hole droplets in semiconductors (in Russian). – Moscow: Nauka. – 1988. – 468 P.
- [3] *Rogachev A.A.* Electron-hole liquids in semiconductors. in: Handbook on Semiconductors, Vol.1. Basic Properties of Semiconductors / Ed. by Landsberg P.T. – Elsevier Science Publishers B.V. – 1992. - P.449-487.
- [4] *Vouk M.A.* Conditions necessary for the formation of the electron-hole liquid in diamond and calculation of its parameters // Journal of physics C: Solid state physics. – 1979. – 12. – P.2305-2312.
- [5] *Thonke K., Teofilov N., Zaitsev A.M., et al.* Electron-hole drops in synthetic diamond // Diamond and related materials. – 2000. – 9. – P.428-431.
- [6] *Shimano R., Nagai M., Horiuchi K., Kuwata-Gonokami M.* Formation of a high  $T_c$  electron-hole liquid in diamond // Physical review letters. – 2002. – 88. – №5. – P.057404.
- [7] *Donato M.G., Messina G., Verona Rinati G., et al.* Exciton condensation in homoepitaxial chemical vapor deposition diamond // Journal of applied physics. – 2009. – 106. – P.053528.
- [8] *Lipatov E.I., Tarasenko V.F., Orlovskii V.M., Alekseev S.B.* Luminescence of crystals excited by a KrCl laser and a subnanosecond electron beam // Quantum electronics. – 2005. – 35. – №8. – C.745-748.

<sup>1</sup> This work was supported by Russian Foundation for Basic Research, grant 14-02-31132.

## MECHANISM OF NON-LINEAR SELF-ADDITION FREQUENCIES OF LASER LINES AT POWERFUL ELECTRON-BEAM PUMPING OF $Er:BaY_2F_8$ CRYSTALS

*V.I. BARYSHNIKOV<sup>1-3</sup>, A.V. IVANOV<sup>1</sup>, I.V. SHIPAEV<sup>1</sup>, S.N. VESNINA<sup>1</sup>*

<sup>1</sup>*Irkutsk State Railway University, 15 Chernyshevskogo, Irkutsk, 664074, Russia.*

<sup>2</sup>*Irkutsk Filial of Laser Physics Institute at SB RAS. 130 a, Lermontova, Irkutsk, 664033, Russia.*

<sup>3</sup>*Applied Physics Institute of Irkutsk State University, 20 Gagarin Blvd, Irkutsk, 664003, Russia E-mail: vibh@rambler.ru.*

At nanosecond electron-beam pumping of  $Er:BaY_2F_8$  crystal (concentration of  $Er^{3+} \sim 1$  wt. %) on current density  $> 1,0 \text{ kA/cm}^2$  the generation of IR (2740 nm, 1650 nm, 1230 nm and 850 nm) red (655 nm, 700 nm) green (502 nm, 518 nm and 541 nm, 553 nm) blue (449 nm, 456 nm), violet (407 nm, 414 nm) and UV (378 nm, 382 nm and 315 nm, 320 nm) lines of laser radiation was achieved. In these experiments the small-sized high-current electron-beam accelerator was used with low-inductance cryostat, containing precision system positioning of the aluminum mirror in the open resonator adjusted on full internal reflection of light from the surface of  $Er:BaY_2F_8$  crystal pumping by high-current electron-beam. Observation was produced by system, structure of which contains spectrograph - grating polychromator and pulse color CCD matrix. The separating 4 %-glass plate with *p-i-n* photodiode and oscilloscope were used for kinetic measurements.

At powerful nanosecond electron-beam pumping of  $Er:BaY_2F_8$  crystals the lines of laser radiation in UV - (315 nm, 320 nm and 378 nm, 382 nm), violet – (407 nm, 414 nm) and blue - (449 nm, 456 nm) spectral ranges are not correspond to known radiative electron transitions in  $Er^{3+}$  ions. The analysis has shown, that on high-current electron-beam pumping of  $Er:BaY_2F_8$  crystals the lines of laser radiation at 407 nm, 414 nm and 449 nm, 456 nm are formed by non-linear self-addition of frequencies of complicate green laser lines at 541 nm and 553 nm according to frequency of a laser line at 1650 nm and line at 2740 nm [1]. The laser radiation at 378 nm, 382 nm are formed by non-linear self-addition of frequencies of laser lines at 541 nm and 553 nm to frequency of a laser line at 1230 nm. Then it was determined that UV laser lines at 315 nm, 320 nm are formed by nonlinear self-addition of frequencies of stimulated emission  $Er^{3+}$  lines at 502 nm and 518 nm with frequency of the line at 850 nm.

It was established, that at diode laser pumping of  $Er:BaY_2F_8$  crystals the nonlinear self-transformation occurs only to the participation of frequencies of laser  $Er^{3+}$  lines. The given results are indicate, that laser regular  $Er^{3+}$  ions influence on the nonlinear properties of  $Er:BaY_2F_8$  crystal. The efficiency of self-transformation in UV and violet-blue spectral range at electron-beam pumping of  $Er:BaY_2F_8$  crystals is higher, than at diode laser pumping. Moreover, the efficiency of self-transformation at electron-beam pumping rises with the increase of energy of electrons in the beam.

On the basis of these results it was established, that at electron-beam pumping of  $Er:BaY_2F_8$  crystals the high efficiency of self-transformation of laser  $Er^{3+}$  lines is caused because of the passage of the hyperacoustic pulse, which creates the short live-time displacement of ions  $Er^{3+}$ . Thus in a vicinity of radiating ions  $Er^{3+}$  is induced the electric indignation electric field. As consequence, considerably increase a two order nonlinear susceptibility and thus, at high current nanosecond electron-beam pumping of  $Er:BaY_2F_8$  crystals high efficiency of self-transformation laser  $Er^{3+}$  lines is achieved.

### REFERENCES

- [1]. *V.I. Baryshnikov, V.V. Krivorotova.* Generation of laser lines and nonlinear self-addition their frequencies at powerful electron-beam pumping of  $Er:BaY_2F_8$  crystals. Abstracts, RPC-15, Russia, Tomsk, 63-65(2012).



## THE PROPAGATION OF EXPLOSIVE DECOMPOSITION FRONT IN THEADLIKE SAMPLES OF HEAVY METAL AZIDES INITIATED BY LASER PULSE IN DIFFERENT SPECTRAL AREAS

A. RAZIN, R. AKHMETSHIN, V. TSIPILEV

*National Research Tomsk Polytechnic University, Lenin Avenue, 30, Tomsk, 634050, Russia ,  
[a.v.razin@mail.ru](mailto:a.v.razin@mail.ru), +7(3822)606292*

The velocity of the propagation of explosive decomposition front was originally measured in [1] at the excitation of threadlike crystal of silver azide by the first harmonics of YAG:Nd laser radiation (1064nm, 10ns). The average velocity of decomposition comprised 1.5km/s which is sufficiently slower than detonation velocity. However, this value is greater than that for stationary combustion. The explanation of that phenomenon was given in [1] within the limits of chain (electron-and-hole) mechanism of progress and propagation of explosive decomposition of heavy metal azides.

In [2] explosive decomposition propagation was studied in threadlike crystals and threadlike pressed powders at pulsed laser action (1064nm, 10ns; i. e laser parameters were the same as those in [1]). It was found that average velocity comprised 1.54km/s. In addition, it was learned that decomposition velocity is unstable and can be varied for 2 times. However, pressed powders demonstrate stable average velocity of  $4\div 4.5$ km/s with instability about 10–12%. The difference in decomposition velocity values of crystals and powders cannot be explained within the limits [1].

To clarify the reason for this difference the measurements of explosive decomposition characteristics (explosion initiation threshold, decomposition front velocity, glow intensity from the irradiated area and beyond it) at pulsed laser action (10ns) on the first and fourth harmonics of YAG:Nd laser and first harmonics of CO<sub>2</sub> laser. It was demonstrated that decomposition velocities are not affected by excitation wavelength and comprised  $1.5\pm 1$  km/s and  $4.5\pm 0.5$  km/s for threadlike crystals and threadlike pressed powders, respectively.

The results indicate that nature of decomposition process is common for initiation and decomposition front propagation. It is to be proposed that nature of those processes based on heat generation and transport and the decomposition front propagation is detonative.

### REFERENCES

- [1] B. Aduiev, E. Aluker et al. // Combustion, Explosion and Shock Waves. – 2003. – vol. 39. – № 6, p. 701
- [2] A. Skripin, V. Tsipilev // Russian Physics Journal. – 2009. – vol. 52. – № 8/2, p. 316

## LASER INITIATION OF CRYSTALS OF SILVER AZIDE GROWN IN ELECTRIC FIELD<sup>1</sup>

A.O. TERENTYEVA\*, E.G. GAZENAUER\*, A.Y. MITROFANOV\*, A.S. ZVEREV\*, E.E. SAFONOVA\*, K.S. TUEVA\*

\*Kemerovo State University, Krasnaya 6, Kemerovo, 650043, Russia, [lira@kemsu.ru](mailto:lira@kemsu.ru), +73842588117

This paper presents experimental results of explosive decomposition at laser initiation (first harmonic of YAG:Nd laser excitation) of crystals of silver azide grown in electric field.

The objects of investigation – threadlike crystals of silver azide grown at low noncontact constant electric field (intensity of electric fields –  $10^{-4}$ ,  $10^{-3}$ ,  $10^{-1}$  V/cm) using patented method [1]. The use of method of growing crystal in electric field allows obtaining crystals of the specified sizes and reactionary ability with a minimum content of defects [2]. The crystals (with an average sizes of 10 on  $10^{-1}$  mm<sup>2</sup> and a thickness of 0.03 mm), for both extremities, were glued to a glass support. Initiation was carried out with 10 ns pulses of the first harmonic (1,064 nm) YAG:Nd laser LDPL10M. Initiation exposure was determined using the pyroelectric head PE50BF-DIF-C (Ophir Photonics). Special care was taken to ensure a fairly homogeneous distribution of the excitation intensity over the sample surface. The laser beam was expanded, and only the central part of the beam was used for irradiation of whole crystal. The energy deviation of the initiating pulse did not exceed 3%. Probability of explosion ( $P$ ) was determined using selection of about 10 crystals per exposure value. Simultaneously, the luminescence signal from photomultiplier Hamamatsu H11526-20-NN was measured using Tektronix 3032b oscilloscope.

Experimental results were processed according to the model which proposed in [3]. Figure 1 presents the dependence of the explosion probability ( $P$ ) on initiation exposure ( $H$ ) with approximation for model.

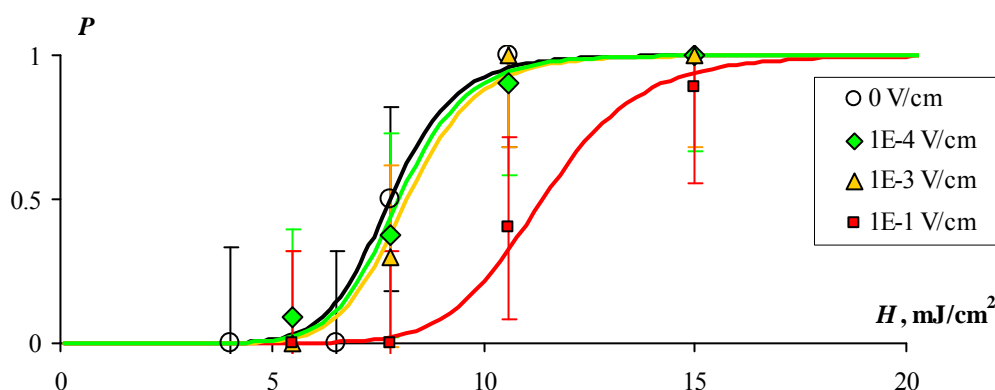


Fig. 1. Dependence of the explosion probability on exposure initiation (1064 nm, 10 ns) of threadlike crystals of silver azide grown up in electric field. Every experimental point is a result of test from a selection of about 10 crystals.

The experimental results of study of the dependence of explosion probability on exposure initiation of threadlike crystals of silver azide shows that sample, grown in electric field intensity  $10^{-1}$  V/m, have higher (approximately in one and a half times as compared to a control crystals threshold of initiation. In addition, in crystals grown in electric field standard deviation of the time for achieve a maximum emission is less than for crystals grown in the usual way.

### REFERENCES

- [1] Gazenaur E.G., Fedorova N.M., Kuzmina L.V., Krashenin V.I. // Method of receipt of threadlike crystals of silver azide. Patent RU №2404296 C1. 20.11.2010. Bulletin 39. 9 p.
- [2] Rodzevich A.P., Gazenaur E.G., Krashenin V.I. // Applied Mechanics and Materials. 2013. V. 379. P. 154-160.
- [3] Aluker E.D., Krechetov A.G., Mitrofanov A.Y., et al. // Molecules. 2013. V. 18. No. 11, P. 14148-14160.

<sup>1</sup> This work was supported by state assignment of Ministry of Education and Science of Russian Federation № 2014/64.

## EFFECT OF LASER RADIATION WAVELENGTH ON ENERGY THRESHOLDS OF INITIATION OF EXPLOSIVES

*R. Akhmetshin\**, A. Razin, A. Skripin, V. Tsipilev, V. Oleshko, V. Zarko

\*Tomsk Polytechnic University, pr. Lenina, 30, Tomsk, 634050, Russia  
[kvant@tpu.ru](mailto:kvant@tpu.ru), +7 (38-22) 60-62-92

Heated centers of various configurations form at laser initiation of explosives. Thus, varying the radiation wavelength results in laser energy localization in a thin subsurface layer of  $< 10^{-4}$  cm (spectral range of “zone-to-zone” absorption), or in “hot spots” of  $\sim 10^{-5}$  cm (spectral range of transparency), or in cylindrical volume with the height of  $10^{-3}$  cm (spectral range of phonon absorption). This brings to the question about the reactive effectiveness of heated centers of different shapes which can be answered after measuring the initiation energy thresholds and kinetic parameters of the explosive decomposition process. Previous studies were performed for primary explosives [1]. It was found that specific heat in heated centers of different shapes makes almost equal value of  $\sim 2700$  J/cm<sup>3</sup>.

In this paper the initiation thresholds were measured and kinetics of decomposition was studied for pressed powders of FTDO (furasan-1,2,3,4-tetrazin-1,3-dioxide) at pulsed laser action by different laser wavelengths: 266 nm (zone-to-zone absorption), 532 nm (transparency range), 1,064 nm (transparency range) and 10,600 nm (phonon absorption). The experiments were carried out for covered samples with the covering pressure of 0.1 GPa (FTDO) and 0.3 GPa (PETN). Laser beam diameter made 1 mm and pulse duration made  $10 \div 25$  ns. The initiation thresholds and approximate specific heats of the centers are presented in Table 1.

Table 1. Energy initiation thresholds (H) and specific energy heat  $\omega$

		10 ns			25 ns
		266 nm	532 nm	1064 nm	10600 nm
PETN	H, mJ/cm <sup>2</sup>	25±20	55±15	60±15	1800±20
	$\omega$ , J/cm <sup>3</sup>	~1900	~1900	~2100	~1800
FTDO	H, mJ/cm <sup>2</sup>	8±2	—	20±6	300±10
	$\omega$ , J/cm <sup>3</sup>	~600	—	~700	~300

Note that evaluated specific heat of different initiation centers (which correspond to different spectral ranges) for every explosive are almost equal when the initiation thresholds are significantly different. Critical value of specific heat for PETN comprised  $\sim 2.0$  kJ/cm<sup>3</sup> and that for FTDO comprised  $0.4$  kJ/cm<sup>3</sup>. Numerical simulation of PETN and FTDO ignition in different spectral ranges was made within the frames of thermal local initiation model. Models of initiation process at laser action were offered.

### REFERENCES

- [1] V. Lisitsyn, V. Tsipilev et al., Comb. Explos. Shock Waves, vol. 47, i. 5 p. 591 (2011)

**BEAM SIZE EFFECT AT LASER INITIATION OF FTDO AND ITS MIXTURES**

*R. Akhmetshin\**, A. Razin, V. Zarko, V. Tsipilev, P. Kalmykov

*\*Tomsk Polytechnic University, pr. Lenina, 30, Tomsk, 634050, Russia*

*[kvant@tpu.ru](mailto:kvant@tpu.ru), +7 (38-22) 60-62-92*

Currently, new energetic materials and its mixtures are being developed to be highly sensitive to laser radiation and insensitive to other actions [1].

One of those energetic materials is furazan-1,2,3,4-tetrazin-1,3-dioxide (FTDO). It is endothermic material with enthalpy of 1,000 cal/g. Pure FTDO is highly sensitive to impact [2]. Therefore, it cocrystallizes with linear nitramine 2,4-dinitro-2,4-diazopentane (DNP) to reduce its impact sensitivity and to keep its energetic characteristics. According to [3] energy thresholds of explosive decomposition of pure FTDO at 1064 nm of laser radiation comprised  $400 \pm \pm 70$  mJ/cm<sup>2</sup>. That means that sensitivity of FTDO which possesses features of secondary explosives is rather high.

In this paper the dependencies of energy threshold initiation of pressed powders of FTDO and its mixtures on laser beam diameter are presented. Note that those dependencies are qualitatively different from those for heavy metal azides [5] and PETN [6]. In particular, beam size effect for pure FTDO and FTDO:DNP (75/25) is less expressed as it was for azides and PETN. The obtained results are discussed with taking into account the radiation diffusion within the samples, conductive and gas dynamic energy drain from the initiation centers. Papers [4 – 6] are the result of this approach.

**REFERENCES**

- [1] *M. Ilyushin, I. Tselinski*, Bull. StPSIT, vol. 35, no. 9, p. 44 (2010)
- [2] *V. Teselkin*, Comb. Explos. Shock Waves, vol. 45, i. 5, p. 632 (2009)
- [3] *V. Oleshko, V. Tsipilev et al.*, J. Rus. Phys., vol 55, no. 11/3, p. 158 (2012)
- [4] *Ye. Aleksandrov, V. Tsipilev*, Comb. Explos. Shock Waves, vol. 17, i. 5, p. 550 (1981)
- [5] *V. Tarzhanov, A. Zinchenko et al.*, Comb. Explos. Shock Waves, vol. 32, i. 4, p. 454 (1996)
- [6] *Ye. ALeksandrov, V. Tsipilev, A. Voznyuk*, Comb. Explos. Shock Waves, vol. 24, i. 6, p. 730 (1989)

**STUDY OF THE LASER SPECTRUM BROADENING DUE TO A SELF-PHASE MODULATION<sup>1</sup>***S.V. ALEKSEEV\**, *M.V. IVANOV\**, *V.F. LOSEV\*\*\***\*Institute of High Current Electronics SB RAS, 2/3 Akademicheskoy Ave., Tomsk, 634055, Russia,  
sergey100@sibmail.com, tel.3822 492547**\*\*Tomsk Polytechnic University, 30 Lenin Ave., Tomsk, 634034, Russia*

Currently in the world the great interest in the design, creation and modernization of ultrahigh power laser systems is appeared. This is due to the fact that obtaining a high-power laser beams expands the opportunities for research in various fields of modern physics. Fundamentally, there are two ways to increase the pulse power output: an increase of the energy and reduction of the pulse duration. The second method is preferable because its implementation does not require the large expenditures. There is the standard method of formation of the short pulse duration in the master oscillator, which for some reason has a limit on the formation of a minimum pulse duration. Thus, in the laser system THL-100 a Ti:Sa master oscillator generates a pulse at the edge of gain profile (950 nm), and due to this its duration is not less than 50 fs. It is far from spectrally limited duration  $\sim 10$  fs. Therefore it is interesting to investigate the possibility of reducing of the spectral-limited pulse by self-phase modulation effects in nonlinear media. Due to this phenomenon the additional spectral components are appeared. This leads to a broadening of the radiation spectrum and to further reduce of the pulse duration. As nonlinear medium we can use a condensed matter and various gases [1,2].

Fig. 1. Spectrum of laser radiation: 1 - initial beam (475 nm, 50 fs), 2 - beam passed through the 65 mm K8.

This paper presents experimental results of the broadening spectrum of the laser radiation at the second harmonic (475 nm) as it passes through different materials. The problems related to the intensity inhomogeneity broadened radiation are discussed. The spectral, temporal and spatial characteristics of the radiation are investigated, as well as the influence of initial chirp on the parameters of the output radiation. Results on a pulse compression due to dispersion compensation of the second and third order are shown. Figure 1 shows a typical spectral broadening of the laser beam as a result of modulation in the glass. It is seen that the spectrum width is increased by 2 times.

## REFERENCES

- [1] *E. Mevel, O. Tcherbakoff, F. Salin, E. Constant // J. Opt. Soc. Am.B. – 2003. – 20. – 105-111.*
- [2] *C. P. Hauri, A. Trisorio, M. Merano, G. Rey, R. B. Lopez-Martens and G. Mourou // Applied Physics Letters. – 2006. – 89. – 151125 (1-5).*

<sup>1</sup> This work was supported by RFBR (projects No. 13-08-00068, 13-08-98038-r\_sibir\_a, 14-08-00511)

## THE INFLUENCE OF INTERSTITIAL IMPURITIES ON THE ADHESION AT THE TiFe $\Sigma 5(310)$ GRAIN BOUNDARY<sup>1</sup>

*S.E. KULKOVA\**, *A. BAKULIN\**, *S. KULKOV\*\**, *S. HOCKER\*\*\**, *S. SCHMAUDER\*\*\**

*\*Institute of Strength Physics and Materials Science SB RAS, pr. Akademicheskoy 2/4, Tomsk, 634021, Russia, kulkova@ms.tsc.ru, +73822286952*

*\*\*National Research Tomsk State University, pr. Lenina 36, Tomsk, 634050, Russia*

*\*\*\*Institute of Materials Testing, Materials Science and Strength of Materials, University of Stuttgart, Pfaffenwaldring 32, D-70569, Stuttgart, Germany*

It is known that hydrogen influences considerably the mechanical properties of materials. Even small concentrations of hydrogen can reduce the mechanical strength and may limit some industrial applications of advanced functional materials. Since TiFe is one of the best hydrogen storage materials, the increase of the resistance of this alloy during hydrogenation is desirable. In this work we investigate the hydrogen sorption properties at the TiFe  $\Sigma 5(310)$  grain boundary (GB) and TiFe(310) free surface (FS) in order to estimate the influence of H on the Griffith work. The calculation of the atomic and electronic structure of TiFe alloy with  $\Sigma 5(310)$  GB and (310) FS was carried out by the plane-wave pseudopotential method. The most preferential positions for H at the GB and FS were determined. It was shown that hydrogen sorption energies at the TiFe  $\Sigma 5(310)$  GB and (310) surface depend strongly on the H local environment. The analysis of electronic properties allows us to establish the microscopic nature of chemical bonding of hydrogen at the interfaces. As shown in Table 1, H decreases the surface energies more significantly than the GB energy, which results in decreasing the Griffith work (negative value of  $\Delta E_{GW}^i$ ) that indicates the decrease of the GB strength. The segregation of H at the GB makes intergranular fracture much easier because the bonding between metal atoms, which are neighbors of H, is weakened. The comparison of results with those obtained for pure Fe was performed. In general, the H segregation behavior confirms it as an embrittler for the TiFe alloy.

Table 1. Segregation energies of H at TiFe  $\Sigma 5(310)$  grain boundary and (310) surface as well as the change of the Griffith work due to H segregation (in J/m<sup>2</sup>).

I-position	$E_{GB}^i$	$E_{FS}^i + E_{FS}$	$\Delta E_{GB}^i$	$\Delta E_{FS}^i$	$E_{GW}$	$E_{GW}^i$	$\Delta E_{GW}^i$
H1	1.38	5.27	-0.23	-0.59	4.25	3.89	-0.36
H2	1.39	5.34	-0.22	-0.52	4.25	3.95	-0.30
H3	1.40	5.39	-0.21	-0.47	4.25	3.99	-0.26
H4	1.52	5.56	-0.09	-0.30	4.25	4.04	-0.21
B1	0.15	5.29	-1.47	-0.57	4.25	5.14	0.89
B2	0.65	5.39	-0.96	-0.47	4.25	4.74	0.49
B3	-0.05	4.74	-1.67	-1.12	4.25	4.79	0.55
B4	1.80	6.69	0.19	0.83	4.25	4.89	0.64

An addition of boron in the intermetallic alloys as was shown in [1] can lead to the improvement of the GB cohesion. In contrast to hydrogen other impurities as boron lead to the opposite effect on the Griffith work. It prefers to segregate towards the grain boundary rather than the surface. Such behavior of B leads to a positive value of  $\Delta E_{GW}^i$  in TiFe similarly as observed for Ni<sub>3</sub>Al [1]. The incorporation of boron in the GB region results in the formation of new bonds and, as consequence, it leads to GB strengthening (Table 1). The estimation of structural and chemical factors and their contributions to the Griffith work was carried out. It was shown that covalently bonded impurities such as boron enhance the cohesion of grain boundaries in the TiFe alloy due to a large contribution of the chemical mechanism to the Griffith work. The interaction energy between B and H was estimated. It was shown that that B and H atoms repel each other at the GB. In general, boron can block the positions which are the most preferential for the H absorption at the grain boundaries which results in an increase of the H sorption in the bulk region.

### REFERENCES

- [1] *Q.M. Hu, R. Yang, D.S. Xu, Y.L. Hao, D. Li. // Phys. Rev. B. – 2003. – V.67. – 224203.*

<sup>1</sup> This work was partially supported by DFG SCHM 746/111-1, 746/133-1 and RSCF

## HIGH POWER ION BEAM TREATMENT OF POLYMER FILMS DEPOSITED ON THE DIELECTRIC SUBSTRATES

V.S. KOVIVCHAK\*\*\*, YU. G. KRYAZHEV\*\*, E.S. MARTYNENKO \*\*\*, E.V. KNYAZEV\*\*

\*Omsk State University, 55a, Mira pr., Omsk, 644077, Russia, [kvs@univer.omsk.su](mailto:kvs@univer.omsk.su), +7(3812)224972

\*\*Omsk Scientific Center of SB RAS, 15, Marks pr., Omsk, 644024, Russia

\*\*\*Institute of Hydrocarbons Processing of SB RAS, 54, Neftezhavodskaya str., Omsk, 644040, Russia

Changes inherent to different classes of materials irradiated by high-power ion beams (HPIB) of nanosecond duration have been comprehensively investigated in metals and alloys. However, only one single work has been devoted to the investigation of the action of HPIB on various polymer materials [1].

In this work, HPIB treatment of chlorinated polyvinyl chloride (CPVC) and polyvinylene chloride - product of CPVC dehydrochlorination was investigated. Taking into account the mobility of chlorine atoms at the conjugation chain, we consider conjugated polyvinylene chloride as reactive carbon precursor. The polyvinylene chloride forms carbon materials as a result of thermal dehydrochlorination with intermolecular condensation under unusually mild thermal treatment conditions according to the following reaction scheme (Fig. 1) [2]:

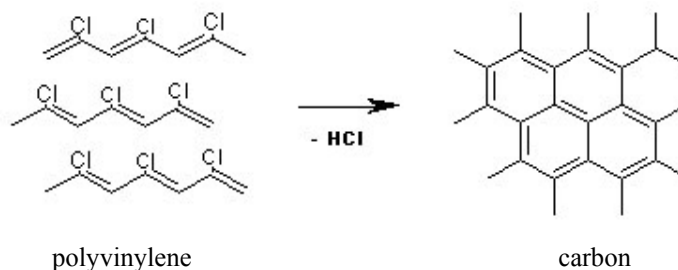


Fig. 1. Reaction scheme of transformation polyvinylene chloride in carbon materials

The rapid energy deposition of HPIB in these polymers resulted in a considerable temperature rise in the surface material and should be accompanied by the formation of carbon materials.

The polymer solution was prepared by dissolving CPVC powder in tetrahydrofuran (THF) and was applied for deposition of films onto substrates by evaporation of the THF. CPVC films were treated by potassium hydroxide solution for the dehydrochlorination.

Irradiation was performed on a Temp accelerator by a proton-carbon (30%  $H^+$  and 70%  $C^+$ ) beam with an average energy of 300 keV, a duration of 60 ns, in the current density range of 20–150 A/cm<sup>2</sup> with a variation in the number of irradiation pulses from 1 to 10. Polymer surfaces were analyzed using a JEOL (JSM-6610LV) scanning electron microscopy with X-ray microanalysis (Inca Energy 350). Specimens were platinum coated to enhance the image features.

Optical inspection of the polymer surfaces irradiated by HPIB generally revealed a more opaque surface with a considerably increased surface roughness. Detailed analysis by scanning electron microscopy indicated that, for investigated materials, surface erosion, ablation and material volatilization had occurred. This is evident as microscopic indentations and bubbles found on the polymer surface. The radiation degradation occurring during irradiation leading to considerable fragmentation of the polymer and the formation of gaseous products (microscopic bubbles in the polymer matrix). Some of these bubbles were partially or fully ruptured.

Some isolated well-faced crystals (characteristic lateral dimension  $\sim$  180 nm) appeared in the film CPVC and polyvinylene chloride after irradiation by HPIB. These crystals consist mainly of carbon according to X-ray microanalysis data. Possible mechanism of used polymer thin films transformations under the action of the HPIB were discussed taking into account the energy loss of carbon and hydrogen ions in the CPVC and polyvinylene chloride.

### REFERENCES

- [1] M. Celina, H. Kudoh, T J Renk, K T. Gillen and R. L. Clough //Polymers for Advanced Technologies. -1996. - V. 9. - P. 38-44.  
 [2] Yu. G. Kryazhev and V. S. Solodovnichenko//Solid Fuel Chemistry. - 2012. - V. 46. - No. 5 - P. 330-337.

## MATHEMATICAL MODELING OF CONVERSION PROCESSES ACCOMPANYING THE DIFFERENT MATERIAL CONJUGATION USING SOLID-PHASE SYNTHESIS AT THE REACTION INITIATION BY SHORT HEAT IMPULSE

*K.A. ALIGOZHINA\**, *A. G. KNYAZEVA\*\**

*\*National Research Tomsk State University, 36, Lenin Street, Tomsk, 634050, Russia, kam.777@mail.ru, +7(952)1760189*

*\*\*Institute of Strength Physics and Materials Science, 2/4, pr. Akademicheskii, Tomsk, 634021, Russia*

Nowadays many ways of material joining exists. Self sustaining high temperature synthesis (SHS) takes a special place. Generally speaking, SHS is the propagation process of chemical reaction wave along reactant mixture to finally solid product or new material formation. Ones distinguish several types of technological processes using SHS. The SHS-welding is one of them. Welding process, when the exothermal reaction propagates in a gap between two specimens that are to be joined, is called SHS-welding. To develop and optimize of SHS technologies it is necessary to understand the physical processes accompanying the chemical reactions and leading to products formation. Because the experimental investigations in this field are quite expensive, the mathematical modeling has a great significance.

It is possible to apply various energy sources for the heating of sample surface. For example, the ignition of condensed matter can be carried out by hot body, heat flux, convective flux etc. Detailed investigation of this problem is described in [1] for various situations. Laser heating is very popular for ignition organization in laboratory investigations and new material synthesis.

For example, models describing selective laser sintering of some powder mixture are given in [2-4]. Advantages of this method of ignition consist in controllability of heat influence parameters and possibility of ignition site formation in required area of a sample. For explosive decomposition of heavy metal azides extensively used laser radiation [5,6]. Many papers were devoted to laser assisted cutting.

The purpose of this work consists in theoretical investigation of heat and kinetic processes accompanying the connective joint formation, when materials with difference properties have been joined. The impulse heat source (for example, laser irradiation) could be used for the reaction assistance.

Mathematical model, which is a basis for numerical investigation of the problem, represents two-dimensional three-layer coupled thermal conductivity problem with chemical heat release source in a middle area. Chemical reaction is described by simple summary scheme. Boundary conditions in the interface are formulated assuming that the contact between connective materials and reagent is ideal. Initiation of the reaction is realized with help of short heat impulse from the surface. That leads to combustion wave formation and its further propagation in the direction of initial substance.

### REFERENCES

- [1] *V. N. Vilyunov, V. E. Zarko // The Ignition of solids. – Elsevier science Ltd, 1989.*
- [2] *B. Xiao, Y. Zhang, Laser sintering of metal powders on top of sintered layers under multiple-line laser scanning // J. Phys. D: Appl. Phys. – 2007. – 40. – № 21. 6725-6734.*
- [3] *T. Chen, Y. Zhang, A partial shrinkage model for selective laser sintering of a two-component metal powder layer // Int. J. of Heat and Mass Transfer. – 2006. – 49. – № 7-8. 1489-1492.*
- [4] *A. V. Koldoba, [et al.], Mathematical modeling of laser sintering of two-component powder mixtures // Keldysh Institute PREPRINTS. – 2009. – 38. 1-15. [In Russian]*
- [5] *V. D. Tsipilev, [et al.], On the question of predetonation stage of explosive decomposition of heavy metal azides. Russian Phys. J. – 2012. – 55. – № 11-3. 240-243.*
- [6] *V.M. Lisitsyn, V. I. Oleshko, V. P. Tsipilev, Initial processes of explosive decomposition of heavy metal azides exposed to pulsed radiation. Russian Phys. J. – 2004. – 48. – № 2. 109-116.*



## THERMODYNAMICAL ANALYSIS OF ORDERING IN A BINARY ALLOY IN PRESENCE OF ELASTIC STRAINS

A.V. ORLOV<sup>1</sup>, V.L. ORLOV<sup>2</sup>, V.P. KRIVOBOKOV<sup>3</sup>, M.A. GUMIROV<sup>4</sup>

<sup>1</sup> Yugra State University, Khanty-Mansiysk, Russia, [a\\_orlov@ugrasu.ru](mailto:a_orlov@ugrasu.ru)

<sup>2</sup> Polzunov Altai State Technical University, Barnaul, Russia, 8-3852-29-09-25 [a\\_v\\_orlov@mail.ru](mailto:a_v_orlov@mail.ru)

<sup>3</sup> Tomsk Polytechnic University, Tomsk, Russia, [krivobokov@tpu.ru](mailto:krivobokov@tpu.ru)

<sup>4</sup> Polzunov Altai State Technical University, Barnaul, Russia, [gumirov71@mail.ru](mailto:gumirov71@mail.ru)

Irradiation and intensive plastic deformation are extreme channels affecting matter. Common for these processes is the introduction of significant portions of energy into the metallic system. However the results of dissipation of this additional energy are different. In the case of irradiation, typically, the material tends to stratify, as well as form discharges where they're not observed in the state of equilibrium. On the other hand, intensive plastic deformation results in the formation of solid solutions, unobtainable through other means. The most probable cause of this difference is the effect of internal strains.

This work presents the results of a calculation for the dependency of the parameter of long-range order on elastic strains for self-ordering alloys at a fixed temperature. We've used the linear thermodynamics approach and compared the calculation with the experimental results for intermetallic compounds.

## COMPUTER MODELING OF AG INTERACTION WITH THE LMO [001] $\text{MnO}_2$ - AND LAO-TERMINATED SURFACES

A.U. ABUOVA<sup>1</sup>, E. A. KOTOMIN<sup>2,4</sup>, T.M. INERBAEV<sup>1</sup>, A.T. AKILBEKOV<sup>1</sup>, YU. A. MASTRIKOV<sup>2,3</sup>, F.U. ABUOVA<sup>1</sup>

<sup>1</sup>L.N. Gumilyov Eurasian National University, Mirzoyan str.2, Astana, Kazakhstan

<sup>2</sup>Institute of Solid State Physics, University of Latvia, Kengaraga str. 8, Riga, Latvia

<sup>3</sup>Materials Science and Engineering Dept., University of Maryland, College Park, USA

<sup>4</sup>Max Planck Institute for Solid State Research, Heisenbergstr.1, Stuttgart, Germany

Metallic silver is a potential component for the SOFC cathode operated at less than 800°C because of its good catalytic activity, high electrical conductivity, and relatively low cost. Different methods have been used to prepare functionalized composite cathodes with improved electrochemical performance and long term stability at reduced operating temperature. [1] In addition, even far below its melting point, silver is relatively mobile. Therefore, these concerns should be addressed prior to a long-term application of silver-based cathodes in SOFCs.

To overcome this problem Zhou *et al.* presented  $(\text{La}_{0.8}\text{Sr}_{0.2})_{0.95}\text{Ag}_{0.05}\text{MnO}_{3-\delta}$  as a high performance intermediate temperature cathode material, in which the contained Ag functions as an effective catalyst through an intercalation/deintercalation mechanism. [2] Under cathodic polarization, Ag moves out of cathode to be deposited as small nanoclusters of Ag metal, leaving the remaining  $(\text{La}_{0.8}\text{Sr}_{0.2})_{0.95}\text{MnO}_{3-\delta}$  as a catalyst carrier. The Ag nanoclusters which are 5–15 nm are very active and stable in catalyzing the cathode reaction even at a reduced temperature. Under anodic polarization, the Ag moves back into the deficient sites of the LSM. This permits an easy regeneration method to restore Ag nanoclusters which may become degraded over time by fusing together, thereby losing the activity.

We present results of *ab-initio* calculations of Ag adsorption on the LMO [001] polar surface. The most energetically favourable adsorption sites on both  $\text{MnO}_2$ - and LaO-terminations have been determined. Electron charge transfer between the adsorbate and the adsorbent has been analyzed. Optimized interatomic distances have been measured.

### REFERENCES

- [1] S. Uhlenbruck, F. Tietz, V. Haanappel, D. Sebold, H.P. Buchkremer, and D. Stover. Journal of Solid State Electrochemistry 8 (2004) 923-927.
- [2] W. Zhou, Z. Shao, F. Liang, Z.-G. Chen, Z. Zhu, W. Jin, and N. Xu. Journal of Materials Chemistry 21 15343-15351.

**WATER ADSORPTION AND OXIDATION AT FLUORINE-DOPED  $\text{Co}_3\text{O}_4$  (100) SURFACE**

G. KAPTAGAI<sup>1</sup>, T.M. INERBAEV<sup>1</sup>, A.T. AKILBEKOV<sup>1</sup>  
YU.A. MASTRIKOV<sup>2</sup>, E.A. KOTOMIN<sup>2,3</sup>, F.U. ABUOVA<sup>1</sup>

<sup>1</sup> L.N. Gumilyov Eurasian National University, Mirzoyan str. 2, Astana, Kazakhstan

<sup>2</sup> Institute of Solid State Physics, University of Latvia, Kengaraga str. 8, Riga, Latvia

<sup>3</sup> Max Plank Institute for Solid State Research, Heisenberg str. 1, Stuttgart, Germany

Electrochemical water splitting has attracted substantial interest in the recent years as a key process in hydrogen production from sunlight and other sources of electricity. Recent experimental studies have demonstrated that  $\text{Co}_3\text{O}_4$  is high-promising anode material for electrochemical water splitting due to its high catalytic activity in the oxygen evolution reaction (OER) [1]. In this context, understanding the interaction of  $\text{Co}_3\text{O}_4$  surfaces with water is an essential preliminary step that can help to shed light on the atomic scale reaction mechanisms. Our attention is focused on investigation of  $\text{Co}_3\text{O}_4$  (100) surface which are the most abundantly presented in  $\text{Co}_3\text{O}_4$  nanoparticles [2]. Density functional method is applied to describe thermodynamics of electrocatalytic water splitting on the  $\text{Co}_3\text{O}_4$  (100) surface. We calculated free energy changes along the reaction pathway using the computational standard hydrogen electrode (SHE) allowing us to replace a proton and an electron with half a hydrogen molecule at  $U = 0$  V vs SHE. The analysis performed for the free energies is at standard conditions ( $\text{pH} = 0$ ,  $T = 298.15$  K) and  $U = 0$ .

Using accurate DFT+U calculations, we shown that water adsorbs dissociatively on  $\text{Co}_3\text{O}_4$  on the (100) surface. From the computed free-energy changes along the OER, we found that the (100) surface is catalytically inactive. Fluorine doping of  $\text{Co}_3\text{O}_4$  nanoparticles drastically changes their interaction with water. In our investigations solvent effects are generally expected to be small for neutral species, the neglect of the water environment is a rather drastic approximation, for which the main justifications are that it provides a qualitative description of experimentally observed trends, and it is the first step toward more complete treatments that include the solvent.

## REFERENCES

[1] I. C. Man, H.-Y. Su, F. Calle-Vallejo, H. A. Hansen, J. I. Martínez, N. G. Inoglu, J. Kitchin, T. F. Jaramillo, J. K. Nørskov, and J. Rossmeisl “Universality in Oxygen Evolution Electrocatalysis on Oxide Surfaces” *ChemCatChem* (2011) **3**, 1159 – 1165.

[2] F. Zasada, W. Piskorz, S. Cristol, J.-F. Paul, A. Kotarba, and Z. Sojka “Periodic Density Functional Theory and Atomistic Thermodynamic Studies of Cobalt Spinel Nanocrystals in Wet Environment: Molecular Interpretation of Water Adsorption Equilibria” *J. Phys. Chem. C* (2010), **114**, 22245–22253.

## THE FORMATION OF CRYSTALLINE STRUCTURES IN THIN FILMS OF TITANIUM DIOXIDE

A. YU. STEPANOV, L. V. SOTNIKOVA, A. A. VLADIMIROV

Kemerovo State University, Red 6 lab.1306, Kemerovo, 650043, Russia Federation, tonystep1110@gmail.com, 8-950-580-06-15

In the present work the processes of formation of titanium dioxide thin films by the method of activated chemical decomposition of the precursor films - polietoksititana were investigated. The dependencies of the thickness and composition of  $\text{TiO}_2$  films from titanium precursor concentration and radiation dose were obtained. The optical properties, phase composition and texture of the resulting films were studied by spectrophotometry, X-ray diffraction (XRD), atomic force microscopy (AFM). The  $\text{TiO}_2$  films obtained by thermal decomposition of the precursor as a comparative sample were used.

Thin oxide films are used in various fields of industry, science and technology. Now a new fields of films using in transparent electronics materials and in protective coatings for flexible and touch displays are successfully developed. The commercially attractive technique of production of such materials are based on solutions using, methods that do not require high energy costs. The titanium dioxide can be used as a material for creating the transparent semiconductor films due to it is inexpensive, chemically resistant material with unique optical, photocatalytic and antibacterial properties. Therefore it is interesting to study the process of formation of  $\text{TiO}_2$  films from solution by decomposition of organic or organometallic compounds under the action of heat, ultraviolet or electron irradiation.

The solutions of titanium chloride in ethanol with the concentration of 50, 20, 10, 5 and 2 mass.% were used to produce the films of polietokstitana with different thicknesses. The substrates glass plates (2.5 x 2.5 cm) were coated by 0.3 ml of a titanium chloride solution. Then the substrates with solution was placed on a horizontal table centrifuge; rotation speed 6000 rev/min, time of centrifugation 10 min. For formation of  $\text{TiO}_2$  films the obtained samples were subjected by gamma irradiation, UV irradiation or pyrolysis. The irradiation of samples was made on irradiator RHM- $\gamma$ -20 with a source  $^{60}\text{Co}$  or by UV-exposition with DRT – 125 lamp, or by thermolysis of samples in a muffle furnace at  $T = 500^\circ\text{C}$ . Fig. 1. shows the typical AFM images of the surface of the resulting films.

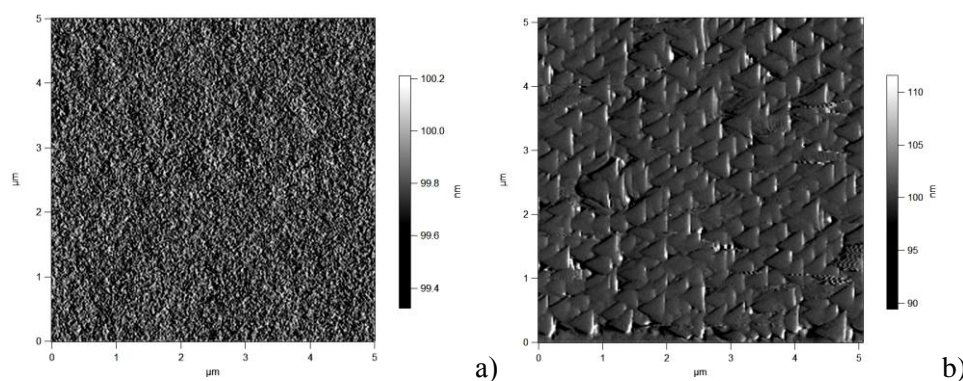


Fig. 1. AFM images of  $\text{TiO}_2$  films obtained by: a) gamma irradiation; b) pyrolysis.

The AFM images show that the texture of films of  $\text{TiO}_2$  depends on the conditions of formation. The films of  $\text{TiO}_2$  formed under irradiation conditions have a smooth surface (value of roughness around 0.16 nm). The average value of roughness of  $\text{TiO}_2$  films that were obtained by pyrolysis is equal  $\sim 5$  nm, with an average size of triangular grain 350 nm. The thickness of the obtained films of  $\text{TiO}_2$  are varied in interval of 50-300 nm in depending on the solution concentration. The films of  $\text{TiO}_2$  with  $h \approx 50$  nm have the metallic color in reflected light, the more thicker films were colored according to laws of light interference in the films. The films of  $\text{TiO}_2$  were obtained which painted in the colors of appropriate entire range of visible light. The pyrolytic films were obtained with uniform color and having a high reflectance. The direct transitions energy values was calculated with using of transmission spectra of  $\text{TiO}_2$  films with a thickness  $\approx 50$  nm and correspond to value of the band gap  $E = 3.9$  eV. The resulting value is significantly greater when the tabulated values for the rutile ( $E = 3.0$  eV), anatase ( $E = 3.2$  eV), brookite ( $E = 3.4$  eV) and possibly are connected with the presence of internal stresses in the film.

## REACTION OF H-ATOMS FROM HYDROGEN PLASMA WITH THE SURFACE OF $\alpha$ -Al<sub>2</sub>O<sub>3</sub> STIMULATED BY UV LIGHT

*D.V. GRANKIN*

*Pryazovskyi State Technical University, Universitetska St., 7, Mariupol, 87500, Ukraine, denis\_grankin@mail.ru, +380629446178*

In the conditions of radiation influences the breaking of chemical bonds, excitation of the electron and nuclear subsystems of wide bandgap materials occurs. The probability of these processes depends on the energy dissipation rate of interaction of particles with a solid or on the efficiency of the energy accommodation. The phonon channel is considered the main channel of the accommodation of the collision energy of atomic particles with solids, although the existence of non-equilibrium chemoelectronic phenomena, such as heterogeneous chemiluminescence (HCL), chemoemission, chemoconductivity etc., indicates the existence of the electron channel of accommodation.

The aim was to detect the influence of UV irradiation on the intensity of HCL of wide-gap solid  $\alpha$ -Al<sub>2</sub>O<sub>3</sub> and investigate the electron channel of the energy accommodation of recombination of H-atoms on its surface.

In the experiments, when the atoms source switched on, the HCL was observed (Fig. 1), which intensity increased over time as the surface filling with atoms and reached a steady value. The stationary HCL intensity of  $\alpha$ -Al<sub>2</sub>O<sub>3</sub> depended on the flux density of atoms and increased with its growth. HCL is a consequence of electronic excitation of the surface during heterogeneous recombination of atoms and indicates the presence of the accommodation of energy of reaction on the surface of  $\alpha$ -Al<sub>2</sub>O<sub>3</sub> via the electronic channel.

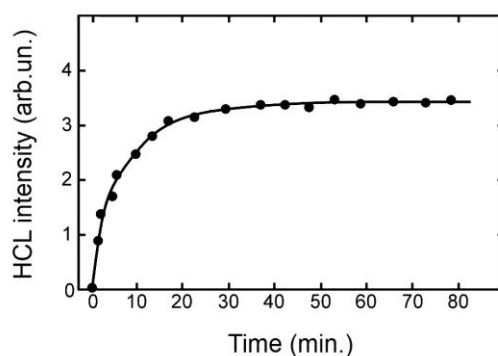


Fig. 1. The time dependence of the HCL intensity of  $\alpha$ -Al<sub>2</sub>O<sub>3</sub>, which is excited by H-atoms.  $j_H = 1 \cdot 10^{16} \text{ cm}^{-2} \text{ s}^{-1}$ ,  $T = 300 \text{ K}$ .

It was observed, when the sample was irradiated with UV light, an increase in the luminescence intensity of the sample, which is determined by the chemical excitation of the surface, in comparison with HCL of unexcited by UV light  $\alpha$ -Al<sub>2</sub>O<sub>3</sub>.

It was found the dependence of the intensity of HCL of  $\alpha$ -Al<sub>2</sub>O<sub>3</sub> on the level of electronic excitation with UV light, which is indicating the participation of the crystal's electronic states in the accommodation of energy of heterogeneous reaction of H-atoms recombination. The UV irradiation resulted in an increase of more than an order of magnitude of the luminescence intensity, which is determined by the chemical excitation of the surface, in comparison with HCL of unexcited by UV light  $\alpha$ -Al<sub>2</sub>O<sub>3</sub>.

The micromechanisms of the transfer of energy of vibrational excitation to the electronic subsystem of the crystal were considered. The kinetic mechanism of excitation of the solid by ionizing atomic fluxes and under the action of UV light was developed. It is shown that in this case the relaxation processes (accommodation via the electronic channel) determine the rate of chemical reaction on the surface. It is concluded that the increase in the rate of accommodation of energy of chemical reaction on the investigated wide-gap sample due to the ionizing radiation can lead to an increased rate of radiation-stimulated processes on the surface and in the bulk of the crystal.

Thus, stabilization of vibrational excitations on the surface or in the solid can be effective due to the energy accommodation of interaction via the electronic channel which efficiency for solids in a metastable state is very high. In the course of radiation influences in the path of the particles arise the electron excitations, and in this regard the electrons on traps can act as catalysts for the relaxation processes in solid.

## FORMATION OF THERMALLY STABLE LAYERED SYSTEM

*A.K. ZHUBAEV, A.S. NURTAZINA*

*Aktobe Regional State University, 34, A.Moldagulova str., Aktobe, 030000, Kazakhstan, mosslab.kz@km.ru*

In the present work the investigations of thermally induced processes of phase formation in two-layered systems Sn(4  $\mu\text{m}$ ) – Fe(10  $\mu\text{m}$ ), obtained by ion-plasma sputtering; have been carried out by methods of Mössbauer spectroscopy at  $^{119}\text{Sn}$  nuclei.

Tin layers were deposited on one side of prepared Armco Iron foils by magnetron sputtering. The thickness of layers was chose so as average values of Tin atoms volume concentrations are situated in two-phase regions of phase diagram, which include  $\alpha\text{-Fe}(\text{Sn})$  solid solution and intermetallide. Prepared samples were subjected to subsequent isothermal annealing in vacuum at 700°C temperature with duration up to 20 h.  $^{119}\text{Sn}$  Mössbauer transmission measurements at room temperature have been carried out. Fitting of experimental spectra were spent by method of model decoding of spectra (for  $^{119}\text{Sn}$ ), realized in program complex MSTools.

The spectrum obtained after annealing for  $t_{\text{ann}}=0.5$  h has a complex form, representing a superposition of several partial spectra, among which there is distinguished a doublet analogous to that observed in the spectrum of the layered system after annealing at 550°C [1]. Besides the doublet, the experimental spectrum contains sextets with large hyperfine fields and a partial spectrum with a large intensity in the central part. With increasing time of annealing, there occurs a decrease in the intensity of the doublet and an increase in the intensity of the additional sextets.

Based on the model identification of all experimental Mossbauer spectra of the  $^{119}\text{Sn}$  nuclei, we obtained the dependence of the relative intensity of partial spectra for the resultant phases (or the relative content of Mossbauer atoms in different phases) on the temperature of annealing (Fig.).

As a result of the study by the methods of Mossbauer spectroscopy at the nuclei of  $^{119}\text{Sn}$  of the layered system Sn(4  $\mu\text{m}$ )–Fe(10  $\mu\text{m}$ ) after sequential thermal annealings at temperature of 700°C, the formation of intermetallic compounds FeSn and Fe<sub>3</sub>Sn<sub>2</sub> and an  $\alpha\text{-Fe}(\text{Sn})$  solid solution has been established. It has been shown that the nature of the phase transformations in this system is determined by changes in the local concentration of tin in the sample in the process of the interdiffusion of the components. Thermally stable spatially inhomogeneous systems Fe<sub>3</sub>Sn<sub>2</sub>/ $\alpha\text{-Fe}(\text{Sn})$  have been obtained.

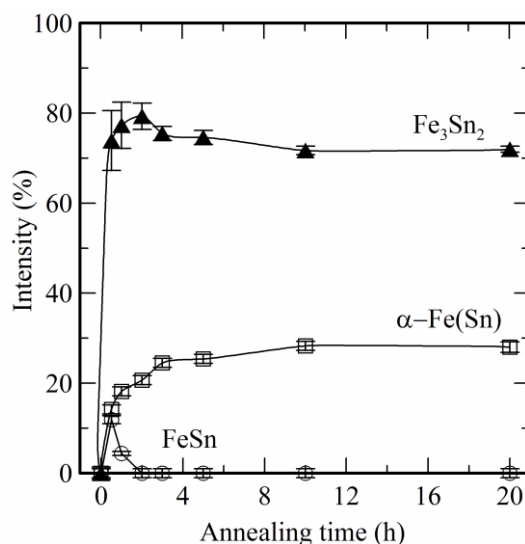


Fig. Dependence of the relative intensities  $I$  of the partial Mossbauer spectra of the  $^{119}\text{Sn}$  nuclei in different phases on the time of the thermal annealing  $T_{\text{ann}}$  at 700°C

### REFERENCES

- [1] *Zhubaev A.K.* Thermal stabilization of FeSn– $\alpha\text{-Fe}(\text{Sn})$  layered system. – 3<sup>rd</sup> International Congress on Radiation Physics and Chemistry of Condensed Matter, High Current Electronics and Modification of materials with particle Beams and Plasma Flows (September 17-21, Tomsk, Russia). Abstracts. P.104.

## EFFECT OF AG NANOPARTICLES ON THE CHARACTERISTICS OF COLOR CENTERS PRODUCED WITH A MICROWAVE RADIATION IN LiF FILMS

*O.I. SHIPILOVA,\* A.A. CHERNYH, A.A. KOLOMYLTSEV, A.O. KHOROSHIKH*

*\*Irkutsk St. University, 1, K.Marx Str., Irkutsk, 664003, Russia, e-mail: 4me4you@bk.ru. 89500910363*

The experiments on producing the F - color centers in thin LiF films, and studies the influence of metal nanoparticles (NPs) on their properties are presented. These films are promising for elaboration of the tunable lasers in the red region of the spectrum. As well the nanoscale layers of metal and semiconductor NPs in the LiF crystals and films are promising for the development of composite materials and development of integrated switches to create optoelectronic components.

Samples of the films were formed by the thermal vacuum deposition on substrates manufactured of silicate glass. Substrate was heated to 500 K in the process of the film deposition. The film thickness was controlled by batch masses of the evaporated components and it was in the range of 90-700 nm. In the LiF film, the metal NPs were synthesized from the flux of Ag atoms, which was produced in the process of thermal evaporation on parallel time with LiF.

For creating the F- color centers, film LiF containing the Ag nanoclusters was placed in a microwave plasma - discharge that was produced with a radiation of 2450 MHz frequency ( $\lambda = 12$  cm). The sample was exposed to ultraviolet and X-ray radiation from the plasma. The absorbed dose was controlled by the irradiation time, which ranged from 90 to 450 seconds. The degree of staining the samples was measured by studying a signal transmitted through the stained samples. Probe samples were taken to determine the discharge region, where the coloring occurs most intensively, they were the LiF tablets of 0.5 mm thickness and 5 mm diameter. A set of the samples was distributed uniformly across the diameter of the plasma reactor aligned to microwave emitter. The resulting distribution of the transmitted signal shown in Figure 1, which shows that a higher concentration of the color centers is observed in samples near the magnetron. Furthermore, it is seen that concentration of the color centers increases with the irradiation time.

In order to understand effect of the presence of metal nanoparticles on the characteristics of the color centers in the LiF films, the absorption spectrum of the film with the NPs was measured that is shown in Figure 2 a. Then, the absorption spectrum of the LiF film, containing both the Ag NPs and color centers, was measured. Further, the spectrum of the film with the NPs only was subtracted from the spectrum of the film containing both the NPs and color centers, i.e. spectrum of coloration in the presence of the Ag NPs was obtained (Figure 2 b). When comparing the resulting spectrum with the spectrum given in Figure 2 a, it's clearly seen that the Ag NPs have some influence on the absorption spectrum of the color centers.

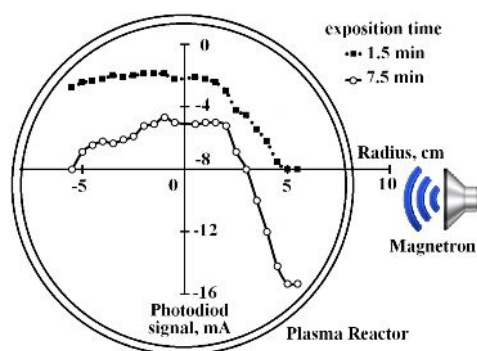


Fig.1

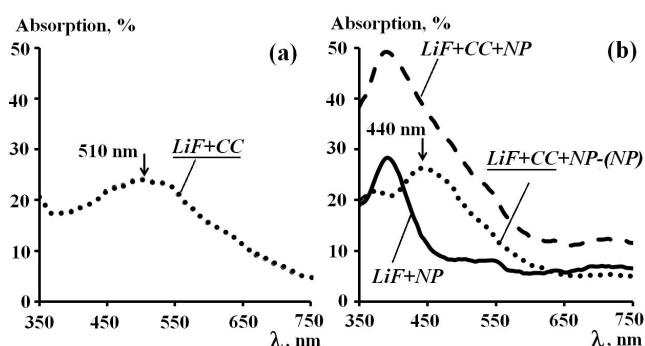


Fig.2

Namely, there observed a 70 nm shift of the F- center spectrum maximum towards the large wavelength. We assume that this shift affects the luminescent properties of the color centers.

## INTERRELATION BETWEEN THE REACTION AND DIFFUSION DURING GRADIENT STRUCTURE FORMATION OF SURFACE LAYER UNDER PARTICLE BEAM ACTION

*ASFANDYAR KHAN\**, *KNYAZEVA ANNA\*\**

*National Research Tomsk Polytechnic University, Lenina Avenue, 30, 634050, Tomsk, Russia,  
\*asfandyarmath@awkum.edu.pk, +79528915085, \*\*anna-knyazeva@mail.ru*

The particle beam action on the materials leads to surface activation, surface structure and properties change. It connects not only with mass transfer process, but with chemical reactions occurring in surface layer. Especially it relates to intermetallic systems [1, 2] (intermetallides are chemical compounds between different metals), where the chemical reactions have own features. The conditions of reactions implementation are irreversible, and their kinetics is not obvious [3]. The models of surface layer formation for intermetallic systems were suggested in [4, 5]. Here we will try reflecting the irreversible conditions for the reactions and mass transfer and take into consideration the finiteness of relaxation time for diffusion flux.

The purpose of this work consists of theoretical investigation of influence of particle beam form on new phase and free implemented particles distribution in surface layer and stresses and strain evaluation due to composition change in isothermal approximation. In this work, the total isothermal problem is formulated to describe the composition change in surface layer during particle beam action. Only one reaction is taken into account. The analytical solutions for some limiting cases are presented. The total problem is solved numerically. Firstly we stop on the simple problems constructed in classical approximation. Then we formulate the problem on new phase formation in surface layer during particle beam action for irreversible conditions. We will show the difference between reaction dynamics accompanying reversible diffusion and irreversible one using simple models. We describe the diffusion and reaction zone change when the source type varies. Finally we demonstrate the stresses and strains evolution in treated surface layer with constant and changing properties. The examples of stresses and strains calculations in the system are presented.

### REFERENCES

- [1] *Cordts B., M.Ahmed, D.I.Potter* // Limiting compositions and phase transformations resulting from implanting aluminum into nickel, Nuclear instruments and methods, (1983) , 209-210 , pp873-879
- [2] *Zhang T., Y.Wu, Y. Zhang etc.* // Phase transition and diffusion of Ni atoms in aluminum during implantation, Vacuum, (2012) , 65, pp.127-132
- [3] *Kurzina I.A., Kozlov E.V., Sharkeev Yu.P.* // Gradient surface layers on the base intermetallic particles. Synthesis, Structure, Properties (in Russian), Tomsk, (2013). izd-vo NTL, – 260 p.
- [4] *A.G. Knyazeva, Yu.P. Sharkeev, I.A. Kurzina, I.A. Bozhko* // Proc. of 8th Int. Conf. on Modification of Materials with Particle Beams and Plasma Flows. (2006), pp.219-221
- [5] *Knyazeva A.G.* // Simulation of intermetallic phase formation in surface layer during ion beam implantation (in Russian), - in Materials of International Conference “Chemical and Radiation Physics”, Russia, Moscow, August, (2009), 25-29 , pp.125-129



## EQUIDISTANT SERIES OF «EDGE» EMISSION IN CdS AT HIGH EXCITATION INTENSITY

*N. K. MOROZOVA\**, *A. A. KANAKHIN\**, *V. G. GALSTYAN\*\**, *A. S. SHNITNIKOV\**

*\*National Research University "Moscow Power Engineering Institute", Krasnokazarmennaya 14, Moscow, 111250, Russia,  
+74953601163, morozovank@mail.ru*

*\*\* Shubnikov Institute of Crystallography, Russian Academy of Sciences, Leninskiy prospekt 59, Moscow, 119333, Russia*

The nature of equidistant band series in CdS photoluminescence spectra near the fundamental absorption edge is studied. Spectra have been examined at 80 and 300 K for vapor-grown monocrystals characterized by various deviation from stoichiometry. The luminescence has been excited using a 337.1-nm nitrogen laser. Excitation intensity has been varied within a range of  $G = (10^{25} - 10^{27}) \text{ cm}^{-3} \text{ s}^{-1}$ . The crystal structure of the samples has been taken into consideration. A series of equidistant emission bands having a leading line of 514 nm (80K) is investigated. Just this band group in the green spectral range under a high excitation intensity had been earlier described as one of basic series edge emission (EE) in CdS, associated with the complex of intrinsic point defects. According to conventional interpretation, the EE CdS decays already at (150 – 200) K and under an excitation intensity  $G \geq 10^{24} \text{ cm}^{-3} \text{ s}^{-1}$ .

Our experiments have shown the absence of green edge emission for samples characterized by excess sulfur – CdS and CdS·S crystals even at  $G = 10^{22} \text{ cm}^{-3} \text{ s}^{-1}$  and 80K. However in CdS·Cd crystals equidistant band series of green edge emission is present. As the excitation density increases, intensity of luminescence for this bands grows, the band width is reduced, while the spectral position remains constant. Their emission exceeds in intensity the exciton luminescence of CdS(O) samples under  $G \geq 10^{24} \text{ cm}^{-3} \text{ s}^{-1}$ . The band series spectral position is independent on the concentration of oxygen solved in the crystals which affects the position of CdS(O) exciton bands in the blue spectral range in according to the band anticrossing theory [1,2]. At a temperature of 300 K the series leading line of CdS·Cd crystals is shifted to 532 nm.

A singular emission band 525-537 nm (300 K) has been observed earlier [2,3] in cathodoluminescence (CL) spectra for CdS(O) crystals. Appearance of green band in impulse CL at an energy density of  $0.2 \text{ J/cm}^2$  by an information layer depth of  $125 \mu\text{m}$  is accompanied by exuding of Cd. Excessive cadmium shows segregates on the surface and CdO crystals grows from them.

The used photoluminescence technique with a thin information layer is favorable to study the crystal surface. Additional information has been obtained from visual inspection of this surface exposed to the SEM beam with  $G \geq 10^{24} \text{ cm}^{-3} \text{ s}^{-1}$ . According to SEM data, initial CdS(O) crystals have block-like structure with hexagonal blocks extended in the growing direction [0001]. CdS(O) blocks demonstrate a weak red glow while local areas radiate bright green light. Exciton luminescence of CdS(O) as basic surface can not give local areas emission. The observed local emission may be attributed only to exciton band 530 nm (300K) or to the band series with leading line 514-nm (80 K). Crystals of cubic form, (2 – 3)  $\mu\text{m}$  in size, are revealed in SEM. Therefore, the series of exciton bands is generated by CdO. The conditions of free growth provide formation of perfect unstrained high-purity CdO crystals.

As noted in [2-4], the luminescence band ~530 nm (300 K) correlates to the width of CdO direct band gap (~ 2.3 eV at 300 K). The carried out study of photoluminescence spectra for CdO bulk crystals has enabled to define more exactly the spectral position of exciton bands, the thermal band gap coefficient ( $3.7 \cdot 10^{-4} \text{ eV/grad}$ ) and LO phonon energy (~35 meV).

### REFERENCES

- [1] *N. K. Morozova, N. D. Danilevich, A.A. Kanakhin // Phys. Stat. Sol. C.– 2010. – 7.– No. 6. pp. 1501-1503*
- [2] *Morozova N. K., Mideros D. A., Danilevich N. D. // Oxygen in Optic of Compounds II-VI of View of Theory Anticrossing zones. – LAP Germany, 2013, [in Russian].*
- [3] *N. K. Morozova, N. D. Danilevich, V. I. Oleshko, and S. S. Vil'chinskaya // Izvestiya vysshikh uchebnykh zavedenii. Elektronika. – 2012. – №6 (98). pp. 3-9.*
- [4] *E. Menendez-Proupin, G. Gutierrez, E. Palmero, J. L. Pena // Phys.Rev B. – 2004. – 70. – 035112*

**MODERN TRENDS AND DEVELOPMENT IN HIGH-DOSE LUMINESCENT MEASUREMENTS**

V.KORTOV, S.NIKIFOROV, S.ZVONAREV, YU.USTYANTSEV

Ural Federal University, Mira Street, 19, Ekaterinburg, 620002, Russia, [uskortov@mail.ru](mailto:uskortov@mail.ru), +7.343.375-44-43

At present there is an intensive development of radiation technologies employing high-dose radiation to modify material properties, sterilize medical products and to perform other industrial processes. High-dose detectors are used in radiation monitoring of nuclear power station (NPS) equipment and storages for spent nuclear fuel. Such detectors are necessary also after large accidents at NPS (like Chernobyl and Fukushima). In most cases measurement of radiation doses as high as several dozens or hundreds of kGy is required.

This talk presents the results of thermoluminescent and dosimetric property investigations of some high-dose detectors. On the basis of this analysis one can conclude:

- At present several successful researches on luminescent and dosimetric properties of some materials suitable for high-dose detector manufacture have been carried out. A number of such materials can be expected to increase, as there is no tissue equivalence requirement for high-dose luminescent detectors.
- Highly sensitive luminescent detectors (e.g.  $\alpha$ -Al<sub>2</sub>O<sub>3</sub>:C, LiF:Mg,Cu,P) can be used to measure both low doses in personal radiation monitoring and high doses in radiation technologies.
- Crystals with deep traps are very prospective for high-dose measurements, because efficient filling of the deep traps starts with high-dose irradiation. Deep traps exist in non-irradiated  $\alpha$ -Al<sub>2</sub>O<sub>3</sub>:C crystals (TLD-500 detectors) and are found after intensive irradiation under high-temperature heating. It was shown that TL peak height at T<sub>m</sub>=430 K of TLD-500 detectors changes linearly in the range from 1,5 kGy to 80 kGy.
- High-dose detectors should be radiation-resistant. Higher radiation resistance is typical for low-dimensional materials (glass, ceramics), nano- and hetero-structures.
- A great role in the change of TL and dosimetric properties of detectors after high-dose irradiation is played by the processes of new trapping center formation including those with the aggregate defects involved.
- It is necessary the development of special annealing procedures after high-dose detector irradiation.

The existing experimental challenges in development and use of high-dose TL detectors are not significant and will be resolved.

## CONTROLLABLE MICROSTRUCTURE GROWTH ON LIQUID METAL SURFACES UNDER PULSED ACTION<sup>1</sup>

*A.N. PANCHENKO, D.E. GENIN, D.V. BELOPLOTOV, YU.N. PANCHENKO*

*Institute of High Current Electronics SB RAS, Akademichesky av., 2/3, Tomsk, 634055, Russia,  
e-mail: [alexei@loi.hcei.tsc.ru](mailto:alexei@loi.hcei.tsc.ru), phone: +7 3822 492392*

Results of experimental study of pulsed action on different liquid metals is presented. It was found that microstructure with controllable size can be formed during laser ablation and (or) pulsed action of arc discharge on liquid metal surface. Multi-pulsed irradiation of liquid metal samples (Ga, Ga-In alloy, In, Pb, Zn, Roze alloy, Wood alloy) was performed by ns pulses of Nd:YAG, N<sub>2</sub> or excimer lasers (2–20 ns, 1064, 337, 308, 222 nm, 3 J/cm<sup>2</sup>) and fs pulses of Ti:Sapphire laser (60 fs, 475 nm, 0,1–2,5 mJ, 0,3–5 J/cm<sup>2</sup>) in a vacuum or in different reactive gases (air, SF<sub>6</sub>, NF<sub>3</sub>, N<sub>2</sub>). It was found that in chemically active gases microstructures are formed on the irradiated area with the rate of ~5–20 mm/pulse. The microstructure length can exceed 1 mm after ~200 laser pulses.

Similar results were obtained under arc discharge action. The discharge was formed between needle and liquid metal surface in air using different pulsed generators. The discharge current amplitude and duration were varied from 0.1 to 100 Hz and from 10 to 200 A, respectively. Microstructures formed in the course of laser and arc discharge action are shown in Fig. 1.

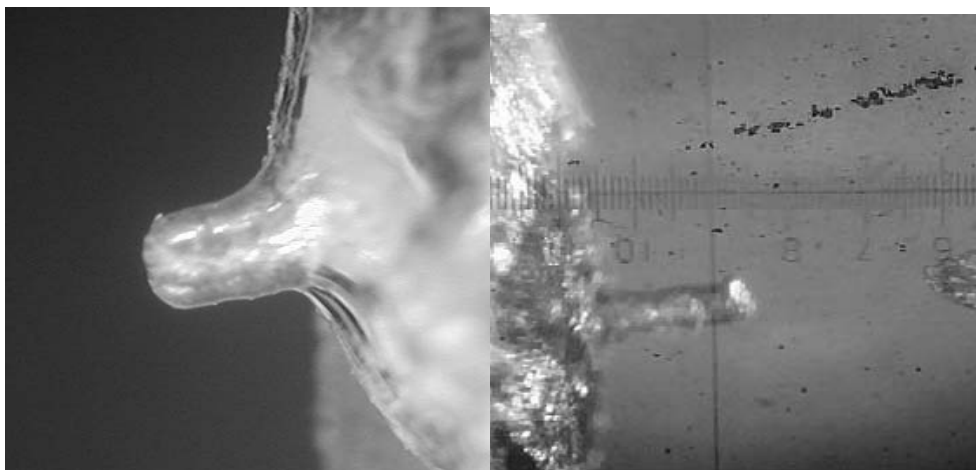


Fig. 1. Microstructure formed on liquid Gallium after 50 pulse of the Ti:Sapphire laser (left) and on Rose alloy after 200 pulses of an arc discharge. The structure lengths in both cases are 1 mm

It was found the microstructure forms and sizes are easily to control. Comparison of the structure growth parameters under the action of ns, fs laser pulses and arc discharges is made. Grows rates of the microstructures are measured and factors limiting there sizes are discussed. The microstructures are found to consist of a thin metal oxide (nitride, fluoride) layer filled with liquid metal.

<sup>1</sup> This work is performed in the framework of the State task for HCEI SB RAS, project №9.5.2

## SIMULATION OF CHARGING AND CATHODOLUMINESCENCE AFTERGLOW OF NANOSTRUCTURED ALUMINA UNDER IRRADIATION BY NANOSECOND ELECTRON BEAM<sup>1</sup>

*T.V. SHTANG, V.S. KORTOV, S.V. ZVONAREV*

*Ural Federal University named after the first President of Russia B.N. Yeltsin, Institute of Physics and Technology, Mira Street 21, Ekaterinburg, 620002, Russia, t.v.shtang@gmail.com*

The aim of the research is to simulate charging and cathodoluminescence decay kinetics with irradiation of crystalline and nanostructured anion-defective  $\text{Al}_2\text{O}_3$  samples with a nanosecond electron beam. Calculations are based on the following physical concepts:

1. Some electrons penetrate to a depth of about tens of microns when dielectric is exposed to short pulses of electrons with energies of  $\sim 100 - 150$  keV. They expend their energy on atom ionization and creation of electron-hole pairs. Ionization density with these energies is high due to fast formation of charge carriers in the bulk of material. After thermalization, most of these carriers effectively fill electron and hole traps with different energies. Charging of the surface and the subsurface layer occurs, the resulting charge produces an electric field which causes a shift of energy levels in the band structure of the material due to the Poole-Frenkel effect. A significant decrease in energy depth of traps occurs and probability of electron delocalization increases under the action of electric field with intensity over  $10^6$  V/cm.

2. The rest of the charge carries recombine with a luminescence center or ionized defect. Excitation of a glow center occurs, when this kind of defect captures an electron. Relaxation of glow center is accompanied by luminescence.

Taking into account these processes, the algorithms and programs were developed for calculation of parameters of surface layer charging and pulse cathodoluminescence (PCL) decay kinetics in dielectrics. Computer simulation was performed for single-crystalline and nanostructured alumina with excitation parameters: electron energy  $E_0 = 130$  keV, current density  $j = 60$  A/cm<sup>2</sup>, and pulse duration  $t = 1$  ns. The calculations have shown that while subsurface alumina layers are being charged, the internal electric field forms in it, its intensity grows monotonically with depth increase to the stationary value at a depth of about  $40 \mu\text{m}$ . The accounted features of nanostructured state do not affect the magnitude of the electric field intensity under irradiation of dielectrics with an electron beam with energy of 130 keV. The energy trap depth is reduced by 0,1 eV with the electric field intensity of  $6,75 \cdot 10^4$  V/cm.

In  $\alpha\text{-Al}_2\text{O}_3$  single-crystals F-center PCL decay time is in the millisecond interval. If the particle size decreases in nanostructured  $\alpha\text{-Al}_2\text{O}_3$ , F-center luminescence decay time decreases to microseconds under pulsed excitation with an electron beam. Electron scattering on the nanoparticle boundaries increases and the particle size decrease is accompanied by electron relaxation rate rise. This rate increase reduces the PCL decay time.

<sup>1</sup> This research project has been supported by grant of the President of Russian Federation (MK-4696.2013.2) and by UrFU under the Framework Programme of development of UrFU through the «Young scientists UrFU» competition.

## RADIATION DEFECTS IN LITHIUM FLUORIDE CRYSTALS INDUCED BY FAST IONS<sup>1</sup>

*A. AKILBEKOV\**, *R. ZABELS\*\**, *A. DAULETBEKOVA\**, *A. RUSSAKOVA\**, *M. BAIZHUMANOV\**, *R. ASSYL BAYEV\**,

*M. ZDOROVETS\*\*\**

\**L.N. Gumilyov Eurasian National University, 2 Myrzoyana Str, Astana, 010008, the Republic of Kazakhstan, [akiekov\\_at@enu.kz](mailto:akiekov_at@enu.kz), +7(7172) 709527*

\*\**Institute of Solid State Physics, University of Latvia, 8 Kengaraga Str., Riga LV-1063, Latvia*

\*\*\**Institute of Nuclear Physics, Astana branch, 3/1 Abylaikhan Av., Astana, 010008, the Republic of Kazakhstan,*

Fast ions are an excellent tool for the creation of nanostructures on the surface and in the bulk of solids. Formation of single defects and bulk nanostructures in LiF crystals, irradiated with swift Kr ions (C-60, Astana) of different energy and dose under normal and oblique incidence, were investigated by AFM, SEM, optical spectroscopy (absorption and luminescence spectra), nanoindentation and thermal annealing. In case of normal ion beam incidence the two structural zones can be distinguished: one enriched with dislocations and another exhibiting features of mosaic-type bulk nanostructure. The observed effects have a threshold nature in terms of energy loss and fluence.

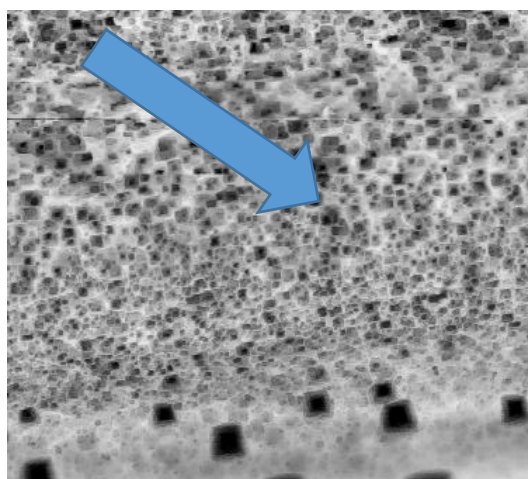


Fig. 1. AFM image of ion induced structures on profile surface obtained by cleaving along the ion path. Irradiation was performed to fluence  $10^{14} \text{cm}^{-2}$  Kr ions 150MeV, under incidence angle  $30^\circ$ .

The samples irradiated at angles other than normal have a similar division into zones, but are oriented in the direction of the ion beam. Variation in thickness of the irradiated layer in dependence on the angle of incidence can be observed.

Thermal annealing enabled to estimate the thermal stability of nanostructures and thermal diffusion of anion vacancies, which actively participate in the process of aggregation of electronic color centers.

<sup>1</sup> This work was supported by grant of MES the Republic of Kazakhstan

## THE FUTURE OF X-RAY COMPUTED TOMOGRAPHY IN THE DENTISTRY<sup>1</sup>

*M.B. PUTRIK\**, *J.E. LAVRENTYEVA\*\**, *V.YU. IVANOV\**

*\*Ural Federal University named after the first President of Russia B.N. Yeltsin, Mira street 19, Yekaterinburg, 620002, Russia, pmb-88@mail.ru, +7(912) 68-27-287*

*\*\*Private dental clinic «Uraldent», Frolova street 29, Yekaterinburg, 620028, Russia*

The traditional X-ray tomography (cone beam computed tomography or spiral computed tomography) is widely used in the dentistry nowadays because it gives essential information for dentists to diagnose illnesses and to plan treatment. Continuous hardware and software development of x-ray scanners allows us to do almost everything: processing of different cross-section images, 3D models, virtual planning etc. It becomes obvious today that the resolution of images provided with traditional computed tomography (approximately 300  $\mu\text{m}$  pixel size) is not enough for modern dentistry. That's why we have focused our investigation on the microcomputed tomography (micro CT).

The tooth was scanned at the SkyScan (BRUKER-MICROCT, Belgium) with following parameters: voltage 50 kV, 23  $\mu\text{m}$  pixel size, 11 Mp x-ray detector resolution. This scanner has a unique x-ray source with variable scanning geometry – it allows to adjust X-ray peak energy to keep the output power constant [1]. The result of the tooth scanning can be used for different dentistry applications: analysis of caries-removal techniques [2], assessment of the reliability radiographic bone density determination [3], survey of complex morphology of the root canal system [4]. Micro CT is applicable only for sample scanning.

We offer a 3D method of modeling tooth impression based on the micro CT data. Dentists can make a tooth impression hand-made or using a 3D optical camera which is expensive. Our method can replace these techniques because of high resolution of micro CT images comparable with optical images (Fig. 1 a). The surface of the impression is automatically designed at each cross-section of the tooth by our software and then 3D model is created (Fig. 1 b). After that 3D model may be converted to the STL format and manufactured by 3D printer.

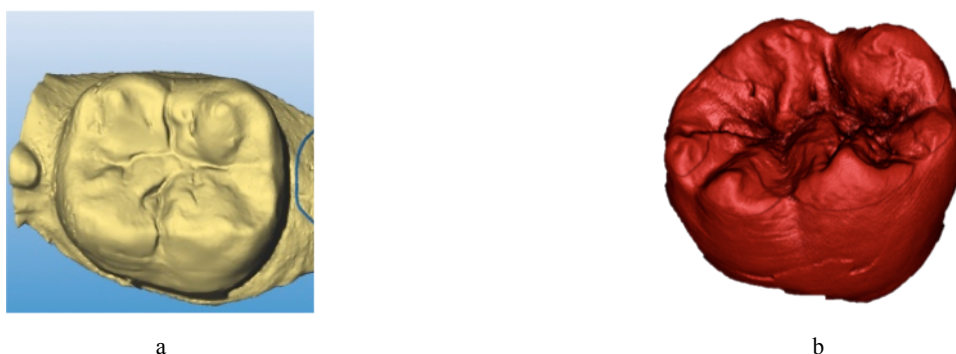


Fig. 1. High resolution tooth images: a – optical image obtained by 3D optical camera CEREC (Sirona GmbH, Germany), b – surface created by our software and imported in the OsiriX software

Suggested method can be used for rapid design of temporary crowns, inlays and onlays. Precious tooth surface quality is very important in surgical guides modeling because it provides the safety of dental implantation. As a result, application of the high resolution micro CT will make new technologies in the clinical dentistry.

The authors are grateful to B.V. Shulgin and I.N. Antsygin for discussing results and work assistance.

### REFERENCES

- [1] *Web resource:* <http://www.skyscan.be/products/1272.htm>
- [2] *Aline de A. Neves, Eduardo Coutinho, Jan De Munck, Bart Van Meerbeek / Caries-removal effectiveness and minimal-invasiveness potential of caries-excitation techniques // Journal of dentistry: Elsevier. – 2011. – № 39. Pages 154-162.*
- [3] *González-García R, Monje F. / The reliability of cone-beam computed tomography to assess bone density at dental implant recipient sites: a histomorphometric analysis by micro-CT // Clin. Oral. Impl. Res.: John Wiley & Sons Ltd. – 2012. Pages 1-9.*
- [4] *P. Verma, R.M. Love / A Micro CT Study of the mesiobuccal root canal morphology of the maxillary first molar // International Endodontic Journal: John Wiley & Sons Ltd. – 2010. – Volume 44. – Issue 3. Pages 210-217.*

<sup>1</sup> This work was partially supported by the Program of Development of Ural Federal University

## THE SENSOR MATERIAL AND DEVICE FOR EXPLOSIVES DETECTION

A.A. BARANOVA, K.O. KHOKHLOV

*Ural Federal University named after the first President of Russia Boris Yeltsin, Mira, 21, Ekaterinburg, 620002, Russia,  
wobbulator@yandex.ru, ph. 8 (343) 3754711*

In recent decades, in the world there has increased the activity of various extremist organizations, which to achieve their goals commit terrorist acts leading to the large number of victims and causing material damage. The problem of operative detection of explosives (HE) is quite relevant. That is why in recent time studies for creation new methods and explosives detection tools are intensively carried out in many countries. The most of the existing methods of HE detection require sampling and sample preparation, in this regard, it causes interest to the HE remote detection methods for detection of their vapors and particles, which present in certain amounts.

Detection tools can be divided into two groups. In the basis of the first one is physical processes of electromagnetic or corpuscular radiation interactions with chemical elements which are part of HE. Specific changes in the characteristics of probing HE, changes in physical fields of different nature allow to determine their presence and concentration with sufficiently high reliability. Detection tools that realize this principle, are often used stationary, they are expensive, in some cases, such tools require compliance with the radiation safety standards and regulations of manipulations with radioactive radiation sources. In the basis of the second group is chemical processes of interaction of HE or vapor generated by them with chemically active materials. And besides there are visually observed the changes in properties of material, indicating to HE presence. A disadvantage of such detection tools is no possibility of determining the HE amount and therefore the application of such tools is only possible as indicators.

Among of these and other methods of HE detection, methods of direct and remote determination of HE vapor are considered as the most promising. In this regard, new materials, whose luminescent properties are significantly changed in contact with HE vapors, are intensively studied. As a sensor material it is used a polymeric material which is sensitive to trinitrotoluene (TNT) vapor and its derivatives. It has been investigated optical spectral and radiation optical properties of this luminescent material, and has been revealed significant changes in luminescent properties as a result of pulsed electron beam pre-irradiation. Sensor material can be used as a detecting device of large dose electron radiation.

The optical spectroscopy results of this material, which has been exposed to different types radiations, indicate that ability of the material to register HE vapors decreases or disappears under the irradiation. It is obvious that irradiation leads to destruction of chemical bonds of material and, consequently, the concentration of compound molecules, which form the luminescent properties of the material decreases and, as a result, - the reduction of photo-luminescent properties. On the other hand, irradiation may leads or contributes to the formation of additional levels of nonradioactive recombination of electron excitations in the material band gap. It is necessary to take into consideration that we talk about surface luminescence centers and luminescence quenching and the energy of creation, destruction and transformation of these centers is much smaller than for the volume centers.

On the basis of this sensor material the device for HE and ionizing radiation detection has been developed. The main task of this device is luminescence quenching registration of sensor material in contact with air which contains nitro HE vapors.

Device functions: blowing air through the sensor element which contains a luminescent material; impact of light source with an excitation wavelength on the sensor element for the occurrence of luminescence; the luminescence intensity measurement by the photosensitive element and tracking the dynamics of luminescence intensity changes over time. The device is operated under control of program, the algorithm provides multiple operating modes (configuration, calibration, measurement etc.).

### REFERENCES

- [1] Caron T., Guillemot M., Montmeat P., Veignal F., Perraut F., Prene P., Serein-Spirau F. // Ultra trace detection of explosives in air: Development of a portable fluorescent detector. – *Talanta* 81, 2010, p. 543-548.
- [2] Anzenbacher Jr. P., Mosca L., Palacios, M.A., Zyryanov G.V., Koutnik, P. // Iptycene-based fluorescent sensors for nitroaromatics and TNT. – *Chemistry - A European Journal*, 2012, 18 (40), p. 12712-12718
- [3] Mosca L., Koutnik P., Lynch V.M., Zyryanov G.V., Esipenko N.A., Anzenbacher P. // Host-guest complexes of pentyptycene receptors display edge-to-face interaction – *Crystal Growth and Design*, 2012, 12 (12), p. 6104-6109.

## SINGLE CRYSTAL GROWTH OF BaBrI:Eu HIGH LIGHT YIELD SCINTILLATORS

*A.I. RUSAKOV, A.O. VASILKOVSKIY, A.A. SHALAEV*

*Vinogradov Institute of Geochemistry SB RAS, Favorski Str. 1a, Irkutsk, 664033, Russia, e-mail: [rusakov@igc.irk.ru](mailto:rusakov@igc.irk.ru)*

Inorganic scintillators are used for the detection of ionizing radiation and are widely applied in such areas as physics, medicine, geology and others. Of these, alkaline earth halide scintillators have received great attention during the past few years due to their high light yield close to the theoretical limit. Currently, one of the most commercially available and effective scintillator is LaBr<sub>3</sub>:Ce. It's fast (30 ns decay time), and has also a good light yield (73,000 photons / MeV) and energy resolution (2.7 - 3.2%) [1]. Unfortunately, it is not produced at the price low enough to be used in great quantities and one of the materials that can replace it is BaBrI:Eu<sup>2+</sup> [2].

We consider the problem of obtaining single crystals BaBrI doped with divalent Eu and study their scintillation and optical properties. BaBrI:Eu<sup>2+</sup> is one of the most promising new scintillator materials. The light yield of our sample obtained from the X-ray luminescence spectrum is 60,000 ± 3000 photons / MeV.

In crystal growing special attention was paid to the preparation of raw materials. The starting materials were BaBr<sub>2</sub>·2H<sub>2</sub>O, BaI<sub>2</sub>·2H<sub>2</sub>O и EuBr<sub>3</sub>. The reagents are premixed at the ratio of about 1:1. The concentration of Eu in the starting mixture was about 5 mol.%. For removing water and hydroxyl groups the raw materials were placed into the quartz ampoule and then were slowly heated in vacuum. The modes of drying materials were selected according to differential scanning calorimetry spectroscopy (data was obtained by A.K. Subanakov, BINM SB RAS).

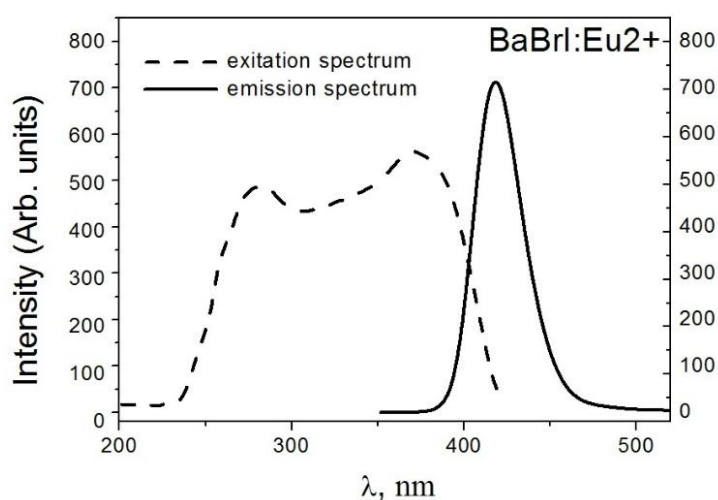


Fig.1 Excitation and emission spectra of BaBrI:Eu<sup>2+</sup> at room temperature.

The crystals were grown from the melt using the vertical Bridgman technique in the multizone thermal facility. The growth rate was 1mm/h and the temperature gradient about 15 °C/cm. For the crystals obtained excitation and emission spectra were measured (Fig.1). According to the spectra obtained Eu is included in the lattice in the divalent state. The scintillation decay time was measured and the sample density calculated.

Further research will be aimed at improving the optical characteristics of crystals BaBrI:Eu<sup>2+</sup>.

### REFERENCES

- [1] *P.R. Menge, G. Gautier, A. Iltis, C. Rozsa, V. Solovyev*, // Nuclear Instruments and Methods in Physics Research Section A 579 (2007) 6–10.
- [2] *E.D. Bourret-Courchesne, G. Bizarri, S.M. Hanrahan, G. Gundiah, Z. Yan, S.E. Derenzo*, // Nuclear Instruments and Methods in Physics Research A 613 (2010) 95–97



## SOME ASPECTS OF POLYMER ION BEAM ANALYSIS<sup>1</sup>

*S.S.ZYRYANOV\**, *O.V.RYABOUKHIN*, *F.G.NESHOV*, *A.V.KRUZHALOV\**

*\*Ural Federal University, ul.Mira,19, Yekaterinburg, 620002, Russia, stepan.fti@mail.ru, +7 (343) 375-47-11*

There are some features in using ion beam analysis for polymer films to be taken to consideration. First of all, the destruction of polymer with releasing of volatile degradation products which lead to its composition changing. Secondly, a low thermal conductivity of polymer films which may affect thermal induced changing of polymer under the ion beam irradiation with high current. Other two features are the non-Rutherford scattering of charged particles with energy of about 1 MeV per nuclon which requires special processing of experimental spectra in programs like SIMNRA or RUMP and the difficulty of identification of high mass elements with neighboring atomic numbers using RBS or NBS methods.

A 3 MeV He<sup>+</sup> ion beam was used both for degradation and characterization of Polyethylene Terephthalate (PET) film, the thickness was 2,5 nm. To widen the possibilities of elemental analysis *in situ* we used both Rutherford Backscattering Spectrometry (RBS), which transforms to Nuclear Backscattering Spectrometry (NBS) at the energy E<sub>α</sub> = 3 MeV and elastic recoil detection (ERD) methods at the same time, combining them with Particle Induced X-ray Emission (PIXE). RBS (NBS) was used for carbon and oxygen analysis, ERD for hydrogen analysis and PIXE for impurity heavy ion detection. PET films was placed on rotating frame to minimize heating during irradiation. Also it allowed to enlarge the irradiated surface to control fluence range from 10<sup>11</sup> to 10<sup>16</sup> cm<sup>-2</sup>. Detection angle were 160° for RBS and 30° for ERD. PIXE detector was placed in vacuum chamber near the sample. Fig.1 shows the changing of NBS spectra after irradiation of PET sample and decreasing of oxygen concentration.

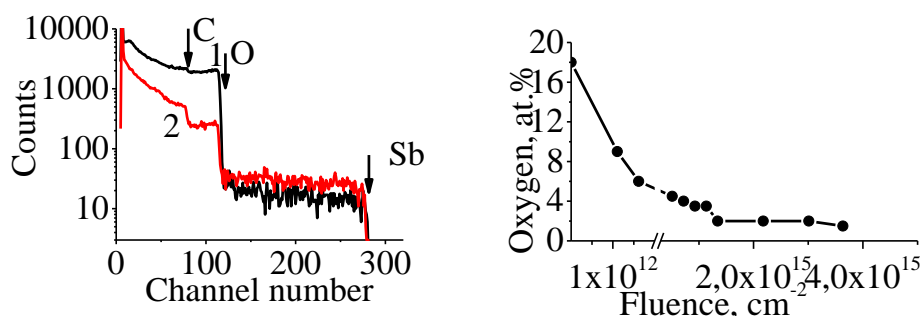


Fig. 1. RBS spectra for He<sup>+</sup> 3MeV on the PET film at the beginning (1) and at the fluence of 10<sup>15</sup> cm<sup>-2</sup> (2) and changing of oxygen concentration during irradiation. Heavy impurity (Sb) is seen in RBS spectra.

After He<sup>+</sup> ion irradiation we notice changing of the yield of backscattered particles from irradiated sample. It shows the reduced concentration of carbon and oxygen. At the fluence of 5·10<sup>15</sup> cm<sup>-2</sup> the concentration of oxygen approaches to 2 at.% (instead of 18 at.% in unirradiated sample), carbon and hydrogen show less depletion and have concentration of 18 at.% instead of 24 at.% for hydrogen and 38 at.% instead of 45 at.% for carbon. Volatile degradation products escape from irradiated surface most in form of H<sub>2</sub>, O<sub>2</sub>, CO and CO<sub>2</sub> [1,2]. Element losses have different rates and different stabilization levels. Ion beam irradiation also lead to concentration of heavy ion impurity because it doesn't leave the sample as C, O, H. The element forming this impurity (Sb) was determined using PIXE. The PET films show a color change after high dose irradiation. As for the mechanical properties, the irradiation also causes the fragility of sample.

So, as we see as the result of this work, degradation processes during irradiation are dose-dependend and are still incompletely understood. Combination of different experimental methods and *in situ* approach can show the evolution of chemical and elemental composition in low-dose area. The control of PET films degradation during irradiation and ion implantation is an important thing in commercial application when you need to get specified characteristics (structure or composition).

### REFERENCES

- [1] *M.B.Lewis, E.H.Lee //Nucl. Instr. Meth. B 61 (1991) 457/*  
 [2] *D.K.Avasthi, J.P.Singh, A.Biwas, S.B.Bose // Nucl. Instr. Meth.B 146 (1998) 504.*

<sup>1</sup> This work was supported by UrFU grant for young scientists

## PHOTOLUMINESCENCE OF NANOSIZED $Zn_2SiO_4:Mn$ PRODUCED BY TOP-DOWN AND BOTTOM-UP METHODS<sup>1</sup>

*K.A. PETROVYKH\*\*\*, A.A. REMPEL\*\*\*, V.S. KORTOV\**

*\*Ural Federal University named after the first President of Russia B.N. Yeltsin, 19 Mira Str., Ekaterinburg, 620002, Russia*

*\*\*Institute of Solid State Chemistry UB of the RAS, 91 Pervomaiskaya Str., Ekaterinburg, 620990, Russia  
kspetrovyh@mail.ru, +7-922-104-90-62*

Nanosized zinc orthosilicate activated with manganese,  $Zn_2SiO_4:Mn$ , has a higher radiation stability and adhesion to the substrate, along with higher intensity and saturation of luminescence comparing to bulk material. Hence it is a promising photo- and cathodophosphor for modern plasma displays and lighting devices [1, 2]. There are a lot of methods of  $Zn_2SiO_4:Mn$  producing, which have its own advantages and features. An industrial technology is based on a solid-state reaction of powder precursors sintering at high temperature. However in this case it is failed to manage controlling particle size and morphology and obtaining nanosized material. Thus new modern methods to produce nanostructured  $Zn_2SiO_4:Mn$  are needed. In this work nanosized  $Zn_2SiO_4:Mn$  was synthesized by two ways: high-energy ball-milling of microcrystalline powder (“top-down” technology) and sol-gel method using organic precursors (“bottom-up” technology).

The main goal was to study the photoluminescence (PL) of nanosized  $Zn_2SiO_4:Mn$ , reveal the features and compare results obtained for each of producing methods mentioned above.

High-energy ball-milling of microcrystalline  $Zn_2SiO_4:Mn$  powder was carried out in a planetary ball mill [3]. The result is a monodisperse powder with particles of about 30 nm, which form agglomerates of up to 400 nm. By sol-gel method followed by annealing  $Zn_2SiO_4:Mn$  nanopowder with a particle size of about 120 nm was obtained. Analysis of the diffraction patterns showed that the material is multiphase.

All the samples of nanosized  $Zn_2SiO_4:Mn$  exhibit a green photoluminescence with an emission wavelength maximum of about 515 nm. However in the case of the material prepared by ball milling, there is a significant lower PL intensity comparing with the microcrystalline powder. The intensity of emission is probably influenced by the presence of deformations in the destroyed crystallites that may lead to an increased probability of nonradiative transitions. Indeed, after the additional annealing partial recovery of the PL intensity is observing. On the other hand, the nanopowders synthesized by the sol-gel method, exhibit intense PL intensity comparable to material obtained by solid-phase technology and higher than PL intensity of  $Zn_2SiO_4:Mn$  obtained by ball-milling. One must note the PL of the samples strongly depends on the concentration of the activator and phase composition. Thus the dependence of the PL intensity on the synthesis conditions is observed. It is shown that the sol-gel technology of nanosized phosphor producing has advantages in terms of technology (simplicity, the ability to control the synthesis conditions) and allows obtaining the material with high emission intensity.

### REFERENCES

- [1] *Feldman C., Jüstel T., Ronda C.R., and Schmidt P.J.* // Adv. Funct. Mater. – 2003. – V. 13. – №. 7. P. 511-516.
- [2] *Morell A. and Khiati N.El.* // J. Electrochem. Soc. – 1993. – V. 140. – № 7. P. 2019-2022.
- [3] *Петровых К.А., Ремпель А.А., Кортвов В.С. и др.* // Неорган. матер. – 2013. – Т. 49. – № 10. С. 1099-1103.

<sup>1</sup> This work was supported in part by the Ural Branch of the Russian Academy of Science (project no. 12-II-234-2003)

## SPECTRAL AND TEMPORAL CHARACTERISTICS OF RADIATION DEFECTS IN THIN FILMS OF LITHIUM FLUORIDE<sup>1</sup>

*V.P. DRESVYANSKIY\**, *V.L. PAPERNY\*\**, *E.V. MILYUTINA\*\*\**, *N.L. LAZAREVA\*\*\**, *A.L. RAKEVICH\**, *O.I. SHIPILOVA\*\**,  
*E.F. MARTINOVICH\*\*\**

*\*Irkutsk Branch of the Institute of Laser Physics SB RAS, 130a Lermontov Str., Irkutsk, 664033, Russia,*

*filial@ilph.irk.ru, 8(3952)512160*

*\*\* Irkutsk State University, 1, K.Marx Str., Irkutsk, 664003, Russia*

The literature describes a number of radiation-optical technologies, which use the color centers produced in the thin films of dielectric inorganic compounds, or in surface or inner layers of the monocrystals. Thin films of lithium fluoride recorded images formed with nanometer spatial resolution in the X-rays or other ionizing radiation rays [1]. In [2] implemented microprinted direct recording on a thin layer of monocrystal using extremely shortwave ultraviolet radiation from laser-induced plasma, focused using a Schwarzschild objective.

This paper presents the results of studies of lithium fluoride thin films obtained by the thermal vacuum deposition on a substrate made of silicate glass. The substrate temperature during the deposition of lithium fluoride was set in the range from 100 to 500 deg. Film thickness, depending on the task, ranged 90-700 nm. Structure of the films, their spectra and kinetics of photoluminescence before and after irradiation with X-rays were investigated experimentally. Studies were carried out on the topology SPM Certus Light Company NanoScan Technologies. Study spectral and temporal characteristics of luminescence of the obtained films were performed by highly sensitive scanning confocal fluorescence microscope with picosecond time resolution MicroTime 200 by PicoQuant GmbH with spatially-selective time-correlated single photon counting. The microscope allowed us to register and reconstruct a microscopic images inside the irradiated volume of the medium by the fluorescent emission at 10 nm scanning step with selection of images in the luminescence decay time. Measuring spectral- kinetic characteristics were performed at excitation of luminescence by picosecond laser pulses with a wavelength of 405 and 470 nm. The photoluminescence spectra were recorded with Ocean Optics spectrometer 65000 coupled with microscope MicroTime 200. To suppress the excitation radiation scattered with the sample, the luminescence was detected through filters with cut-off wavelength of 430 nm and 500 nm, respectively.

The results showed that the obtained films contain grains of 30 - 200 nm size. Unexposed films show weak photoluminescence with the main non-elementary band emission with a maximum at 510 nm. After irradiation, the total luminescence intensity increased by an order of value due to the formation of  $F_2$  and  $F_3^+$  color centers with their characteristic luminescence bands. However, the decay times were markedly different from the values characteristic of single crystals. The reasons for the decrease in the lifetime of the excited states and other properties of the synthesized films are examined.

### REFERENCES

- [1] *Monteali R.M., Bonfigli F., Vincenti M.A., Nichelatti E. // Nuovo Cimento della Societa Italiana di Fisica. C. – 2013. V. 36 – №2. P. 35–42.*
- [2] *[2] Barkusky F., Peth C., Mann K. // Review of Scientific Instruments. – 2005. – V. 76. P. 105102*

<sup>1</sup> This work was supported by the Programme No. 13 of Presidium of RAS, project № 4.12 and by Programme of RAS No. II.8.1, project № 6.

**PHYSICAL PROPERTIES OF FERROALLOY SLAGS***O.R. SARIYEV\*, A.M. AKUOV\*, E.U. ZHUMAGALIYEV\***\*Aktobe Regional State University named after K.Zhubanov, 34, A.Moldagulova av., Aktobe, 030000, Kazakhstan,  
[rafhatsson@mail.ru](mailto:rafhatsson@mail.ru), +7-701-642-23-08*

The article presents the results of laboratory experiments to determine the slag physical characteristics, such as viscosity, crystallization temperature, specific to the production of refined grades of ferrochrome, ferro-titanium and carbon ferromanganese with additions of boron-containing fluxes. There are graphs of temperature dependence of viscosity and calculations of values of activation energy of slag viscous flow. In practice, explored properties of slag play an important role in the processes between the metal and slag.

## REFERENCES

- [1] Toporishev G.A. // Trudy ChEMK. –1975. -№4. Pages 72-75.
- [2] Voskoboinikov V.G. // Svoistva zhidkikh domennykh shlakov. Spravochnik. –Moscow, Metallurgiya, 1975.
- [3] Unigovskiy Ya.B., Pavlov V.A., Lutsenko V.T. // Sovershenstvovanie tekhnologii ferrosplavov. –1981. Pages 15-19.
- [4] J. Frenkel // Journal of Physics. -1945. -Volume 9. -№5. Pages 385-391.
- [5] Semik I.P. // Stal. -1949. -№1. Pages 18-27.
- [6] Lapin V.V. // Stal. -1965. -№11. Pages 1008-1014.
- [7] Zhilo N.L. // Snizhenie poter pri proizvodstve ferrosplavov. -1982. Pages 17-23.
- [8] Suchilnikov S.I., Sokolov V.E., Voinov V.V. // Izvestiya VUZov. Chernaya metallurgiya. -1961. -№10. Pages 42-45.
- [9] Belyankin D.S., Bogolyubov V.V., Lapin V.V. // DAN SSSR. –1949. -Volume LXV. -№5. Pages 56-64.
- [10] Mikhailov V.V., Bratchikov S.G. // Trudy UPI. -1957. -№67. Pages 174-180.
- [11] Yestropyev K.C., Toropov N.A. // Khimiya i fizicheskaya khimiya silikatov. – GIL po stroitelnyim materialam, 1956.
- [12] Gantserovskiy O.G., Khitrik S.I., Chepelenko Yu.V. // Proizvodstvo ferrosplavov. -1976. – №3. 56-65.
- [13] Gavrilov V.A., Gasik M.I. // Silikotermya margantsa. –Sistemniye tekhnologii, 2001.
- [14] Gabdullin T.G., Takenov T.D., Baisanov S.O., Buketov E.A. // Fiziko-khimicheskie svoistva marganzevykh shlakov. –Alma-ata, Nauka, 1984.
- [15] Sariev O.R., Tolymbekov M.Zh., Kim A.S., Nurgali N.Z. // Vliyanie osnovnosti shlakov na protsessy fazoobrazovaniya pri vyplavke margantsevykh splavov // Sbornik materialov II Mezhdunarodnoi nauchnoi konferentsii “ Innovatsionnoe razvitiye i vostrebovanost nauki v sovremennom Kazakhstane”. -2008. –Volume 2. Pages 96-98.

## EFFECT OF HYDROGEN ON THE CORROSION OF TITANIUM AS THEY ARE PROCESSED BY IONIZING RADIATION

*A.M.LIDER\**, *A.V. PANIN\*\**, *V.V. LARIONOV\**, *G.V.GARANIN\**

*\*Tomsk Polytechnic University, 30, Lenin, Tomsk, 634050, Russia, E-mail: lider@tpu.ru, +7 3822 705012*

*\*\* Institute of Strength Physics and Materials Science of Siberian Branch Russian Academy of Sciences, 2/4, pr. Akademicheskii, Tomsk, 634021, Russia*

One of the actual research fields is the studies of hydrogen corrosion caused by radiation effects during irradiation of hydrogen saturated metals. Studies of corrosion resistance of such films as well as their microstructure evolution studies are conducted for the purpose of developing new technologies of creating coatings with prescribed corrosion properties and parameters. These studies represent an actual issue. In order to obtain and study protective coatings the rectangular planar BT-01 titanium samples with the size of 50 x 50 mm, thickness 0.7 – 10 mm were used. Irradiation was performed by X-ray quanta and by continuous and impulse electron beam (IEB). The influence was performed one-sidedly as well as from two sides of the sample with energy density from 12 to 25 J/sm<sup>2</sup>. Electron current density comprised from 10 to 50 A/sm<sup>2</sup>, electrons energy – 18 keV, and pulse width – 50 ms. During continuous electron irradiation the electrons energy comprised 30 keV with the current 2 μA/sm<sup>2</sup>. During the studies of X-ray influence the samples were open air irradiated on the X-ray setup (voltage U = 120 kV, current 5 μA, tungsten cathode) with the irradiation dose equal to 5·10<sup>4</sup> rad. On the surface of X-ray irradiated titanium voids and craters initiation is noticeable. The voids and craters are about 20 μm in size, with ragged edges and contain partial ejection of metal matter. This effect increases surface roughness and leads to increase of hydrogen absorption during hydrogenation [1]. Thickness of the layer which is subjected to corrosion during X-ray quanta irradiation is increasing dependent on the thickness of oxide layer, energy and irradiation dose. Accompanying this hydrogen yield from the irradiated side as well as from the opposite side is observed in hydrogen saturated titanium with oxide. This testifies that energy transfer from electrons and X-ray quanta takes place in excitation conditions in the whole hydrogen subsystem of titanium. Corrosion effects are intensified and developing in such a way that the irradiation process in the modes under study does not lead to protective films formation. Certain interest represents the fact that elimination of products of organic aggregates from surfaces of the samples under study takes place. With the electron energy increase the surface washing leads to decrease of roughness and increase of hardening of the surface layer of material. Electron-beam processing leads to high speed surface melt (108–1010 K/sec) and further crystallization of surface layer with thickness of 2–5 μm. As a result of fast crystallization (with the speed about 107 K/sec) the surface acquires high finish. After irradiation the grain boundaries appear on the surface, the size of which varies from 2 up to 10 μm. Nonregular folded structure is being formed within the grains including acicular formations. The grains are uniformly distributed along the surface of the alloy. For the irradiation dose of 15 J/sm<sup>2</sup> the grains of the size of about 2 μm are met on the surface. As the irradiation dose increases the size of the grains enlarges. Thus, with the dose of 20 J/sm<sup>2</sup> the grains of the size less than 5 μm are not met any longer. With increase of energy density of the beam (15 – 24 J/sm<sup>2</sup>) the height and length of folds on the sample surface gradually increases. It is necessary to mention that folded relief is being formed extremely on uniformly. In the first place, the grains appear (grains agglomerates) which lack folding. In the second place, alongside with coarse folds, more fine folded structure appears. Hydrogen permeability and physical and mechanical properties of titanium irradiated by IEB lead to abrupt decrease of electronic density of material which is related to development of microstructure of the surface and internal stresses which in their turn occur during impulse heating and rapid cooling of titanium alloy. With increase of introduced energy up to 20 J/sm<sup>2</sup> the material surface layer hardening is in two times more than in comparison with initial state. At the same time during X-ray radiation with the same energy density titanium fracture occurs in case when its thickness is less than 1 μm.

### REFERENCES

- [1] Chernov I.P., Ivanova S.V., Koval N.N., Larionov V.V., Lider A.M., Pushilina N.S. *Properties and Structural State of the Surface Layer in a Zirconium Alloy Modified by a Pulsed Electron Beam and Saturated by Hydrogen* // *Technical Physics*, 2012, Vol. 57, № 3, pp. 392–398.

## FEMTOSECOND LASER MODIFICATIONS OF SODIUM FLUORIDE<sup>1</sup>

*L.I. BRYUKVINA, A.A. POPOV, A.V. KUZNETSOV, E.F. MARTYNOVICH*

*Irkutsk Branch of Institute of Laser Physics of SB RAS, Lermontjva Str130A, Irkutsk, 664033, Russia,  
E-mail: [baikal@ilph.irk.ru](mailto:baikal@ilph.irk.ru), (395-2)512160*

Femtosecond lasers have used as universal tools for microstructuring of lithium fluoride (LiF) by direct writing procedures [1-3]. However no papers on recording optical waveguides and micro-components in sodium fluoride (NaF), though this material is close on the properties to lithium fluoride.

We received and investigated color centers (CCs) in femtosecond laser filaments in NaF crystal. Conditions of receiving of spurs with CCs in NaF were: titan sapphire femtosecond laser, lens of  $f=33$  cm, duration of an pulse is 30 fs, frequency of following is 1000 Hz, energy of pulse 0,56 мДж. The radiation time is approximately 5 sec (number of the received pulses about 5000). Length of a way of a femtosecond beam into crystal about 1 cm. Radiation of femtosecond beams was focused by a lens at the following distances from an entrance surface (right side of fig.1a) of a crystal: 1st spur (bottom of fig.1a) – 5 mm in a crystal, the 2nd spur – 10 mm in a crystal, the 3rd spur (top of fig.1a) – 15 mm (10 mm in a crystal plus 5 mm behind the crystal). CCs in spurs were investigated by means of the confocal microscope MT 200. Image and luminescence of CCs in single spur are presented.

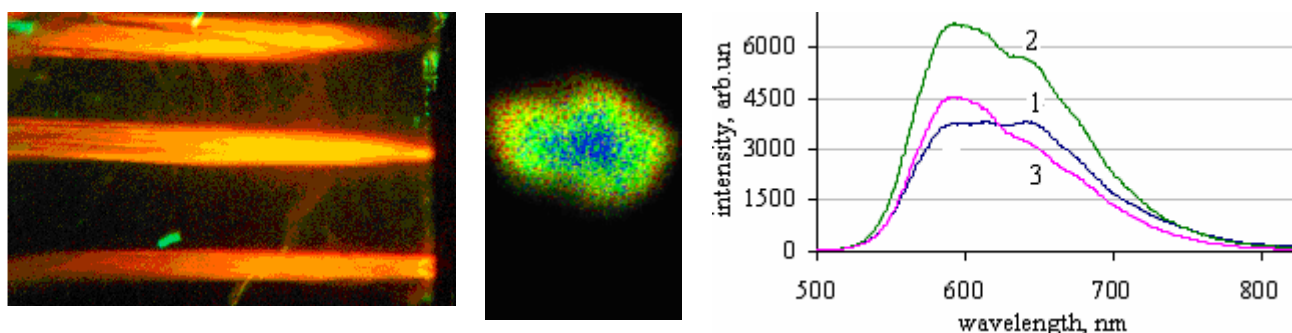


Fig. 1. The image by digital camera of spurs with CCs in sodium fluoride (a) the image by confocal microscope of cross sections of the single spur (b) CCs luminescence from the center of single spur to its periphery at  $\lambda_{\text{ex}}=470$  nm (c)

It was established that CCs in sodium fluoride are created same by femtosecond pulses as well as under the influence of other types of radiation exposure. At excitement by picosecond pulse laser radiation with  $\lambda_{\text{max}}=470$  nm luminescence of  $F_3^+$  and  $F_2$  CCs with maximums of 590 and 650 nm, respectively, was revealed. The decay times of a luminescence were  $\tau_1=4.10$  ns ( $F_3^+$ ) and  $\tau_2=9.43$  ns ( $F_2$ ). The luminescence with  $\lambda_{\text{max}}=720$  nm, the corresponding  $F_2^*$  CCs in  $\gamma$ -irradiated NaF with magnesium and hydroxyl impurities, was revealed in femtosecond irradiated NaF crystals at excitement by laser radiation with  $\lambda_{\text{max}}=640$  nm. Efficiency of CCs formation on the cross section of the single spur with CCs was investigated. It is established that density of simple and aggregate CCs in the center of spur is more, than on the periphery of the spur. The fig. 1c is demonstrated that there are high concentrations of CCs in the range of 550÷800 nm in the center of single spur (fig. 1c). The wide column of luminescence spectrum of  $F_3^+$ ,  $F_2$  and more complicated aggregate CCs (fig 1c), and also light-scattered defects, not divided into separate maximums, testifies to it.

### REFERENCES

- [1] T. Kurobori, K. Kawamura, M. Hirano and H. Hosono // *Phys.: Condens. Matter.* – 2003. – V. 5. – P. L399–L405.
- [2] L.C. Courrol, R.R. Salmad, L. Gomes, I.M. Ranieri, S.L. Baldochi, A.Z. Freitas, N.D. Vieira Jr. // *Opt. Express* – 2004. – V. 12. – P. 288–293.
- [3] L.I. Bryukvina, A.L. Rakevich, E.F. Martynovich // *Russian Physics Journal* – 2012. – V. 55. – № 11/3. P. 29–33.

<sup>1</sup> This work was supported by the Presidium of RAS (Programme No. 13, project No 4.12) and by the Siberian Branch of RAS (Programme No. II.8.1, project No 6)

## ROLE OF HF MOLECULE IN RADIATION MODIFICATION OF LiF CRYSTAL WITH HYDROXYL IMPURITY<sup>1</sup>

*L.I. BRYUKVINA, E.F. MARTYNOVICH*

*Irkutsk Branch of Institute of Laser Physics of SB RAS, Lermontjva Str130A, Irkutsk, 664033, Russia,*

*E-mail: baikal@ilph.irk.ru, (395-2)512160*

The radiation-chemical transformations taking place in crystals of alkaline fluorides with impurity of free hydroxyl ions and in complexes with metals were widely studied nearly thirty years ago. In Alekseev P. D. works (for example, in [1]) the turning point of view about the nature of the radiation-induced centers with  $800\div 4000\text{ cm}^{-1}$  IR absorption bands as complexes with hydrogen bond (H-bond) was stated. These conceptions have received the further development in works of authors [3-6]. An important role in formation of complexes with H-bond belongs to the product of hydroxyl decomposition under radiation found by us in LiF crystal – to a molecule of hydrogen fluoride (HF) with a  $4096\text{ cm}^{-1}$  absorption band. The absorption spectrum of  $\gamma$ -irradiated crystal in which HF molecule was formed is given in fig. 1.

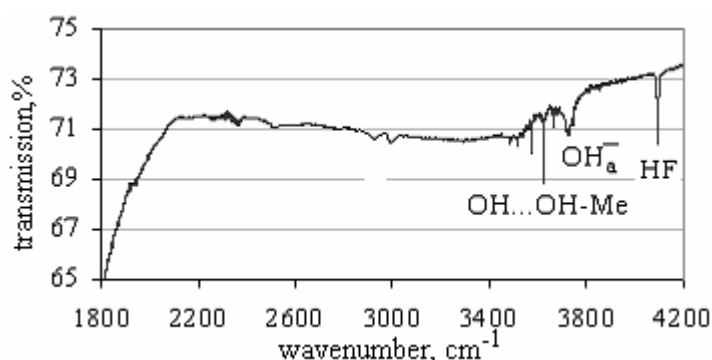
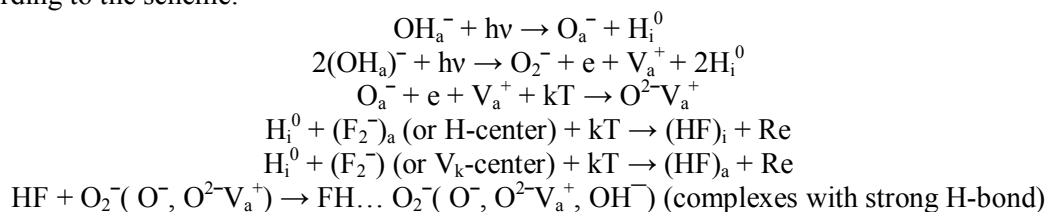
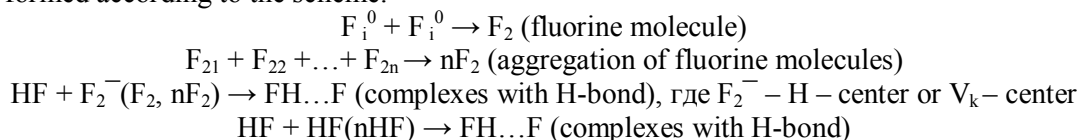


Fig. 1. IR spectrum of  $\gamma$ -irradiated LiF crystal with hydroxyl and magnesium impurities (dose of irradiation is  $1.5 \cdot 10^3\text{ C/kg}$ )

The molecule of HF participates in radiation-chemical and radiation-thermal transformations with formation of complexes with H-bond, preventing thereby a recombination of electronic and hole primary defects and promoting increase in efficiency of formation of the color centers. Complexes with H-bond of a HF molecule with oxygen products of a hydroxyl radiolysis and with hydroxyl ( $\nu=1700\div 2300\text{ cm}^{-1}$ ) are created according to the scheme:



Complexes with H-bond of the strong and weak types of HF molecules with radiation-created halogen defects are formed according to the scheme:



### REFERENCES

- [1] P.D. Alekseev, G.I. Baranov, E.P. Kurakina, K.A. Maltsev // Phys. Stat. Sol. (b). – 1983. – V.120. – №2. P. K119-K121.
- [2] V.V. Bryukvin, L.I. Bryukvina // Zhurnal Prikladnoi Spektroskopii. – 1987. – V. 47. – № 2. P. 254-259.
- [3] L.I. Bryukvina // Russian Physics Journal. – 1988. – №9. P. 101-103.
- [4] L.I. Bryukvina, V.M. Khulugurov, I.A. Parfianovich // Optika i Spektroskopiya. – 1987. – V. 63. – № 1. P. 207-210.
- [5] L.I. Bryukvina, V.M. Khulugurov, I.A. Parfianovich // Zhurnal Prikladnoi Spektroskopii. – 1988. – V.48. – №2. P. 322-324.

<sup>1</sup> This work was supported by the Presidium of RAS (Programme No. 13, project No 4.12) and by the Siberian Branch of RAS (Programme No. II.8.1, project No 6)

## ELECTRICAL AND PHOTOELECTRIC PROPERTIES OF POLYCRYSTALLINE DIAMOND FILMS, DEPOSITED BY ABNORMAL GLOW DISCHARGE

A.V.GAYDAYCHUK, A.V.KABYSHEV, F.V.KONUSOV, S.A.LINNIK, G.E.REMNEV

Tomsk Polytechnic University, Lenin ave. 30, Tomsk, 634050, Russia, E-mail: konusov@hvd.tpu.ru

In the last few decades, diamond films grown by chemical vapor deposition arouse ever greater interest because of its outstanding mechanical, optical, chemical and thermal properties. Among the various diamond film deposition methods, there are microwave plasma, hot filament, arc-jet and glow discharge chemical vapor deposition (CVD) to be marked out. But each of them has a number of disadvantages MPCVD has a high cost and limited maximal deposition area, as for HFCVD the growth rate is low and constant replacement of filaments is necessary, the disadvantages of arc-jet CVD method are small deposition area and high gas consumption. We submit a new discharge system for diamond film deposition at AC abnormal glow discharge [1]. In this process the discharge in form of a plasma line operates between two small electrodes, and the interelectrode spacing reaches 20 cm. The electrodes are moved away from the substrate and do not contaminate the film.

In this work the electrical and photoelectrical characteristics and the peculiarities of conduction mechanisms of polycrystalline diamond films deposited with abnormal glow discharge were investigated. Diamond films deposition from the alternating high-current glow discharge plasma [1].

Transport charge at surface dark and photoconduction of diamond films due to the continuous nature of the polycrystalline diamond films of the energy distribution of localized states induced in band gap by defects of various kinds. Dominated by *n*-type conductivity and photoconductivity activation component is implemented and the hopping mechanism with the participation of states localized in the band gap near the Fermi level. Activation transport is realized in the exchange of charge carriers between the allowed bands and levels of activation energy  $\epsilon = 0.007-0.21$  eV, which have weakly populated and a considerable spread in their parameters. Thermal quenching of photoconductivity was manifested. Hopping transport dominates in the temperature range 300-600 K. The density of states, on which the hopping conduction is significant and is in  $N(E_F) = 10^{17}-10^{21}$  eV<sup>-1</sup> cm<sup>-3</sup>, its change in the films due to the content of defects inhomogeneously distributed in grain boundaries. When light irradiation the states density increases in 3-5 times, and the probable length of the jumps for the photoconductivity decreased slightly by 1-3 nm. Spectral distribution centers photosensitivity correlated with the distribution of deep band gap localized determining the absorption spectra.

### REFERENCES

- [1] Linnik S.A., Gaydaychuk // Diamond and Related Materials. – 2013. – V. 32. – P.43–47.



## THE DEFECTS IN LiF CRYSTALS, OBTAINED BY MODIFICATION OF $F_3$ - CENTER <sup>1</sup>

*I.G. PRIMAK, L.I. SHCHEPINA*

*Applied Physics Institute of Irkutsk State University, Blvd Gagarin, 20, Irkutsk, 664003, Russia, schepina@api.isu.ru,*

In the second half of the XX century there were a large number of investigations that was devoted to the spectroscopy of metallic colloids, induced by the ionized irradiation or heavy ions in alkali halide crystals. However the question about the seeds for nanosize Li colloids is still open. Authors [1] assumed that two or more spatially correlated  $F_3$ -centers can fulfill the role of such a seed. Besides previously authors of [2-4] were made several assumptions that have not yet received the experimental or theoretical evidence. Based on these assumptions, we decided to model the possible modifications of the spatial configuration of  $F_3$ -center, that may be occur when the sample with pre-induced  $F_3$ -centers is irradiated by light. In essence, modifications are the spatial shift of lithium, leading to formation of minimum size aggregate.

Modeling was carried out in the framework of the pseudopotential theory using the supercell geometry (we used super cell size  $4 \times 4 \times 4$  atoms). The pseudopotentials were generated using Vanderbilt code version 7.3.5. Energy transaction was 30 Rydberg. Modeling was performed using the open-source software [5]. The supercell consisted of 29 pairs Li-F, 3 anion vacancies, 3 unpaired lithium cations. The number of valence electrons ranged from 232 to 238. In accordance with assumptions [2-4] we have considered the following options for the spatial arrangement of the lithium core: plane of anions, plane of cations and anion vacancy. The density of states and the total energy of the system for different charge states of supercell: +3,+2,+1,0,-1,-2,-3 (0-electrically neutral supercell) were calculated for these spatial configurations. In addition to the above spatial configurations, the same values have been calculated for the "initial" configuration: lithium core is still located in a regular lattice site.

For all charge states of the supercell the resulting differences of the total energy between initial and modified state of system were minimal for the configuration "lithium core is shifted to the plane, defined by anion vacancies. This means that after the light absorption the most probable spatial location of shifted lithium is plane (111). According to our assumption in this case semi metallic bonding with the nearest cations can take place. Furthermore only for above spatial configuration differences of the total energy system between initial and modified special decreases more than twice, when supercell charge varies from +3 to -1. Therefore for samples with pre-induced  $F_3$ -centers under irradiation the probability of lithium displacement to the plane defined by anion vacancies significantly increase. The highest value of DOS (8650) was found for same configuration (charge state of supercell +3).

The deepest levels in the band gap correspond to the configuration "the lithium core spatially located on the plane, defined by cations". The density of electron states of these levels decreases as 11,6:8,9:5,1:3,4:1 with increasing negative charge of the supercell. The above defect configurations can localize 4, 3, 2, 1, 0 electrons, respectively.

Most probable plane of the spatial localization of the displaced lithium is the plane of anionic vacancies (111). The lithium shift results in forming of doublet levels in the band gap and of semi metallic bounding displaced lithium with closest to him cations. These centers can be a seed for nanosize lithium colloids.

### REFERENCES

- [1] *A. Lushchik, Ch. Lushchik, K. Schwartz, et al // Phys. Rev.B. – 2007. – V.134. – №5. P. 054114(1)-054114(11).*
- [2] *L.F. Vorozheykina, N.G. Politov // Electronic and ionic processes in solids. – Mecnieraba, 1971. P. 36-87.*
- [3] *Y. Farge // Phys. Rev.B. – 1970. – V.1. – №12. P. 4797-4802.*
- [4] *B.D. Lobanov, V.M. Kostyukov, N.T. Maksimova et al // Solid State Physz.. – 1995. – V.37. – №9. P. 2445-2449.*
- [5] *Paolo Giannozzi et al // Journal of Physics: Condensed Matter. – 2009. – V.21. – №39. P. 395502.*

<sup>1</sup> This work was supported by Ministry of Education and Science Russia. Goszadaniya № 091-14-105.

## SUBSTITUTIONAL IMPURITIES INFLUENCE ON HYDROGEN SORPTION PROPERTIES OF TITANIUM AND ZIRCONIUM<sup>1</sup>

*E.V. TUCH\**, *T.I. SPIRIDONOVA\*\**, *A.V. BAKULIN\**, *S.E. KULKOVA\**

*\*Institute of Strength Physics and Materials Science, pr. Akademicheskoy 2/4, Tomsk, 634021, Russia, kulkova@ms.tsc.ru, +73822286952*

*\*\*National Research Tomsk Polytechnic University, pr. Lenina 30, Tomsk, 634050, Russia*

It is known that IVB group metals have the similar phase transitions and widely used for industrial applications. Titanium is advanced metal with an excellent high strength-to-weight ratio and corrosion resistance. Its alloys are used from medicine to aerospace. Zirconium has a very low thermal-neutron capture cross-section, high melting point as well as high corrosion resistance and biocompatibility. It is widely used in nuclear power engineering, medicine and chemical production. It is known that hydrogen does not dissolve appreciably in these metals at room temperature. The formation of a hydride phase results in brittle behavior of metals. Since Zr is used in nuclear power engineering, the main factor initiating degradation of the zirconium materials under operating conditions is hydrogen, which forms during corrosion process and is absorbed in zirconium alloy. On other hand with increasing temperature, more hydrogen dissolves in the titanium matrix that lead to its ductile behavior. Therefore, one effective approach to improving the hydrogen embrittlement is to increase the solubility of hydrogen and restrain the formation of metal hydrides. The influence of impurities on hydrogen sorption in metal hexagonal phase was studied by the projector augmented wave method within density functional theory. The supercell approach was applied in order to decrease the concentration of impurity and H. The supercell includes 8 lattice positions as shown in Fig. 1a. It contains one impurity and hydrogen atom. The position of H is placed at the center of the interstice (octahedral or tetrahedral). We consider the impurity atom as the nearest neighbors of hydrogen. The interaction energy was calculated using following equation:

$$\Delta E = [E(N, X, H) + E(N)] - [E(N, X) + E(N, H)], \quad (1)$$

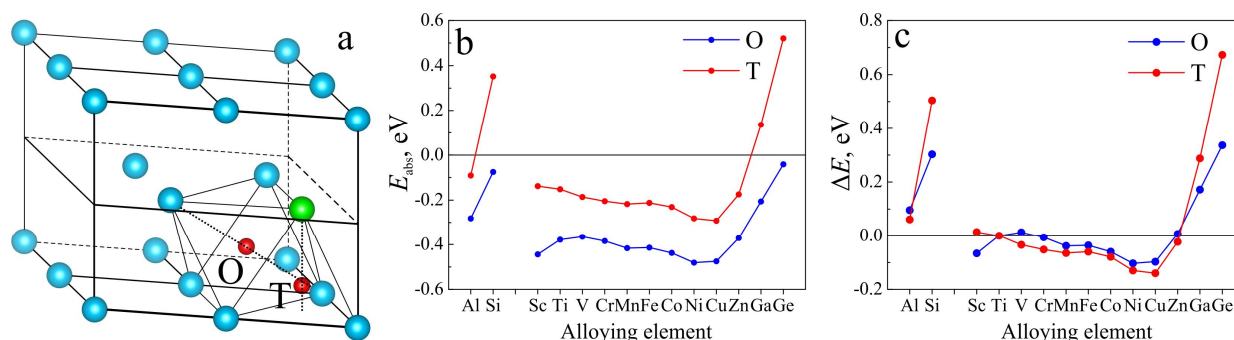


Fig. 1. Atomic structure of supercell for  $\alpha$ -Me (a) and absorption (b) and interaction energies (c) between the solute and hydrogen occupying an octahedral and a tetrahedral interstice in  $\alpha$ -Ti.

Our calculations show that hydrogen prefer to be absorbed in the octahedral site rather than in the tetrahedral one (Fig. 1b). The calculation of the interaction energy between hydrogen and impurities (Fig. 1b) demonstrates that transition metals attract mainly hydrogen, while simple metals repel hydrogen that is consistent with the conclusion of [1] for  $\alpha$ -Ti. Analysis of the density of states show that in the case of transition metal a strong hybridization of  $s$ -H orbitals with metal  $s, d$ -orbitals is observed. In the case of simple metal the hybridization of its  $s$ -orbitals with  $s$ -H orbitals leads to splitting of their valence band into two band (bonding and antibonding) and although hybridization contributes little to the binding energy, but due to the Pauli principle, the contribution to kinetic energy increases. This leads to a positive energy  $\Delta E$  and to repulsive interaction between the simple metal and hydrogen. The relationship between impurity trapping of hydrogen in both metals us discussed.

### REFERENCES

- [1] *Hu Q.M., Xu D.S., Yang R., Li D., Wu W.T.* // Phys. Rev. B. – 2002. – V. 66. – P. 064201-1-8.

<sup>1</sup> This work was supported by RSCF

**OPTICAL AND THERMOLUMINESCENCE PROPERTIES OF LiF:Mg,Cu SINGLE CRYSTALS**

*A. SHALAEV, N. BOBINA, A. PAKLIN, R. SHENDRIK AND A. NEPOMNYASHCHIKH*

*Vinogradov Institute of Geochemistry SB RAS, Favorski Str. 1a, Irkutsk, 664033, Russia, e-mail: alshal@igc.irk.ru  
Irkutsk State University, Faculty of Physics, Gagarin Blvd. 20, Irkutsk, 664003, Russia*

Thermoluminescent detectors based on the lithium fluoride are widely applied in dosimetry [1]. The results of optical and spectroscopic studies on LiF:Cu and LiF: Mg,Cu, single crystals are presented in this work. Besides, it reveals the influence of copper and magnesium impurities on the thermoluminescent (TL) processes and the influence of magnesium concentration on the radiation sensitivity of crystals LiF:Mg,Cu.

The growth of LiF:Cu<sup>+</sup> single crystals is difficult because of copper instability in the monovalent state. Copper monovalent ions are actively reduced to metal or oxidized to two-valence state. We managed to grow crystals of lithium fluoride doped with copper in the monovalent state [2]. Crystal growth was carried out by the Czochralski method. To avoid monovalent copper reduction the resistive nichrome heater and metal elements of thermal screens were used. CuCl and MgF<sub>2</sub> were utilized as the source of copper and magnesium for crystal doping. The chemical composition of mixtures and crystals was determined by the atomic absorption spectrometry method. The single crystals LiF:Mg,Cu were grown with varying concentrations of Mg (0.2% and 0.05%); the copper content makes up 0.001%. The spectroscopic (optical absorption, photoluminescence) studies of LiF:Cu crystals were conducted to prove the presence of copper in the monovalent state after doping. The emission peak at 400 nm and excitation peak at 275 nm in LiF crystals doped with copper are attributed to Cu<sup>+</sup> impurities. The monovalent copper is detected in the grown crystals by excitation band at 275 nm. Magnesium was added after the proof of the monovalent state of copper in crystals LiF.

The efficiency of thermoluminescence in crystals LiF:Cu,Mg was evaluated. The TL sensitivity LiF:Mg,Cu with 0.05% Mg content is noticeably reduced as compared to the samples doped with 0.2% Mg. The glow curves structure is not changed, but the relation of peak intensity varies. The TL sensitivity of phosphor rises with increasing heating number and remains stable after several readouts. Four or five readouts are enough for TL sensitivity of the thermoluminophor becomes constant. Perhaps the proper selection of thermal mode will improve the TL capability of detectors.

## REFERENCES

- [1] Horowitz, Y. S. // Radiation Protection Dosimetry. – 2013. – Volume 153. – № 1 . Pages 1-22.  
[2] Непомнящих, А.И. // Оптика и спектроскопия, – 2011. – том 111. – № 3, с. 442-445.

## TEMPERATURE DESTRUCTION OF RADIATION DEFECTS IN CALCIUM FLUORITE, STRONTIUM FLUORITE AND BARIUM FLUORITE DOPED WITH TRIVALENT RARE-EARTHS IONS

*T.YU. SIZOVA, E.A.RADZHABOV*

*\*Vinogradov institute of Geochemistry SB RAS, Favorsky street 1A, Irkutsk, 664033, Russia, sizova@igc.irk.ru*

It is known that the X-irradiation of CaF<sub>2</sub> containing certain rare earths ions (La, Ce, Gd, Tb and Lu) or yttrium which have low third ionization potentials produces an photochromic color center (PC center) [1, 2]. The photochromic centers can be considered as a trivalent rare-earth ion next to an anion vacancy (intrinsic defects which is not created by x-irradiation in the undoped crystals) with one (PC<sup>+</sup> center) or two (PC center) trapped electrons [3].

In our studies it was shown that after X- irradiation at 80 K the optical absorption of PC<sup>+</sup> centers is observed in CaF<sub>2</sub> and SrF<sub>2</sub> doped with Ce<sup>3+</sup> and Tb<sup>3+</sup>. At temperatures in the ranges 350–450 K in CaF<sub>2</sub>-Ce and CaF<sub>2</sub>-Tb PC<sup>+</sup> centers are transforms into PC centers. All colour centers decay upon heating of the crystals to approximately 600 K.

The SrF<sub>2</sub> crystals doped with Ce and Gd cannot be colored by X-irradiation at room. For the BaF<sub>2</sub> crystals doped with Ce and Tb irradiated at 80 K, absorption bands are observed at energies of 2.25 and 3.60 eV. These absorption bands are assigned to F- and V<sub>k</sub>-centers [4]. However these bands have a higher optical density than the absorption bands of PC<sup>+</sup> centres in CaF<sub>2</sub> and SrF<sub>2</sub> crystals and lie in the region of the absorption bands of PC<sup>+</sup> centres. In our previous studies it was shown that efficiency of the formation of the photochromic centers decreases from CaF<sub>2</sub> to SrF<sub>2</sub> [2, 5]. Probably absorption bands of F- and V<sub>k</sub>-centers overlap the absorption bands of PC<sup>+</sup> centres in BaF<sub>2</sub> crystals.

Crystals of CaF<sub>2</sub>, SrF<sub>2</sub> and BaF<sub>2</sub> doped with 0.1 to few mol. percent CeF<sub>3</sub> and TbF<sub>3</sub> were grown in vacuum in graphite crucible by Stockbarger method. The crystals were irradiated at 80 or 300K by X-rays from a Pd tube operating at 35 kV and 20 mA. Optical absorption was measure by Perkin-Elmer Lambda 950 spectrophotometer.

### REFERENCES

- [1] C. R. A. Catlow // *J.Phys. C:Solid State Phys.*-1979.- 12.- 969
- [2] T. Y. Bugayenko, E. A. Radzhabov // *Physics of the Solid State.*-2008.- 50.- 1671
- [3] D. L. Staebler, S. E. Schnatterly, W. Zernik // *IEEE Journal of Quantum Electronics.*-1968.- QE-4.- 575
- [4] E. A. Radzhabov, A. Shalaev, A. I. Nepomnyashikh // *Radiation Measurement.*-1998.- 29.-307
- [5] T. Sizova, E. Radzhabov // *IEEE Transaction on Nuclear Science.*-2012.- 59/5.- 2098 – 2101.

## CHEMICAL PROCESSES UNDER RADIATION PROCESSING OF MILK<sup>1</sup>

*A.A.BARANOVA, V.V.EMELYANOV, E.A.SAVATEEVA, N.E.MAKSIMOVA,  
N.N.MOCHULSKAYA, A.V.KRUZHALOV, V.A.CHERESHNEV*

*Ural Federal University named after the first President of Russia Boris Yeltsin, Mira, 21, Ekaterinburg, 620002, Russia,  
wobbulator@yandex.ru, ph. 8 (343) 3754711*

Actuality. Today in 69 countries over 80 different types of foods are processed by radiation. The volume of radiation sterilization services market is about 12-15 billion dollars.

Radiation-induced conversions of proteins, lipids, nucleic acids and carbohydrates are well studied. However, there is a few information about the features of radiation and chemical processes in foods containing dozens of different chemical components. Explanation of the features of radiation and chemical transformations of food components and pharmaceutical products will allow to determine the radiation doses and modes more soundly. Insufficient consideration of these factors, in addition to the main antiseptic effect, causes changes of organoleptic qualities, some consumer properties and possibly appearance of toxic substances because of radiation-chemical-biological reactions of proteins, carbohydrates, lipids, vitamins, etc. In view of the above the study of the theoretical foundations of food and pharmaceuticals radiation processing for subsequent widespread adoption is extremely important.

In Ural Federal University there is an experience of medical products radiation processing. There were studied the possibility of accelerator microtron (10 MeV) for using to study the effect of sterilizing doses on survival of different microorganisms species, on stability of various packaging types, on possibility to extend the shelf life of food and to reduce the risk of contamination with pathogenic microorganisms.

We have chosen milk as the first object of this study. The generally accepted method of the milk microbiological safety providing is pasteurization.

Materials and methods. The object of the study is drinking milk with fat content of 2.5%. To assess changes in consumer qualities of product during radiation processing it was carried out milk irradiation by using URT-02 installation. The general technical data of URT-02 are: accelerating voltage is up to 200 kV, pulse width at half-maximum is 34 ns, frequency is 250 Hz, electron beam size is 220x30 mm<sup>2</sup>, beam current density is up to 0.3 A/cm<sup>2</sup>, radiation dose rate at 5 cm (when using the accelerator at 50 Hz) is 21 kGy/min. The radiation dose was 10 kGy.

Results and discussion. According to data presented in the table, the irradiation of milk at 10 kGy dose resulted in statistically significant increase in acidity that exceed the level permitted by regulations. Milk acidification by irradiation may be associated with a variety of radiation and chemical processes: triglycerides hydrolysis and fatty acids release, fragmentation of chain fatty acids molecules and formation of short chain fatty acids (C3-C6), lowering medium pH significantly.

### Conclusions.

Investigations of radiation and chemical transformations of food components and pharmaceuticals under radiation processing is an important interdisciplinary problem of considerable practical importance.

Radiation processing of milk with 10 kGy dose results in significant activation of LPO products and accumulation of cytotoxic products in milk.

In order to develop an efficient and safe method of milk radiation processing it is promising to use radiation doses up to 10 kGy with comprehensive assessment of biochemical and microbiological parameters.

### REFERENCES

- [1] *Sharpaty V.A.* // Radiation chemistry of biopolymers. GEOS, Moscow, 2008. 208 p.
- [2] *Kudryashov Y.B.* // Radiation biophysics (ionizing radiation). Moscow: Fizmatlit, 2004. 448 p.
- [3] *Emelyanov V.V., Maximova N.E., Mochulskaya N.N., Chereshev V.A.* // Non-enzymatic glycosylation of proteins: chemistry, pathophysiology, perspective correction / Issues. biol., med. and pharm. chemistry. 2010. № 1. P. 3 – 15.
- [4] *Macej O.D., Jovanovic S.T., Denin J.D., Djurd J.* // The influence of high temperatures on milk proteins / Chem. Ind. 2002. V.56, № 3. R. 123 - 132.
- [5] *Hramtsov A.G., Pavlov V.A., Nesterenko P.G.* // Processing and use of whey. Technological notebook. M. Rosagropromizdat. 1989. 272 p.

<sup>1</sup> This work was supported by a RFBR grant A № 13-03-01100.

## RADIATION OPTICAL EFFECTS IN COMMERICALLY SiO<sub>2</sub>:Ge FIBERS

A.V. ISHCENKO\*, A.N. TCHEREPANOV\*, A.S. VOKHMINTSEV\*, I.A. WEINSTEIN\*, B.V. SHULGIN\*,  
L.N. SHALIMOV\*\*, N.G. MANKO\*\*, A.N. SHTYKOV\*\*, G.V. SHESTAKOV\*\*, E.K. CHISTYAKOVA\*, A.A. SHONOKHOVA\*

\*Ural Federal University named after the first President of Russia B.N. Yeltsin,  
Mira 19, Yekaterinburg, 620002, Russia, a-v-i@mail.ru, +7(343) 375-93-74

\*\* FSUE Scientific and Production Association of automatics named after academician N.A. Semikhatov  
Mamin-Sibiryak Str., 145, Yekaterinburg, 620075, Russia, okba@bk.ru, +7(343) 350-56-76

Doped quartz optical fibers are being used in optical communication systems and other devices for over 40 years. Optical fiber gyroscopes and distributed optical fiber sensors of external physical effects for continuous monitoring of the controllable parameters are produced based on doped quartz optical fibers. Present work is dedicated to investigation of radiation optical properties of SiO<sub>2</sub>:Ge glass fibers produced by Fujikura and Corning Glass. Distribution of Ge dopant characteristics in core and cladding of quartz fiber were determined using EDX methods. Ge dopant luminescence was observed in fiber. It is shaped in rings with most intense luminescence zone in core centre border areas (Fig. 1, a), as was determined using SEM methods. New method of determination the Ge dopant distribution in core and cladding cross sectional profile of silica fiber glass was presented [1].

Thermoluminescence and light storage processes in fibers affected by x-ray radiation were investigated. The parameters of charge carrier traps were calculated. TL fiber three-dimensional (3D) image is presented on Fig. 1, b.

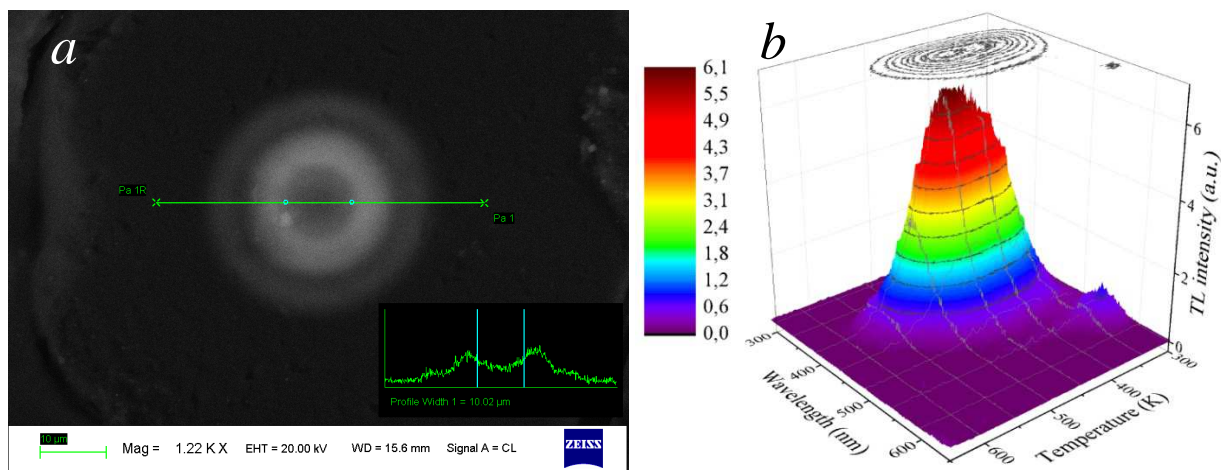


Fig. 1. Fiber quartz core luminescence intensity distribution profile (a) and TL 3D image (b) of Fujikura LWP fiber

There are two bands of luminescence with 400 nm and 550 nm maxima, which appear in different temperature stimulation conditions. Approximation procedure of lines mentioned above was provided. It has been determined for the first band:  $E_{\max}=3.09$  eV (401 nm) and  $\text{FWHM}=0.55$  eV; for the second one:  $E_{\max}=2.26$  eV (549 nm) and  $\text{FWHM}=0.25$  eV.

In addition cathode pulse luminescence spectra were investigated. Obtained results are discussed taking into account well-known models [2, 3].

### REFERENCES

- [1] B.V. Shulgin, A.V. Ishchenko, A.N. Tcherepanov, L.N. Shalimov, N.G. Manko, A.N. Shtykov, G.V. Shestakov, E.K. Chistyakova // Application for invention № 2013142549. 17.09.2013.
- [2] H.-J. Fitting, T. Barfels, A.N. Trukhin, B. Schmidt, A. Gulans, A. von Czarnowski // *Journal of Non-Crystalline Solids*, 2002. Vol. 303 P. 218–231.
- [3] A.F. Zatsepin, H.-J. Fitting, V.S. Kortov, V.A. Pustovarov, B. Schmidt, E.A. Buntov // *Journal of Non-Crystalline Solids*, 2009. Vol. 355. P. 61–67.

## RADIATION RESISTANCE OF LIGHT-EMITTING DIODES BASED ON AlGaAs-HETEROSTRUCTURES TO FAST NEUTRON AND ELECTRON RADIATION

*P.V. RUBANOV\*, A.V. GRADOBOEV\*\**

*\*National Research Tomsk Polytechnic University, Institute of Non-Destructive Testing, Lenin Avenue, 30, Tomsk, 634050, Russian Federation, e-mail: sopromatchik@rambler.ru, +7(952)1520235*

*\*\*Yurga Institute of Technology (branch) of National Research Tomsk Polytechnic University, Yurga, Russian Federation e-mail: gradoboev1@mail.ru, +7(913)8668405*

The resistance of LED based on AlGaAs-heterostructures to fast neutron and electron radiation is to be investigated in the work.

As research objects LED based on AlGaAs-heterostructures batch-produced in a single technological cycle were used. The radiation was performed in a passive power supply mode.

LED radiation has been found out not to result in considerable changes of current-voltage and capacitance-voltage characteristics that coincides with the known studies [1, 2].

Fig. 1a shows the general character of the change in LED emission intensity under electron radiation after preliminary fast neutron radiation is seen to be constant for the area with high electron injection and to follow in two phases as well as under electron radiation only. Similar results were obtained for the area with low electron injection. At the first stage the observed decrease in emission intensity is described by the relation (1).

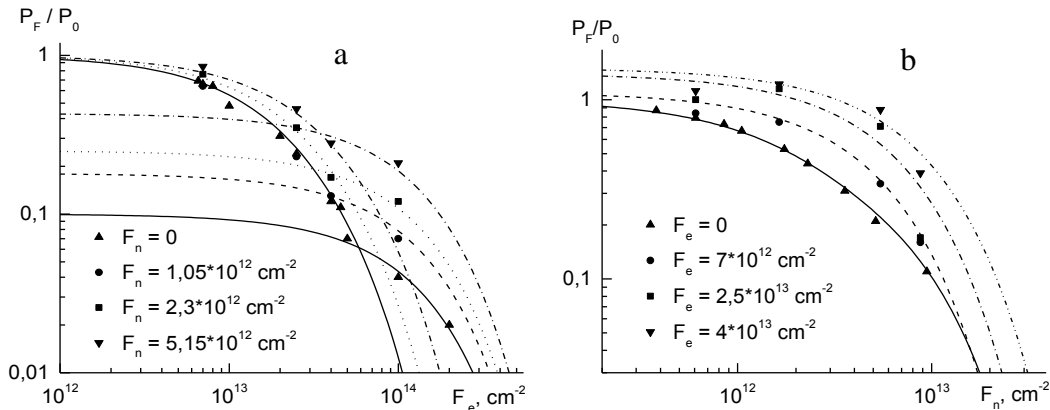


Fig. 1. The change in emission intensity in the area with high injection under: a) electron radiation of LED, after preliminary fast neutron radiation; b) fast neutron radiation of LED after preliminary electron radiation

$$\frac{P_F}{P_0} = \begin{cases} 0,5 \cdot \exp(-K_1 \cdot F) + 0,5 \cdot \exp(-K_2 \cdot F) \\ A \cdot \exp(-K_3 \cdot F) \end{cases}, \quad (1)$$

where  $P_F$ ,  $P_0$  – emission intensity before and after radiation;  $A$ ,  $K_1$ ,  $K_2$  and  $K_3$  – proportionality constants;  $F$  – fluence of fast neutrons or electrons, correspondingly.

Fig. 1b shows the change in LED emission intensity in the area with high electron injection under fast neutron radiation in accordance with preliminary electron radiation. As one can see, a sharp renewal of emission intensity decreased after electron radiation is observed after the subsequent neutron radiation of LED. As long as the neutron fluence is rising, LED emission intensity is falling.

The presented results make it possible to conclude:

1. The preliminary fast neutron radiation raises the radioresistance of LED to the subsequent electron radiation several times.

2. The preliminary electron radiation of LED leads to the renewal of emission intensity under the subsequent fast neutron radiation.

3. Under coupled fast neutron and electron radiation of LED there is no additive degradation of emission intensity as the results of such impact depend on the factor sequence.

### REFERENCES

- [1] *Selesnev D.V.* // Candidate of Science Thesis. – M.: MGUPI, 2006. 124 p.
- [2] *Gradoboev A.V., Rubanov P.V.* // XI International Conference «Physics of Solids» (FTT-11). 9 – 12 June Ust-Kamenogorsk. – Ust-Kamenogorsk, 2010.

## PHOTOLUMINESCENCE SPECTROSCOPY OF CHARGE-TRANSFER PROCESSES IN OXIDE COMPOUNDS $\text{Ni}_x\text{Mg}_{1-x}\text{O}^1$

V.N. CHURMANOV\*, V.I. SOKOLOV\*\*, V.A. PUSTOVAROV\*, V.YU. IVANOV\*, N.B. GRUZDEV\*\*, N. MIRONOVA-ULMANE\*\*\*

\* Ural Federal University, Mira str. 19, Yekaterinburg, 620002, Russia, e-mail: chenov@olympus.ru, phone: +79126382765

\*\* Institute of Metal Physics UB RAS, S. Kovalevskaya str. 18, Yekaterinburg, 620990, Russia

\*\*\* Institute of Solid State Physics, University of Latvia, Kengaraga str.8, Riga, LV-1063, Latvia

The study of the real electronic spectrum of antiferromagnetic crystal of NiO is an actual problem of the solid state physics. Solid solution  $\text{Ni}_x\text{Mg}_{1-x}\text{O}$  may be used as good model system to receive the additional information about optical transitions in NiO.  $\text{Ni}_x\text{Mg}_{1-x}\text{O}$  solid solutions were studied in the present work using optical spectroscopy methods. For better understanding of properties it is significant to distinguish p-d and d-d charge transfer (CT) transitions [1]. The photoluminescence (PL) measurements were made on the samples of solid solutions  $\text{Ni}_x\text{Mg}_{1-x}\text{O}$  ( $x = 0.01, 0.04, 0.09, 0.43$  and  $0.74$ ) with rock salt crystal structure in the energy range of 3,7 – 12 eV. The measurements of PL spectra under soft X-ray (XUV) excitation were made on a SUPERLUMI station (HASYLAB (DESY), Hamburg). The time-resolved photoluminescence spectra as well as the photoluminescence decay kinetics under XUV excitation has been measured on a BW3 beam line by a VUV monochromator (Seya-Namioka scheme) equipped with microchannel plate-photomultiplier (MCP 1645, Hamamatsu).

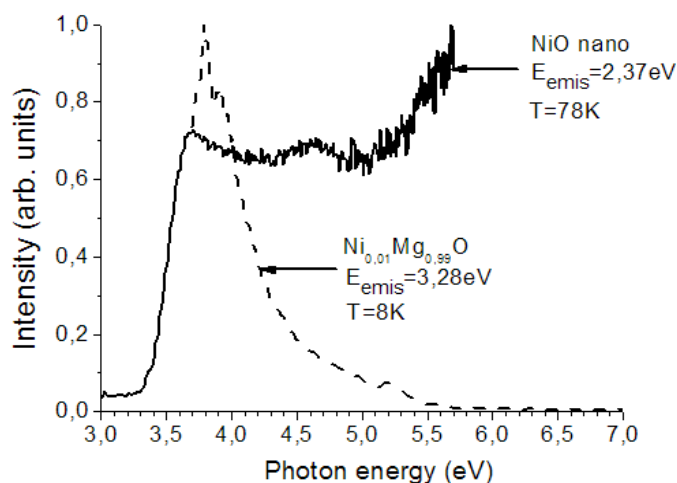


Figure 1. Photoluminescence excitation spectra of  $\text{Ni}_{0.01}\text{Mg}_{0.99}\text{O}$  and NiO nano [2]. Emission energies  $E_{\text{emis}}=3.28$  eV and 2,37 eV correspondingly.

Fig.1 represents PL excitation spectra of  $\text{Ni}_{0.01}\text{Mg}_{0.99}\text{O}$  and NiO nano. One can notice that the edge of excitation spectrum of NiO nano very well coincides with PL excitation spectrum of  $\text{Ni}_{0.01}\text{Mg}_{0.99}\text{O}$ . Transfer energy of electron from p-shell of oxygen to d-shell of nickel determines the edge of CT band. Since the vicinity of Ni-ions in NiO and  $\text{Ni}_{0.01}\text{Mg}_{0.99}\text{O}$  is almost identical: ion  $\text{Ni}^{2+}$  is surrounded by six ions of  $\text{O}^{2-}$ ; distance between  $\text{Ni}^{2+}$  and  $\text{O}^{2-}$  is 2,088 Å in NiO, 2,105 Å in  $\text{Ni}_{0.01}\text{Mg}_{0.99}\text{O}$ , we expect the same transfer energy of electron in these compounds. For small Ni concentrations in  $\text{Ni}_x\text{Mg}_{1-x}\text{O}$  we consider only p-d CT transitions  $d^8 + \hbar\omega \rightarrow d^9 + h$ , whereas d-d CT transitions have small chance of existence. Thus observed coincidence between the edge of PL excitation spectrum of  $\text{Ni}_{0.01}\text{Mg}_{0.99}\text{O}$  and NiO provides reliable confirmation that the edge of PL excitation band in NiO arises due to p-d CT transitions.

### REFERENCES

- [1] V. Sokolov, V. Pustovarov, V. Churmanov et al // Phys. Rev. B. – 2012. – V.86. – 115128.  
 [2] V. Sokolov, V. Pustovarov, V. Churmanov et al // IOP Conf. Series: M. Science and Eng. – 2012. – V.38. – 012007.

<sup>1</sup> This work was partially supported by the Ural Branch of RAS (grant № 12-u-2-1030) and the Ministry of Education and Science of Russian Federation (the basic part of the government mandate). Also this research project has been supported by UrFU under the Framework Programme of development of UrFU through the «Young scientists UrFU» competition.



## PHOTOLUMINESCENCE OF CoO EXCITED BY SYNCHROTRON RADIATION<sup>1</sup>

V.N. CHURMANOV\*, V.I. SOKOLOV\*\*, V.A. PUSTOVAROV\*, V.YU. IVANOV\*, N.B. GRUZDEV\*\*, P.S. SOKOLOV\*\*\*,  
A.N. BARANOV\*\*\*

\* Ural Federal University, Mira str. 19, Yekaterinburg, 620002, Russia, e-mail: chenov@olympus.ru, phone: +79126382765

\*\* Institute of Metal Physics UB RAS, S. Kovalevskaya str. 18, Yekaterinburg, 620990, Russia

\*\*\* Lomonosov Moscow State University, Moscow, 119991, Russia

Investigation of energy spectrum of 3d-transition metal oxides is the actual problem of the condensed matter physics. Experimental researches of interband transitions of NiO and CoO oxides are realized by the methods of optical spectroscopy and inelastic X-ray scattering. Recently the interesting results were achieved in connection with the observation of photoluminescence (PL) and photoluminescence excitation (PLE) spectra of NiO using synchrotron radiation (DESY, Hamburg) [1,2]. The most of experimental studies of CoO were focused on cathodoluminescence [3], but investigation of photoluminescence has not been carried out up to date. High intensity of synchrotron radiation improves significantly possibilities of PL observation and allows us to observe photoluminescence of CoO for the first time. The samples of CoO were the tablets which have been pressed from the Sigma Aldrich powder.

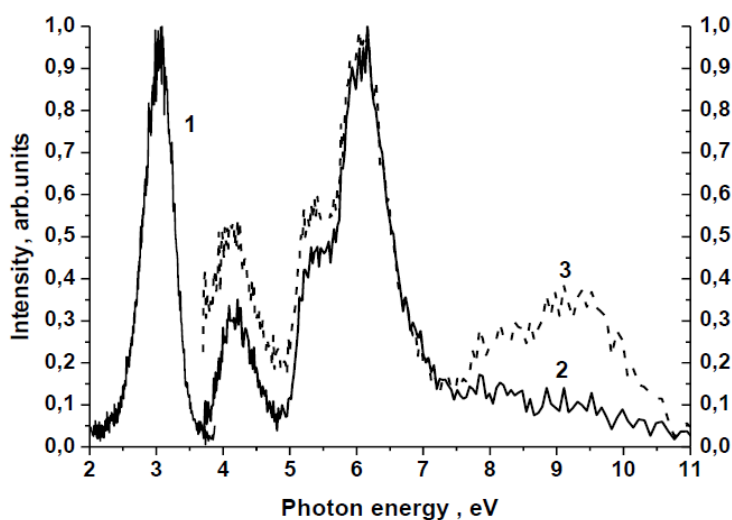


Figure 1. Low-temperature ( $T=8\text{K}$ ) time-resolved CoO luminescence. 1 - PL (fast window),  $E_{\text{exc}}=6,2\text{eV}$ ; 2, 3 – PLE spectra (fast and time-integrated windows correspondingly),  $E_{\text{emis}}=3\text{eV}$ .

Fig. 1 represents PL and PLE spectra of CoO at impulse excitation with length of the impulse of 1 ns. PL and PLE spectra were registered in two temporary windows: fast (1-5 ns) and slow (50-60ns) and also in the time-integrated window (1-80ns). The decay of PL was observed in time interval of 1-80 ns. The PL spectrum presents the wide band in the interval of 2,5-3,5 eV, whose intensity was changing in dependence on excitation energy. The PLE spectra differ significantly for the fast, slow and time-integrated registration. As soon as no experimental PLE spectra in the region of interband transitions for CoO are described in the literature, the preliminary results are interpreted in comparison with the PL and PLE spectra of NiO [1]. Difference between obtained PLE spectra of CoO and PLE spectra of NiO is small. Therefore we expect similar structure of the valence band states for CoO and NiO. Further detailed analysis of PL and PLE spectra of CoO on the basis of cluster model is required.

### REFERENCES

- [1] V. Sokolov, V. Pustovarov, V. Churmanov et al // Phys. Rev. B. – 2012. – V.86. – 115128.
- [2] V. Sokolov, V. Pustovarov, V. Churmanov et al // IOP Conf. Series: M. Science and Eng. – 2012. – V.38. – 012007.
- [3] C. Dias-Guerra, J. Piqueras // Solid State Commun. – 1997. – V.104. – pp. 763-767.

<sup>1</sup> This work was partially supported by the Ural Branch of RAS (grant № 12-u-2-1030) and the Ministry of Education and Science of Russian Federation (the basic part of the government mandate). Also this research project has been supported by UrFU under the Framework Programme of development of UrFU through the «Young scientists UrFU» competition.

## SIMULATION OF RADIATION EFFECTS ON SiO<sub>2</sub>/Si STRUCTURES

*G.M. ZAYATS\**, *A.F. KOMAROV\*\**, *F.F. KOMAROV\*\**, *S.A. MISKIEWICZ\*\**, *V.V. MICHAILOV\*\**

*\*Institute of Mathematics, Academy of Sciences of Belarus, 11 Surganov Street, Minsk, 220072, Belarus, math@im.bas-net.by, 80172841701*

*\*\*Institute of Applied Physics Problems, 7 Kurchatov Street, Minsk, 220108, Belarus*

The problem of forecasting and control of bipolar and CMOS ICs radiation resistance is of great importance today. An aim of this work is to develop efficient mathematical model as well as software for simulation of the processes described in [1], where a physical model of the accumulation of radiation induced electric charge in the dielectric of SiO<sub>2</sub>/Si structure and its subsequent discharge due to the tunnel discharging and thermal emission is presented. Developed mathematical model is the system of equations [1, 2] describing the free electron and hole kinetics, the kinetics of hole charge accumulated on the shallow and deep trap levels and the electric field intensity in dielectric layer. The tunnel discharge of the captured hole charge in the dielectric layer is described in [3]. Potential distribution in MOS structure in the presence of charge in dielectric layer and on the surface states is given by electro neutrality. The software to evaluate the dependence of radiation-induced changes in the threshold voltage of MOS structures, charge and potential distribution on the ionizing radiation has been developed.

The calculations presented in figures 1 and 2 are performed for various concentration of deep and shallow trap levels and based on the following values: the mobility of the charge carriers  $\mu_n=10^2 \text{ cm}^2\text{V}^{-1}\text{s}^{-1}$  and  $\mu_p=0,6 \times 10^{-3} \text{ cm}^2\text{V}^{-1}\text{s}^{-1}$ , the boron concentration in the semiconductor  $N_B=10^{15} \text{ cm}^{-3}$ , the temperature  $T=300\text{K}$ , the gate material is the polysilicon doped by the phosphorus. The obtained results demonstrate high adequacy of the model to the experimental data.

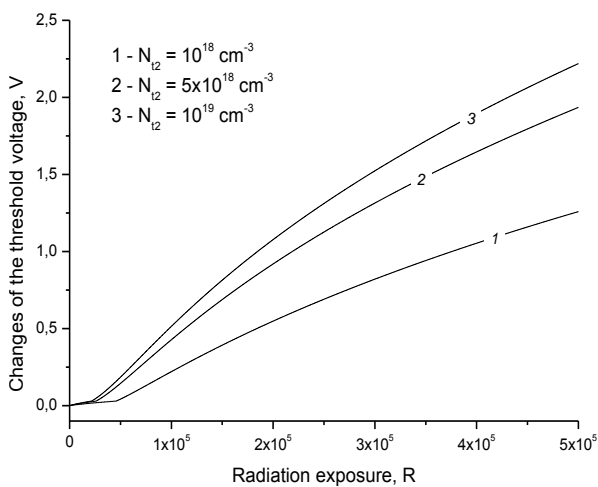


Fig.1. Dependence of the radiation-induced changes of the threshold voltage of the MOS structure on the ionizing radiation dose for the different concentrations of the deep trap levels  $N_{12}$ . The concentration of the shallow trap levels  $N_{11}=10^{18} \text{ cm}^{-3}$

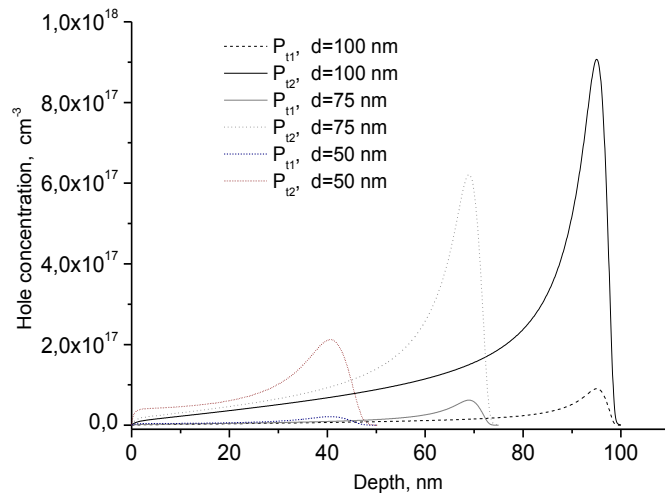


Fig. 2. Hole charge distribution on the deep and shallow trap levels for the different values of dielectric layer thickness. The concentration of deep trap levels  $N_{12}=10^{19} \text{ cm}^{-3}$  and shallow trap levels  $N_{11}=10^{18} \text{ cm}^{-3}$ .

### REFERENCES

- [1] *M.N. Levin, A.V. Tatarintsev, V.A. Makarenko, V.G. Gitlin // Microelectronics. – 2006. – 35. – 5. 382 - 391.*
- [2] *G.M. Zayats, F.F. Komarov, A.F. Komrov, S.A. Miskiewicz // Reports of NAS of Belarus. – 2013. – 57. – 3. 53 - 57.*
- [3] *P.J. MCWhorter, S.L. Miller, W.M. Miller // IEEE Trans. Nuclear Physics. – 1990. – 37. – 6. – 1682 – 1689.*

## INDIRECT STUDY OF OPTICAL PROPERTIES OF VOLUENTARY INIT OF PETN AT MIXING IT WITH ABSORPTIVE ADDITIVES (SOOT AND ALUMINIUM)

*V.A. OVCHINNIKOV\**, *V.P. CIPILEV\*\**

*\*Tomsk Polytechnic University, pr. Lenin 30, Tomsk, 634050, Russia, vladislav\_ovchin@mail.ru, +7(983)230-02-18*

*\*\* Tomsk Polytechnic University, PR. Lenin 45, Tomsk, 634034, Russia*

Laser initiation thresholds of pressed powders of PETN at laser wavelengths which correspond to its transparency spectral range depend on the irradiance distribution which is determined by both radiation absorption and diffusion on heterogeneities and within the matrix of the sample. Therefore, optical properties of explosives and effect of heterogeneities on its optical properties are to be studied to describe the initiation mechanism. Adding soot and aluminium additives allows better varying the absorption index of voluuntary unit of PENT than any other methods. However, to obtain absolute values of absorption and scattering index of voluuntary unit precise solution of radiation transport equation is required. Mie theory easily demonstrates that dependency of absorption index on absorptive additives is linear, whereas, the dependency of scattering index on the diffusive reflection coefficient is more complicated due to the failure of single diffusion theory. Moreover, aluminium particles possesses effective diffusion cross-section and it is to result in significant change in diffusive properties of voluuntary unit.

Aim of this paper is the determination of optical properties of voluuntary units of explosives.

The following steps were made to achieve this aim:

1. Diffusive reflection coefficients were measured for PETN with different concentration of soot and aluminium additives. Also, those coefficients were obtained from Monte Carlo simulation data with taking into account the absorption cross section calculated within the frames of Mie theory.
2. The correlation between incident energy density of laser radiation and volumetric irradiance of subsurface layers, and different additives concentration were obtained.
3. Calculated dependencies of reflection coefficients on photons survivability were conferred with experimental dependencies of reflection coefficients on additives concentration. As the result, optical properties of PETN matrix were obtained.

Table 1. The dependency of diffusion reflection coefficient for samples with different concentration of soot at the wavelength of 532 nm (diffusive index of matrix is 1,000 cm<sup>-1</sup>)

Mass concentration, %	Reflection coefficient RC, %	$\Delta$ RC, % confidence interval (P = 0.97)	Absorption index, cm <sup>-1</sup>	Mie absorption index, cm <sup>-1</sup>
0.5	13	0.283713	270	236
0.25	15.50642	0.865161	198	118
0.125	28.11818	0.633895	75	59

Additives concentration was within the range of 0.025 – 0.1 % what allowed to neglect radiation diffusion on them, because diffusion cross section of the matrix centers is high. Therefore, inverse problem solution demonstrated that low pressed explosives possess spherical indicatrix. Moreover, effectiveness of laser energy absorption of every concrete particle starts decreasing with additives concentration increase (>0.1 %) and diffusion coefficient decrease even when the total absorption index is being increased. Linearization of dependency of absorption index on soot concentration and its approximation to zero concentration allowed obtaining the absorption index of pure PETN.

Obtained optical properties are necessary for simulation of self-sustaining decomposition within the frames of local heat explosion initiation theory and other theories.

### REFERENCES

- [1] *Ovchinnikov V.A., Yakovlev A.N., Cipilev V.P. Simulation of radiation diffusion in scattering media of different thickness// Izvestiya vusov. Fizika – 2012. – 55. – № 11/3. 162 p.*
- [2] *Ovchinnikov V.A., Yakovlev A.N., Cipilev V.P. On the question of the optical properties of pentaerythritol tetranitrate pressed powders// Izvestiya vusov. Fizika – 2012. – 55. – № 11/3. 167 p.*

## PROBABILITY OF TRANSITIONS IN COLOR CENTERS OF SAPPHIRE CRYSTALS IRRADIATED BY FAST NEUTRONS

*N.L. LAZAREVA<sup>1,2</sup>, A.L. RAKEVICH<sup>1</sup>, E.F. MARTYNOVICH<sup>1,2</sup>*

<sup>1</sup>*Irkutsk Branch of Institute of Laser Physics SB RAS,  
130a Lermontov Str., Irkutsk, 664033 Russia, [filial@ilph.irk.ru](mailto:filial@ilph.irk.ru), ph: 83952512160*

<sup>2</sup>*Irkutsk State University, 20, Gagarin Blvd, Irkutsk, 664003 Russia*

A number of color centers have a multilevel scheme of the energy levels in the neutron- irradiated sapphire. It allows the emission of luminescence in multiple quantum transitions [1]. In the present paper we investigate the dynamics of picosecond excitation transfer within such a center, the nature of which is not yet determined. Its characteristic feature is a narrow zero-phonon line with a maximum at 755 nm, associated with long-wavelength transitions  $1 \rightarrow 2$  (absorption) and  $2 \rightarrow 1$  (luminescence). This line appears only at temperatures close to the boiling point of liquid nitrogen (Fig. 1).

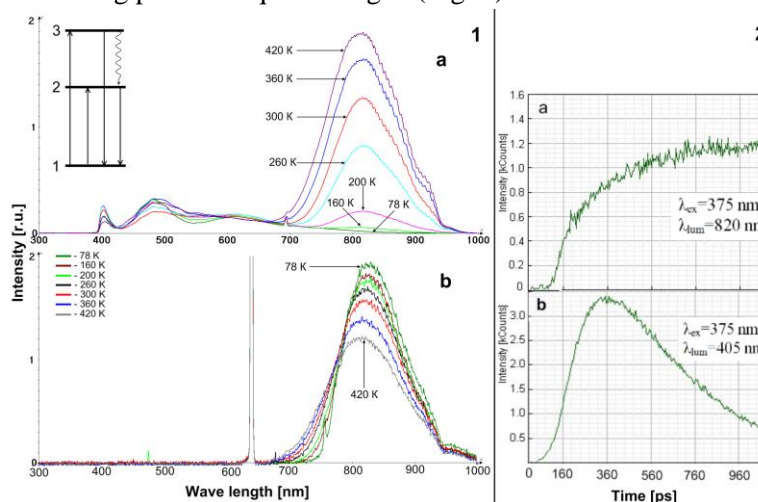


Fig. 1 - 1 - sapphire luminescence spectra excited by laser radiation with wavelength of 375 nm (a) and of 640 nm (b) at different temperatures; 2 - the kinetics of rise and decay of the luminescence at 405 nm (b) and 820 nm (a) when excited at 375nm. T = 300K

Studies were carried out using confocal scanning fluorescence microscope MicroTime 200 with picosecond time resolution, that works in the mode of time-correlated single photon counting. This microscope was equipped with Ocean Optics 65000 spectrofluorimeter. Studied center is excited by picosecond laser radiation with a wavelength of 375 nm in a high energy transition  $1 \rightarrow 3$ . The luminescence was detected through an interference filter having a bandwidth limit at a wavelength of 400 nm. Rate of energy transfer was investigated in a low-energy state in the channel of  $3 \rightarrow 2$ . For this purpose the change of population at level 3 was monitored. In this transition, the luminescence is not registered. But the dynamics of changes in the population of level 3 can be monitored, observing the luminescence kinetics in the band of 405 nm (band is partially cut by optical filter). This corresponds to the transition  $3 \rightarrow 1$ . Fig. 1.2b shows the rise and decay of the emission intensity with time in this transition. The view of this curve reflects the time dependence of the 3<sup>rd</sup> level population. Programmatic analysis of the kinetics of luminescence showed that the electron lifetime at 3<sup>rd</sup> level is 320 ps. This time is determined by the probabilities of two transitions: radiative  $3 \rightarrow 1$  and nonradiative  $3 \rightarrow 2$ . To determine of these probabilities the temperature dependences were measured in the range of 78-420 K (Fig. 1.1). Kinetics of the luminescence in Fig. 1.2a confirms that the level 2 is really populated by non-radiative transitions  $3 \rightarrow 2$ .

This work was partially supported by the project № 4-12 of RAS Presidium Program № 13 and the project II.10.1.6 Program of Base Research RAS 2013-2016.

### REFERENCES

1. *E.F.Martynovich, V.A.Grigorov, A.G.Tokarev, S.A.Zilov, V.M.Nazarov. Luminescence of color centers in  $\alpha$ -Al<sub>2</sub>O<sub>3</sub>. In the book: Fluorescent receivers and transmitters of ionizing radiation. Galanin M.D. (Ed.). Novosibirsk, 1985, p. 132-136.*

## OPTICALLY STIMULATED LUMINESCENCE OF ACTIVATED NaF CRYSTALS

*M.M. KIDIBAEV, G.S. DENISOV, A.S. BEKTASHOV*

*Institute of Physical and Technical Problems and Materials Science NAS KR,*

During optically stimulated luminescence charges release from one or several catchers. The released charges can be caught by other catchers (bimolecular reaction). For quantitative description of processes occurring in crystals during decoloration by visible light a mathematical model has been developed.

Let's mark through  $n$  a concentration of charges in deeper catchers, and through  $N$  – a concentration of charges in other shallower catchers in a crystal. Under the light action the carriers migrate from one catcher to another (with probability  $\alpha$  and  $\beta$ ) or they are recombined (with probability  $\gamma$  and  $\varepsilon$ ).

A process of variation of these carriers concentrations can be described by the following differential equations system:

$$\begin{cases} \frac{dn}{dt} = \alpha N - (\beta + \gamma)n, \\ \frac{dN}{dt} = -(\alpha + \varepsilon)N, \end{cases}$$

where  $\alpha$ ,  $\beta$ ,  $\gamma$  and  $\varepsilon$  are velocity constants (probable migrations per time unit), characterizing the processes of charges carriers migration.

Depending on concrete physical processes some parameters can be neglected. Namely, the electrons released from shallow catchers are caught by the deeper ones, but not vice versa, so it is assumed that  $\beta = 0$ .

The solution of differential equations system can have the following view:

$$\begin{cases} N = N_0 e^{-b_1 t}, \\ n = n_0 + a (1 - e^{-b_1 t}) - (a + n_0)(1 - e^{-b_2 t}), \end{cases}$$

Here the velocity parameter of accumulation by the carriers charge is  $b_1 = \alpha$ , and a parameter of decay –  $b_2 = \gamma$ ,  $N_0$  and  $n_0$  – are electrons concentrations in deep and shallow catchers respectively at  $t = 0$ ;  $a$  – maximum accessible concentration (not taking into account initial quantity  $n_0$ ).

Subject to parameters  $a$ ,  $b_1$ , and  $b_2$ , the OSL curve form will be different. When finding pointed parameters it becomes possible to make conclusions of physical processes occurring in crystals.

The OSL of nominally pure and activated crystals NaF has been studied. In Fig. 2 the points show experimental data. In compliance with parameters  $N_0$ ,  $b_1$ ,  $n_0$ ,  $b_2$  were found in environment MATLAB for fast and slow components.

The solution of differential equations allows passing on from qualitative description of OSL process to quantitative description. All found coefficients have a clear physical meaning.

## APPLICATION OF THE EMISSION IR SPECTROSCOPY METHOD TO STUDY THE STATE OF OXIDE FILMS ON THE ION-MODIFIED SURFACE.

*L.P.NEKRASOVA, R.A.VALIKOV, N.V.VOLKOV, I.V.OLEINIKOV*

*National Research Nuclear University MEPhI (NRNU MEPhI), highway Kashirskoe, Moscow, Russia,  
[NVVolkov@mail.ru](mailto:NVVolkov@mail.ru), 8-903-507-61-98*

The task of improving the properties of oxide compounds Be, Al, Ti, Fe, Cu, Mo, Zr and stabilization of their structural-phase state is currently important, because usual methods to obtain thermally stable, radiation-resistant compounds with desired properties is impossible.

Thereby we propose used ion beam radiation with wide energy spectrum (gaussian distribution) and average energy 6-20 keV for modification properties of oxide films. Experiments show, that simultaneous impact of ions with different energy significantly increases modification zone and reduce stress and density of radiation defects in modification layer. Under radiation ion beam with wide energy spectrum system "multilayer films – oxide – metal substrate", atoms of multilayer film penetrate into the oxide, at the expense of radiation-induced processes, and defect free doped its to a depth of 1  $\mu\text{m}$  with a concentration higher, than the solubility limit. In result complex simultaneous alloying of oxide films, created new states (physicochemical, electrophysical), which impossible obtaine other methods. For example, revealed. That in result simultaneous alloying system "ZrO<sub>2</sub>-film – Zr-substrate" atoms Al, Fe, Mo, Y to a depth of 100 nm were formed multilayer gradient layers, formed oxides and intermetallic compounds of Zr<sub>3</sub>Al, ZrFe<sub>2</sub>, ZrMo<sub>2</sub>, which enhance the properties of products (improved corrosion resistance and wear resistance claddings from zirconium alloys).

By IR spectroscopy shows the principal possibility of identifying the states of oxide films on polycrystalline metal substrate, which will improve the technology to produce and control oxide films with desired properties.

## INVESTIGATION OF LUMINAIRE TEMPERATURE CONDITIONS AT DIFFERENT CURRENTS IN LEDS

*S.Y.GURIN\**, *B.P.GRICENKO\*\*\**

*\*National Research Tomsk Polytechnic University, Lenina Avenue, 30, Tomsk, 634050, Russian Federation*

*\*\* Institute of Strength Physics and Materials Science, Tomsk, Russian Federation*

The purpose of this project was to investigate the temperature conditions of Cree[1] LEDs, depending on impressed current. The basic idea was to obtain dependencies that could be used to select the optimal operating mode for getting the most LED lamp efficiency.

Calculation of thermal conditions was held with the help of a special software application SolidWorks Flow Simulation. In the course of research 5 PCBs mounted on the aluminum housing of the designed luminaire were calculated. On each board different current from 0.35A to 1.5A was impressed. LED quantity on PCBs was chosen so that the luminous flux was the same on all the boards - 12klm.

After the calculations the graphs, reflecting energy efficient and economic characteristics of the luminaire were obtained. Figure 1 shows the dependence of the luminous efficiency on the current.

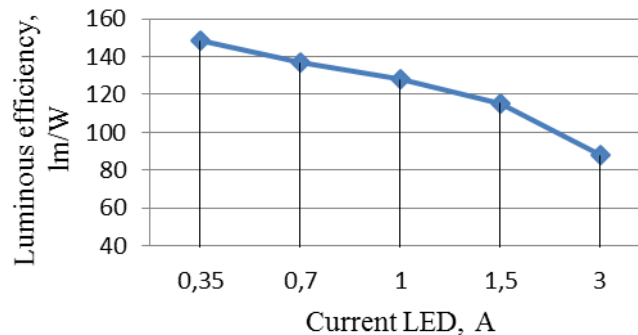


Fig. 1 Dependence of the luminous efficiency of LEDs from the LED current.

The data were analyzed and the following conclusions were made:

- the calculation of LEDs thermal condition (especially, powerful) and the choice of a suitable cooling system is one of the main criteria in the design of a reliable and durable LED lighting system;
- the maximum life span of LEDs is achieved while its working at low currents;
- price reduction of the luminaire by increasing LEDs operating current leads to significant decrease of the luminous efficiency.

### REFERENCES

- [1] <http://cree.com/LED-Components-and-Modules/Products/XLamp/Discrete-Directional/XLamp-XML>

## THE LABORATORY DEVICE FOR MEASURING THE PROPAGATION VELOCITY OF ULTRASONIC WAVES IN HYDROGENATED METALS<sup>1</sup>

*A.M. LIDER, V.V. LARIONOV, G.V. GARANIN*

*Tomsk Polytechnic University, 30, Lenin, Tomsk, 634050, Russia, E-mail: lider@tpu.ru, +7 3822 705012*

Development of nuclear power engineering, rocket and aircraft production requires improvement of identification methods for hydrogen embrittlement of titanium products in order to increase their rupture life, exclude and prognose hydrogen degradation of products [1]. Application of ultrasonic Rayleigh waves (URW) in metals for diagnostic purposes is conditioned by peculiarities of such waves: 1) the possibility to measure acoustic signal from any point of surface sample in which the wave propagates, 2) relatively high concentration of energy in wave due to small layer of wave localization. Application of URW in many cases is accompanied by contradictory effects. For example, decrease of material density leads to decrease of URW propagation velocity. At the same time formation of metal hydrides can lead to its increase as well as to its decrease [1]. In order to solve such tasks the laboratory device was designed, its scheme is discussed in the report. Titanium BT1-0 samples in the form of rectangular sheets with the size of 90×40×3 mm along different directions of parent sheet rolling were used for studies. Integral hydrogen content in titanium samples was controlled by melting performed on the setup produced by RHEN 602 LECO. Several parties of identical titanium samples were produced. Thereafter, they were hydrogenated to different concentrations on the setup PCI 6GasReactionController subjected to Sieverts method. After hydrogenation the ultrasonic waves` propagation velocity was measured. Thereafter each sample hydrogenated to necessary concentration was subjected to elongation that lead to rupture. In a number of experiments hydrogenation and ultrasonic waves velocity measurements were performed sequentially on the same sample. Sample elongation that lead to rupture was performed on the test unit ComTen-95. In order to measure hydrogen embrittlement of metal ultrasonic waves velocity was measured, standard dependency of ultrasonic waves velocity in metal on hydrogen concentration in metal was built. Diagram of standard dependency has increasing and decreasing diagram legs. Tangent lines are built to both diagram legs, the crosspoint of these lines is identified. A perpendicular is dropped from the tangent lines crosspoint on the hydrogen concentration axis. The crosspoint of the perpendicular and the hydrogen concentration axis determines the concentration of hydrogen in metal from which embrittlement of titanium alloy begins. With increase of hydrogen concentration in the test sample within the range of concentrations from 0 to ~ 0,20 weight percents ultrasonic waves velocity increases linearly. BT1-0 titanium alloy hydrogenation within the given interval of concentrations leads to increase of inner stresses, increase of elastic modulus (and, respectively to increase of ultrasonic propagation velocity). Decrease of Rayleigh waves velocity within the range of hydrogen concentration from 0,20 to 0,60 weight percents in the sample is conditioned by defects forming and considerable decrease of material strength property. In order to compare the results obtained by ultrasonic method and loading (elongation) of samples method, the dependency (the right scale) of change of relative stretching to rupture of a sample during elongation due to hydrogen concentration in titanium alloy was studied. Samples were subjected to elongation that lead to rupture after change of ultrasonic waves` velocity propagation in them. Size  $\epsilon$  is practically linearly decreasing with the increase of hydrogen concentration in material until hydrogen embrittlement condition occurs. With further increase of hydrogen concentration its size does not change and constitutes 1,5 ÷ 2 %. During all experiments there is correlation observed between relative change of Rayleigh wave velocity along the sample length and hydrogen concentration. The more hydrogen concentration in BT1-0 titanium is the more graph of function indexes deviation which reflects dependence between relative value of Rayleigh wave velocity and location of transducer in hydrogenated samples is. The developed technique allows conducting measurements of hydrogen concentration in light alloys based on ultrasonic waves` propagation velocity. The efficiency of measurements depends on the choice of autocirculation frequency, locating distance between the receiver and transducer and is controlled by the means of correlation between ultrasonic waves velocity and value reverse to autocirculation frequency.

### REFERENCES

- [1] *Lider, A.M., Kroening M.X, Larionov, V.V., Garanin, G.V. // Technical Physics. – 2011. – Volume 56. – № 11. pp. 1630–1634.*

<sup>1</sup> This work was supported by goszadaniye «Nauka» № 0.1325.2014.



**RESEARCH OF THE ANISOTROPY RELAXATION TIME OF RHODAMINE 6G FLUORESCENCE IN SAMPLES OF CEREBROSPINAL FLUID OF PATIENTS WITH DISEASES OF THE CARDIOVASCULAR SYSTEM.**

*A.V. BARTUL\**, *S. A. ZILOV\**, *A. L. RAKEVICH\**, *V. V. KOVALEV\*\**

*\*Institute of Laser Physics of Siberian Branch of Russian Academy of Sciences, Irkutsk, Russia, E-mail: [sigruna\\_nano@bk.ru](mailto:sigruna_nano@bk.ru), 8-983-249-03-14*

*\*\*Irkutsk State Medical Academy of Continuing Education, Irkutsk, Russia.*

Application of fluorescence methods for the diagnostics and prediction of diseases is of great interest. Confocal fluorescence microscopy can provide understanding of many processes in complex biological systems. Investigation of human cerebrospinal fluid with confocal fluorescence microscopy allows carry out express analysis to diagnose problems and to assess the severity of the disease.

Pathologies of the cerebrospinal fluid with various diseases are studied in a large number of research works. However the results of a study of cerebrospinal fluid viscosity with confocal fluorescence microscopy with high temporal resolution are not covered in the current literature. The results of measurements of this parameter in the dynamics of the disease seem to be very interesting for assessment of the severity of the pathological process and for prognosis.

Research of cerebrospinal fluid samples was done on a confocal laser fluorescence microscope MicroTime 200, PicoQuant GmbH. Changing of the viscosity of the medium can be observed with Brownian motion of impurity test particles. We used Rhodamine 6G molecules as test particles. Measured parameter (the anisotropy relaxation time of the fluorescence of Rhodamine 6G molecules) is associated with the rotational diffusion of Rhodamine molecules and, hence, with viscosity of the medium.

We have investigated cerebrospinal fluid of patients with various diseases of the cardiovascular system. Our experiments showed that the value of the anisotropy relaxation time depends on the severity of pathology.

## SPACE RADIATION CHARGING EFFECTS OF DIELECTRIC MATERIALS: TESTING METHODS AND APPARATUS

A. A. CHIGORKO

*National Research Tomsk Polytechnic University, Institute of Non-Destructive Testing, 30, Lenin av., Tomsk, 634050, Russia,  
chigorko@gmail.com, (3822) 41-76-54*

Dielectric materials on spacecraft surfaces being exposed to magnetospheric plasma build up quite a few charge. Spacecraft charging causes difference in the electrostatic potential of a spacecraft surfaces with respect to the surrounding plasma or between parts of the spacecraft (differential charging). The most dangerous effect of spacecraft charging is perhaps the resulting electrostatic discharge (ESD) which may cause degradation of spacecraft components or even malfunctions of electronics.

There are several forms of ESD:

- 1) Surface discharge (flash-over) – propagates from a starting point to the closest electric ground;
- 2) Blow-off – emission of negative charges (electrons) into space;
- 3) Bulk discharge (punch through) – classic breakdown of a dielectric material.

The testing of dielectric materials is required to predict the ability of material to build up charges and the possibility of following ESD.

Experimental test stand [1] is used to simulate relevant space conditions (electron irradiation, vacuum, temperature) and observe charging and discharging of the materials under these conditions.

The testing stand has the following main components:

- Cylindrical vacuum chamber made of stainless steel;
- Electron gun with energy range from 70 to 300 keV;
- Oil-free pumping system including turbomolecular and cryogenic pumps which ensures a pressure of the order of  $10^{-6}$  Torr;
- Specimen holder with temperature regulation;
- Measuring tools specific to the electrostatic studies such as current probes and surface potential probes.

The combination of well-known and developed testing methods is used. The following material properties and charging/discharging parameters can be measured during the testing:

- 1) Bulk electrical resistivity, measured by conventional “capacitor method” or more accurate charge storage method [2] using picoammeter with 10fA resolution;
- 2) Surface electrical resistivity;
- 3) Radiation induced conductivity;
- 4) Surface potential, measured with electrostatic surface potential probe;
- 5) Discharge current, measured with 1 GHz oscilloscope and non-contacting current probes with bandwidth of 120 MHz and 1 GHz;
- 6) Visual observance and discharge monitoring with hi-speed videcamera.

Thus, the significance of radiation testing of dielectrics used for space is shown. Basic values, such as bulk resistivity, surface potential and discharge parameters, are observed. Testing methods and apparatus for radiation charging are given. Main features of the new testing stand for radiation charging of dielectrics are shown.

### REFERENCES

- [1] A. A. Chigorko, Y. A. Bezhaev, A. A. Lukashchuk // Testing. Diagnostics. – 2012. – № 3 (165) – p.45-48
- [2] A. R. Frederickson, C. E. Benson // Nuclear Instruments and Methods in Physics Research. – 2003 – vol. 208 – p. 454-460.

## ADVANCED ${}^6\text{LiF-ZnS(Ag)}$ THERMAL NEUTRON DETECTOR

*I. DUBTSOV\**, *L. ANDRUSCHENKO\**, *V. TARASOV\**, *O. SHPILINSKAJA\*\**, *L. TREFILOVA\**,  
*V. YAKOVLEV\*\*\**, *V. LISITSYN \*\*\**, *A.DUDNIK\*\*\*\**

*\*Institute for Scintillation Materials, 60 Lenin Avenue, Kharkov 61001, Ukraine, [dubcov@isma.kharkov.ua](mailto:dubcov@isma.kharkov.ua), +38(057)3410246*

*\*\*Institute for Single Crystals of NASU, 60 Lenin Avenue, Kharkov 61001, Ukraine,*

*\*\*\*Tomsk Polytechnic University, 30 Lenin Avenue, Tomsk 634034, Russian Federation*

*\*\*\*\*V.N. Karazin National University, 4, Svoboda Square, Kharkov 61022, Ukraine*

A composite scintillator  ${}^6\text{LiF-ZnS(Ag)}$  has been used for more than a century to detect thermal neutrons. According to the reaction  ${}^6\text{Li} + n \rightarrow \tau (2.74 \text{ MeV}) + \alpha (2.06 \text{ MeV})$ ,  ${}^6\text{LiF}$  converts a thermal neutron into  $\tau$  (2.74 MeV) and  $\alpha$  (2.06 MeV) particles which make  $\text{ZnS(Ag)}$  respond with scintillations.

The sizes of  ${}^6\text{LiF}$  and  $\text{ZnS(Ag)}$  grains are crucial to the registration efficiency of the composite scintillator. Nanotechnology has made it possible to obtain disperse powders of  ${}^6\text{LiF}$  and  $\text{ZnS(Ag)}$  with optimal sizes of the grains, which has dramatically improved the parameters of  ${}^6\text{LiF-ZnS(Ag)}$  composite scintillator, making it a perfect substitute for  ${}^3\text{He}$  nuclide – a rare and expensive gas. The optimal sizes of  ${}^6\text{LiF}$  and  $\text{ZnS(Ag)}$  grains 600-800 nm and 7-9  $\mu\text{m}$ , respectively were determined by a computer and experimental modeling. The ratio of  ${}^6\text{LiF}$  and  $\text{ZnS(Ag)}$  in an epoxy matrix was 1:4:1, respectively. The neutron detector consists of five layers of  ${}^6\text{LiF-ZnS(Ag)}$  composite scintillator separated by four organic glass plates with the dimensions of  $40 \times 25 \times 3 \text{ mm}^3$  (Fig.1). The thermal neutron registration efficiency of 200 $\mu\text{m}$  thick  ${}^6\text{LiF-ZnS(Ag)}$  layer was 29.5%. The organic glass plates act as light conductors and neutron retarders. Tetratex was used as a light-reflecting element and FEU photomultiplier R1307 as a photodetector. This solid-state detector is simple and reliable in service, has a low sensitivity to gamma radiation and the high registration efficiency (75%) of the gas-filled  ${}^3\text{He}$  detector.

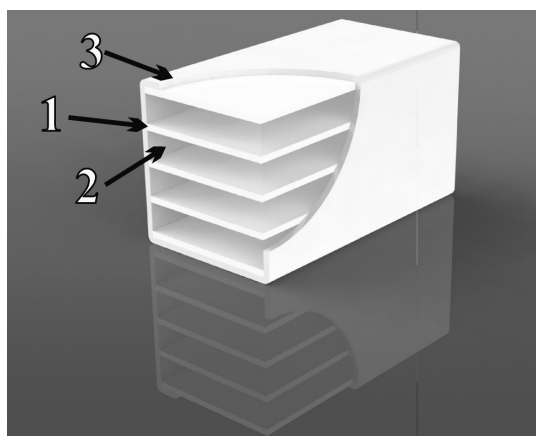


Рис. 1. The structure of  ${}^6\text{LiF-ZnS(Ag)}$  thermal neutron detector  
1-  ${}^6\text{LiF-ZnS(Ag)}$  layer, 2 - organic glass plate, 3 - light-reflector

## AUTHOR INDEX

<b>A</b>			
Abadias G.	284	Bagdasarov G.A.	61
Abashev R.M.	419, 434	Baizhigitova B.A.	443
Abdullin E.N.	48, 49, 119, 133	Baizhumanov M.	501
Abidzina V.	306, 318	Baklanova I.V.	406
Abuova A.U.	490	Baksht E.Kh.	53, 155, 158, 171, 177
Abuova F.U.	490, 491	Baksht R.B.	58, 68, 69
Aduev B.P.	459, 463, 464, 476, 477	Baktybekov K.	457
Aihaiti Yisihaketu	103	Bakulin A.V.	486, 514
Aimaganbetova Z.K.	445, 447	Baldanov B.B.	402
Akhmadeev Yu.H.	215, 219, 281, 345	Balesin M.E.	181, 191
Akhmetshin R.	481, 483, 484	Balykov D.V.	461, 470
Akilbekov A.T.	301, 490, 491, 501	Balzovskii E.V.	174
Aksenova T.I.	333	Banokina T.I.	154
Akuov A.M.	508	Barakhvostov S.V.	66, 212
Aleksandrov V.V.	56	Baranov A.N.	423, 521
Alekseev S.V.	119, 468, 485	Baranova A.A.	503, 517
Alekseev V.	450	Baratova A.	457
Alexeenko V.M.	126	Barchenko V.T.	230, 235, 240, 382
Aligozhina K.A.	488	Barengolts S.A.	31, 40, 157
Alontseva D.L.	348	Barmina A.A.	445
Amirova A.A.	410	Bartul A.V.	404, 529
Anan'ev V.A.	437, 438, 442	Baryshevsky V.	391
Anan'eva M.V.	458, 461, 470	Baryshnikov V.I.	480
Ananin P.S.	258	Basalai A.V.	271, 302
Andre Y.-B.	182	Bataev V.A.	289
Andreev M.V.	201	Batoroev S.B.	402
Andreev Yu.A.	84	Baymagambetov K.N.	410
Andreev Yu.M.	283, 471, 472	Bazarov B.G.	275, 321
Andruschenko L.	531	Bazarova J.G.	275, 321
Anishchik V.M.	384	Bazelyan E.M.	183
Anshakov A.S.	211	Beilin L.	83
Antonov O.	62	Beketov I.V.	186
Antonyuk V.I.	265	Beklemishchev A.V.	130
Aoufi A.	451, 452, 465	Bekmyrza K.Zh.	428
Arantchouk L.	182	Bektashov A.S.	525
Arestov S.I.	342	Belaya M.	306, 318
Arkipov V.	391	Belenko A.A.	193
Arteev M.S.	111, 202	Beloglazova P.A.	327
Artemenko S.N.	91, 92, 93, 94, 96, 98, 111	Belokurov G.M.	476
Artyomov A.P.	57	Belomytsev S.Ya.	155
Artyomov K.P.	430, 449	Beloplotov D.V.	149, 151, 164, 167, 499
Asainov O.Kh.	294	Belous N.	391
Assylbayev R.	501	Belyi A.V.	309
Astashynski V.M.	245, 270, 271, 300, 302	Beniyash A.	213
Astrakchantsev N.V.	210	Berezneeva E.V.	327, 365
Astrelin V.T.	17, 241	Bestetti M.	364
Aubakirova R.K.	397	Bleykher G.A.	251
Avdeev S.M.	479	Bobina N.	515
Avgustinovich V.A.	91, 93, 94, 98, 111	Bogomaz A.A.	63, 77
Azarkevich E.I.	186	Boichenko S.V.	404
		Bokhan P.A.	122, 173
		Bolbukov V.P.	217, 221
		Boldarev A.	72
<b>B</b>		Bolotov A.V.	341
Babinov N.A.	235	Bolshakov M.A.	46, 47, 88, 179, 193
Badmaeva I.N.	335	Boltachev G.S.	37
Bagazeev A.V.	186		

Boreysho A.S.	191	<b>D</b>	
Borisov D.P.	237	Dabagov S.B.	430
Borodin E.N.	246	Damamme G.	451, 452, 465
Borovikova A.P.	460, 461, 470	Dampilon B.V.	293, 313, 314
Botov M.A.	429	Dasheev D.E.	320, 335, 355, 356
Bozhenko A.K.	344	Datsko I.M.	74, 76
Bozhko I.A.	363	Dauletbekova A.K.	301, 501
Brele Y.	182	Daurenbekov D.H.	428
Brunella M.F.	364	Davydenko V.I.	17
Bryukvina L.I.	510, 511	Deichuly M.P.	81
Budilov V.V.	273, 337, 383	Dektyarev S.V.	258
Budin A.V.	63	Demidenko V.V.	295
Budovskih E.A.	288	Denisov G.S.	525
Bugaev A.S.	223, 227, 298	Denisov V.V.	215, 219, 220, 238, 281
Bui B.	125	Denisova Yu.A.	309, 345, 346
Bukharkin A.A.	180, 474	Devyatkov V.N.	21, 24, 50, 242
Bulanov S.S.	61	Dian Zhang	110
Buldakov M.A.	179	Dik A.V.	430
Bulusheva L.G.	393	Dmitrieva N.M.	176
Bumagina A.I.	247, 257, 258, 259, 260, 344	Dobrovolskiy A.	33
Burachenko A.G.	153, 155, 158, 171, 177, 479	Dolgachev A.V.	453
Buranov S.N.	162	Dolgachev V.A.	475
Burdovitsin V.A.	214, 232, 304	Donskoy M.	83
Bureyev O.A.	222, 375	Dorozhko A.V.	296
Burlakov R.B.	250	Dorzhiiev A.D.	356
Bychkov Yu.I.	200	Dorzhiieva S.G.	275, 321
Bykov N.M.	143	Doyle S.	374
Bykov Y.A.	183	Dresvyanskiy V.P.	404, 468, 469, 507
Bystritskii Vit.M.	436	Dubtsov I.	531
Bystritsky V.M.	436	Dudarev E.F.	290
Bytzenko O.A.	248, 254, 310	Dudkin G.N.	60, 196, 197, 436
<b>C</b>		Dudnik A.	531
Carbonne J.	182	Durakov V.G.	293, 313, 314, 369, 370, 371
Chaikovsky S.A.	57, 58, 59, 68, 69, 74, 76, 78, 131, 157	Dushkin I.V.	311
Chebodaeva V.V.	366	Dzhumaev P.S.	252, 316
Chen Lin	115	<b>E</b>	
Chepak-Gizbrekht M.V.	269	Efimov S.	62
Cherdizov R.K.	60, 75, 124	Efremov A.M.	84
Cherdyntseva N.V.	179	Ehrenberg H.	275
Cherenda N.N.	245, 270, 271, 302	Eltchaninov A.A.	52, 87, 97
Cherepenin V.A.	108	Emelyanov V.V.	517
Chereshnev V.A.	517	Emelyanova O.V.	252
Chernov I.P.	312, 327, 365	Emlin R.V.	13
Chernyavski A.V.	330	Engelko V.I.	248, 254, 310
Chernyh A.A.	495	Enikeev N.A.	252
Chertov A.A.	20	Ermilov I.V.	145
Chigorko A.A.	530	Ermolaev V.N.	333
Chimitova O.D.	275	Ermolaev Yu.V.	333
Chingina E.A.	54, 212	Erofeev E.V.	292
Chistyakova E.K.	518	Erofeev M.V.	158, 171, 277, 282, 315
Chukin A.V.	354	Eroshenko A.Yu.	289
Chumakov Y.A.	478	Esarey E.	61
Chumerin P.Yu.	104, 105, 106	Evdokimov A.A.	399, 400
Churmanov V.N.	423, 520, 521	Evdokimov I.M.	191
Cikhardt J.	60, 75	<b>F</b>	
Cipilev V.P.	523	Faleev V.A.	211
Cordova S.R.	125	Farafonov D.S.	166
Cuneo M.E.	125	Fedin I.V.	292

Fedorischeva M.V.	325	Grishkov A.A.	51, 155
Fedorov S.V.	353	Gritsenko B.P.	287
Fedorov V.M.	80, 95	Gromov A.N.	248, 254, 310
Fedunin A.V.	57	Gromov V.E.	343
Filatov I.E.	203, 204	Gruner F.R.	125
Filipowicz M.	436	Gruzdev N.B.	423, 520, 521
Focia R.J.	125	Gubanov V.P.	104
Fortuna S.V.	289	Guchenko S.A.	389
Fowler W.A.	125	Gudimova E.Yu.	266, 276
Frangulyan T.S.	330	Gugin P.P.	122, 173
Frants O.B.	71, 73, 341	Gul'kin A.V.	27
Frolov E.N.	430	Gumirov M.A.	489
Frolova V.P.	225, 331	Gunin A.V.	113
Fursov F.I.	60, 75, 124	Guo Fan.	115
<b>G</b>		Gurevich A.V.	170
Galkin P.S.	367	Gurin S.Y.	527
Galstyan V.G.	497	Gurinovich A.	391
Ganchenkova M.G.	252	Gurnevich E.	391
Ganina I.I.	410	Gurovich V.T.	62, 159
Gao Y.	244	Guselnikov A.	391
Garanin G.V.	509, 528	Gusev A.I.	117, 120, 129
Gasilov V.	72	Gushchina N.V.	278, 319
Gavrilov N.V.	28, 222, 354	Gushenets V.I.	33, 223, 227
Gavrilyk A.O.	441	<b>H</b>	
Gaydaychuk A.V.	512	Hocker S.	486
Gazenauro E.G.	466, 482	Hojatzadeh K.	142
Gazi S.	436	Houard A.	182
Geddes C.G.R.	61	Huran J.	436
Geiman V.G.	341	Hutsel B.T.	125
Genin D.E.	479, 499	<b>I</b>	
Gerasimov D.Yu.	399, 400	Ibrayeva A.	444
Gering G.I.	262	Ievlev V.M.	264
Geyman V.G.	71	Ignatov A.A.	369, 370, 371
Ghyngazov S.A.	330	Igumnov V.S.	98
Ginzburg N.S.	79, 101	Il'ves V.G.	406, 418
Girsova N.V.	287	Il'eva A.E.	291
Glazkov R.N.	49	Ilyakova N.N.	455
Glukhov I.A.	289	Inerbaev T.M.	490, 491
Glushko Yu.A.	396, 397	Ionov I.V.	229, 377
Gnusov S.F.	293, 313, 314, 369, 370, 371	Isaenko L.I.	421
Golkovski M.G.	289	Isaev Yu.N.	42
Golosov E.V.	351, 352	Isakova Y.I.	14
Goncharov A.	33	Ishchenko A.V.	518
Gorbunov S.P.	130	Ivanov A.A.	474
Gorev S.A.	91, 94	Ivanov A.V.	480
Gorina S.G.	435	Ivanov G.A.	462
Gorodetskiy D.V.	393	Ivanov I.A.	18
Gorokhov V.V.	162	Ivanov I.E.	112
Grabovetskaya G.P.	299	Ivanov M.V.	119, 485
Grabovskii E.V.	56, 183	Ivanov N.G.	119, 133, 192
Gradoboev A.V.	338, 339, 519	Ivanov S.N.	138, 139
Grankin D.V.	493	Ivanov V.V.	184, 185, 186
Gribov A.N.	183	Ivanov V.Ya.	11, 26
Gricenko B.P.	527	Ivanov V.Yu.	423, 424, 440, 502, 520, 521
Grigoriev A.N.	70, 278	Ivanov Yu.F.	280, 287, 288, 308, 309, 315, 340, 343, 345, 346, 349, 398
Grigoriev S.N.	217, 221	Ivashov R.V.	244
Grigoriev S.V.	22, 23, 242	Ivshutenko A.S.	405, 413
Grigoriev V.P.	16, 19		
Grigoryev D.V.	332, 479		
Grippa A.	431, 450		

<b>J</b>			
Jiang Ping	114	Khrushchev K.A.	13
Johnston M.D.	125	Khusainov U.G.	337
Ju J.C.	86	Kidibaev M.M.	525
Jun Zhan	110	Kiefer M.L.	125, 126
		Kim A.A.	126, 127
		Kirm M.	421
<b>K</b>		Kiseleva M.S.	448
Kabyshev A.V.	329, 512	Kisil E.	450
Kachalkov A.A.	121	Kislitsin S.B.	265
Kado T.	362	Kiziridi P.P.	34
Kagadei V.A.	292	Klimov A.I.	85, 89, 97
Kaigorodova L.I.	278, 319	Klimov A.S.	232
Kainarbai A.Zh.	428	Klir D.	60, 75
Kalashnikov M.P.	325, 363, 398	Klopotov A.A.	308, 340
Kalashnikov S.V.	390	Klopotov V.D.	340
Kalenskii A.V.	458, 459, 460, 461, 470	Knyazev E.V.	250, 487
Kalin B.A.	252, 286, 316	Knyazeva A.G.	218, 269, 307, 381, 473, 478, 488
Kalinin Yu.G.	56	Knyazeva Anna	496
Kalmykov P.	467, 484	Knyazeva I.R.	88, 185
Kalushevich A.A.	373	Kocharovskaya E.R.	79, 101
Kamenetskikh A.S.	354	Kochumeev V.A.	106
Kaminsky V.L.	93, 111	Koketai T.A.	443, 444
Kamrikova A.	425	Kokh K.A.	283, 472
Kanaev G.G.	109	Kokhanenko A.P.	332
Kanakhin A.A.	497	Kokshenev V.A.	60, 75, 124, 146
Kandaurov I.V.	18, 241	Koleukh D.S.	184
Kanygin M.A.	393	Kolganova Yu.L.	376, 401
Kaplas T.	391	Kolmogorov A.V.	17
Kaptagai G.	491	Kolobov Y.R.	351, 352
Karelin V.I.	156, 162, 163	Kolomiets M.D.	43, 44, 170
Karnaukhov E.I.	70	Kolomytsev A.A.	495
Karner T.	426	Kolubaev E.A.	346
Kartaev E.V.	361	Komarek A.	275
Kartashov I.N.	99	Komarov A.F.	522
Kashin O.A.	326	Komarov F.F.	522
Kashukov S.V.	255	Komarova E.G.	366
Kasyanov V.S.	244, 341	Kondratiev S.S.	126
Kaykanov M.I.	30	Konev V.Yu.	113
Kazakov A.V.	214	Konig K.	404
Kazimirov A.I.	292	Konovalev I.N.	199
Kereya A.V.	46, 47, 88	Konusov F.V.	329, 512
Khaltanova V.M.	335, 355	Kopysheva A.K.	410
Khaltarov Z.M.	355	Korchuganov A.V.	420
Khamzakhan G.	131	Korepanov V.	425
Khan A.	496	Kornienko V.N.	108
Khanefit A.V.	453, 462, 475	Kornilov S.	213
Kharlov A.V.	118, 132, 194	Korolev Yu.D.	71, 73, 244, 341
Khartaeva E.Ch.	402	Korotaev A.D.	237, 357, 360, 379
Khasanov O.L.	398	Korotaev A.G.	332
Khaylov I.P.	14	Kortov V.S.	5, 417, 433, 498, 500, 506
Khein A.T.	252, 316	Koryashov I.A.	180, 474
Khimich I.N.	344	Koryukin V.I.	36
Khishchenko K.V.	56, 64	Koryukina E.V.	35, 36
Khmel S.Ya.	395	Korzhenko D.V.	228
Khodanovich M.Yu.	46, 47	Korzhova V.V.	388
Khokhlov K.O.	503	Koshelev V.I.	81, 82, 84
Kholodnaya G.E.	30, 189, 190	Kostyrya I.D.	153, 168, 169
Khoroshikh A.O.	495	Kotko A.S.	264
Khoruzhii V.D.	312	Kotomin E.A.	301, 490, 491
Khristenko Yu.F.	363	Koval N.N.	15, 21, 24, 50, 53, 209, 215, 220, 238, 272, 287, 345, 365, 373, 374, 412
Khromushin I.V.	333		

Koval T.V.	109, 175	Kuzmina L.V.	466
Koval'chuk O.B.	104	Kuzmitski A.M.	270, 271, 300, 302
Kovalchuk A.N.	377	Kuznetsov A.V.	404, 510
Kovalchuk B.M.	52, 60, 84, 118, 140, 141	Kuznetsov A.Y.	429
Kovalev R.I.	463, 477	Kuznetsov D.L.	204
Kovalev V.V.	529	Kuznetsov V.M.	237
Kovalskiy S.S.	215, 219, 220, 238	Kuznetsov V.V.	59
Kovivchak V.S.	250, 261, 487	Kuznetsova N.S.	187, 195
Kovsharov N.F.	367, 368	Kvasov N.T.	432
Kozhevnikov V.Yu.	176		
Kozhova V.V.	387	<b>L</b>	
Kozlov M.	62	Labetskaya N.A.	57, 58, 68, 69, 74, 76
Kozyrev A.V.	53, 176, 243, 249	Labetsky A.Yu.	60, 75, 124
Krashenin V.I.	466	Landl N.V.	71, 73, 244, 341
Krasik Y.E.	62, 83, 159	Lanskii G.V.	283, 471, 472
Krasnikov V.S.	246, 255	Larionov V.V.	509, 528
Krasov V.I.	210	Larour J.	182
Krastelev E.G.	144, 188	Laskovnev A.P.	271, 302
Kravarik J.	60, 75	Latyshev A.N.	264
Kravchenko K.A.	193	Laurynas V.Ch.	389
Krechetov A.G.	454, 455, 456	Lavrentyeva J.E.	502
Kruger L.D.	437, 438, 442	Lavrinovich A.V.	20, 121
Kruger V.G.	458, 461, 470	Lavrinovich I.V.	134, 135
Krivobokov V.P.	251, 489	Lavrukhin M.A.	122, 173
Krukovski A.	72	Lazar K.S.	303
Krukovskiy K.V.	287, 326	Lazarev S.V.	435
Krupovich N.V.	240	Lazareva N.L.	507, 524
Krutenkova E.P.	46, 47	Le V.M.	324
Krutikov V.I.	184	Lebedev I.N.	193
Krutsilina E.A.	300	Lebedev N.V.	210
Kruzhalov A.V.	505, 517	Leckbee J.	125, 126
Kryazhev Yu.G.	412, 487	Lee J.-G.	184
Krylov A.R.	436	Lee M.-K.	184
Krylova N.Y.	314	Leemans W.P.	61
Krysina O.V.	209, 280, 349, 365, 373, 374	Legostaeva E.V.	366
Kryukova O.N.	307	Leks A.G.	63
Kryzhevich D.S.	420	Leonova L.Y.	264
Kubes P.	60, 75	Leont'ev V.V.	63
Kudabaeva M.S.	46, 47	Leont'eva-Smirnova M.V.	252, 316
Kudiyarov V.N.	365	Leshkevich S.S.	284
Kukhta V.	123, 362	Levashov P.R.	56
Kuleshov A.K.	41, 300	Levko D.	159
Kulikov V.D.	305	Leyvy A.Ya.	245, 253
Kulkov S.	486	Li Hongtao	114
Kulkova S.E.	486, 514	Li W.	86
Kulyashova K.S.	396, 397	Liangji Zhou	116
Kumpyak E.V.	118	Lider A.M.	509, 528
Kun Liu	148	Ligachev A.E.	351, 352
Kurakina N.K.	77	Likholobov V.A.	412
Kuralbayeva G.A.	410	Liming Guo	107
Kurkan I.K.	51, 52, 143	Lin Chen	116
Kurkuchekov V.V.	18, 241	Linnik S.A.	41, 512
Kurmaev N.E.	60, 75, 124	Lipatov E.I.	479
Kushchev S.B.	264	Lipchak A.I.	28
Kuskova N.I.	76	Lisenkov A.A.	230
Kutenkov O.P.	46, 47, 88, 90, 179, 193	Lisenkov V.V.	165
Kuterbekov R.A.	428	Lisitsyn V.	531
Kuzelev M.V.	99	Liskov I.Y.	476, 477
Kuzhir P.	391	Litovko I.	33
Kuzmichev A.I.	234	Liu Hongwei	114
Kuzmin V.I.	361	Liu Jinfeng	114



Loginov S.V.	65, 128	Metel A.S.	216, 217, 221
Lomaev M.I.	149, 150, 151, 154, 164, 167, 177, 196, 197	Michailov K.A.	261
Long F.W.	125	Michailov V.V.	522
Lopatin I.V.	175, 209, 215, 219, 238, 281	Michalchenko A.A.	361
Lopatin V.V.	180, 187, 195, 249, 435, 474	Mikhailova D.	275
Losev V.F.	119, 133, 192, 198, 283, 468, 471, 472, 485	Miklin M.B.	437, 438, 442
Lotkov A.A.	266	Mikolaychuk M.A.	218
Lotkov A.I.	268, 272, 276, 326	Mikov A.V.	242
Lotova G.Z.	152	Milman I.I.	418, 419, 434, 440
Lubenko D.M.	283, 471, 472	Milonov A.S.	335, 356
Lucero D.J.	125	Milyutina E.V.	507
Lurie S.A.	394	Mingaleev A.R.	78
Lushchik A.	426	Mironova-Ulmane N.	520
Lushchik Ch.	426	Mishin I.P.	299
Lyamina G.V.	291	Mishin S.N.	78
Lysitsin V.M.	422	Miskiewicz S.A.	522
Lysyk V.V.	467	Mitichkin A.	431
Lyubutin S.K.	117, 120	Mitrofanov A.Yu.	453, 454, 455, 482
<b>M</b>		Mochulskaya N.N.	517
Ma H.	160	Moiseeva M.A.	468
Ma Xun	114	Moiseikin E.V.	419, 434
Maaroos A.	426	Molchanov P.	391
Mahinko F.F.	319	Moroz V.N.	454
Maikut S.A.	234	Morozov P.A.	13
Makarov A.S.	429	Morozova N.K.	497
Makarov A.V.	336	Morozova N.N.	343
Makarova A.F.	403	Moskvin P.V.	22, 23, 242
Makarova E.B.	334	Mozharovsky S.M.	319
Makovsky M.M.	233	Mulville T.D.	125
Maksimenko S.	391	Munasbaeva K.K.	333
Maksimova N.E.	517	Murakami K.	285
Malygina I.Yu.	336	Murzakaev A.M.	186, 411
Mamaev A.S.	375	Mussina G.I.	443
Mamaeva A.A.	397	Muzyukin I.L.	12, 38, 212
Mambetova K.M.	342	Mysyrowicz A.	182
Mamontov Y.I.	129	<b>N</b>	
Manko N.G.	518	Nagayev K.A.	66, 212
Mao H.-S.	61	Nalivaiko V.I.	361
Markov A.B.	279, 328, 364	Naumenko I.A.	316
Martemyanov S.M.	180, 474	Nechaev B.A.	60, 196, 197, 436
Martens V.Ya.	233	Nekrasova L.P.	526
Martynenko E.S.	487	Nelubina N.V.	476
Martynovich E.F.	404, 468, 469, 507, 510, 511, 524	Nemirovich-Danchenko N.M.	46, 47
Mastrikov Yu.A.	490, 491	Nepomnyashchikh A.	515
Matys V.G.	296, 297	Neshov F.G.	505
Mayer A.E.	246	Neyfeld V.V.	325
Mayer P.N.	246	Neyman A.A.	267, 272
Mazarakis M.G.	125, 126	Nguyen Bao Hung	175
Mcdaniel D.H.	125	Nguyen Man' Hung	109
Mckee G.R.	125	Nielsen D.S.	125
Mckennee J.	125	Nighmatullin R.M.	103
Medovnik A.V.	214	Nikiforov S.A.	203, 204
Medvedev A.I.	186	Nikiforov S.V.	5, 417, 433, 498
Meisner L.L.	266, 267, 268, 272, 276, 323	Nikitenkov A.N.	311
Meisner S.N.	268, 323	Nikitenkov N.N.	239, 311, 344
Melnik Yu.A.	217, 221	Nikitin A.P.	459, 460, 463, 464, 476, 477
Menshakov A.I.	28	Nikitin D.S.	408
Mesyats G.A.	10, 39, 119, 436	Nikitin I.V.	233
		Nikolaev A.G.	225, 298, 331
		Nikolaychuk G.A.	230

Nikulin S.P.	29	Paperny V.L.	130, 210, 507
Nomoev A.V.	390, 392	Paranin S.N.	184
Novikov M.V.	49	Parfenova E.S.	381
Novikov S.A.	91, 93, 94, 111	Pashpekin A.S.	456
Novikov V.	72	Pavlenko A.V.	70, 278
Nurakhmetov T.N.	428	Pavlenko T.S.	382
Nurmukhametov D.R.	463, 464, 476, 477	Pavlinsky A.V.	200, 201
Nurtazina A.S.	494	Pavlov A.P.	229
<b>O</b>			
Ochirov V.D.	320	Pavlov S.K.	295, 329, 407
Ogorodnikov A.S.	175	Pazyzbek S.	428
Ogorodnikov I.N.	421, 427, 440, 448	Pedin N.N.	140, 141
Okano M.	285	Pedos M.S.	120, 129, 137
Okotrub A.V.	391, 393	Pegel I.V.	51, 85, 90
Oks E.M.	33, 214, 223, 225, 227, 231, 232, 298, 304, 331	Pen'kov F.M.	436
Okunkova A.A.	353	Peresipkin A.S.	105, 106
Oleinik G.M.	56	Peresipkin A.V.	104
Oleinikov I.V.	526	Petikar P.	425
Oleshko V.I.	435, 467, 483	Petin V.K.	20, 121
Oleynik G.M.	183	Petkun A.A.	82, 84
Oliver B.V.	125	Petrenko M.D.	440
Olkhovskaya O.G.	56, 61, 72	Petrikova E.A.	280, 288, 345, 346, 349
Omelkov S.I.	421	Petrov V.I.	328
Orcikova H.	60	Petrovykh K.A.	506
Oreshkin E.V.	157	Petukevich M.S.	398
Oreshkin V.I.	57, 58, 59, 68, 69, 74, 76, 127, 134, 157	Philippov A.V.	436
Orlikov L.N.	342	Pichugin V.F.	386
Orlov A.V.	489	Pikulev A.A.	236
Orlov V.L.	489	Pikuz S.A.	78
Orlovskii V.M.	172	Pinaev G.A.	361
Osintseva A.L.	336	Pinchuk M.E.	63, 77
Oskirko V.O.	229	Ping Yan	147, 148, 205
Oskomov K.V.	277, 315	Pinzhin Yu.P.	357, 379
Ostapenko M.G.	266, 276	Plokhoi V.V.	278
Ostashev V.Ye.	80, 95	Plotnikov S.A.	334, 378
Othman H.A.	422	Pogorelko V.V.	256
Ovcharenko N.	431, 450	Point G.	182
Ovcharenko V.E.	309	Pol'skii V.I.	316
Ovchinnikov O.V.	264	Poleeva N.V.	454
Ovchinnikov S.V.	357, 379	Polisadova E.F.	422, 439
Ovchinnikov V.A.	523	Poltavtseva V.P.	265
Ovchinnikov V.V.	278, 319	Polukonova A.E.	335
Oztarhan A.	331	Polyakov O.V.	393
Ozur G.E.	25, 34	Ponomarev A.V.	129
<b>P</b>			
Padalko V.N.	60, 196, 197, 436	Ponomarev D.V.	30, 189, 190
Pak A.Ya.	401	Poplavsky V.V.	296, 297
Pak V.H.	441, 274, 324	Popov A.A.	510
Paklin A.	515	Popov A.I.	426
Pan E.S.	46, 47	Popova E.V.	264
Panarin V.A.	172, 236	Porter J.L.	125
Panchenko A.N.	150, 177, 199, 499	Portnov D.S.	186
Panchenko N.A.	150	Postnov V.V.	383
Panchenko Yu.N.	119, 192, 198, 200, 201, 499	Potekaev A.I.	290, 340
Panichkin A.V.	397	Potyomkin G.V.	351, 352
Panin A.V.	509	Pozubenkov A.A.	63
Panova T.V.	250, 261, 262	Pribytkov G.A.	387, 388
		Primak I.G.	513
		Puchikin A.V.	198, 200
		Pugovkin M.M.	368
		Punanov I.F.	13
		Purans J.	301
		Pushilina N.S.	327, 365

Pushkarev A.I.	14	Saigash A.S.	376, 405
Pustovarov V.A.	418, 421, 423, 424, 427, 520, 521	Sainova A.B.	397
Putrik M.B.	502	Sakharchuk Y.P.	456
<b>R</b>		Saladukhin I.A.	284
Rabotkin S.V.	368, 377	Salimi K.G.	396
Radko S.I.	211	Samoylenko G.M.	92, 96
Radnaev B.R.	402	Sarapulova A.E.	275
Radzhabov E.A.	516	Sariyev O.R.	508
Raharjo P.	285	Sasorov P.V.	56, 61
Rakevich A.L.	404, 507, 524, 529	Sataeva G.E.	410
Rakhadilov B.K.	27, 322	Savage M.E.	125
Rakhmatullin I.A.	403	Savateeva E.A.	517
Ramazanov I.S.	273	Savitskii A.P.	387, 388
Ramazanov K.N.	273, 337, 350, 383	Savkin K.P.	223, 225, 231, 298, 385
Ratakhin N.A.	60, 119	Savostikov V.M.	290
Rau A.G.	396	Sazonov R.V.	30, 189, 190
Razin A.	481, 483, 484	Schamiloglu E.	83
Remnev A.G.	249	Schanin P.M.	24, 215, 219
Remnev G.E.	30, 41, 189, 190, 295, 327, 329, 351, 352, 407, 432, 512	Scherbinin S.V.	181, 191
Rempe N.	213	Schmauder S.	486
Rempel A.A.	506	Schroeder C.B.	61
Repin P.B.	162	Schuvalov E.N.	196, 197
Rezac K.	60, 75	Sedin A.A.	188
Rezvova M.A.	274	Sednev V.V.	338, 339
Rhee C.-K.	184	Sedunova I.N.	427, 448
Ribalko E.V.	363	Seitov A.S.	333
Rodzevich A.P.	466	Semenov A.P.	358, 359
Romanchenko I.V.	102, 113, 137	Semenov D.B.	130
Romanov I.	72	Semenova I.A.	358
Romanov I.V.	332	Semin V.O.	267, 272
Romanov N.A.	392	Semjonova Yu.N.	46, 47, 88
Romanov V.Ya.	396	Sergachev D.V.	361
Romanova V.M.	78	Sergeev A.S.	79
Rongyao Fu.	148, 205	Sergeev V.P.	325, 363
Rostov V.V.	43, 44, 45, 85, 87, 97, 102, 113, 137, 179, 193	Sergeyev D.M.	445, 447
Rousskikh A.G.	58, 59, 68, 69	Serikbayeva G.D.	445
Rovbut A.Y.	284	Seropyan G.M.	412
Roznowski S.A.	125	Serykau A.	318
Rubanov P.V.	519	Shalaev A.A.	504, 515
Rubshtein A.P.	334, 378	Shalimov L.N.	518
Rud A.D.	76	Shalnov K.	362
Rukin S.N.	117, 120, 137	Shamiankou U.	306, 318
Rusakov A.I.	504	Shamiankova A.	306, 318
Rusalsky D.P.	41	Shandrikov M.V.	298, 385
Russakova A.	501	Shanenkov I.I.	376, 401, 413
Rutberg Ph.G.	63	Shao T.	148, 160, 244
Ryabchikov A.I.	247, 257, 258, 259, 260	Sharkeev Yu.P.	289, 366, 396, 397
Ryaboukhin O.V.	505	Sharypov K.A.	43, 44, 45, 101, 102, 137, 138, 139
Rybka D.V.	153, 174	Shchepina L.I.	513
Ryzhov V.V.	178	Shejan V.P.	303
<b>S</b>		Shekhovtsov V.V.	224
Sadykov A.F.	170	Shelkovenko T.A.	78
Sadykova A.G.	79, 170	Shemyakin I.A.	71, 73, 244, 341
Sadykova B.M.	428	Shendrik R.	515
Saenko M.Yu.	191	Shestakov G.V.	518
Safonova E.E.	482	Shibitov Yu.M.	156
Sagymbaeva Sh.Zh.	446	Shipaev I.V.	480
		Shipilova A.V.	377
		Shipilova O.I.	495, 507
		Shirvanyanz G.G.	254
		Shishlov A.V.	60, 75, 124

Shiyan V.P.	109	Spirin A.V.	184
Shklyaev V.A.	155, 165, 166, 178	Stepanov A.Yu.	492
Shlapakovski A.	83	Stepanov K.I.	413
Shmelev D.L.	31, 32, 40	Stepanova E.N.	299
Shnitnikov A.S.	497	Stepanova O.M.	77
Shonokhova A.A.	518	Stepchenko A.S.	104, 143
Shpak V.G.	43, 101, 102, 137, 138, 139	Stoltzfus B.	125
Shpilinskaja O.	531	Strelkov P.S.	112
Shtang T.V.	500	Struve W.E.	125
Shtykov A.N.	518	Stygar W.A.	125
Shuba M.	391	Sukhikh L.G.	449
Shugurov V.V.	15, 209, 345, 346, 365, 373	Sukhushin K.N.	84
Shulepov I.A.	290, 344	Sukovaticin Yu.A.	68
Shulepov M.A.	172, 277, 315, 332	Sulakshin S.A.	15, 23, 24
Shulgin B.V.	518	Sun Y.	160, 244
Shulov V.A.	248, 254, 310	Surdo A.I.	418, 419, 434
Shumeiko D.V.	112	Surkov Yu.S.	203, 204
Shunailov S.A.	43, 44, 45, 79, 101, 102, 136, 137, 170	Suslov A.I.	150
Shunkeyev K.Sh.	445, 446, 447	Sutygina A.N.	344
Shunkeyev S.K.	446	Svechkanova A.A.	409
Shvayko V.N.	456	Svetlichnyi V.A.	283, 471, 472
Shymanski V.I.	270, 407, 432	Svirko Y.	391
Sidelev D.V.	372, 380	Synebryukhov V.A.	126
Sigfusson I.N.	311, 312	Sypchenko V.S.	239, 311
Sigfusson T.I.	239		
Sila O.	60, 75	<b>T</b>	
Sivin D.O.	247, 257, 258, 259, 260, 344	Tabachenko A.N.	290
Sivkov A.A.	276, 399, 400, 401, 403, 405, 408, 409, 413	Tagayeva B.S.	443, 444
Sivov Yu.A.	312	Tarakanov V.P.	80, 212
Sizova T.Yu.	516	Tarasenko V.F.	53, 149, 150, 151, 153, 154, 155, 158, 164, 167, 168, 169, 171, 174, 177, 196, 197, 199, 236, 277, 282, 315, 332, 479
Skakov M.K.	27, 322	Tarasov V.	531
Skripin A.	483	Tardiveau P.	161
Skripkin N.I.	104	Tcherepanov A.N.	518
Skripnikova N.K.	224	Terentyeva A.O.	455, 482
Skuratov V.A.	317	Teresov A.D.	242, 272, 280, 287, 288, 299, 309, 343, 345, 346, 349, 398, 412
Slabodchikov V.A.	379	Teryaev A.D.	310
Slesarev A.I.	418	Teryaev D.A.	248, 254, 310
Slinko V.N.	104, 105, 106	Tilikin I.N.	78
Slovikovsky B.G.	120	Timoshenkov S.P.	120
Smirnov V.P.	183	Timoshenkova O.R.	411
Smirnyagina N.N.	320, 335, 355, 356, 358, 359	Ting Shu.	107
Smoljakova M.Y.	351, 352	Tkachenko A.V.	349
Smorudov G.V.	118	Tkachenko D.V.	234
Sobolev A.B.	429	Tkachenko S.I.	56, 66
Soboleva N.N.	336	Tolkachev O.S.	308
Sochugov N.S.	229, 368	Tolstokulakov A.M.	313
Sokolov P.S.	423, 521	Totmeninov E.M.	85, 89, 90
Sokolov V.I.	423, 520, 521	Trefilova L.	431, 450, 531
Sokovnin S.Yu.	181, 191, 406, 418	Trenikhin M.V.	412
Sokullu E.	331	Trenkin A.A.	156, 163
Soloviev A.A.	229, 367, 368	Trifonov S.A.	230
Solovyev A.A.	377	Truhachev F.	318
Sorokin D.A.	149, 151, 154, 164, 167, 196, 197	Trunev Yu.A.	18, 241
Sorokin S.A.	9, 67	Tscherbakov M.G.	191
Sorokova S.N.	347	Tsipilev V.P.	467, 481, 483, 484
Sosnin E.A.	236	Tskhai S.	159
Sosnin K.V.	343	Tsoy N.V.	118
Sotnikova L.V.	492		
Spiridonova T.I.	514		

Tsuchiya T.	362	Vladimirov A.B.	334, 378
Tsybul'skiy L.Yu.	234	Vlasov M.I.	418, 419, 434
Tsygankov R.V.	85, 87	Voitsekhovskii A.V.	332
Tsygvintsev I.	72	Vokhmitsev A.S.	518
Tsyranov S.N.	117, 120	Volkov E.N.	68
Tsyrenov D.B-D.	359	Volkov N.B.	54, 66, 212
Tuch E.V.	514	Volkov N.V.	286, 526
Tueva K.S.	482	Volokitin G.G.	224
Tugushev V.I.	188	Volokitin O.G.	224, 308, 340
Tukshaitov R.H.	103	Volosova M.A.	217, 221
Tuleushev Yu.Zh.	436	Volzhaninov D.	12
Tupikova O.S.	257, 380	Vorobyov M.S.	15, 23, 24, 53
Tupitsyn A.V.	456	Voronov A.V.	363
Tupitsyna I.A.	439	Vostrov D.O.	427, 448
Turek K.	60		
Turmyshev I.S.	212, 411	<b>W</b>	
Tuseyev T.	333	Wakeland P.E.	125
Tussupbekova A.K.	443	Wang Lingyun	114
Tverdokhlebova A.V.	268, 323	Webb T.J.	125
Tyunkov A.V.	231, 298, 385	Weinstein I.A.	518
Tyurin Yu.I.	239, 311, 312		
<b>U</b>		<b>X</b>	
Udovichenko S.Yu.	240	Xiaoping Zhang	100
Uemura K.	123, 249, 274, 285, 362	Xie Weiping	114, 115
Uglov V.V.	41, 245, 270, 271, 284, 300, 302, 317, 407, 432	Xueke Che	148
Ugodnikov G.G.	204	Xuzhe Xu	147
Uimanov I.V.	32, 38, 39, 40	<b>Y</b>	
Ul'ynov A.V.	80, 95	Yagafarov I.I.	383
Ulmaskulov M.R.	43, 44, 45, 101, 102, 136, 137	Yakovlev E.V.	279, 328, 364
Umnov S.P.	294	Yakovlev V.	431, 450, 531
Urazova A.S.	193	Yakovlev V.V.	215, 220
Urbakh A.E.	211	Yakovlev V.Yu.	418, 448
Urbakh E.K.	211	Yakushin V.L.	252, 316
Usikov A.I.	399, 400	Yalandin M.I.	43, 44, 45, 79, 101, 102, 137, 170
Usmanov B.F.	383	Yalovets A.P.	245, 253, 255, 256
Usseinov A.	301	Yampolskaya S.A.	200
Ustyantsev Yu.	5, 498	Yang H.W.	86
Uvarin V.V.	204	Yang W.	160
<b>V</b>		Yangmei Li.	100
Vafin R.K.	350	Yanin S.N.	228
Vagin E.S.	16	Yano K.	123
Valiev D.T.	439	Yaohong Sun.	147, 148, 205
Valiev R.Z.	252	Yapparov R.Sh.	286
Valikov R.A.	286, 526	Yashin A.S.	286
Valko N.G.	384	Yastremskii A.G.	192, 200
Vasil'chenko E.	426	Yatom S.	159
Vasil'ev I.P.	330	Yazawa N.	123
Vasileva O.V.	42	Ye Min. Soe	353
Vasiliev S.V.	126	Yinghui Gao	148, 205
Vasilkovskiy A.O.	504	Yuan Jianqiang	114
Vasilyev S.A.	193	Yudin A.S.	187, 195
Vekselman V.	159	Yue Zhao	116
Vershinin G.A.	262	Yurchenko V.I.	106
Vesnina S.N.	480	Yurjev Y.N.	372, 380
Vilkhivskaya O.V.	239, 311, 344	Yurov V.M.	389
Vizir A.V.	223	Yuryeva A.V.	251
Vladimirov A.A.	492	Yushkov G.Yu.	223, 225, 298, 331
		Yushkov Yu.G.	91, 93, 94, 98, 111, 231
		Yuzhang Yuan	110

<b>Z</b>			
Zabels R.	501	Zhumagaliyev E.U.	508
Zaitcev D.A.	380	Zhunusbekov A.M.	428
Zakharov A.N.	367	Zhuravlev M.V.	295
Zakharova M.A.	266	Zhuravlev P.G.	461, 470
Zakrevsky D.E.	122, 173	Ziganshin A.I.	313, 314
Zamoshchina T.A.	88	Zilov S.A.	404, 469, 529
Zarko V.E.	467, 473, 483, 484	Zimin V.P.	226
Zarva D.B.	27	Ziska D.	125
Zaslavsky V.Yu.	79, 101	Zlotski S.V.	284, 317
Zavatskiy O.N.	389	Zolnikov K.P.	420
Zayats G.M.	522	Zolotov I.V.	337
Zdorovets M.	501	Zolotukhin D.B.	231, 304
Zemskov Yu.A.	38, 212	Zorin V.B.	78
Zhang C.	160	Zorkaltseva M.Yu.	82, 84
Zhang J.	86	Zotova I.V.	79, 101
Zhanturina N.N.	446, 447	Zou Wenkang	115
Zherlitsyn A.A.	52, 140, 141	Zubarev N.M.	10, 37
Zherlitsyn A.G.	109, 303	Zubareva O.V.	37
Zhevnyak V.D.	274, 324	Zuev M.G.	406
Zhidkov M.V.	351, 352	Zvekov A.A.	459, 463, 464
Zhigalin A.S.	58, 59, 68, 69	Zverev A.S.	453, 454, 455, 482
Zhiqiang Li.	107	Zvigintsev I.L.	19
Zhmurikov E.I.	263	Zvonarev S.V.	5, 498, 500
Zhorov A.A.	439	Zybin K.P.	170
Zhubaev A.K.	494	Zykov I.Yu.	458, 459, 460
Zhukovskii Yu.F.	301	Zyryanov S.S.	505
		Zyul'kova L.A.	243